DTIC FILE COPY.

MARINE PHYSICAL LABORATORY
SCRIPPS INSTITUTION OF OCEANOGRAPHY

San Diego, California 92152

DTIC FILE COPY.

AD-A201 977

Comparison of Swallow Float, Ocean Bottom Seismometer, and Sonobuoy Data in the VLF Band

G. L. D'Spain and W. S. Hodgkiss

DTIC
ELECTE
NOV 16 1988
S D
H

MPL TECHNICAL MEMORANDUM 404

MPL-U-32/88

Approved for public release; distribution unlimited.

88 11 16 035

SECURITY CLASSIFICATION OF THIS PAGE

ADA201977

REPORT DOCUMENTATION PAGE

1a. REPORT SECURITY CLASSIFICATION UNCLASSIFIED	1b RESTRICTIVE MARKINGS
2a. SECURITY CLASSIFICATION AUTHORITY	3. DISTRIBUTION/AVAILABILITY OF REPORT Approved for public release; distribution unlimited.
2b. DECLASSIFICATION/DOWNGRADING SCHEDULE	
4. PERFORMING ORGANIZATION REPORT NUMBER(S) MPL TECHNICAL MEMORANDUM 404 [MPL-U-32/88]	5. MONITORING ORGANIZATION REPORT NUMBER(S)
6a. NAME OF PERFORMING ORGANIZATION Marine Physical Laboratory 6b. OFFICE SYMBOL (If applicable) MPL	7a. NAME OF MONITORING ORGANIZATION Office of Naval Research Department of the Navy
6c. ADDRESS (City, State, and ZIP Code) University of California, San Diego Scripps Institution of Oceanography San Diego, CA 92152	7b. ADDRESS (City, State, and ZIP Code) 800 North Quincy Street Arlington, VA 22217-5000
8a. NAME OF FUNDING/SPONSORING ORGANIZATION Office of Naval Research 8b. OFFICE SYMBOL (If applicable) ONR	9. PROCUREMENT INSTRUMENT IDENTIFICATION NUMBER N00014-87-K-0010
8c. ADDRESS (City, State, and ZIP Code) Department of the Navy 800 North Quincy Street Arlington, VA 22217-5000	10. SOURCE OF FUNDING NUMBERS PROGRAM ELEMENT NO. / PROJECT NO. / TASK NO. / WORK UNIT ACCESSION NO.
11. TITLE (Include Security Classification) COMPARISON OF SWALLOW FLOAT, OCEAN BOTTOM SEISMOMETER, AND SONOBUOY DATA IN THE VLF BAND	
12. PERSONAL AUTHOR(S) G. L. D'Spain and W. S. Hodgkiss	
13a. TYPE OF REPORT tech memo 13b. TIME COVERED FROM _____ TO _____ 14. DATE OF REPORT (Year, Month, Day) September 1988 15. PAGE COUNT 564	
16. SUPPLEMENTARY NOTATION	
17. COSATI CODES FIELD / GROUP / SUB-GROUP	18. SUBJECT TERMS (Continue on reverse if necessary and identify by block number) Swallow floats, ocean bottom seismometers, sonobuoy, spectral differences

19. ABSTRACT (Continue on reverse if necessary and identify by block number)

Very low frequency (VLF) data collected concurrently by three sets of instruments, the Marine Physical Laboratory's freely drifting Swallow floats, an array of ocean bottom seismometers (OBSs) deployed by Prof. Dorman's group at Scripps Institution of Oceanography, and sonobuoys from the Naval Air Development Center, are compared. The data were collected in April and May, 1987, near the site of Deep Sea Drilling Project hole 469, 32.5° N, 120.5° W.

In order to make the data comparisons quantitative, the OBS and sonobuoy data were resampled to a sampling frequency of 50 Hz and the time bases for the three sets of instruments were aligned using coherent arrivals. Spectra, spectral differences, and coherence squared estimates were calculated and plotted. The results indicate that the Swallow float geophone data are consistent (that is, the spectra from different instruments

20. DISTRIBUTION/AVAILABILITY OF ABSTRACT ☐ UNCLASSIFIED/UNLIMITED ☒ SAME AS RPT ☐ DTIC USERS	21. ABSTRACT SECURITY CLASSIFICATION UNCLASSIFIED
22a. NAME OF RESPONSIBLE INDIVIDUAL	22b. TELEPHONE (Include Area Code) / 22c. OFFICE SYMBOL MPL

DD FORM 1473, 84 MAR 83 APR edition may be used until exhausted. All other editions are obsolete

SECURITY CLASSIFICATION OF THIS PAGE

* U.S. Government Printing Office: 1986—607-044

of the same type do not differ within the confidence limits of the spectral estimates) as are most of the OBS vertical-axis geophone data. The inter-Swallow-float coherences are significantly different from zero at frequencies thought to be broadcast by the research vessels in the experiment. The inter-vertical-axis-OBS coherences are also significantly different from zero at frequencies below 6 Hz as well as at the ship frequencies. The high coherences below 6 Hz is probably due to the close spacing of the OBSs in the experiment.

On the other hand, the OBS horizontal-axis geophone data from different instruments can vary over several tens of decibels in spectral level, the OBS hydrophone time series contain 0.5-second spikes of various amplitudes, and the sonobuoy data appear to suffer from some type of contamination below 10 Hz. The sonobuoy contamination has the same appearance as that due to flow noise.

DTIC COPY INSPECTED 6

Accession For
NTIS GRA&I ☑
DTIC TAB ☐
Unannounced ☐
Justification
By
Distribution/
Availability Codes
Dist | Avail and/or Special
A-1

Comparison of Swallow Float, Ocean Bottom Seismometer, and Sonobuoy Data in the VLF Band

G. L. D'Spain and W. S. Hodgkiss

Marine Physical Laboratory
Scripps Institution of Oceanography
San Diego, CA 92152

ABSTRACT

Very low frequency (VLF) data collected concurrently by three sets of instruments, the Marine Physical Laboratory's freely drifting Swallow floats, an array of ocean bottom seismometers (OBSs) deployed by Prof. Dorman's group at Scripps Institution of Oceanography, and sonobuoys from the Naval Air Development Center, are compared. The data were collected in April and May, 1987, near the site of Deep Sea Drilling Project hole 469, 32.5°N, 120.5°W.

In order to make the data comparisons quantitative, the OBS and sonobuoy data were resampled to a sampling frequency of 50 Hz and the time bases for the three sets of instruments were aligned using coherent arrivals. Spectra, spectral differences, and coherence squared estimates were calculated and plotted. The results indicate that the Swallow float geophone data are consistent (that is, the spectra from different instruments of the same type do not differ within the confidence limits of the spectral estimates) as are most of the OBS vertical-axis geophone data. The inter-Swallow-float coherences are significantly different from zero at frequencies thought to be broadcast by the research vessels in the experiment. The inter-vertical-axis-OBS coherences are also significantly different from zero at frequencies below 6 Hz as well as at the ship frequencies. The high coherences below 6 Hz is probably due to the close spacing of the OBSs in the experiment.

On the other hand, the OBS horizontal-axis geophone data from different instruments can vary over several tens of decibels in spectral level, the OBS hydrophone time series contain 0.5-second spikes of various amplitudes, and the sonobuoy data appear to suffer from some type of contamination below 10 Hz. The sonobuoy contamination has the same appearance as that due to flow noise.

September 5, 1988

Table of Contents

Introduction

I. Data Resampling

II. Time Series
- i) April Deployment
  - a) Swallow Float Time Series
  - b) Ocean Bottom Seismometer Time Series
  - c) Sonobuoy Time Series
- ii) May Deployment
  - a) Swallow Float Time Series
  - b) Ocean Bottom Seismometer Time Series

III. Time Series Alignment
- i) April Deployment
- ii) May Deployment

IV. Velocity and Pressure Spectral Estimates
- i) April Deployment
  - a) Midwater Swallow Float Spectra
  - b) Ocean Bottom Seismometer Spectra
  - c) Sonobuoy Spectra
- ii) May Deployment
  - a) Midwater Swallow Float Spectra while the Float was Descending
  - b) Additional Midwater Swallow Float Spectra
  - c) Bottom-Mounted Swallow Float Spectra
  - d) Ocean Bottom Seismometer Spectra

V. Spectral Differences
  - a) Spectral Differences between Instruments of the Same Type
  - b) Spectral Differences between a Bottom Swallow Float and the Midwater Floats
  - c) Spectral Differences between a Bottom Swallow Float and the OBSs
  - d) Spectral Differences between the Midwater Swallow Floats and the OBSs
  - e) Spectral Differences between the Midwater Swallow Floats and the Sonobuoys
  - f) Spectral Differences between the OBS Hydrophones and the Sonobuoys

g) Spectral Differences between a Descending Swallow Float and One at Depth
h) Spectral Differences between a Descending Swallow Float and the Sonobuoys
i) Spectral Differences between Swallow Float Data in April and in May

VI. Coherence Squared Estimates
a) Coherence Squared Estimates between Two Midwater Swallow Floats
b) Coherence Squared Estimates between Two Ocean Bottom Seismometers
c) Coherence Squared Estimates between Two Sonobuoys
d) Coherence Squared Estimates between a Midwater Swallow Float and an OBS
e) Coherence Squared Estimates between a Midwater Swallow Float and a Sonobuoy

Acknowledgements

References

Appendix - Calibration Curves

Figures

Introduction

This progress report presents results from the initial attempts to inter-compare Swallow float geophone data, Naval Air Development Center (NADC) sonobuoy data, and ocean bottom seismometer (OBS) geophone and hydrophone data. These data were collected during the April and May, 1987 deployments of the Swallow floats. Important details on the two sea trips, as well as on the three sets of instruments, are contained in "Freely drifting Swallow float array: April, 1987 Trip report" [1] and "Freely drifting Swallow float array: May, 1987 Trip report" [2].

The three sets of instruments measure different quantities and attempts to inter-compare the sensor systems' data must take this into account. The Swallow float geophones are water-particle-velocity sensors, i.e. they measure the three components of velocity, v_x^w, v_y^w, and v_z^w, where the superscript indicates that the measurements are made in the water-column. From the power spectra of the three components of particle velocity, the equivalent plane wave pressure power spectrum can be derived [3]. The sonobuoys measure water-column pressure, p, as do the two types of hydrophones attached to the ocean bottom seismometers. The OBS geophones measure the three components of sediment velocity, v_x^s, v_y^s, and v_z^s.

The Swallow float data were recorded during two 24-hour periods in 1987, starting at 07:54, 22 April, and at 09:56, 5 May. In April, the midwater floats were neutrally buoyant at about 400 meters depth; in May, the floats were ballasted for about a 1800-meter depth. Useable data were obtained from five midwater column Swallow floats and two bottom Swallow floats during the April deployment and from six midwater floats and three bottom floats during the May trip.

Most of the OBS events which were recorded during these two periods of time are listed in Table 1. These instruments rested on the sediment-covered bottom, at about 3800 meters depth. Data were collected from nine properly functioning instruments and have been provided to us by Dr. L. Dorman and his research team.

The NADC sonobuoys were only deployed during the April trip. They were tethered to a surface-drifting float by a 140-meter cable. Seven of the eight ship-launched sonobuoys operated successfully during an eight-and-a-half-hour period, starting at 17:03, 22 April. Some of the sonobuoy data, recorded in analog form, were subsequently digitized at 20 kHz. Data recorded during an 18-minute period, from 19:26 to 19:44, 22 April, by two sonobuoys have been given to us by NADC. We have requested additional digitized data, including data from the twelve, concurrently deployed, air-launched sonobuoys.

In this report, the conversion between time and Swallow float record number was made assuming that the first record written was record number 1. However, the first record written to tape was actually record 0. In addition, when the floats were synchronized, their microprocessor program spent a half-second in initialization, preceeded by a 120 msec delay. Therefore, a 45.62-second offset must be made to the Swallow time base assumed in this report in order to obtain the true float time base. However, this offset does not affect any of the results presented herein since the time base alignment in Section III implicitly takes it into account.

Note that all times given above and in the following sections are in local Pacific Daylight Time. To get Greenwich Mean Time, add seven hours.

I. Data Resampling

In order to make quantitative comparisons between the various sets of data, the OBS time series, sampled at 128 Hz, and the sonobuoy time series, sampled at 20 kHz, had to be resampled in order to match the 50 Hz sampling frequency of the Swallow float data. This section describes how this was done.

The OBS data were resampled in four steps; interpolation by a factor of five was done to go from a sampling frequency of 128 Hz to 640 Hz, low-pass filtering and desampling by a factor of 8 was next done to go from 640 Hz to 80 Hz, and, finally, these two steps were repeated in order to go from 80 Hz to 400 Hz to 50 Hz. Interpolation was done using a sinc function with 17 coefficients. The 128-coefficient, finite-impulse-response, equal-ripple, digital filter used in the low-pass filtering operation was designed using the Remez exchange algorithm. The filter had a transition (from pass band to stop band) width of 0.03 fractional sampling frequency, a ripple deviation in the pass band of 0.0039 dB and a -67.04 dB ripple deviation in the stop band. The transfer function of the total four-step resampling operation is shown in Figure I.1. Frequencies above 20 Hz are attenuated due to the finite transition width of the filter.

To verify that the OBS resampling process was behaving properly, spectra calculated from time series sampled at the original 128 Hz were plotted, from 0 to 25 Hz, on top of spectra estimated from time series resampled to 50 Hz. Figure I.2 shows the results of a typical comparison. Most of the perceptible differences occur above 22 Hz, as expected from the transfer function of the resampling process. Some of the differences are also due to the slightly different total duration of the time series considered in each case.

The 20 kHz sonobuoy data were also resampled in a four-step process. Two identical steps of low-pass filtering and desampling by a factor of five, to go from 20 kHz to 4 kHz to 800 Hz, were followed by two identical steps of filtering and desampling by a factor of four, to go from 800 Hz to 200 Hz to 50 Hz. The two equal ripple digital filters used in the process also had 128 coefficients and transition widths of 0.03 fractional sampling frequency. The filter used prior to desampling by five had ripple deviations in the pass band and stop band of 0.0035 dB and -67.98 dB, respectively, and the filter used prior to desampling by four had deviations in the pass band and stop band of 0.0037 dB and -67.40 dB. The transfer function of the sonobuoy resampling process is shown in Figure I.3.

II. Time Series

Selected time series from each of the sensor systems are presented in this section. Data collected during the April deployment are presented first, followed by data from the May deployment.

i) April Deployment

a) Swallow Float Time Series

Swallow float records 547 through 558, which were recorded between 14:44 and 14:53, 22 April, appear in Figures II.1 to II.5. Only the data from the midwater floats are presented; both of the bottom Swallow floats' data were contaminated by tether effects during this time. This block of records was written before the floats had reached their equilibrium depth. The very low frequency (about 0.4 Hz), flow-induced float rocking is evident on the horizontal geophone components. The one-to-two-second duration arrivals occuring ten seconds into some of the records are caused by the 8 kHz localization ping issued by each float every 12 records. These time series are plotted because the ship-generated signal, becoming predominant in record 553 on the z axes, was used to align the Swallow float and the OBS time series in the April experiment.

Swallow float records 927 through 938, recorded approximately between 19:29 and 19:38, 22 April, are plotted in Figures II.6 to II.10, for all properly operating midwater floats. The clipped arrivals in records 927 and 929 are from two 5-lb TNT detonations, shots #4 and #5, deployed from the Melville [1]. The clipped arrivals on the horizontal geophone axes in records 931 and 932 are probably due to the Narragansett.

b) Ocean Bottom Seismometer Time Series

The four-component time series recorded by ocean bottom seismometers 05 and 06 during events 87 and 88 are plotted in Figures II.11 and II.12. Only these two OBSs recorded events 87 and 88. The events' starting times were 14:31 and 14:46, 22 April. (Refer to Tables I.8 and I.9 in the May Swallow float trip report [2] for the starting times of *all* events recorded while the Swallow floats were in the water in April and May). These time series are presented because the Narragansett-generated signal at the end of event 88 was used to align the ocean bottom seismometer time base with that of the Swallow floats during the April experiment (see the following section).

The four-component OBS time series for events 105 through 112, each 29 seconds in duration, are plotted in Figures II.13 through II.21. The events were recorded 15 minutes apart starting at 19:01 (Table 1). The time series amplitude is normalized by the value given at the top of each figure. Event 107 is studied further in the following sections since it was recorded during the time period for which sonobuoy data were available (19:26 through 19:44) as well as during the time period for the recording of Swallow float record 930, presented in Figures II.6 through II.10. For a discussion of the quality of the OBS data, see the May trip report [2].

c) Sonobuoy Time Series

Four minutes of sonobuoy time series are presented in Figures II.22 and II.23 for two sonobuoys, channels 20 and 21. Note that each figure shows *three* minutes of data, recorded between the beginning of the two times listed in the figures, and that the two figures have a two-minute overlap. The abscissa in the figures has a length of 45 seconds, in order to be consistent with the Swallow float and OBS time series plots. Again, the amplitude has been normalized by the value given at the top of each plot.

The two arrivals due to the two TNT shots #4 and #5 are clearly recorded. These arrivals allow the Swallow float and sonobuoy time series to be aligned, as discussed in the next section. The low frequency oscillation in sonobuoy 20's time series starting about 35 seconds into time 19:29 may be caused by the

140-meter-long sonobuoy tether. Sonobuoy 20 data also show a few spurious spikes which are probably not of acoustic origin since they were not recorded by sonobuoy 21.

ii) May Deployment

a) Swallow Float Time Series

Selected time series, records 1044 through 1055, written by the midwater Swallow floats during the May deployment are presented in Figures II.24 through II.29. This period of time, from 22:59 through 23:08, 5 May, was chosen for plotting because of the simultaneous recording of the three-minute OBS event 313 and because of the presence of a coherent arrival, thought to be ship-generated, near the end of record 1048 on the horizontal Swallow float geophone components.

b) Ocean Bottom Seismometer Time Series

Events 311 (179 seconds of data starting at 17:01, 5 May) and 313 (179 seconds of data starting at 23:01, 5 May) recorded by the ocean bottom seismometers are plotted in Figures II.30 through II.38. Event 311 was recorded during the time when bottom-mounted Swallow float 11 was apparently uncontaminated by its tether. (Float 11 time series are presented in Figures X.9c of the May trip report [2]). Event 313 was recorded within an hour after the research ship, the Scorpius, had steamed across the array. Therefore, the coherent arrival ten to fifteen seconds into event 313, most prominently recorded on the vertical geophone axes of OBSs' 02, 04, 06, and 13, was probably ship generated. It is *assumed* that this coherent arrival is the same one recorded on the Swallow floats' horizontal axes in record 1048. This assumption allows the Swallow float and OBS time series to be approximately aligned so that inter-comparisons between data taken at the same time can be made. Since only spectral differences, and not coherences, between the two sensors have been attempted for the May trip data, the need to align the time bases accurately can be relaxed by assuming that the noise is stationary over the remaining (and unknown) period of time offset between the time series.

III. Time Series Alignment

Coherence squared estimates, presented in Section VI, are dependent upon the time offset between the two time series under consideration. That is, $\gamma^2(\tau) = \gamma^2(0)\left[1-\frac{\tau}{T}\right]$, where τ is the time offset between the time series, T is the time period for each segment of data being transformed, and γ is the frequency-dependent coherence function. Therefore, in order to obtain maximum coherence squared estimates, the three sensor systems' time series must be aligned.

i) April Deployment

In the April trip, the recording of the TNT explosions allow for the time bases of the Swallow floats and the sonobuoys to be aligned. Unfortunately, the ocean bottom seismometers did not record any of the explosions. A complete search of the OBS time series has been performed in order to find alternate coherent arrivals with which to align the time bases. The only candidate in the April data, a Narragansett-generated arrival, appears at the end of event 88 in OBSs' 05 and 06 time series and in record 553 of the Swallow float data. (See the time series plots in Section II). Figures III.1 through III.10 show the results of cross-correlating the midwater Swallow float time series in record 553 with the last 44 seconds of event 88. A peak consistently occurs at a lag of just over -6 seconds in the plots showing the cross-correlation of the Swallow float axes with the OBSs' vertical axes, the uppermost plot in each figure. Therefore, the first sample point of record 553 corresponds to a sample taken just about 129 seconds into event 88.

The delay estimated in the previous paragraph includes the delay due to the difference in propagation path lengths from the Narragansett to the two sets of instruments. To estimate the path difference, the approximate Swallow float location was gotten from linearly interpolating between the location where the floats were deployed and where they were retrieved after recall (re Figure I.1 of [1]). The location of the Narragansett was known from intermittent log entries (see Figures II.1 of [1]) and the OBS locations were known from very accurate GPS position fixes (re Figures I.5 and I.6 of [1]). The estimated path length difference causes approximately a one second difference in the arrival of the signal at the two sensor systems. Therefore, a sample recorded at the beginning of record 553 was recorded at about the same time as a point 128 seconds into event 88. This implies that the ocean bottom seismometer time base measures the time of Swallow float synchronization to be 07:53:20, 22 April, which is well within the accuracy of the logged Swallow float synchronization time of 07:54 since the time was simply read from a wrist watch.

Because of the impulsive nature of the TNT explosion, the Swallow float and sonobuoy time bases can be easily aligned by eye using the time series plots in Section II. From Figure II.22, the arrival of the first explosion in the sonobuoy data occurred at 19:29:19.3 and the second one arrived at 19:30:15.9. The arrival times were gotten from the first large impulsive arrival. However, both explosions recorded by both sonobuoys show a small precursor arriving 1.8 seconds before the main pulse train. Since the Swallow float time series show no such precursor clearly, the arrival time of the main impulsive arrival was used.

The arrivals of the explosions in the Swallow float data are most clearly recorded on the vertical geophone component. Since the floats each have independent internal clocks which drift slightly with respect to one another (less than a second in 24 hours), the explosions' arrival times can vary between floats due both to differences in propagation distances and to relative clock drift. From the inter-float localization ping data (see [1], Section VII), floats 0 and 1 show very little relative clock drift. Because of that, and because the explosions' arrival times measured from these two floats' data are about the average of the arrival times for all midwater Swallow floats, floats 0 and 1 were chosen for determining the arrival times. (Actually, the maximum difference in arrival times between each of the Swallow floats for a given shot was only 0.8 seconds). The two detonation arrivals are at 19:29:52.0 and 19:30:48.5 from Swallow floats' 0 and 1 z-axis data. This results in a 32.7-second time offset between between the Swallow float and the sonobuoy time bases. From the geometry of TNT explosions #4 and #5 (Figures II.6 and II.7 of [1]) with respect to the estimated positions of the Swallow floats (from Figure I.1 of [1]) and the sonobuoys (from Figure I.3 of [1]), no significant time delay due to propagation path differences appears to exist. Therefore, according to the sonobuoy time base, the Swallow floats were not synchronized at 07:54, but rather at 07:53:27.3, 22 April. This implies that a 7.3-second offset occurs between the OBS and the sonobuoy time

bases.

ii) May Deployment

The coherent ship-generated arrival in the May data discussed in section II can be used to align the Swallow float and OBS time bases. Since coherence squared estimates are not presented for the May data, the alignment of the time series can be done more roughly. The coherent arrival time, as measured by the Swallow floats, was gotten from float 3's y axis where it was most clearly recorded. It is at about 23:02:35, 5 May. The time of arrival in the OBS data is quite variable, differing by up to five seconds. This variability cannot be explained by a difference in propagation distance; the OBSs were closely spaced in the experiment [1] in order to study slowly propagating Scholte waves. Also, relative OBS clock drifts cannot explain the difference; timing offsets due to clock drift were less than one second. The arrival time recorded by the OBSs was taken to be ten seconds into event 313, i.e. at 23:01:10. The resulting time offset is 85 seconds. Therefore, the OBS time base measures the float synchonization time to be at 09:54:35, 5 May, rather than at 09:56.

Initial attempts at aligning the time series using impulse response estimation techniques have been made. Figure III.11 shows the result of estimating the time offset between the two sonobuoys by estimating the impulse response between them. According to an article by P. Roth [4], and to numerical simulations, the impulse response has a larger signal-to-noise ratio than the cross correlation as long as the two time series can be approximately aligned beforehand (i.e. as long as the initial time offset is less than about one-fourth the duration of the impulse response function. In Figure III.11, note how the envelope of the impulse response amplitude tapers towards the center of the plot, due to degradation caused by the increasing time offset). The sonobuoy data were recorded using the same time base for all ship-launched sonobuoys. Any time offset between sonobuoys 20 and 21 is therefore due to a difference in propagation time from a coherent source to the sensors. The period of time chosen for estimating the impulse response in Figure III.11 corresponds to the time of arrival of the second TNT detonation in the sonobuoy time series. The maximum amplitude in the figure occurs at an offset of 0.6 seconds, indicating an inter-sonobuoy distance offset of 900 meters with respect to the TNT shot location. Careful measurement of the arrival times from the time series in Figure II.22 show about a 0.5 second offset. Since the two sonobuoys were deployed at the same location [1], they had to drift apart by at least 900 meters during the two-and-a-half hour period after they were deployed. This impulse-response estimation technique may be used to fine-tune the time offsets between two sensors once gross offsets in the time bases have been removed and the locations of the instruments (for the sonobuoys and the Swallow floats) have been determined.

IV. Velocity and Pressure Spectral Estimates

i) April Deployment

a) Midwater Swallow Float Spectra

Swallow float geophone velocity spectra and derived pressure spectra for records 927 through 932 and for record 1600 for all properly operating midwater floats in the April trip are presented in Figures IV.1 through IV.10. (Note that the spectral estimate for float 3 in record 932 cannot be made because of a missing resynchronization character in the record's data, re Figure V.1a of [1]). The spectral estimates are calculated by dividing 40.96 seconds of data in each record, starting three seconds into each record in order to avoid tape recorder contamination, into seven 10.24-second segments overlapped by 50 %, windowing each segment with a Kaiser-Bessel window of α equal 2.5, Fourier transforming, and then incoherently averaging the resulting seven spectra. The spectral estimates, with 90 % confidence limits of approximately + 3.3 dB to - 2.3 dB, are properly normalized to give units of dB re 1 $(m/sec)^2/Hz$ or dB re 1 $(\mu Pa)^2/Hz$.

Records 927 through 932 (19:29 through 19:33, 22 April) were recorded while the Narragansett was 2000 to 2500 meters away towing the Argotec source [1]. The source was broadcasting at about 16 Hz until around 19:32, when the frequency was changed to 50 Hz. Records 927, 923, and 929 contain the two TNT explosions. Record 1600 was recorded during the early morning hours of 23 April, at 03:53, presumably during a quiet period. However, as mentioned in the April trip report [1], the Melville was stationed over the center of the deployment area during this period. The lumps of energy seen in record 1600's spectra (Figures IV.6 through IV.10) between 7 and 10 Hz, 15 to 20 Hz, and at 23 Hz are probably ship generated.

b) Ocean Bottom Seismometer Spectra

In Figures IV.11 through IV.19, the spectral estimates for the 29-second-long event 107 for all properly operating ocean bottom seismometers are presented. These estimates were derived following the procedure described above for the Swallow float spectra, with two differences. The first three seconds of the event were not skipped and since the event is only 29 seconds long, only four 10.24-second segments, rather than seven, were available for transforming and averaging. The spectral estimates therefore have a wider 90 % confidence interval, from + 4.7 dB to - 2.9 dB. Spectral estimates were also calculated using 5.12-second segments, giving less frequency resolution, but allowing for an average of ten spectra rather than four. The estimated spectral levels in both cases were almost identical.

The hydrophones installed on the ocean bottom seismometers were of two types; OBSs 01, 05, and 06 were equipped with the ultra-low-frequency differential pressure transducers of the Cox-type design and the other instruments were fitted with the regular OBS hydrophones (see [2] for references). All instruments had identical three-component geophones. The Cox-type hydrophone on OBS 01 did not operate properly, the one on OBS 05 stopped recording sometime between the April and May Swallow float deployments, and the time series recorded by the regular hydrophones on OBSs 02, 08, 12, 13, and 14 were contaminated by spikes spaced every half second, yielding the peaks every 2 Hz in the spectra. Since the Cox-type hydrophones appear to be noisy above a few Hz [2], only the regular hydrophone on OBS 04 appears to have recorded uncontaminated data above a few hertz.

The OBS geophone spectral level estimates are quite variable, both between levels reported on a given component by different instruments and by different components of a given instrument. These variations can be seen more clearly in the plots of the next section. Reasons for the variation in the spectral levels are still being invesigated by Dr. Dorman's research group [private communication]. His group has thus far focused most of their attention on the vertical geophone component [private communication], which appears to record more consistent spectral levels, except those from OBSs 05 and 06 during event 107. Also, calibration for the OBS-sediment coupling has been done only for the z geophone component [5]. Figure IV.20 reproduces Figure 3.7 from reference [5], which shows the correction to the OBS

vertical geophone spectra to account for the OBS-sediment coupling. This correction has not been made in the spectral estimates presented here. It amounts to at most an 8 dB adjustment in the vertical component spectral levels around 20 Hz, where a resonance in the OBS-sediment coupling occurs.

The OBS spectra from event 107 and the Swallow float spectra during record 930 show similar broad peaks at about 14 Hz, 17 Hz, 18 Hz, and 23 Hz. These peaks are probably due to the Narragansett. Very little indication of the Argotec source is present, either because of a weak signal or because the source frequency had already been changed to 50 Hz. Data recorded earlier (in record 921) did show a 16 Hz, Argotec-generated peak on the z axis of the Swallow float geophones, although it was weak [1]. The overall spectral levels will be discussed in the next section on spectral differences.

c) Sonobuoy Spectra

The estimated pressure spectra from the data recorded by the two sonobuoys, channels 20 and 21, are shown in Figures IV.21 and IV.22. These spectral estimates were calculated following the procedure used in calculating the Swallow float spectra, after taking the first 40.96 seconds of data from each of the four minutes of data listed in the figures. Note that, as discussed in the Appendix, the sonobuoy calibration curves below 5 Hz were empirically derived. Therefore, the spectral plots below 5 Hz are only rough approximations. The sonobuoy spectra do not show any of the peaks in common with the Swallow float and OBS data. The especially predominant spectral peak at 23 Hz in the Swallow float and OBS data does not appear in the sonobuoy spectra, except during 19:32 for sonobuoy 20. The lack of the peak is somewhat disturbing, although it is possible that the sonobuoys were in a shadow zone with respect to the source (presumably the Narragansett) during this time. The sonobuoys were at approximately 130 meters depth, whereas the midwater Swallow floats were at 400 meters and the bottom-mounted instruments were at 3800 meters. What is more disturbing is the large difference in spectral levels, especially at the upper end of the frequency band, reported by the two sonobuoys. This will be better illustrated in the next section. Also, there is a significant variation in the shape and level of sonobuoy 20's spectra from one minute to the next.

ii) May Deployment

a) Midwater Swallow Float Spectra while the Float was Descending

Spectral estimates from periodic samples of the data recorded by Swallow float 2 while it descended to its equilibrium depth at 1800 meters are shown in Figures IV.23 through IV.26. These estimates were made in order to see how relative flow past the Swallow floats affects the spectra. From the change in the travel time of the surface reflection of the 8 kHz localization ping [2] over time, the rate of descent, and thus the relative flow, during each of the four records in Figures IV.23 through IV.26 can be derived. It was 0.08 m/sec during record 200, 0.05 m/sec during record 400, 0.03 m/sec during record 600, and about 0.0004 m/sec during record 800. For reference, currents near the ocean floor are typically on the order of a few centimeters per second. Because of float rocking, induced by pressure differences due to the relative flow, the signals from the horizontal axes of the geophone are clipped during records 200 and 400. Therefore, only the z axis spectral levels should be considered. The vertical axis spectra for the four records are plotted together in Figure IV.27. As is evident in the figure, a relative flow of 0.08 m/sec can increase the particle velocity spectral levels by over 20 dB below 10 Hz. At a relative flow of 0.05 m/sec, the increased levels are only slightly reduced, but only occur below 2 to 3 Hz. An initial attempt to model these spectral level increases due to relative flow by considering the advection of turbulent velocity fluctuations past the geophone [6] has been weakly successful. One problem with the model is that the predicted levels depend heavily on the amount of turbulent energy dissipation per unit mass, which is unknown.

b) Additional Midwater Swallow Float Spectra

A six-record sequence of spectra from the midwater Swallow floats, from 1047 to 1052, are shown in Figures IV.28 through IV.33. (The interval of records plotted for float 8 are from 963 to 968, written at the same time as records 1047 to 1052; both floats 8 and 9 data contained time offsets in May due to being resynchronized [2]). Record 1050 was recorded at about the same time as the data starting a minute into OBS event 313. The Scorpius had steamed across the OBS array about an hour previously, traveling northeast at about 10 km/hr (5.5 knots). No obvious peak in the spectra occurs at the blade rate frequency of the ship, predicted to be between 19.5 and 21 Hz. However, spectral energy does appear around 13 Hz, most predominantly in record 1050, and at 7 Hz, mostly in record 1051. Spectral peaks at about 0.5 Hz are due to float rocking, and the peaks below 5 Hz in floats' 3, 7, and 8 spectra are generated by their cassette tape recorders [2].

A final six-record sequence of midwater Swallow float spectra, from record 1527 through 1532 (1443 through 1448 for float 8), are given in Figures IV.34 through IV.38. (Note that Swallow float 0 had stopped recording data by this time [2]). The data were recorded at the same time as the data after a minute into OBS event 315. Spectral peaks at 9, 12.6, 18, and 20 Hz appear rather consistently in the data. The Scorpius was 30 km from the array at this time.

c) Bottom-Mounted Swallow Float Spectra

An interval of data, records 566 through 571, recorded when bottom-mounted Swallow float 11 was uncontaminated by tether effects, was analyzed. Spectral estimates are given in Figures IV.39a through IV.39f. The midwater floats had unfortunately not yet reached their ballasted depth when these records were written, but the ocean bottom seismometers recorded event 311 during this time. Twenty seconds after the beginning of event 311 corresponds in time to the beginning of record 569. Again, the spectra contain a peak at 12.6 Hz. The Scorpius was a horizontal distance of 7.4 km from float 11 and 4.4 km from the OBS array at this time. Differences in spectral levels recorded by the Swallow float and the OBSs will be discussed in the next section.

d) Ocean Bottom Seismometer Spectra

Spectral estimates from the OBS data collected during the May deployment of the Swallow floats are now presented, in Figures IV.40 through IV.65. The pieces of data selected for analysis, starting 23 seconds into event 311, 68 seconds into event 313, and 68 seconds into event 315, correspond to the times of Swallow float records 569, 1050, and 1530, respectively, with a three-second delay (re Table 1). A Dirac delta impulse at 0 Hz in some of the spectra, e.g. the pressure spectra for OBS 05, indicate that data were not recorded by that component. (Other apparent problems with the OBS data are discussed in reference [2]). The OBS spectra also appear to show a peak at 12.6 Hz. A peak at 20 Hz also appears in some of the spectra.

V. Spectral Differences

A comparison of the spectral levels reported by the various instruments is most easily done by plotting spectral differences. These plots are now presented.

a) Spectral Differences between Instruments of the Same Type

In order to illustrate the consistency between the levels reported by instruments of the same type, spectral differences (from data taken at the same time) between midwater Swallow floats and other midwater Swallow floats, ocean bottom seismometers and other ocean bottom seismometers, and between the two sonobuoys, are plotted in Figures V.1 through V.31. The Swallow float spectral difference plots, in Figures V.1 through V.8, show that these instruments consistently report approximately the same spectral levels. Variations from zero in the figures are generally within the confidence limits expected from the variance in the spectral estimates. The difference in levels on the x axes of two floats may show a net offset, but the y axes' difference shows an offset of opposite sign. If the compass heading information had been used to align the geophones' horizontal axes, these offsets would not exist. The difference plots involving one of the floats with a noisy cassette tape recorder, i.e. floats 3, 7, and 8, show the 0.5, 2, and/or 3 Hz peak(s) on the horizontal axes mentioned in the previous section.

The OBS spectral differences calculated from data taken in events 107 and 315 are shown in Figures V.9 through V.27. OBS 04 was used as reference since, as mentioned in the previous section, its hydrophone data was of the highest quality of all the ocean bottom seismographs and its geophone data appeared to be uncontaminated. The hydrophone spectral differences show the relatively low quality of the data, although with some effort in removing the contaminating half-second spikes in OBSs' 02, 08, 12, 13, and 14 time series, useable data may result. The vertical axes differences are quite consistent (except for those of OBSs 01, 05 and 06 in event 107), and are remarkably consistent below 6 Hz. The horizontal axes' differences are another story; variations of up to 40 dB are not uncommon. (Note that for some components in some of the figures, i.e. the z axes' difference of Figures V.11 and V.12, the y axes' difference in Figure V.13, and the x axes' difference of Figure V.15, the spectral difference appears to not be plotted. In these cases, the spectral difference was greater than 40 dB over the whole frequency range. The lack of a plot for the pressure difference in Figure V.19, on the other hand, was due to the malfunction of the hydrophone on OBS 05 sometime between the April and May sea trips. Therefore, spectral differences greater than 40 dB over the whole frequency range occur only in event 107, which was 29 seconds long, and not in events of 179 seconds duration). The large variations in levels on the horizontal axes are not random; this will be discussed later in part c of this section. However, note that when using OBS 08 as reference in comparison with OBSs 12, 13 and 14, in Figures V.25 through V.27, the spectral differences on the horizontal axes are much more consistent. It also appears that the data is of generally higher quality in event 315 than in event 107; this may be a result of the short duration of event 107.

The comparison of the spectral levels reported by the two sonobuoys for which we have data are in Figures V.28 through V.31. Above 1 Hz, the difference between the two sonobuoys appears to increase with increasing frequency, and is generally less than 15 dB, except during 19:32. The difference between the two sonobuoys also increases as a function of time for the four consecutive minutes analyzed here, making a sudden jump to a 20 dB difference during 19:32, in Figure V.31. This spectral difference may be due to differences in the sonobuoy locations with respect to a sound source; the arrival times of TNT shot #5, as discussed at the end of Section III, suggest a sensor separation of at least 900 meters. The difference may also be due to a degradation in sonobuoy 20's sensitivity. Data from other sonobuoys, as well as localizing the sonobuoys using the 8 kHz ping issued by the Swallow floats, would help distinguish between these possible explanations.

b) Spectral Differences between a Bottom Swallow Float and the Midwater Floats

The spectral differences between data from bottom-mounted Swallow float 11 and the midwater Swallow floats' data during the May deployment are presented in Figures V.32 through V.36. The data from float 11 were taken during a period of time when contamination from the float's tether does not

appear to be present. Unfortunately, the midwater floats had not yet reached their equilibrium depth at this time, and float 11's data were tether-contaminated for the remainder of the deployment after the midwater floats had reached equilibrium. The comparison is therefore between data taken at different times. The spectral levels above 5 Hz heard by float 11 are about 10 dB less than those on the midwater floats (which are 1800 meters in depth). Below 5 Hz, the differences gradually decrease to zero. This may be a result of possible residual tether contamination in float 11's data, or of the decreasing ability of the sound channel to trap acoustic energy with decreasing frequency.

c) Spectral Differences between a Bottom Swallow Float and the OBSs

The ocean bottom seismometers recorded event 311 during the time when float 11 appears to be unaffected by its tether. The spectral differences are shown in Figures V.37 through V.45. The Swallow float derived pressure spectrum and the OBS hydrophone spectrum, specifically the spectrum for OBS 04 since its data was of the best quality, are both measures of the acoustic power in the water column near the ocean-sediment interface; the difference in Figure V.39 shows that the OBS hydrophone hears spectral levels about 15 dB higher than the Swallow float, except near the tape-recorder-induced peak at 0.5 Hz in float 11's spectrum. This difference may be due to improper calibration of one of the instruments. It may also be due to the difference in heights above the ocean bottom of the two sensors; the bottom Swallow floats were connected to their anchors by 4.57-meter-long tethers in May whereas the OBS hydrophones are only about a half meter or so above the ocean-sediment interface. The difference in levels may indicate that the Swallow float was about one skin depth from the bottom (one skin depth implies an 8.7 dB difference in levels). However, this skin depth, z_s, must be independent of frequency, i.e. $k_t z_s \approx 1$ for all frequencies. The difference in spectral levels doesn't appear to be due to a difference in flow noise contamination; it doesn't have the right frequency dependence. Likewise, the method of deriving the pressure spectrum from the velocity power spectra for the Swallow float data over-estimates, not under-estimates, the spectral levels when curvature of the wave field is important [7].

Although the Swallow float geophones measure water particle velocity and the OBS geophone measures sediment particle velocity, the z axes' spectral levels can be compared since vertical particle velocity is continuous across the water-sediment interface. The Swallow float's vertical axes levels are about 10 dB less than those of the ocean bottom seismometers across the whole frequency range plotted. This difference is consistent with the difference in the pressure spectra discussed in the previous paragraph; the possible explanations for the difference given there hold here also.

The horizontal axes' differences, although variable, are around zero above 5 to 10 Hz. At lower frequencies, one of two situations occur; either the levels on the OBS horizontals are 15 to 30 dB *greater* than Swallow float 11's spectral levels below 8 to 10 Hz, or the OBS horizontals have increasingly *lower* spectral levels than the Swallow float horizontals with decreasing frequency; i.e. a few dB lower at 5 Hz increasing to around 30 dB lower at 1 Hz. This suggests that the spectral levels reported by the OBS horizontal components are of two types. One or both of the two types may result from some characteristic form of contamination, e.g. the lower spectral levels may result from the OBS geophone not being level because of a sticky gimbal mechanism. A geophysical explanation for this pattern doesn't appear likely.

d) Spectral Differences between the Midwater Swallow Floats and the OBSs

The differences of the midwater Swallow float spectral levels and the OBS spectral levels for data recorded at the same time are plotted in Figures V.46 through V.79. Swallow float 2 and OBS 04 are used as references in most of the plots. The differences in the pressure spectra for the regular OBS hydrophones and the derived pressure spectra of the Swallow floats hover around zero for most of the comparisons (ignoring the spike contamination). This is also true of the vertical geophone axes' spectral levels (again ignoring those spectra that are obviously contaminated). One typical pattern in the comparison of the horizontal components' data taken in April (record 930 versus event 107 in Figures V.46 through V.60) shows positive differences (levels greater on the OBSs than on the Swallow floats) below 5 to 6 Hz, a drop to negative differences between 6 and 10 Hz, and a gradual decrease in differences with increasing frequency starting between about 10 and 15 Hz. This pattern may be offset in the positive or negative direction. For

the comparison of the horizontals' data taken in May (record 1530 versus event 315 in Figures V.61 through V.79), the difference on the horizontals may be significantly non-zero only below 5 to 10 Hz. A downward-going spike at about 0.5 Hz in the difference plots with float 2's spectra as reference is evidence of tape-recorder-induced contamination in the Swallow float spectra even for floats with quiet tape recorders. The 0.5-Hz spike is consistently greatest in amplitude on the x axis.

e) Spectral Differences between the Midwater Swallow Floats and the Sonobuoys

Figures V.80 through V.90 show the results of comparing midwater Swallow float derived pressure spectra with sonobuoy spectra. (Figure V.80 shows some of the spectral differences plotted on the same scale as the previous plots in this section). The comparison is only approximate below 5 Hz since the sonobuoy calibration curve is derived empirically. The difference plots show three distinct slopes in three frequency ranges; above about 10 Hz, the spectral difference is almost independent of frequency; between 4 and 10 Hz, the spectral difference has a slope of maybe -3 dB/Hz; and below 3 to 4 Hz, the slope of the difference is about -9 dB/Hz. A hump around 5 Hz appears to be a characteristic feature of the difference plots.

Much further work remains to be done in order to understand the differences between the spectral levels reported by the Swallow floats and the sonobuoys. The simultaneous calibration of the two sets of instruments, to be conducted in Hotham Sound possibly sometime this year, will certainly help answer some of the questions. However, these preliminary results indicate that the sonobuoys are contaminated by flow noise below 10 Hz. Evidence for this is that the frequency dependence of the Swallow float-sonobuoy spectral difference plots is about that expected for flow noise (see parts g and h of this section), and the midwater Swallow float-OBS spectral difference plots show comparable spectral levels for the derived pressure-hydrophone and the vertical geophone axes except at the float rocking frequency of about 0.5 Hz. Above 10 Hz, the Swallow floats and the sonobuoys report about the same spectral levels if the levels from the two sonobuoys are averaged.

f) Spectral Differences between the OBS Hydrophones and the Sonobuoys

The OBS hydrophone-sonobuoy spectral difference plots, Figures V.91 through V.100, show results similar to those discussed in the previous paragraph. A slight modification might be that, using the highest quality hydrophone data set collected by the regular OBS hydrophone on instrument 04, the spectral difference (Figures V.93 and V.100) has a frequency dependence of approximately 1 dB/Hz for frequencies greater than 2 Hz.

g) Spectral Differences between a Descending Swallow Float and One at Depth

In order to get some idea of the effects on recorded noise levels of water flow around the Swallow floats, spectral differences were calculated between data taken by float 2 while it descended to depth (records 200, 400, 600, and 800) and data it recorded much later in the May deployment (record 1530). These plots are shown in Figures V.101 through V.104. At record 200, the float was descending at a rate of 0.08 m/sec; in record 400, at a rate of 0.05 m/sec; in record 600, 0.03 m/sec; and at rate of 0.0004 m/sec in record 800. In record 1530, the float was no longer descending in the water column, but some small relative flow may have existed due, for example, to propagating internal waves. The geophone signals on the horizontal axes are clipped in records 200 and 400; the clipping, among other things, causes increased levels above 21 to 22 Hz. Note that float rocking at 0.5 Hz is strongly excited when relative flow is present, even on the vertical geophone axis. A secondary, rocking-induced peak at about 1 Hz is also present on the horizontal axes.

The important feature to note from these plots is that the frequency dependence of flow noise contamination in the Swallow float spectra is akin to that shown by the spectral differences between the Swallow floats and the sonobuoys in part e of this section. The plots of the z axes' spectral differences in Figures V.101 and V.102 and the Swallow float-sonobuoy spectral differences in Figure V.80 have a similar shape, apart from the float rocking resonances below 1 Hz.

h) Spectral Differences between a Descending Swallow Float and the Sonobuoys

To further illustrate the point made in the previous paragraph, spectral estimates taken during record 200 by float 2 in the May deployment were subtracted from the spectral estimates from the April deployment of the sonobuoys. The results are shown in Figures V.105 through V.108, using both float 2's derived pressure spectral estimate and the float's vertical axis spectral estimate (where clipping was not occurring) as reference. Figure V.105 shows the remarkable agreement between float 2's derived pressure spectral estimate when the relative flow was about 0.08 m/sec and sonobuoy 20's spectral estimate in the frequency range of 3 to 20 Hz. Above 20 Hz, float 2's spectrum is contaminated due to signal clipping, and below 3 Hz, another effect appears to become dominant. Note that the sharp increase in the spectral difference below 3 Hz is interrupted by the two troughs at about 0.5 and 1 Hz which are caused by float rocking. The overall impression gotten from these plots is that the sonobuoy data appear to be flow contaminated. Sonobuoy tether strumming may be present, which may cause the change in the spectral difference slope below 3 Hz.

i) Spectral Differences between Swallow Float Data in April and in May

The final plots of this section, Figures V.109 through V.114, compare the ambient noise spectral levels recorded by the midwater Swallow floats in the April deployment with those recorded in May. Both sets of data which are compared were written during the early morning hours of the two deployments, when the research vessel which deployed the Swallow floats was far from the float array. However, as mentioned previously, the research vessel the Melville remained close to the Swallow float array for most of the April deployment [1]. This is the main reason for the appearance of the spectral difference plots. The ship-generated peaks at about 9 Hz, between 15 and 20 Hz, and at 23 Hz are especially predominant on the vertical axes, indicating that the ship wasn't too far from overhead. The difference in deployment depths, in April the floats were ballasted to 400 meters and in May they were deployed at around 1800 meters, may have also contributed to the 5-to-10 dB increase above 5 Hz in April's derived pressure spectral levels versus those in May.

VI. Coherence Squared Estimates

The coherence function is akin to a normalized cross correlation function done on a per frequency basis. The magnitude squared of the coherence function estimates is presented in this section since it is an easily interpretable quantity; it represents the fraction of the power in one time series which is due to the power in another time series at a given frequency [4]. First, the estimates are presented between sensors of the same type, followed by the inter-sensor estimates.

a) Coherence Squared Estimates between Two Midwater Swallow Floats

The coherence squared estimates between two midwater Swallow floats are shown in Figures VI.1 through VI.9. The estimates were made by decomposing 43.52 seconds of data in a record into sixteen 5.12-second segments overlapped by 50 %. This segment duration is half that used in the spectral estimates of Section IV so that more averaging could be done. The segments were windowed with a Kaiser-Bessel window of α equal to 2.5, Fourier transformed, and then incoherently averaged to obtain the cross- and auto-spectral estimates needed to calculate the coherence. Assuming the sixteen averages are independent, then if the true coherence squared is actually zero, the estimate will be greater than 0.3 less than 10 % of the time.

The coherence squared estimates between the functioning midwater Swallow floats in April are presented in Figures VI.1 through VI.3. The time chosen for processing, record 930, was written after clipping due to the TNT explosion in record 929 and before ship-generated clipping in record 931. As mentioned previously, both OBS event 107 and sonobuoy time 19:31 were written during this time.

No relative offsets between the Swallow floats' time bases have been made prior to calculating the coherences. The inter-float 8 kHz ping data [1] indicate that the relative float clock drifts were small, especially between floats 0 and 1, and between floats 3 and 5. Adjustments to the time base alignments will be made once the floats have been localized since inter-float ping arrival differences can be used to estimate relative clock drift. However, it appears that the present coherence squared estimates are probably well within 90 % of their maximum value.

The coherence between two vertical geophone axes can be quite large at certain frequencies. The peaks at 17 and 23 Hz are the most prominent, appearing on many of the other inter-component comparisons as well, but other peaks at 12 Hz, 20 Hz, and 22 Hz occur frequently. In the coherence squared plots between two horizontal components, the 23 Hz peak also occurs, but the 17 Hz peak is not at all prominent. Rather, a very large peak occurs at 18 Hz, notably between floats 3 and 5. This difference between the vertical-component coherences and the horizontal-component coherences is somewhat surprising. These peaks in the plots are assumed to be due to coherent arrivals from the Narragansett. (Melville-generated noise may also contribute to the large coherences; however, the Melville was about 8.6 km from the Swallow float array during this time whereas the Narragansett was about 2.1 km away). In addition, significant coherences can exist between two horizontal axes in the 4 to 12 Hz frequency range.

Large coherence squared estimates can occur around 0.5 Hz, especially between floats 3 and 5 as seen in Figures VI.3i through VI.3k. This is most likely due to tape-recorder-induced float rocking; the first 3 seconds of the record, which are the most strongly affected by rocking, were not skipped so that an average of sixteen segments, each 256 points long, could be made. However, the noise from the Narragansett may also contribute; spectral lines at 0.2 and 0.9 Hz were identified in the ship's noise field using a Clevite hydrophone and a General Radio spectrum analyzer. The excitation of float rocking due to acoustic arrivals is presently under investigation.

The coherence squared estimates between inter-midwater-Swallow-float data collected in May, 1987, in record 1530, are shown in Figures VI.4 through VI.9. These data were collected near daybreak of 6 May. The coherences are, in general, much lower than in the April, record 930, data due to the lack of an identifiable coherent noise source. A comparison of float 2's x axis with float 3's y axis, Figure VI.4i, shows a broad, significant level of coherence between 4 and 15 Hz. A few peaks of significant coherence, at 9, 10, 12, 12.5, 17, and 18 Hz, often appear.

b) Coherence Squared Estimates between Two Ocean Bottom Seismometers

Figures VI.11 through VI.24 display the coherence between the ocean bottom seismometer geophone and hydrophone components in the April, event 107, data. The results for the inter-hydrophone comparisons probably should be ignored until further processing to remove the spike contamination is done. The plots have half the frequency resolution of the Swallow float coherence plots; since event 107 was only 29 seconds long, the segment length was decreased to 2.56 seconds, allowing for an average of 21 FFTs with 50 % overlap. Because of the shorter segment length, the coherence estimates are more strongly affected by time base offsets. The table in Figure VI.10 gives the seconds and milliseconds of the starting recording times of the OBS events in April and May in order to determine the magnitudes of the relative time base offsets. For most of the inter-OBS comparisons, the offset is small, reducing the coherence squared by less than 10 %. In some cases, e.g. between OBS 04 and 08 and between OBS 08 and 13, the time difference is significant. Taking the relative offset into account can have a dramatic effect in these cases; aligning the time bases of OBS 04 and OBS 08 causes a large increase in coherence between the two vertical geophone axes below 6 Hz (Figure VI.18 versus VI.17), but the alignment of OBS 08 and OBS 13 time bases results in a *decrease* in coherence below 6 Hz on the vertical components (Figure VI.24 versus Figure VI.23).

The most dramatic aspect of the coherence function between two ocean bottom seismometers is the large coherence squared values (greater than 0.8) below 6 Hz on the inter-vertical-geophone-component plots. For noise sources modeled as isotropic, independent, homogeneously-distributed point sources radiating into an isotropic, homogeneous medium, the spatial correlation function has the form, $\frac{\sin(kx)}{kx}$, where x is the inter-element spacing and k is the wave number component in the direction of x. The close spacing of the instruments in the array can therefore contribute to the large coherences at the lowest frequencies. The large coherences may also be a result of a concentrated ambient noise source; Prof. Dorman has proposed that a sediment pond near the study site may have allowed ambient noise created near the ocean surface to be coupled into Scholte wave energy in the ocean-sediment-interface waveguide. The horizontal geophone components generally do not show a corresponding large coherence at the low frequencies, except for the x axes of OBSs 01 and 02, Figure 11. This is probably indicative of the large variation in spectral levels on the horizontals, as discussed in Section IV, although the fact that the horizontal components are non-rotated also contributes to lower coherences.

The horizontal component comparisons do show significant coherence squared levels, mostly above 15 Hz. The peak around 23 Hz, also seen on the midwater-Swallow-float coherence plots, is striking. Peaks at 19 and 22 Hz appear commonly.

The coherence squared estimates for the OBS data in May, Figures VI.25 through VI.35 for event 311 and Figures VI.36 through VI.48 for event 315, again show the large coherences on the vertical component comparisons below 6 Hz. The x-axis versus x-axis coherences can many times also show significant coherences below 6 Hz. The reason why large coherences below 6 Hz appear on the x-axes comparisons and not on the y axes plots is not yet understood. A coherence peak at 12.5 Hz appears often in the plots for event 315, as it did in the midwater Swallow float plots.

Note that the coherence squared estimates for May were calculated using the same procedure followed in the Swallow float coherence function estimation, i.e. sixteen 5.12-second segments were FFT'd and averaged.

c) Coherence Squared Estimates between Two Sonobuoys

Following the procedure used in the Swallow float coherence function estimation, the coherences between the two sonobuoys, channels 20 and 21, were estimated. The results for four consecutive minutes, 19:29 through 19:32, are presented in Figures VI.49 and VI.50. Time 19:31 corresponds to Swallow float record 930 and to OBS event 107. Remarkably, none of the coherence squared plots show significant coherence, except at 0 Hz and maybe at 2 Hz, even though TNT explosions arrived in 19:29 and 19:30 (Figures II.15 and II.16) and the Narragansett was close enough to cause large coherences between the midwater Swallow floats (Section VIa). Since all the ship-launched sonobuoys' data were recorded using the same time base, relative time offsets could not occur. The time offsets due to a difference in path length from a source to the two sonobuoys, as mentioned in Section III, does not appear to be sufficiently

large to account for the lack of coherence. No explanation for the low coherences, except for poor quality data (re the intermittent down-going spikes in sonobuoy 20's time series; Figures II.15 and II.16), is known at this time. The analysis of more digitized data from the other functioning sonobuoys in April will provide a better basis for drawing conclusions.

d) Coherence Squared Estimates between a Midwater Swallow Float and an OBS

The coherence squared estimates between data recorded by the midwater Swallow floats and the ocean bottom seismometers in April, 1987, are shown in Figures VI.51 through VI.63. The first sample of the Swallow float data segments was recorded 7.5 seconds after the beginning of record 930; these data were recorded at the same time as OBS event 107. The procedure for calculating the coherence estimates was identical to that used in making the coherence estimates between two ocean bottom seismometers' data in event 107 (Section VIb).

The largest coherence squared estimates in Figures VI.51 through VI.63 consistently occur when the data from the vertical axis of the Swallow float geophones are compared to the OBS data (i.e. in those figures whose figure number is appended with a "k"). In these comparisons, peaks of significant coherence occur at 17, 22, and especially 23 Hz; peaks also sometimes occur around 14 and 19 Hz. A peak at 11 Hz appears quite often when the Swallow floats' vertical axes are compared to the OBSs' vertical axes; a peak at about 12 Hz sometimes occurs when the floats' vertical axes are compared to the OBS hydrophone data. Note that the high level of coherence seen in the inter-OBS comparison plots at frequencies below 6 Hz is not present in these figures.

Some peaks of significant coherence appear when the horizontal axes' data from the Swallow floats are compared to the OBS data, noteably at 17, 18, and 23 Hz. The peak at 23 Hz is especially dominant in Figure 61.i, where the x axis of float 2 is compared to OBS 04 data. It does not appear in the comparison of float 2's y axis data with that of OBS 04, in Figure 61.j. Therefore, the level of significance of the coherence peaks when the instruments' horizontal axes are involved is probably dependent upon the axes' spatial orientation.

e) Coherence Squared Estimates between a Midwater Swallow Float and a Sonobuoy

Finally, Figures VI.64 through VI.67 show the coherence squared estimates between the midwater Swallow floats and the sonobuoys. The coherence is insignificant across the frequency band plotted, as expected from the low coherences in the inter-sonobuoy comparisons in Section VIc. Again, as in Section VIc, the explanation for low coherence cannot be time base misalignment; both the Swallow floats and the sonobuoys record clearly the two TNT shots, #4 and #5 [1], whose arrival times can be used to align the instruments' time series (Section III).

Acknowledgements

We would like to thank the other members of the Swallow float team, Lee Culver, Marvin Darling, and Greg Edmonds for their countless contributions to the project. We would like to thank Dr. Dorman and the members of his research group, Allan Sauter and Tony Schreiner, for providing us with the ocean bottom seismometer data. Our thanks also go out to Jim McEachern and the Naval Air Development Center for giving us the digitized sonobuoy data.

This work was supported by the Office of Naval Research, Code 1125, under contract N00014-87-K-0010.

References

[1] G. L. D'Spain, R. L. Culver, W. S. Hodgkiss, and G. L. Edmonds, "Freely drifting Swallow float array: April, 1987 trip report" MPL Tech. Mem. 397, Marine Physical Laboratory, Scripps Institution of Oceanography, San Diego, CA (1987).

[2] G. L. D'Spain, R. L. Culver, W. S. Hodgkiss, and G. L. Edmonds, "Freely drifting Swallow float array: May, 1987 trip report" MPL Tech. Mem. 402, Marine Physical Laboratory, Scripps Institution of Oceanography, San Diego, CA (1988).

[3] R. L. Culver, "Infrasonic ambient ocean noise spectra from freely drifting sensors" SIO Ref. 85-22, Marine Physical Laboratory, Scripps Institution of Oceanography, San Diego, CA (1985).

[4] P. R. Roth, "Effective measurements using digital signal analysis" I.E.E.E. Spectrum, April, (1971).

[5] A. W. Sauter, "Studies of the upper oceanic floor using ocean bottom seismometers" Ph.D dissertation, University of California, San Diego, (1987).

[6] G. L. D'Spain, "Effect of turbulence on the Swallow float geophones" Marine Physical Laboratory, Scripps Institution of Oceanography, San Diego, CA (in press).

[7] G. L. D'Spain, "The calculation of acoustic pressure spectra from particle velocity spectra revisited" Marine Physical Laboratory, Scripps Institution of Oceanography, San Diego, CA (in press).

Appendix - Calibration Curves

Calibration curves for the five types of transducers installed on the three sets of instruments, including the effects of amplifiers and anti-aliasing and notch filters, are plotted in this appendix. The curves for the Swallow float geophone channels (in Figure A1), the OBS geophone channels (in Figure A2), the regular OBS hydrophone channel (in Figure A3), and the Cox-type differential pressure transducer channel (in Figure A4), have been presented elsewhere (see Appendix 1 of [1] or [2], Appendix 3 of [2], and the list of references in [2]). Again, note that no correction for the coupling between the ocean bottom seismometers and the sediment has been included.

The calibration curve for sonobuoy 20 is given in Figure A5. Each sonobuoy has its own calibration curve, but the curves differ by less than a dB in the frequency band of interest here. The calibration curve was derived from amplitude calibration data at 5, 10, and 30 Hz provided by the Naval Air Development Center. A quadratic interpolation using these three data points was used to create the calibration curve above 5 Hz. Below 5 Hz, the curve was empirically derived from the data, which is known to be contaminated by system noise [Jim McEachern; private communication]. Therefore, sonobuoy spectral levels reported in Section IV below 5 Hz are only approximate.

OBS Events and Swallow Float Records April, May 1987

(Times are in local Pacific Daylight Time; add 7 hours to get GMT).

OBS Event		Date	Approx Time (hr:min) of First Sample	Duration of Event (sec)	Swallow Float Record No. (@)
073		4-22	11:01	179	250 (+ 10 sec)
085	*	4-22	14:01	179	490 (+ 10 sec)
087	*	4-22	14:31	179	530 (+ 10 sec)
088	*	4-22	14:46	179	550 (+ 10 sec)
097		4-22	17:01	179	730 (+ 10 sec)
105		4-22	19:01	29	890 (+ 10 sec)
106		4-22	19:16	29	910 (+ 10 sec)
107		4-22	19:31	29	930 (+ 10 sec)
108		4-22	19:46	29	950 (+ 10 sec)
109		4-22	20:01	29	970 (+ 10 sec)
110		4-22	20:16	29	990 (+ 10 sec)
111		4-22	20:31	29	1010 (+ 10 sec)
112		4-22	20:46	29	1030 (+ 10 sec)
113		4-22	21:01	29	1050 (+ 10 sec)
114		4-22	21:16	29	1070 (+ 10 sec)
115		4-22	21:31	29	1090 (+ 10 sec)
116		4-22	21:46	29	1110 (+ 10 sec)
117		4-22	22:01	29	1130 (+ 10 sec)
118		4-22	22:16	29	1150 (+ 10 sec)
119		4-22	22:31	29	1170 (+ 10 sec)
120		4-22	22:46	29	1190 (+ 10 sec)
121		4-22	23:01	179	1210 (+ 10 sec)
133	*	4-23	02:01	179	1450 (+ 10 sec)
145		4-23	05:01	179	1690 (+ 10 sec)
157	*	4-23	08:01	179	1930 (+ 10 sec)
309		5-5	11:01	179	88 (+ 25 sec)
310	*	5-5	14:01	179	328 (+ 25 sec)
311		5-5	17:01	179	568 (+ 25 sec)
312	*	5-5	20:01	179	808 (+ 25 sec)
313		5-5	23:01	179	1048 (+ 25 sec)
314	*	5-6	02:01	179	1288 (+ 25 sec)
315		5-6	05:01	179	1528 (+ 25 sec)
316	*	5-6	08:01	179	1768 (+ 25 sec)
317		5-6	11:01	179	2008 (+ 25 sec)

(*) These events were only recorded by instruments 5 and 6.

(@) These times were gotten after aligning the time bases of the Swallow floats with the OBSs (re Section III). In April, the OBS time base records the time of Swallow float synchronization as 07:53:20, 22 April; in May, the time of Swallow float synchronization, according to the OBS time base, was 09:54:35, 5 May.

Table 1

Addendum 1: Aligning the Swallow Float and OBS Time Bases in May, 1987

The recording by the Swallow floats of the P wave arrival from an earthquake in the Aleutian Islands during the May, 1987 deployment [1] has resulted in a correction to the alignment of the time bases of the Swallow floats and the ocean bottom seismometers for this experiment (re Section III.ii of this report). Using the origin time of the magnitude 6.3 earthquake, gotten from the May, 1987 monthly listing of the "Preliminary Determination of Epicenters" by the National Earthquake Information Center, and a standard-earth-model-based computer program to calculate the travel time, the predicted time of arrival of the P wave at the Swallow float/OBS study site (32.5° N, 120.5° W) is 21:14:42 local time. The P wave arrival is clearly recorded on the vertical components of all midwater Swallow float geophones at about 43 seconds into record 905. This implies that the Swallow float synchronization time according to the world-wide standard time base was 09:55:14 on 5 May, or 39 seconds after the time deduced in Section III.ii. The assumption in Section III.ii that the arrival in event 313 of the OBS data corresponded to the ship-generated arrival in record 1048 of the Swallow float data must have been incorrect. A further search of the time series has resulted in the identification of three small arrivals on the z axes of OBSs 5 and 6 during event 316 which correspond to arrivals in Swallow float records 1767 through 1770 [1]. The time base alignment using these sets of arrivals is qualitatively consistent with the alignment using the Aleutian Islands earthquake P wave arrival, assuming that the ocean bottom seismometer time base is approximately (within a few seconds) the same as the worldwide standard time base. Efforts are presently in progress to quantitatively align the time bases using these arrivals. The recording in the Swallow float data of the P wave arrival from an earthquake in Honshu, Japan during the April, 1987 experiment has verified the Swallow float/OBS time base offset determined in Section III.i; the P wave arrival time measured in the Swallow float data and corrected for the time base offset agrees within one second of the predicted standard-earth-model-based arrival time [1].

Addendum 2: Correction to the Swallow Float Calibrated Spectra

Recent calibration measurements of the Swallow float geophone signal conditioning electronics have determined that seven RC circuits in the system, previously assumed to have an insignificant effect in the frequency band of interest, actually have a noticeable effect on the calibration curve, and thus the calibrated Swallow float geophone spectra [2]. Below is a plot showing the amount to be added to the Swallow float spectra presented in this report in order to obtain the true calibrated spectral levels.

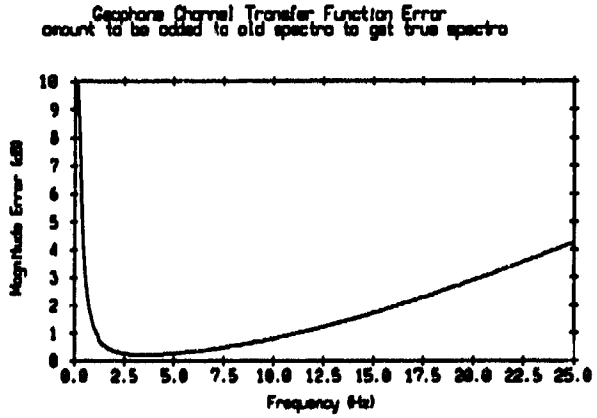

[1] G. L. D'Spain and W. S. Hodgkiss, "Earthquake arrivals in the Swallow float data" Marine Physical Laboratory, Scripps Institution of Oceanography, San Diego, CA (in preparation).

[2] G. L. D'Spain, G. L. Edmonds, and W. S. Hodgkiss, "Calibration of the Swallow float VLF data acquisition system" Marine Physical Laboratory, Scripps Institution of Oceanography, San Diego, CA (in preparation).

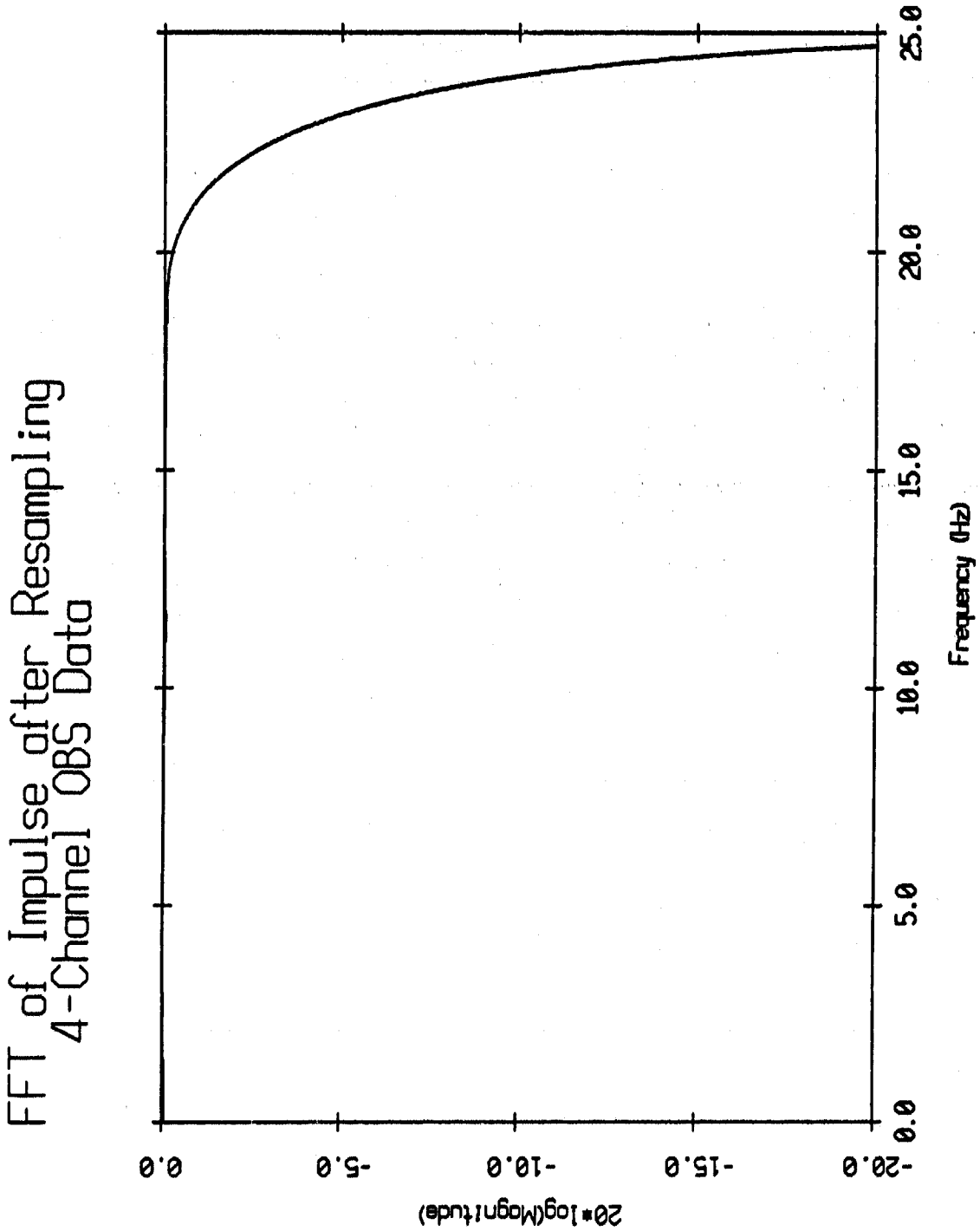
FFT of Impulse after Resampling
4-Channel OBS Data
20*log(Magnitude)
0.0
-5.0
-10.0
-15.0
-20.0
0.0
5.0
10.0
15.0
20.0
25.0
Frequency (Hz)

Figure I.1

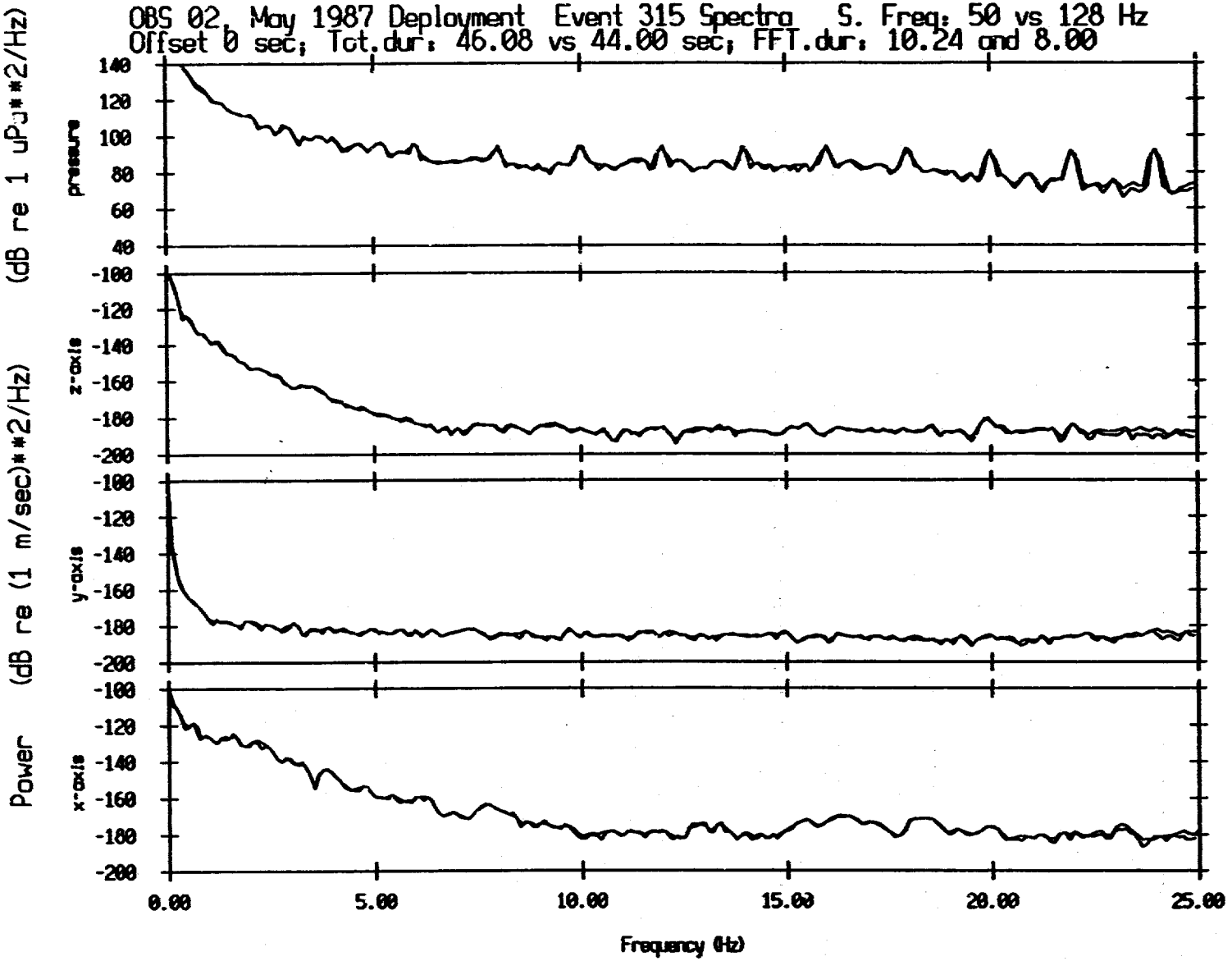
OBS 02, May 1987 Deployment Event 315 Spectra S. Freq: 50 vs 128 Hz
Offset 0 sec; Tot.dur: 46.08 vs 44.00 sec; FFT.dur: 10.24 and 8.00
Power (dB re (1 m/sec)**2/Hz) (dB re 1 uPa**2/Hz)
pressure
z-axis
y-axis
x-axis
140
120
100
80
60
40
-100
-120
-140
-160
-180
-200
0.00
5.00
10.00
15.00
20.00
25.00
Frequency (Hz)

Figure 12

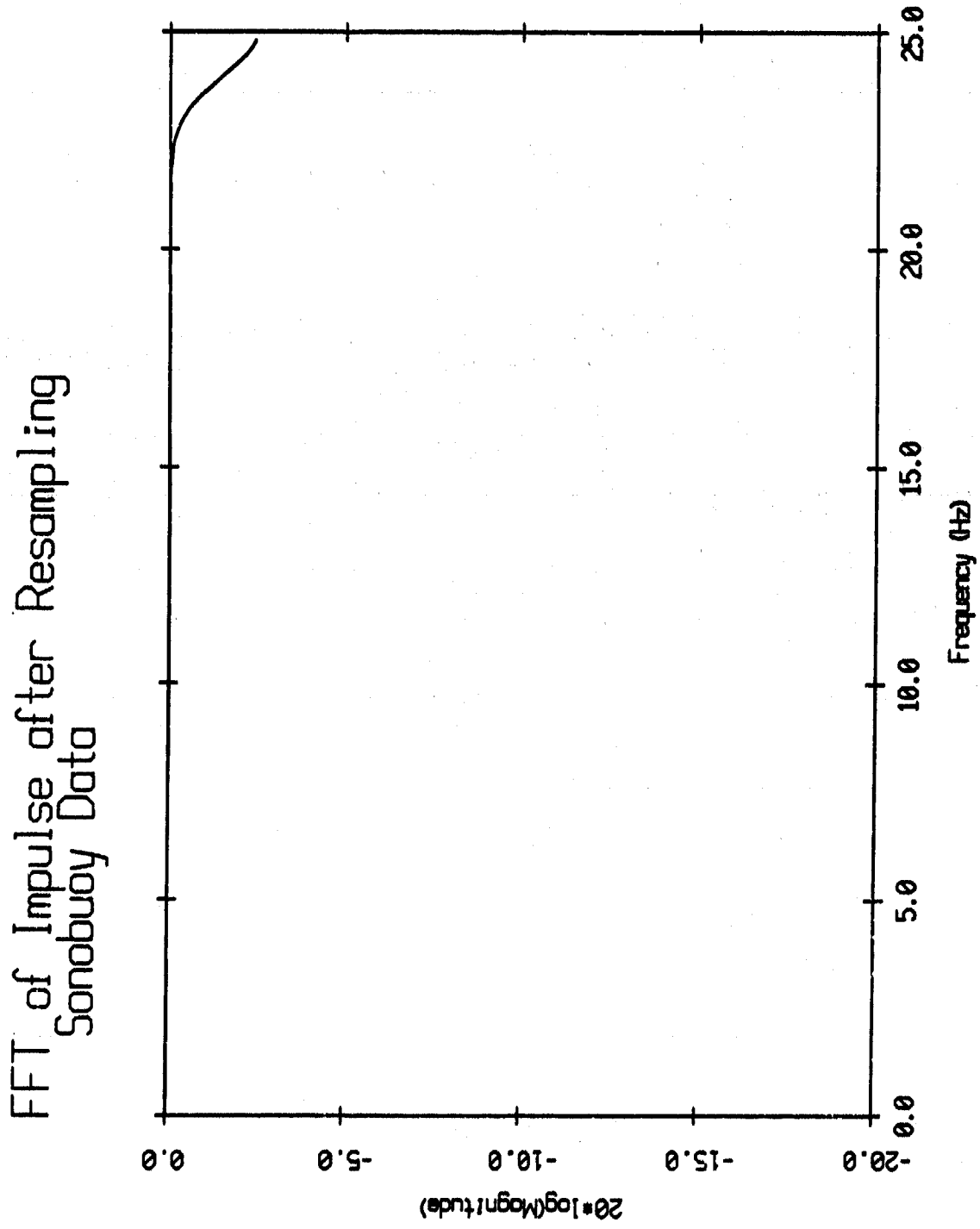
FFT of Impulse after Resampling
Sonobuoy Data
20*log(Magnitude)
0.0
-5.0
-10.0
-15.0
-20.0
0.0
5.0
10.0
15.0
20.0
25.0
Frequency (Hz)

Figure I.3

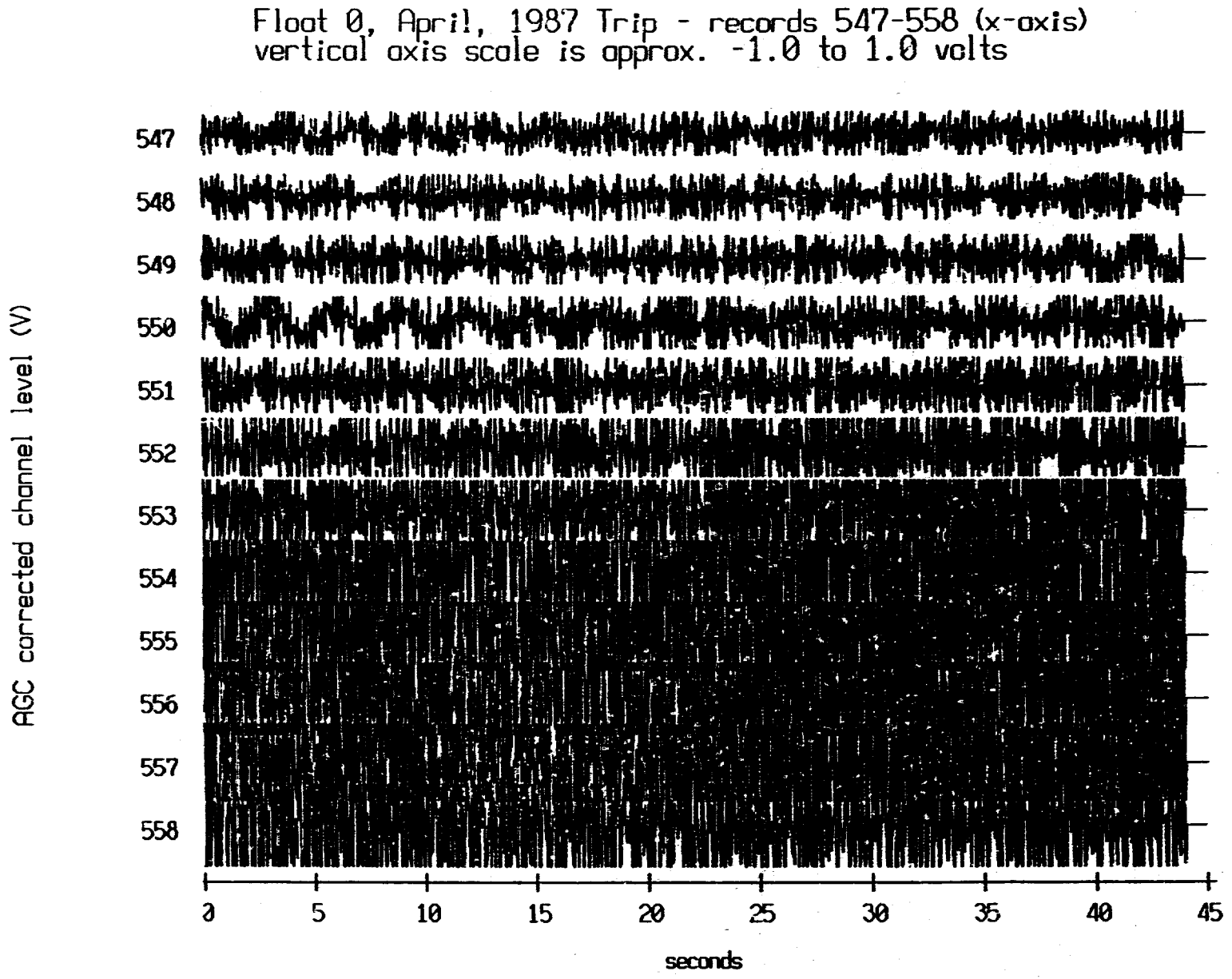
Float 0, April, 1987 Trip - records 547-558 (x-axis)
vertical axis scale is approx. -1.0 to 1.0 volts
AGC corrected channel level (V)
547
548
549
550
551
552
553
554
555
556
557
558
0
5
10
15
20
25
30
35
40
45
seconds

Figure II.1i

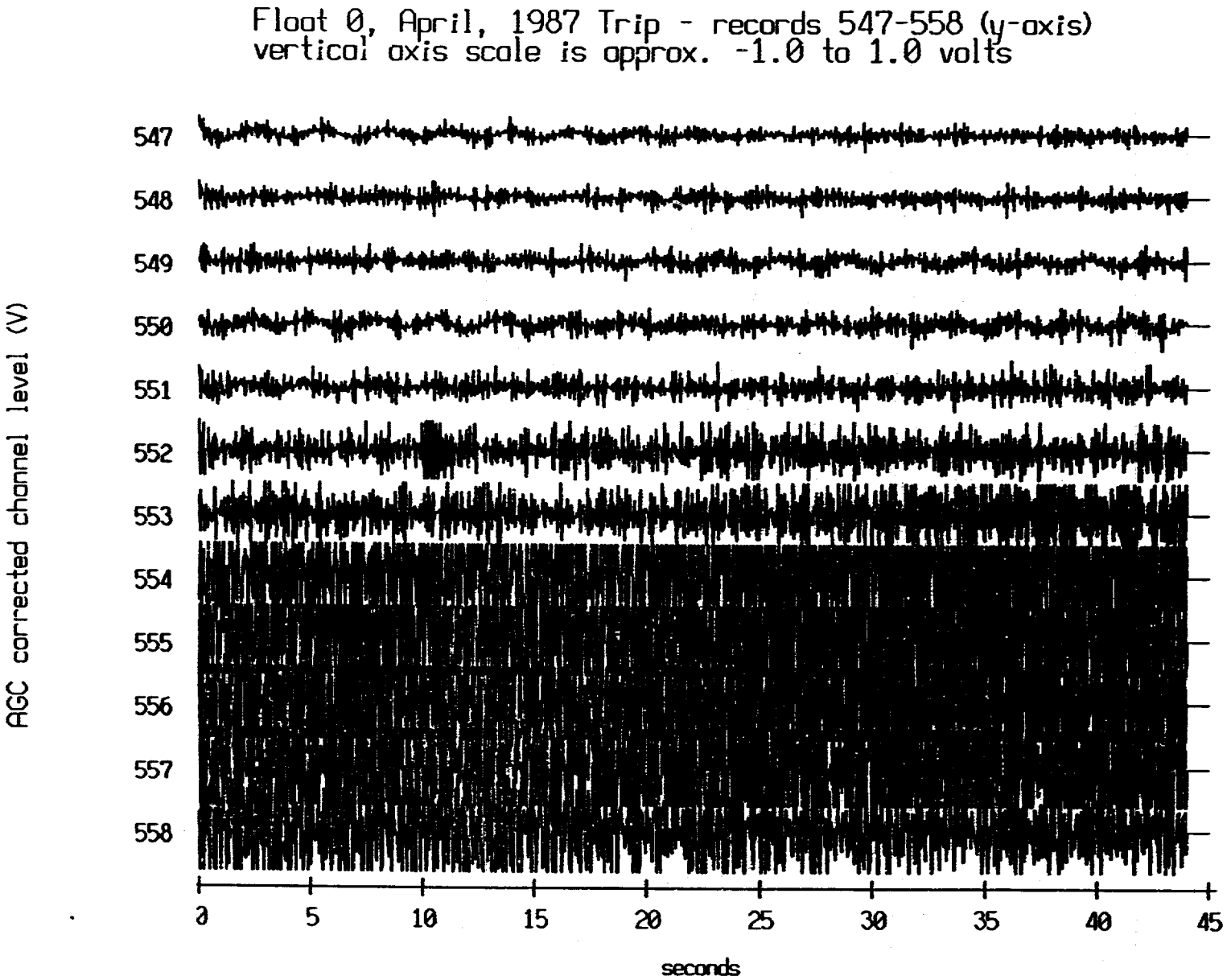
Float 0, April, 1987 Trip - records 547-558 (y-axis)
vertical axis scale is approx. -1.0 to 1.0 volts
AGC corrected channel level (V)
547
548
549
550
551
552
553
554
555
556
557
558
0
5
10
15
20
25
30
35
40
45
seconds

Figure II.1

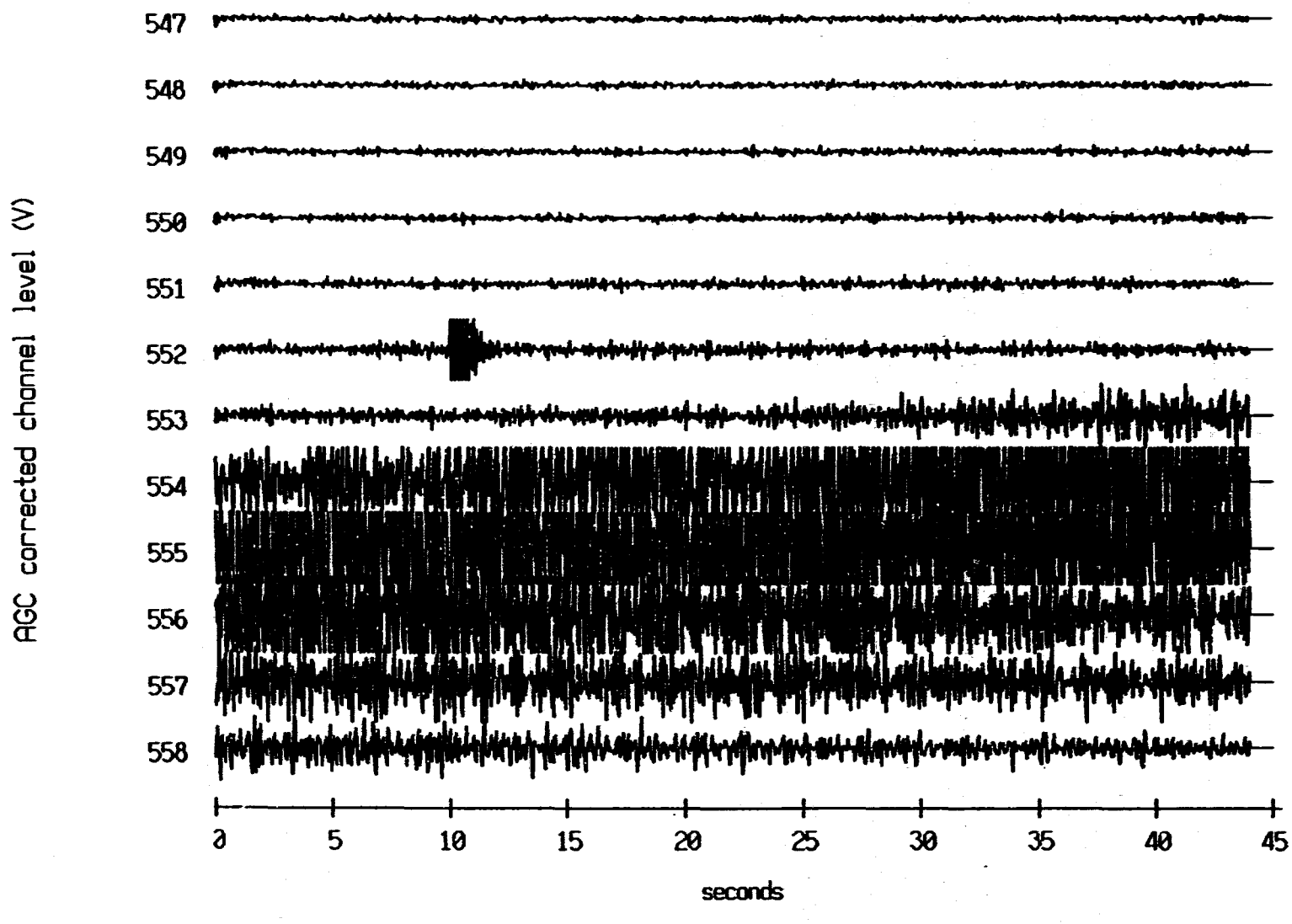
Float 0, April, 1987 Trip - records 547-558 (z-axis)
vertical axis scale is approx. -1.0 to 1.0 volts
547
548
549
550
551
552
553
554
555
556
557
558
AGC corrected channel level (V)
0
5
10
15
20
25
30
35
40
45
seconds

Figure II.1k

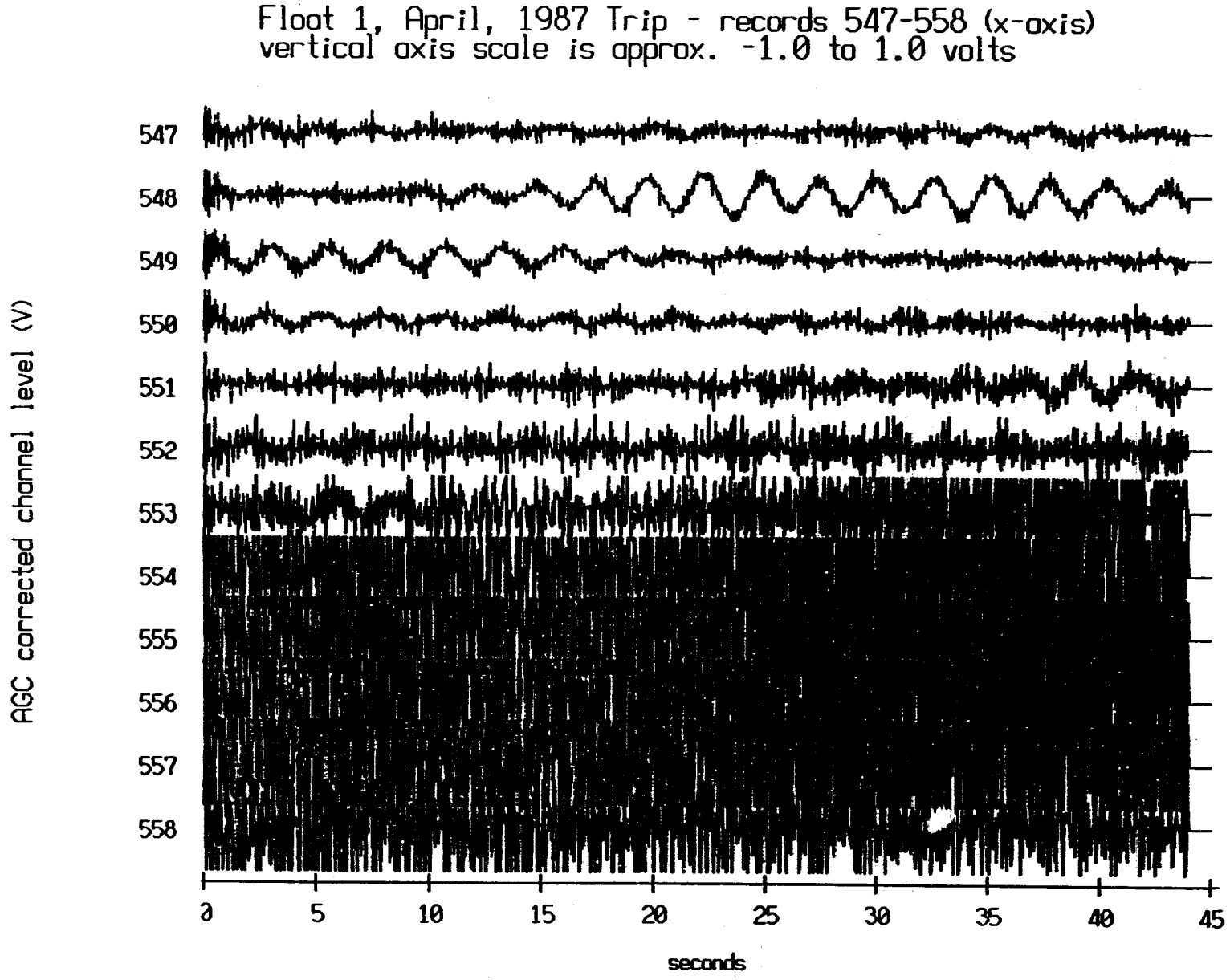
Float 1, April, 1987 Trip - records 547-558 (x-axis)
vertical axis scale is approx. -1.0 to 1.0 volts
AGC corrected channel level (V)
547
548
549
550
551
552
553
554
555
556
557
558
0
5
10
15
20
25
30
35
40
45
seconds

Figure II.21

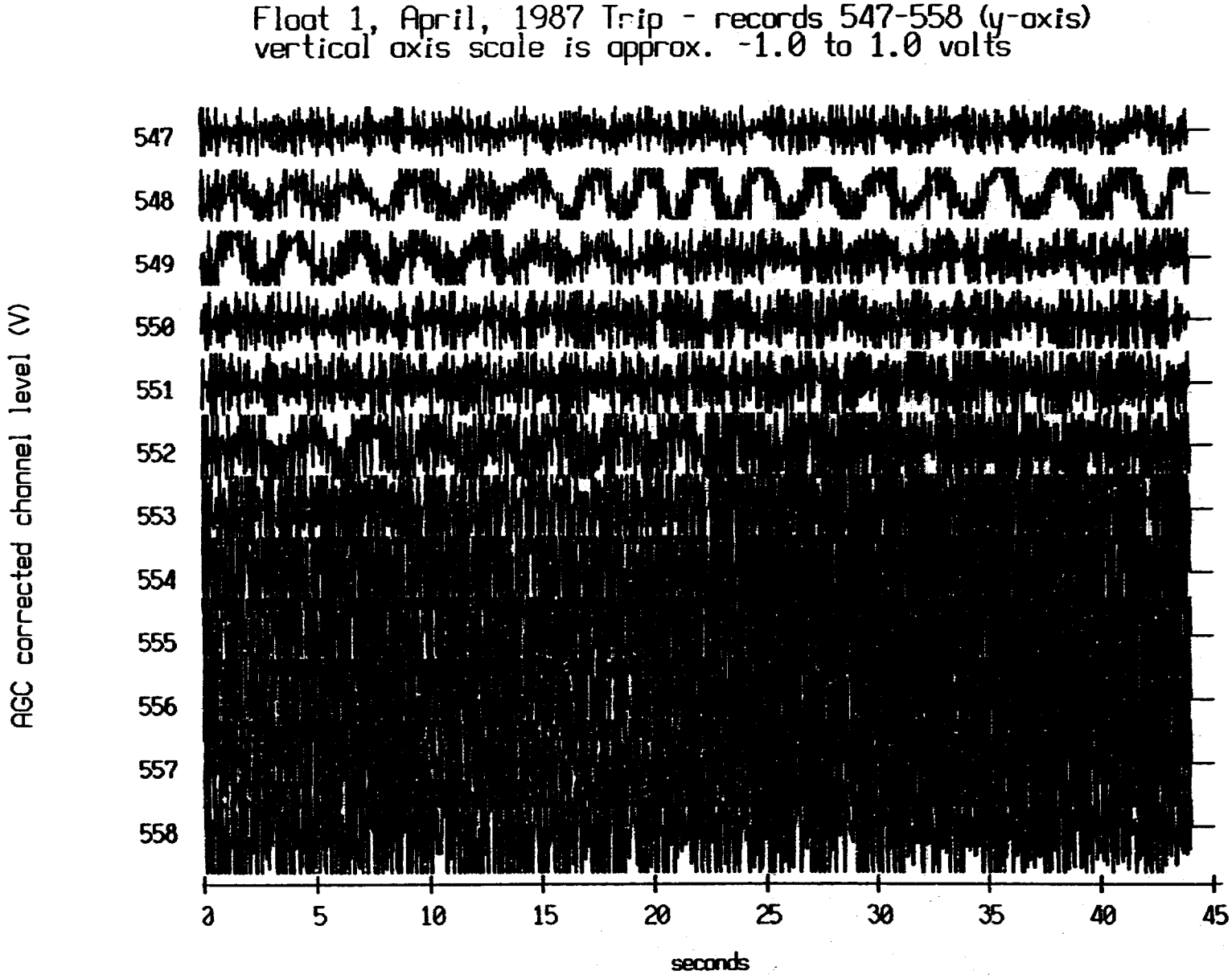
Float 1, April, 1987 Trip - records 547-558 (y-axis)
vertical axis scale is approx. -1.0 to 1.0 volts
AGC corrected channel level (V)
547
548
549
550
551
552
553
554
555
556
557
558
0
5
10
15
20
25
30
35
40
45
seconds

Figure II.2j

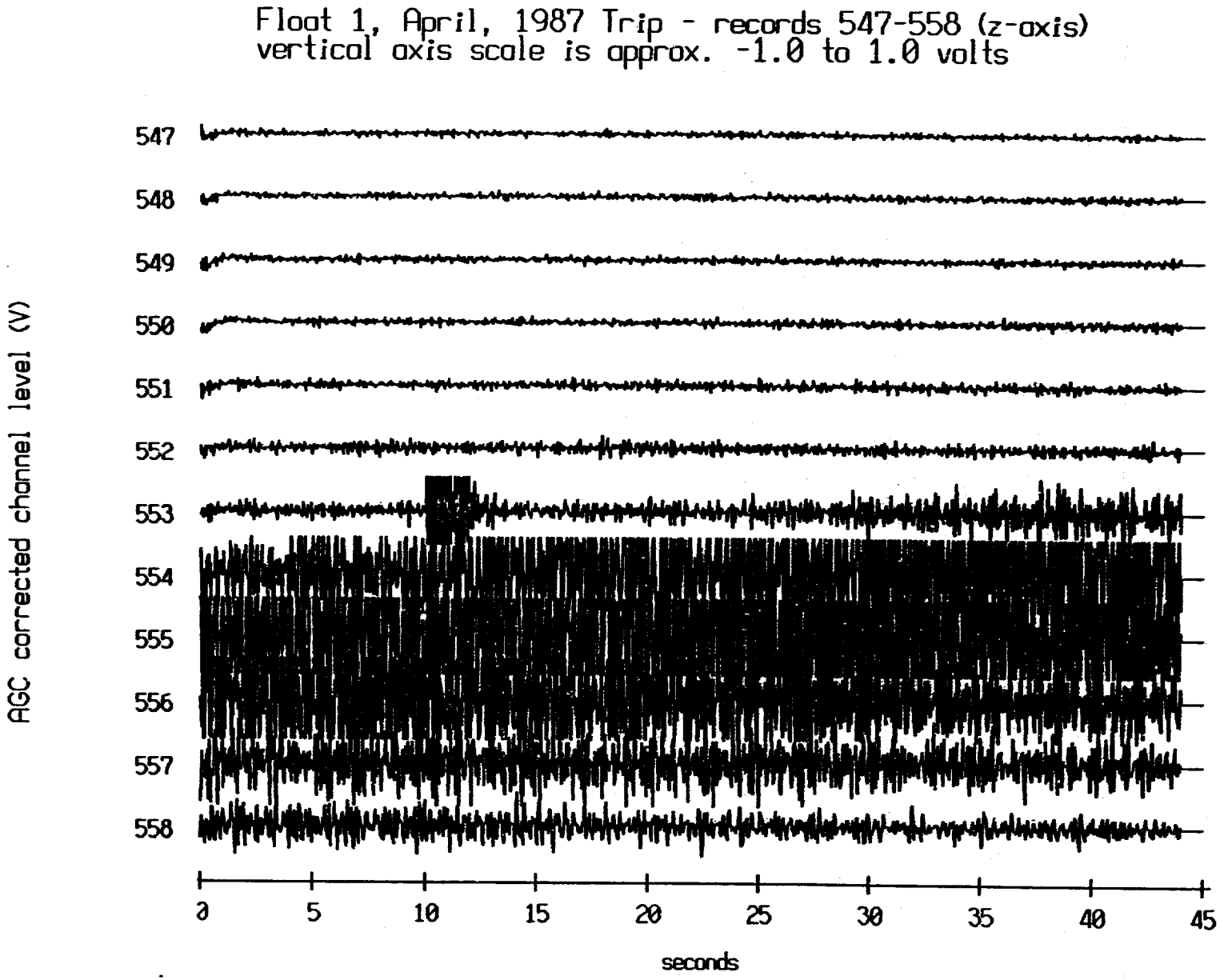
Float 1, April, 1987 Trip - records 547-558 (z-axis)
vertical axis scale is approx. -1.0 to 1.0 volts
AGC corrected channel level (V)
547
548
549
550
551
552
553
554
555
556
557
558
0
5
10
15
20
25
30
35
40
45
seconds

Figure II.2k

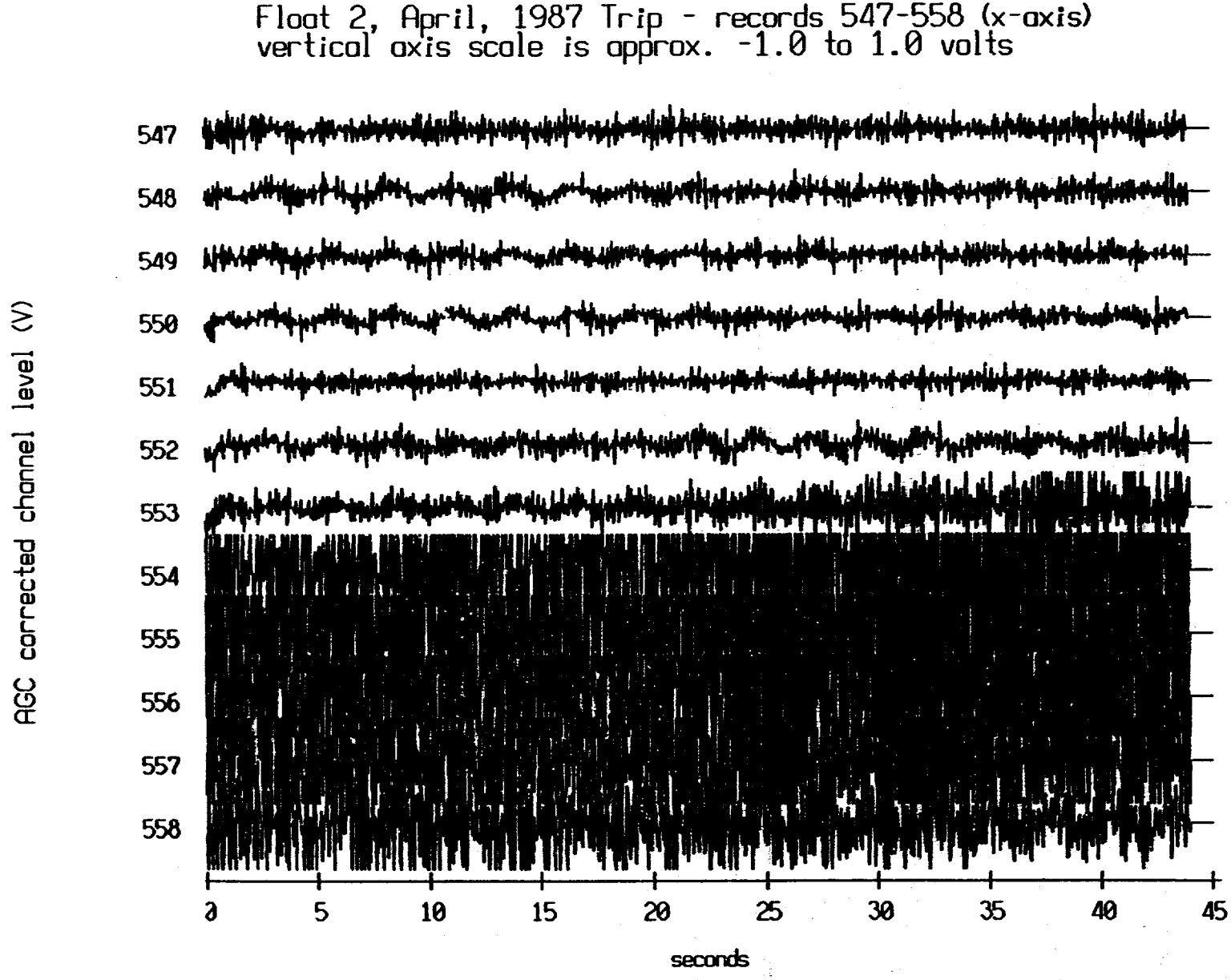
Float 2, April, 1987 Trip - records 547-558 (x-axis)
vertical axis scale is approx. -1.0 to 1.0 volts
AGC corrected channel level (V)
547
548
549
550
551
552
553
554
555
556
557
558
0
5
10
15
20
25
30
35
40
45
seconds

Figure II.3i

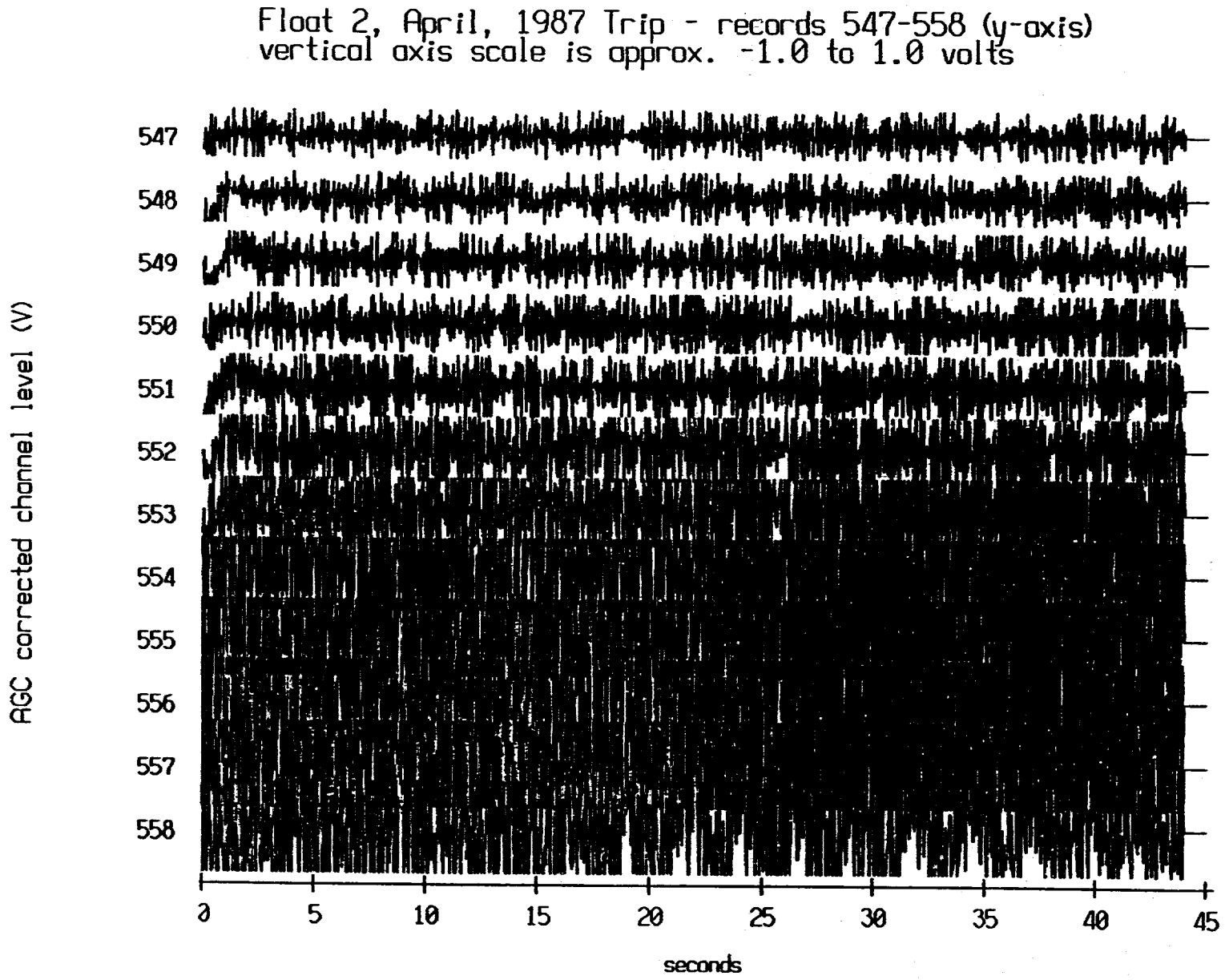
Float 2, April, 1987 Trip - records 547-558 (y-axis)
vertical axis scale is approx. -1.0 to 1.0 volts
AGC corrected channel level (V)
547
548
549
550
551
552
553
554
555
556
557
558
0
5
10
15
20
25
30
35
40
45
seconds

Figure II.3j

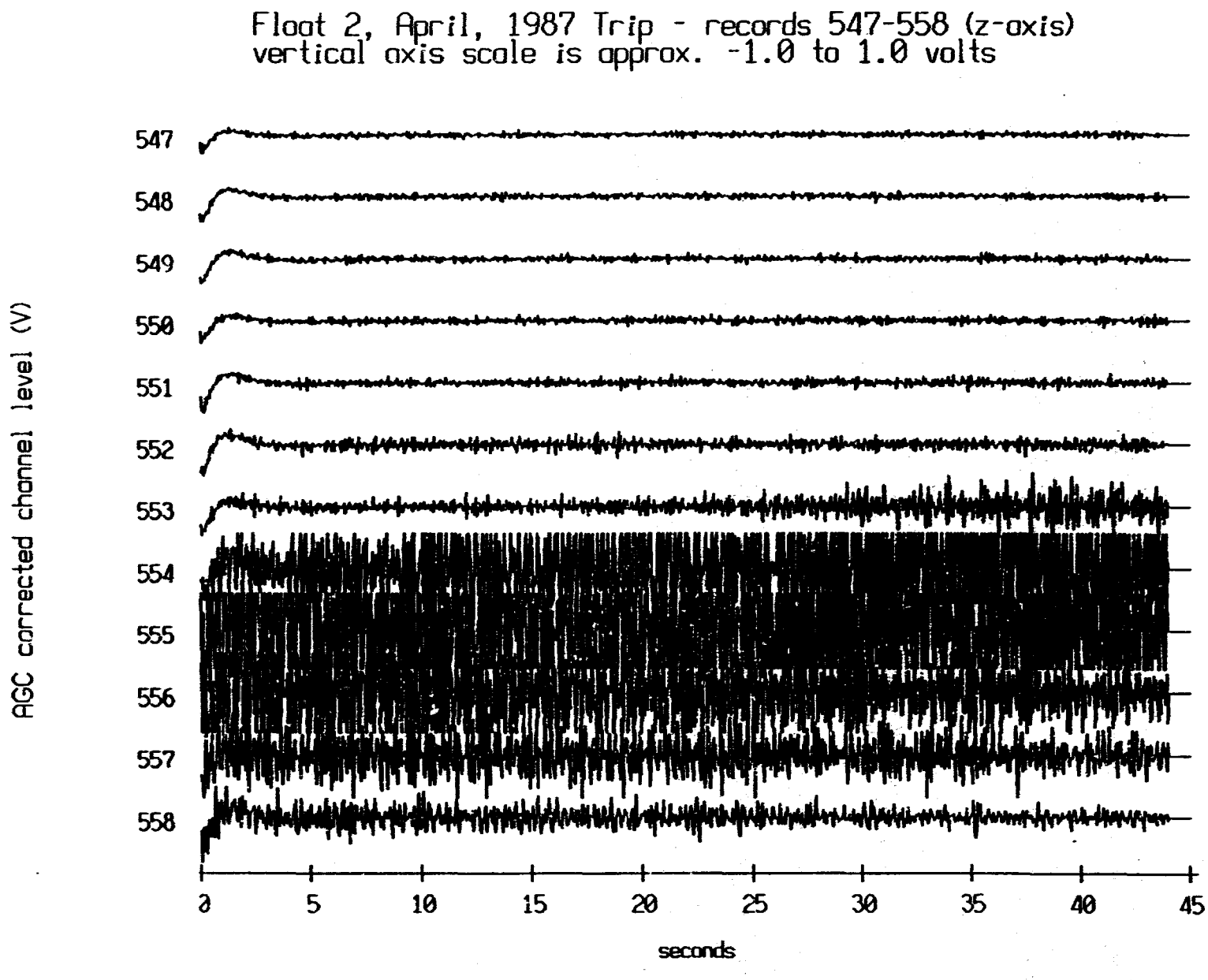
Float 2, April, 1987 Trip - records 547-558 (z-axis)
vertical axis scale is approx. -1.0 to 1.0 volts
AGC corrected channel level (V)
547
548
549
550
551
552
553
554
555
556
557
558
0
5
10
15
20
25
30
35
40
45
seconds

Figure II.3k

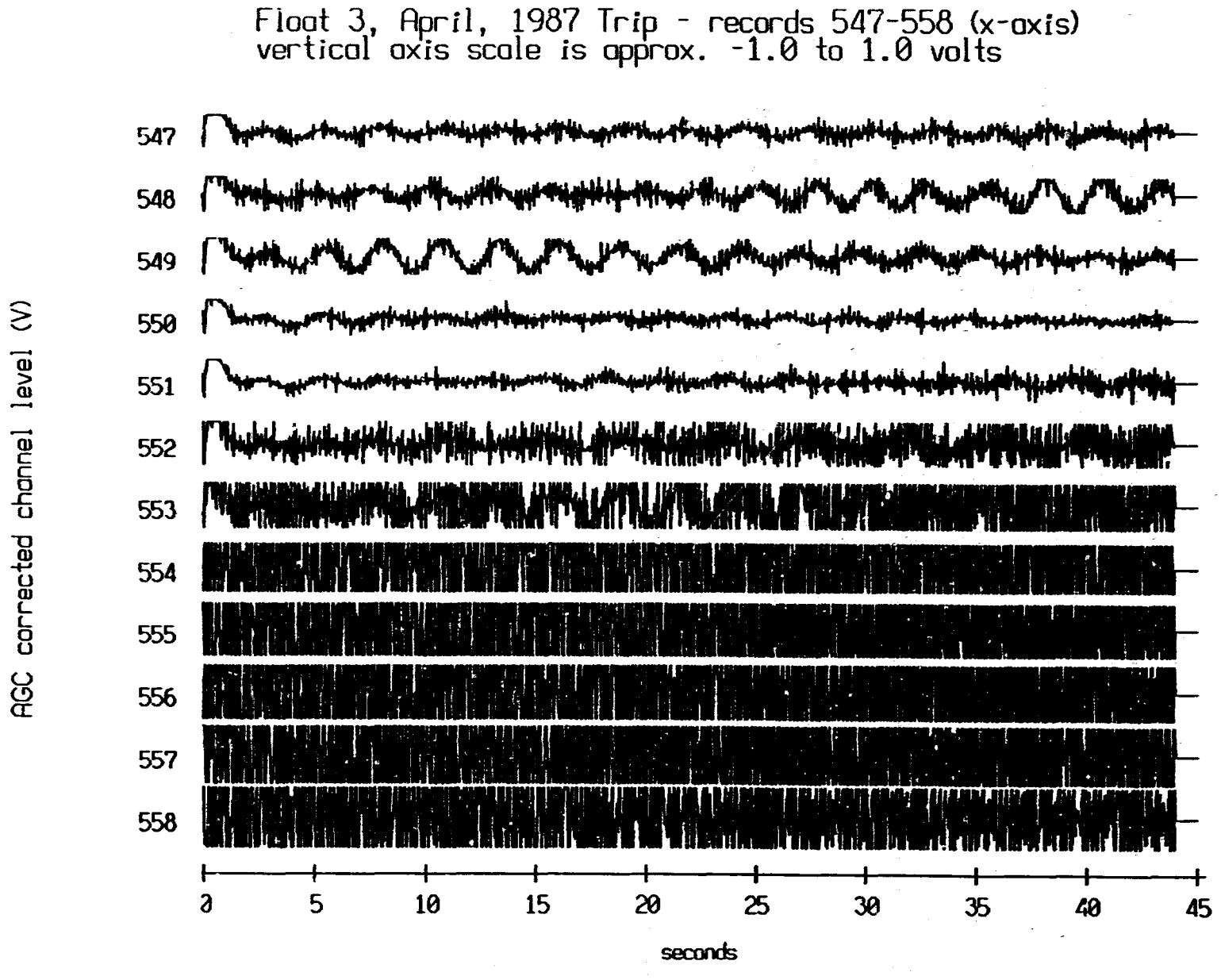
Float 3, April, 1987 Trip - records 547-558 (x-axis)
vertical axis scale is approx. -1.0 to 1.0 volts
AGC corrected channel level (V)
547
548
549
550
551
552
553
554
555
556
557
558
0
5
10
15
20
25
30
35
40
45
seconds

Figure II.4i

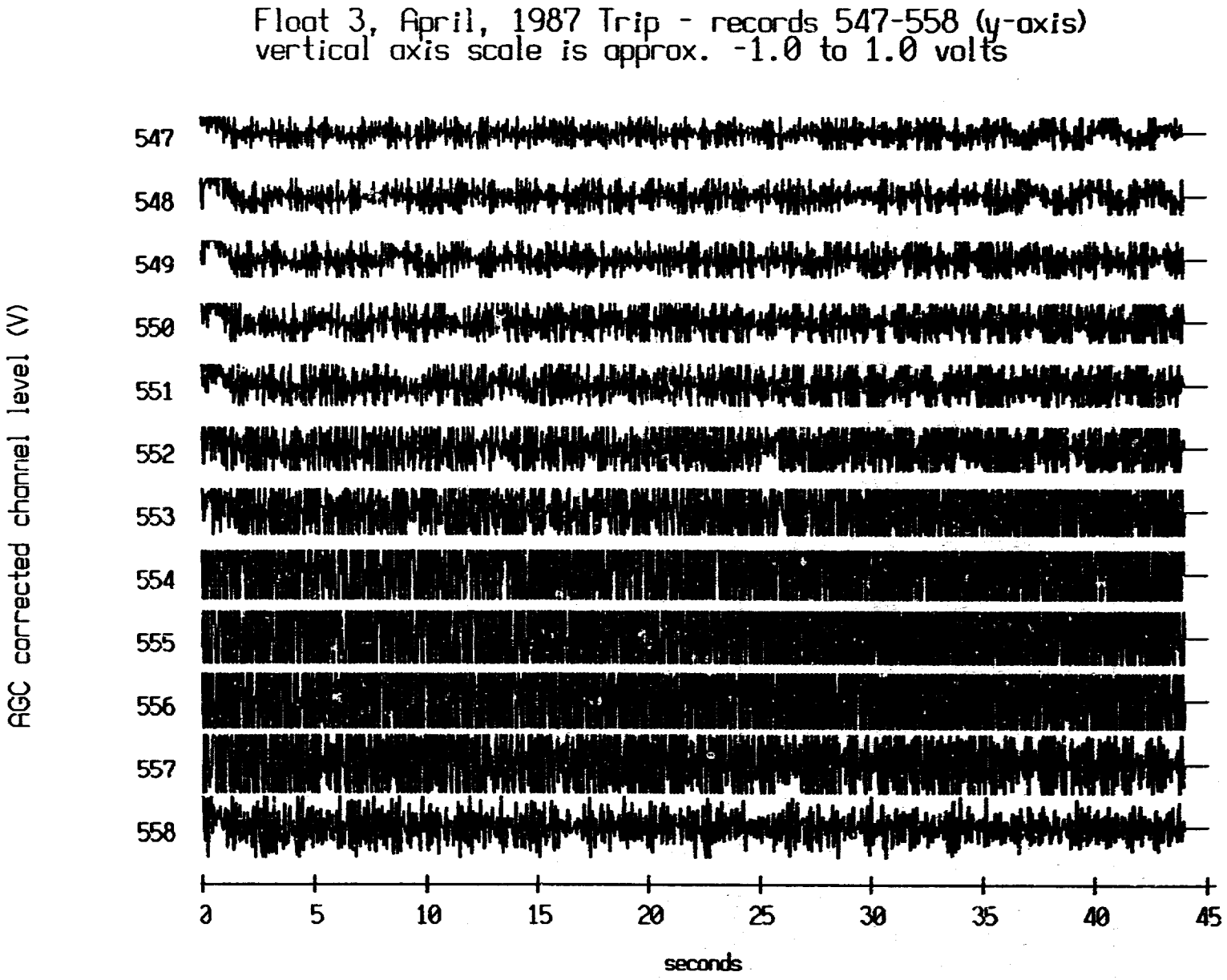
Float 3, April, 1987 Trip - records 547-558 (y-axis)
vertical axis scale is approx. -1.0 to 1.0 volts
AGC corrected channel level (V)
547
548
549
550
551
552
553
554
555
556
557
558
0
5
10
15
20
25
30
35
40
45
seconds

Figure II.4j

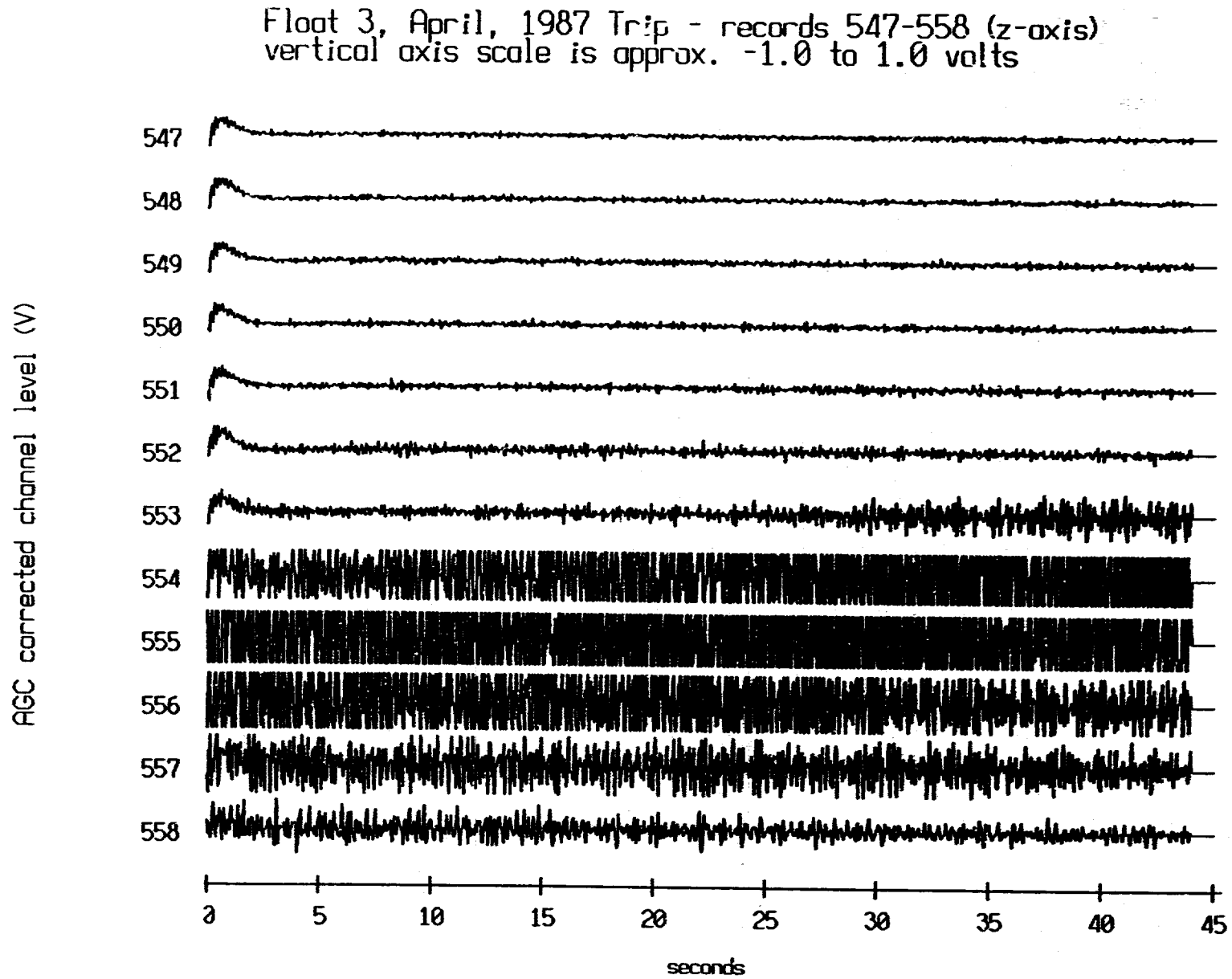
Float 3, April, 1987 Trip - records 547-558 (z-axis)
vertical axis scale is approx. -1.0 to 1.0 volts
AGC corrected channel level (V)
547
548
549
550
551
552
553
554
555
556
557
558
0
5
10
15
20
25
30
35
40
45
seconds

Figure II.4k

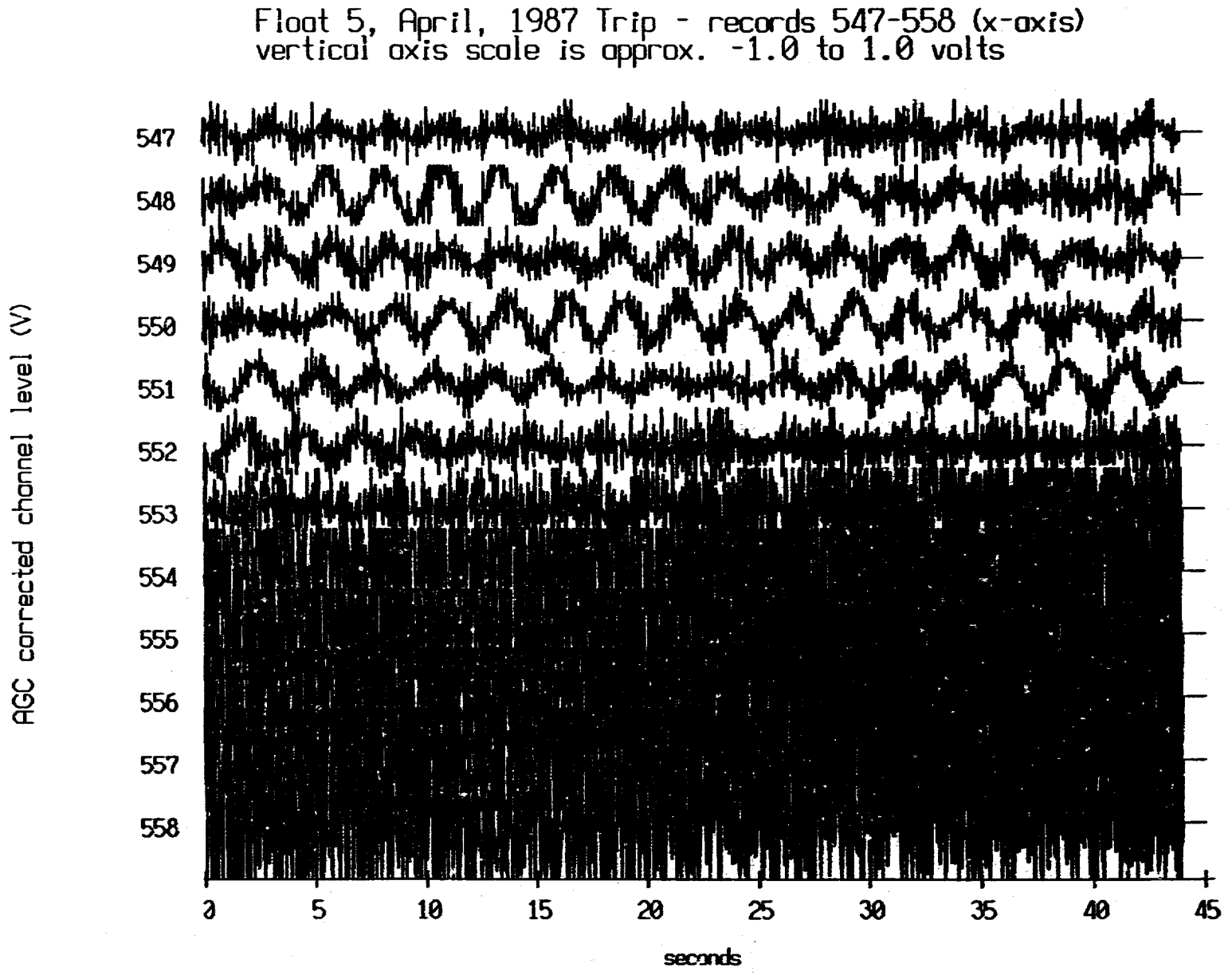
Float 5, April, 1987 Trip - records 547-558 (x-axis)
vertical axis scale is approx. -1.0 to 1.0 volts
AGC corrected channel level (V)
547
548
549
550
551
552
553
554
555
556
557
558
0
5
10
15
20
25
30
35
40
45
seconds

Figure II.5i

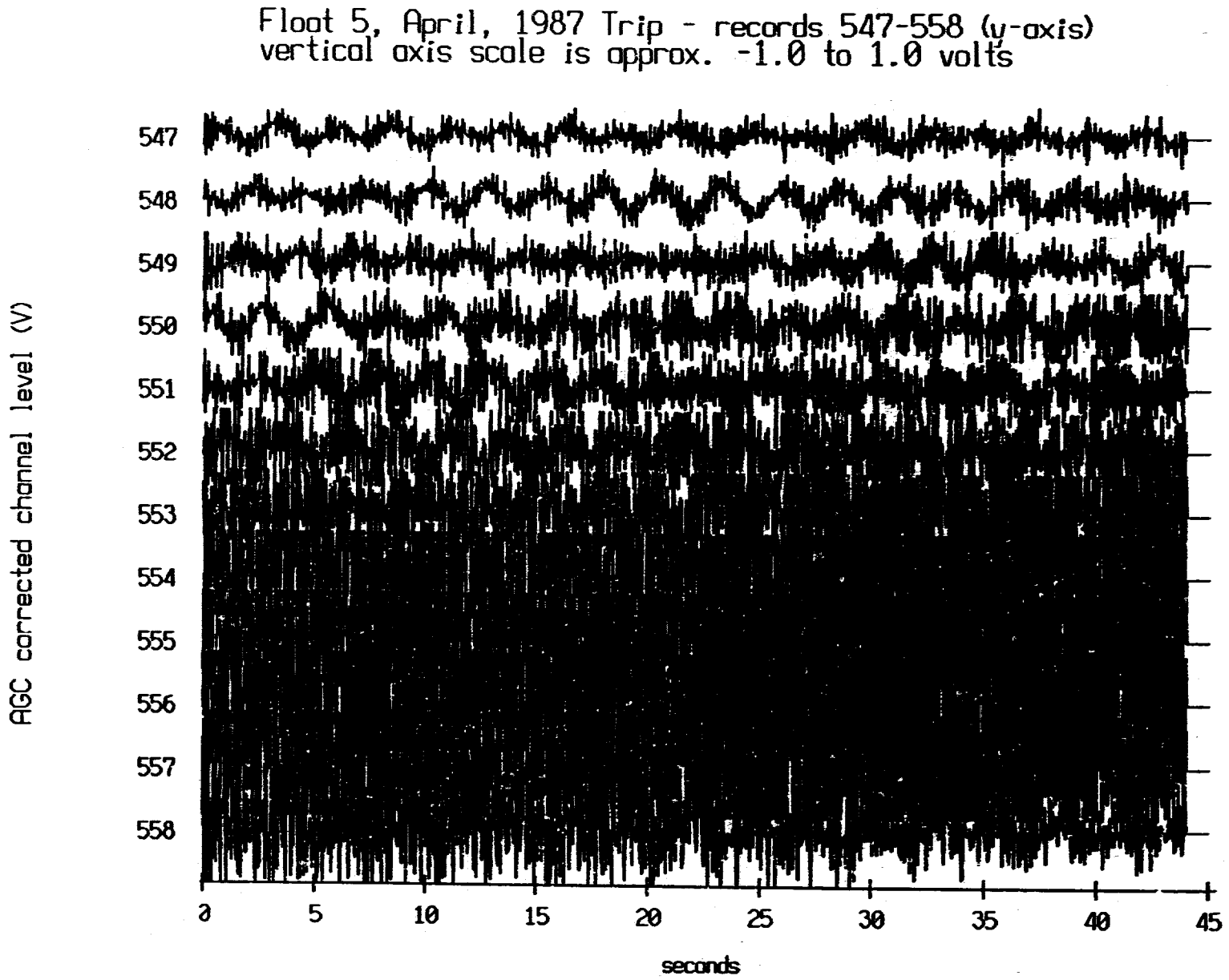
Floot 5, April, 1987 Trip - records 547-558 (y-axis)
vertical axis scale is approx. -1.0 to 1.0 volts
AGC corrected channel level (V)
547
548
549
550
551
552
553
554
555
556
557
558
0
5
10
15
20
25
30
35
40
45
seconds

Figure II.5j

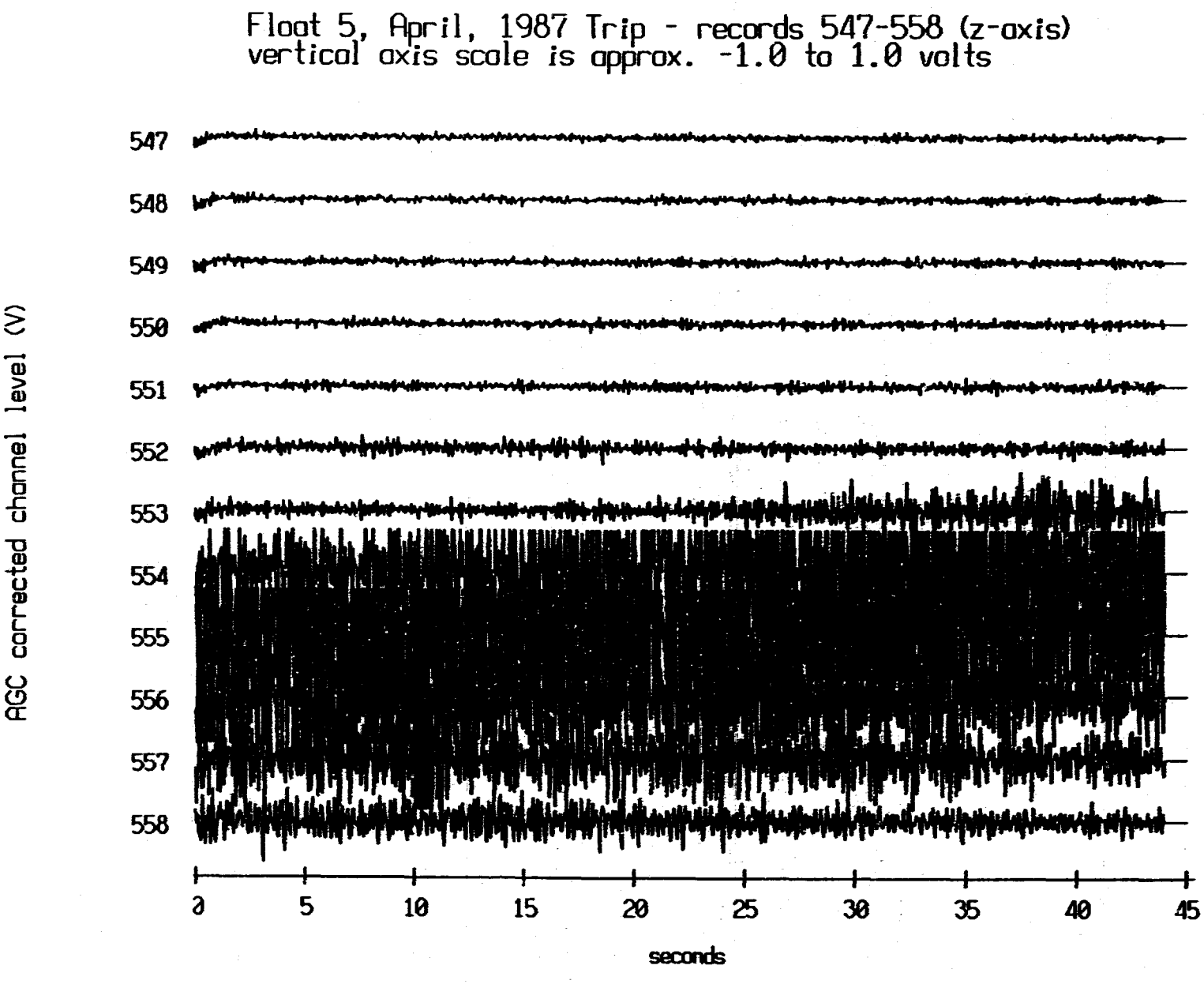
Float 5, April, 1987 Trip - records 547-558 (z-axis)
vertical axis scale is approx. -1.0 to 1.0 volts
AGC corrected channel level (V)
547
548
549
550
551
552
553
554
555
556
557
558
0
5
10
15
20
25
30
35
40
45
seconds

Figure II.5k

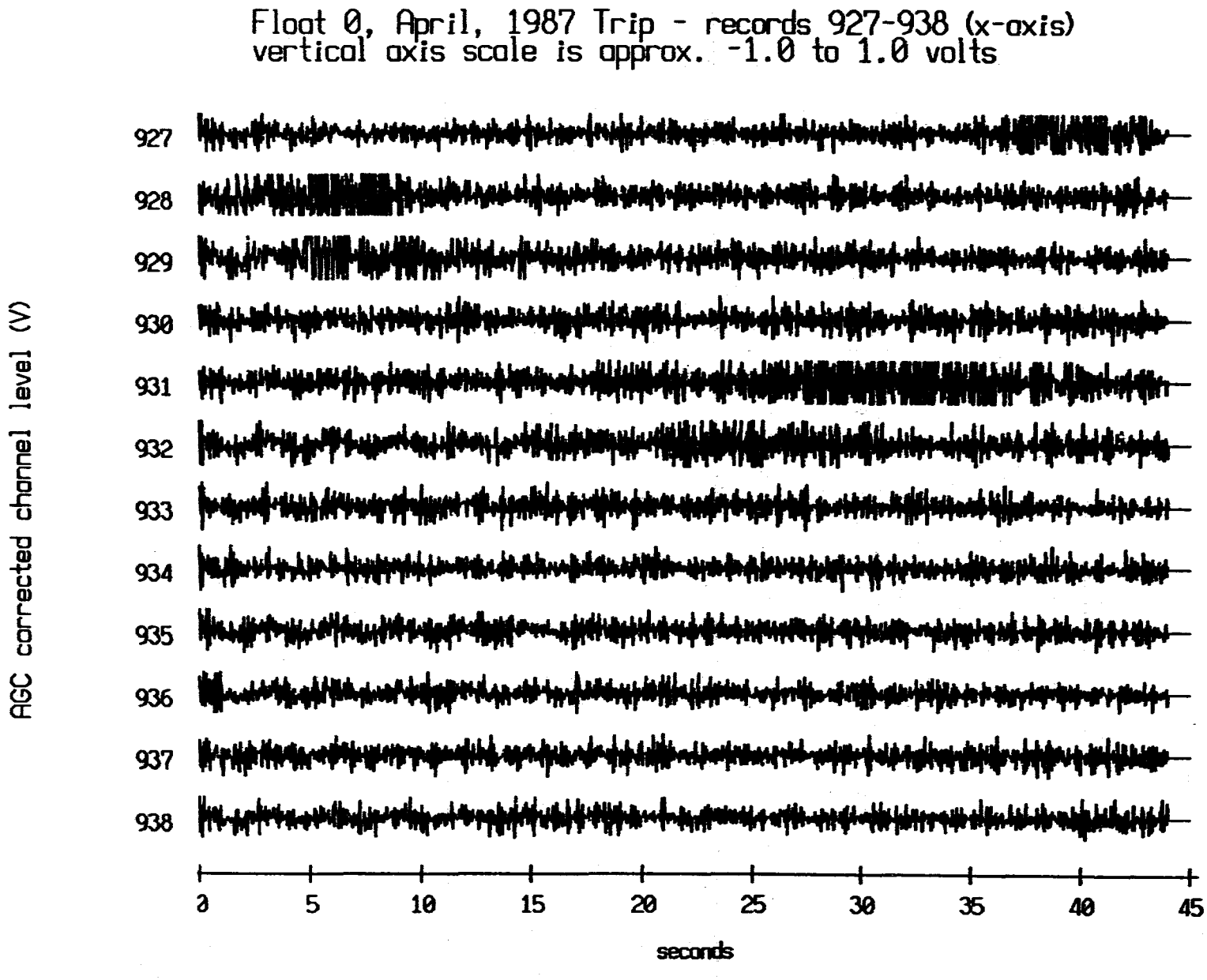
Float 0, April, 1987 Trip - records 927-938 (x-axis)
vertical axis scale is approx. -1.0 to 1.0 volts
AGC corrected channel level (V)
927
928
929
930
931
932
933
934
935
936
937
938
0
5
10
15
20
25
30
35
40
45
seconds

Figure II.6i

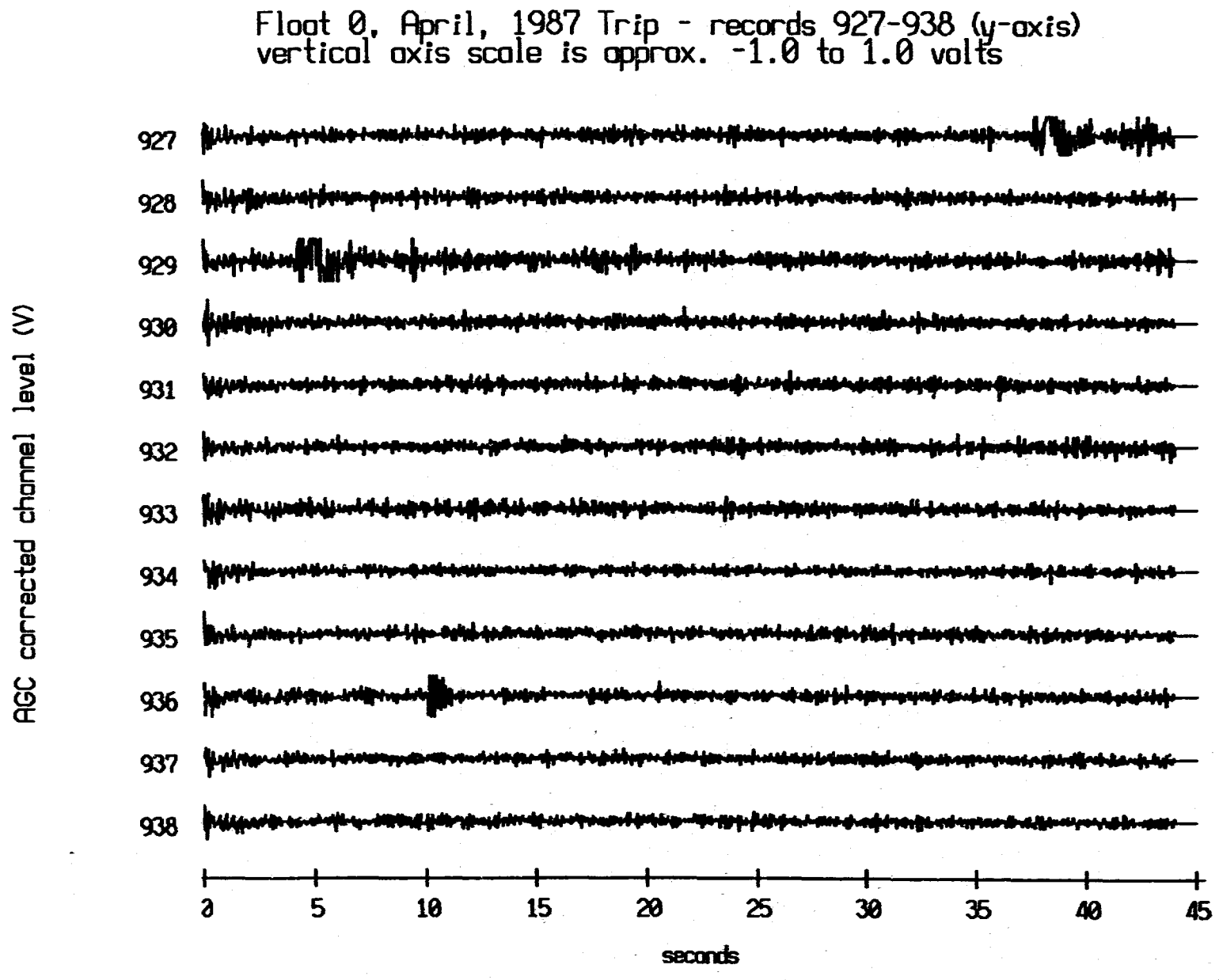
Float 0, April, 1987 Trip - records 927-938 (y-axis)
vertical axis scale is approx. -1.0 to 1.0 volts
927
928
929
930
931
932
933
934
935
936
937
938
AGC corrected channel level (V)
0
5
10
15
20
25
30
35
40
45
seconds

Figure 11.6j

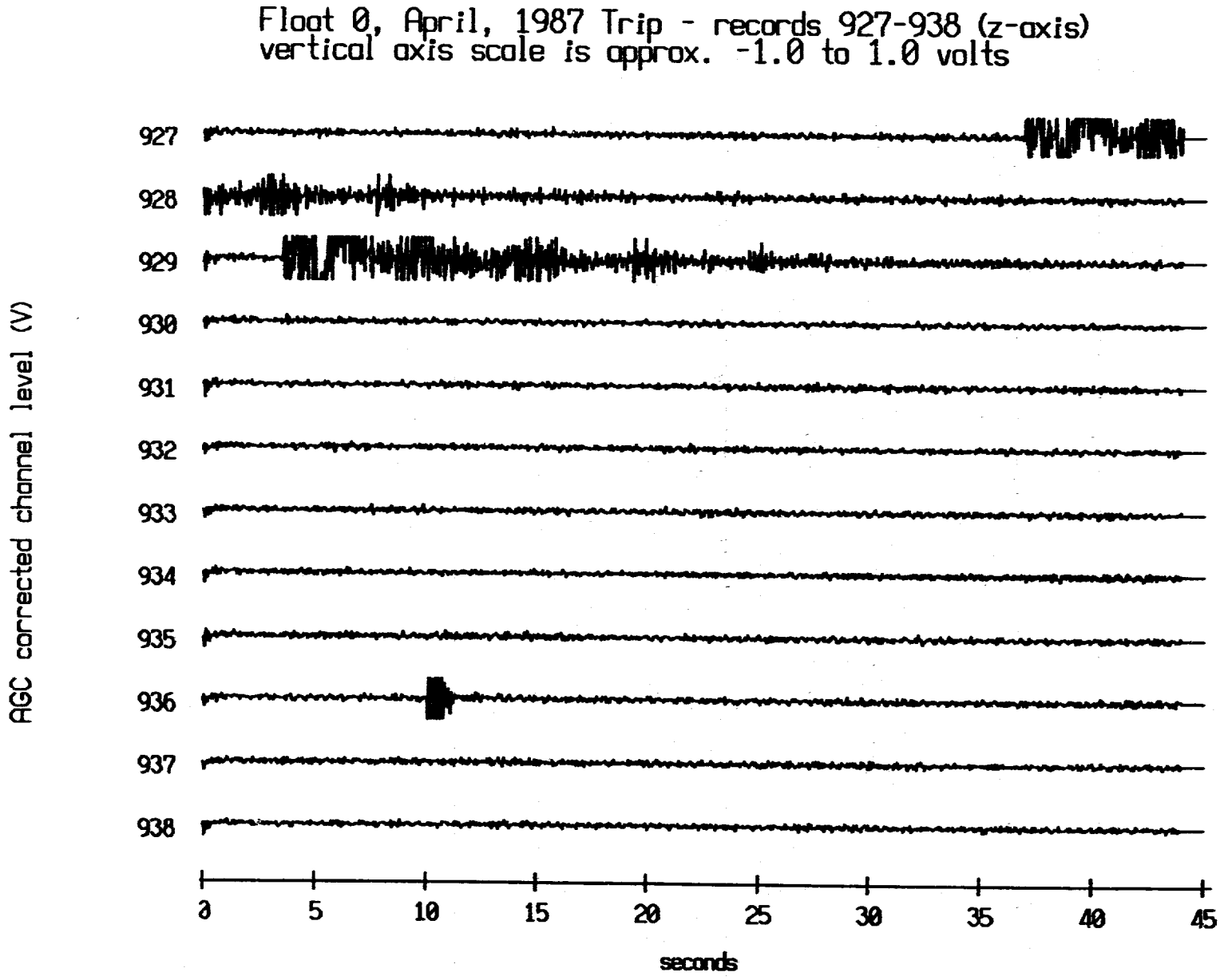
Float 0, April, 1987 Trip - records 927-938 (z-axis)
vertical axis scale is approx. -1.0 to 1.0 volts
AGC corrected channel level (V)
927
928
929
930
931
932
933
934
935
936
937
938
0
5
10
15
20
25
30
35
40
45
seconds

Figure II.6k

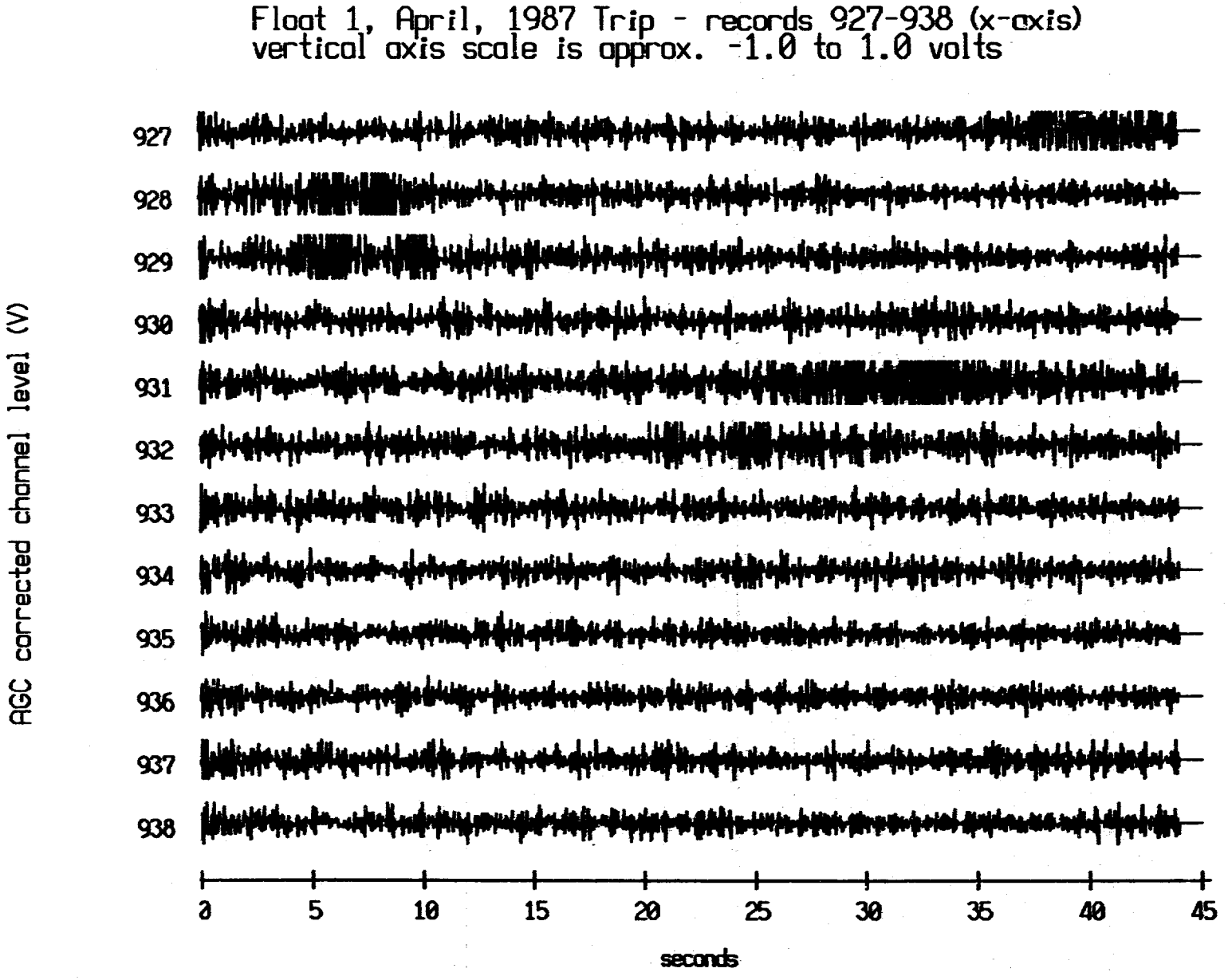
Float 1, April, 1987 Trip - records 927-938 (x-axis)
vertical axis scale is approx. -1.0 to 1.0 volts
AGC corrected channel level (V)
927
928
929
930
931
932
933
934
935
936
937
938
0
5
10
15
20
25
30
35
40
45
seconds

Figure II.7i

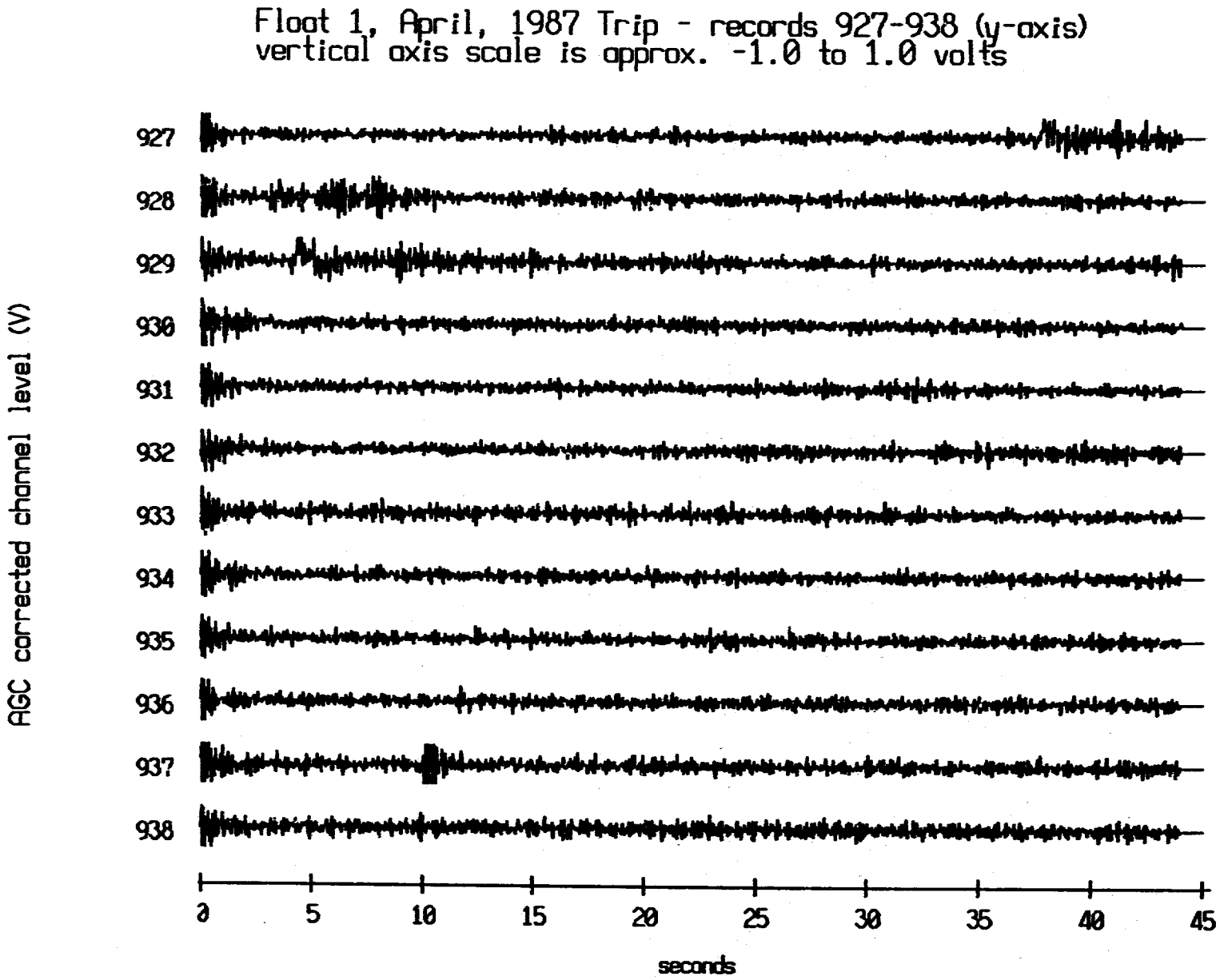
Float 1, April, 1987 Trip - records 927-938 (y-axis)
vertical axis scale is approx. -1.0 to 1.0 volts
927
928
929
930
931
932
933
934
935
936
937
938
AGC corrected channel level (V)
0
5
10
15
20
25
30
35
40
45
seconds

Figure II.7j

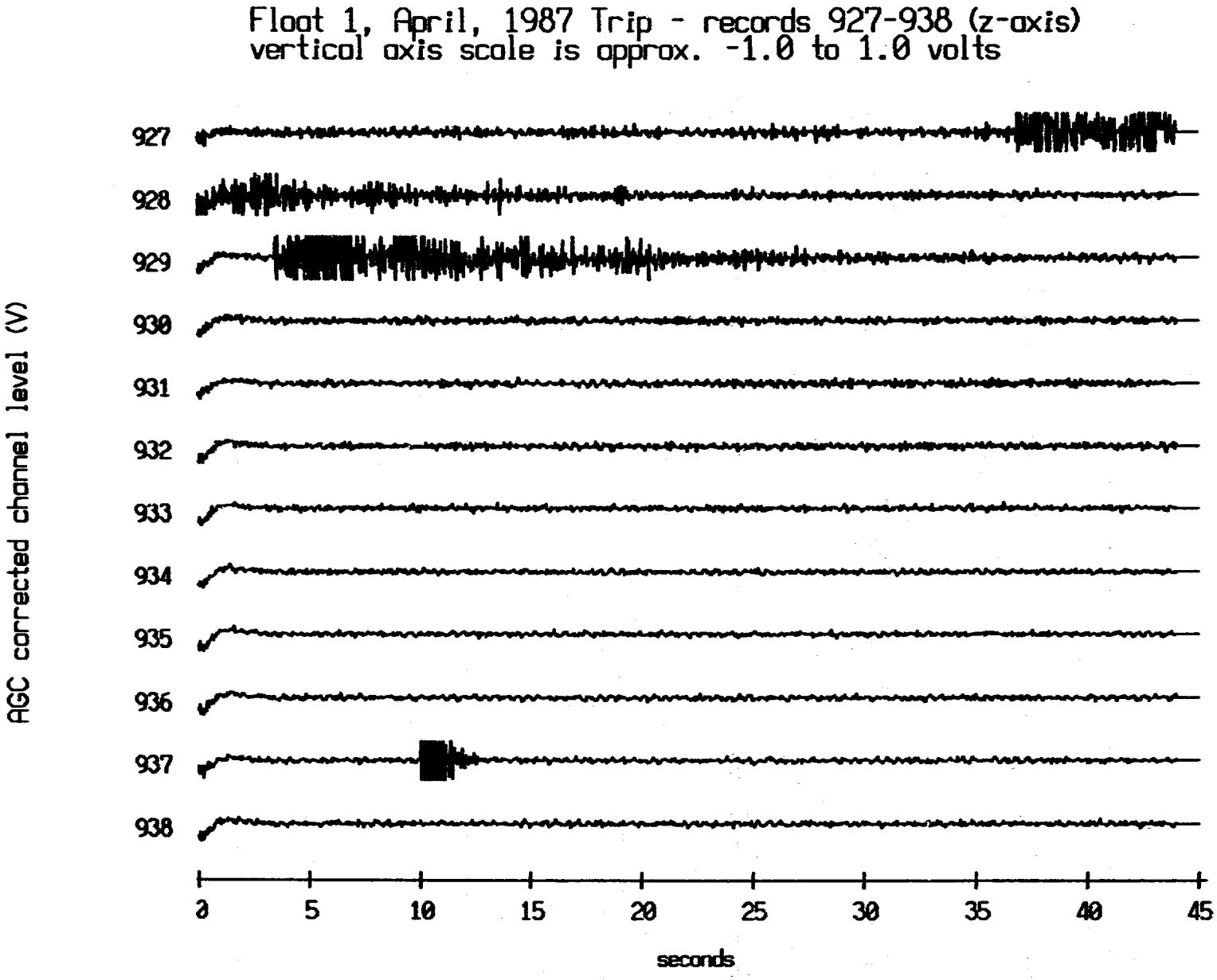
Float 1, April, 1987 Trip - records 927-938 (z-axis)
vertical axis scale is approx. -1.0 to 1.0 volts
AGC corrected channel level (V)
927
928
929
930
931
932
933
934
935
936
937
938
0
5
10
15
20
25
30
35
40
45
seconds

Figure II.7k

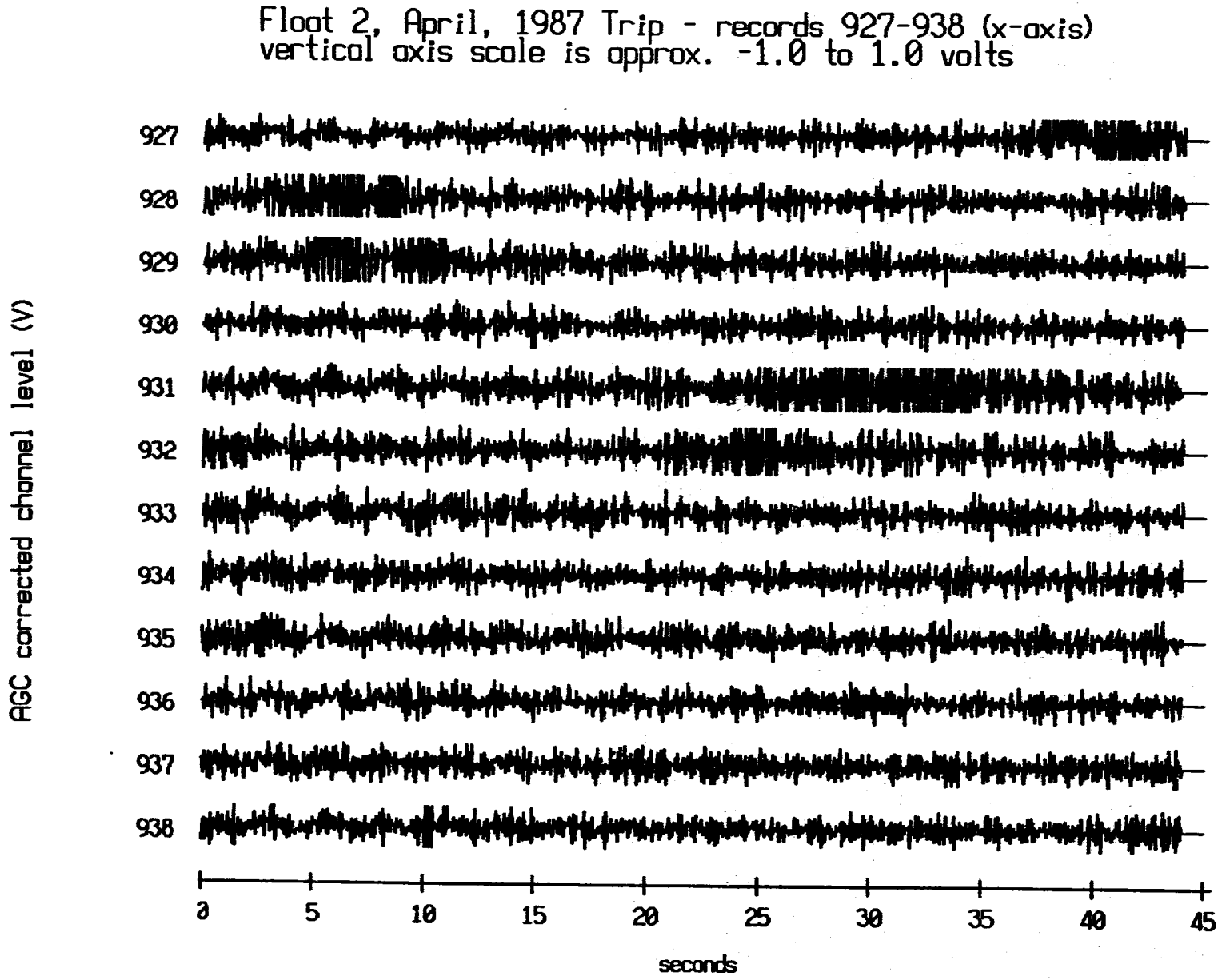
Float 2, April, 1987 Trip - records 927-938 (x-axis)
vertical axis scale is approx. -1.0 to 1.0 volts
AGC corrected channel level (V)
927
928
929
930
931
932
933
934
935
936
937
938
0
5
10
15
20
25
30
35
40
45
seconds

Figure II.8i

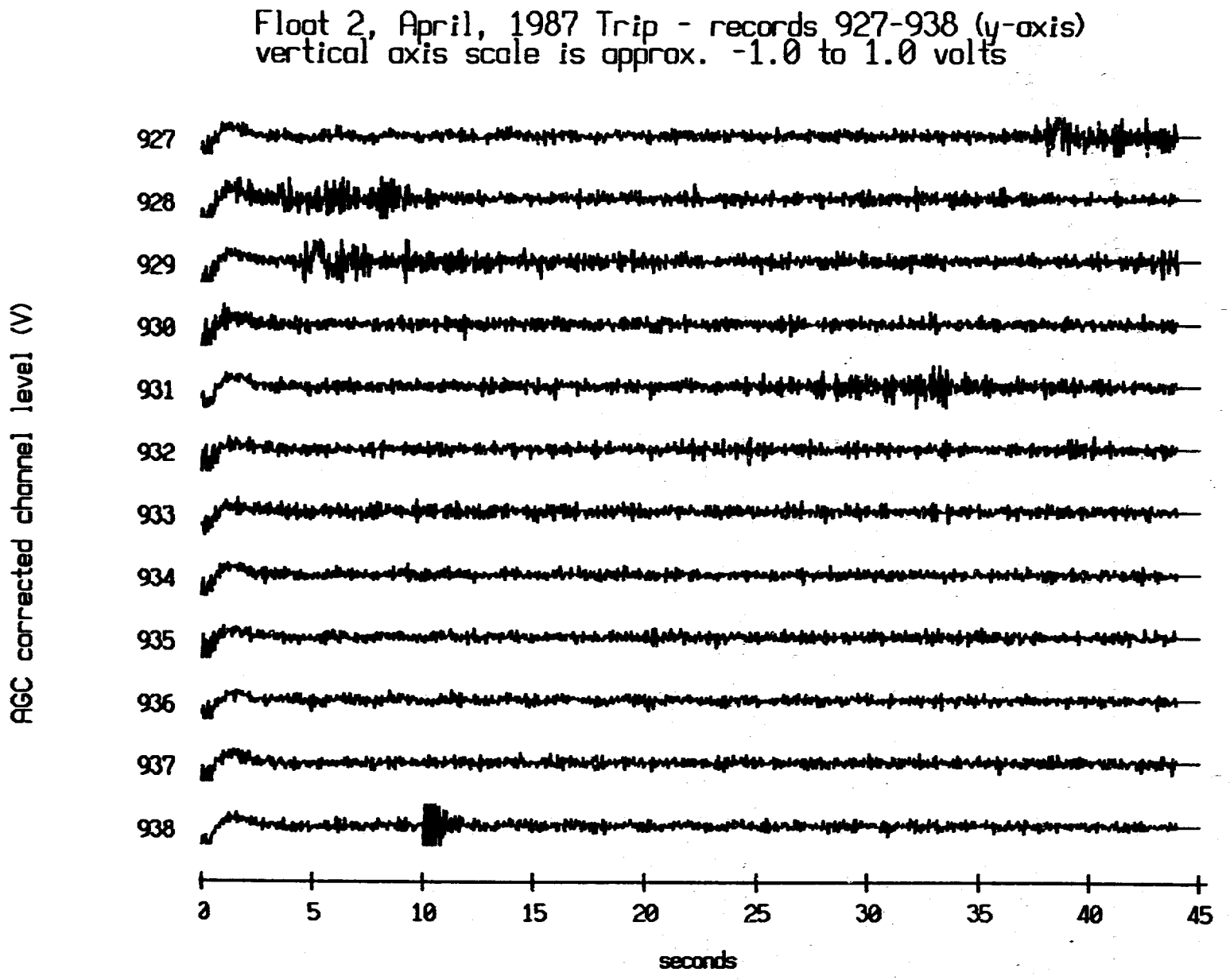
Float 2, April, 1987 Trip - records 927-938 (y-axis)
vertical axis scale is approx. -1.0 to 1.0 volts
927
928
929
930
931
932
933
934
935
936
937
938
AGC corrected channel level (V)
0
5
10
15
20
25
30
35
40
45
seconds

Figure 11.5j

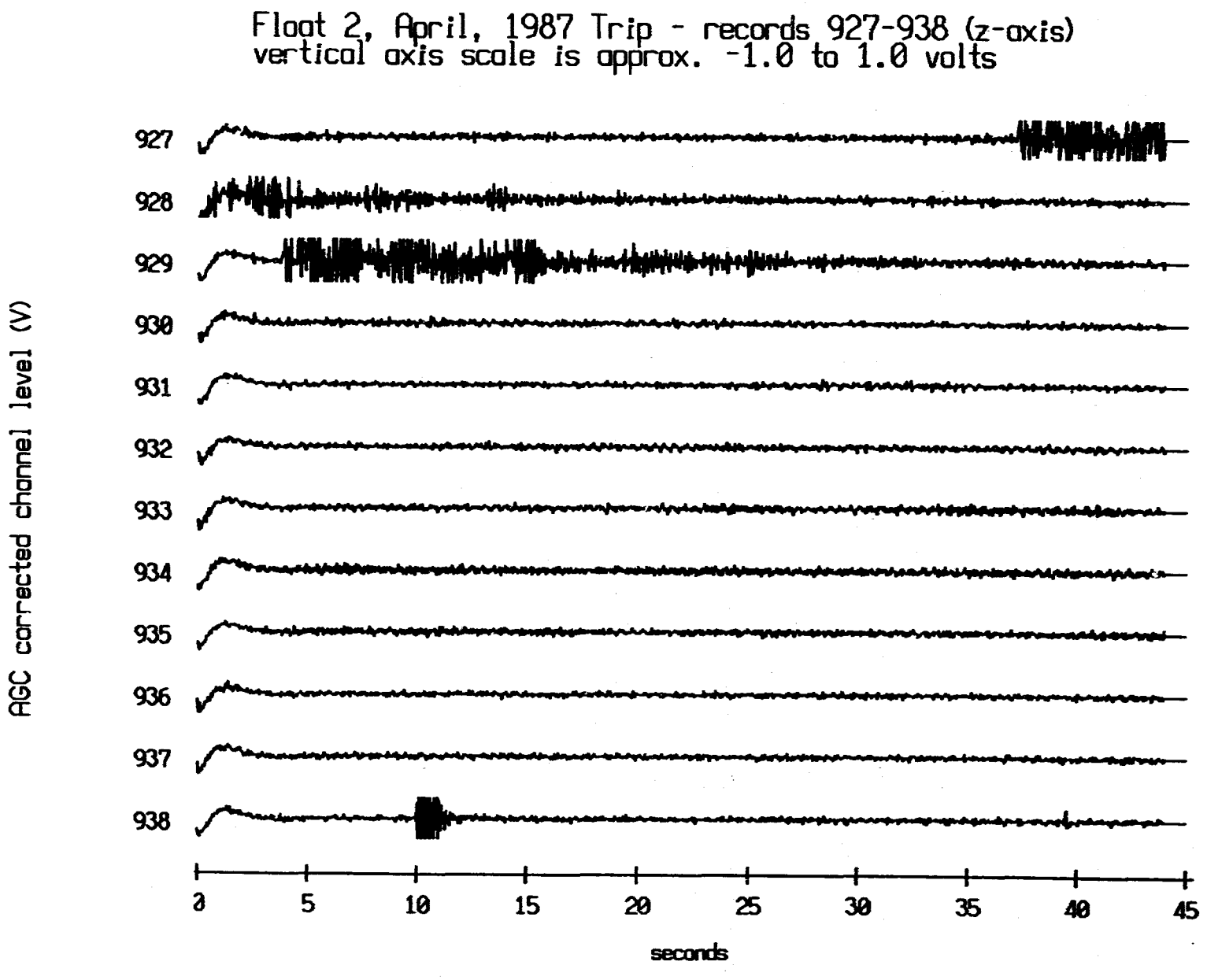
Float 2, April, 1987 Trip - records 927-938 (z-axis)
vertical axis scale is approx. -1.0 to 1.0 volts
AGC corrected channel level (V)
927
928
929
930
931
932
933
934
935
936
937
938
0
5
10
15
20
25
30
35
40
45
seconds

Figure II.8k

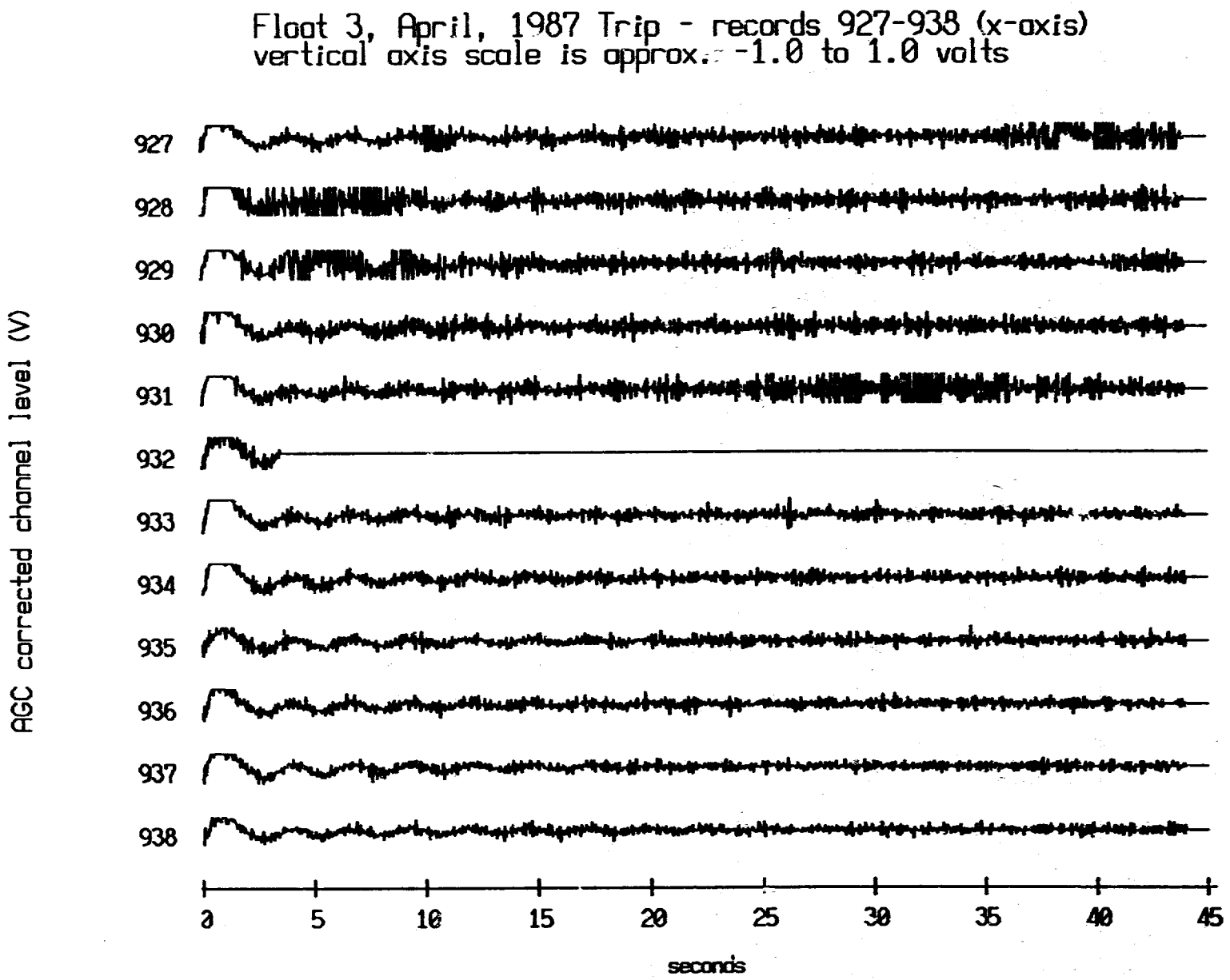
Float 3, April, 1987 Trip - records 927-938 (x-axis)
vertical axis scale is approx. -1.0 to 1.0 volts
927
928
929
930
931
932
933
934
935
936
937
938
AGC corrected channel level (V)
0
5
10
15
20
25
30
35
40
45
seconds

Figure II.9i

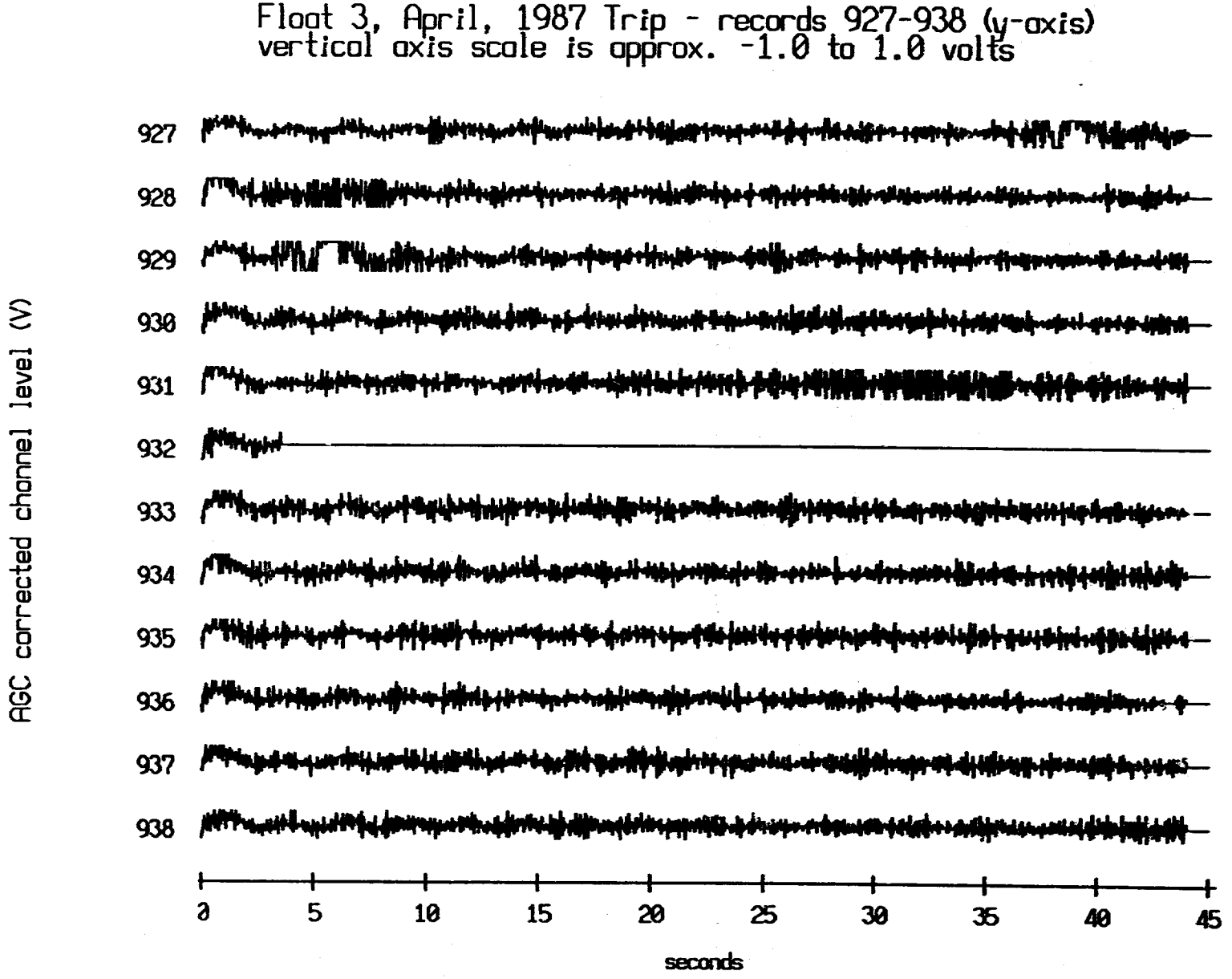
Float 3, April, 1987 Trip - records 927-938 (y-axis)
vertical axis scale is approx. -1.0 to 1.0 volts
AGC corrected channel level (V)
927
928
929
930
931
932
933
934
935
936
937
938
0
5
10
15
20
25
30
35
40
45
seconds

Figure II.9j

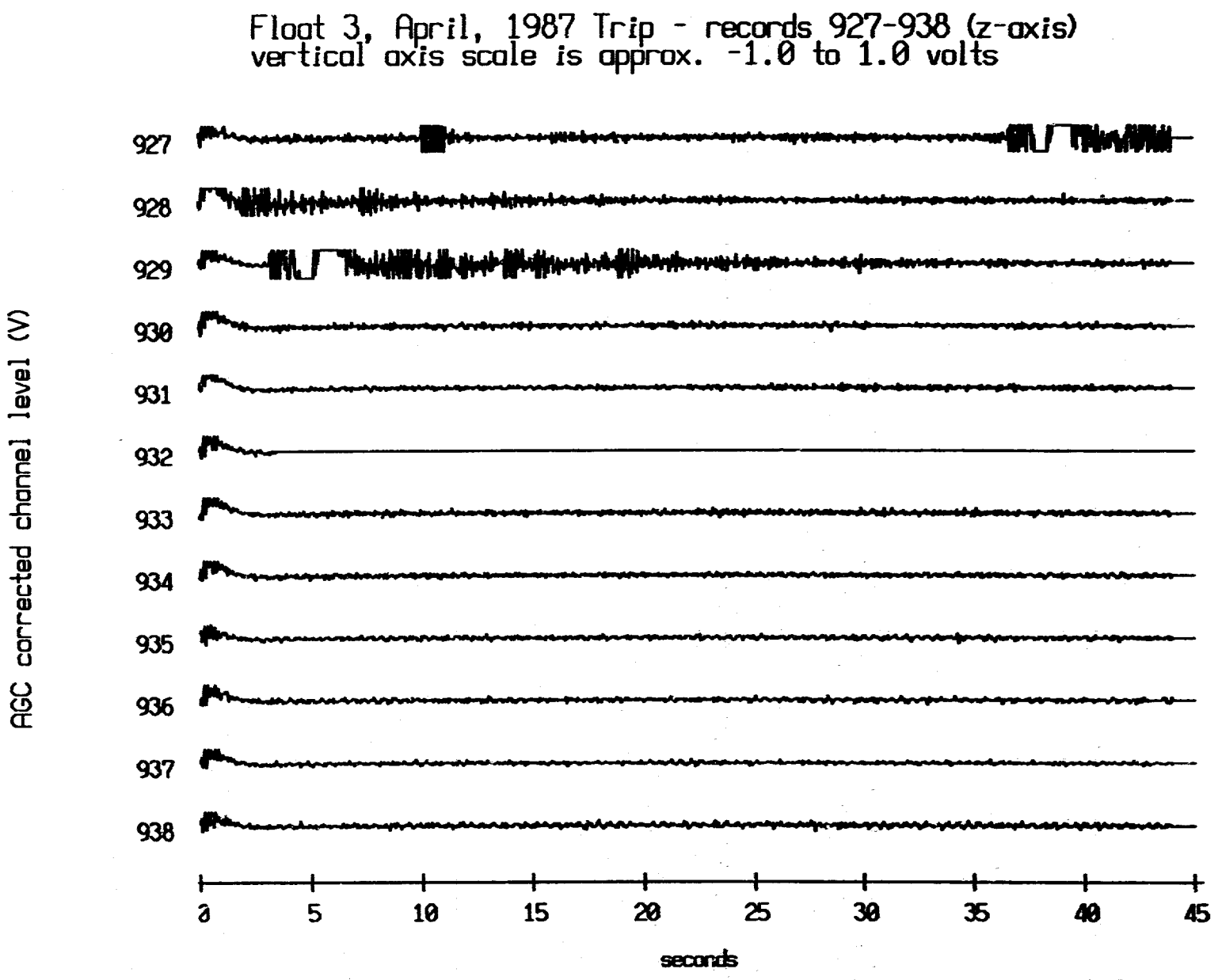
Float 3, April, 1987 Trip - records 927-938 (z-axis)
vertical axis scale is approx. -1.0 to 1.0 volts
AGC corrected channel level (V)
927
928
929
930
931
932
933
934
935
936
937
938
0
5
10
15
20
25
30
35
40
45
seconds

Figure II.9k

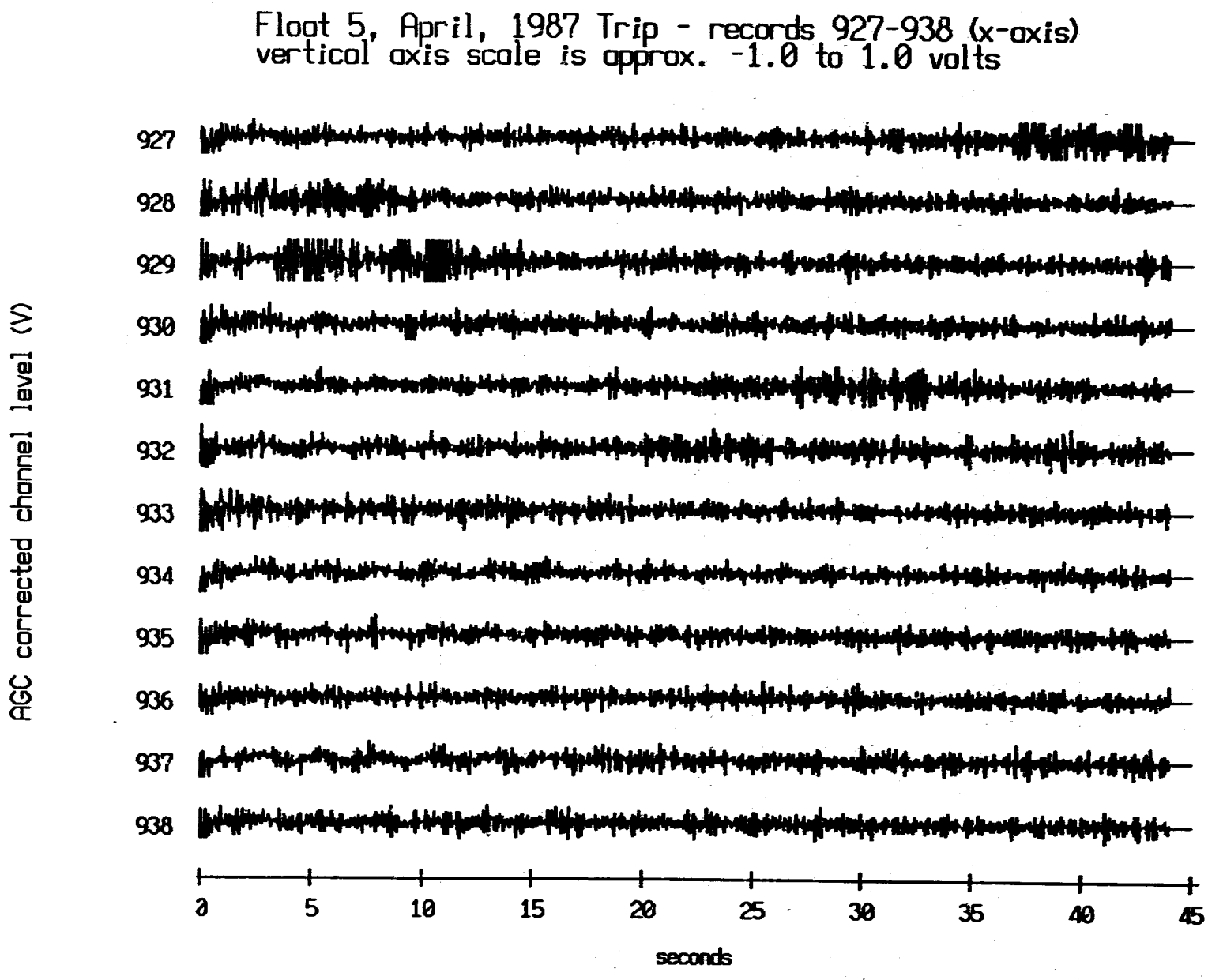
Float 5, April, 1987 Trip - records 927-938 (x-axis)
vertical axis scale is approx. -1.0 to 1.0 volts
AGC corrected channel level (V)
927
928
929
930
931
932
933
934
935
936
937
938
0
5
10
15
20
25
30
35
40
45
seconds

Figure II.10

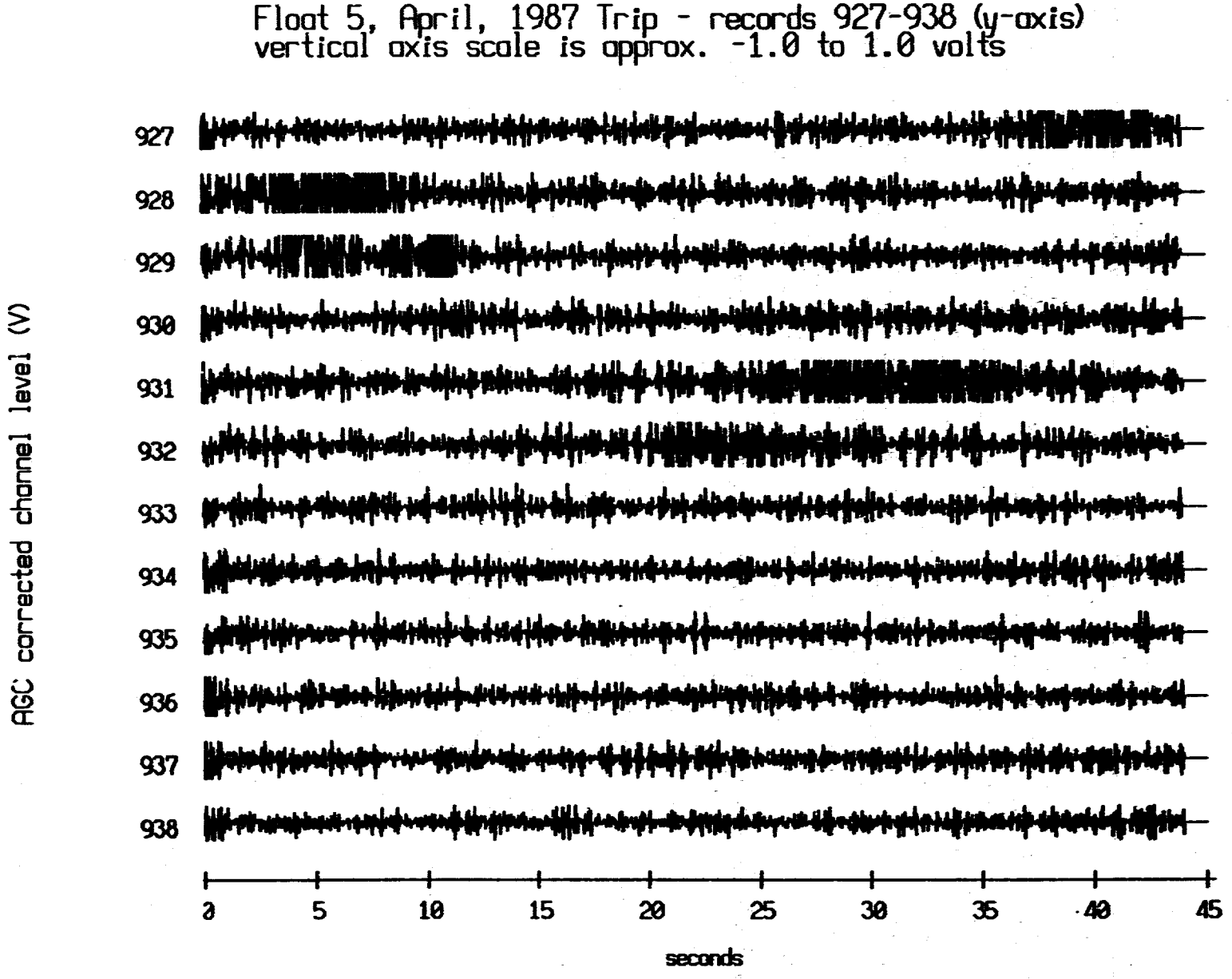

Figure II.10j

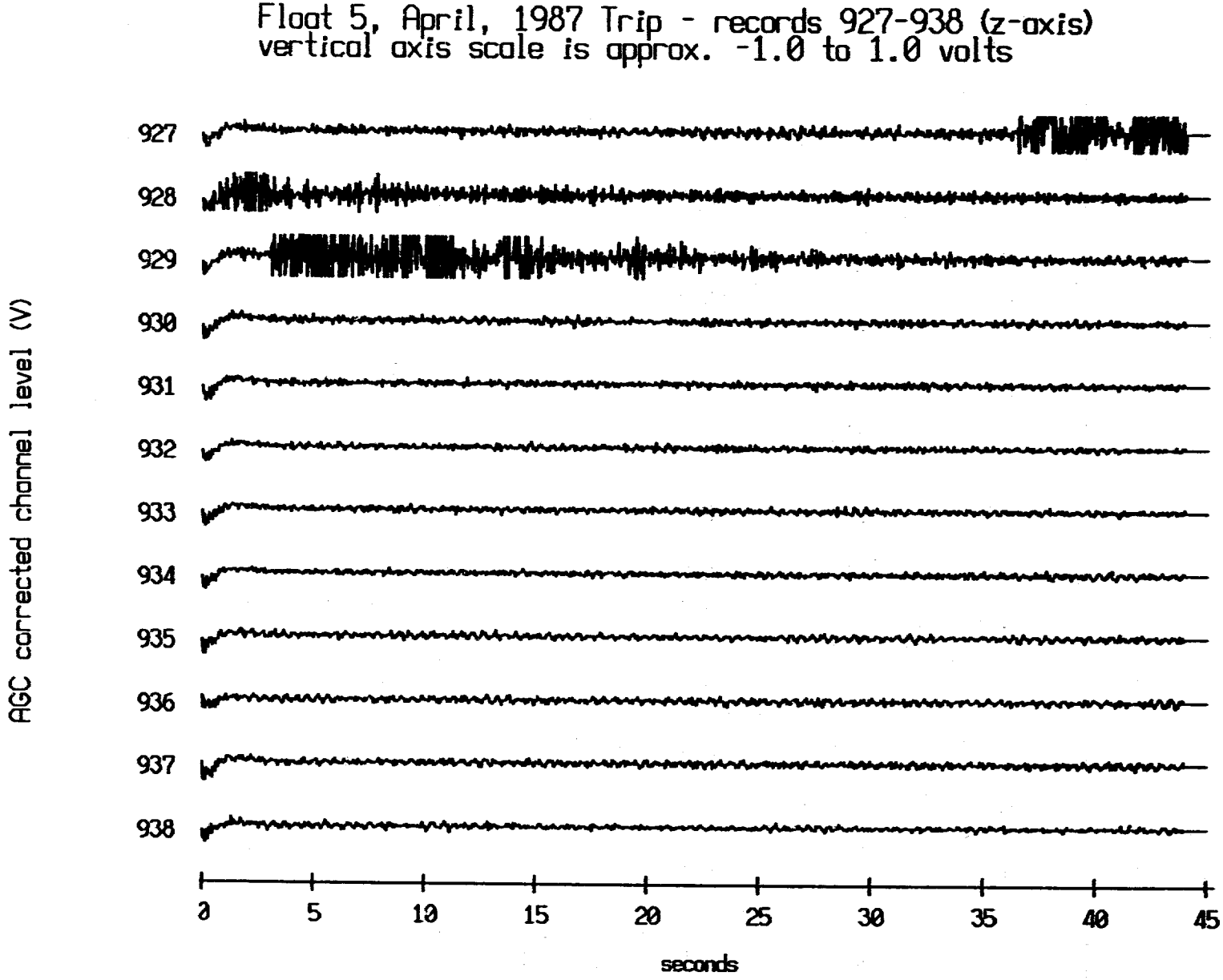

Figure II.10k

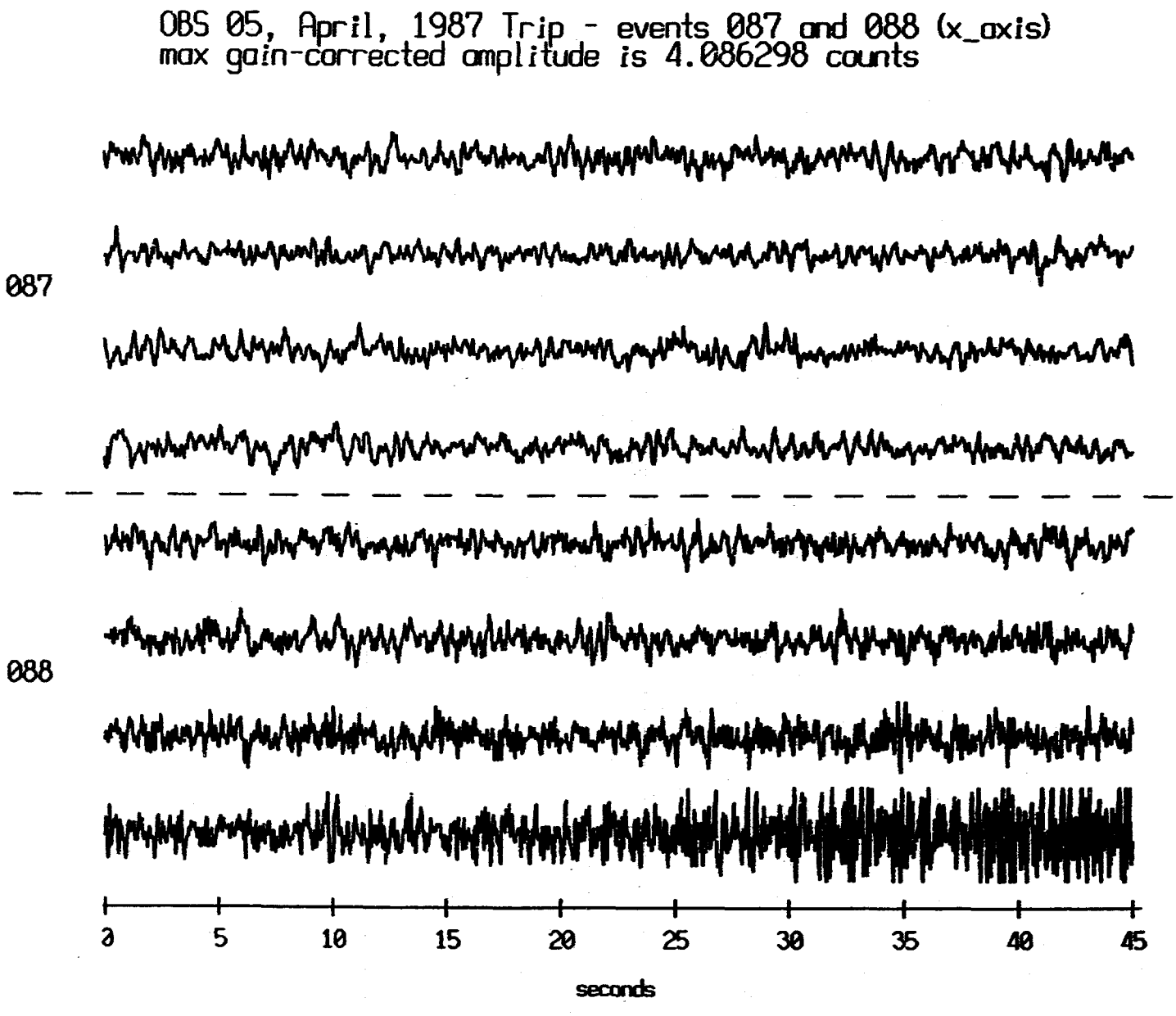

Figure II.11i

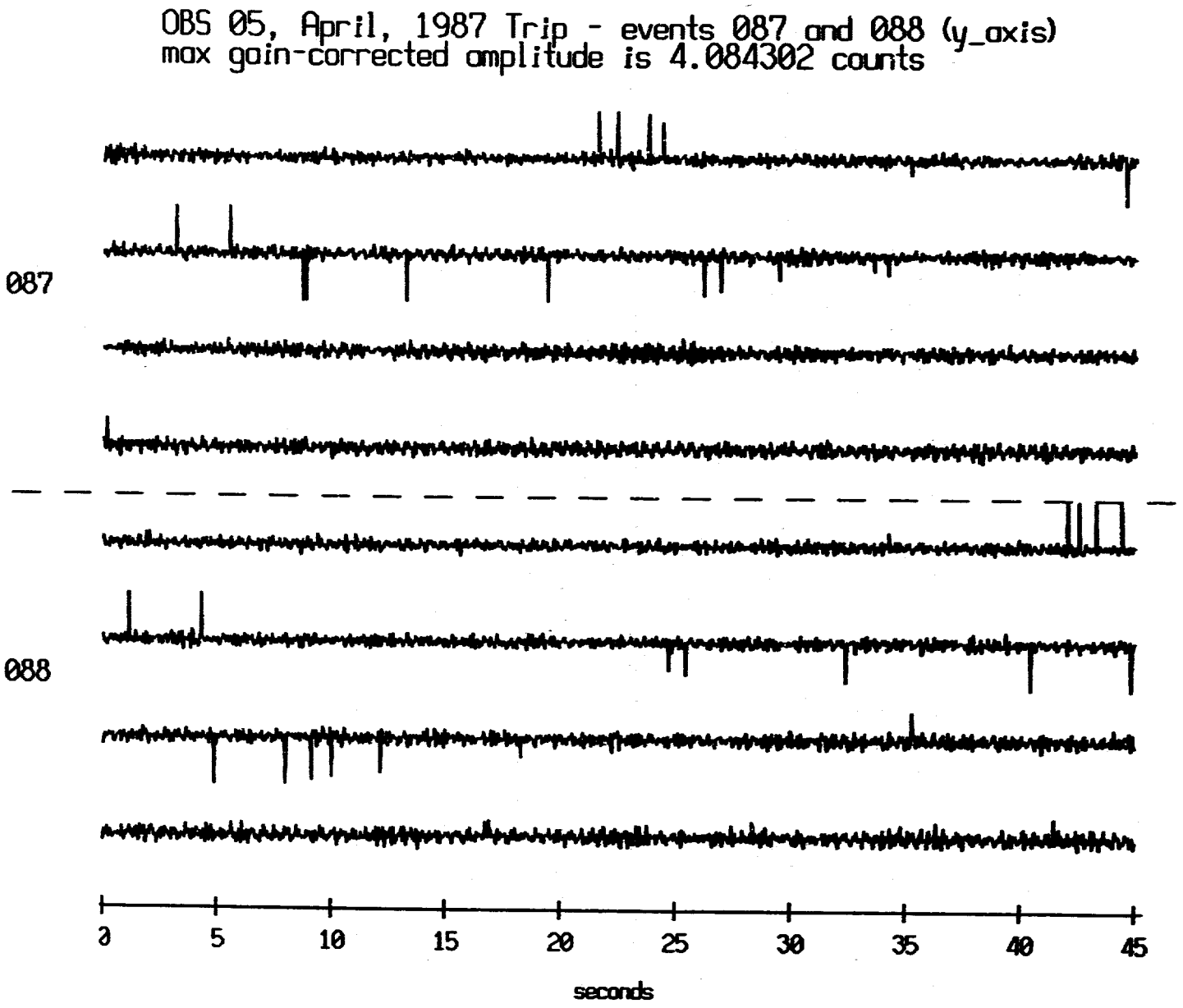
OBS 05, April, 1987 Trip - events 087 and 088 (y_axis)
max gain-corrected amplitude is 4.084302 counts
087
088
Normalized channel level
0
5
10
15
20
25
30
35
40
45
seconds

Figure III.j

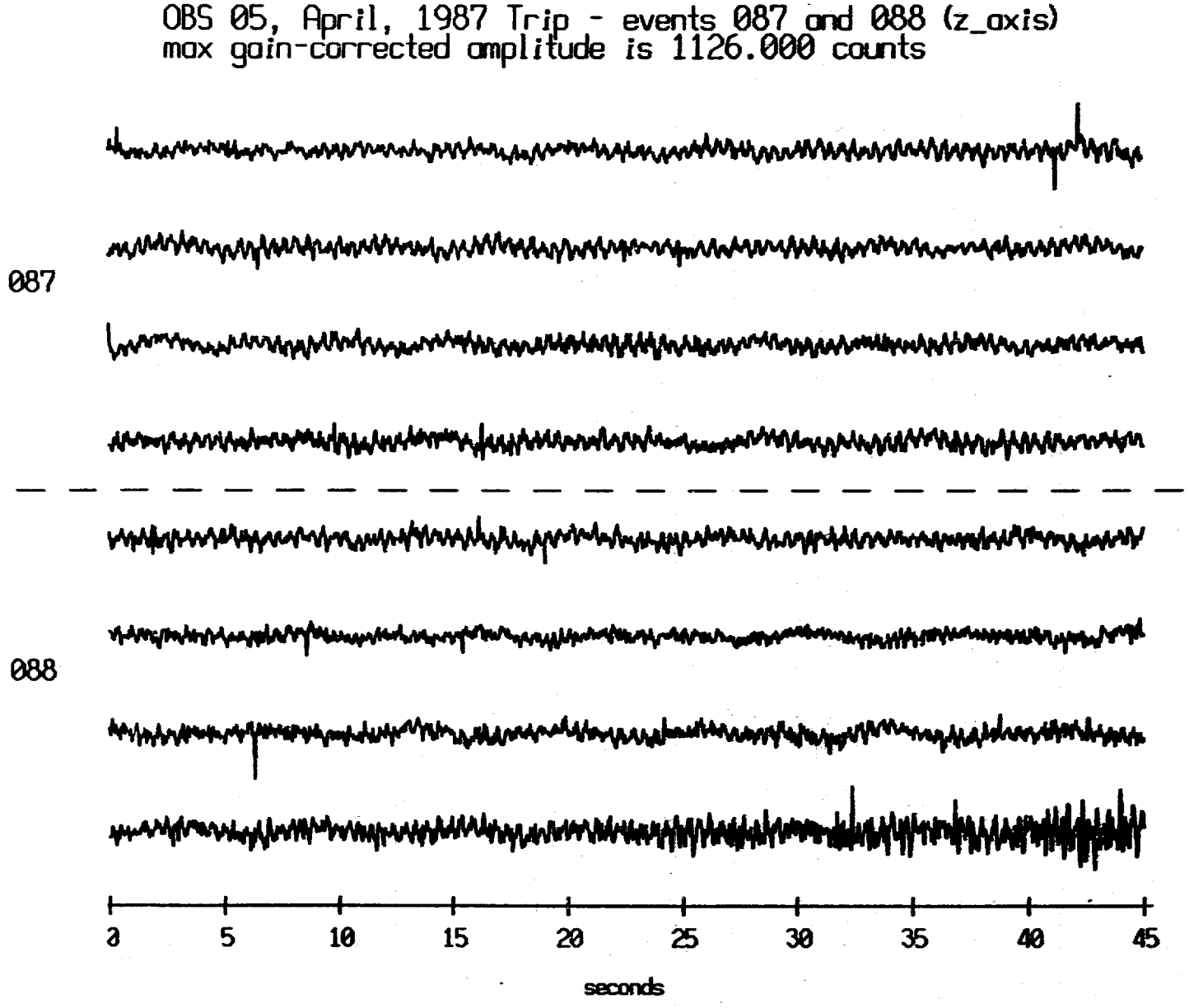

Figure II.11k

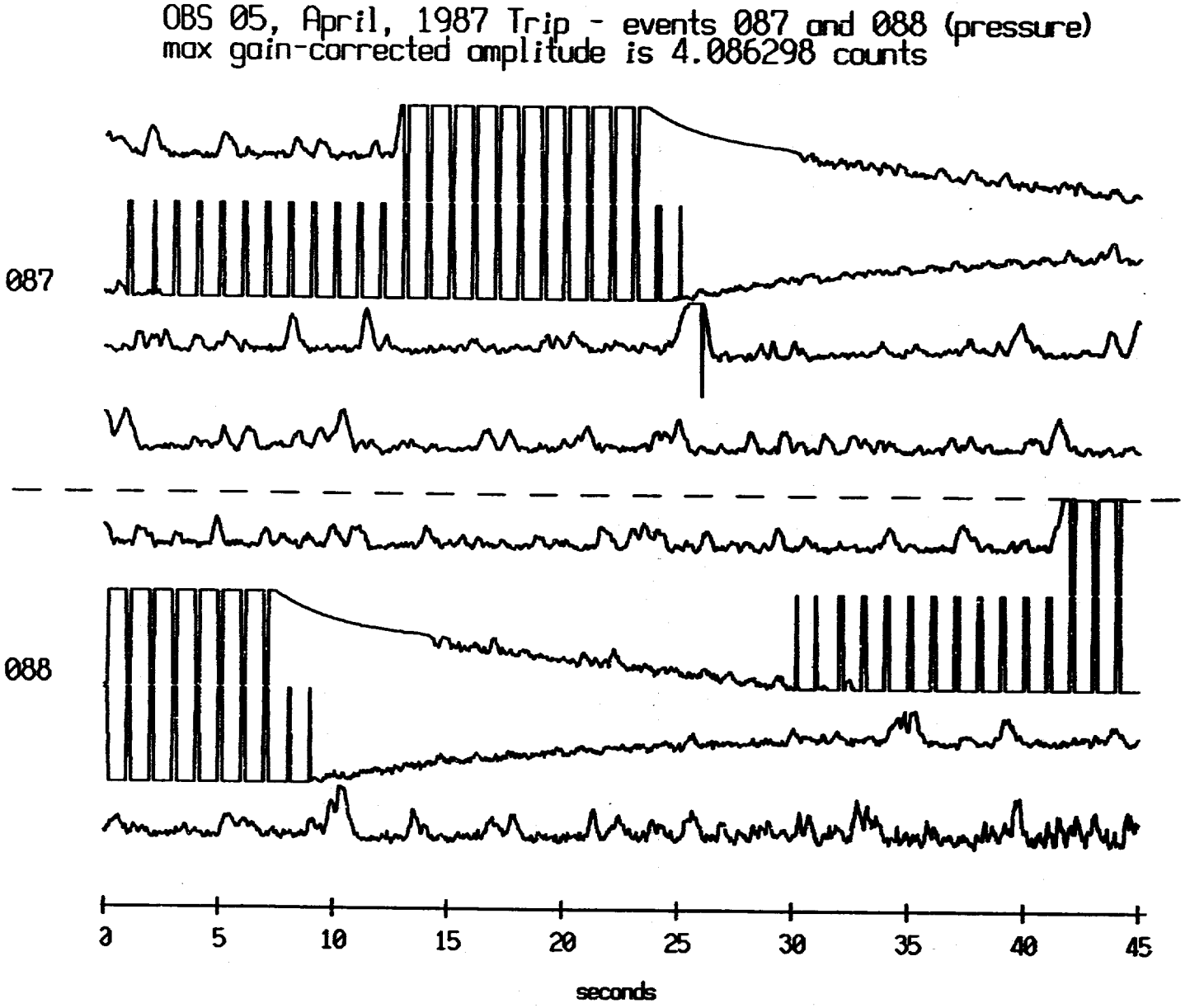
OBS 05, April, 1987 Trip - events 087 and 088 (pressure)
max gain-corrected amplitude is 4.086298 counts
087
088
Normalized channel level
0
5
10
15
20
25
30
35
40
45
seconds

Figure II.11

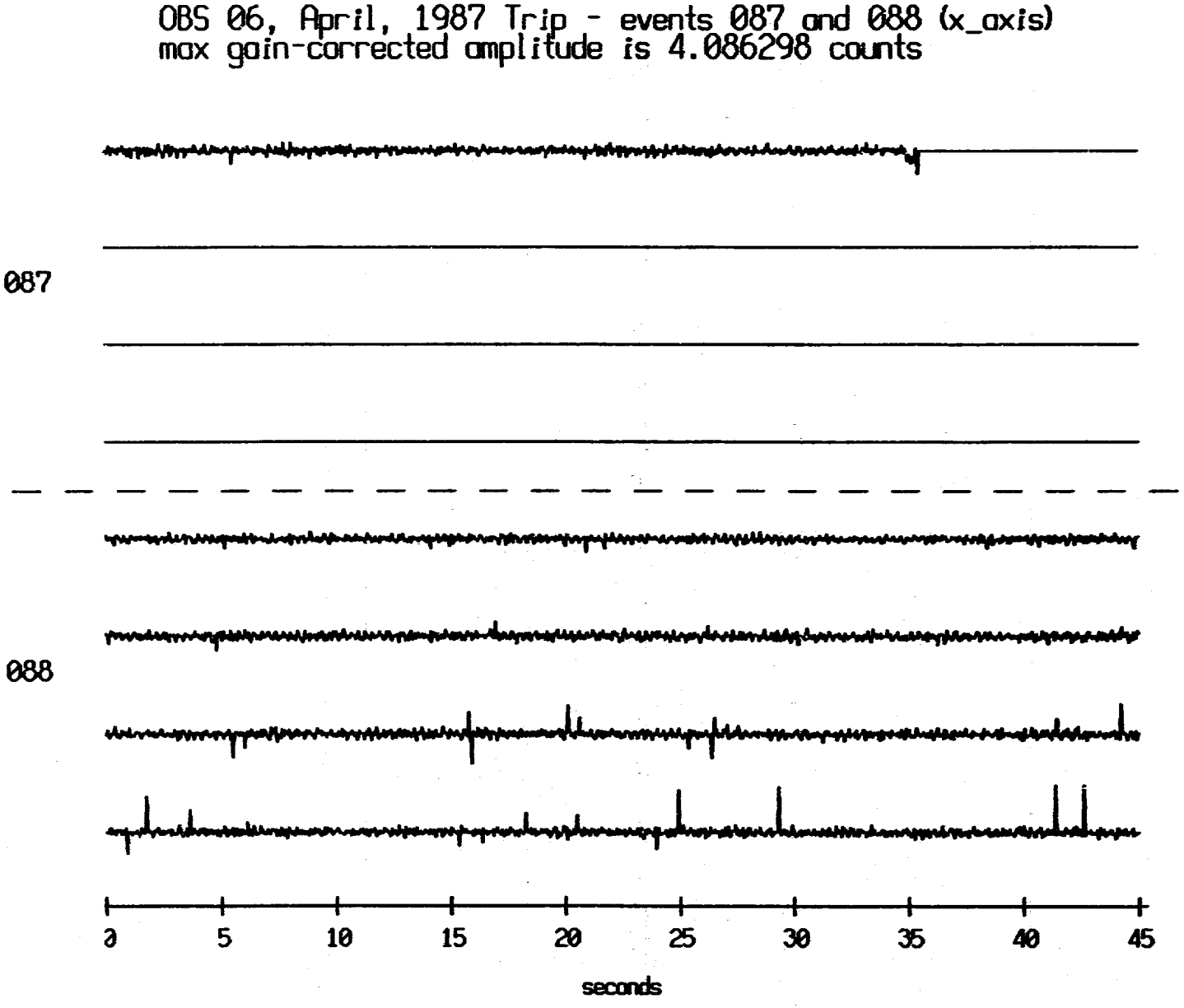

Figure II.12i

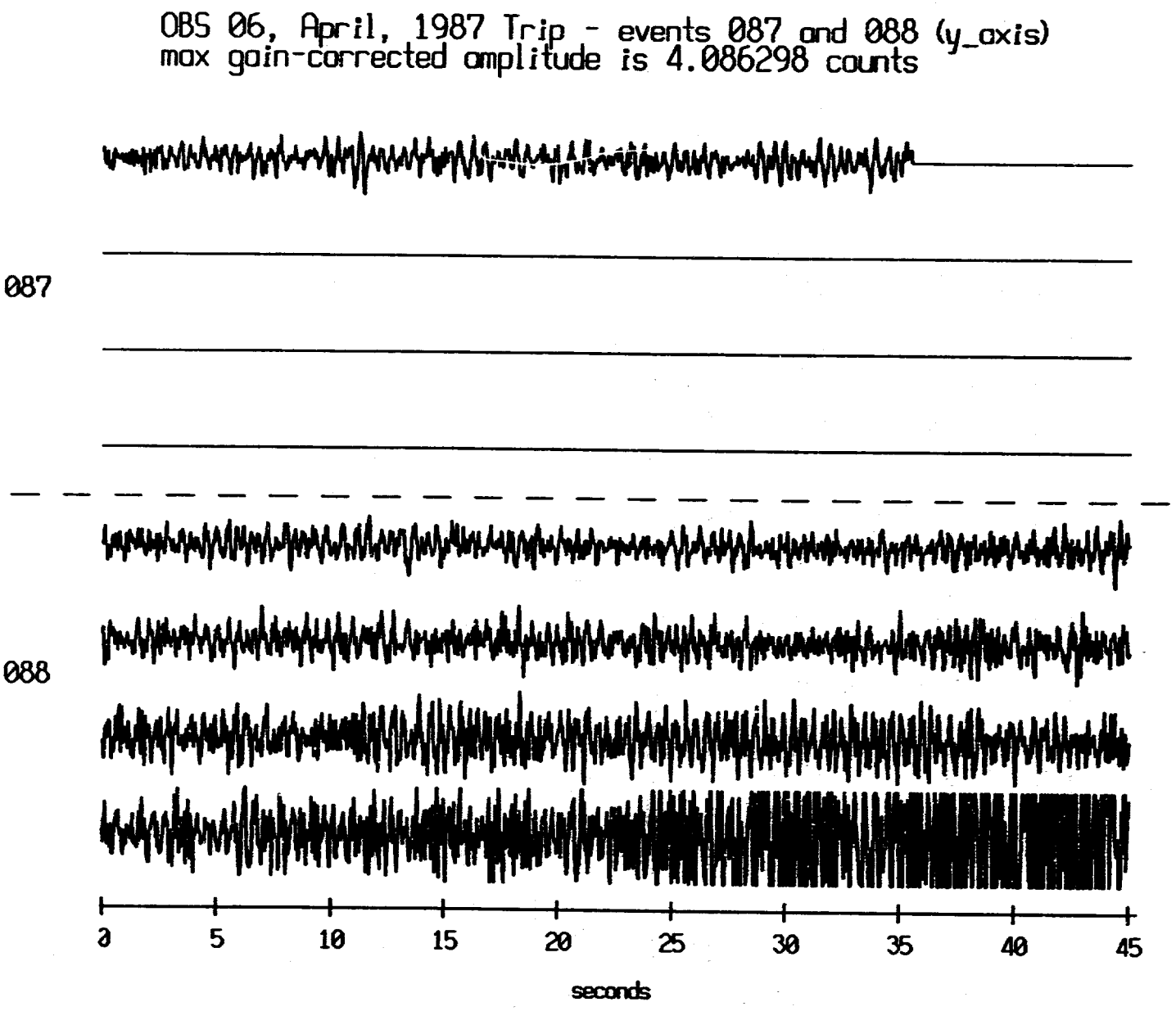

Figure III.2j

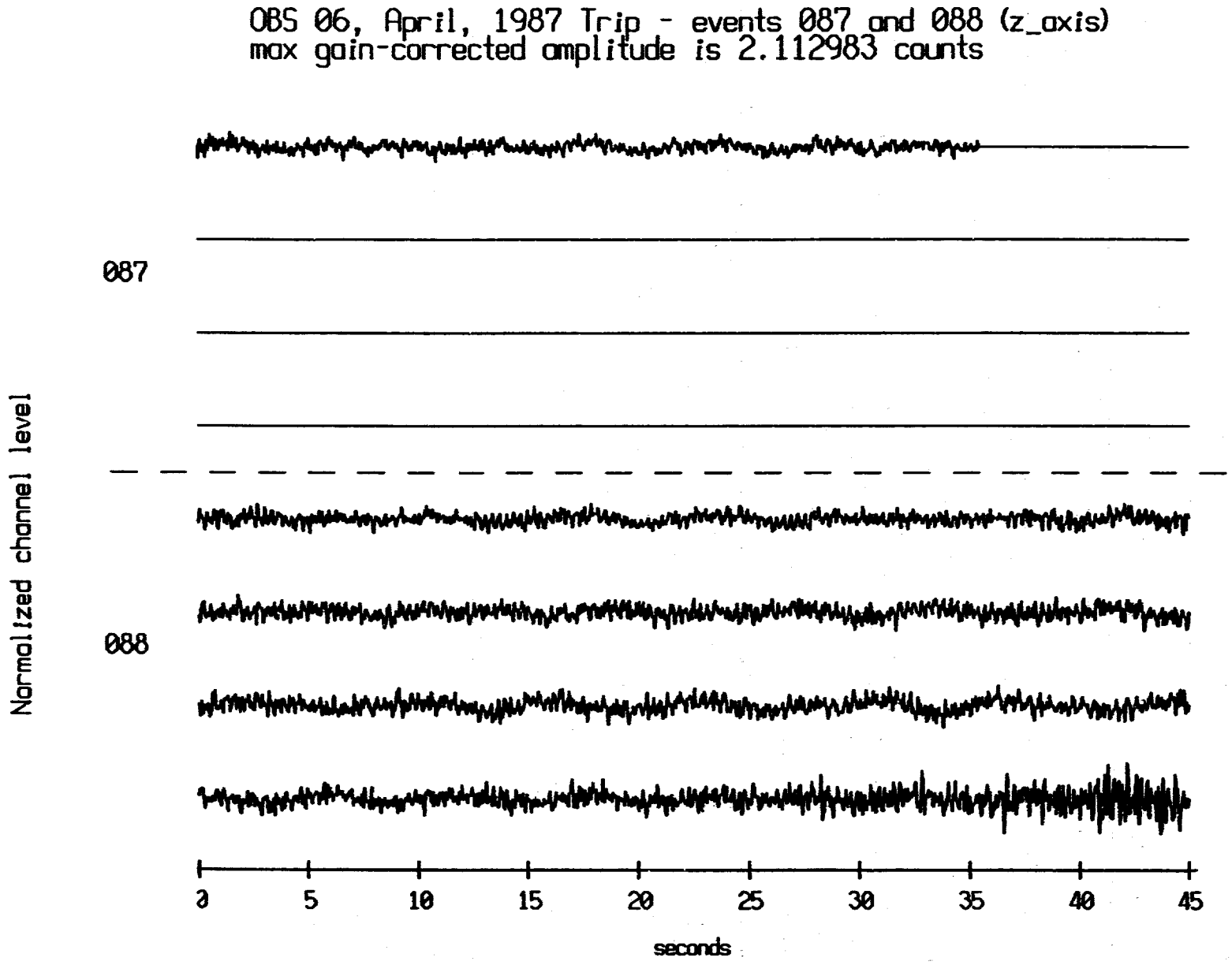

Figure II.12k

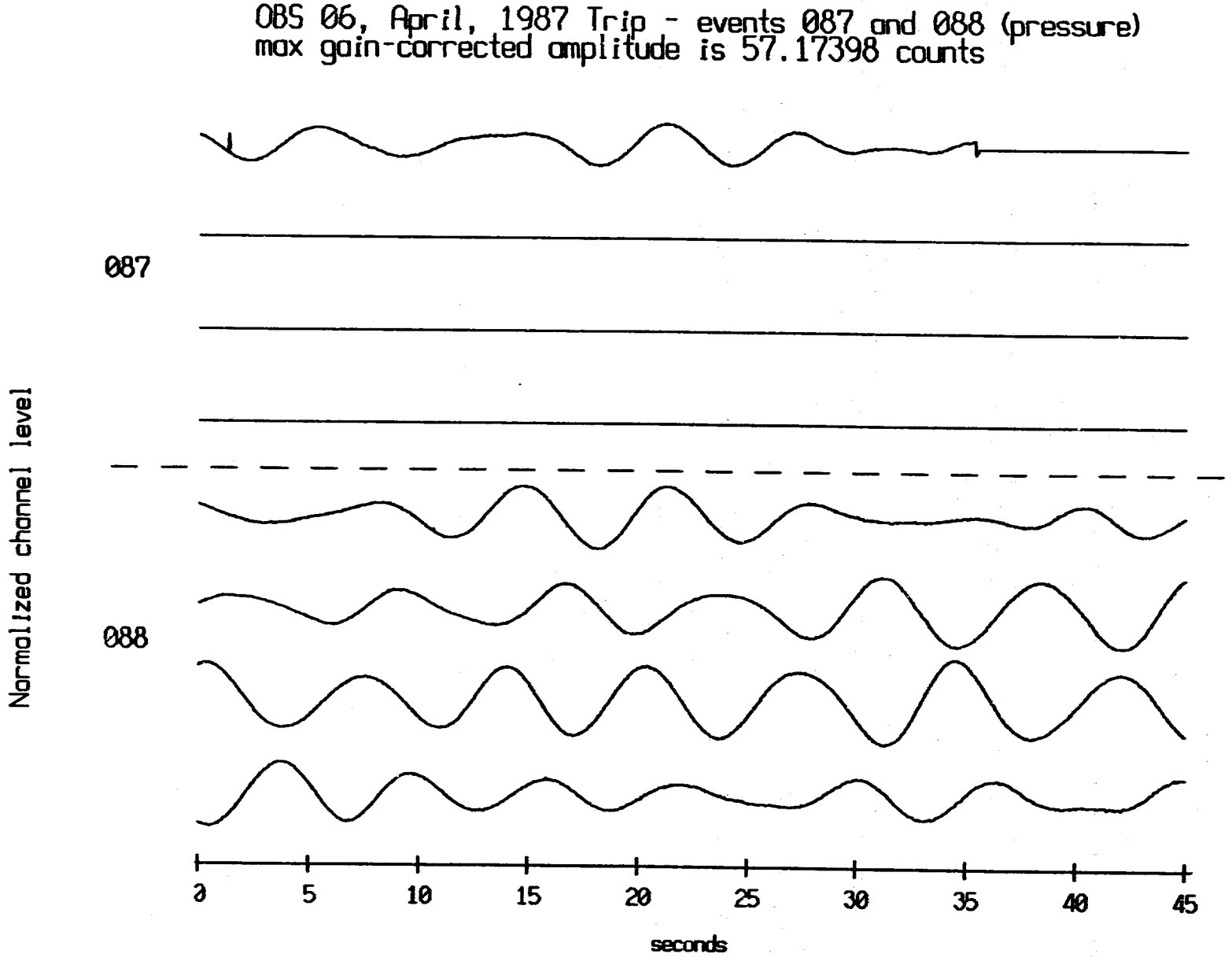

Figure II.12l

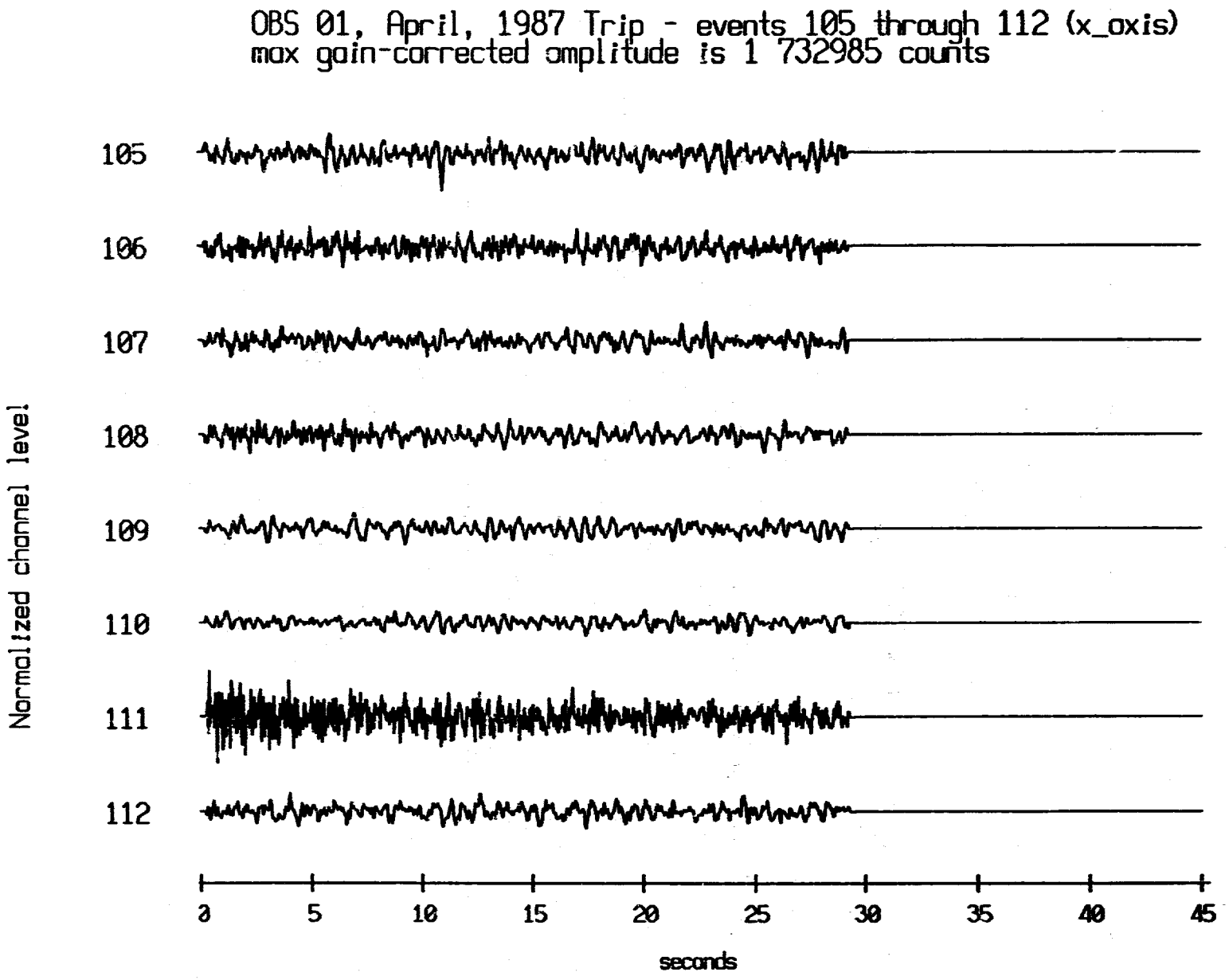

Figure II.13i

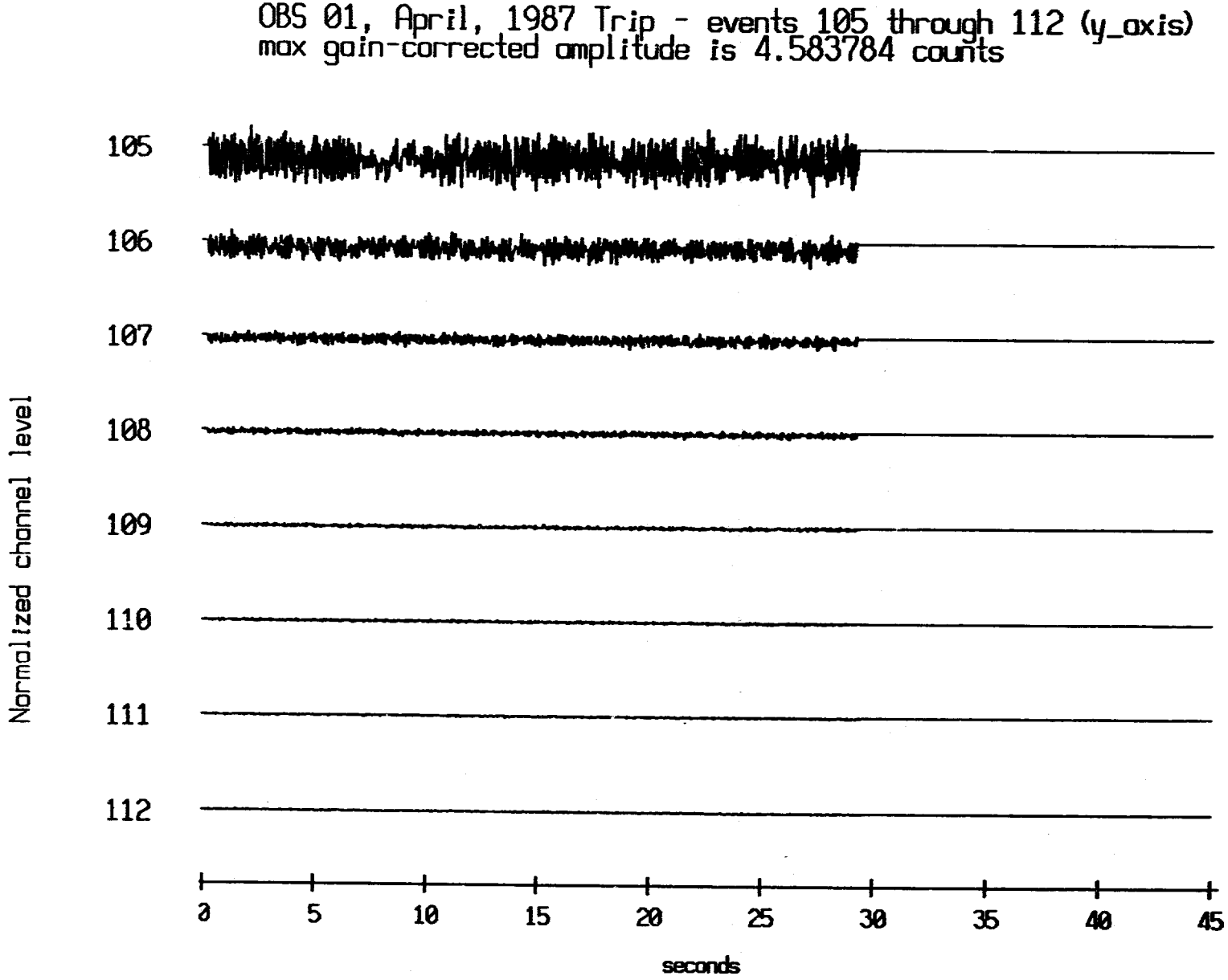

Figure II.13j

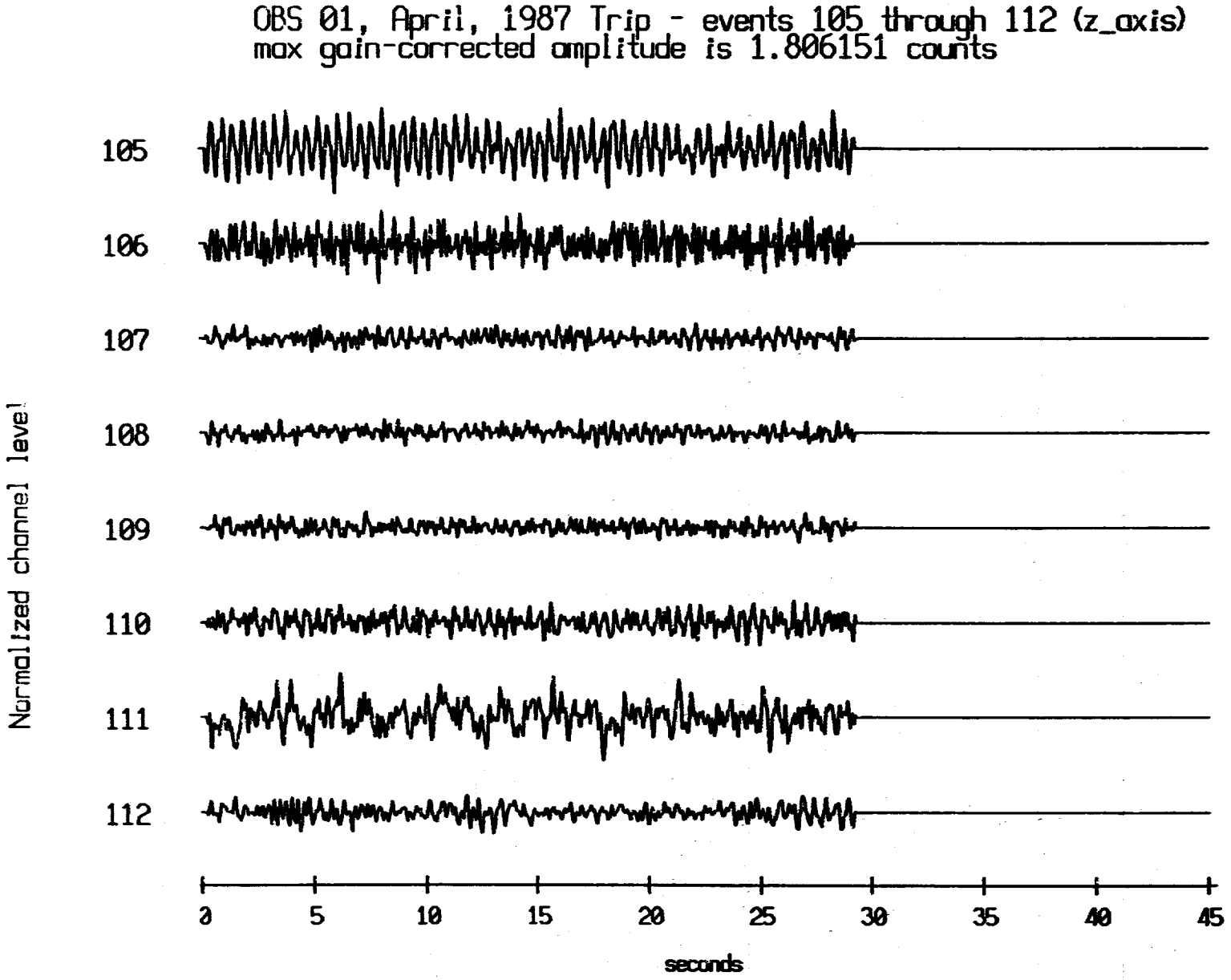

Figure II.13k

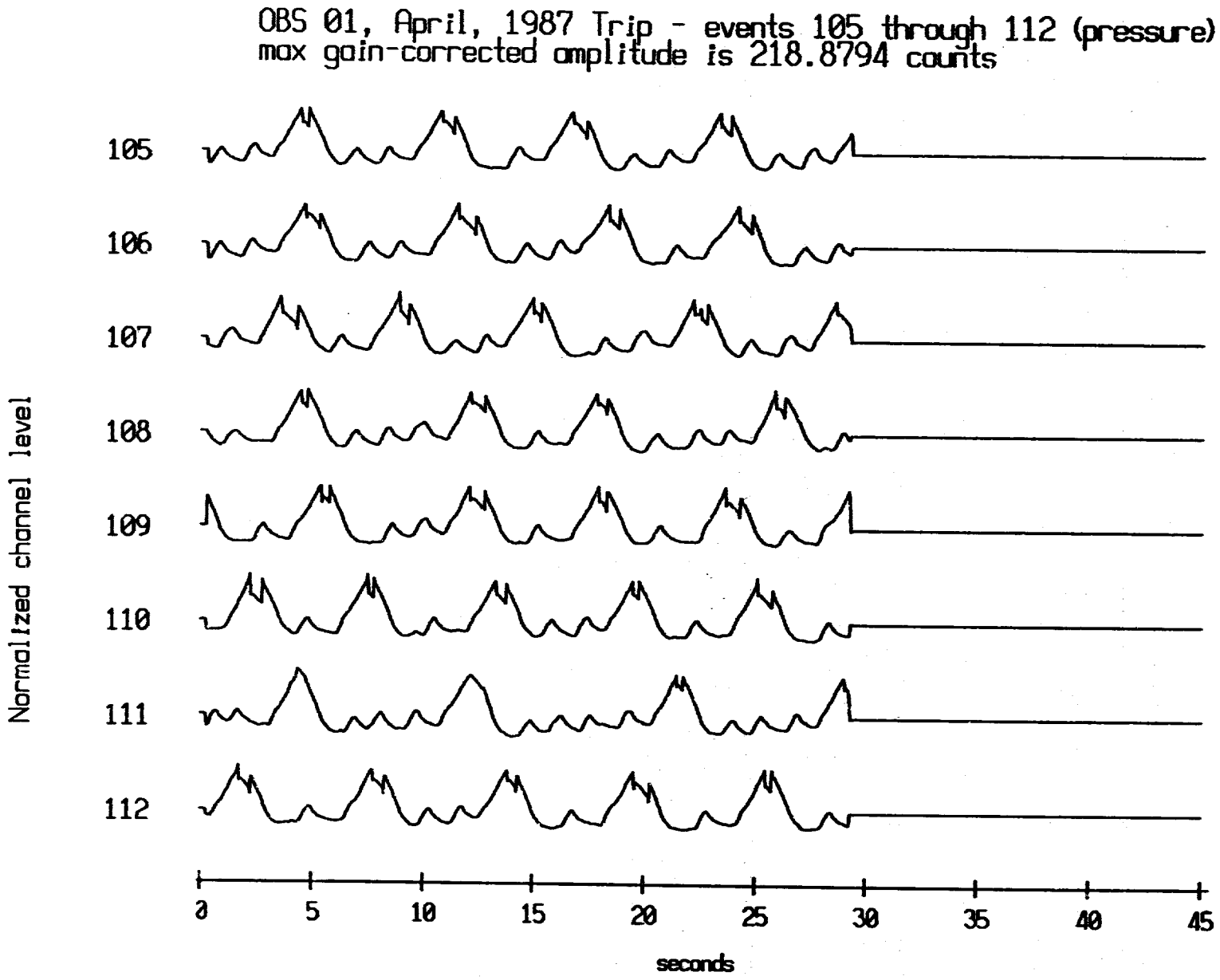

Figure II.13l

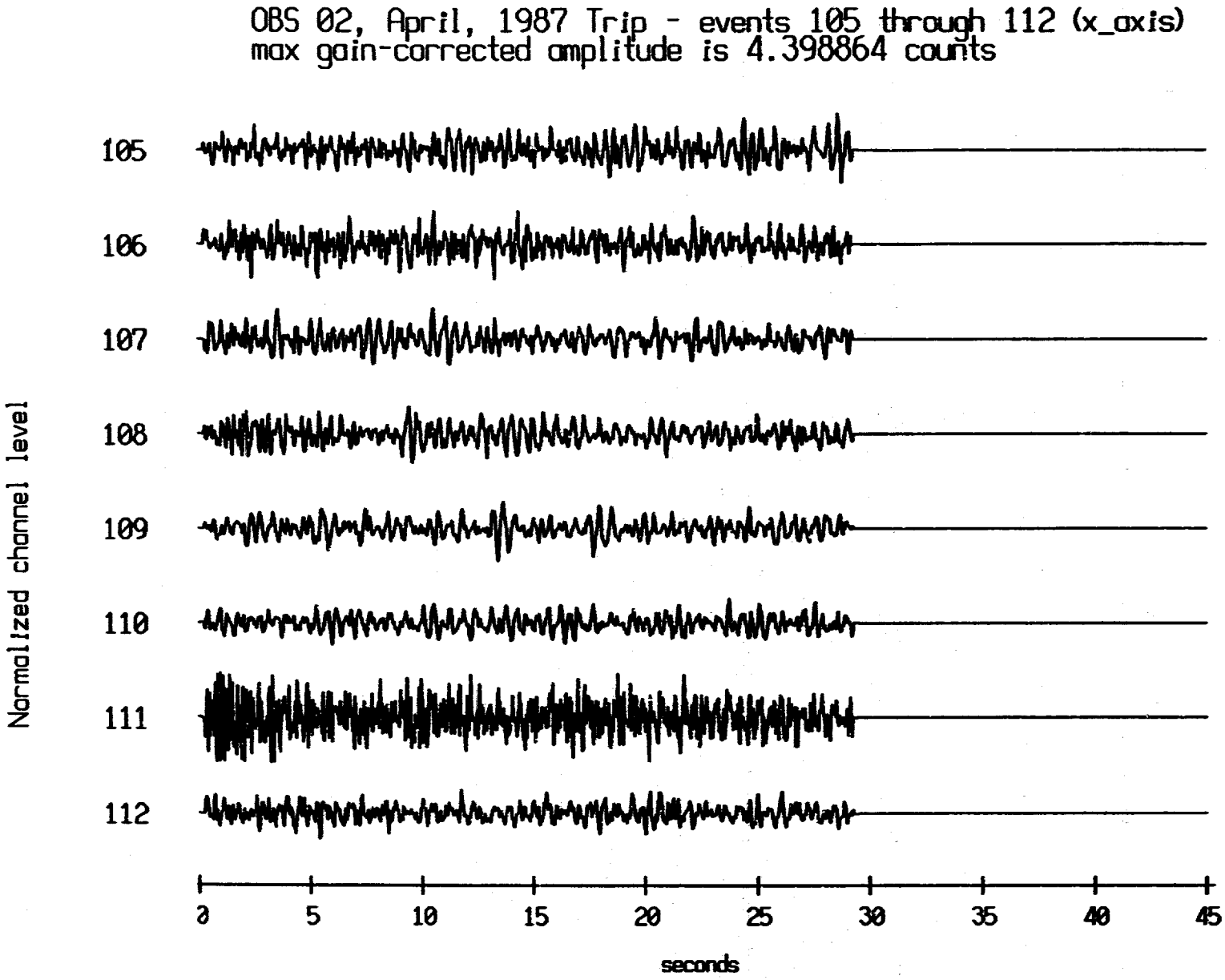

Figure II.14i

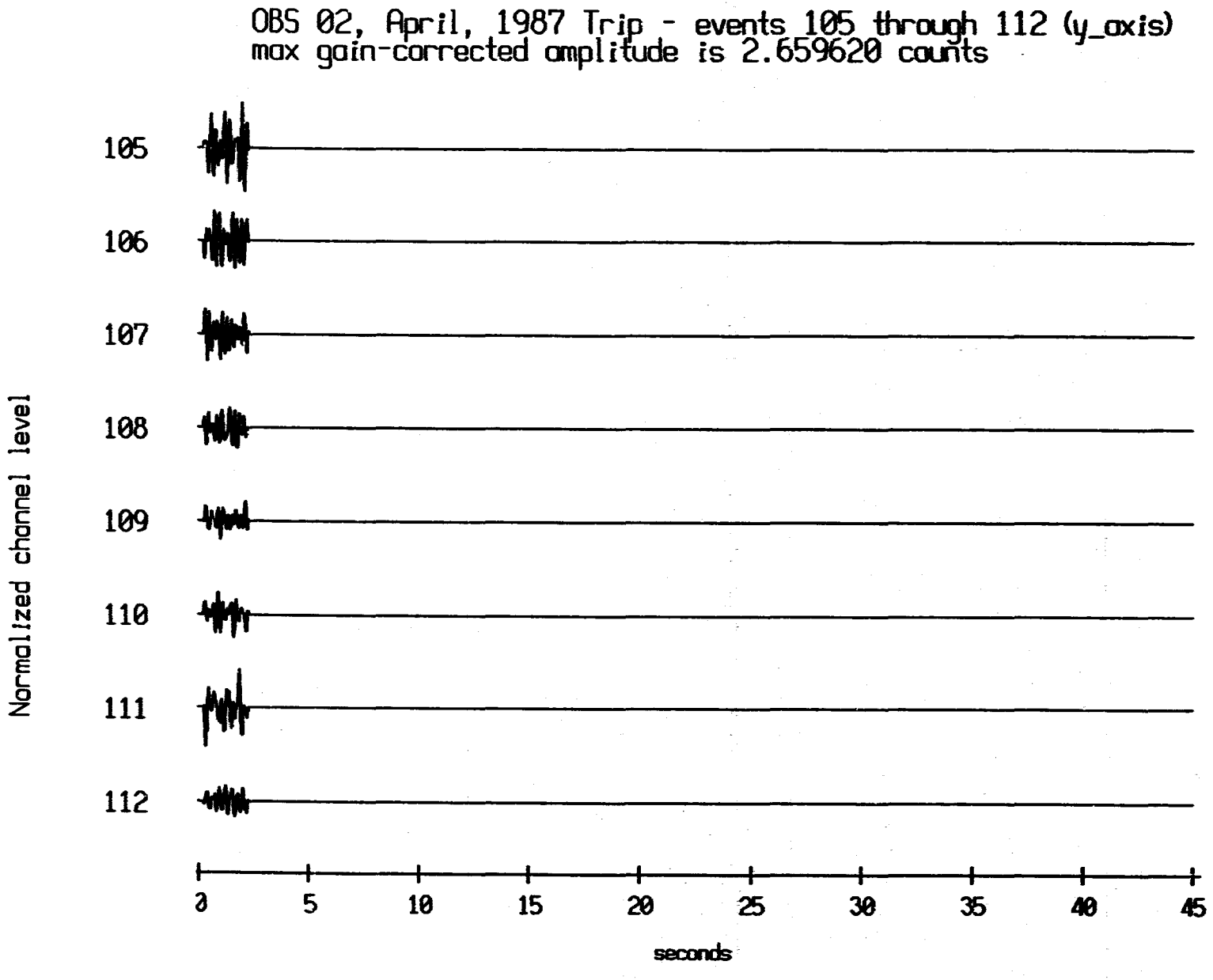

Figure II.14j

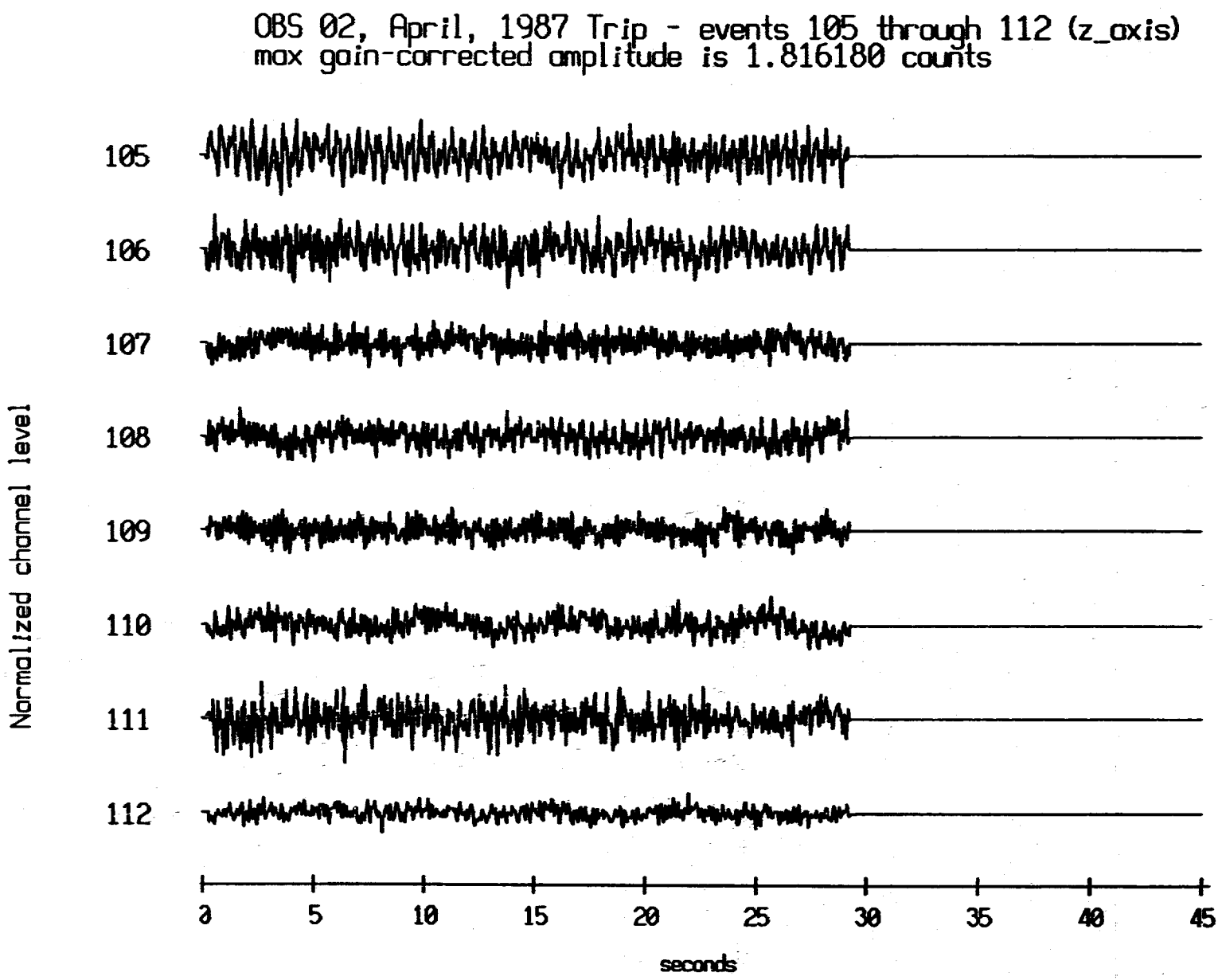

Figure II.14k

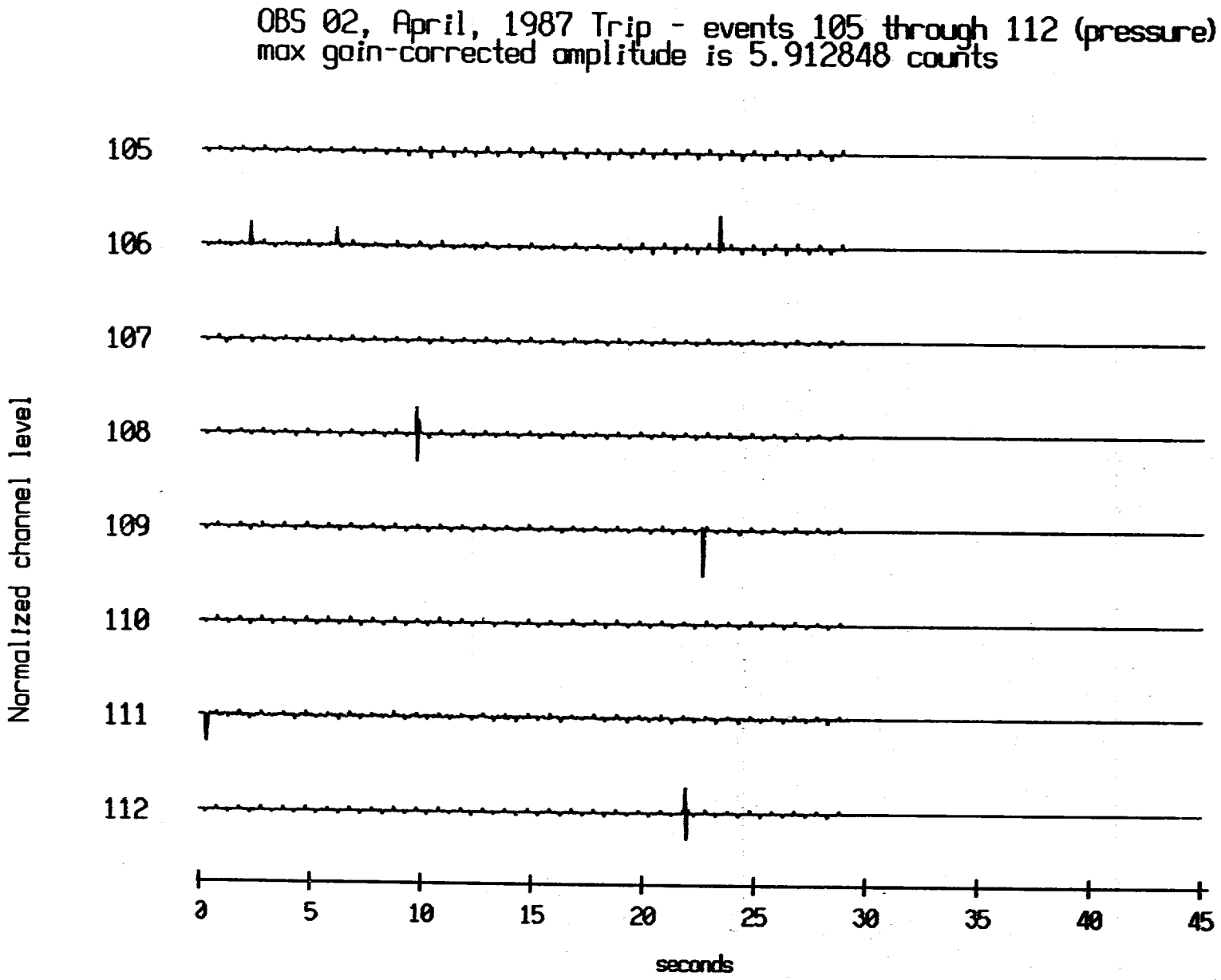
OBS 02, April, 1987 Trip - events 105 through 112 (pressure)
max gain-corrected amplitude is 5.912848 counts
105
106
107
108
109
110
111
112
Normalized channel level
0
5
10
15
20
25
30
35
40
45
seconds

Figure II.14

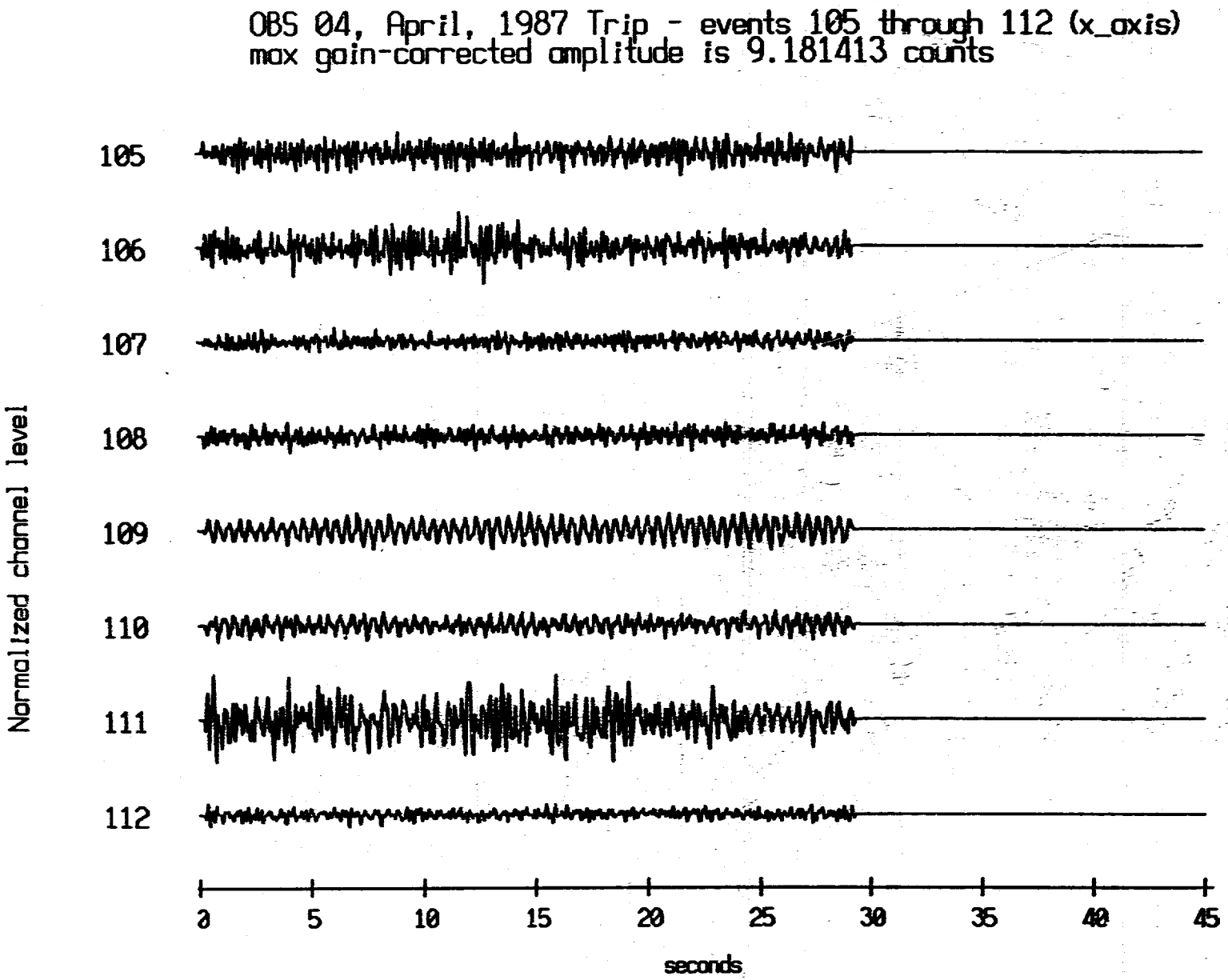

Figure II.15i

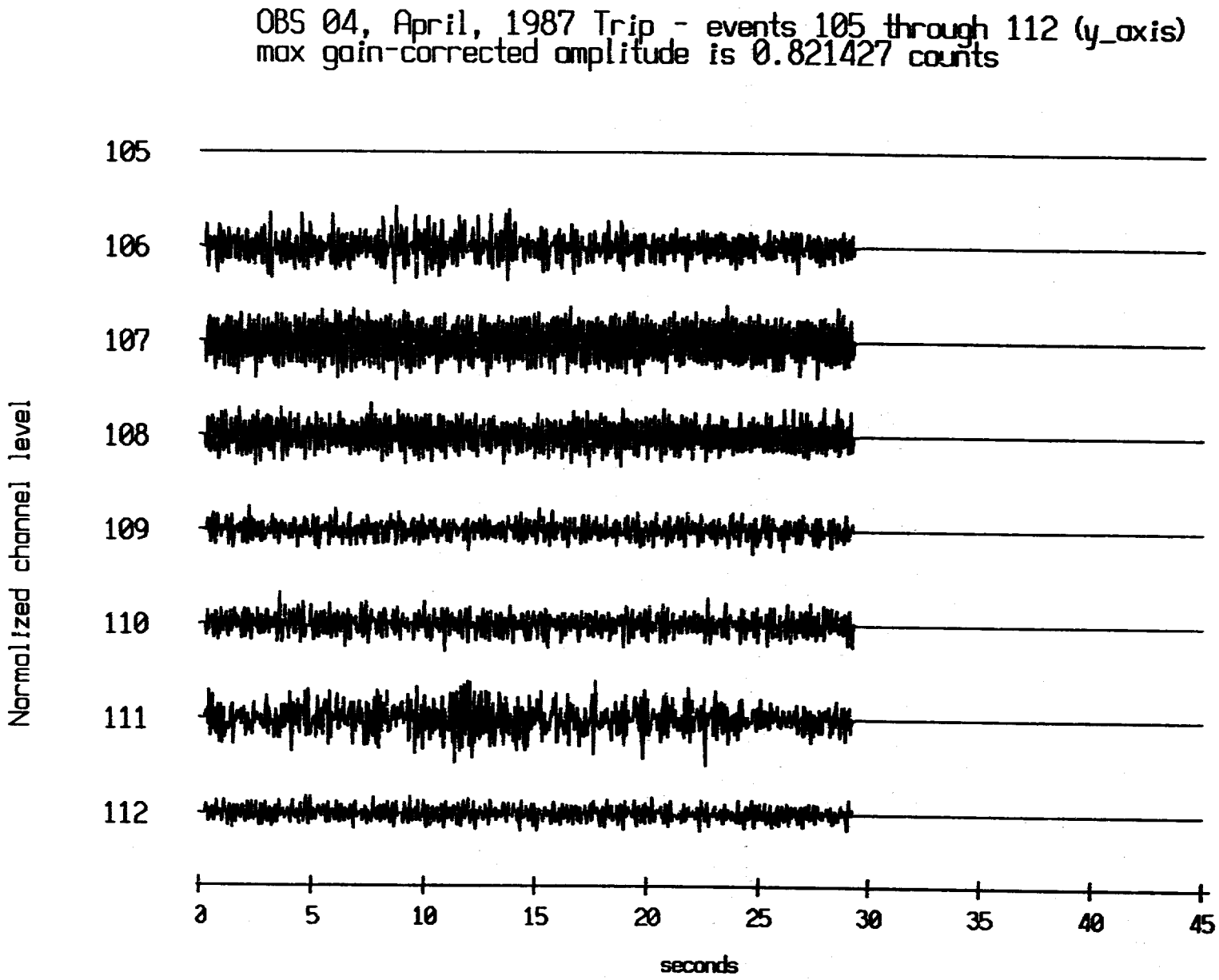

Figure II.15j

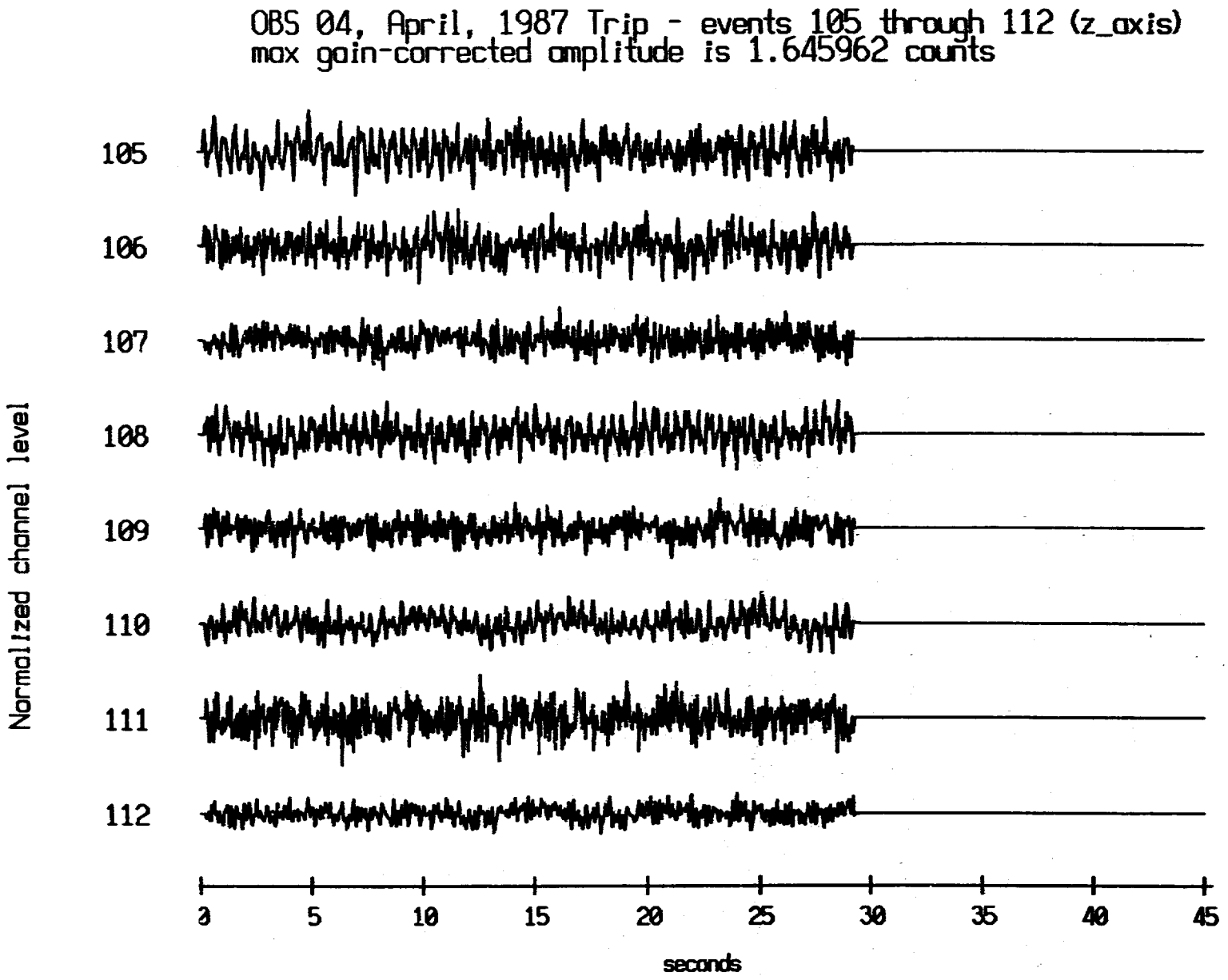

Figure II.15k

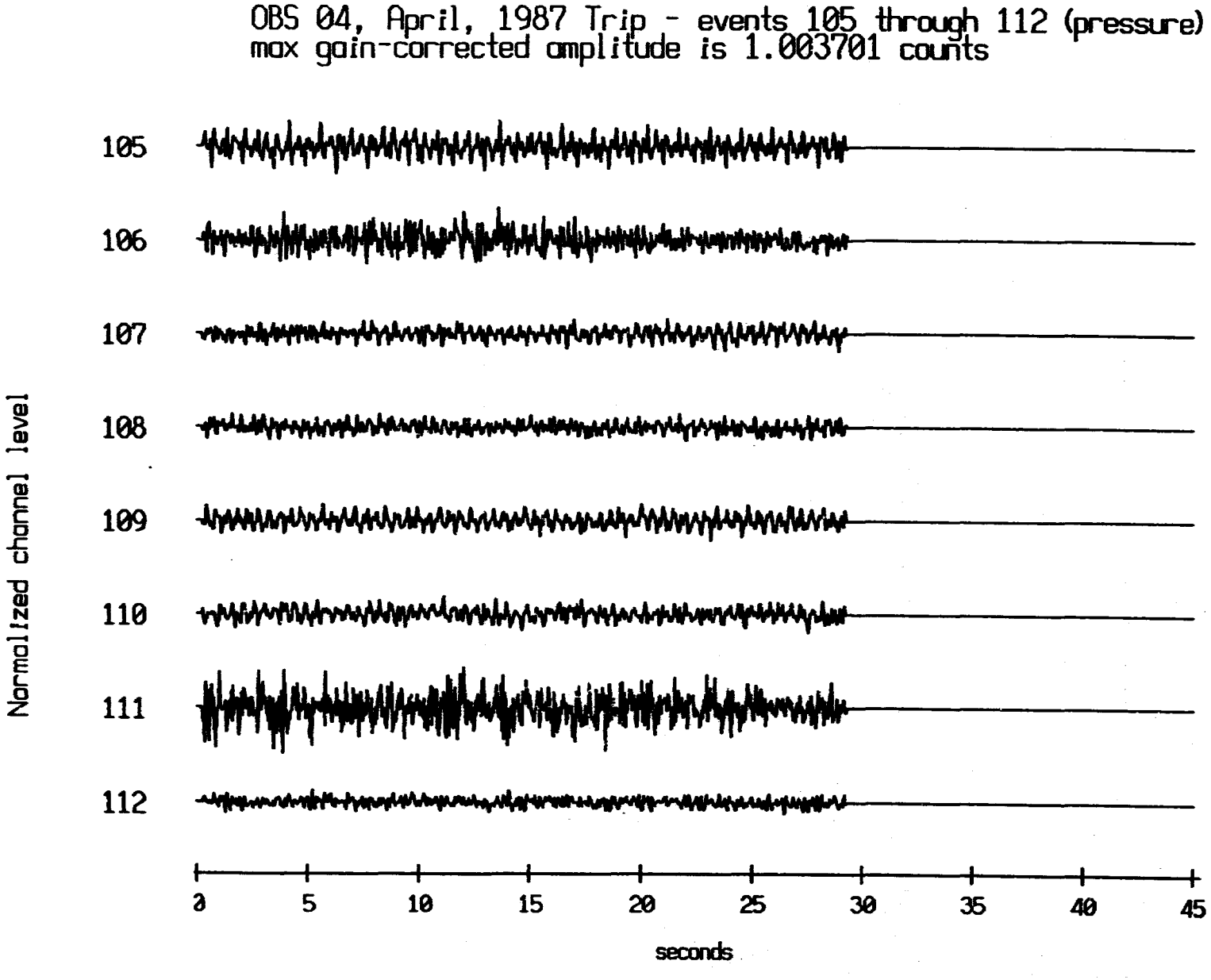

Figure II.15l

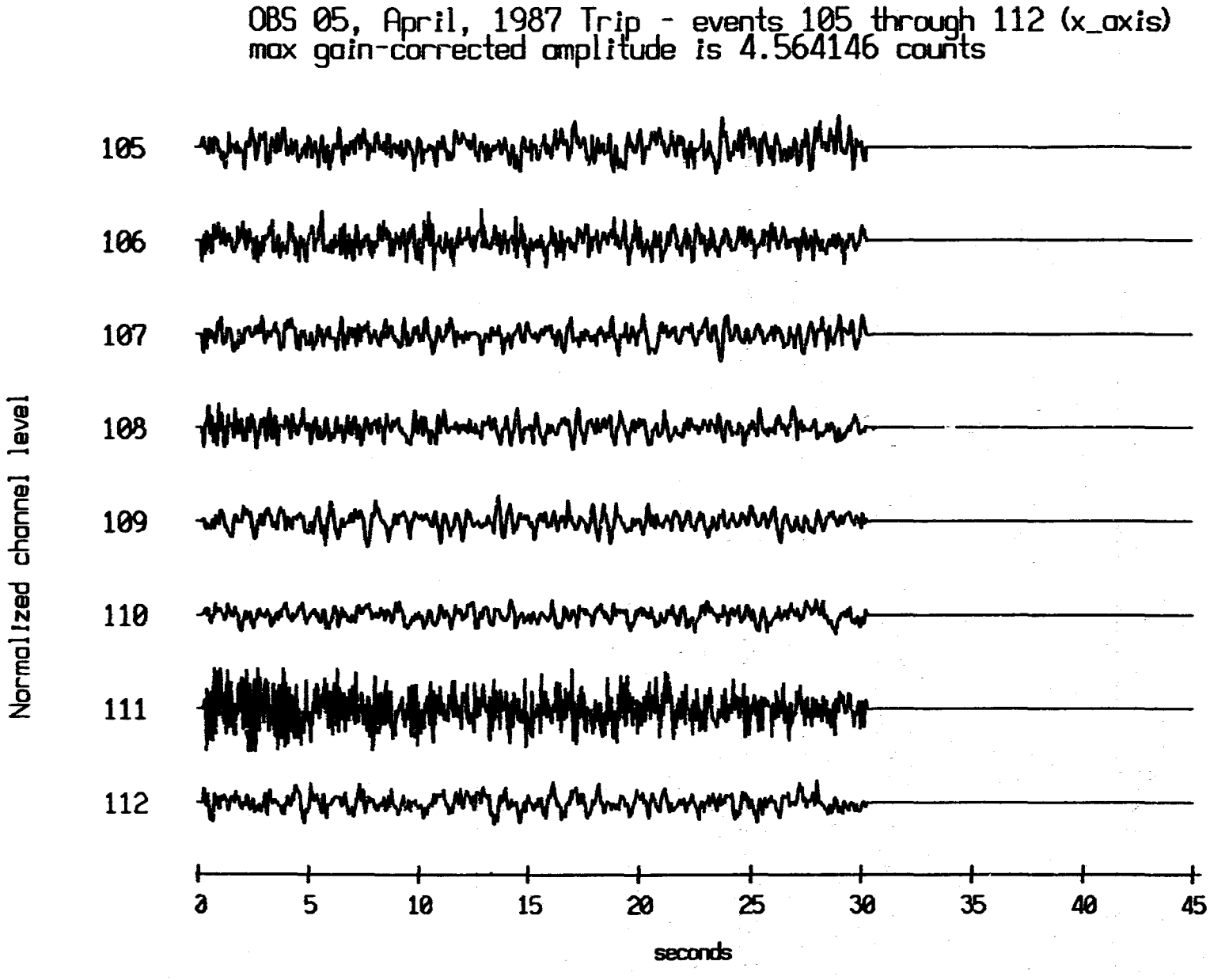

Figure II.16i

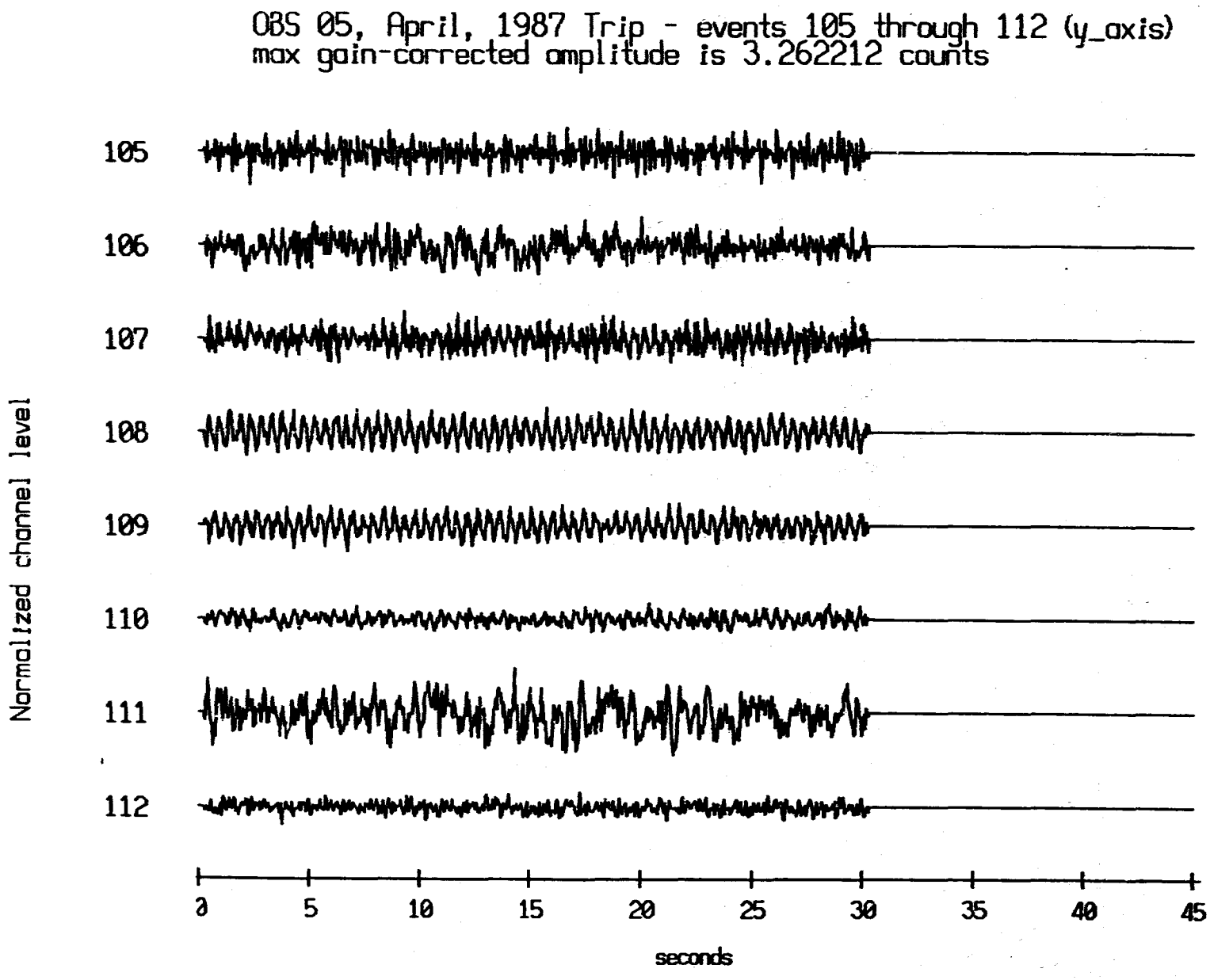

Figure II.16j

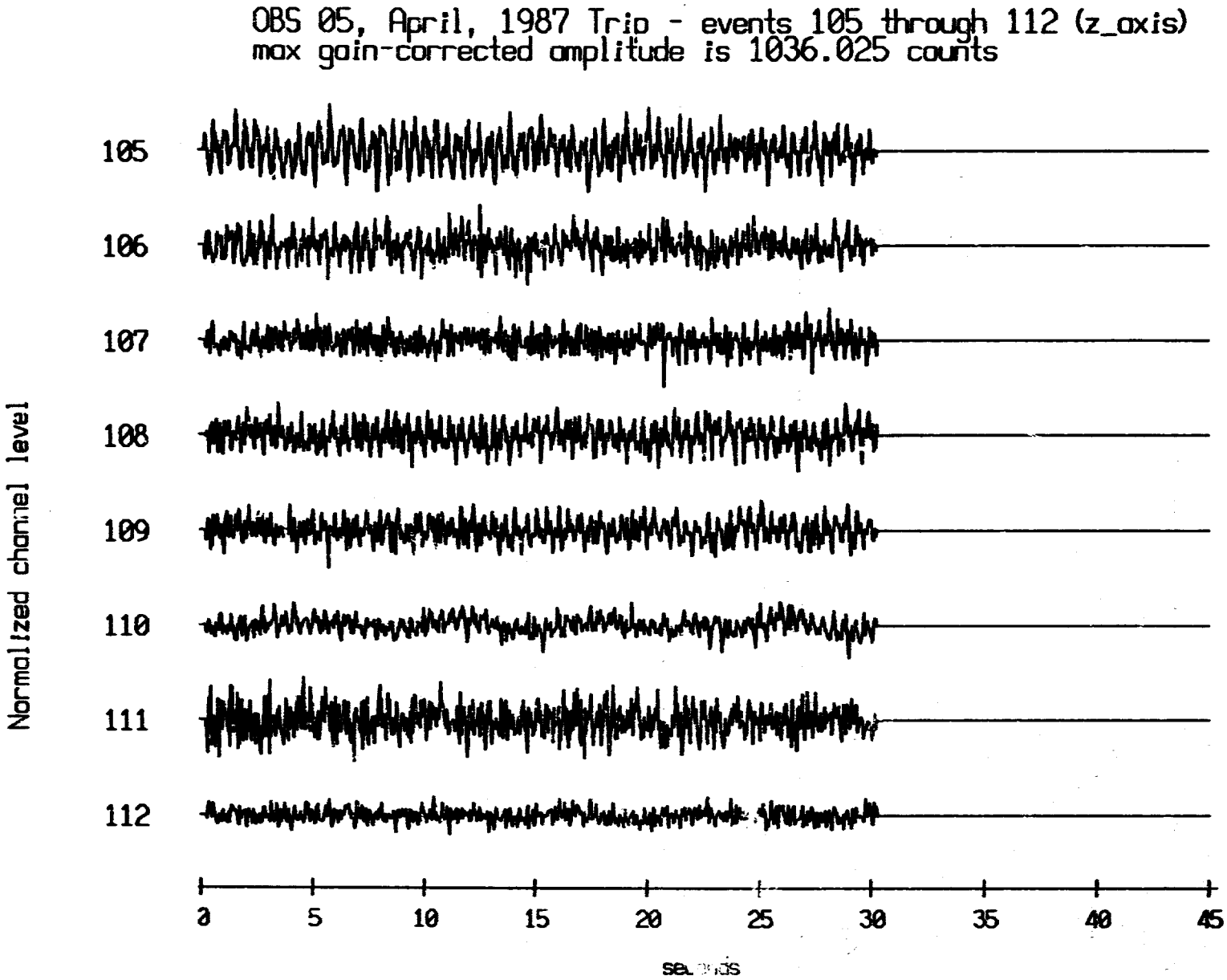

Figure II.10k

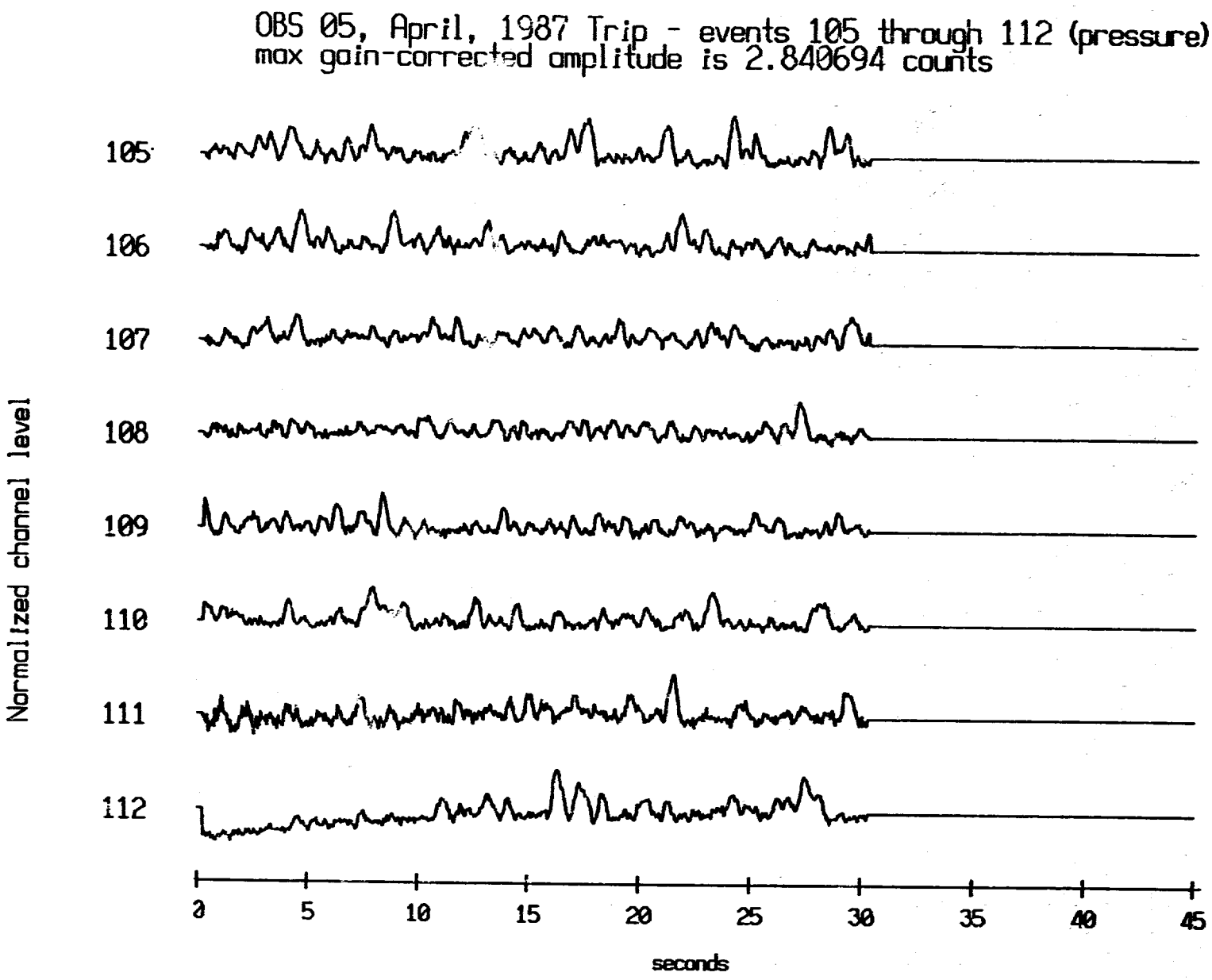
OBS 05, April, 1987 Trip - events 105 through 112 (pressure)
max gain-corrected amplitude is 2.840694 counts
105
106
107
108
109
110
111
112
Normalized channel level
0
5
10
15
20
25
30
35
40
45
seconds

Figure II.61

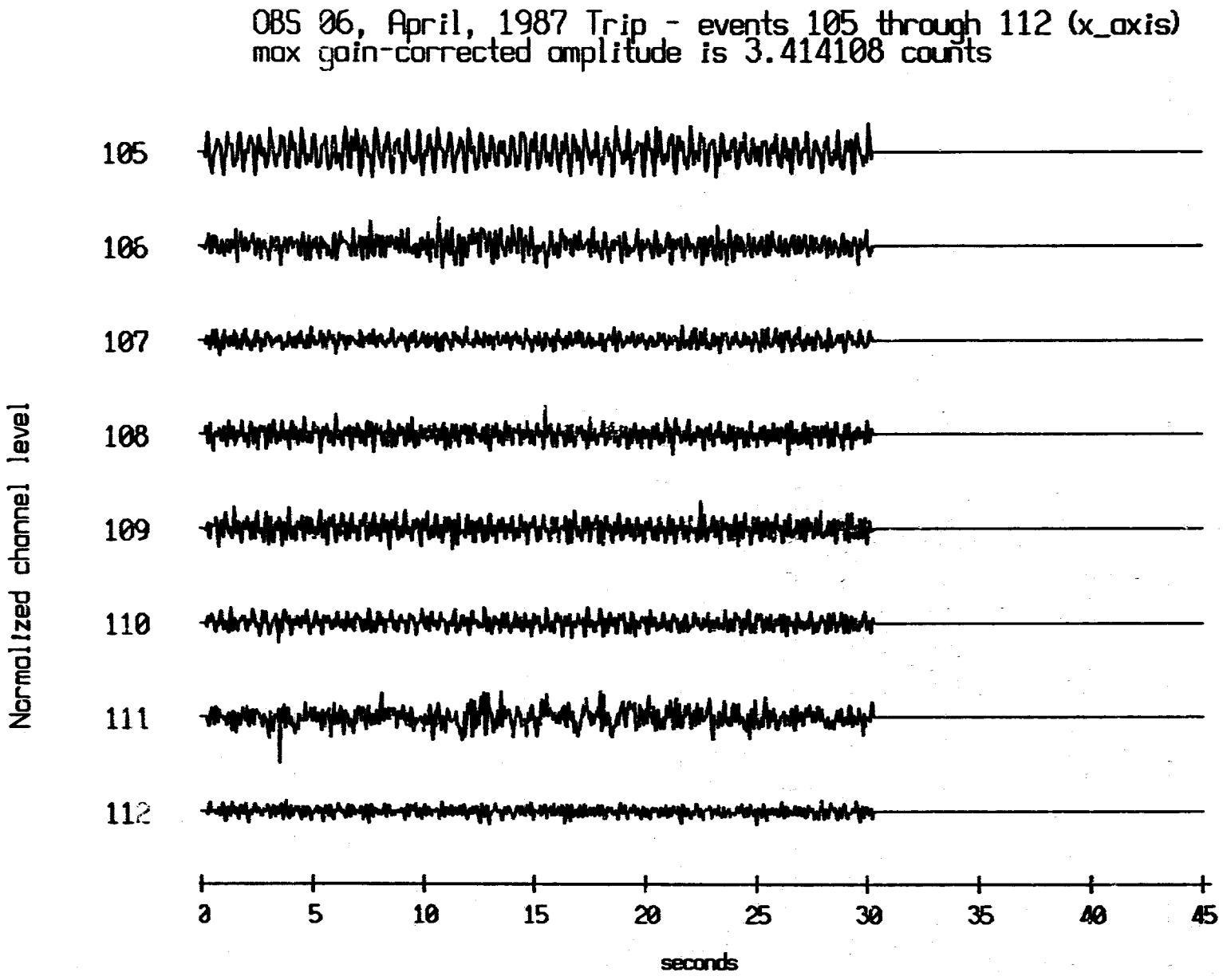
OBS 06, April, 1987 Trip - events 105 through 112 (x_axis)
max gain-corrected amplitude is 3.414108 counts
105
106
107
108
109
110
111
112
Normalized channel level
0
5
10
15
20
25
30
35
40
45
seconds

Figure II.7i

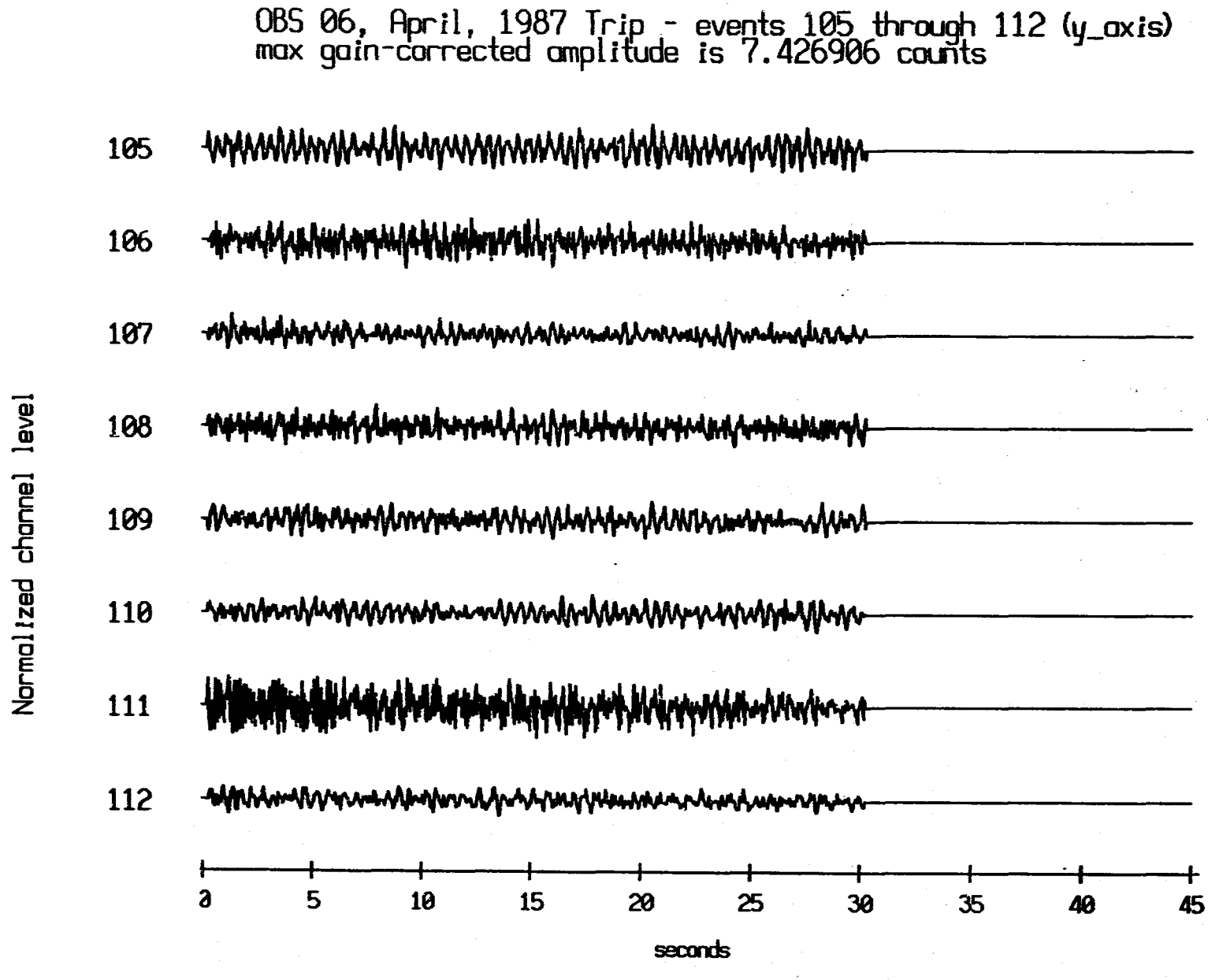

Figure II.17j

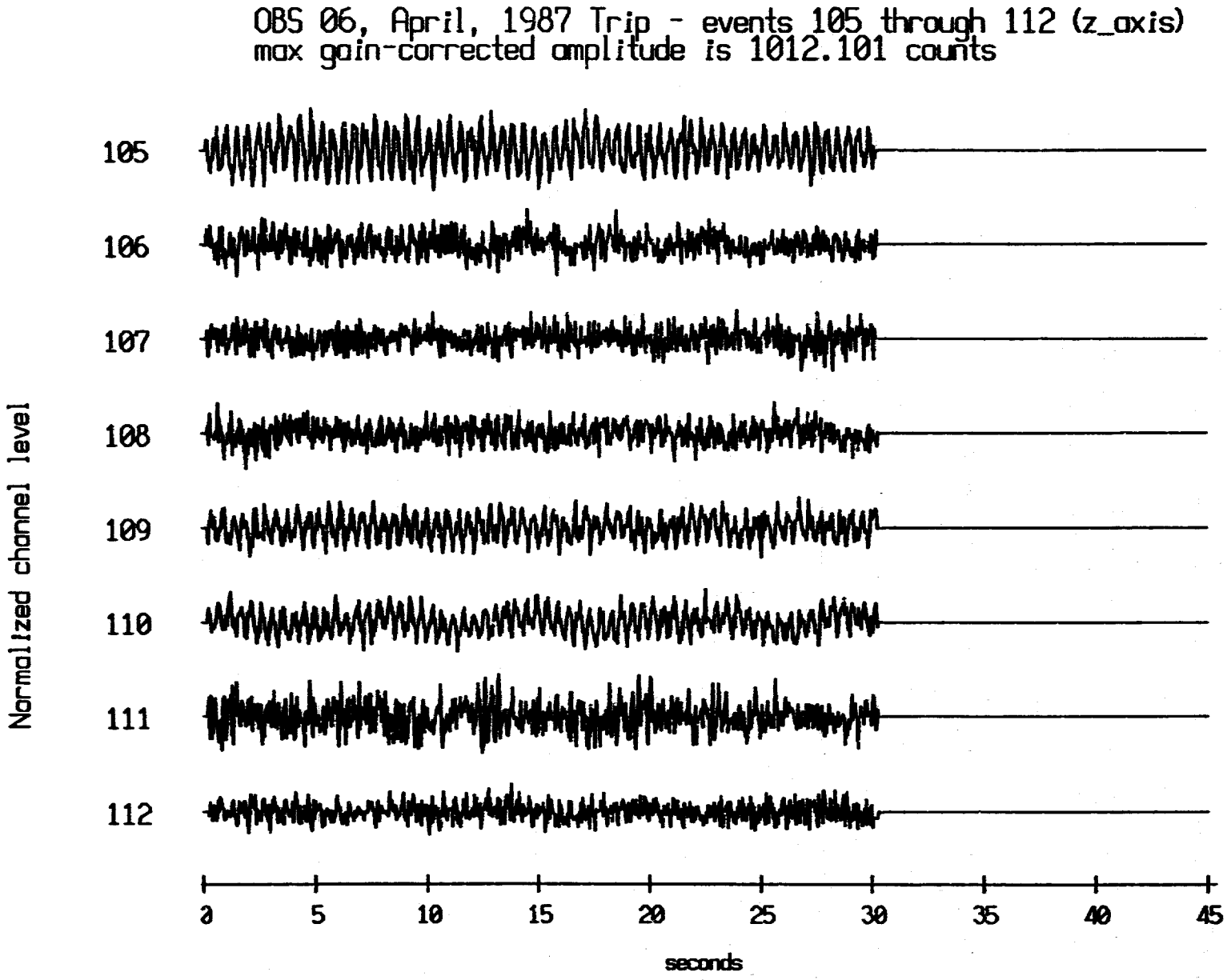

Figure II.17k

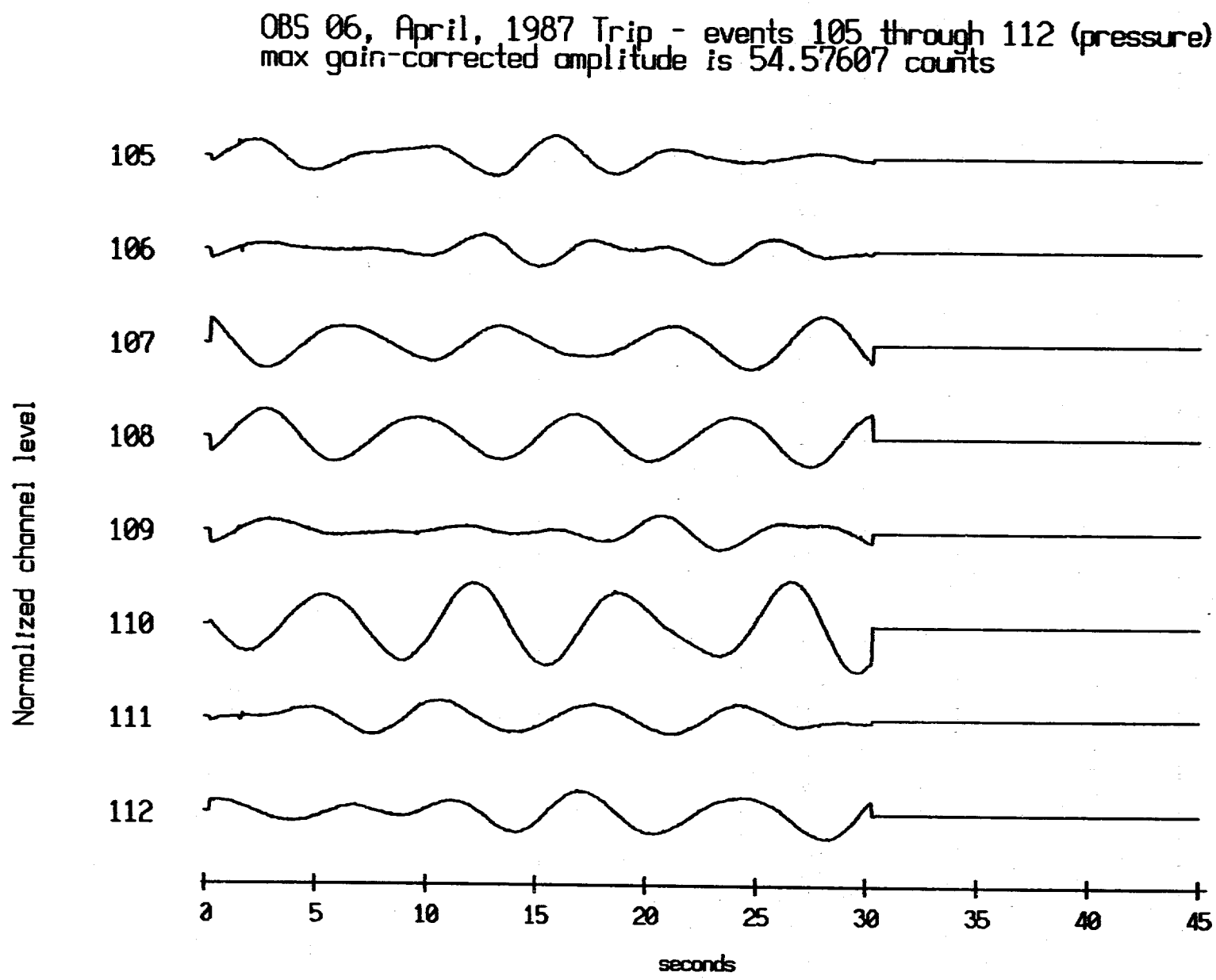
OBS 06, April, 1987 Trip - events 105 through 112 (pressure)
max gain-corrected amplitude is 54.57607 counts
105
106
107
108
109
110
111
112
Normalized channel level
0
5
10
15
20
25
30
35
40
45
seconds

Figure II.17

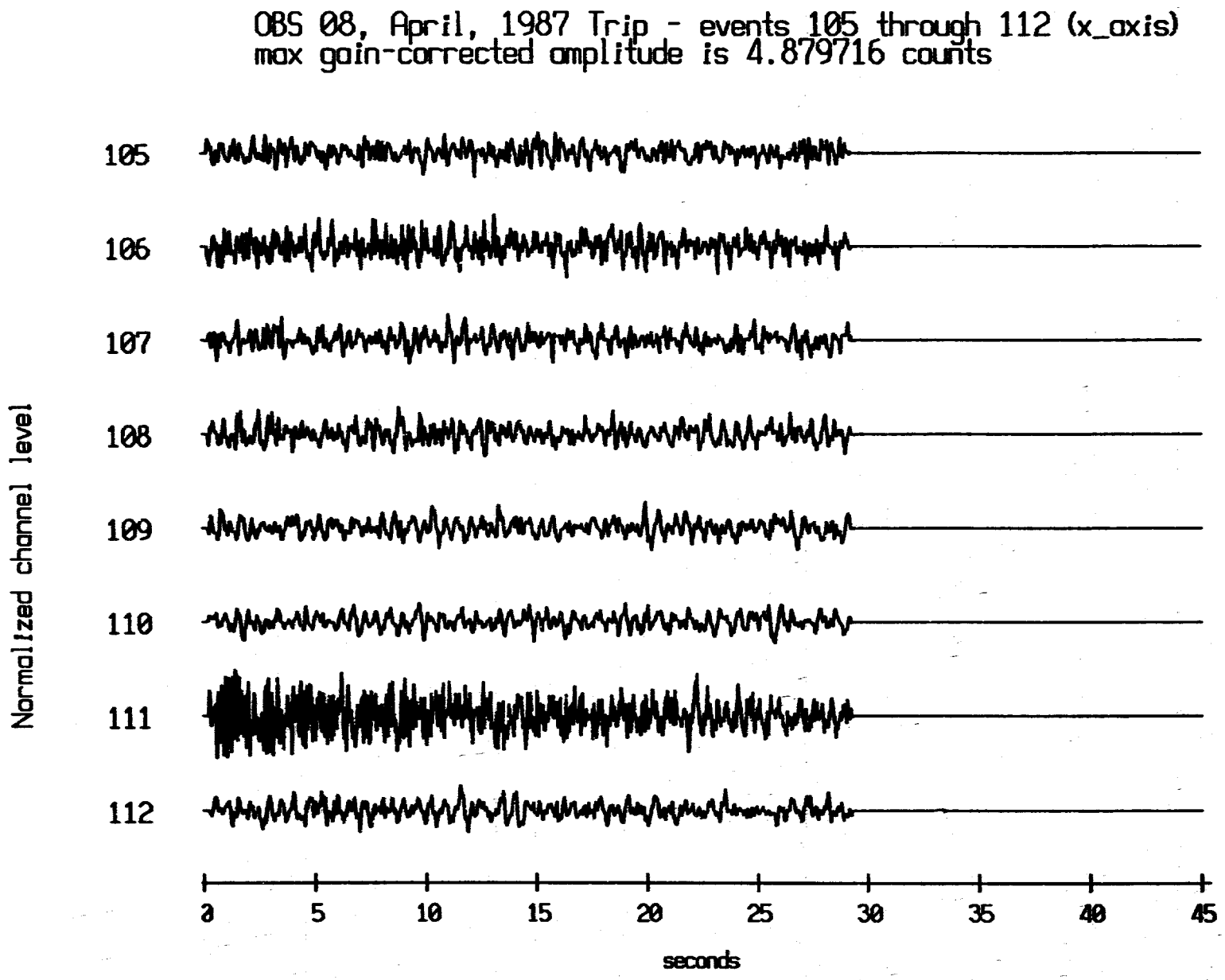

Figure II.18i

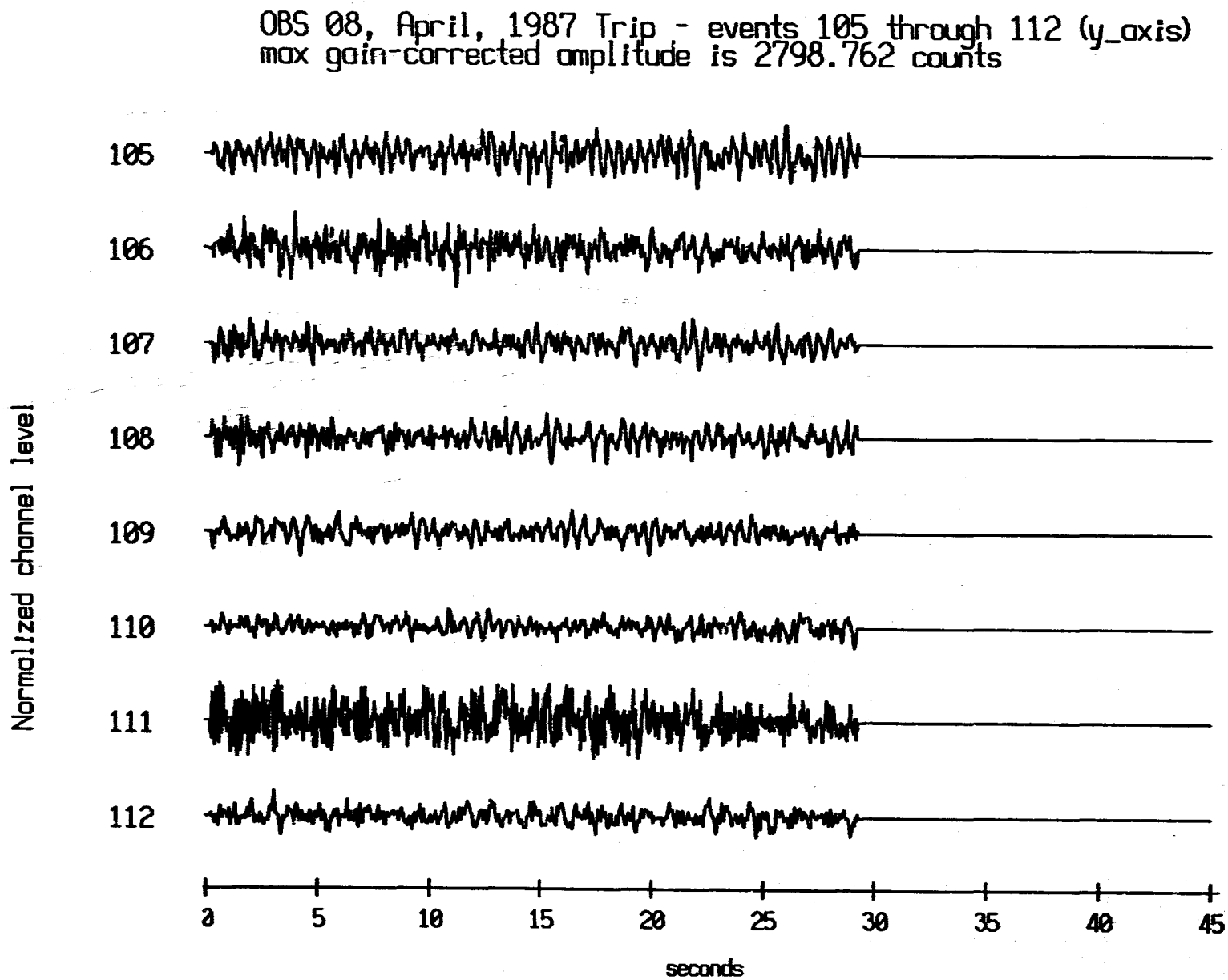

Figure II.18j

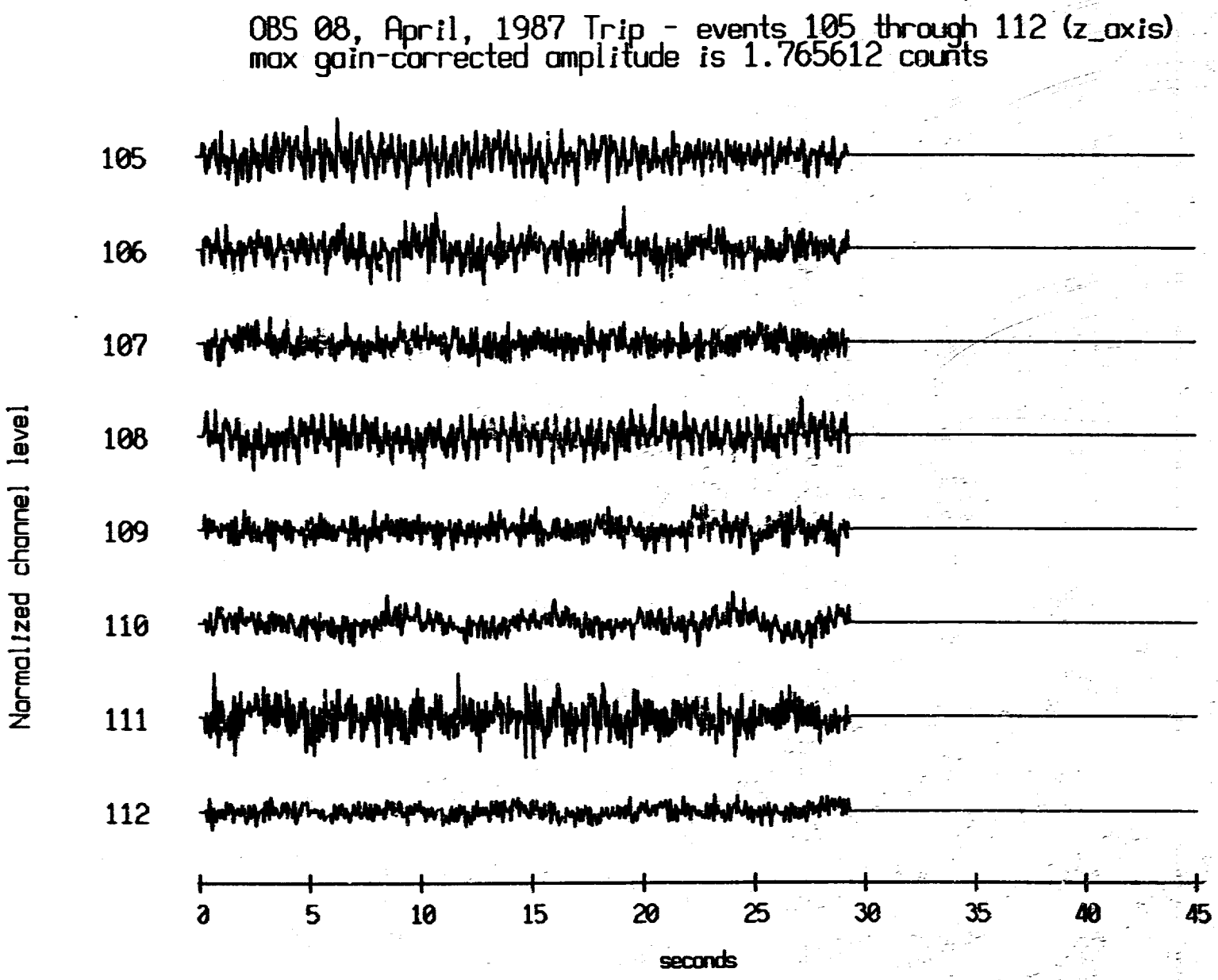

Figure II.18k

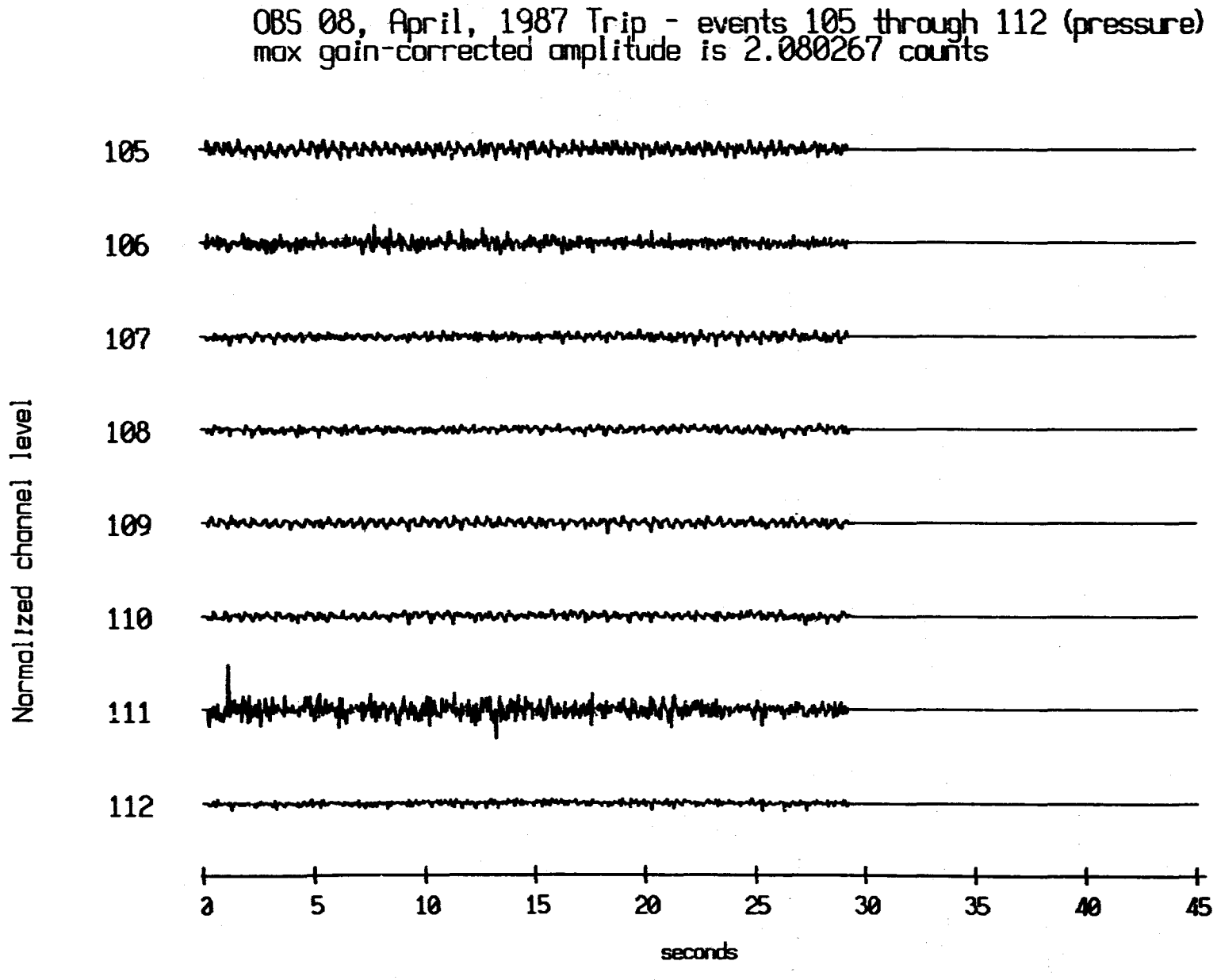
OBS 08, April, 1987 Trip - events 105 through 112 (pressure)
max gain-corrected amplitude is 2.080267 counts
105
106
107
108
109
110
111
112
Normalized channel level
0
5
10
15
20
25
30
35
40
45
seconds

Figure II.18

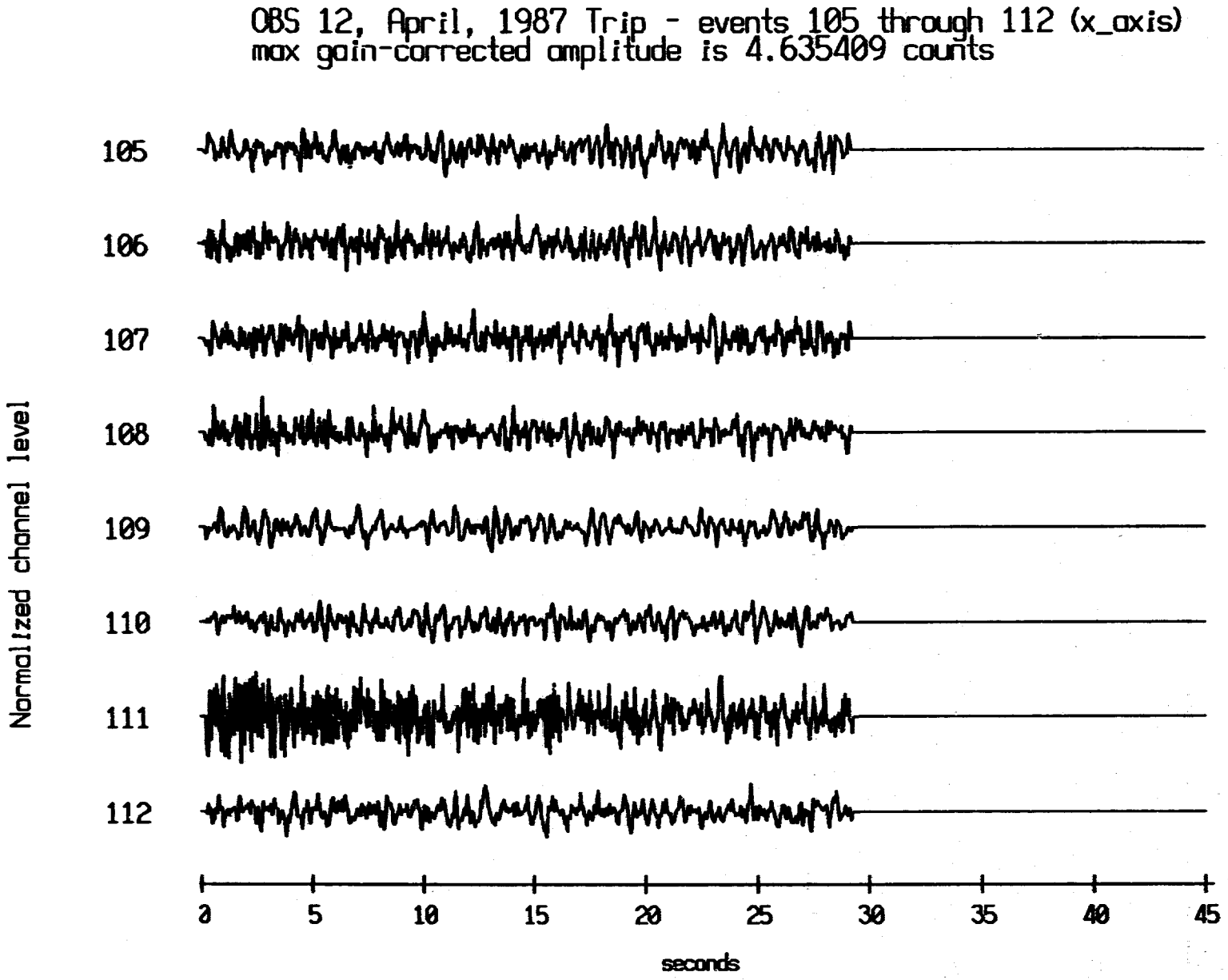

Figure II.10i

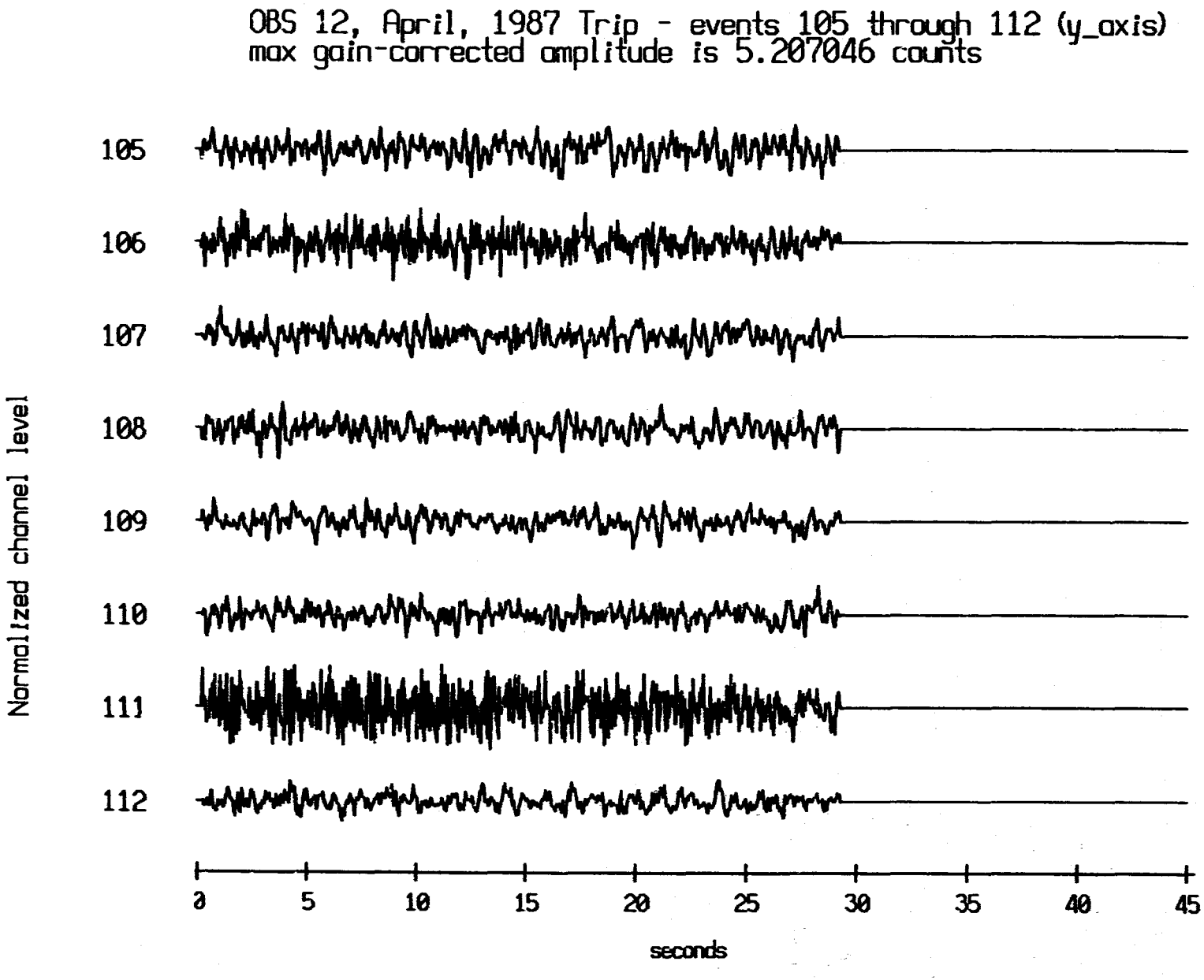

Figure II.19j

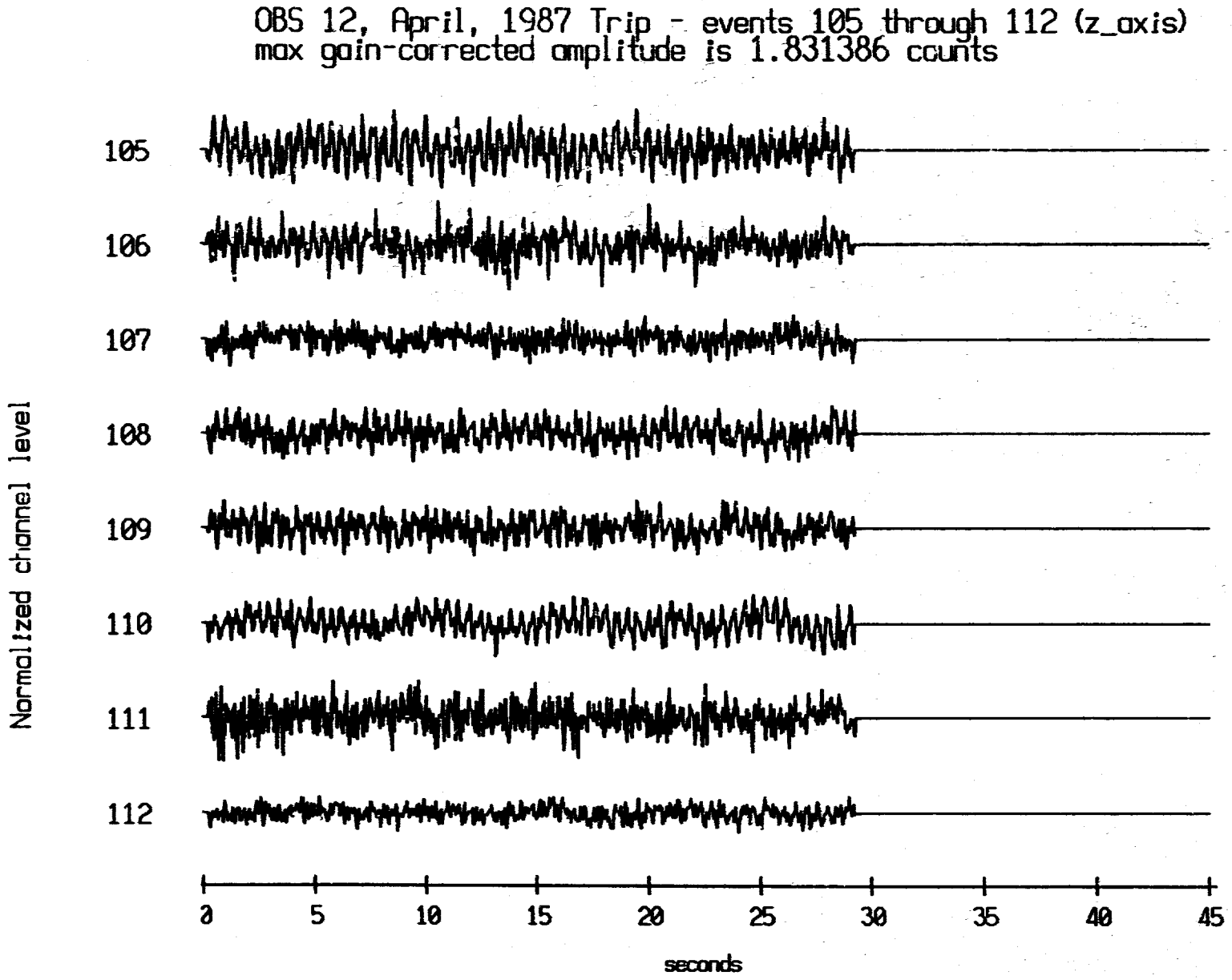

Figure II.19k

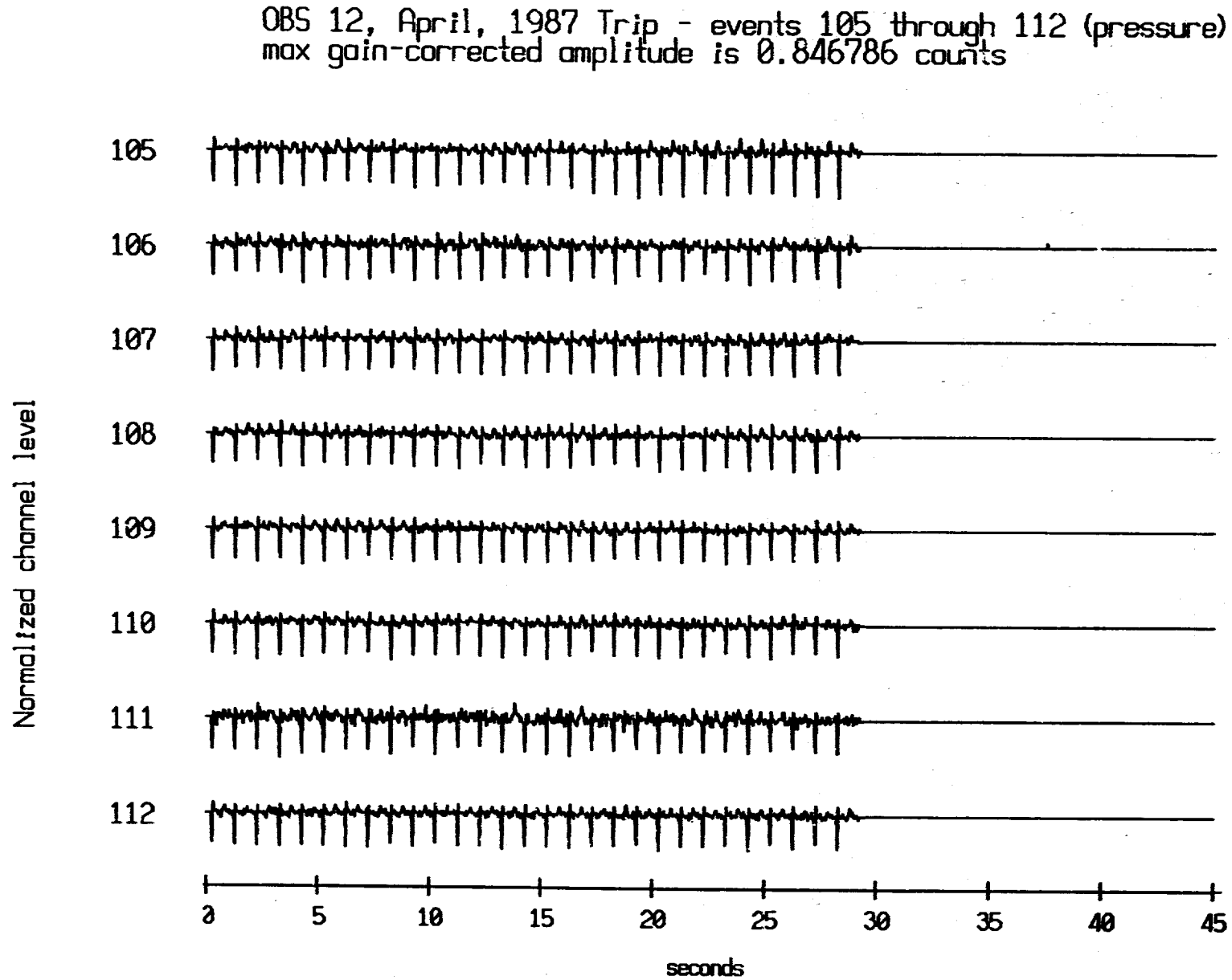

Figure II.19l

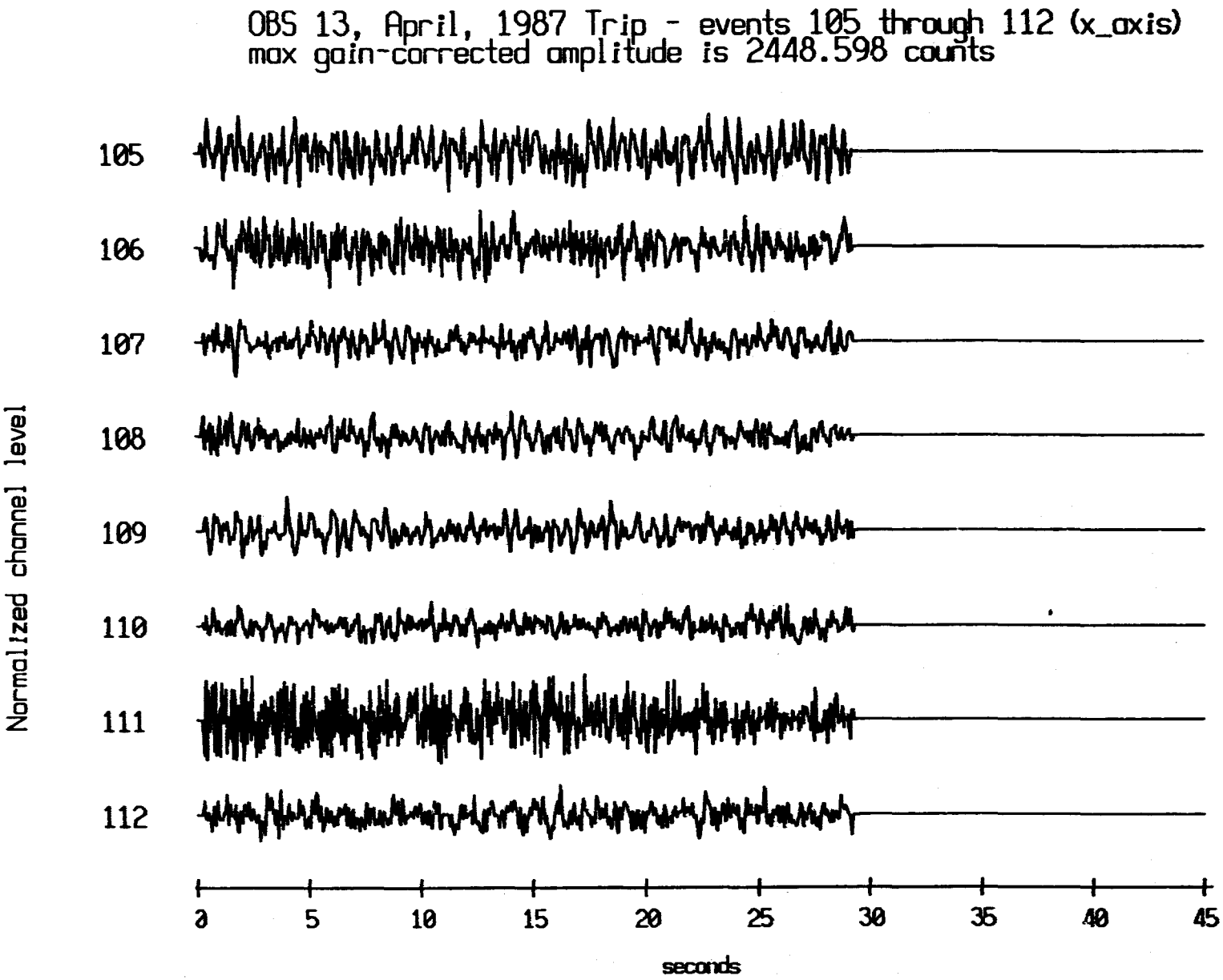

Figure II.20i

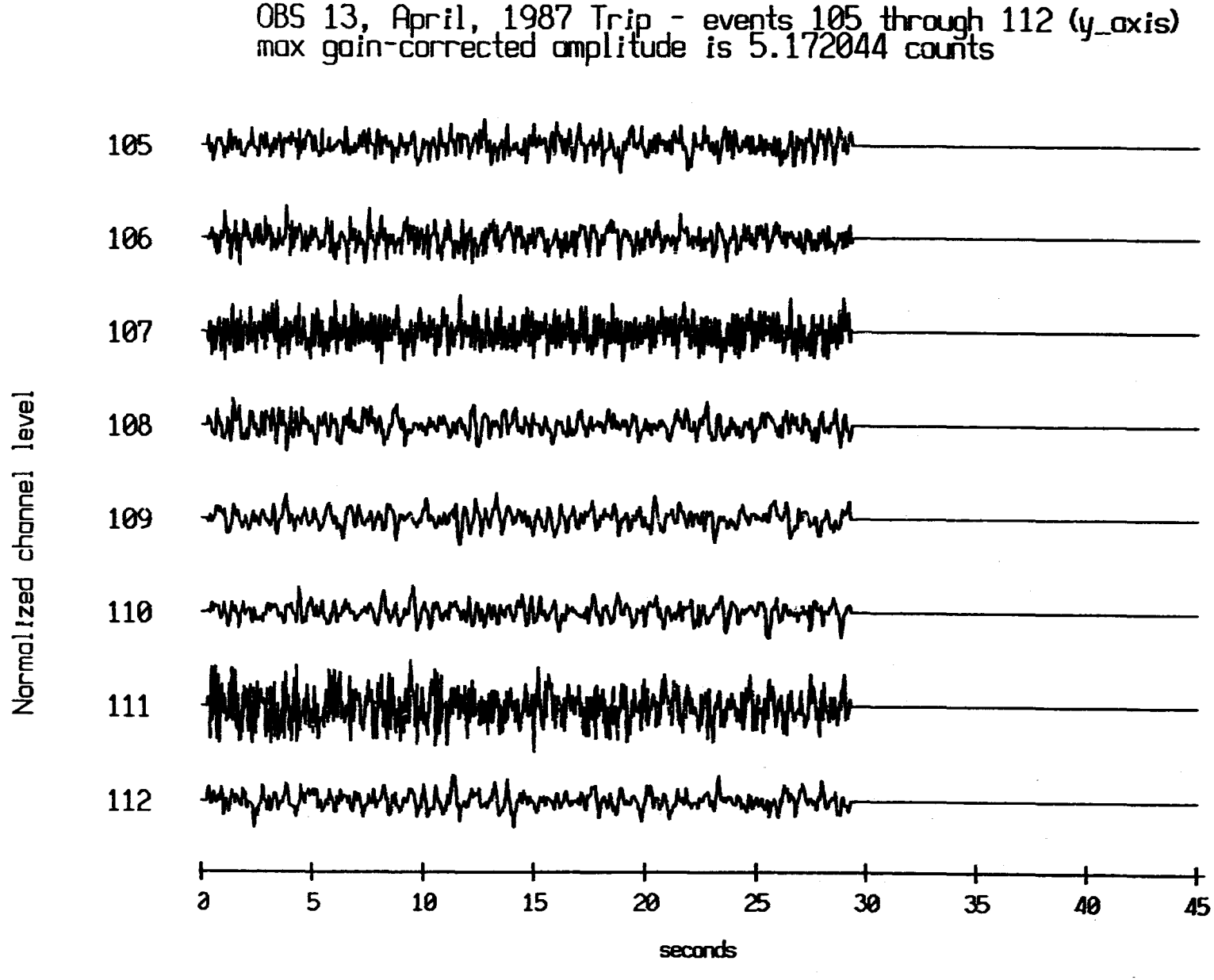

Figure II.20j

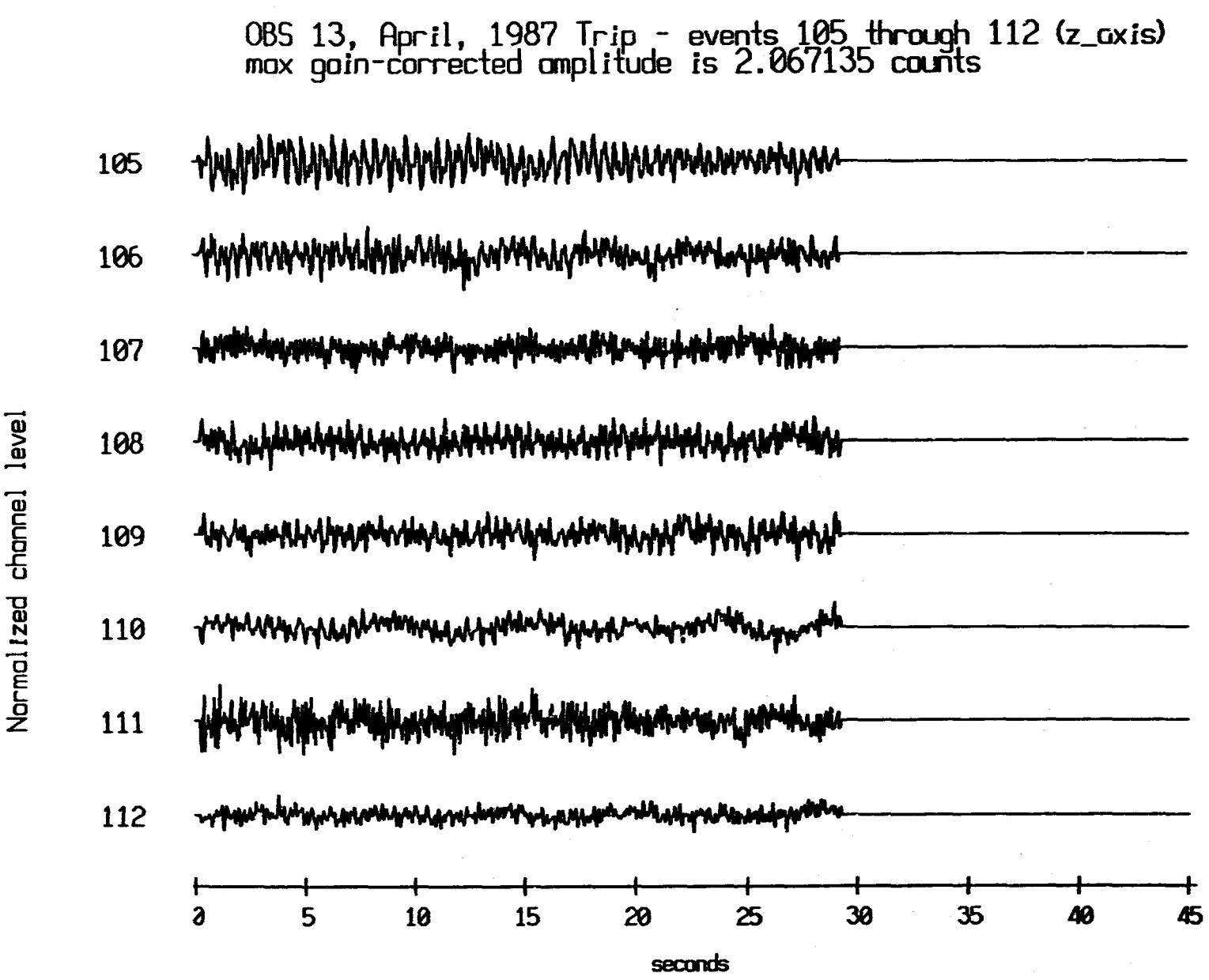

Figure II.20k

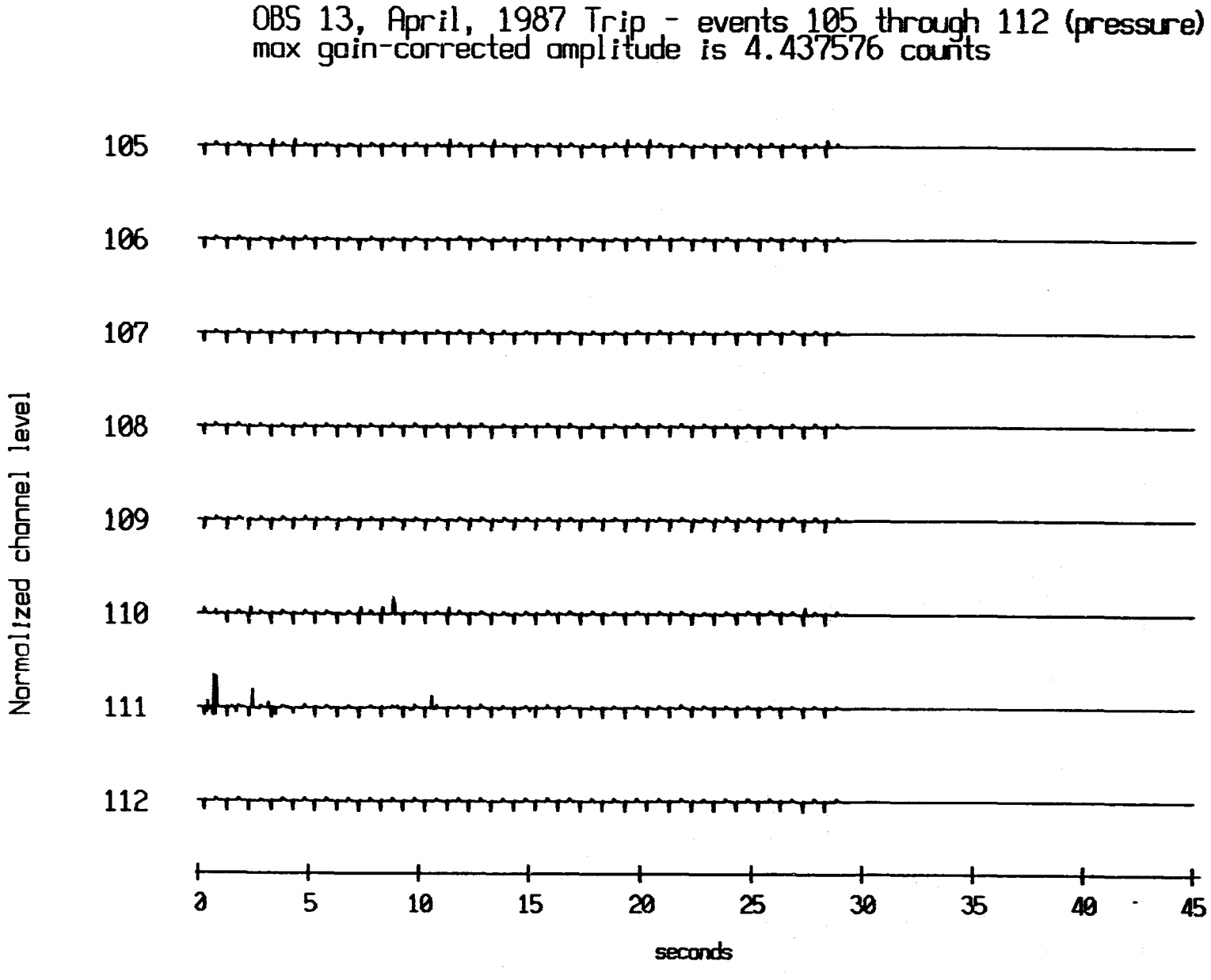
OBS 13, April, 1987 Trip - events 105 through 112 (pressure)
max gain-corrected amplitude is 4.437576 counts
105
106
107
108
109
110
111
112
Normalized channel level
0
5
10
15
20
25
30
35
40
45
seconds

Figure II.20

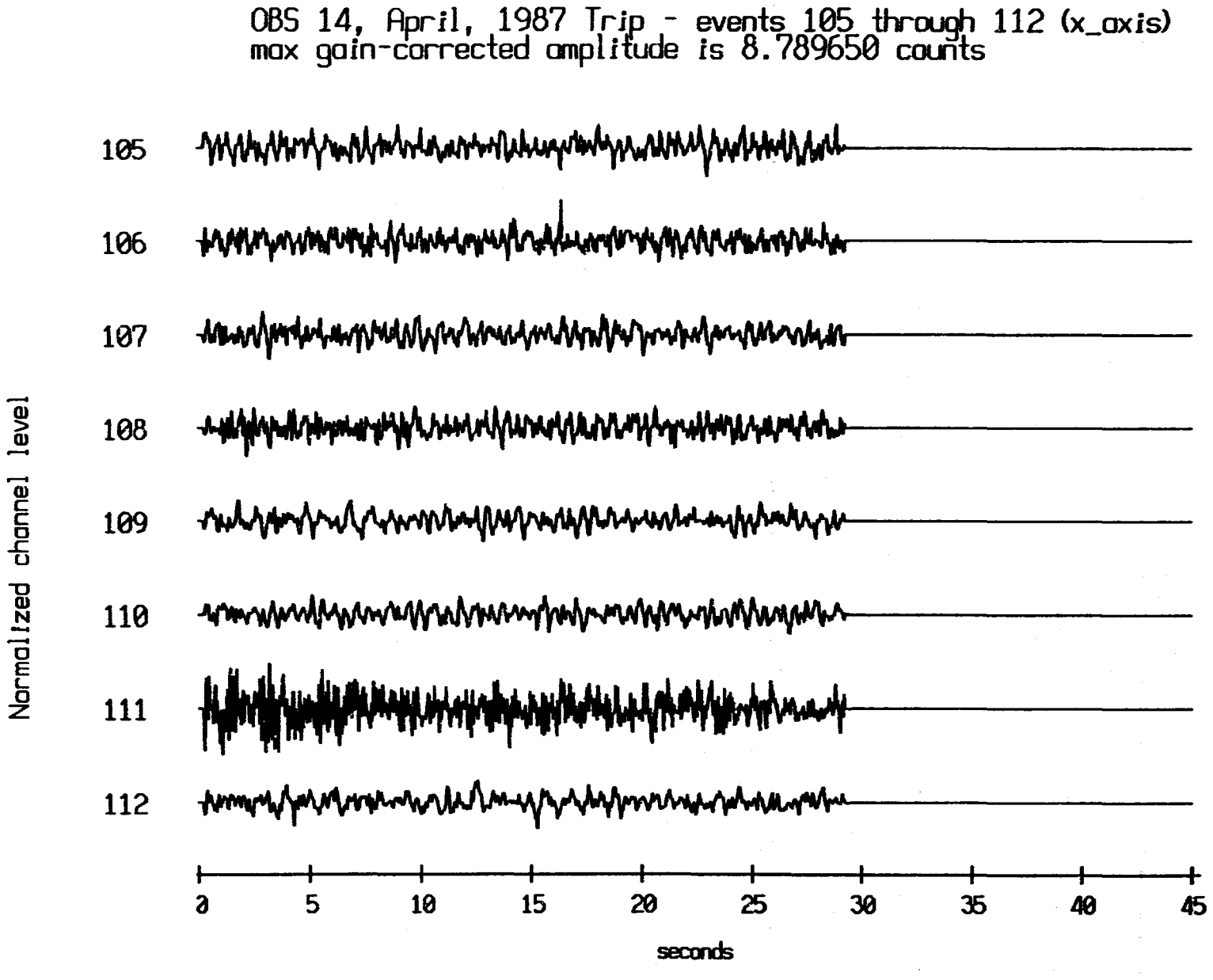

Figure II.21i

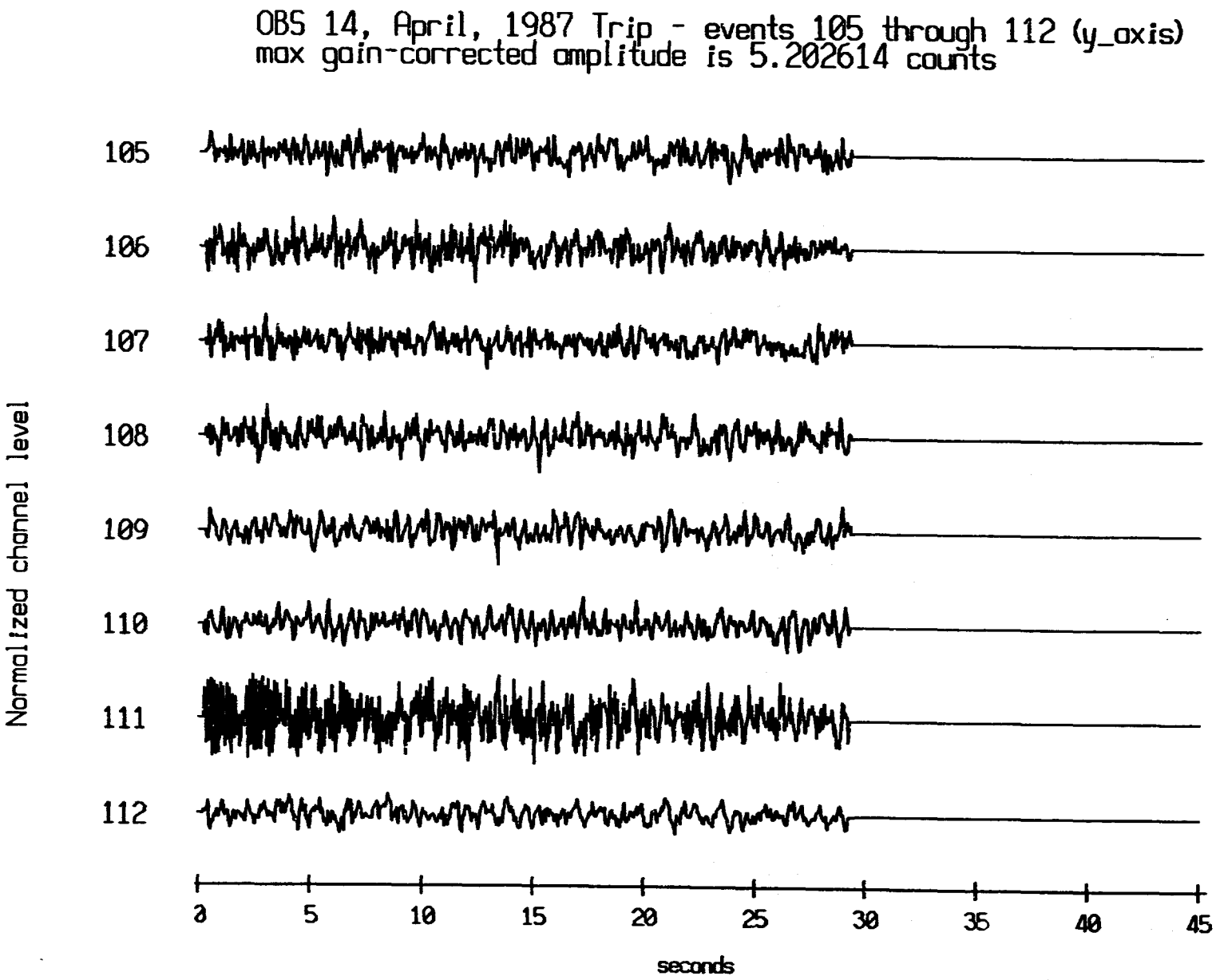

Figure II.21j

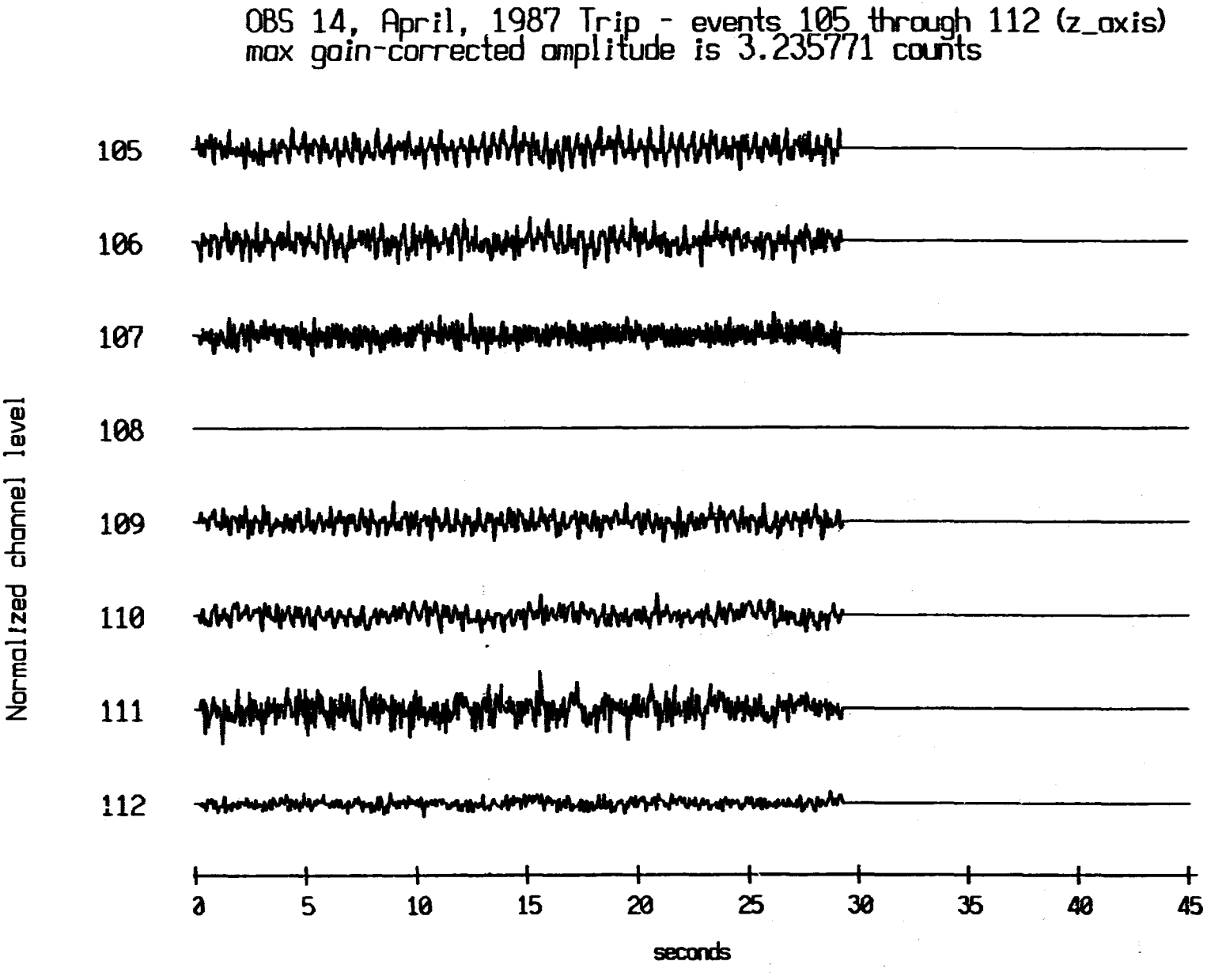

Figure II.21k

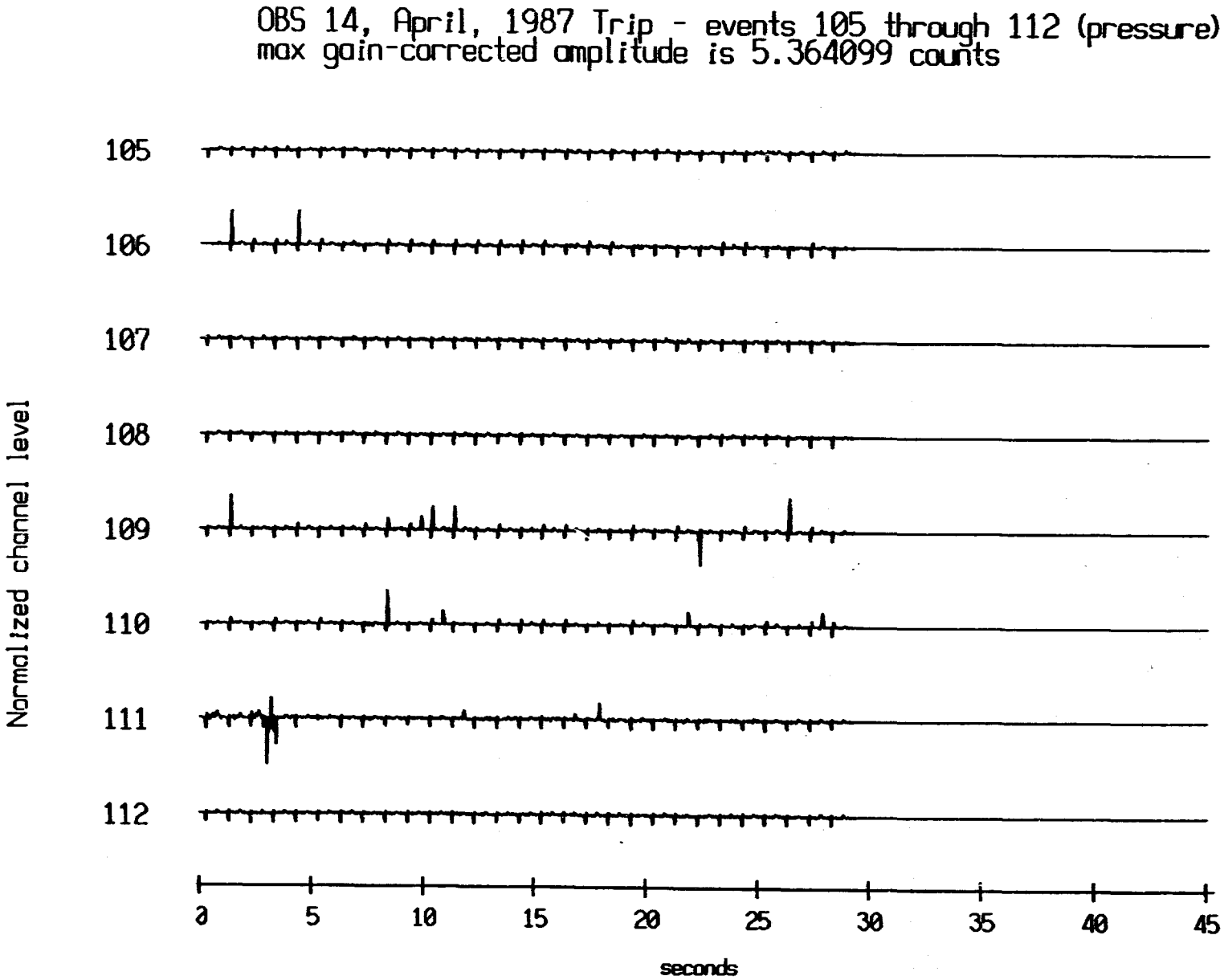
OBS 14, April, 1987 Trip - events 105 through 112 (pressure)
max gain-corrected amplitude is 5.364099 counts
105
106
107
108
109
110
111
112
Normalized channel level
0
5
10
15
20
25
30
35
40
45
seconds

Figure II.21

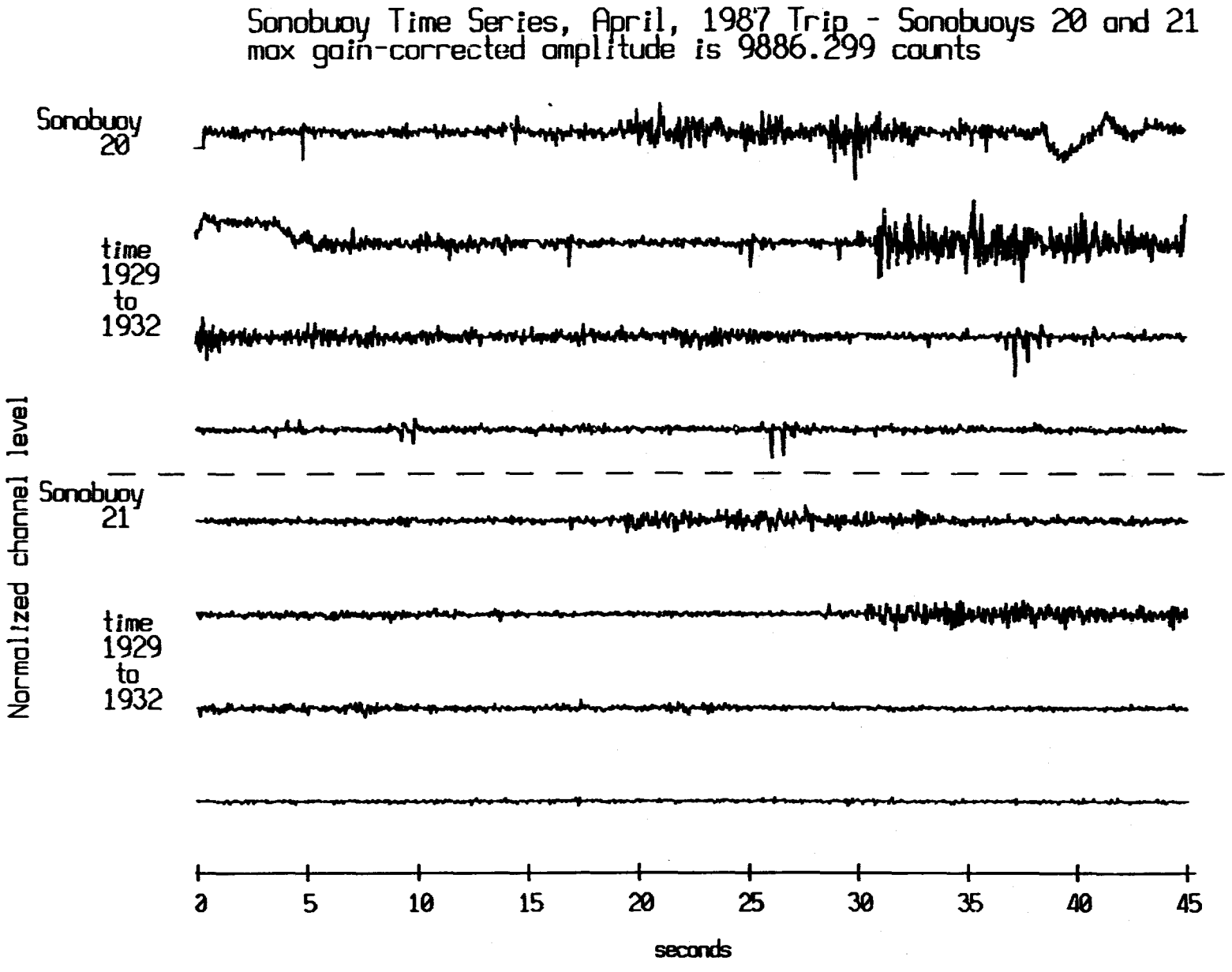
Sonobuoy Time Series, April, 1987 Trip - Sonobuoys 20 and 21
max gain-corrected amplitude is 9886.299 counts
Sonobuoy 20
time 1929 to 1932
Sonobuoy 21
time 1929 to 1932
Normalized channel level
0
5
10
15
20
25
30
35
40
45
seconds

Figure II.22

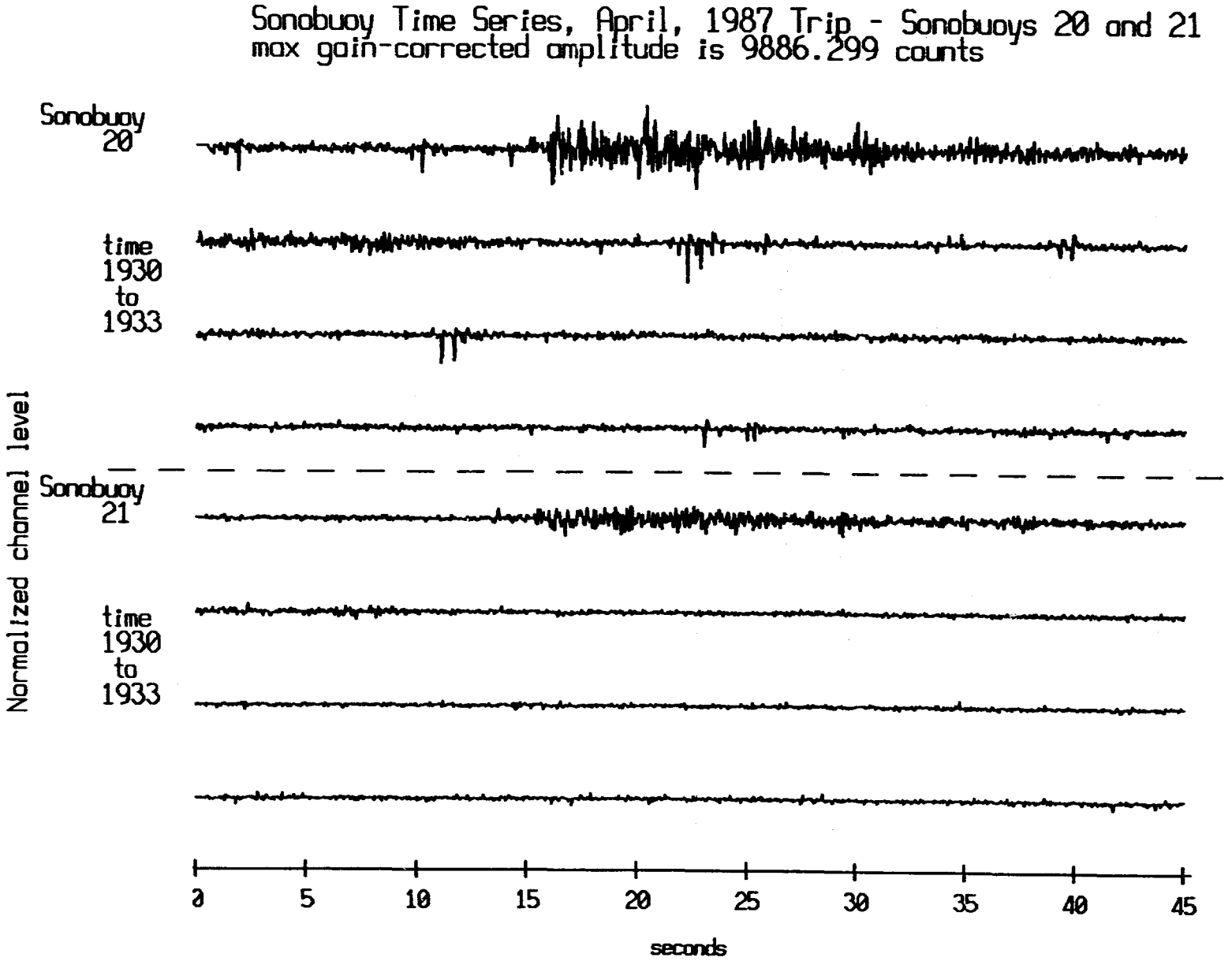
Sonobuoy Time Series, April, 1987 Trip - Sonobuoys 20 and 21
max gain-corrected amplitude is 9886.299 counts
Sonobuoy 20
time 1930 to 1933
Sonobuoy 21
time 1930 to 1933
Normalized channel level
0
5
10
15
20
25
30
35
40
45
seconds

Figure II.23

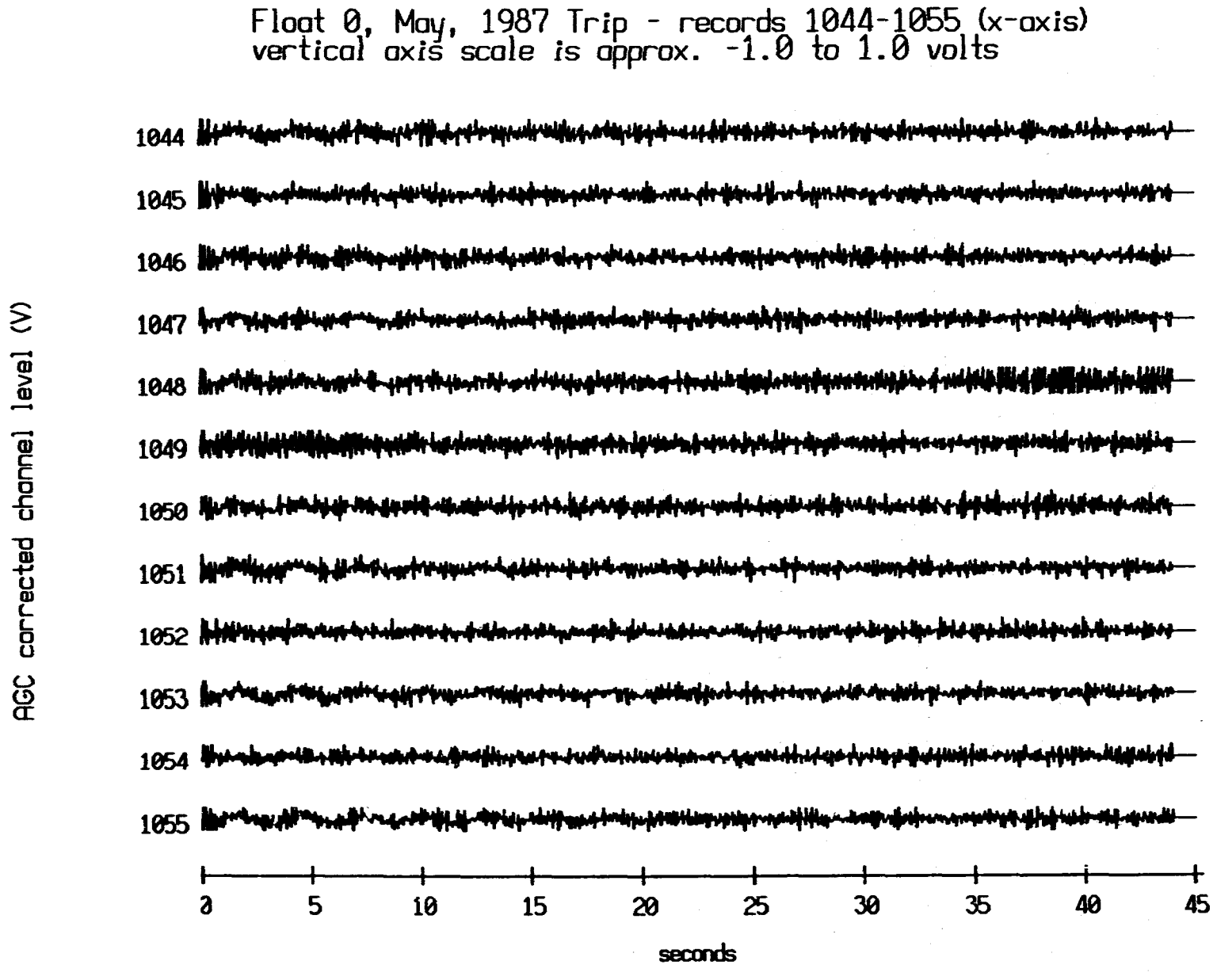

Figure II.24i

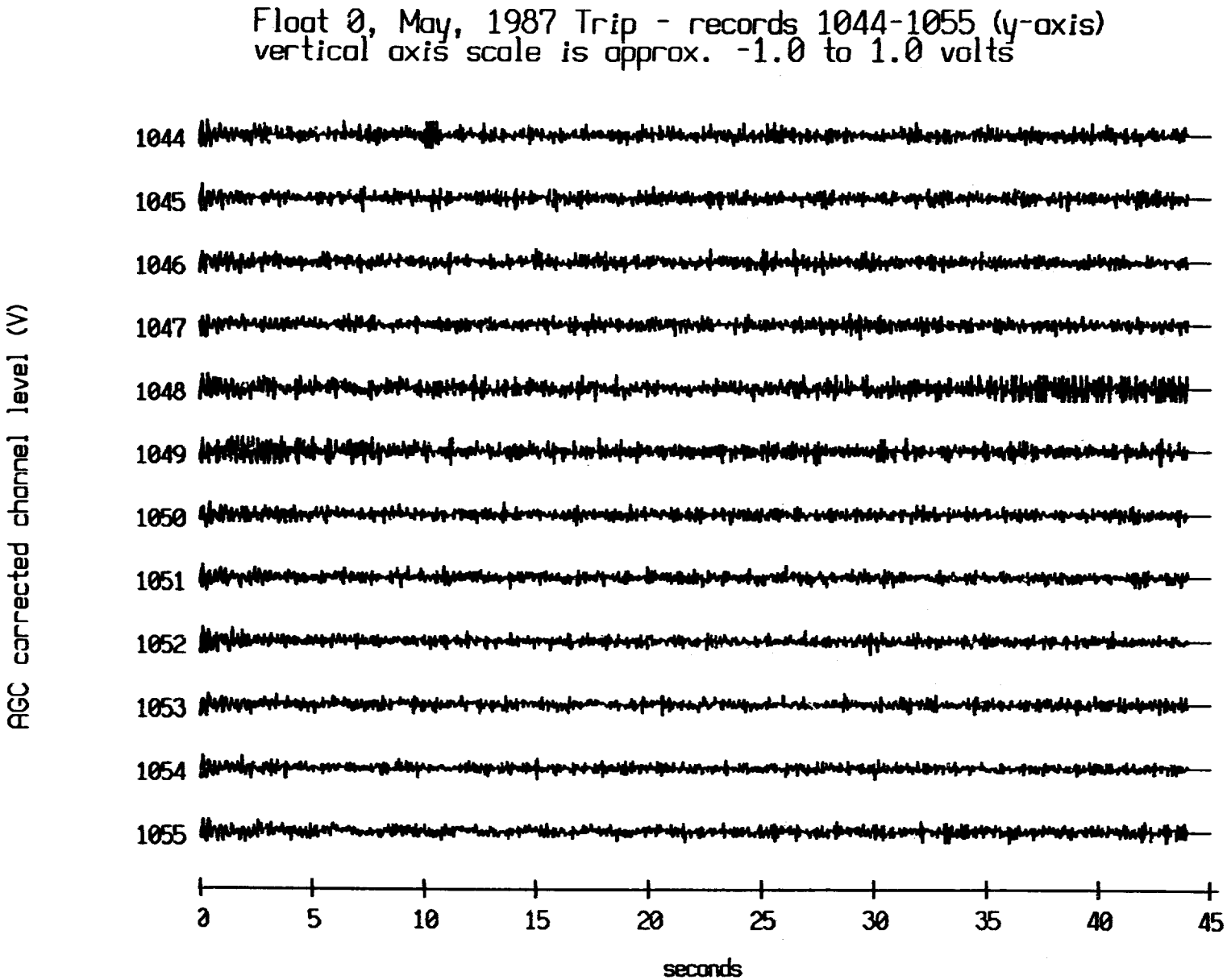

Figure II.24j

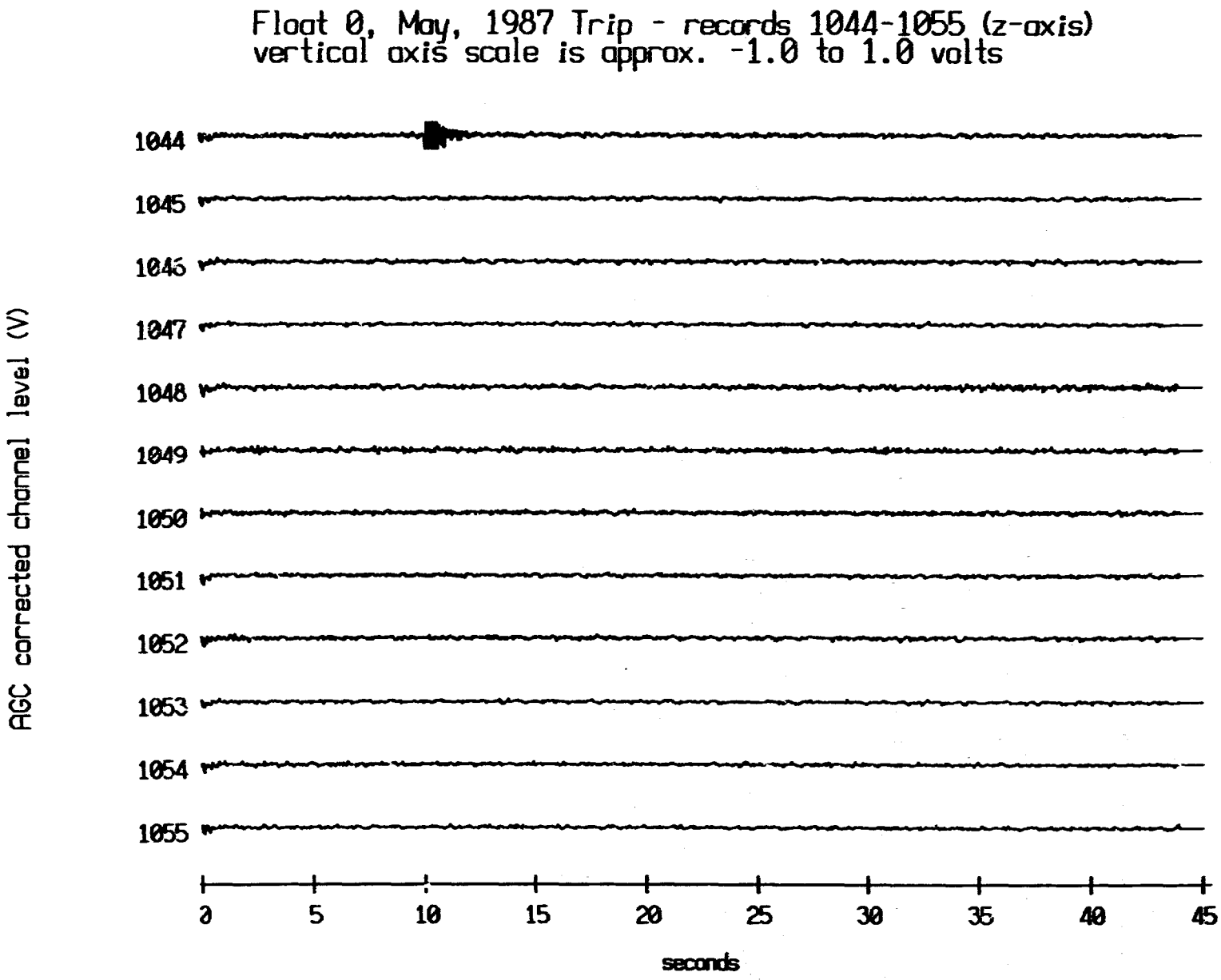

Figure II.24k

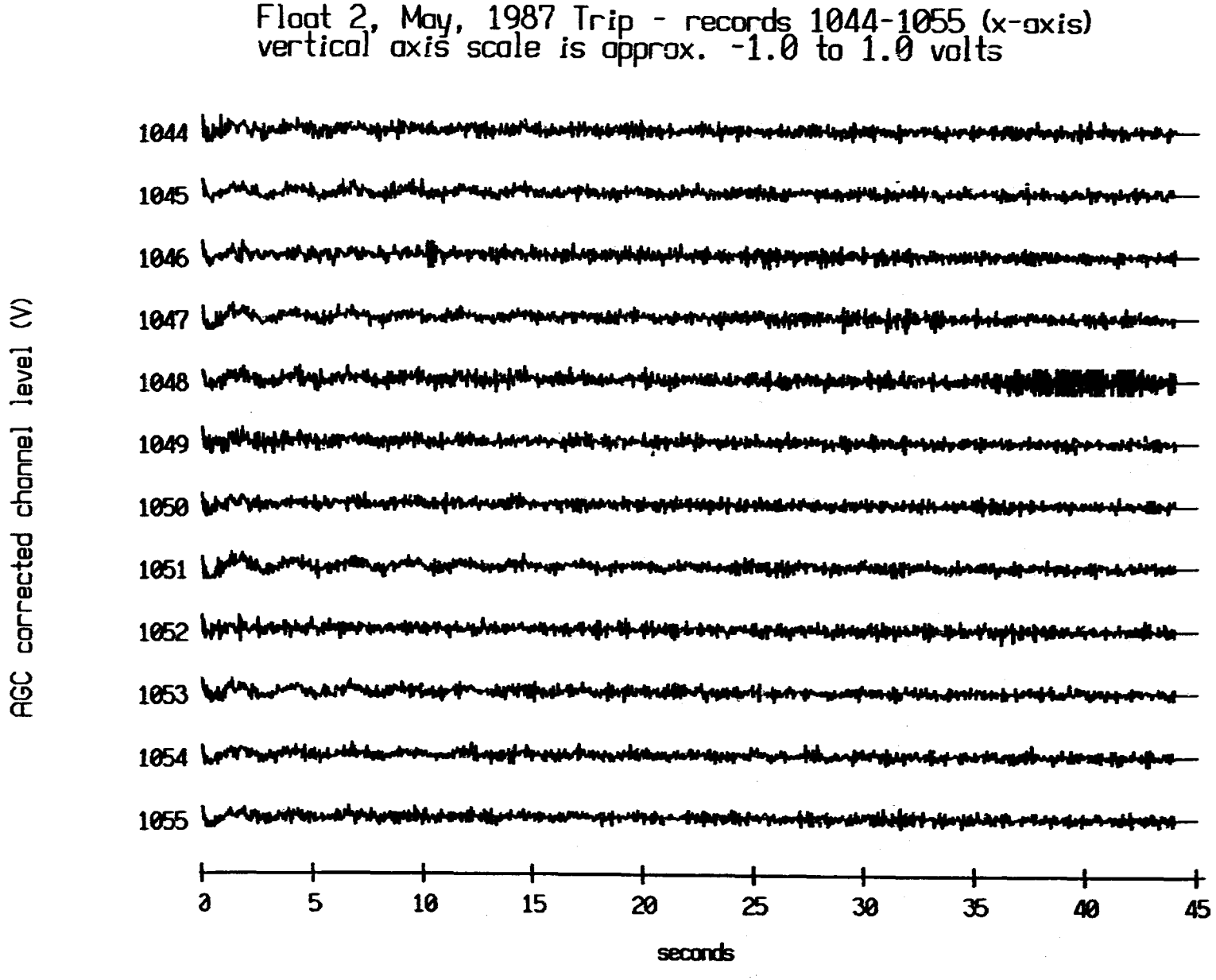

Figure II.25i

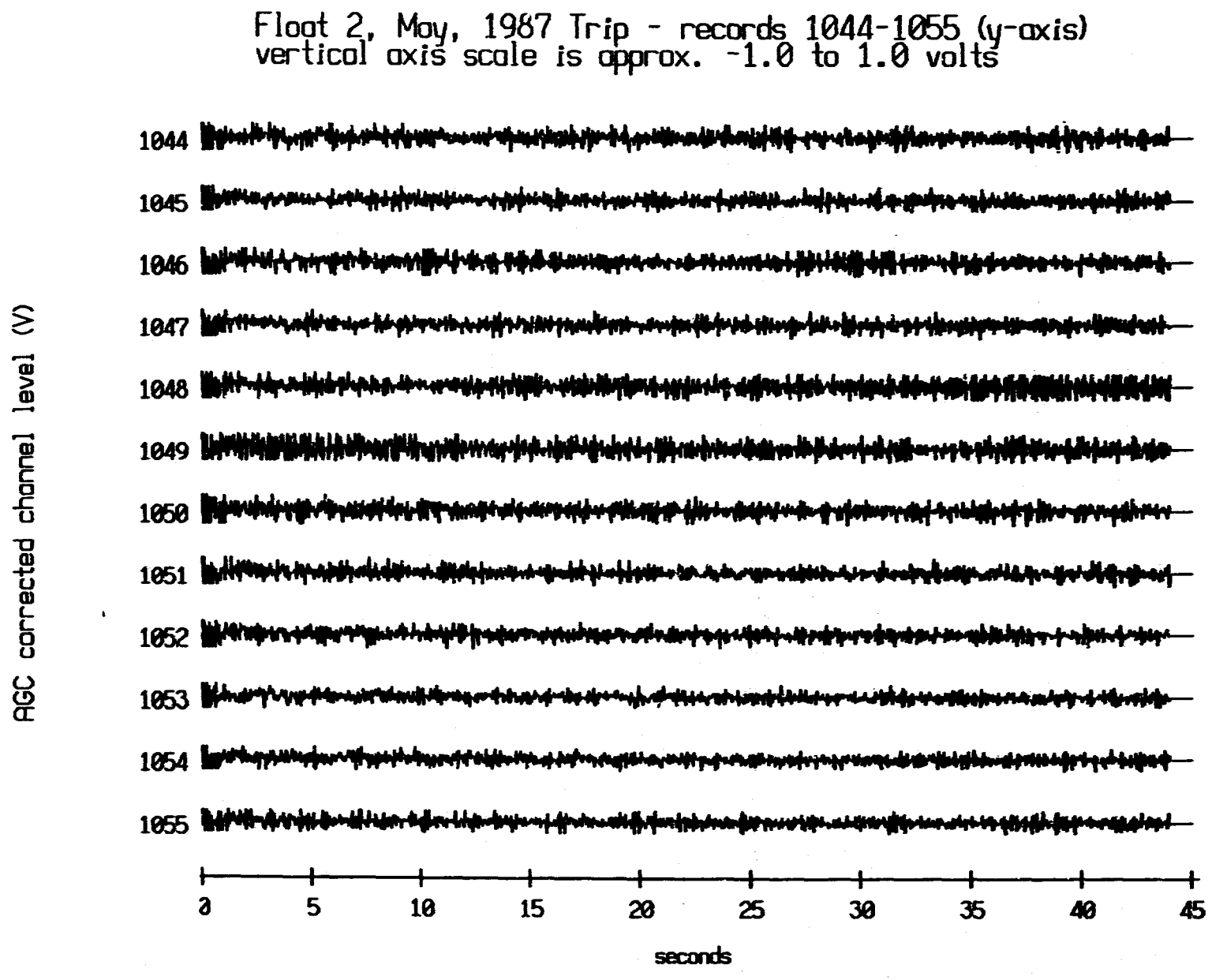

Figure II.25j

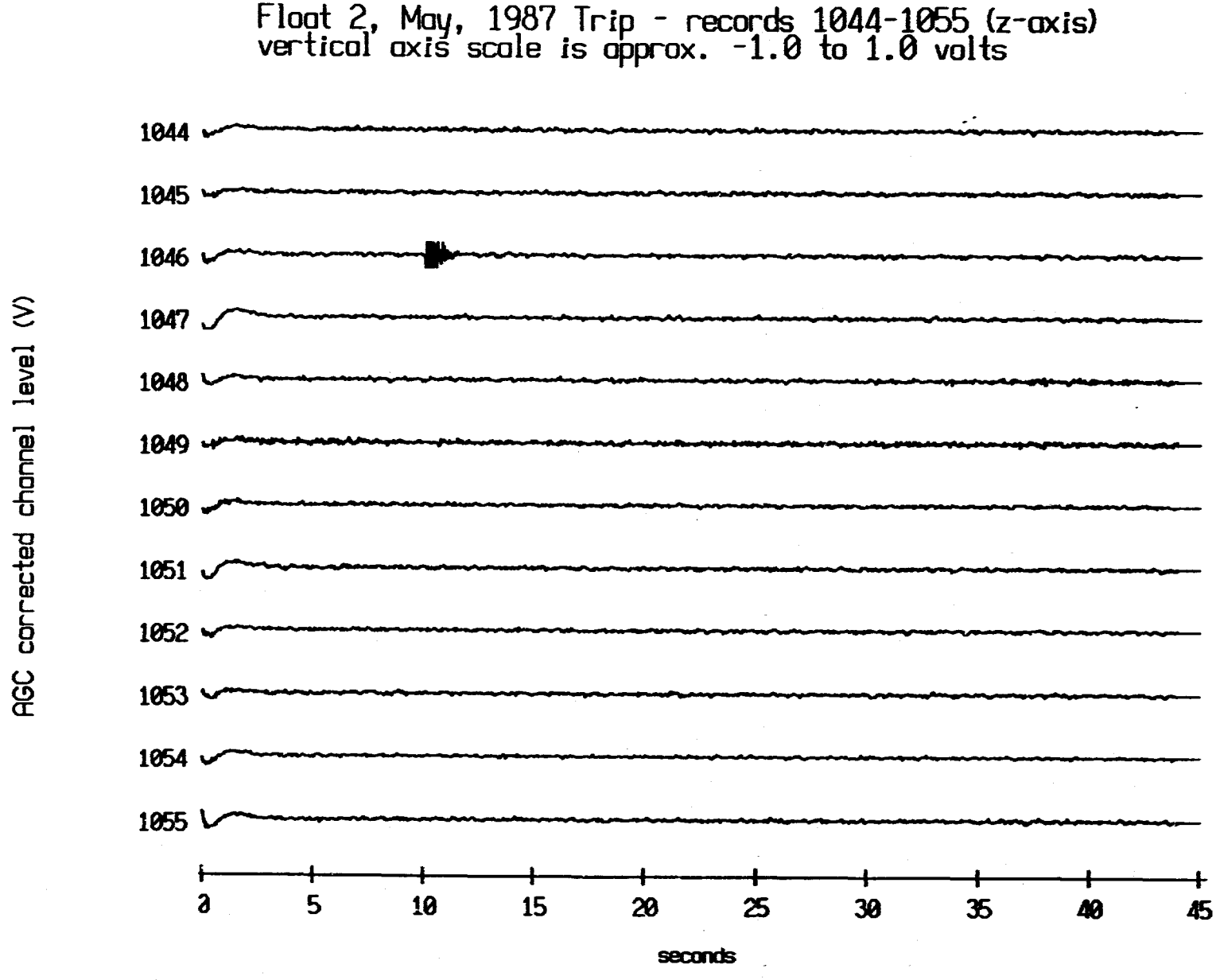

Figure II.25k

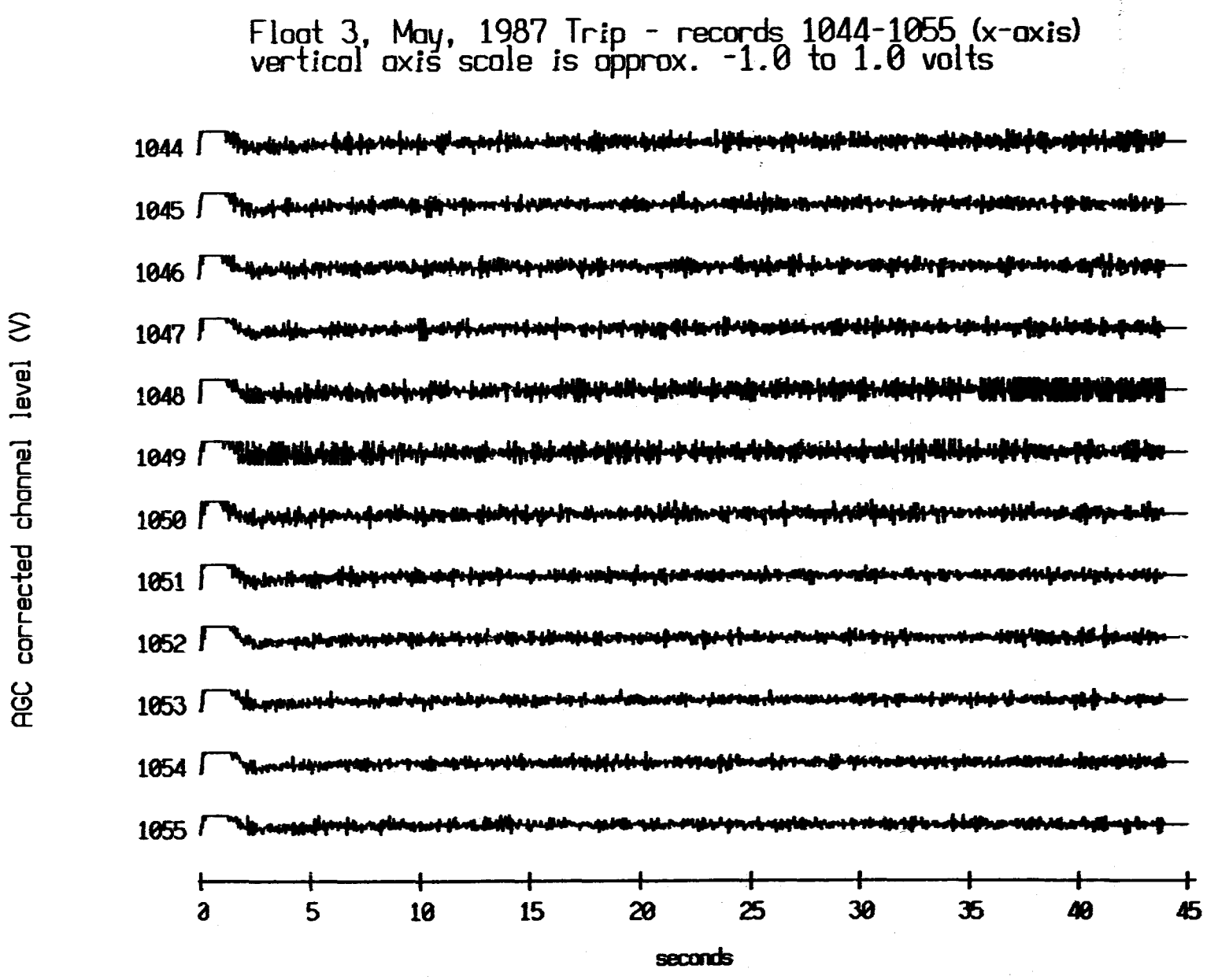

Figure II.26i

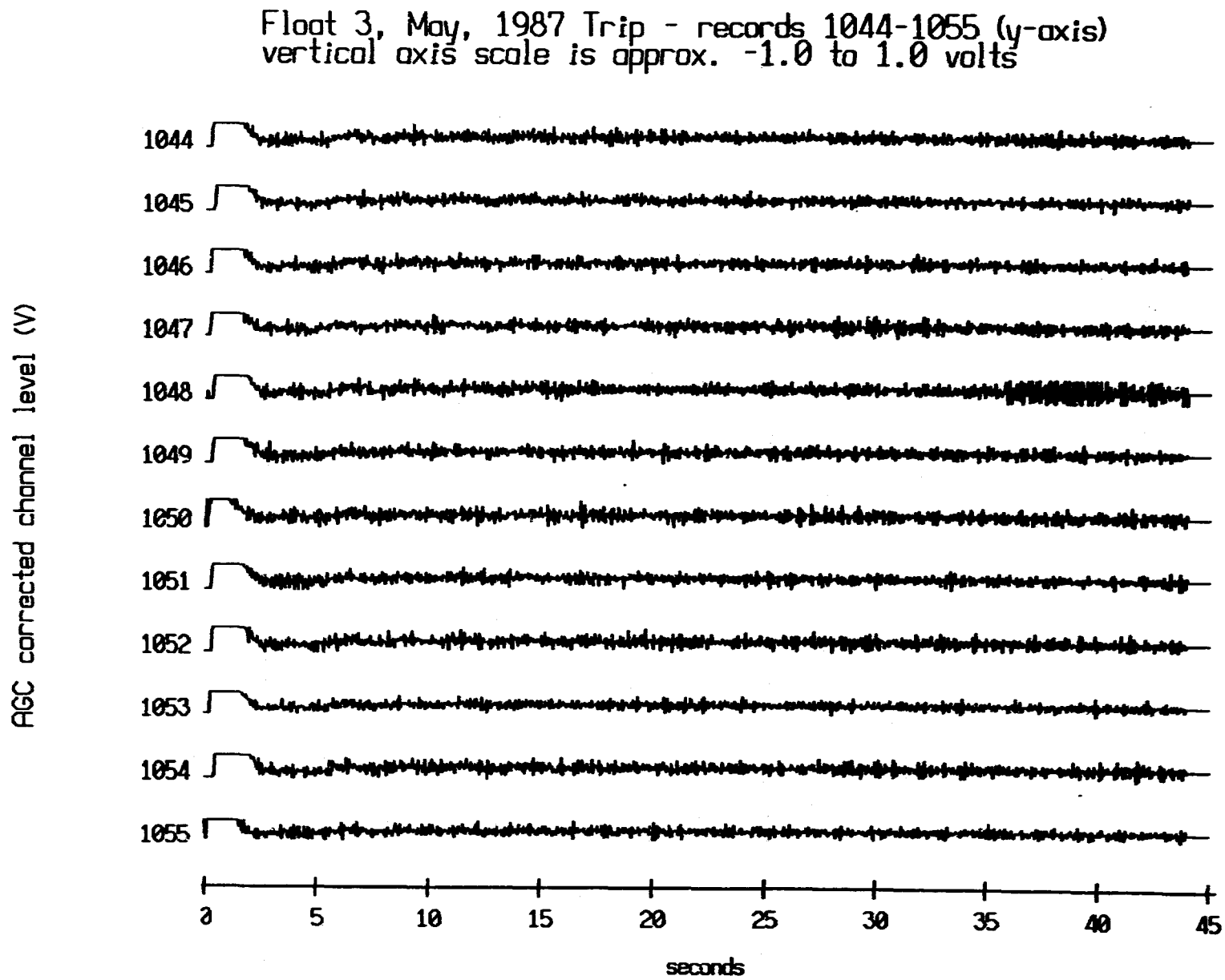

Figure II.26j

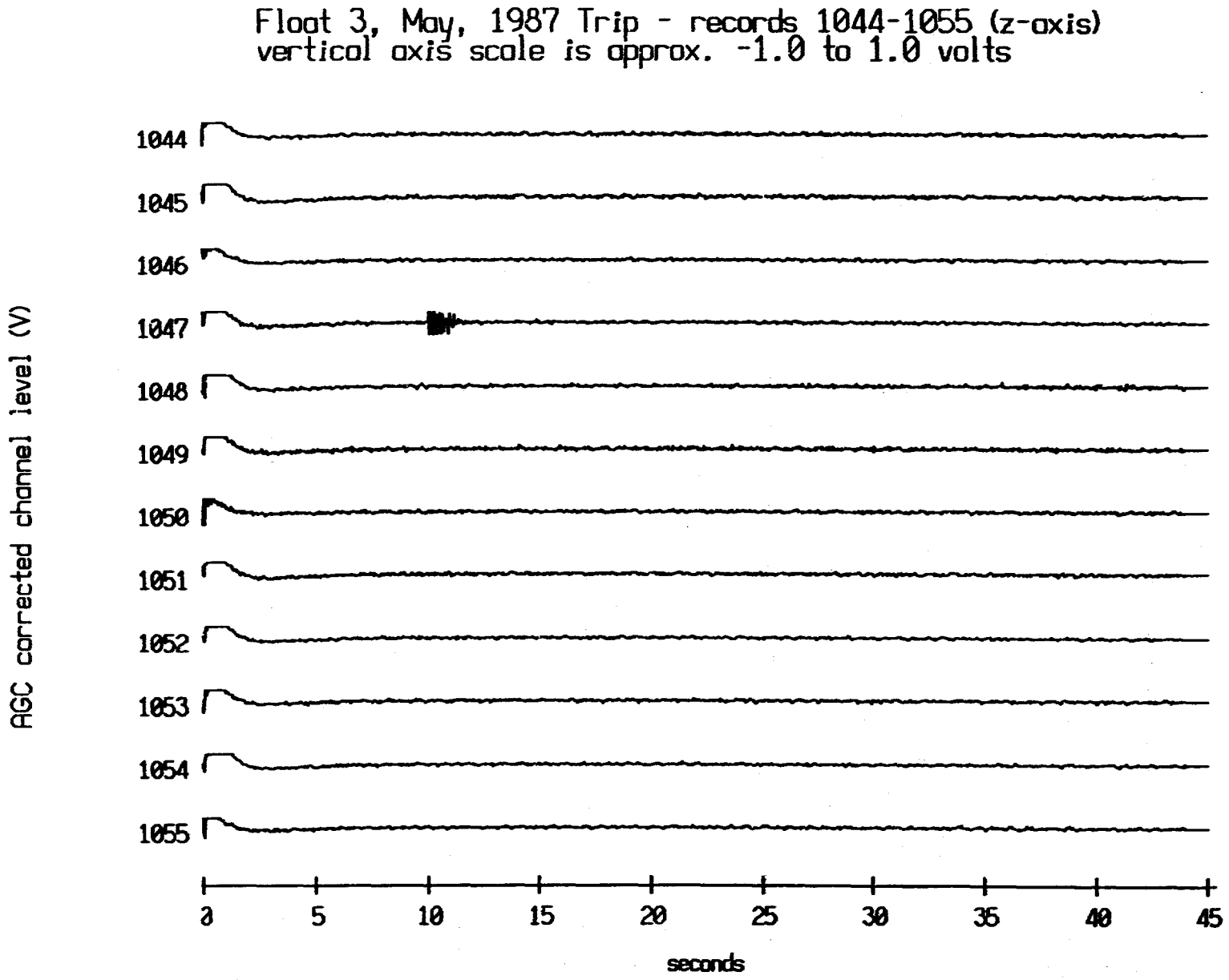

Figure II.26k

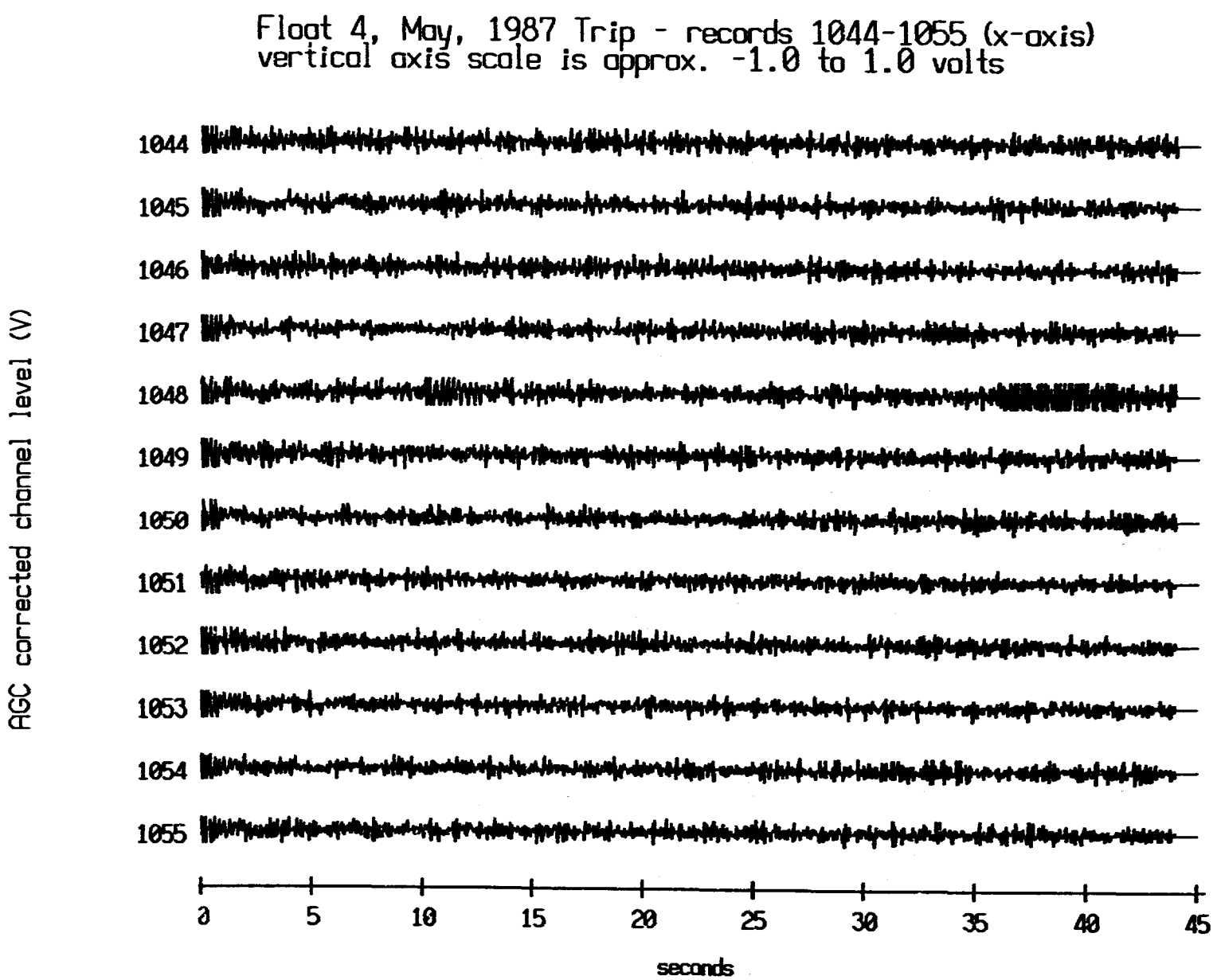

Figure II.27i

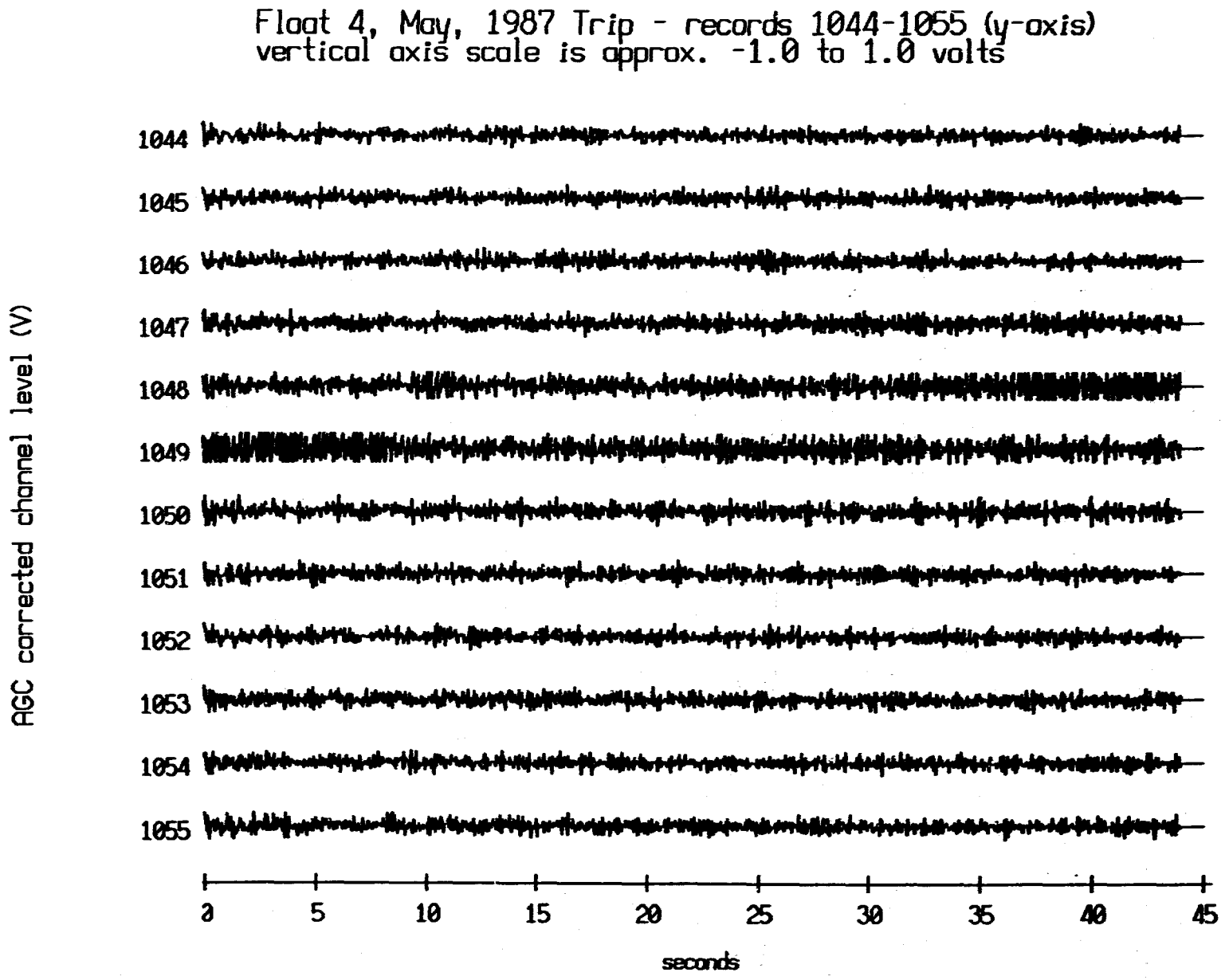

Figure II.27j

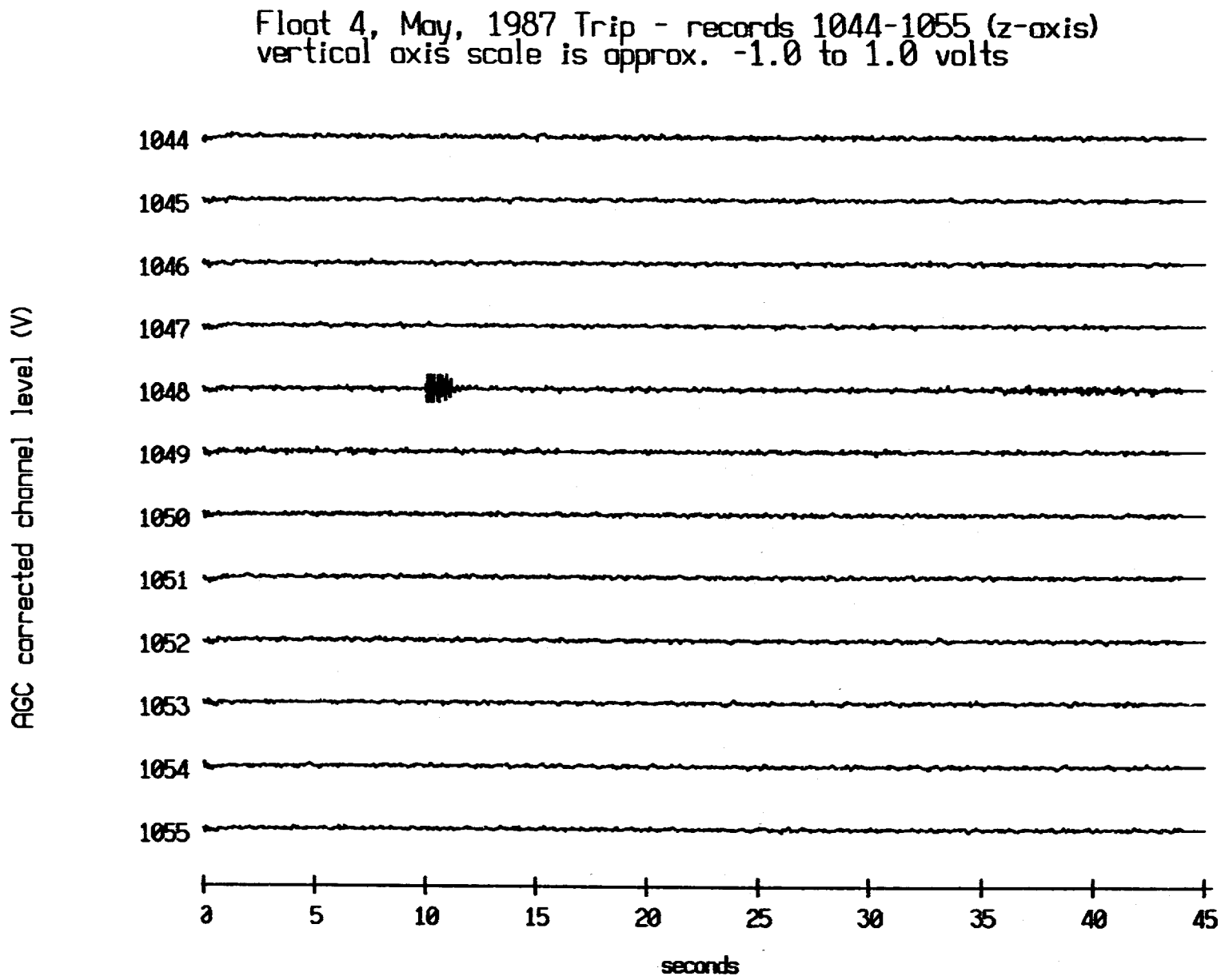

Figure II.27k

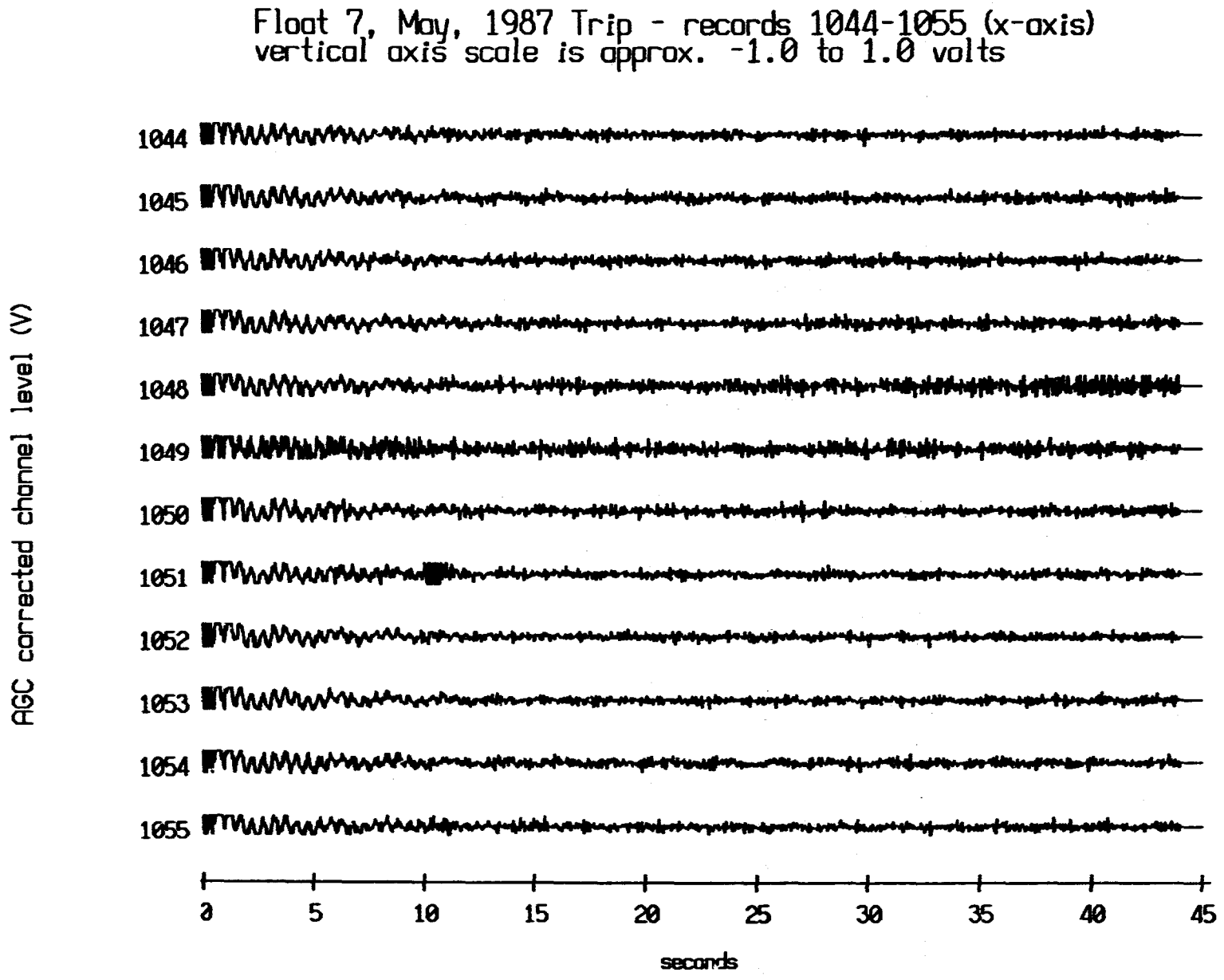

Figure II.28i

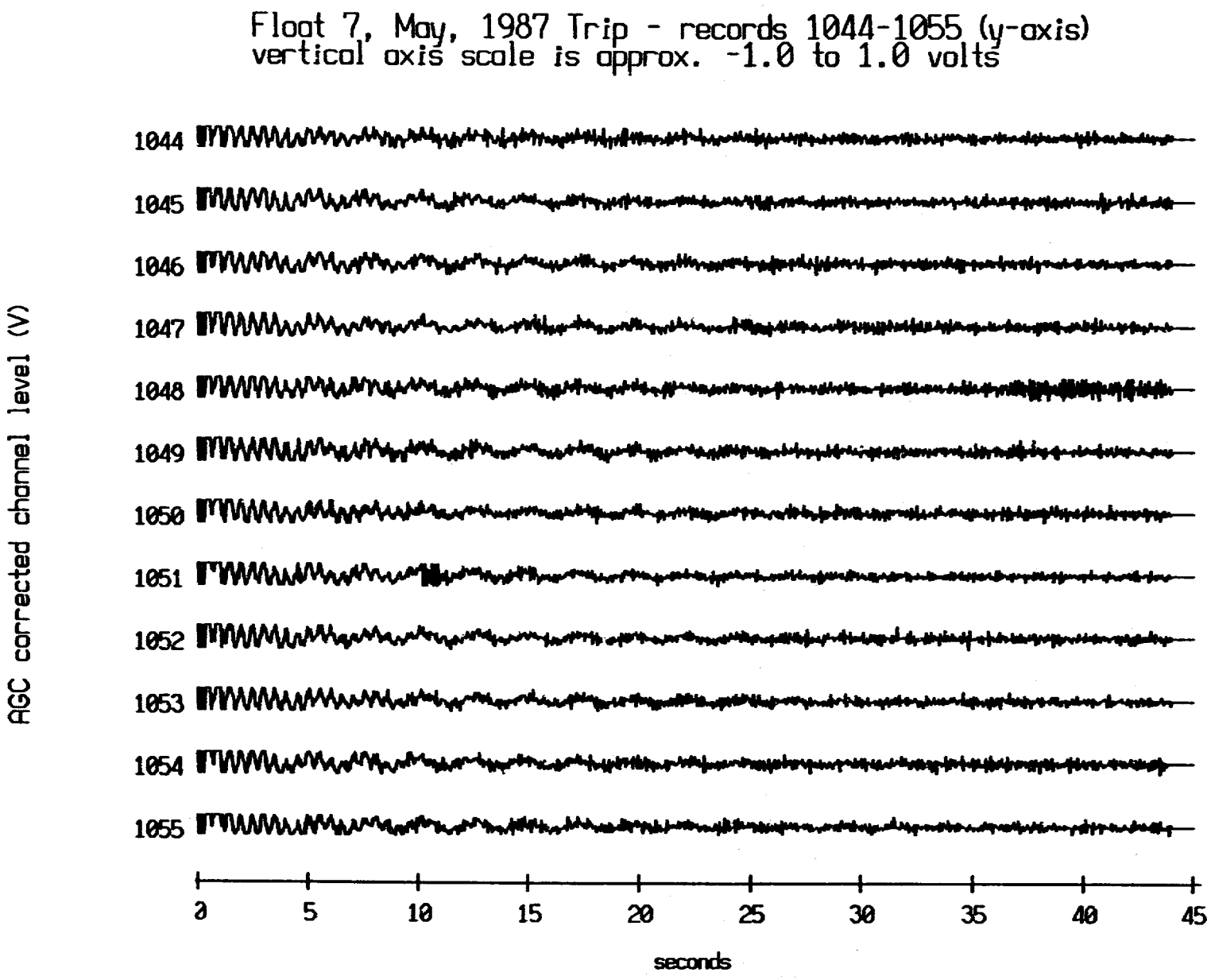

Figure II.28j

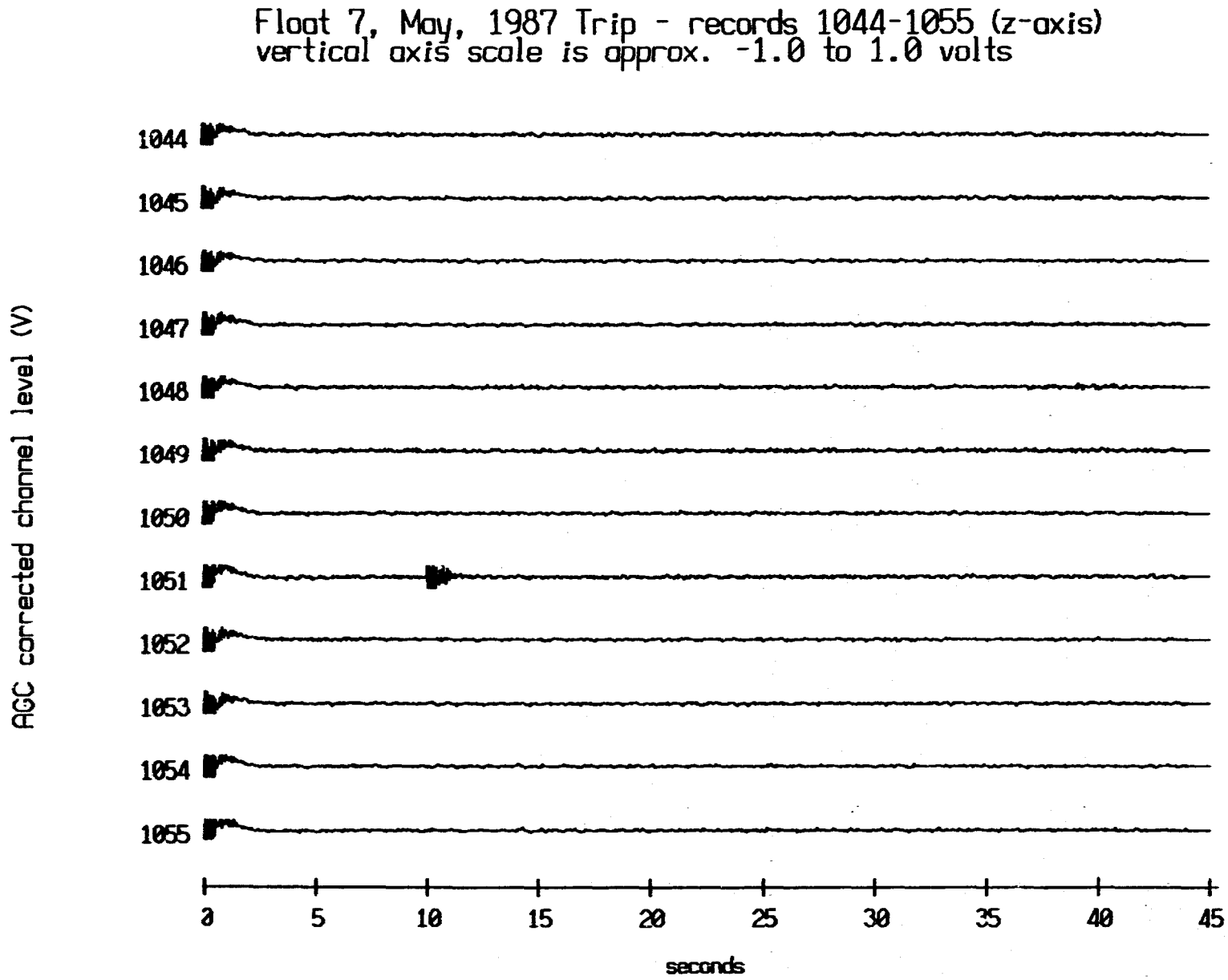

Figure II.28k

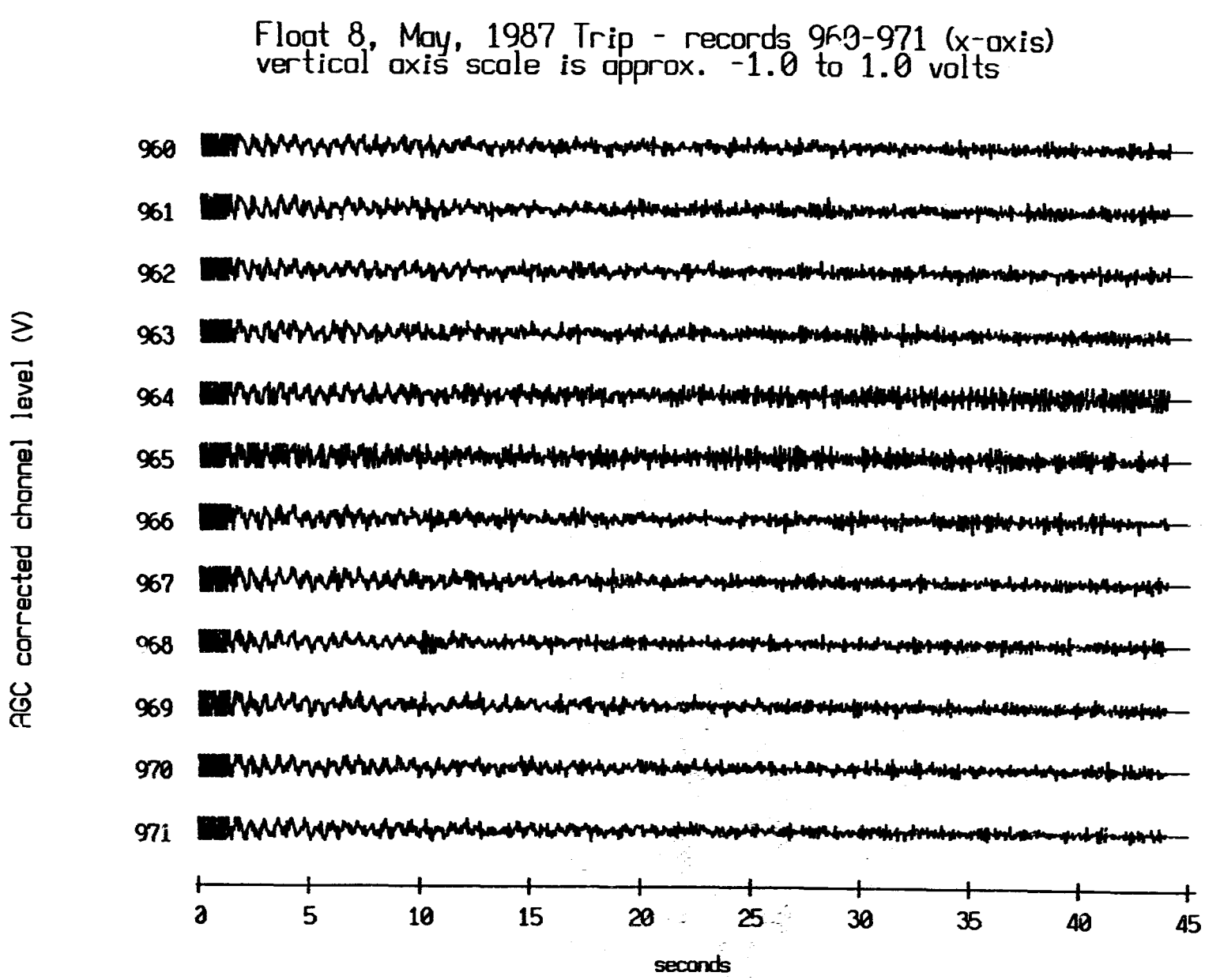

Figure II.29i

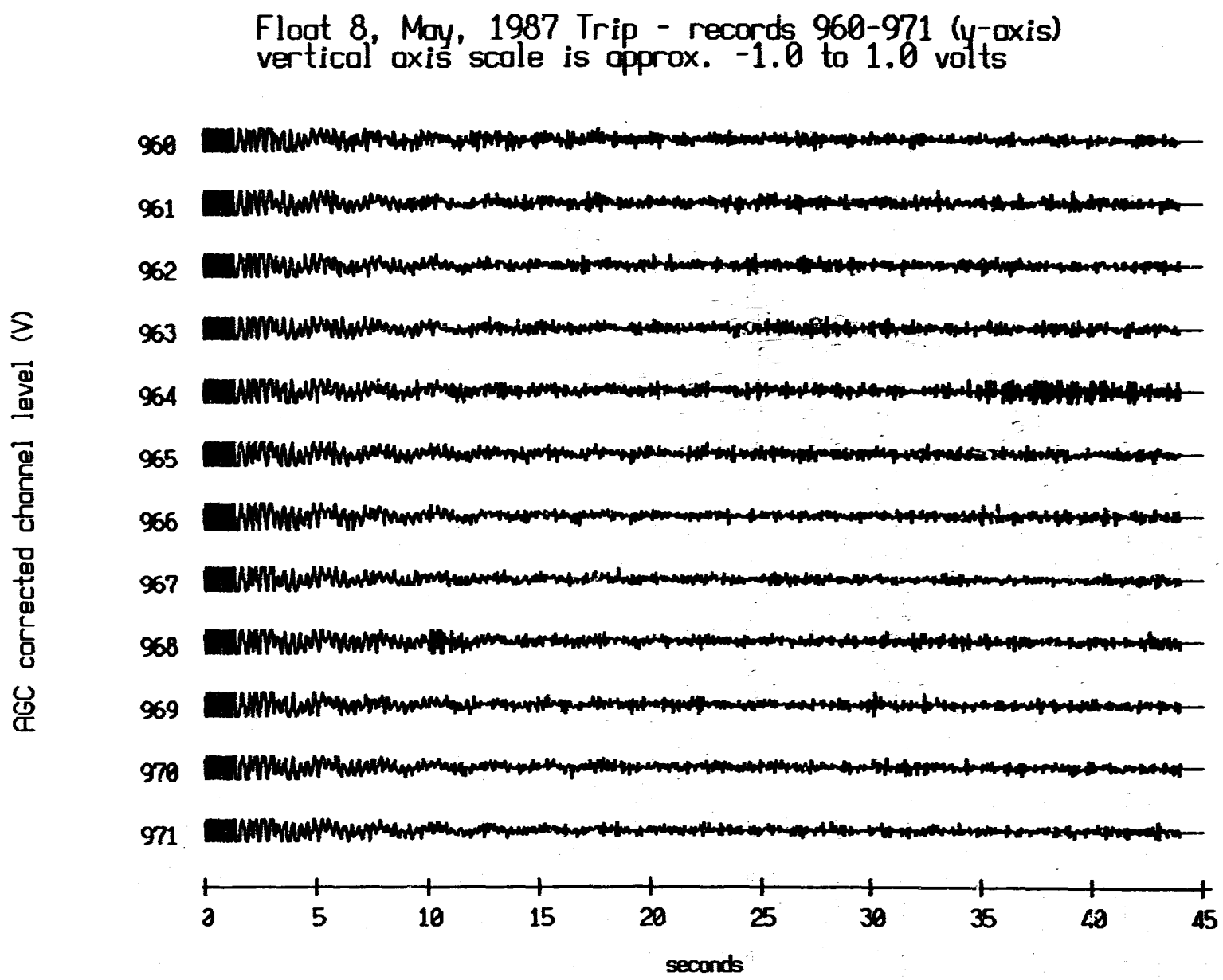

Figure II.29j

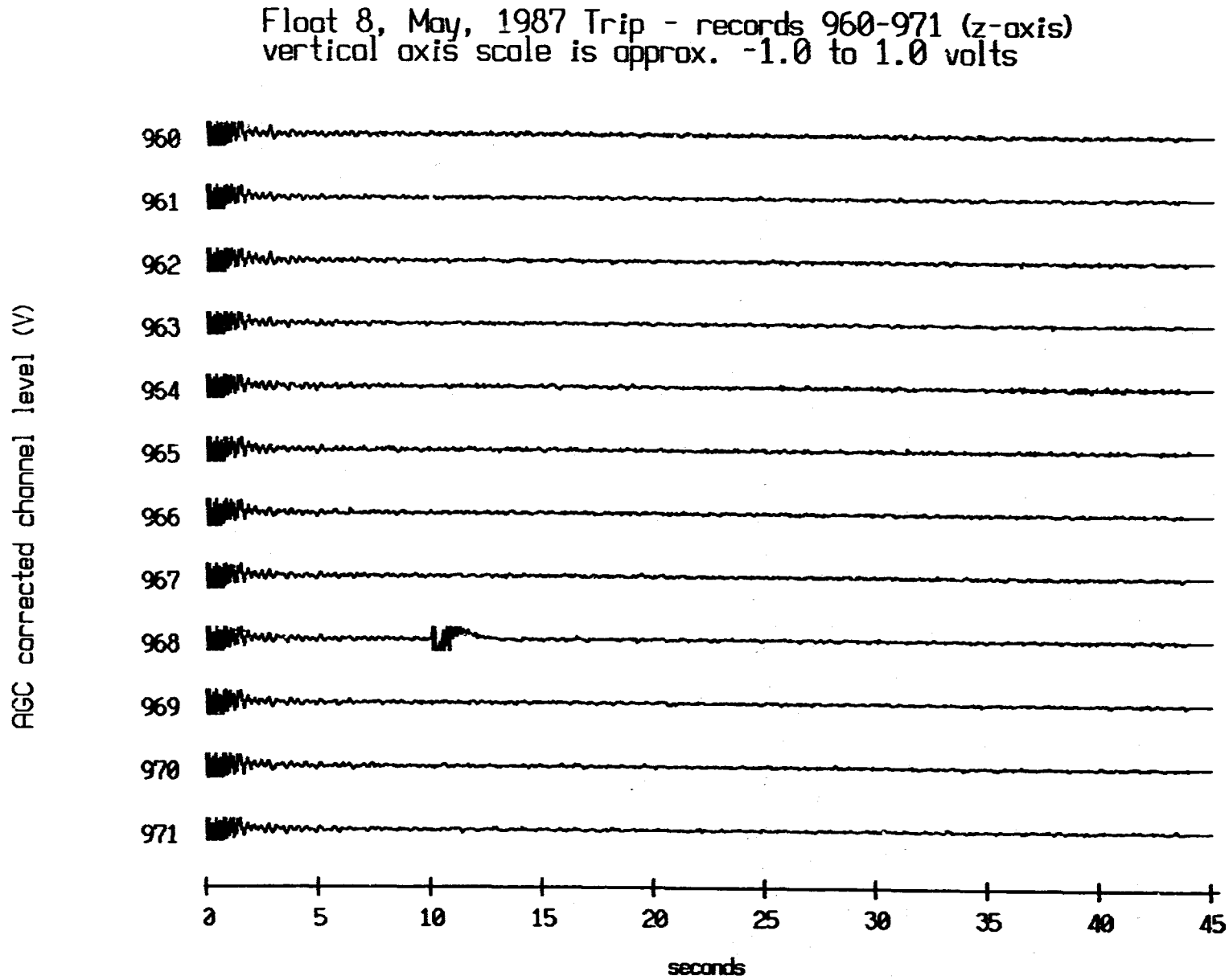

Figure II.20k

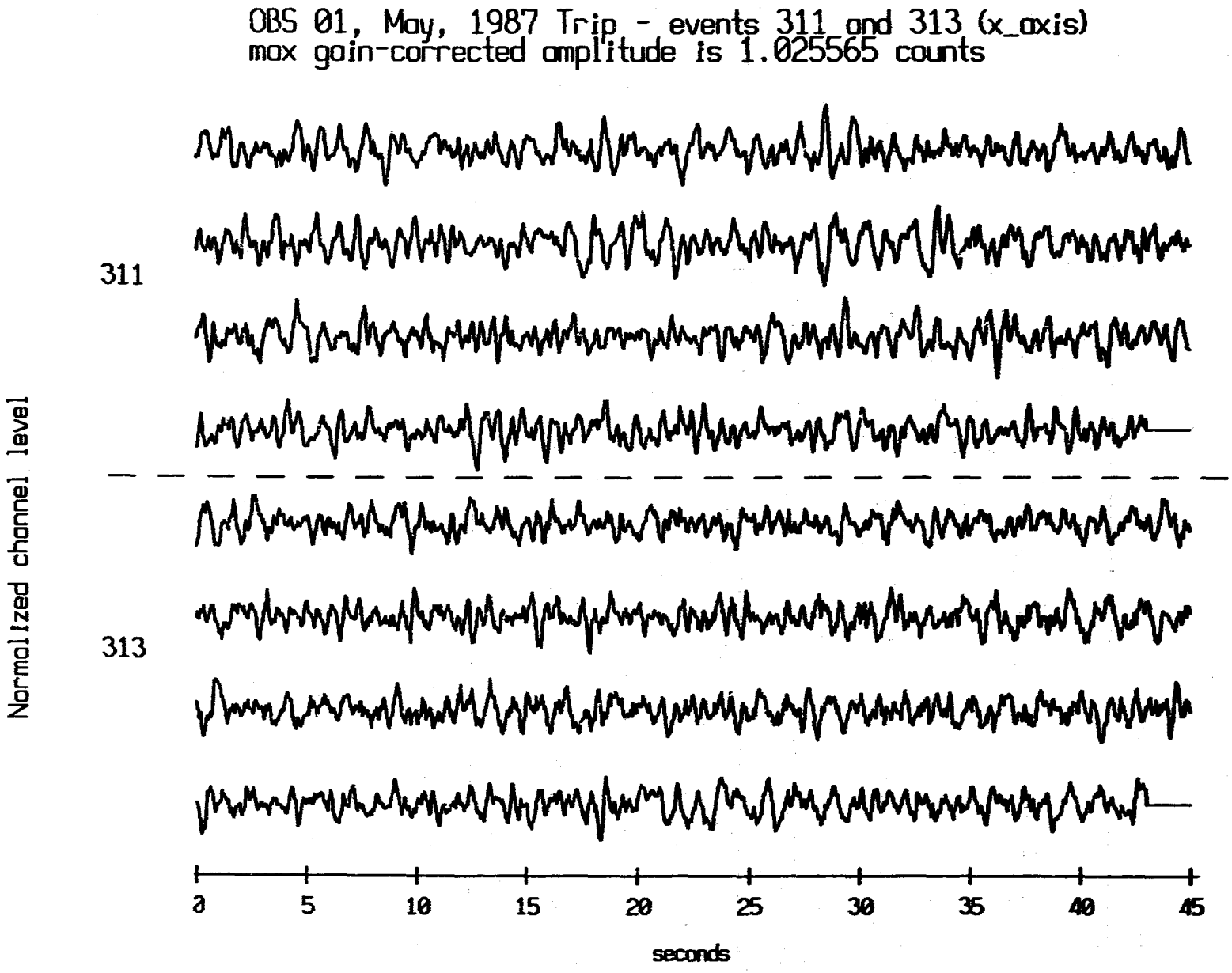

Figure II.30i

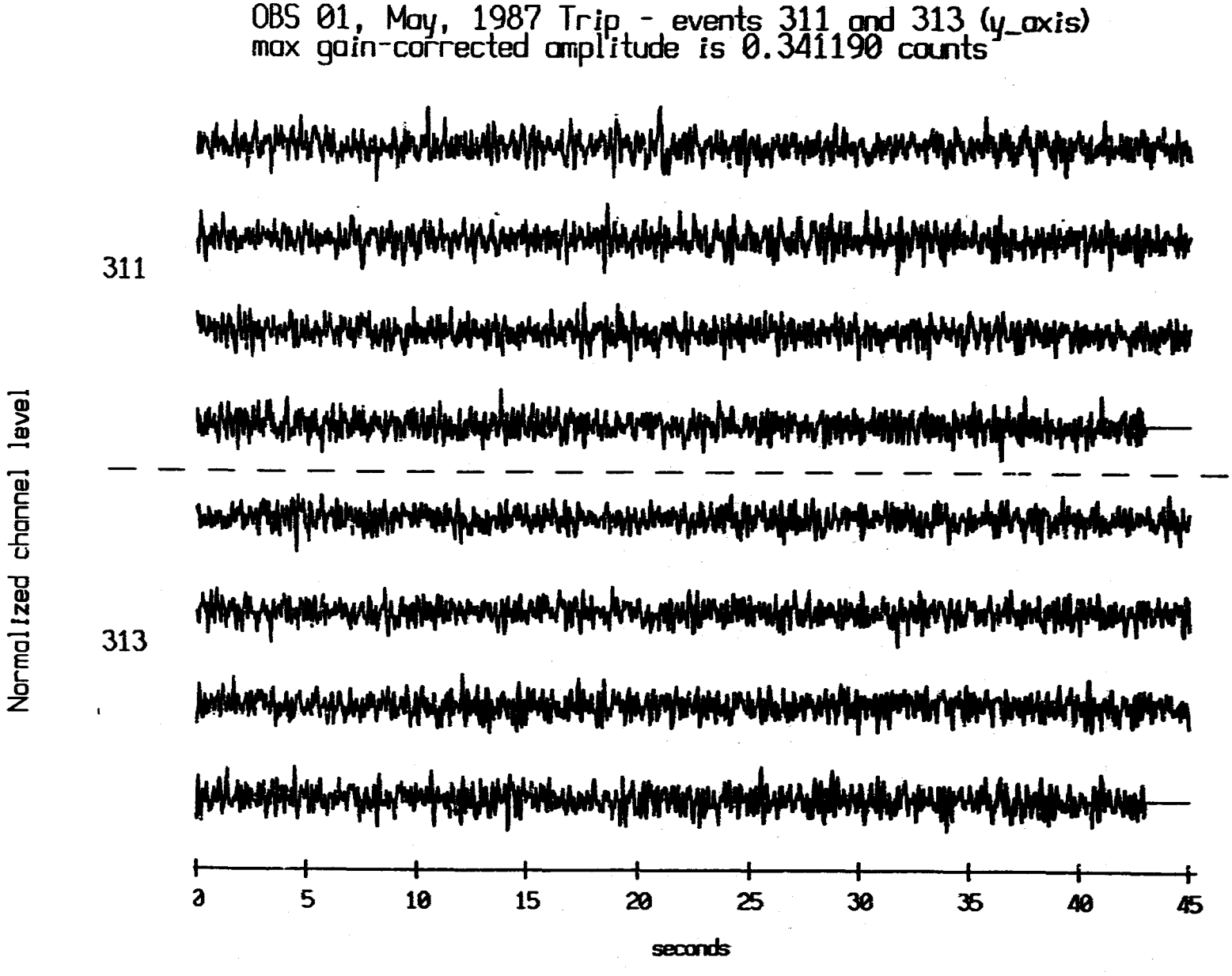

Figure II.30j

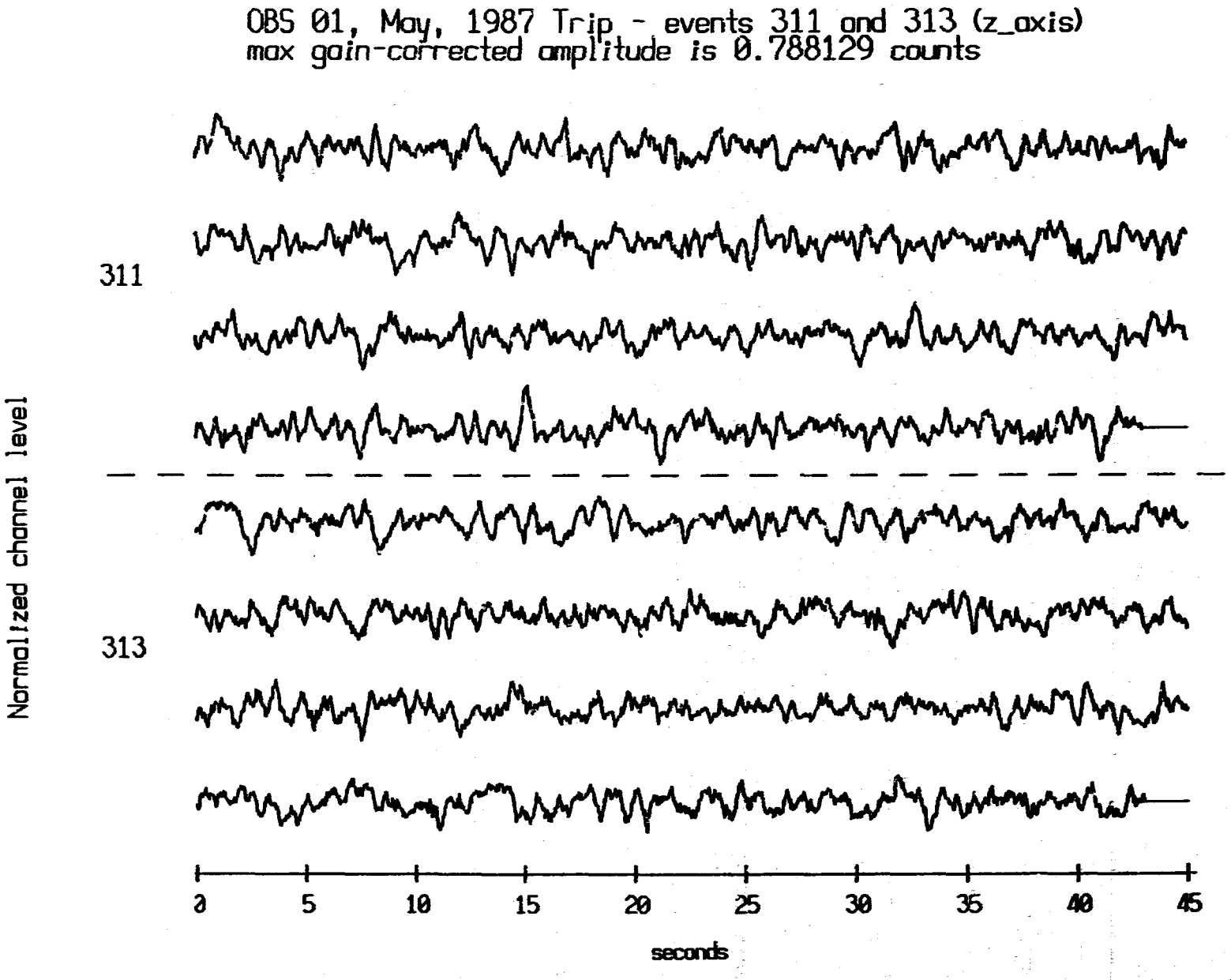

Figure II.30k

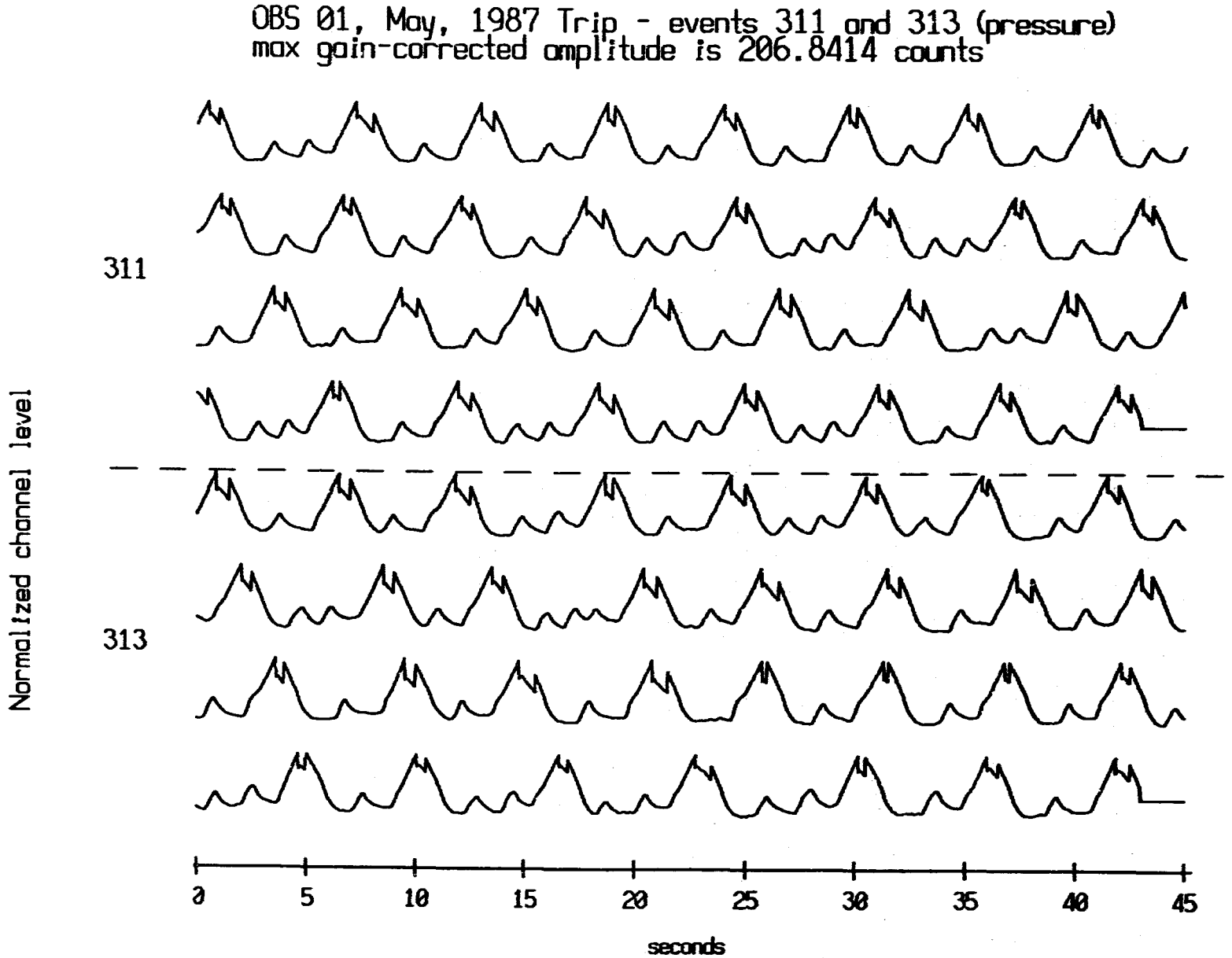

Figure II.301

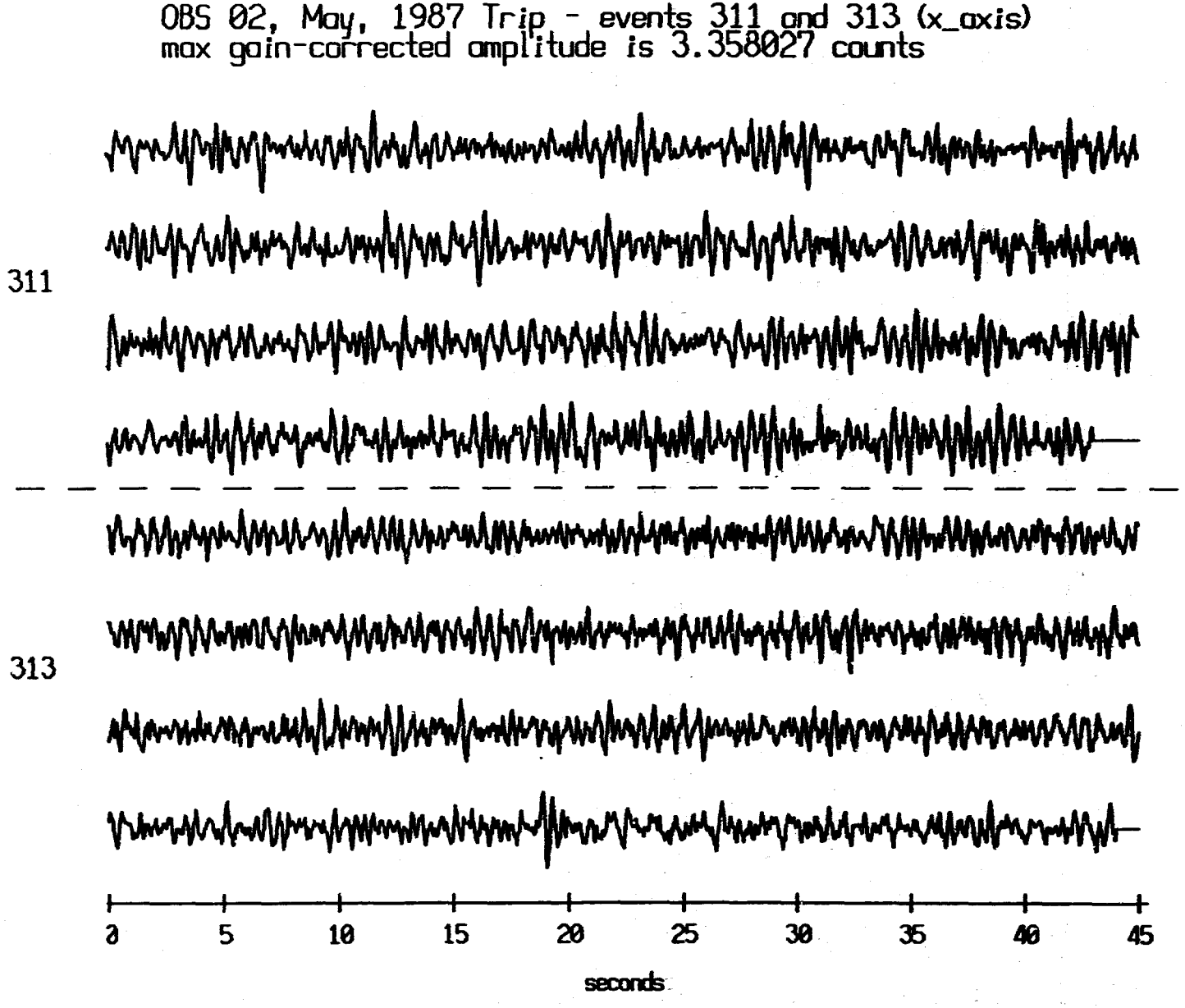

Figure II.31i

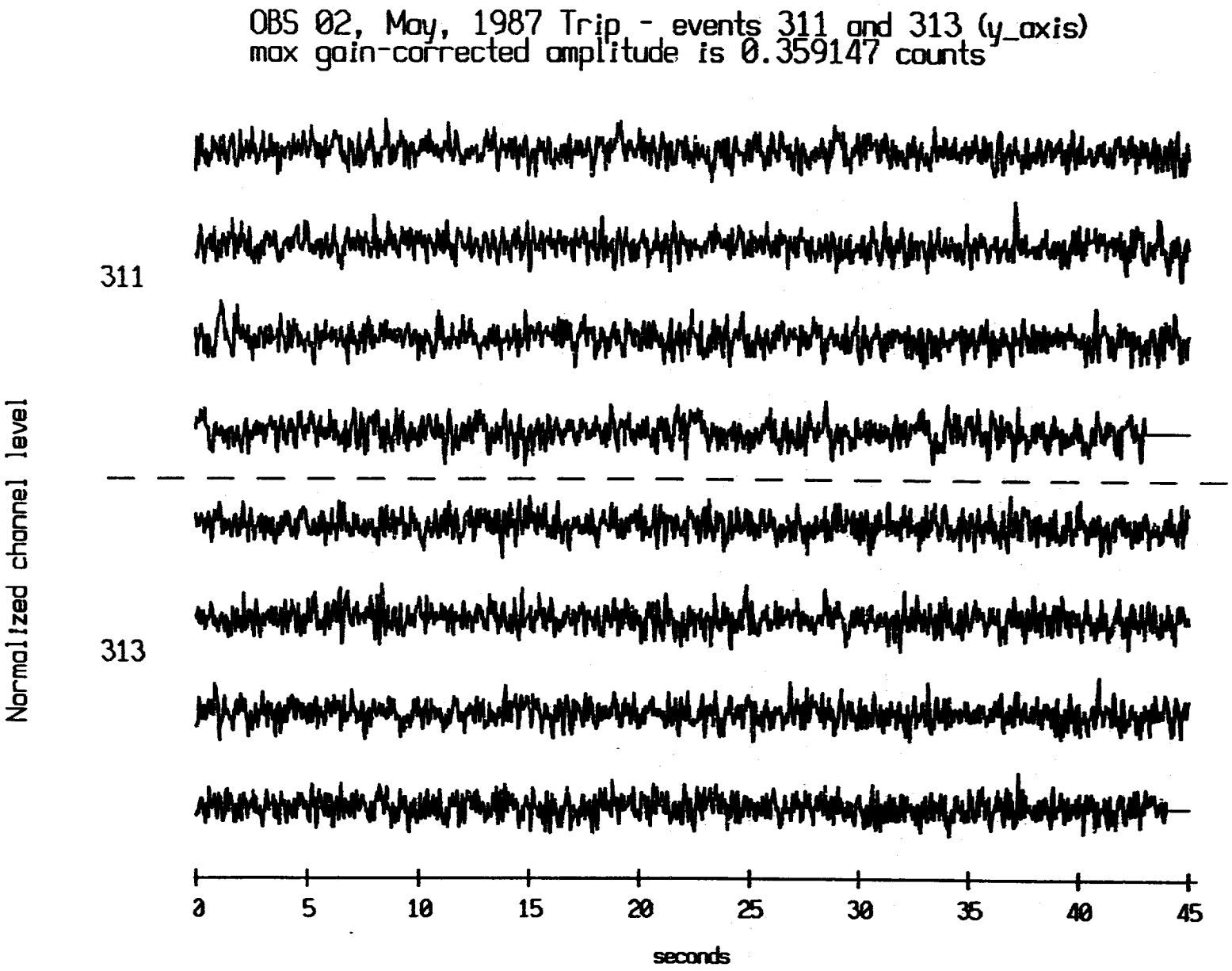

Figure II.31j

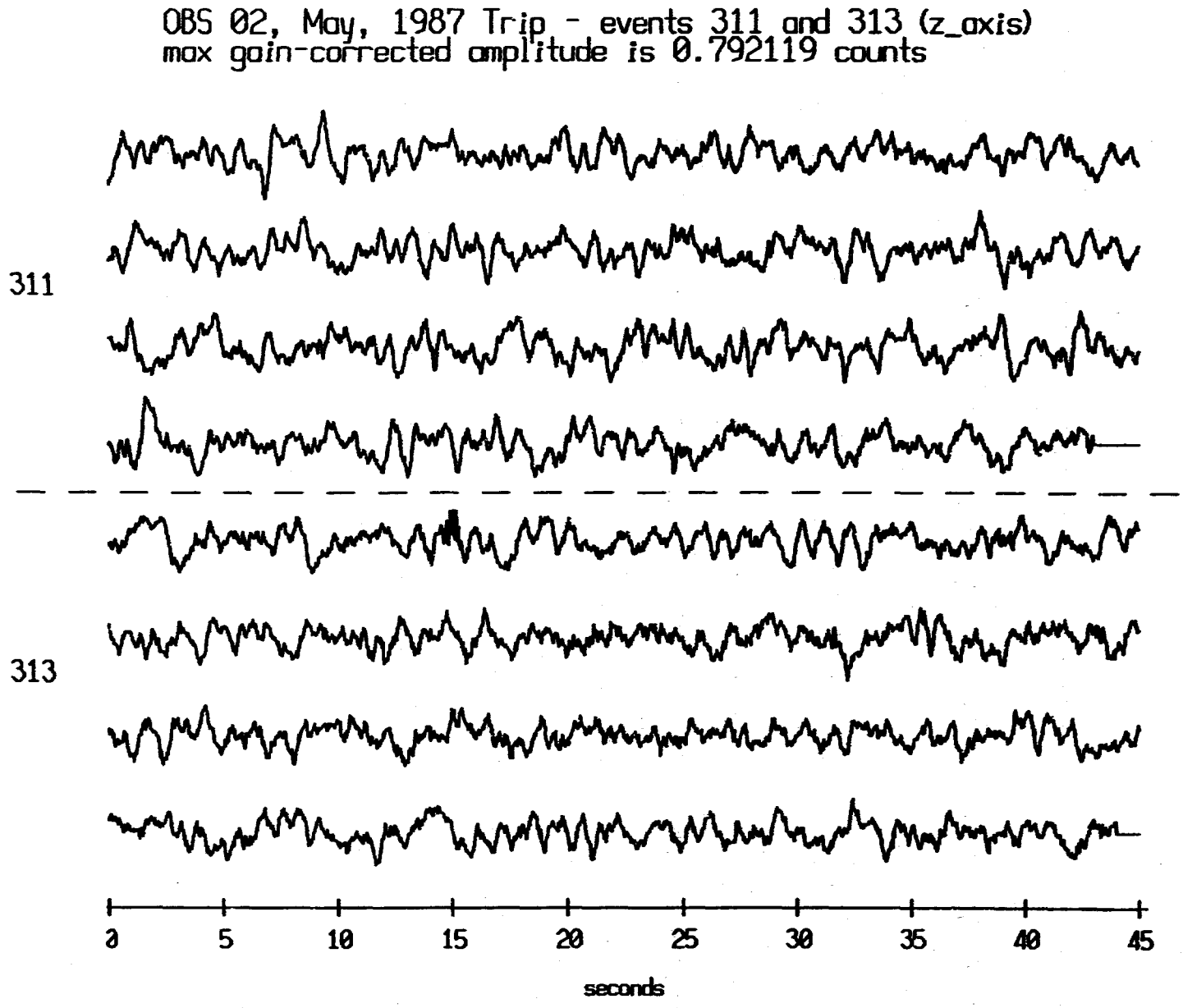

Figure II.31k

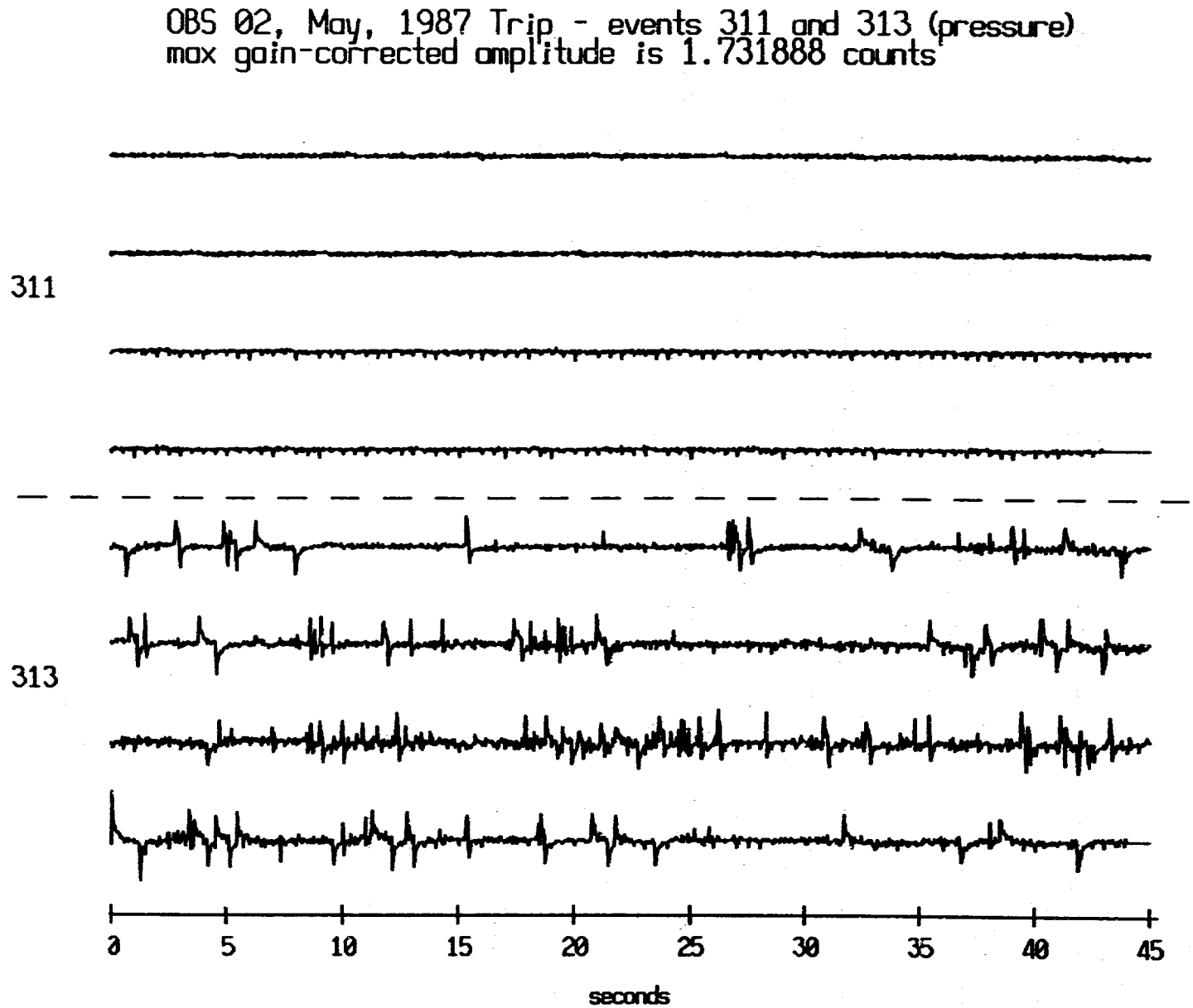

Figure II.31l

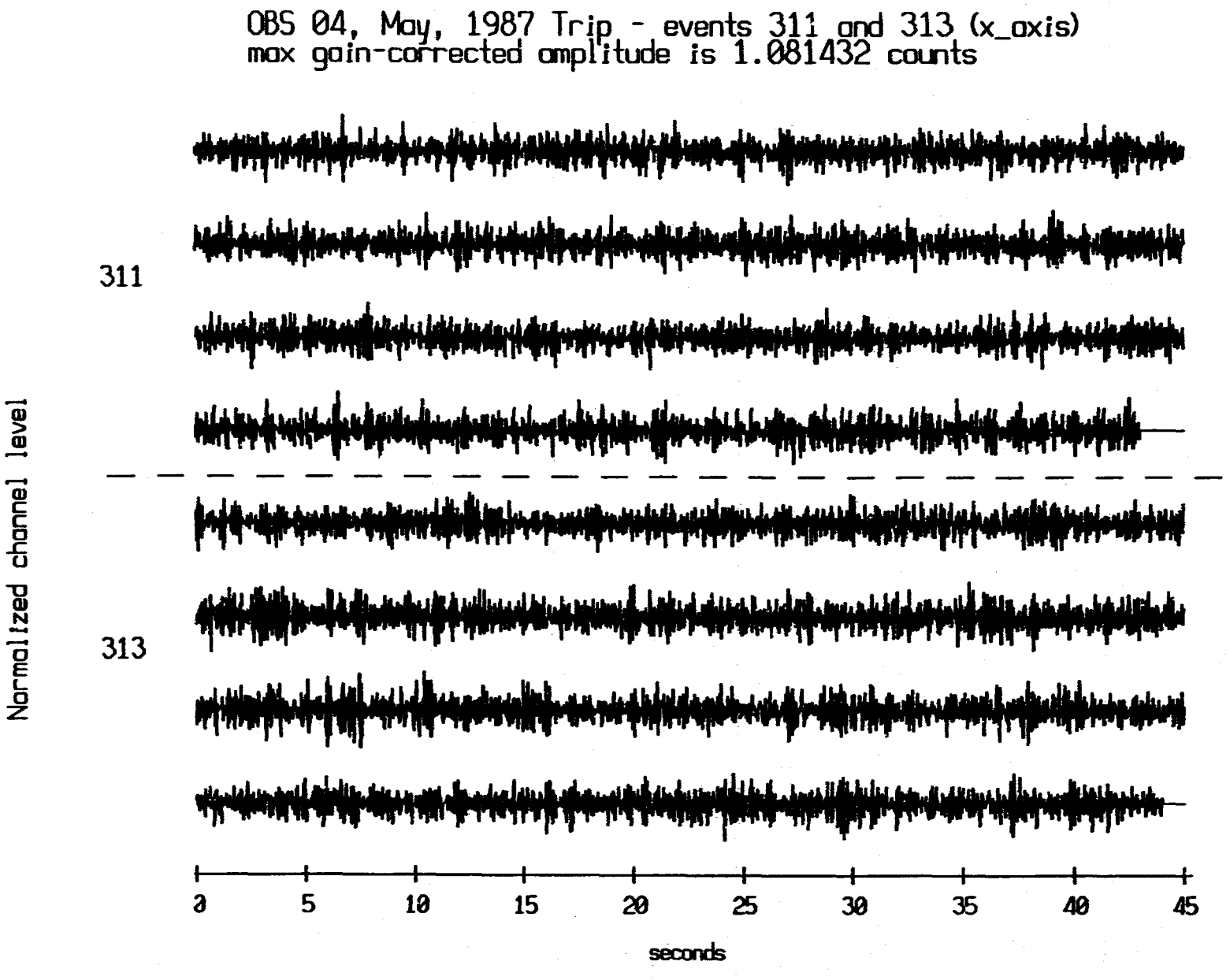

Figure II.32i

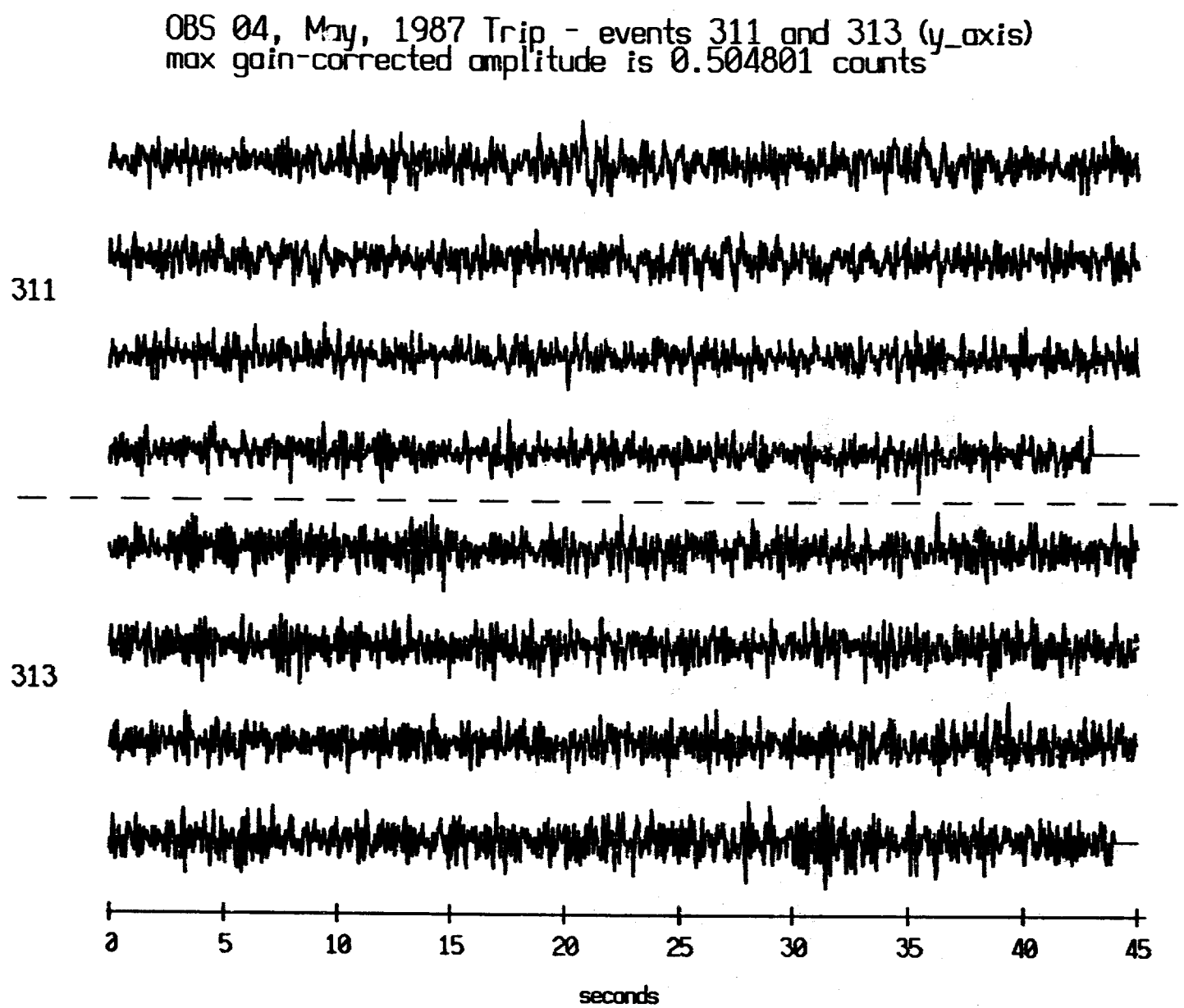

Figure II.32j

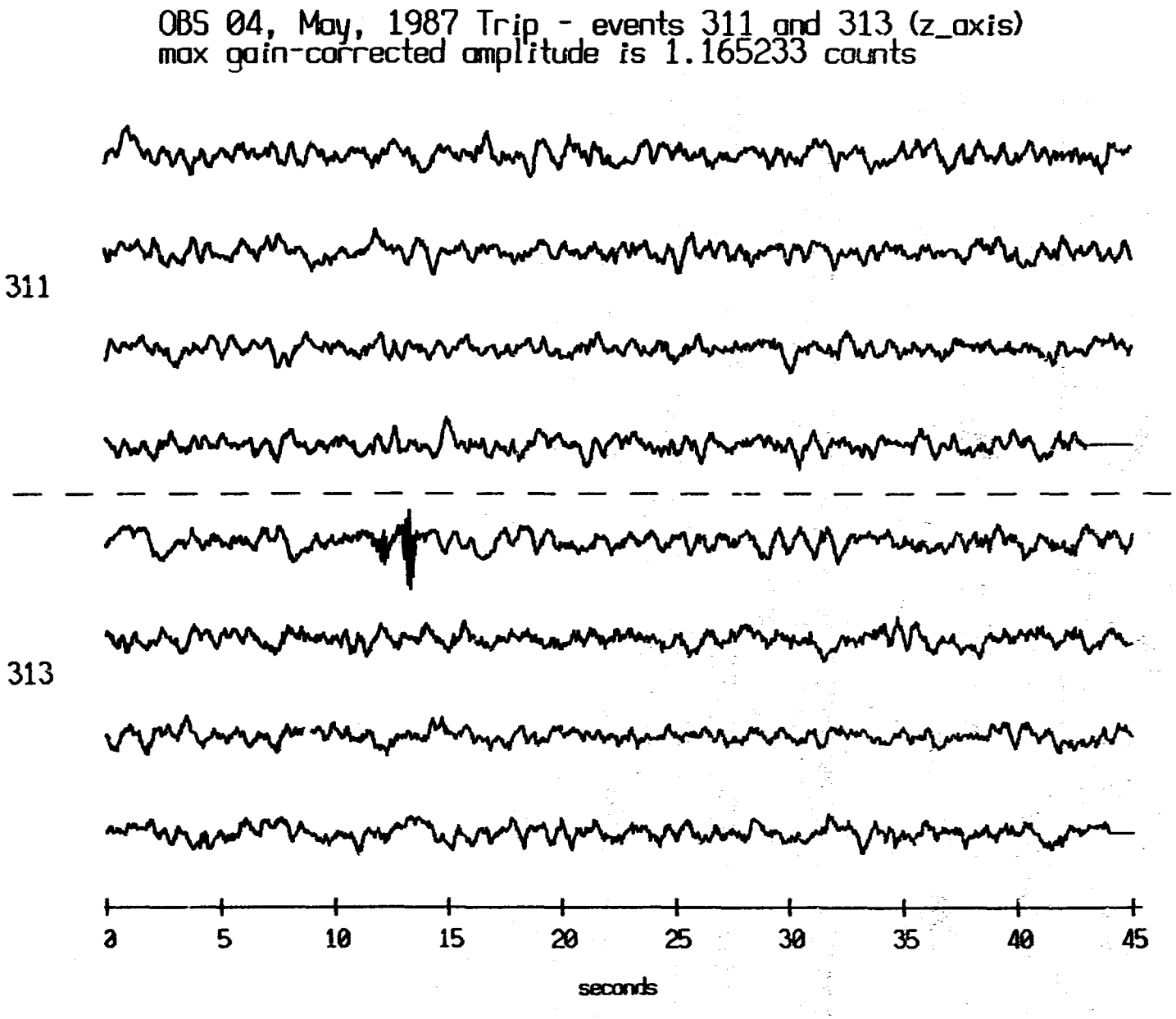

Figure II.32k

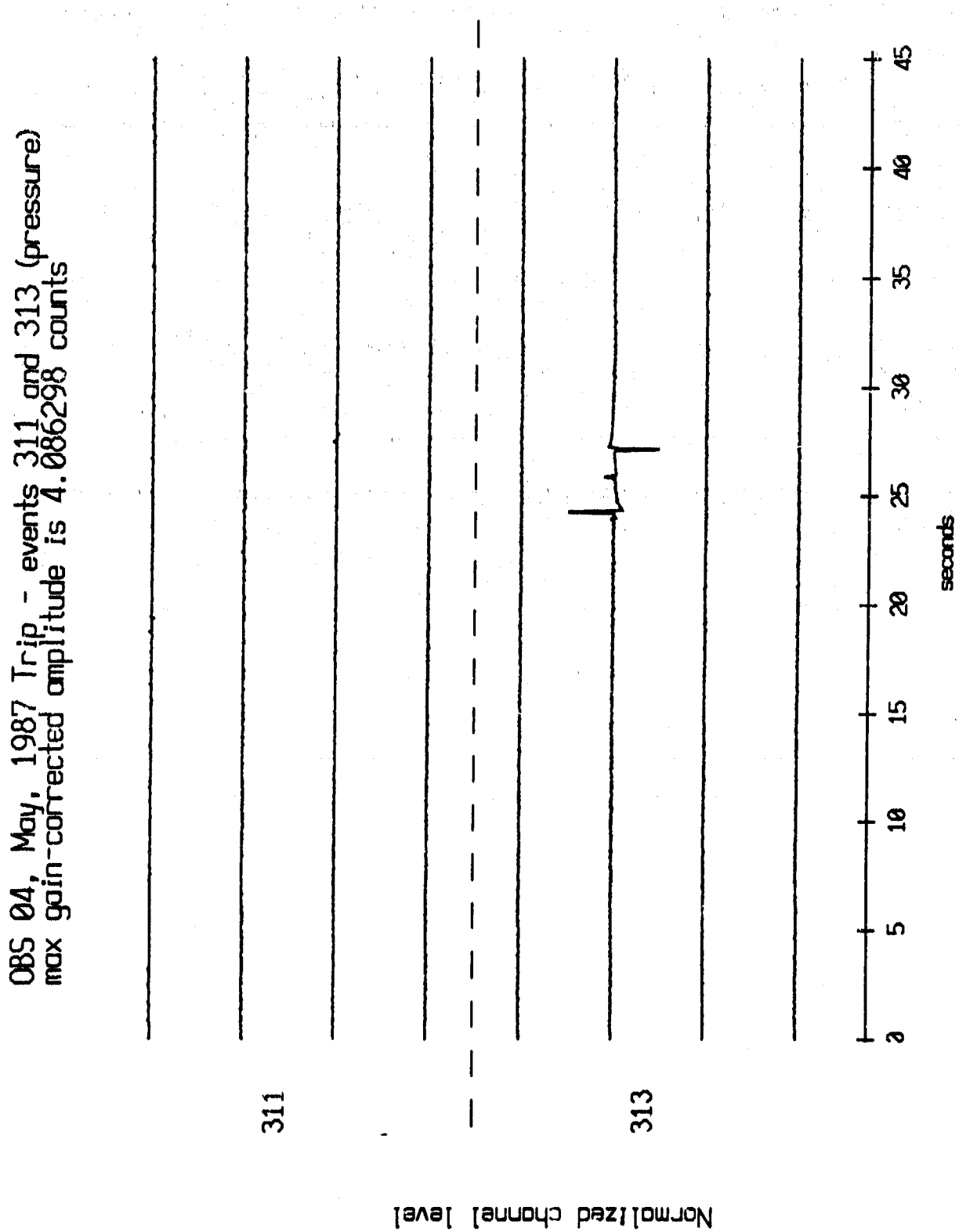

Figure II.321

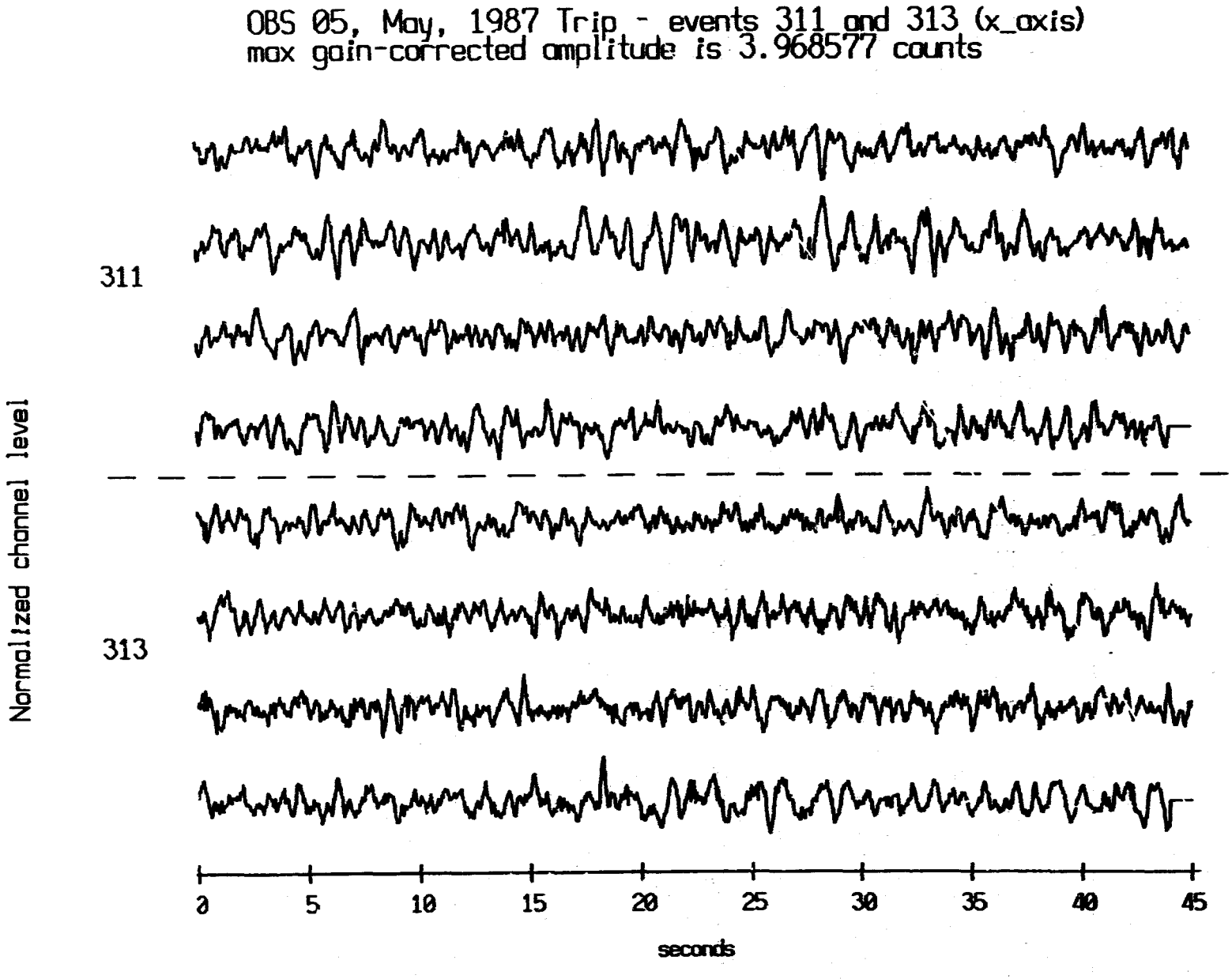
OBS 05, May, 1987 Trip - events 311 and 313 (x_axis)
max gain-corrected amplitude is 3.968577 counts
311
313
Normalized channel level
0
5
10
15
20
25
30
35
40
45
seconds

Figure II.31

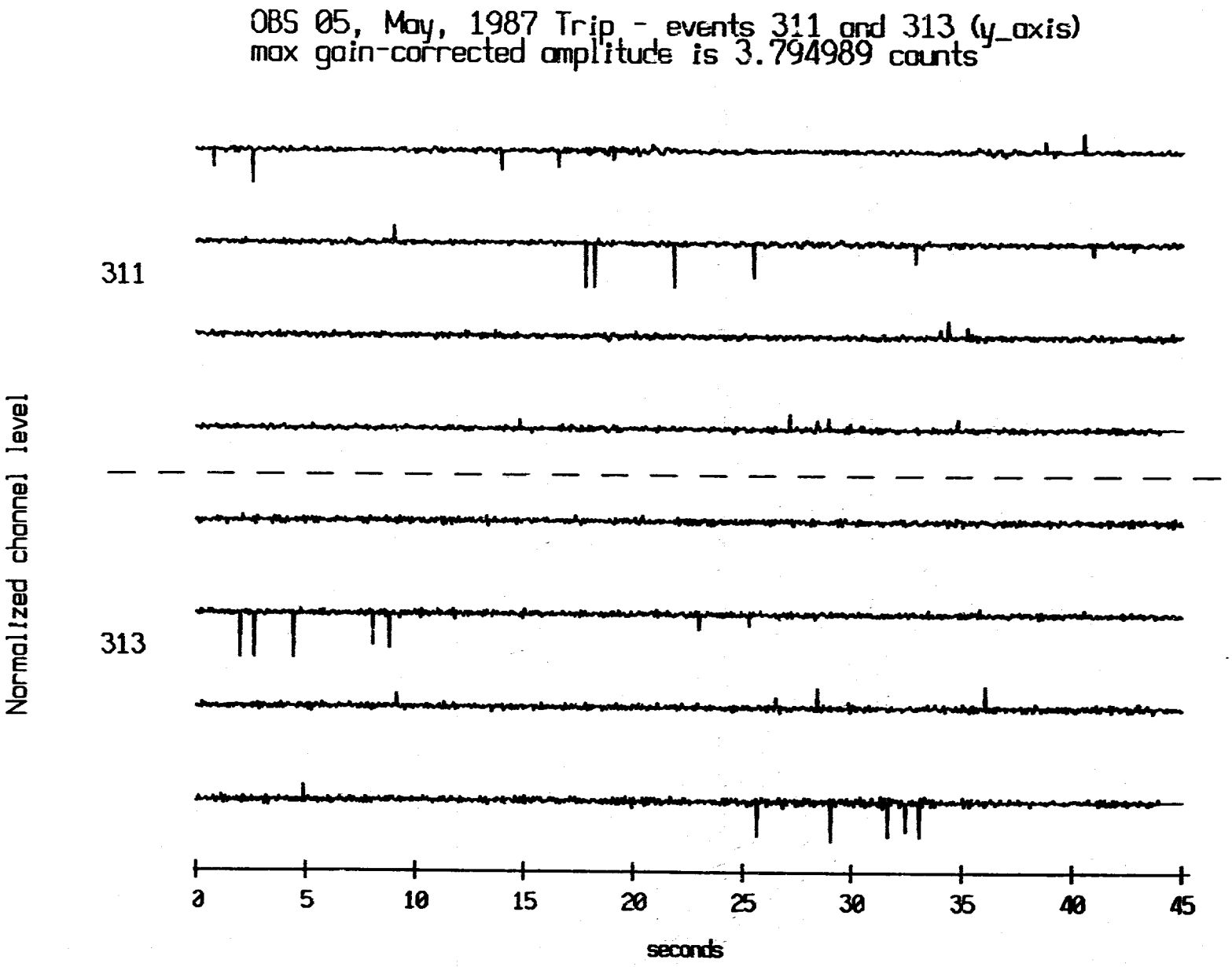

Figure II.33j

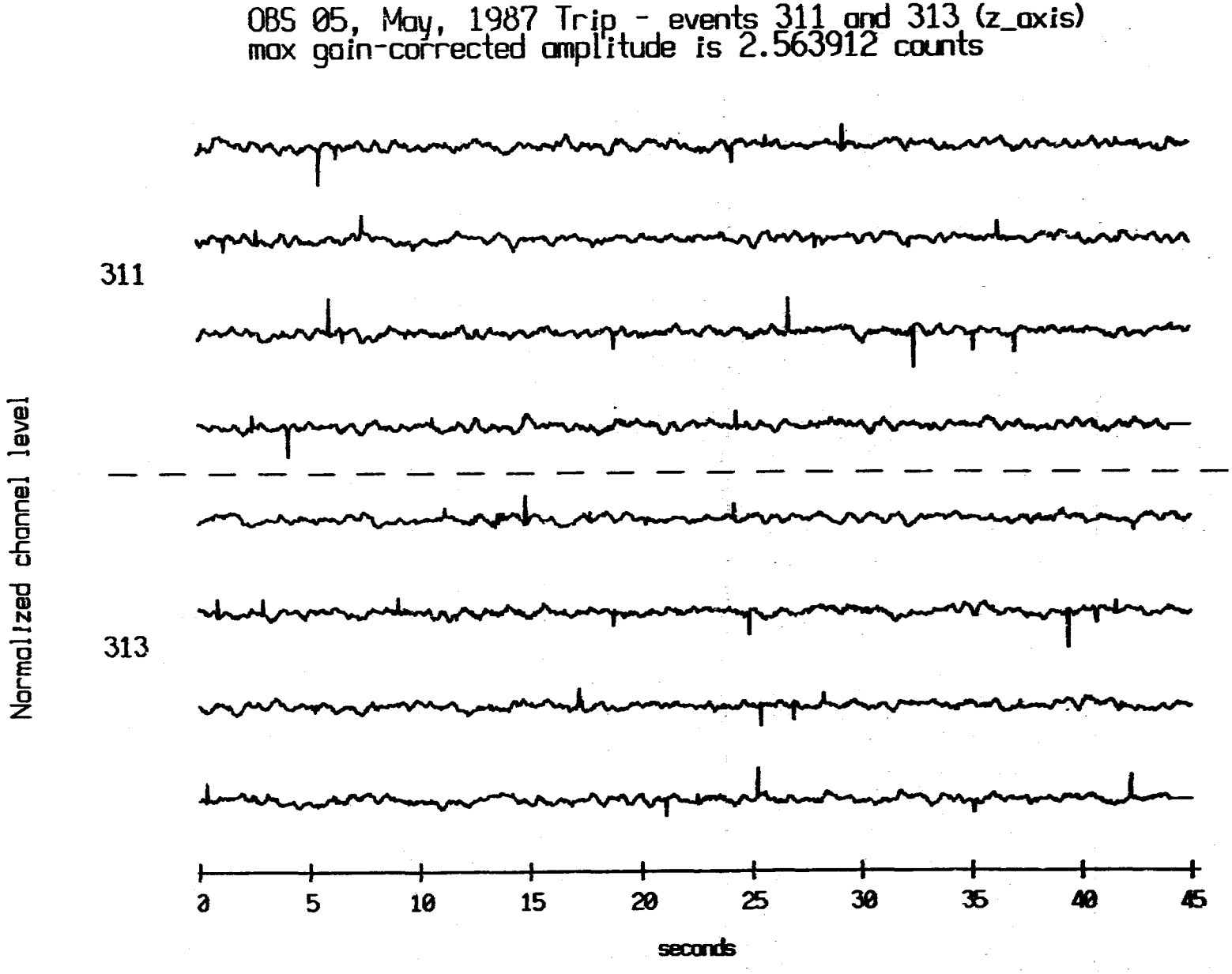

Figure II.33k

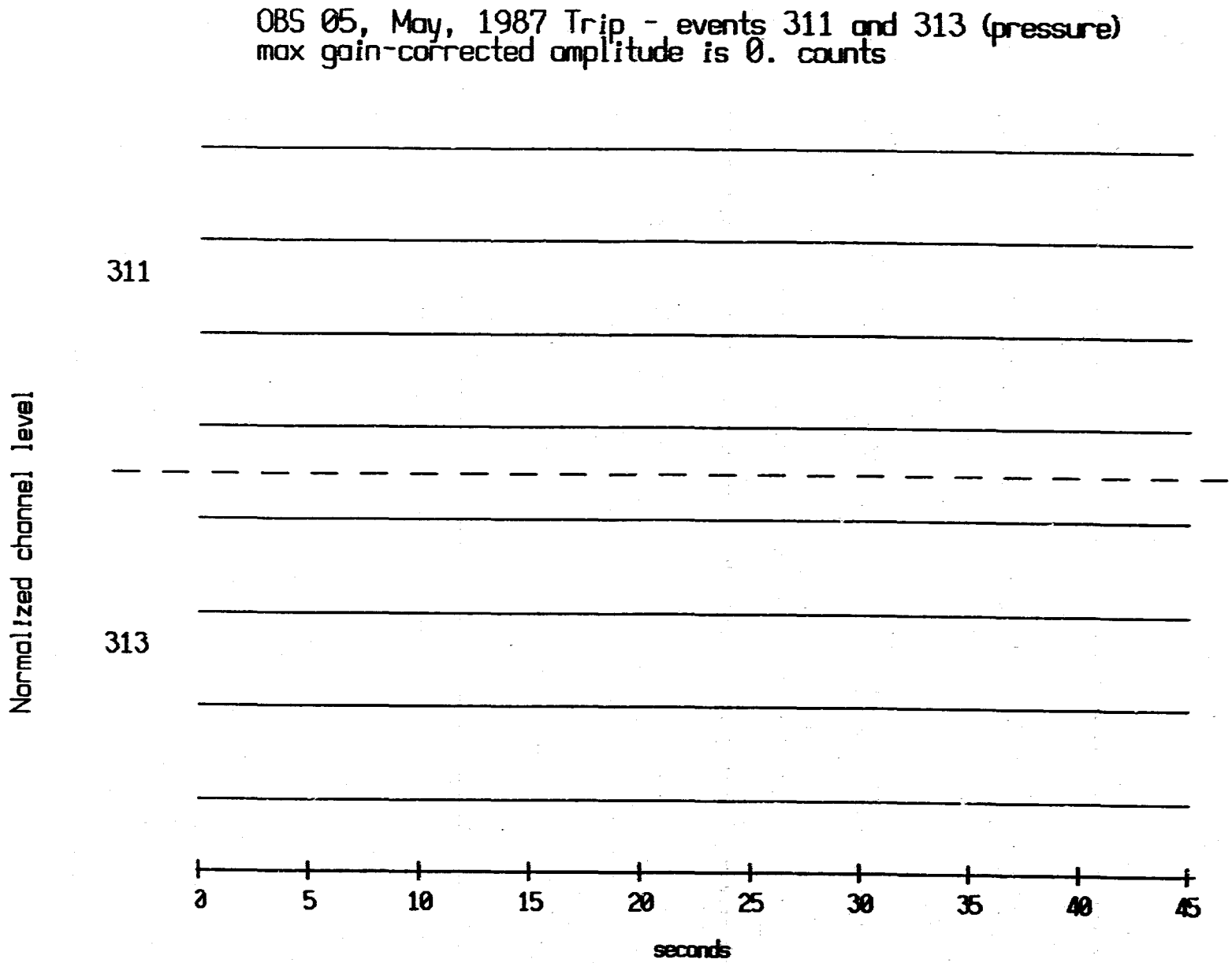

Figure II.33l

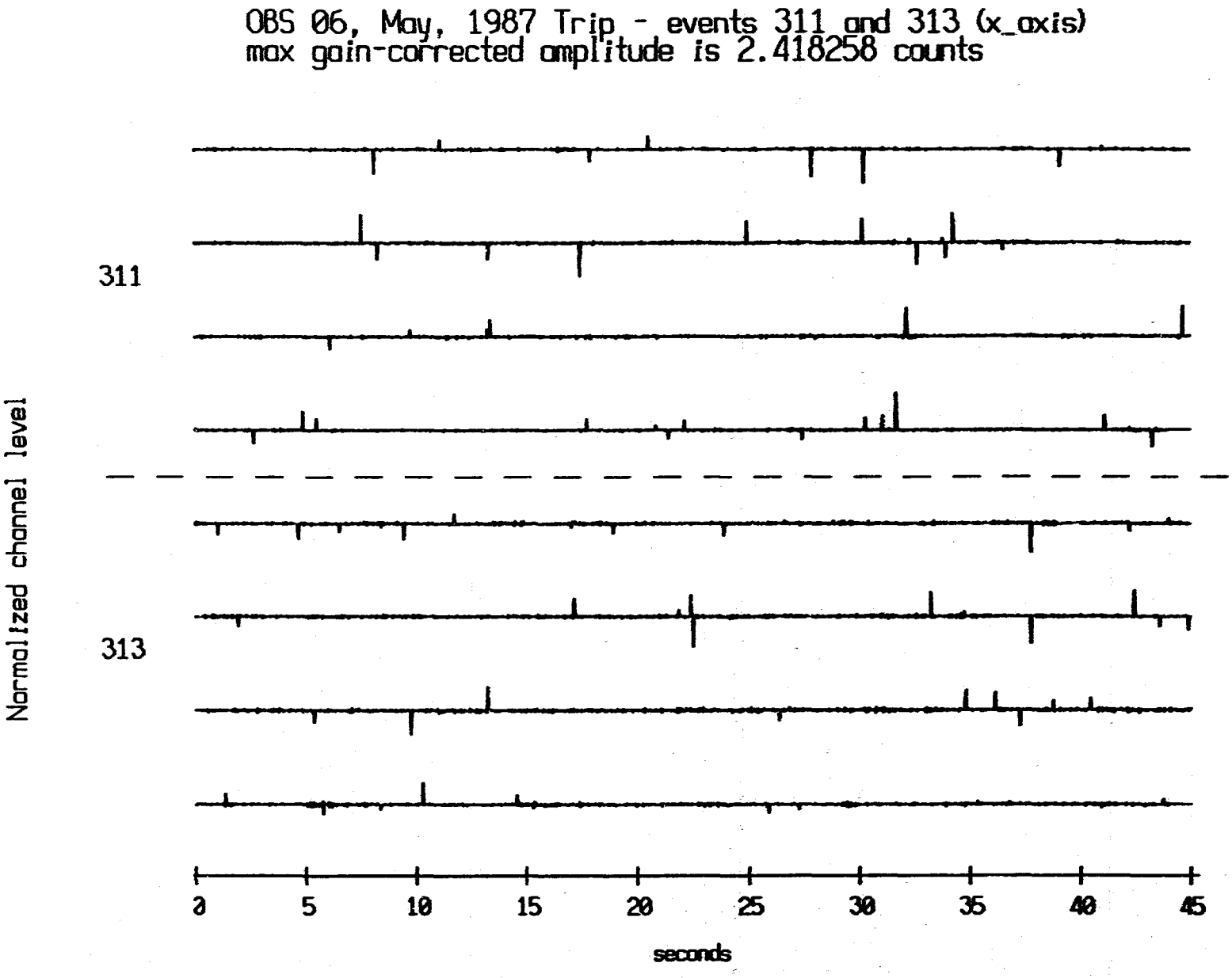

Figure II.34i

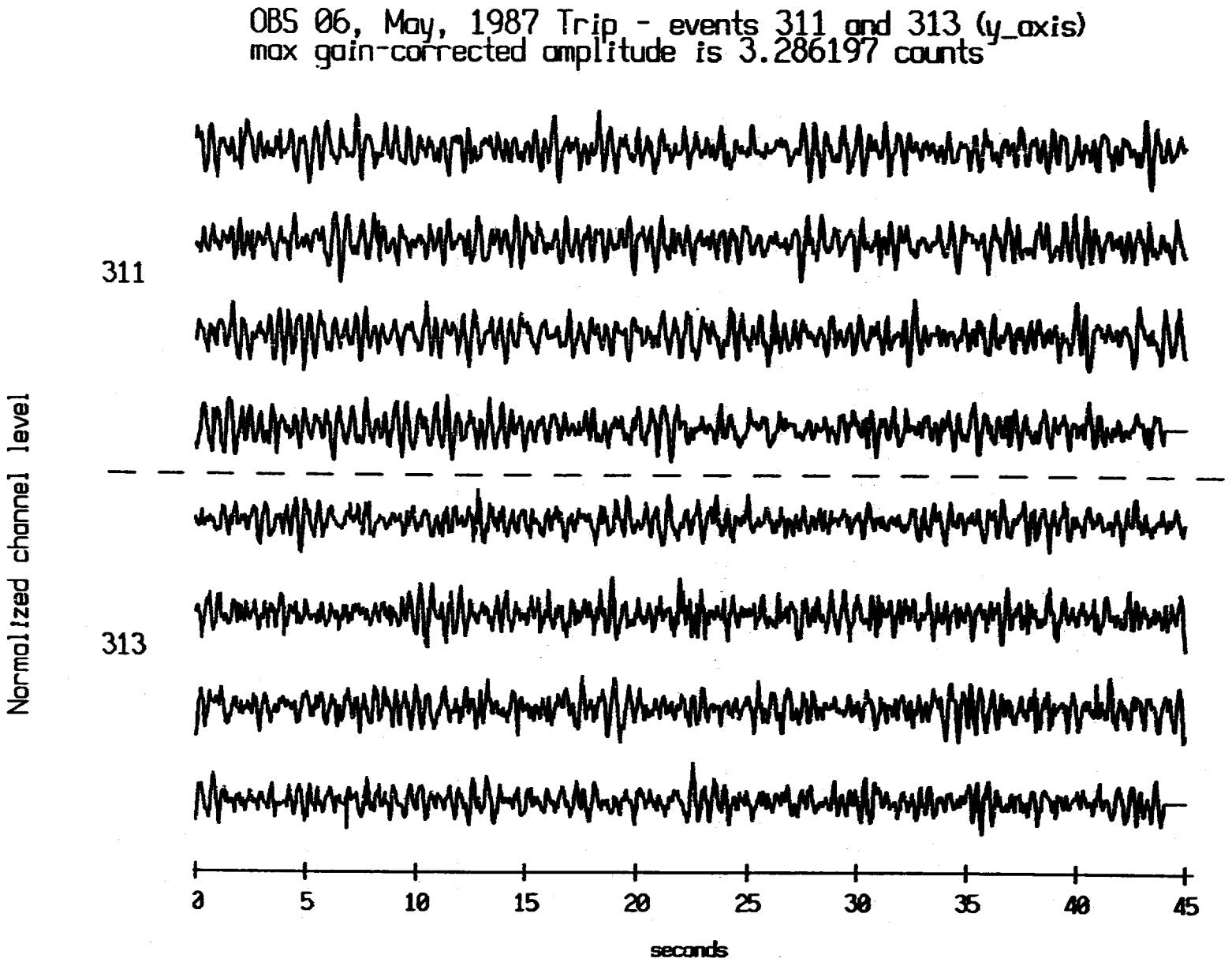

Figure II.34j

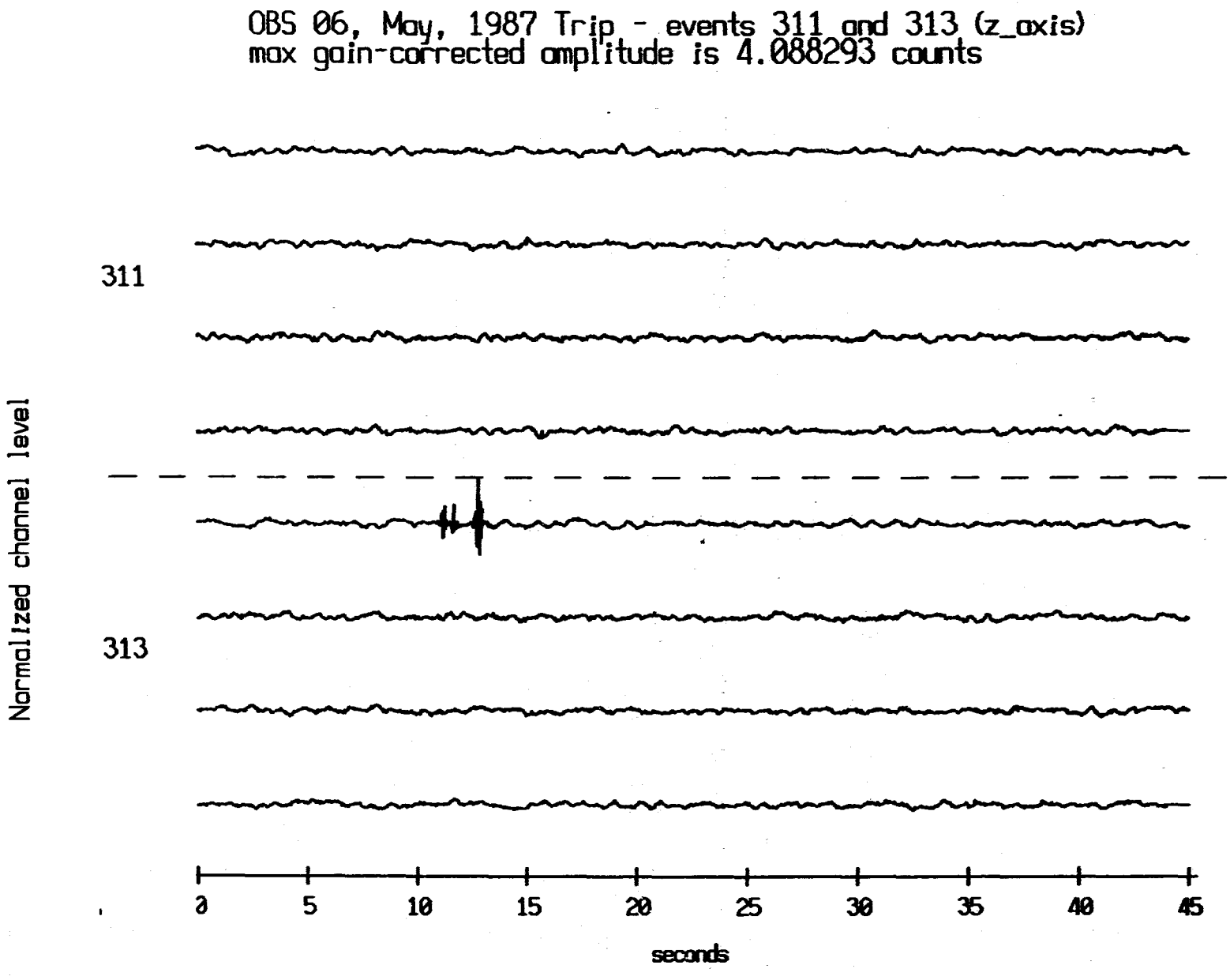

Figure II.34k

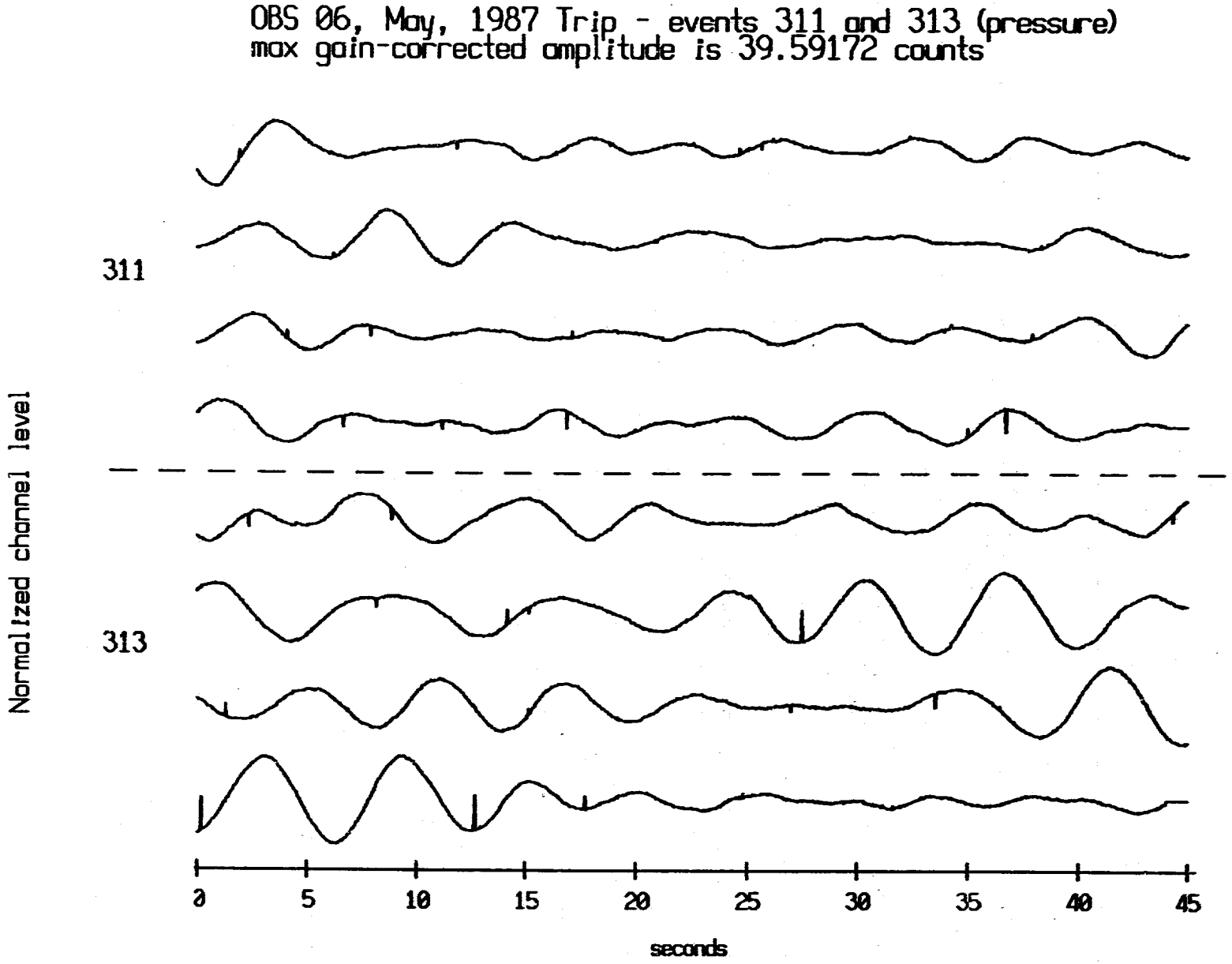
OBS 06, May, 1987 Trip - events 311 and 313 (pressure)
max gain-corrected amplitude is 39.59172 counts
311
313
Normalized channel level
0
5
10
15
20
25
30
35
40
45
seconds

Figure II.34

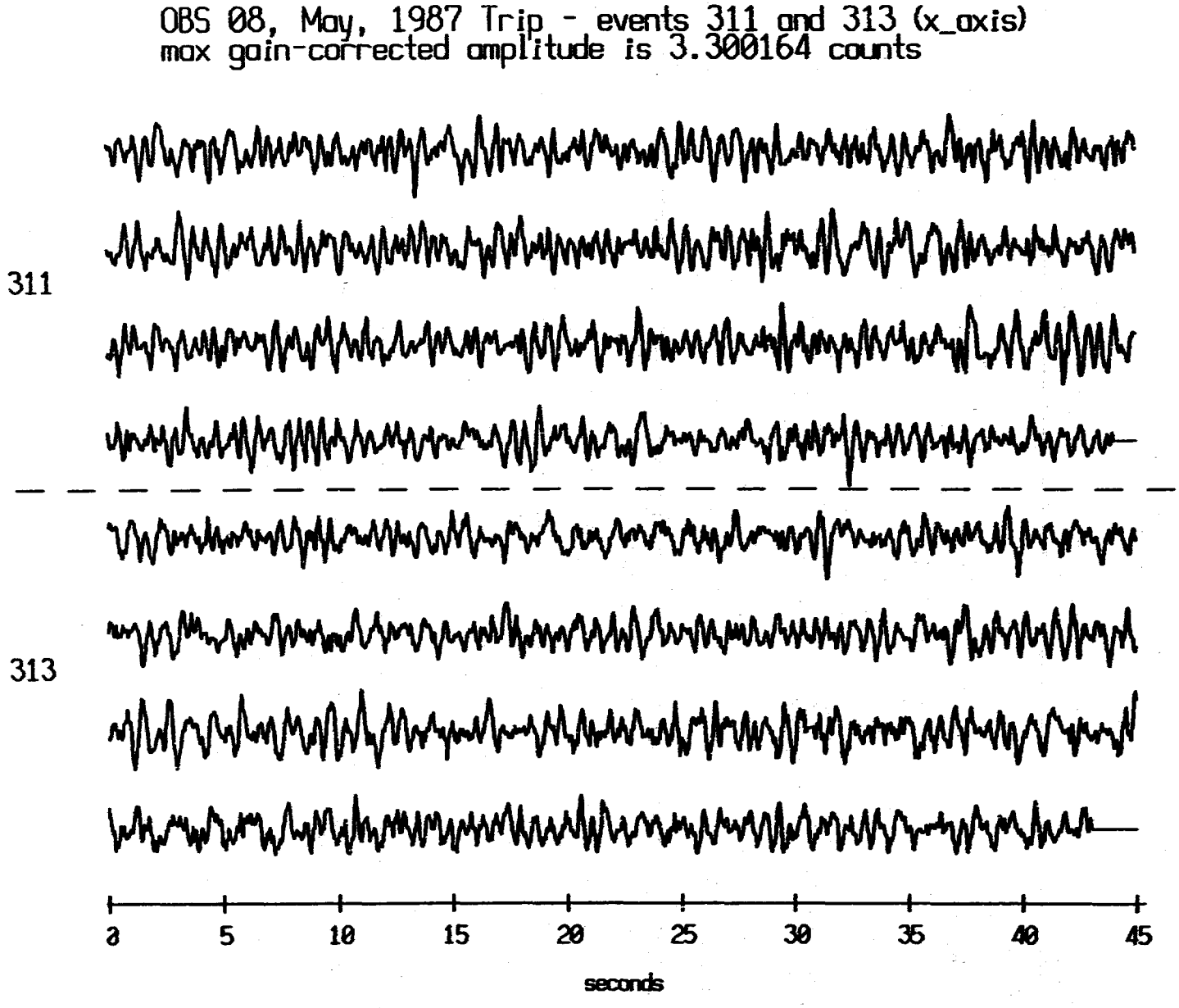

Figure II.35i

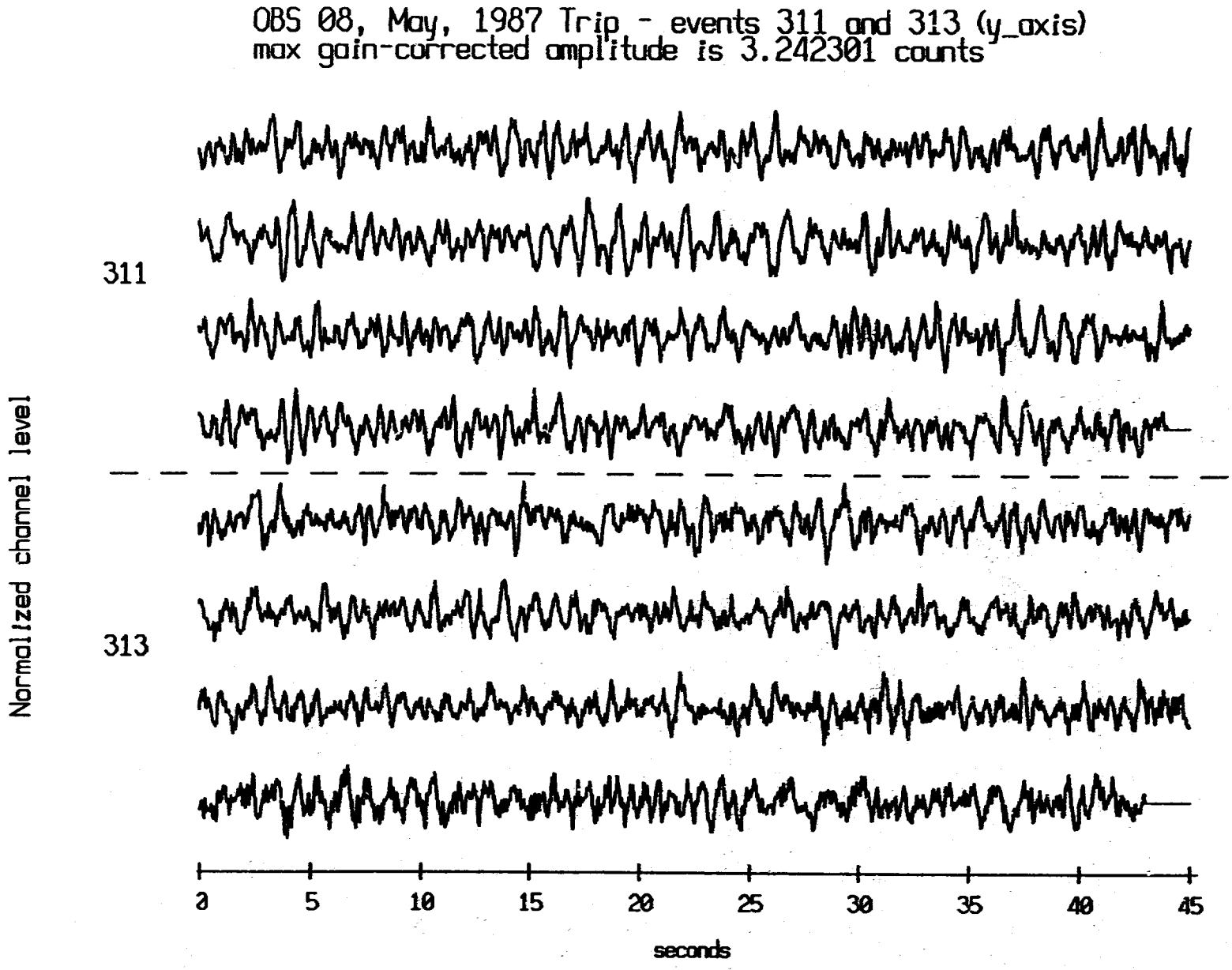

Figure II.35j

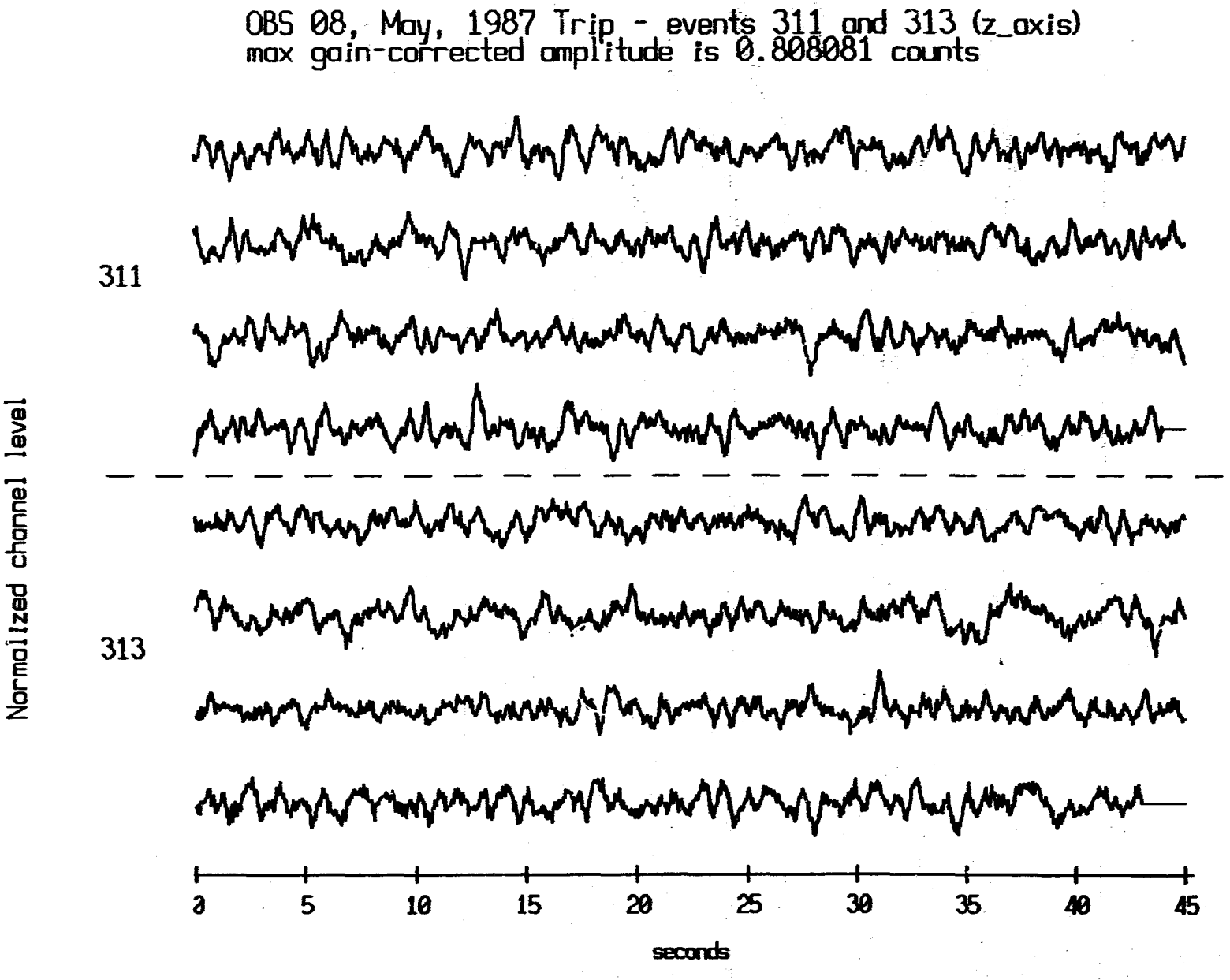

Figure II.35k

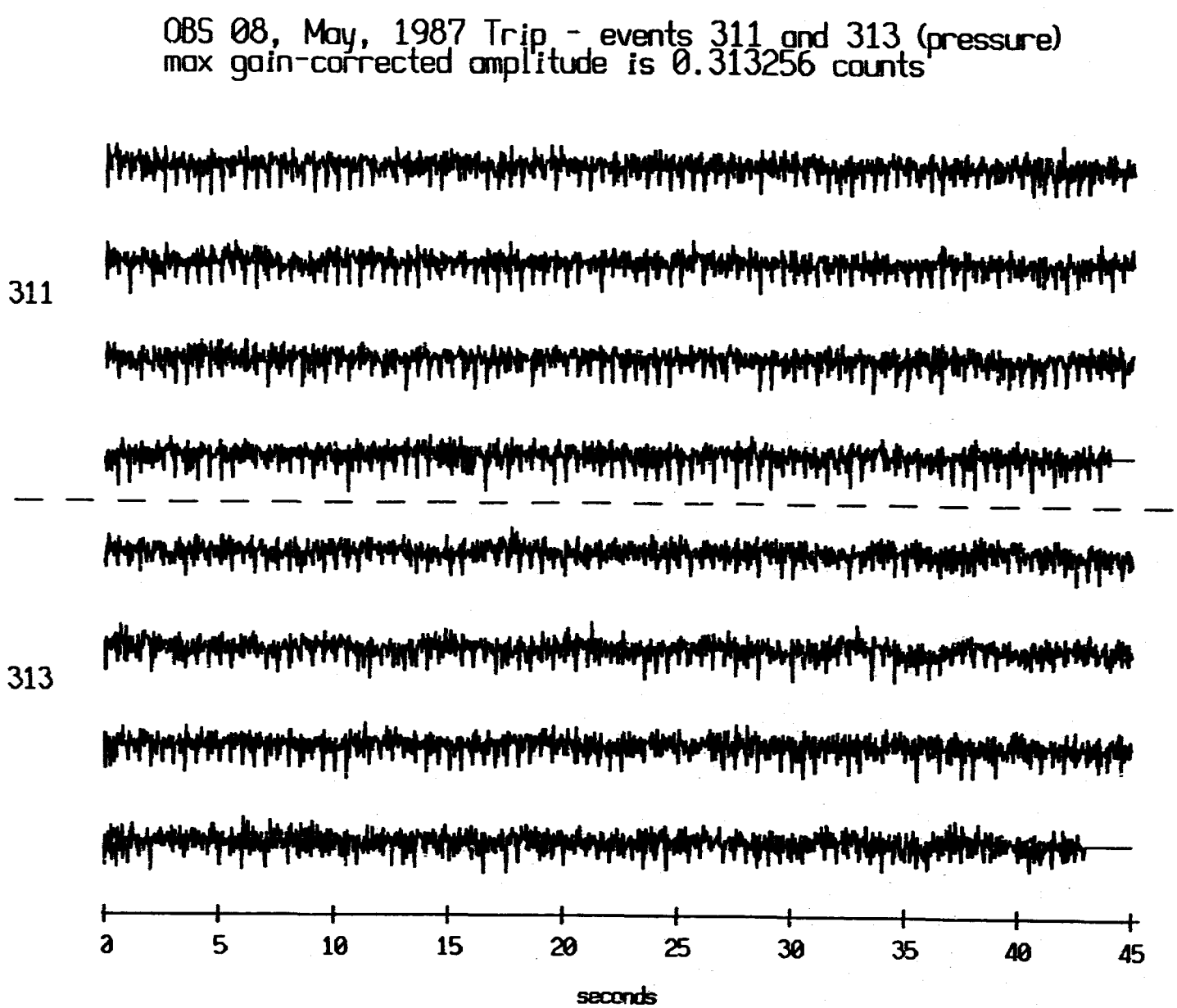

Figure II.35l

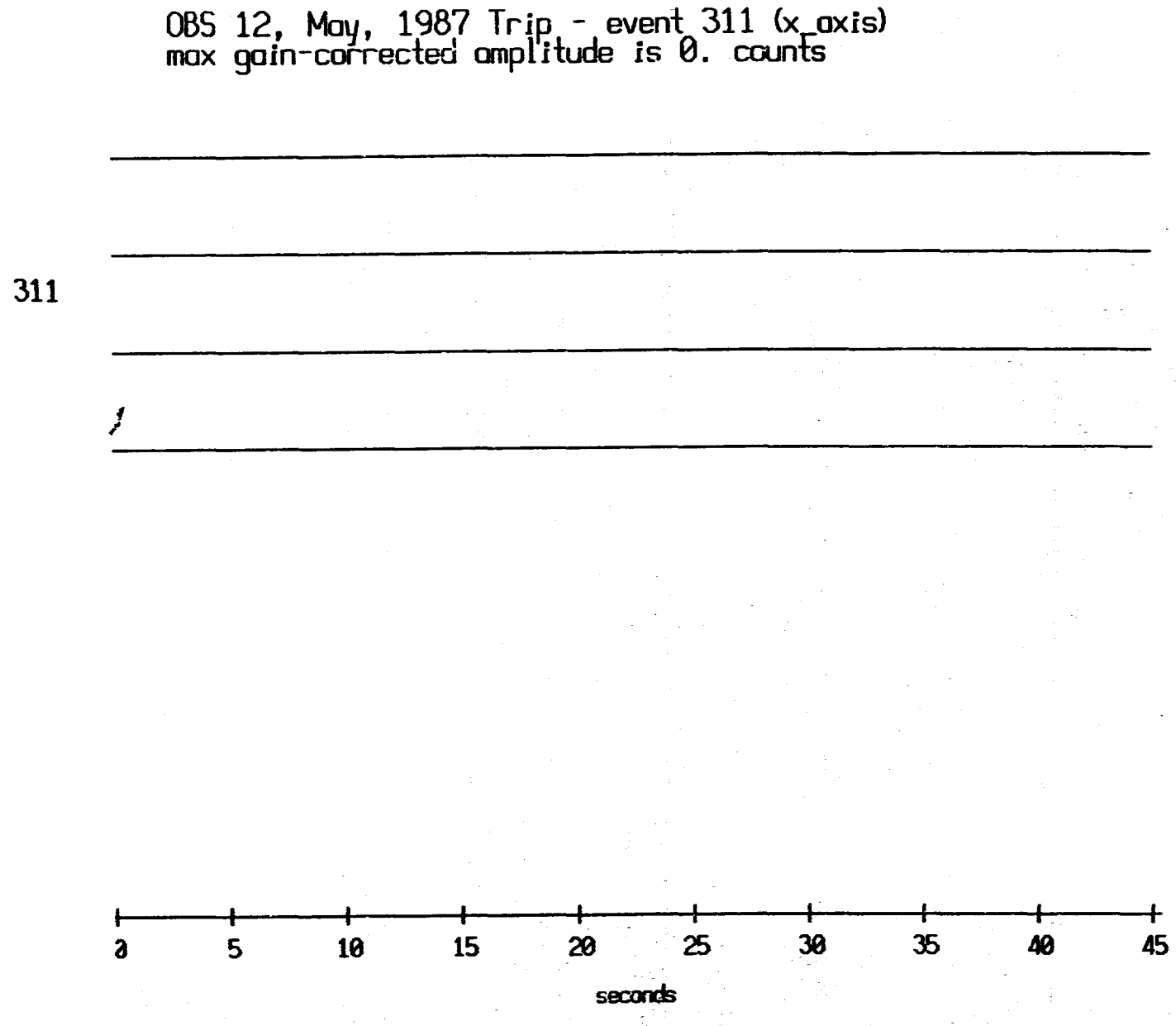

Figure II.36i

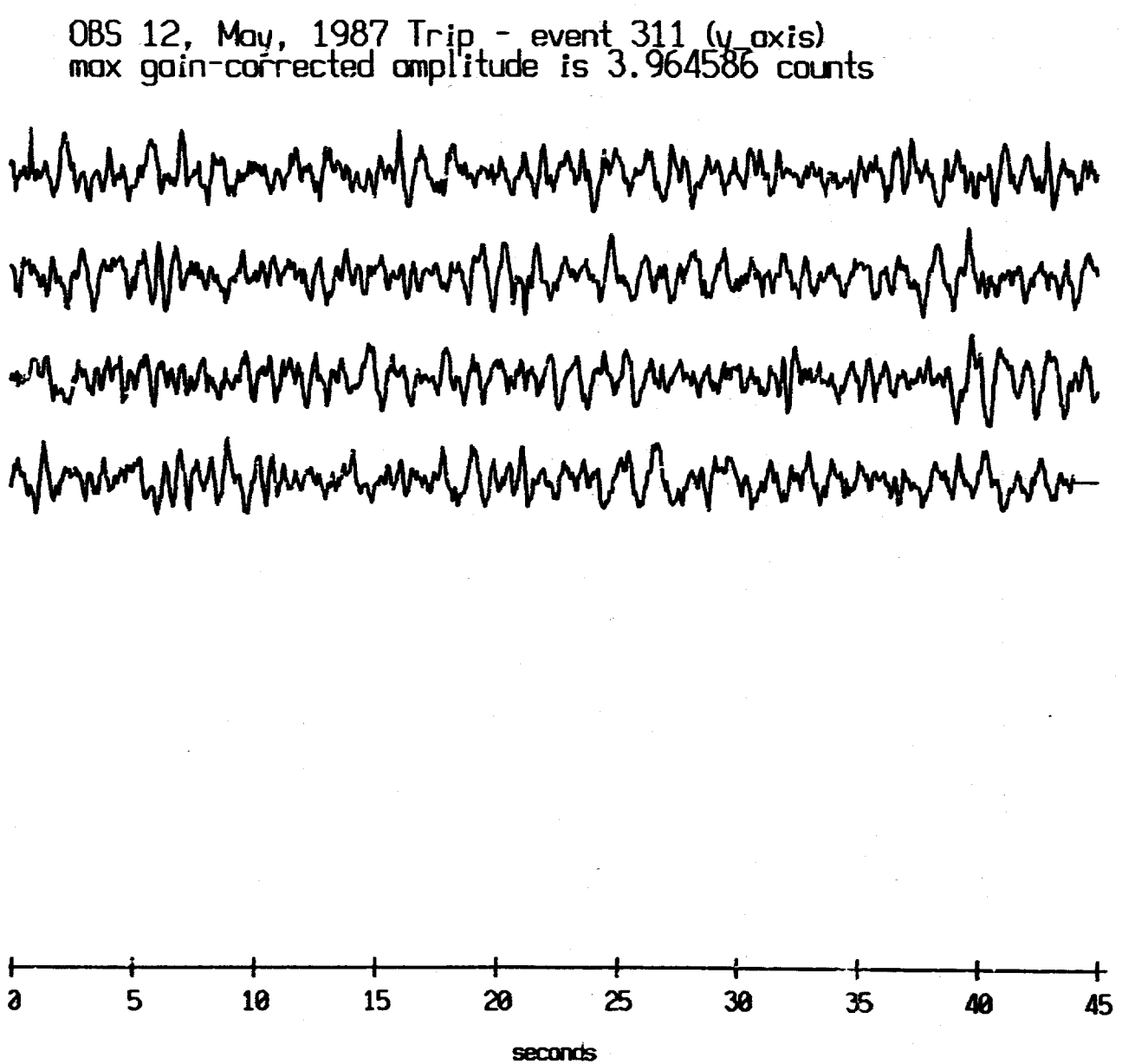

Figure II.36j

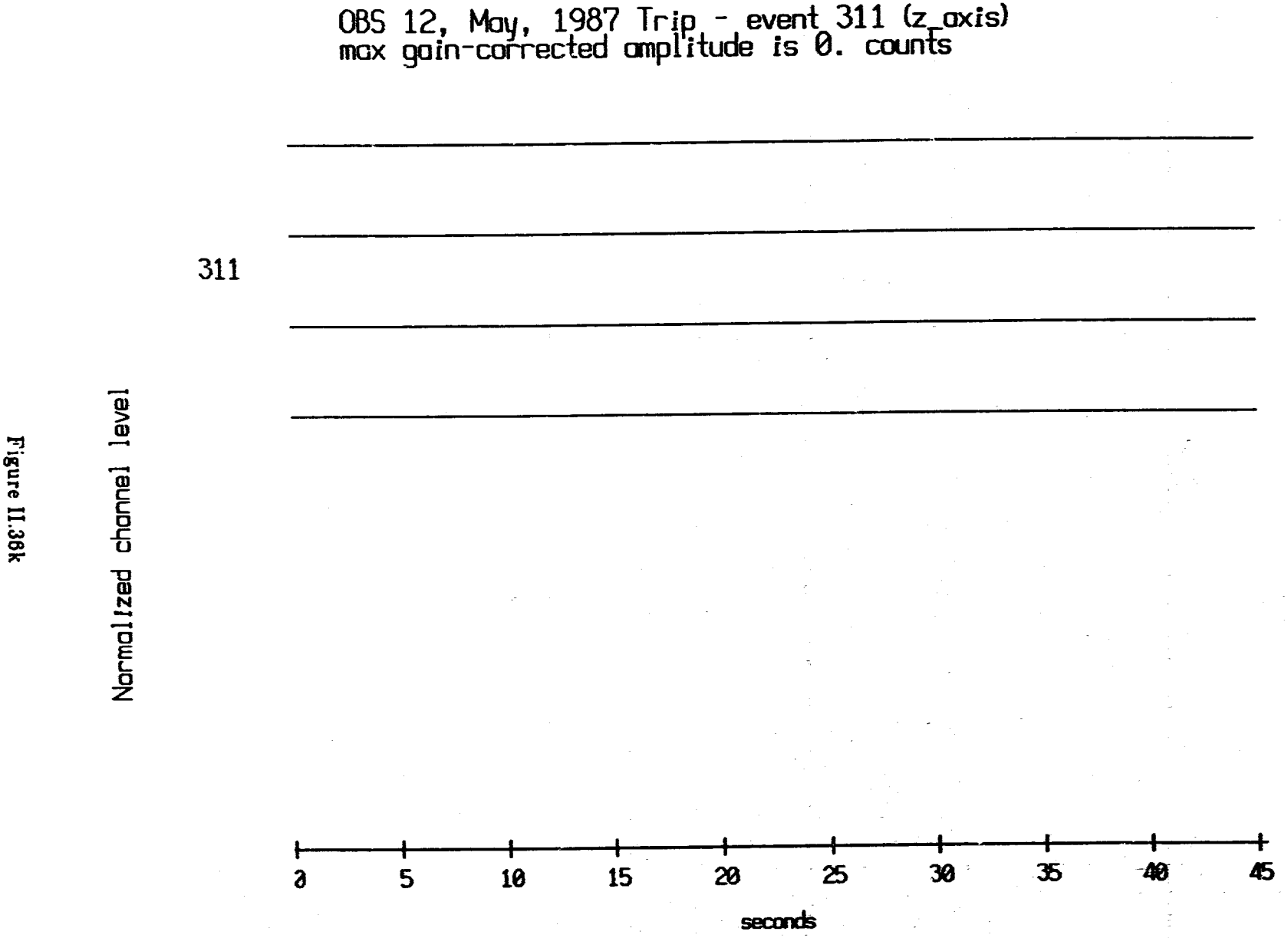

Figure II.36k

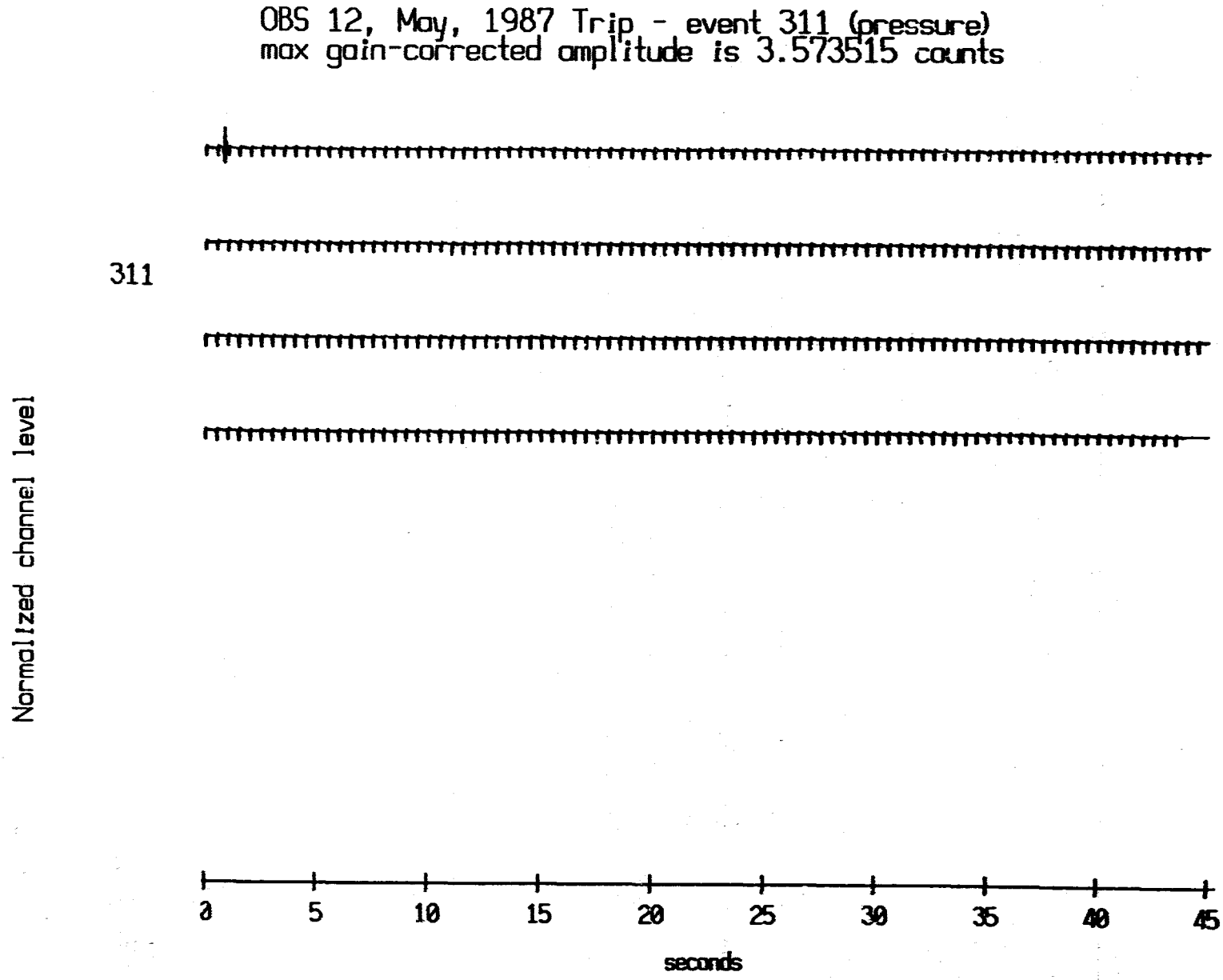

Figure II.361

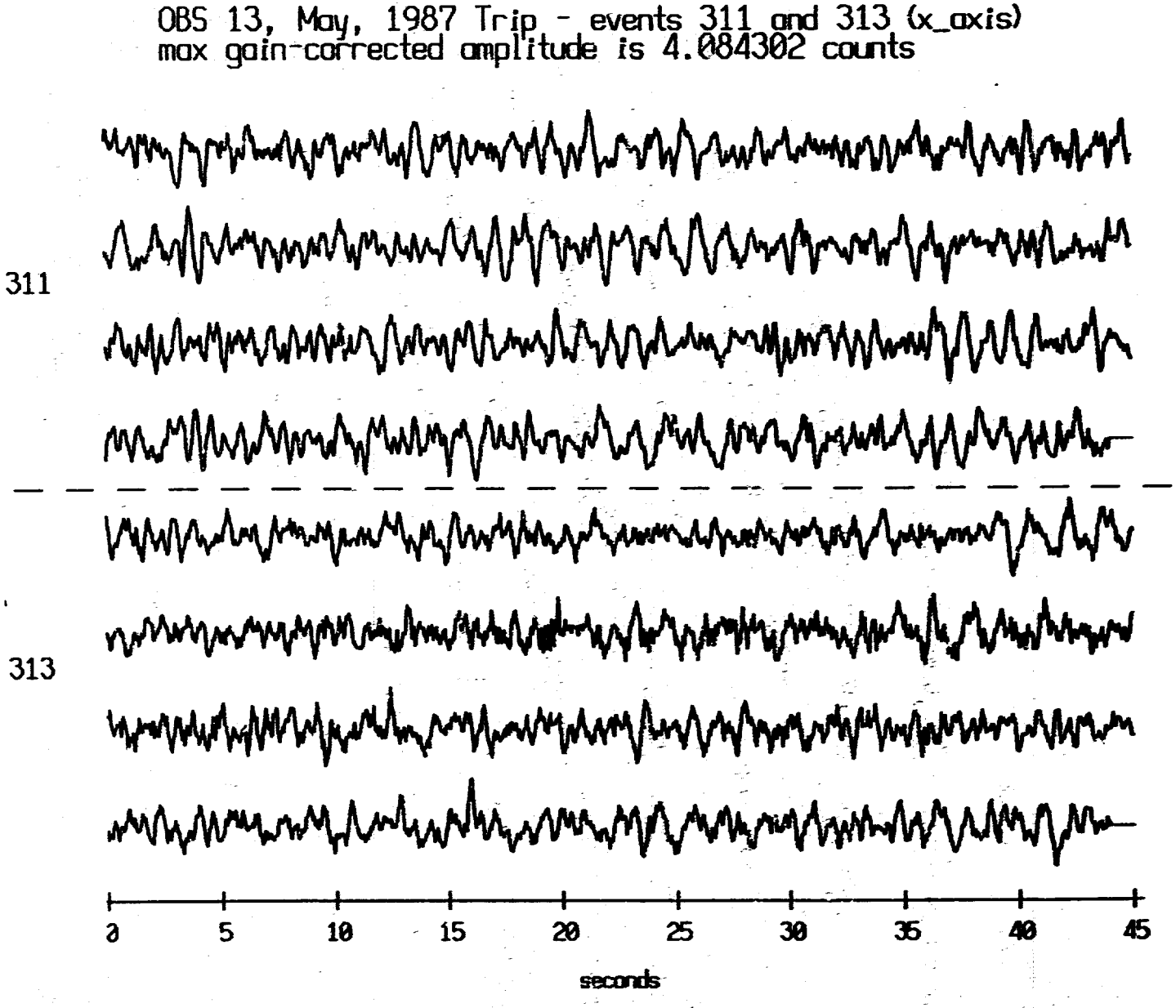

Figure II.37i

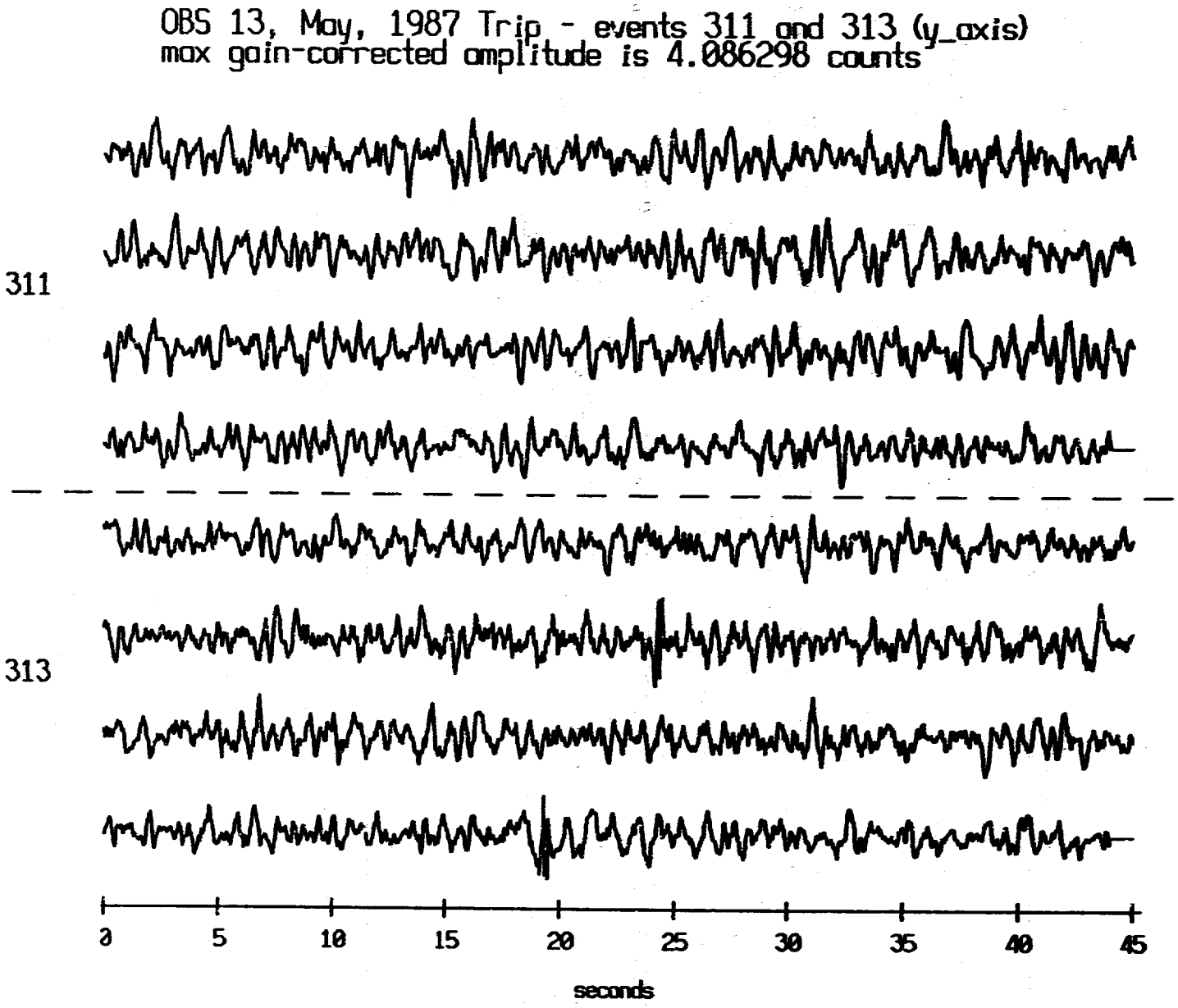

Figure II.37j

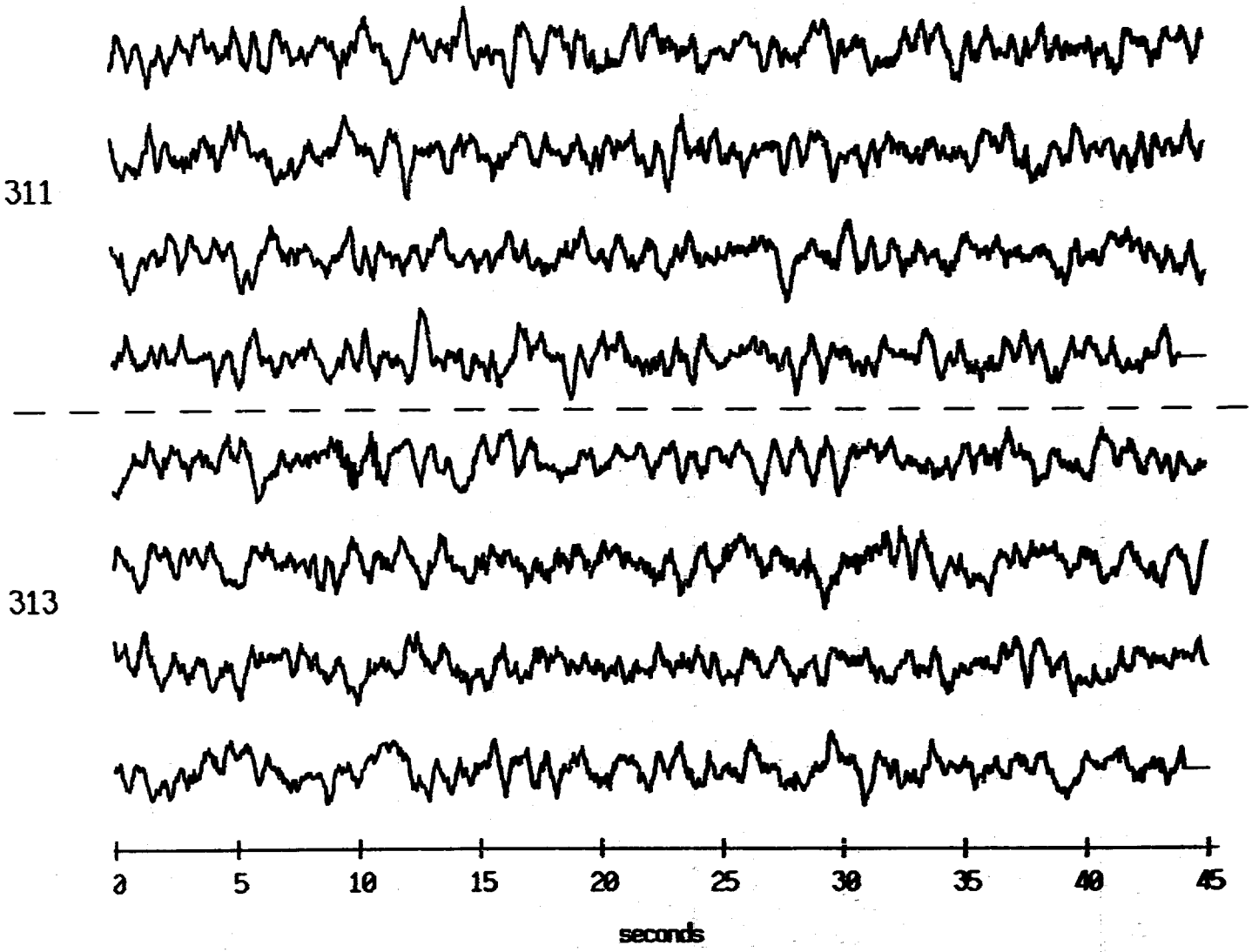

Figure II.37k

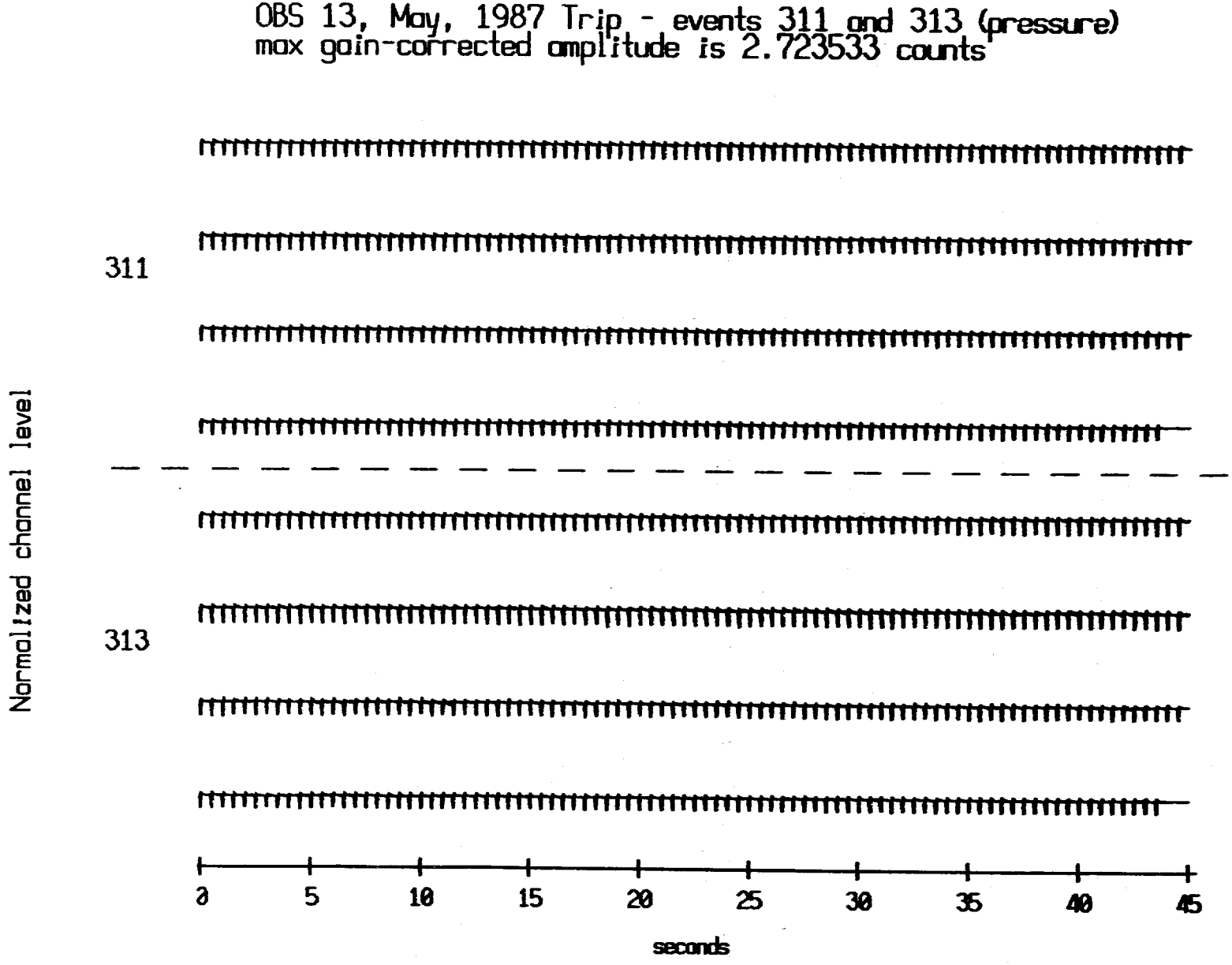

Figure II.37l

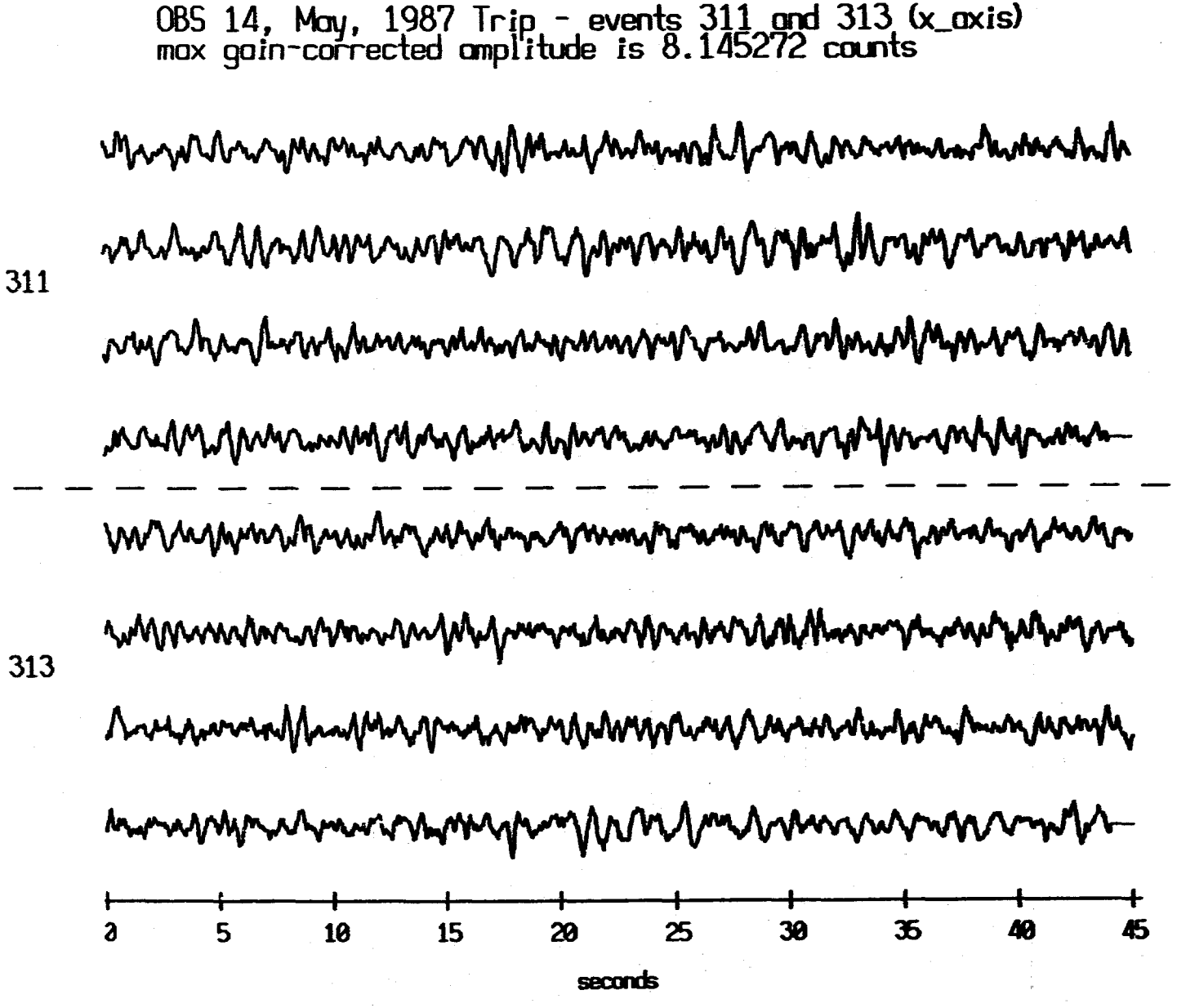

Figure II.38i

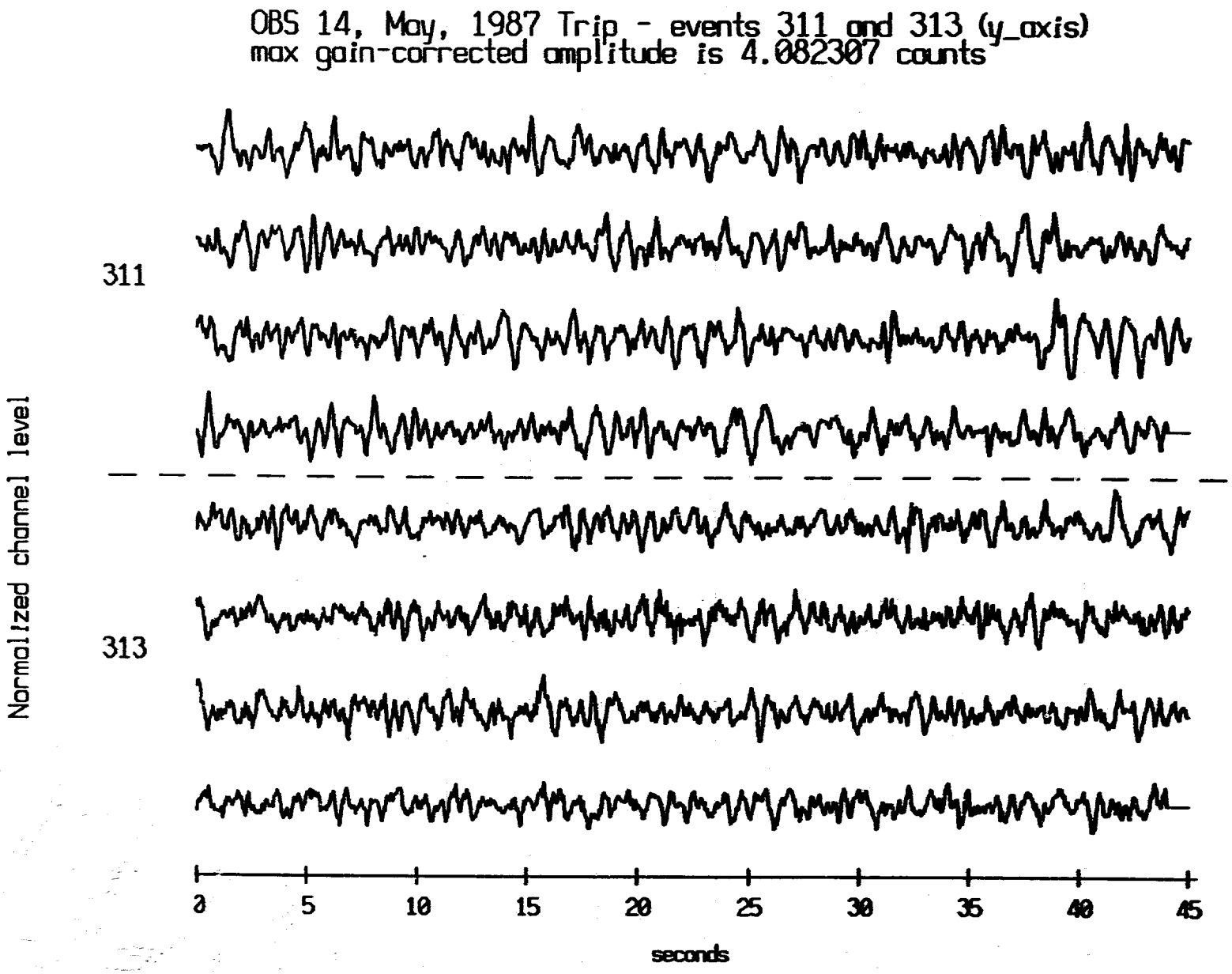

Figure II.38j

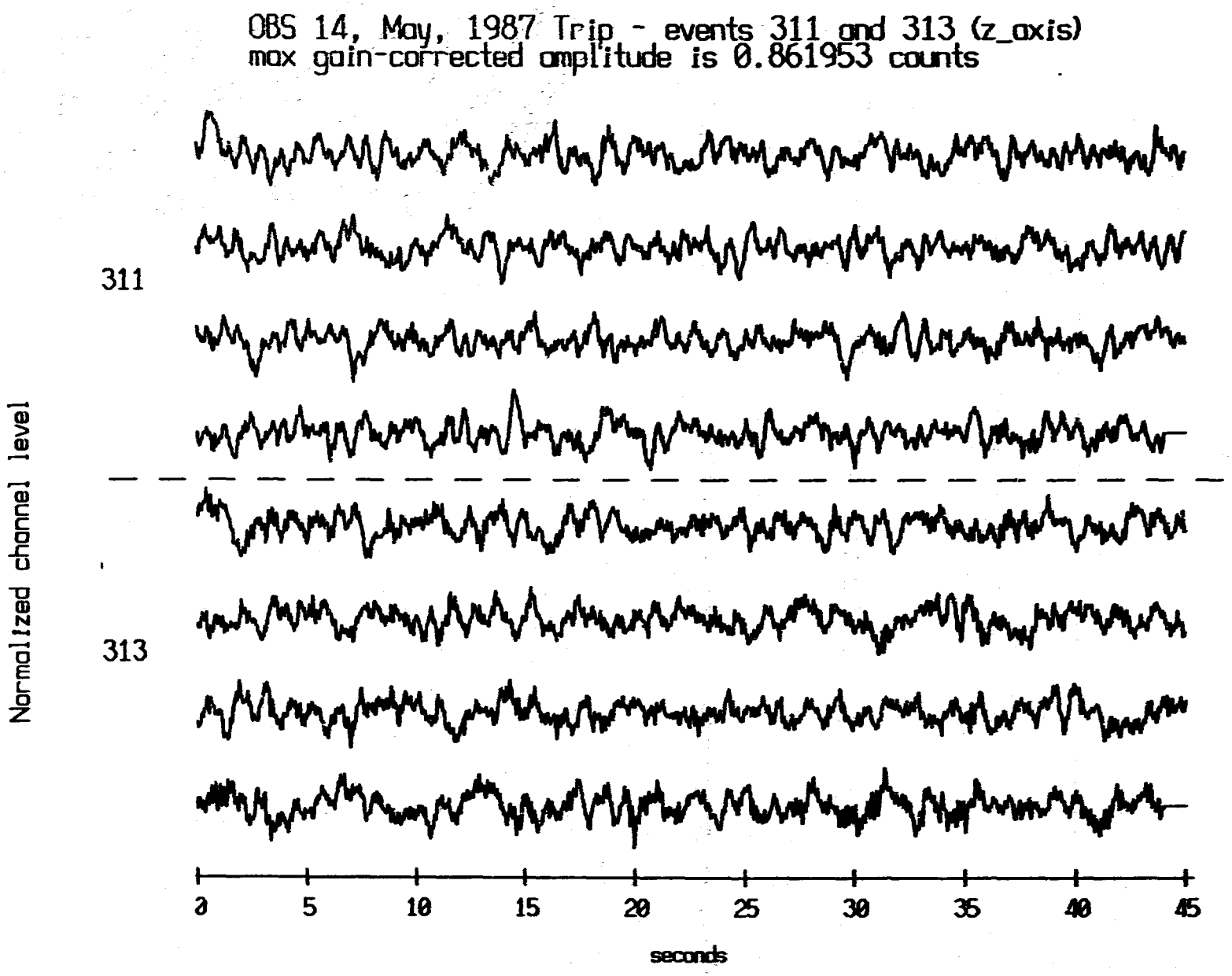

Figure II.38k

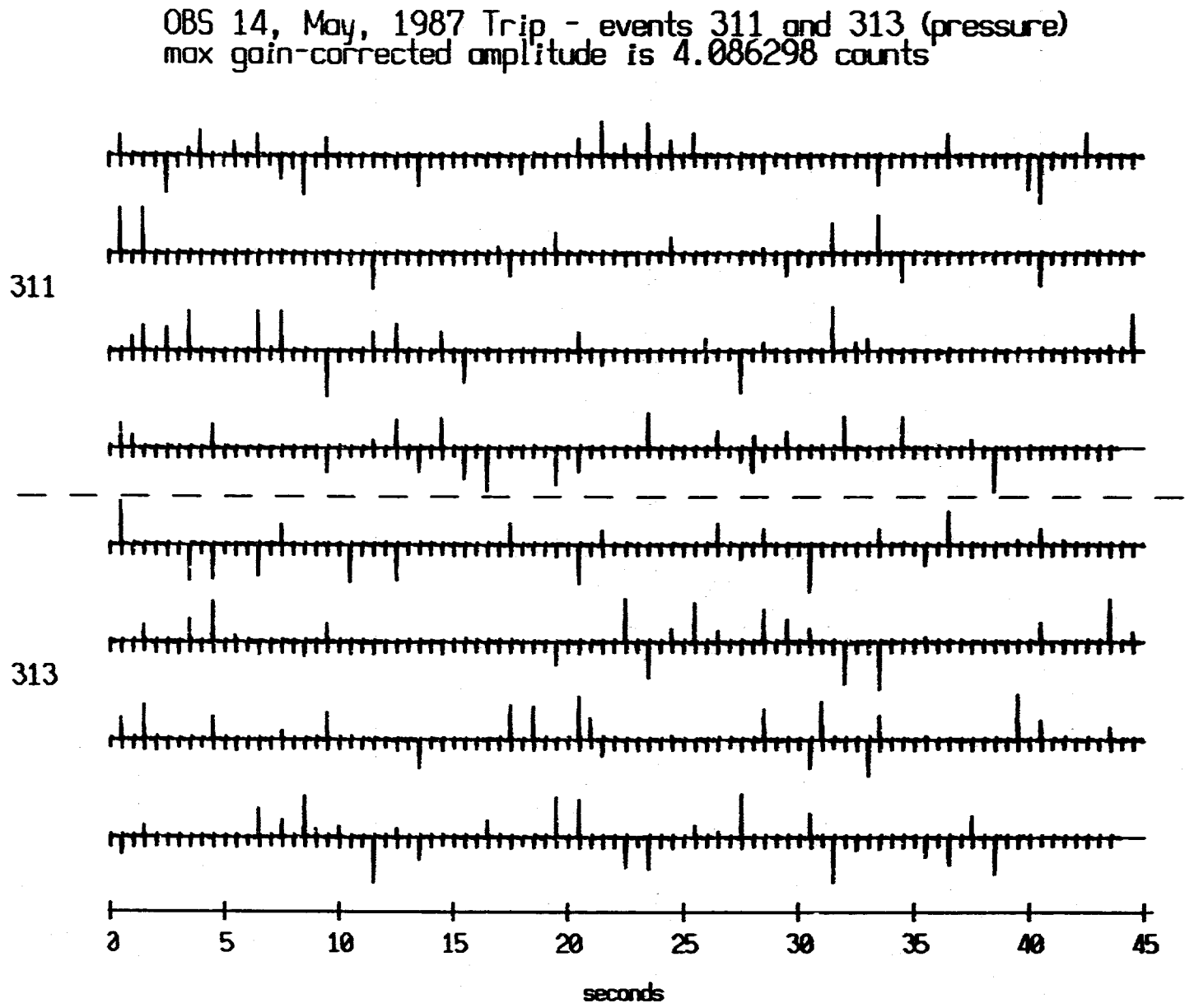
OBS 14, May, 1987 Trip - events 311 and 313 (pressure)
max gain-corrected amplitude is 4.086298 counts
311
313
Normalized channel level
0
5
10
15
20
25
30
35
40
45
seconds

Figure II.38

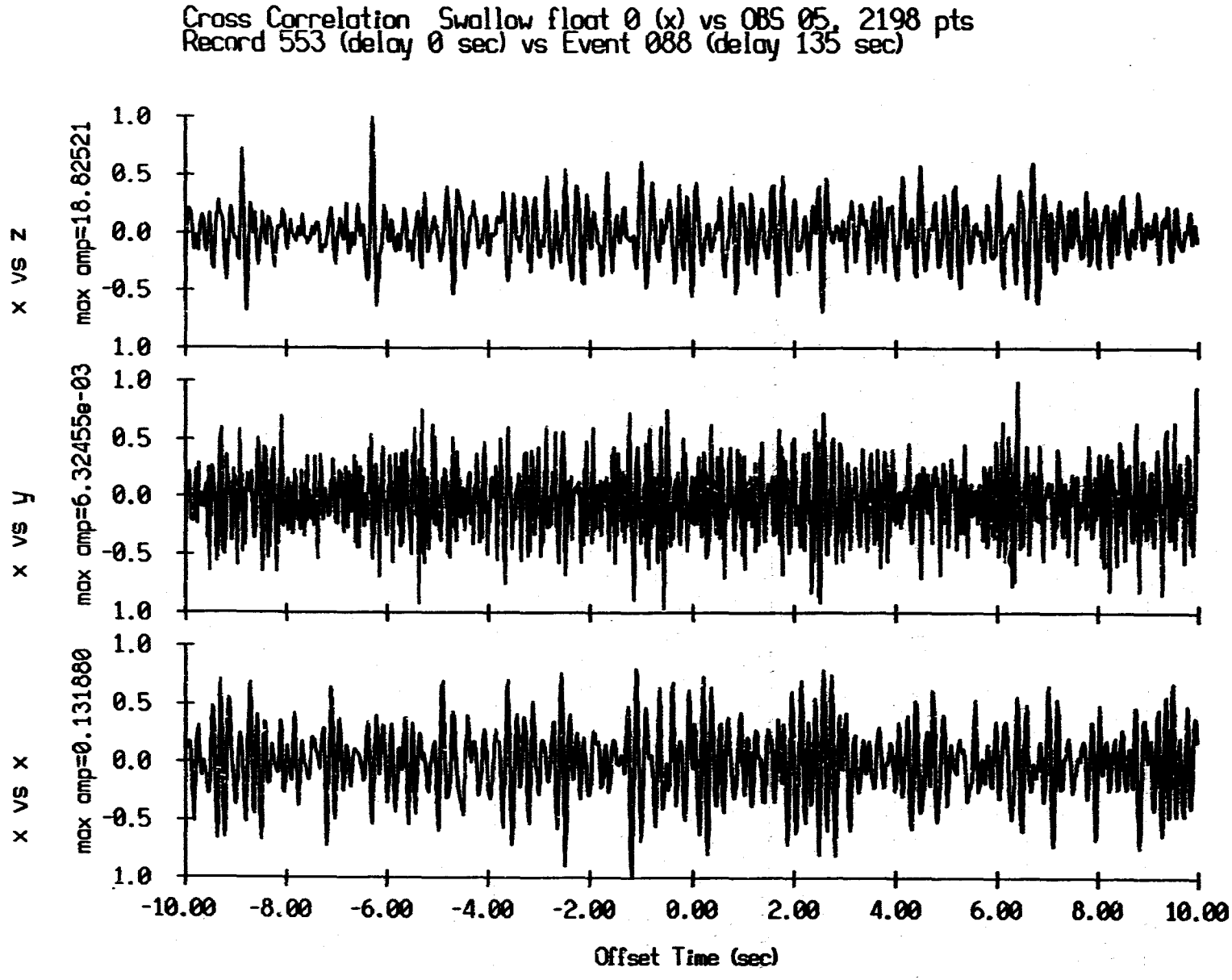

Figure III.11

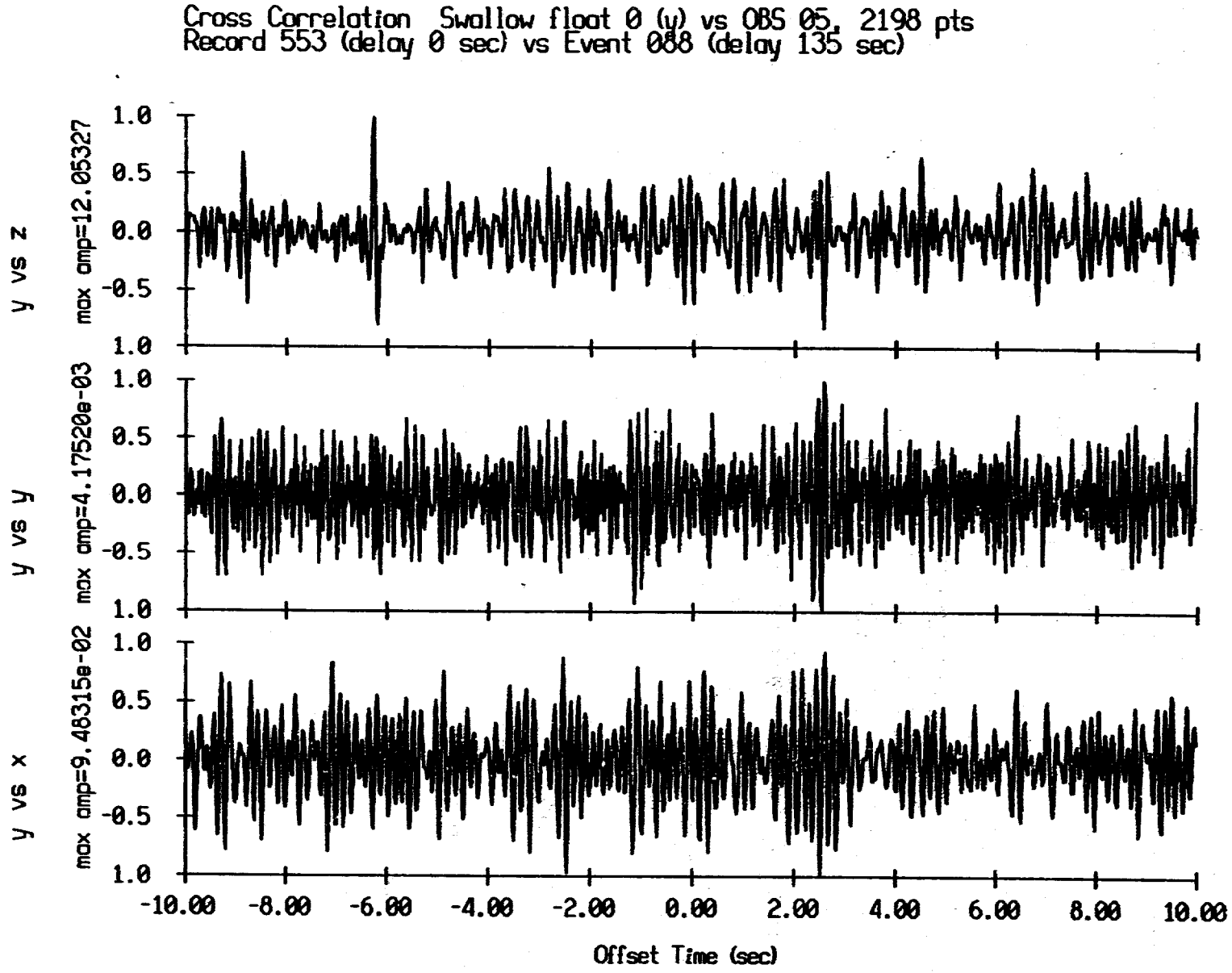

Figure III.1j

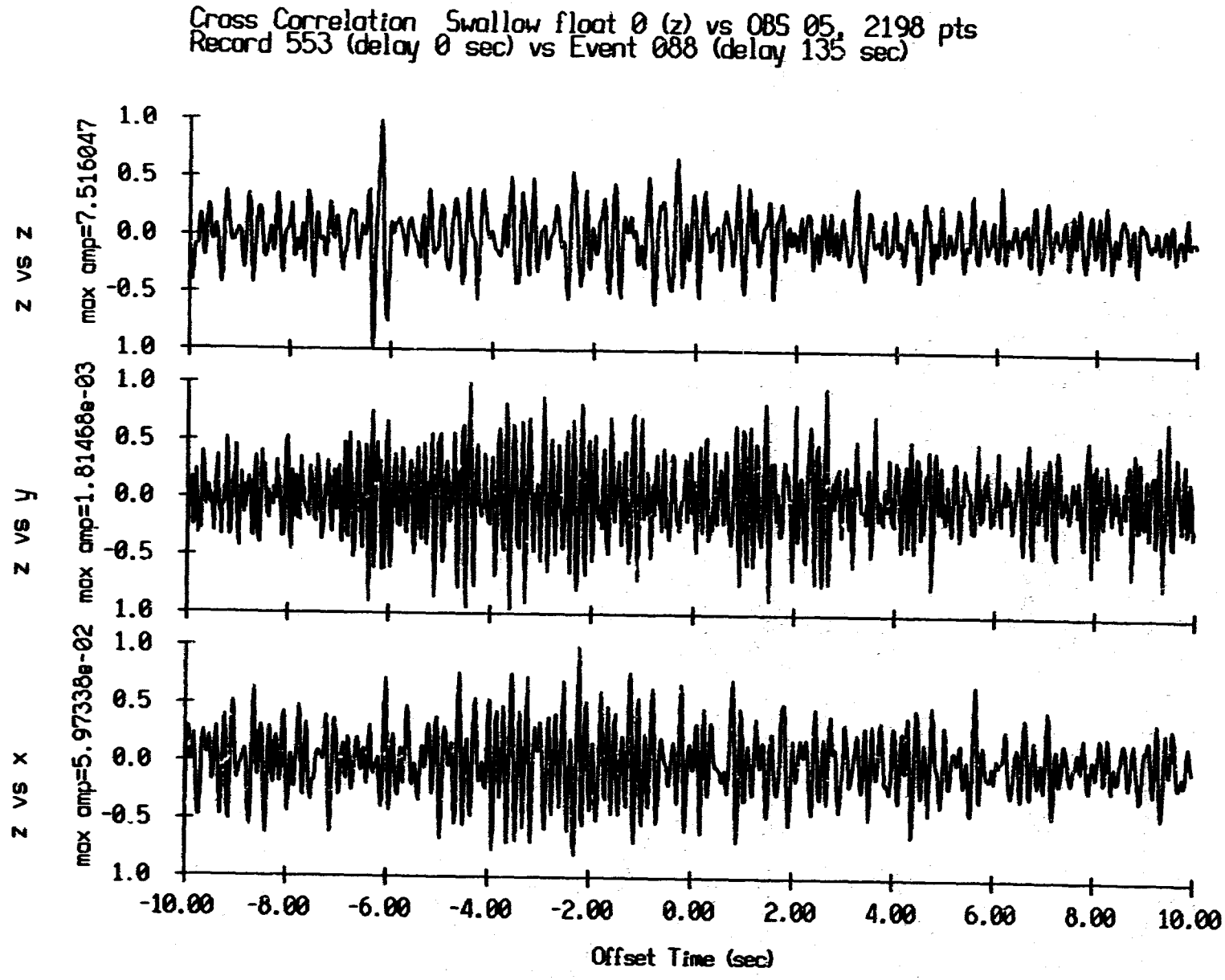

Figure III.1k

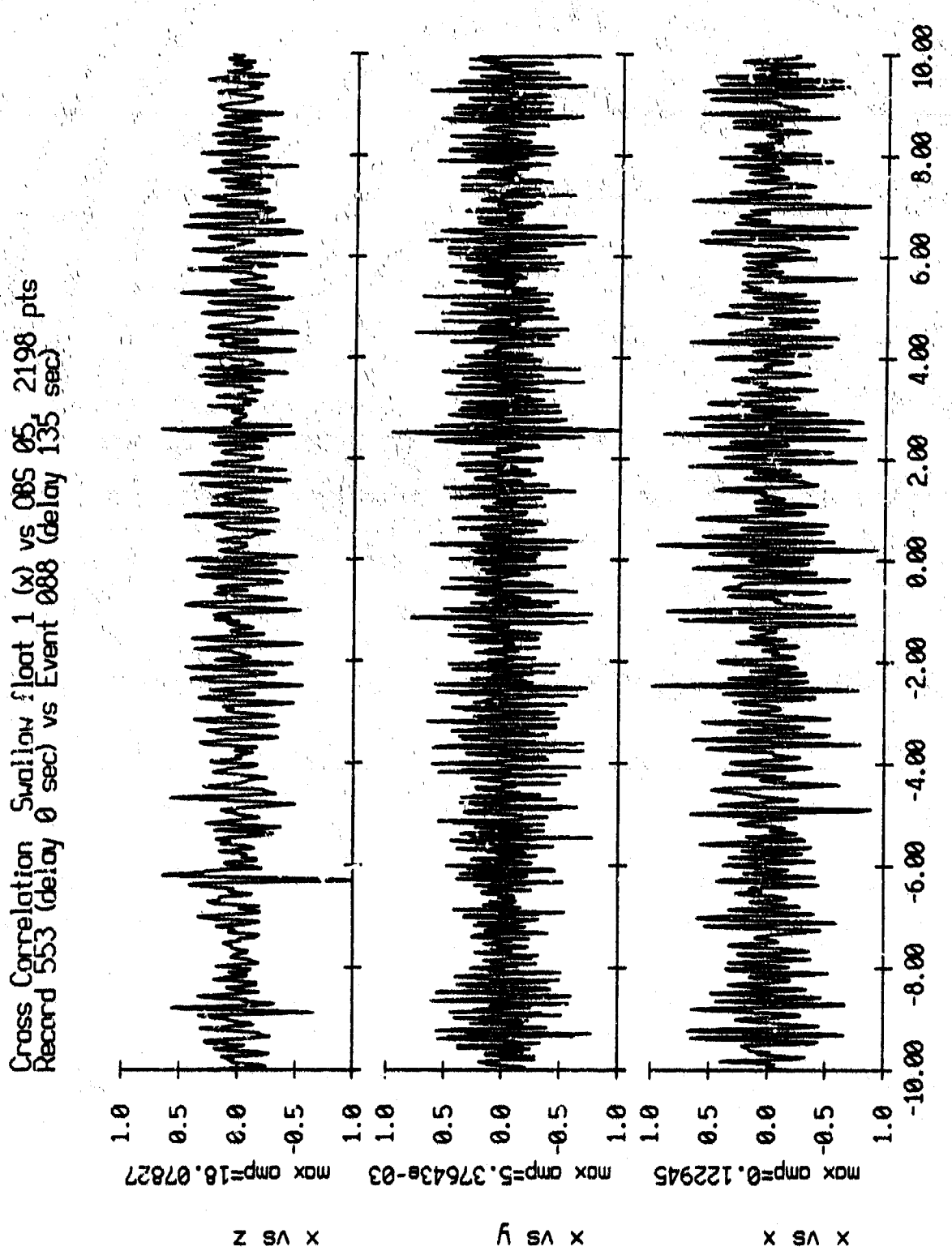

Figure III.2i

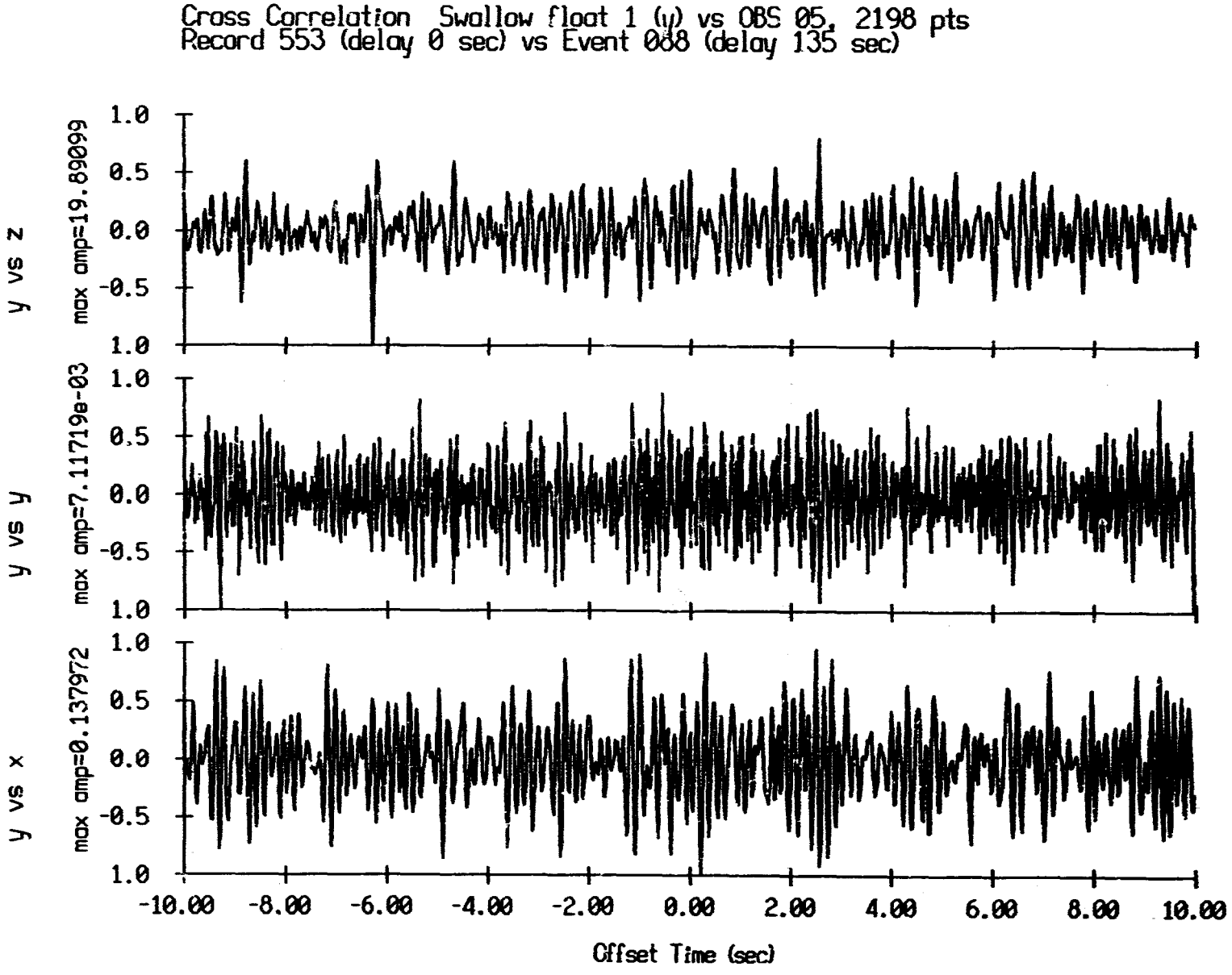

Figure III.2j

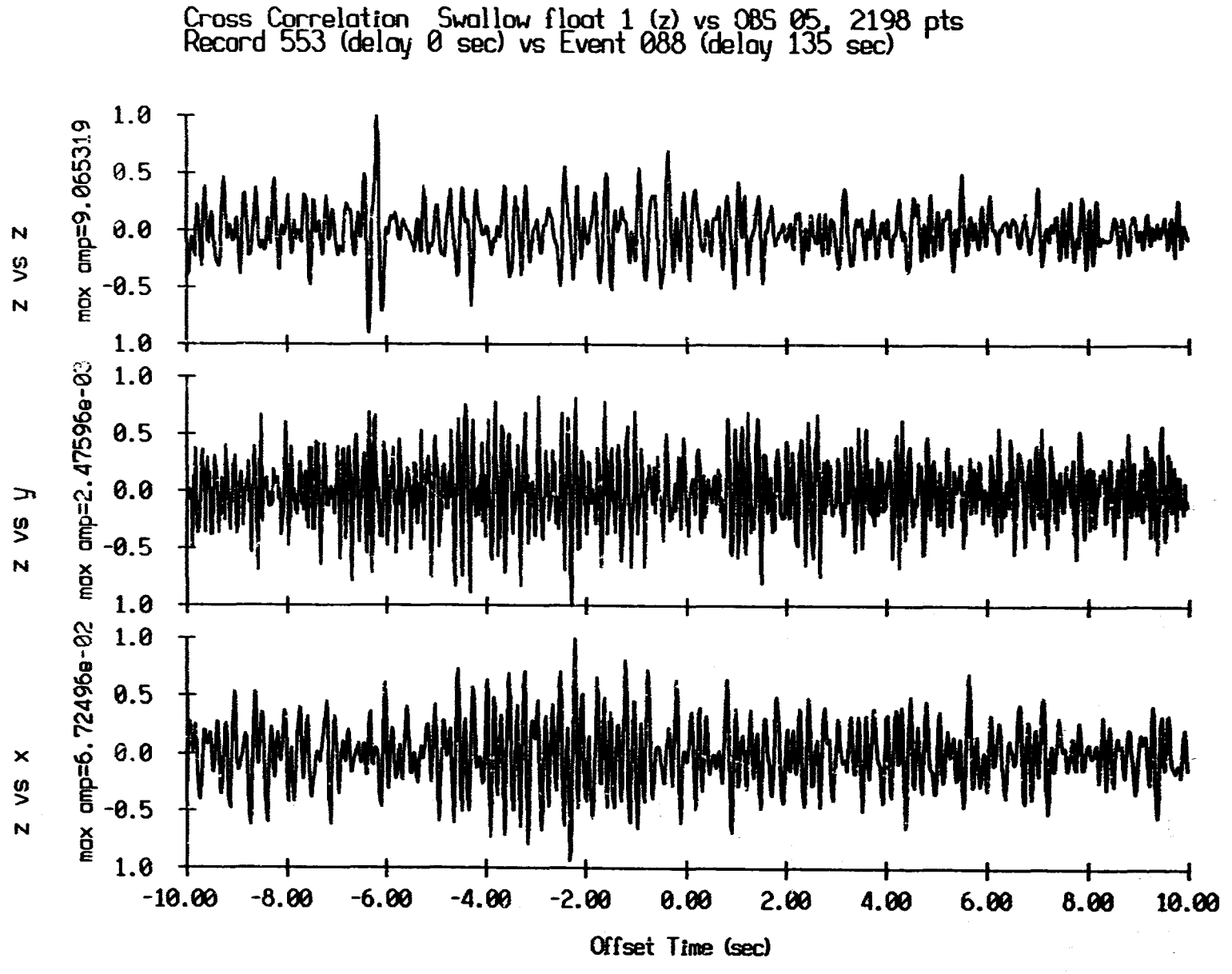

Figure III.2k

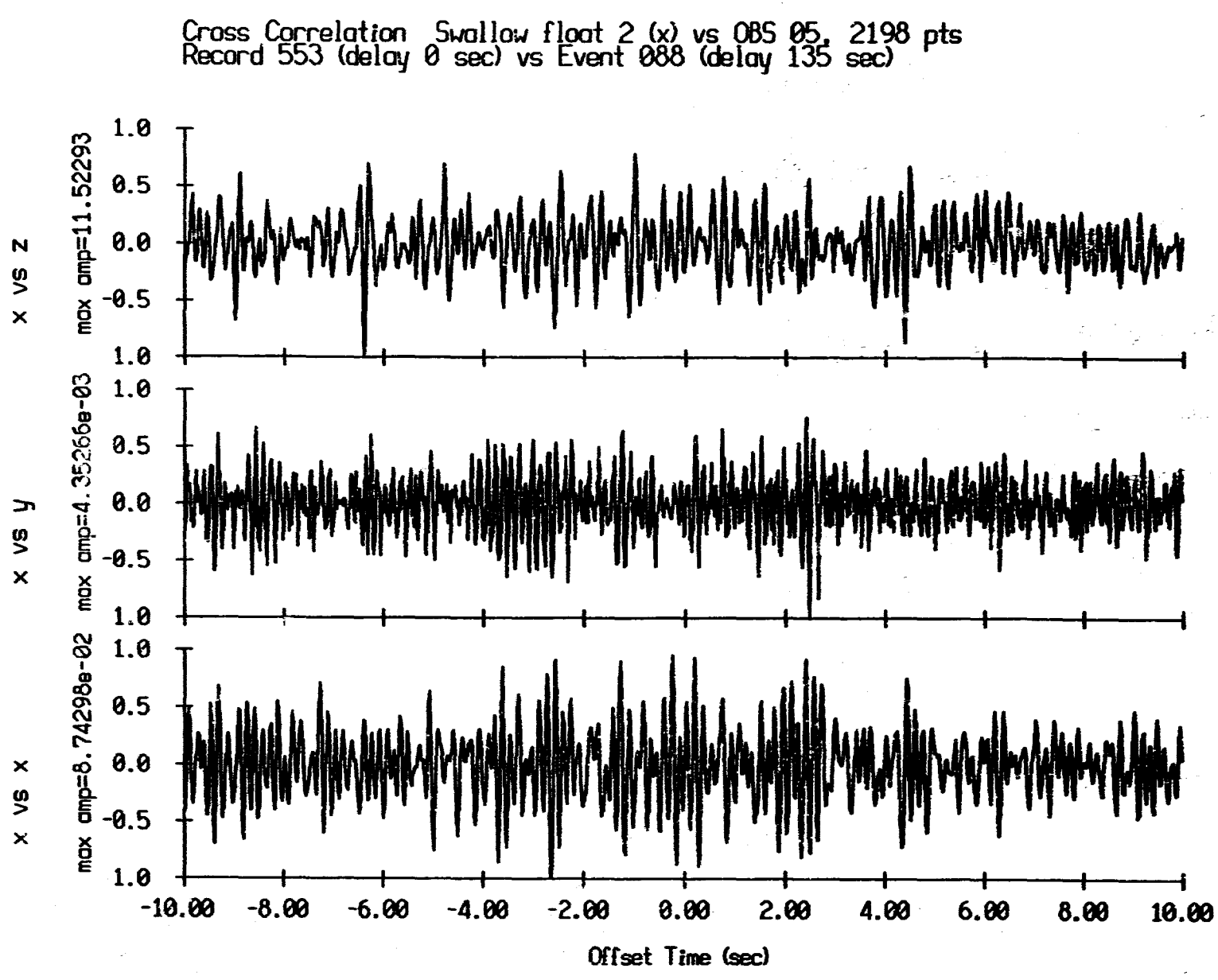

Figure III.31

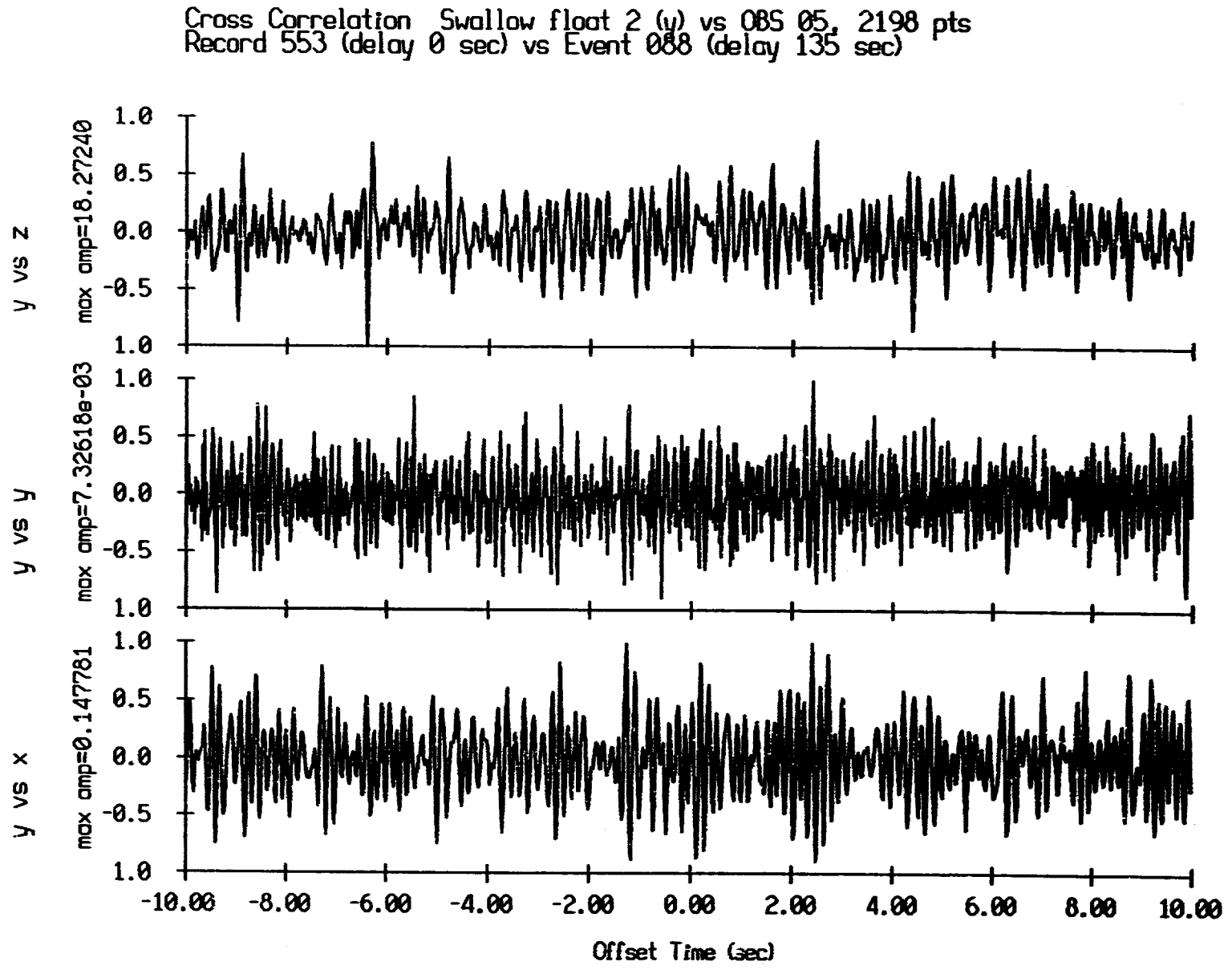

Figure III.3j

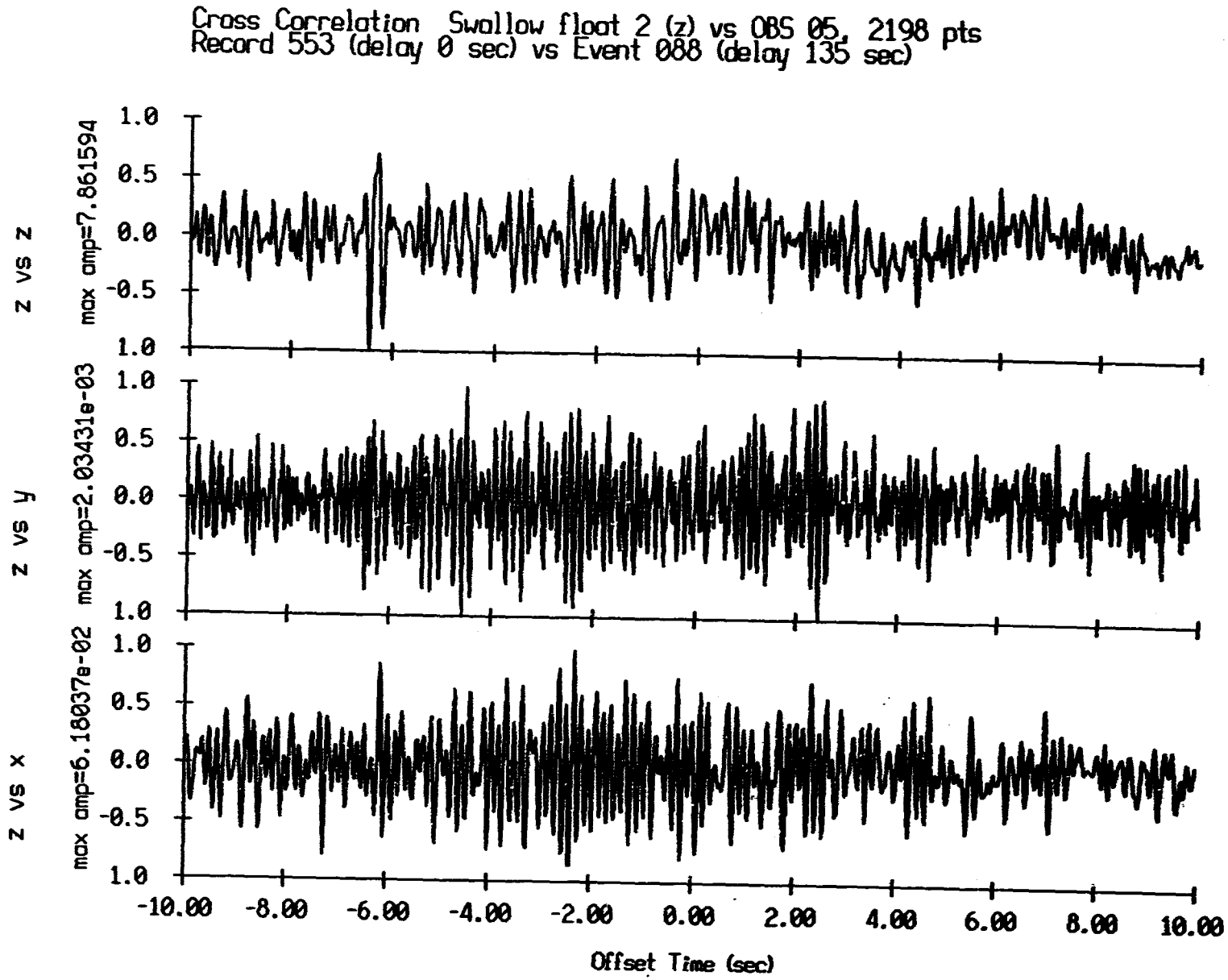

Figure III.3k

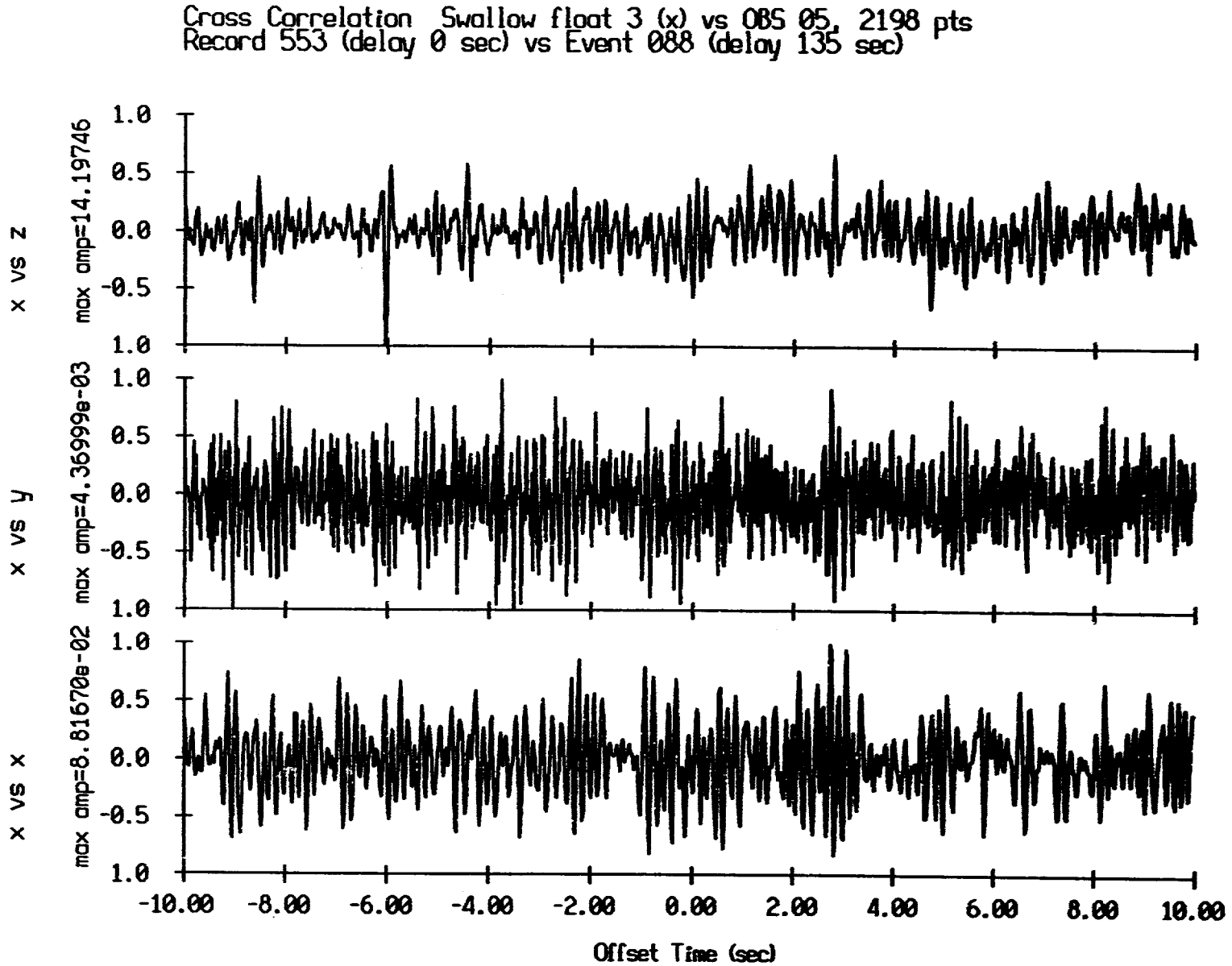

Figure III.4i

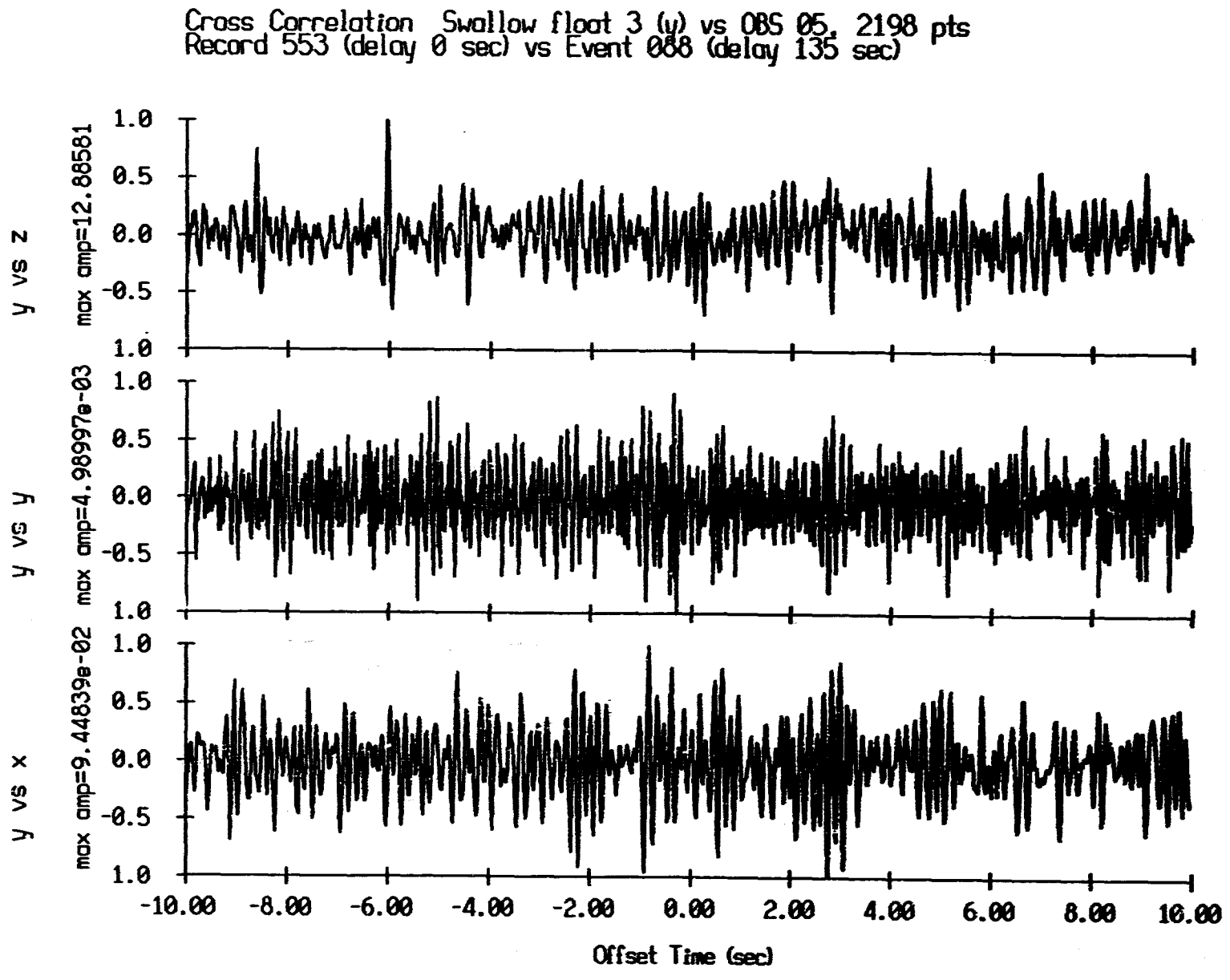

Figure III.4j

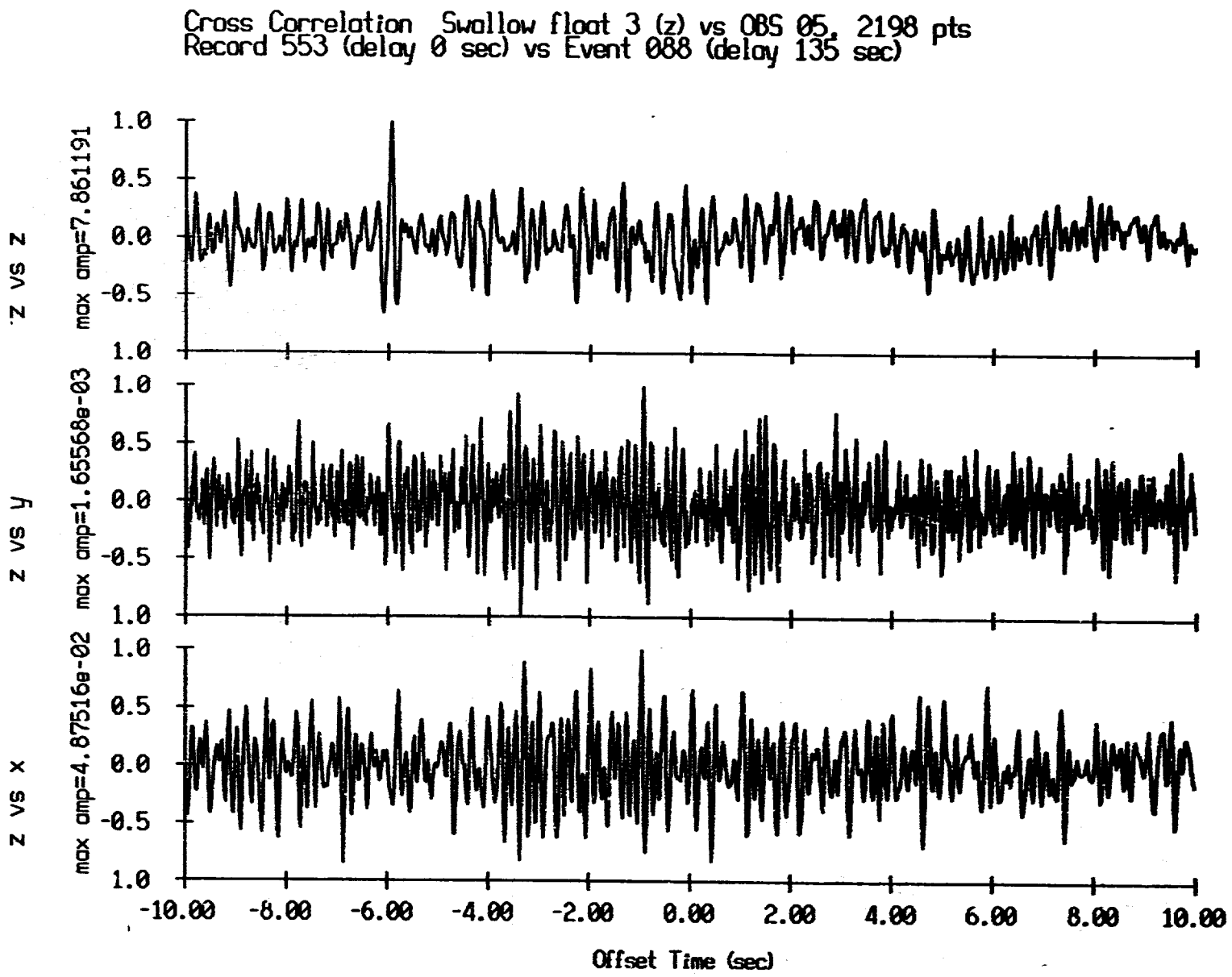

Figure III.4k

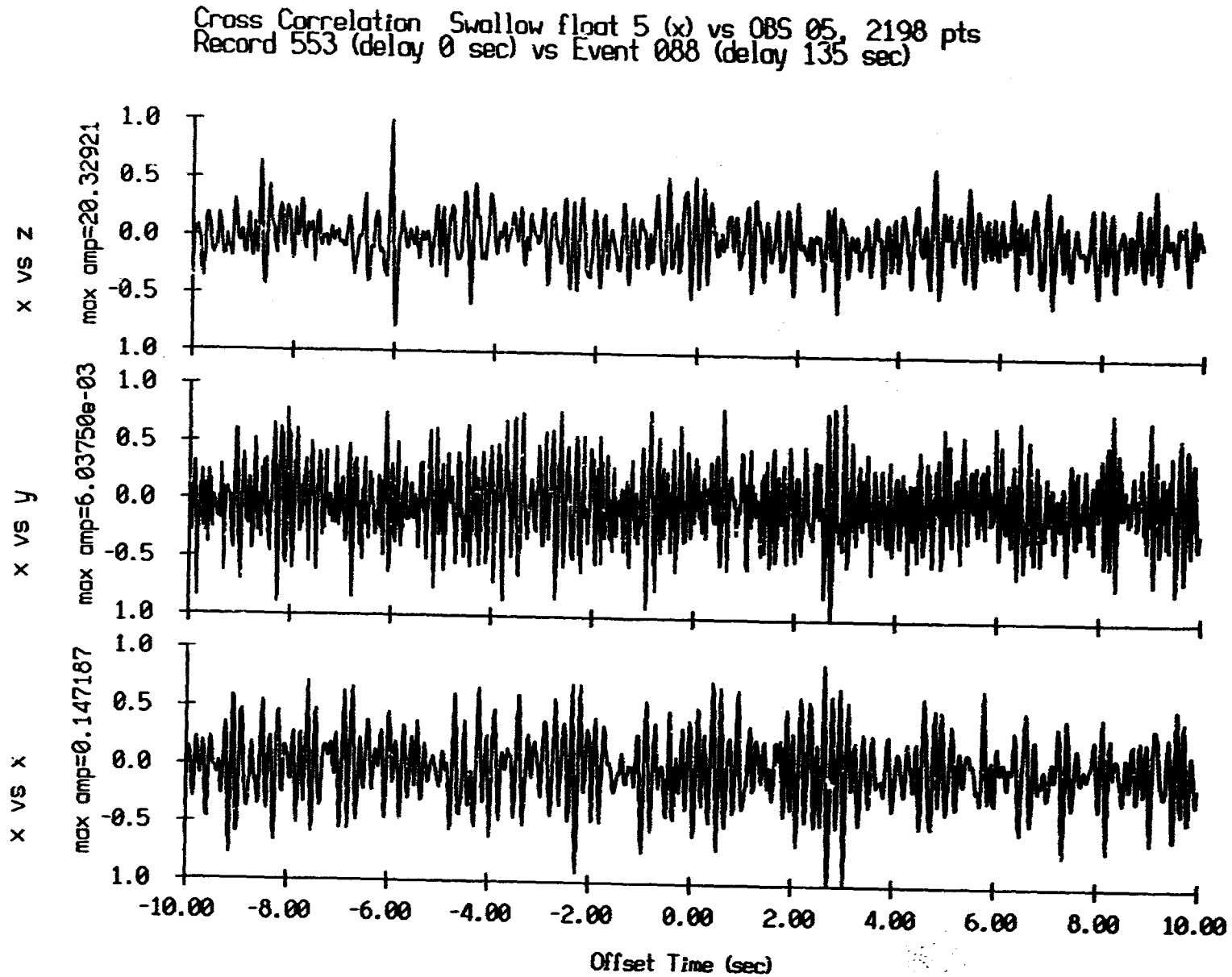

Figure III.5i

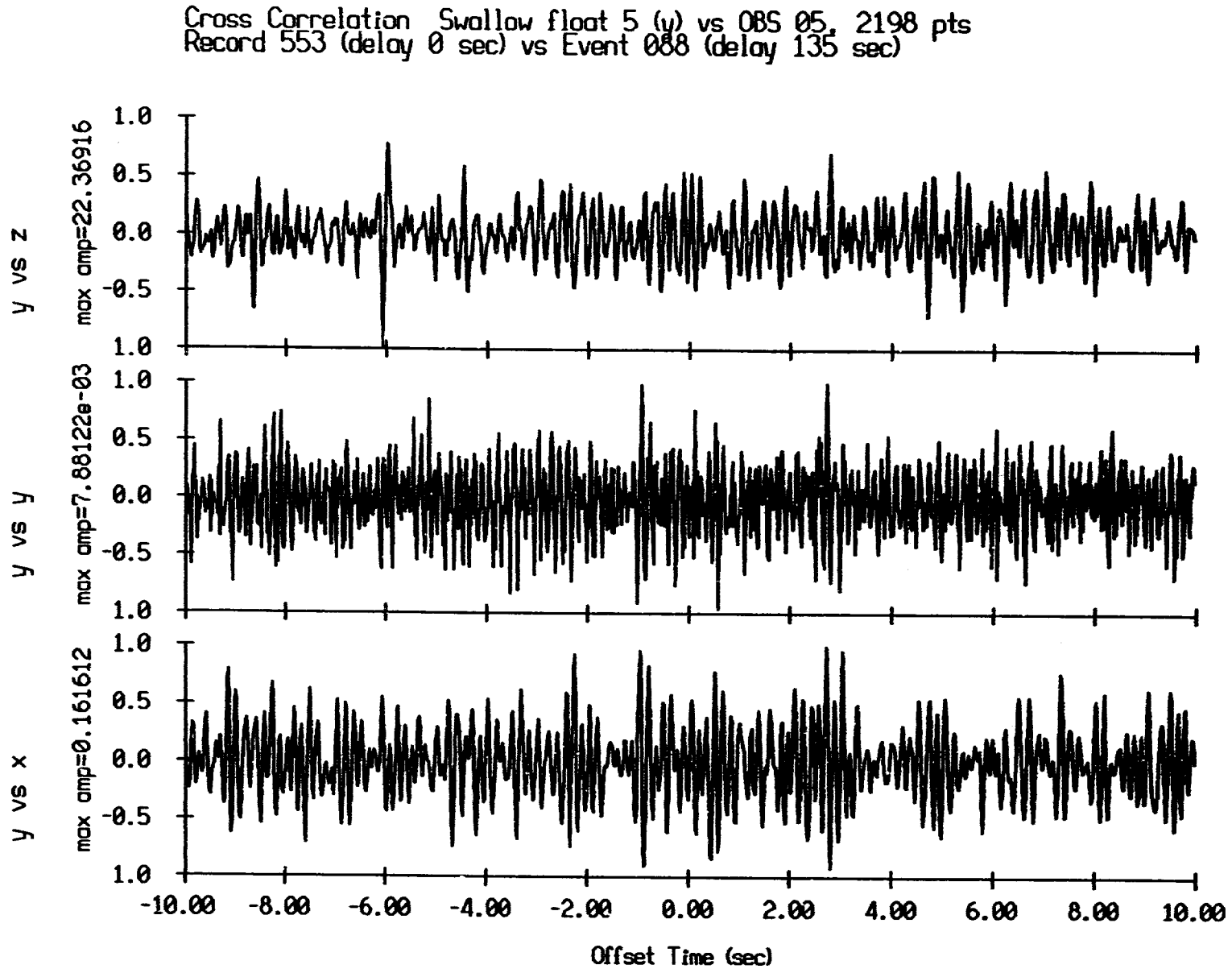

Figure III.5j

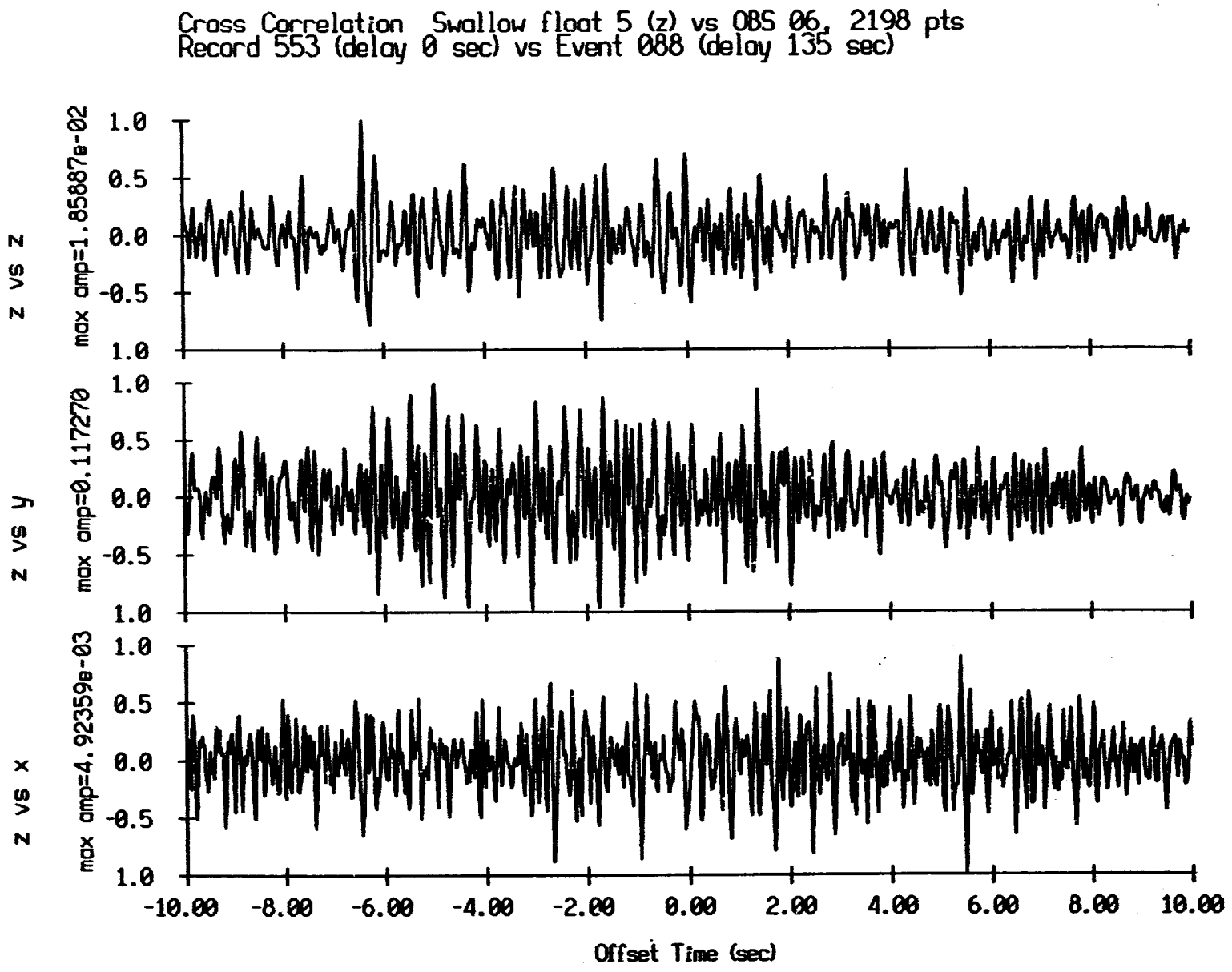

Figure III.5k

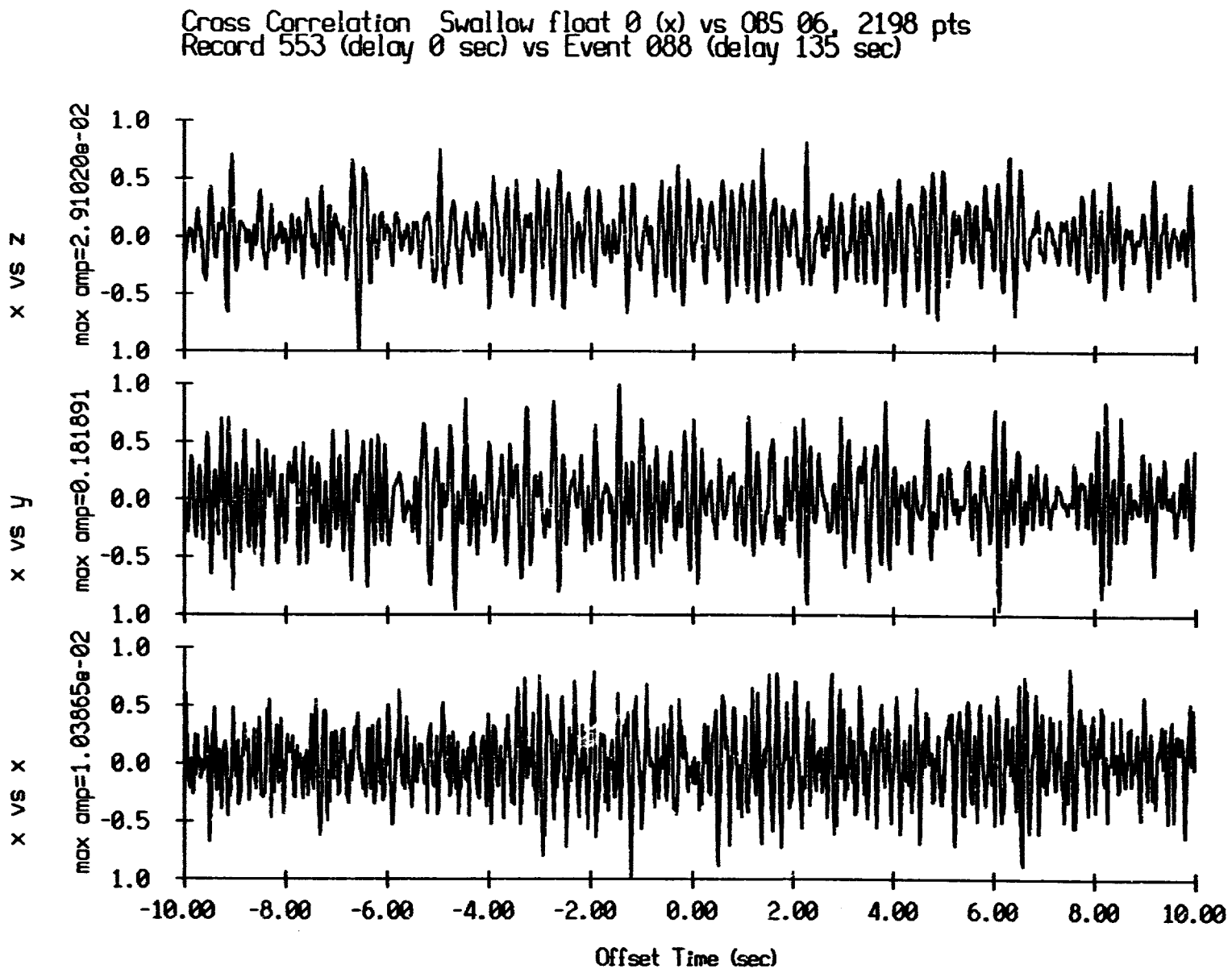
Cross Correlation Swallow float 0 (x) vs OBS 06, 2198 pts
Record 553 (delay 0 sec) vs Event 088 (delay 135 sec)
x vs z
max amp=2.91020e-02
x vs y
max amp=0.181891
x vs x
max amp=1.03865e-02
1.0
0.5
0.0
-0.5
-1.0
-10.00
-8.00
-6.00
-4.00
-2.00
0.00
2.00
4.00
6.00
8.00
10.00
Offset Time (sec)

Figure III.6

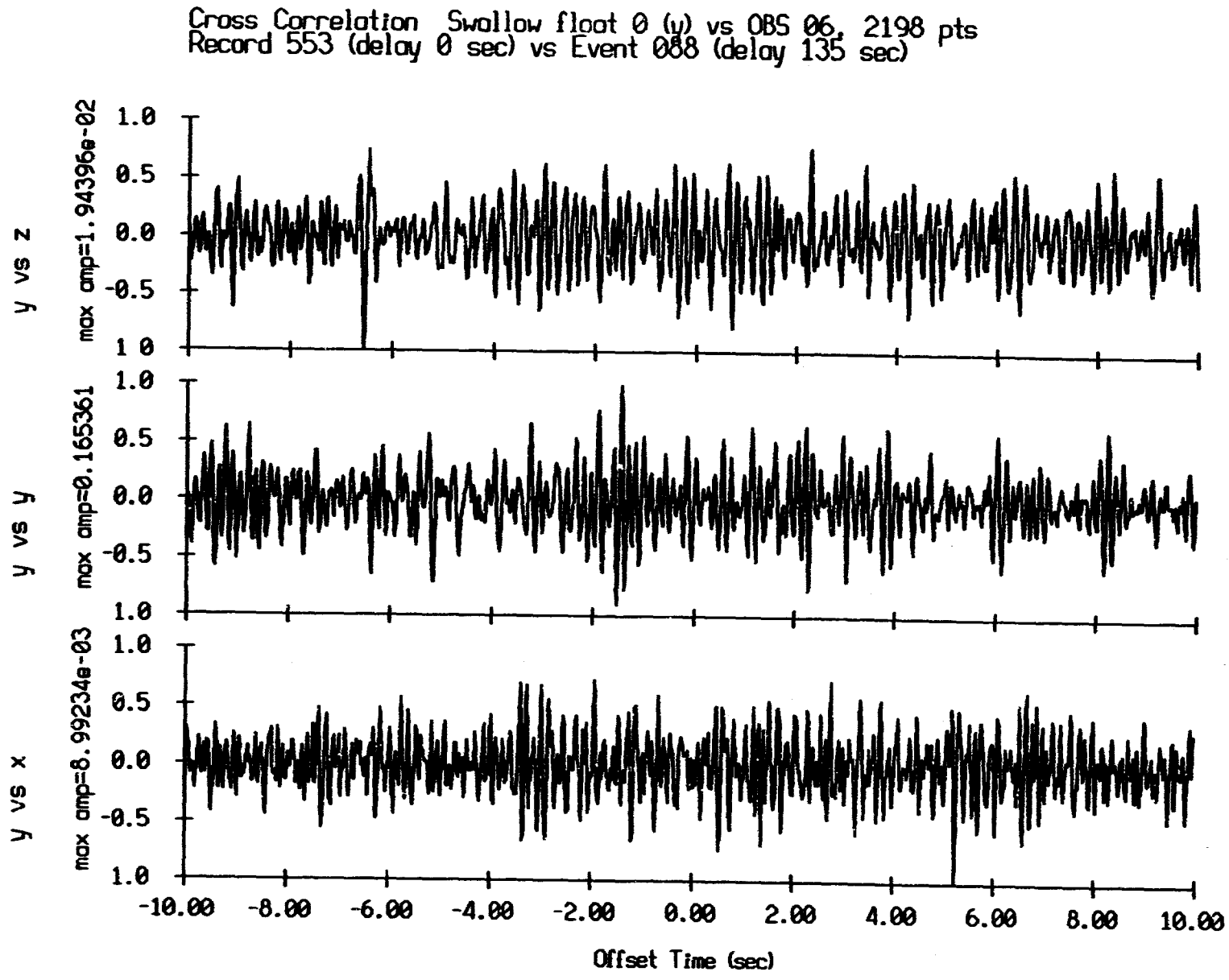

Figure III.6j

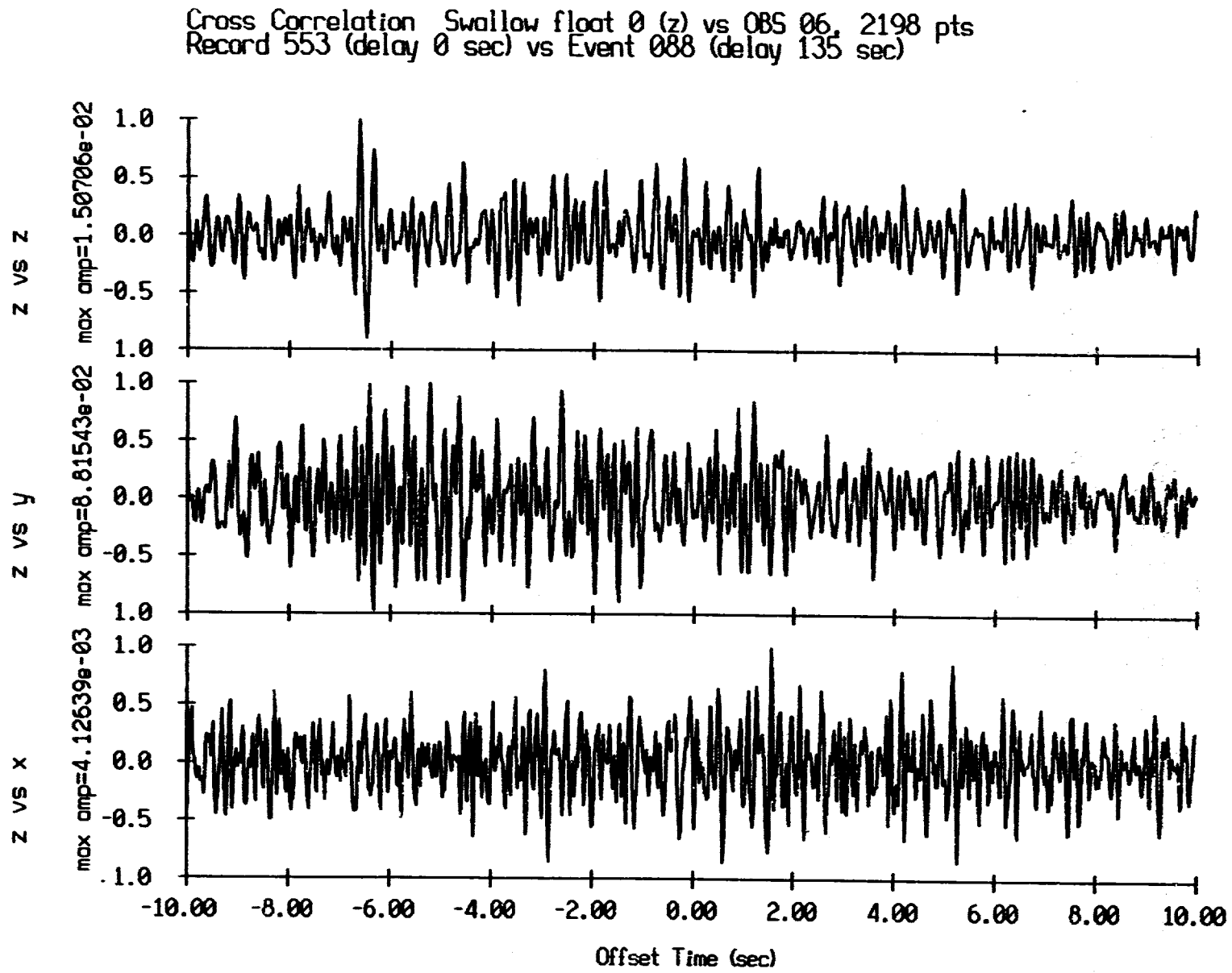

Figure III.6k

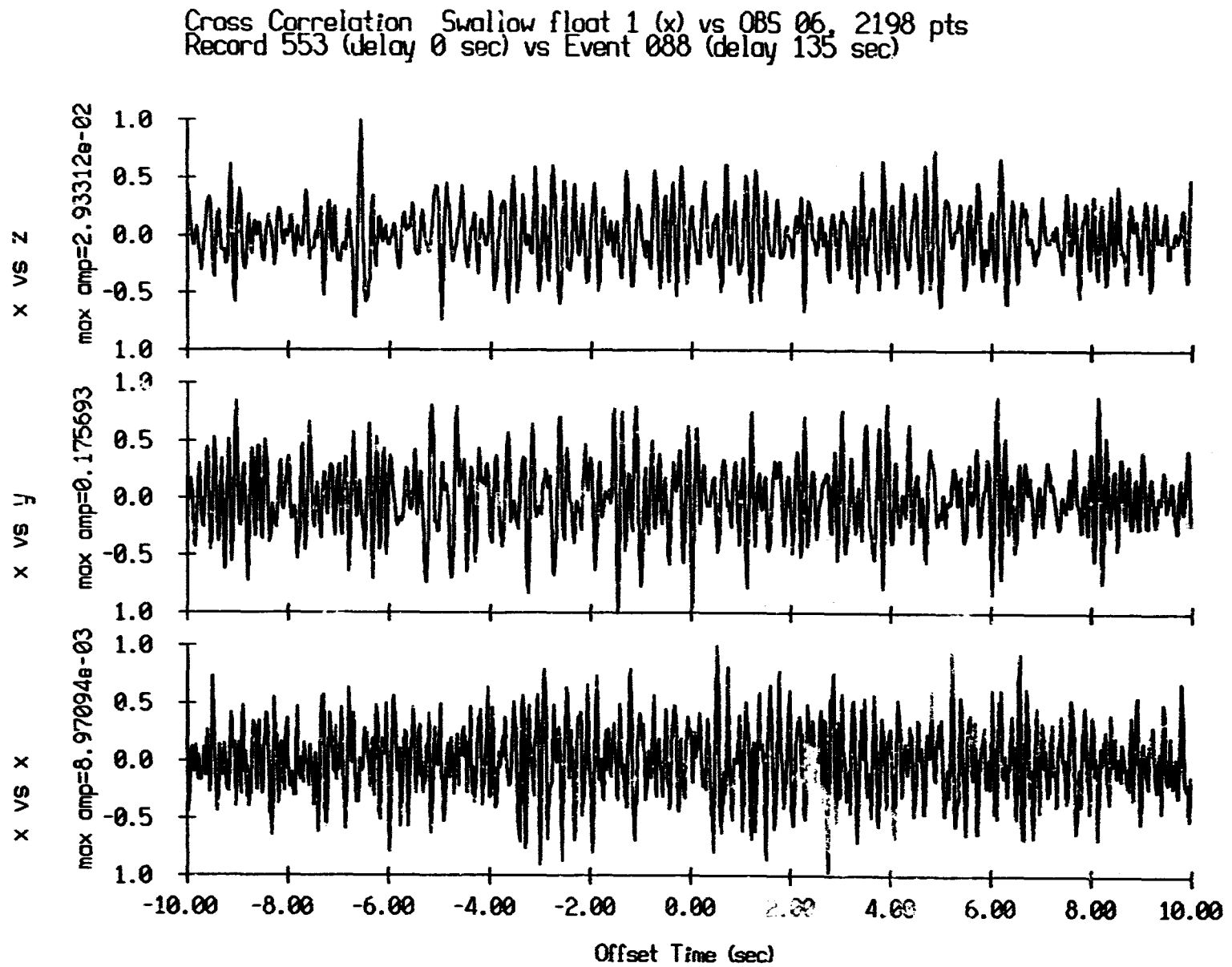

Figure III.7i

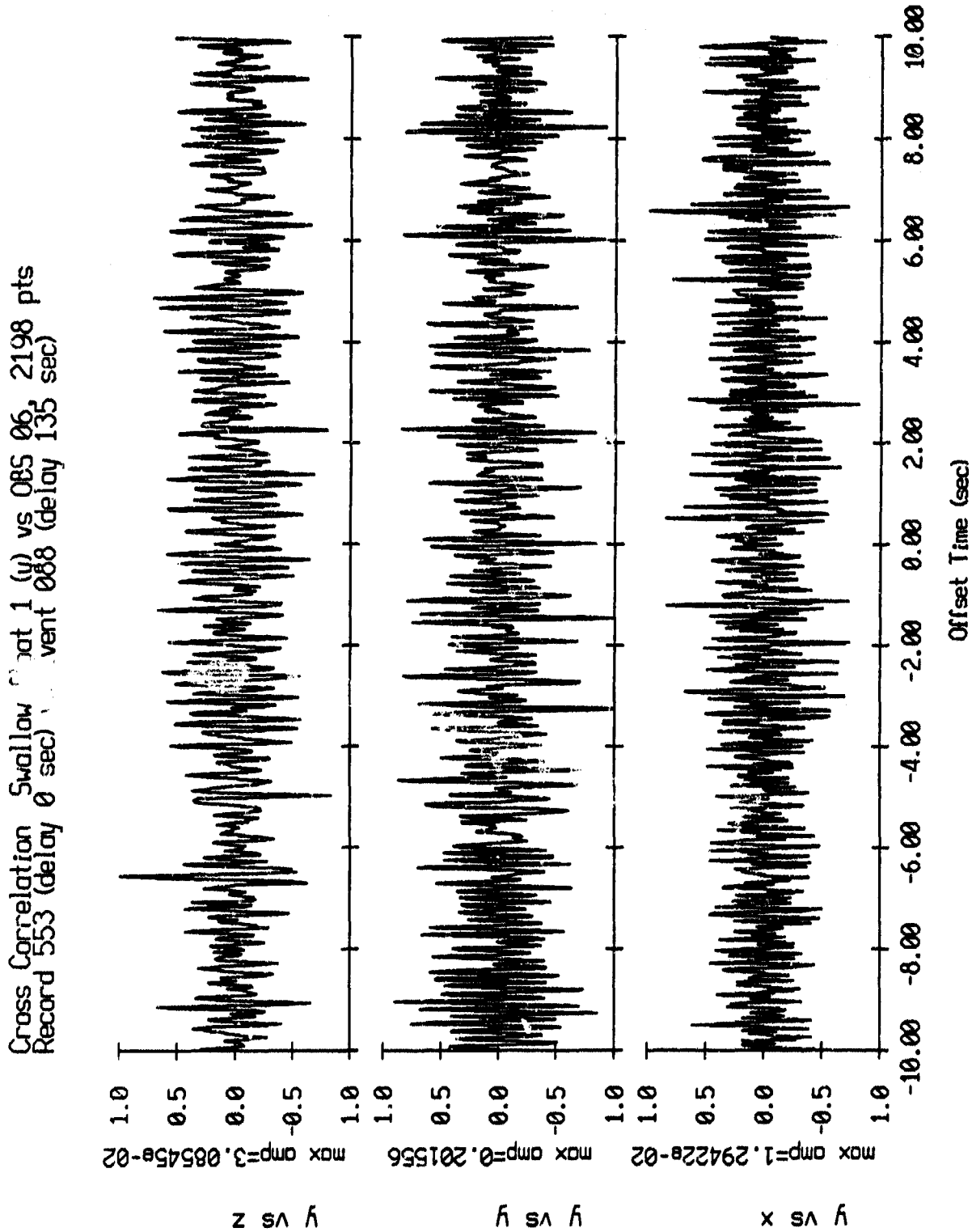

Figure III.7j

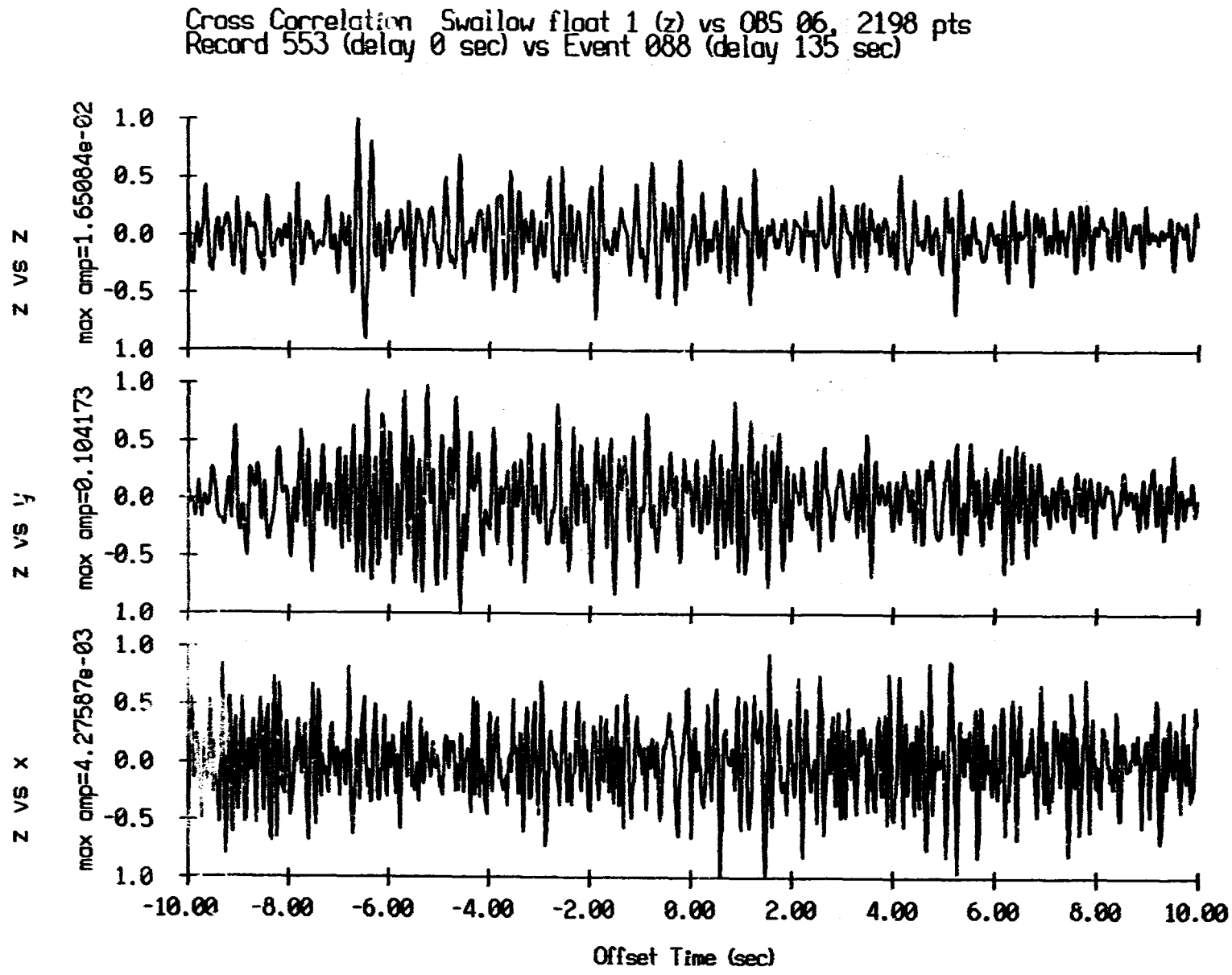

Figure III.7k

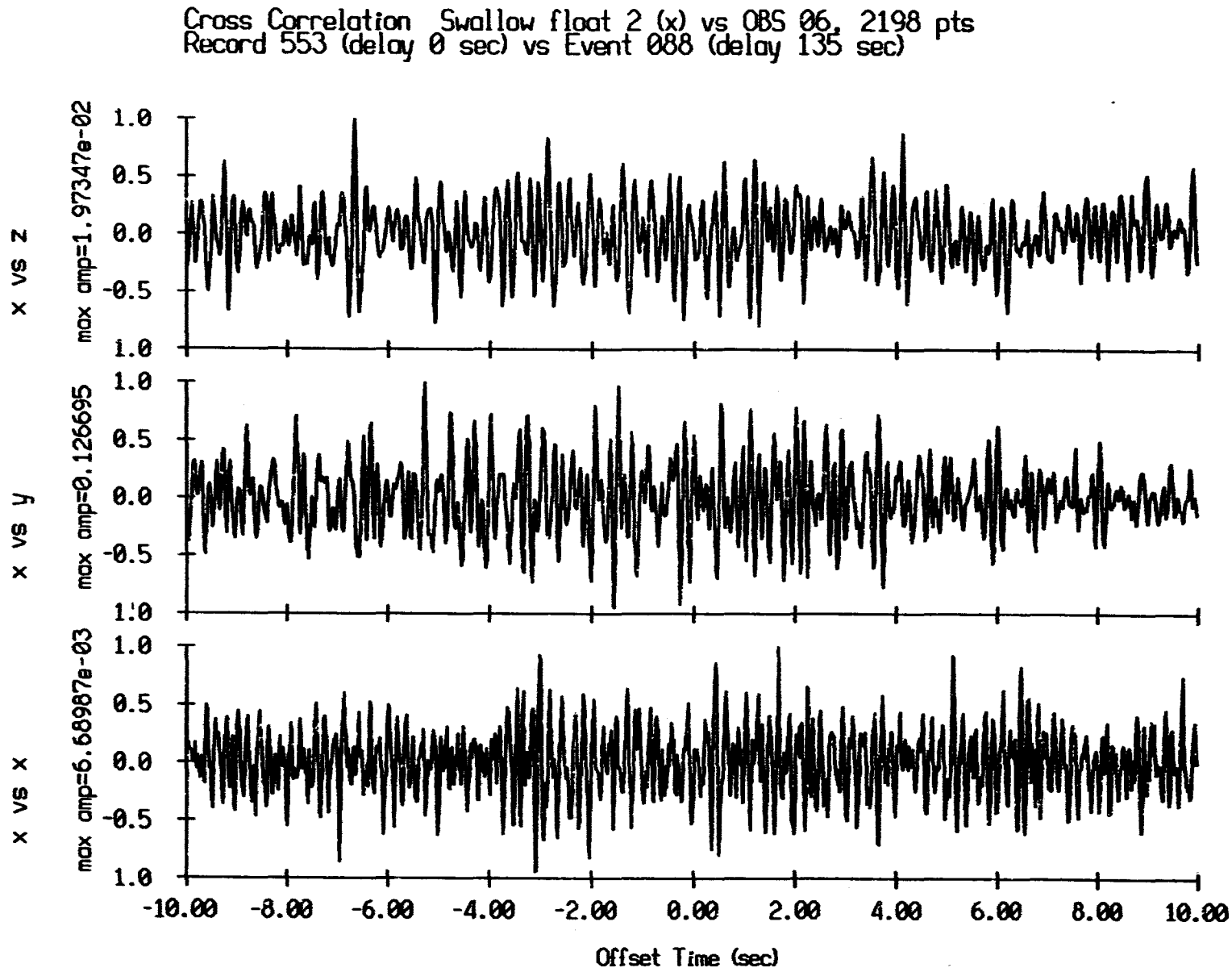

Figure III.8i

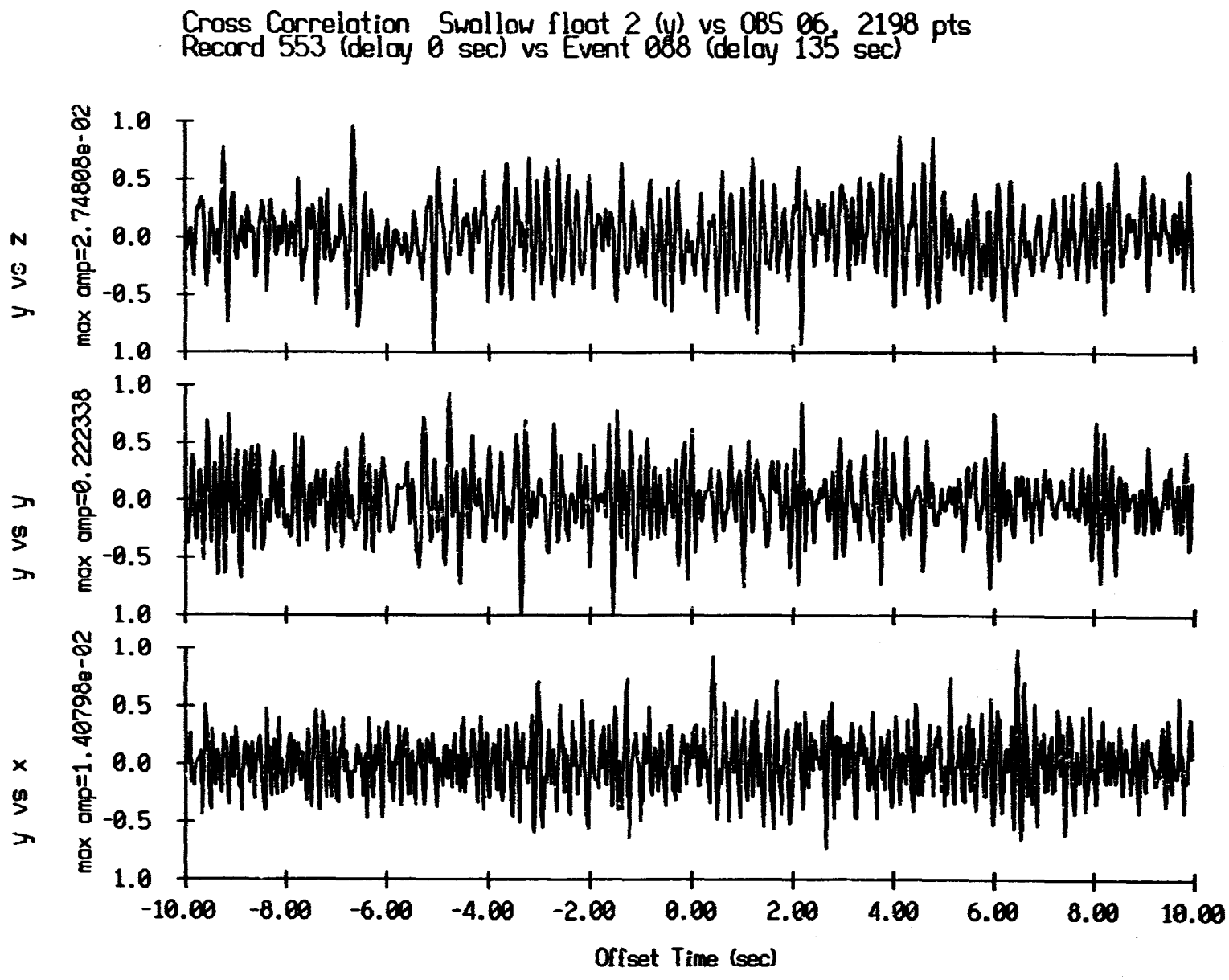

Figure III.8j

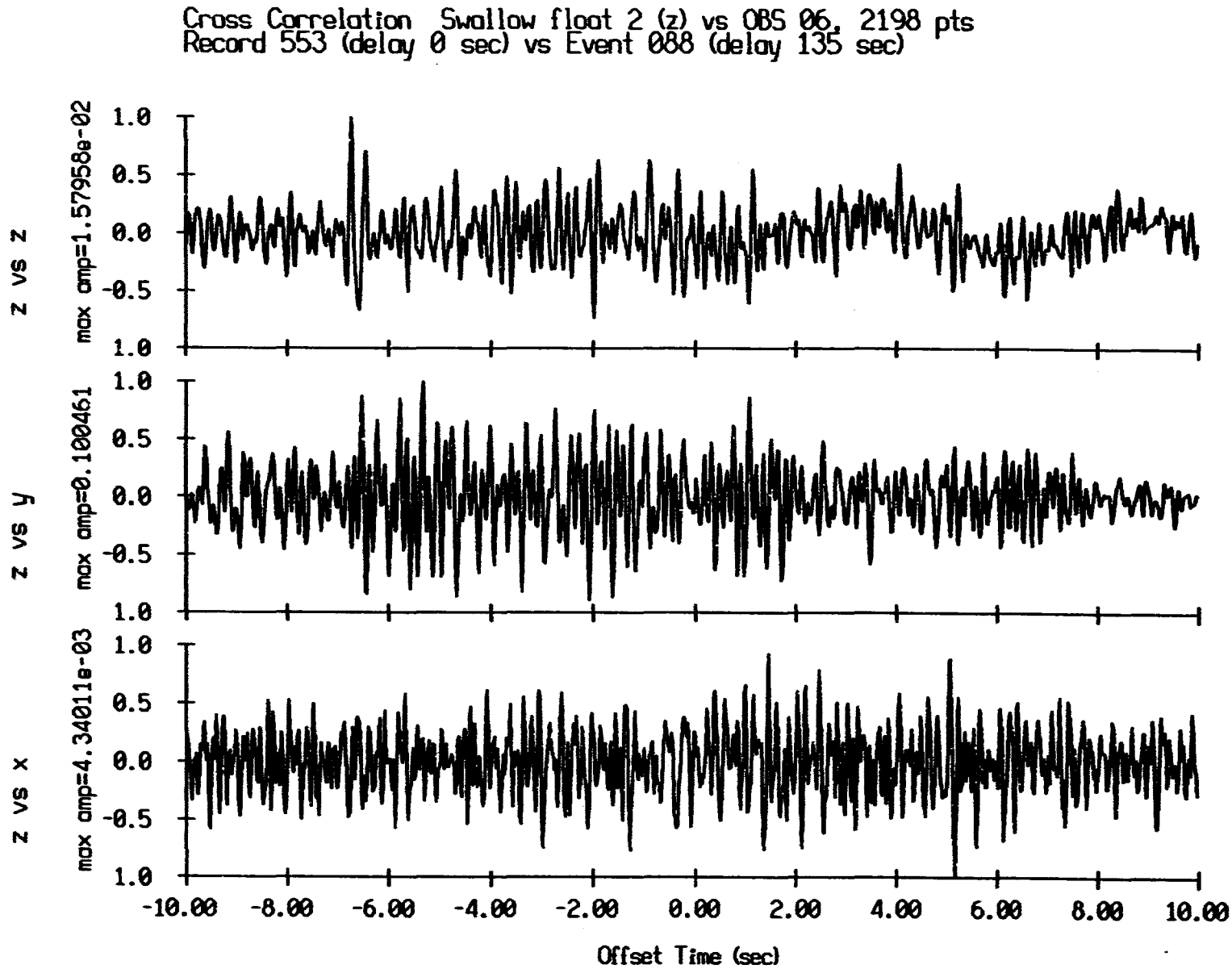

Figure III.8k

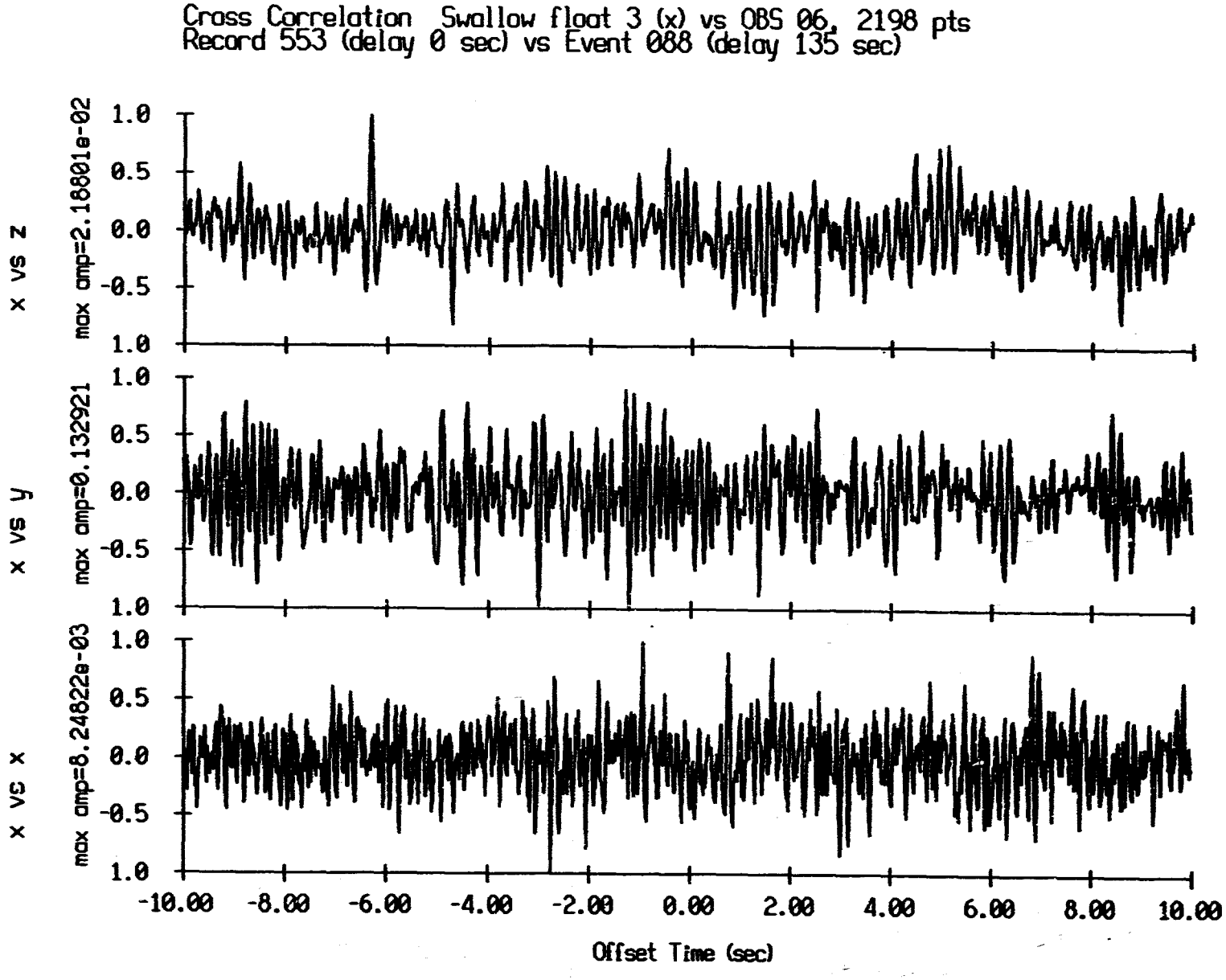

Figure III.9i

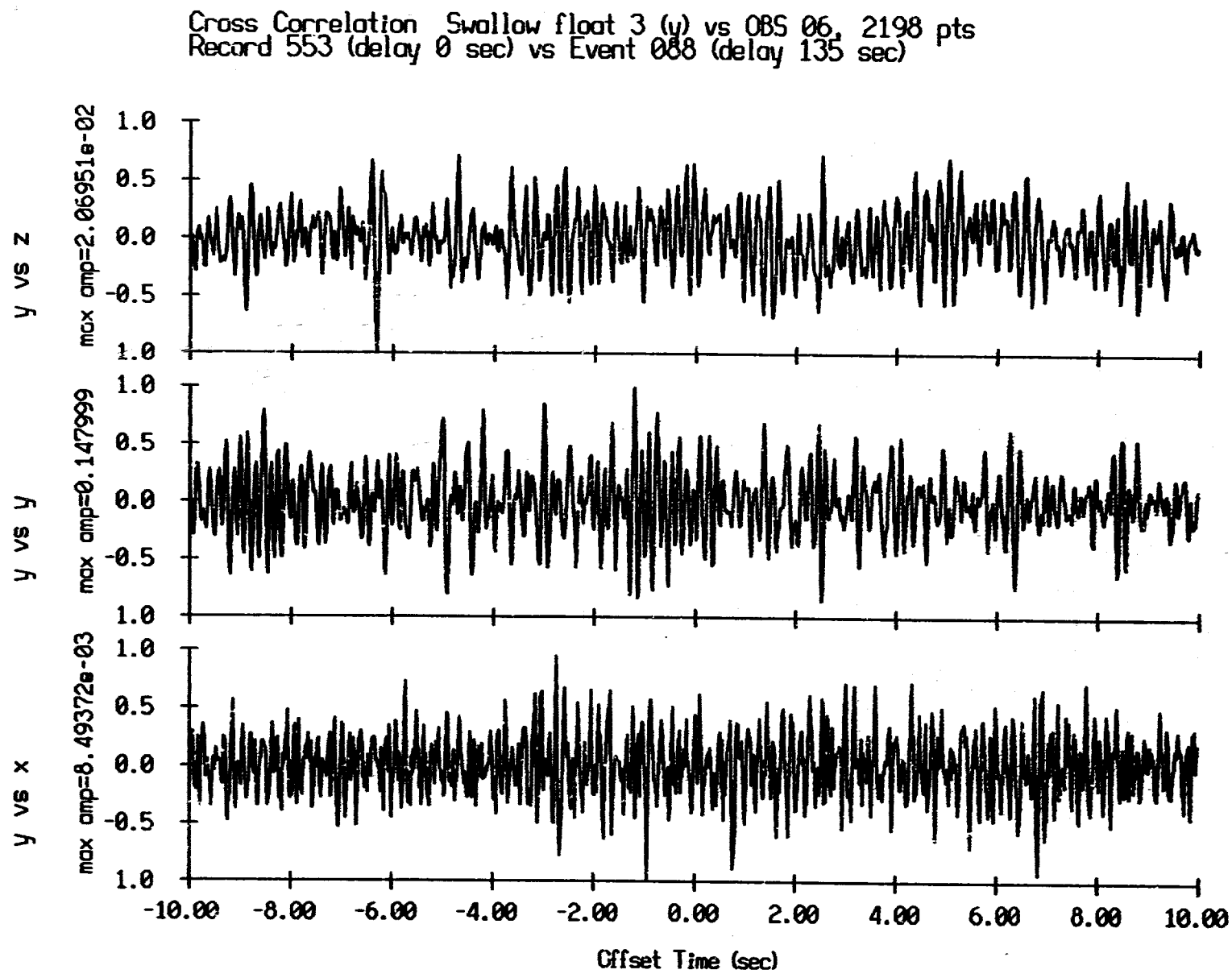

Figure III.9j

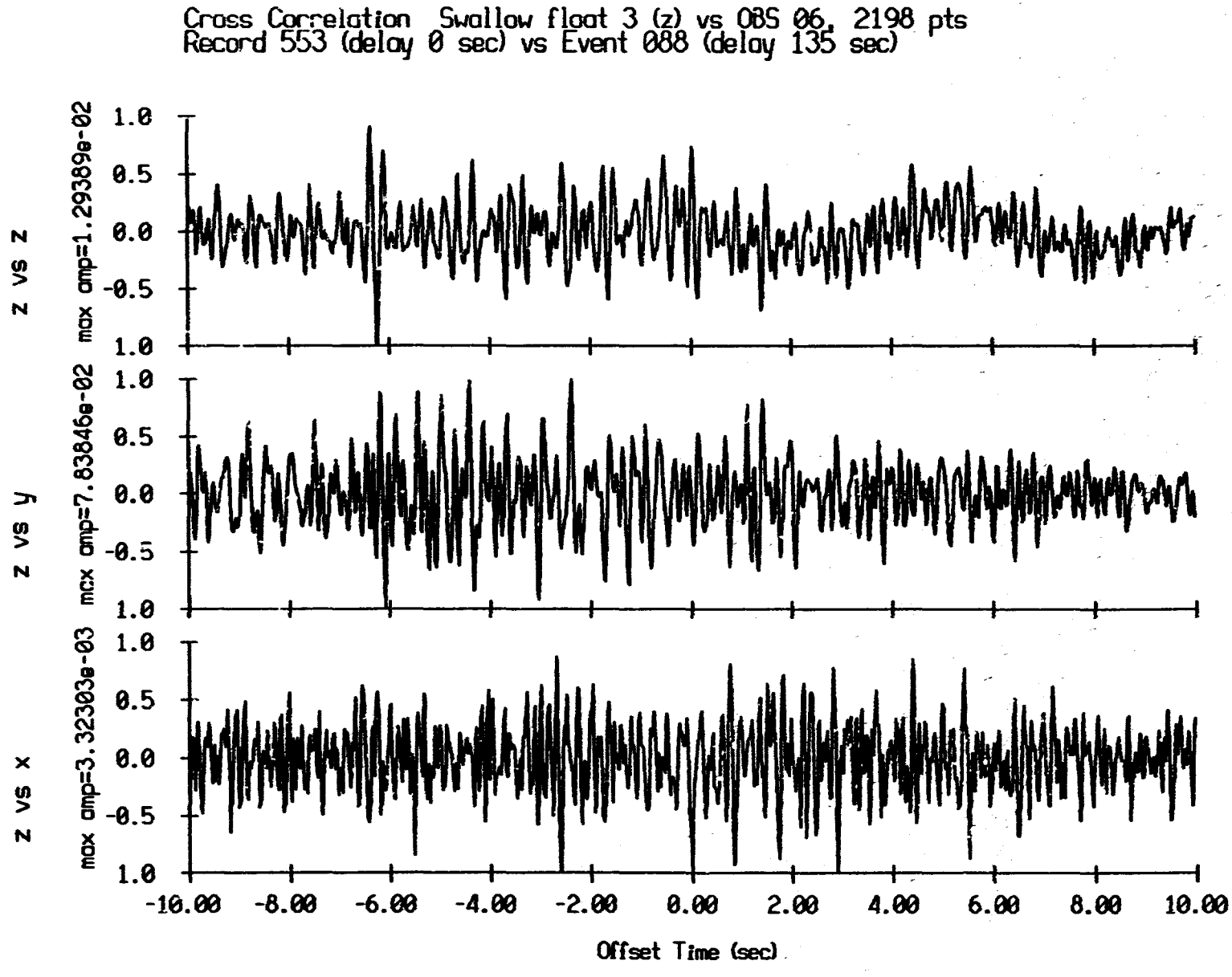

Figure III.9k

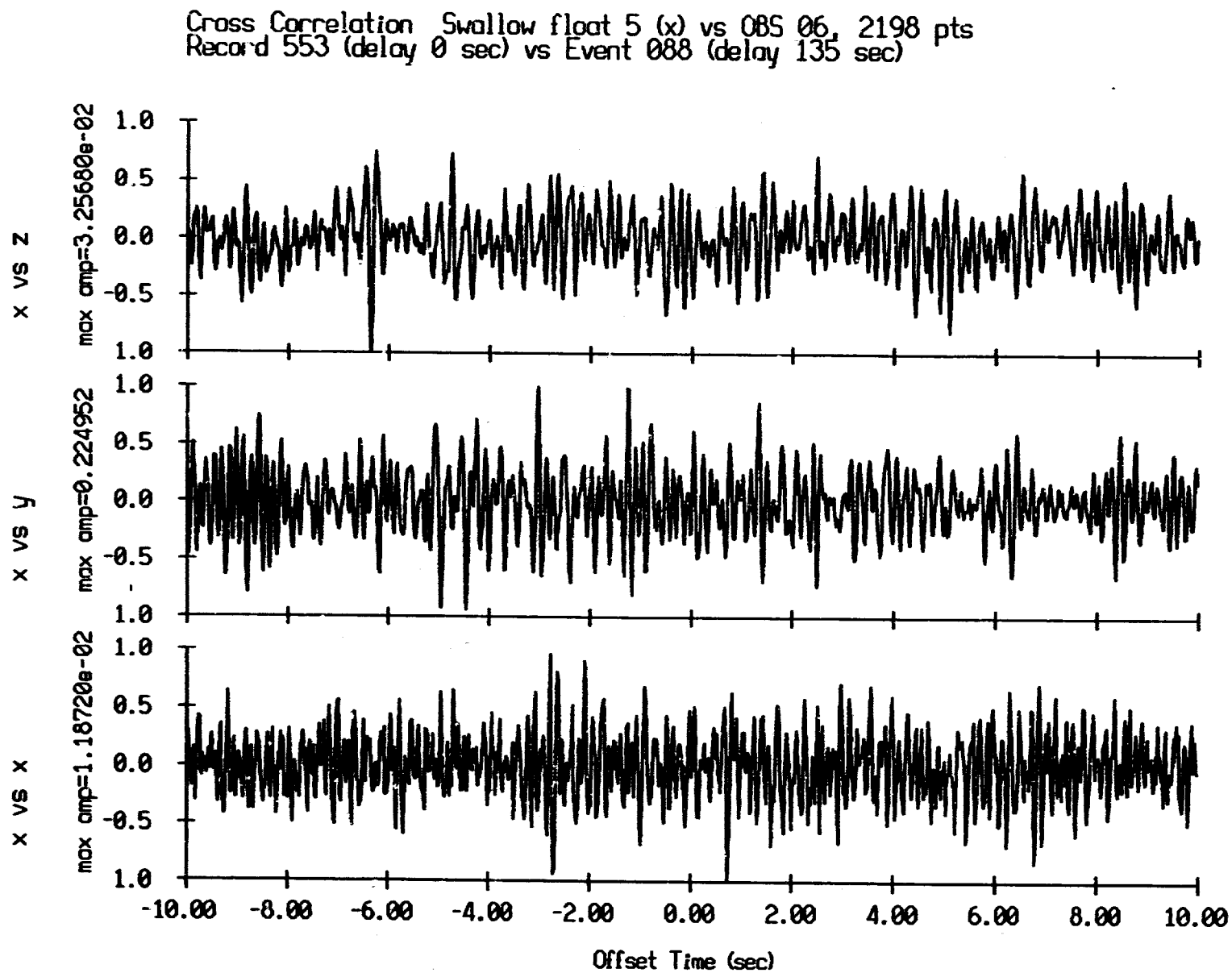

Figure III.10i

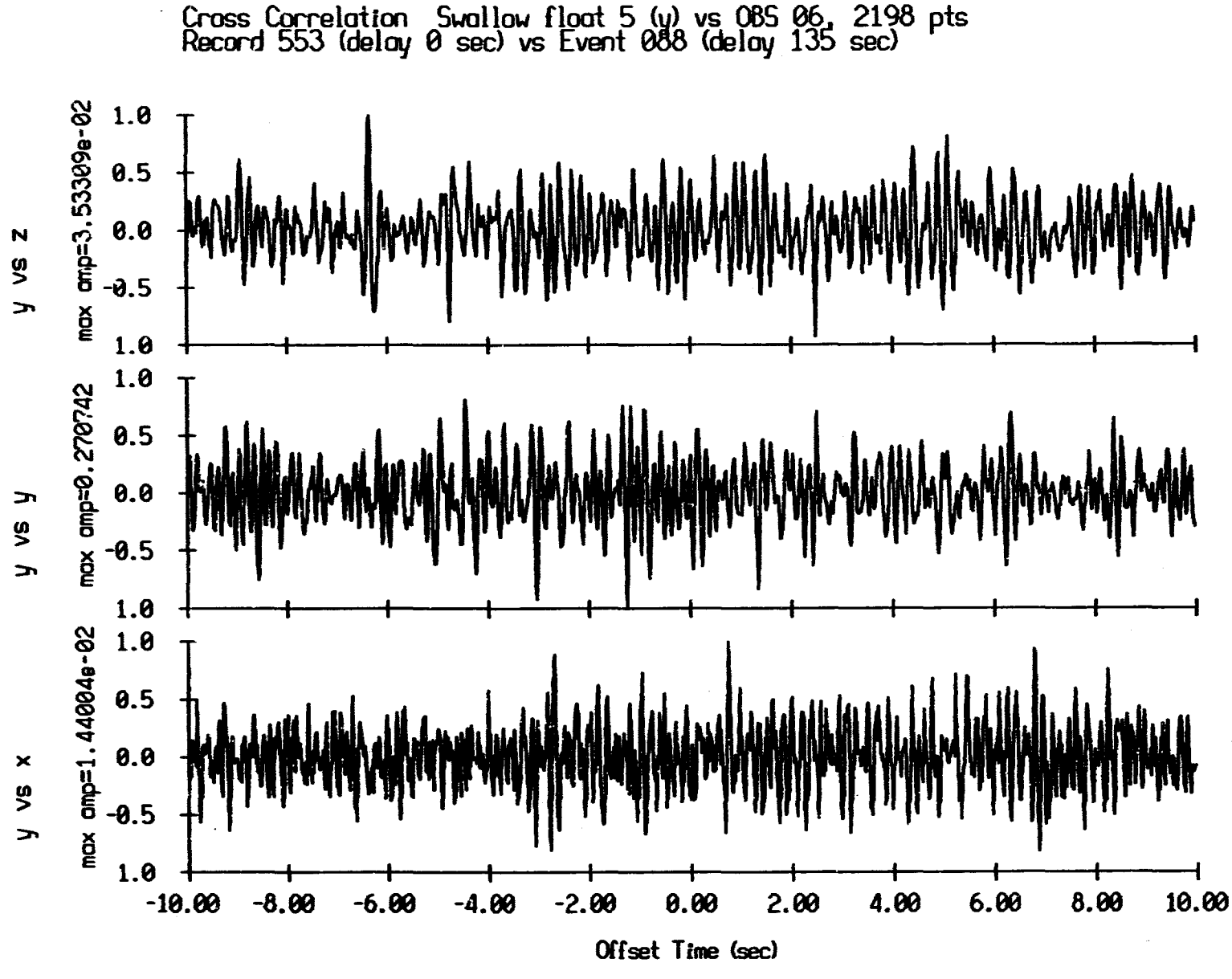

Figure III.10j

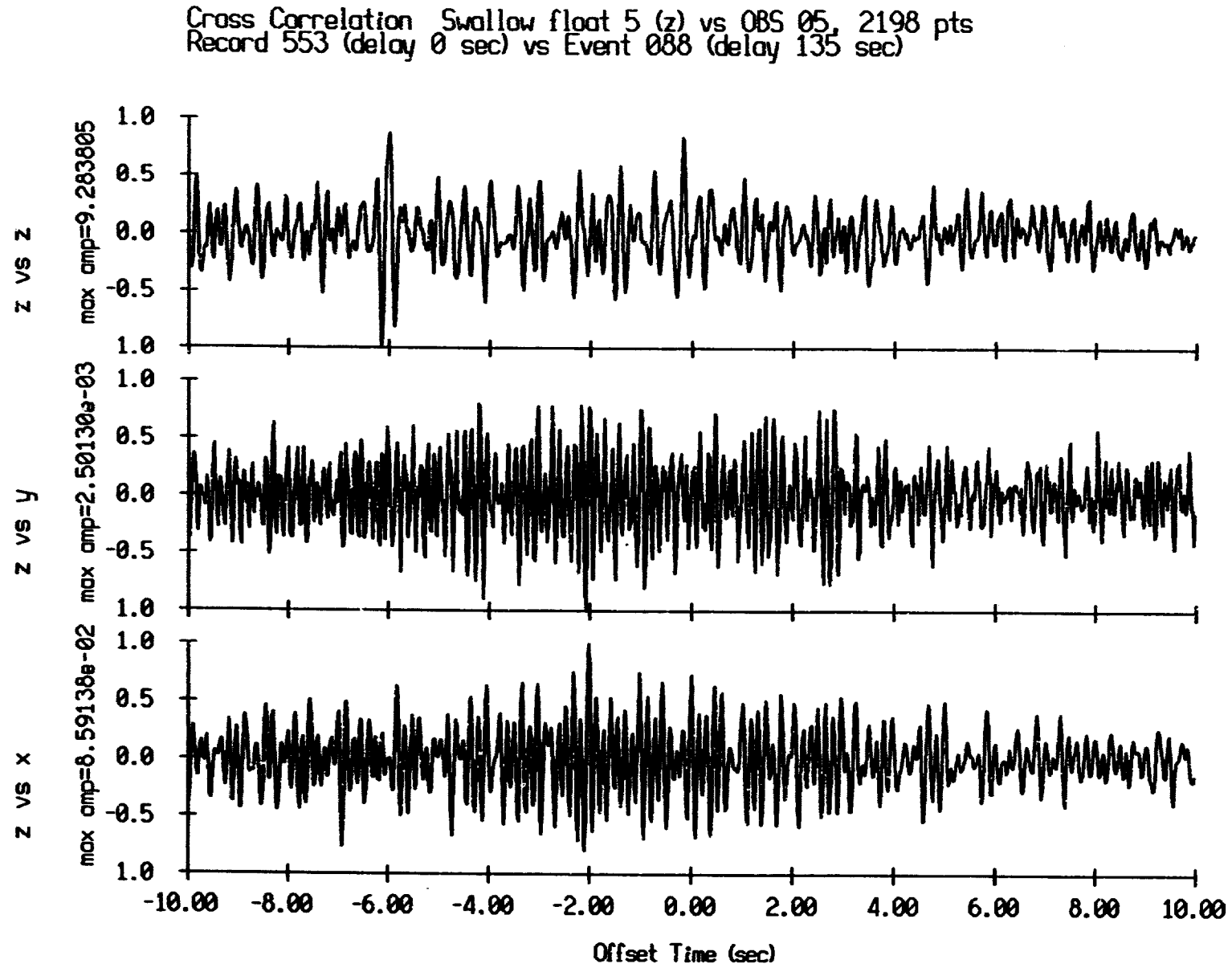

Figure III.10k

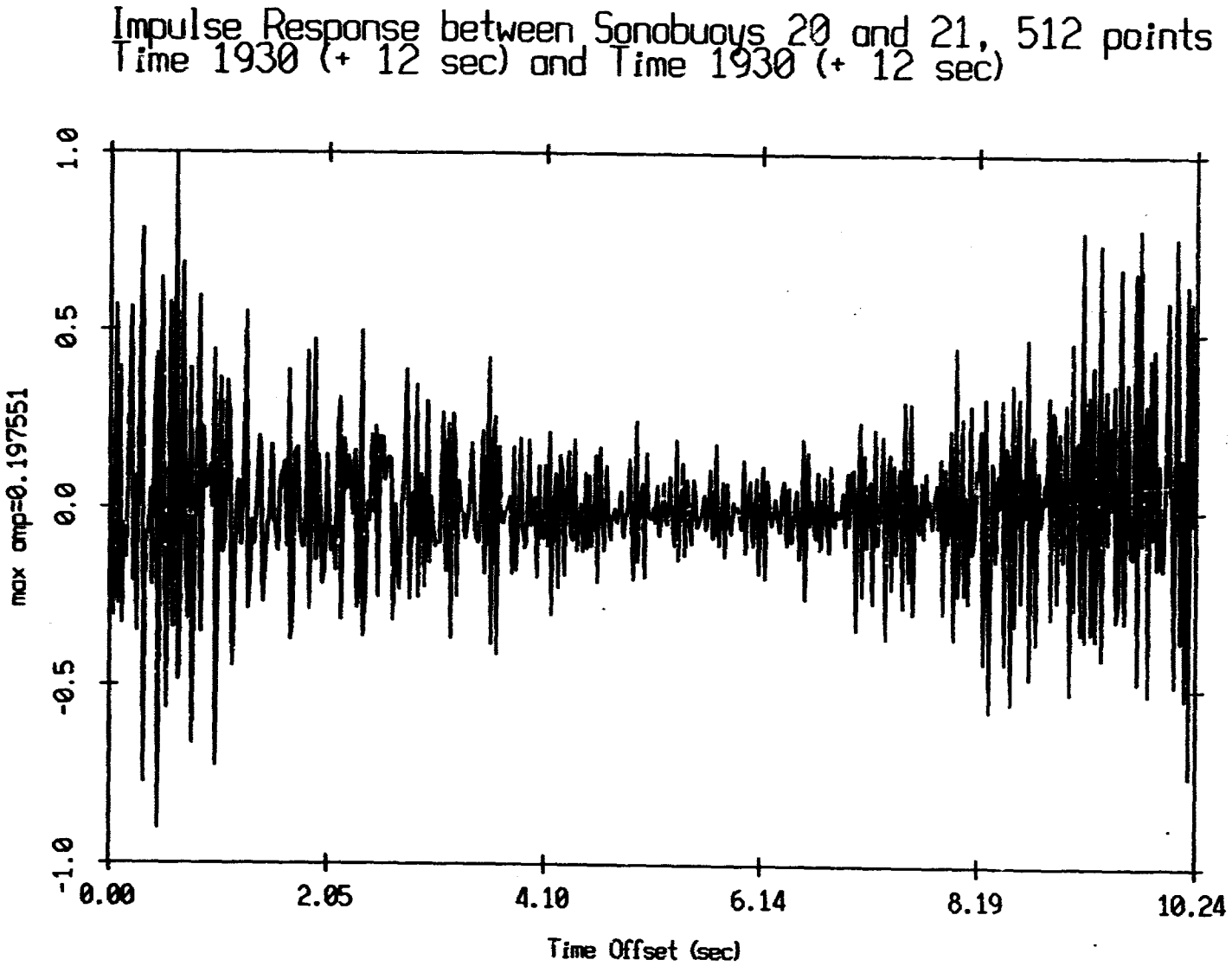

Figure III.11

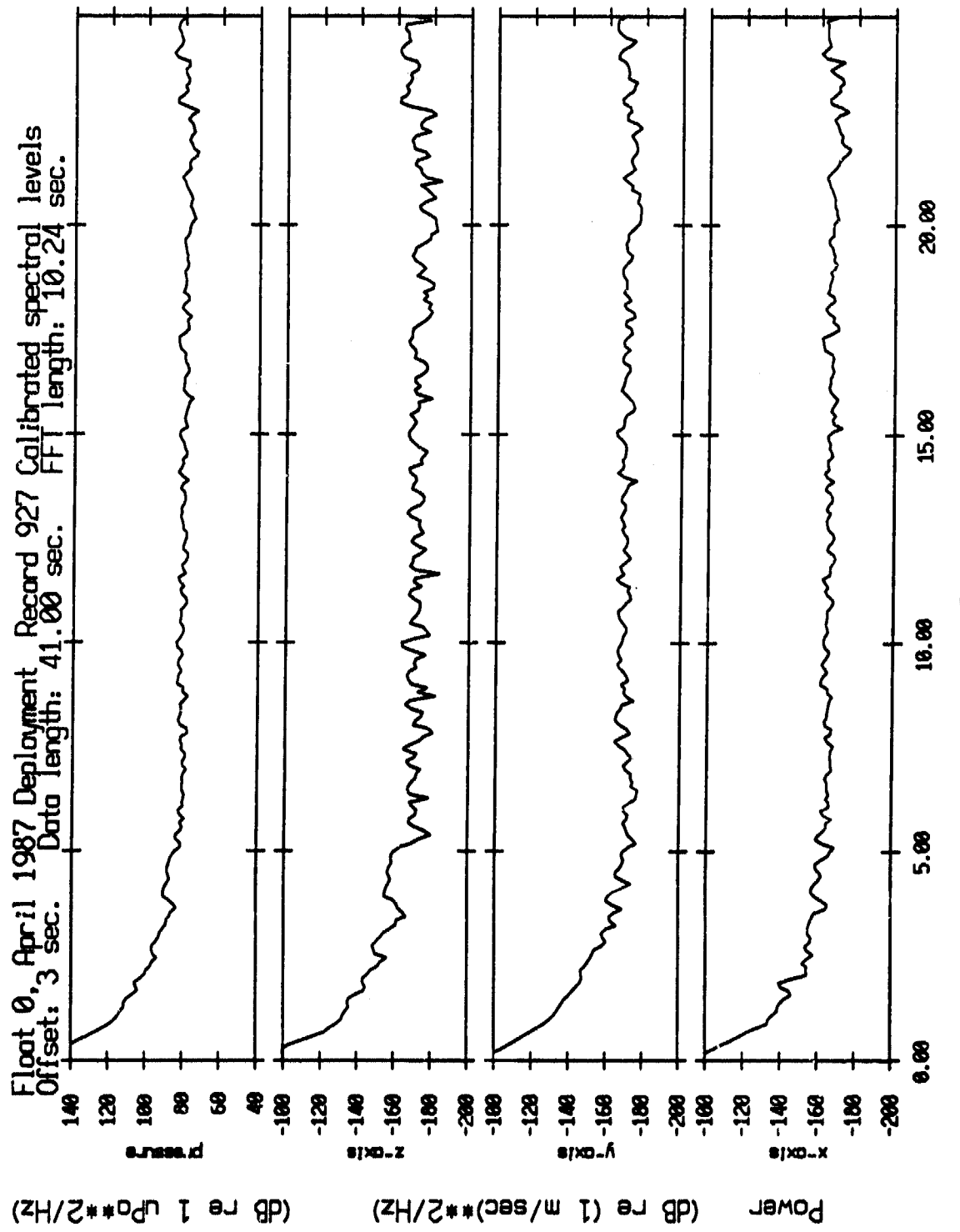
Float 0, April 1987 Deployment Record 927 Calibrated spectral levels
Offset: 3 sec. Data length: 41.00 sec. FFT length: 10.24 sec.
pressure
z-axis
y-axis
x-axis
Power (dB re (1 m/sec)**2/Hz)
(dB re 1 uPa**2/Hz)
Frequency (Hz)
0.00
5.00
10.00
15.00
20.00

Figure IV.1a

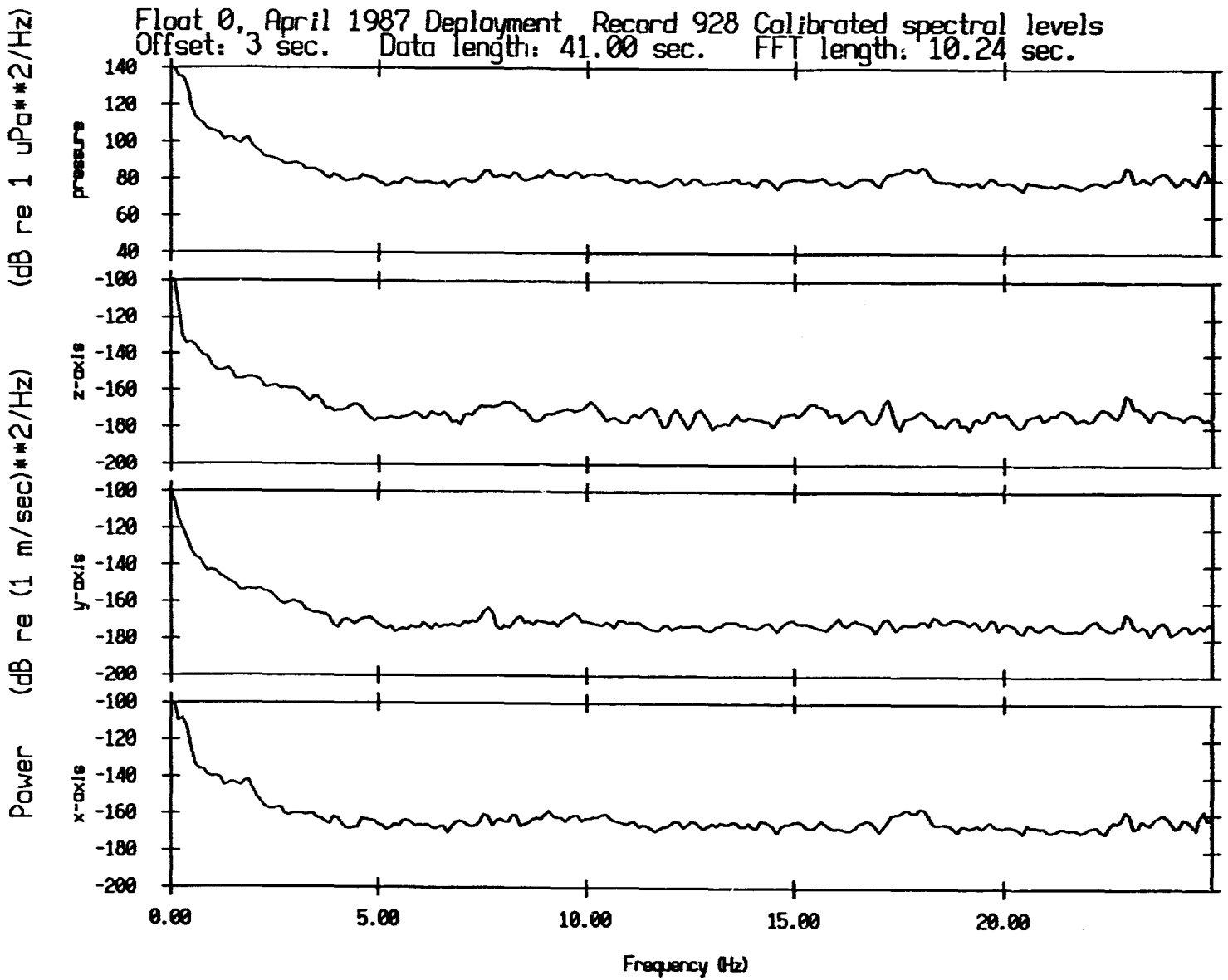
Float 0, April 1987 Deployment Record 928 Calibrated spectral levels
Offset: 3 sec. Data length: 41.00 sec. FFT length: 10.24 sec.
Power (dB re (1 m/sec)**2/Hz) (dB re 1 uPa**2/Hz)
pressure
z-axis
y-axis
x-axis
140
120
100
80
60
40
-100
-120
-140
-160
-180
-200
0.00
5.00
10.00
15.00
20.00
Frequency (Hz)

Figure IV.1b

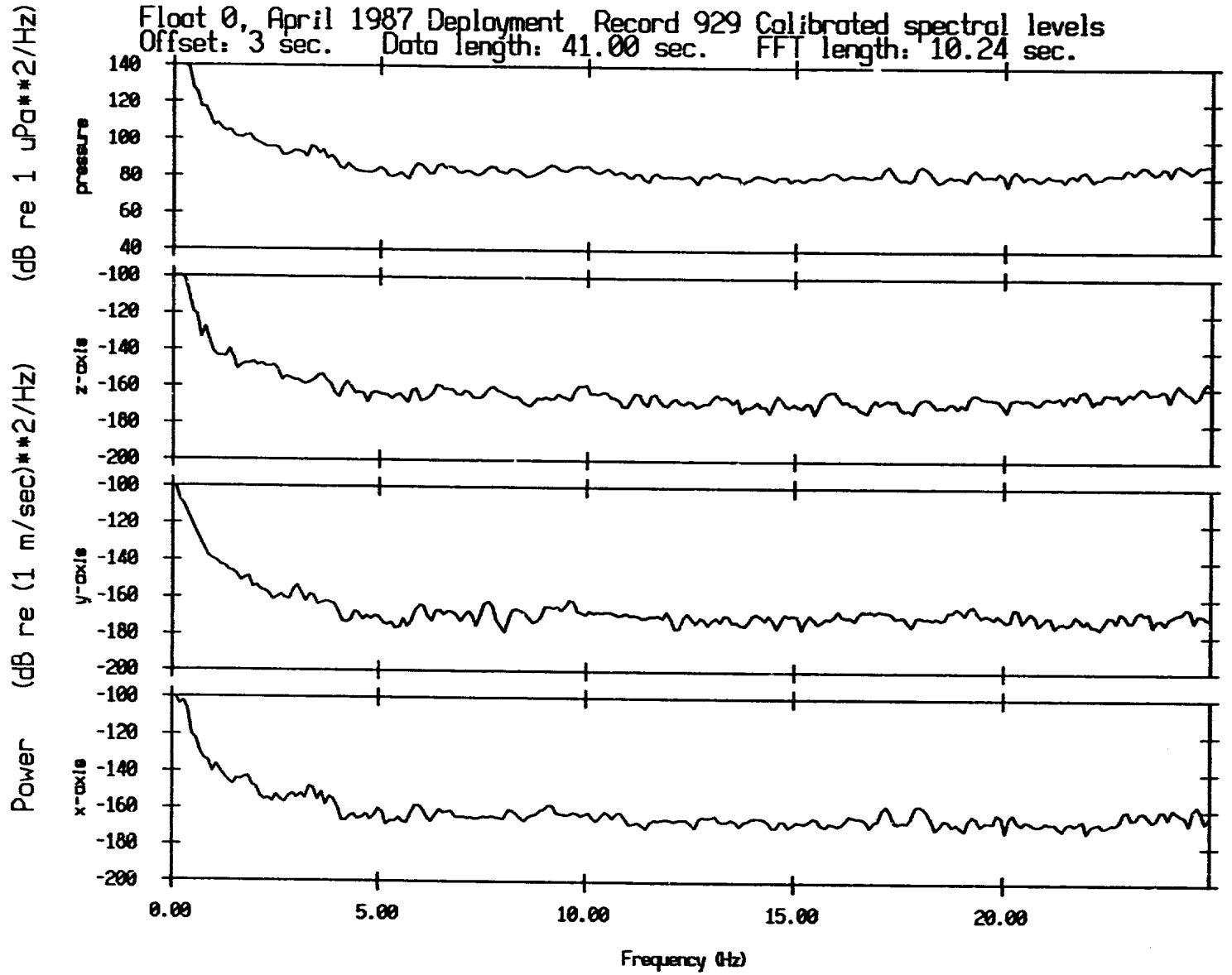
Float 0, April 1987 Deployment Record 929 Calibrated spectral levels
Offset: 3 sec. Data length: 41.00 sec. FFT length: 10.24 sec.
Power (dB re (1 m/sec)**2/Hz) (dB re 1 uPa**2/Hz)
pressure
z-axis
y-axis
x-axis
140
120
100
80
60
40
-100
-120
-140
-160
-180
-200
0.00
5.00
10.00
15.00
20.00
Frequency (Hz)

Figure IV.1c

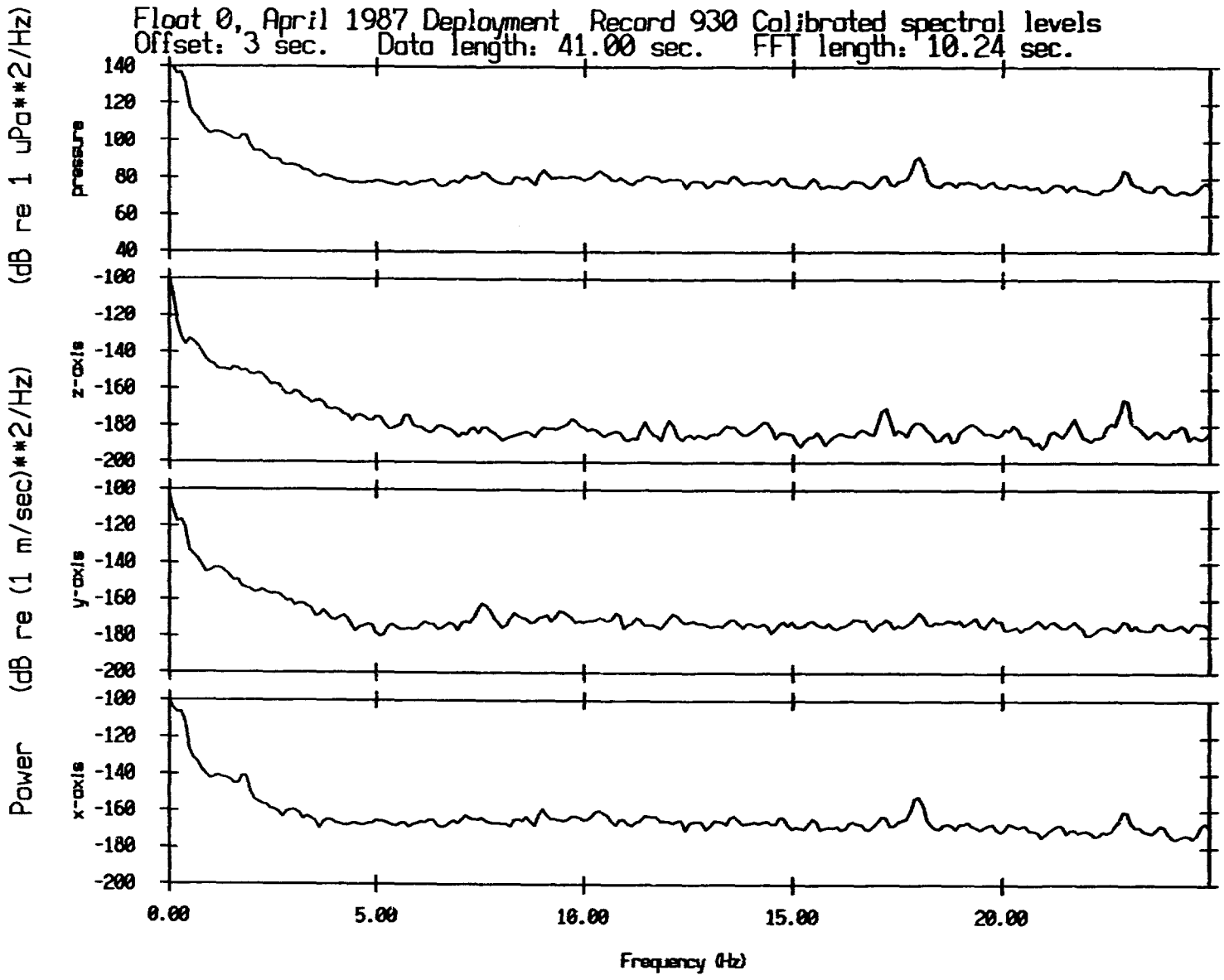
Float 0, April 1987 Deployment Record 930 Calibrated spectral levels
Offset: 3 sec. Data length: 41.00 sec. FFT length: 10.24 sec.
Power (dB re (1 m/sec)**2/Hz) (dB re 1 uPa**2/Hz)
pressure
z-axis
y-axis
x-axis
140
120
100
80
60
40
-100
-120
-140
-160
-180
-200
0.00
5.00
10.00
15.00
20.00
Frequency (Hz)

Figure IV.1d

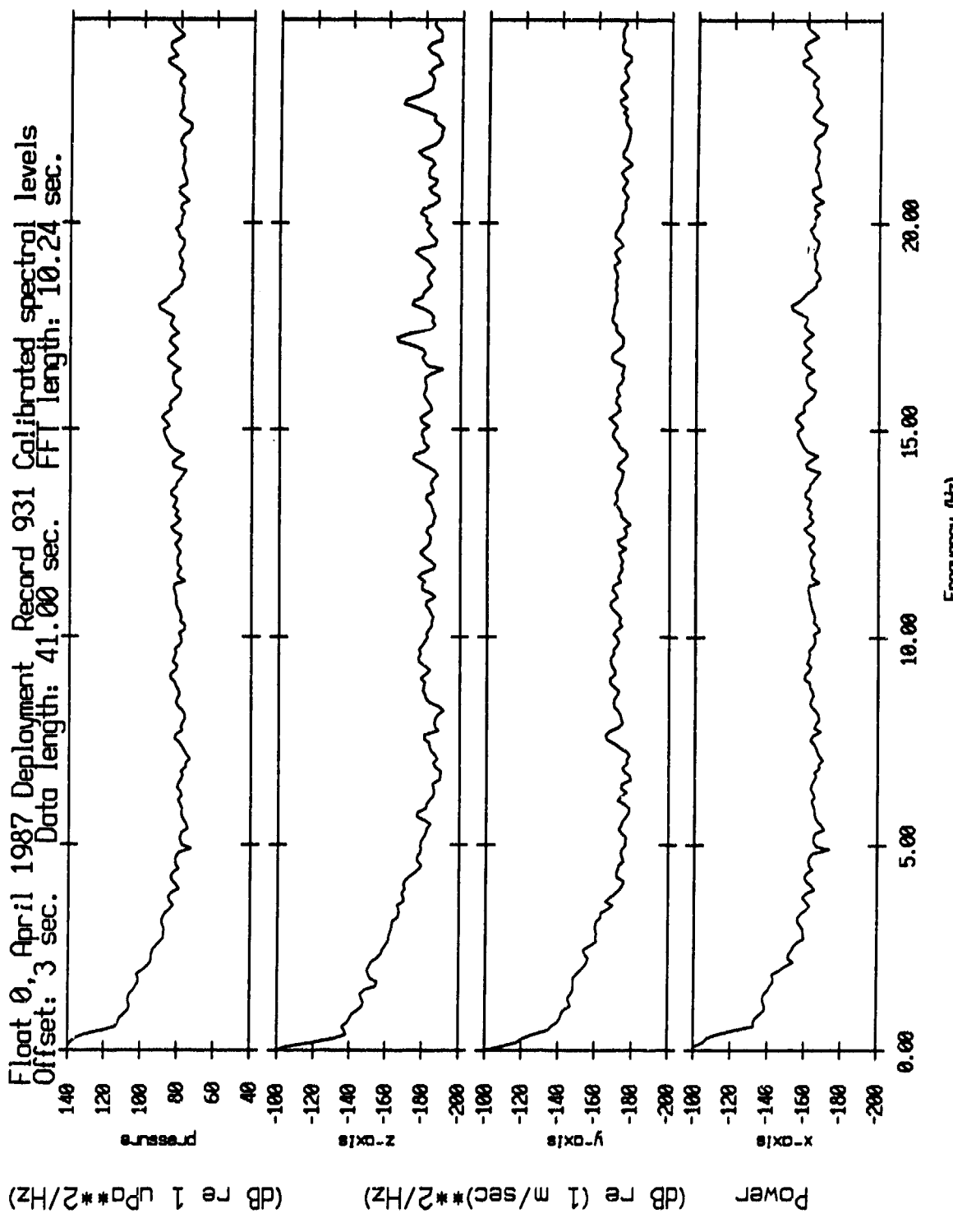
Float 0, April 1987 Deployment Record 931 Calibrated spectral levels
Offset: 3 sec. Data length: 41.00 sec. FFT length: 10.24 sec.
pressure
z-axis
y-axis
x-axis
Power (dB re (1 m/sec)**2/Hz)
(dB re 1 uPa**2/Hz)
Frequency (Hz)
0.00
5.00
10.00
15.00
20.00

Figure IV.1e

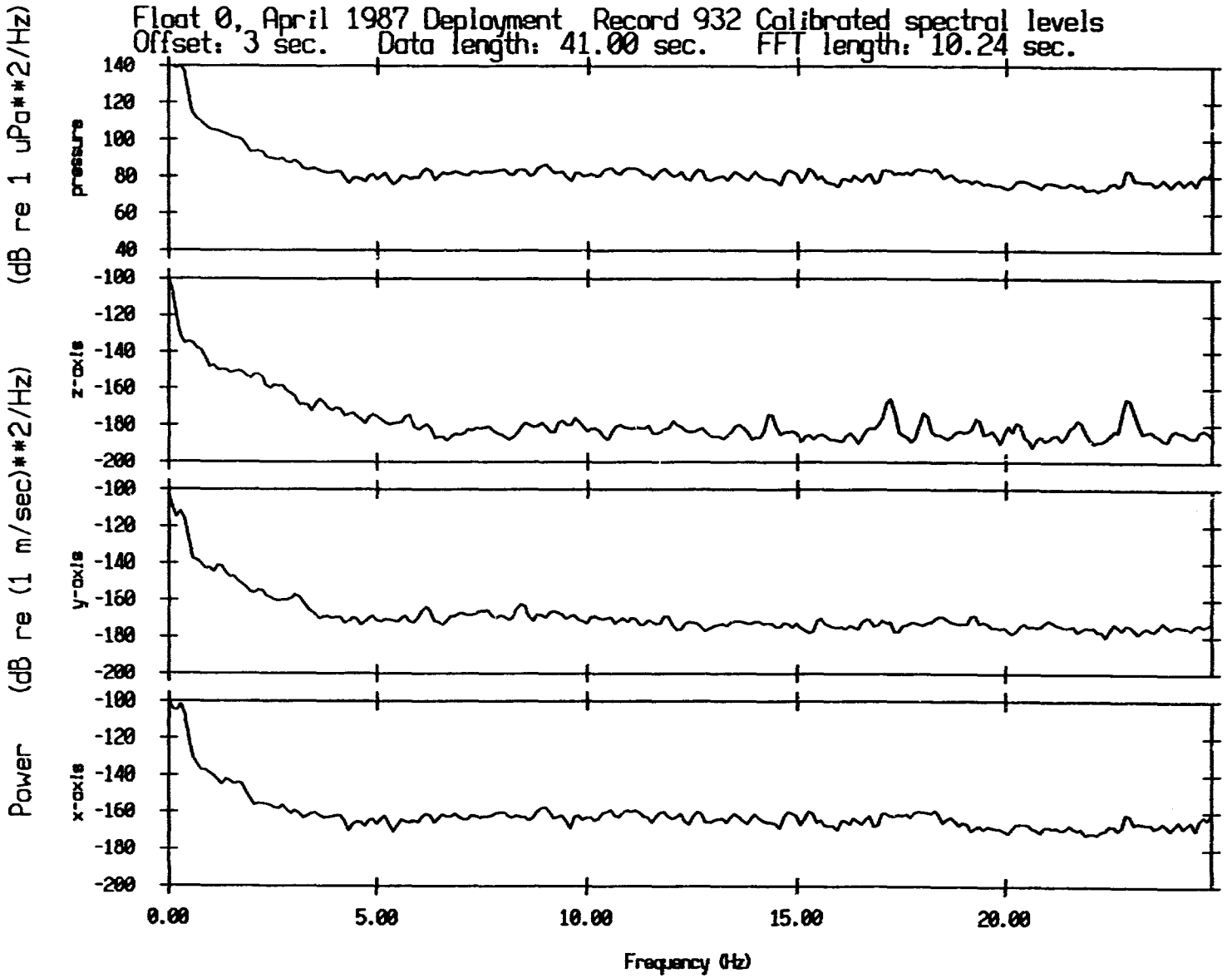
Float 0, April 1987 Deployment Record 932 Calibrated spectral levels
Offset: 3 sec. Data length: 41.00 sec. FFT length: 10.24 sec.
Power (dB re (1 m/sec)**2/Hz) (dB re 1 uPa**2/Hz)
pressure
z-axis
y-axis
x-axis
140
120
100
80
60
40
-100
-120
-140
-160
-180
-200
0.00
5.00
10.00
15.00
20.00
Frequency (Hz)

Figure IV.1f

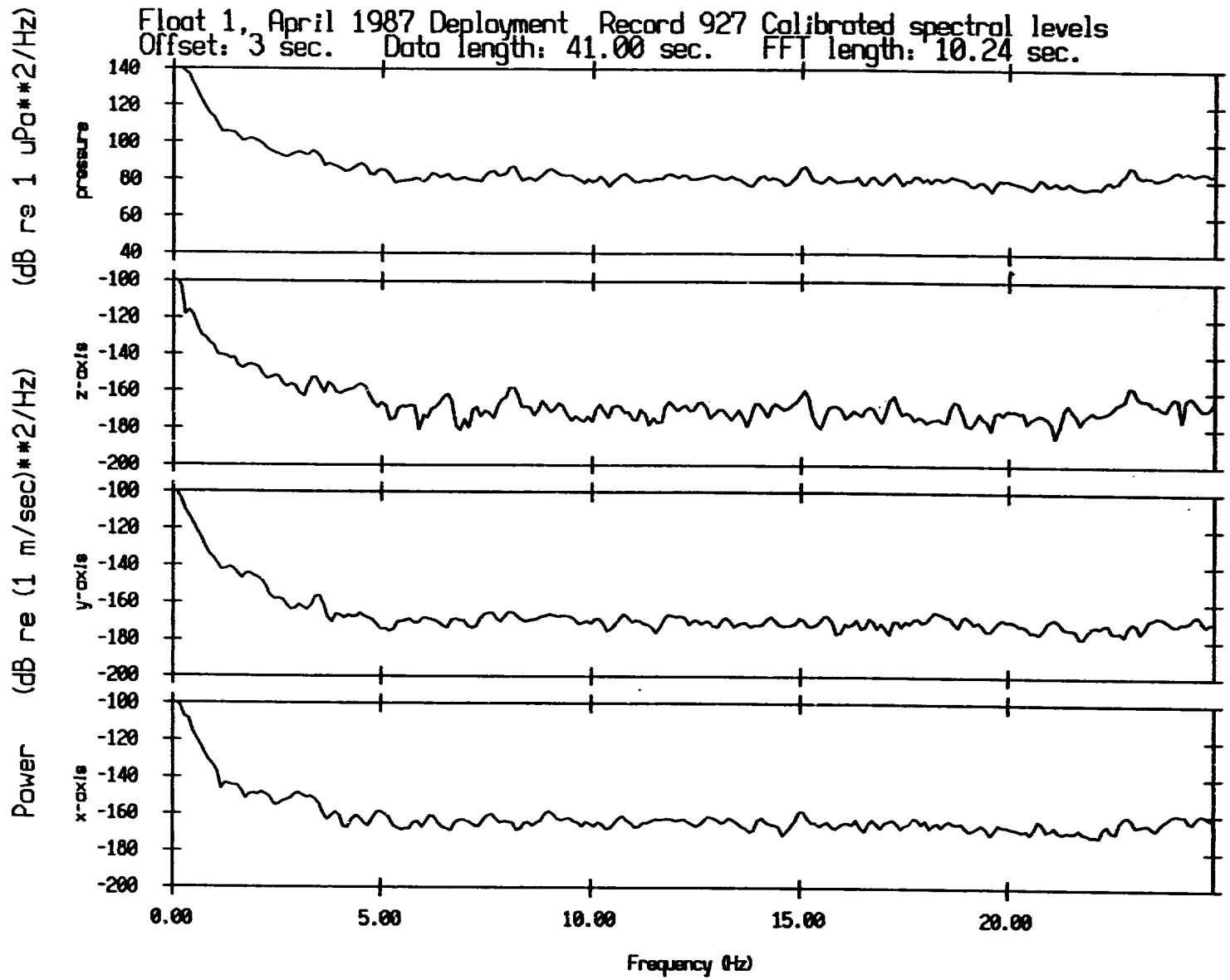
Float 1, April 1987 Deployment Record 927 Calibrated spectral levels
Offset: 3 sec. Data length: 41.00 sec. FFT length: 10.24 sec.
Power (dB re (1 m/sec)**2/Hz) (dB re 1 uPa**2/Hz)
pressure
z-axis
y-axis
x-axis
140
120
100
80
60
40
-100
-120
-140
-160
-180
-200
0.00
5.00
10.00
15.00
20.00
Frequency (Hz)

Figure IV.2a

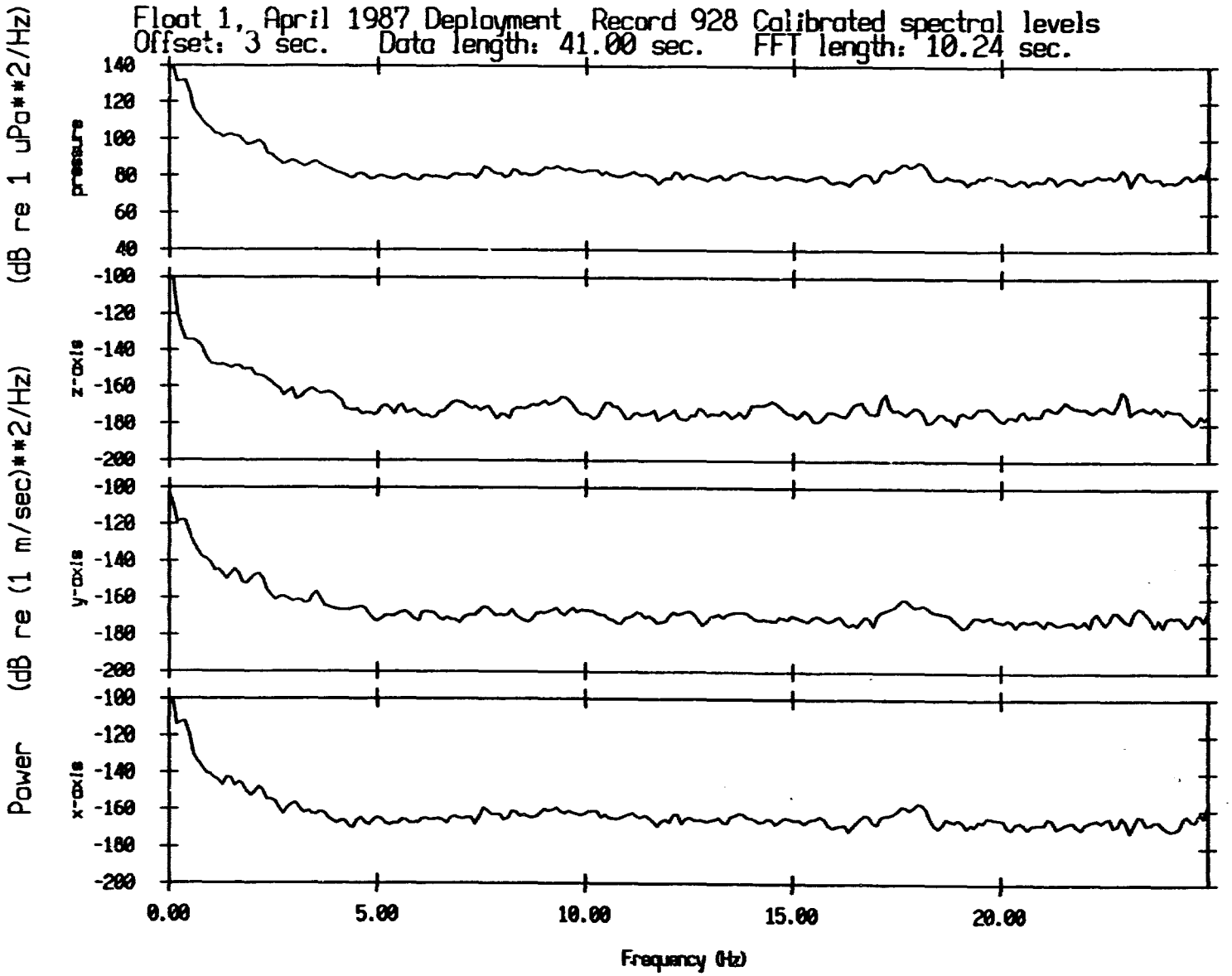
Float 1, April 1987 Deployment Record 928 Calibrated spectral levels
Offset: 3 sec. Data length: 41.00 sec. FFT length: 10.24 sec.
Power (dB re (1 m/sec)**2/Hz) (dB re 1 uPa**2/Hz)
pressure
z-axis
y-axis
x-axis
140
120
100
80
60
40
-100
-120
-140
-160
-180
-200
0.00
5.00
10.00
15.00
20.00
Frequency (Hz)

Figure IV.2b

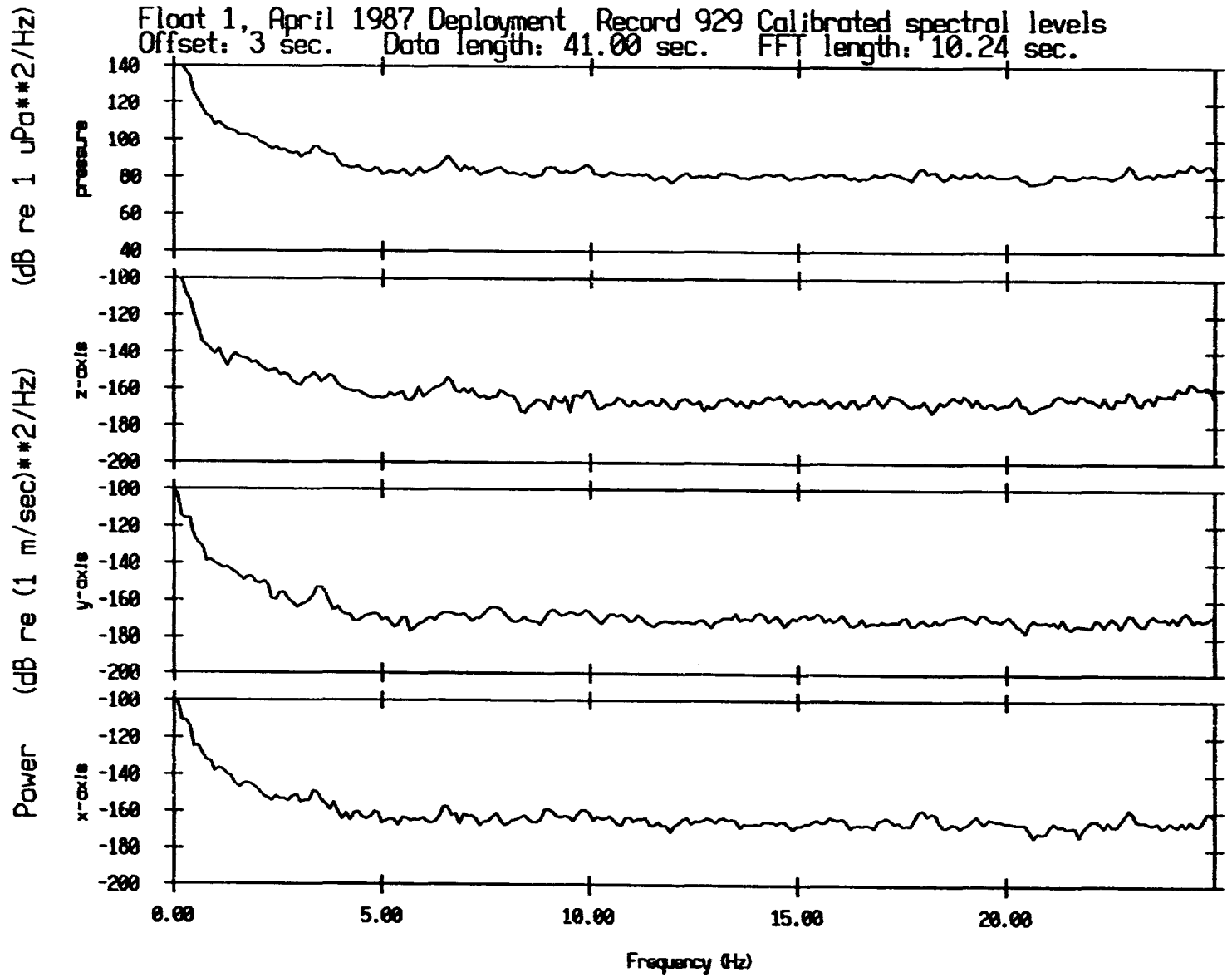
Float 1, April 1987 Deployment Record 929 Calibrated spectral levels
Offset: 3 sec. Data length: 41.00 sec. FFT length: 10.24 sec.
Power (dB re (1 m/sec)**2/Hz) (dB re 1 uPa**2/Hz)
pressure
z-axis
y-axis
x-axis
140
120
100
80
60
40
-100
-120
-140
-160
-180
-200
0.00
5.00
10.00
15.00
20.00
Frequency (Hz)

Figure IV.2c

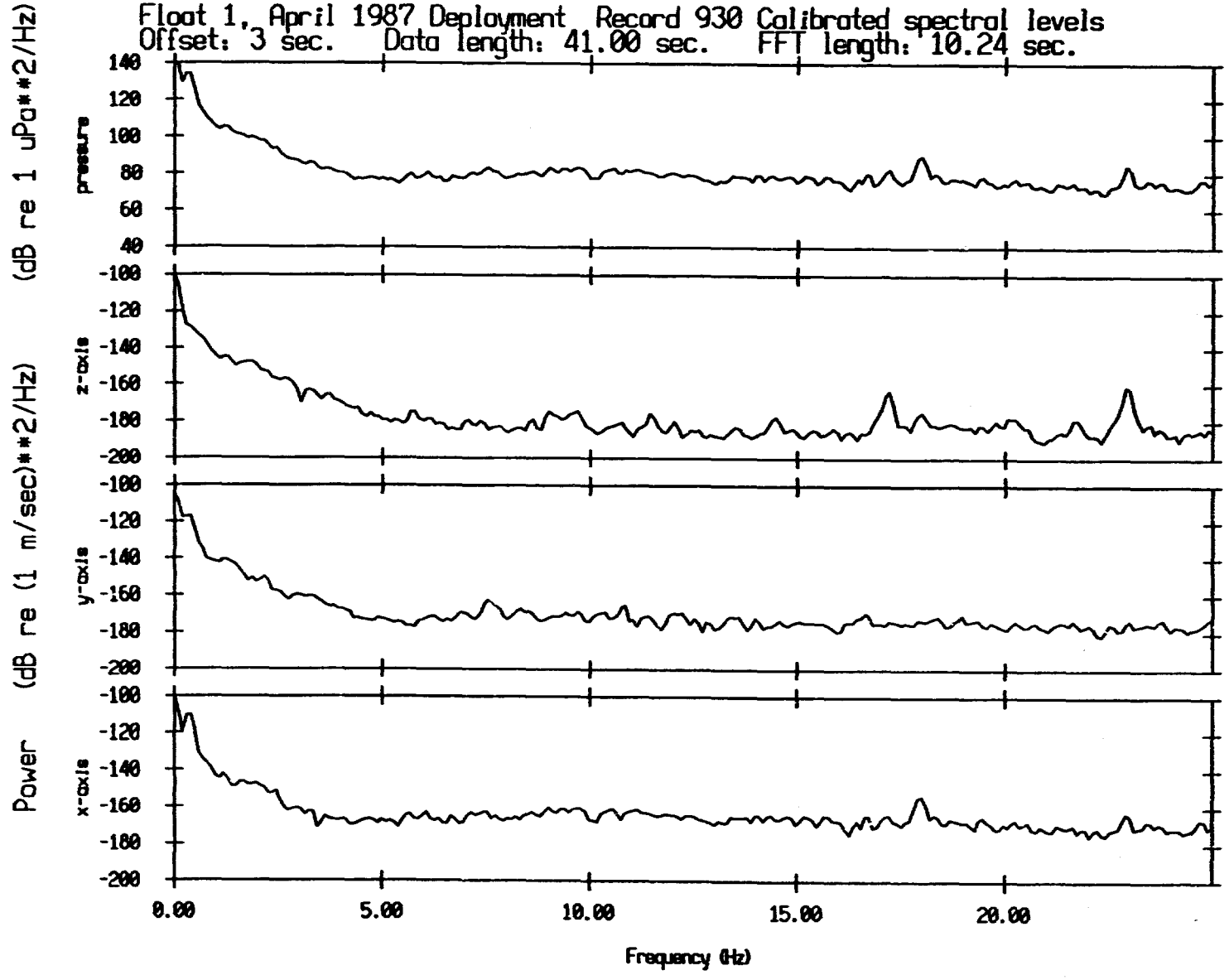
Float 1, April 1987 Deployment Record 930 Calibrated spectral levels
Offset: 3 sec. Data length: 41.00 sec. FFT length: 10.24 sec.
Power (dB re 1 uPa**2/Hz)
pressure
(dB re (1 m/sec)**2/Hz)
z-axis
y-axis
x-axis
140
120
100
80
60
40
-100
-120
-140
-160
-180
-200
0.00
5.00
10.00
15.00
20.00
Frequency (Hz)

Figure IV.2d

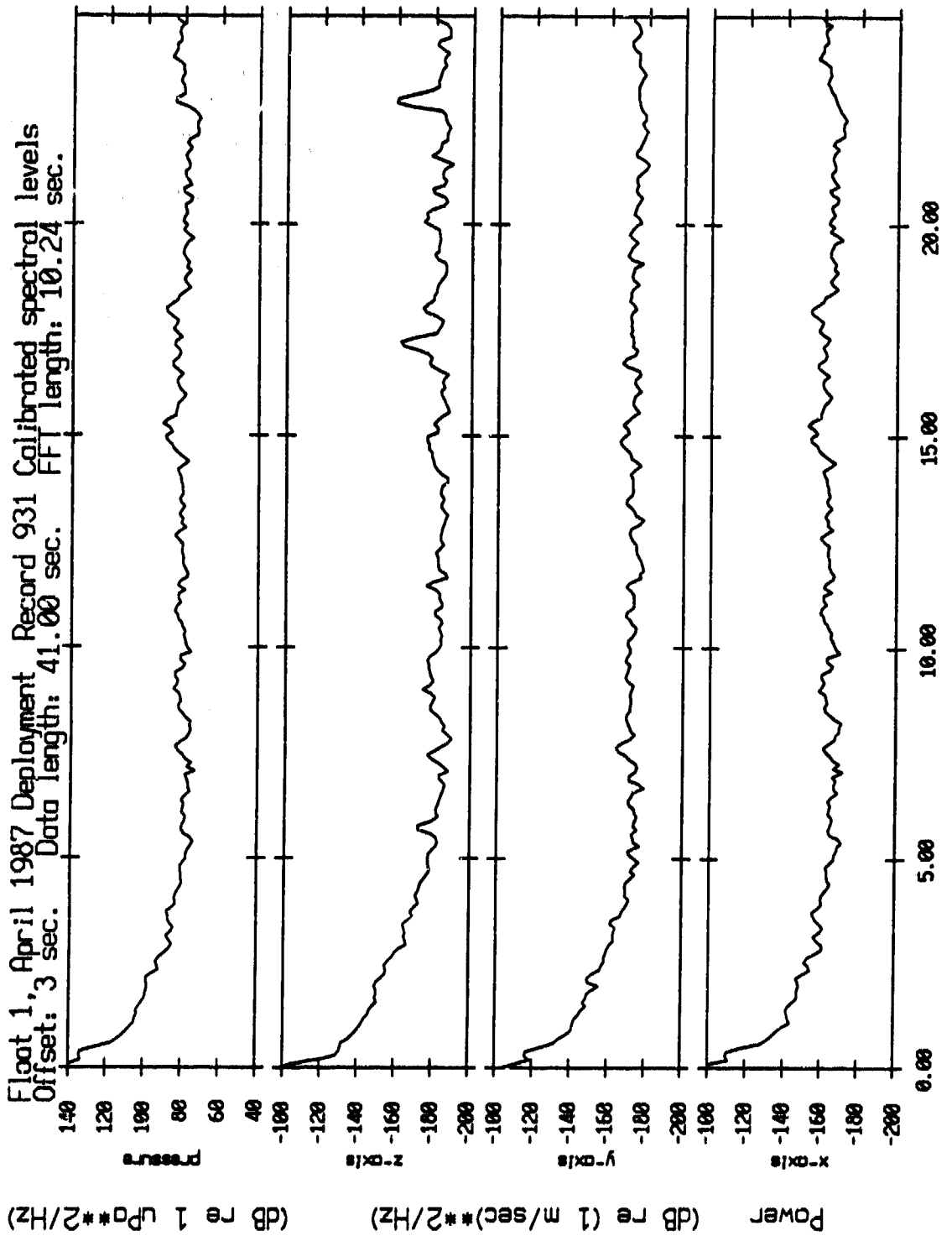
Float 1, April 1987 Deployment Record 931 Calibrated spectral levels
Offset: 3 sec. Data length: 41.00 sec. FFT length: 10.24 sec.
pressure
z-axis
y-axis
x-axis
(dB re 1 uPa**2/Hz)
(dB re (1 m/sec)**2/Hz)
Power
Frequency (Hz)
0.00
5.00
10.00
15.00
20.00

Figure IV.2e

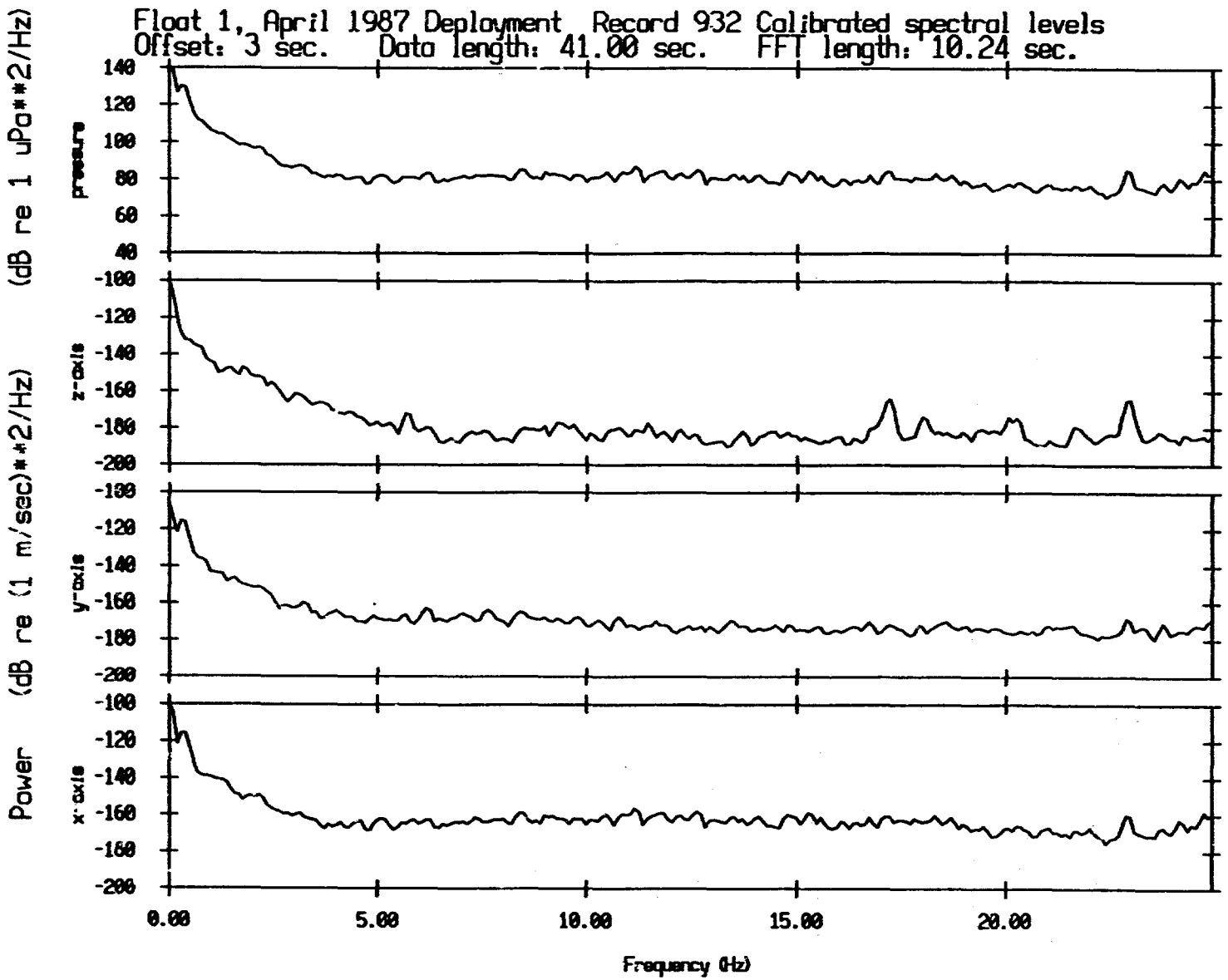
Float 1, April 1987 Deployment Record 932 Calibrated spectral levels
Offset: 3 sec. Data length: 41.00 sec. FFT length: 10.24 sec.
Power (dB re (1 m/sec)**2/Hz) (dB re 1 uPa**2/Hz)
pressure
z-axis
y-axis
x-axis
140
120
100
80
60
40
-100
-120
-140
-160
-180
-200
0.00
5.00
10.00
15.00
20.00
Frequency (Hz)

Figure IV.3f

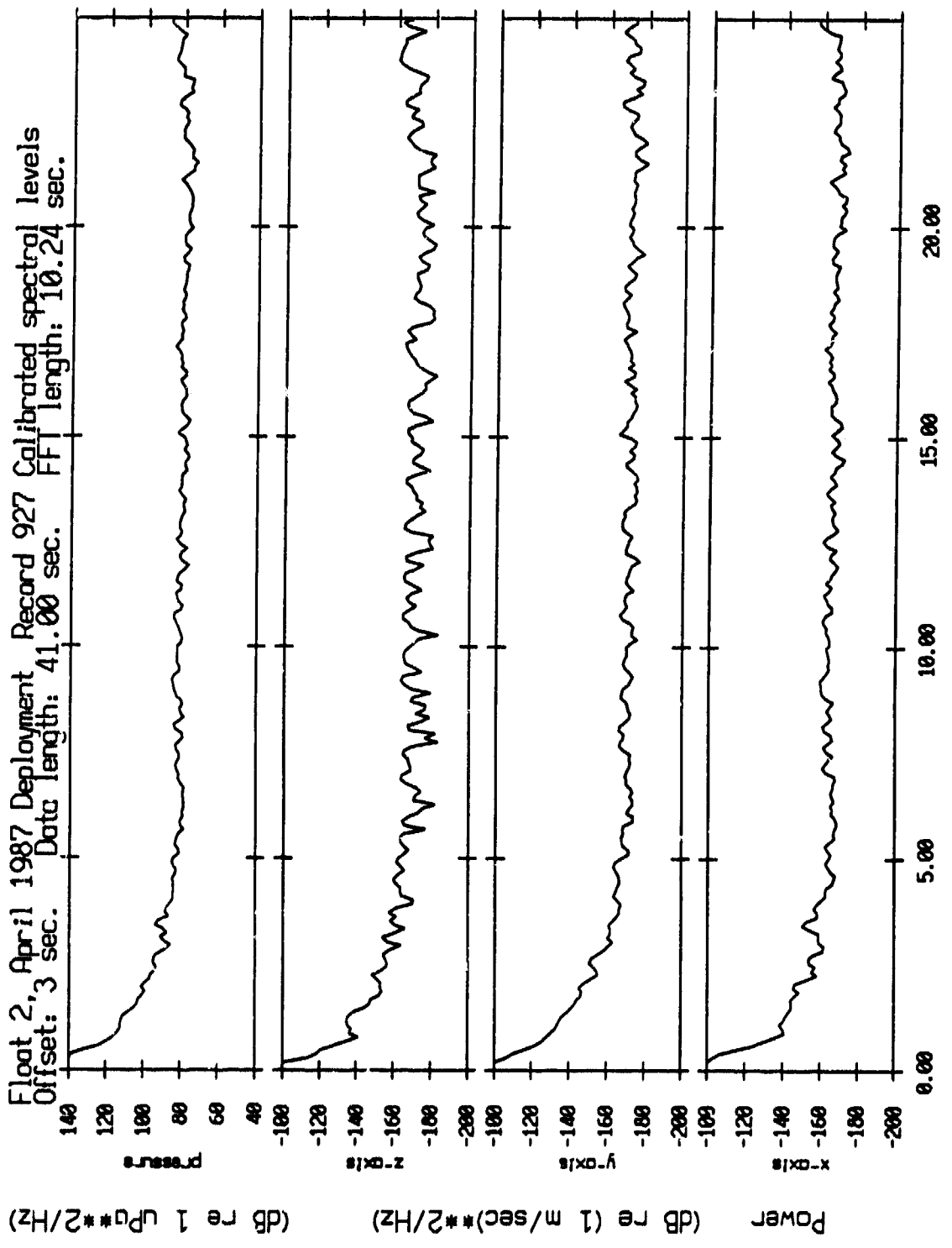
Float 2, April 1987 Deployment Record 927 Calibrated spectral levels
Offset: 3 sec. Data length: 41.00 sec. FFT length: 10.24 sec.
pressure
z-axis
y-axis
x-axis
(db re 1 uPa**2/Hz)
(db re (1 m/sec)**2/Hz)
Power
Frequency (Hz)
0.00
5.00
10.00
15.00
20.00

Figure IV.3a

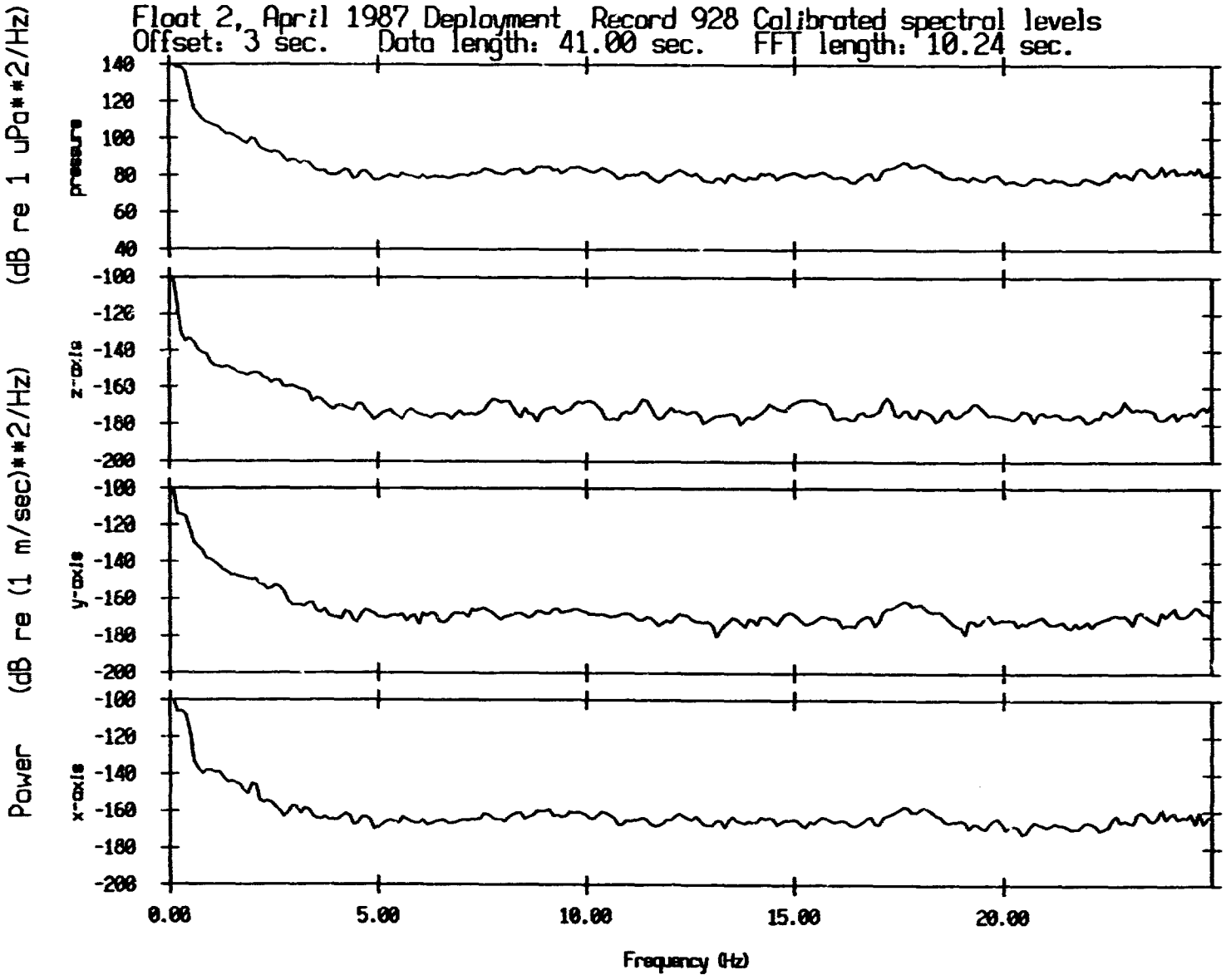
Float 2, April 1987 Deployment Record 928 Calibrated spectral levels
Offset: 3 sec. Data length: 41.00 sec. FFT length: 10.24 sec.
Power (dB re (1 m/sec)**2/Hz) (dB re 1 uPa**2/Hz)
pressure
z-axis
y-axis
x-axis
140
120
100
80
60
40
-100
-120
-140
-160
-180
-200
0.00
5.00
10.00
15.00
20.00
Frequency (Hz)

Figure IV.3b

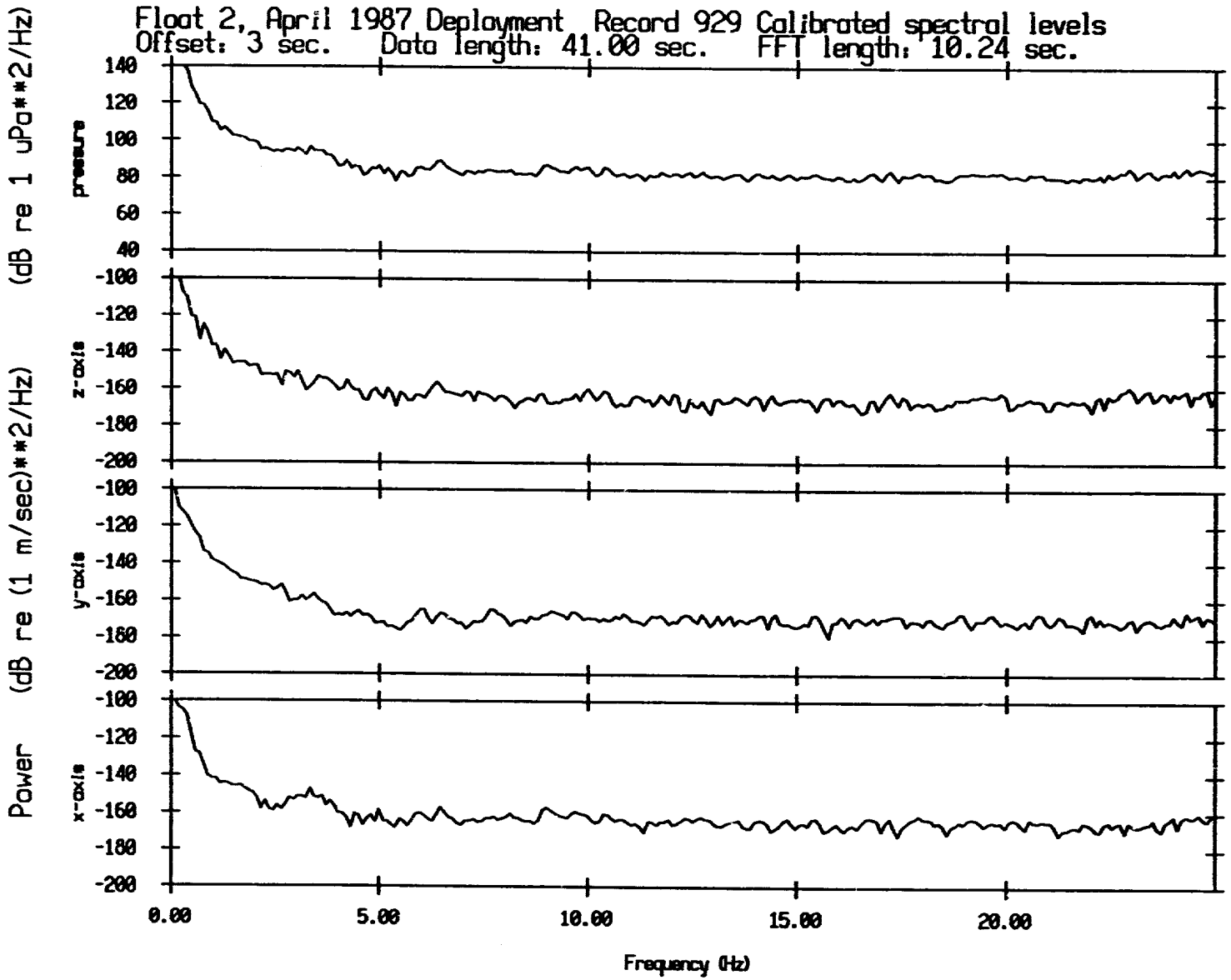
Float 2, April 1987 Deployment Record 929 Calibrated spectral levels
Offset: 3 sec. Data length: 41.00 sec. FFT length: 10.24 sec.
Power (dB re (1 m/sec)**2/Hz) (dB re 1 uPa**2/Hz)
pressure
z-axis
y-axis
x-axis
140
120
100
80
60
40
-100
-120
-140
-160
-180
-200
0.00
5.00
10.00
15.00
20.00
Frequency (Hz)

Figure IV.3c

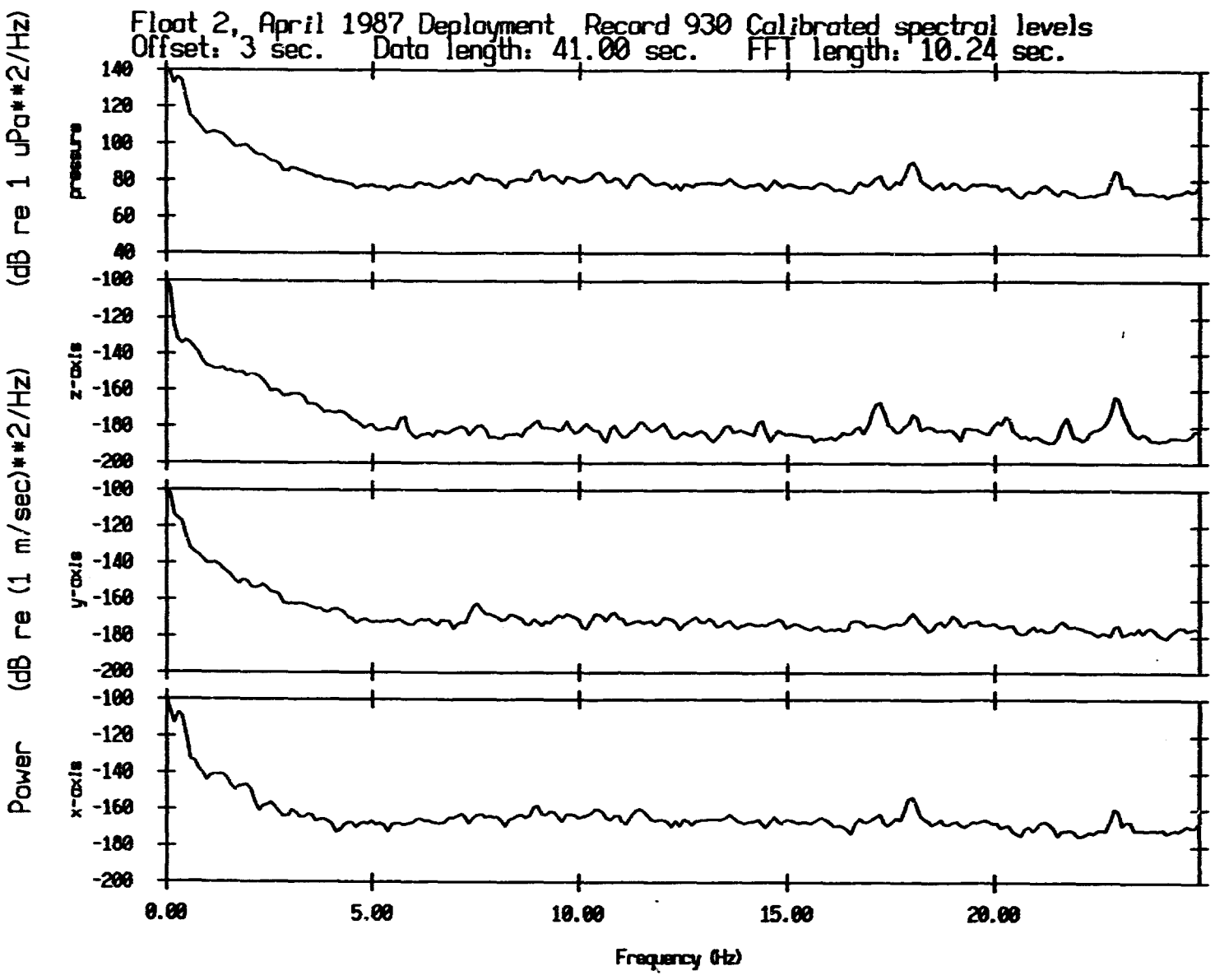
Float 2, April 1987 Deployment Record 930 Calibrated spectral levels
Offset: 3 sec. Data length: 41.00 sec. FFT length: 10.24 sec.
Power (dB re (1 m/sec)**2/Hz) (dB re 1 uPa**2/Hz)
pressure
z-axis
y-axis
x-axis
140
120
100
80
60
40
-100
-120
-140
-160
-180
-200
0.00
5.00
10.00
15.00
20.00
Frequency (Hz)

Figure IV.3d

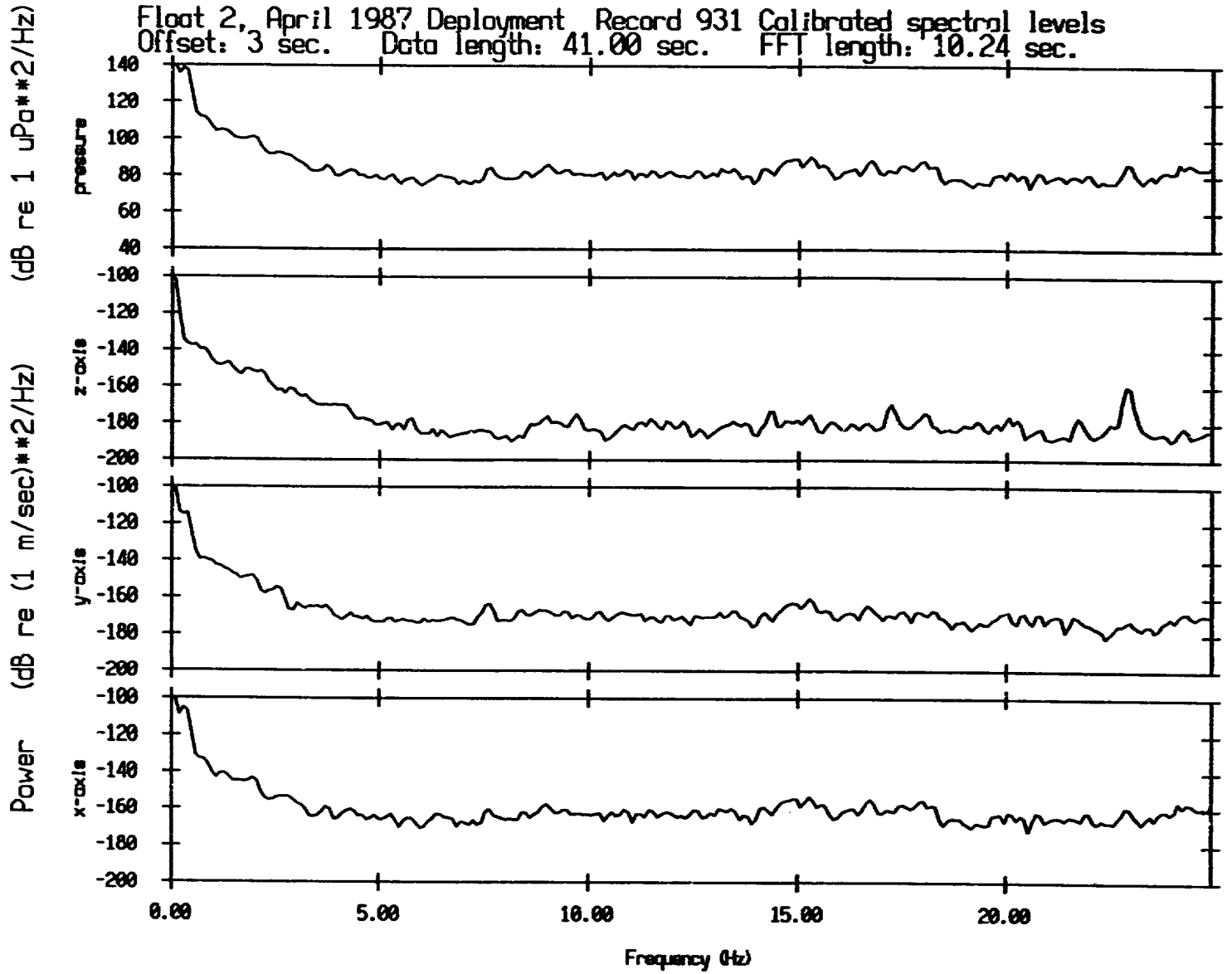
Float 2, April 1987 Deployment Record 931 Calibrated spectral levels
Offset: 3 sec. Data length: 41.00 sec. FFT length: 10.24 sec.
Power (dB re (1 m/sec)**2/Hz) (dB re 1 uPa**2/Hz)
pressure
z-axis
y-axis
x-axis
140
120
100
80
60
40
-100
-120
-140
-160
-180
-200
0.00
5.00
10.00
15.00
20.00
Frequency (Hz)

Figure IV.3e

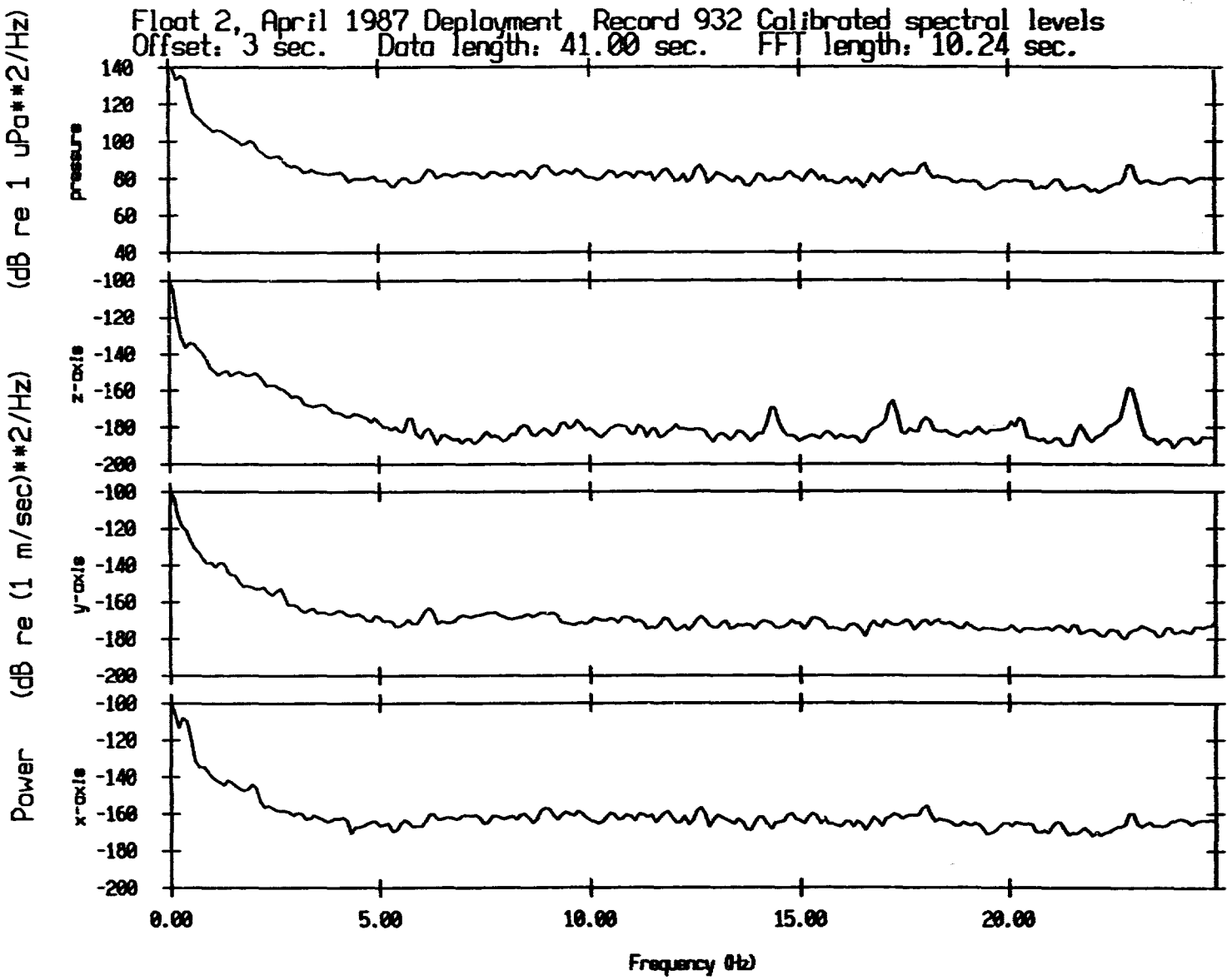
Float 2, April 1987 Deployment Record 932 Calibrated spectral levels
Offset: 3 sec. Data length: 41.00 sec. FFT length: 10.24 sec.
Power (dB re (1 m/sec)**2/Hz) (dB re 1 uPa**2/Hz)
pressure
z-axis
y-axis
x-axis
140
120
100
80
60
40
-100
-120
-140
-160
-180
-200
0.00
5.00
10.00
15.00
20.00
Frequency (Hz)

Figure IV.3f

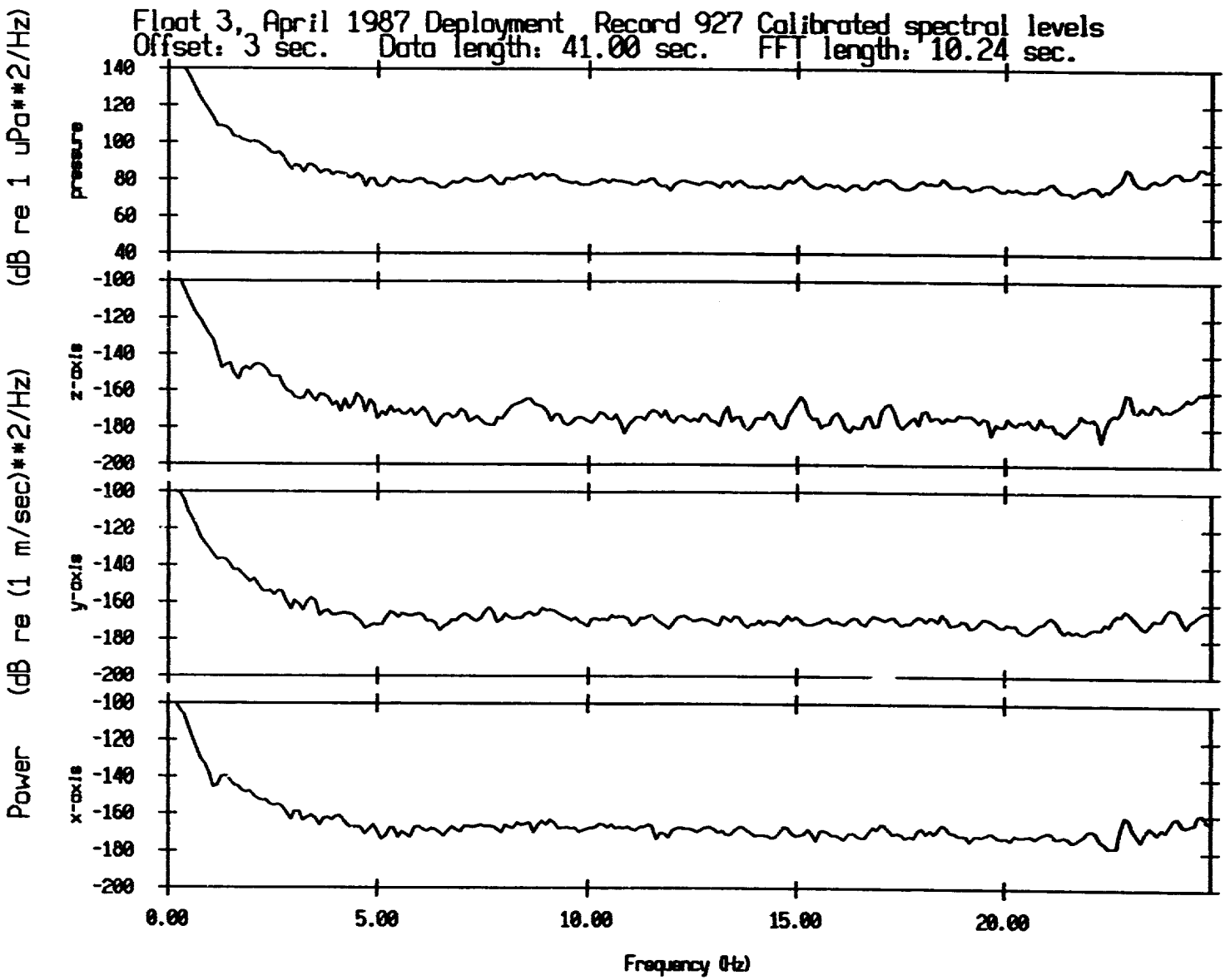
Float 3, April 1987 Deployment Record 927 Calibrated spectral levels
Offset: 3 sec. Data length: 41.00 sec. FFT length: 10.24 sec.
Power (dB re (1 m/sec)**2/Hz) (dB re 1 uPa**2/Hz)
pressure
z-axis
y-axis
x-axis
140
120
100
80
60
40
-100
-120
-140
-160
-180
-200
0.00
5.00
10.00
15.00
20.00
Frequency (Hz)

Figure IV.4a

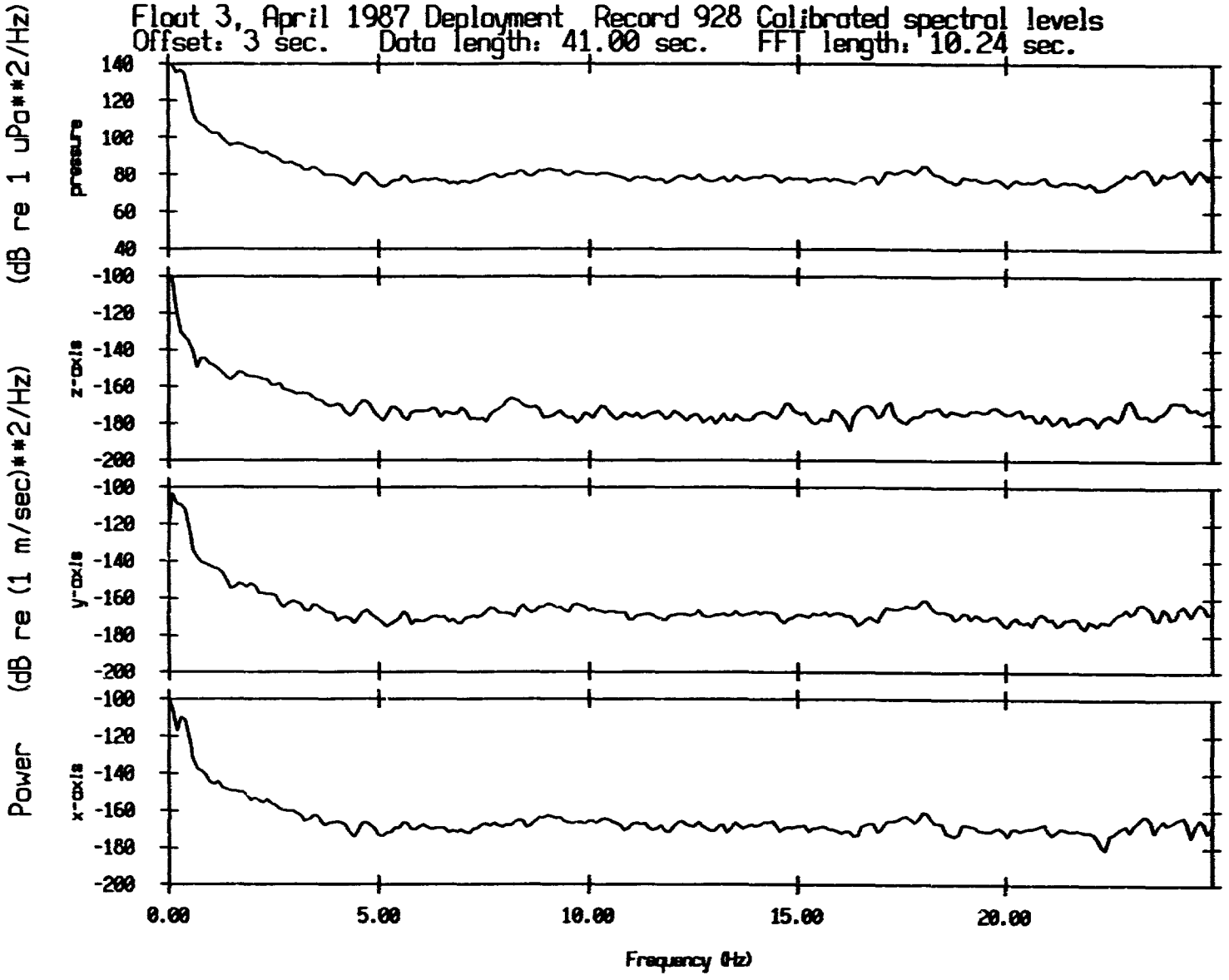
Float 3, April 1987 Deployment Record 928 Calibrated spectral levels
Offset: 3 sec. Data length: 41.00 sec. FFT length: 10.24 sec.
Power (dB re (1 m/sec)**2/Hz) (dB re 1 uPa**2/Hz)
pressure
z-axis
y-axis
x-axis
140
120
100
80
60
40
-100
-120
-140
-160
-180
-200
0.00
5.00
10.00
15.00
20.00
Frequency (Hz)

Figure IV.4b

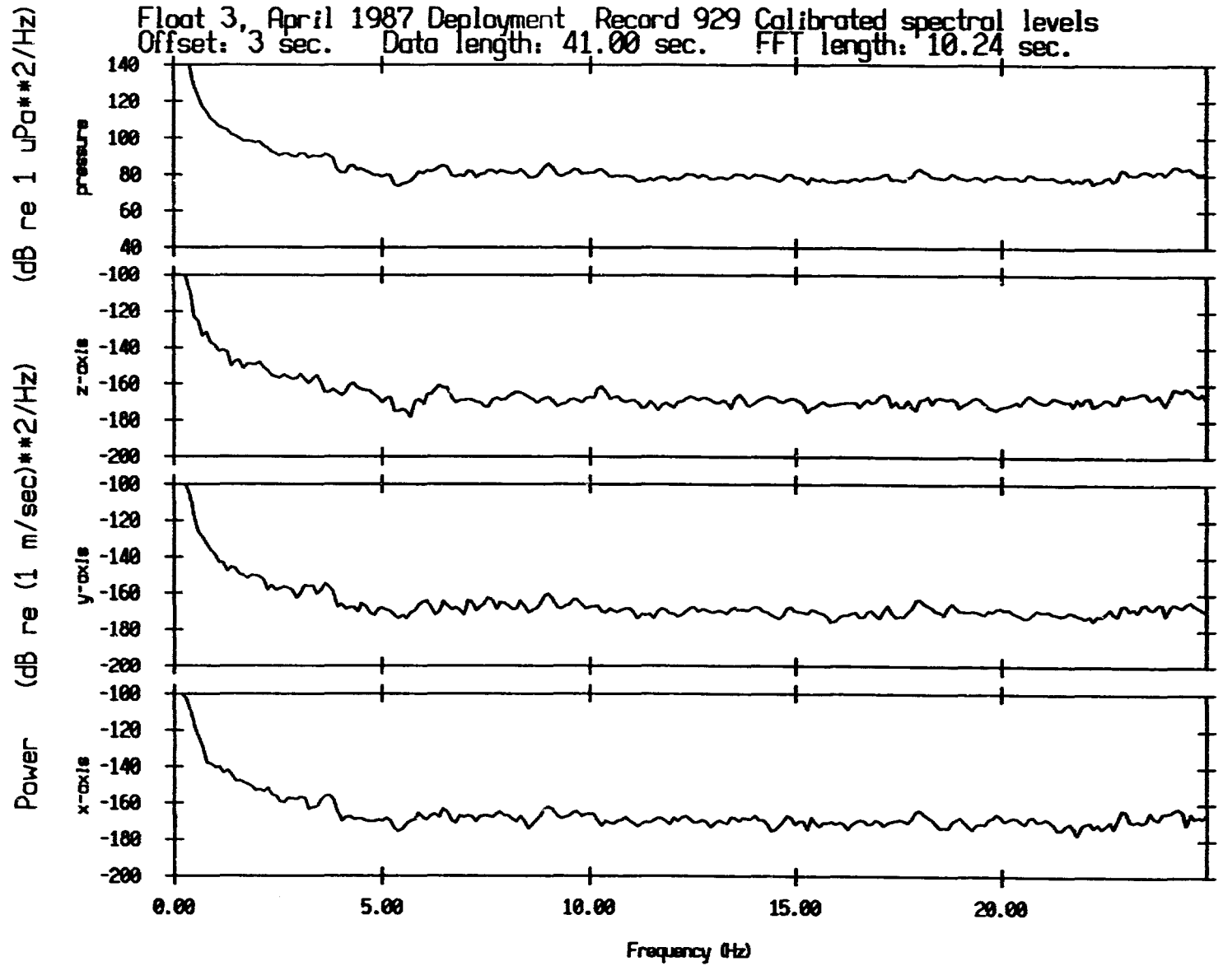
Float 3, April 1987 Deployment Record 929 Calibrated spectral levels
Offset: 3 sec. Data length: 41.00 sec. FFT length: 10.24 sec.
Power (dB re (1 m/sec)**2/Hz) (dB re 1 uPa**2/Hz)
pressure
z-axis
y-axis
x-axis
140
120
100
80
60
40
-100
-120
-140
-160
-180
-200
0.00
5.00
10.00
15.00
20.00
Frequency (Hz)

Figure IV.4c

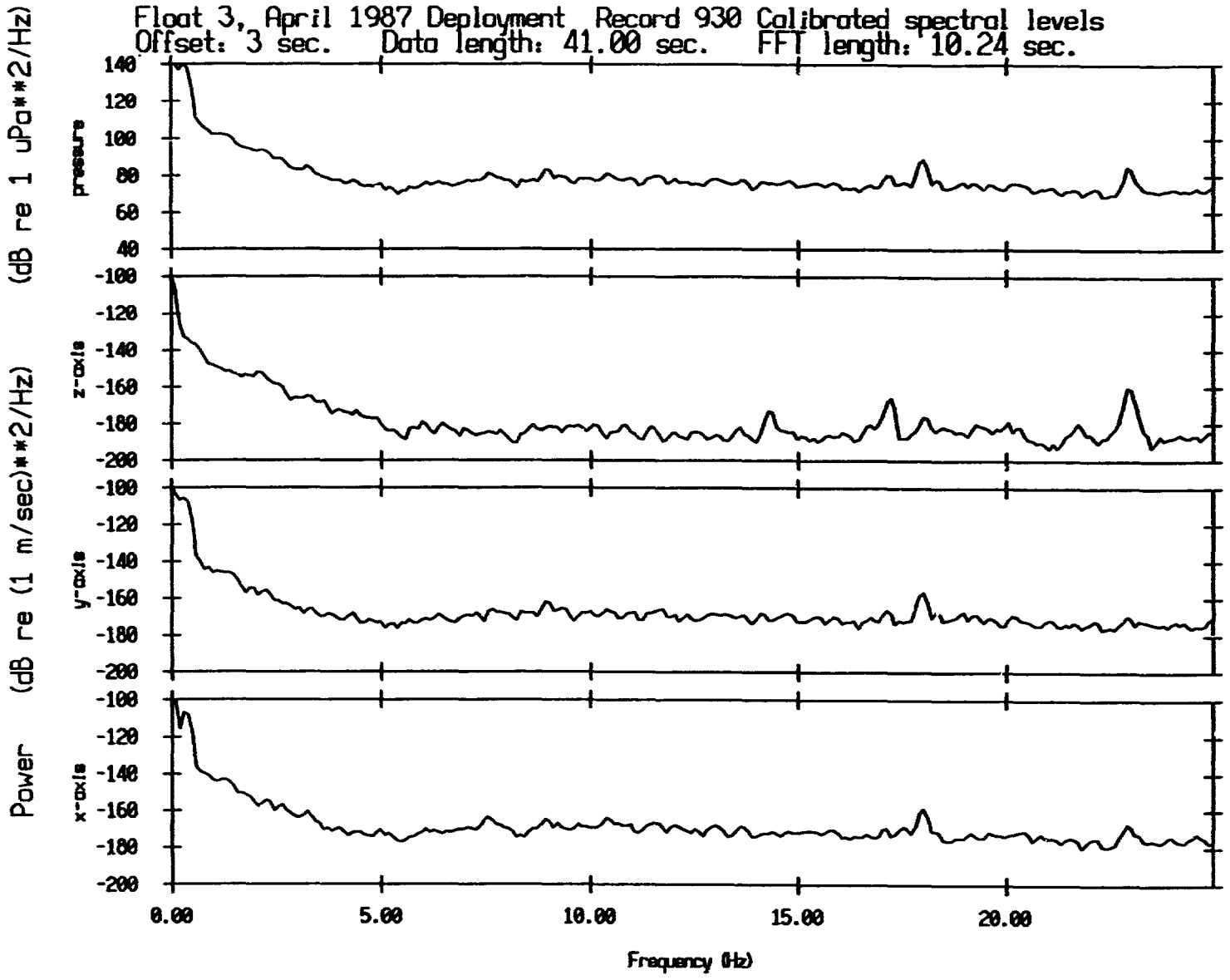
Float 3, April 1987 Deployment Record 930 Calibrated spectral levels
Offset: 3 sec. Data length: 41.00 sec. FFT length: 10.24 sec.
Power (dB re (1 m/sec)**2/Hz) (dB re 1 uPa**2/Hz)
pressure
z-axis
y-axis
x-axis
140
120
100
80
60
40
-100
-120
-140
-160
-180
-200
0.00
5.00
10.00
15.00
20.00
Frequency (Hz)

Figure IV.4d

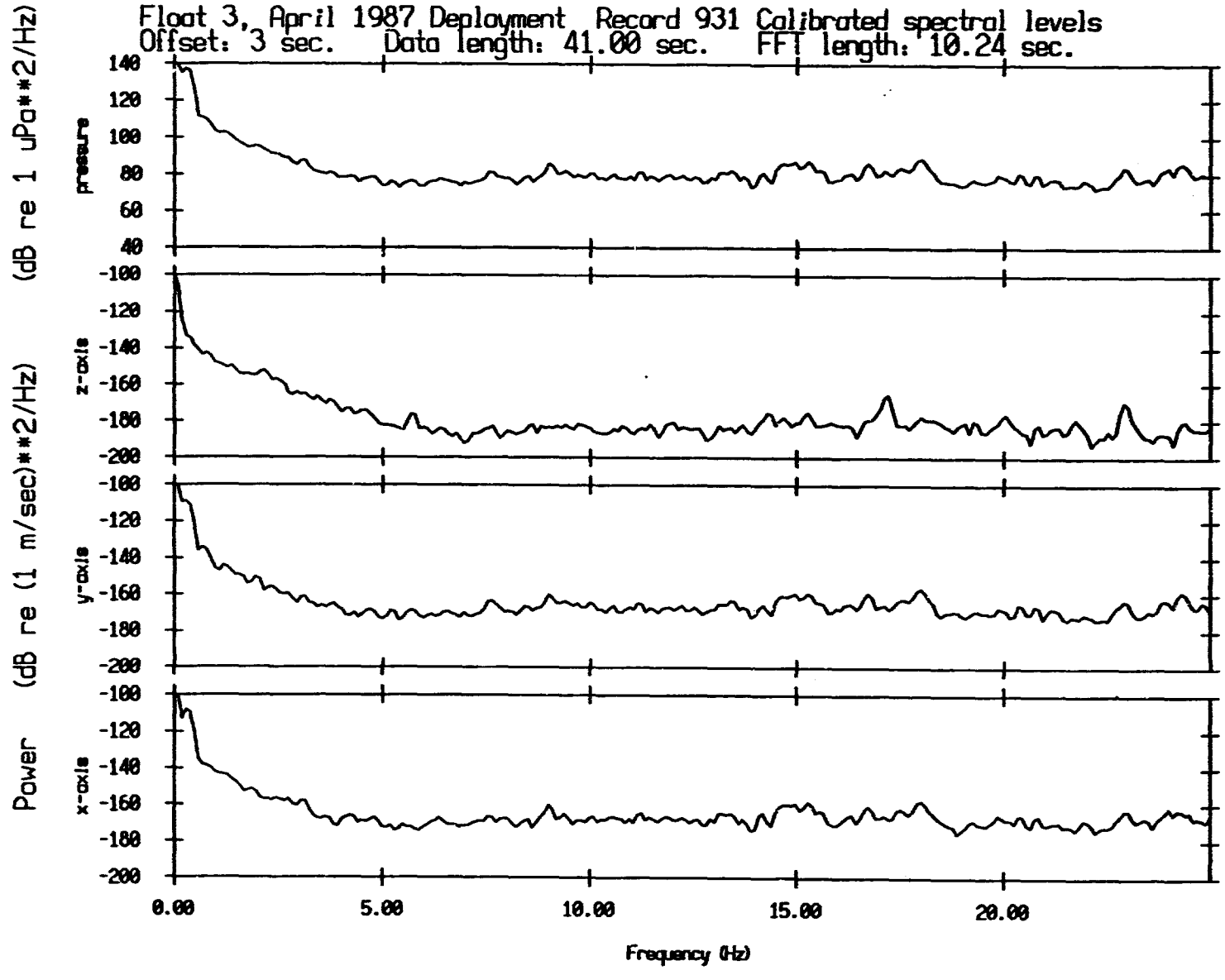
Float 3, April 1987 Deployment Record 931 Calibrated spectral levels
Offset: 3 sec. Data length: 41.00 sec. FFT length: 10.24 sec.
Power (dB re (1 m/sec)**2/Hz) (dB re 1 uPa**2/Hz)
pressure
z-axis
y-axis
x-axis
140
120
100
80
60
40
-100
-120
-140
-160
-180
-200
0.00
5.00
10.00
15.00
20.00
Frequency (Hz)

Figure IV.4e

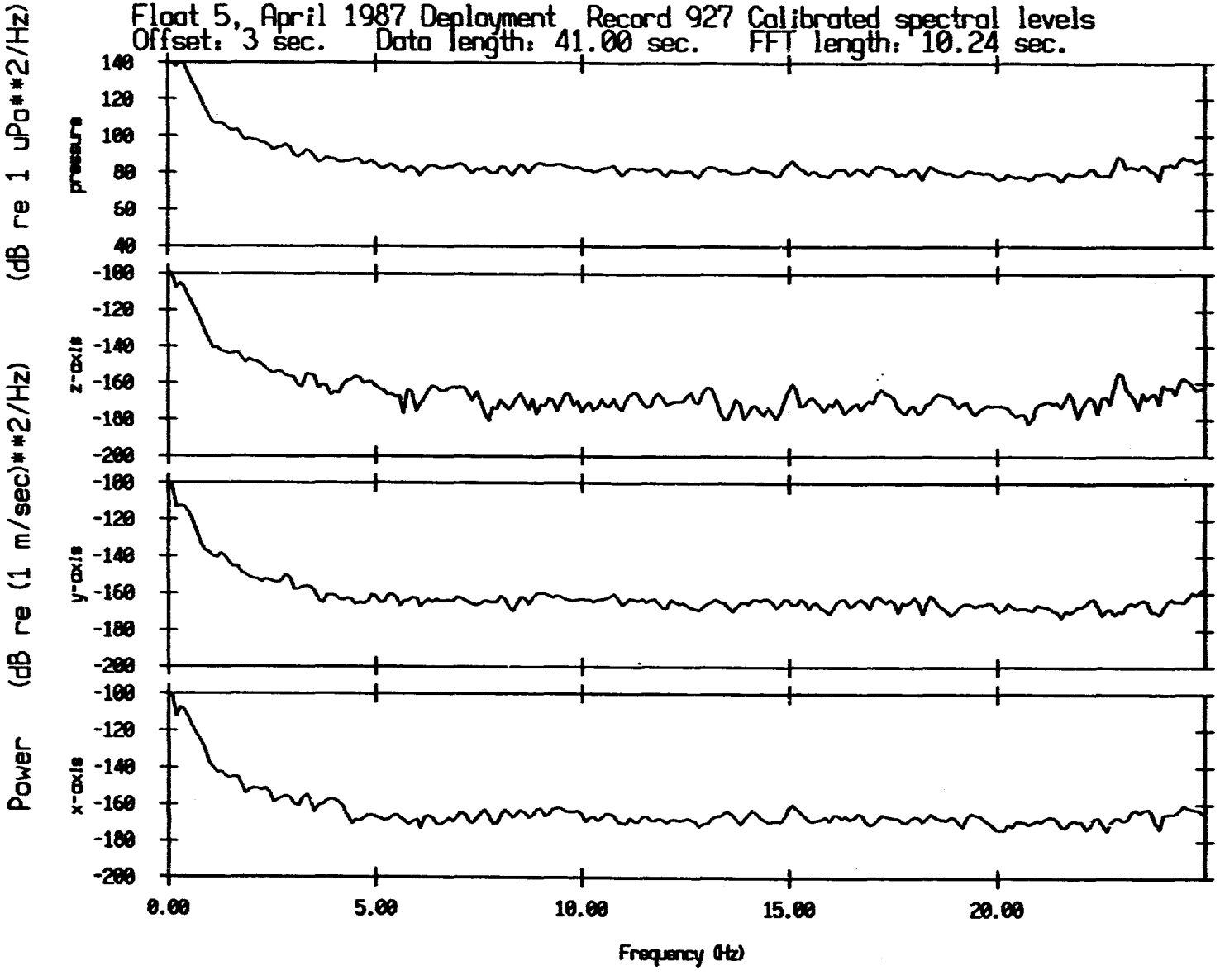
Float 5, April 1987 Deployment Record 927 Calibrated spectral levels
Offset: 3 sec. Data length: 41.00 sec. FFT length: 10.24 sec.
Power (dB re (1 m/sec)**2/Hz) (dB re 1 uPa**2/Hz)
pressure
z-axis
y-axis
x-axis
140
120
100
80
60
40
-100
-120
-140
-160
-180
-200
0.00
5.00
10.00
15.00
20.00
Frequency (Hz)

Figure IV.5a

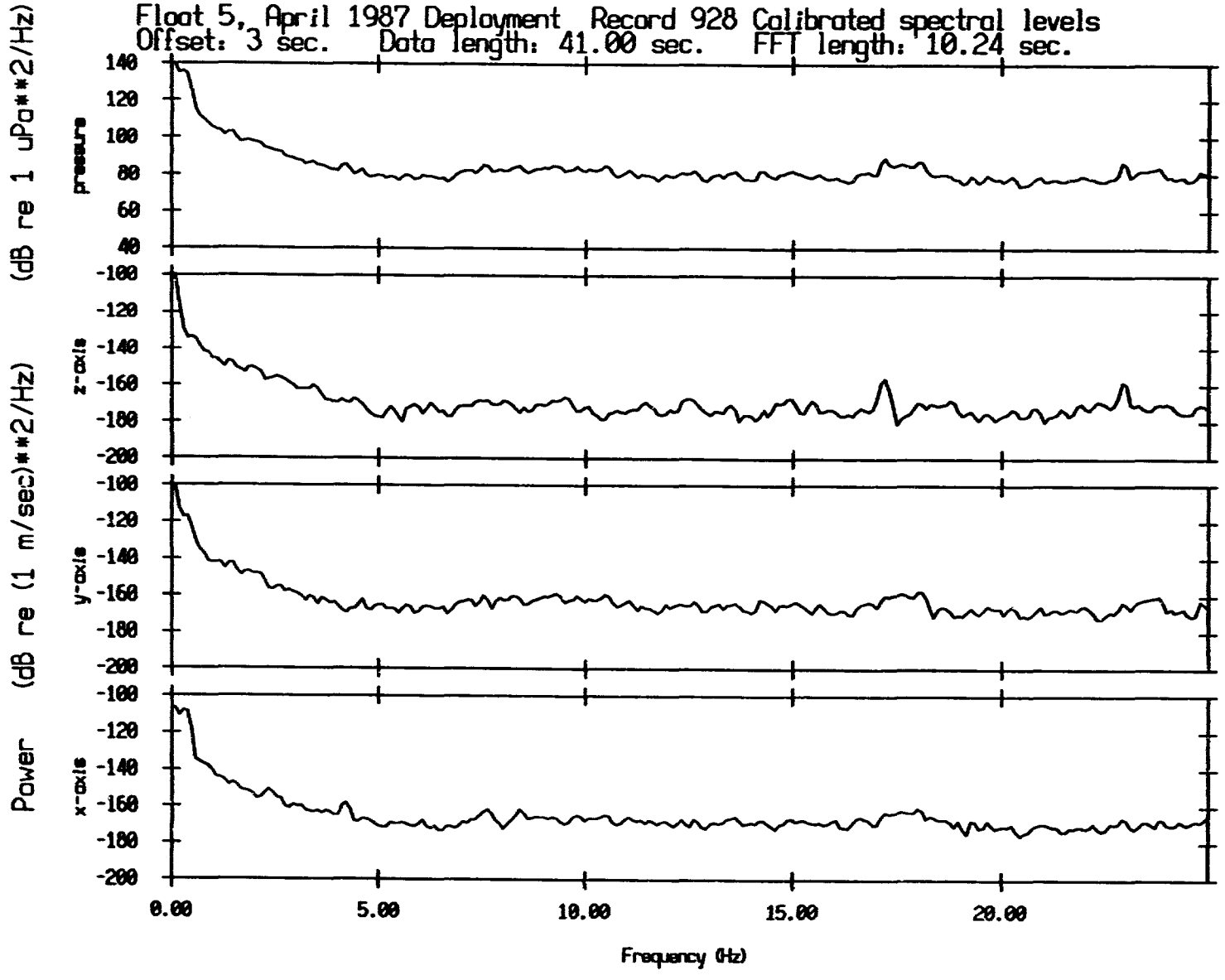
Float 5, April 1987 Deployment Record 928 Calibrated spectral levels
Offset: 3 sec. Data length: 41.00 sec. FFT length: 10.24 sec.
Power (dB re (1 m/sec)**2/Hz) (dB re 1 uPa**2/Hz)
pressure
z-axis
y-axis
x-axis
140
120
100
80
60
40
-100
-120
-140
-160
-180
-200
0.00
5.00
10.00
15.00
20.00
Frequency (Hz)

Figure IV.3b

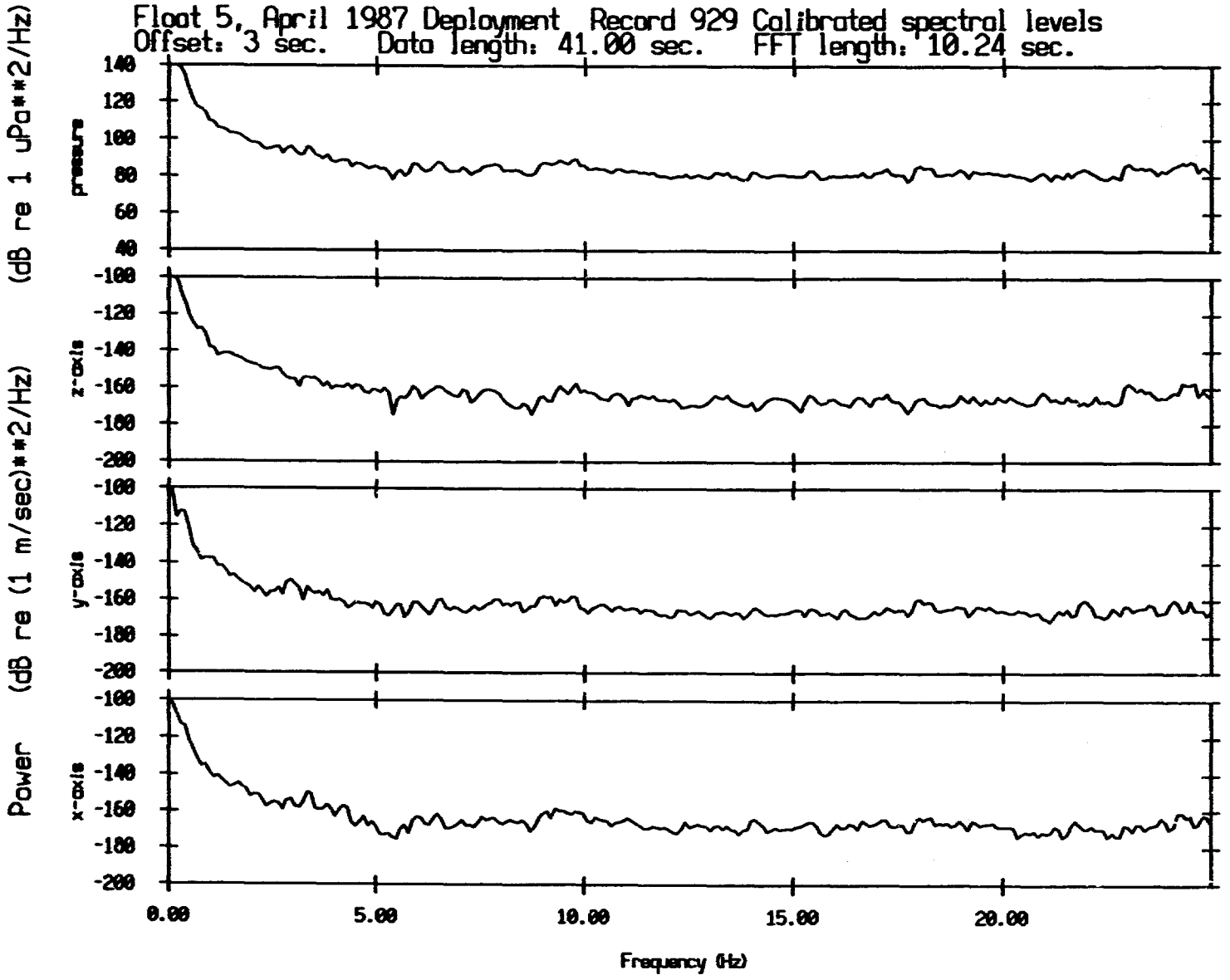
Float 5, April 1987 Deployment Record 929 Calibrated spectral levels
Offset: 3 sec. Data length: 41.00 sec. FFT length: 10.24 sec.
Power (dB re (1 m/sec)**2/Hz) (dB re 1 uPa**2/Hz)
pressure
z-axis
y-axis
x-axis
140
120
100
80
60
40
-100
-120
-140
-160
-180
-200
0.00
5.00
10.00
15.00
20.00
Frequency (Hz)

Figure IV.5c

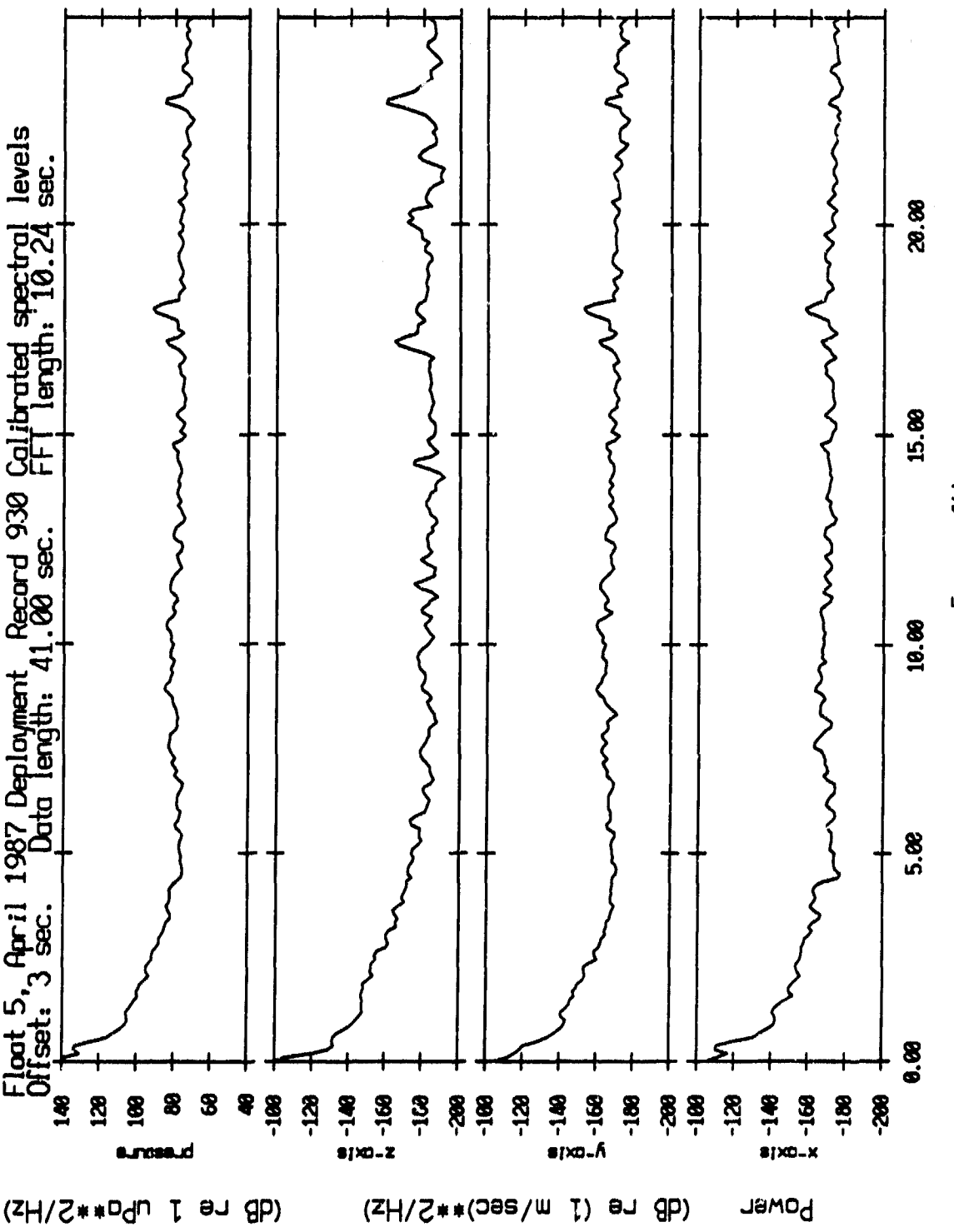
Float 5, April 1987 Deployment Record 930 Calibrated spectral levels
Offset: 3 sec. Data length: 41.00 sec. FFT length: 10.24 sec.
pressure
z-axis
y-axis
x-axis
(dB re 1 uPa**2/Hz)
(dB re (1 m/sec)**2/Hz)
Power
0.00
5.00
10.00
15.00
20.00
Frequency (Hz)

Figure IV.5d

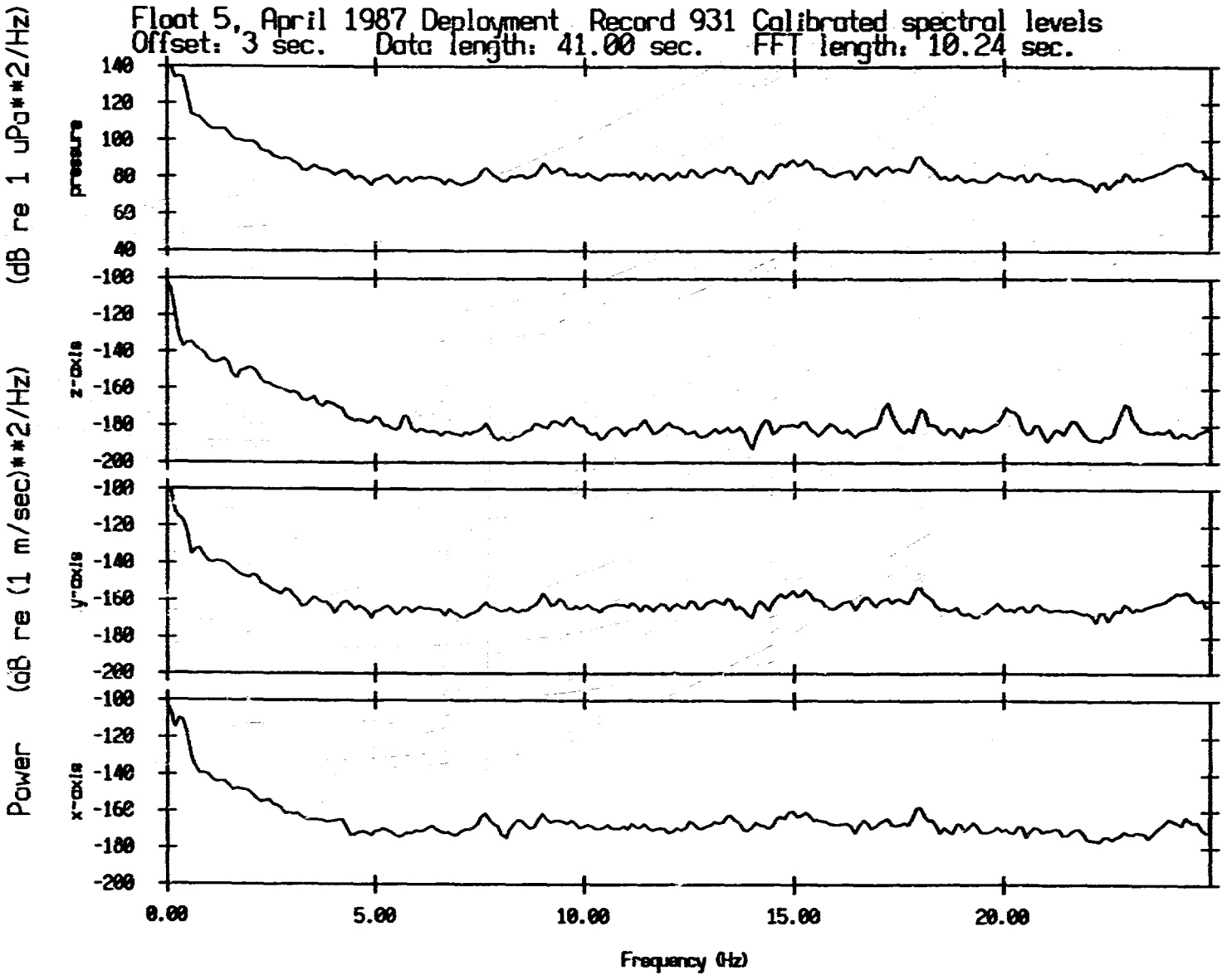
Float 5, April 1987 Deployment Record 931 Calibrated spectral levels
Offset: 3 sec. Data length: 41.00 sec. FFT length: 10.24 sec.
Power (dB re (1 m/sec)**2/Hz) (dB re 1 uPa**2/Hz)
pressure
z-axis
y-axis
x-axis
140
120
100
80
60
40
-100
-120
-140
-160
-180
-200
0.00
5.00
10.00
15.00
20.00
Frequency (Hz)

Figure IV.5e

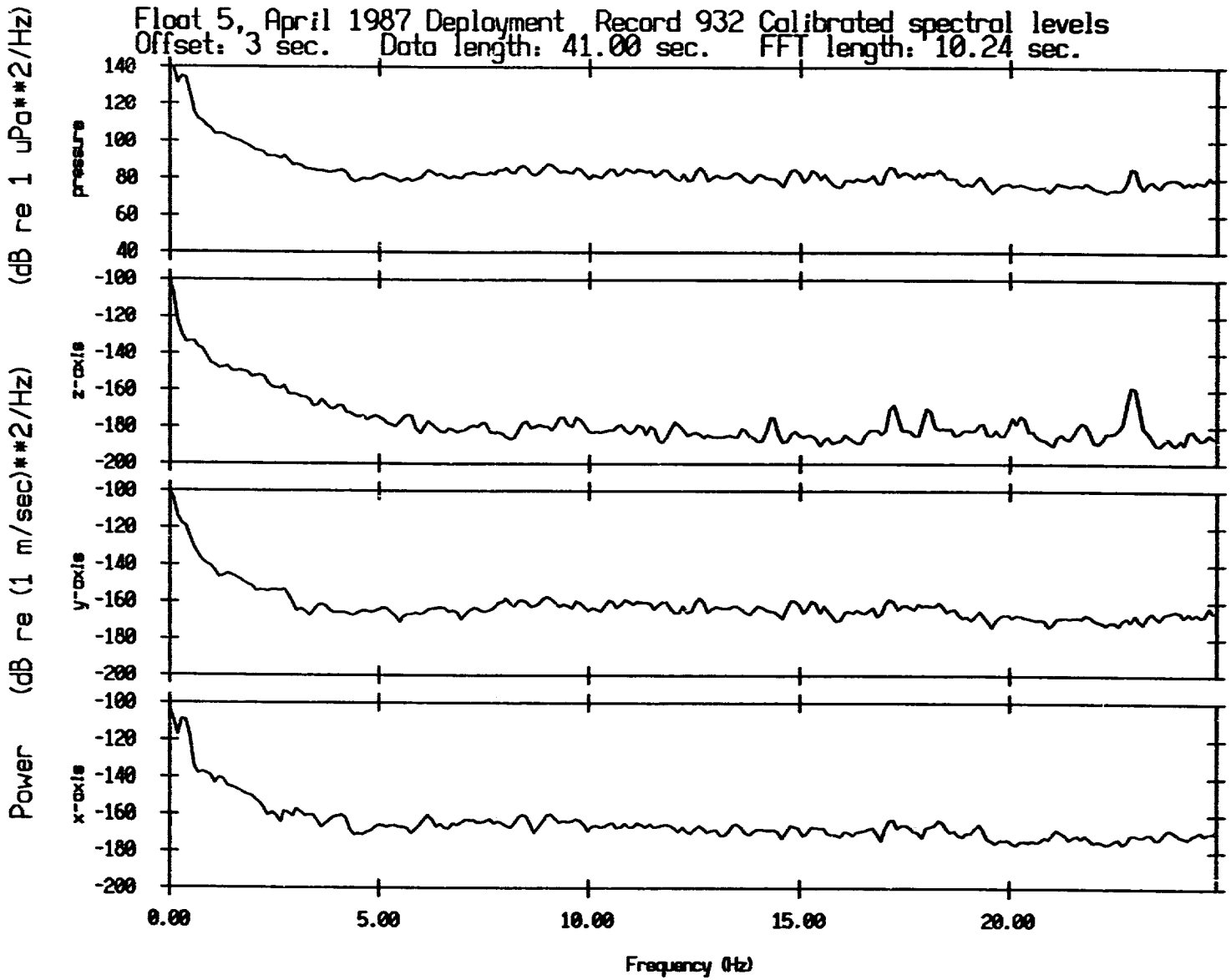
Float 5, April 1987 Deployment Record 932 Calibrated spectral levels
Offset: 3 sec. Data length: 41.00 sec. FFT length: 10.24 sec.
Power (dB re (1 m/sec)**2/Hz) (dB re 1 uPa**2/Hz)
pressure
z-axis
y-axis
x-axis
140
120
100
80
60
40
-100
-120
-140
-160
-180
-200
0.00
5.00
10.00
15.00
20.00
Frequency (Hz)

Figure IV.5f

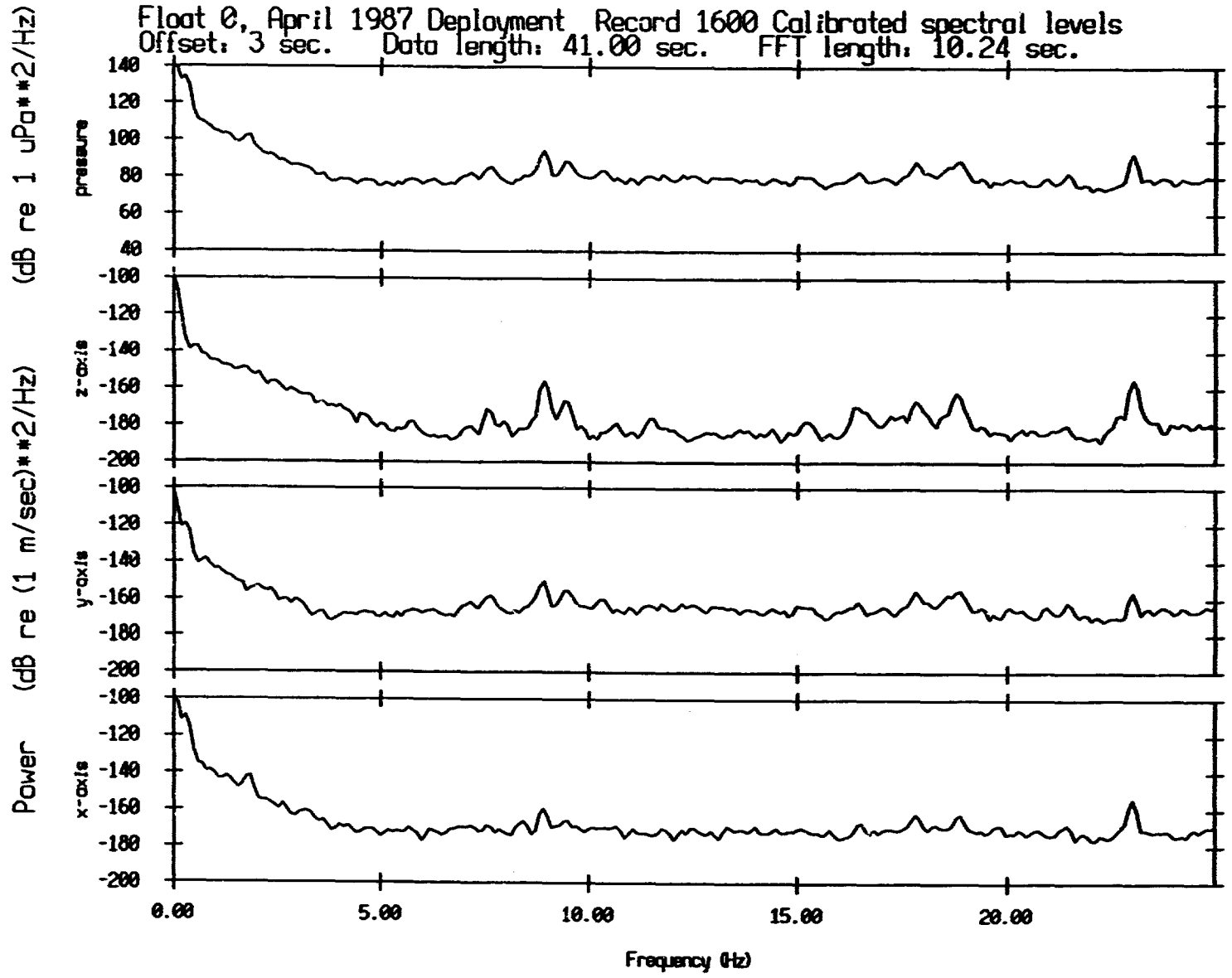
Float 0, April 1987 Deployment Record 1600 Calibrated spectral levels
Offset: 3 sec. Data length: 41.00 sec. FFT length: 10.24 sec.
Power (dB re (1 m/sec)**2/Hz) (dB re 1 uPa**2/Hz)
pressure
z-axis
y-axis
x-axis
140
120
100
80
60
40
-100
-120
-140
-160
-180
-200
0.00
5.00
10.00
15.00
20.00
Frequency (Hz)

Figure IV.8

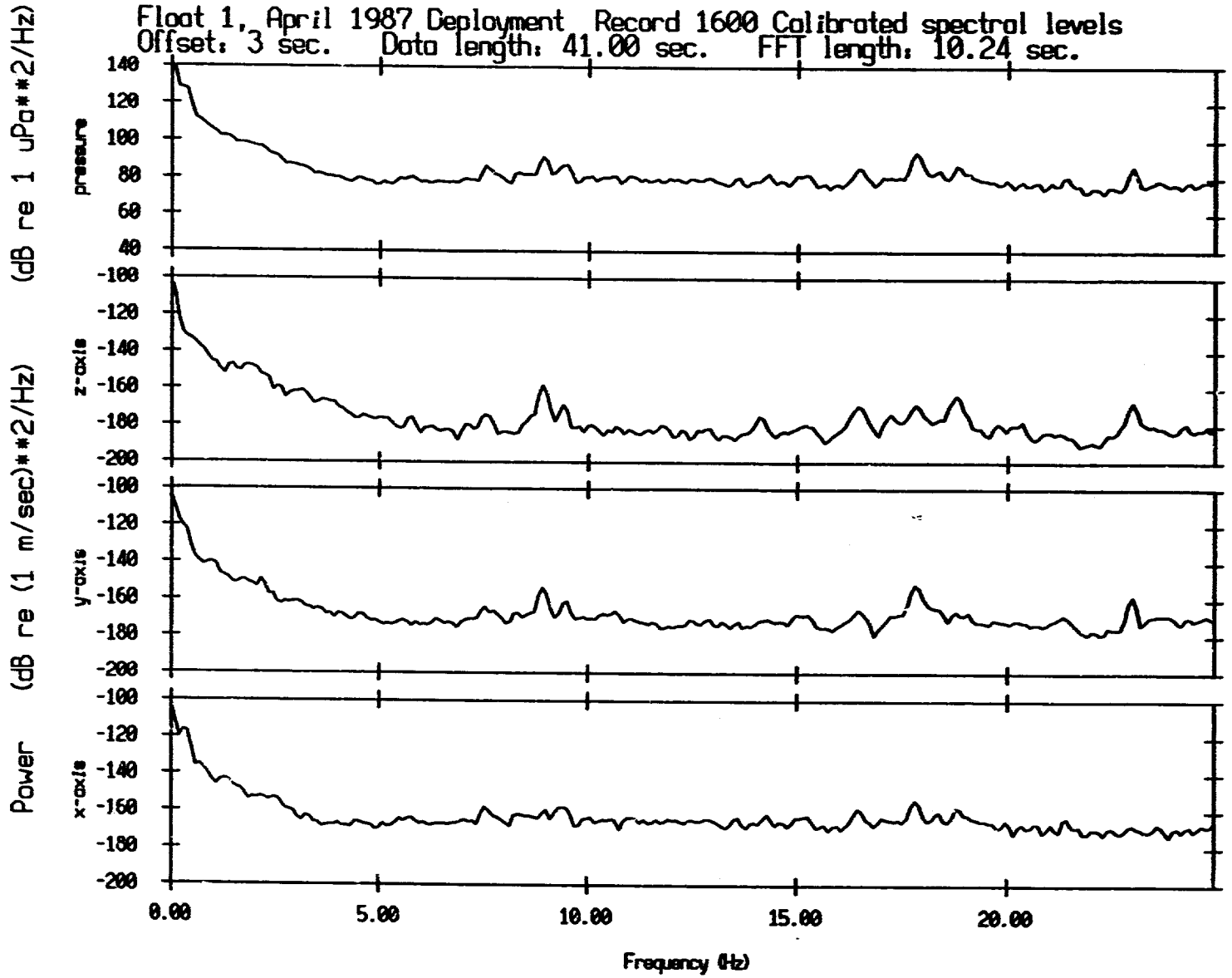
Float 1, April 1987 Deployment Record 1600 Calibrated spectral levels
Offset: 3 sec. Data length: 41.00 sec. FFT length: 10.24 sec.
Power (dB re (1 m/sec)**2/Hz) (dB re 1 uPa**2/Hz)
pressure
z-axis
y-axis
x-axis
140
120
100
80
60
40
-100
-120
-140
-160
-180
-200
0.00
5.00
10.00
15.00
20.00
Frequency (Hz)

Figure IV.7

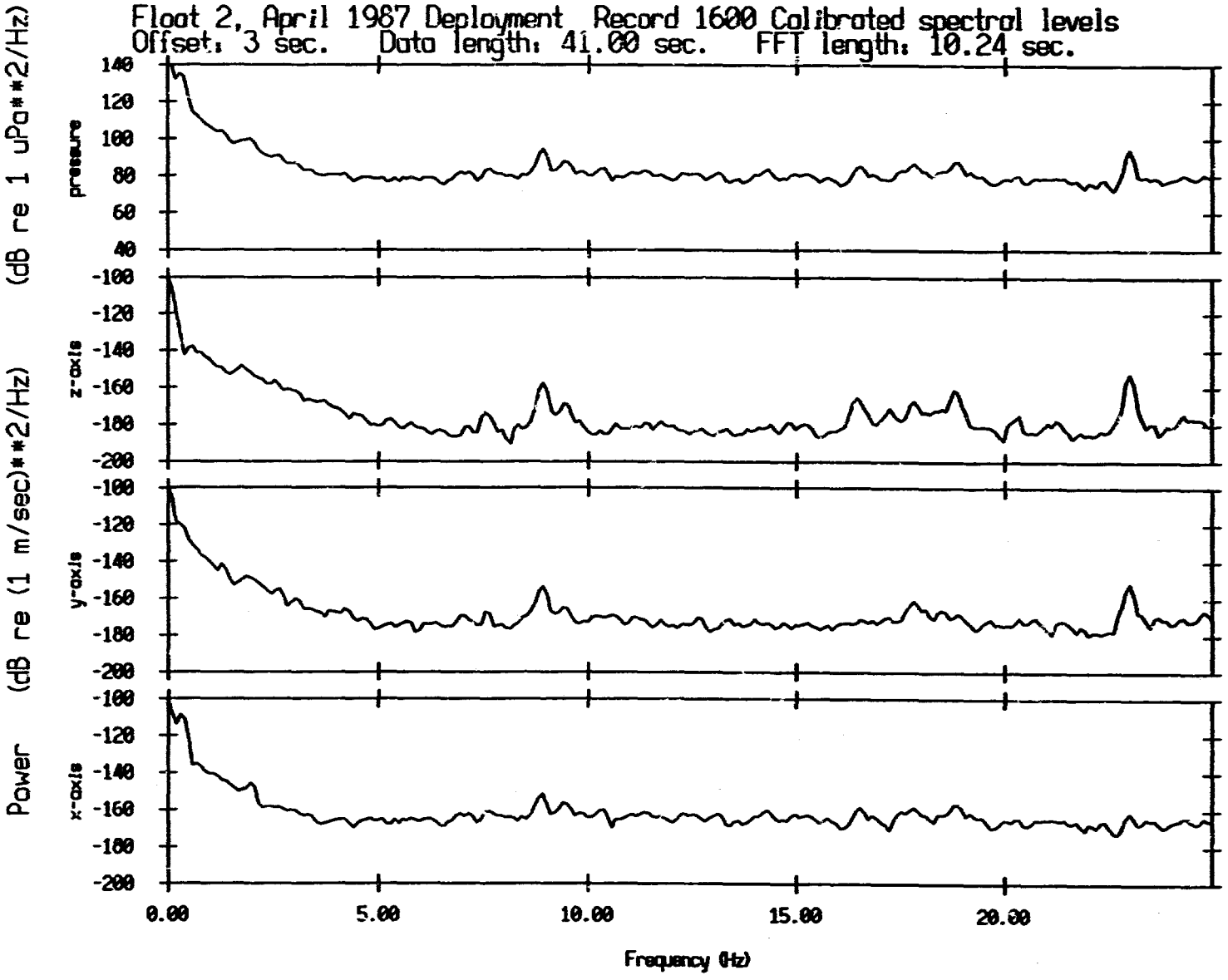
Float 2, April 1987 Deployment Record 1600 Calibrated spectral levels
Offset: 3 sec. Data length: 41.00 sec. FFT length: 10.24 sec.
Power (dB re (1 m/sec)**2/Hz) (dB re 1 uPa**2/Hz)
pressure
z-axis
y-axis
x-axis
140
120
100
80
60
40
-100
-120
-140
-160
-180
-200
0.00
5.00
10.00
15.00
20.00
Frequency (Hz)

Figure IV.8

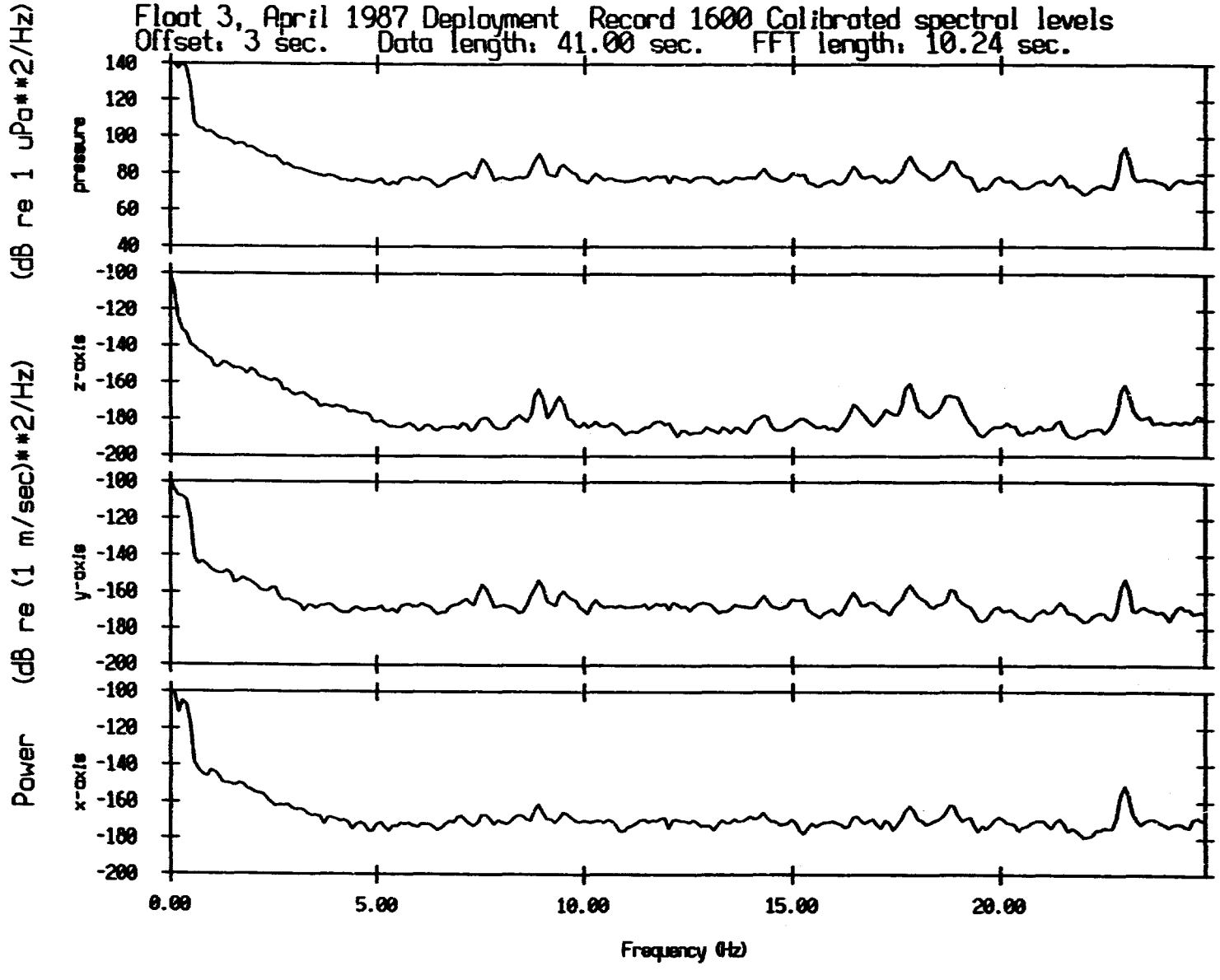
Float 3, April 1987 Deployment Record 1600 Calibrated spectral levels
Offset: 3 sec. Data length: 41.00 sec. FFT length: 10.24 sec.
Power (dB re (1 m/sec)**2/Hz) (dB re 1 uPa**2/Hz)
pressure
z-axis
y-axis
x-axis
140
120
100
80
60
40
-100
-120
-140
-160
-180
-200
0.00
5.00
10.00
15.00
20.00
Frequency (Hz)

Figure IV.9

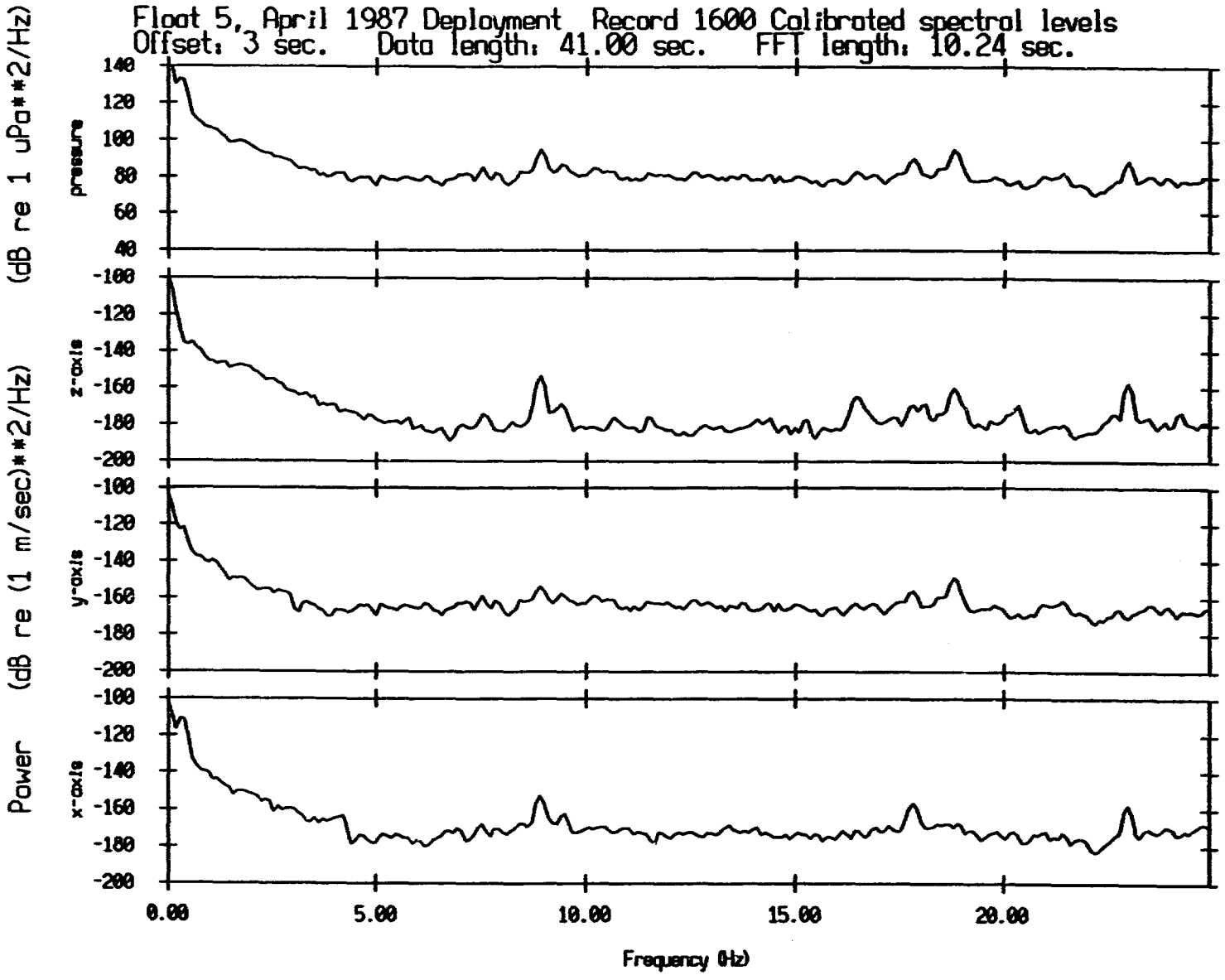
Float 5, April 1987 Deployment Record 1600 Calibrated spectral levels
Offset: 3 sec. Data length: 41.00 sec. FFT length: 10.24 sec.
Power (dB re (1 m/sec)**2/Hz) (dB re 1 uPa**2/Hz)
pressure
z-axis
y-axis
x-axis
140
120
100
80
60
40
-100
-120
-140
-160
-180
-200
0.00
5.00
10.00
15.00
20.00
Frequency (Hz)

Figure IV.10

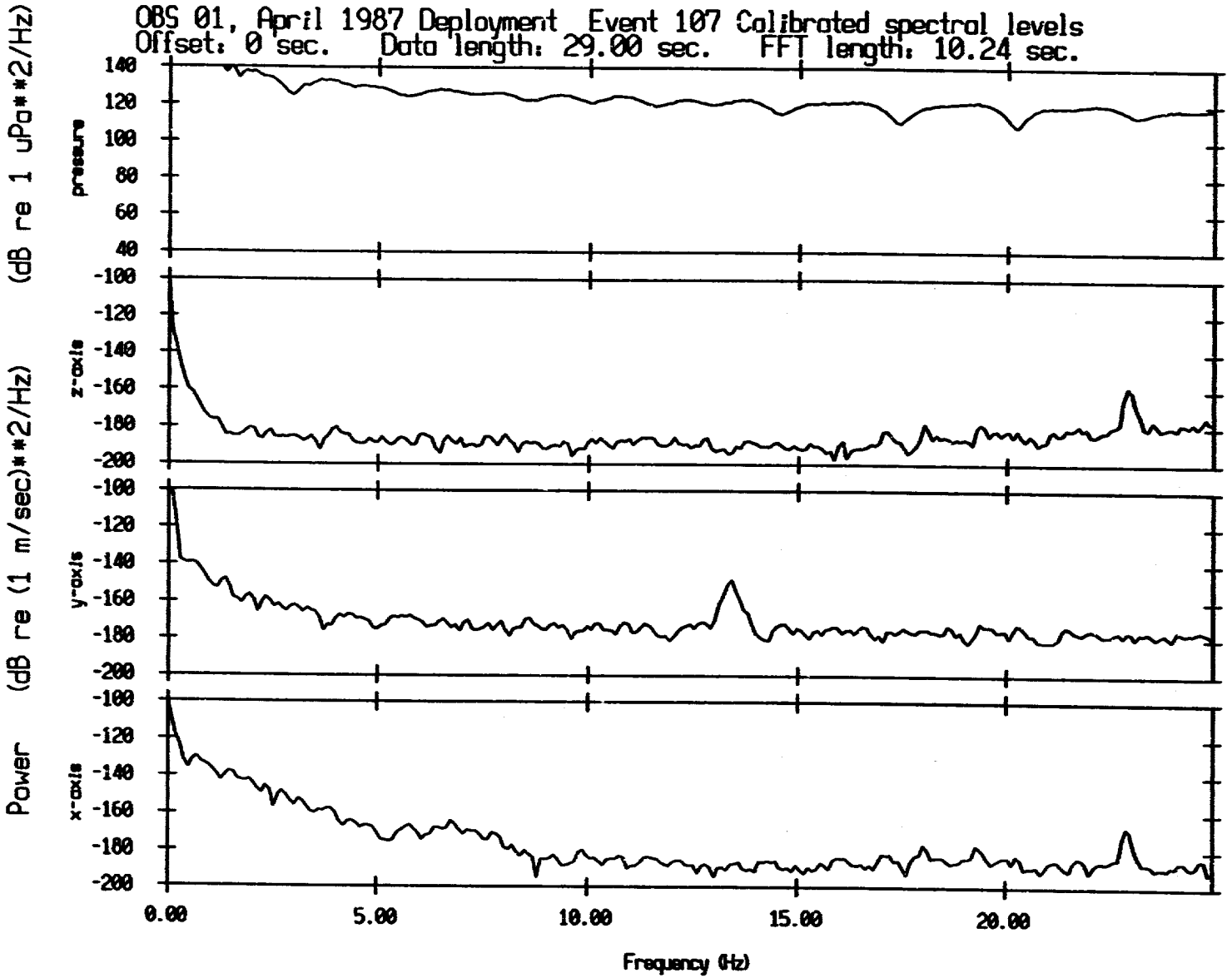
OBS 01, April 1987 Deployment Event 107 Calibrated spectral levels
Offset: 0 sec. Data length: 29.00 sec. FFT length: 10.24 sec.
Power (dB re (1 m/sec)**2/Hz) (dB re 1 uPa**2/Hz)
pressure
z-axis
y-axis
x-axis
140
120
100
80
60
40
-100
-120
-140
-160
-180
-200
0.00
5.00
10.00
15.00
20.00
Frequency (Hz)

Figure IV.11

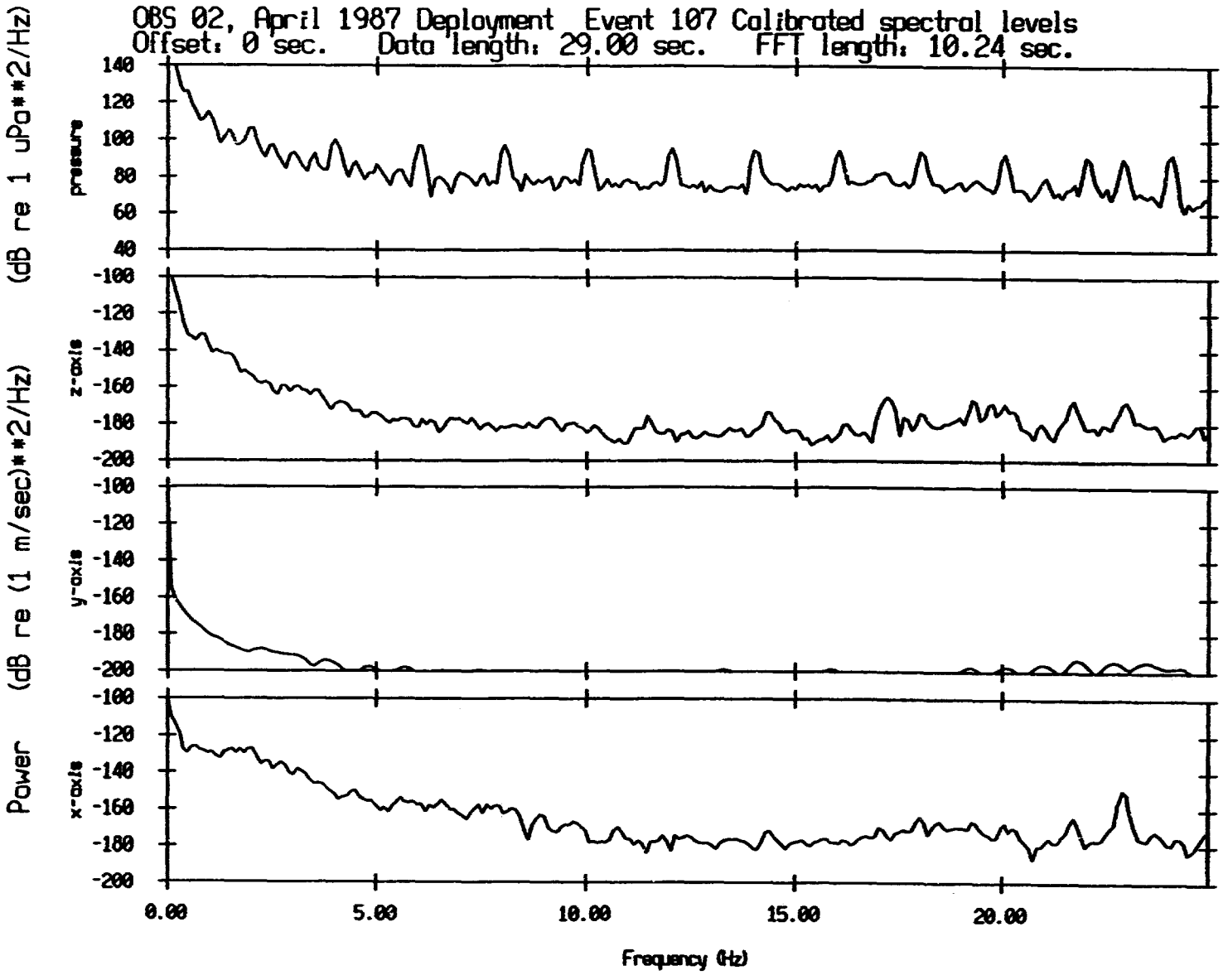
OBS 02, April 1987 Deployment Event 107 Calibrated spectral levels
Offset: 0 sec. Data length: 29.00 sec. FFT length: 10.24 sec.
Power (dB re (1 m/sec)**2/Hz) (dB re 1 uPa**2/Hz)
pressure
z-axis
y-axis
x-axis
140
120
100
80
60
40
-100
-120
-140
-160
-180
-200
0.00
5.00
10.00
15.00
20.00
Frequency (Hz)

Figure IV.12

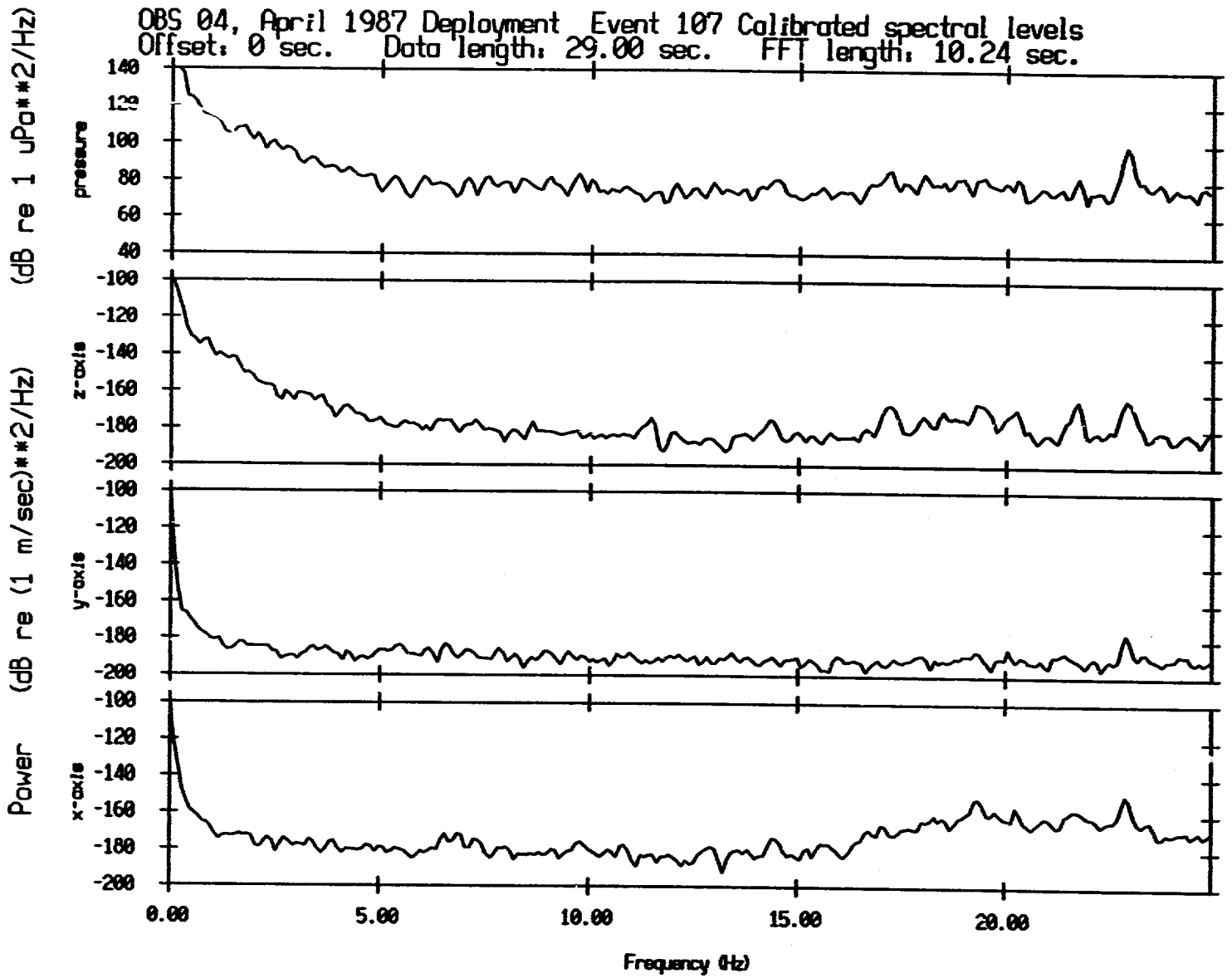
OBS 04, April 1987 Deployment Event 107 Calibrated spectral levels
Offset: 0 sec. Data length: 29.00 sec. FFT length: 10.24 sec.
Power (dB re (1 m/sec)**2/Hz) (dB re 1 uPa**2/Hz)
pressure
z-axis
y-axis
x-axis
140
120
100
80
60
40
-100
-120
-140
-160
-180
-200
0.00
5.00
10.00
15.00
20.00
Frequency (Hz)

Figure IV.13

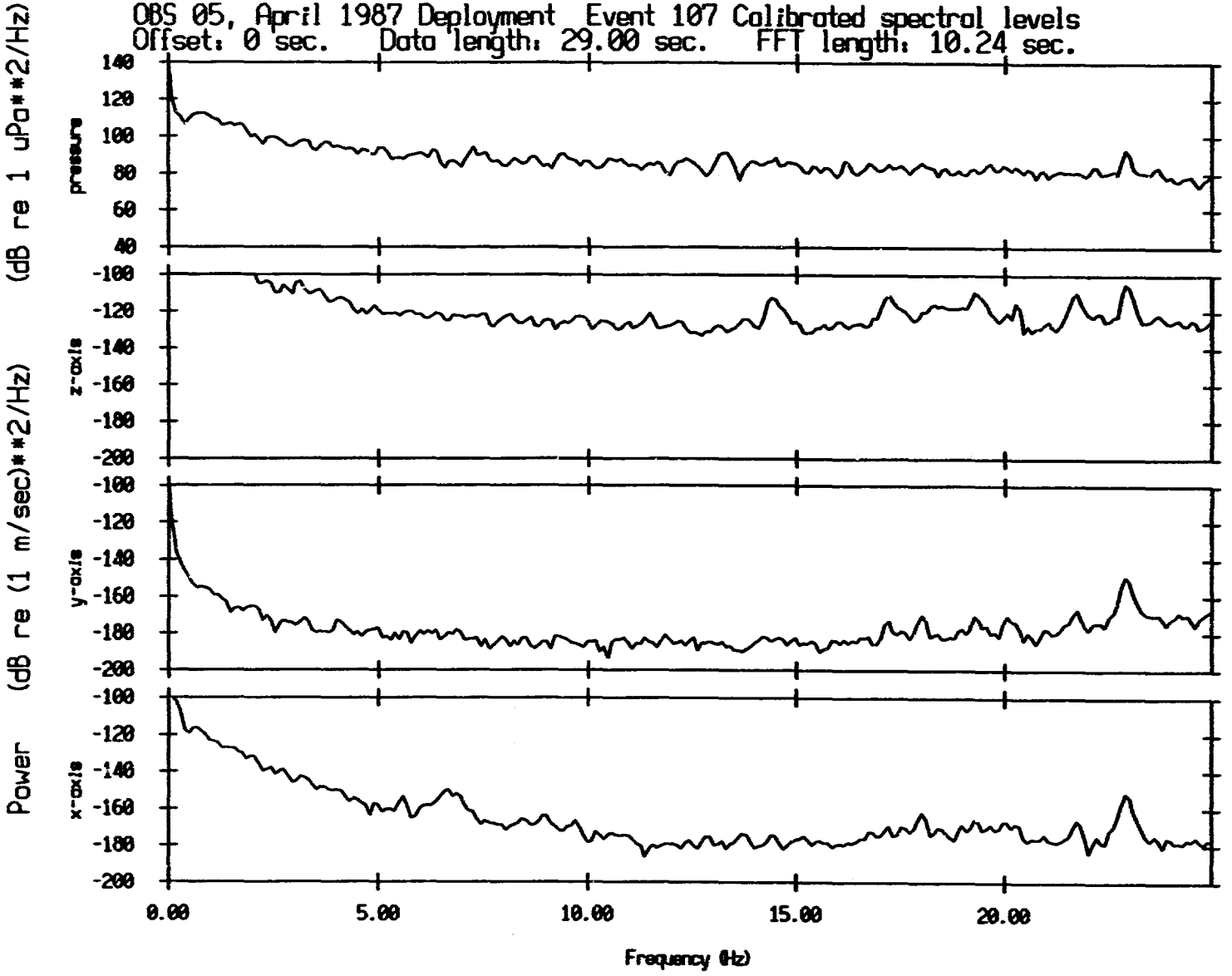
OBS 05, April 1987 Deployment Event 107 Calibrated spectral levels
Offset: 0 sec. Data length: 29.00 sec. FFT length: 10.24 sec.
Power (dB re (1 m/sec)**2/Hz) (dB re 1 uPa**2/Hz)
pressure
z-axis
y-axis
x-axis
140
120
100
80
60
40
-100
-120
-140
-160
-180
-200
0.00
5.00
10.00
15.00
20.00
Frequency (Hz)

Figure IV.14

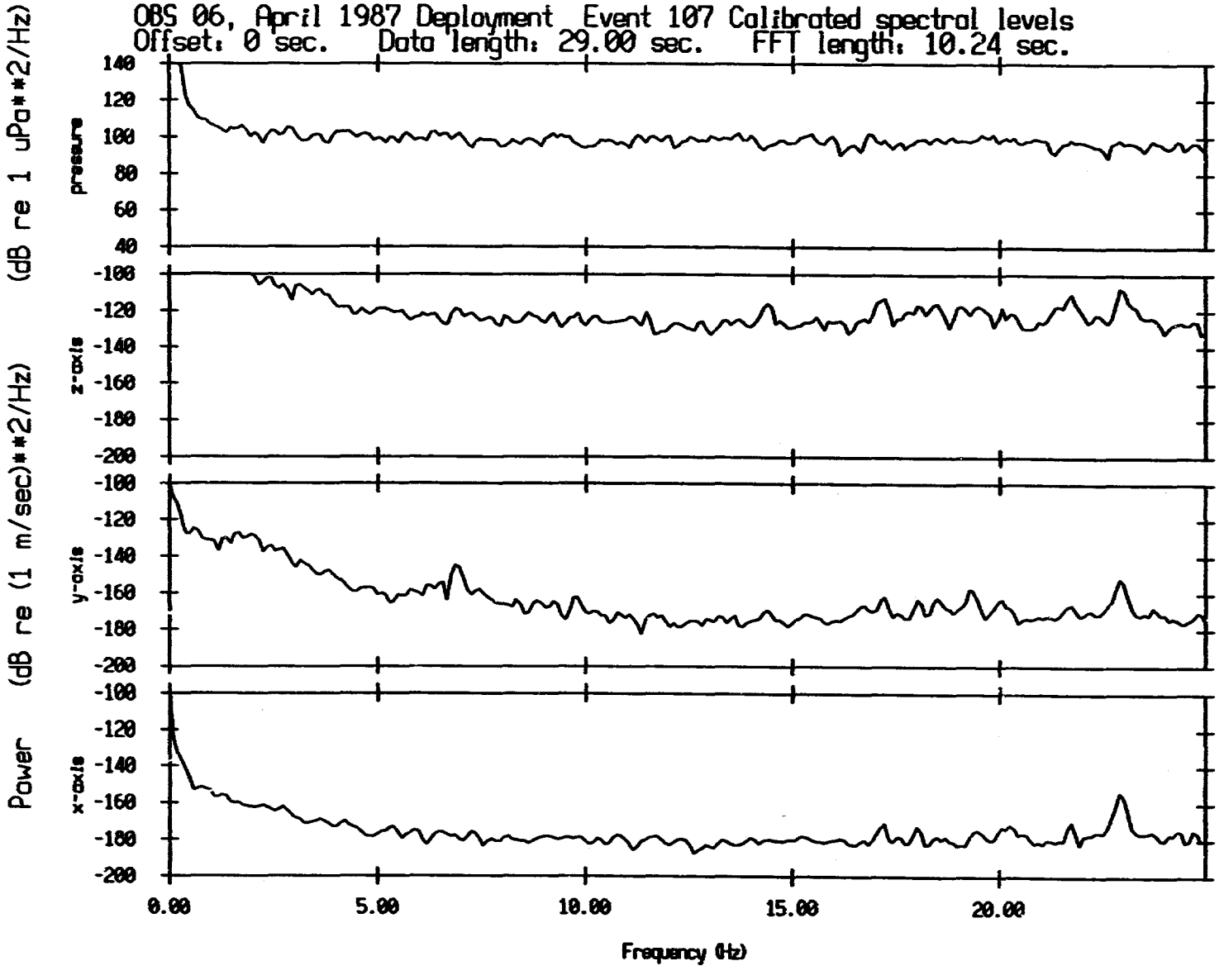
OBS 06, April 1987 Deployment Event 107 Calibrated spectral levels
Offset: 0 sec. Data length: 29.00 sec. FFT length: 10.24 sec.
Power (dB re (1 m/sec)**2/Hz) (dB re 1 uPa**2/Hz)
pressure
z-axis
y-axis
x-axis
140
120
100
80
60
40
-100
-120
-140
-160
-180
-200
0.00
5.00
10.00
15.00
20.00
Frequency (Hz)

Figure IV.15

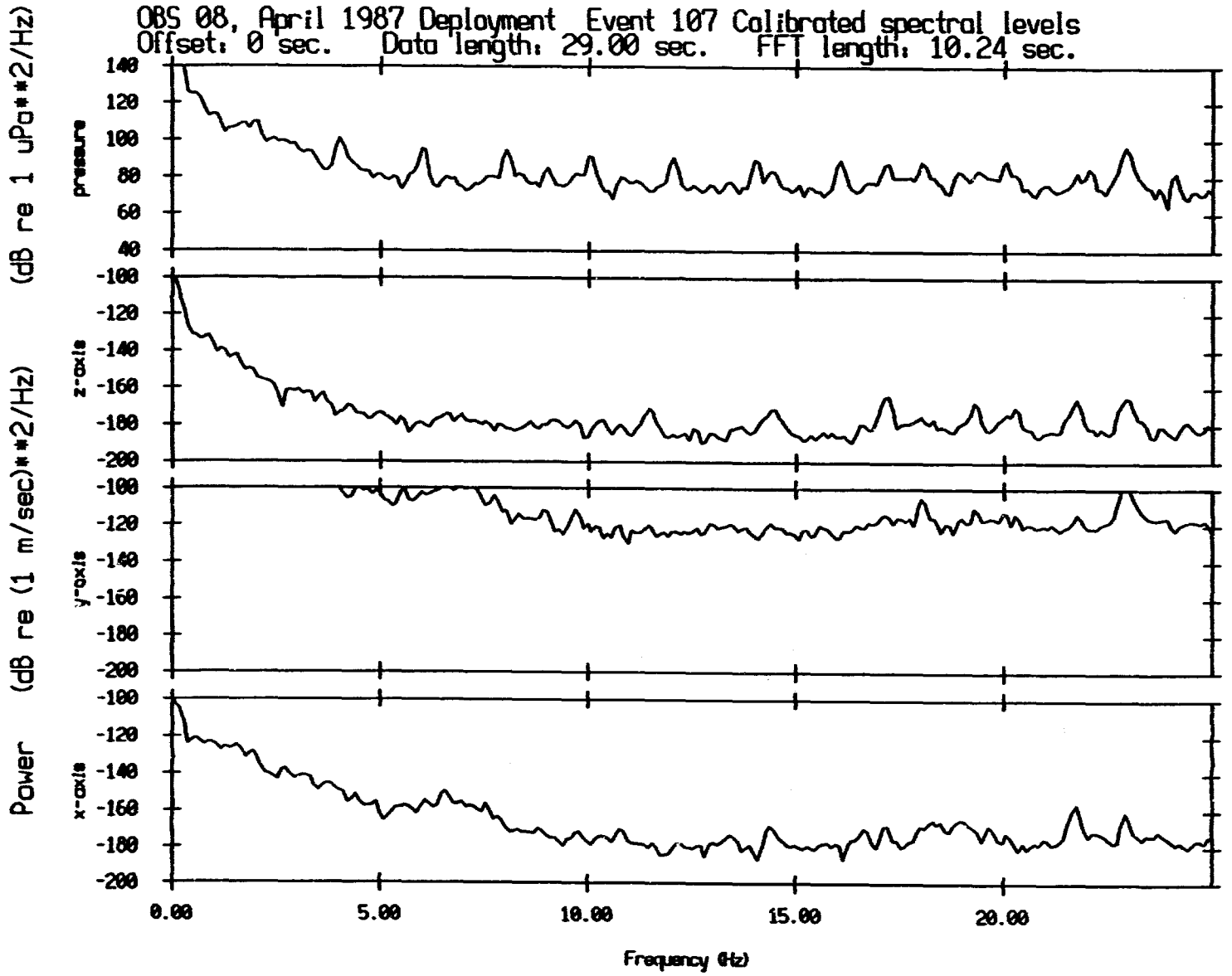
OBS 08, April 1987 Deployment Event 107 Calibrated spectral levels
Offset: 0 sec. Data length: 29.00 sec. FFT length: 10.24 sec.
Power (dB re (1 m/sec)**2/Hz) (dB re 1 uPa**2/Hz)
pressure
z-axis
y-axis
x-axis
140
120
100
80
60
40
-100
-120
-140
-160
-180
-200
0.00
5.00
10.00
15.00
20.00
Frequency (Hz)

Figure IV.16

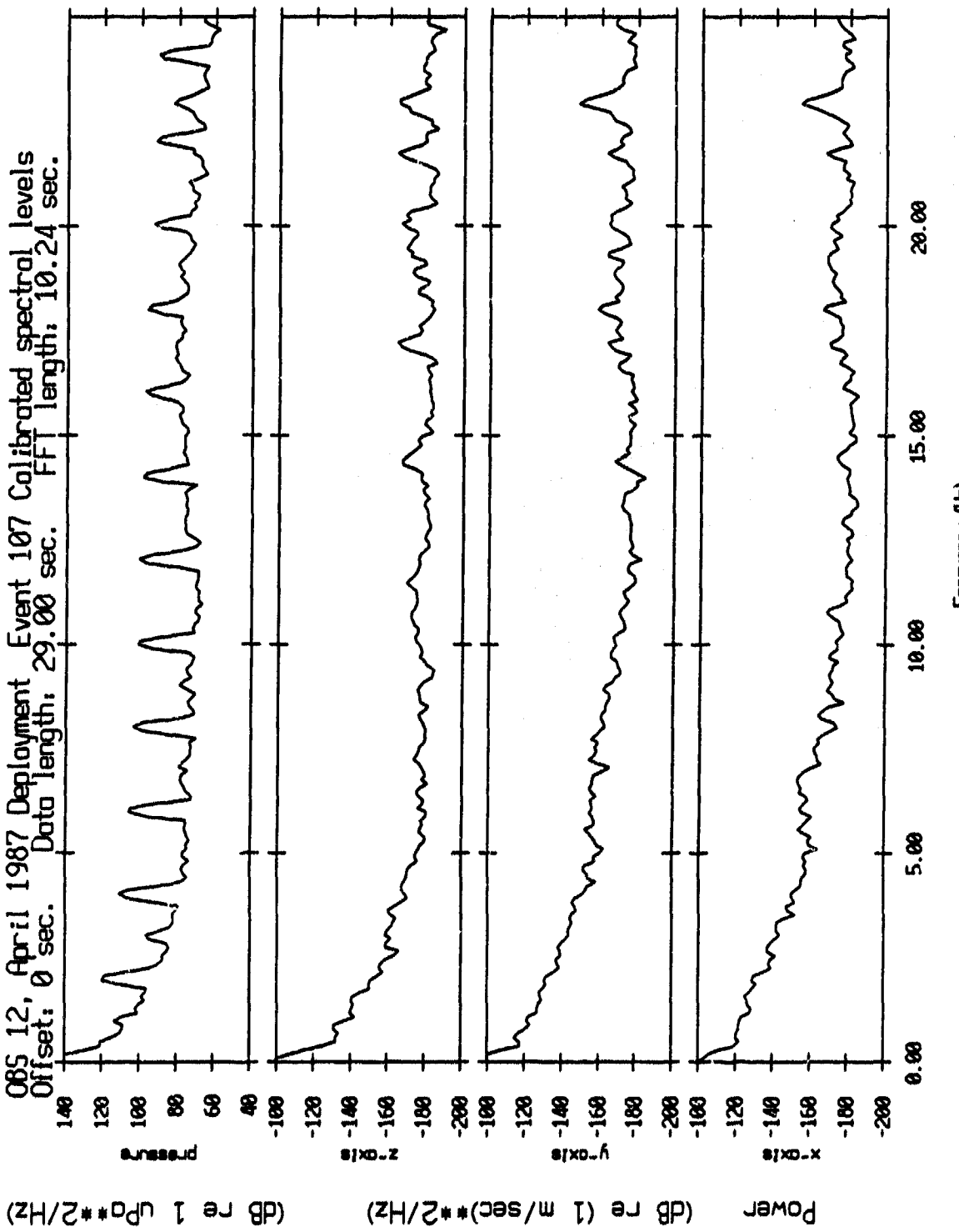
085 12, April 1987 Deployment Event 107 Calibrated spectral levels
Offset: 0 sec. Data length: 29.00 sec. FFT length: 10.24 sec.
pressure
z-axis
y-axis
x-axis
(dB re 1 uPa**2/Hz)
(dB re (1 m/sec)**2/Hz)
Power
Frequency (Hz)

Figure IV.17

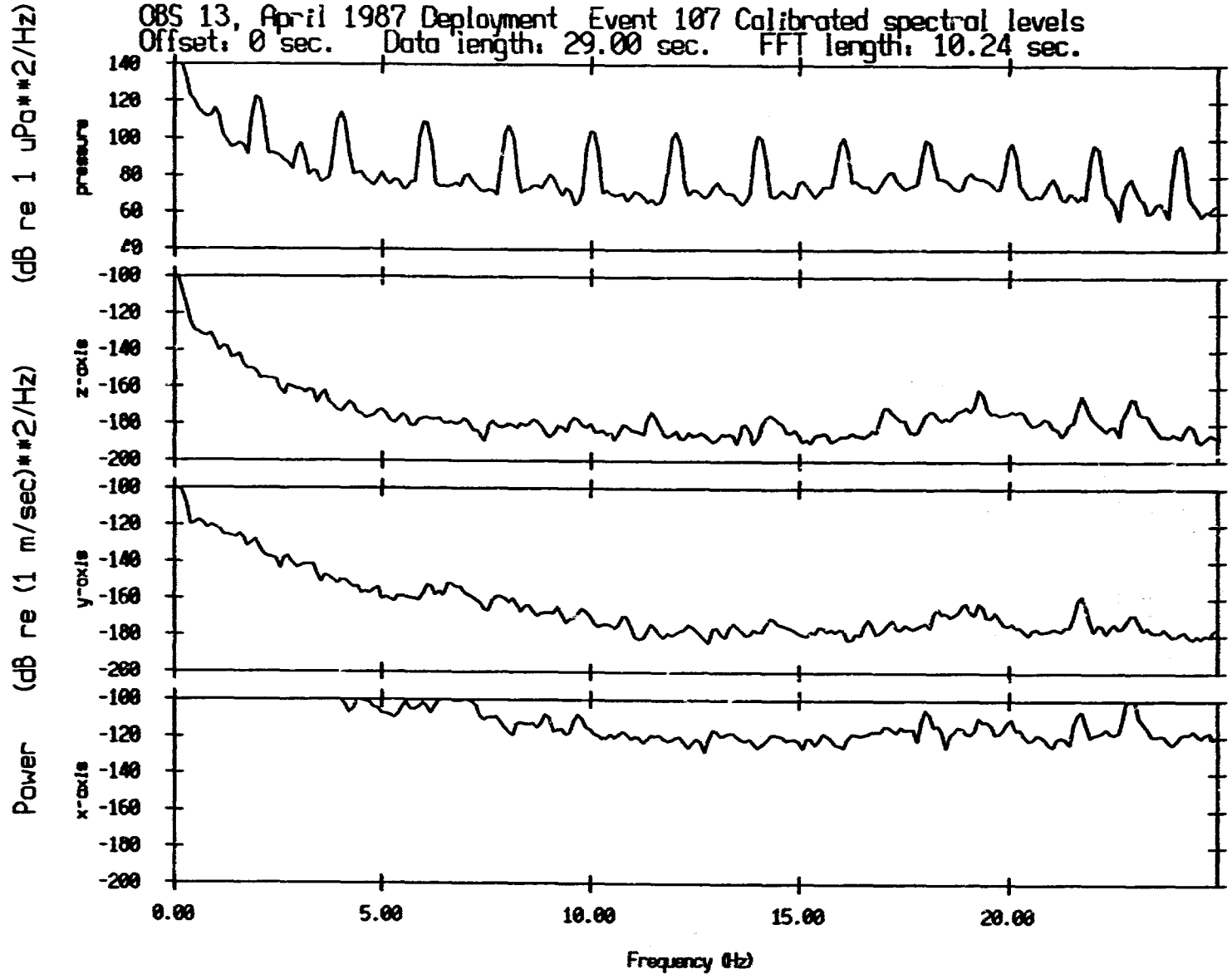
OBS 13, April 1987 Deployment Event 107 Calibrated spectral levels
Offset: 0 sec. Data length: 29.00 sec. FFT length: 10.24 sec.
Power (dB re (1 m/sec)**2/Hz) (dB re 1 uPa**2/Hz)
pressure
z-axis
y-axis
x-axis
140
120
100
80
60
40
-100
-120
-140
-160
-180
-200
0.00
5.00
10.00
15.00
20.00
Frequency (Hz)

Figure IV.18

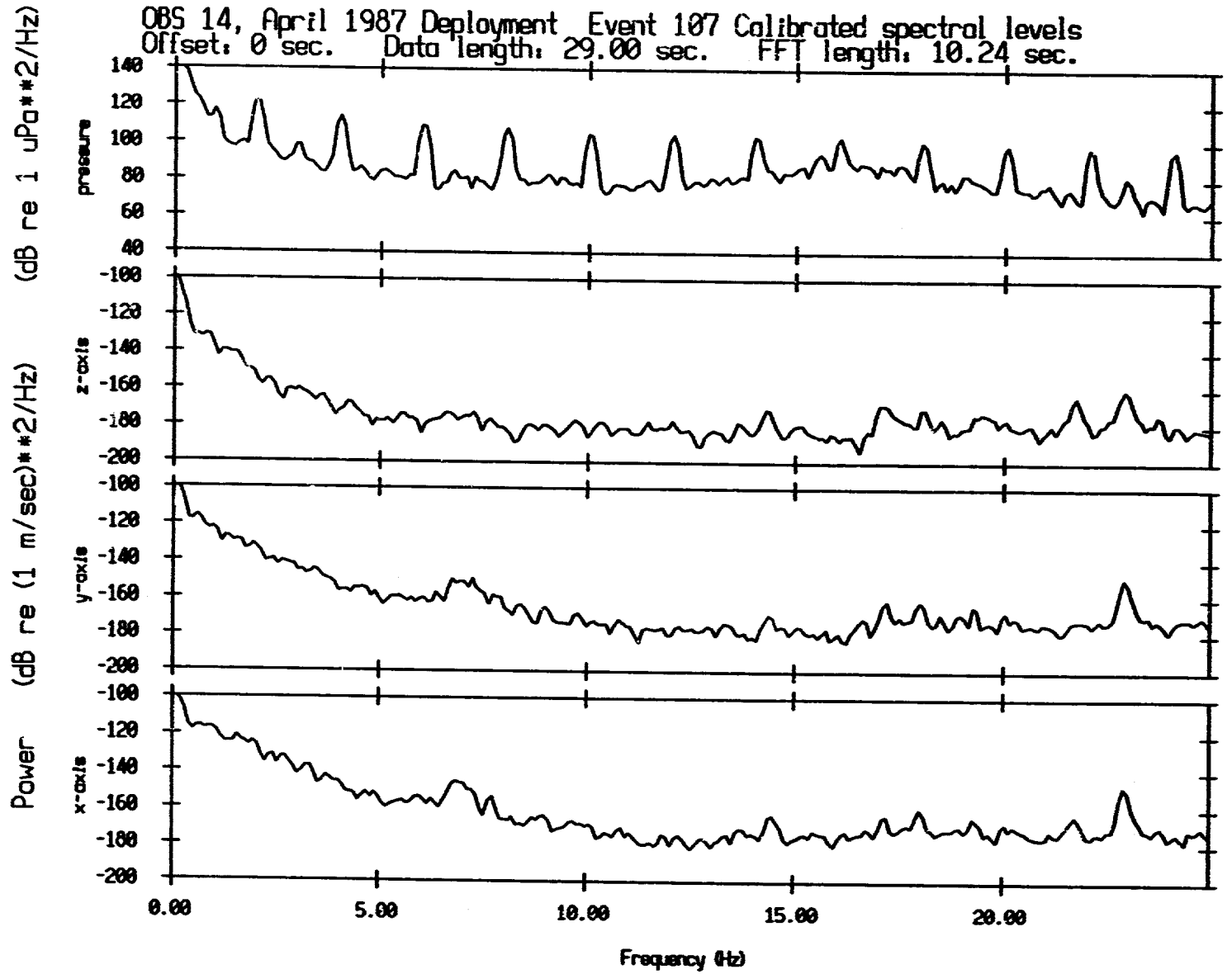
OBS 14, April 1987 Deployment Event 107 Calibrated spectral levels
Offset: 0 sec. Data length: 29.00 sec. FFT length: 10.24 sec.
Power (dB re (1 m/sec)**2/Hz) (dB re 1 uPa**2/Hz)
pressure
z-axis
y-axis
x-axis
140
120
100
80
60
40
-100
-120
-140
-160
-180
-200
0.00
5.00
10.00
15.00
20.00
Frequency (Hz)

Figure IV.19

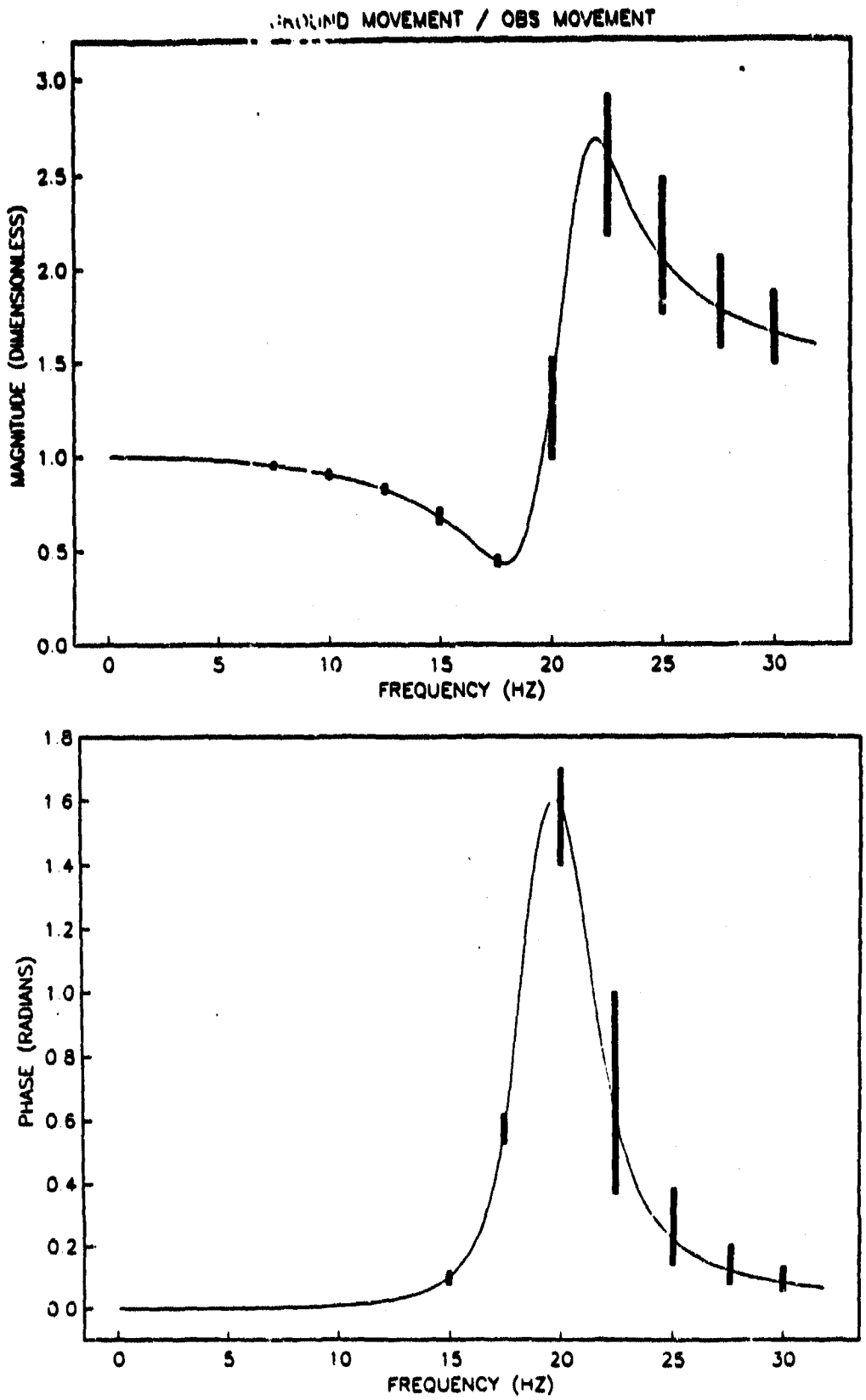

Figure 3.7. Ground motion correction transfer function. This relates the sea floor motion undisturbed by the presence of an OBS to the actual OBS motion recorded at Site 469. The vertical bars represent the uncertainty caused by the standard deviations in the resonance measurements.

Figure IV.20

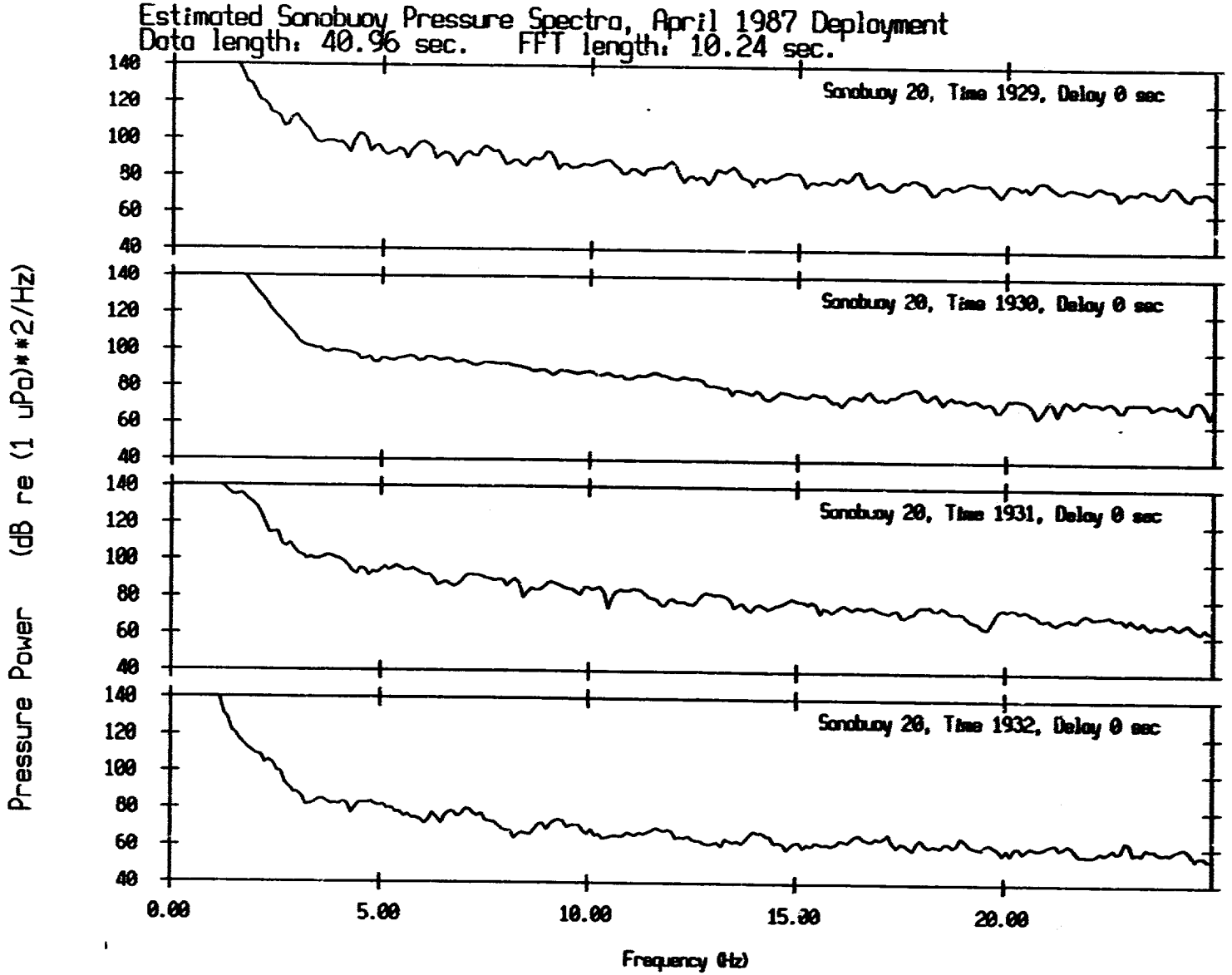
Estimated Sonobuoy Pressure Spectra, April 1987 Deployment
Data length: 40.96 sec. FFT length: 10.24 sec.
Sonobuoy 20, Time 1929, Delay 0 sec
Sonobuoy 20, Time 1930, Delay 0 sec
Sonobuoy 20, Time 1931, Delay 0 sec
Sonobuoy 20, Time 1932, Delay 0 sec
140
120
100
80
60
40
0.00
5.00
10.00
15.00
20.00
Pressure Power (dB re (1 uPa)**2/Hz)
Frequency (Hz)

Figure IV.21

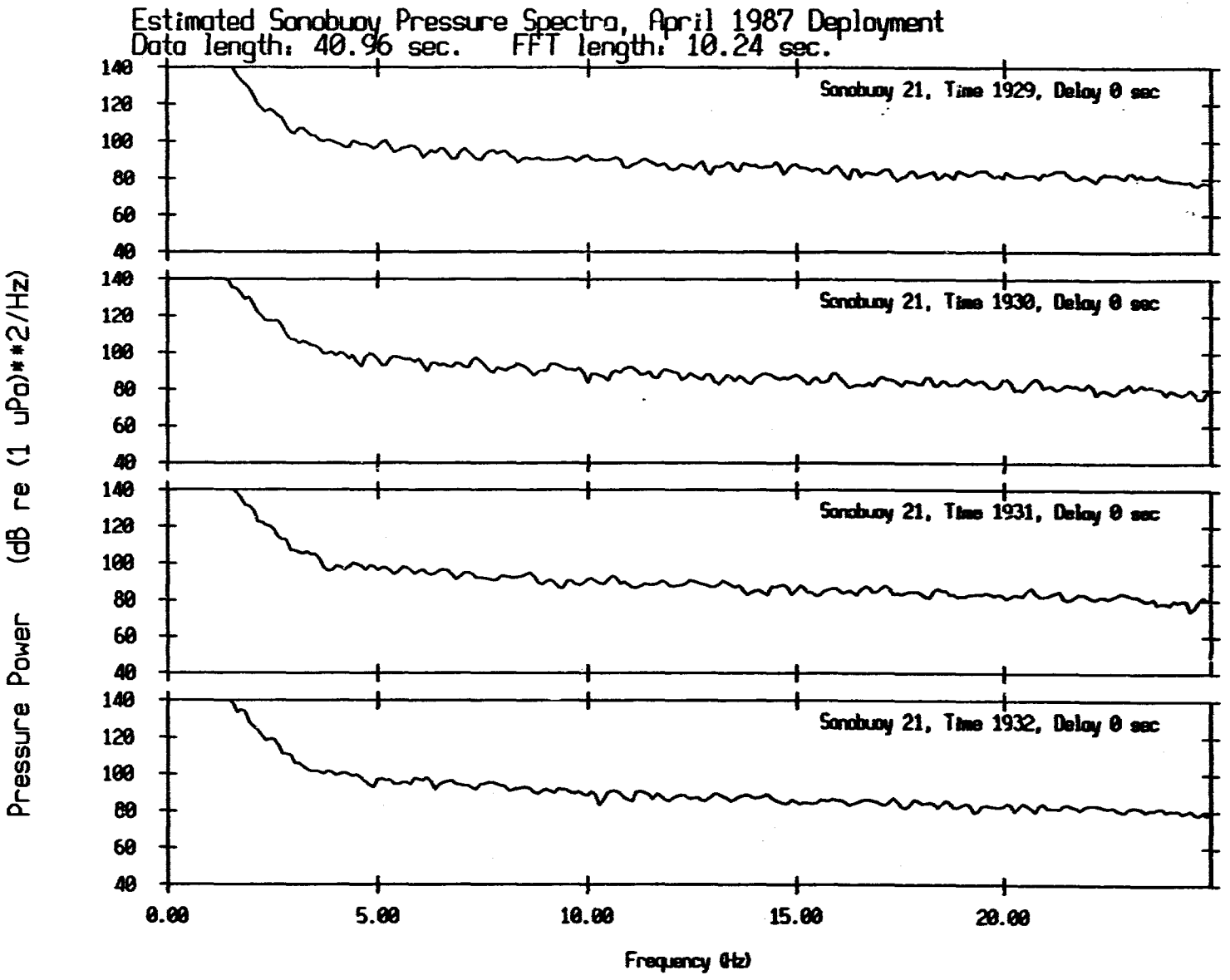
Estimated Sonobuoy Pressure Spectra, April 1987 Deployment
Data length: 40.96 sec. FFT length: 10.24 sec.
Sonobuoy 21, Time 1929, Delay 0 sec
Sonobuoy 21, Time 1930, Delay 0 sec
Sonobuoy 21, Time 1931, Delay 0 sec
Sonobuoy 21, Time 1932, Delay 0 sec
Pressure Power (dB re (1 uPa)**2/Hz)
140
120
100
80
60
40
0.00
5.00
10.00
15.00
20.00
Frequency (Hz)

Figure IV.22

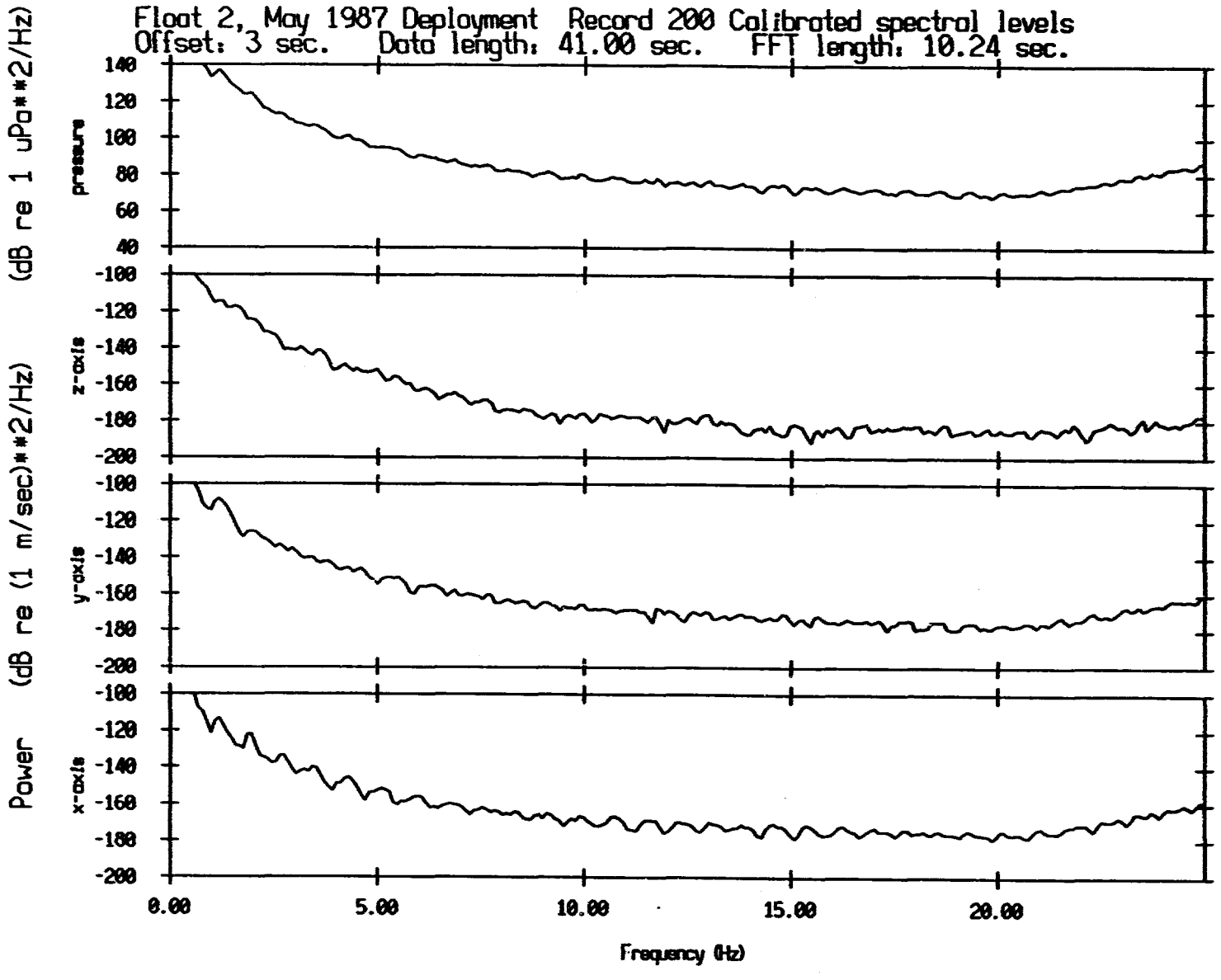
Float 2, May 1987 Deployment Record 200 Calibrated spectral levels
Offset: 3 sec. Data length: 41.00 sec. FFT length: 10.24 sec.
Power (dB re (1 m/sec)**2/Hz) (dB re 1 uPa**2/Hz)
pressure
z-axis
y-axis
x-axis
140
120
100
80
60
40
-100
-120
-140
-160
-180
-200
0.00
5.00
10.00
15.00
20.00
Frequency (Hz)

Figure IV.23

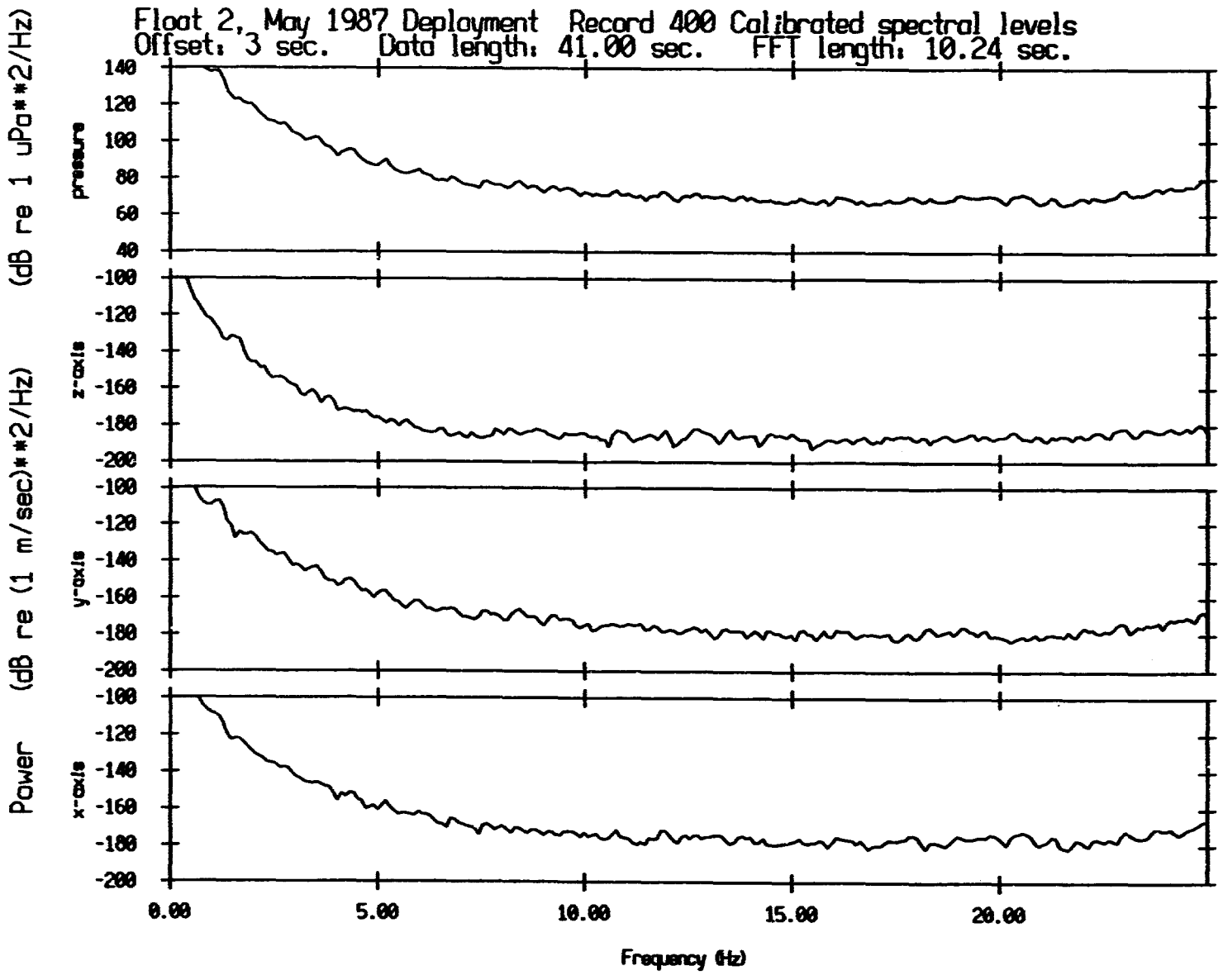
Float 2, May 1987 Deployment Record 400 Calibrated spectral levels
Offset: 3 sec. Data length: 41.00 sec. FFT length: 10.24 sec.
Power (dB re (1 m/sec)**2/Hz) (dB re 1 uPa**2/Hz)
pressure
z-axis
y-axis
x-axis
140
120
100
80
60
40
-100
-120
-140
-160
-180
-200
0.00
5.00
10.00
15.00
20.00
Frequency (Hz)

Figure IV.24

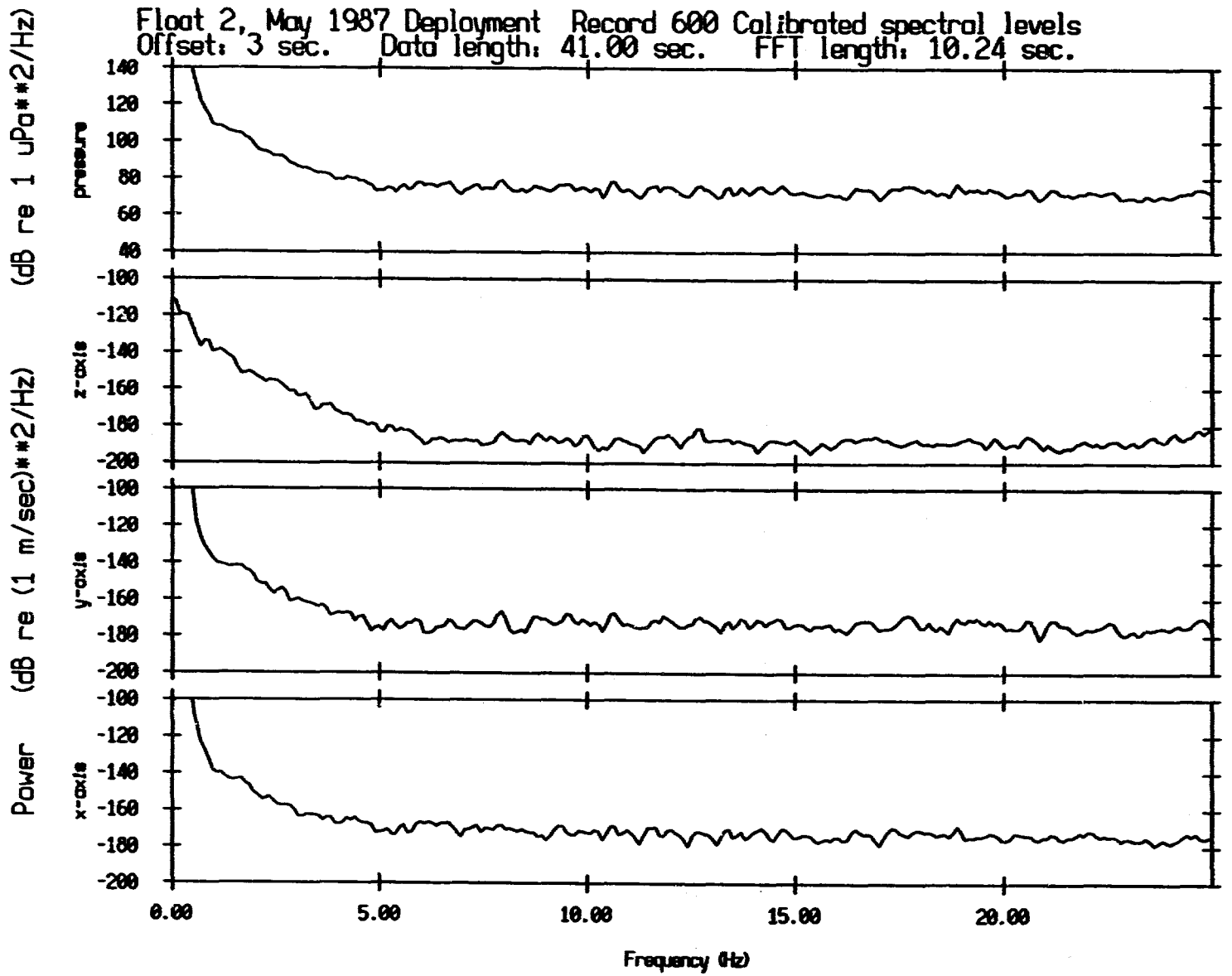
Float 2, May 1987 Deployment Record 600 Calibrated spectral levels
Offset: 3 sec. Data length: 41.00 sec. FFT length: 10.24 sec.
Power (dB re (1 m/sec)**2/Hz) (dB re 1 uPa**2/Hz)
pressure
z-axis
y-axis
x-axis
140
120
100
80
60
40
-100
-120
-140
-160
-180
-200
0.00
5.00
10.00
15.00
20.00
Frequency (Hz)

Figure IV.25

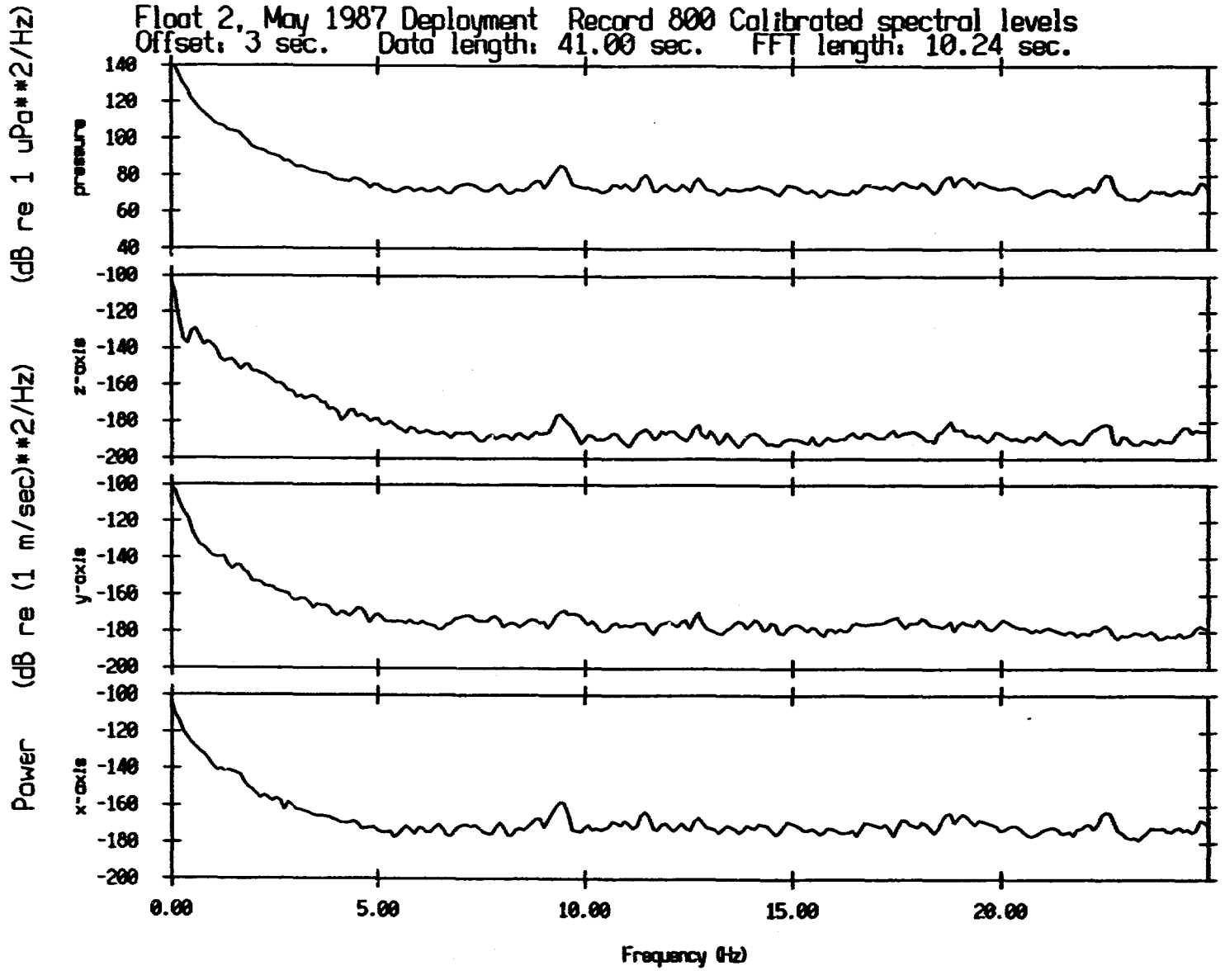
Float 2, May 1987 Deployment Record 800 Calibrated spectral levels
Offset: 3 sec. Data length: 41.00 sec. FFT length: 10.24 sec.
Power (dB re (1 m/sec)**2/Hz) (dB re 1 uPa**2/Hz)
pressure
z-axis
y-axis
x-axis
140
120
100
80
60
40
-100
-120
-140
-160
-180
-200
0.00
5.00
10.00
15.00
20.00
Frequency (Hz)

Figure IV.28

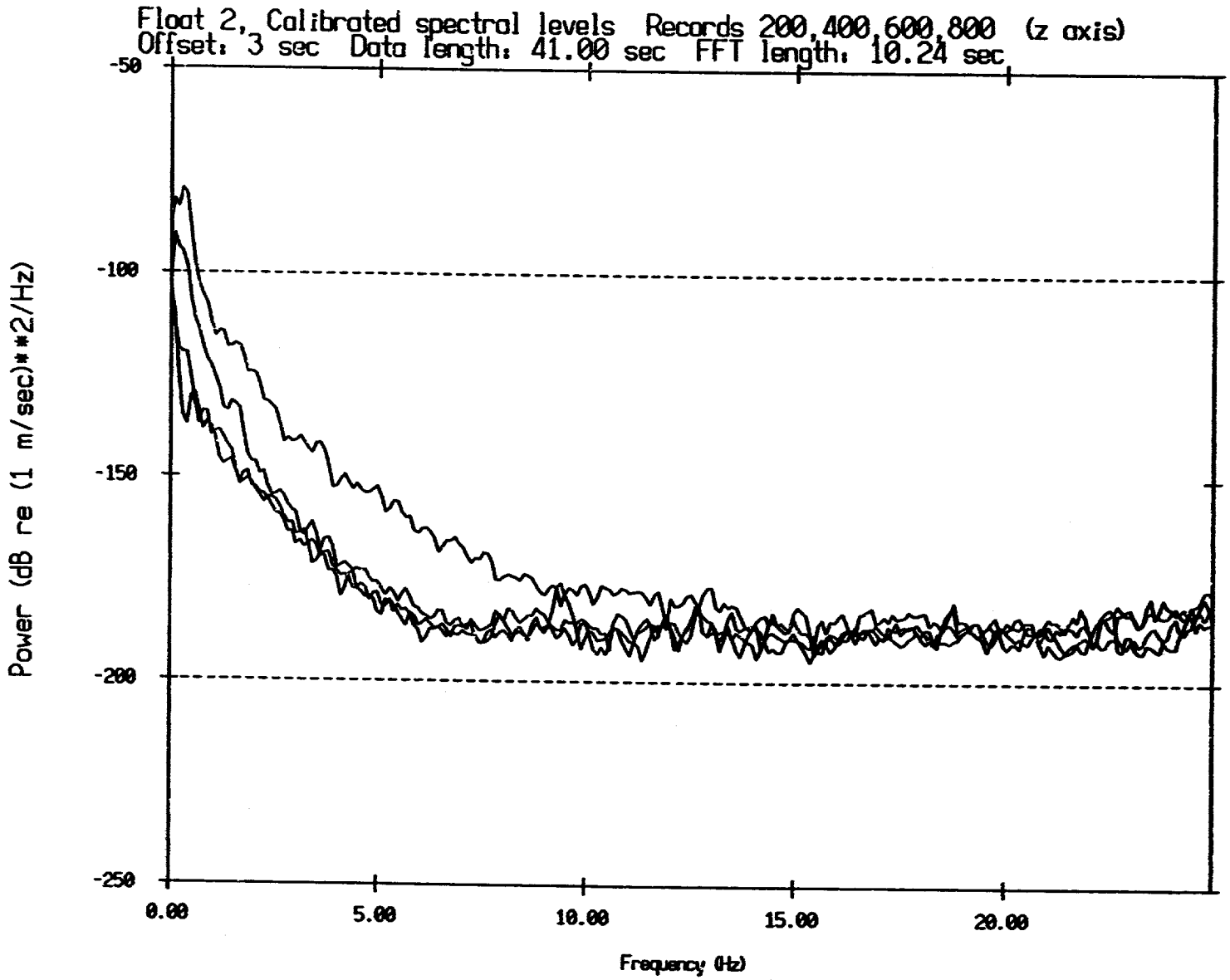
Float 2, Calibrated spectral levels Records 200,400,600,800 (z axis)
Offset: 3 sec Data length: 41.00 sec FFT length: 10.24 sec
-50
-100
-150
-200
-250
Power (dB re (1 m/sec)**2/Hz)
0.00
5.00
10.00
15.00
20.00
Frequency (Hz)

Figure IV.27

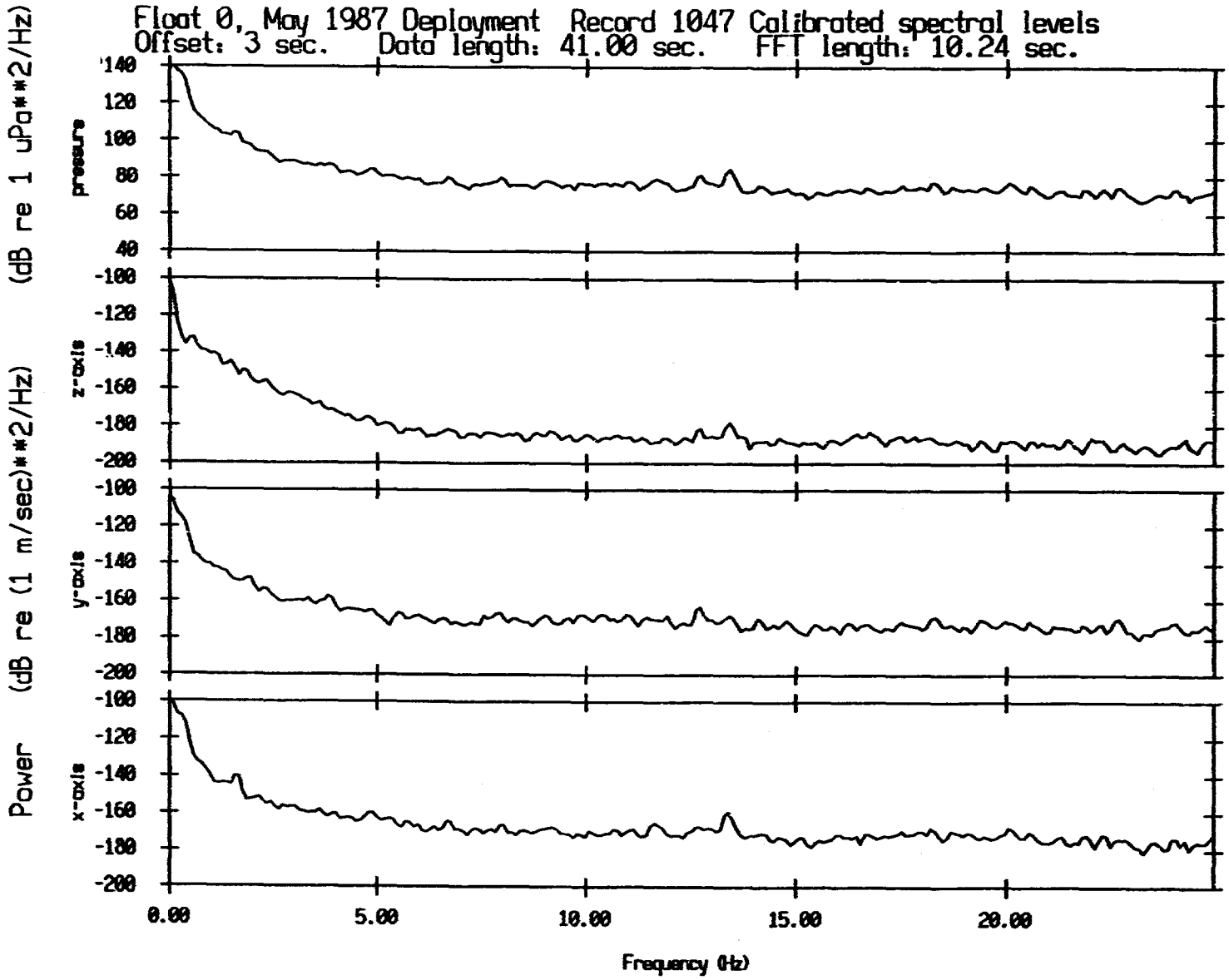

Figure IV.28a

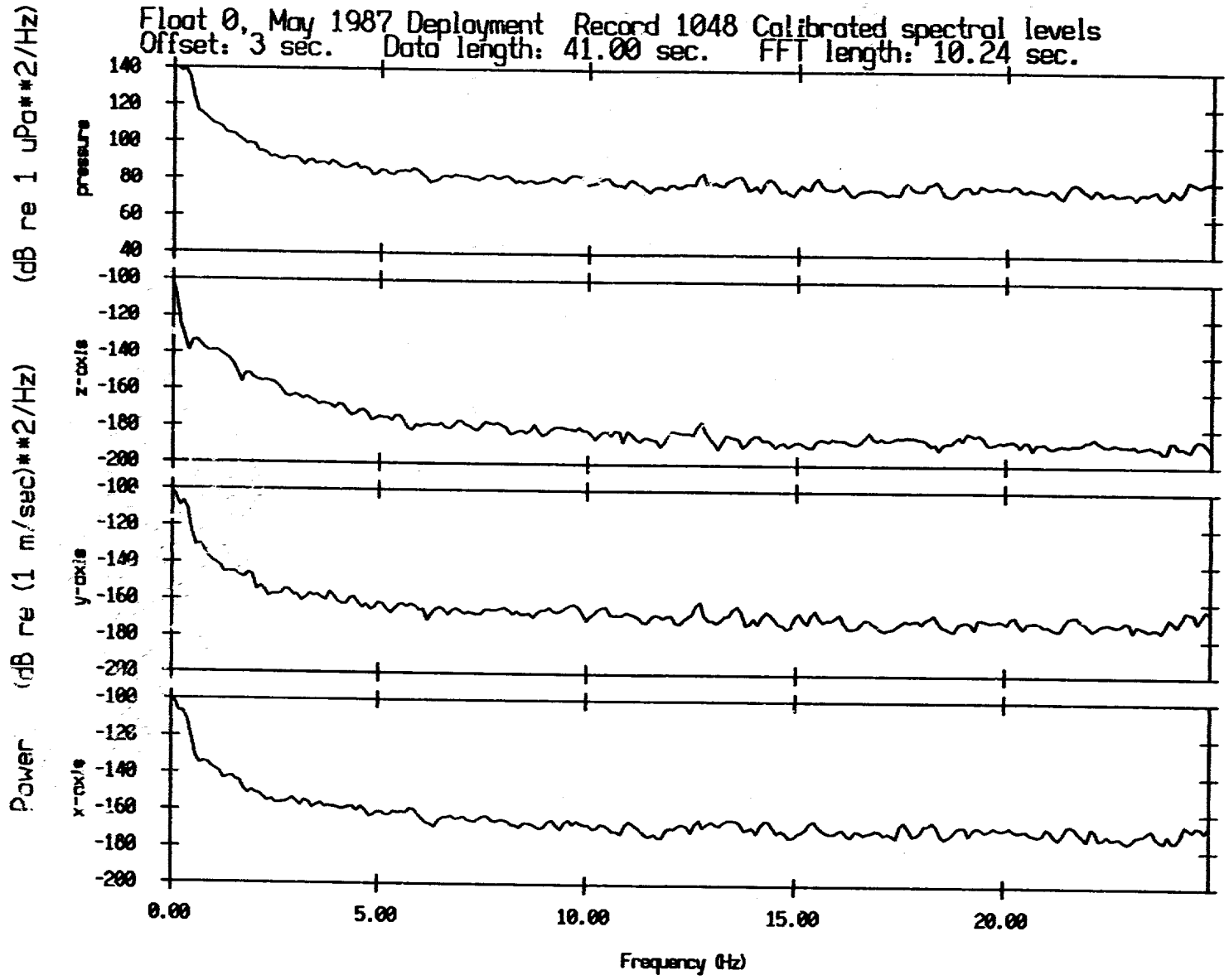

Figure IV.28b

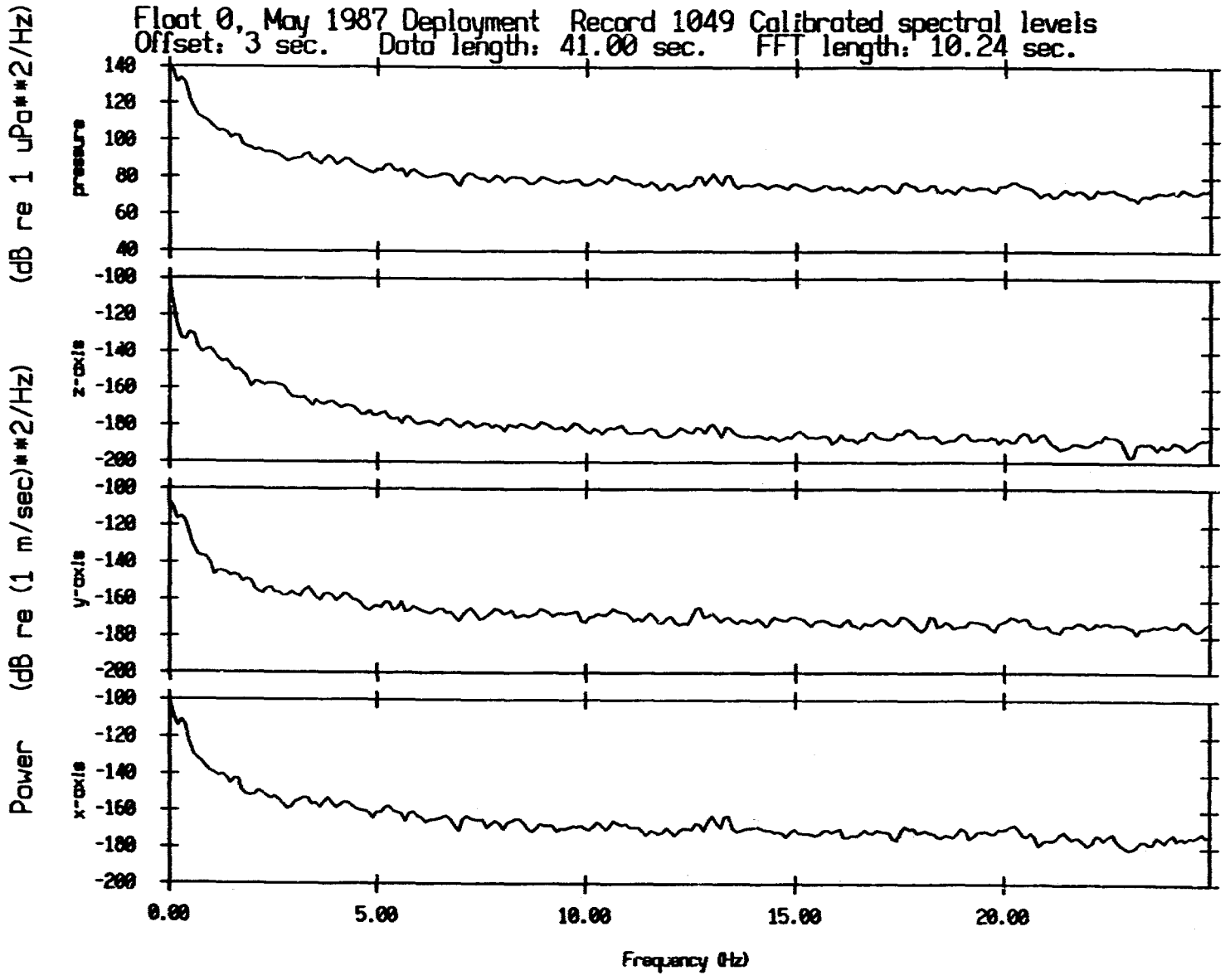

Figure IV.28c

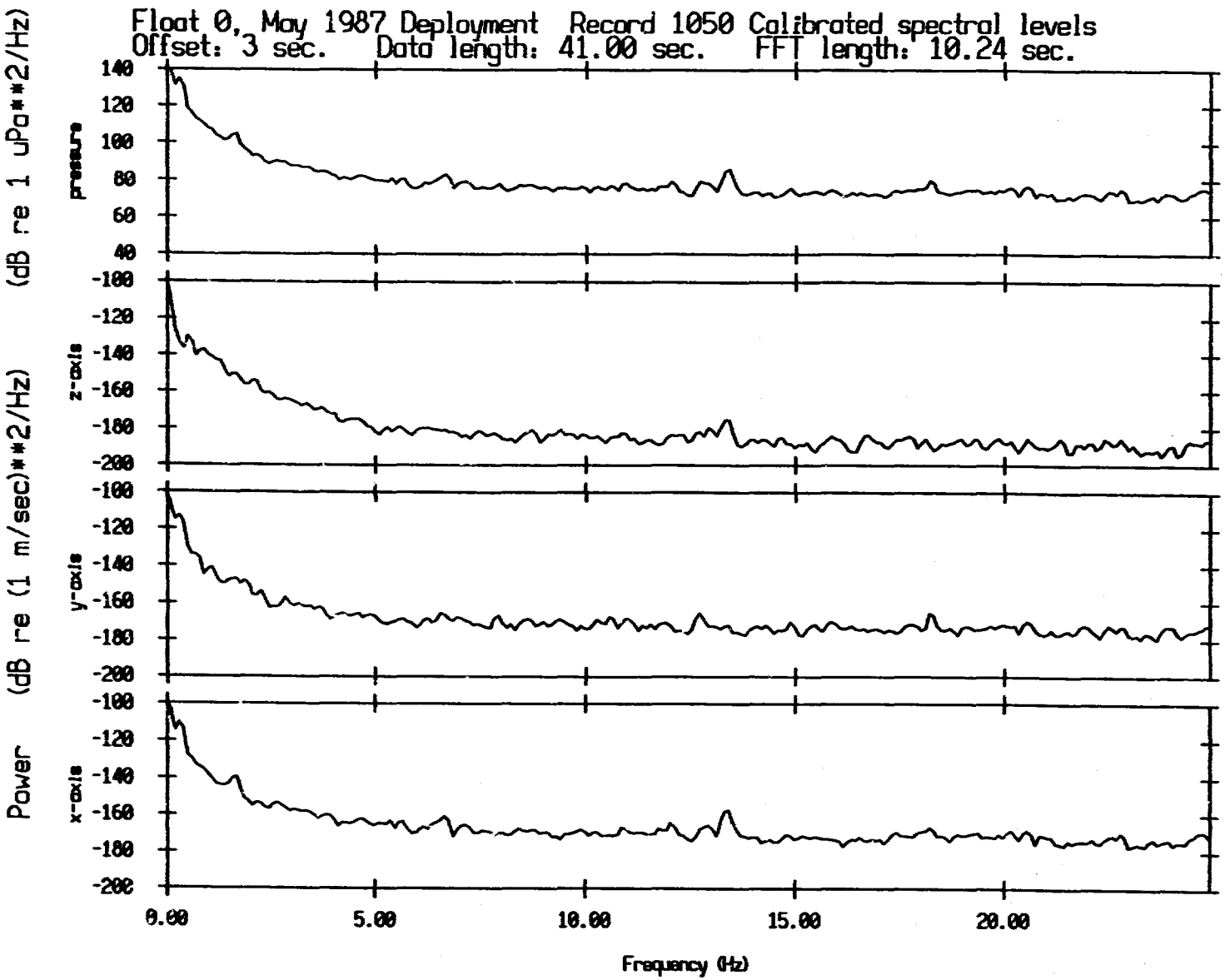

Figure IV.28d

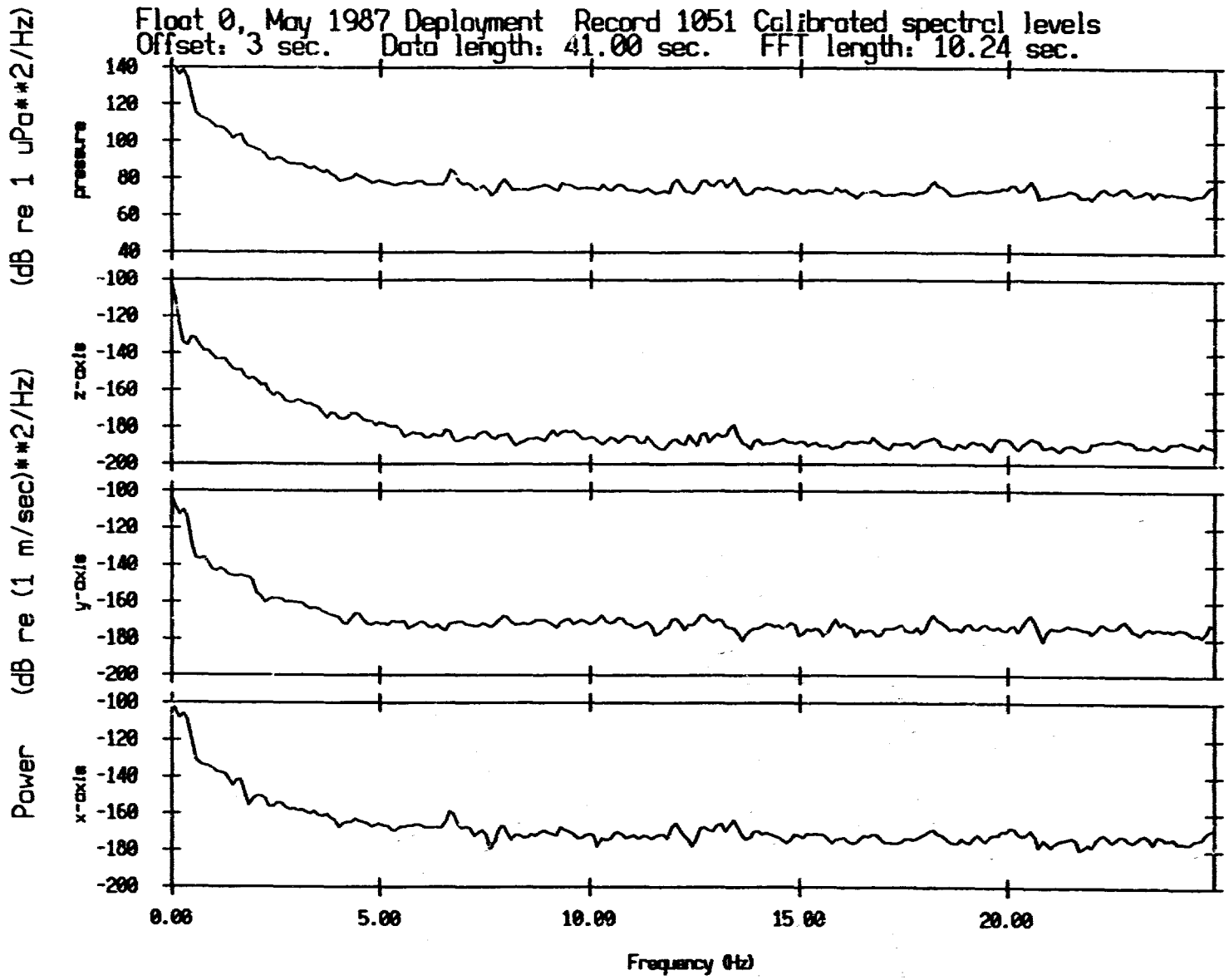

Figure IV.28e

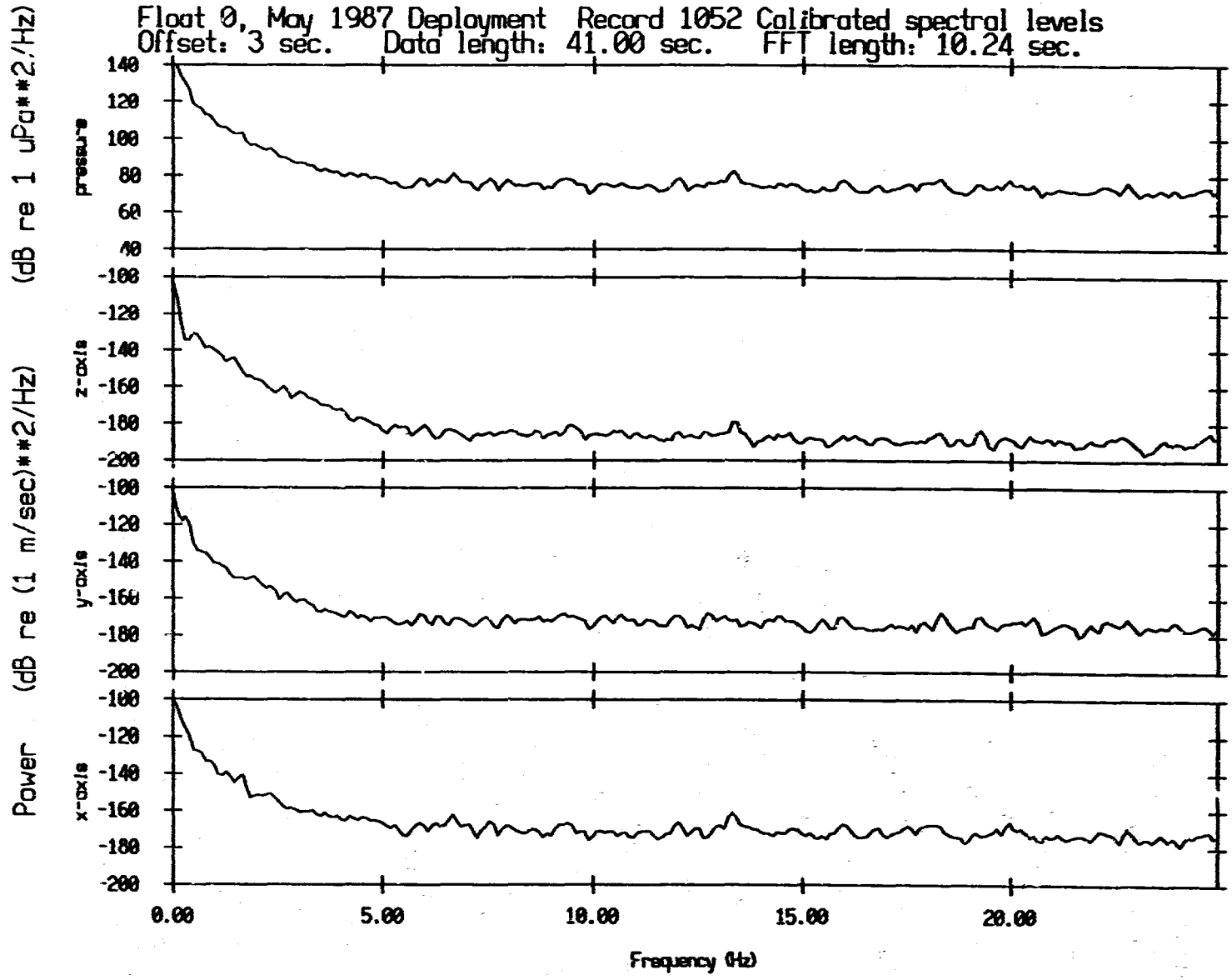

Figure IV.28f

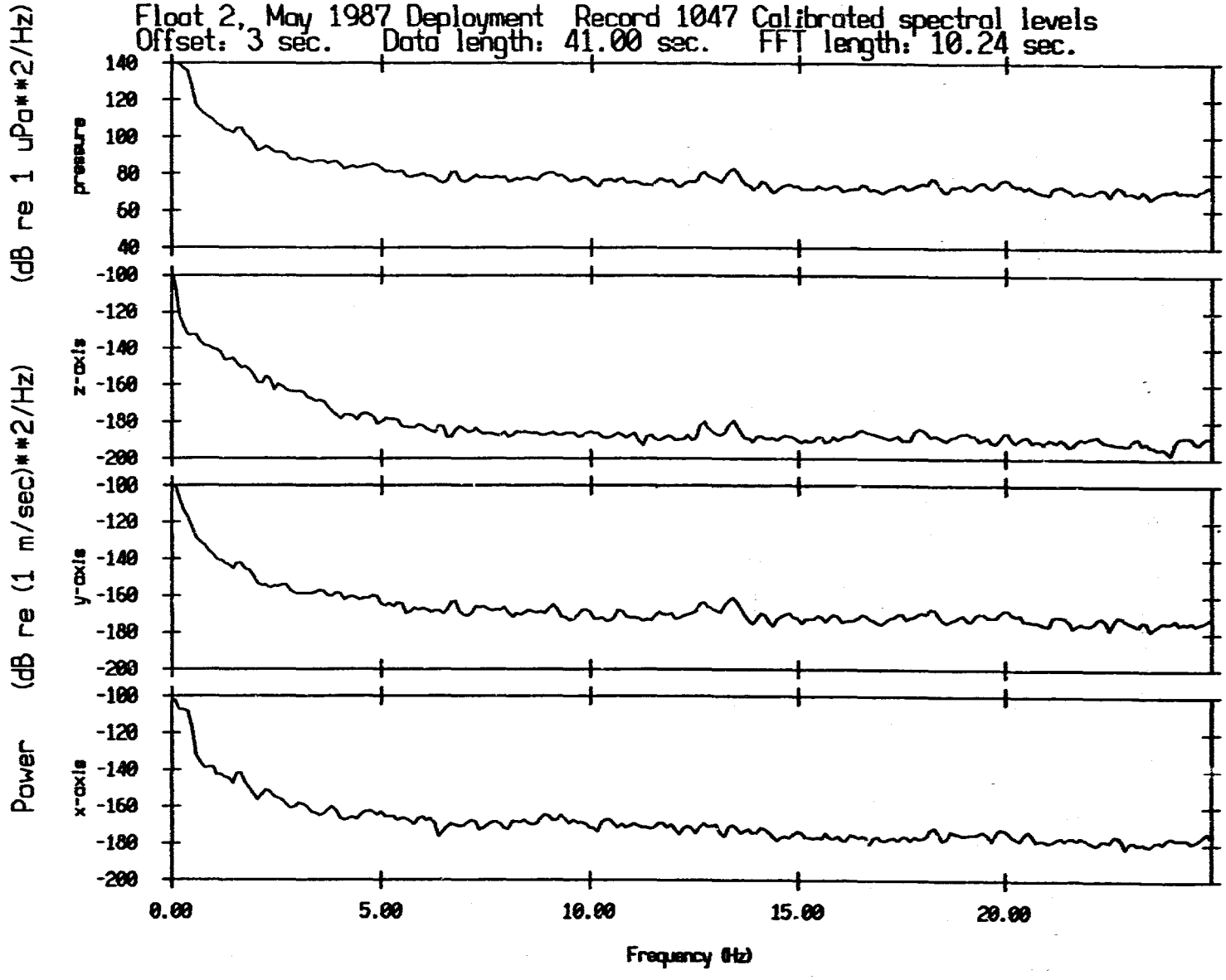

Figure IV.20a

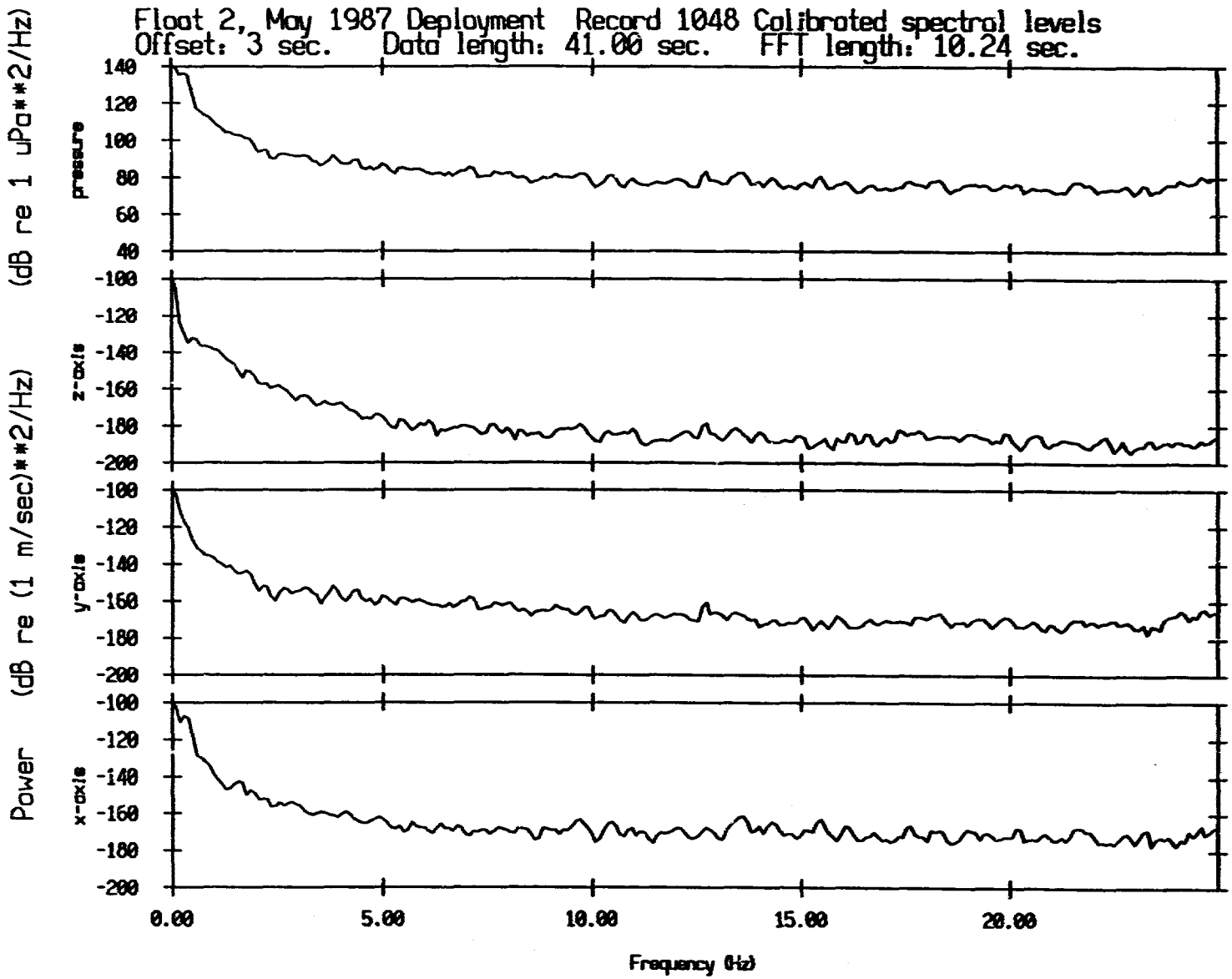

Figure IV.29b

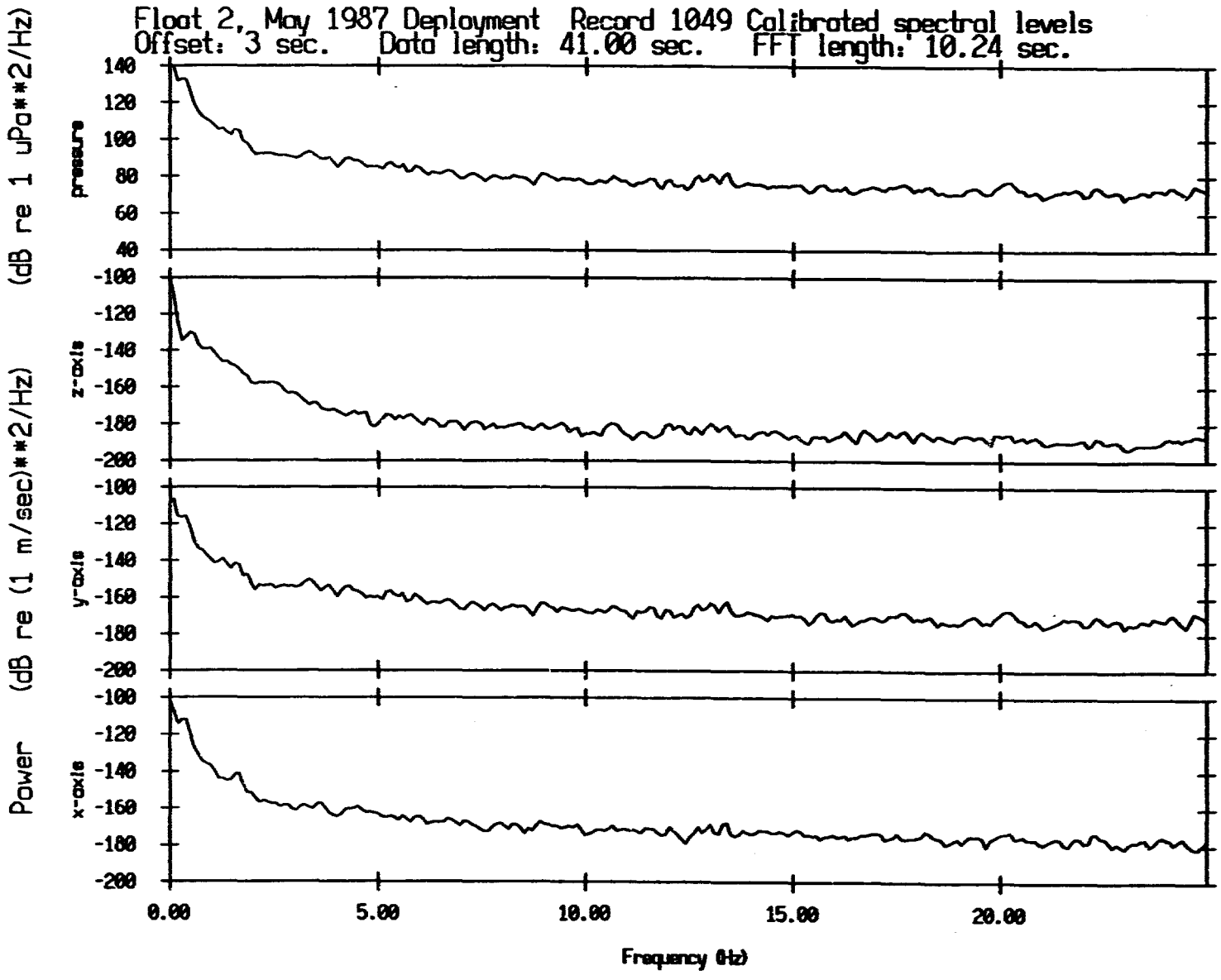

Figure IV.29c

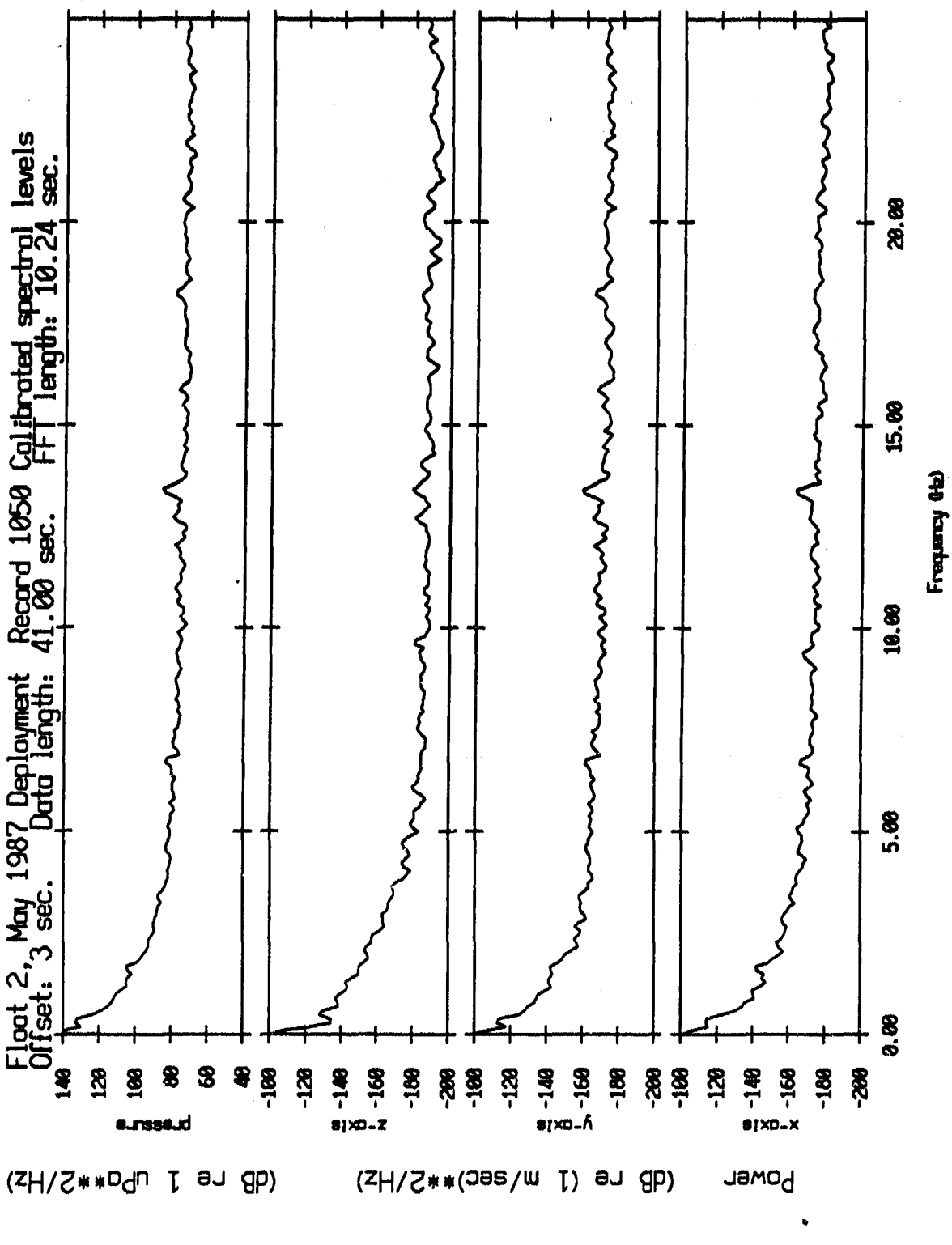

Figure IV.29d

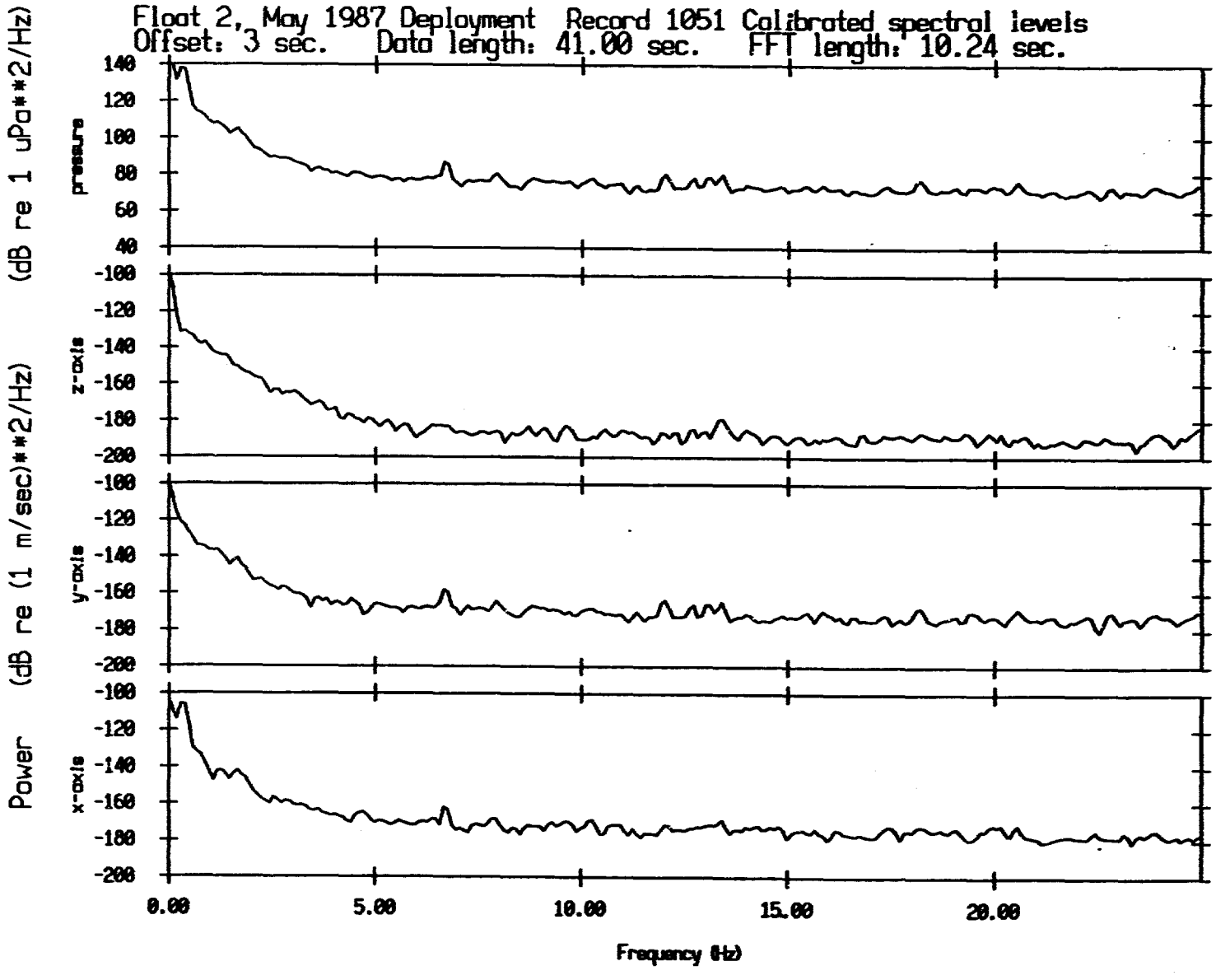

Figure IV.20e

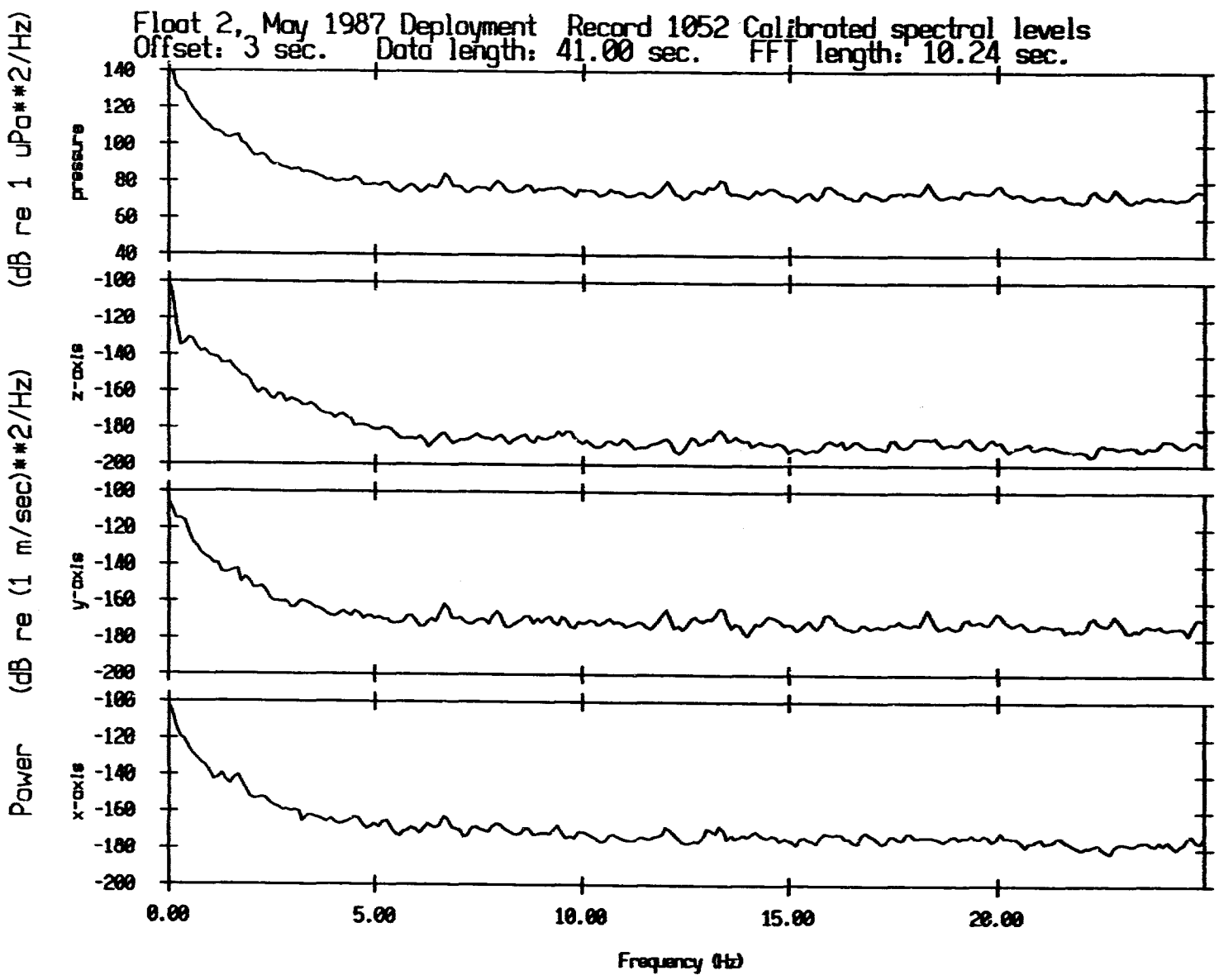

Figure IV.20f

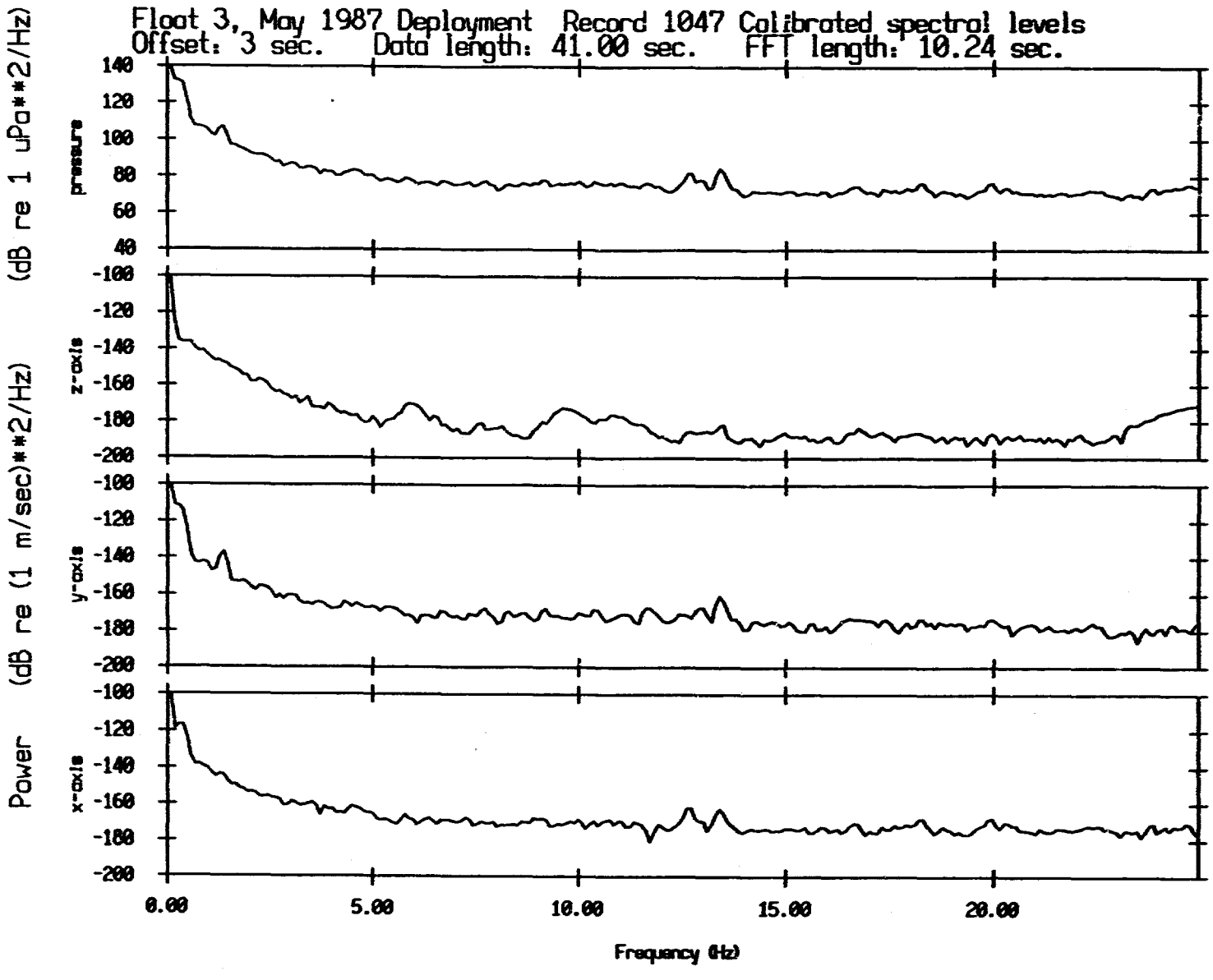

Figure IV.30a

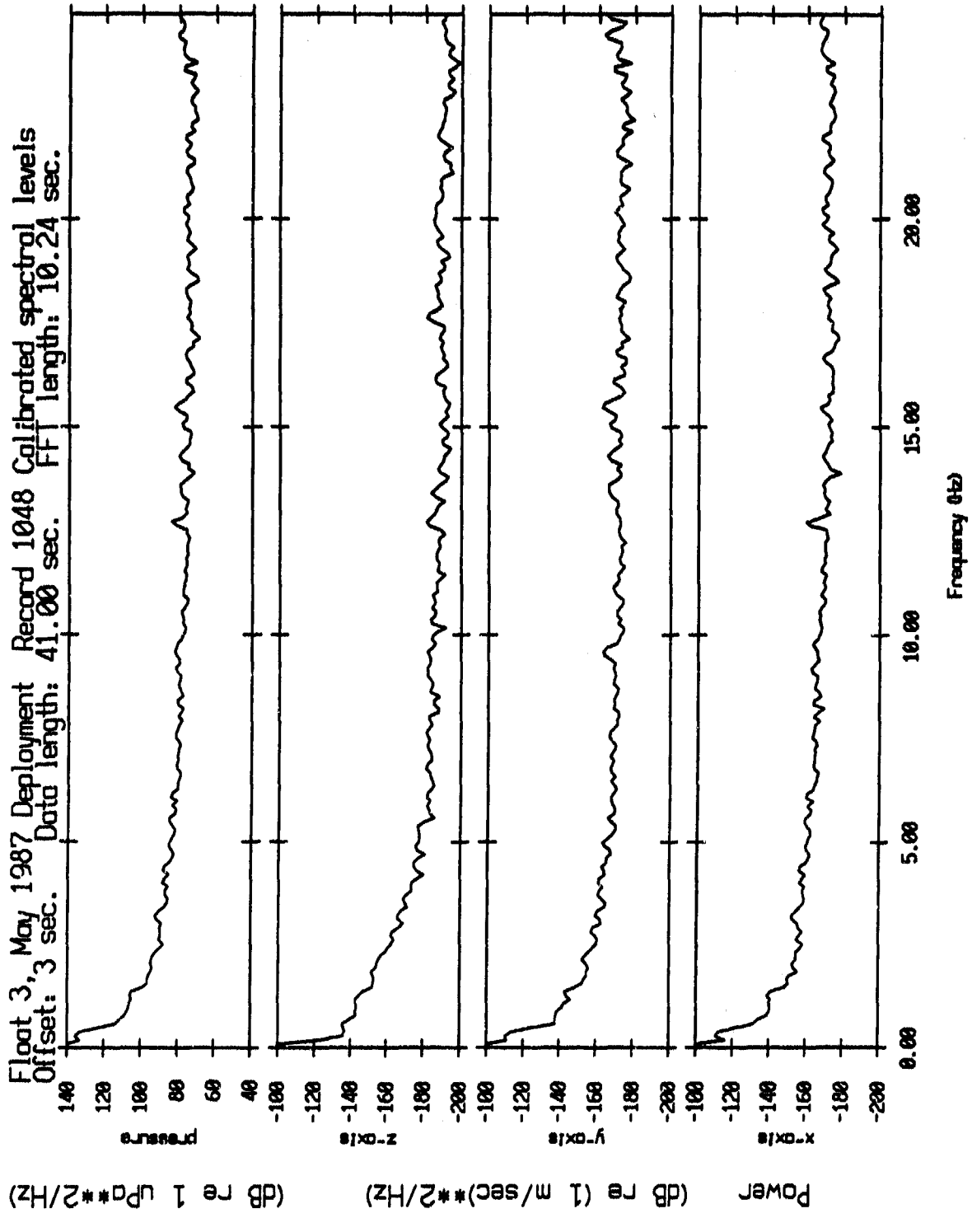

Figure IV.30b

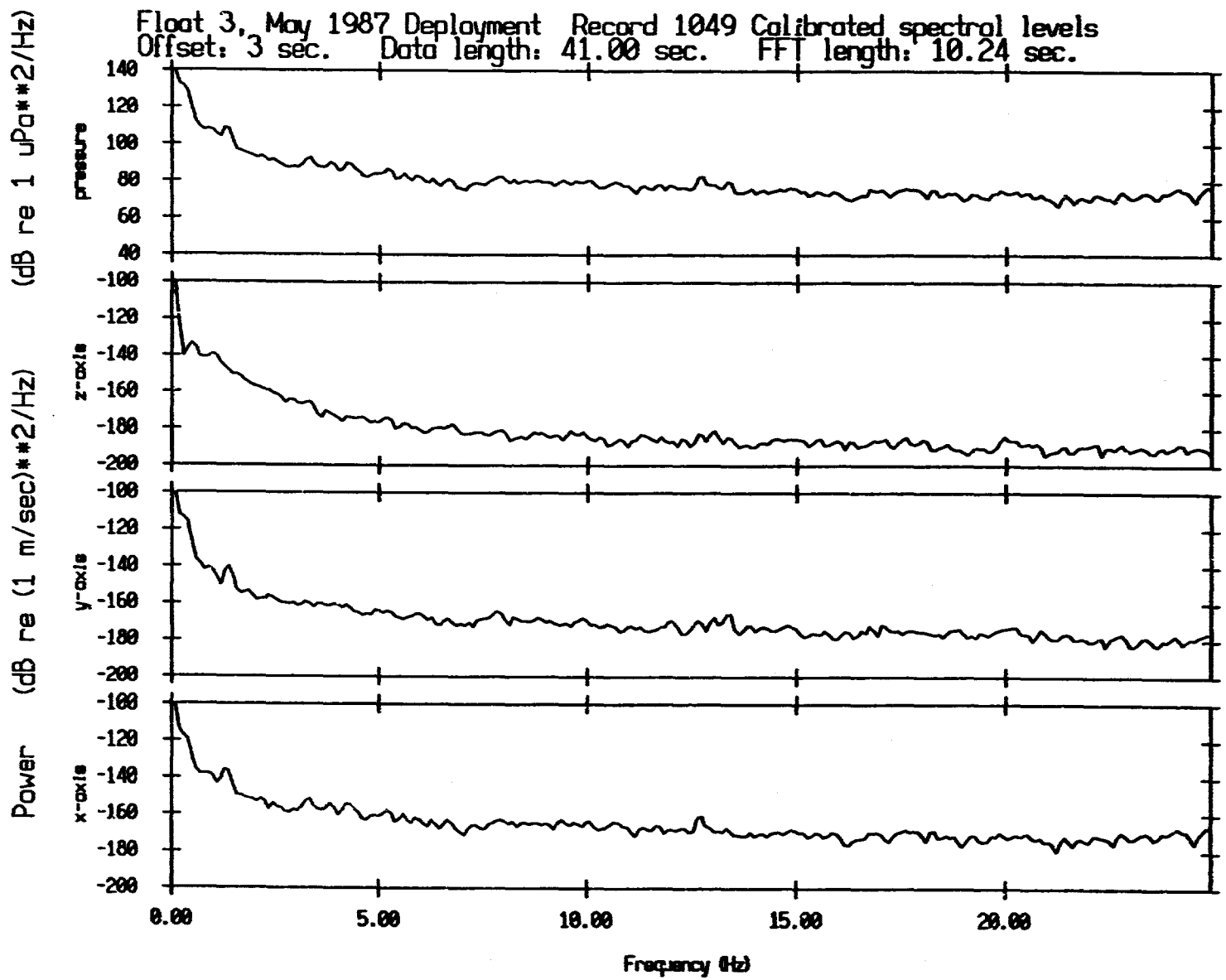

Figure IV.30c

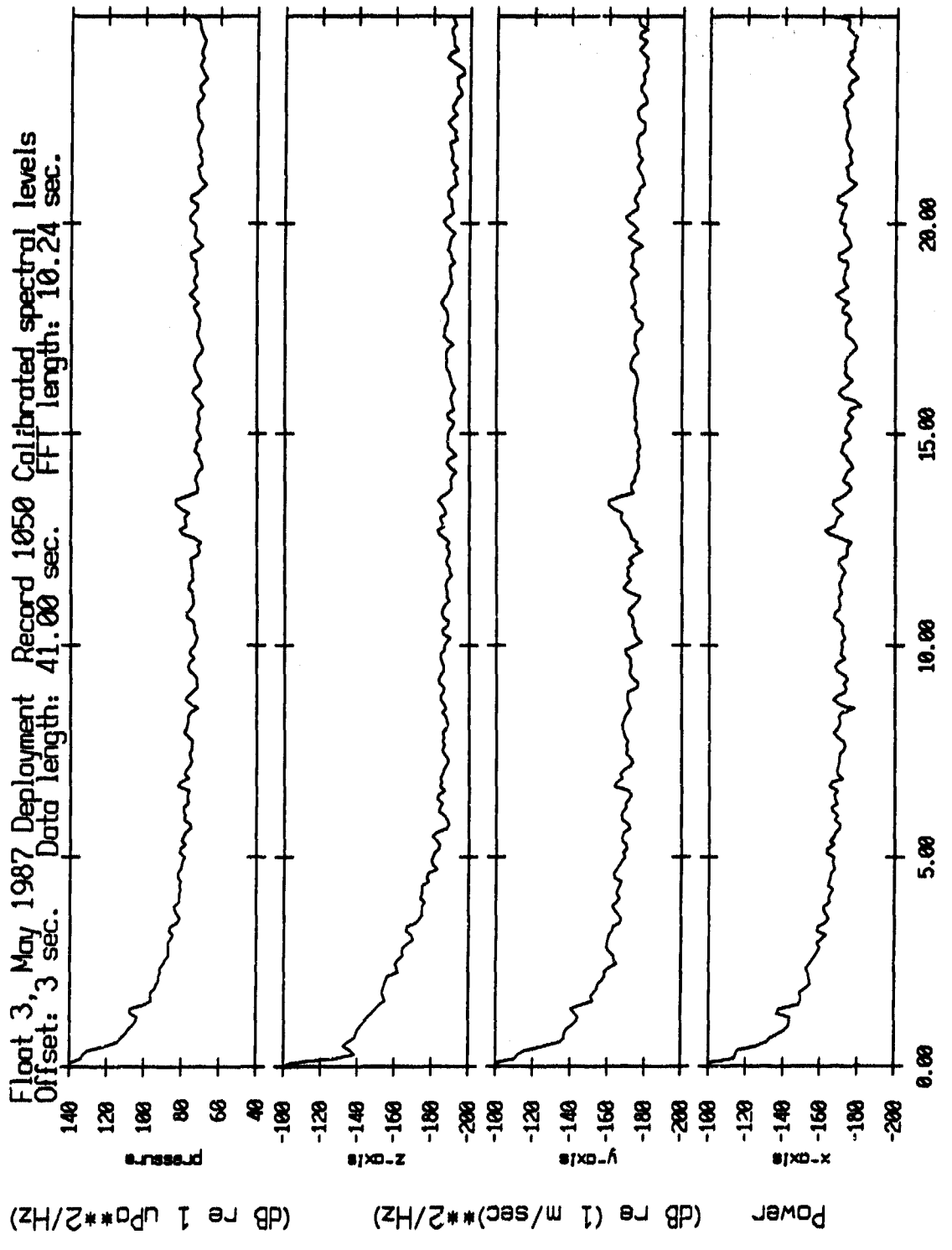

Figure IV.30d

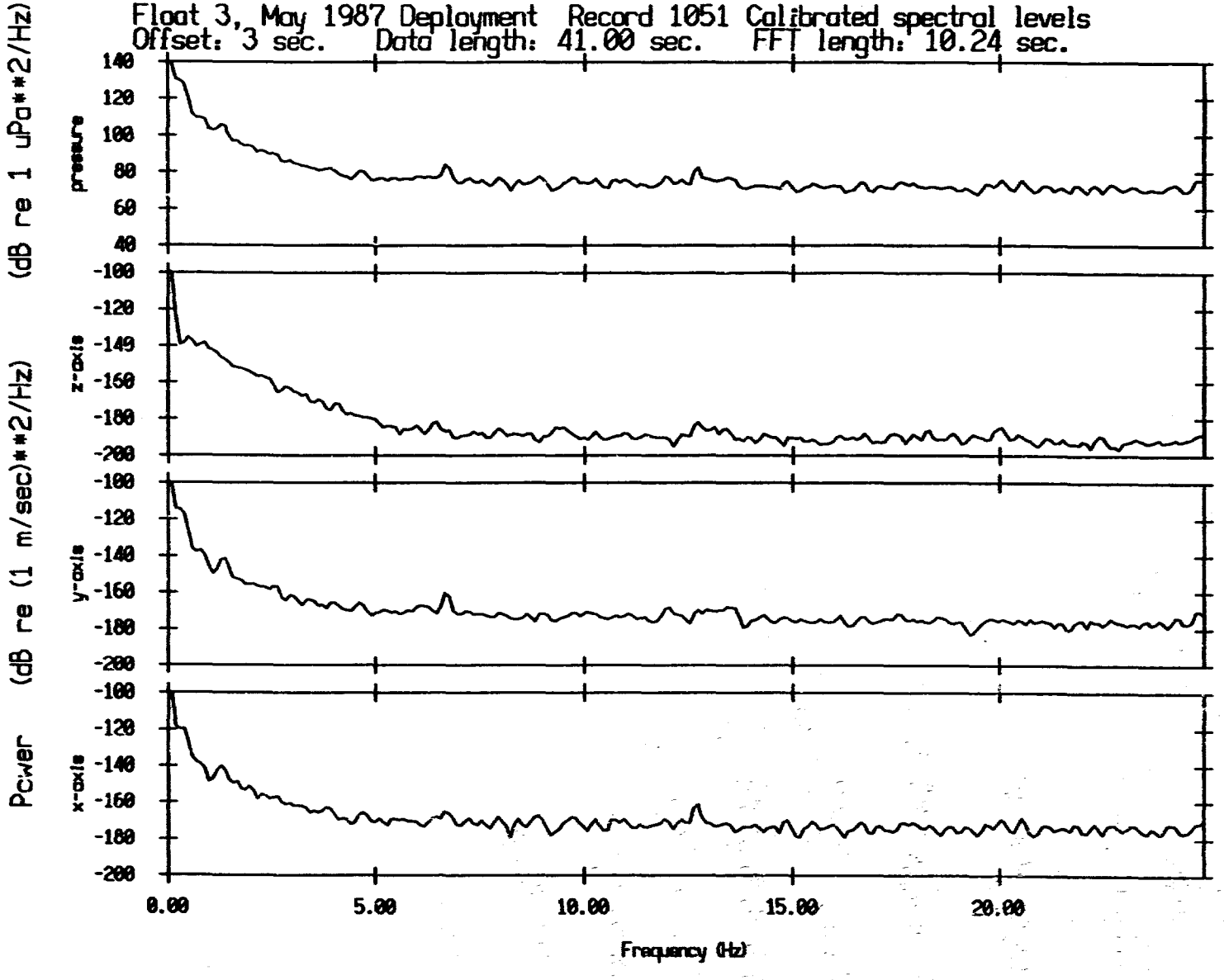

Figure IV.30e

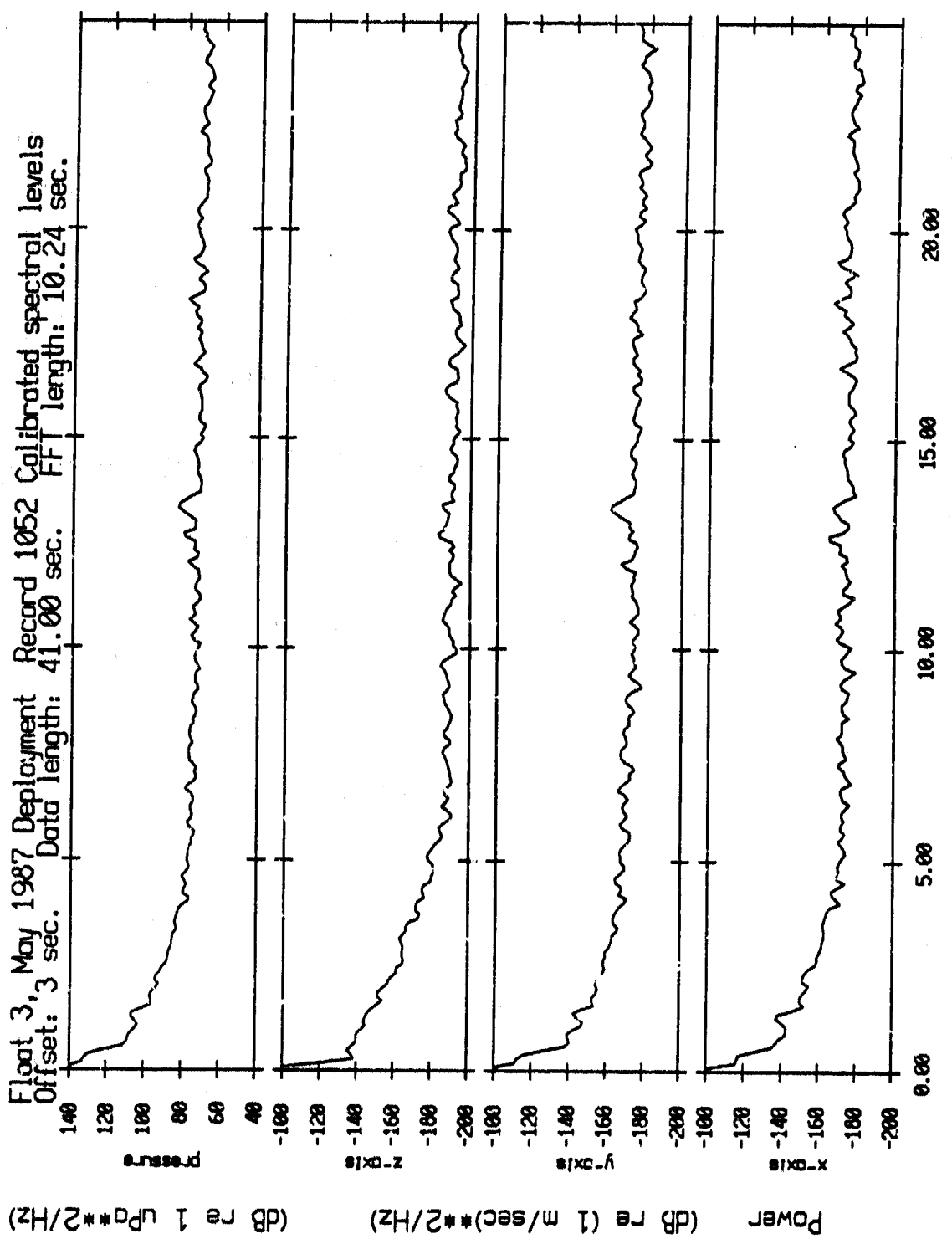

Figure IV.30f

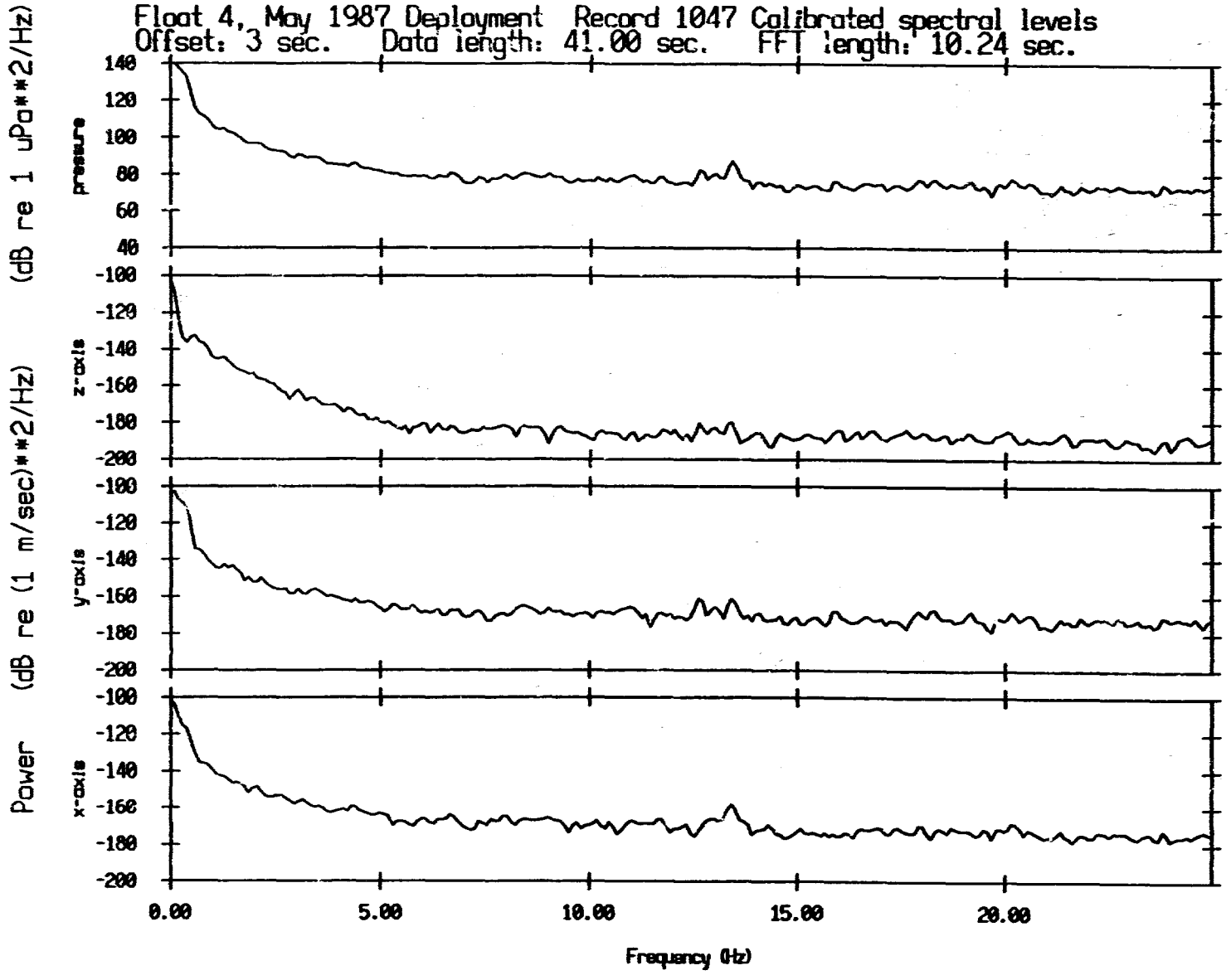

Figure IV.31a

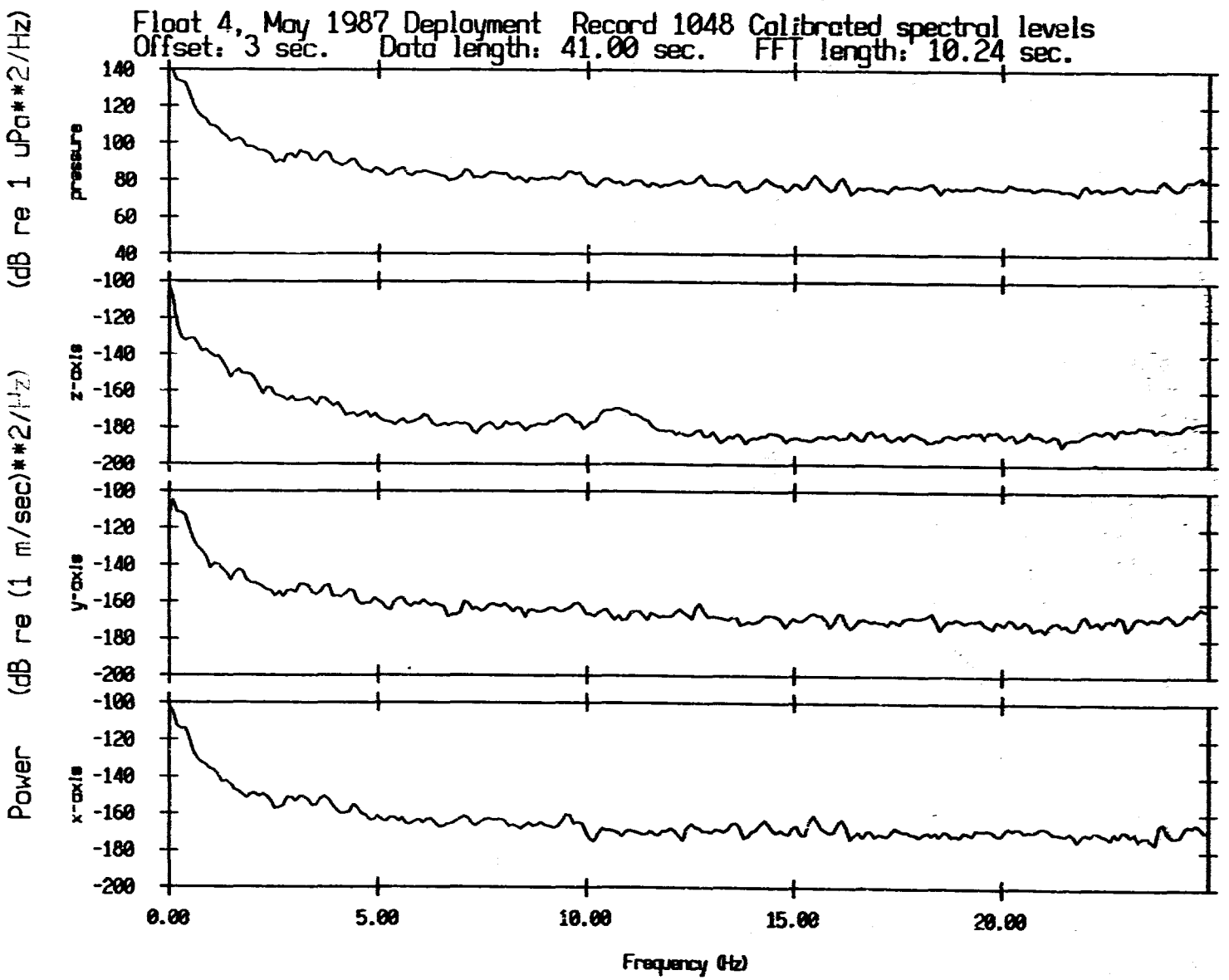

Figure IV.31b

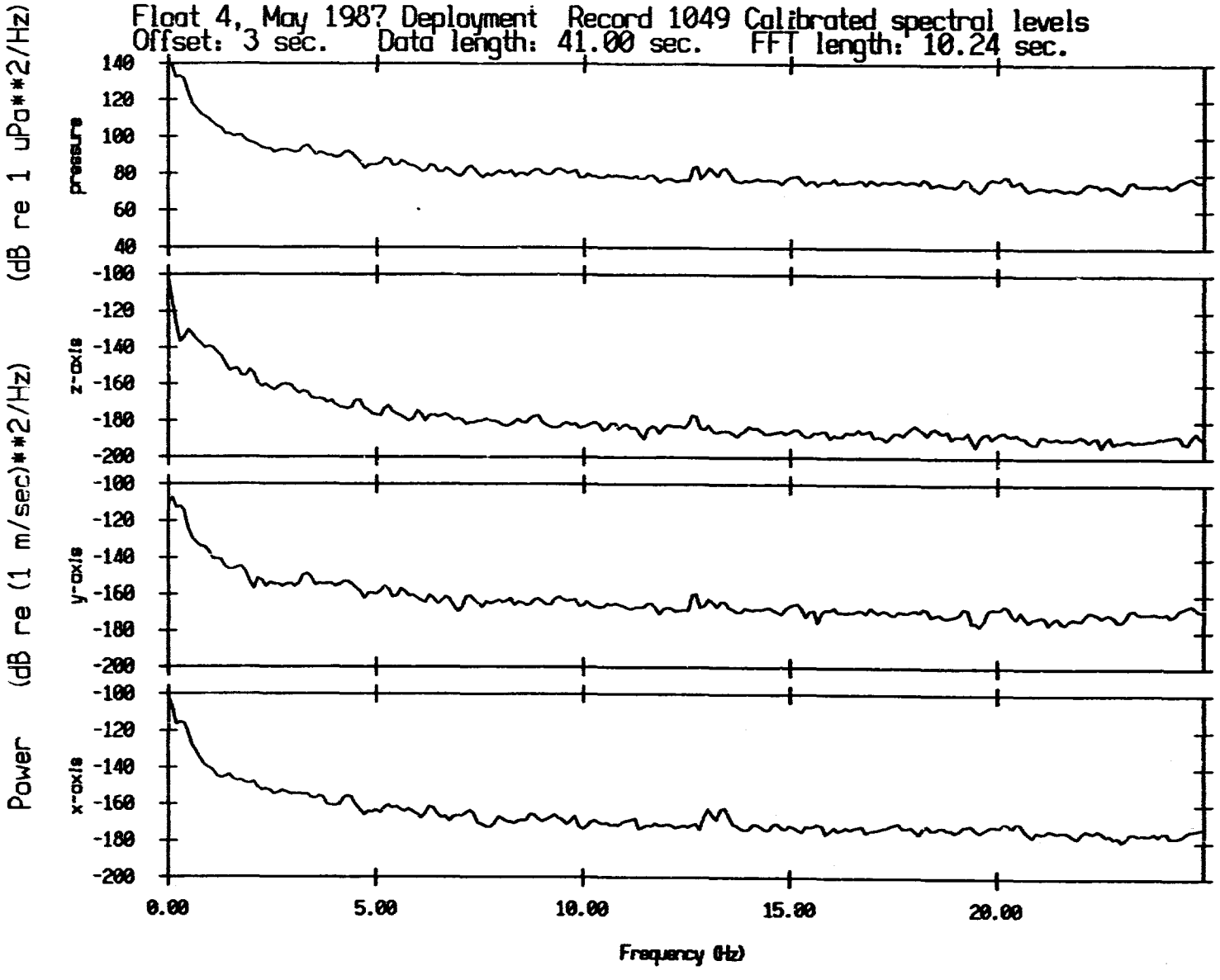

Figure IV.31c

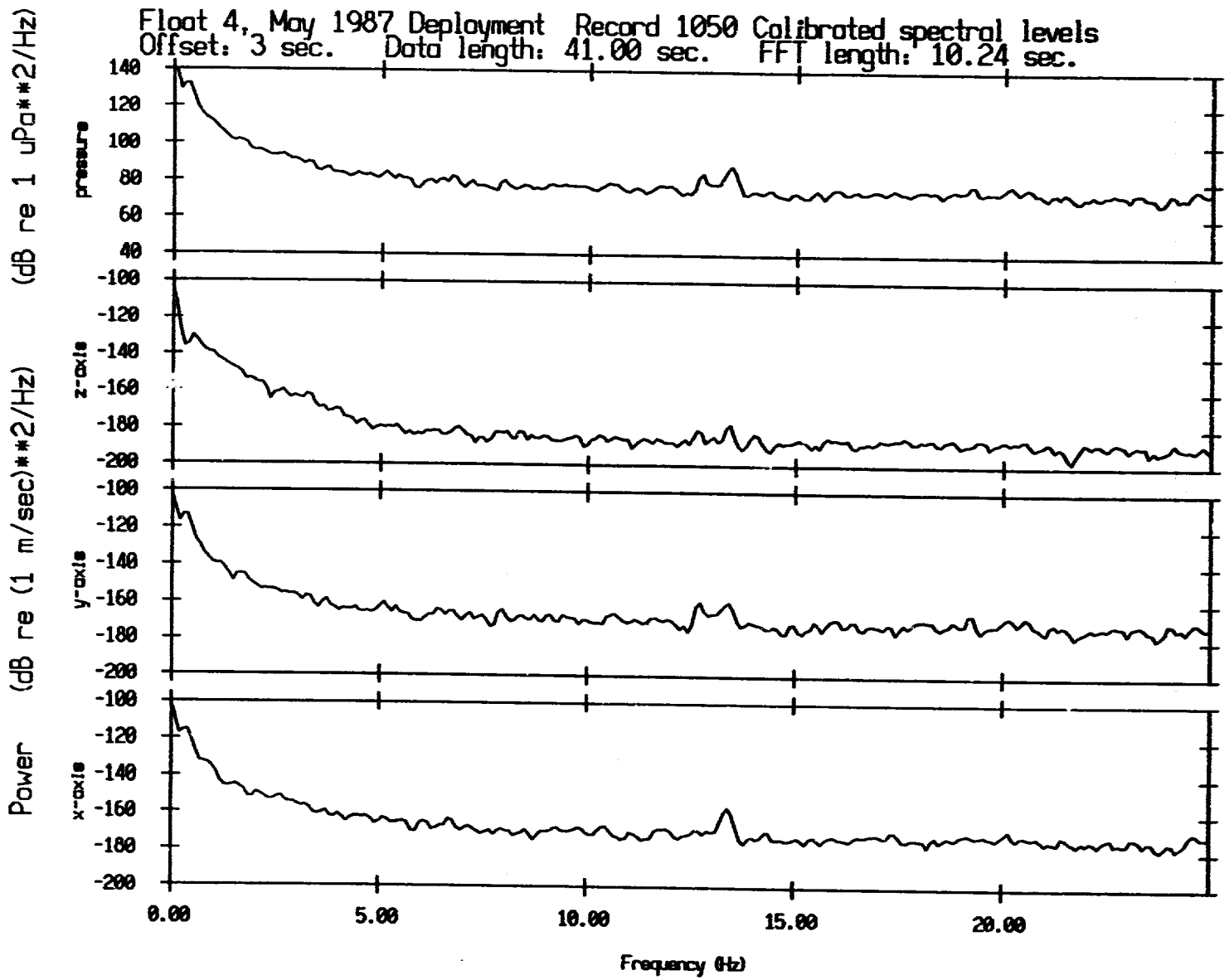

Figure IV.31d

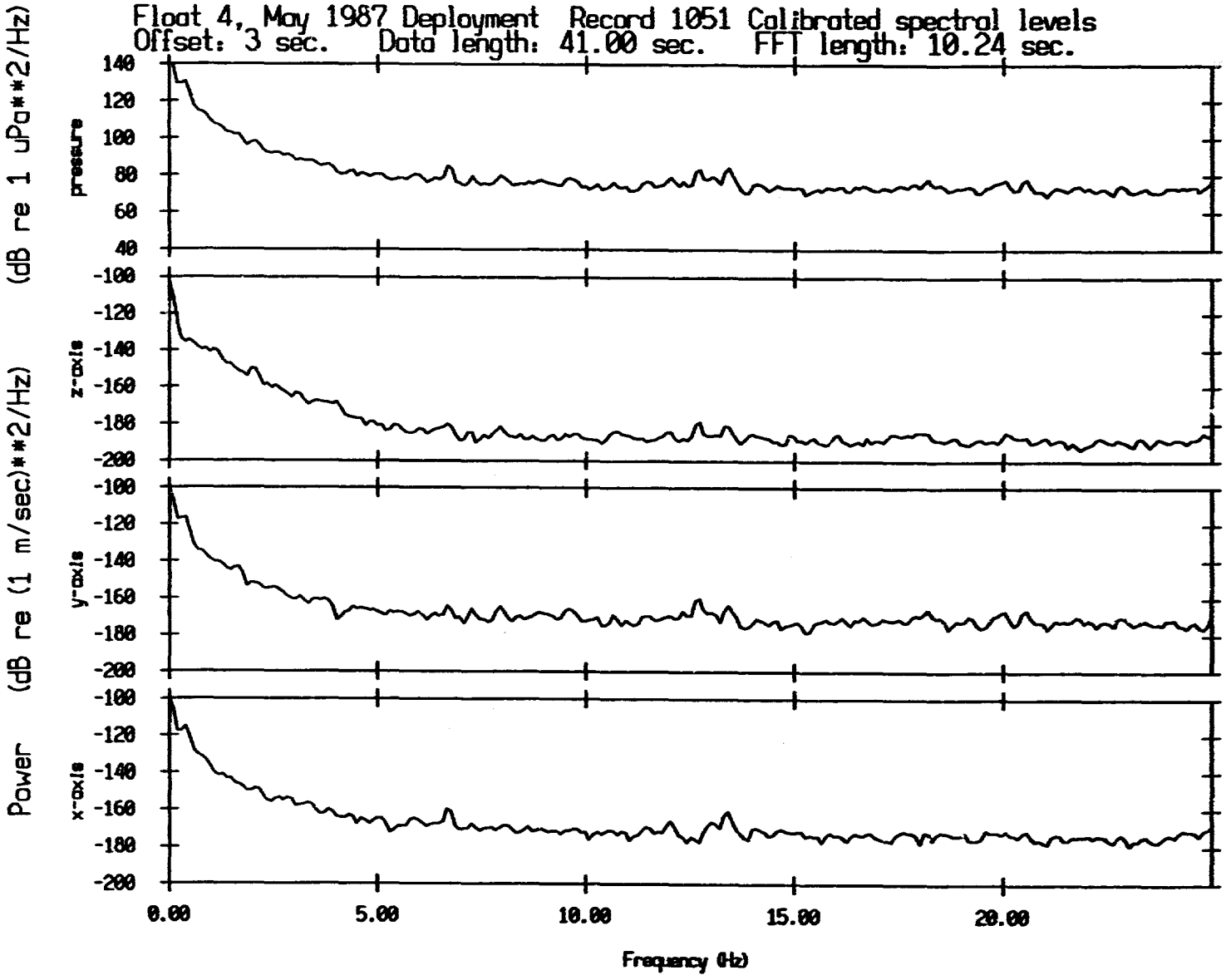

Figure IV.31e

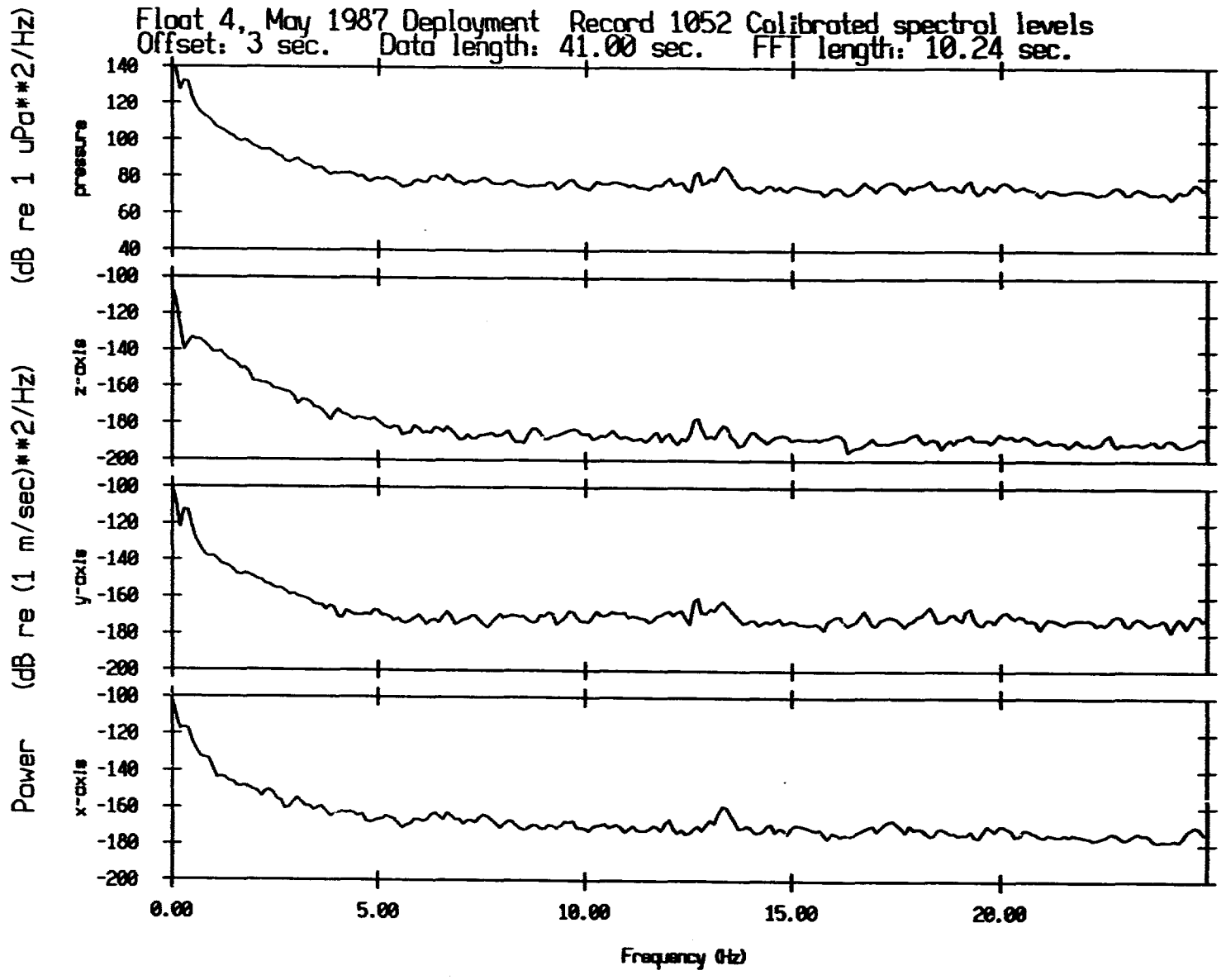

Figure IV.31f

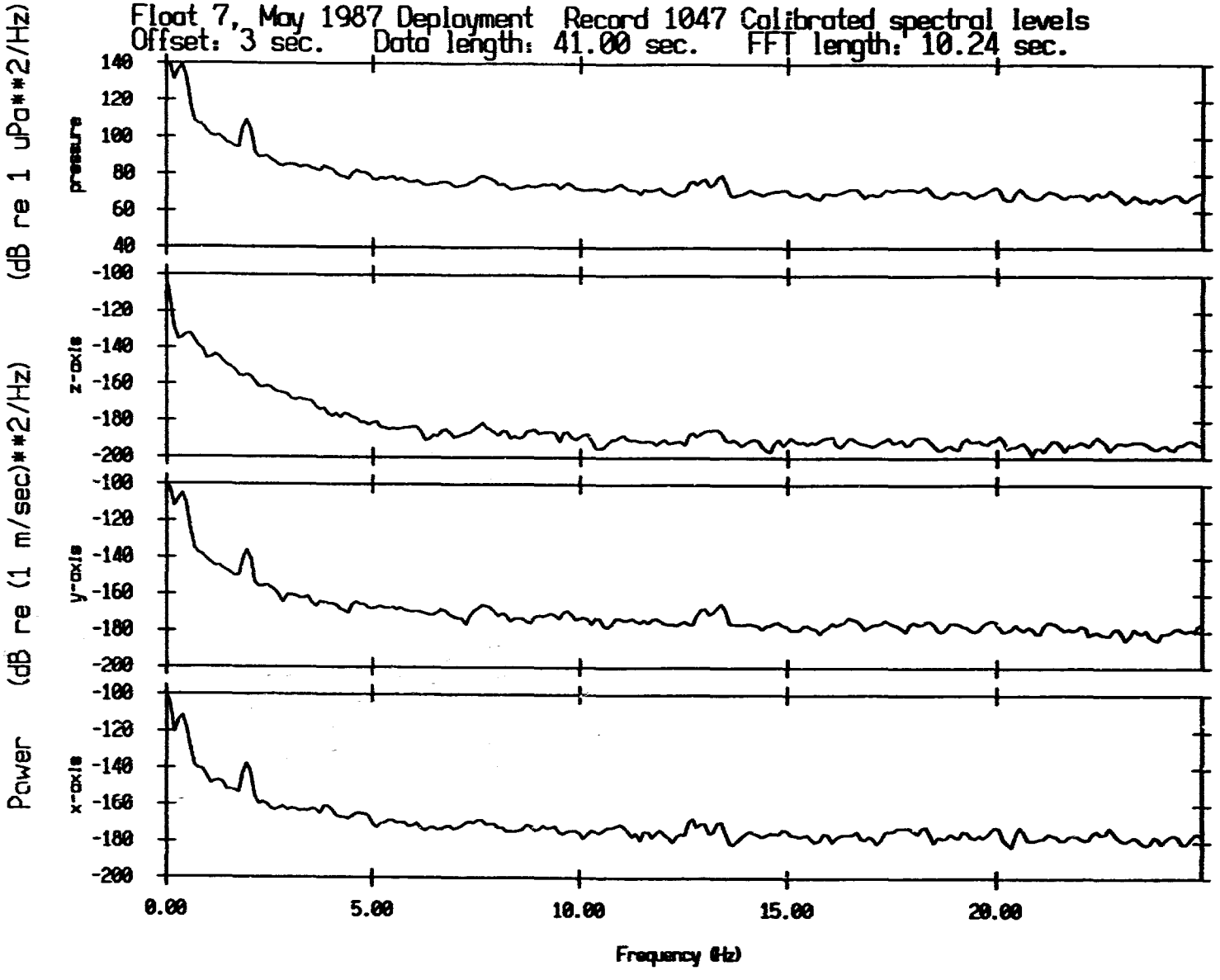

Figure IV.32a

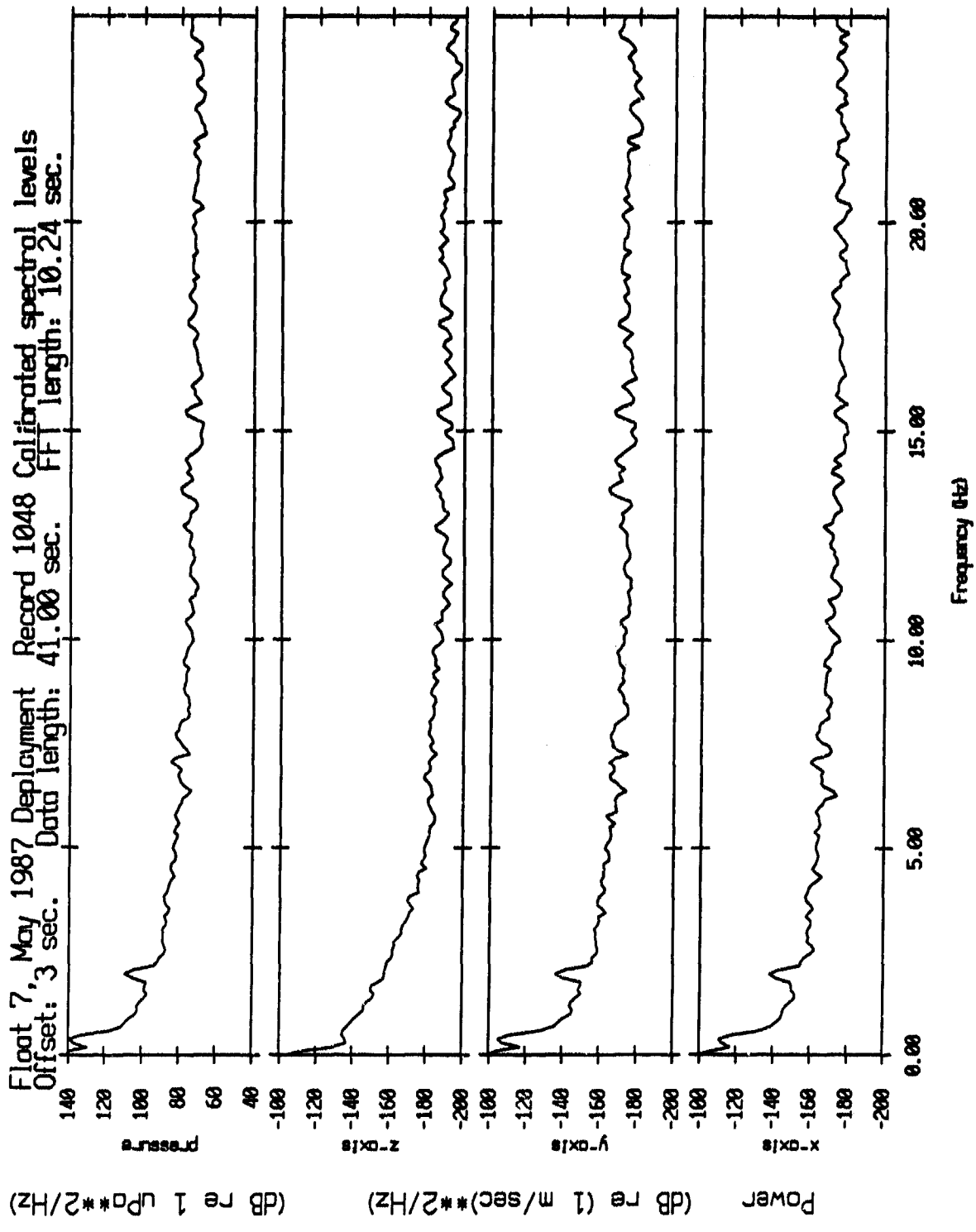

Figure IV.32b

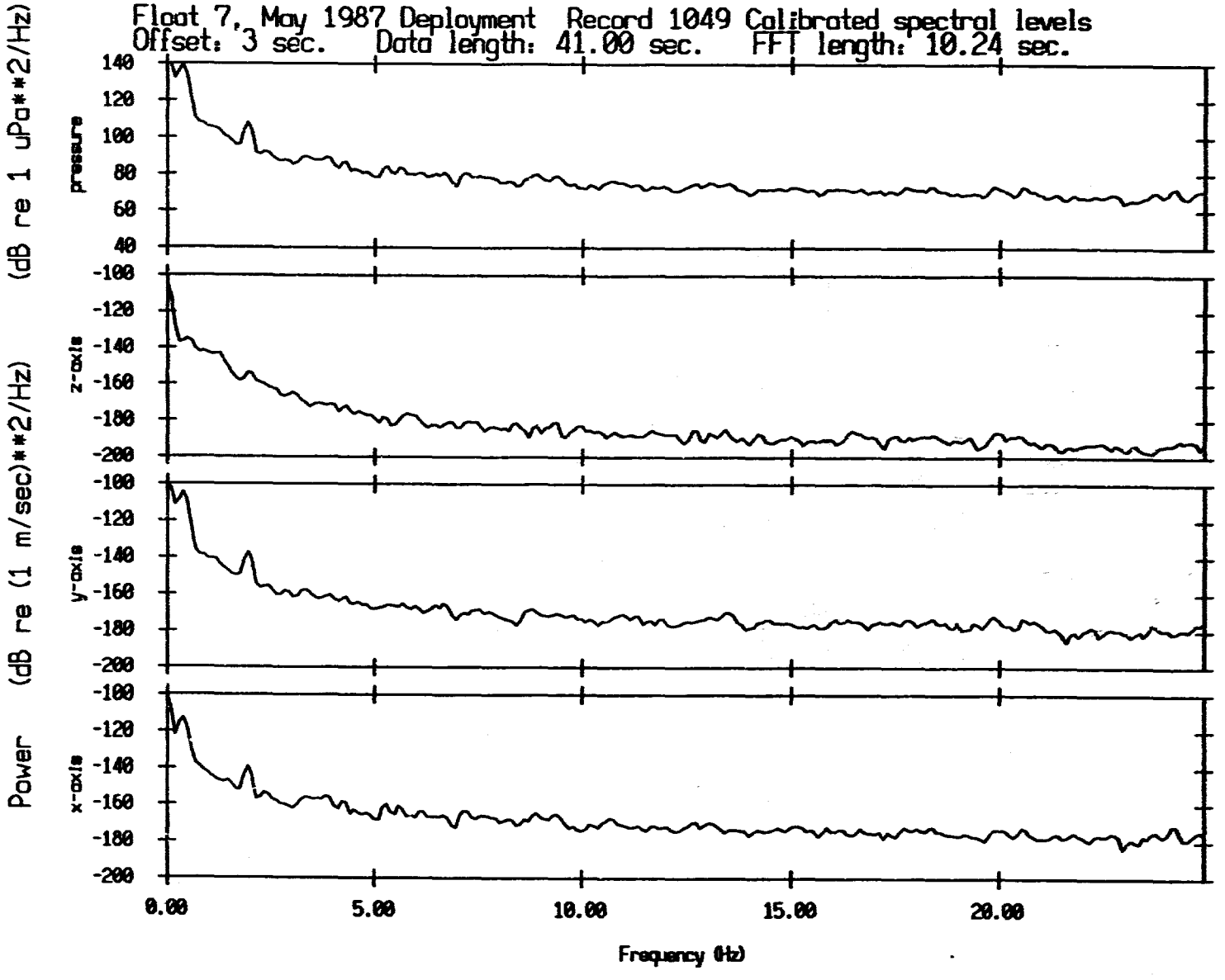

Figure IV.32c

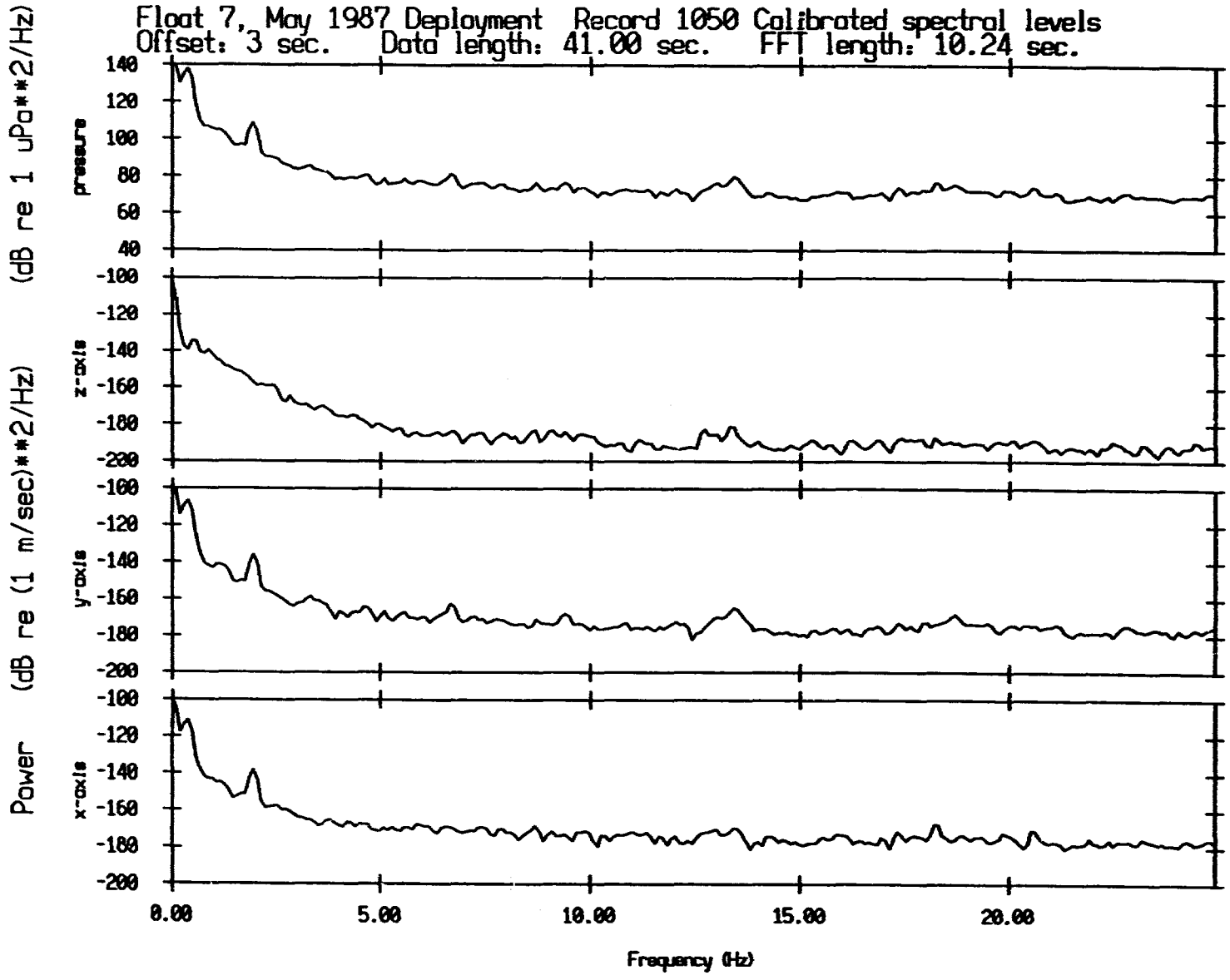

Figure IV.32d

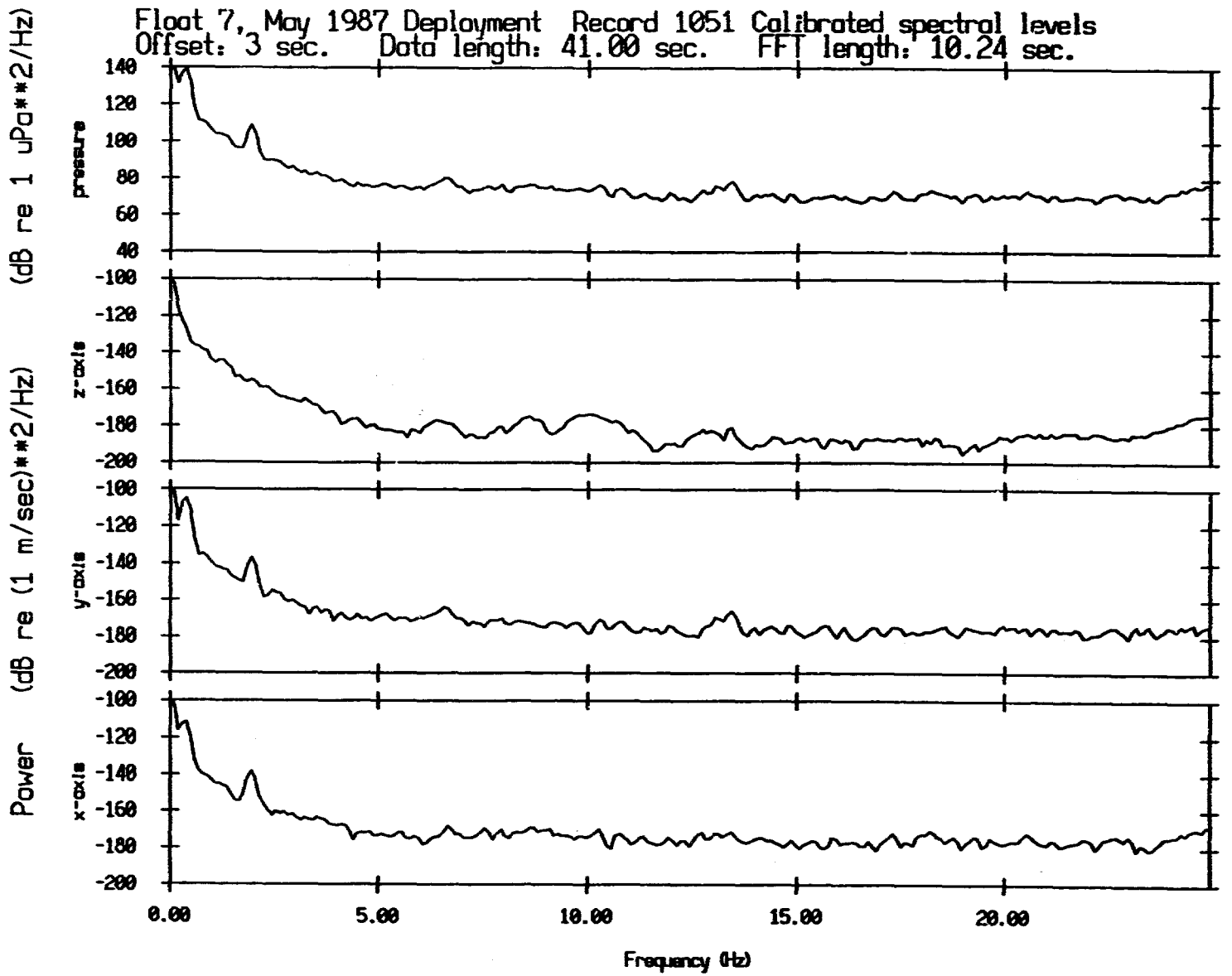

Figure IV.32e

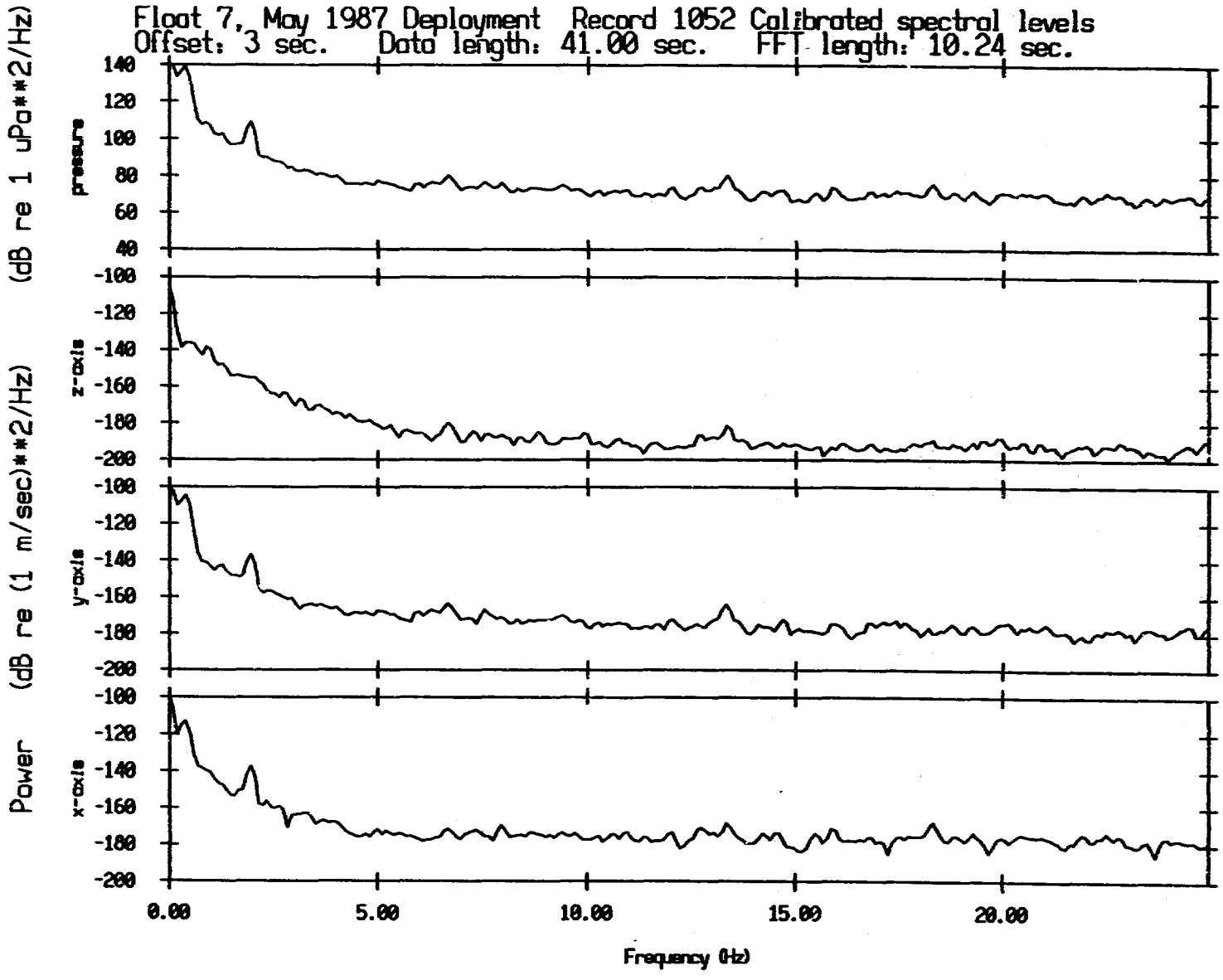

Figure IV.32f

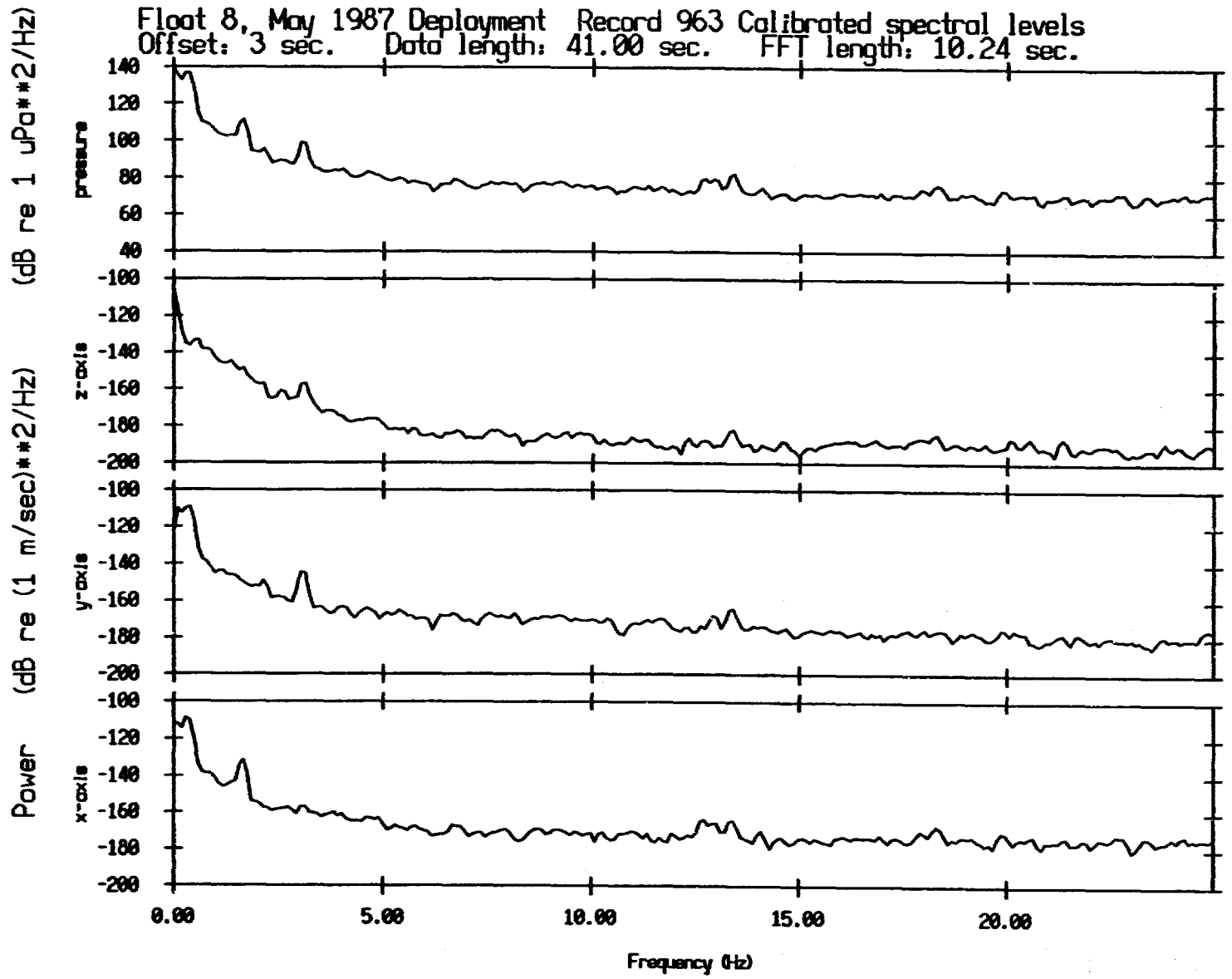

Figure IV.33a

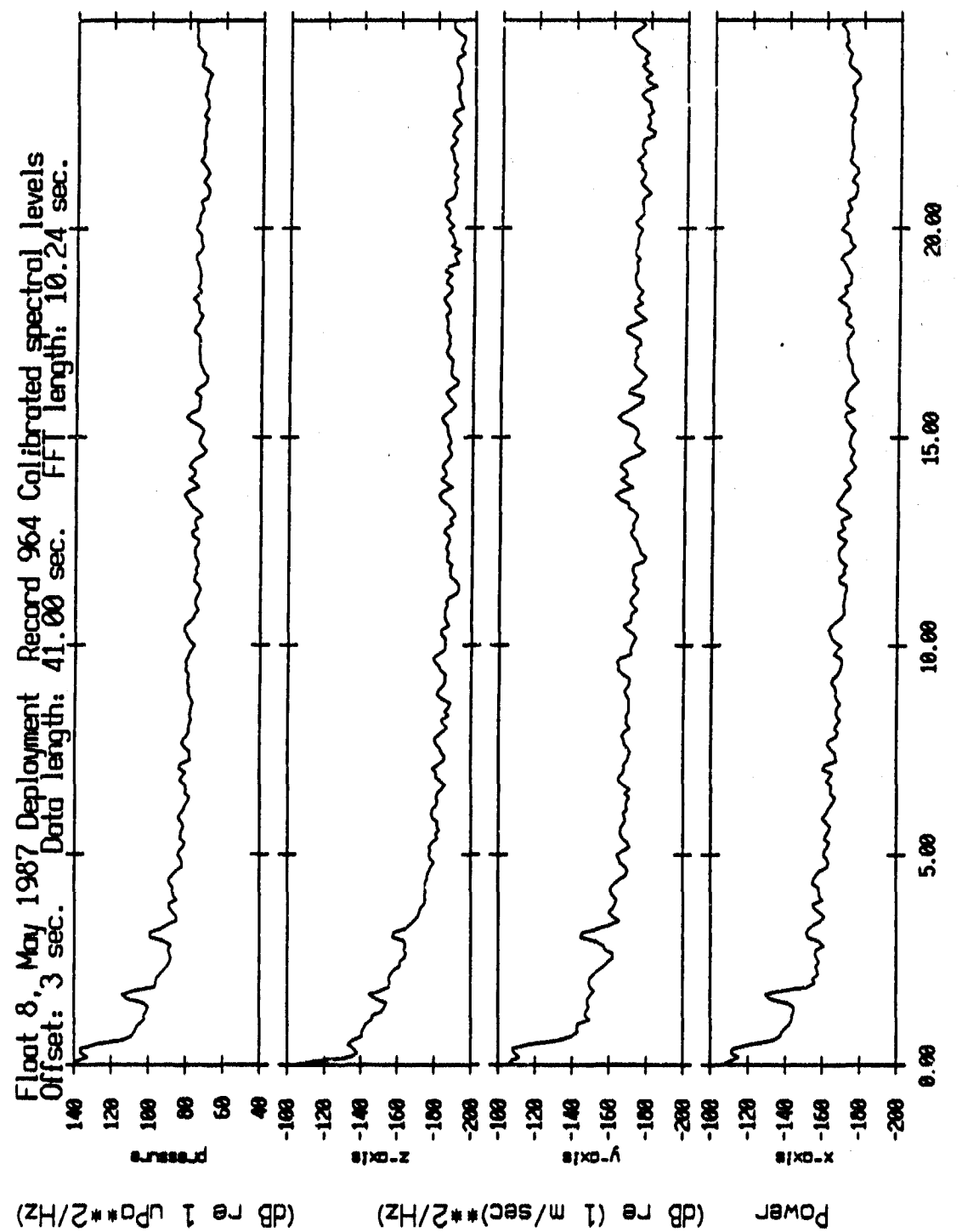

Figure IV.33b

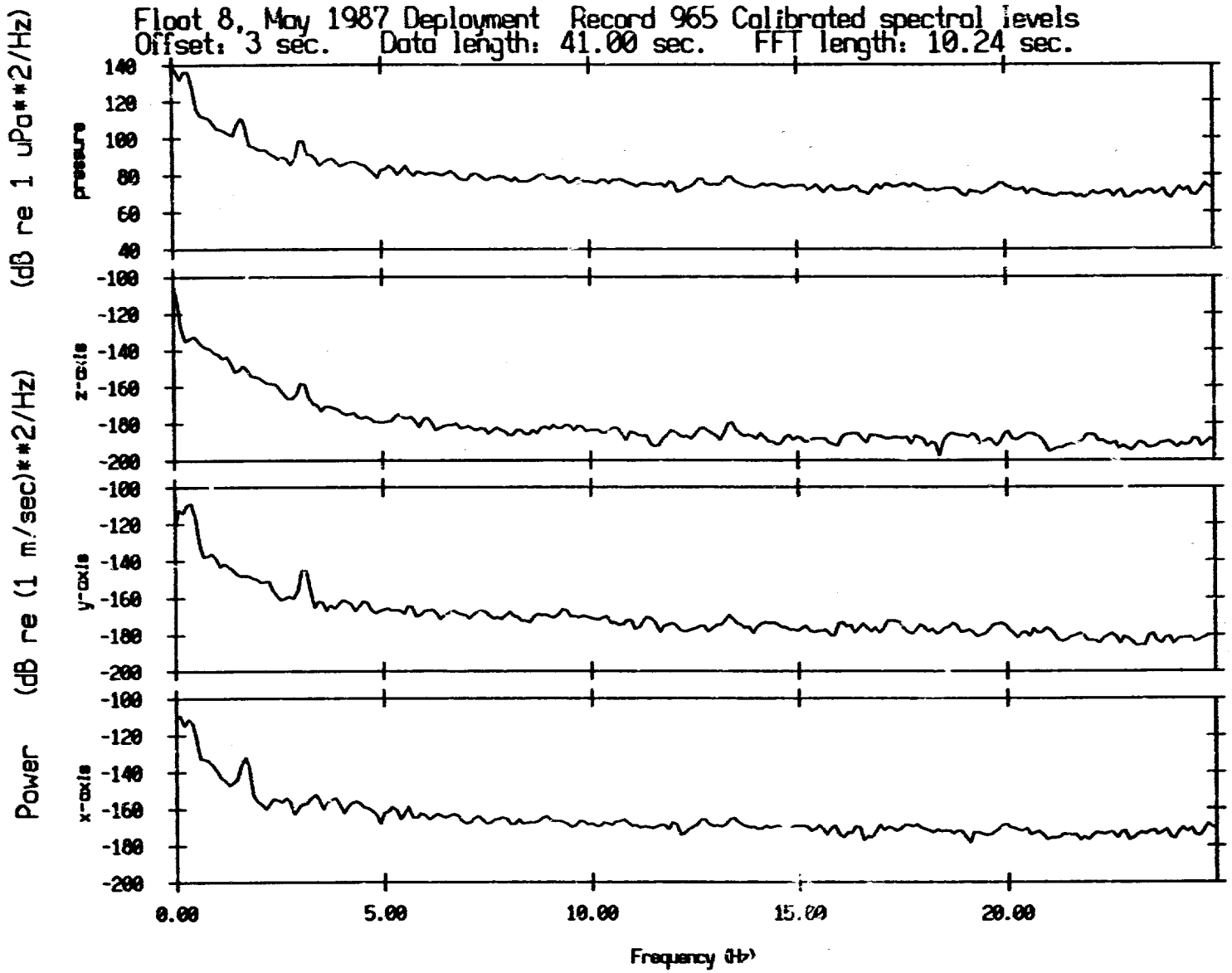

Figure IV.33c

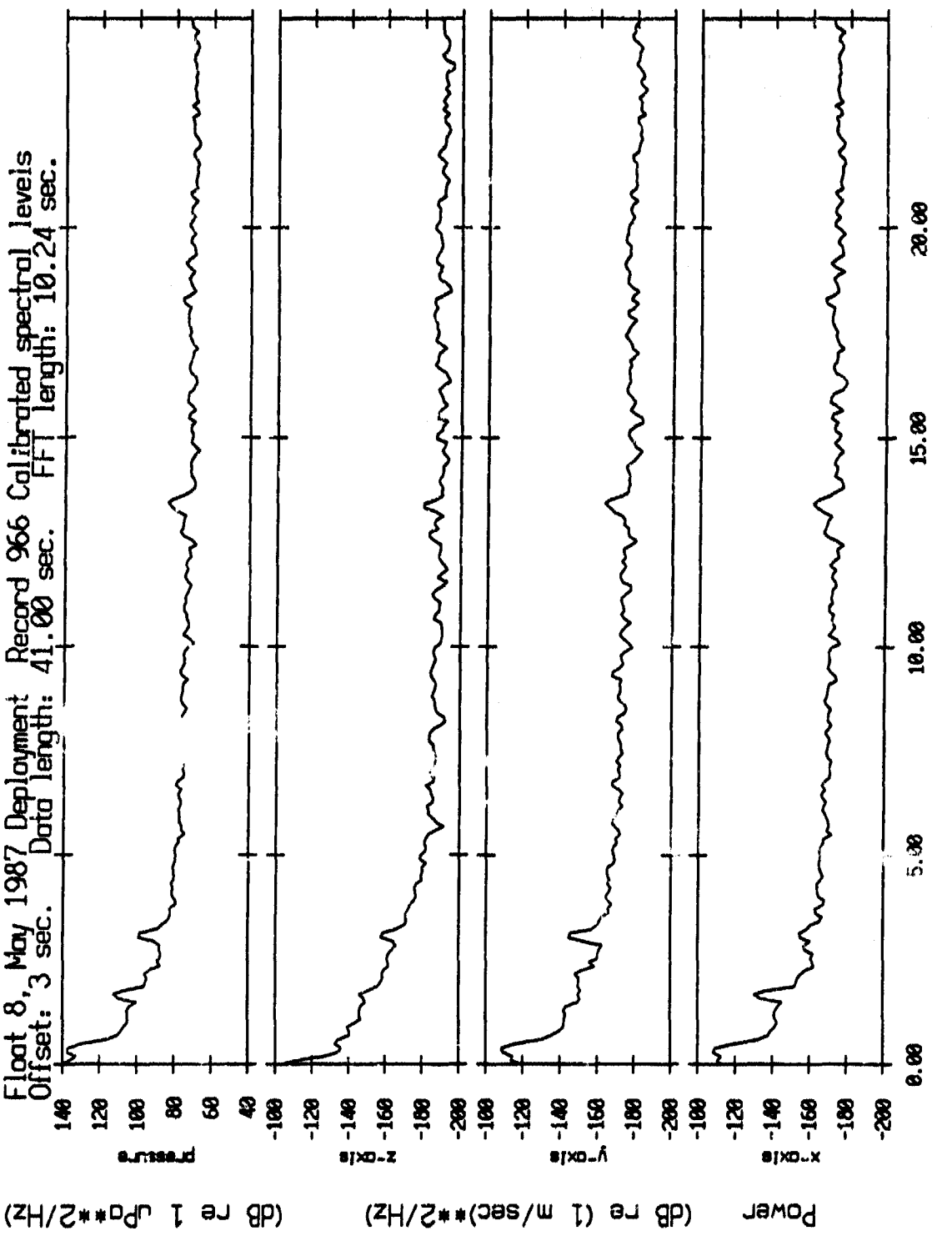

Figure IV.33d

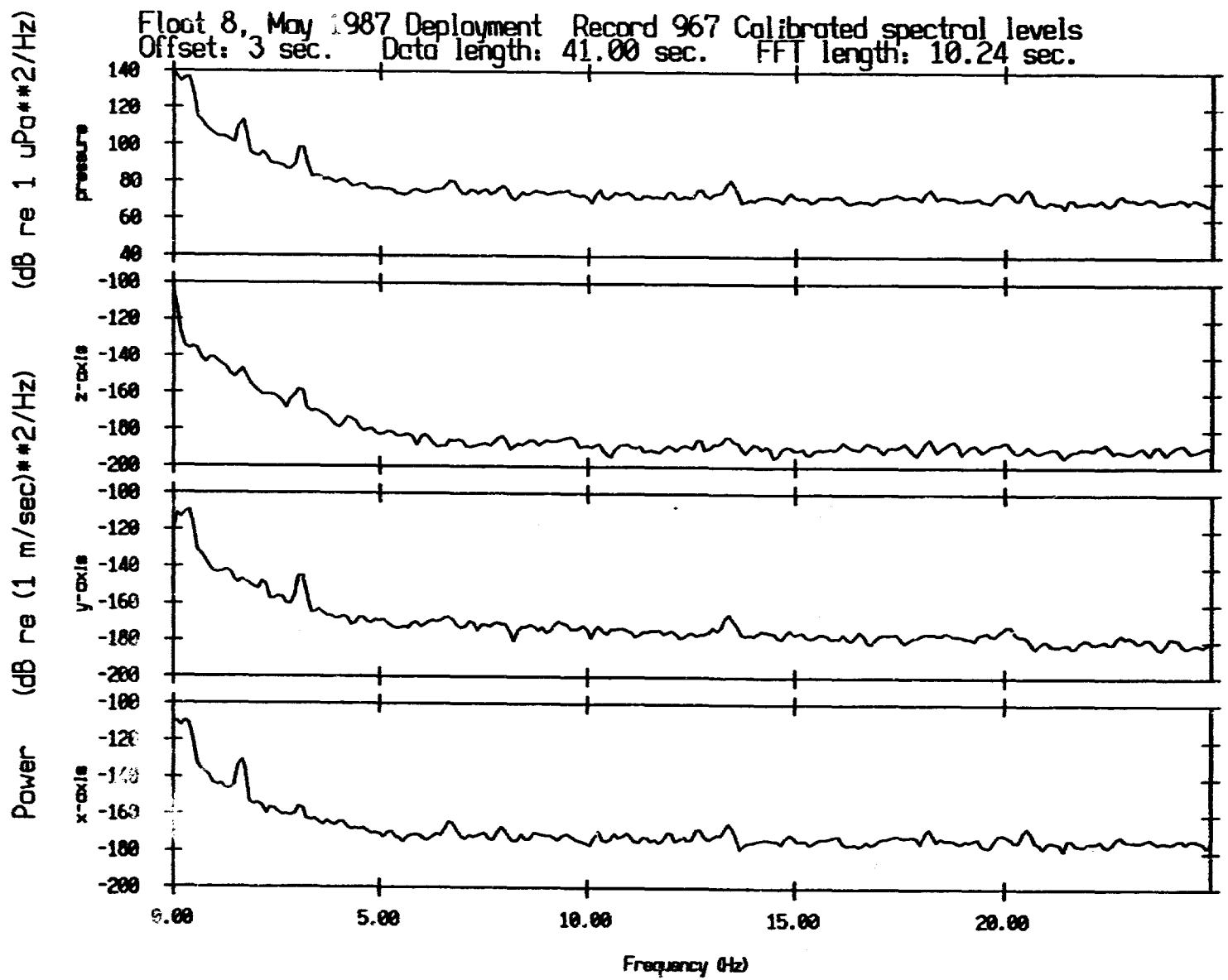

Figure IV.33e

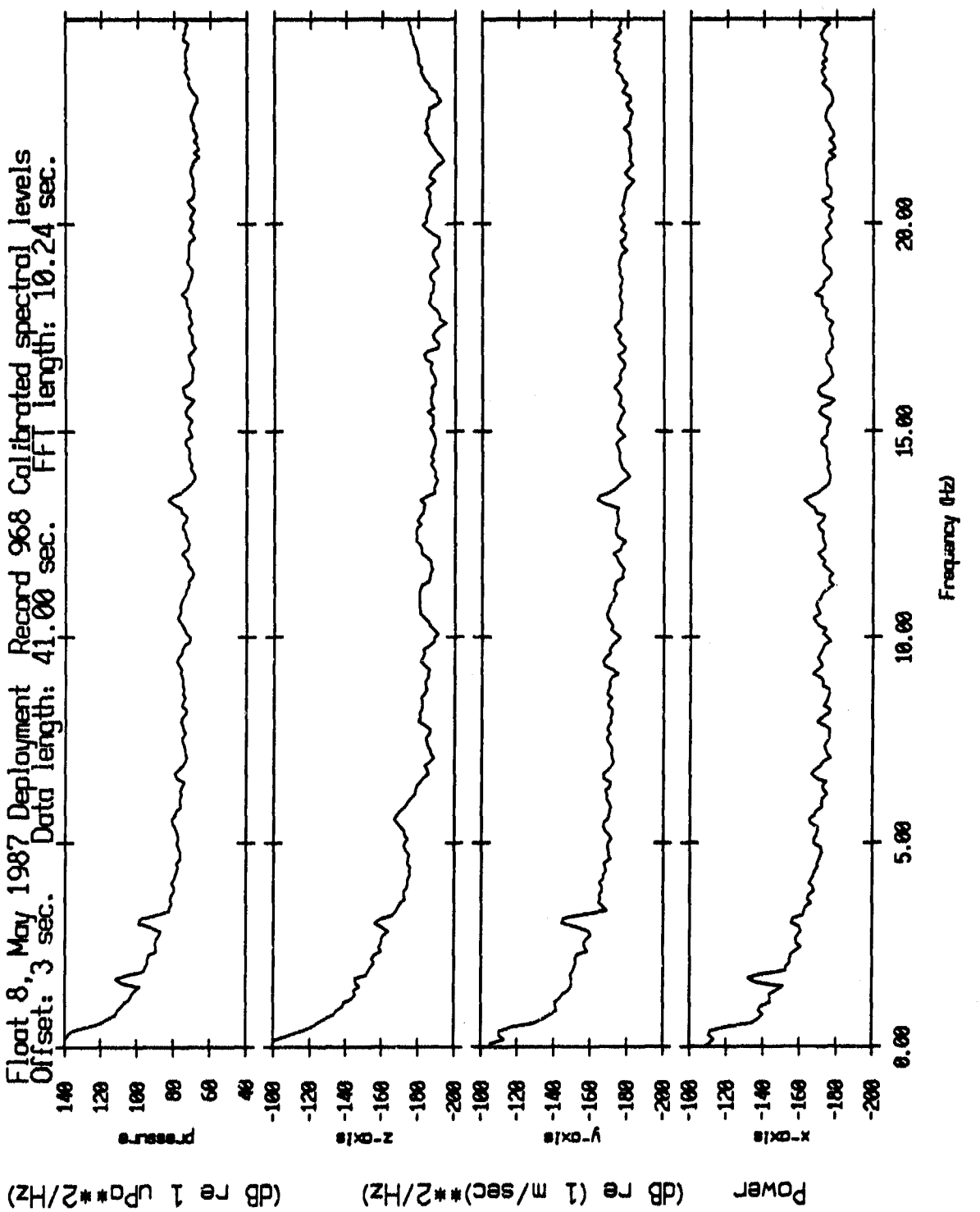

Figure IV.33f

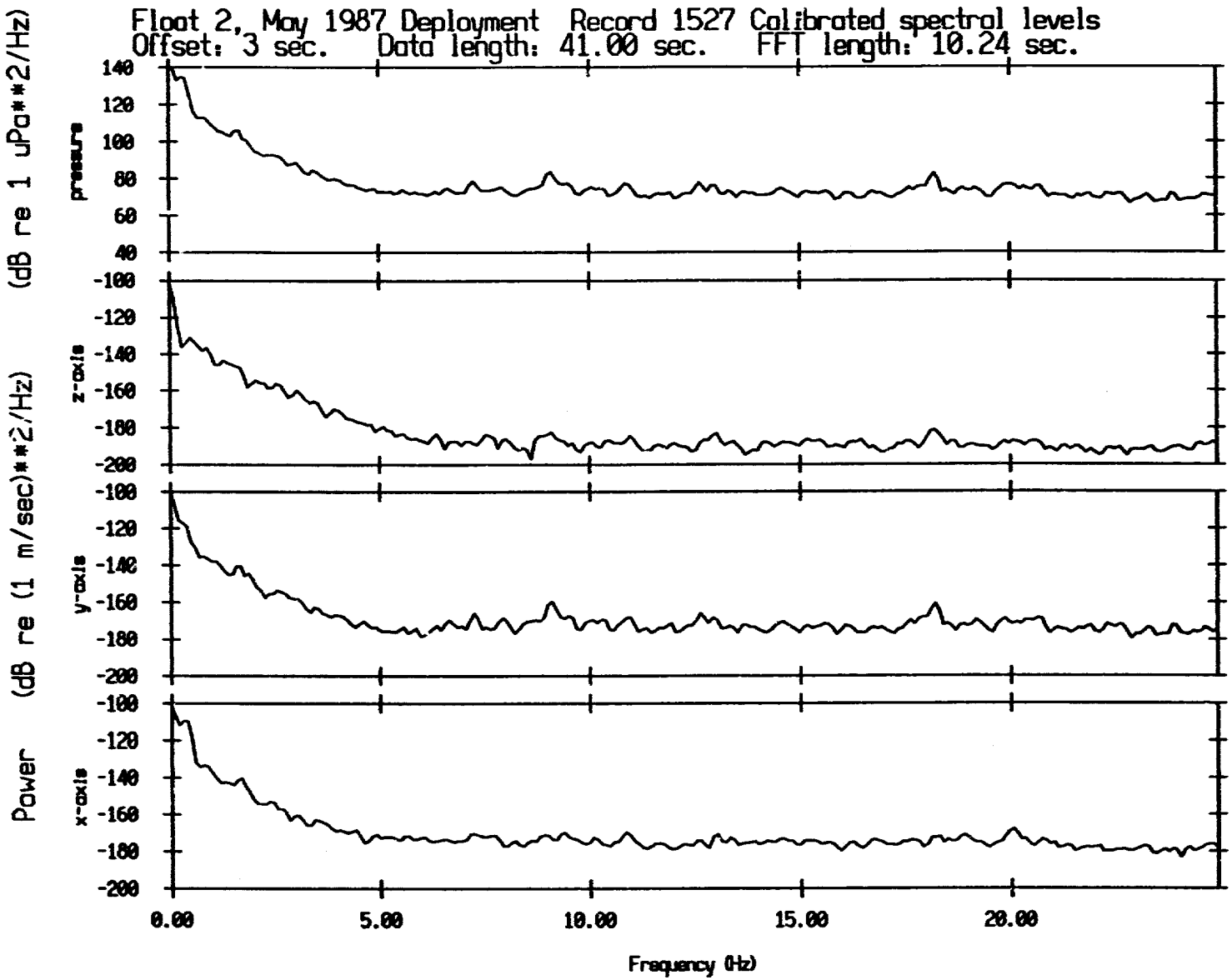

Figure IV.34a

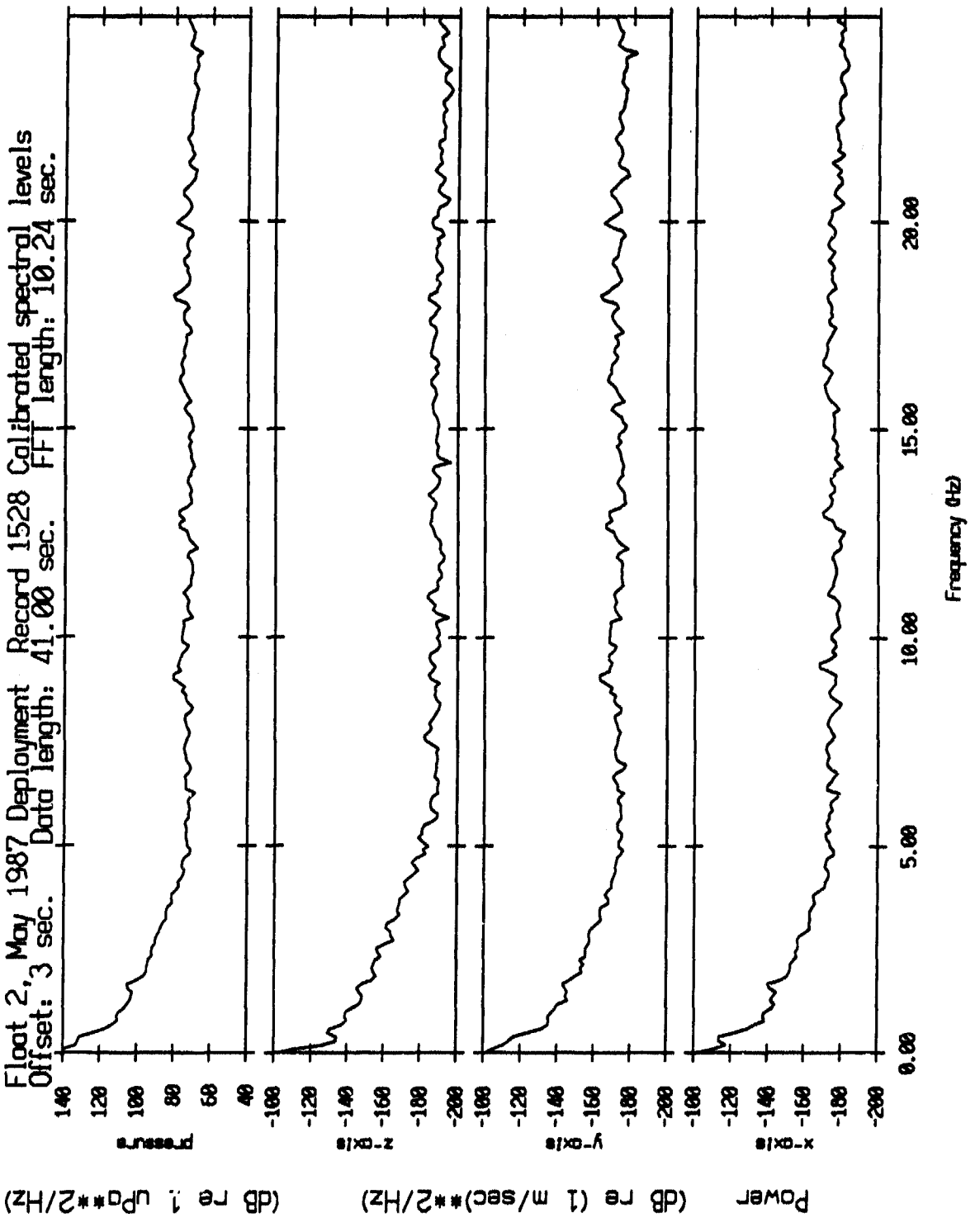

Figure IV.34b

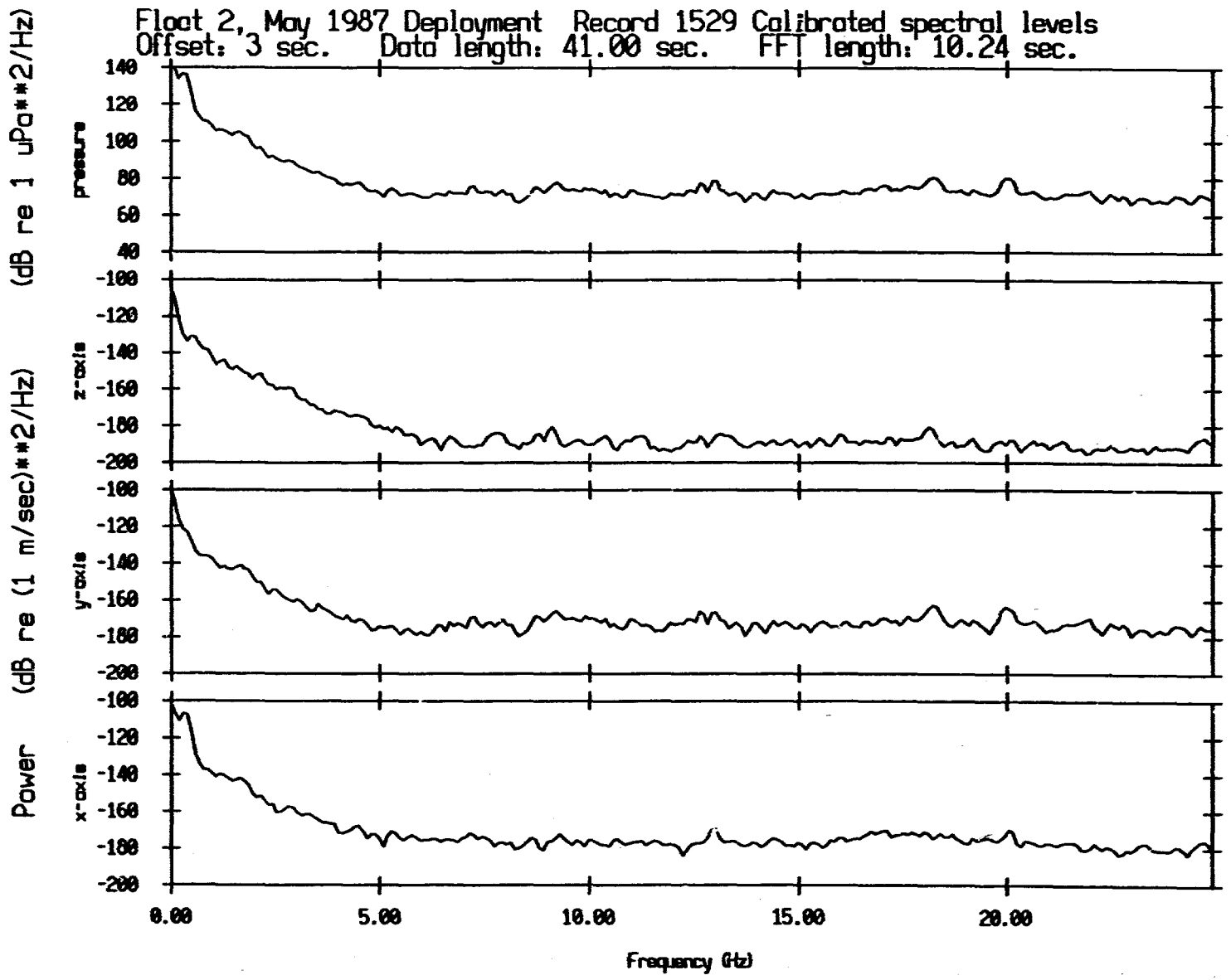

Figure IV.34c

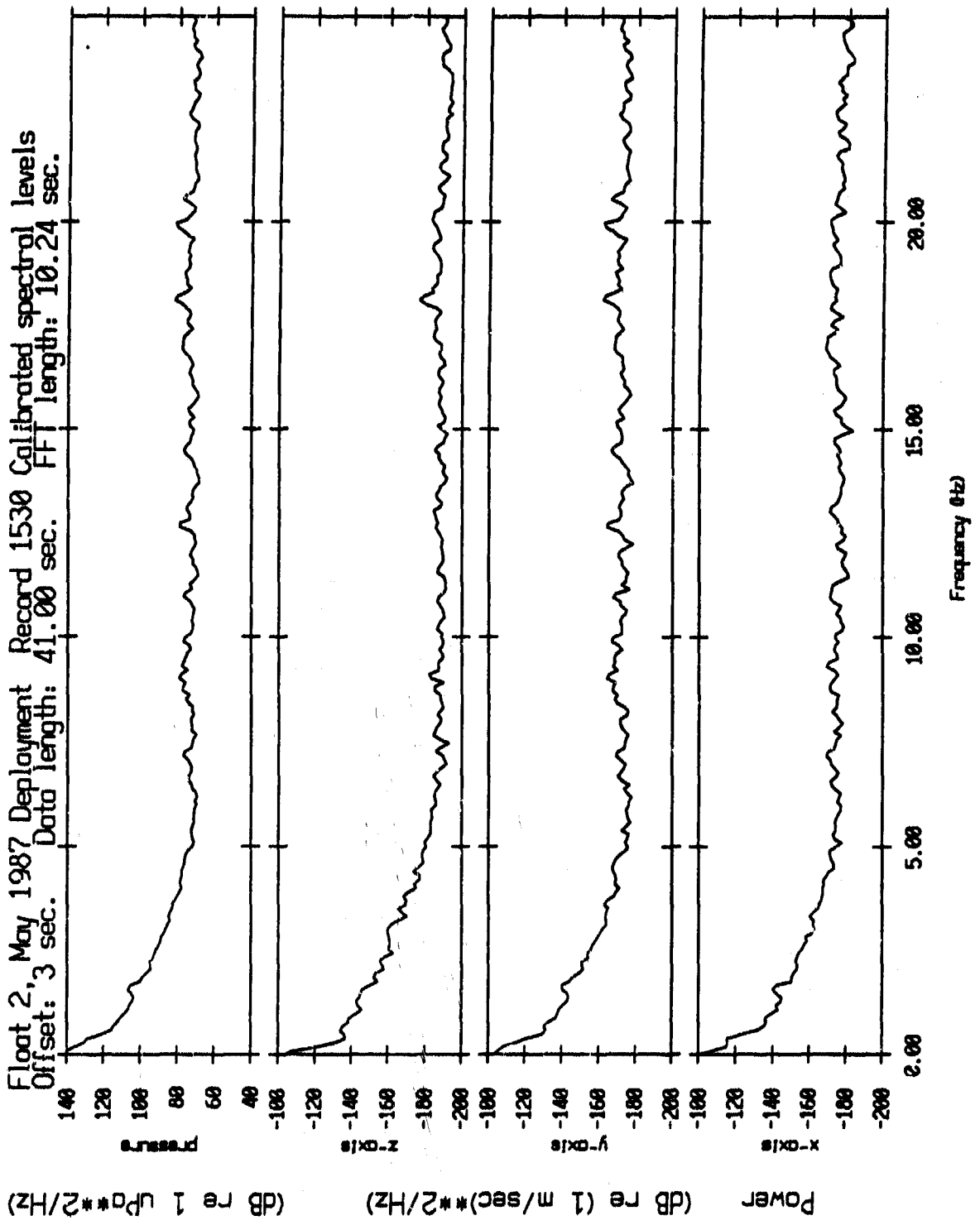

Figure IV.34d

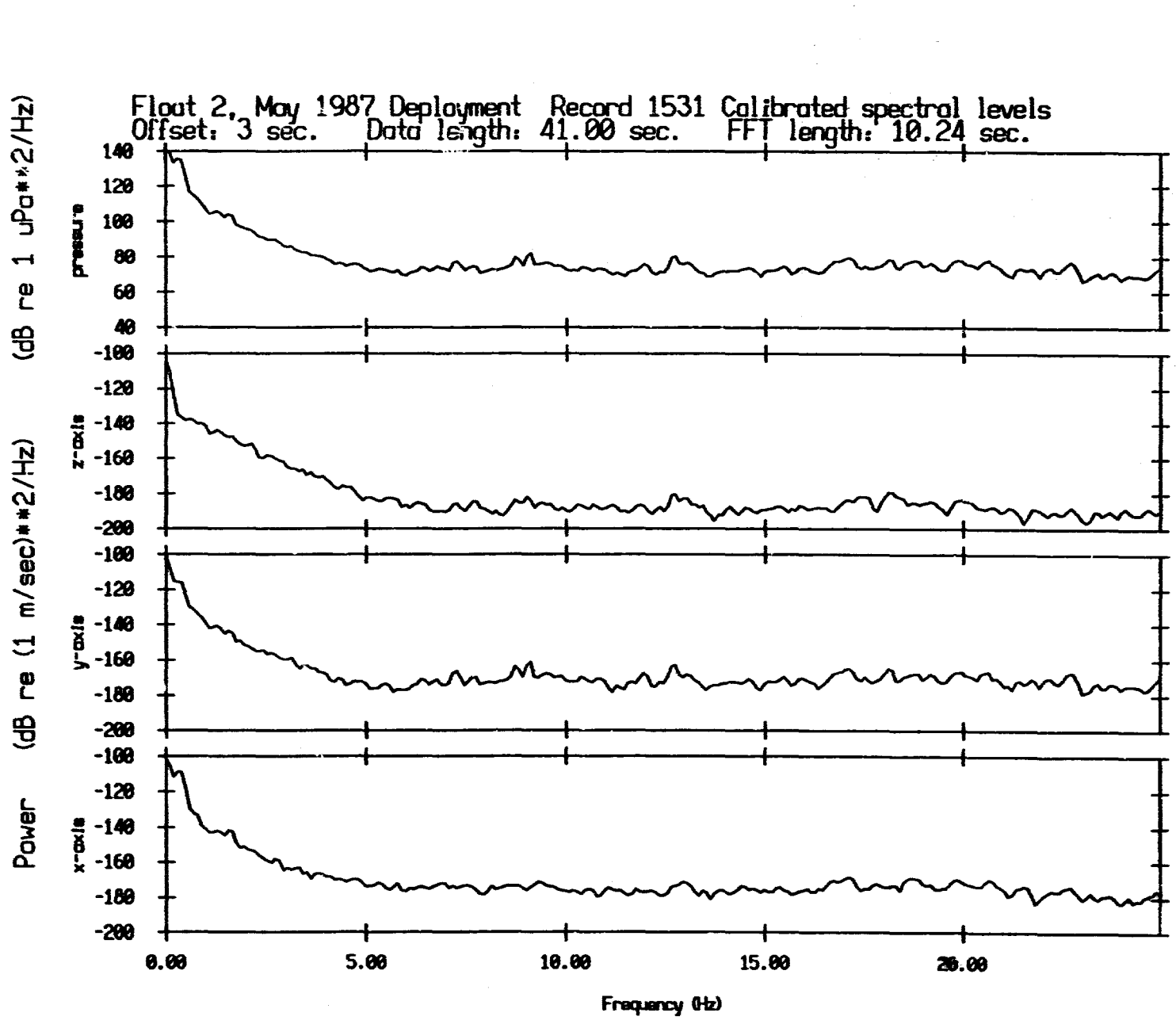

Figure IV.34e

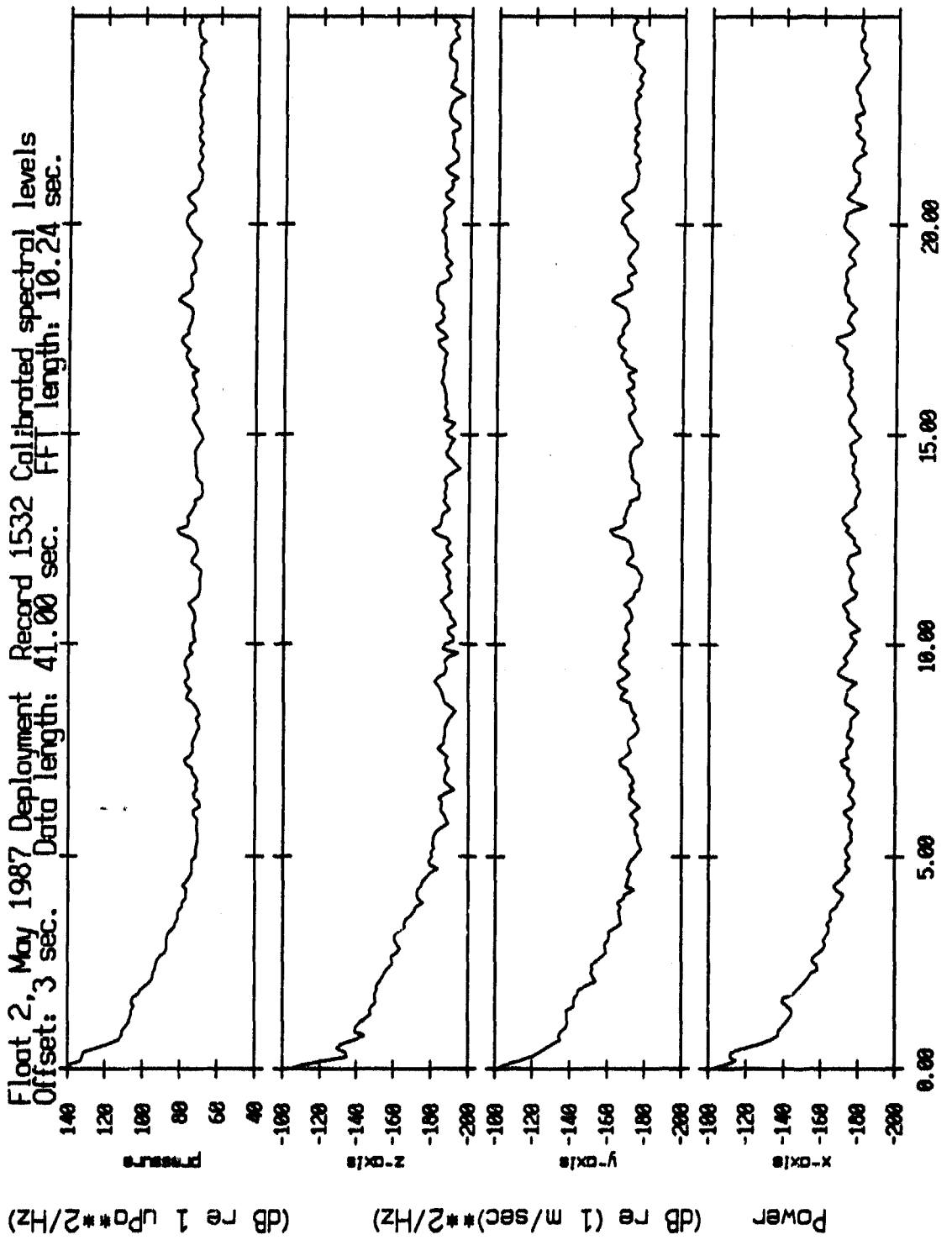

Figure IV.34f

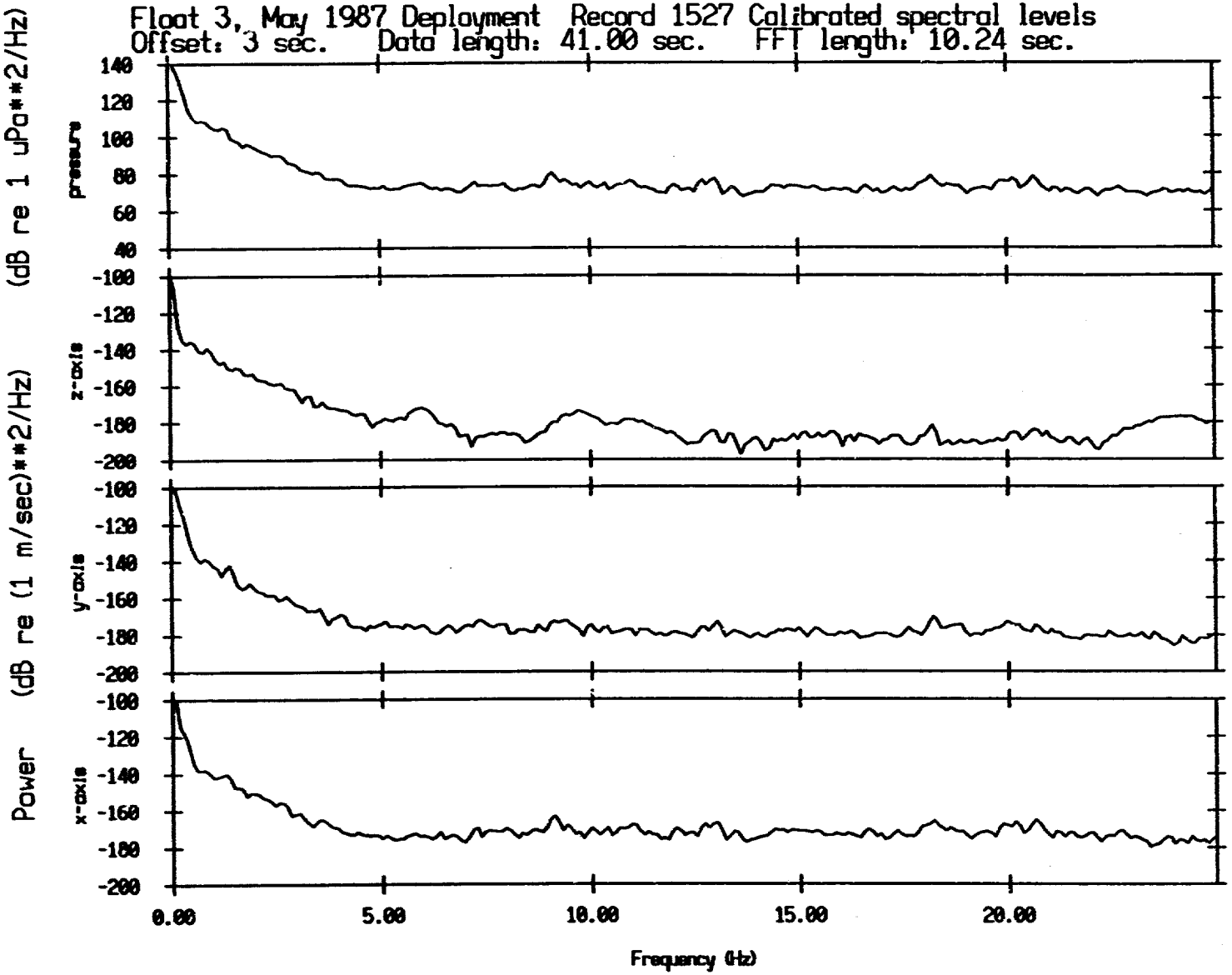

Figure IV.35a

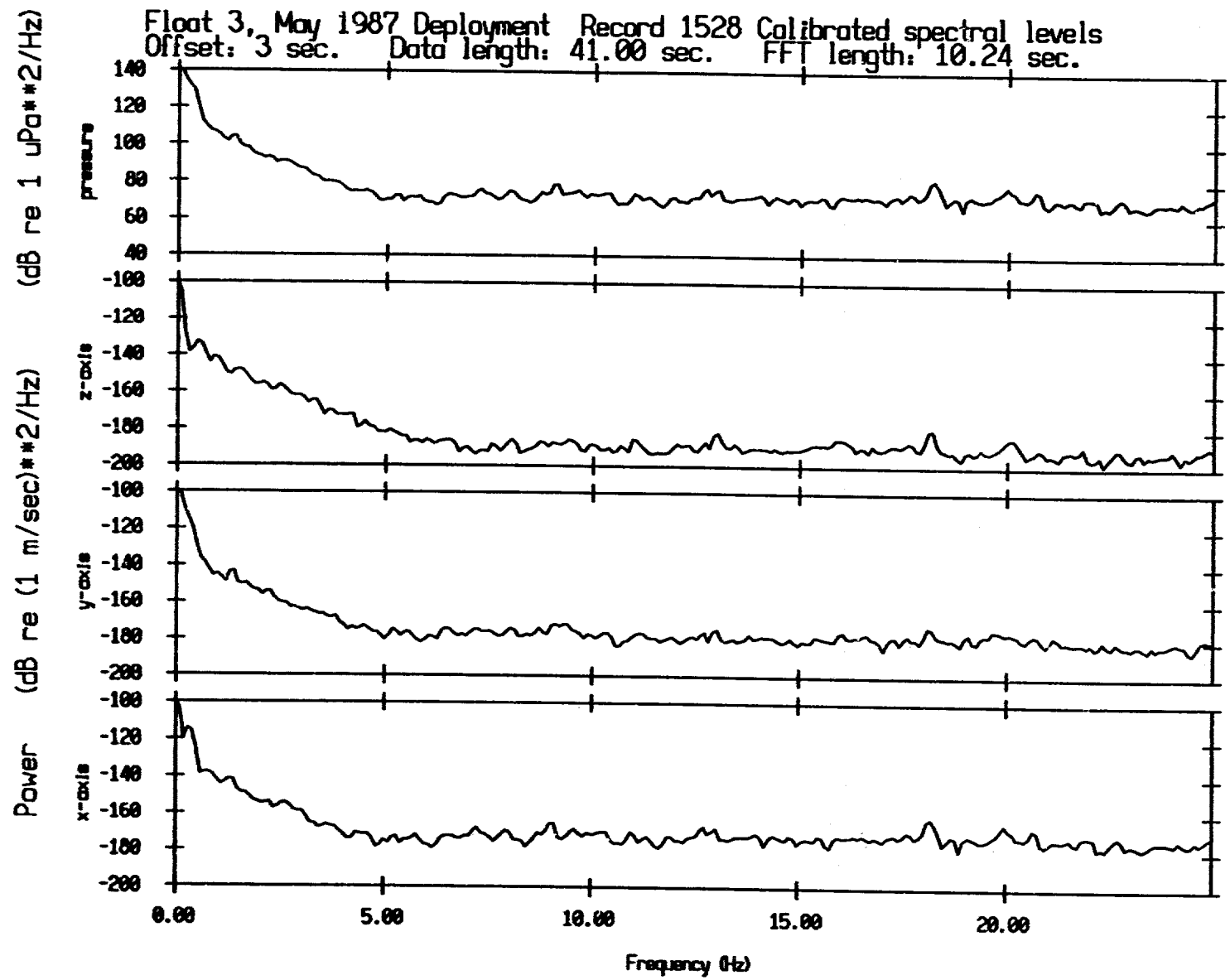

Figure IV.35b

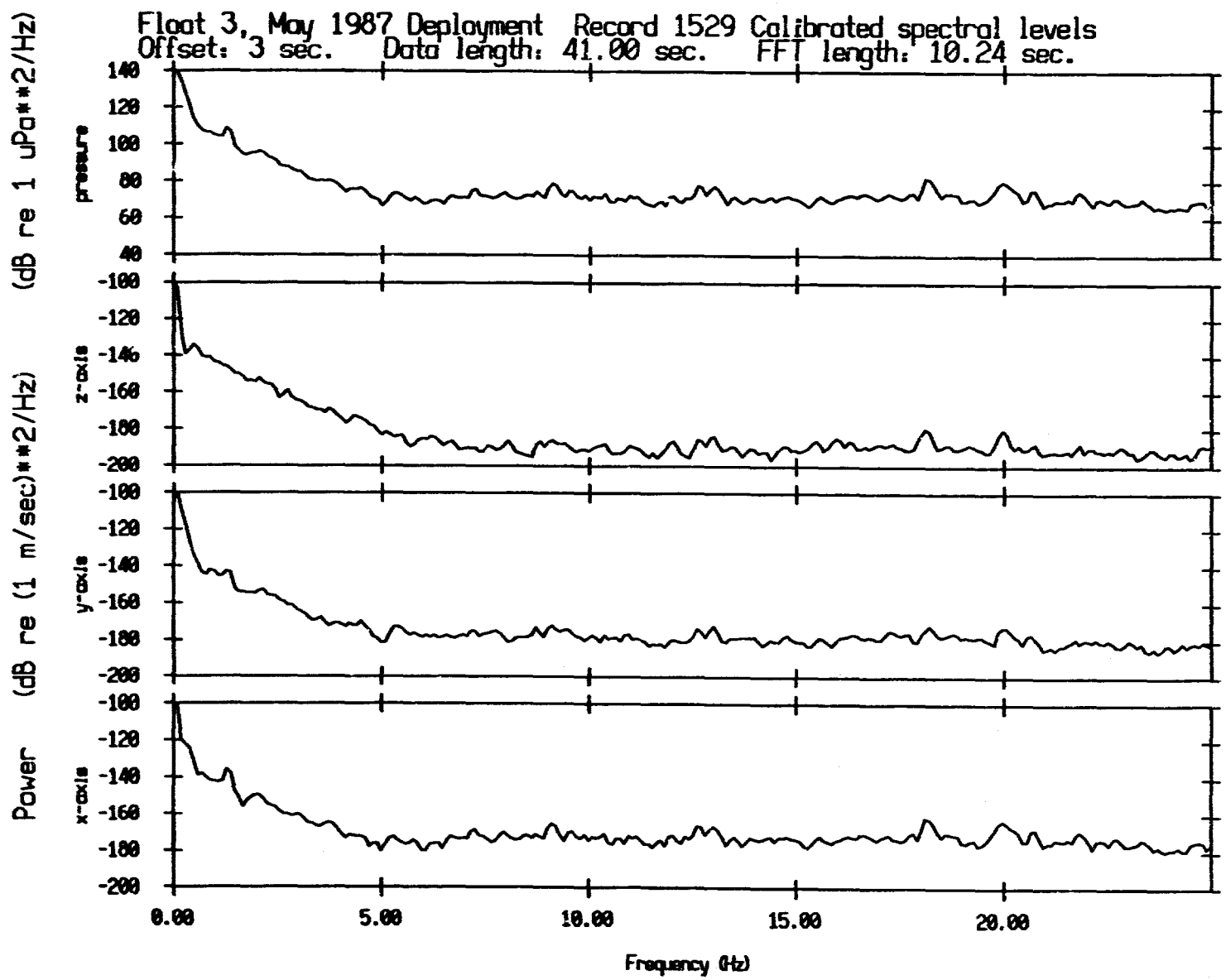

Figure IV.35c

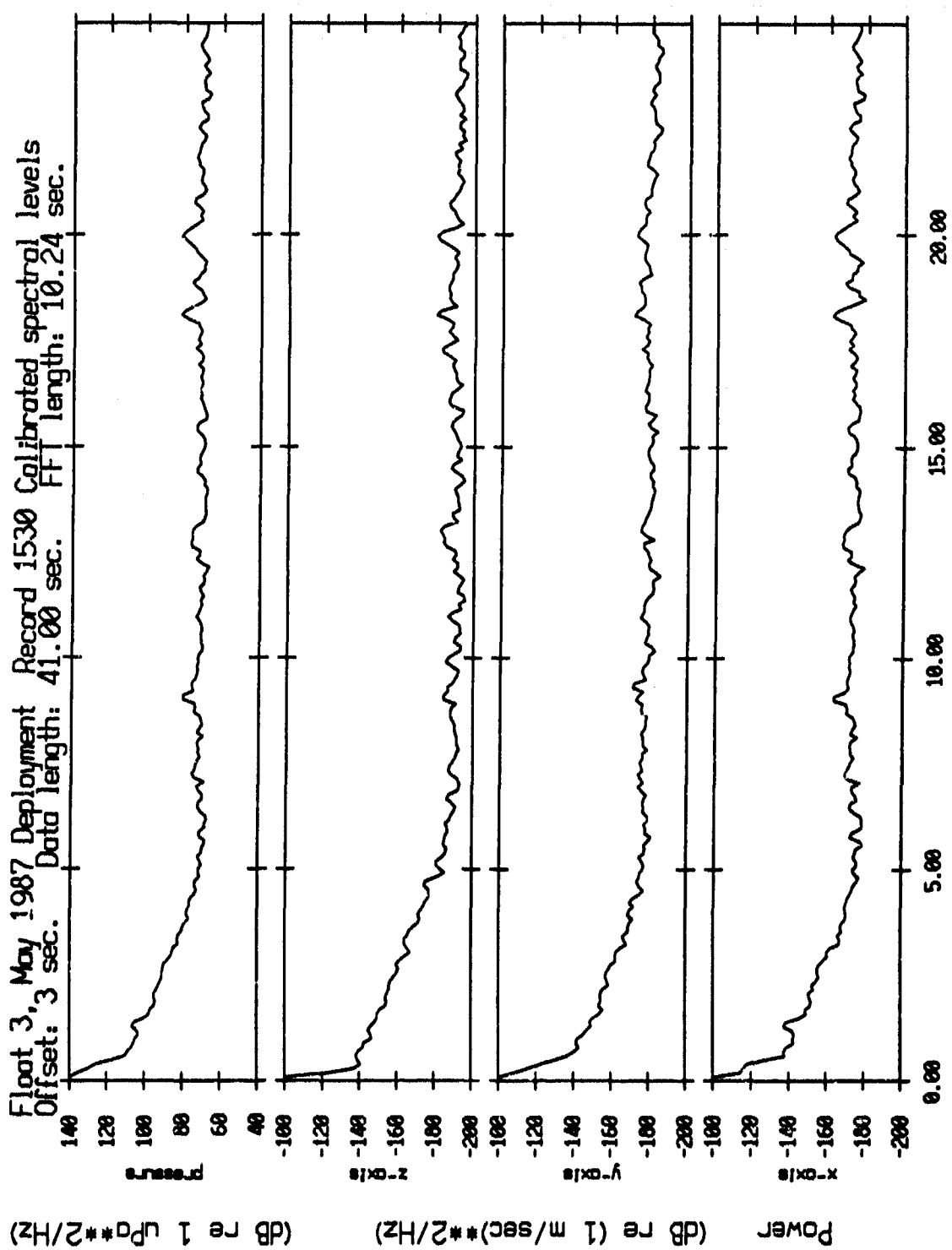

Figure IV.35d

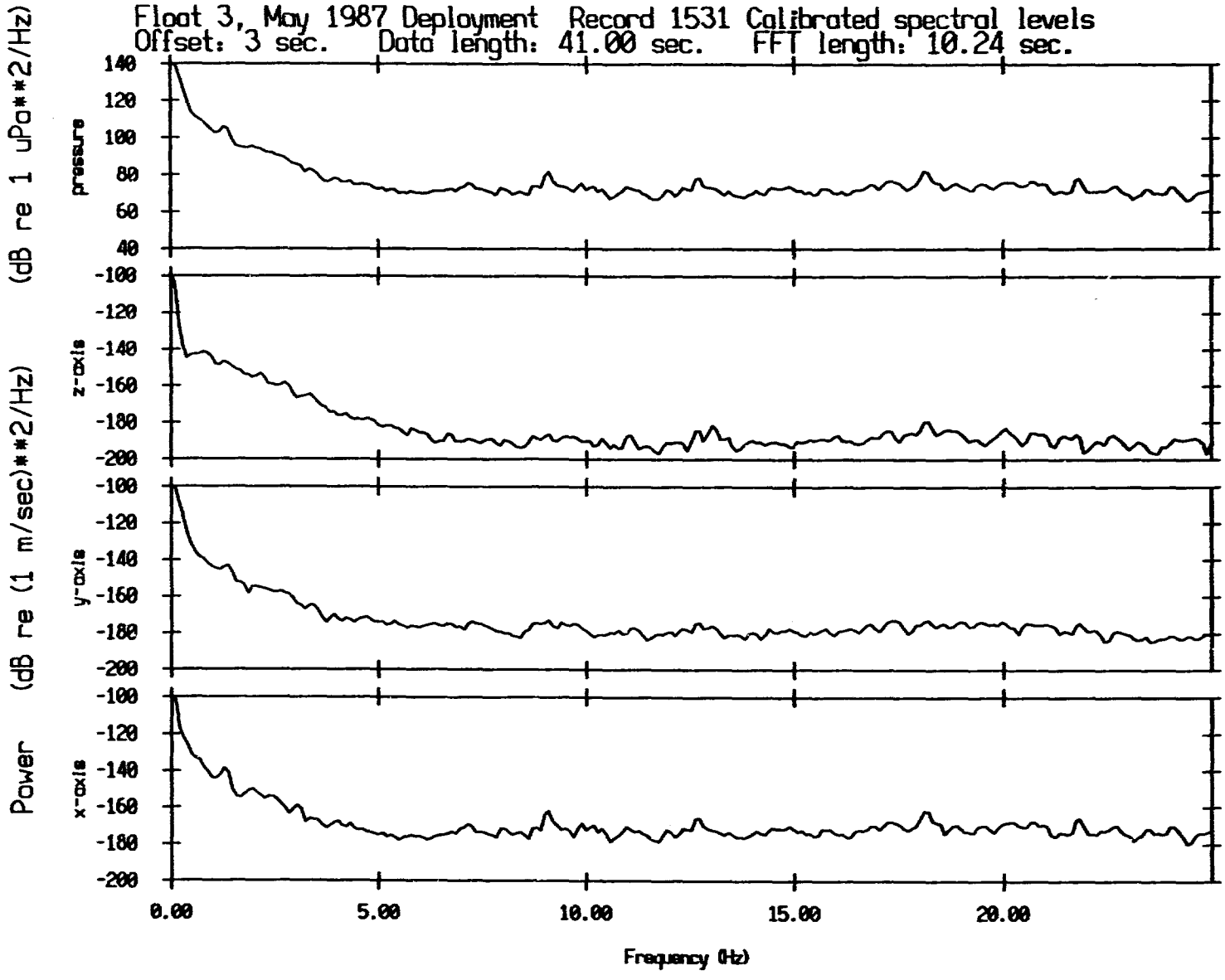

Figure IV.35e

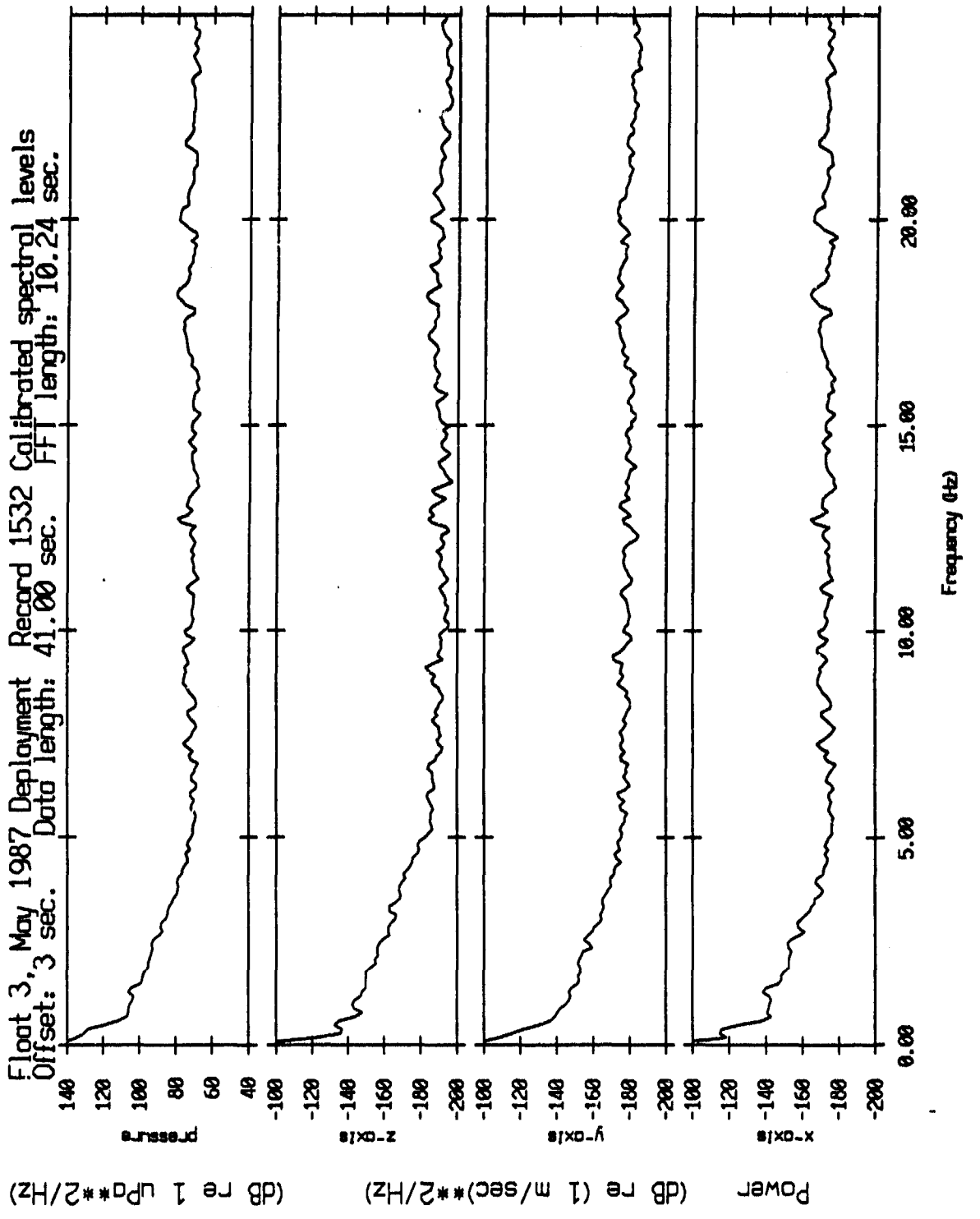

Figure IV.35f

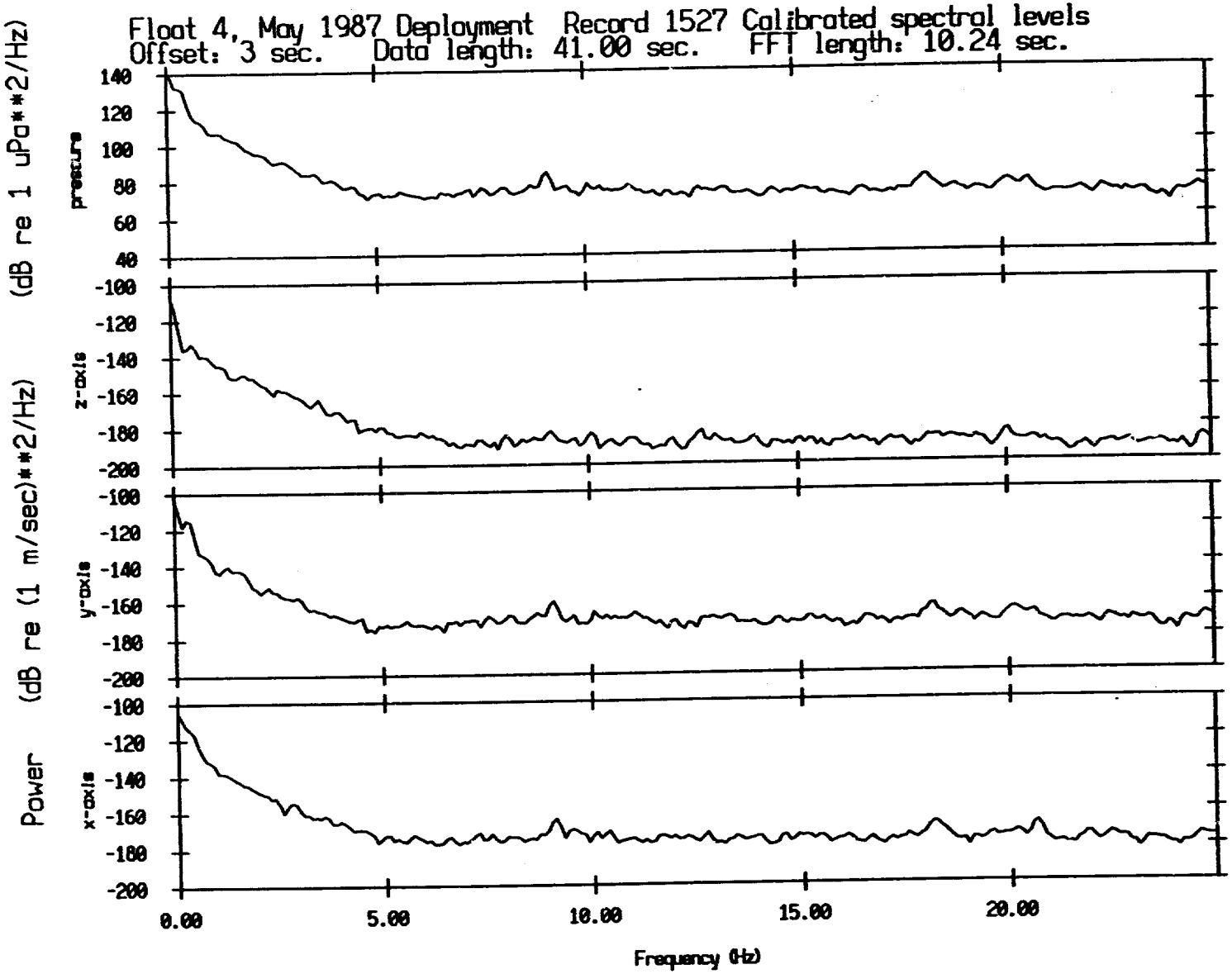

Figure IV.38a

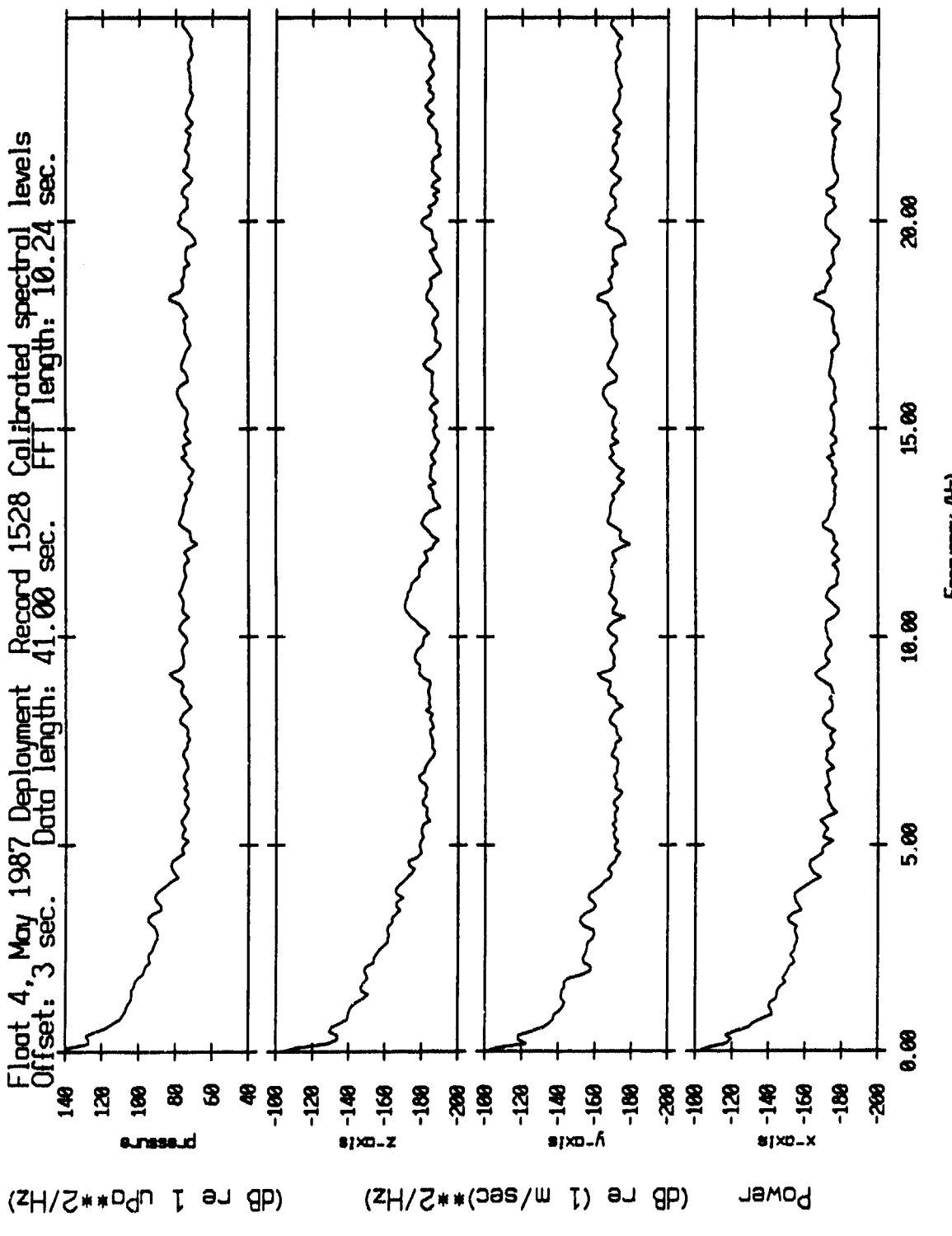

Figure IV.36b

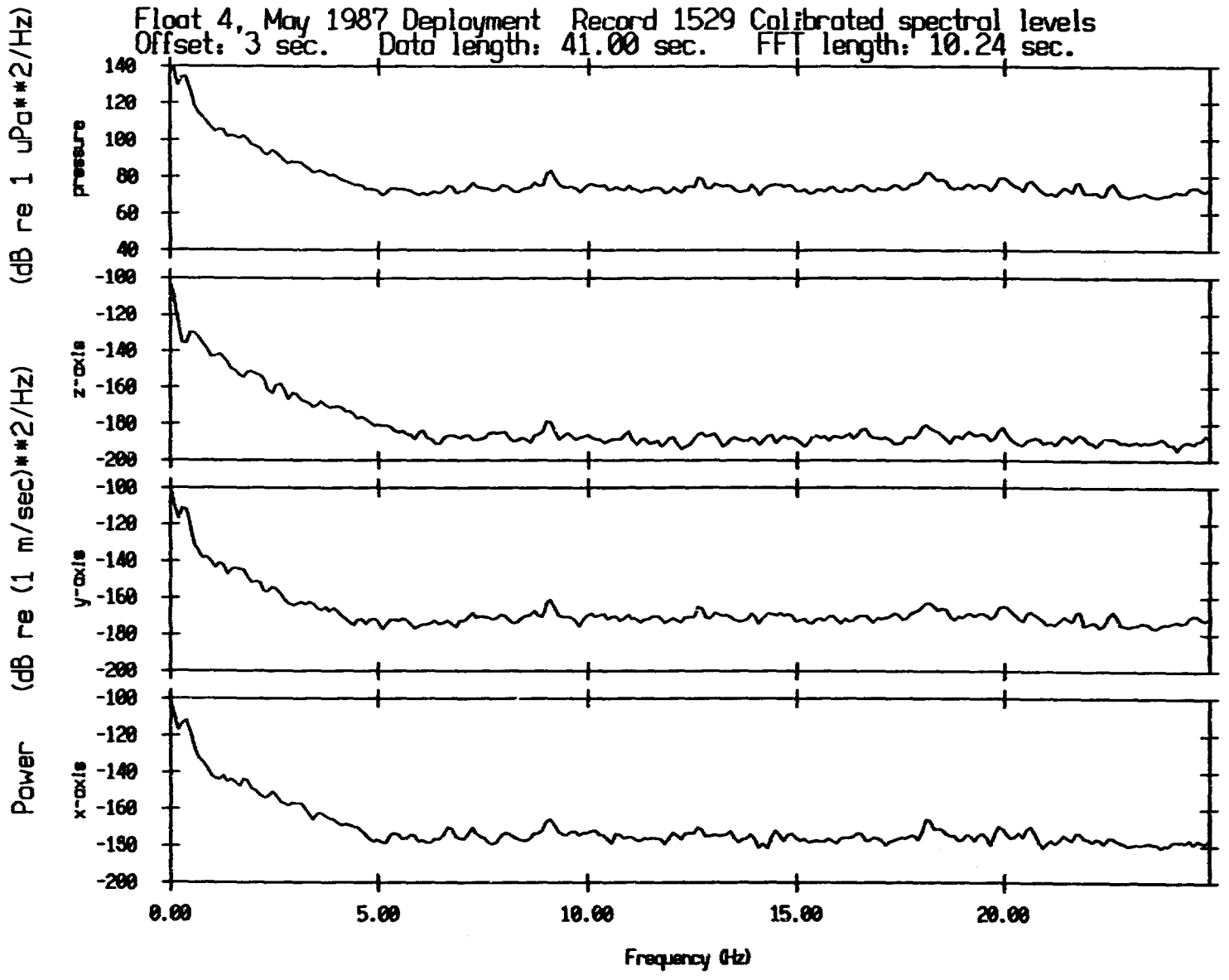

Figure IV.36c

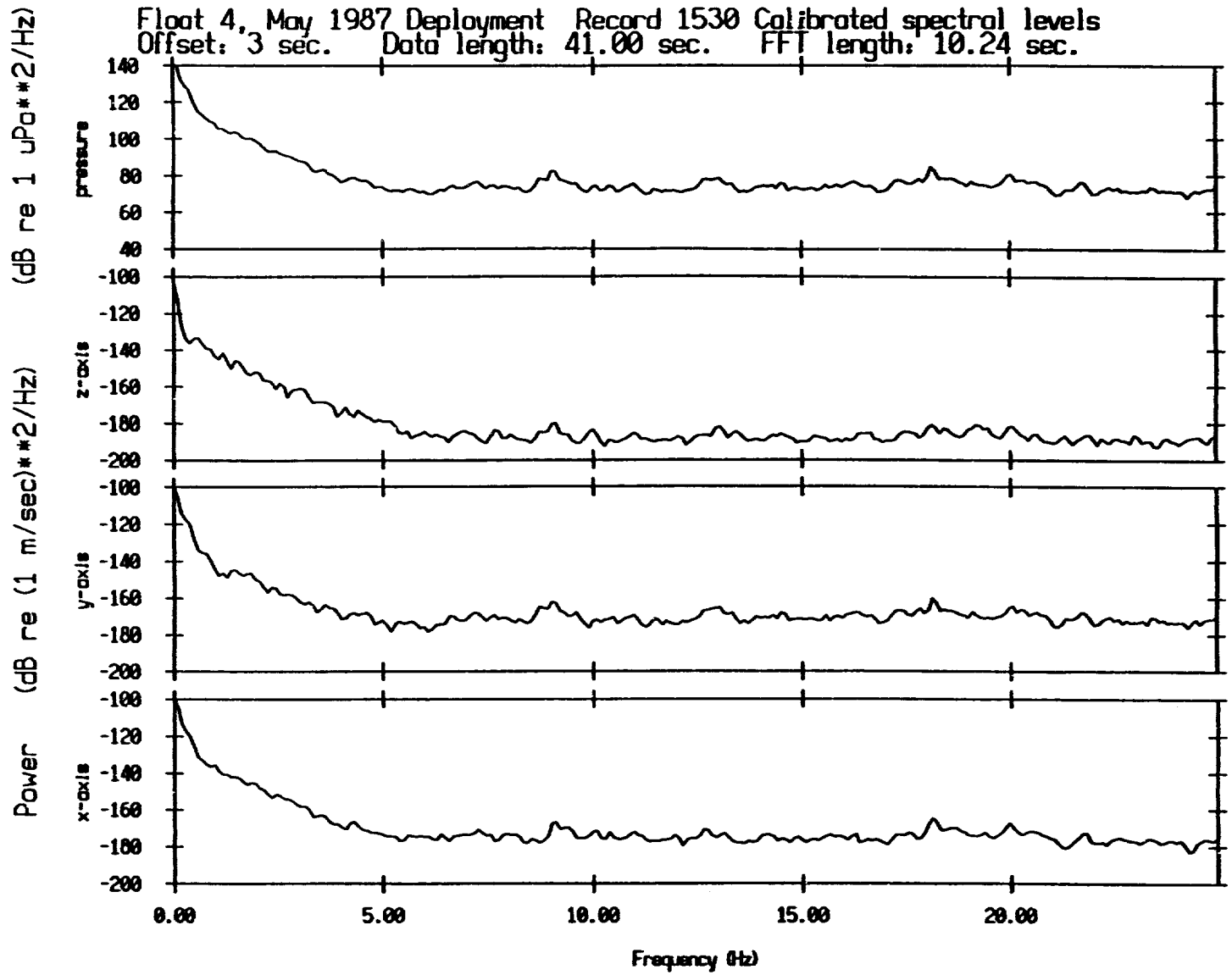

Figure IV.36d

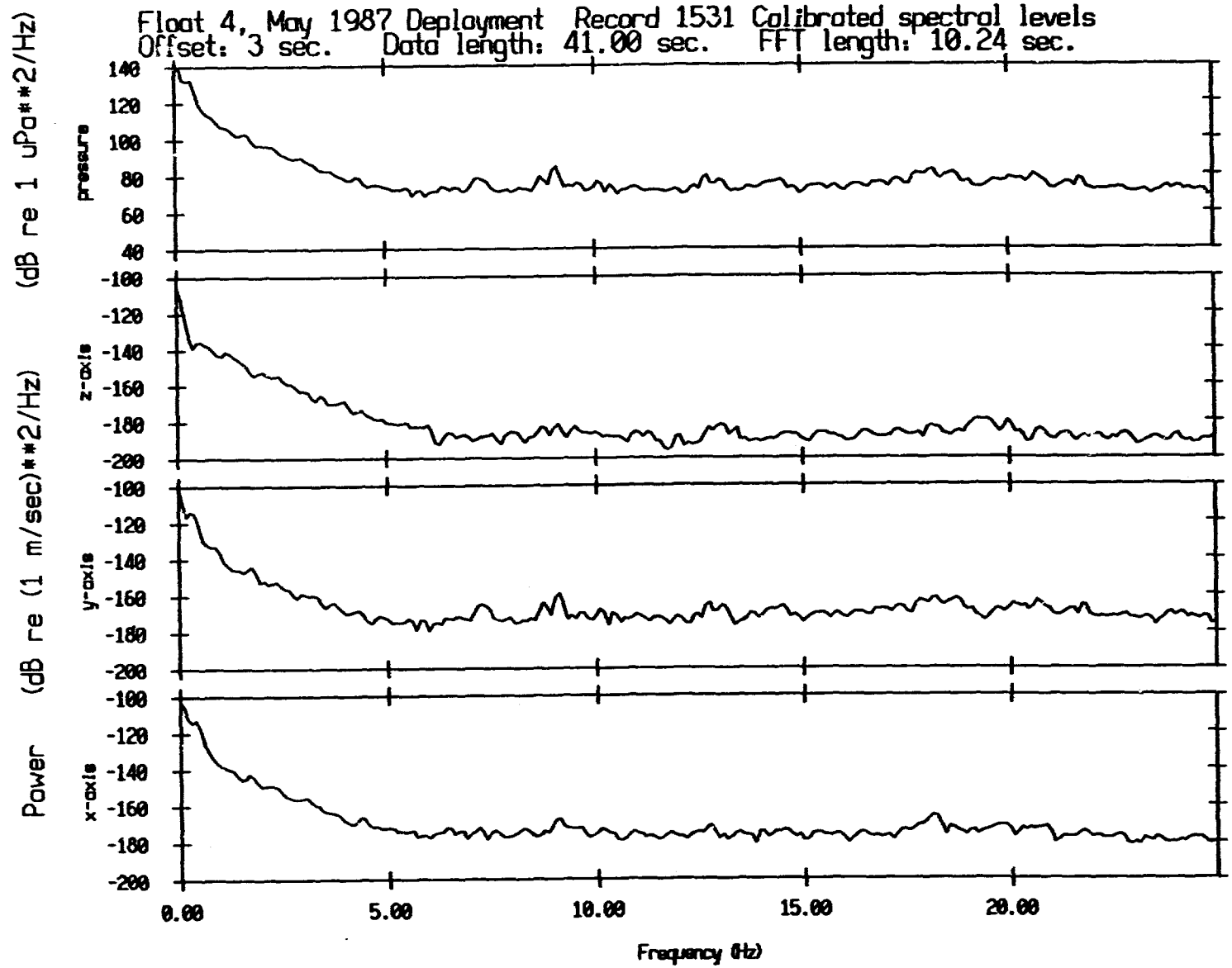

Figure IV.36a

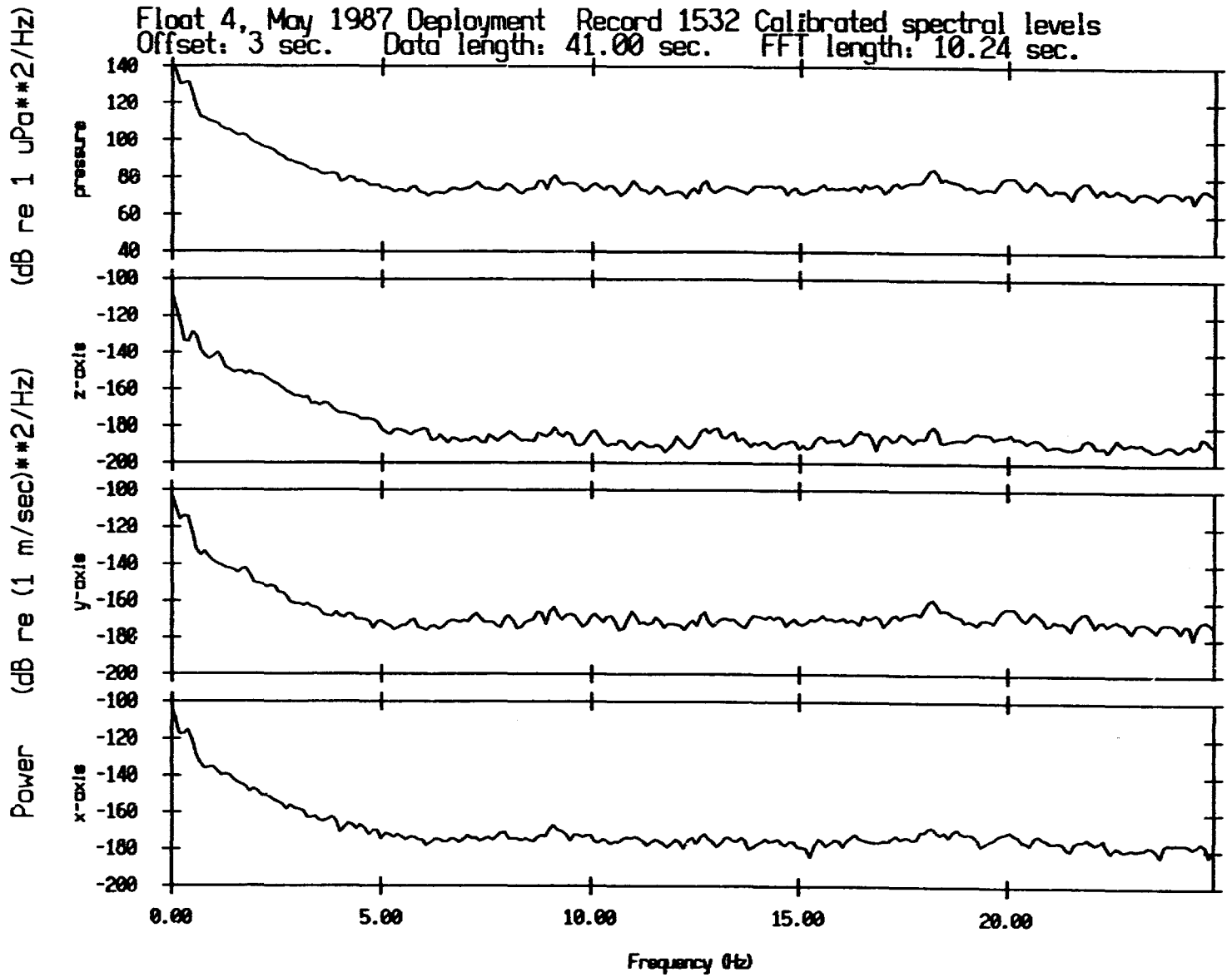

Figure IV.36f

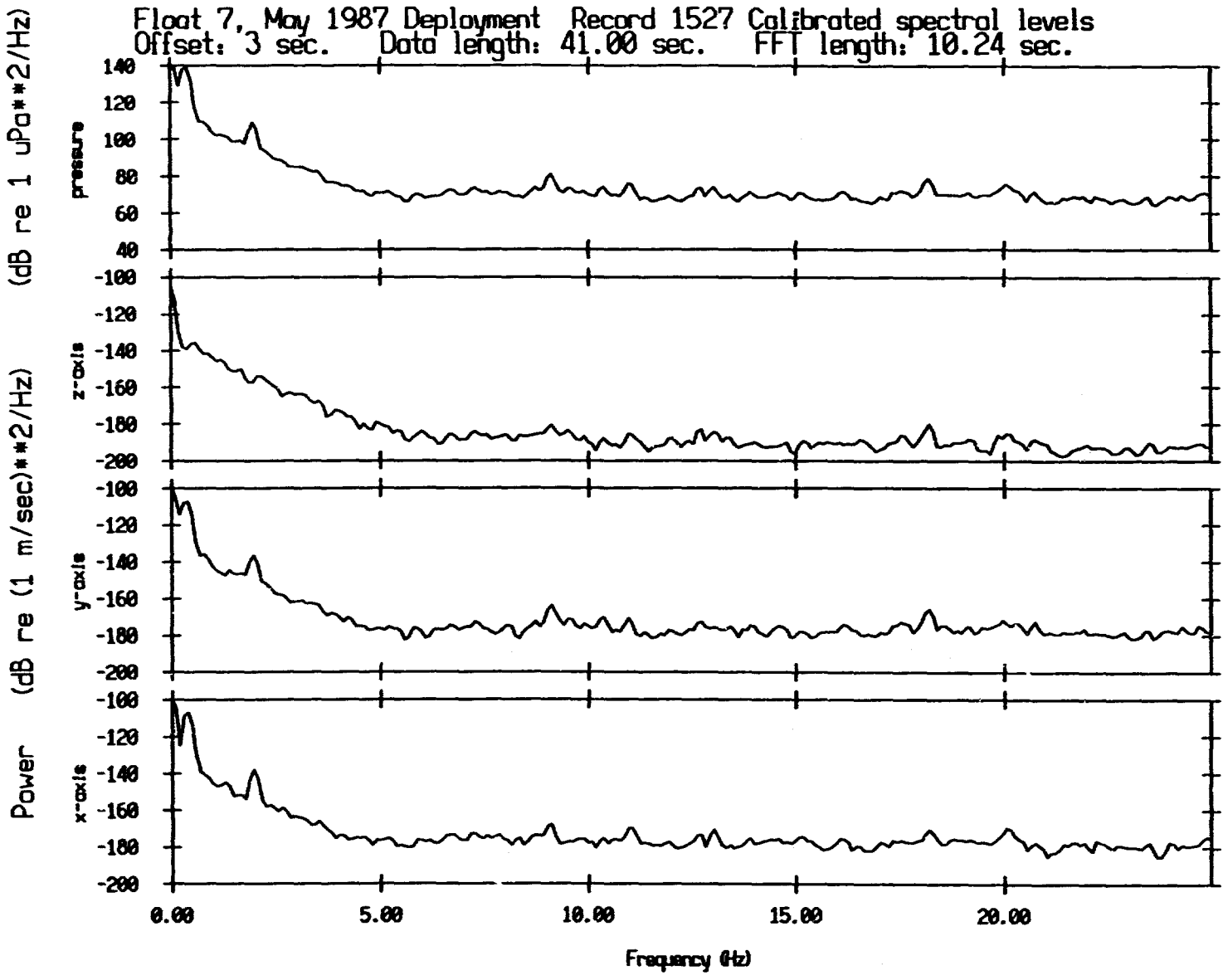

Figure IV.37a

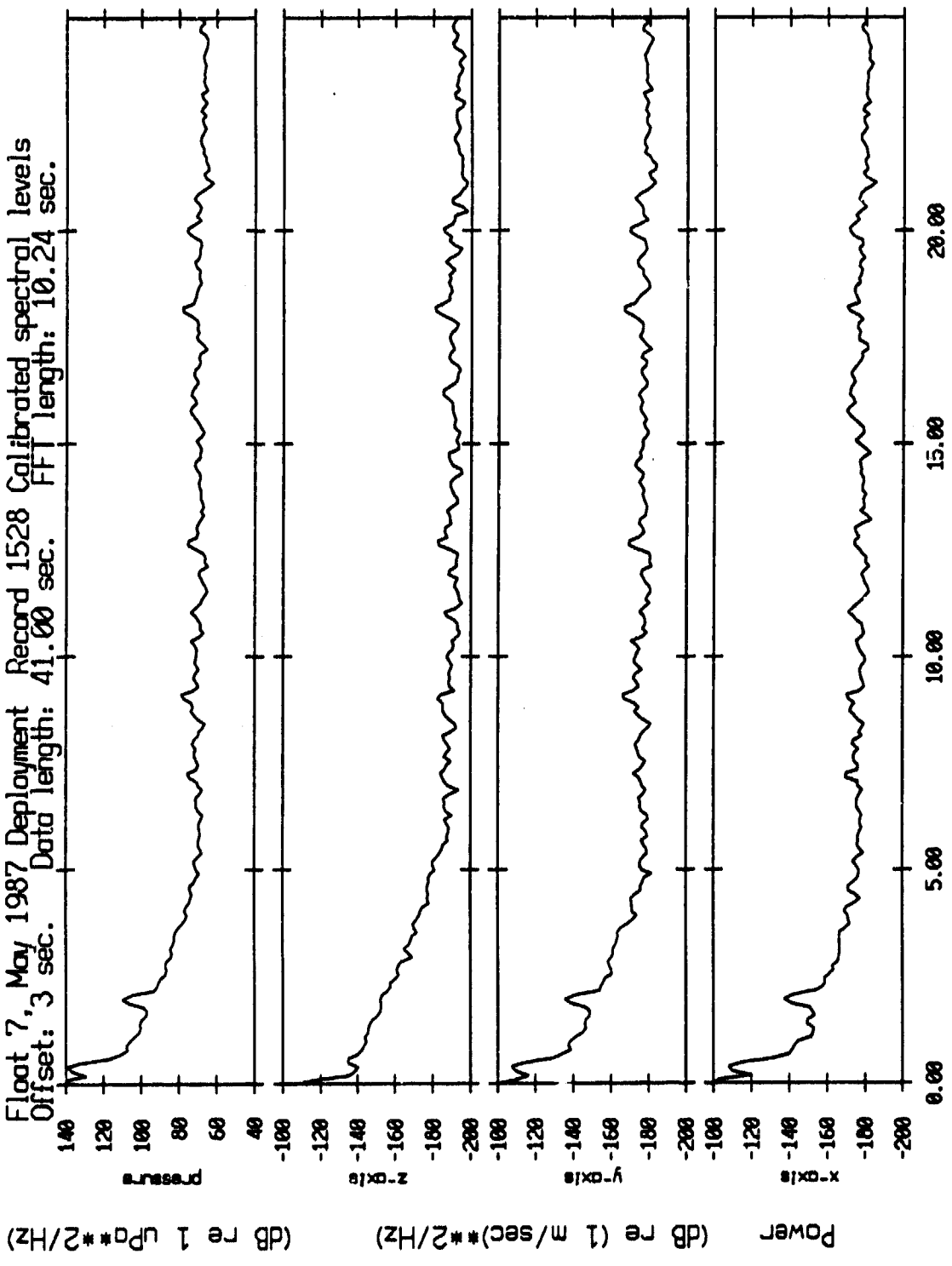

Figure IV.37b

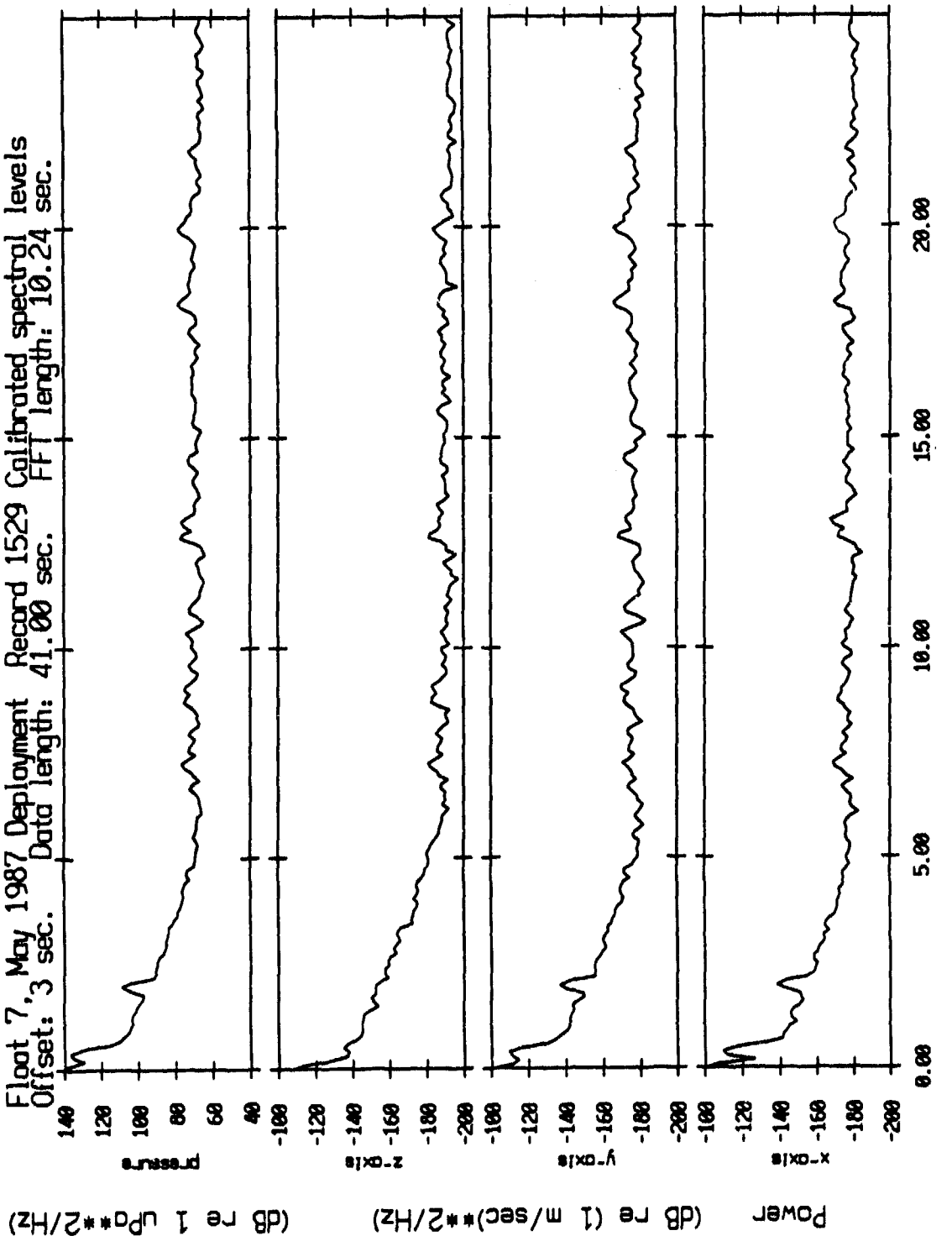

Figure IV.37c

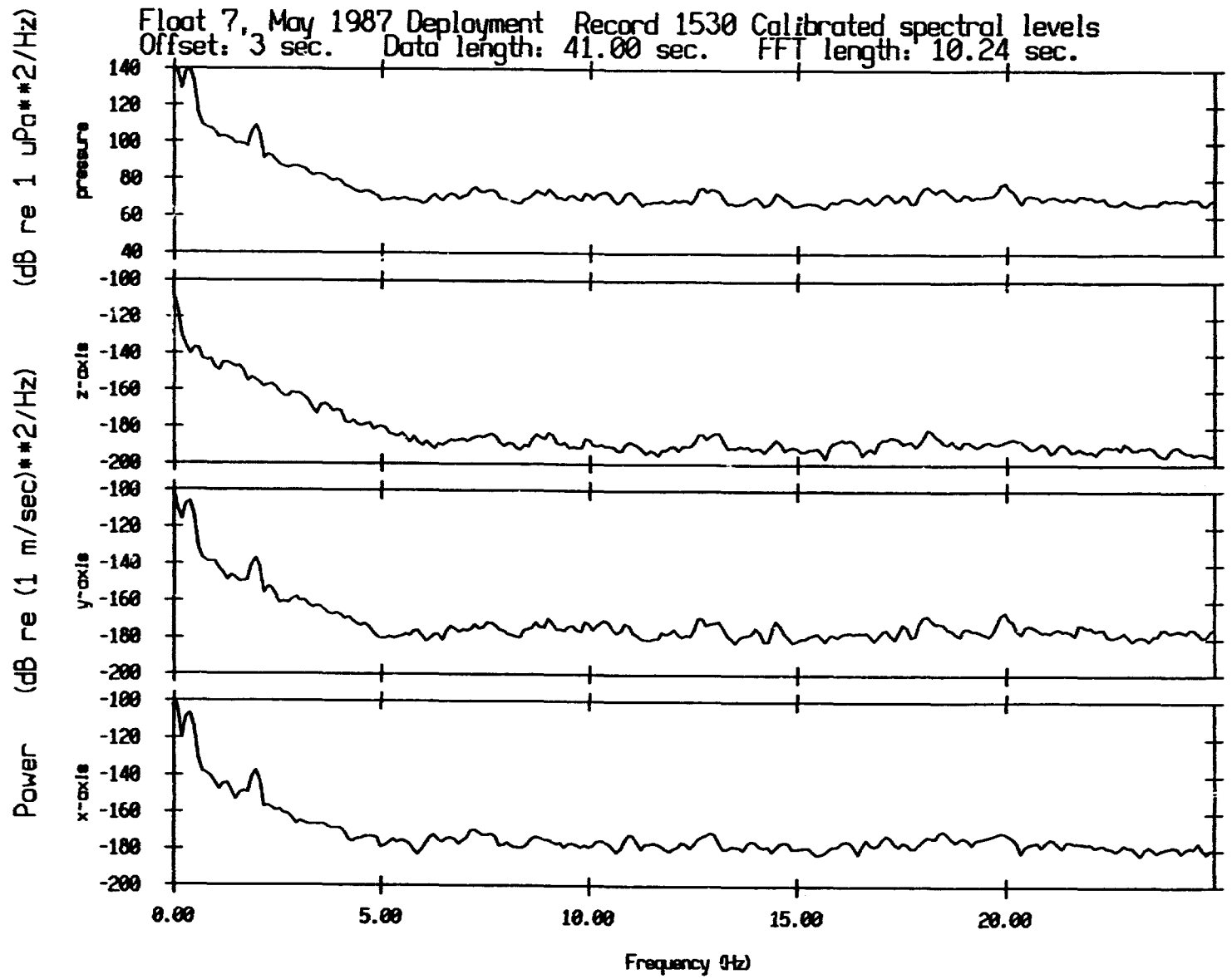

Figure IV.37d

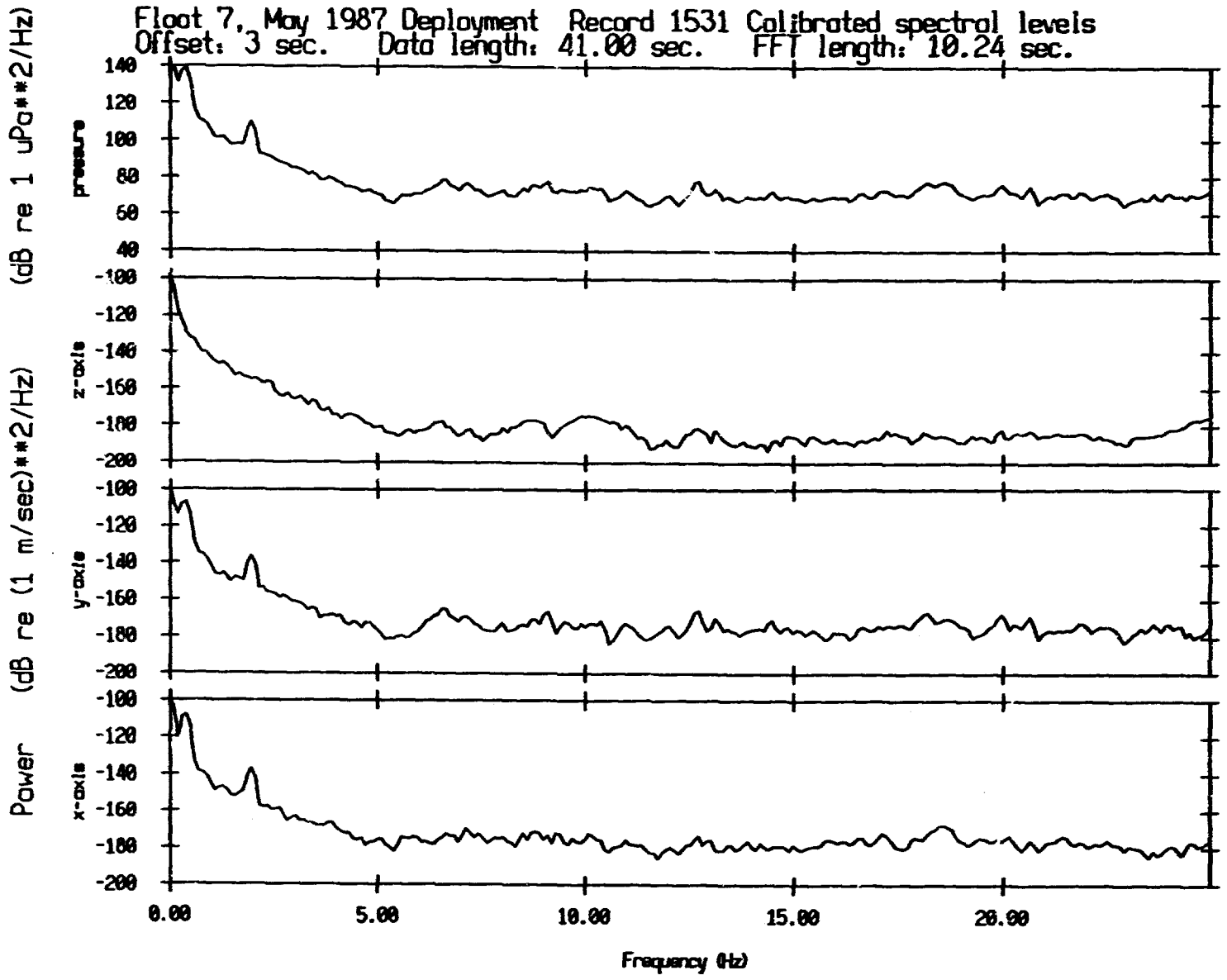

Figure IV.37e

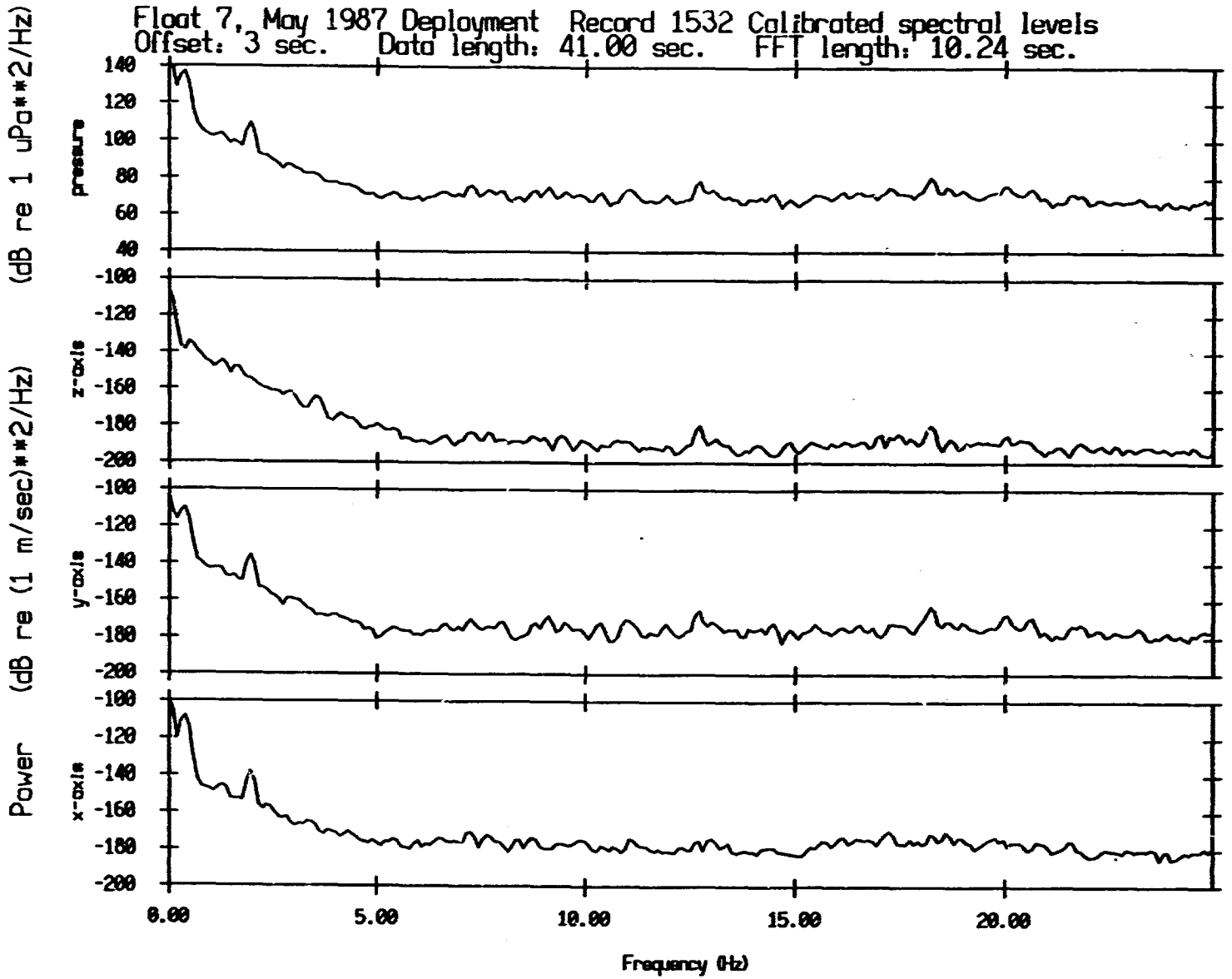

Figure IV.37f

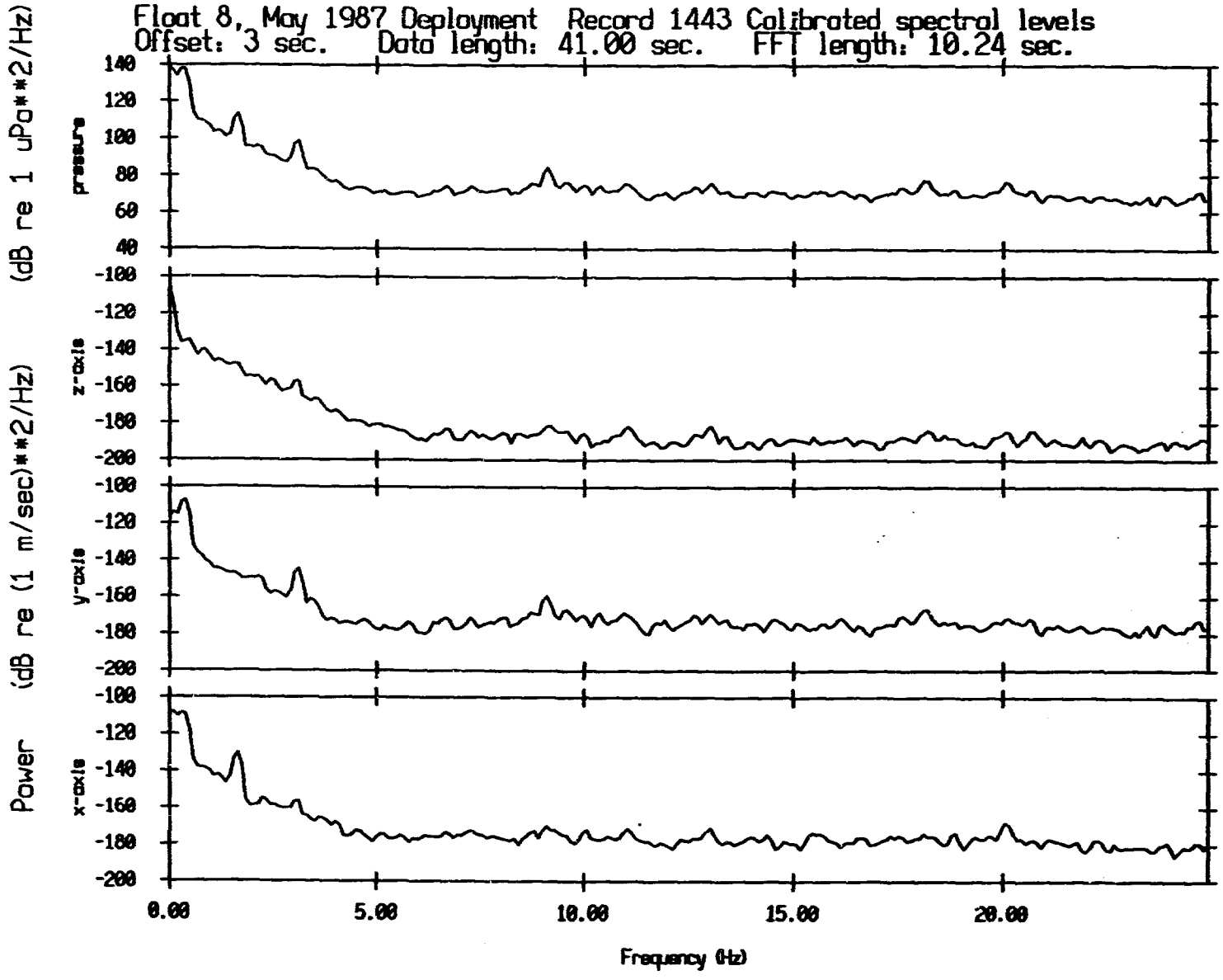

Figure IV.38a

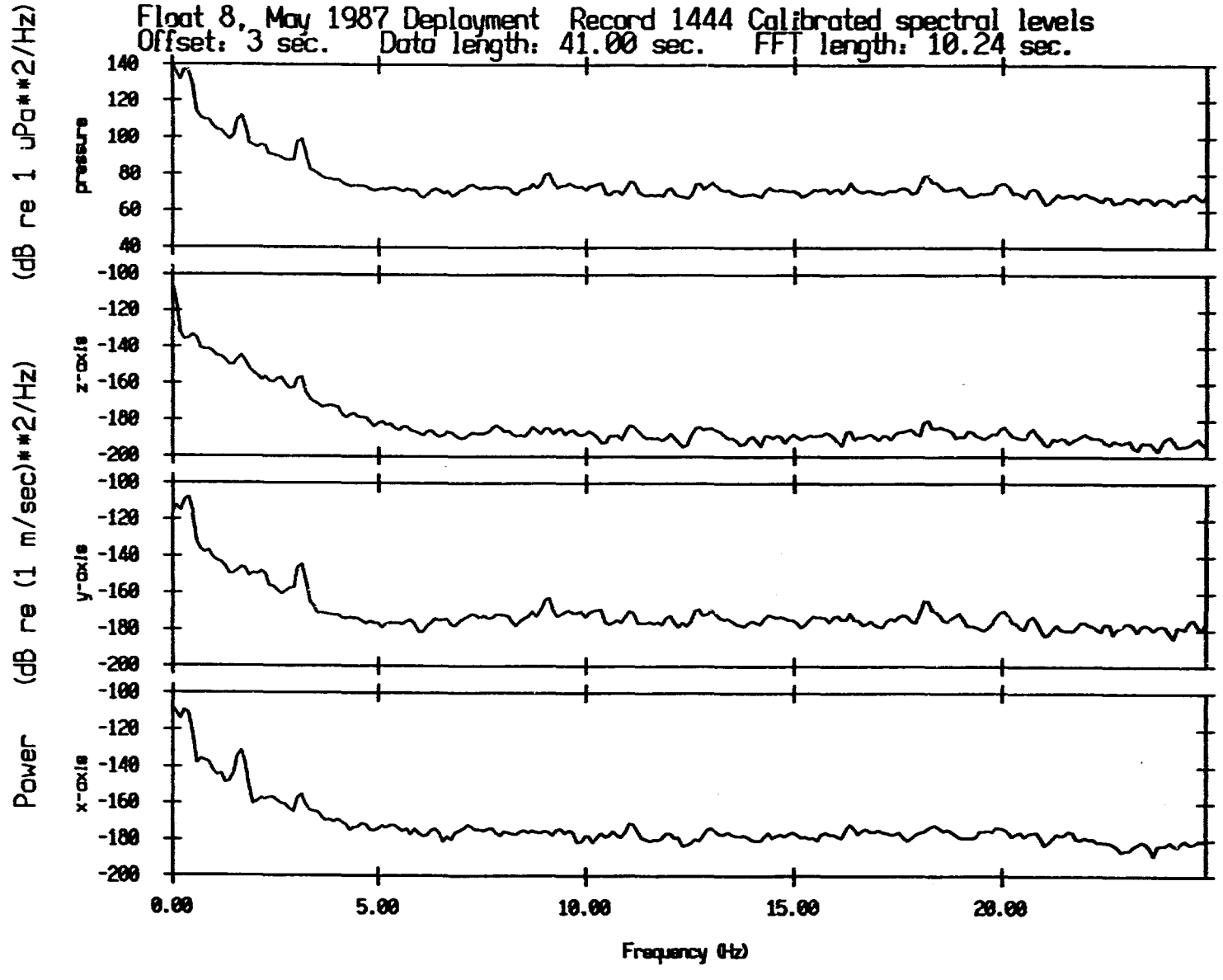

Figure IV.38b

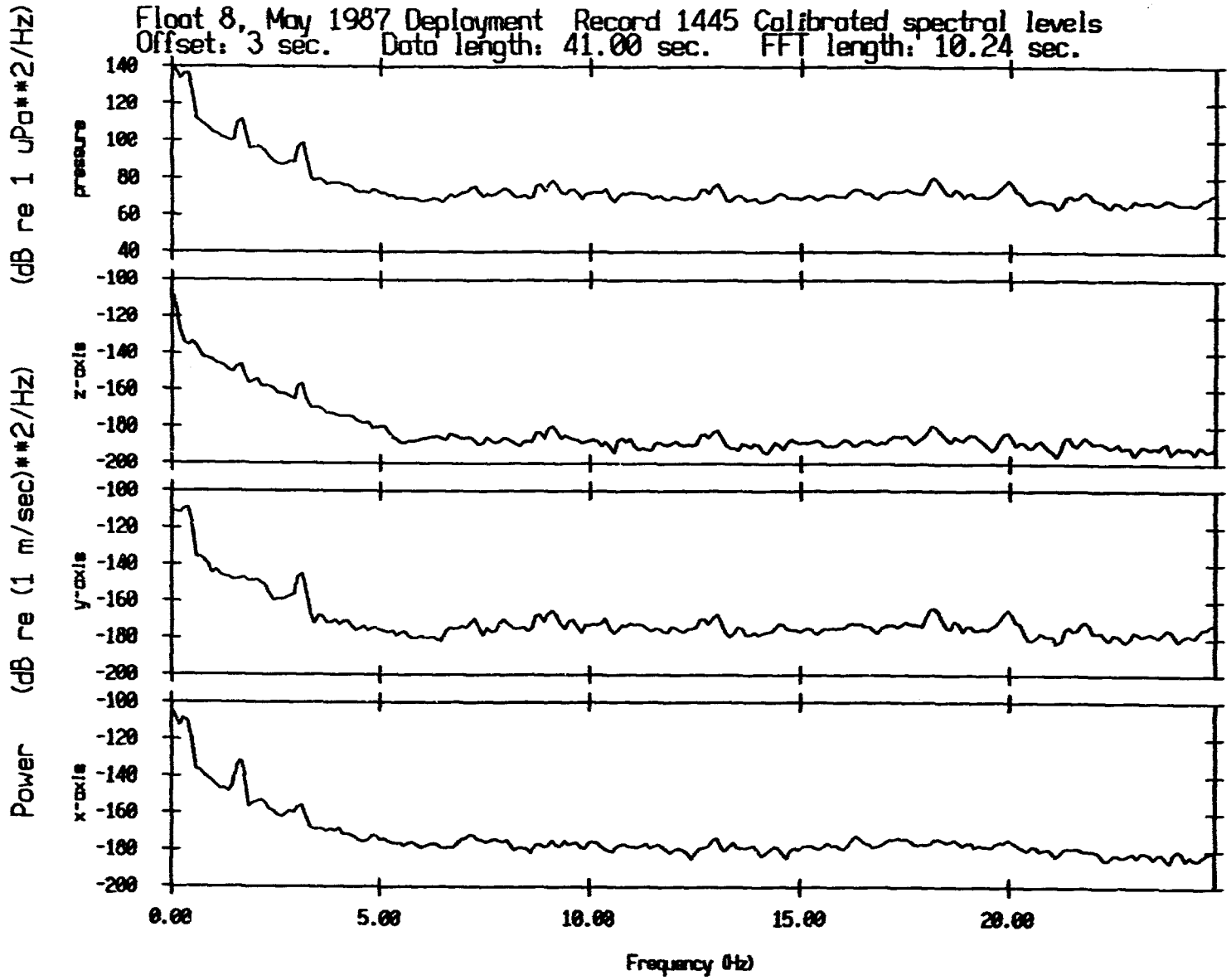

Figure IV.38c

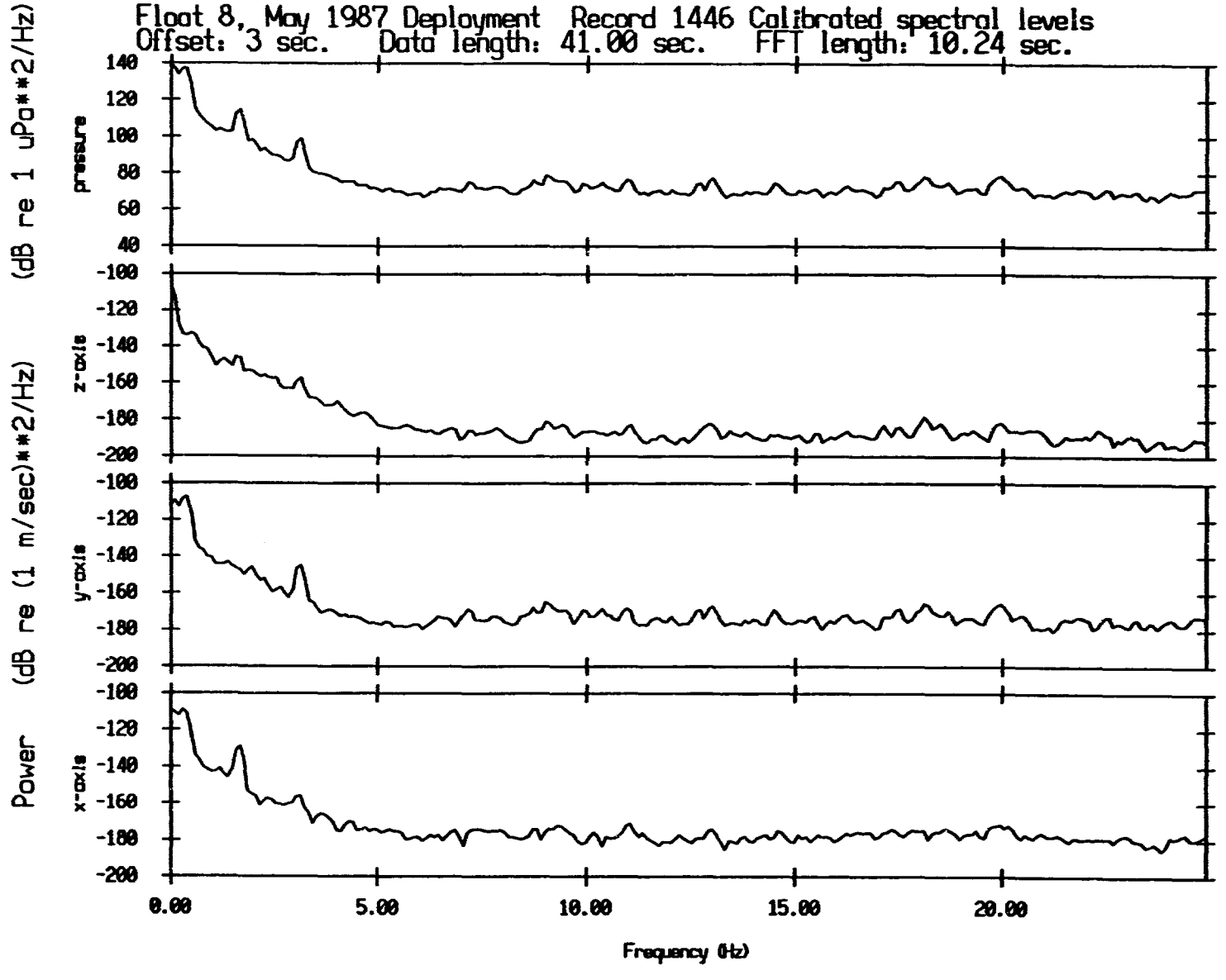

Figure IV.38d

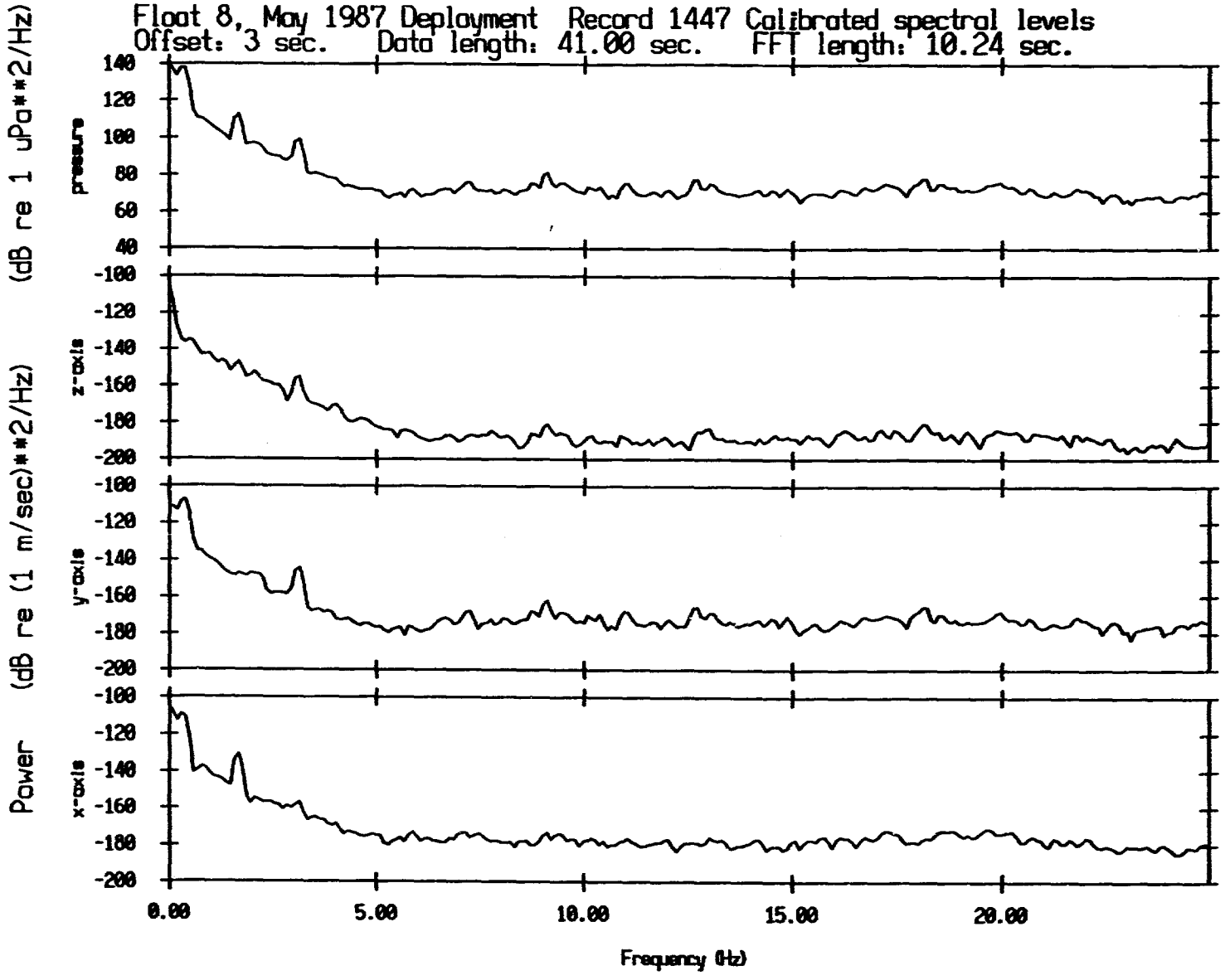

Figure IV.38e

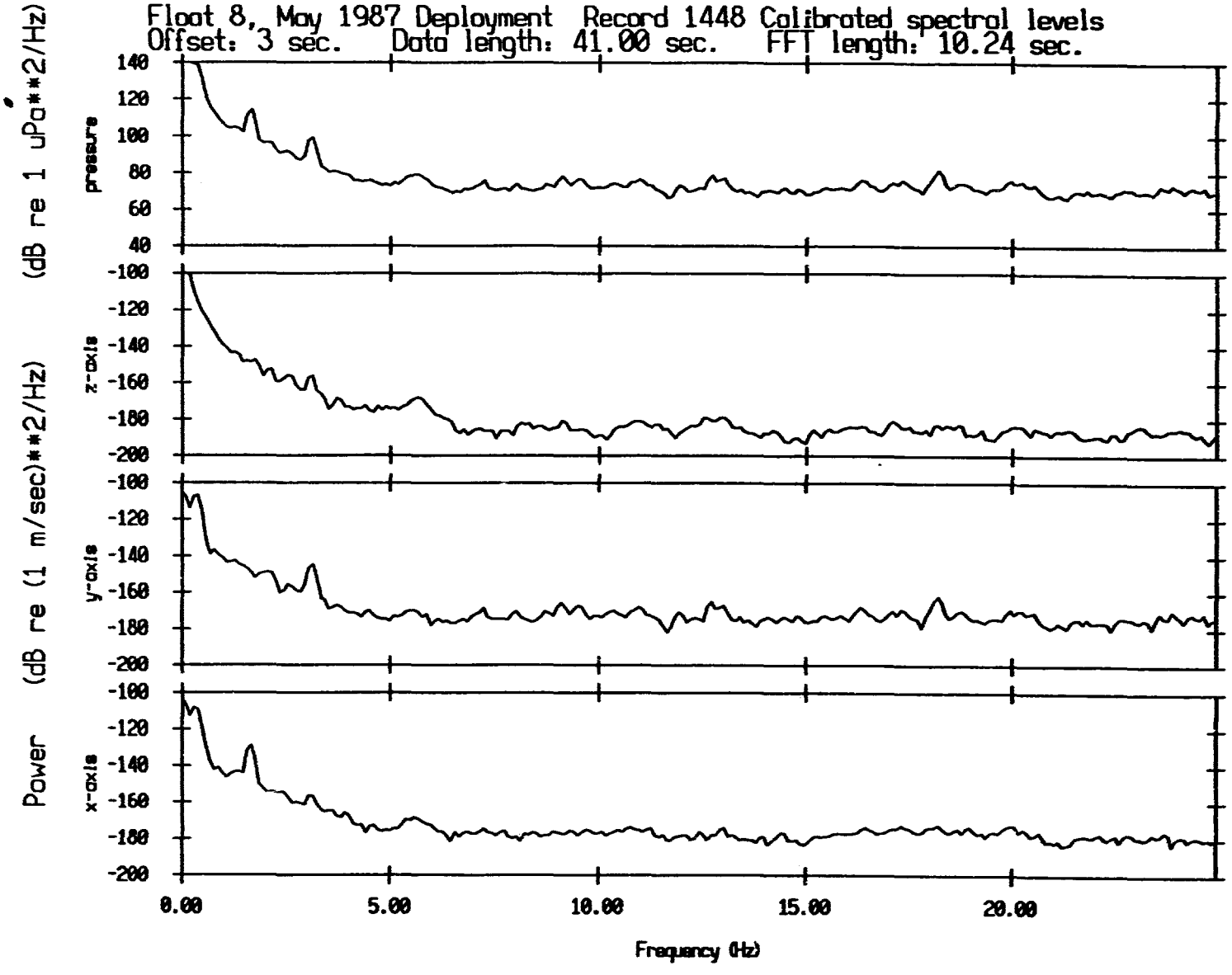

Figure IV.38f

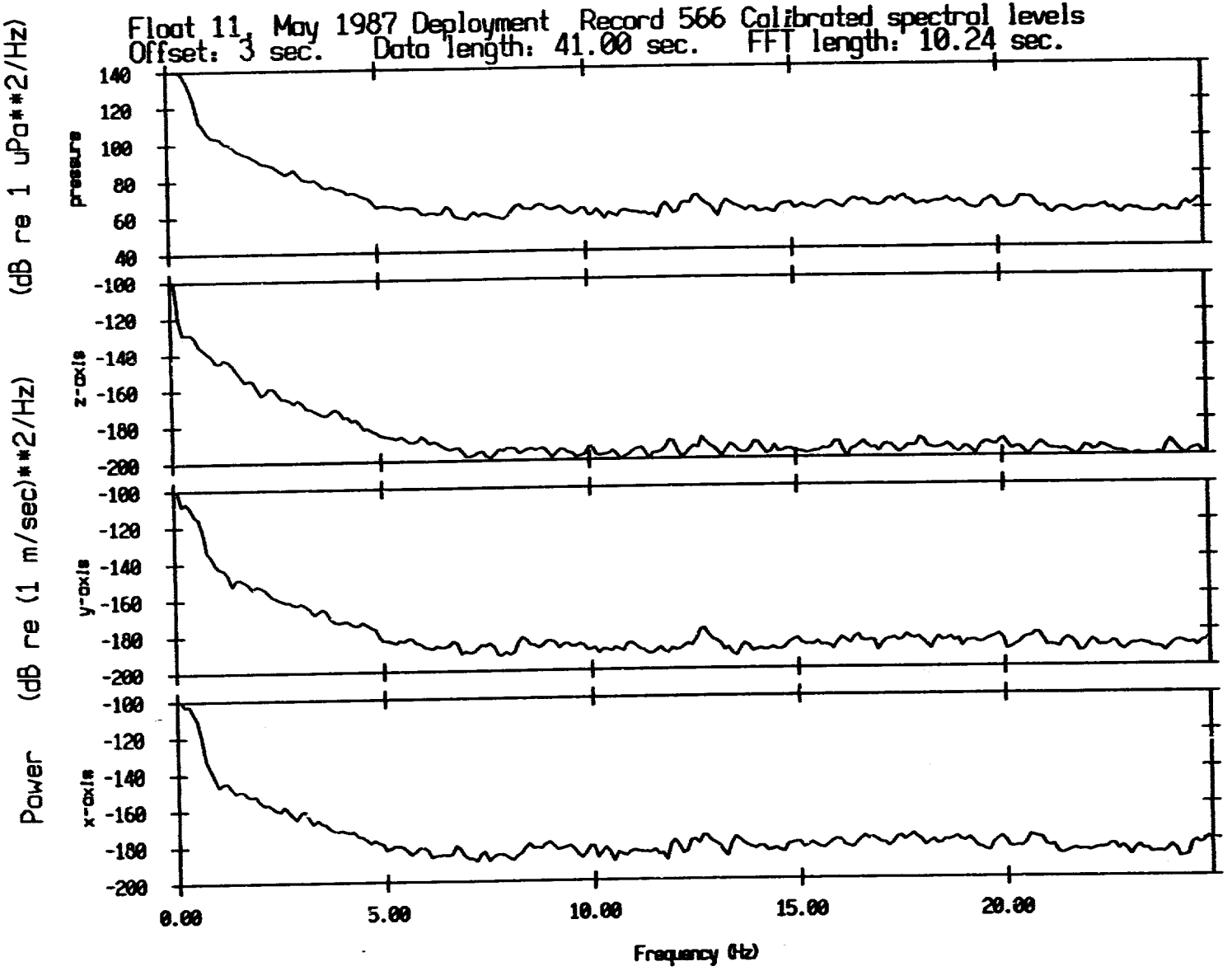

Figure IV.39a

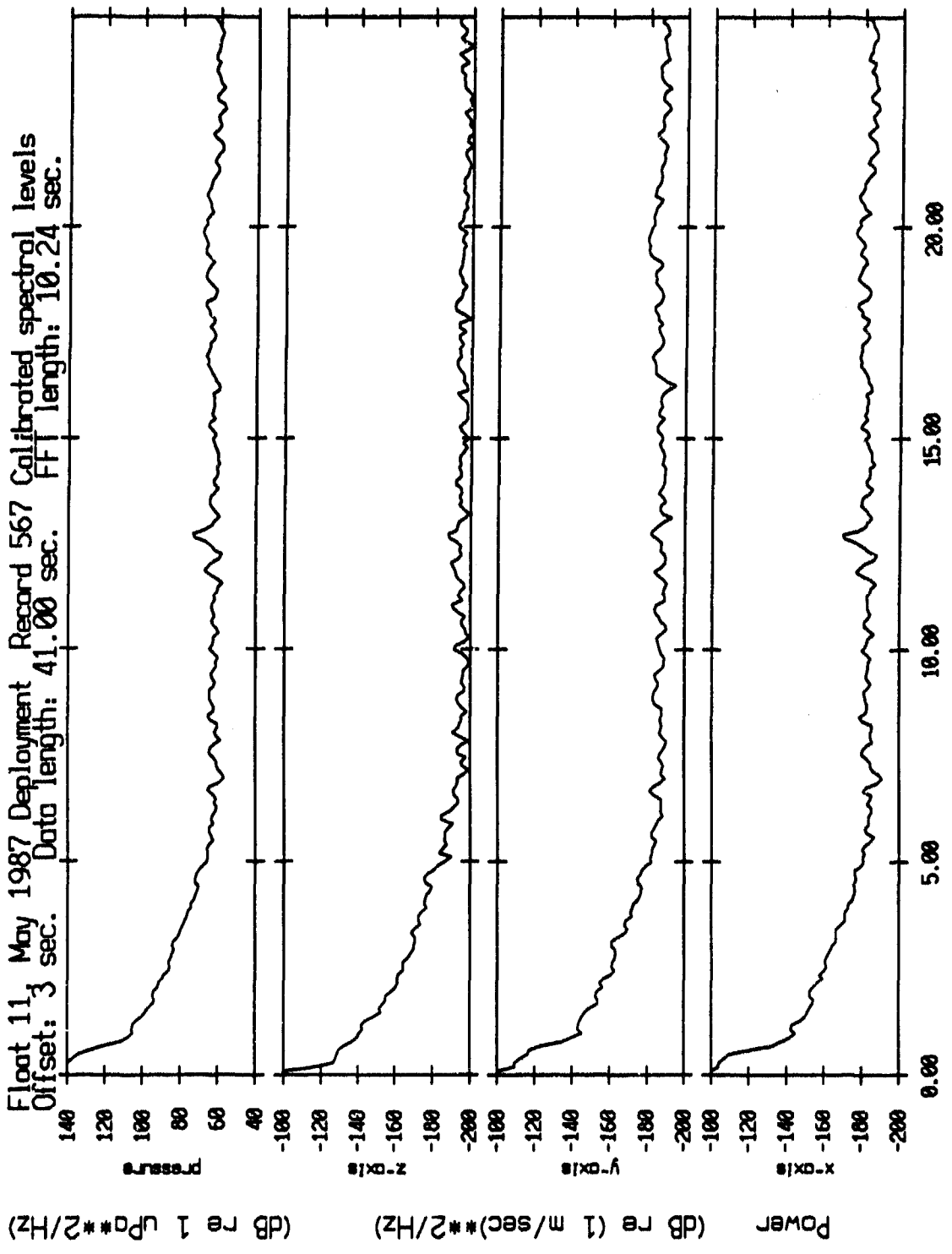

Figure IV.39b

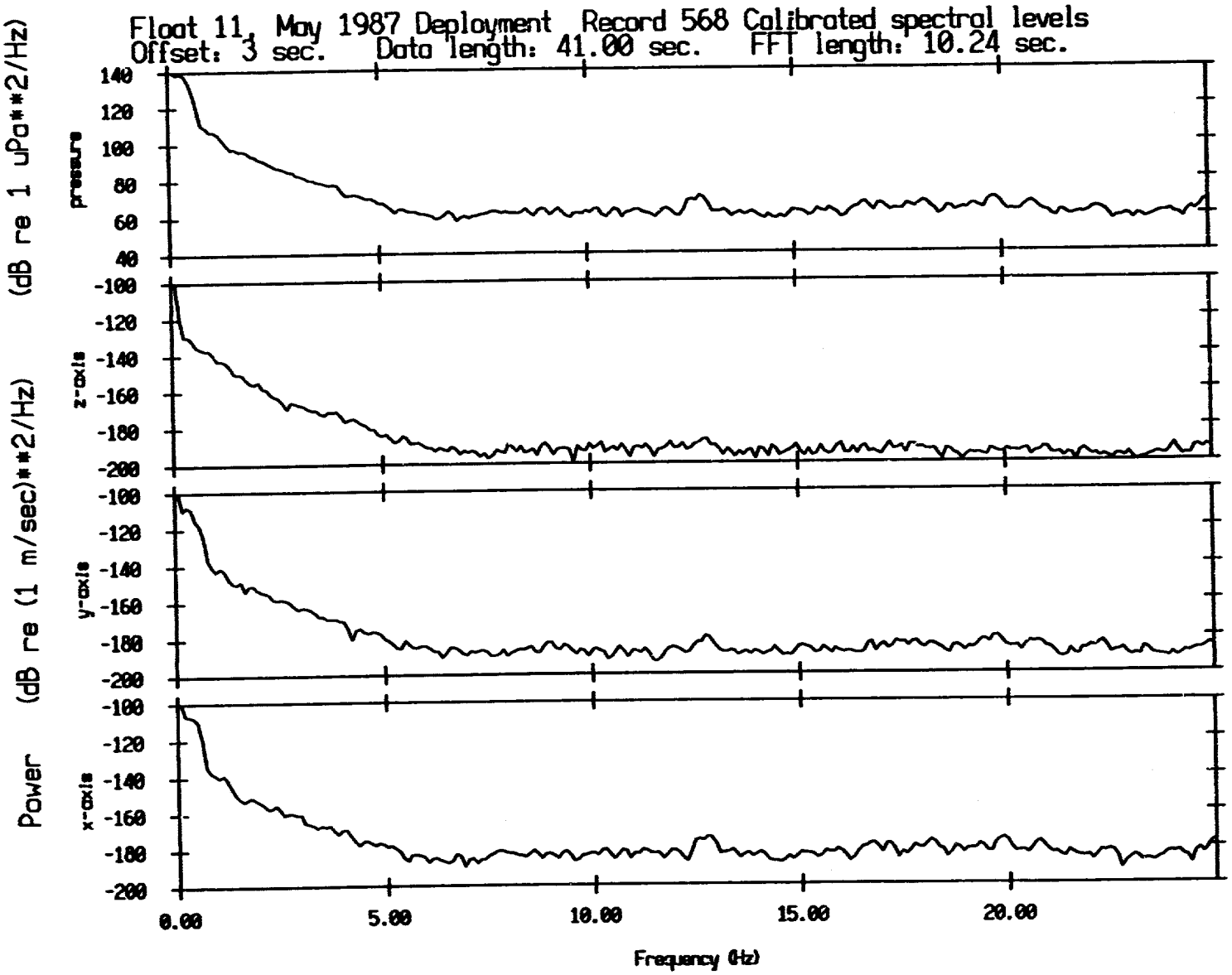

Figure IV.39c

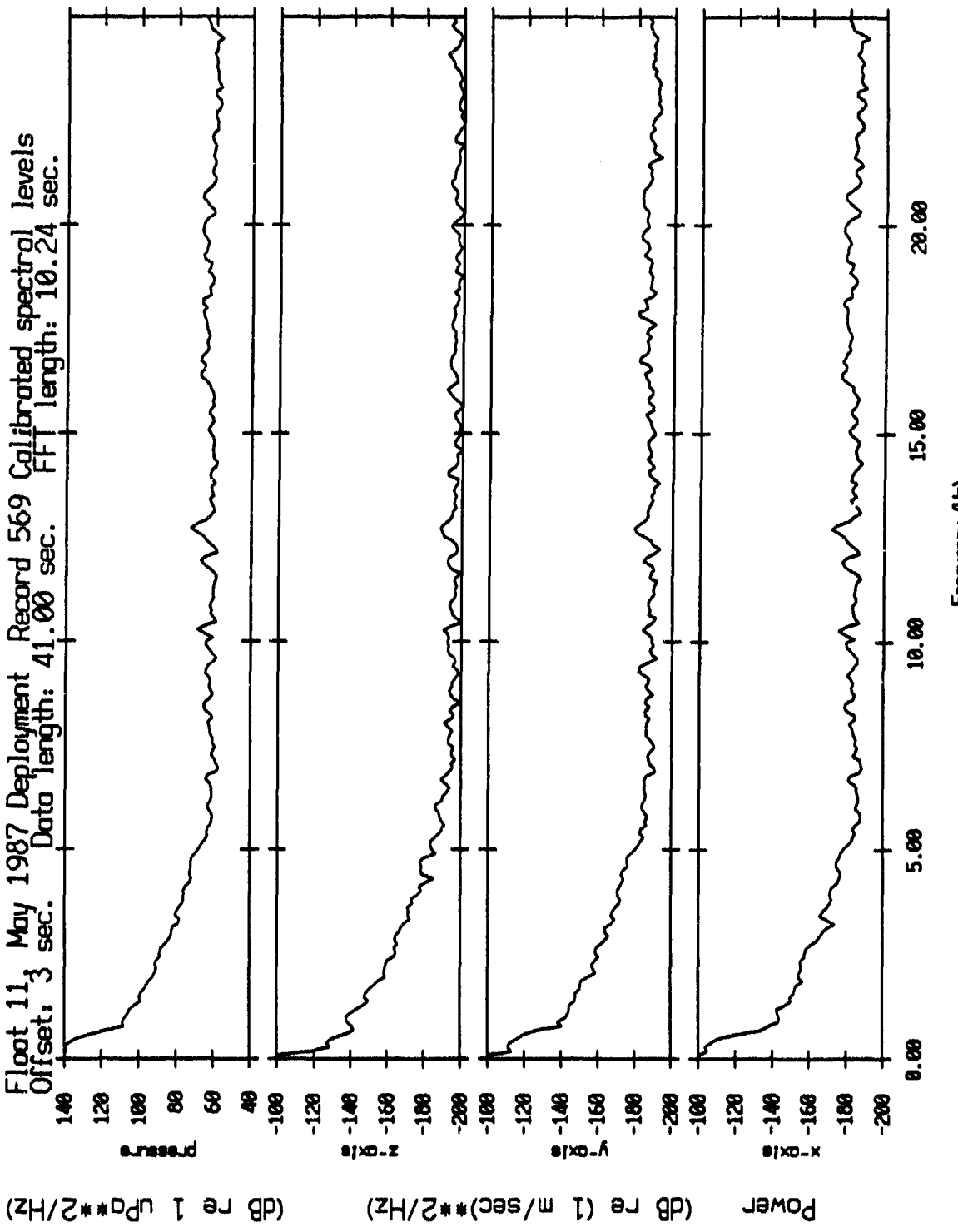

Figure IV.39d

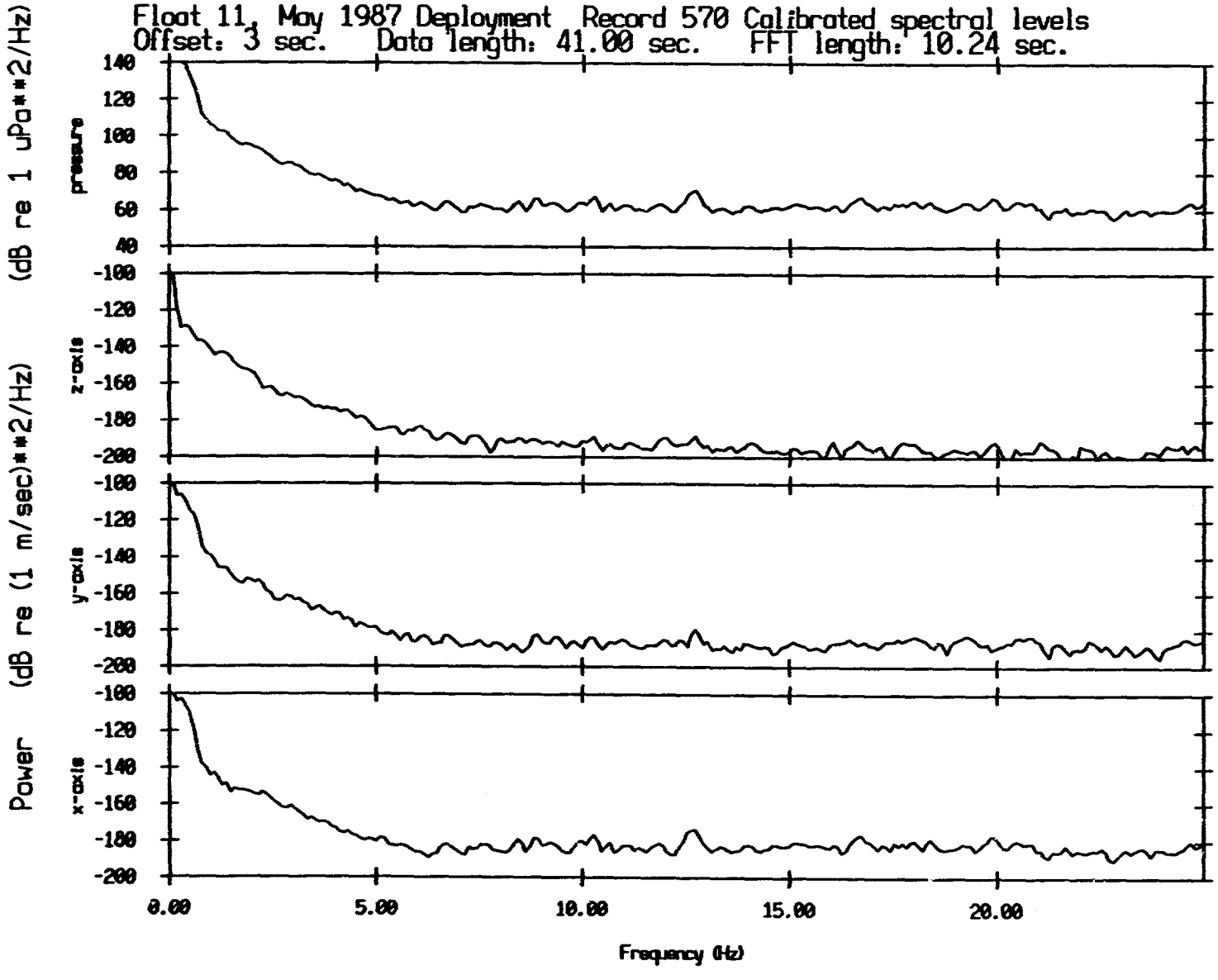

Figure IV.39e

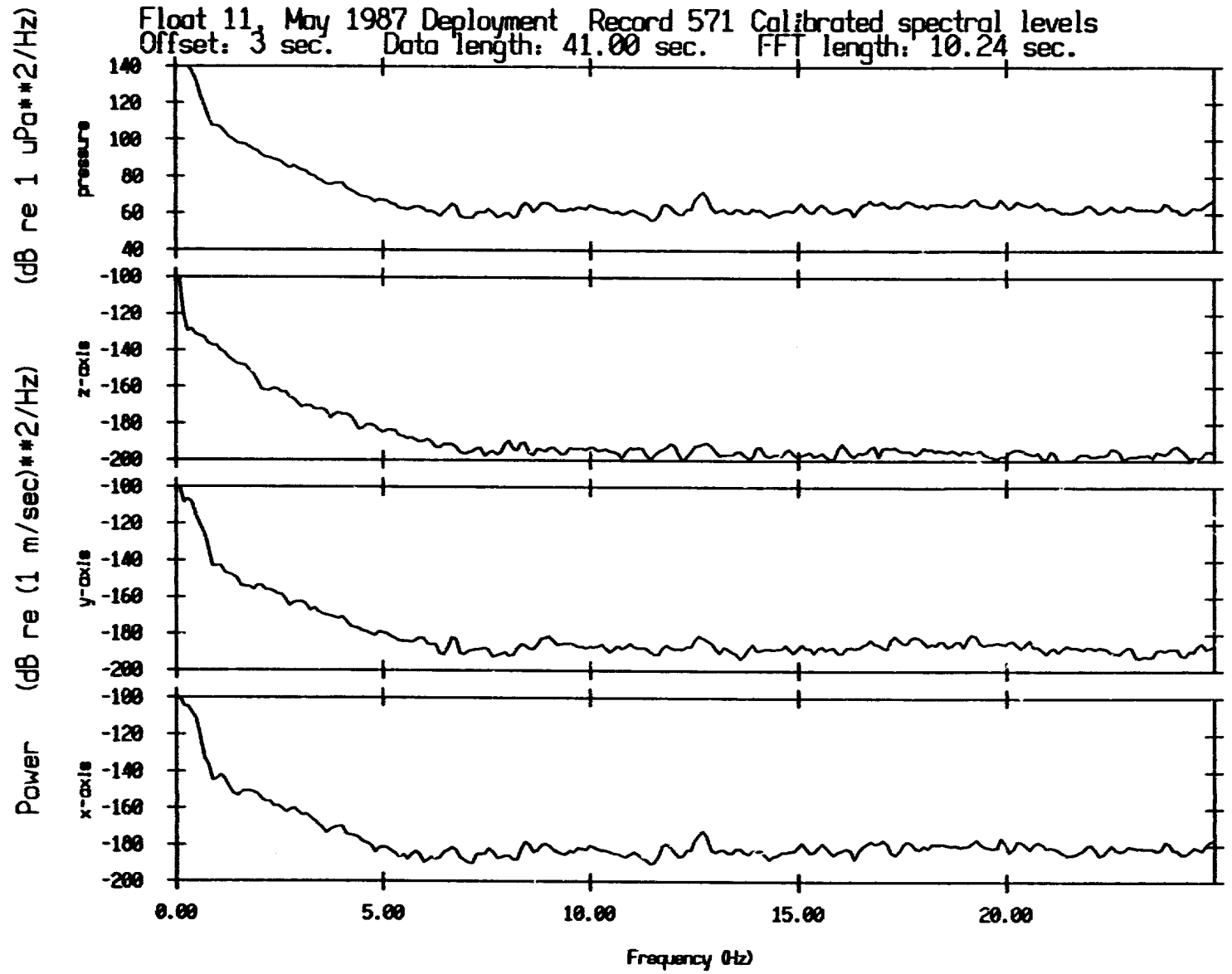

Figure IV.36f

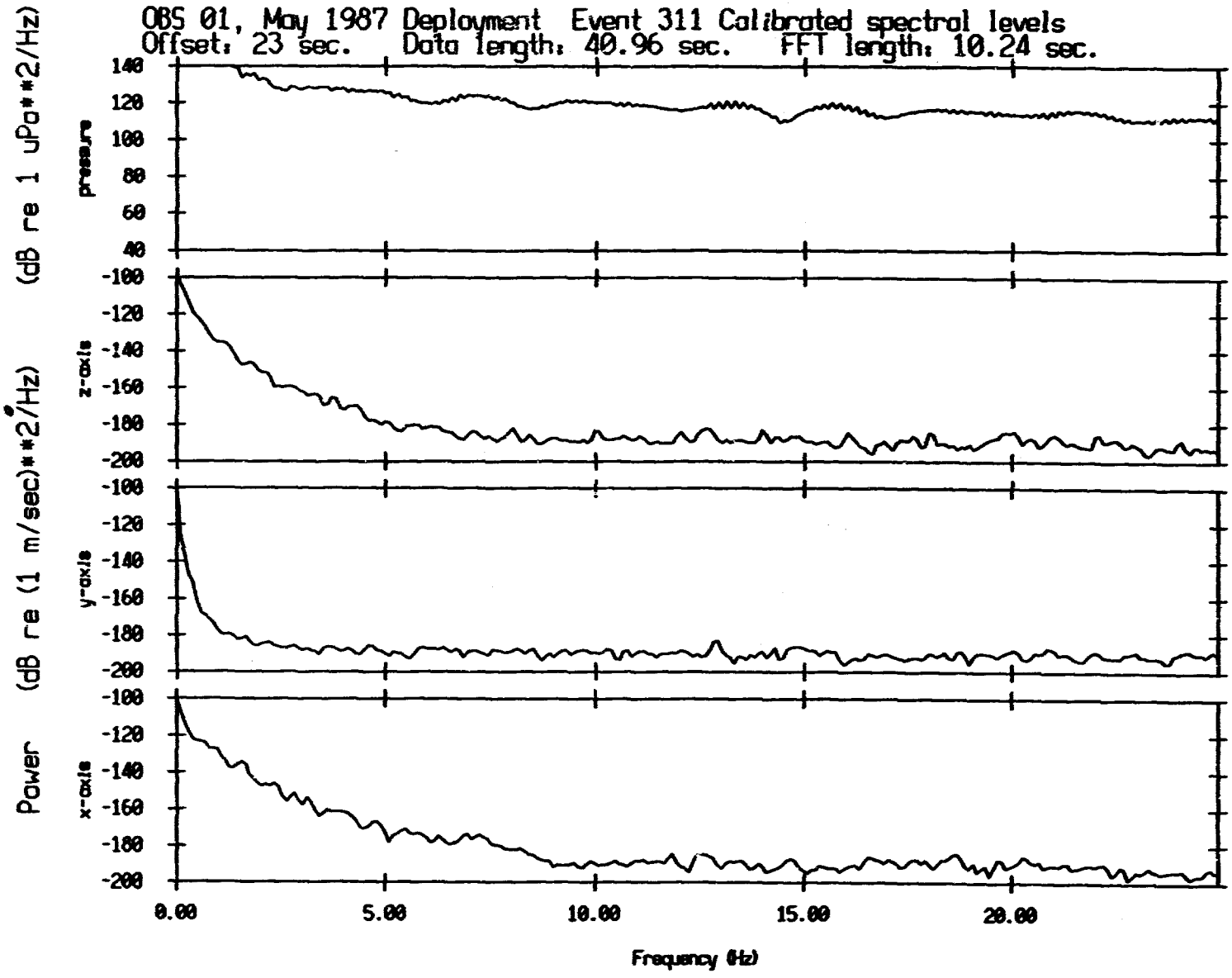
OBS 01, May 1987 Deployment Event 311 Calibrated spectral levels
Offset: 23 sec. Data length: 40.96 sec. FFT length: 10.24 sec.
Power (dB re (1 m/sec)**2/Hz) (dB re 1 uPa**2/Hz)
pressure
z-axis
y-axis
x-axis
140
120
100
80
60
40
-100
-120
-140
-160
-180
-200
0.00
5.00
10.00
15.00
20.00
Frequency (Hz)

Figure IV.40

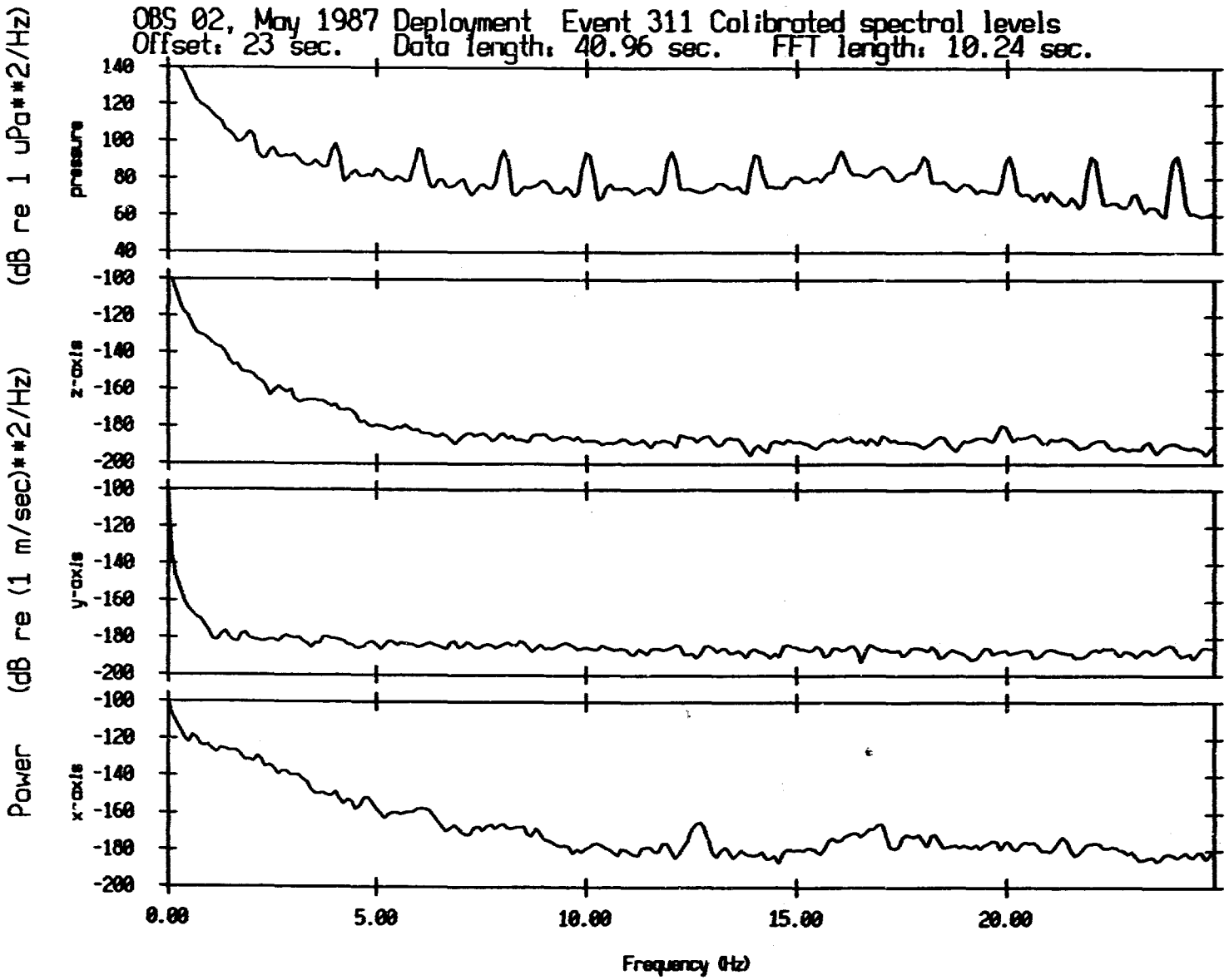
OBS 02, May 1987 Deployment Event 311 Colibrated spectral levels
Offset: 23 sec. Data length: 40.96 sec. FFT length: 10.24 sec.
Power (dB re (1 m/sec)**2/Hz) (dB re 1 uPa**2/Hz)
pressure
z-axis
y-axis
x-axis
140
120
100
80
60
40
-100
-120
-140
-160
-180
-200
0.00
5.00
10.00
15.00
20.00
Frequency (Hz)

Figure IV.41

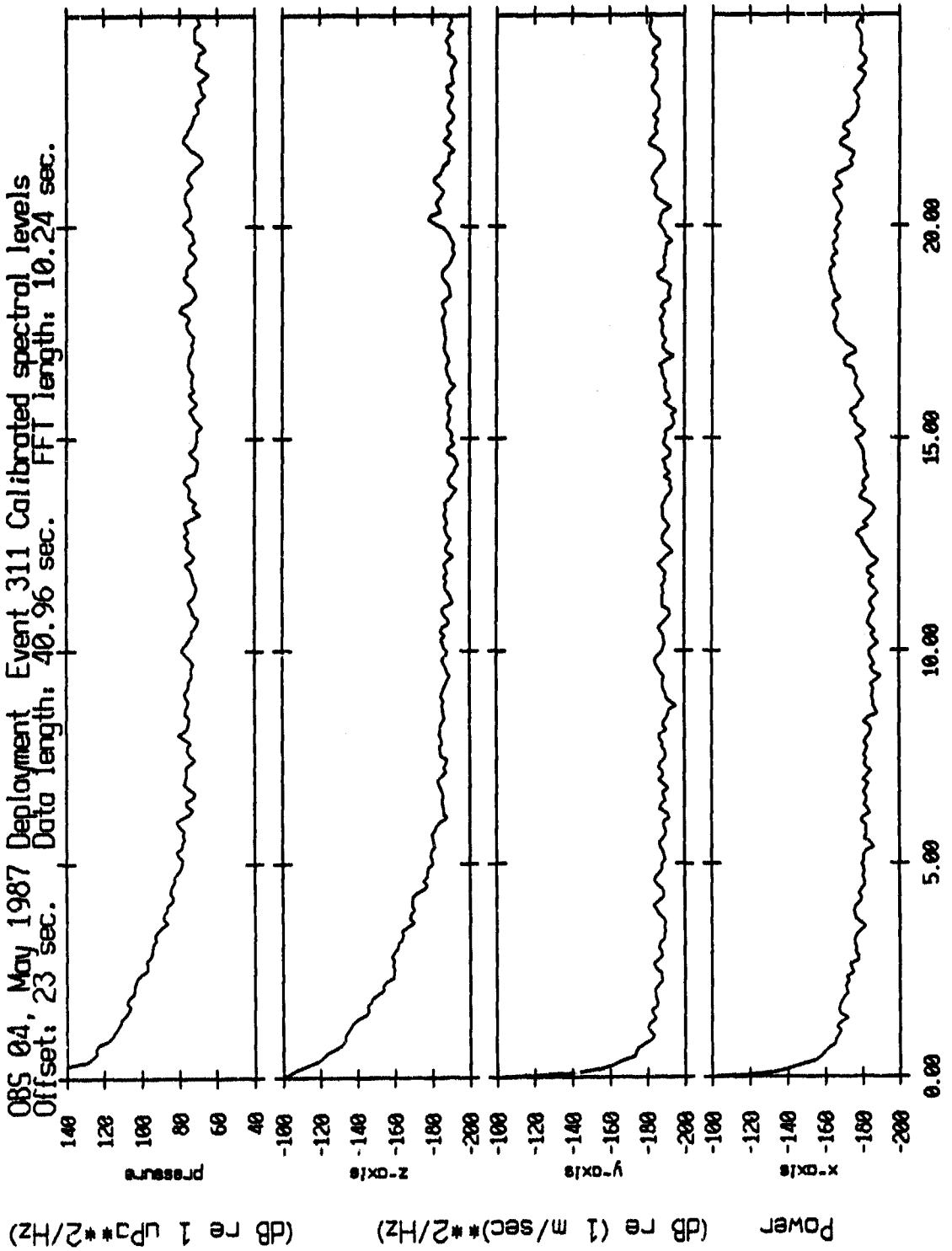
OBS 04, May 1987 Deployment Event 311 Calibrated spectral levels
Offset: 23 sec. Data length: 40.96 sec. FFT length: 10.24 sec.
Pressure
z-axis
y-axis
x-axis
Power
(dB re 1 uPa**2/Hz)
(dB re (1 m/sec)**2/Hz)
Frequency (Hz)
0.00
5.00
10.00
15.00
20.00

Figure IV.42

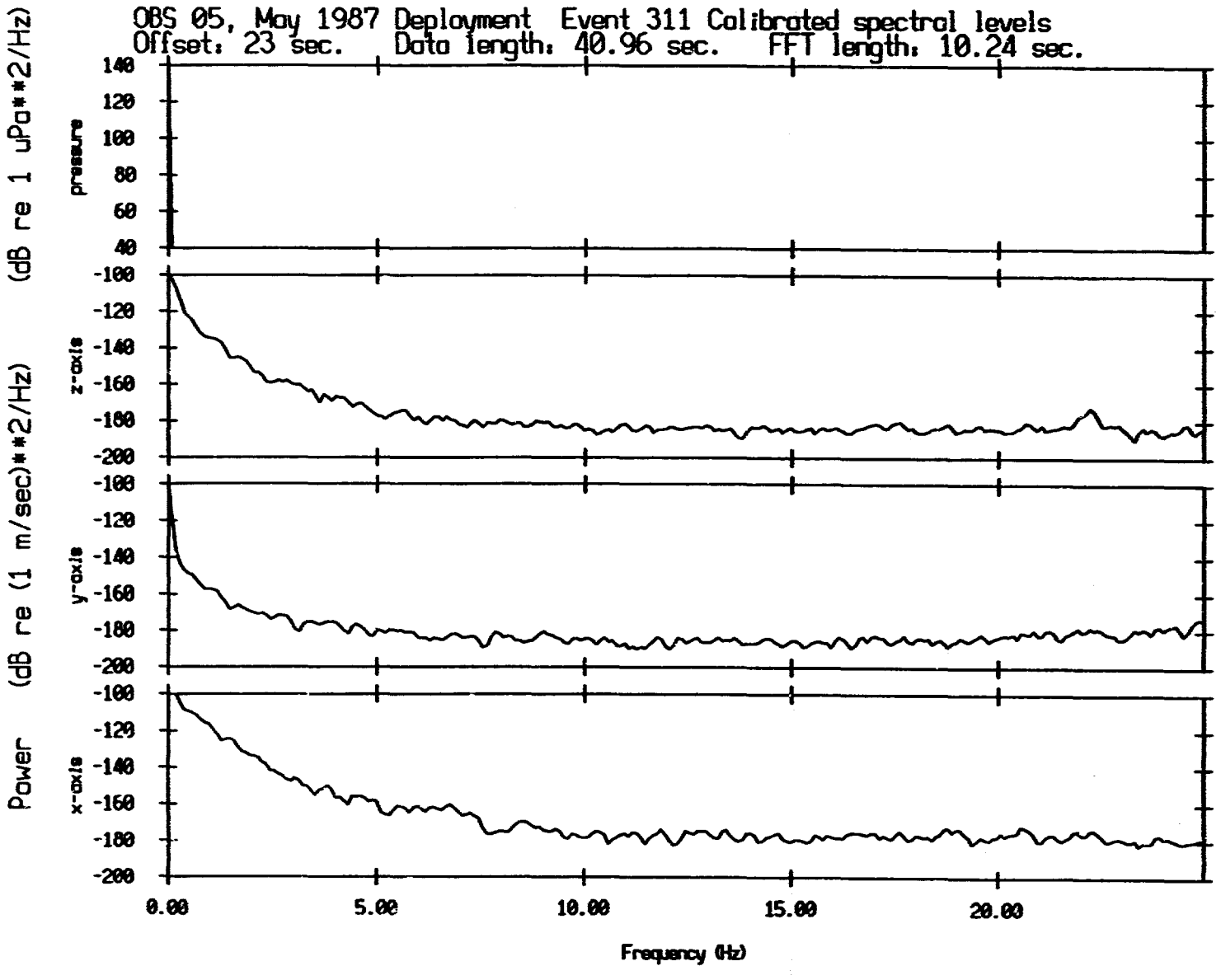
OBS 05, May 1987 Deployment Event 311 Calibrated spectral levels
Offset: 23 sec. Data length: 40.96 sec. FFT length: 10.24 sec.
Power (dB re (1 m/sec)**2/Hz) (dB re 1 uPa**2/Hz)
pressure
z-axis
y-axis
x-axis
140
120
100
80
60
40
-100
-120
-140
-160
-180
-200
-100
-120
-140
-160
-180
-200
-100
-120
-140
-160
-180
-200
0.00
5.00
10.00
15.00
20.00
Frequency (Hz)

Figure IV.43

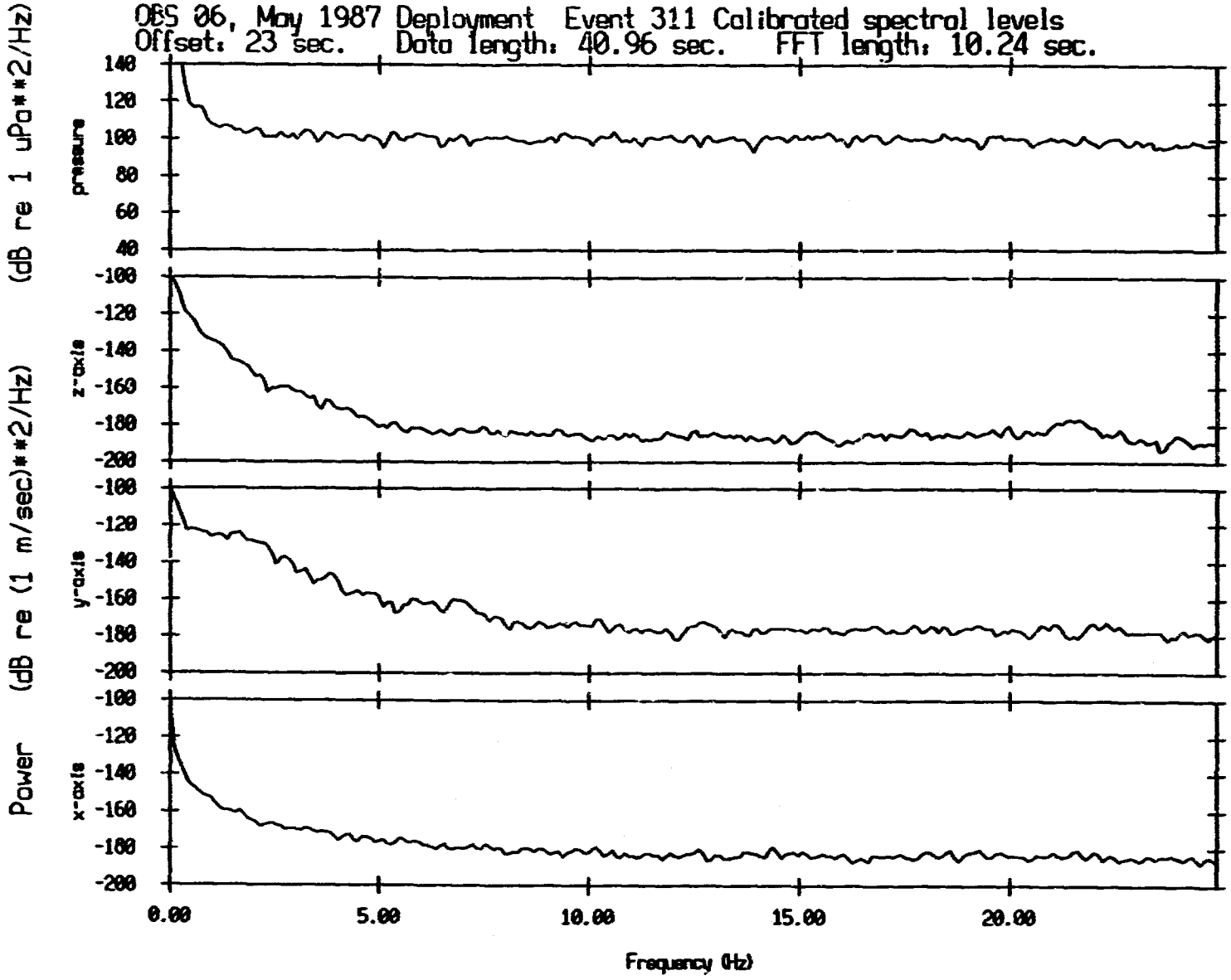
OBS 06, May 1987 Deployment Event 311 Calibrated spectral levels
Offset: 23 sec. Data length: 40.96 sec. FFT length: 10.24 sec.
Power (dB re (1 m/sec)**2/Hz) (dB re 1 uPa**2/Hz)
pressure
z-axis
y-axis
x-axis
140
120
100
80
60
40
-100
-120
-140
-160
-180
-200
0.00
5.00
10.00
15.00
20.00
Frequency (Hz)

Figure IV.44

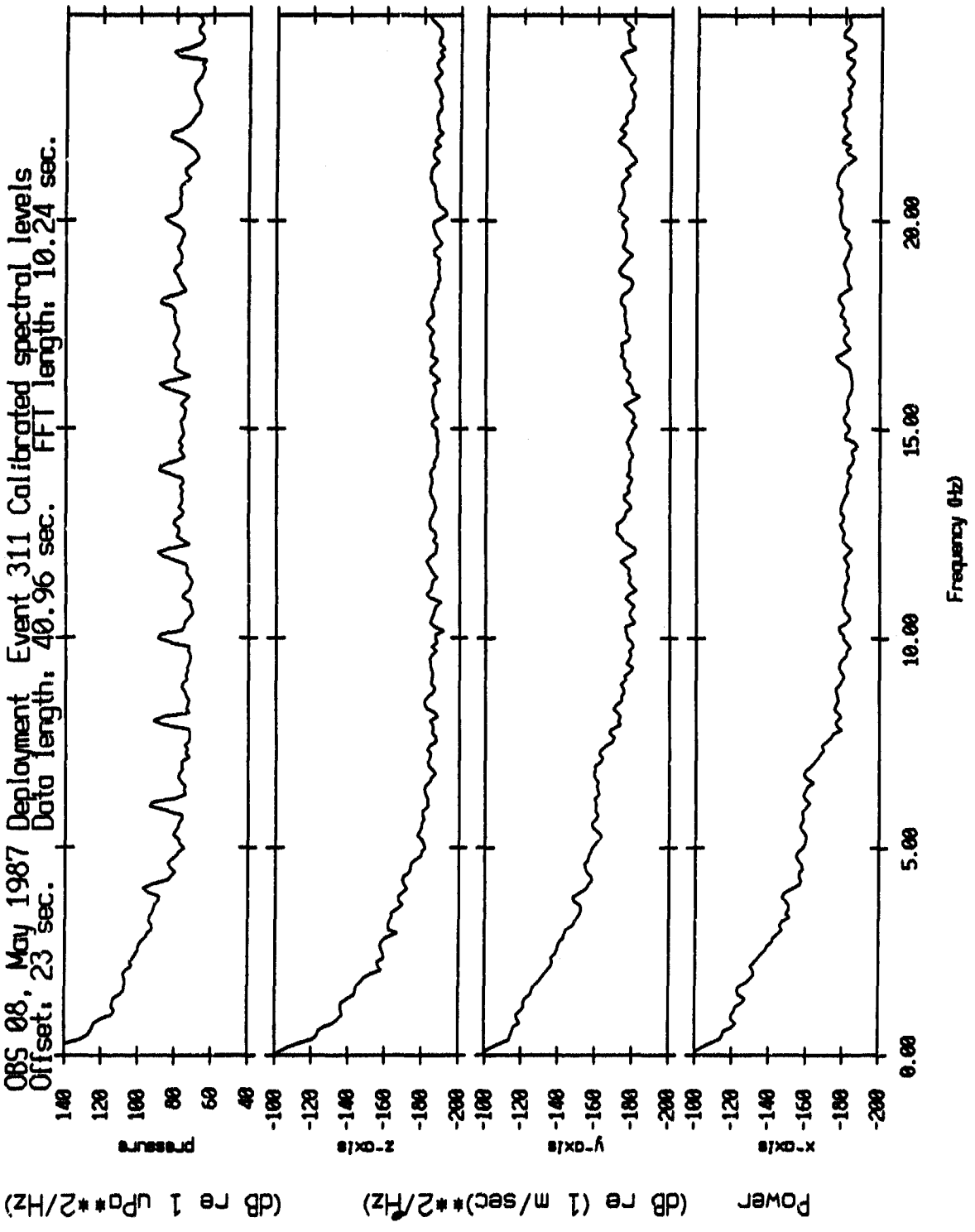
OBS 08, May 1987 Deployment Event 311 Calibrated spectral levels
Offset: 23 sec. Data length: 40.96 sec. FFT length: 10.24 sec.
pressure
z-axis
y-axis
x-axis
Power (dB re (1 m/sec)**2/Hz)
(dB re 1 uPa**2/Hz)
Frequency (Hz)
0.00
5.00
10.00
15.00
20.00

Figure IV.45

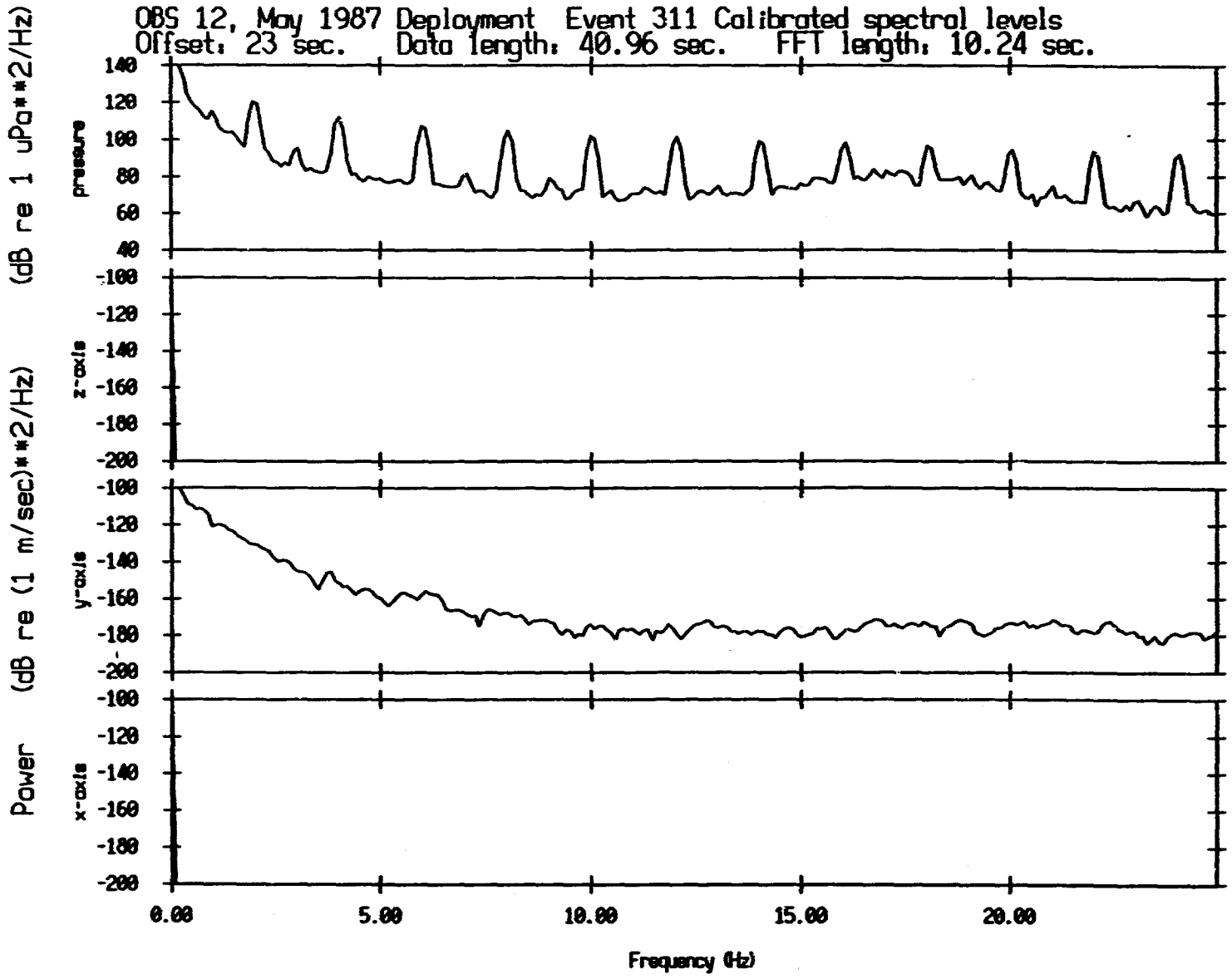
OBS 12, May 1987 Deployment Event 311 Calibrated spectral levels
Offset: 23 sec. Data length: 40.96 sec. FFT length: 10.24 sec.
Power (dB re (1 m/sec)**2/Hz) (dB re 1 uPa**2/Hz)
pressure
z-axis
y-axis
x-axis
140
120
100
80
60
40
-100
-120
-140
-160
-180
-200
0.00
5.00
10.00
15.00
20.00
Frequency (Hz)

Figure IV.46

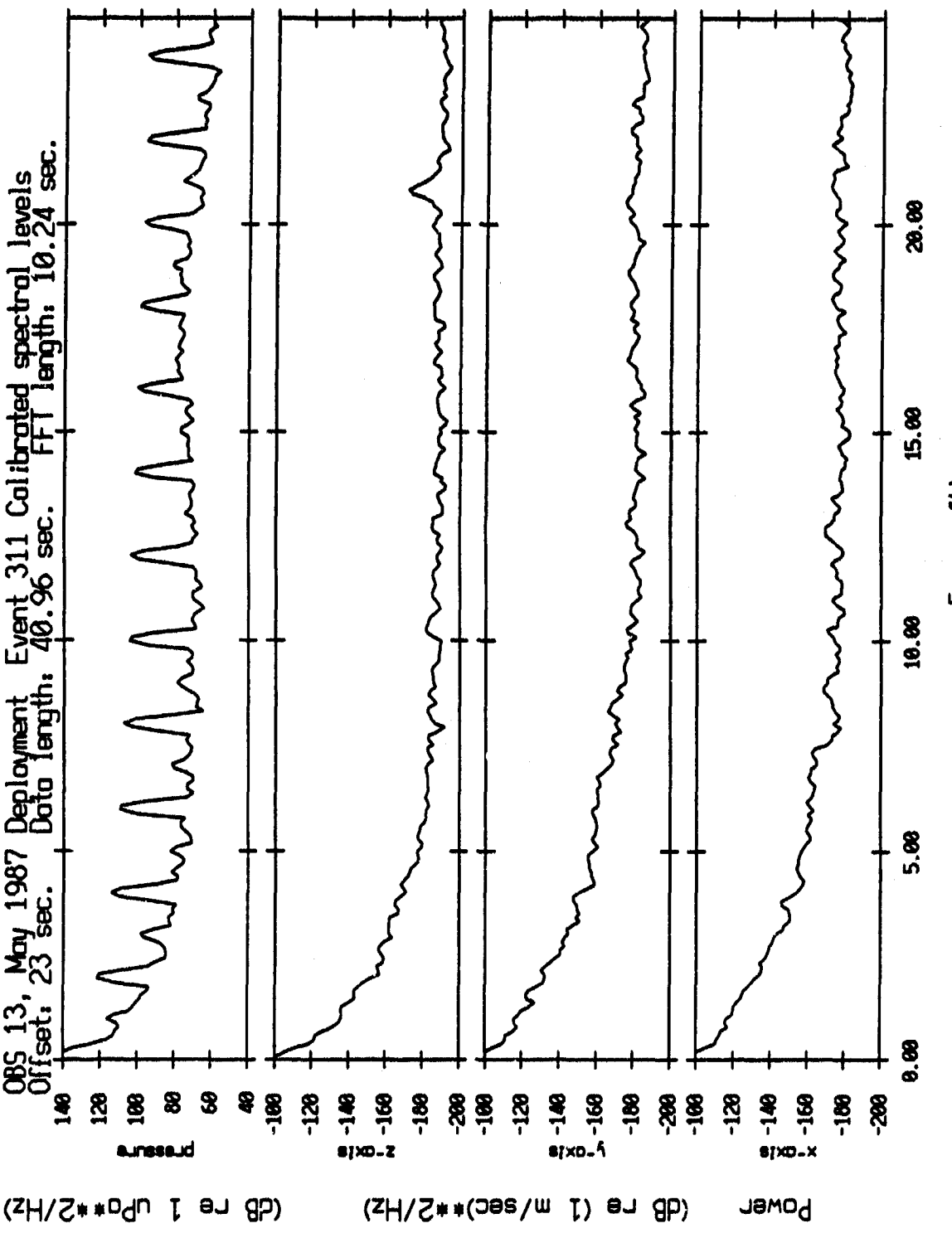
OBS 13, May 1987 Deployment Event 311 Calibrated spectral levels
Offset: 23 sec. Data length: 40.96 sec. FFT length: 10.24 sec.
pressure
z-axis
y-axis
x-axis
(dB re 1 uPa**2/Hz)
(dB re (1 m/sec)**2/Hz)
Power
Frequency (Hz)

Figure IV.47

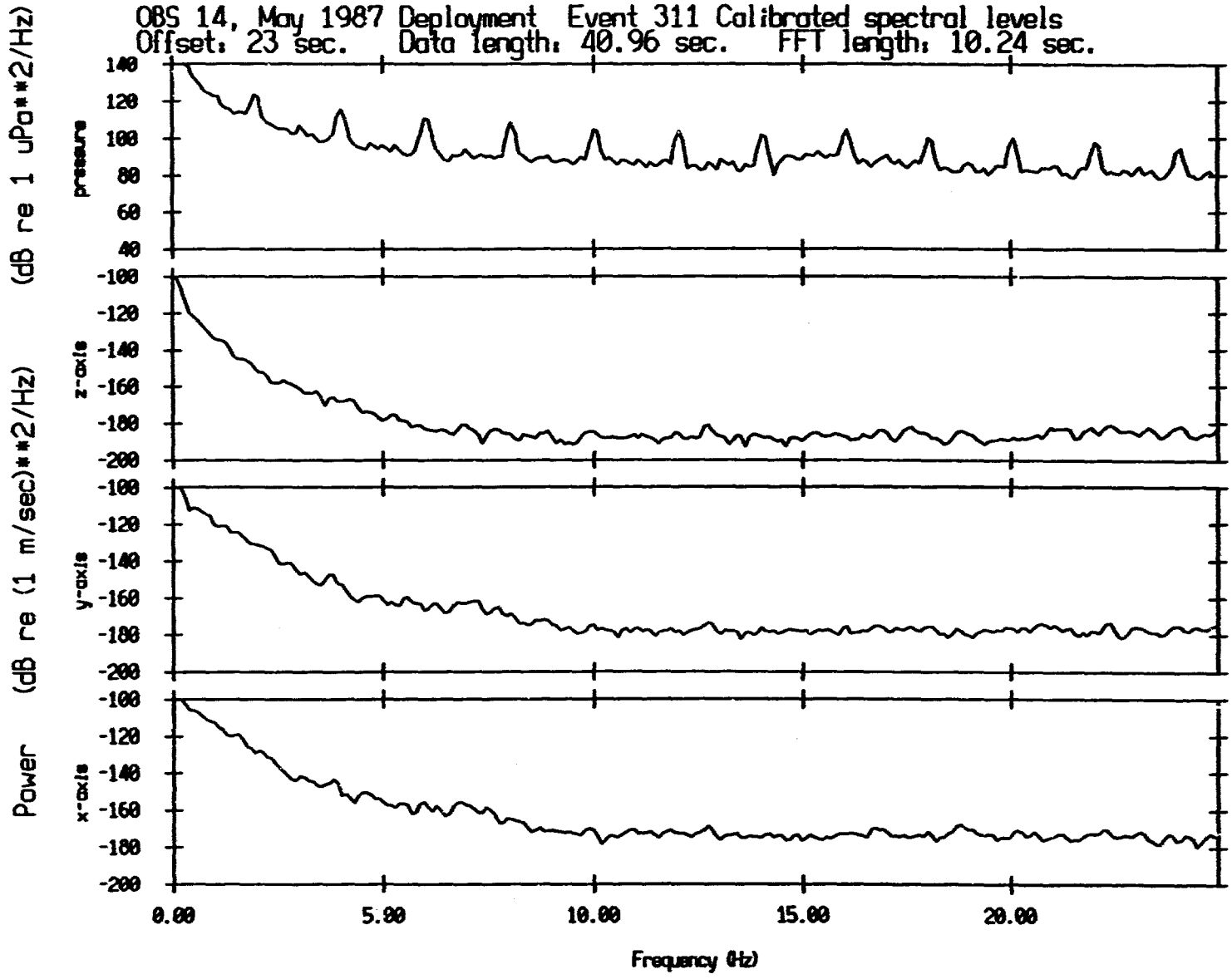
OBS 14, May 1987 Deployment Event 311 Calibrated spectral levels
Offset: 23 sec. Data length: 40.96 sec. FFT length: 10.24 sec.
Power (dB re (1 m/sec)**2/Hz) (dB re 1 uPa**2/Hz)
pressure
z-axis
y-axis
x-axis
140
120
100
80
60
40
-100
-120
-140
-160
-180
-200
0.00
5.00
10.00
15.00
20.00
Frequency (Hz)

Figure IV.48

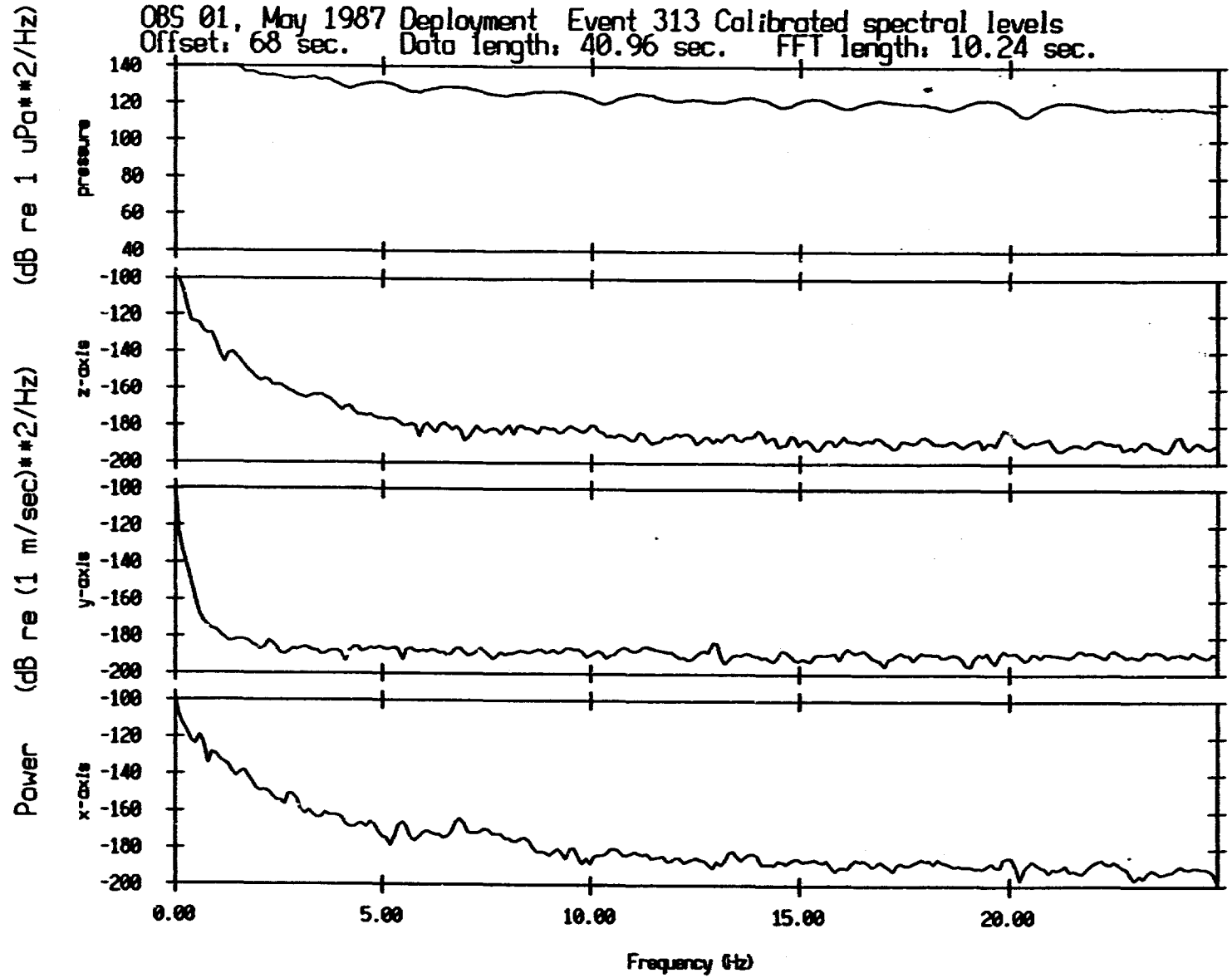
OBS 01, May 1987 Deployment Event 313 Calibrated spectral levels
Offset: 68 sec. Data length: 40.96 sec. FFT length: 10.24 sec.
Power (dB re (1 m/sec)**2/Hz) (dB re 1 uPa**2/Hz)
pressure
z-axis
y-axis
x-axis
140
120
100
80
60
40
-100
-120
-140
-160
-180
-200
0.00
5.00
10.00
15.00
20.00
Frequency (Hz)

Figure IV.49

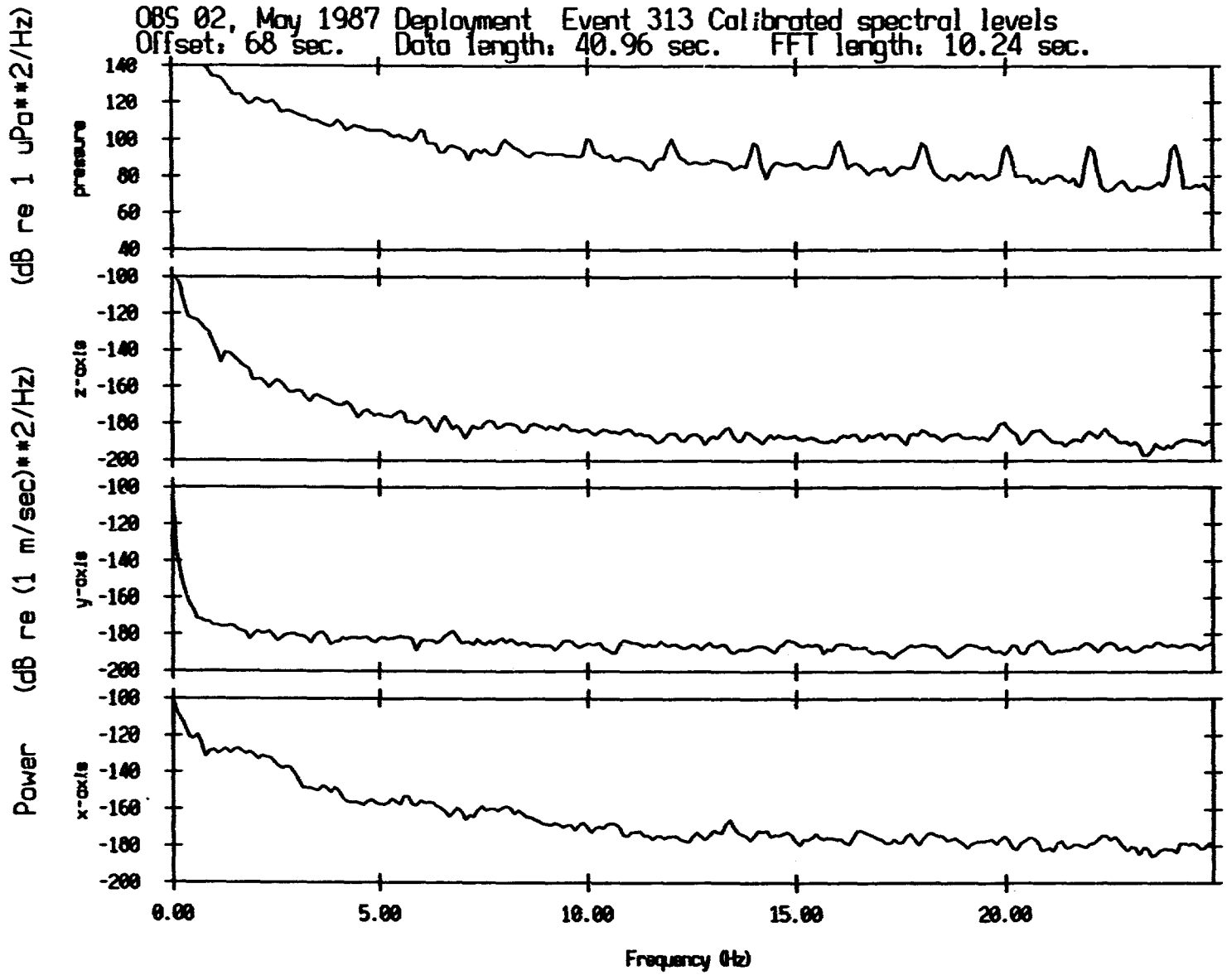
OBS 02, May 1987 Deployment Event 313 Calibrated spectral levels
Offset: 68 sec. Data length: 40.96 sec. FFT length: 10.24 sec.
Power (dB re (1 m/sec)**2/Hz) (dB re 1 uPa**2/Hz)
pressure
z-axis
y-axis
x-axis
140
120
100
80
60
40
-100
-120
-140
-160
-180
-200
0.00
5.00
10.00
15.00
20.00
Frequency (Hz)

Figure IV.50

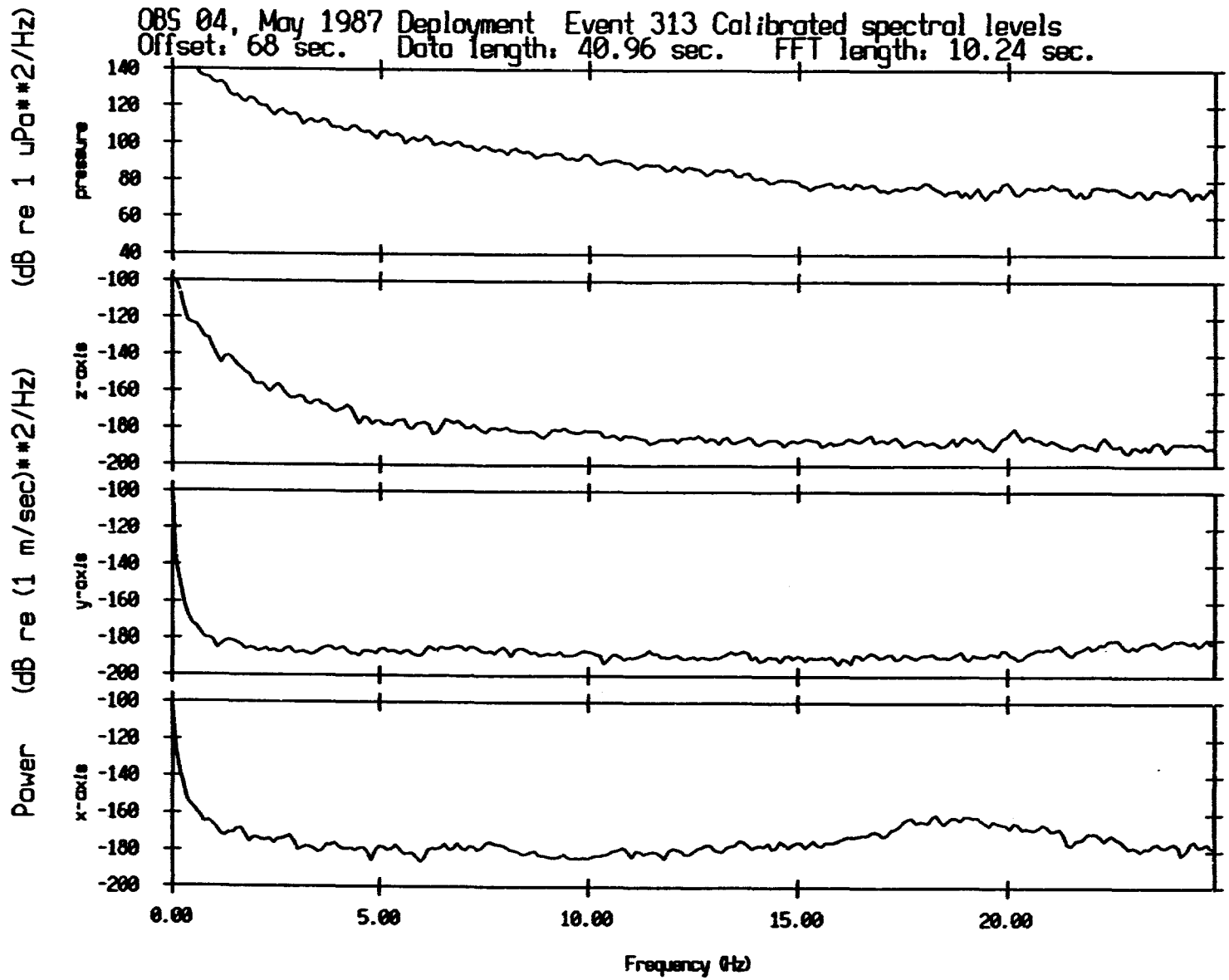
OBS 04, May 1987 Deployment Event 313 Calibrated spectral levels
Offset: 68 sec. Data length: 40.96 sec. FFT length: 10.24 sec.
Power (dB re (1 m/sec)**2/Hz) (dB re 1 uPa**2/Hz)
pressure
z-axis
y-axis
x-axis
140
120
100
80
60
40
-100
-120
-140
-160
-180
-200
0.00
5.00
10.00
15.00
20.00
Frequency (Hz)

Figure IV.51

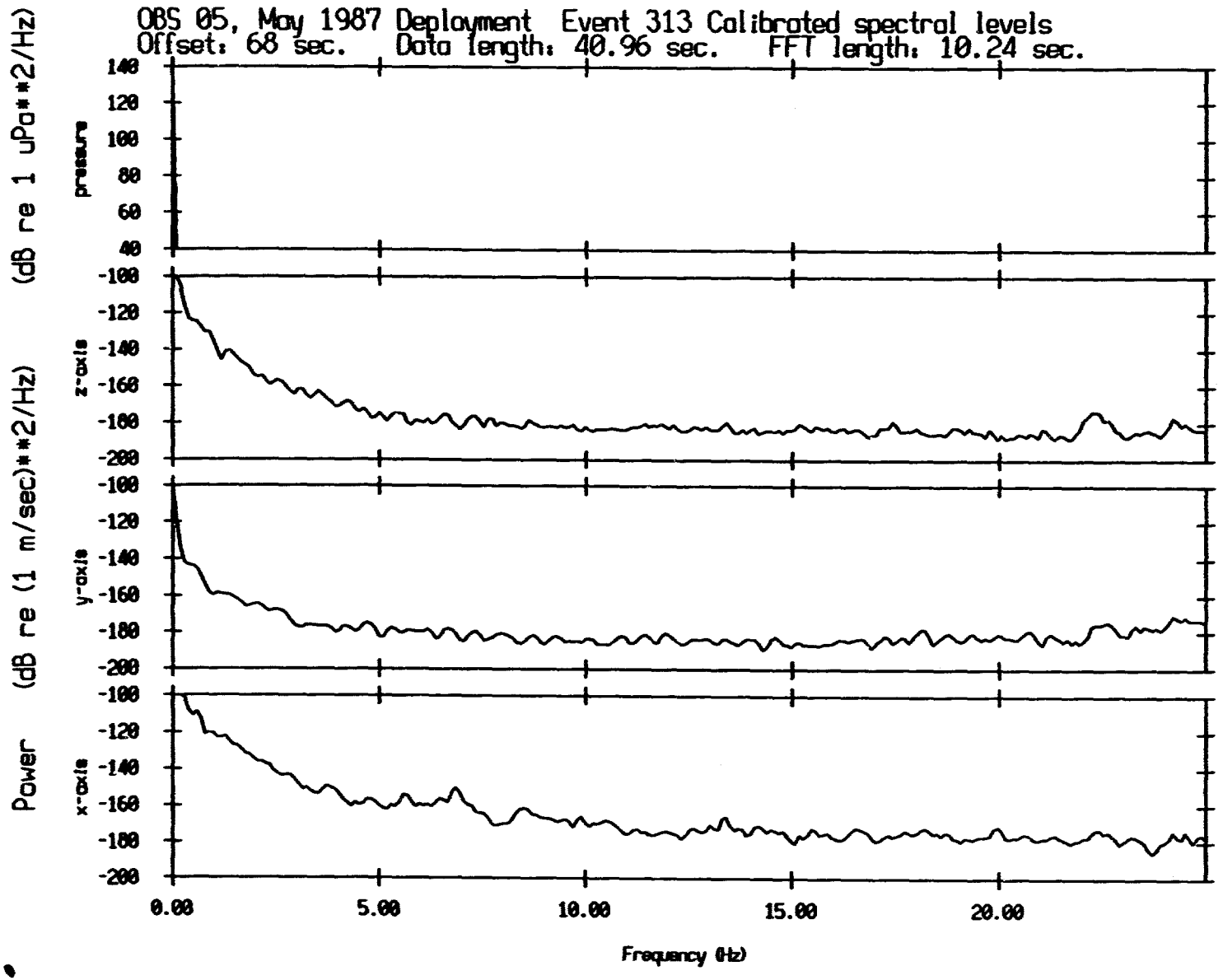
OBS 05, May 1987 Deployment Event 313 Calibrated spectral levels
Offset: 68 sec. Data length: 40.96 sec. FFT length: 10.24 sec.
Power (dB re (1 m/sec)**2/Hz) (dB re 1 uPa**2/Hz)
pressure
z-axis
y-axis
x-axis
140
120
100
80
60
40
-100
-120
-140
-160
-180
-200
0.00
5.00
10.00
15.00
20.00
Frequency (Hz)

Figure IV.52

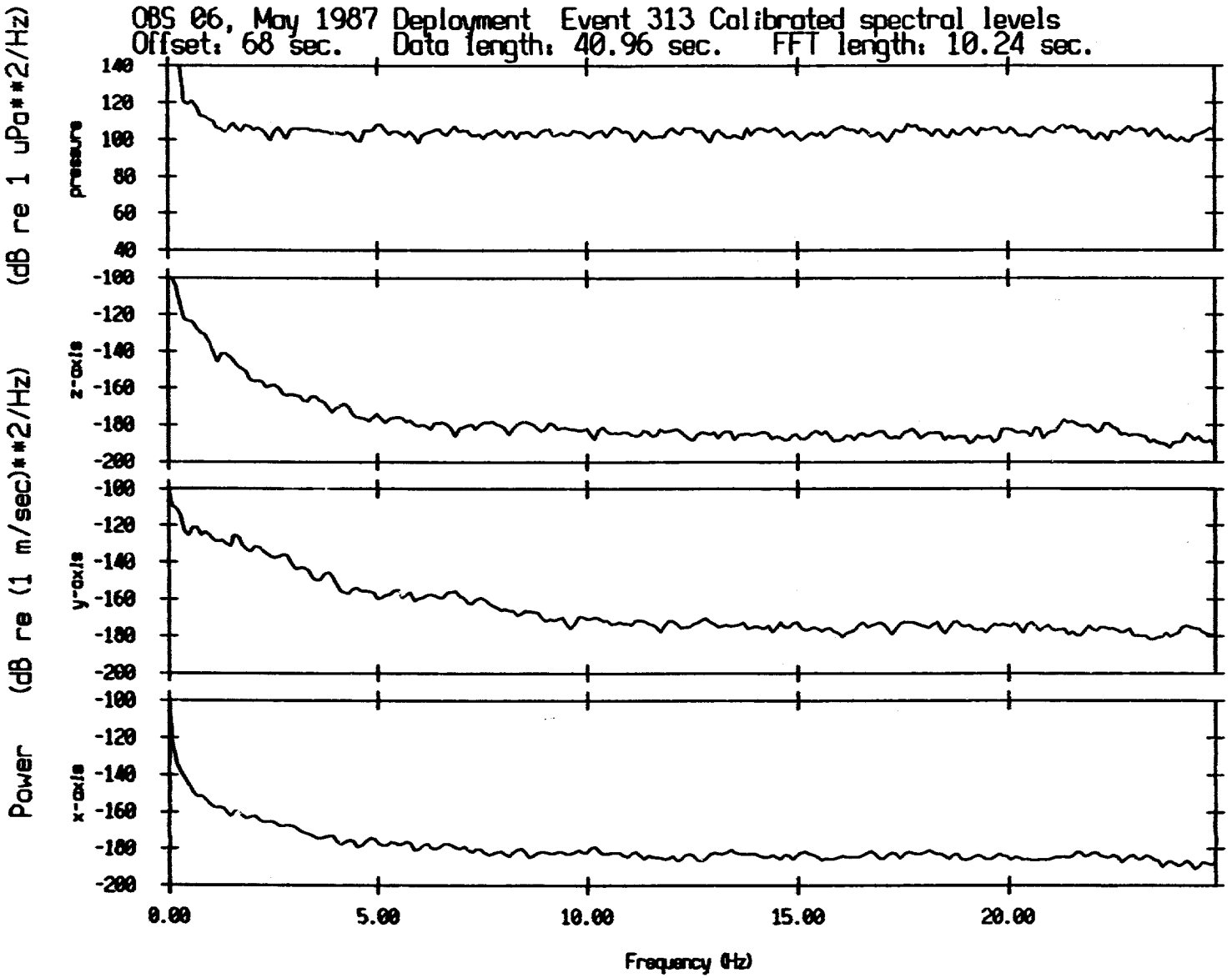
OBS 06, May 1987 Deployment Event 313 Calibrated spectral levels
Offset: 68 sec. Data length: 40.96 sec. FFT length: 10.24 sec.
Power (dB re (1 m/sec)**2/Hz) (dB re 1 uPa**2/Hz)
pressure
z-axis
y-axis
x-axis
140
120
100
80
60
40
-100
-120
-140
-160
-180
-200
0.00
5.00
10.00
15.00
20.00
Frequency (Hz)

Figure IV.53

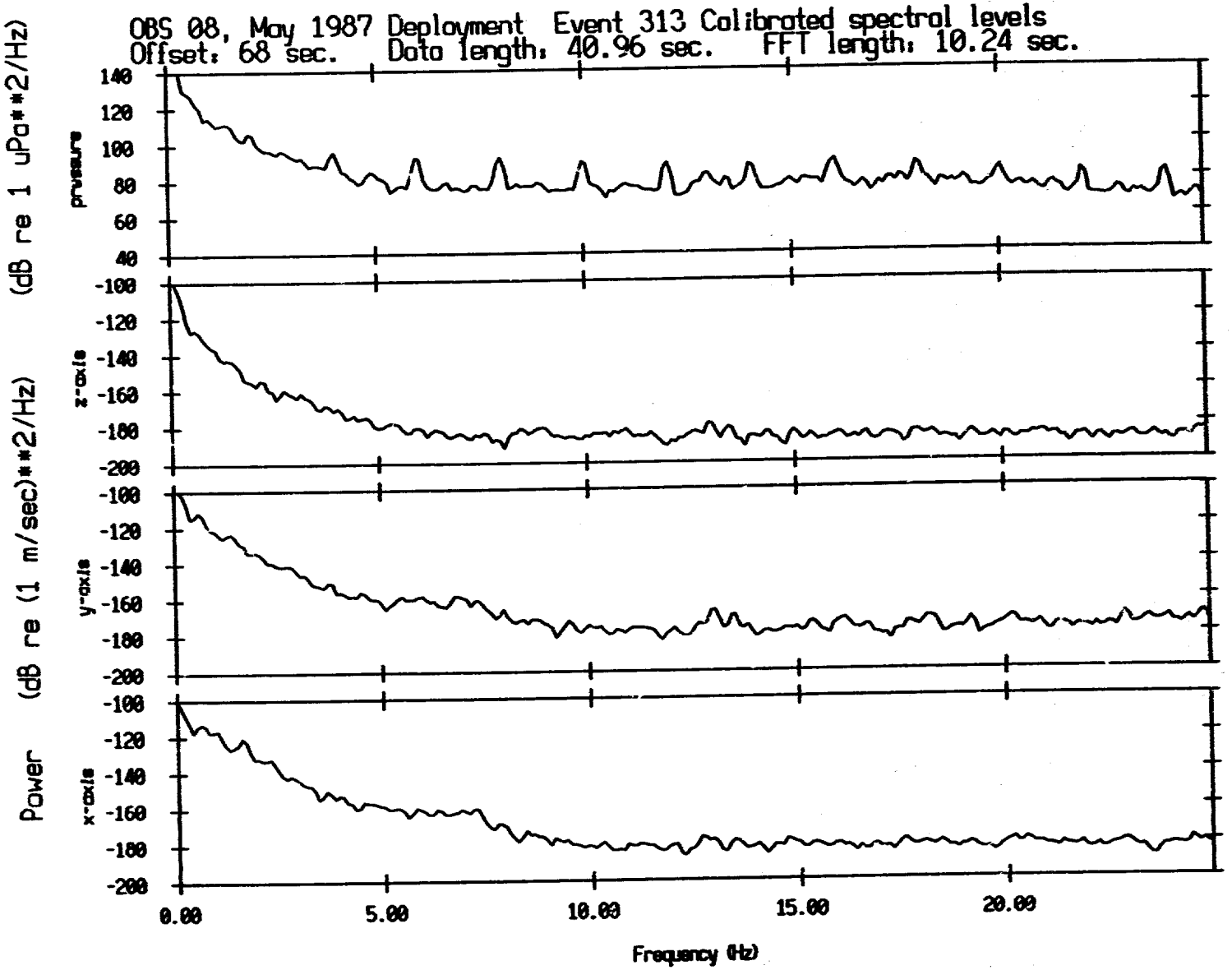
OBS 08, May 1987 Deployment Event 313 Calibrated spectral levels
Offset: 68 sec. Data length: 40.96 sec. FFT length: 10.24 sec.
Power (dB re (1 m/sec)**2/Hz) (dB re 1 uPa**2/Hz)
pressure
z-axis
y-axis
x-axis
140
120
100
80
60
40
-100
-120
-140
-160
-180
-200
0.00
5.00
10.00
15.00
20.00
Frequency (Hz)

Figure IV.54

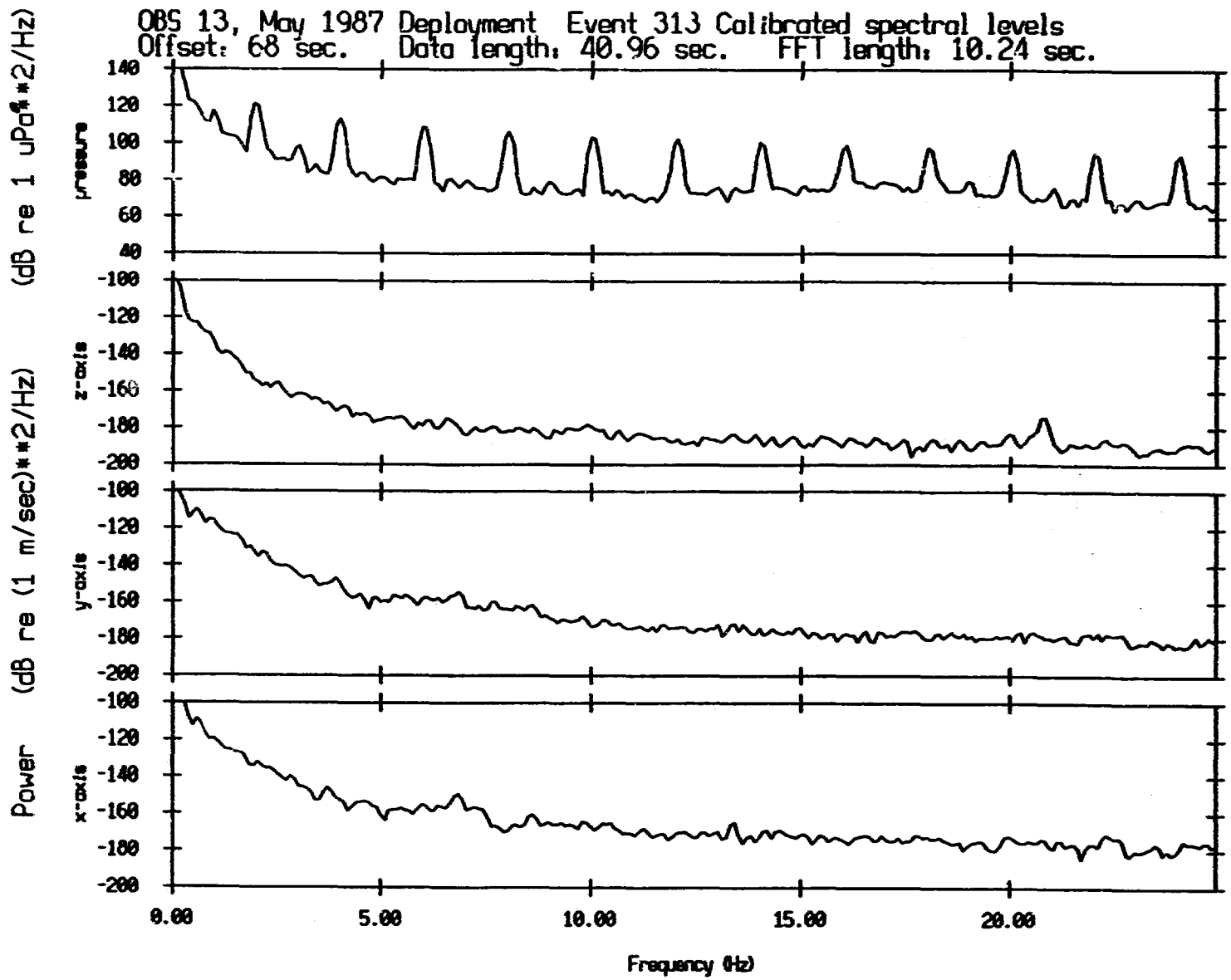
OBS 13, May 1987 Deployment Event 313 Calibrated spectral levels
Offset: 68 sec. Data length: 40.96 sec. FFT length: 10.24 sec.
Power (dB re (1 m/sec)**2/Hz) (dB re 1 uPa**2/Hz)
pressure
z-axis
y-axis
x-axis
140
120
100
80
60
40
-100
-120
-140
-160
-180
-200
0.00
5.00
10.00
15.00
20.00
Frequency (Hz)

Figure IV.55

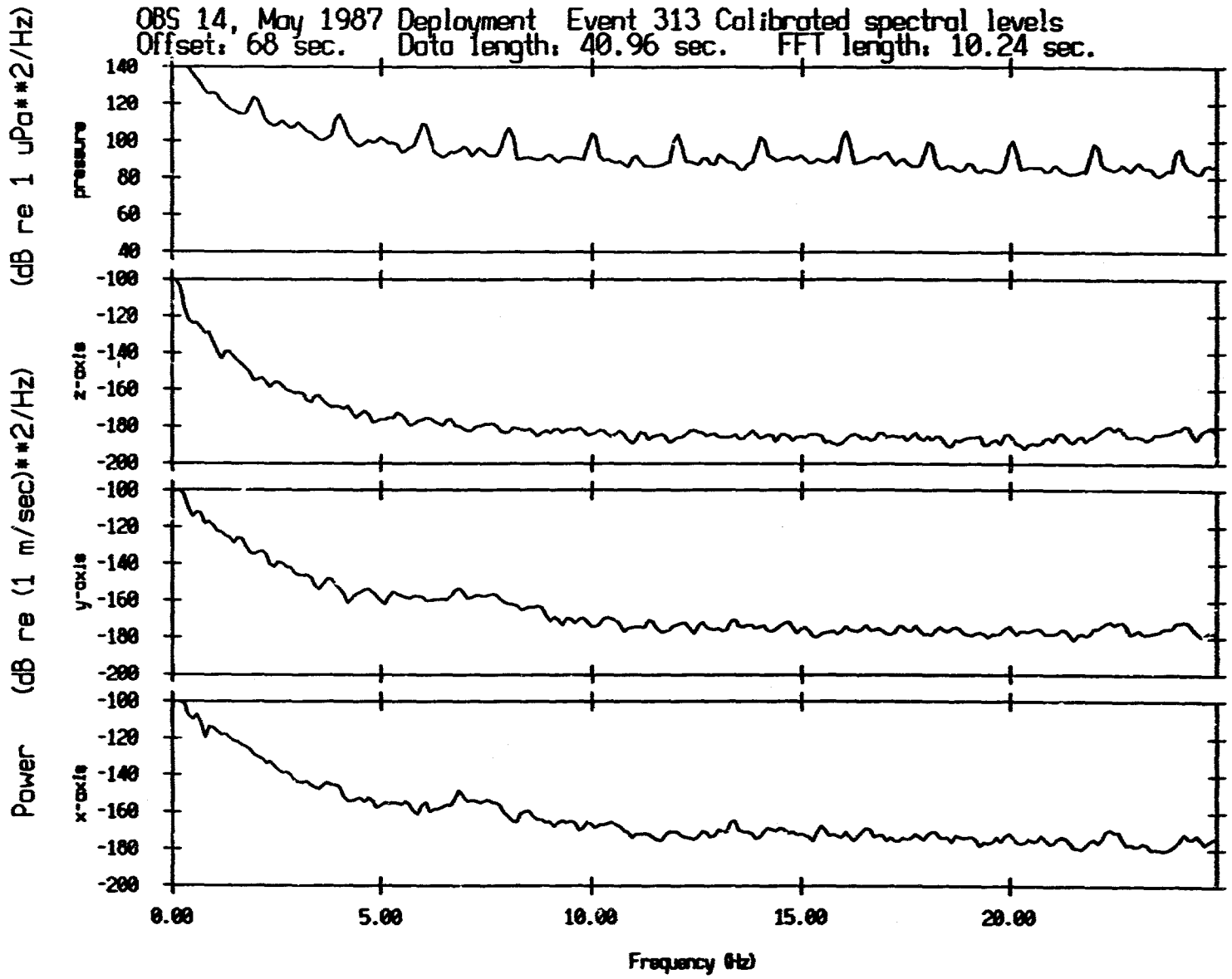
OBS 14, May 1987 Deployment Event 313 Calibrated spectral levels
Offset: 68 sec. Data length: 40.96 sec. FFT length: 10.24 sec.
Power (dB re (1 m/sec)**2/Hz) (dB re 1 uPa**2/Hz)
pressure
z-axis
y-axis
x-axis
140
120
100
80
60
40
-100
-120
-140
-160
-180
-200
0.00
5.00
10.00
15.00
20.00
Frequency (Hz)

Figure IV.58

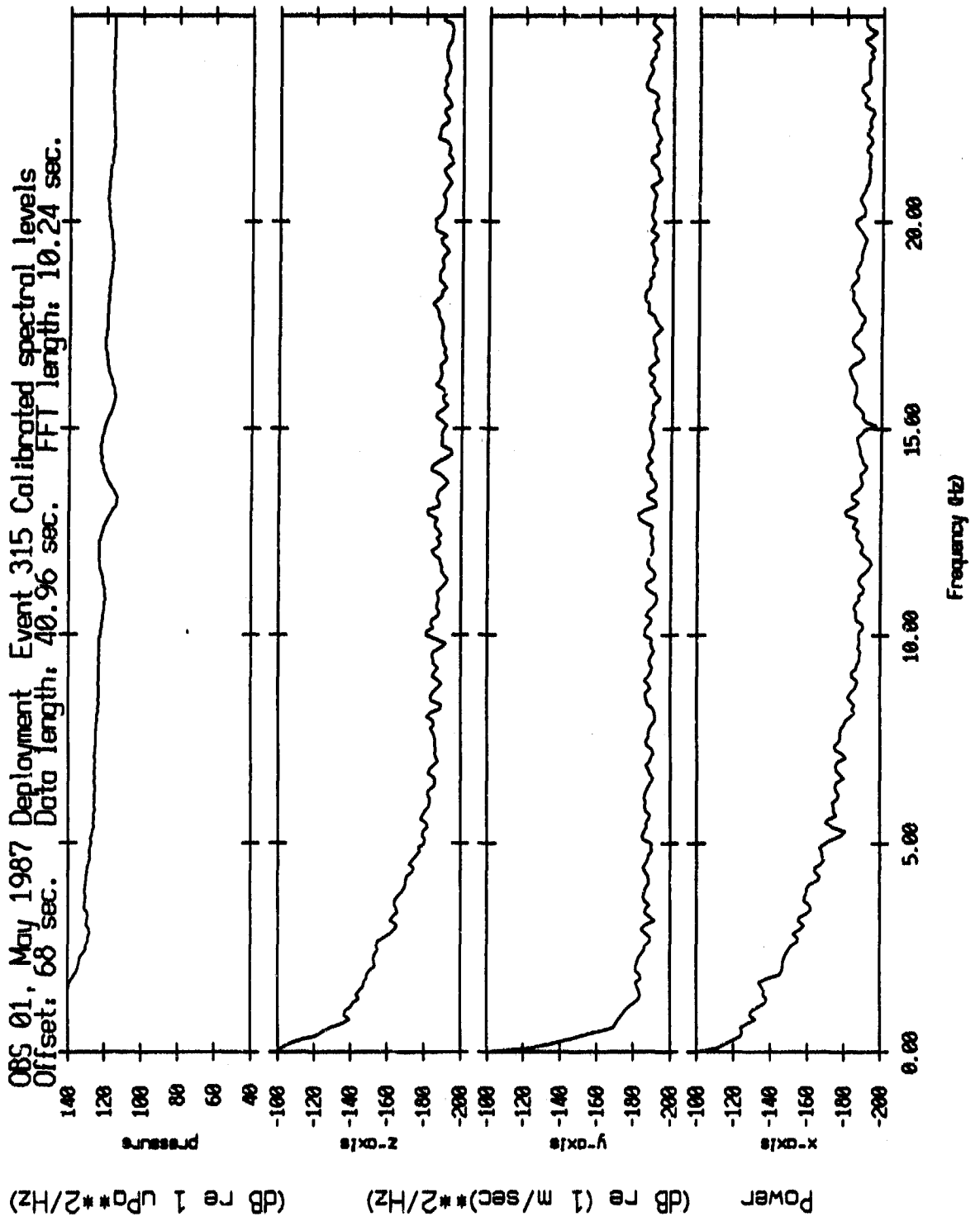
OBS 01, May 1987 Deployment Event 315 Calibrated spectral levels
Offset: 68 sec. Data length: 40.96 sec. FFT length: 10.24 sec.
pressure
z-axis
y-axis
x-axis
Power (dB re (1 m/sec)**2/Hz)
(dB re 1 uPa**2/Hz)
Frequency (Hz)
0.00
5.00
10.00
15.00
20.00

Figure IV.57

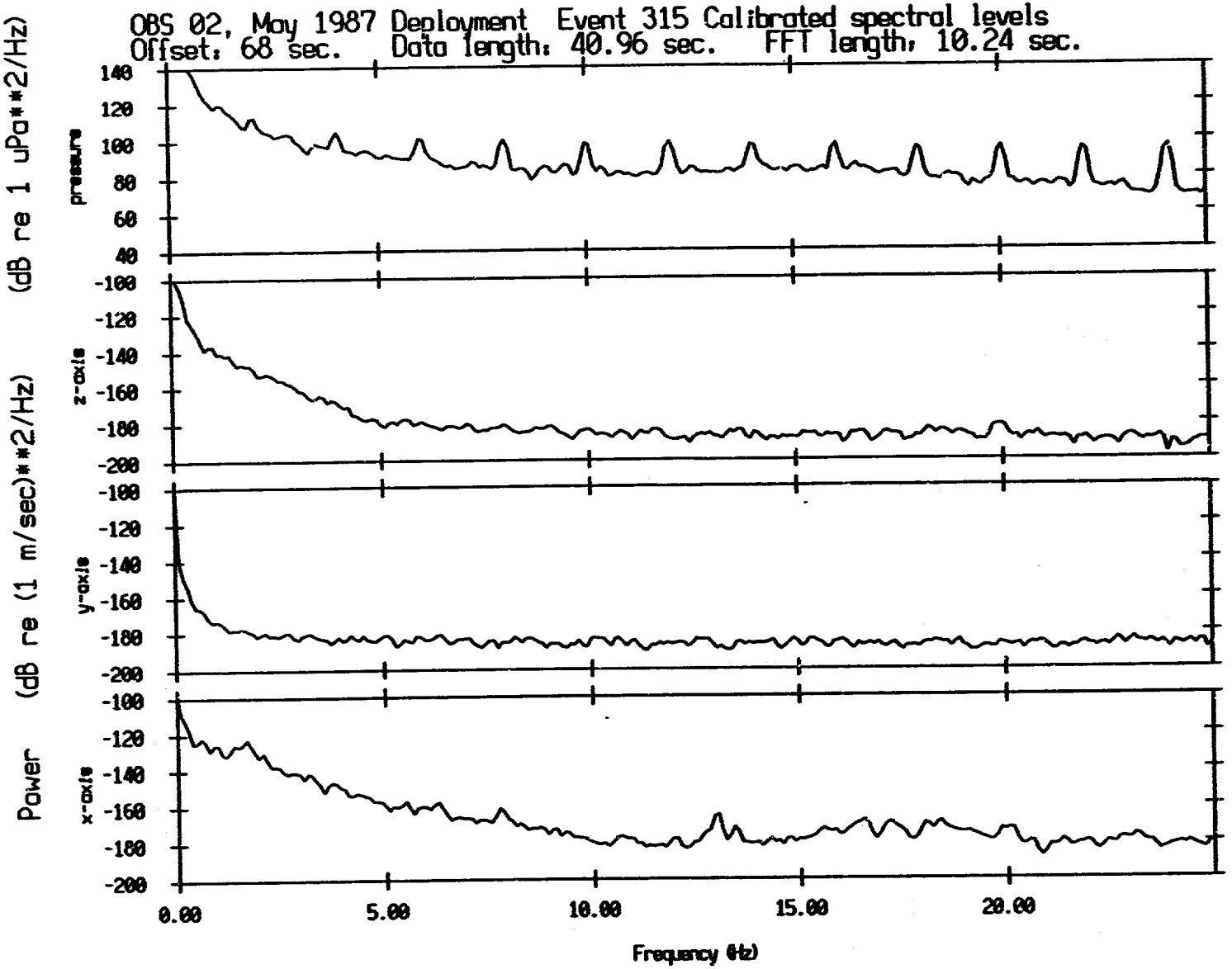
OBS 02, May 1987 Deployment Event 315 Calibrated spectral levels
Offset: 68 sec. Data length: 40.96 sec. FFT length: 10.24 sec.
Power (dB re (1 m/sec)**2/Hz) (dB re 1 uPa**2/Hz)
pressure
z-axis
y-axis
x-axis
140
120
100
80
60
40
-100
-120
-140
-160
-180
-200
0.00
5.00
10.00
15.00
20.00
Frequency (Hz)

Figure IV.58

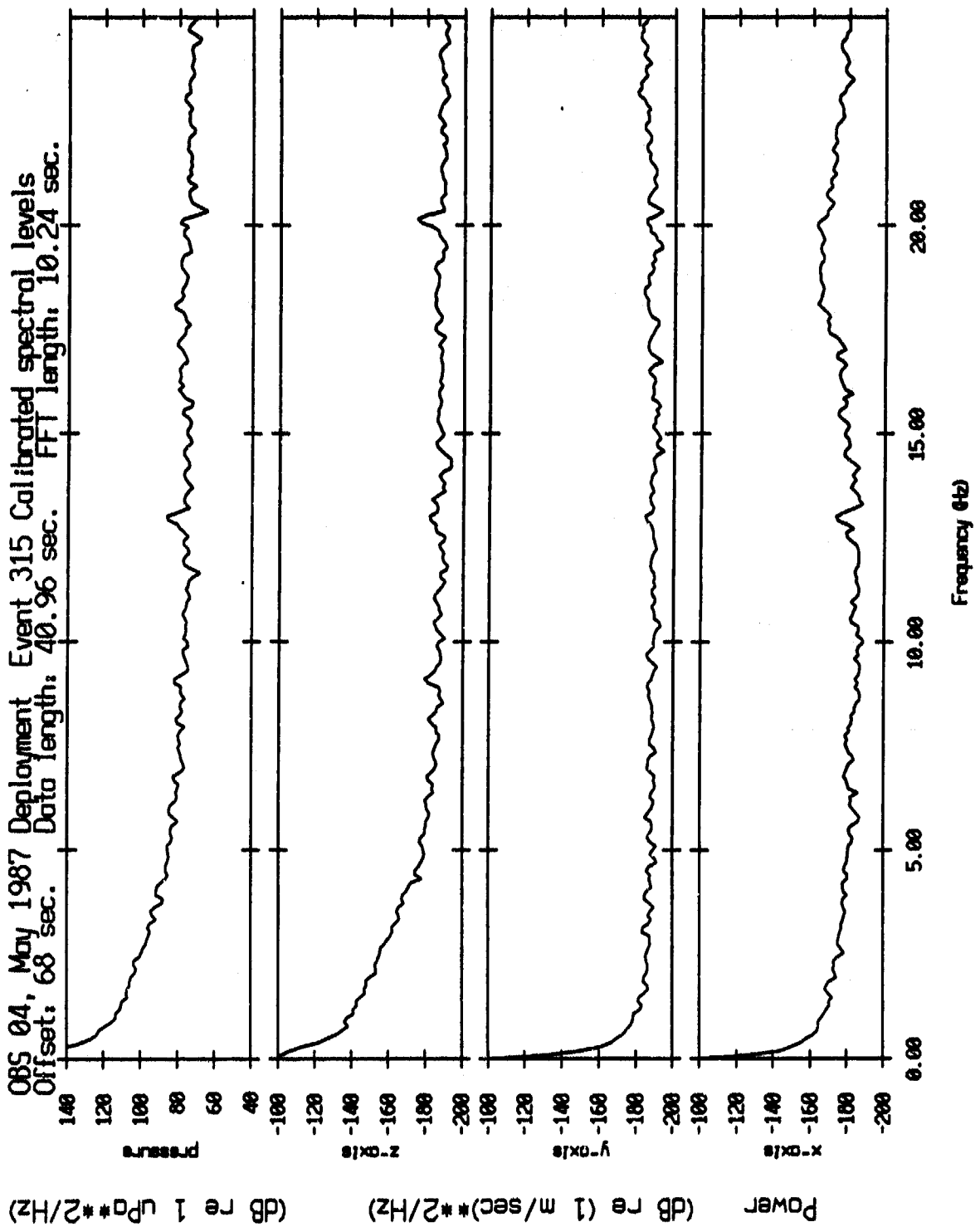
OBS 04, May 1987 Deployment Event 315 Calibrated spectral levels
Offset: 68 sec. Data length: 40.96 sec. FFT length: 10.24 sec.
pressure
z-axis
y-axis
x-axis
Power (db re (1 m/sec)**2/Hz)
(db re 1 uPa**2/Hz)
Frequency (Hz)
0.00
5.00
10.00
15.00
20.00

Figure IV.59

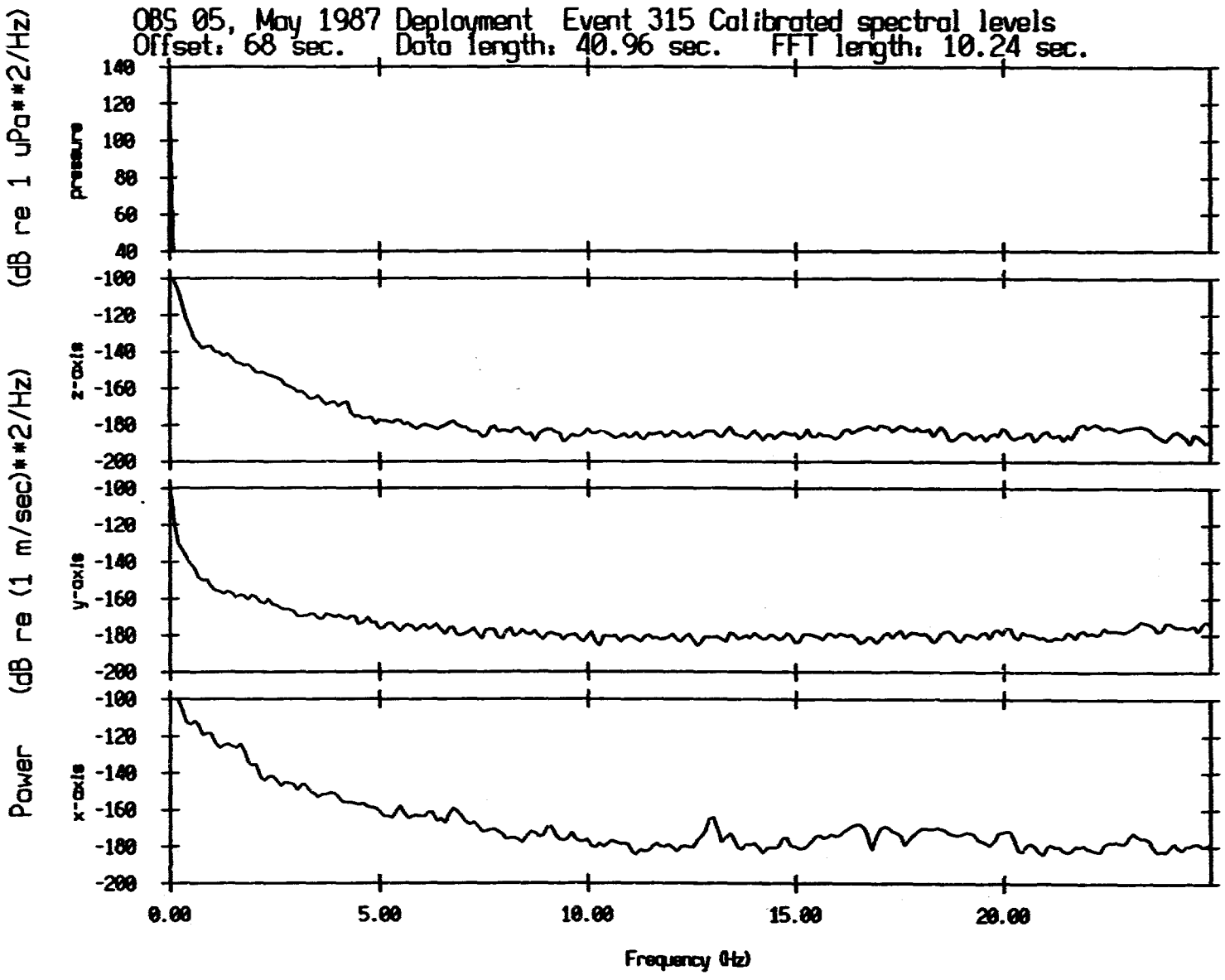
OBS 05, May 1987 Deployment Event 315 Calibrated spectral levels
Offset: 68 sec. Data length: 40.96 sec. FFT length: 10.24 sec.
Power (dB re (1 m/sec)**2/Hz) (dB re 1 uPa**2/Hz)
pressure
z-axis
y-axis
x-axis
140
120
100
80
60
40
-100
-120
-140
-160
-180
-200
0.00
5.00
10.00
15.00
20.00
Frequency (Hz)

Figure IV.80

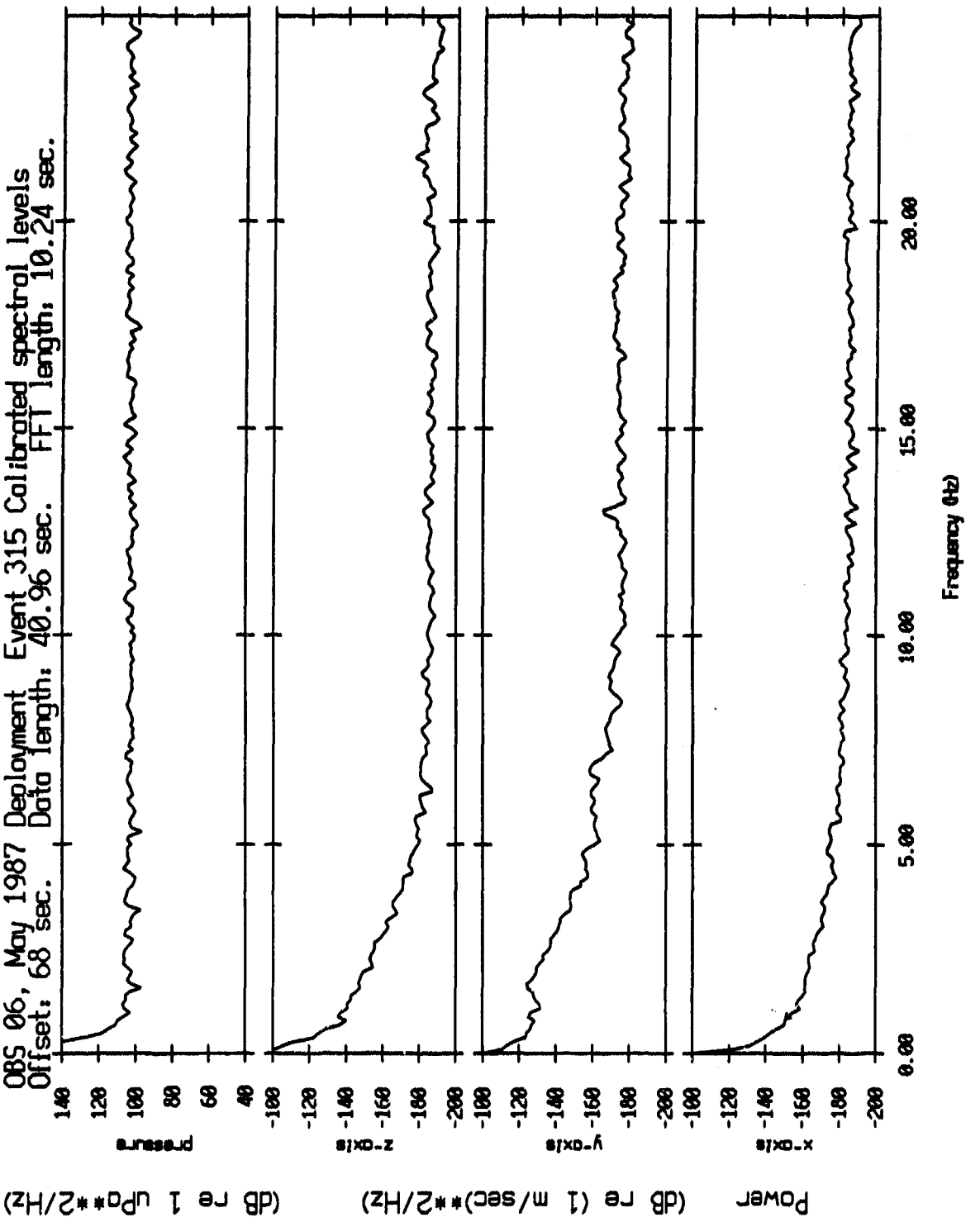
OBS 06, May 1987 Deployment Event 315 Calibrated spectral levels
Offset: 68 sec. Data length: 40.96 sec. FFT length: 10.24 sec.
pressure
z-axis
y-axis
x-axis
(dB re 1 uPa**2/Hz)
(dB re (1 m/sec)**2/Hz)
Power
Frequency (Hz)
0.00
5.00
10.00
15.00
20.00

Figure IV.61

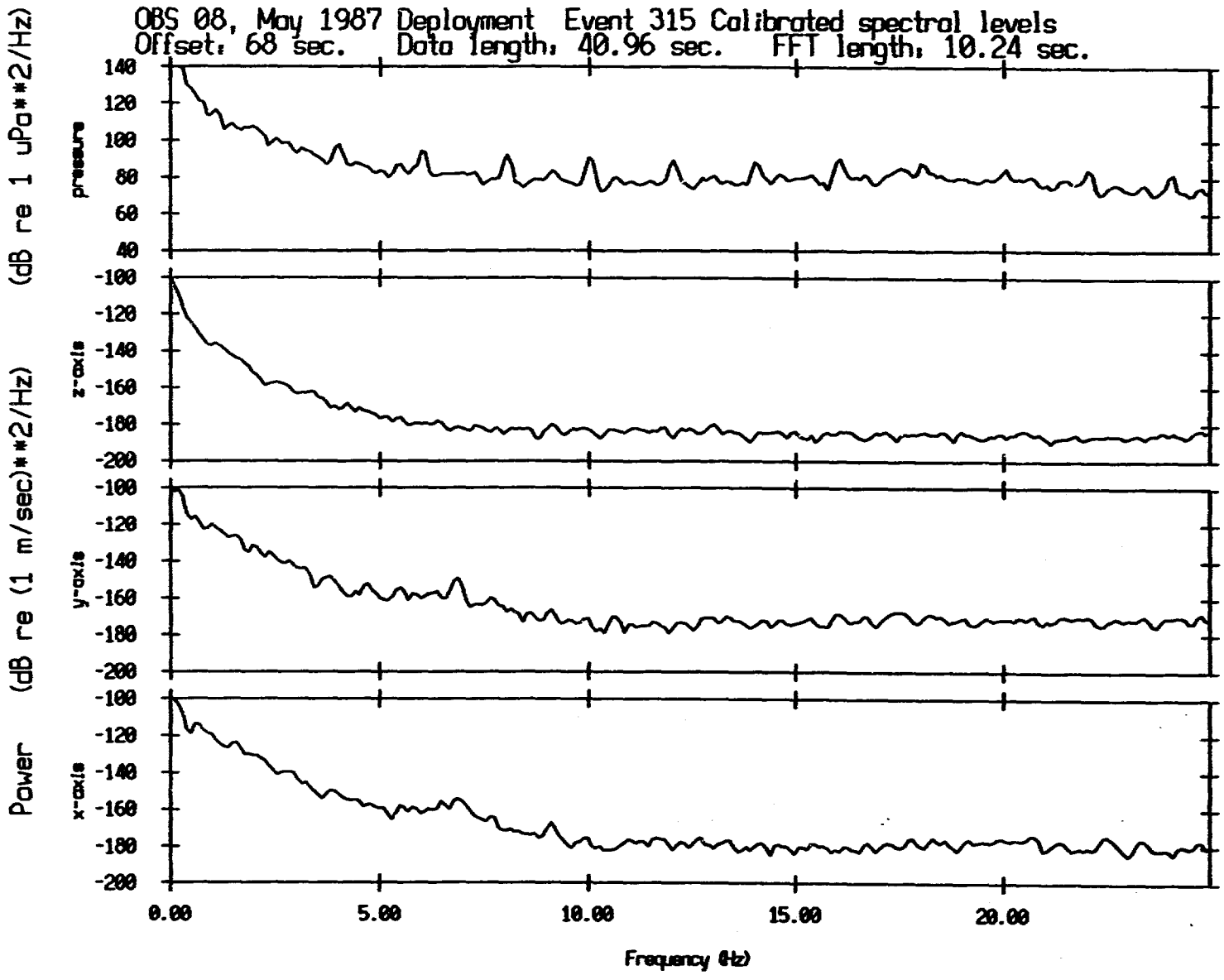
OBS 08, May 1987 Deployment Event 315 Calibrated spectral levels
Offset: 68 sec. Data length: 40.96 sec. FFT length: 10.24 sec.
Power (dB re (1 m/sec)**2/Hz) (dB re 1 uPa**2/Hz)
pressure
z-axis
y-axis
x-axis
140
120
100
80
60
40
-100
-120
-140
-160
-180
-200
0.00
5.00
10.00
15.00
20.00
Frequency (Hz)

Figure IV.02

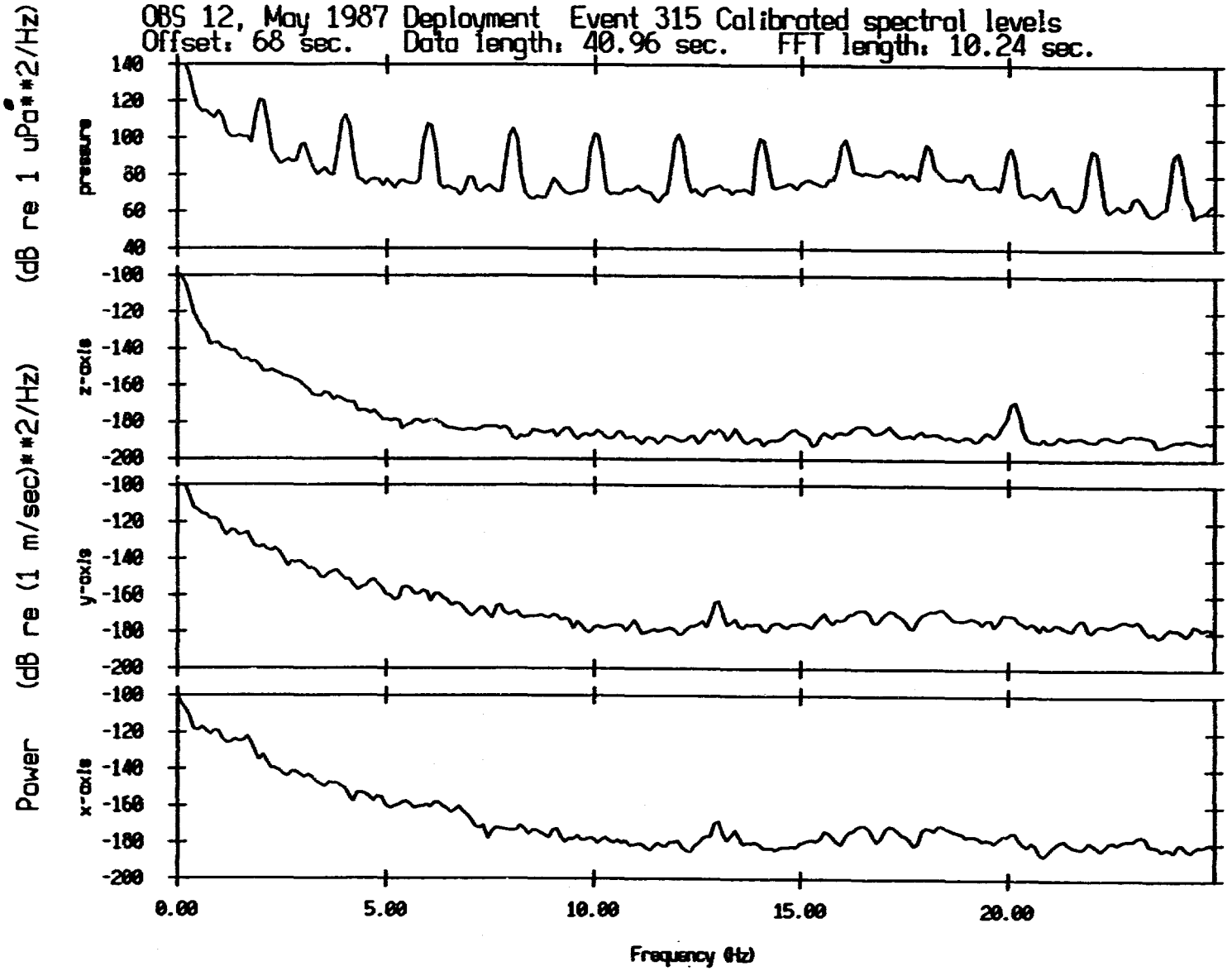
OBS 12, May 1987 Deployment Event 315 Calibrated spectral levels
Offset: 68 sec. Data length: 40.96 sec. FFT length: 10.24 sec.
Power (dB re (1 m/sec)**2/Hz) (dB re 1 uPa**2/Hz)
pressure
z-axis
y-axis
x-axis
140
120
100
80
60
40
-100
-120
-140
-160
-180
-200
0.00
5.00
10.00
15.00
20.00
Frequency (Hz)

Figure IV.63

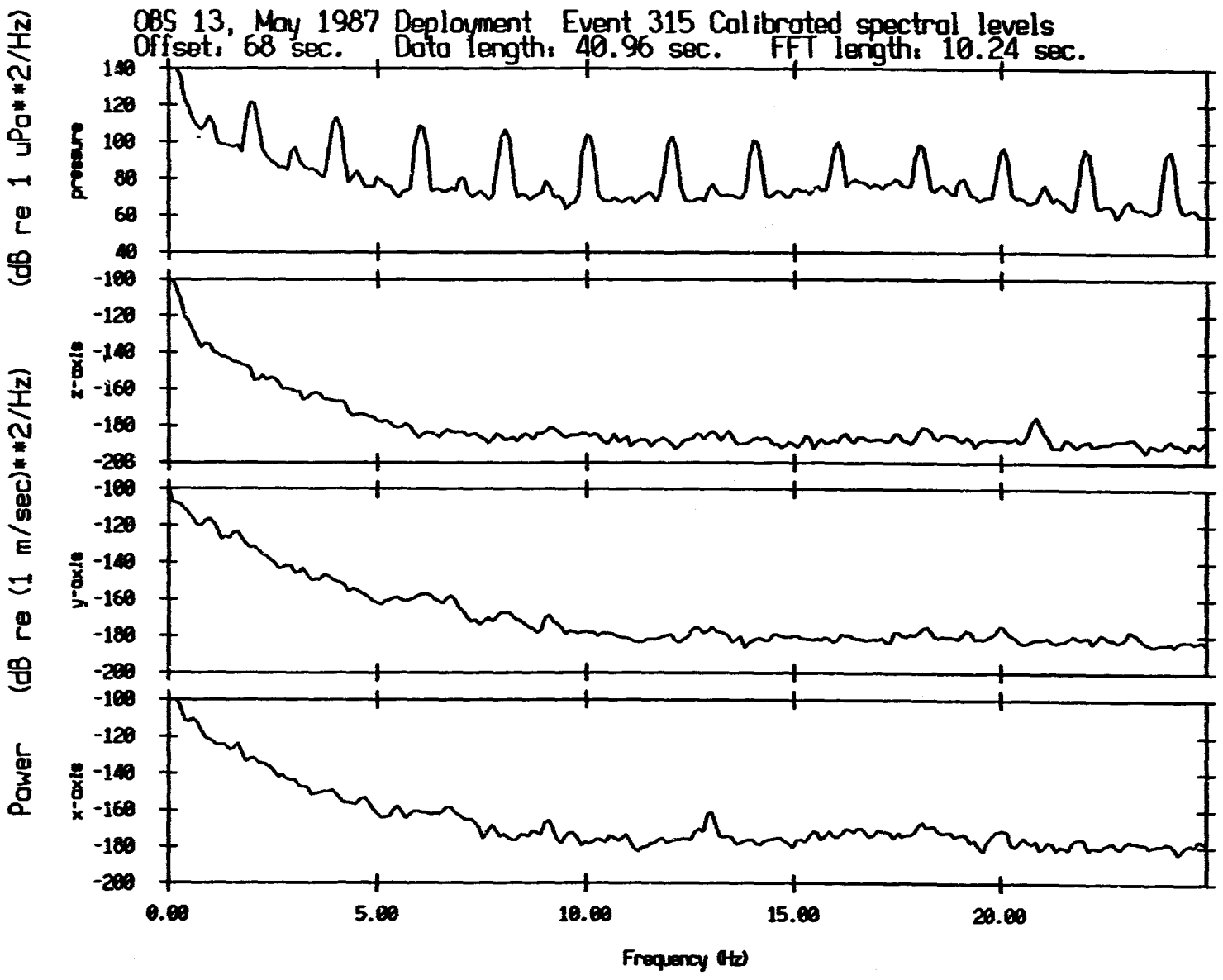
OBS 13, May 1987 Deployment Event 315 Calibrated spectral levels
Offset: 68 sec. Data length: 40.96 sec. FFT length: 10.24 sec.
Power (dB re (1 m/sec)**2/Hz) (dB re 1 uPa**2/Hz)
pressure
z-axis
y-axis
x-axis
140
120
100
80
60
40
-100
-120
-140
-160
-180
-200
0.00
5.00
10.00
15.00
20.00
Frequency (Hz)

Figure IV.84

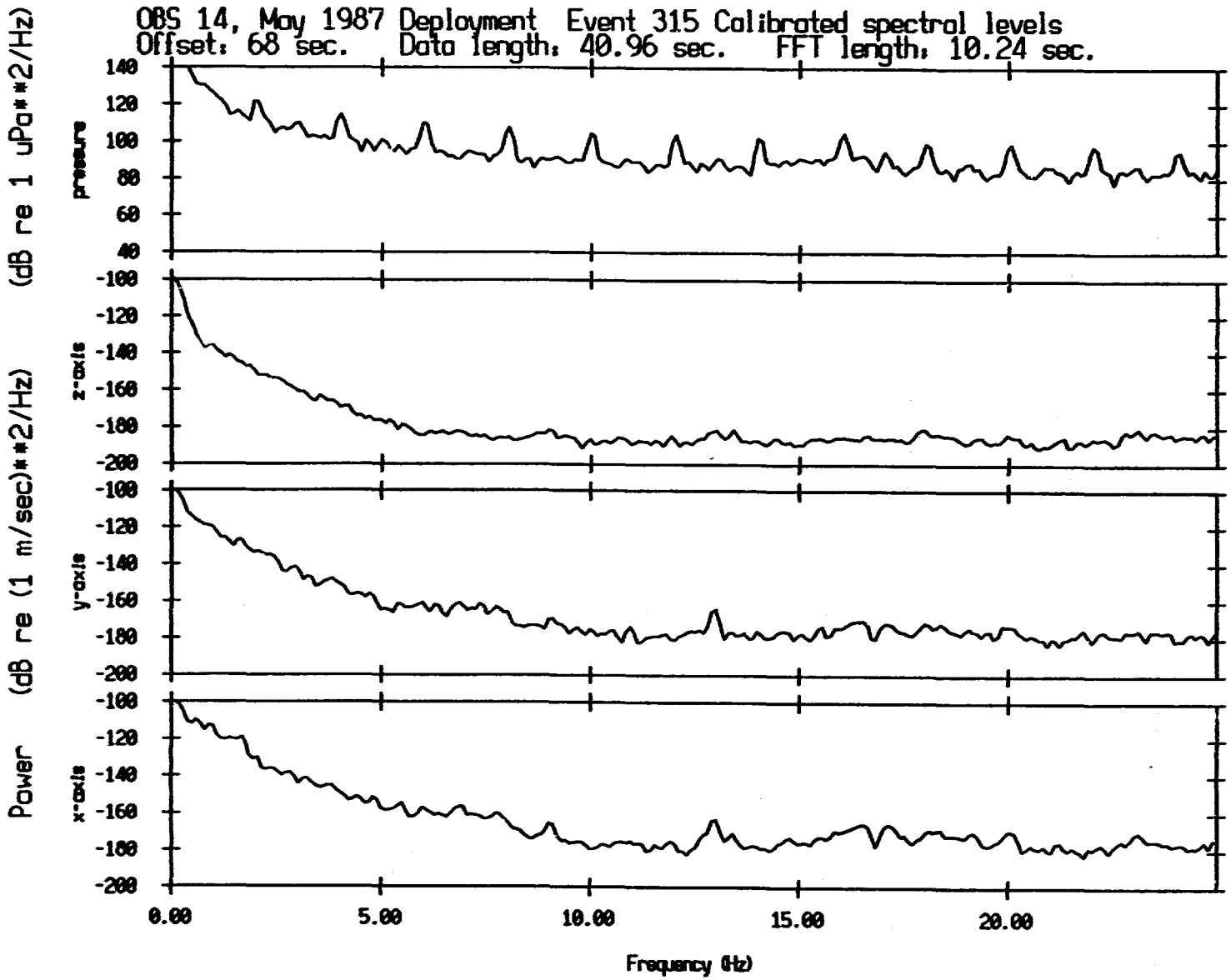
OBS 14, May 1987 Deployment Event 315 Calibrated spectral levels
Offset: 68 sec. Data length: 40.96 sec. FFT length: 10.24 sec.
Power (dB re (1 m/sec)**2/Hz) (dB re 1 uPa**2/Hz)
pressure
z-axis
y-axis
x-axis
140
120
100
80
60
40
-100
-120
-140
-160
-180
-200
0.00
5.00
10.00
15.00
20.00
Frequency (Hz)

Figure IV.85

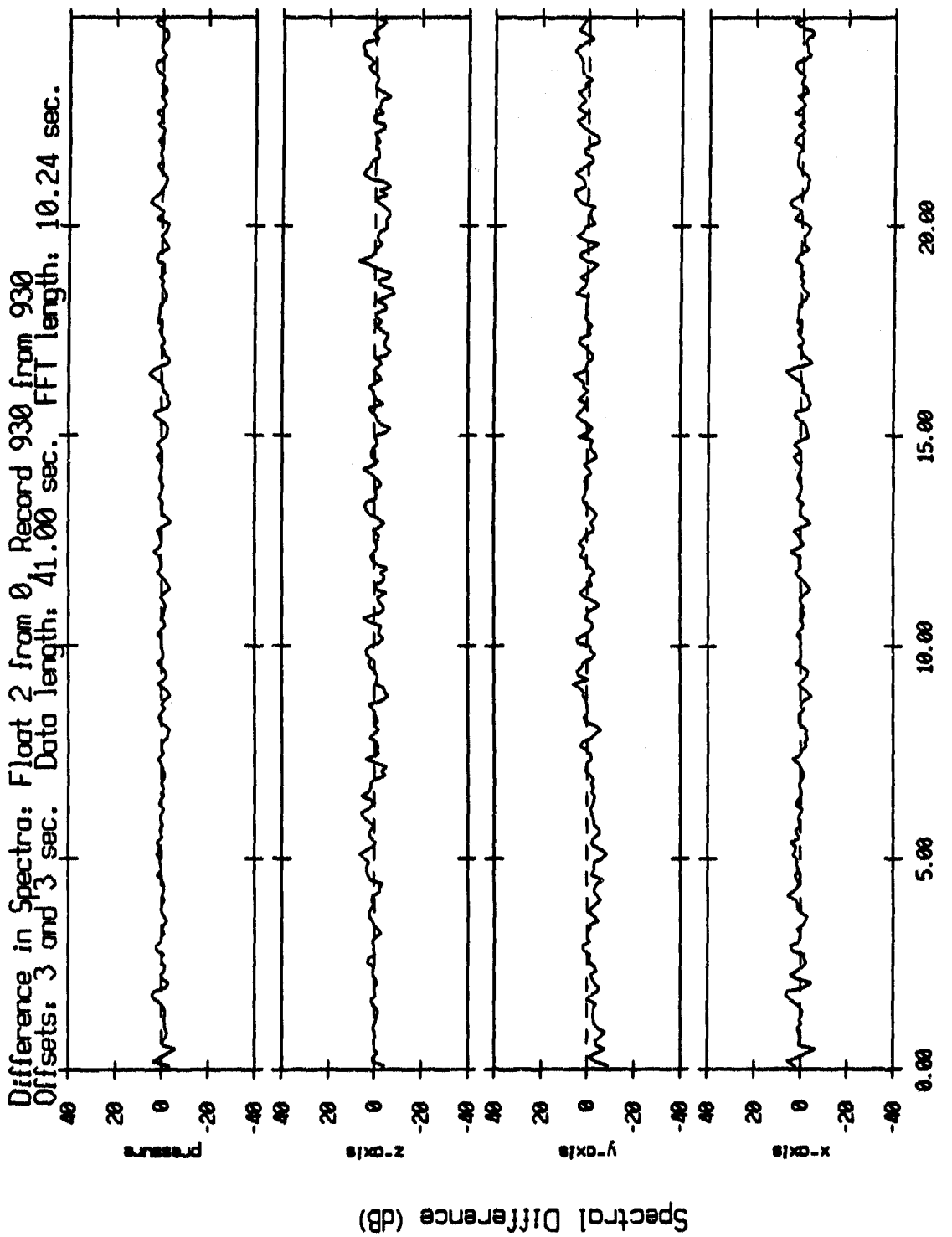
Difference in Spectra: Float 2 from 0, Record 930 from 930
Offsets: 3 and 3 sec. Data length: 41.00 sec. FFT length: 10.24 sec.
pressure
z-axis
y-axis
x-axis
40
20
0
-20
-40
0.00
5.00
10.00
15.00
20.00
Frequency (Hz)
Spectral Difference (dB)

Figure V.1

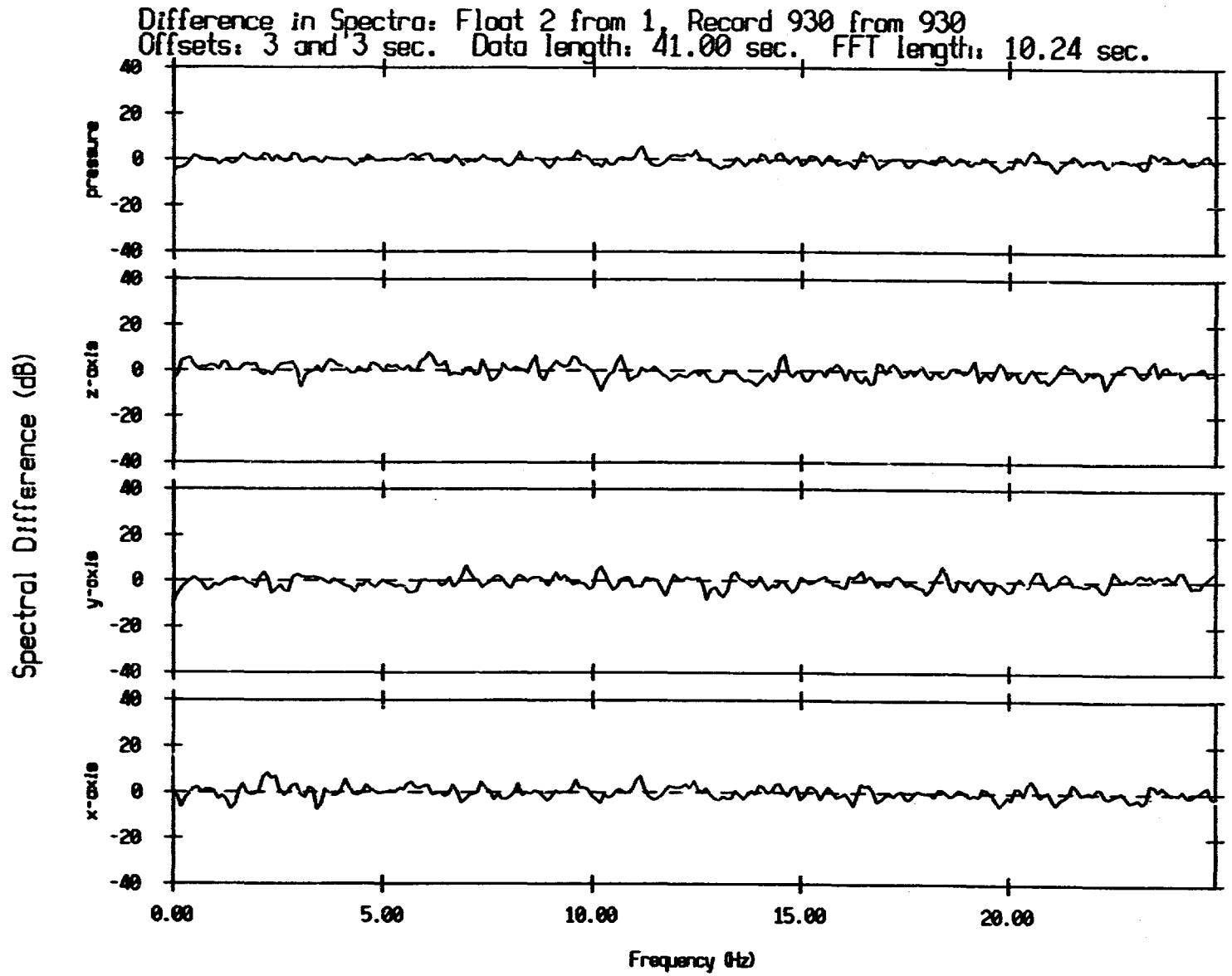
Difference in Spectra: Float 2 from 1, Record 930 from 930
Offsets: 3 and 3 sec. Data length: 41.00 sec. FFT length: 10.24 sec.
Spectral Difference (dB)
pressure
z-axis
y-axis
x-axis
40
20
0
-20
-40
0.00
5.00
10.00
15.00
20.00
Frequency (Hz)

Figure V.2

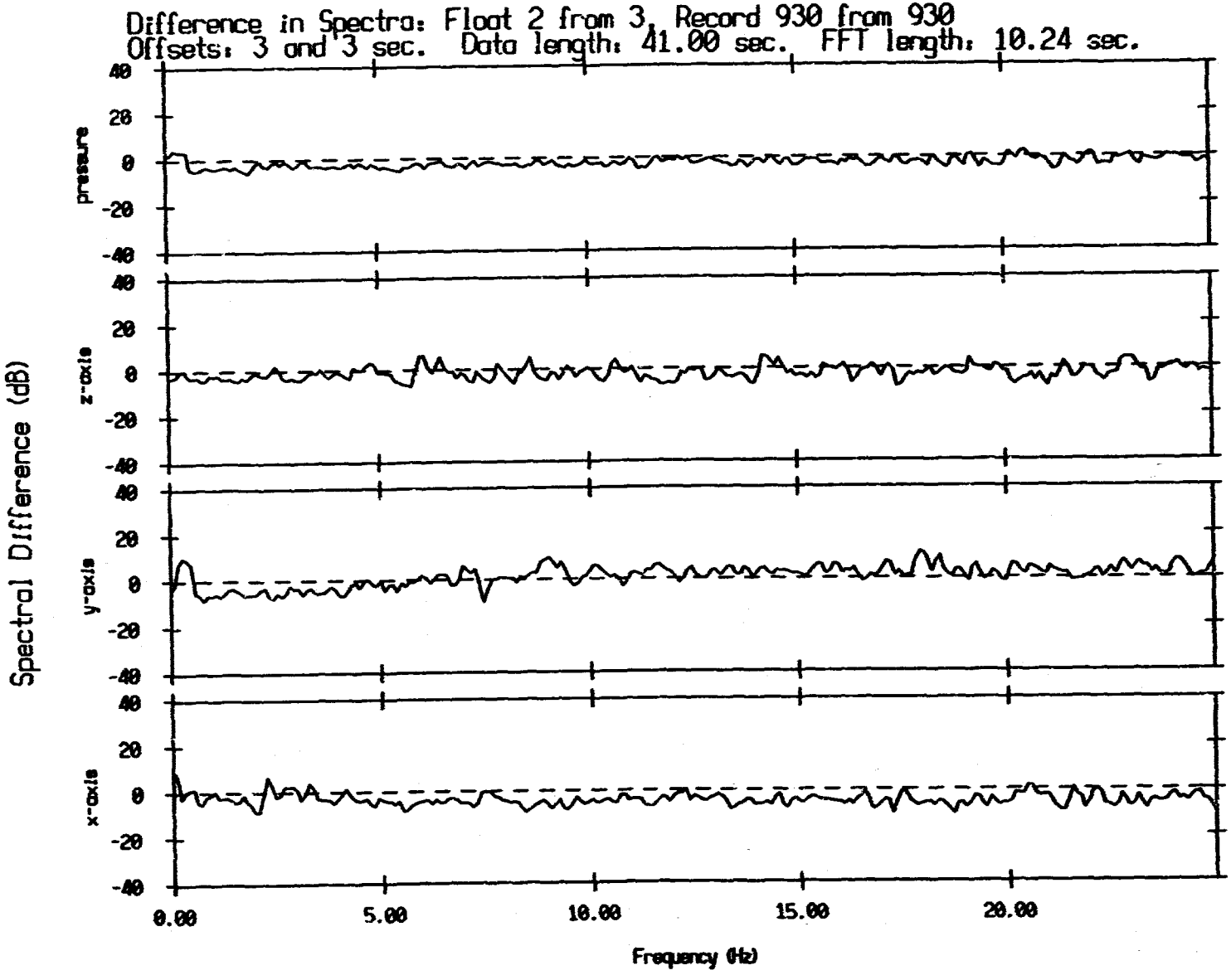
Difference in Spectra: Float 2 from 3, Record 930 from 930
Offsets: 3 and 3 sec. Data length: 41.00 sec. FFT length: 10.24 sec.
Spectral Difference (dB)
pressure
z-axis
y-axis
x-axis
40
20
0
-20
-40
0.00
5.00
10.00
15.00
20.00
Frequency (Hz)

Figure V.3

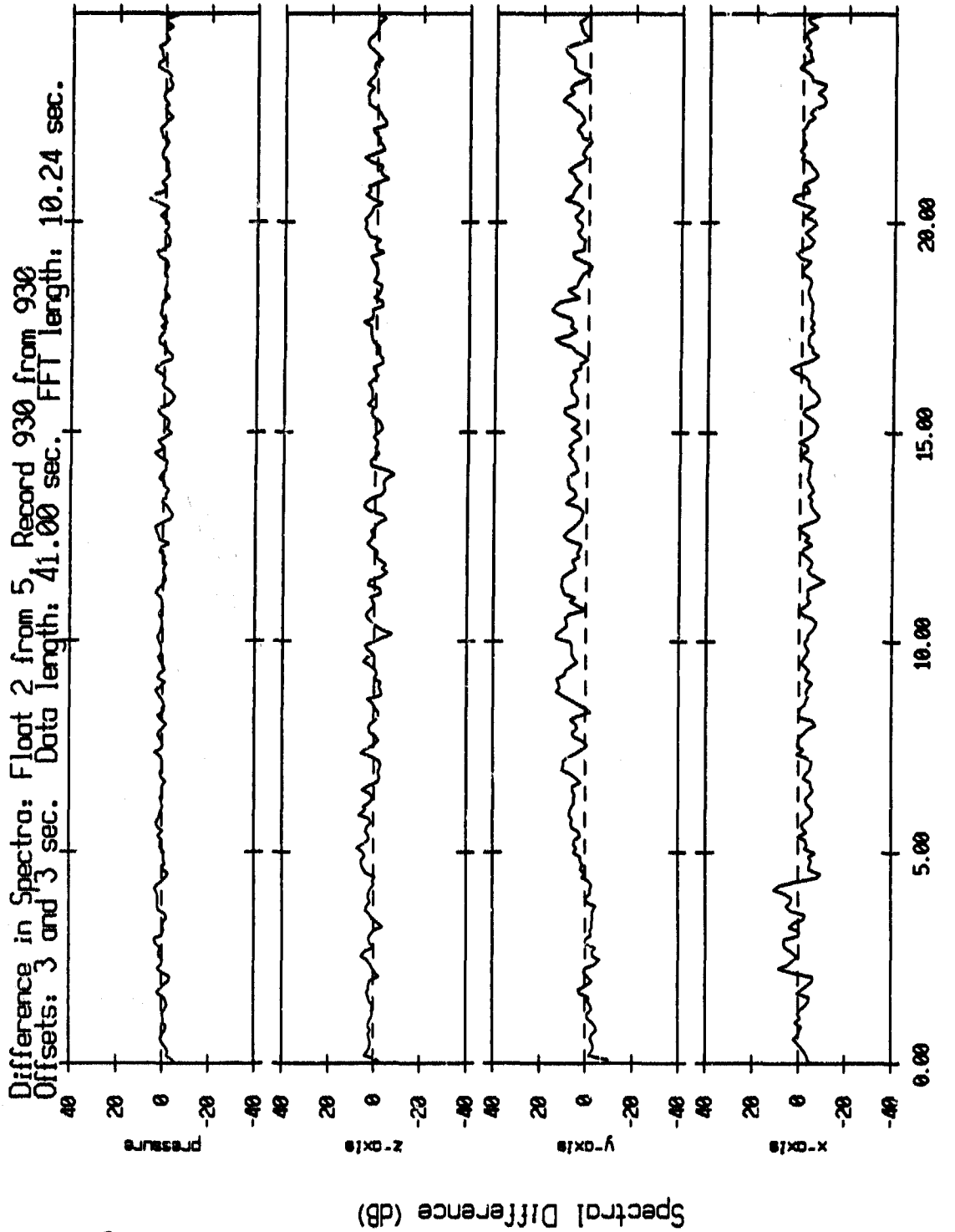
Difference in Spectra: Float 2 from 5, Record 930 from 930
Offsets: 3 and 3 sec. Data length: 41.00 sec., FFT length: 10.24 sec.
pressure
z-axis
y-axis
x-axis
40
20
0
-20
-40
0.00
5.00
10.00
15.00
20.00
Frequency (Hz)
Spectral Difference (dB)

Figure V.4

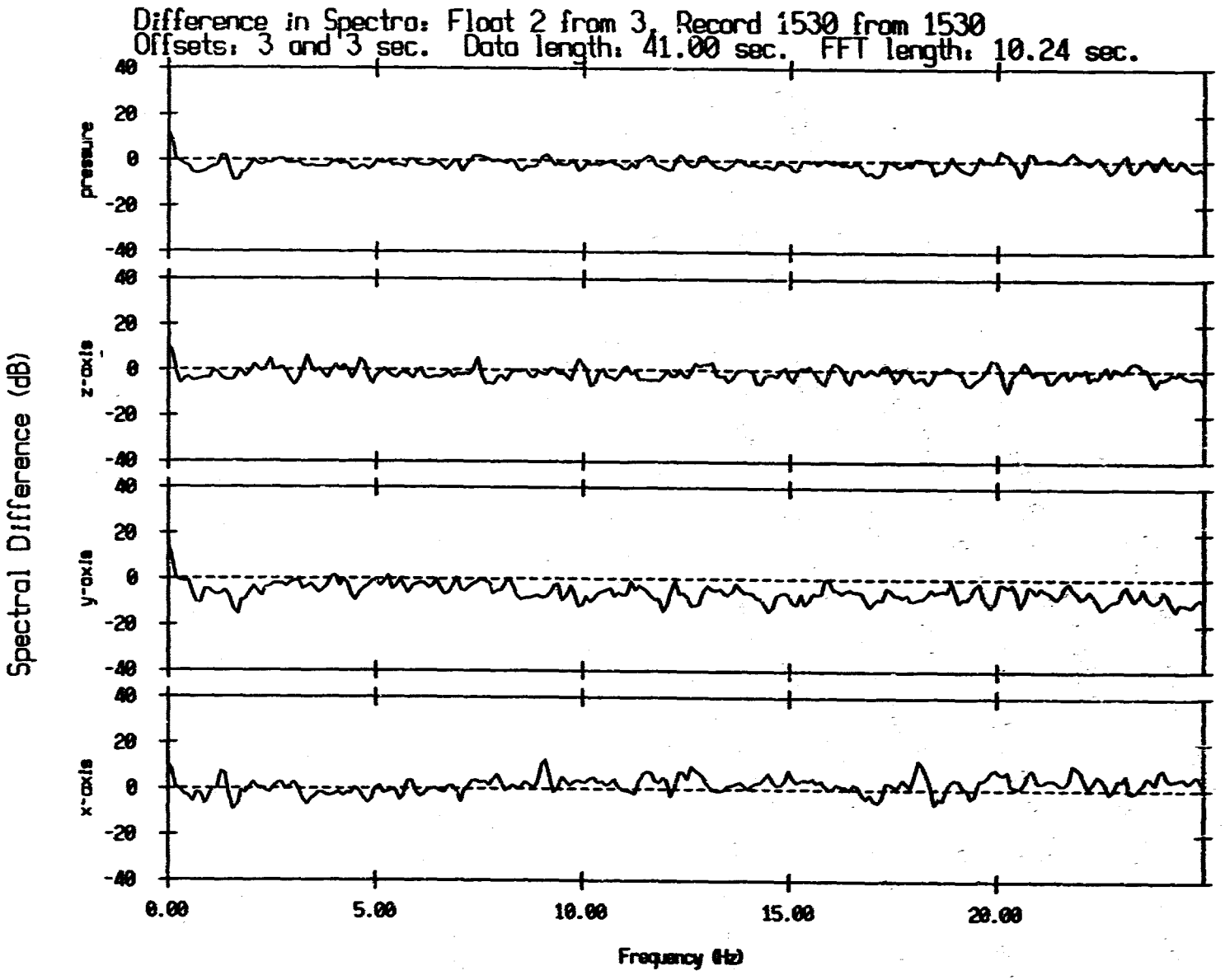
Difference in Spectra: Float 2 from 3, Record 1530 from 1530
Offsets: 3 and 3 sec. Data length: 41.00 sec. FFT length: 10.24 sec.
Spectral Difference (dB)
pressure
z-axis
y-axis
x-axis
40
20
0
-20
-40
0.00
5.00
10.00
15.00
20.00
Frequency (Hz)

Figure V.5

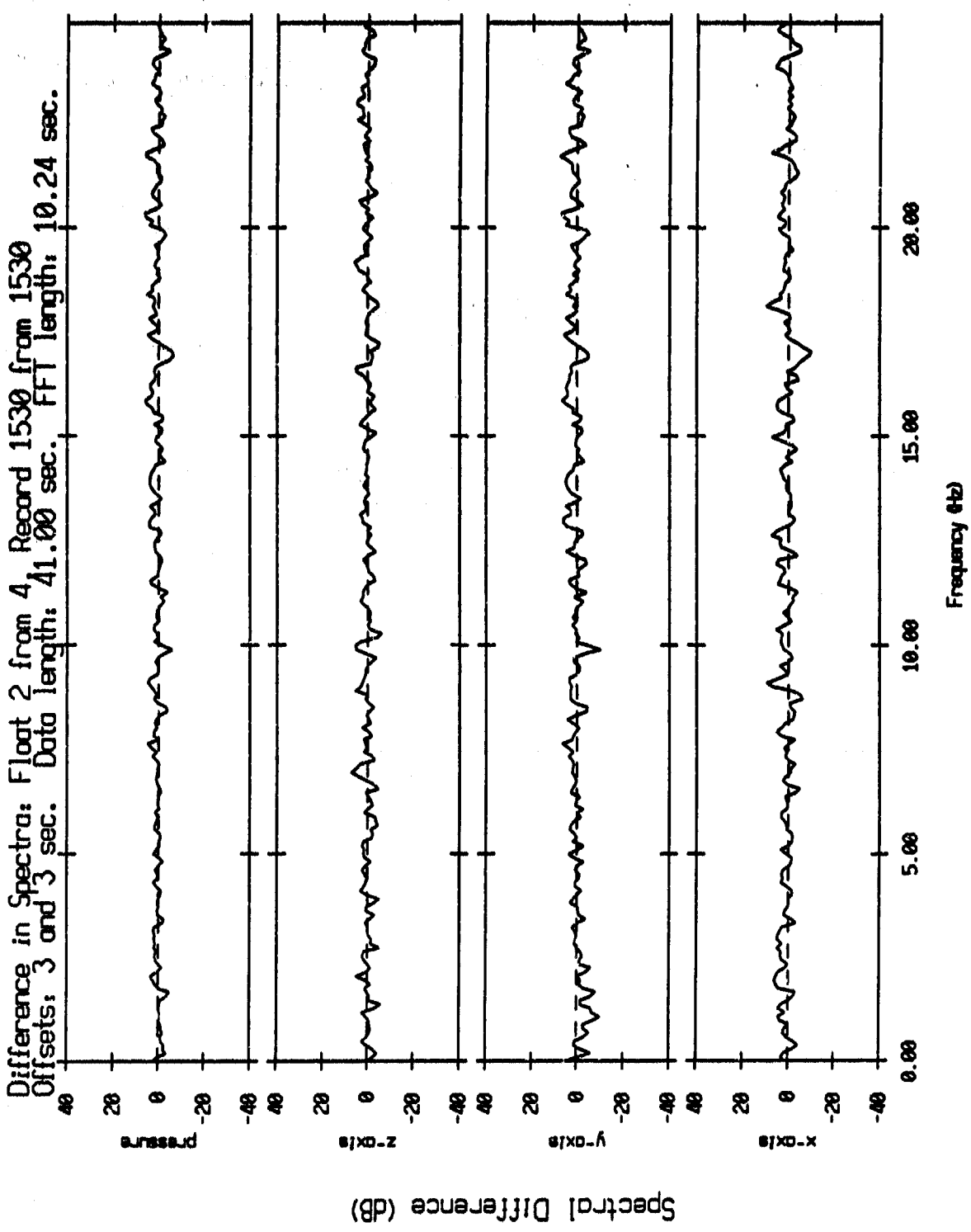
Difference in Spectra: Float 2 from 4 Record 1530 from 1530
Offsets: 3 and 3 sec. Data length: 41.00 sec. FFT length: 10.24 sec.
pressure
z-axis
y-axis
x-axis
40
20
0
-20
-40
0.00
5.00
10.00
15.00
20.00
Frequency (Hz)
Spectral Difference (dB)

Figure V.6

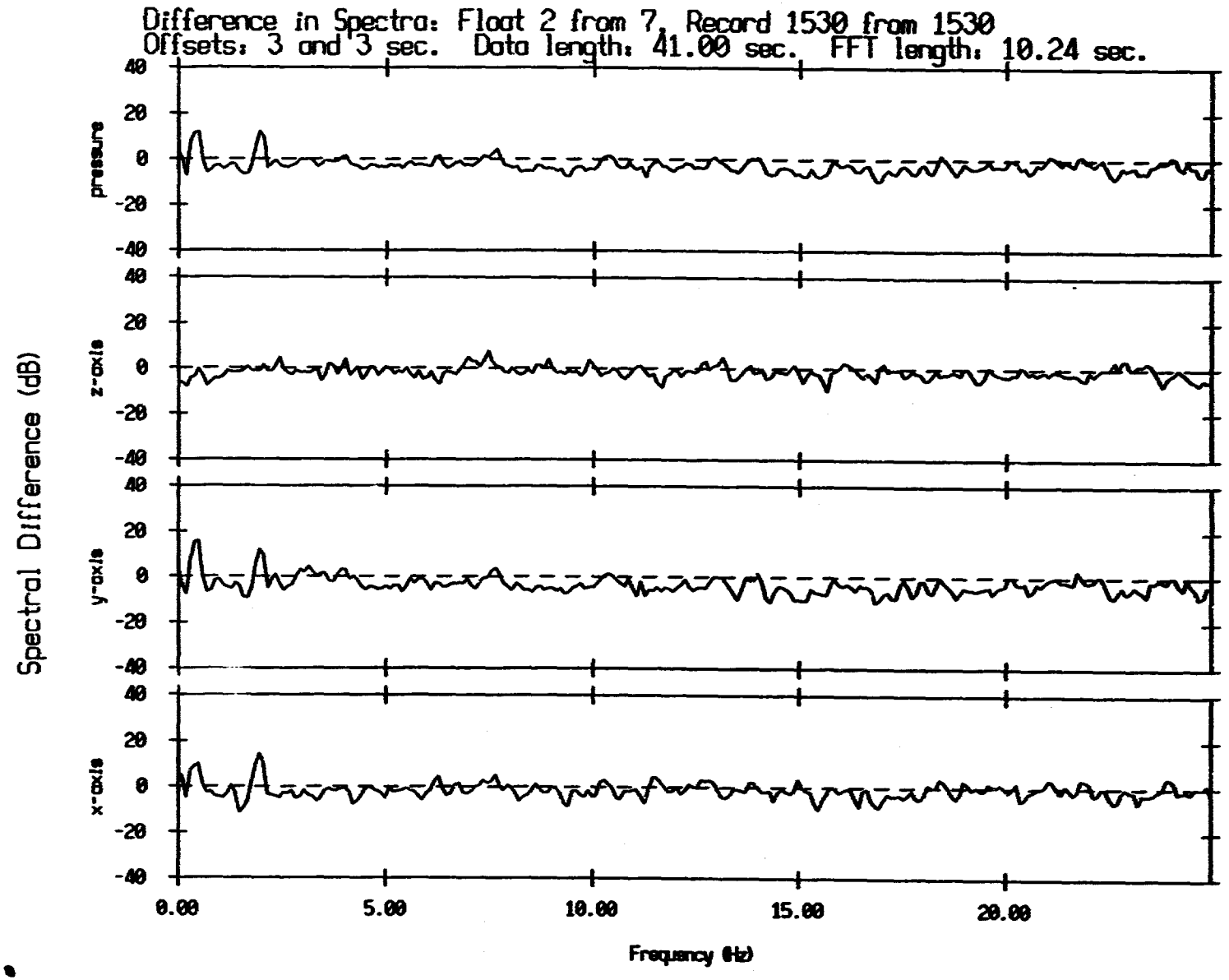
Difference in Spectra: Float 2 from 7, Record 1530 from 1530
Offsets: 3 and 3 sec. Data length: 41.00 sec. FFT length: 10.24 sec.
Spectral Difference (dB)
pressure
z-axis
y-axis
x-axis
40
20
0
-20
-40
0.00
5.00
10.00
15.00
20.00
Frequency (Hz)

Figure V.7

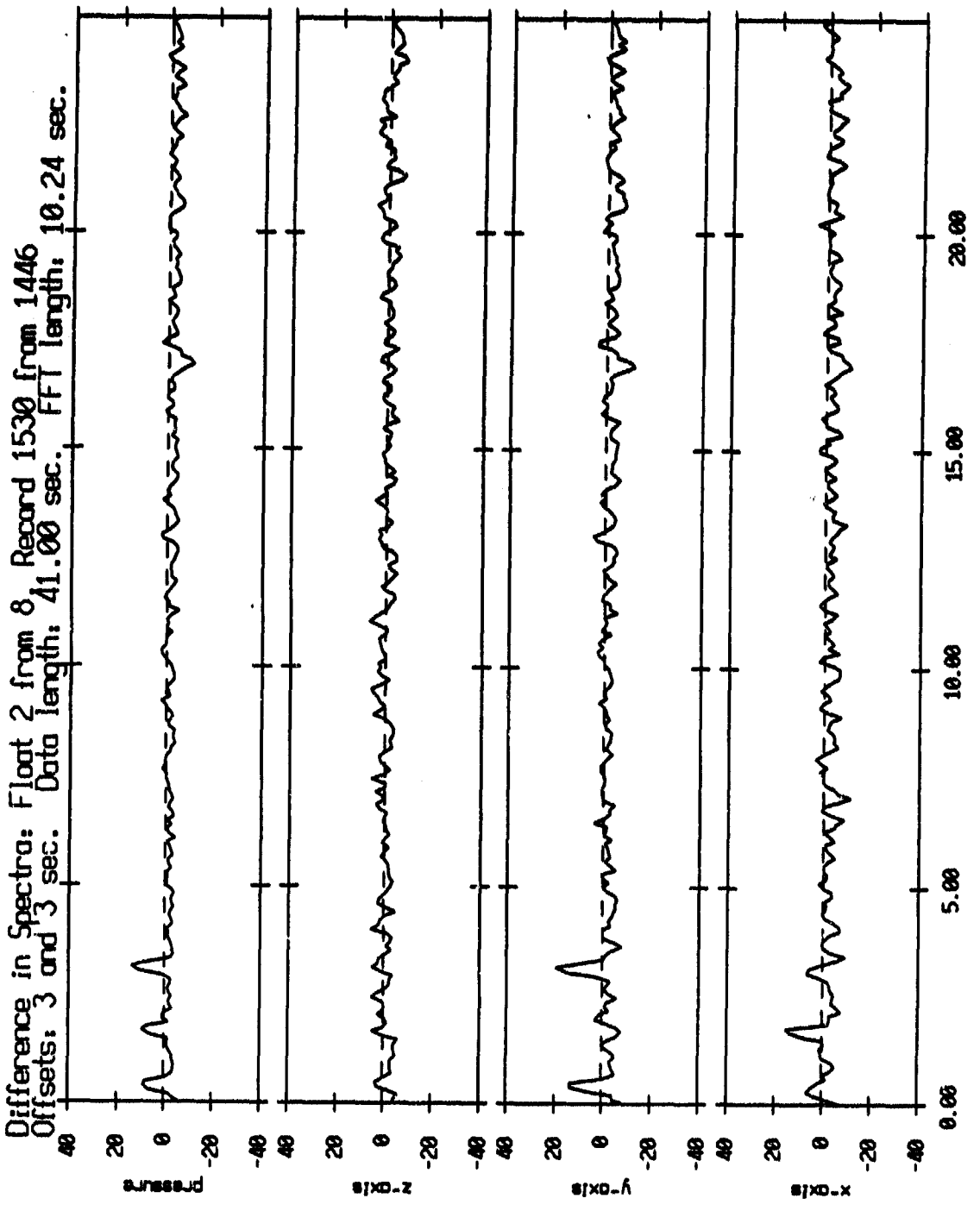
Difference in Spectra: Float 2 from 8 Record 1530 from 1446
Offsets: 3 and 3 sec. Data length: 41.00 sec. FFT length: 10.24 sec.
pressure
z-axis
y-axis
x-axis
40
20
0
-20
-40
0.00
5.00
10.00
15.00
20.00
Frequency (Hz)
Spectral Difference (dB)

Figure V.8

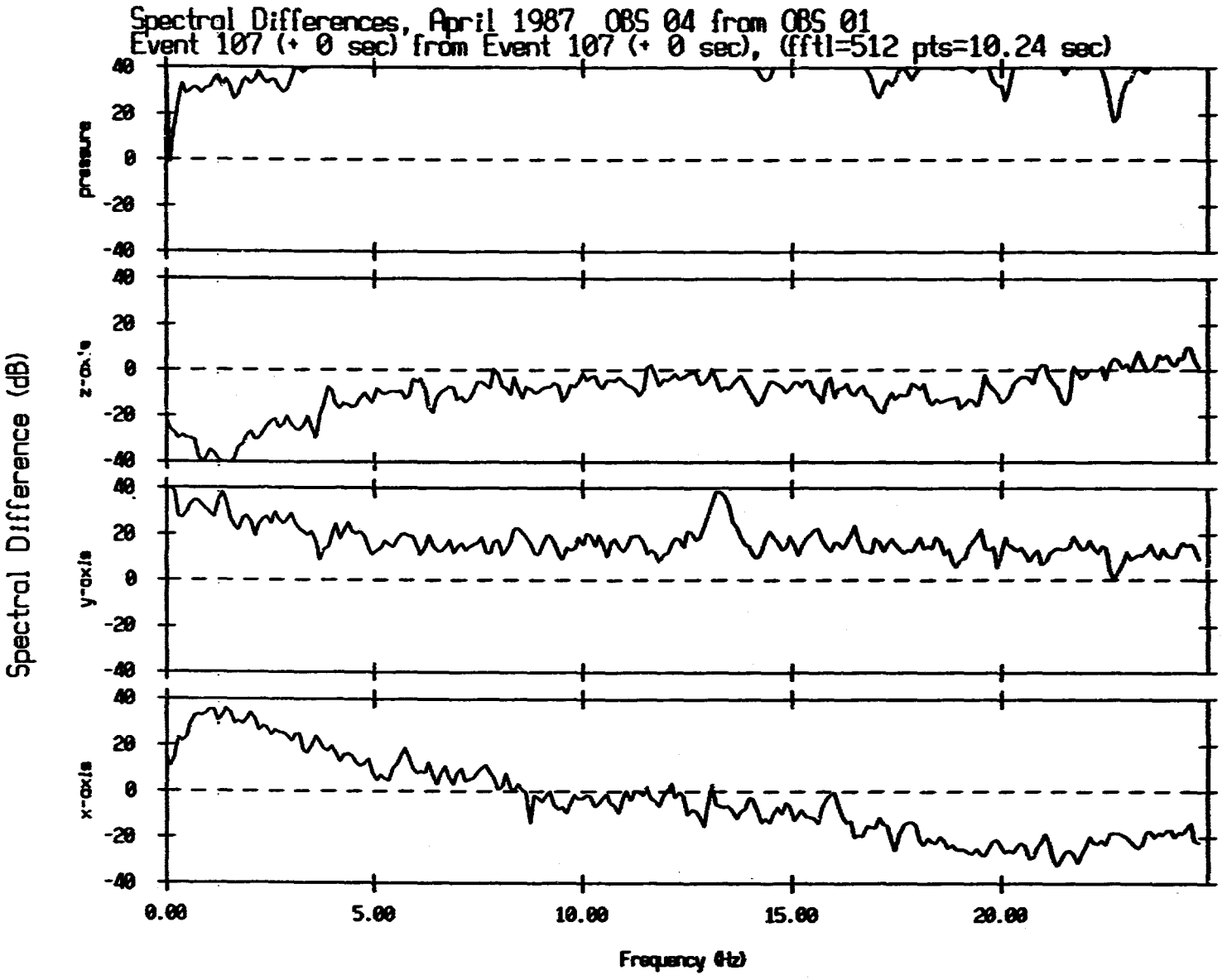
Spectral Differences, April 1987 OBS 04 from OBS 01
Event 107 (+ 0 sec) from Event 107 (+ 0 sec), (fftl=512 pts=10.24 sec)
Spectral Difference (dB)
pressure
z-axis
y-axis
x-axis
40
20
0
-20
-40
0.00
5.00
10.00
15.00
20.00
Frequency (Hz)

Figure V.9

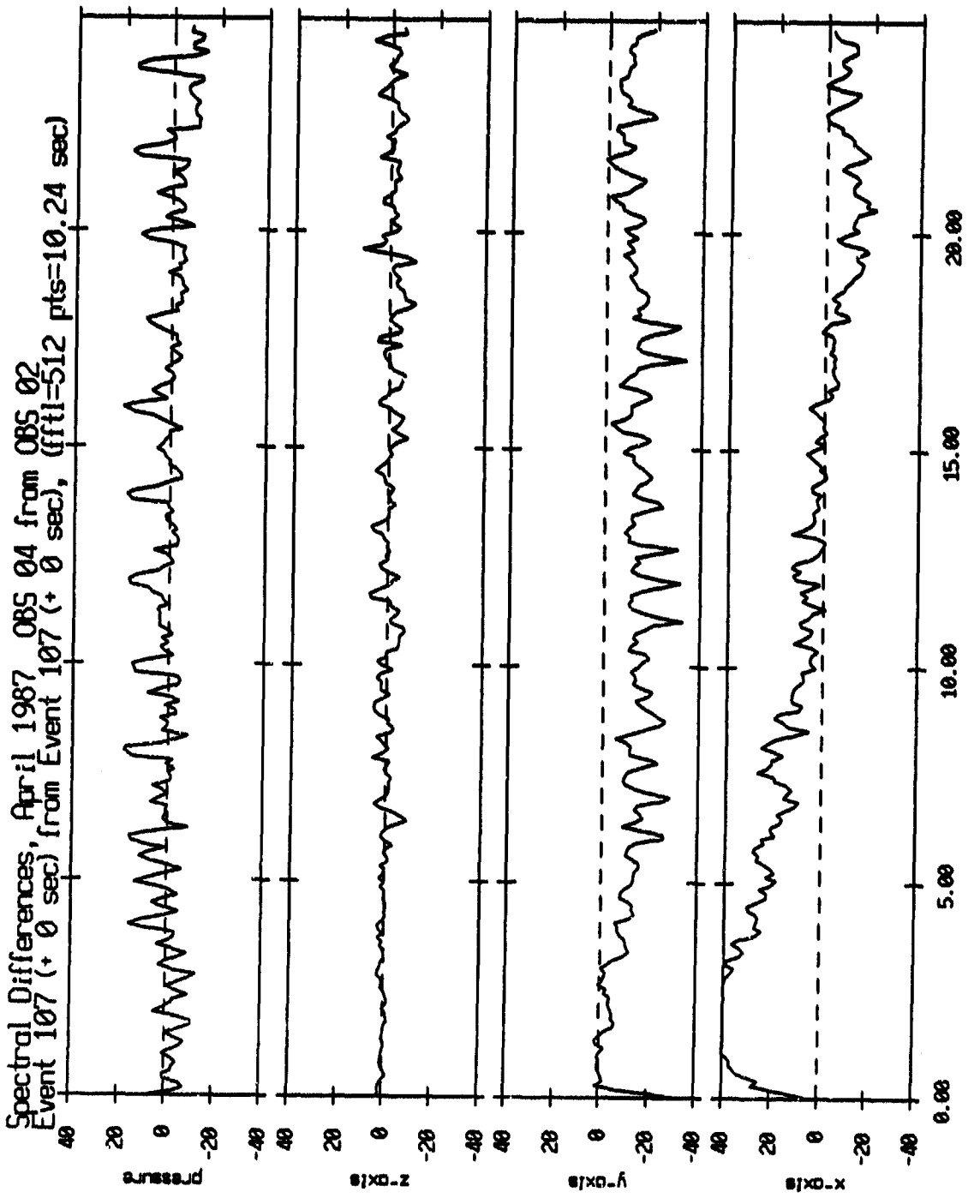
Spectral Differences, April 1987 OBS 04 from OBS 02
Event 107 (+ 0 sec) from Event 107 (+ 0 sec), (fft1=512 pts=10.24 sec)
pressure
z-axis
y-axis
x-axis
40
20
0
-20
-40
0.00
5.00
10.00
15.00
20.00
Frequency (Hz)
Spectral Difference (dB)

Figure V.10

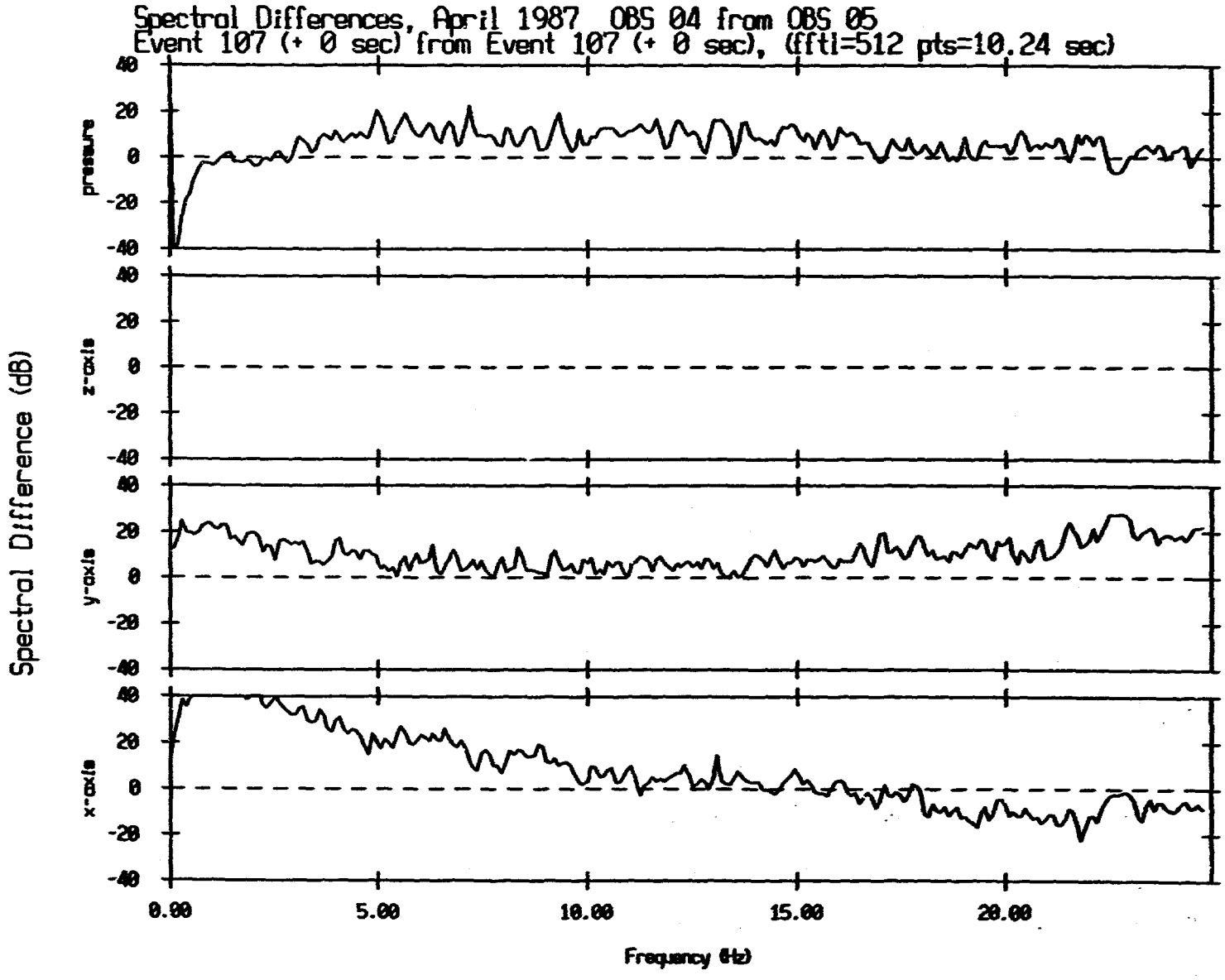
Spectral Differences, April 1987 OBS 04 from OBS 05
Event 107 (+ 0 sec) from Event 107 (+ 0 sec), (fftl=512 pts=10.24 sec)
Spectral Difference (dB)
pressure
z-axis
y-axis
x-axis
40
20
0
-20
-40
0.00
5.00
10.00
15.00
20.00
Frequency (Hz)

Figure V.11

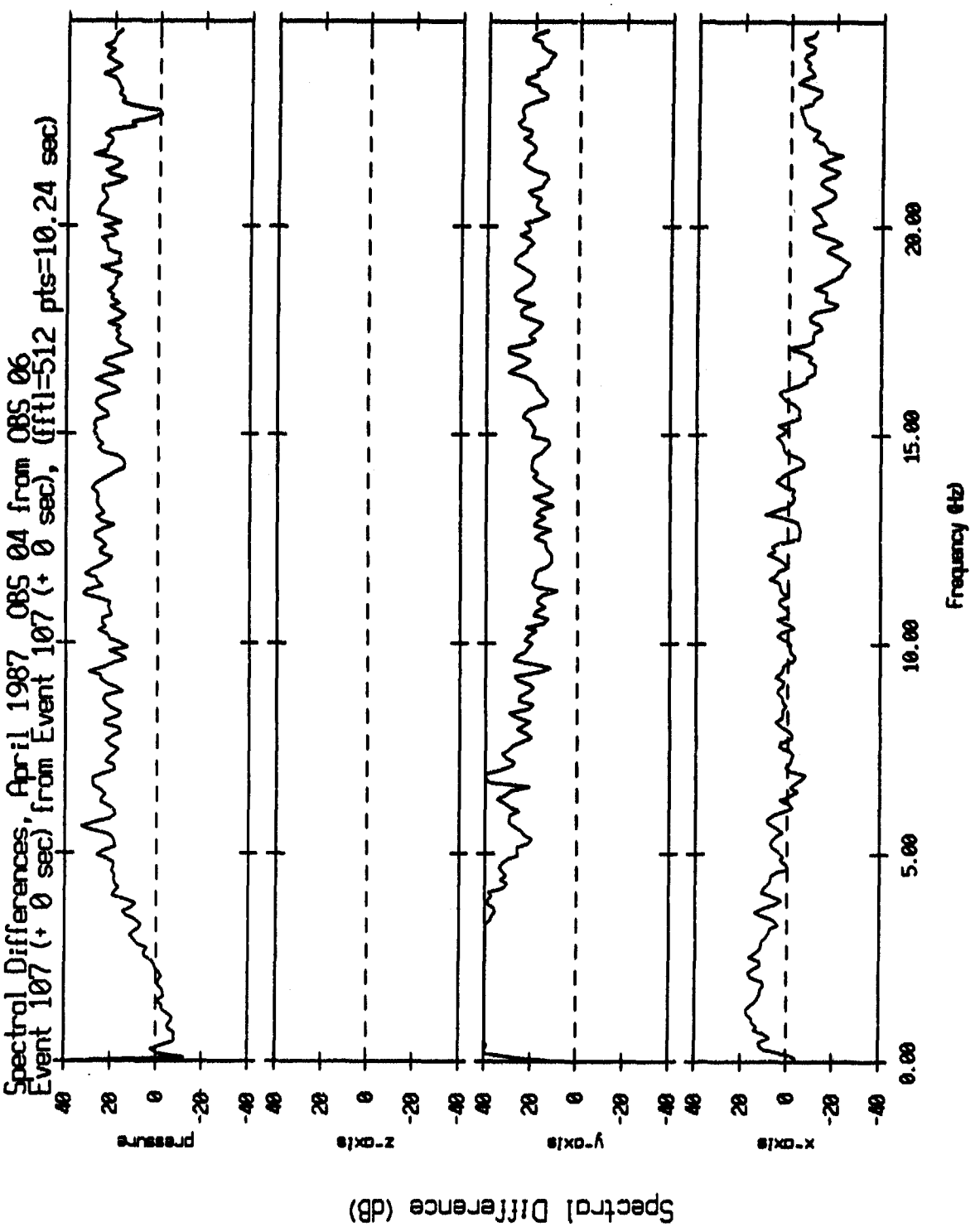
Spectral Differences, April 1987 085 04 from 085 06
Event 107 (+ 0 sec) from Event 107 (+ 0 sec), (fftl=512 pts=10.24 sec)
pressure
z-axis
y-axis
x-axis
40
20
0
-20
-40
0.00
5.00
10.00
15.00
20.00
Frequency (Hz)
Spectral Difference (dB)

Figure V.12

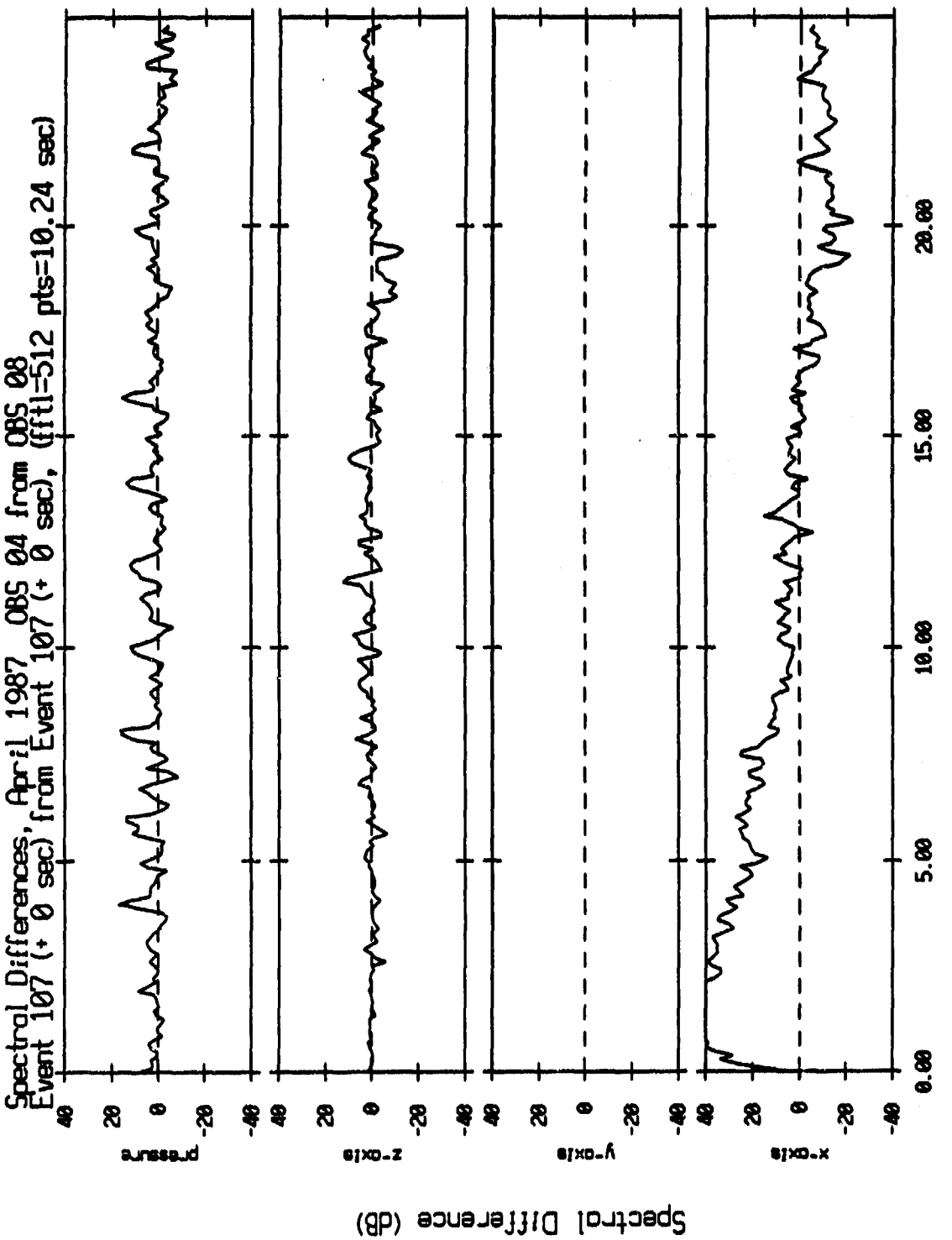
Spectral Differences, April 1987 OBS 04 from OBS 08
Event 107 (+ 0 sec) from Event 107 (+ 0 sec), (fftl=512 pts=10.24 sec)
pressure
z-axis
y-axis
x-axis
40
20
0
-20
-40
0.00
5.00
10.00
15.00
20.00
Frequency (Hz)
Spectral Difference (db)

Figure V.13

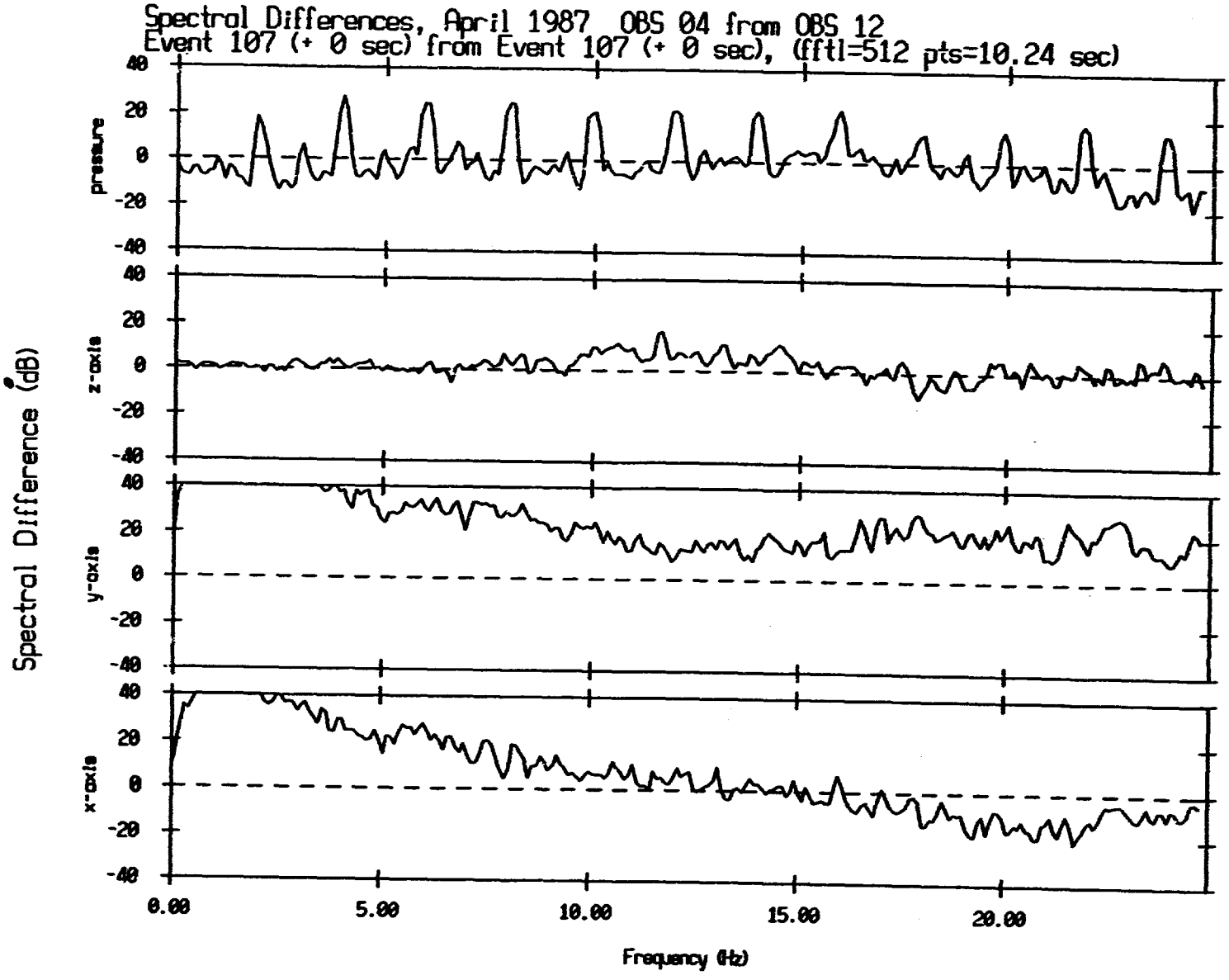
Spectral Differences, April 1987 OBS 04 from OBS 12
Event 107 (+ 0 sec) from Event 107 (+ 0 sec), (fftl=512 pts=10.24 sec)
Spectral Difference (dB)
pressure
z-axis
y-axis
x-axis
40
20
0
-20
-40
0.00
5.00
10.00
15.00
20.00
Frequency (Hz)

Figure V.14

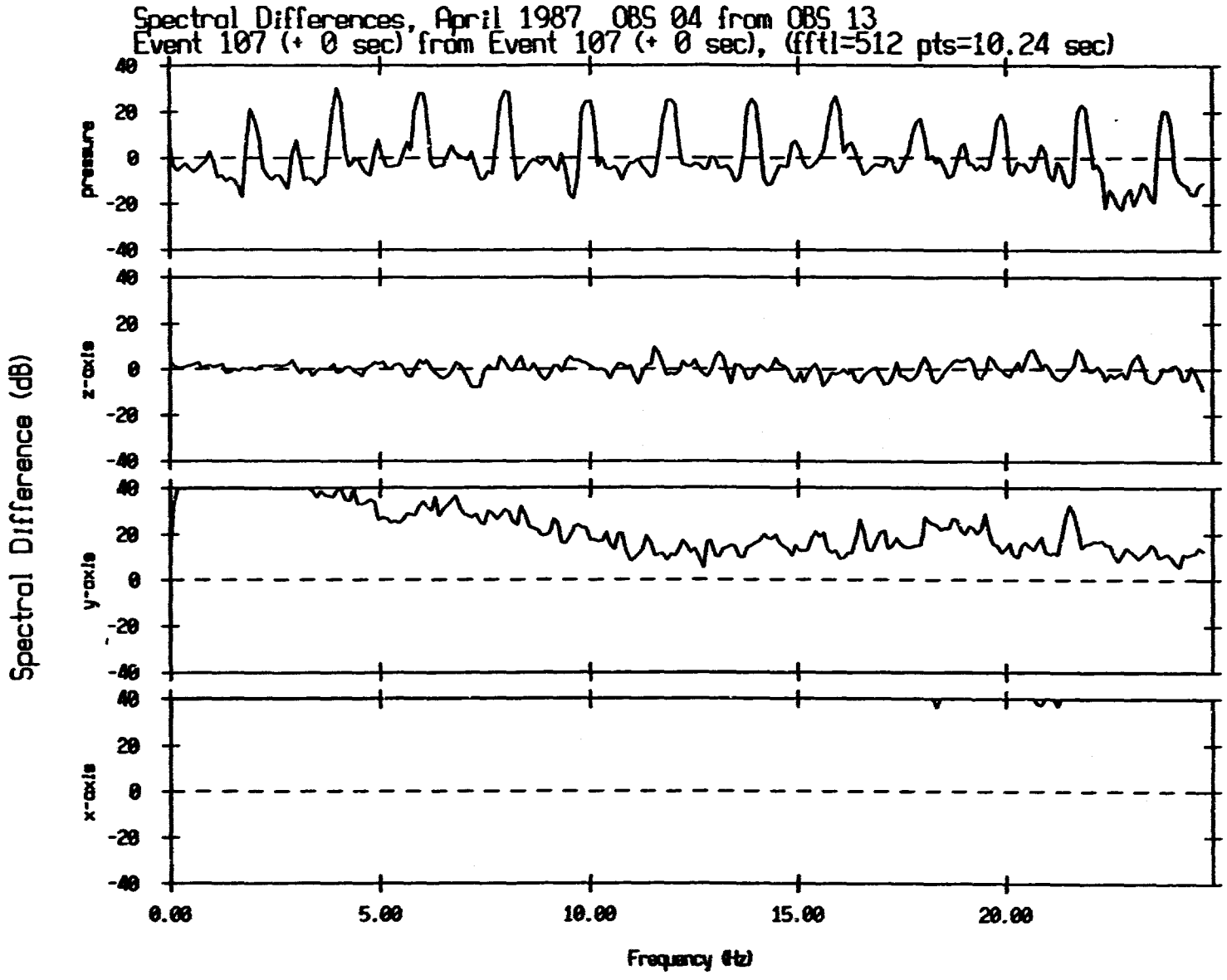
Spectral Differences, April 1987 OBS 04 from OBS 13
Event 107 (+ 0 sec) from Event 107 (+ 0 sec), (fftl=512 pts=10.24 sec)
Spectral Difference (dB)
pressure
z-axis
y-axis
x-axis
40
20
0
-20
-40
0.00
5.00
10.00
15.00
20.00
Frequency (Hz)

Figure V.15

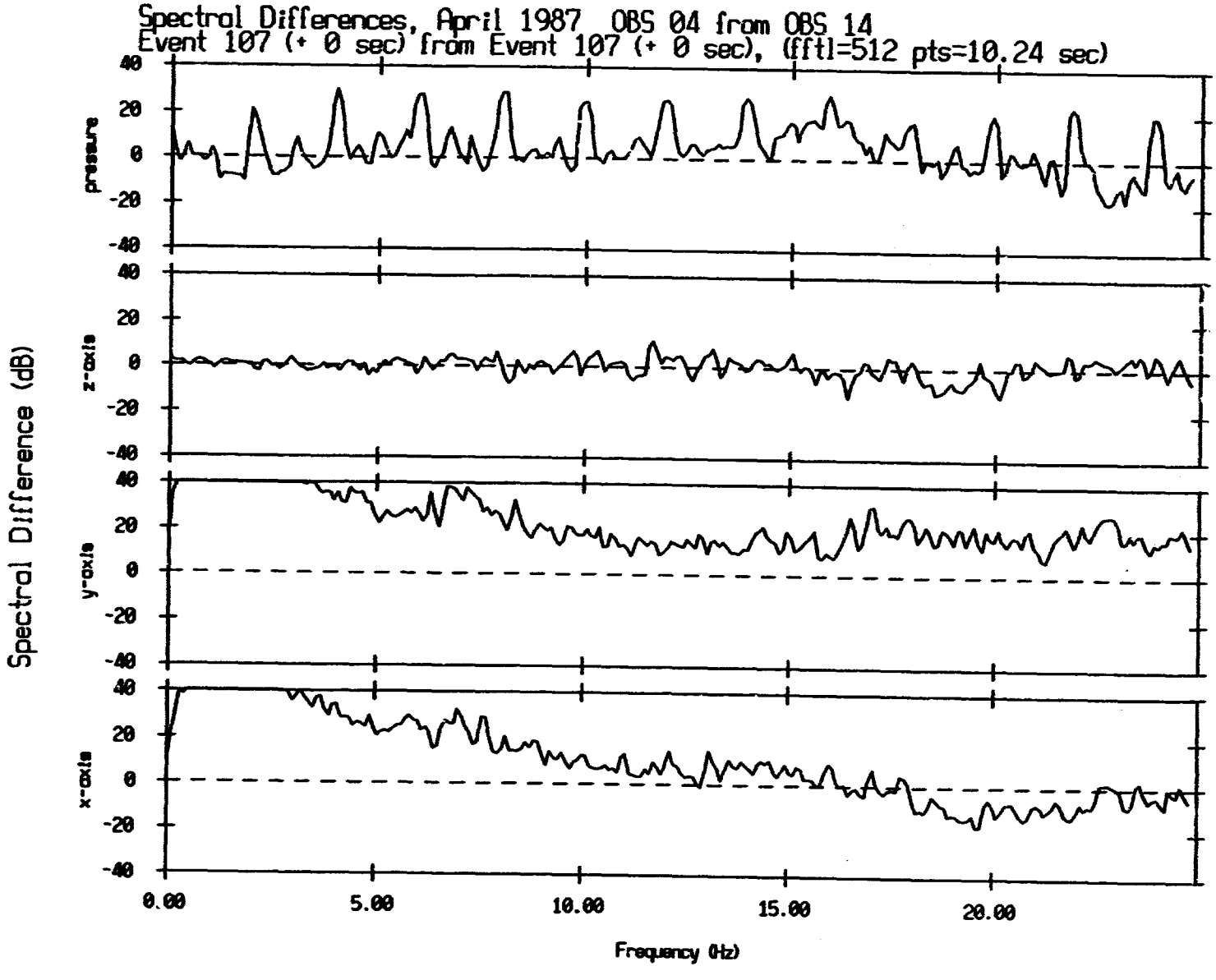
Spectral Differences, April 1987 OBS 04 from OBS 14
Event 107 (+ 0 sec) from Event 107 (+ 0 sec), (fftl=512 pts=10.24 sec)
Spectral Difference (dB)
pressure
z-axis
y-axis
x-axis
40
20
0
-20
-40
0.00
5.00
10.00
15.00
20.00
Frequency (Hz)

Figure V.16

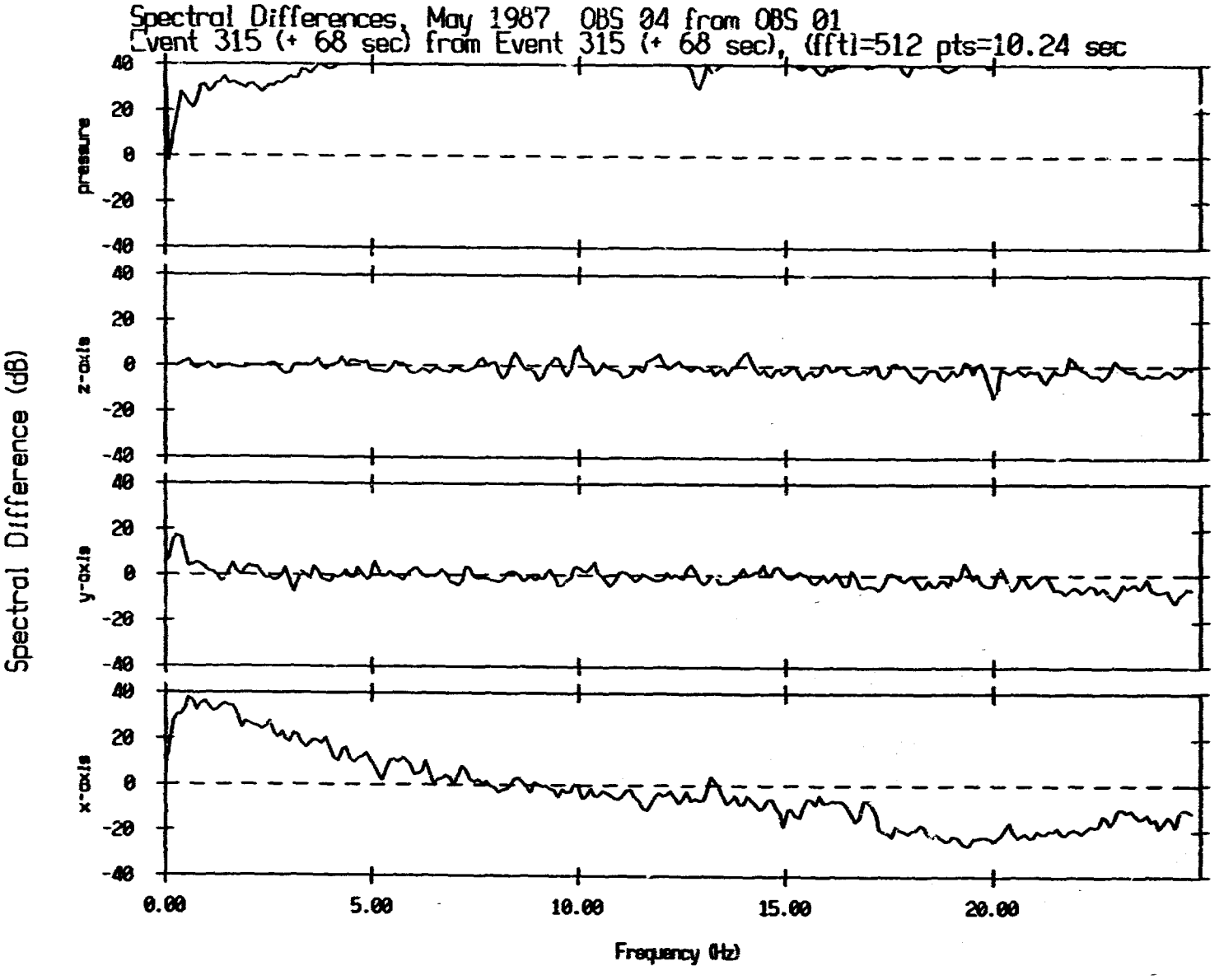
Spectral Differences, May 1987 OBS 04 from OBS 01
Event 315 (+ 68 sec) from Event 315 (+ 68 sec), (fft)=512 pts=10.24 sec
Spectral Difference (dB)
pressure
z-axis
y-axis
x-axis
40
20
0
-20
-40
0.00
5.00
10.00
15.00
20.00
Frequency (Hz)

Figure V.17

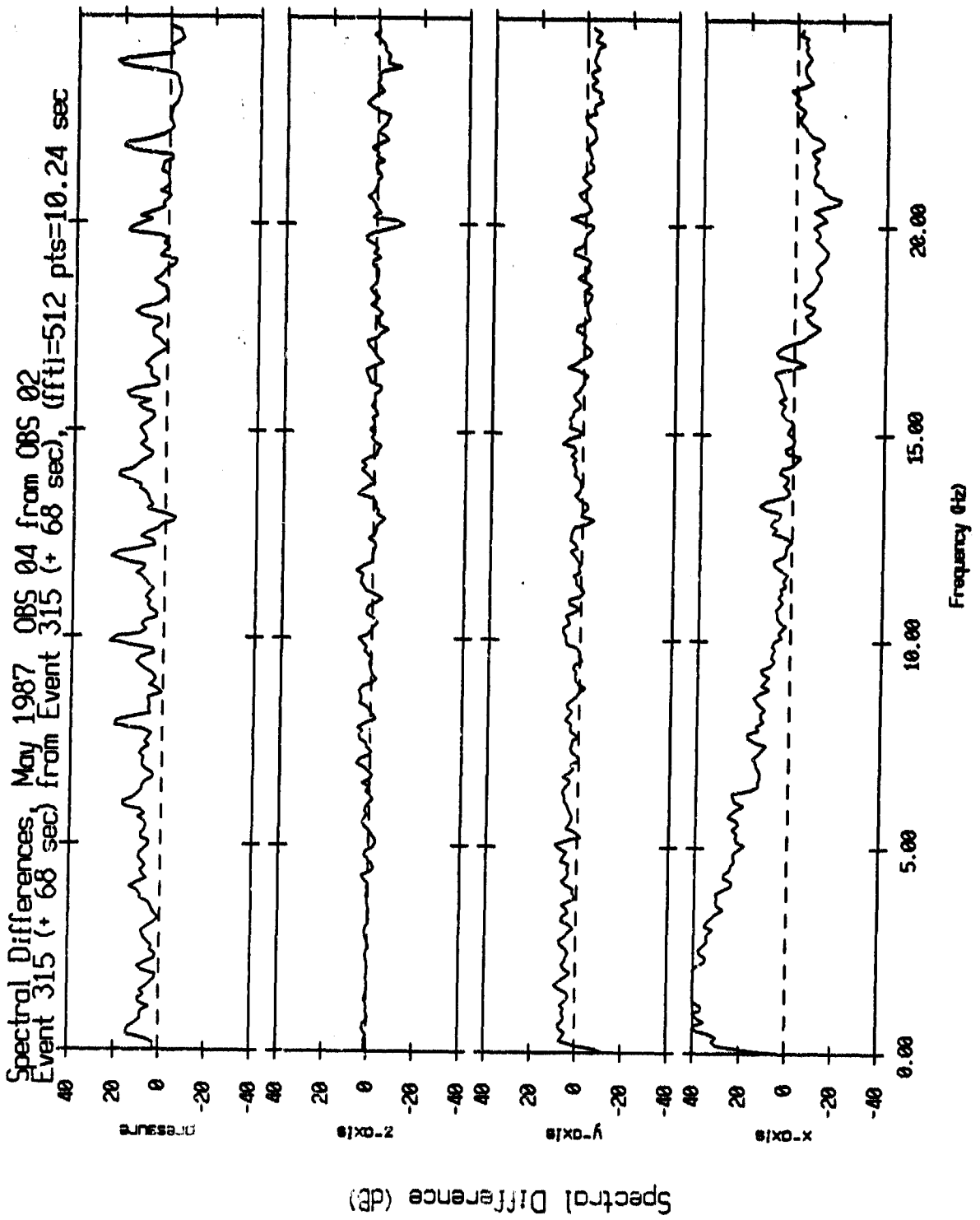
Spectral Differences, May 1987 OBS 04 from OBS 02
Event 315 (+ 68 sec) from Event 315 (+ 68 sec), (fft1=512 pts=10.24 sec
Spectral Difference (dB)
Frequency (Hz)
0.00
5.00
10.00
15.00
20.00
x-ax/s
y-ax/s
z-ax/s
pressure
40
20
0
-20
-40

Figure V.18

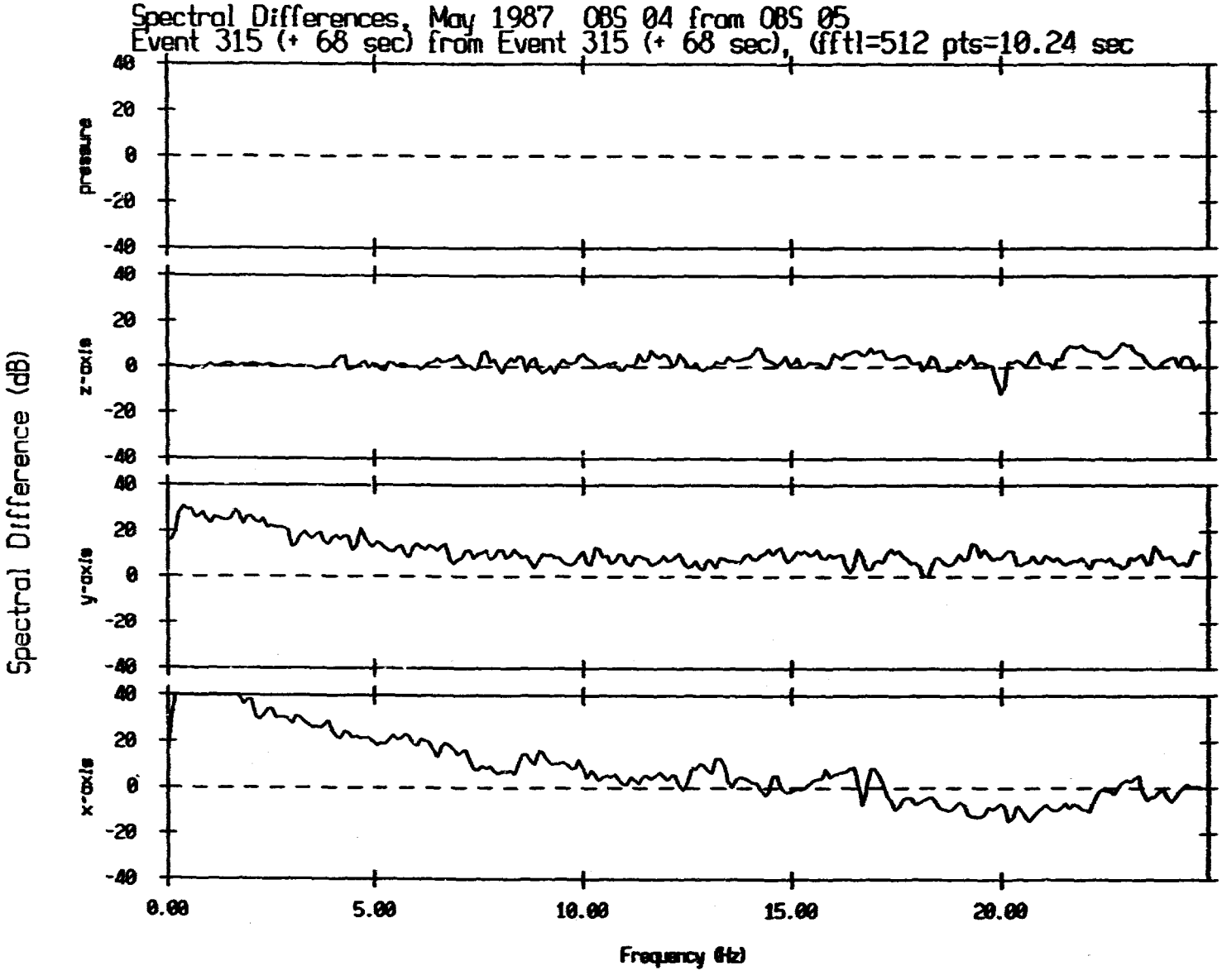
Spectral Differences, May 1987 OBS 04 from OBS 05
Event 315 (+ 68 sec) from Event 315 (+ 68 sec), (fftl=512 pts=10.24 sec
Spectral Difference (dB)
pressure
z-axis
y-axis
x-axis
40
20
0
-20
-40
0.00
5.00
10.00
15.00
20.00
Frequency (Hz)

Figure V.19

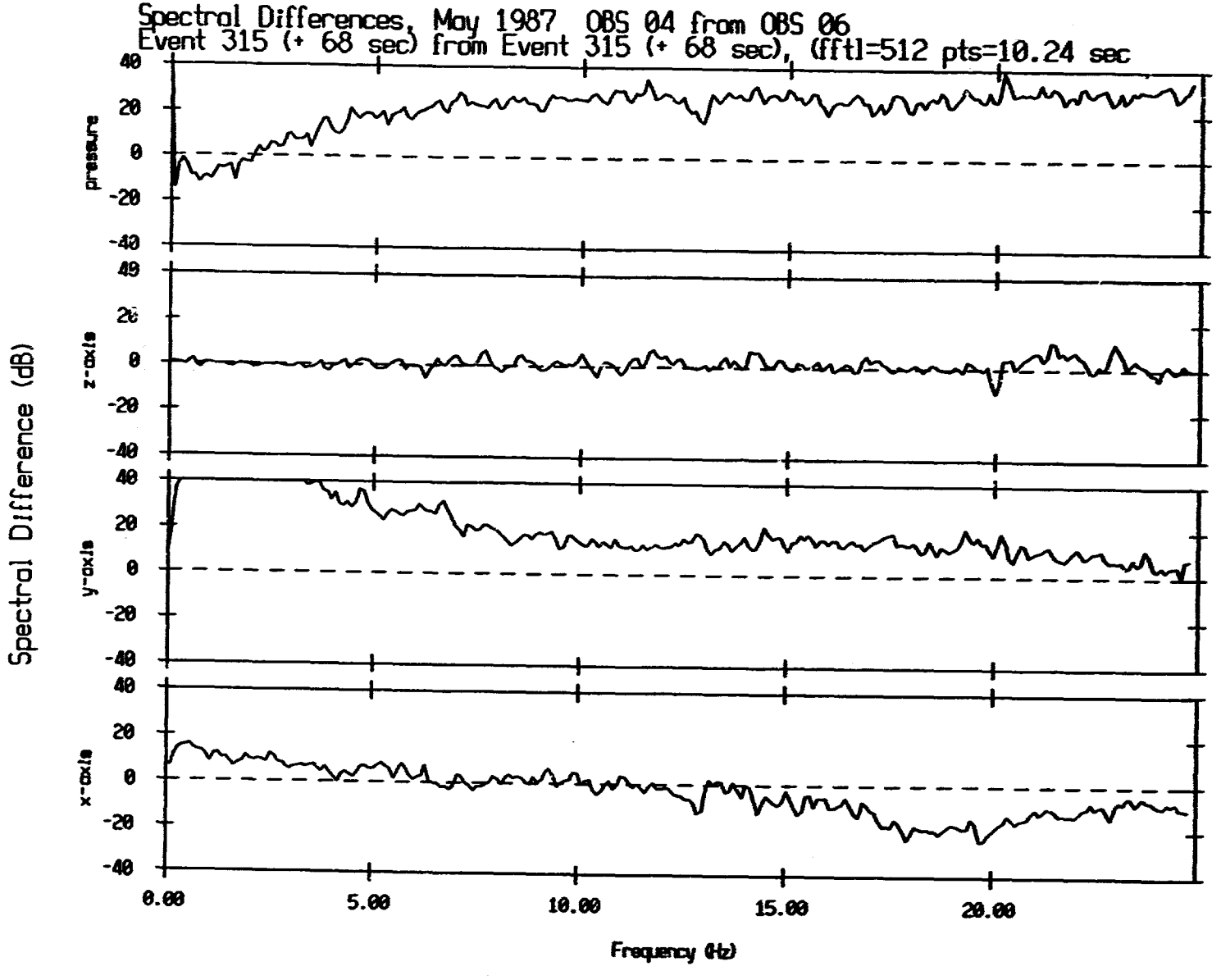
Spectral Differences, May 1987 OBS 04 from OBS 06
Event 315 (+ 68 sec) from Event 315 (+ 68 sec), (fftl=512 pts=10.24 sec
Spectral Difference (dB)
pressure
z-axis
y-axis
x-axis
40
20
0
-20
-40
0.00
5.00
10.00
15.00
20.00
Frequency (Hz)

Figure V.20

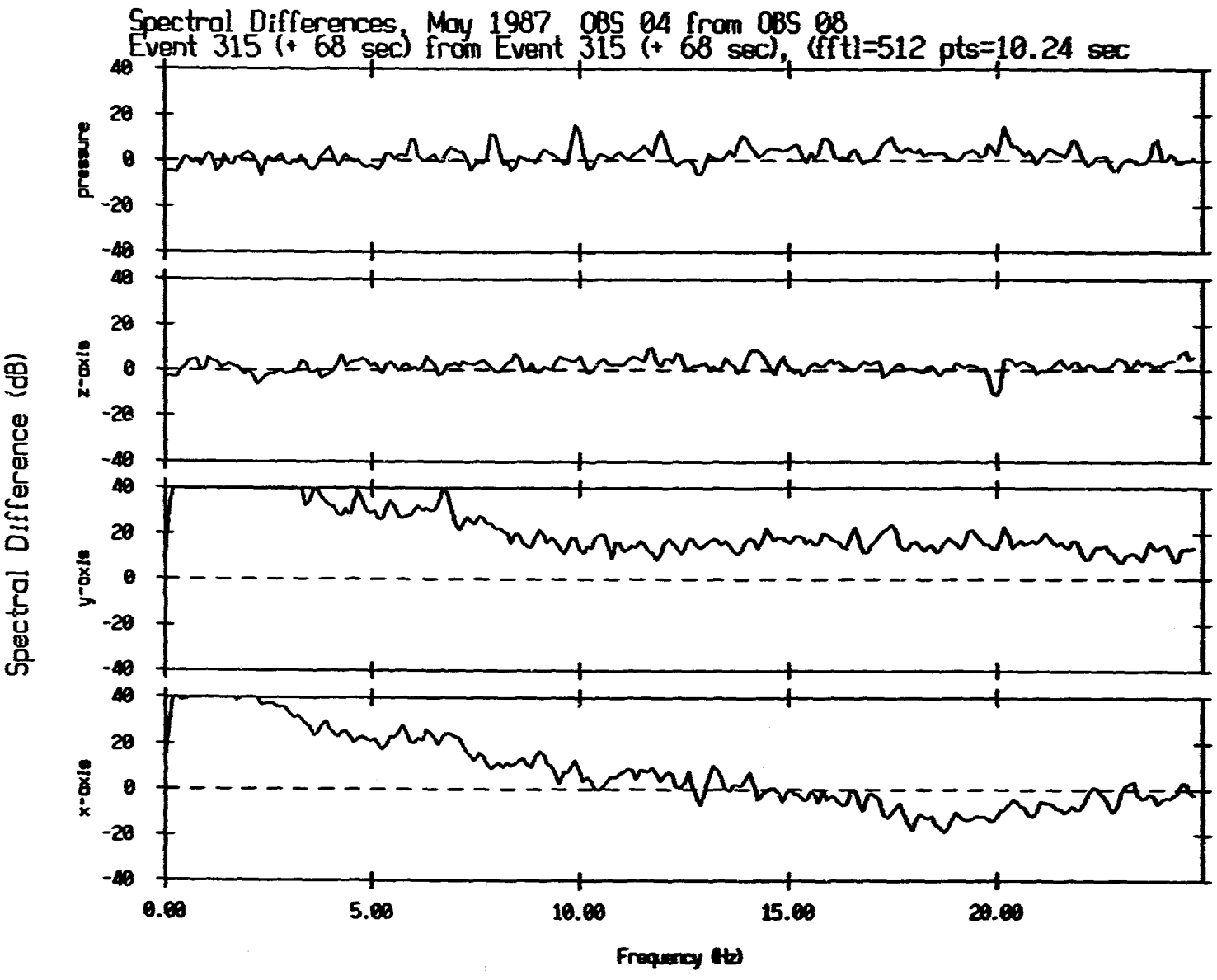
Spectral Differences, May 1987 OBS 04 from OBS 08
Event 315 (+ 68 sec) from Event 315 (+ 68 sec), (fftl=512 pts=10.24 sec
Spectral Difference (dB)
pressure
z-axis
y-axis
x-axis
40
20
0
-20
-40
0.00
5.00
10.00
15.00
20.00
Frequency (Hz)

Figure V.21

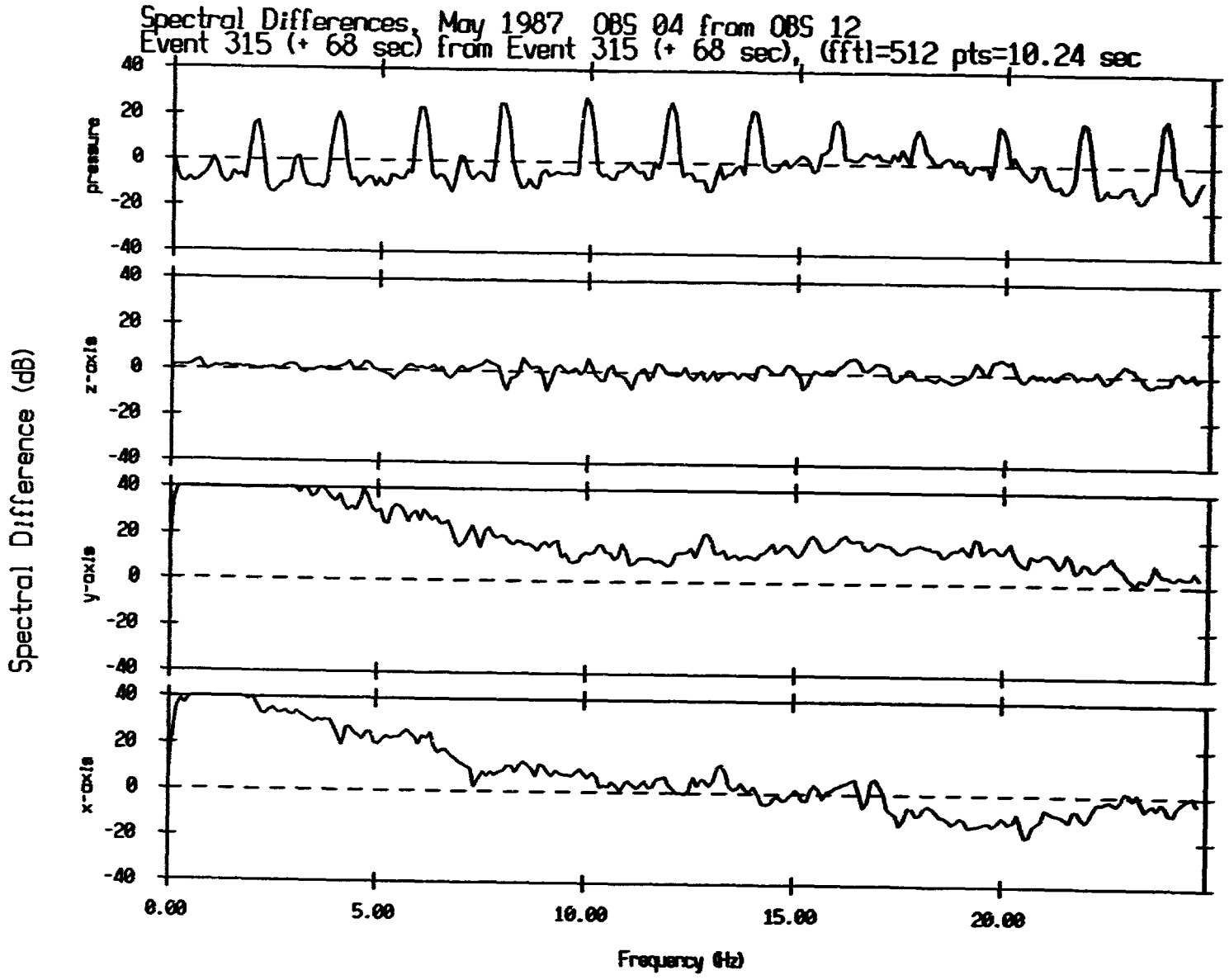
Spectral Differences, May 1987 OBS 04 from OBS 12
Event 315 (+ 68 sec) from Event 315 (+ 68 sec), (fftl=512 pts=10.24 sec
Spectral Difference (dB)
pressure
z-axis
y-axis
x-axis
40
20
0
-20
-40
0.00
5.00
10.00
15.00
20.00
Frequency (Hz)

Figure V.22

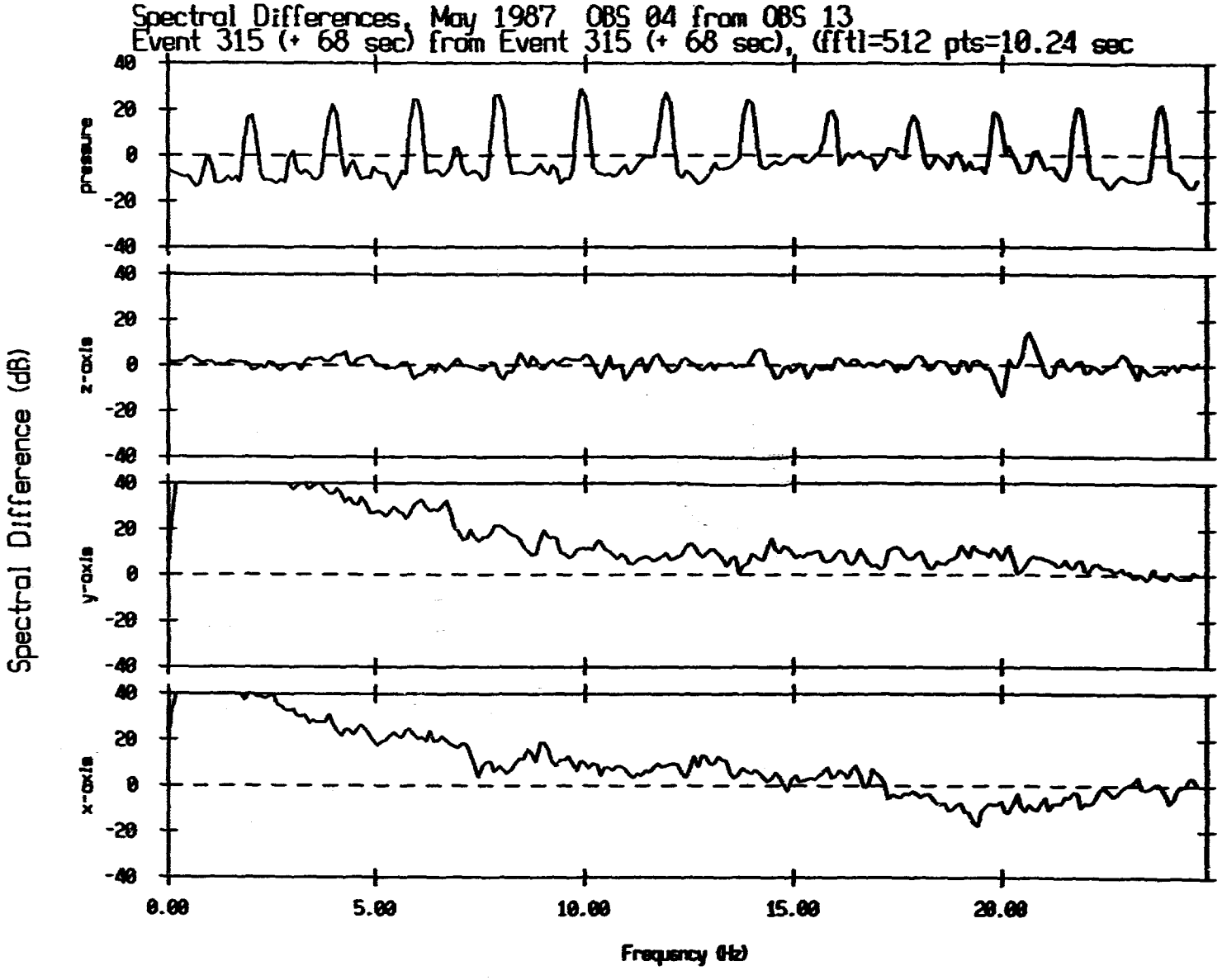
Spectral Differences, May 1987 OBS 04 from OBS 13
Event 315 (+ 68 sec) from Event 315 (+ 68 sec), (fft)=512 pts=10.24 sec
Spectral Difference (dB)
pressure
z-axis
y-axis
x-axis
40
20
0
-20
-40
0.00
5.00
10.00
15.00
20.00
Frequency (Hz)

Figure V.23

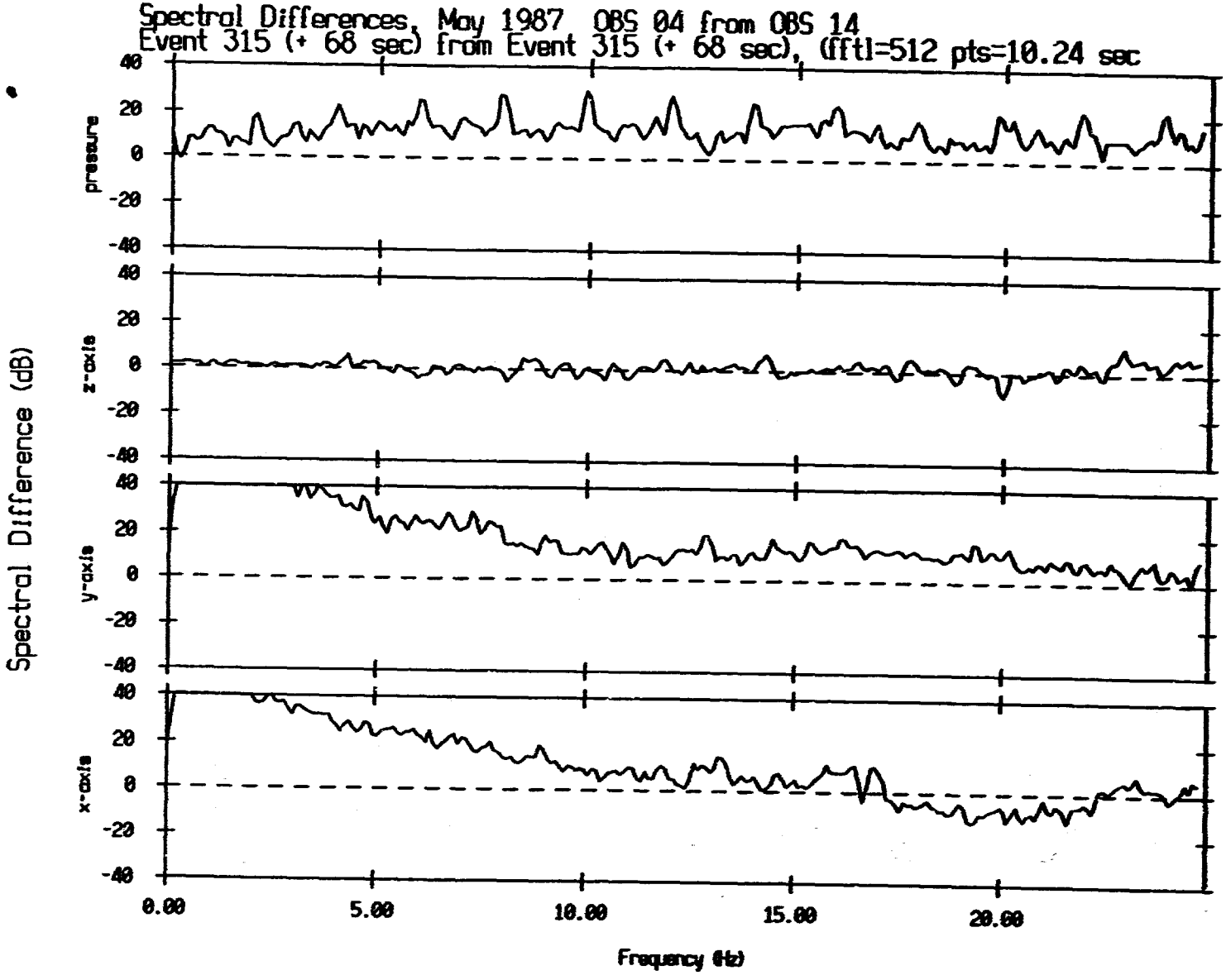
Spectral Differences, May 1987 OBS 04 from OBS 14
Event 315 (+ 68 sec) from Event 315 (+ 68 sec), (fftl=512 pts=10.24 sec
Spectral Difference (dB)
pressure
z-axis
y-axis
x-axis
40
20
0
-20
-40
0.00
5.00
10.00
15.00
20.00
Frequency (Hz)

Figure V.24

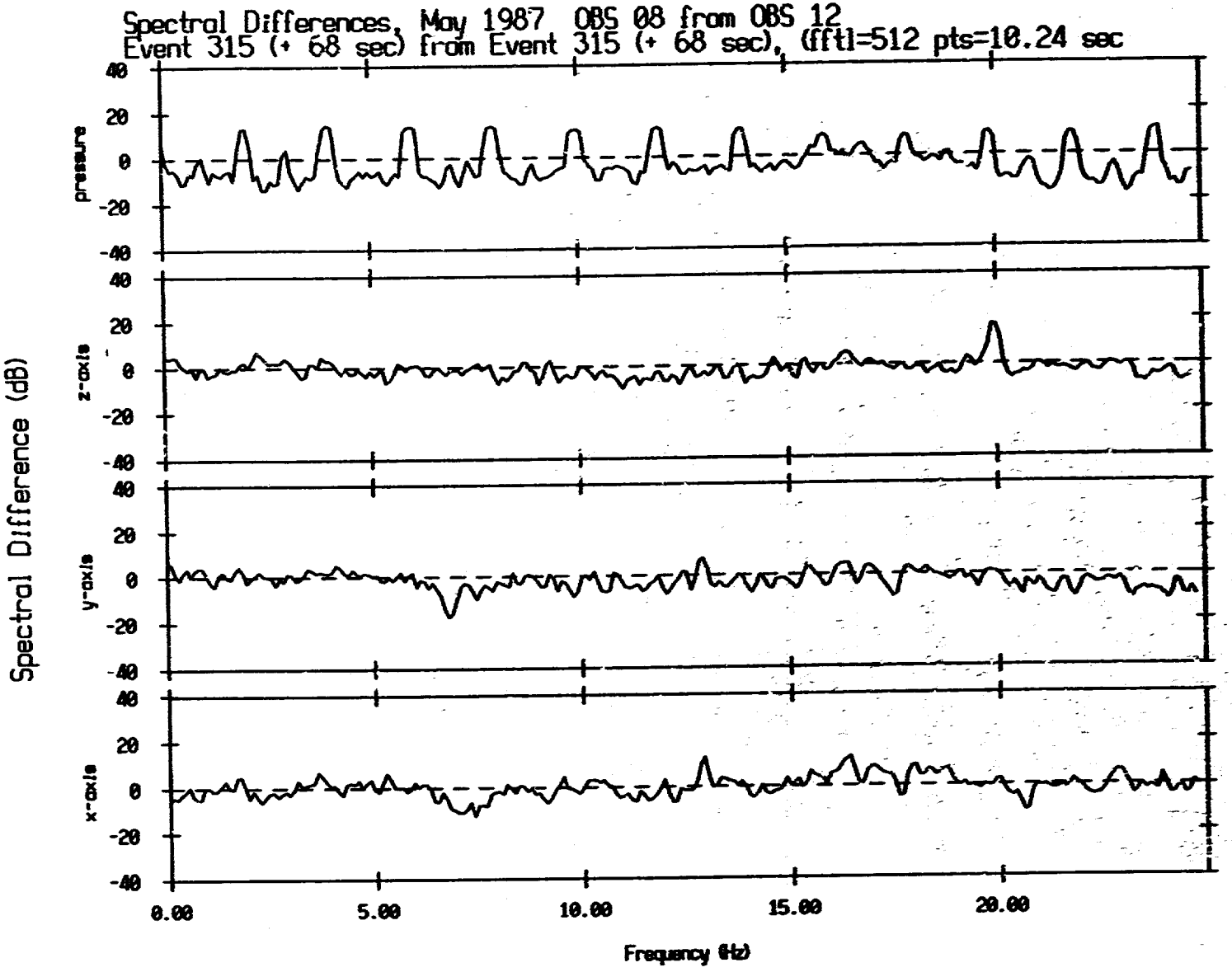
Spectral Differences, May 1987 OBS 08 from OBS 12
Event 315 (+ 68 sec) from Event 315 (+ 68 sec), (fft)=512 pts=10.24 sec
Spectral Difference (dB)
pressure
z-axis
y-axis
x-axis
40
20
0
-20
-40
0.00
5.00
10.00
15.00
20.00
Frequency (Hz)

Figure V.25

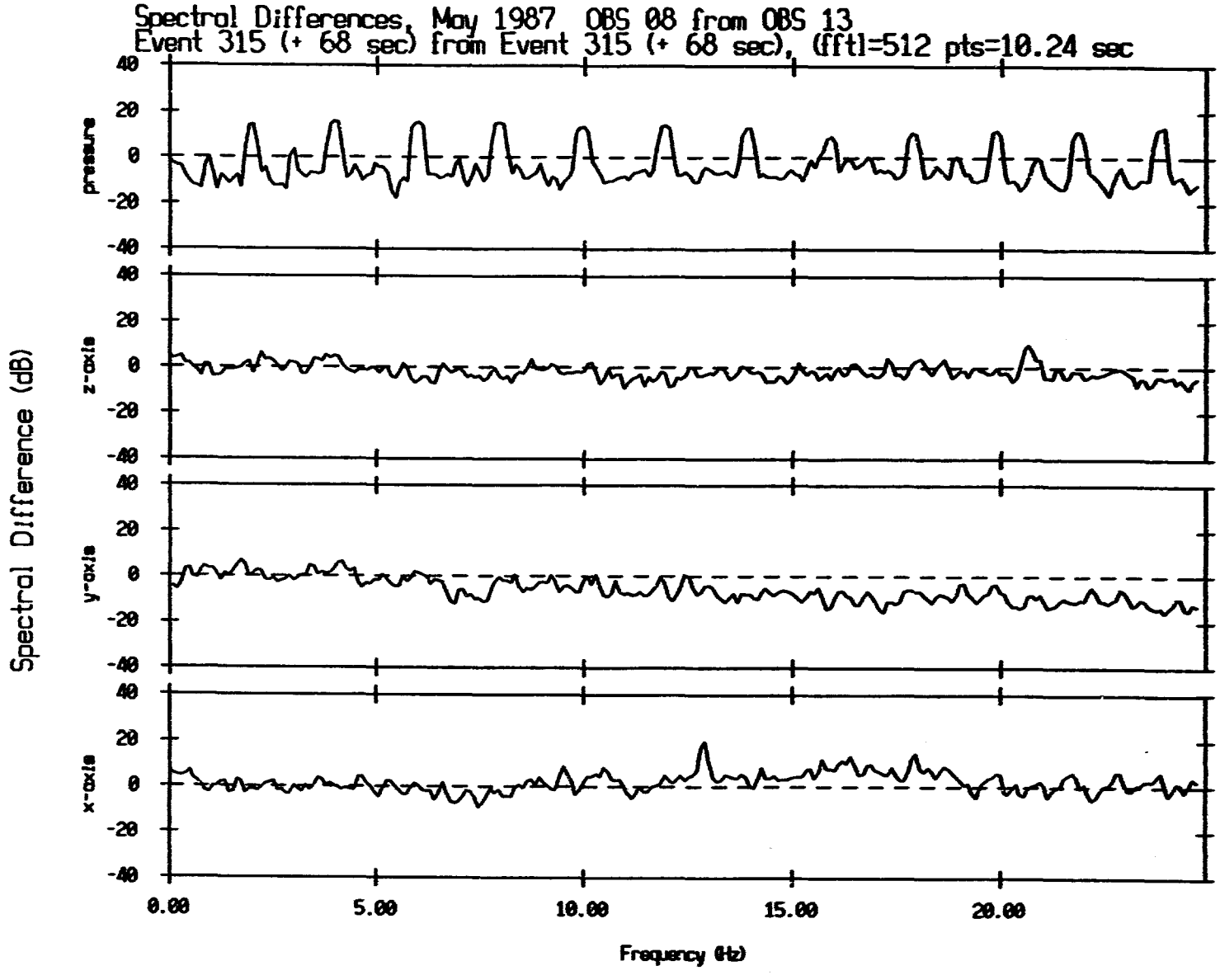
Spectral Differences, May 1987 OBS 08 from OBS 13
Event 315 (+ 68 sec) from Event 315 (+ 68 sec), (fftl=512 pts=10.24 sec
Spectral Difference (dB)
pressure
z-axis
y-axis
x-axis
40
20
0
-20
-40
0.00
5.00
10.00
15.00
20.00
Frequency (Hz)

Figure V.26

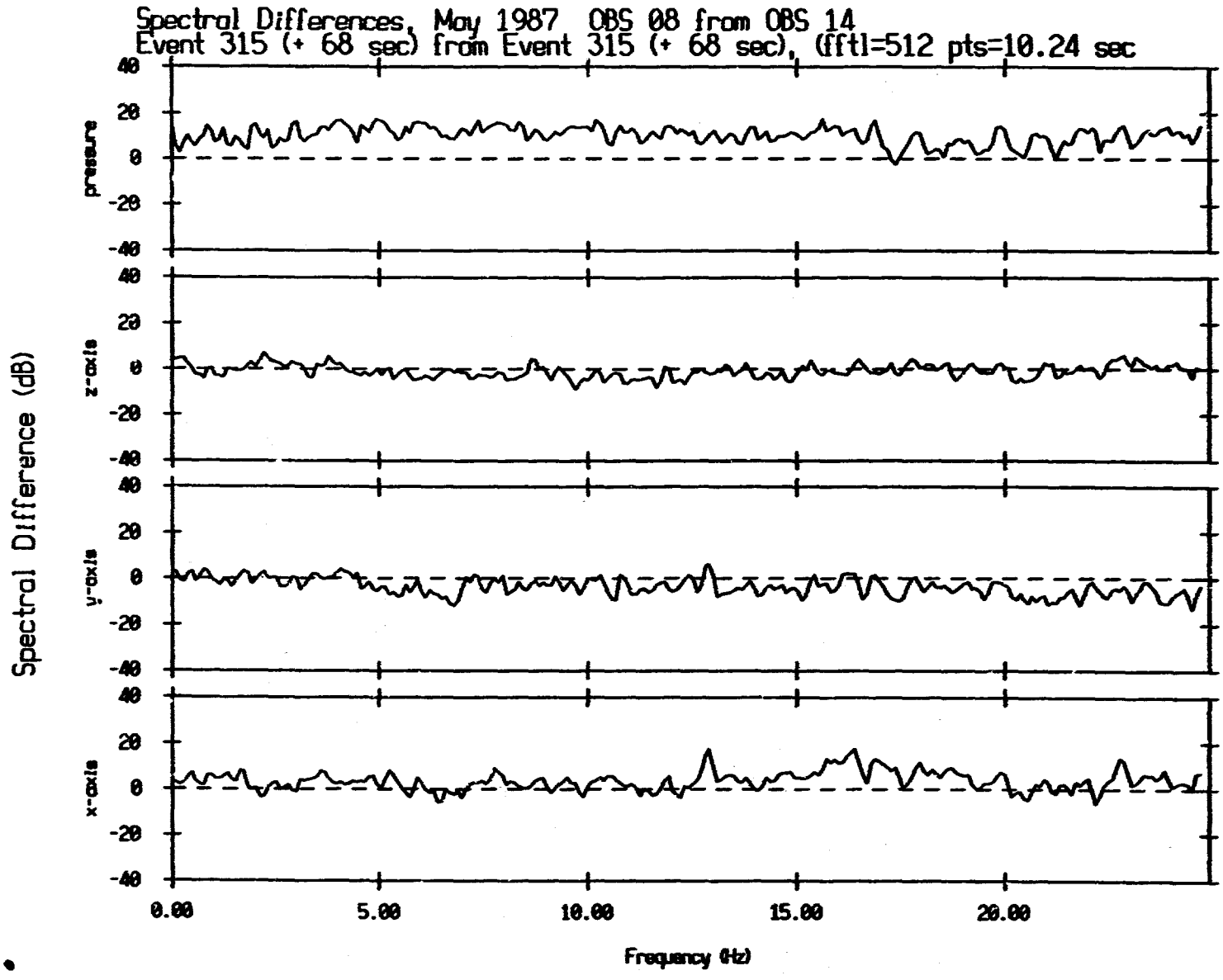
Spectral Differences, May 1987 OBS 08 from OBS 14
Event 315 (+ 68 sec) from Event 315 (+ 68 sec), (fftl=512 pts=10.24 sec
Spectral Difference (dB)
pressure
z-axis
y-axis
x-axis
40
20
0
-20
-40
0.00
5.00
10.00
15.00
20.00
Frequency (Hz)

Figure V.27

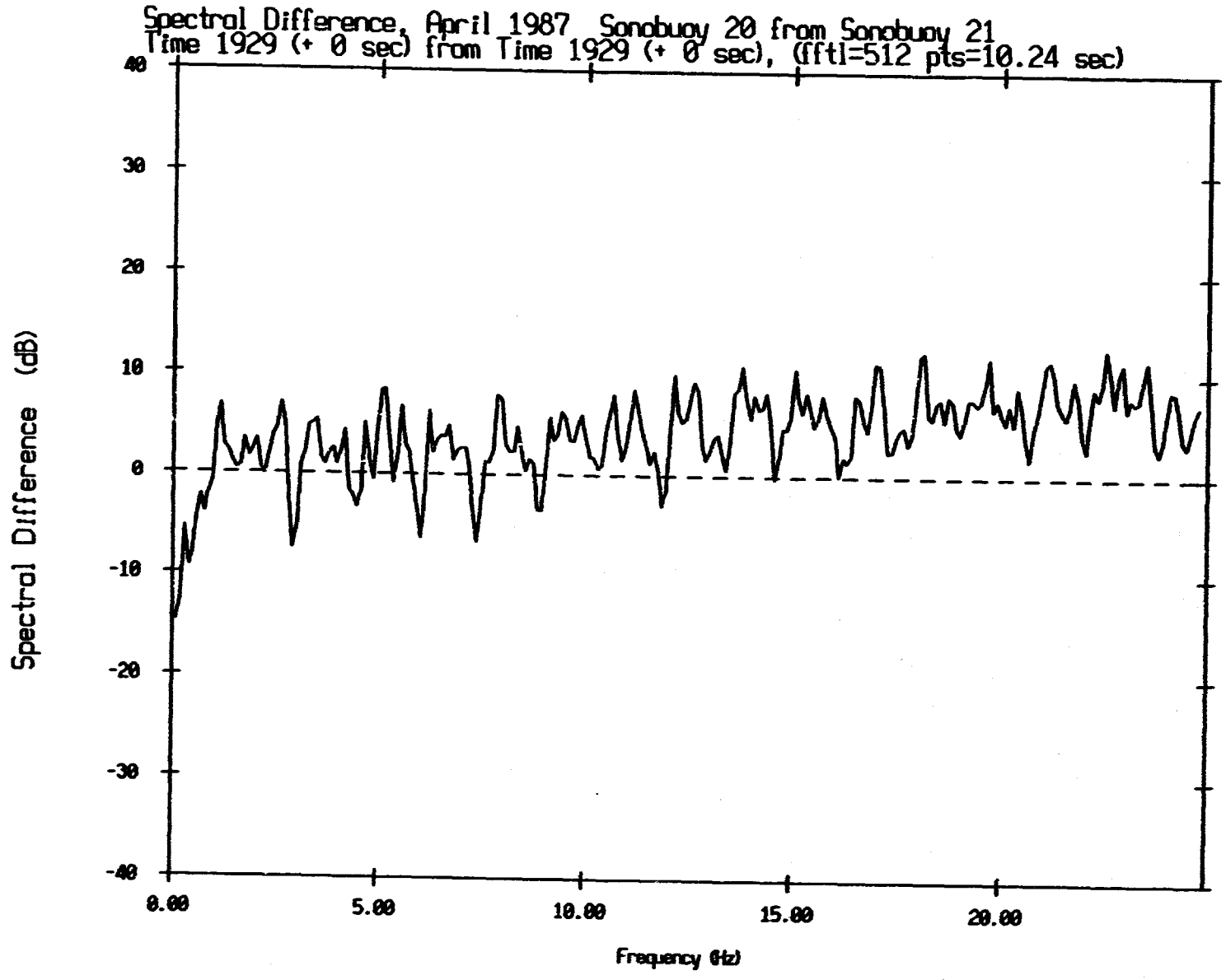
Spectral Difference, April 1987 Sonobuoy 20 from Sonobuoy 21
Time 1929 (+ 0 sec) from Time 1929 (+ 0 sec), (fftl=512 pts=10.24 sec)
Spectral Difference (dB)
40
30
20
10
0
-10
-20
-30
-40
0.00
5.00
10.00
15.00
20.00
Frequency (Hz)

Figure V.28

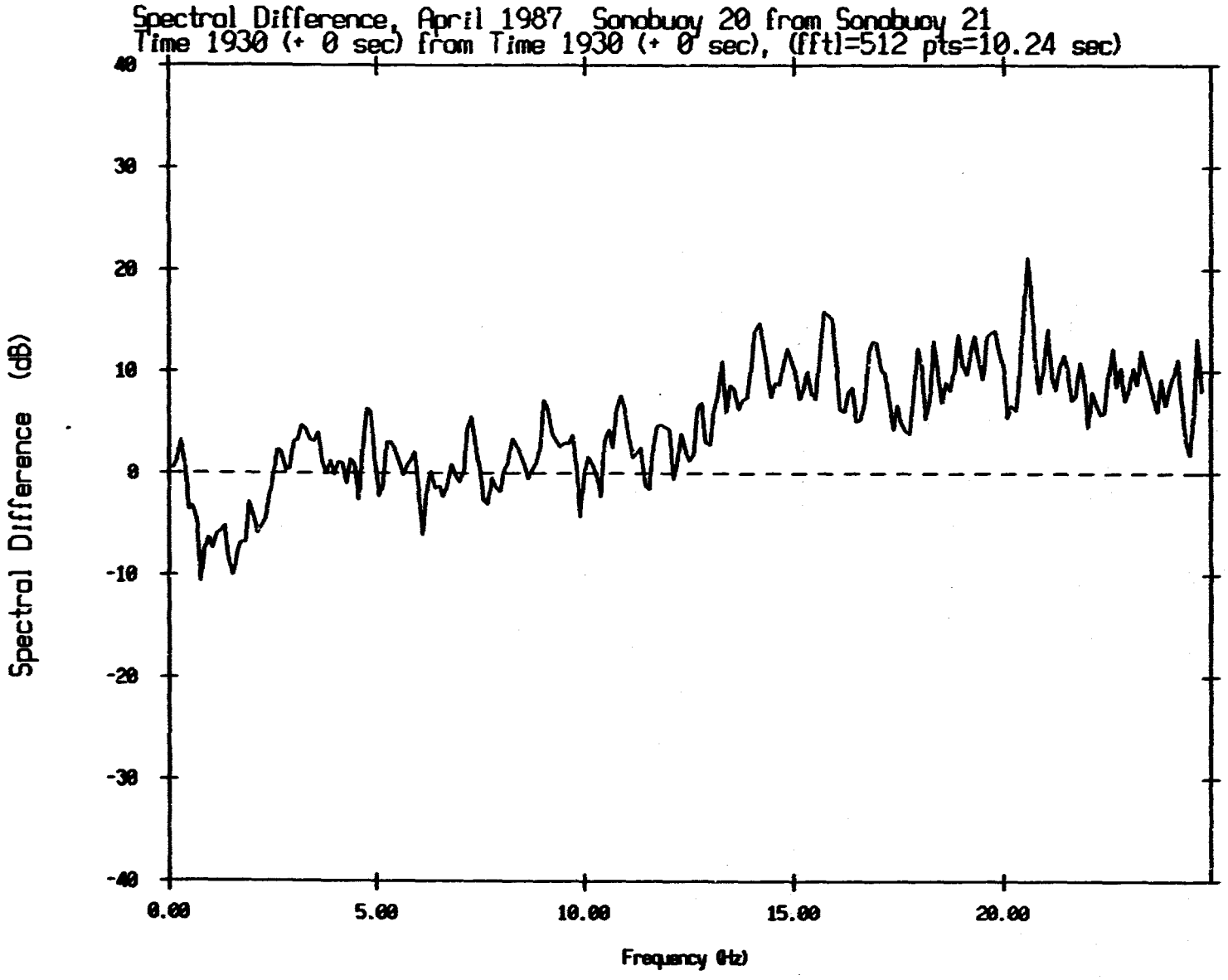
Spectral Difference, April 1987 Sonobuoy 20 from Sonobuoy 21
Time 1930 (+ 0 sec) from Time 1930 (+ 0 sec), (fftl=512 pts=10.24 sec)
Spectral Difference (dB)
40
30
20
10
0
-10
-20
-30
-40
0.00
5.00
10.00
15.00
20.00
Frequency (Hz)

Figure V.29

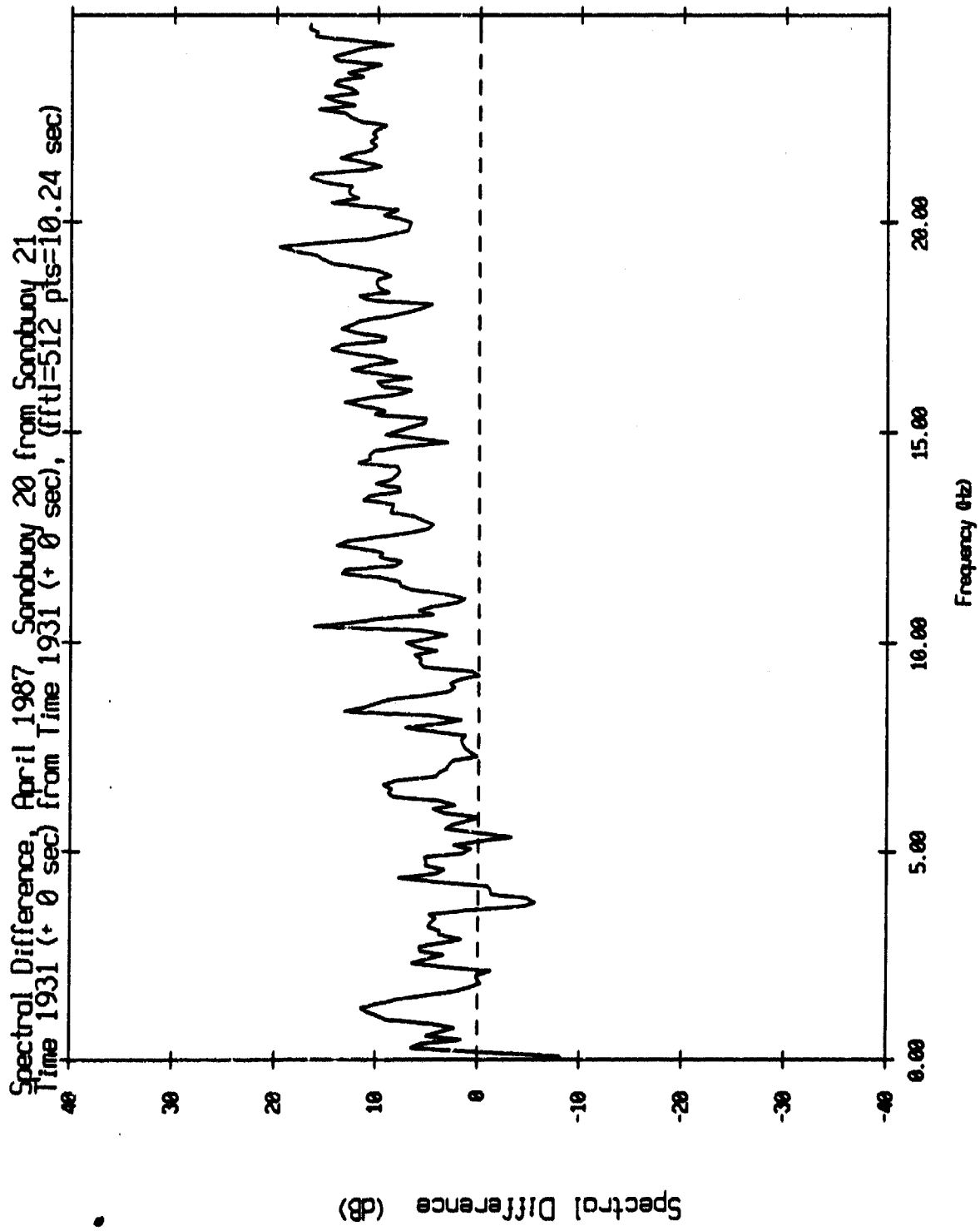
Spectral Difference, April 1987 Sonobuoy 20 from Sonobuoy 21
Time 1931 (+ 0 sec) from Time 1931 (+ 0 sec), (fftl=512 pts=10.24 sec)
Spectral Difference (dB)
40
30
20
10
0
-10
-20
-30
-40
0.00
5.00
10.00
15.00
20.00
Frequency (Hz)

Figure V.30

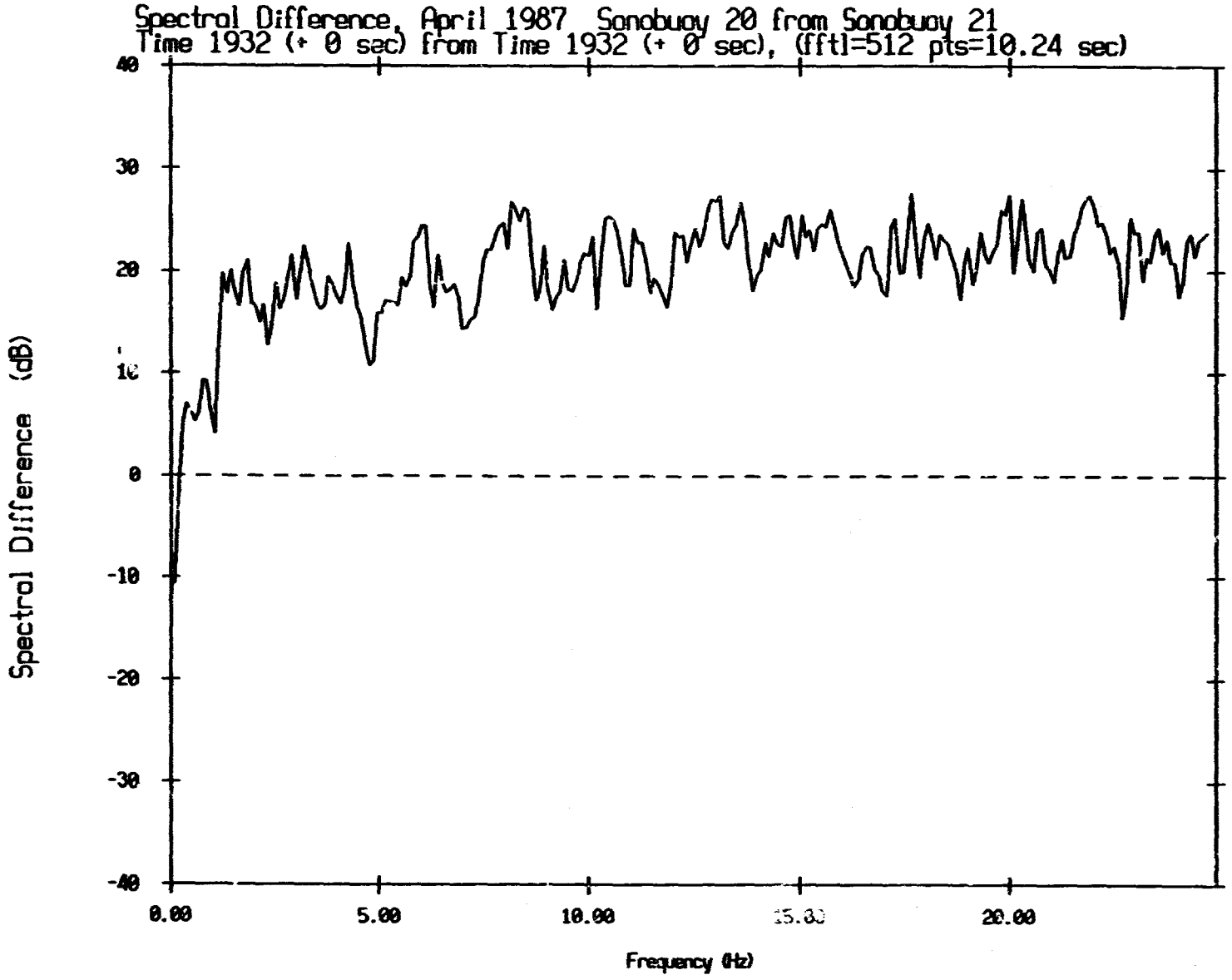
Spectral Difference, April 1987 Sonobuoy 20 from Sonobuoy 21
Time 1932 (+ 0 sec) from Time 1932 (+ 0 sec), (fft=512 pts=10.24 sec)
Spectral Difference (dB)
40
30
20
10
0
-10
-20
-30
-40
0.00
5.00
10.00
15.00
20.00
Frequency (Hz)

Figure V.31

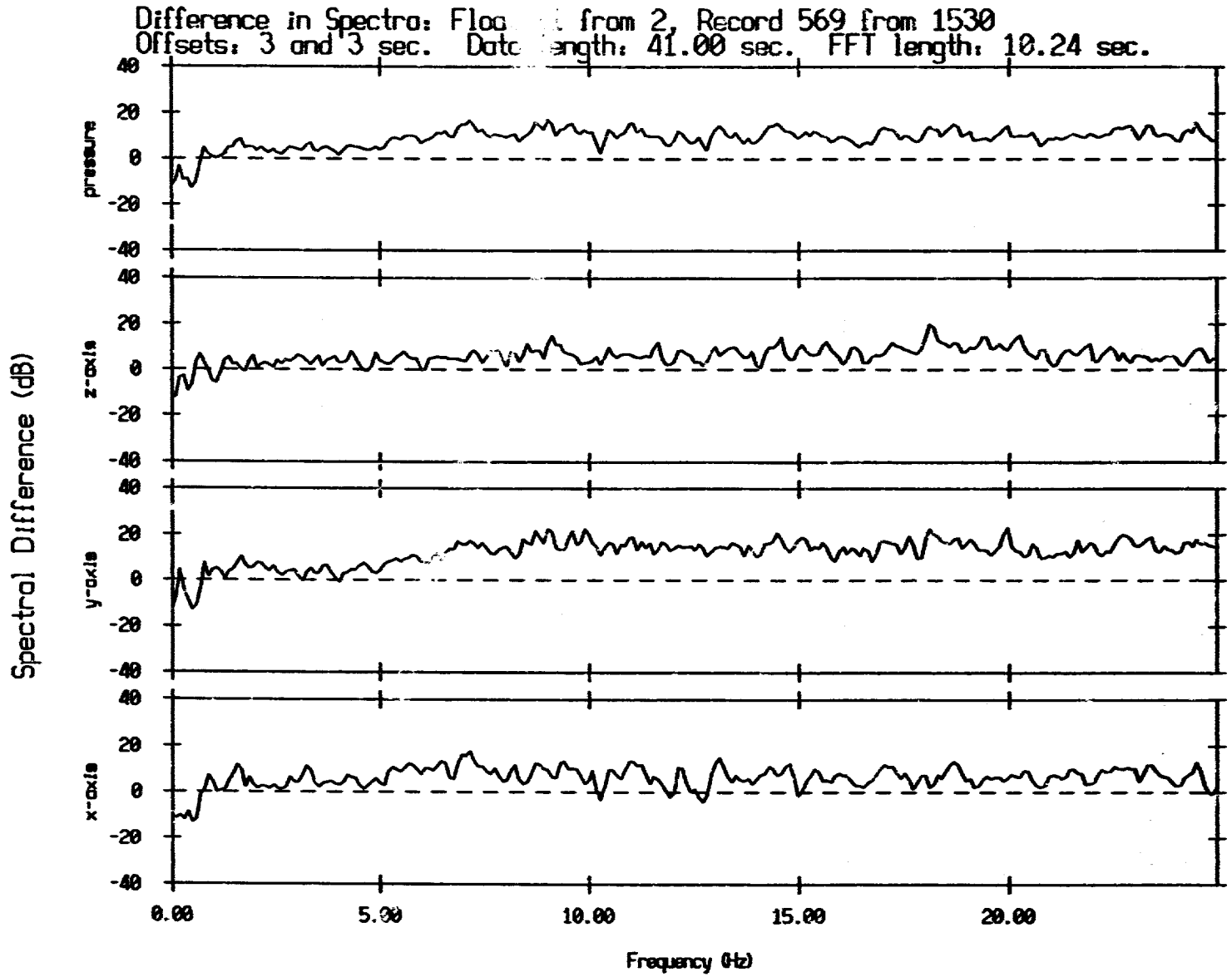
Difference in Spectra: Floc t from 2, Record 569 from 1530
Offsets: 3 and 3 sec. Data length: 41.00 sec. FFT length: 10.24 sec.
Spectral Difference (dB)
pressure
z-axis
y-axis
x-axis
40
20
0
-20
-40
0.00
5.00
10.00
15.00
20.00
Frequency (Hz)

Figure V.32

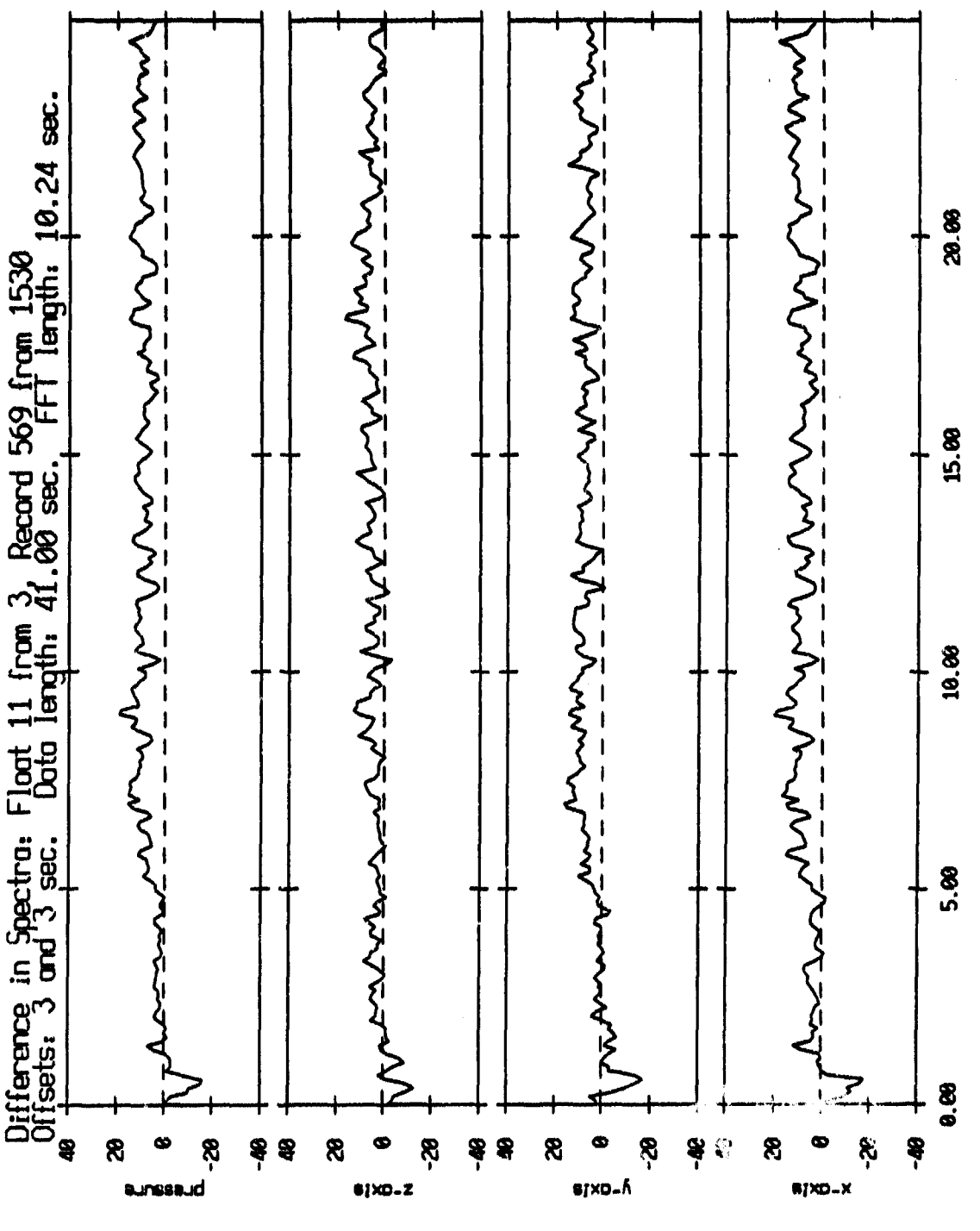
Difference in Spectra: Float 11 from 3, Record 569 from 1530
Offsets: 3 and 3 sec. Data length: 41.00 sec. FFT length: 10.24 sec.
pressure
z-axis
y-axis
x-axis
40
20
0
-20
-40
0.00
5.00
10.00
15.00
20.00
Frequency (Hz)
Spectral Difference (dB)

Figure V.33

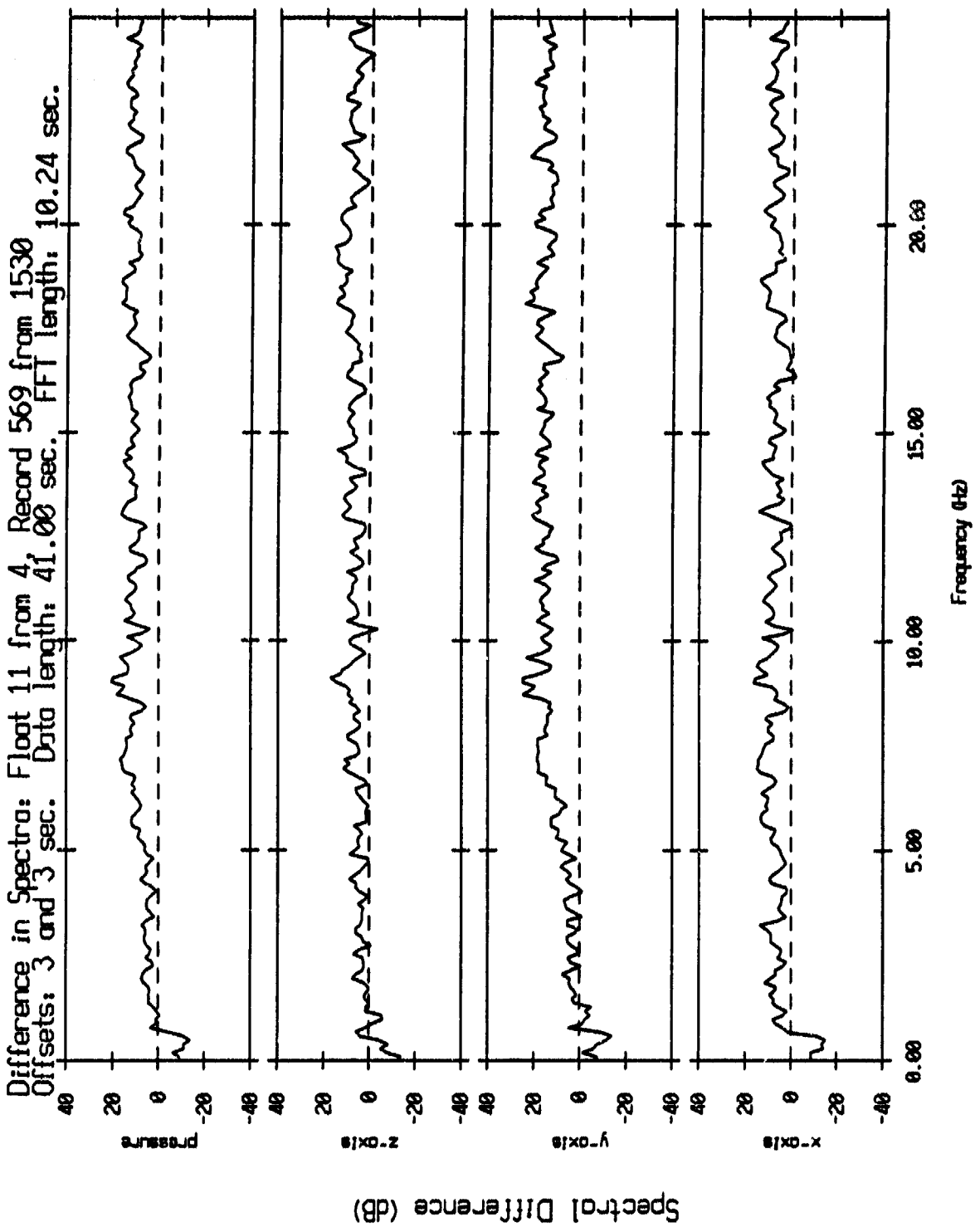
Difference in Spectra: Float 11 from 4, Record 569 from 1530
Offsets: 3 and 3 sec. Data length: 41.00 sec. FFT length: 10.24 sec.
pressure
z-axis
y-axis
x-axis
40
20
0
-20
-40
0.00
5.00
10.00
15.00
20.00
Frequency (Hz)
Spectral Difference (db)

Figure V.34

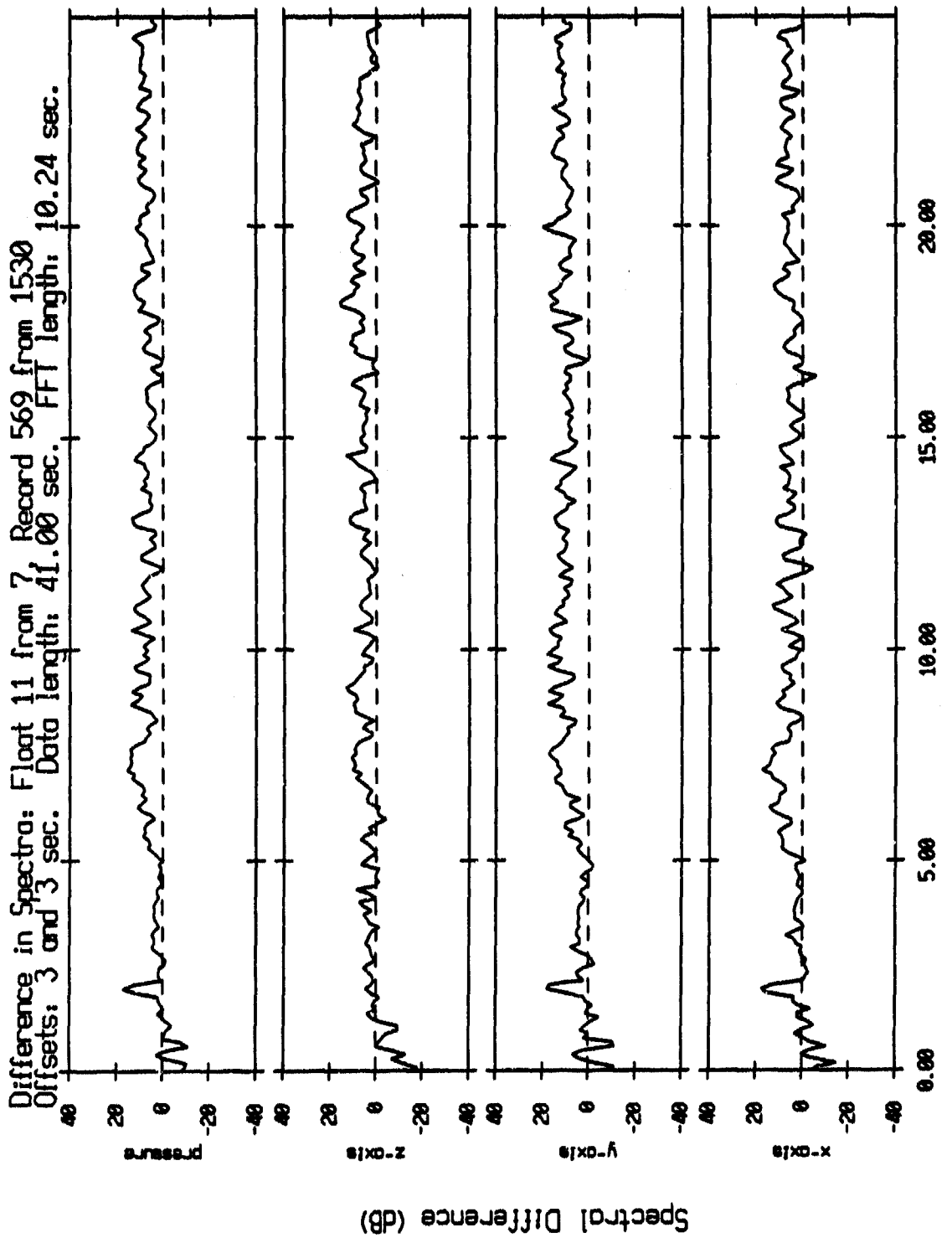
Difference in Spectra: Float 11 from 7, Record 569 from 1530
Offsets: 3 and 3 sec. Data length: 41.00 sec. FFT length: 10.24 sec.
pressure
z-axis
y-axis
x-axis
40
20
0
-20
-40
0.00
5.00
10.00
15.00
20.00
Frequency (Hz)
Spectral Difference (db)

Figure V.35

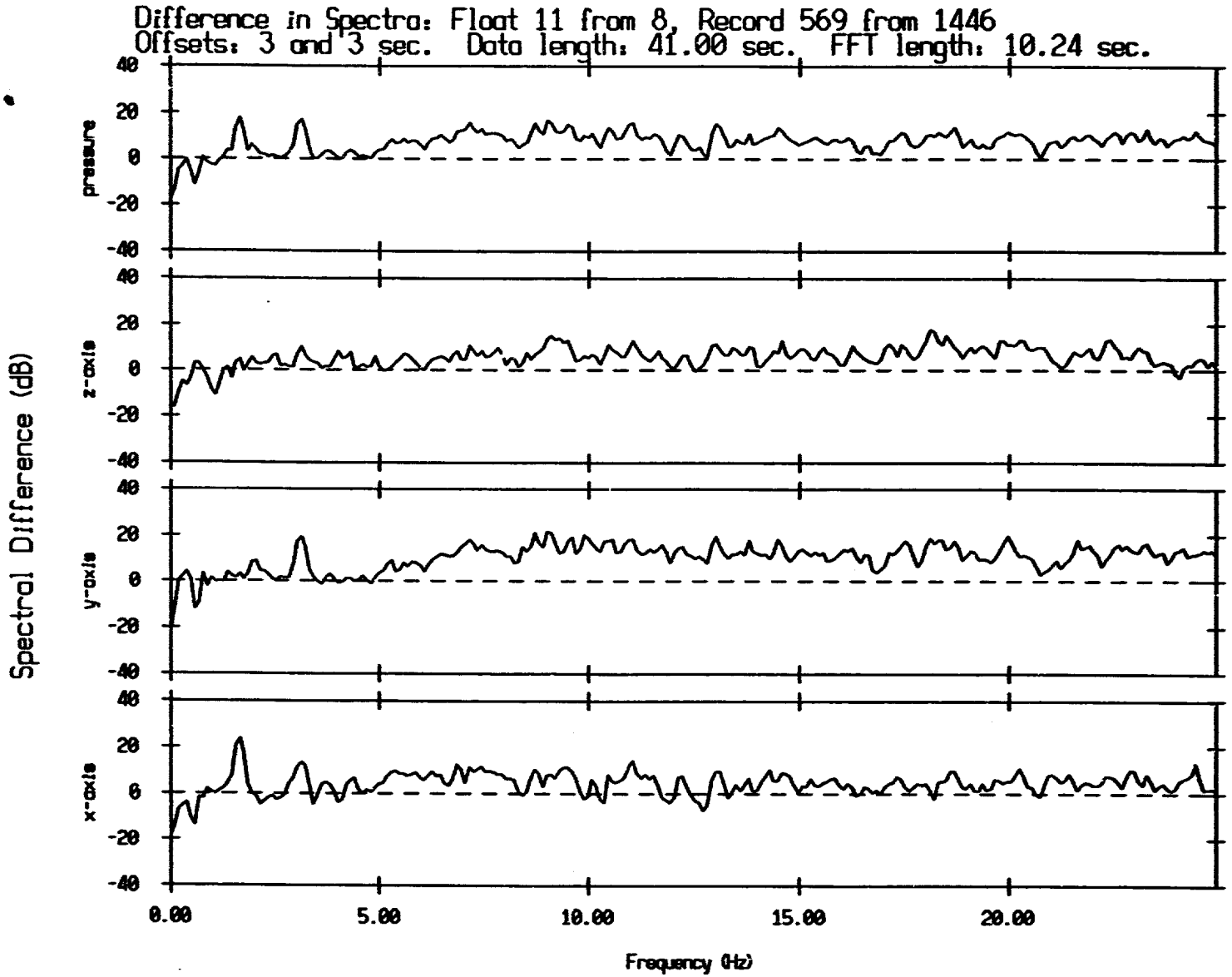
Difference in Spectra: Float 11 from 8, Record 569 from 1446
Offsets: 3 and 3 sec. Data length: 41.00 sec. FFT length: 10.24 sec.
Spectral Difference (dB)
pressure
z-axis
y-axis
x-axis
40
20
0
-20
-40
0.00
5.00
10.00
15.00
20.00
Frequency (Hz)

Figure V.30

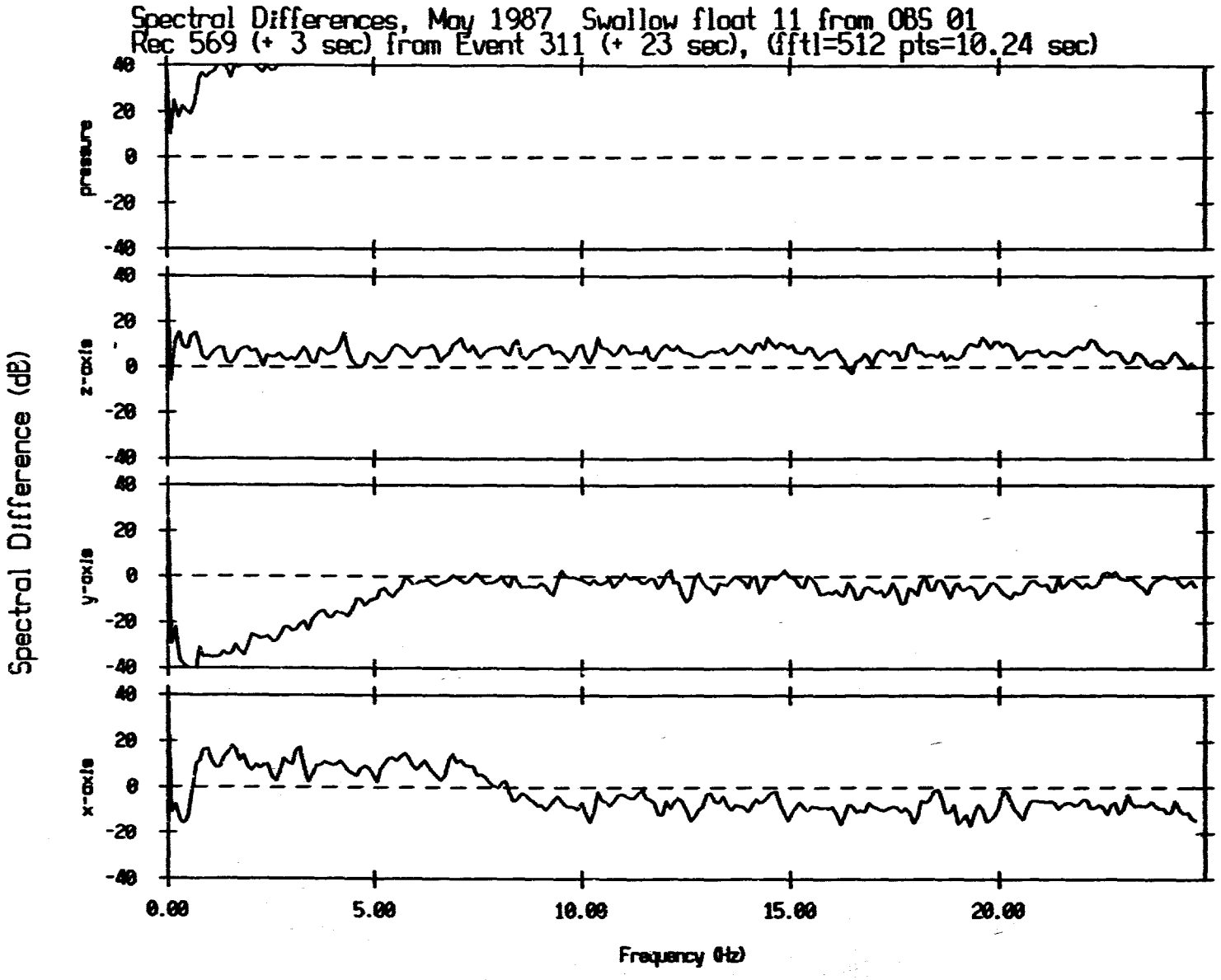
Spectral Differences, May 1987 Swallow float 11 from OBS 01
Rec 569 (+ 3 sec) from Event 311 (+ 23 sec), (fftl=512 pts=10.24 sec)
Spectral Difference (dB)
pressure
z-axis
y-axis
x-axis
40
20
0
-20
-40
0.00
5.00
10.00
15.00
20.00
Frequency (Hz)

Figure V.37

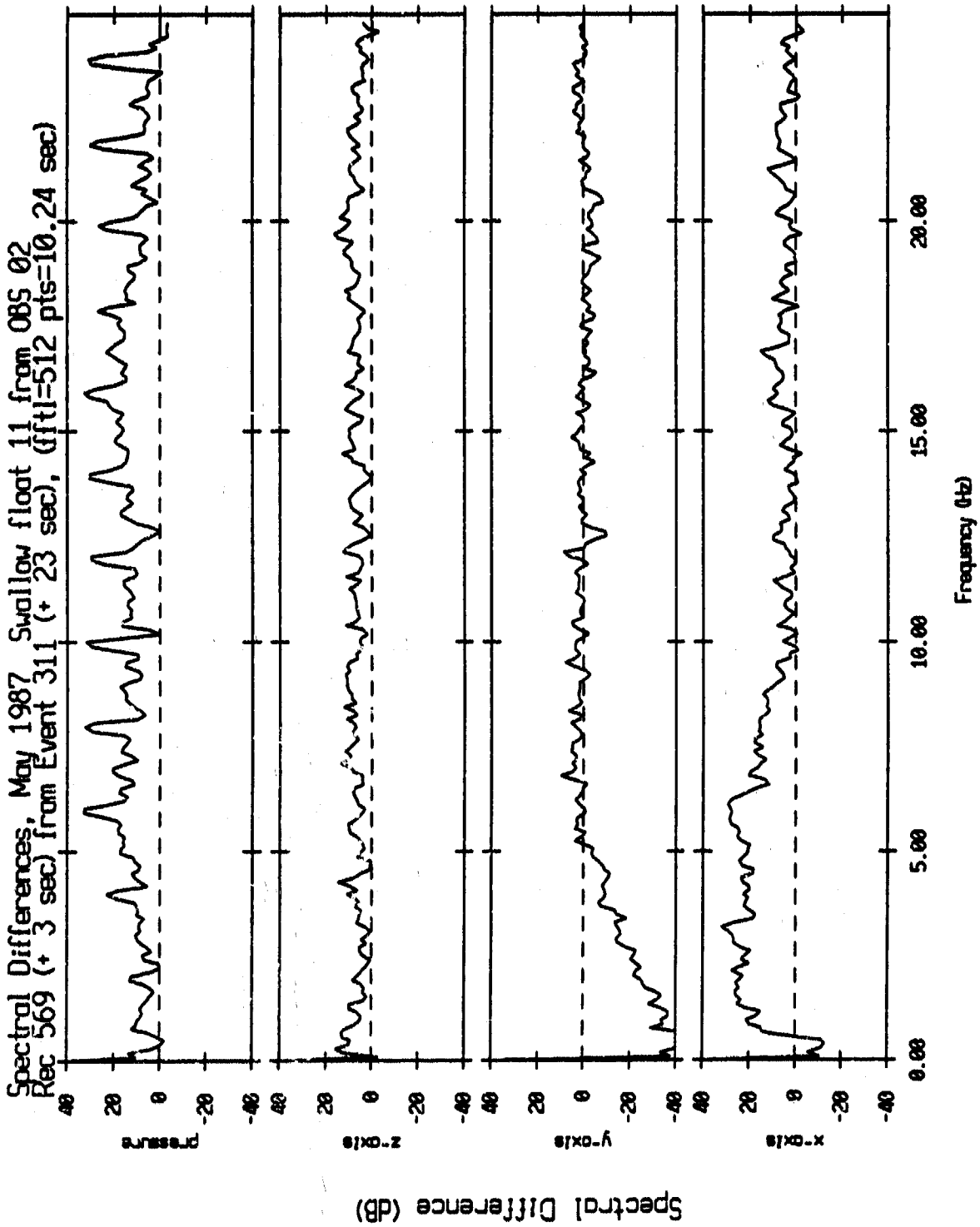
Spectral Differences, May 1987 Swallow float 11 from OBS 02
Rec 569 (+ 3 sec) from Event 311 (+ 23 sec), dfft1=512 pts=10.24 sec)
pressure
z-axis
y-axis
x-axis
40
20
0
-20
-40
0.00
5.00
10.00
15.00
20.00
Frequency (Hz)
Spectral Difference (dB)

Figure V.38

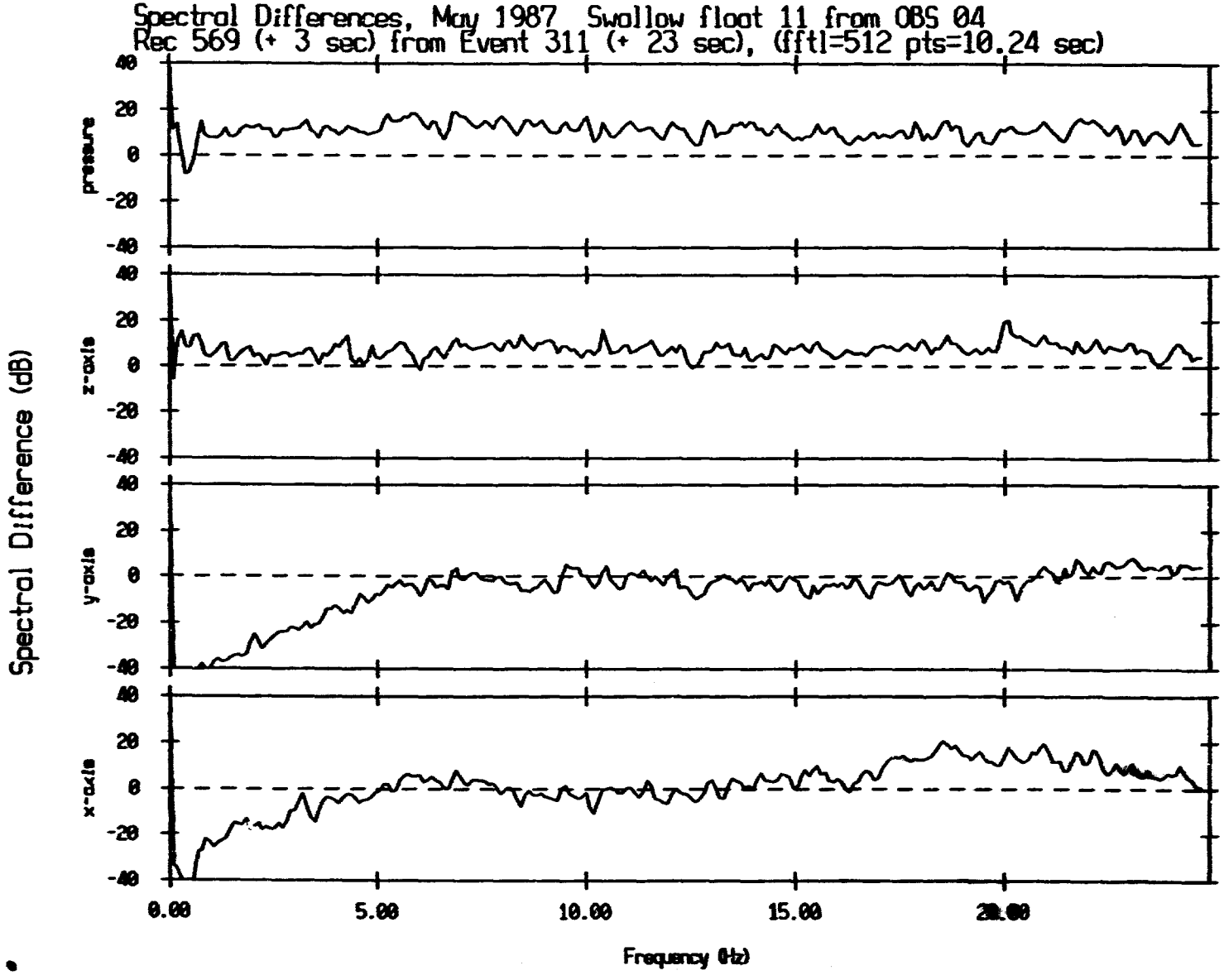
Spectral Differences, May 1987 Swallow float 11 from OBS 04
Rec 569 (+ 3 sec) from Event 311 (+ 23 sec), (fftl=512 pts=10.24 sec)
Spectral Difference (dB)
pressure
z-axis
y-axis
x-axis
40
20
0
-20
-40
0.00
5.00
10.00
15.00
Frequency (Hz)

Figure V.39

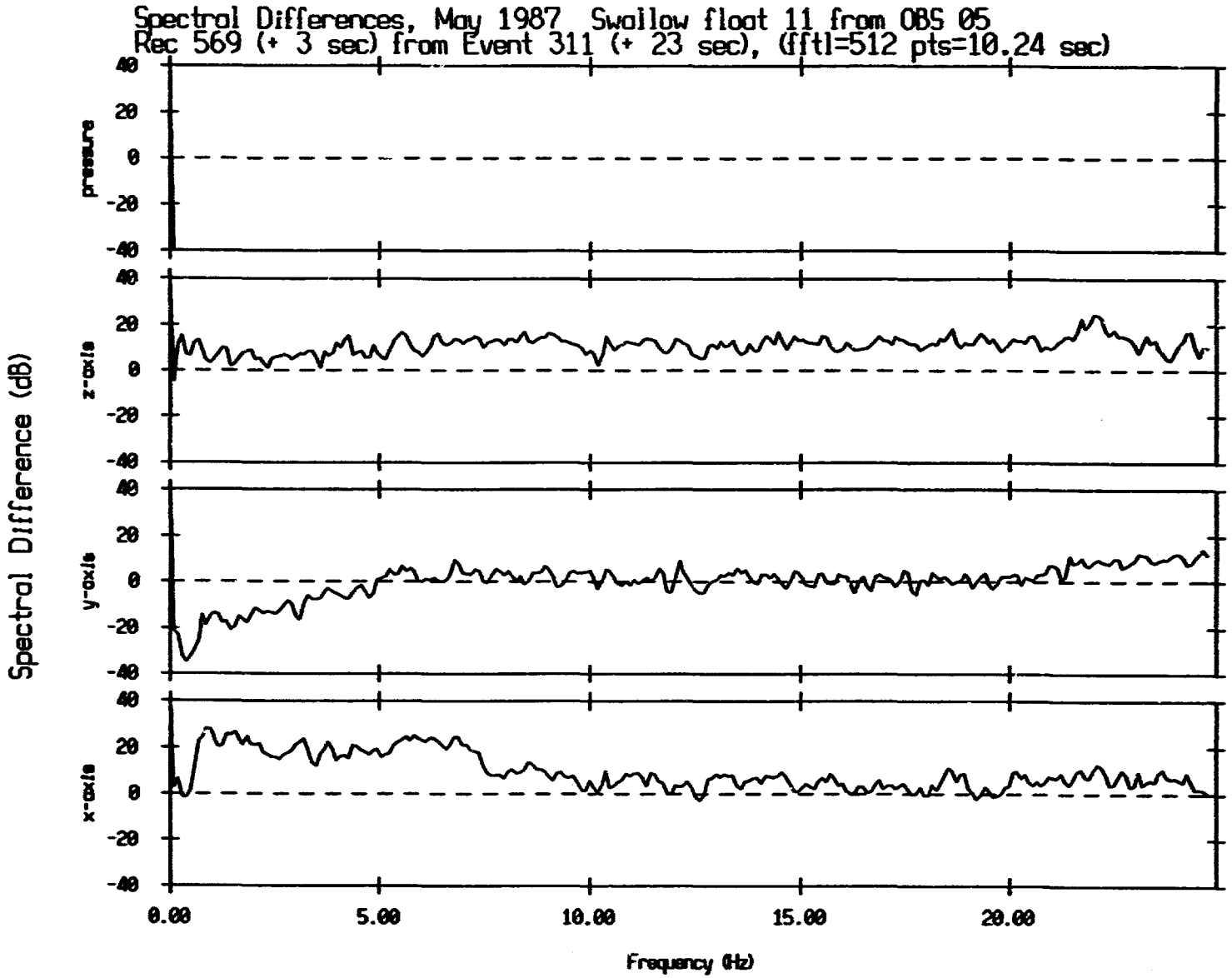
Spectral Differences, May 1987 Swallow float 11 from OBS 05
Rec 569 (+ 3 sec) from Event 311 (+ 23 sec), (fftl=512 pts=10.24 sec)
Spectral Difference (dB)
pressure
z-axis
y-axis
x-axis
40
20
0
-20
-40
0.00
5.00
10.00
15.00
20.00
Frequency (Hz)

Figure V.40

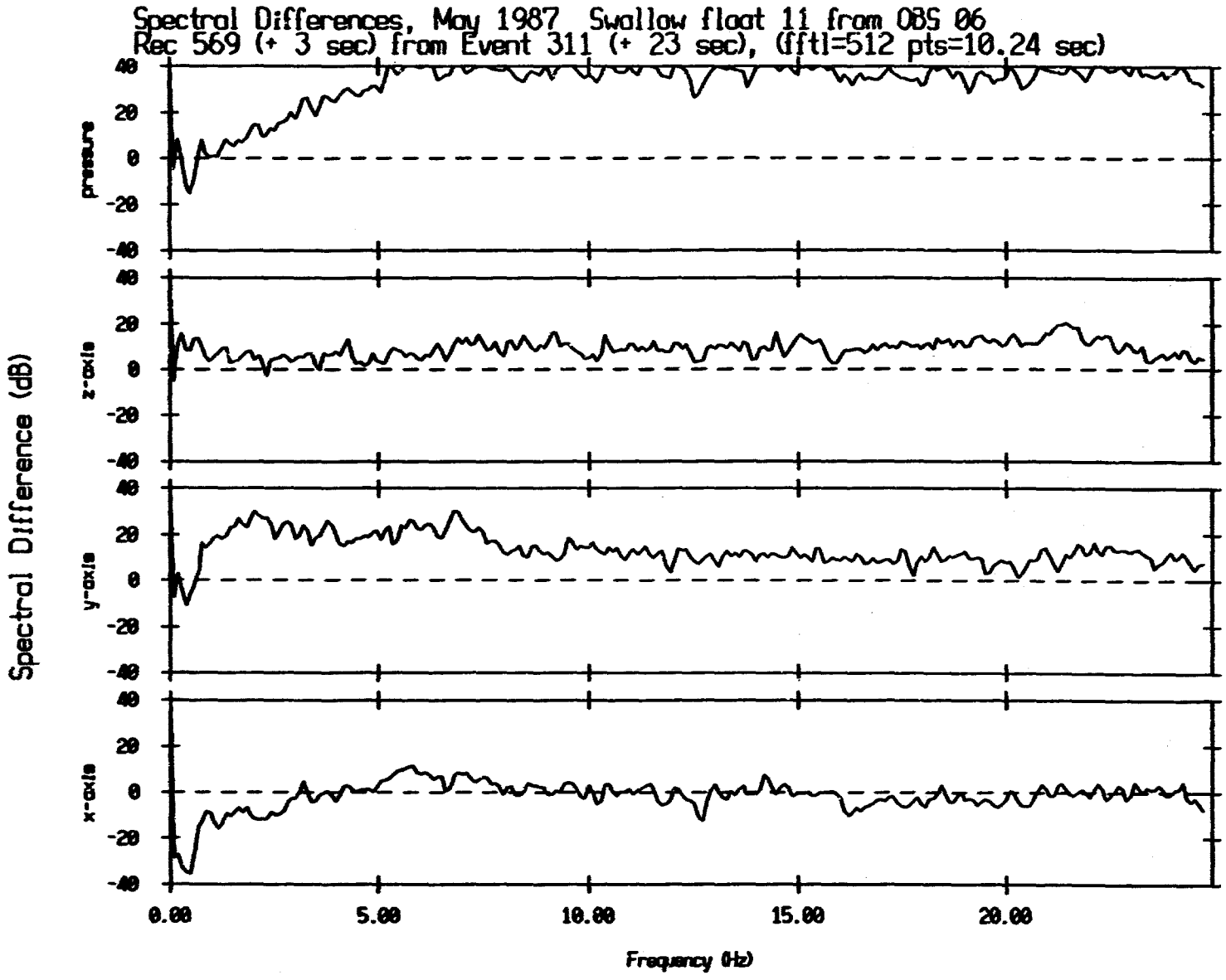
Spectral Differences, May 1987 Swallow float 11 from OBS 06
Rec 569 (+ 3 sec) from Event 311 (+ 23 sec), (fftl=512 pts=10.24 sec)
Spectral Difference (dB)
pressure
z-axis
y-axis
x-axis
40
20
0
-20
-40
0.00
5.00
10.00
15.00
20.00
Frequency (Hz)

Figure V.41

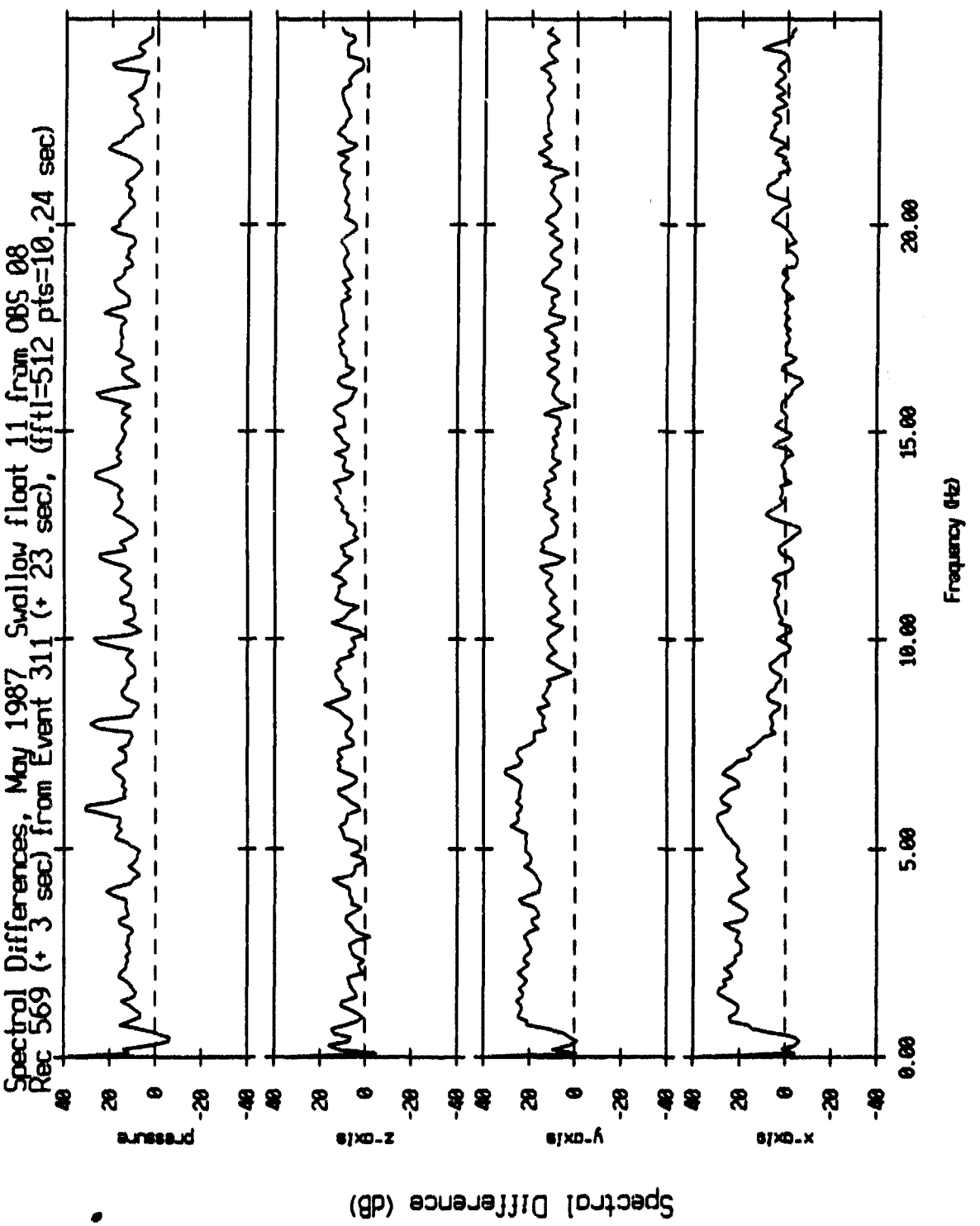
Spectral Differences, May 1987 Swallow float 11 from OBS 08
Rec 569 (+ 3 sec) from Event 311 (+ 23 sec), dft1=512 pts=10.24 sec)
pressure
z-axis
y-axis
x-axis
40
20
0
-20
-40
0.00
5.00
10.00
15.00
20.00
Frequency (Hz)
Spectral Difference (dB)

Figure V.42

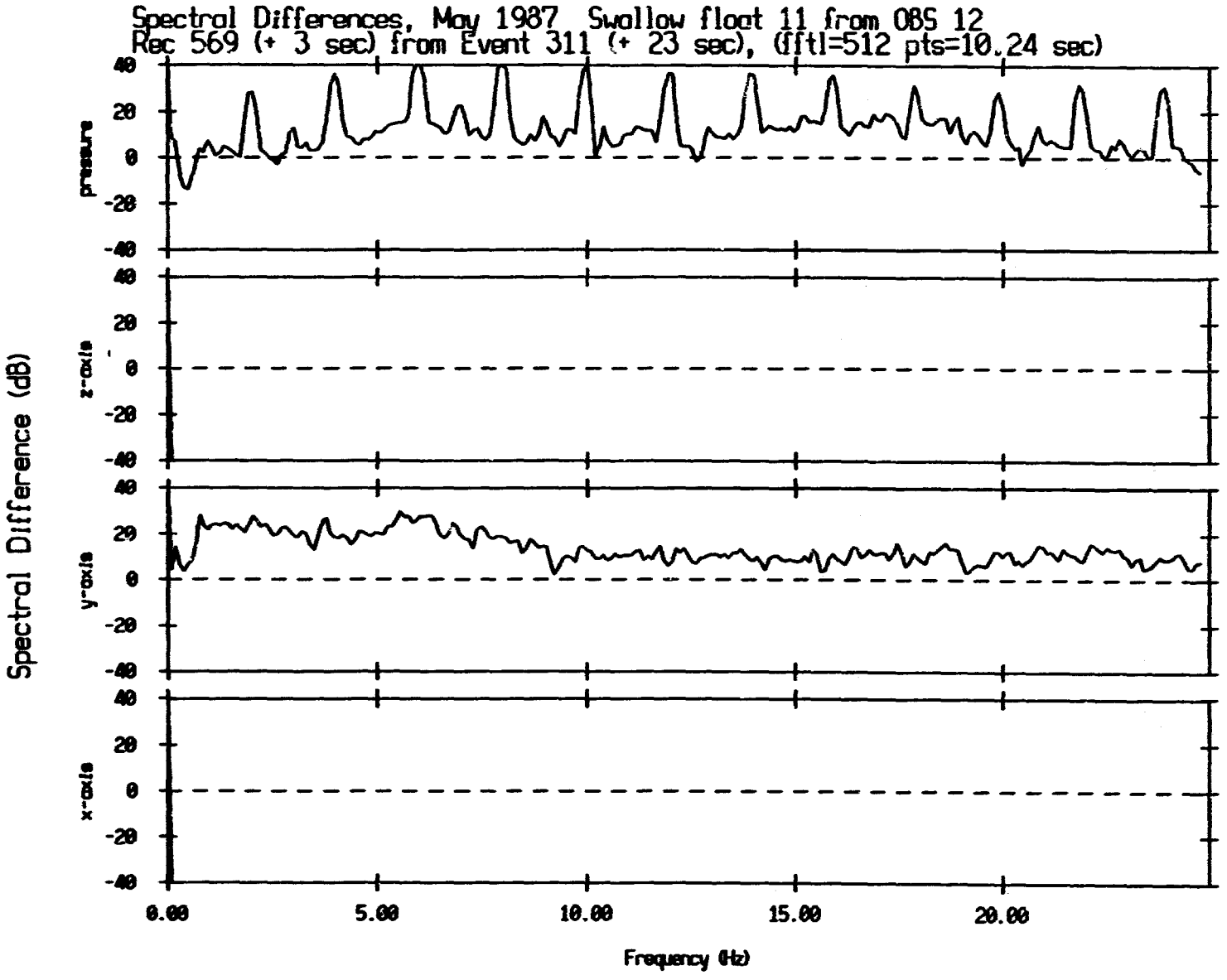
Spectral Differences, May 1987 Swallow float 11 from OBS 12
Rec 569 (+ 3 sec) from Event 311 (+ 23 sec), (fftl=512 pts=10.24 sec)
Spectral Difference (dB)
pressure
z-axis
y-axis
x-axis
40
20
0
-20
-40
0.00
5.00
10.00
15.00
20.00
Frequency (Hz)

Figure V.43

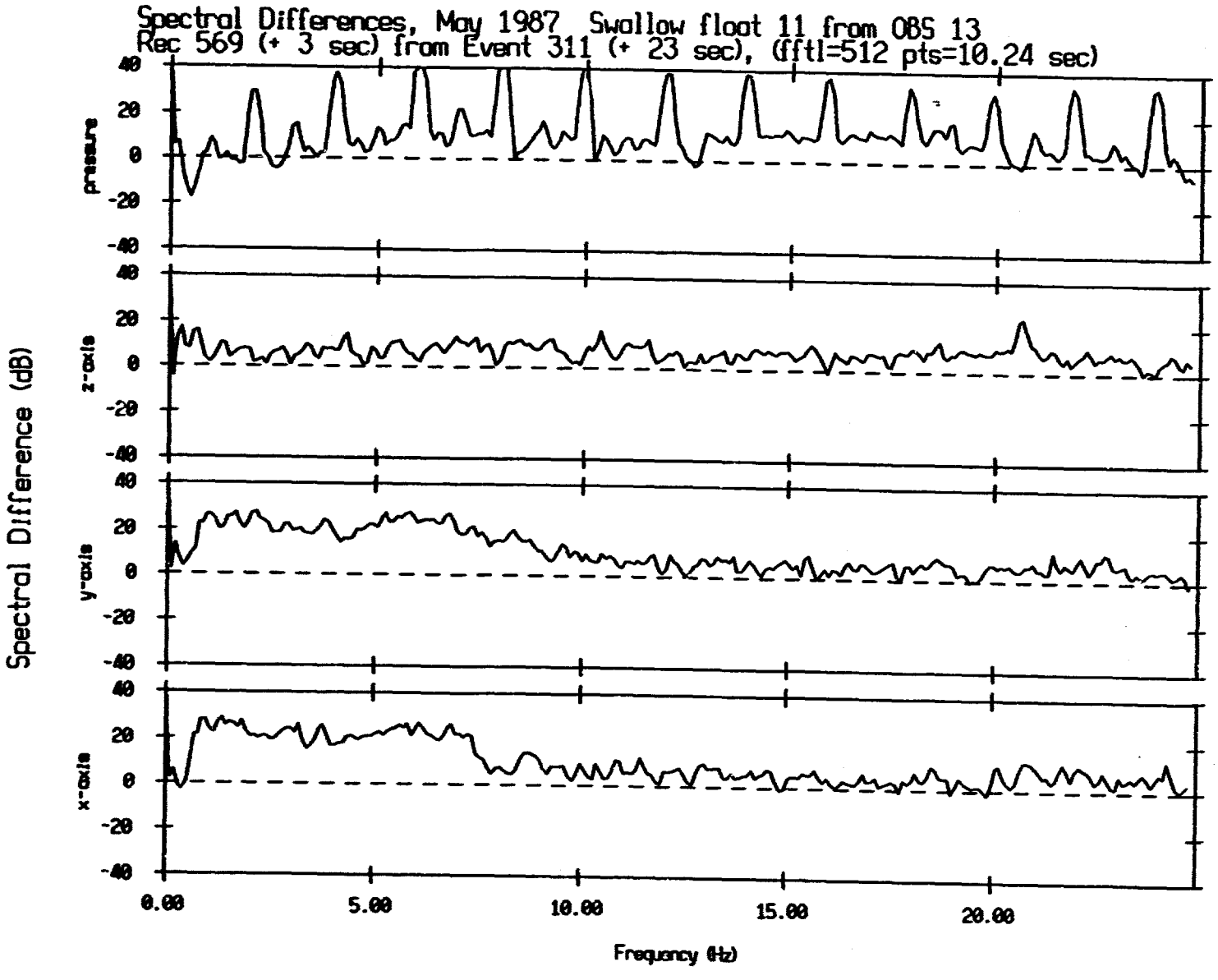
Spectral Differences, May 1987 Swallow float 11 from OBS 13
Rec 569 (+ 3 sec) from Event 311 (+ 23 sec), (fftl=512 pts=10.24 sec)
Spectral Difference (dB)
pressure
z-axis
y-axis
x-axis
40
20
0
-20
-40
0.00
5.00
10.00
15.00
20.00
Frequency (Hz)

Figure V.44

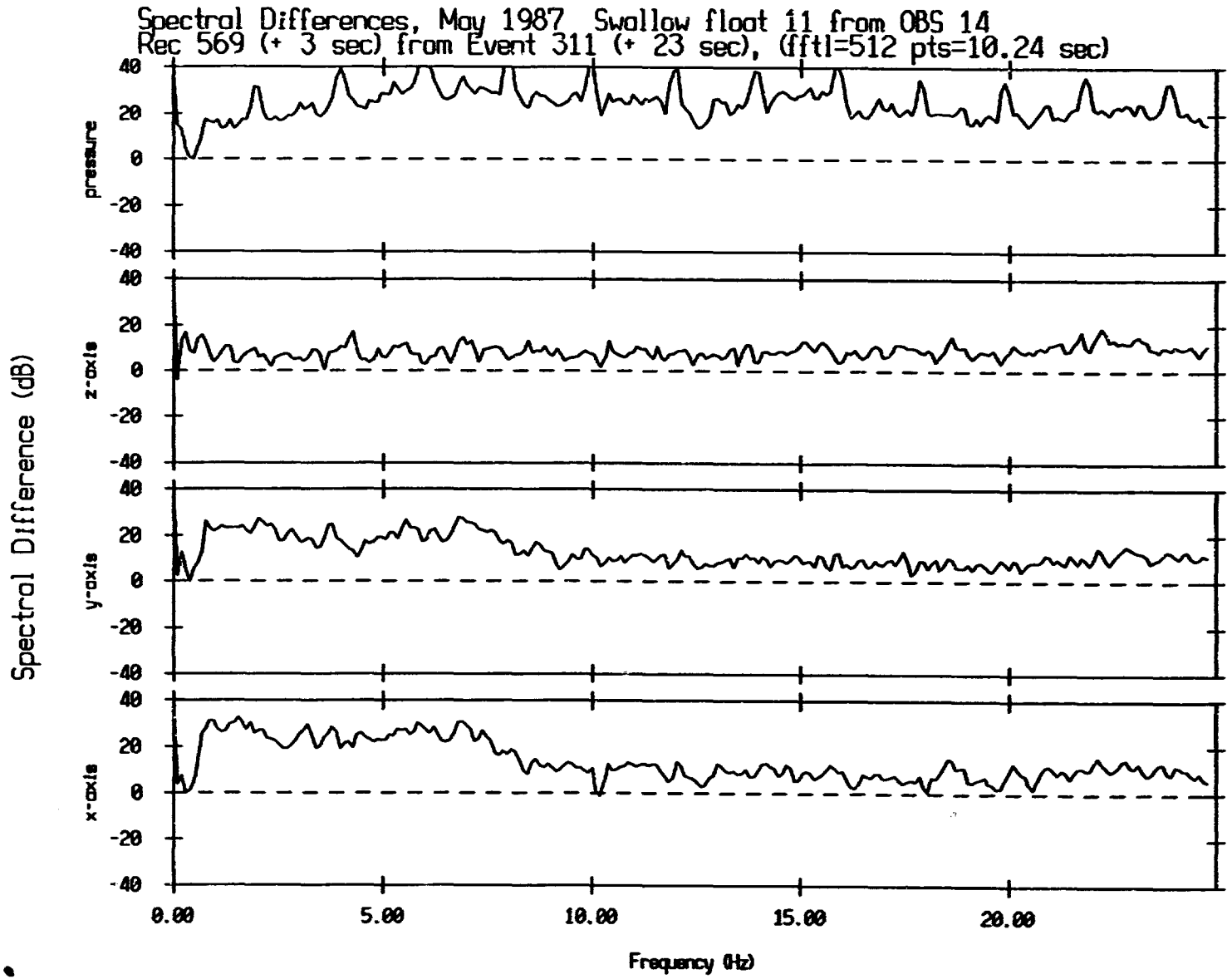
Spectral Differences, May 1987 Swallow float 11 from OBS 14
Rec 569 (+ 3 sec) from Event 311 (+ 23 sec), (fftl=512 pts=10.24 sec)
Spectral Difference (dB)
pressure
z-axis
y-axis
x-axis
40
20
0
-20
-40
0.00
5.00
10.00
15.00
20.00
Frequency (Hz)

Figure V.45

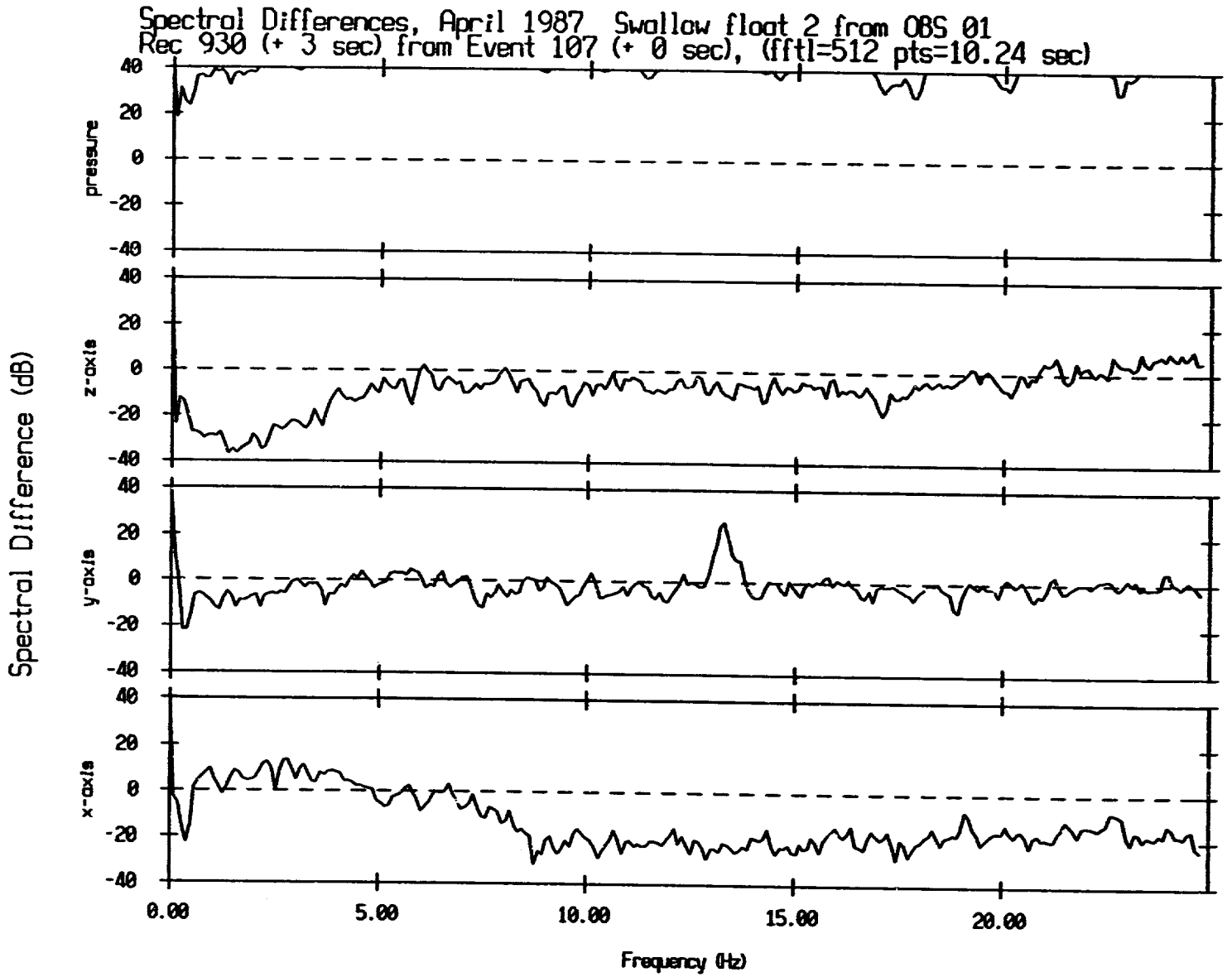
Spectral Differences, April 1987 Swallow float 2 from OBS 01
Rec 930 (+ 3 sec) from Event 107 (+ 0 sec), (fftl=512 pts=10.24 sec)
Spectral Difference (dB)
pressure
z-axis
y-axis
x-axis
40
20
0
-20
-40
0.00
5.00
10.00
15.00
20.00
Frequency (Hz)

Figure V.46

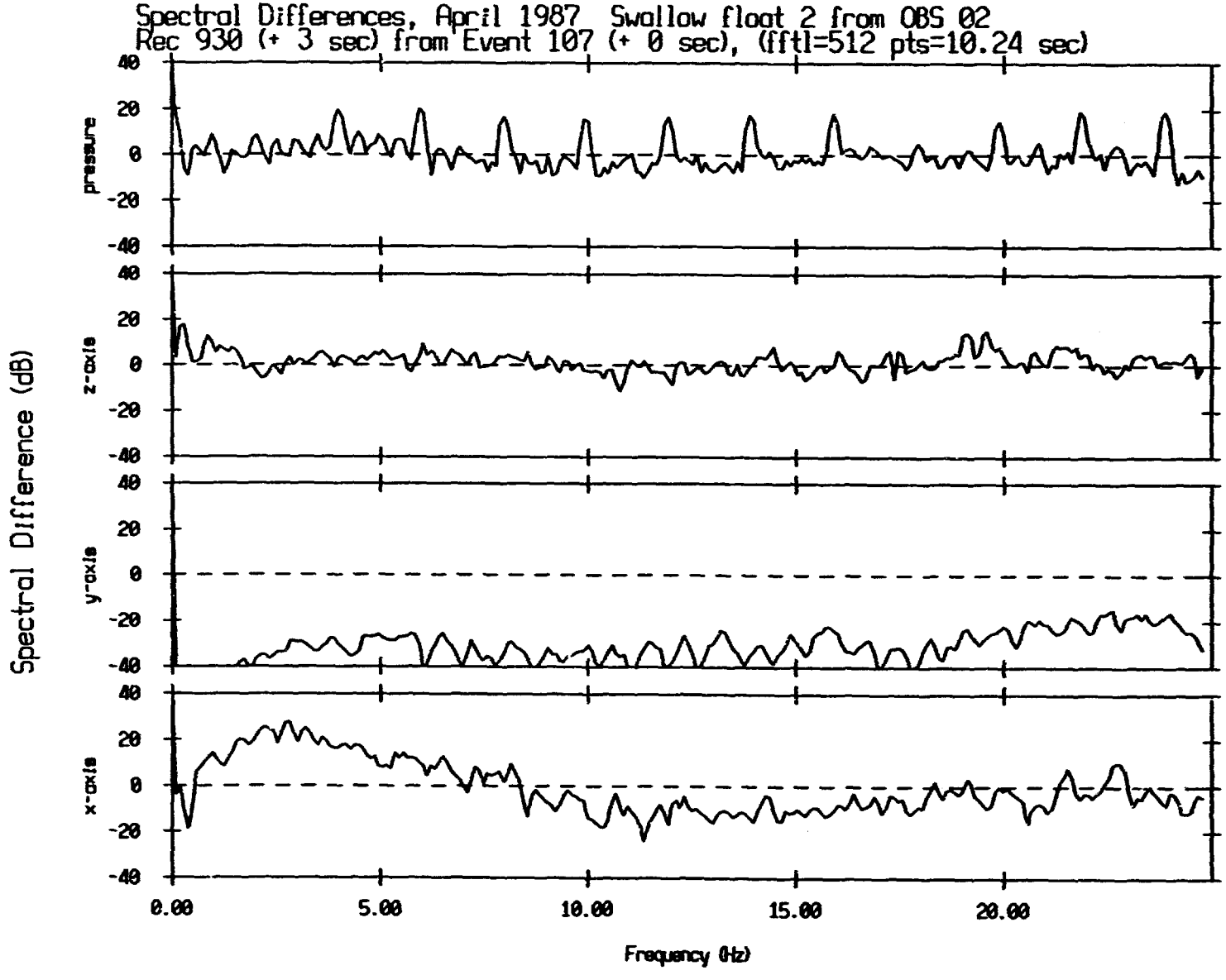
Spectral Differences, April 1987 Swallow float 2 from OBS 02
Rec 930 (+ 3 sec) from Event 107 (+ 0 sec), (fftl=512 pts=10.24 sec)
Spectral Difference (dB)
pressure
z-axis
y-axis
x-axis
40
20
0
-20
-40
0.00
5.00
10.00
15.00
20.00
Frequency (Hz)

Figure V.47

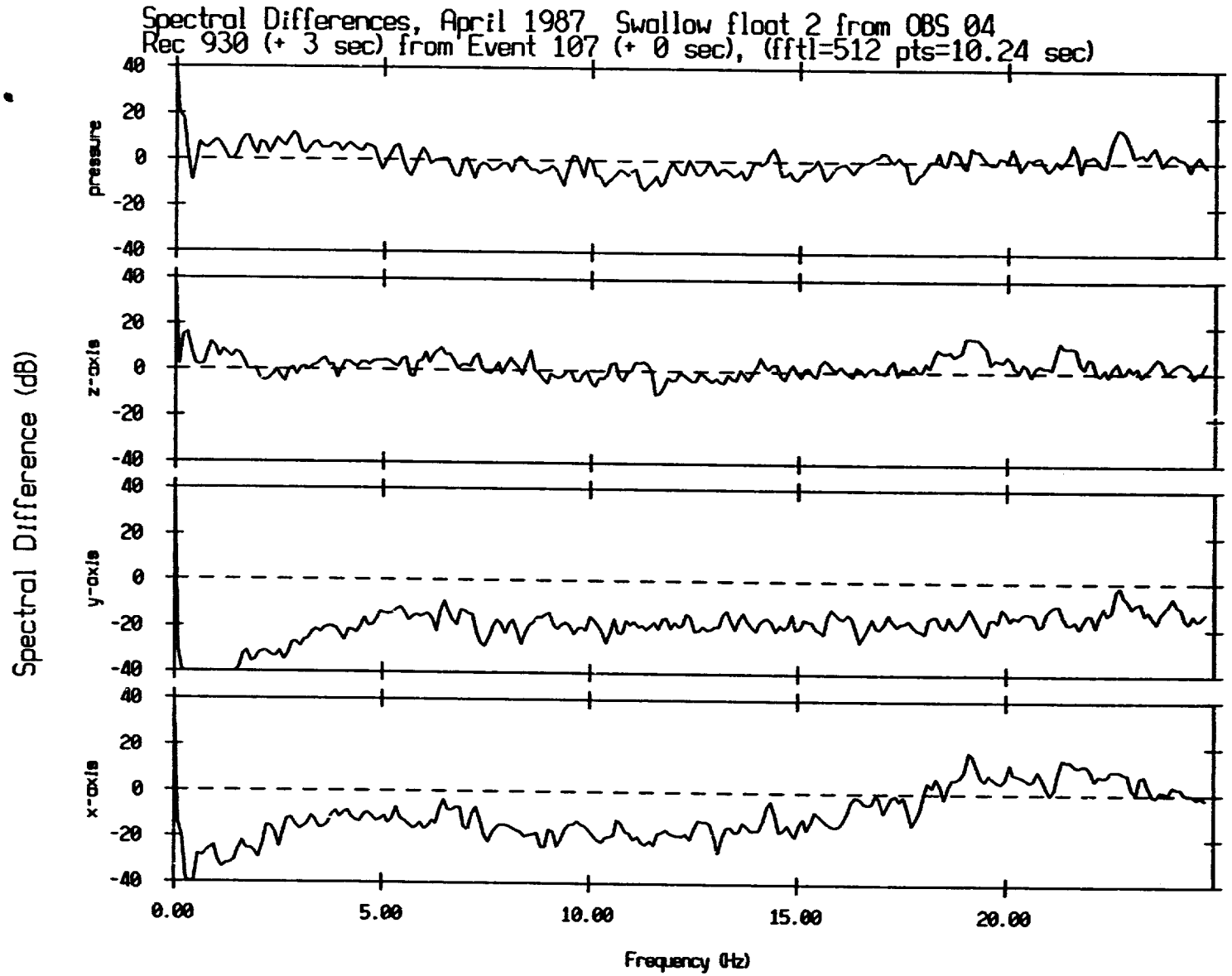
Spectral Differences, April 1987 Swallow float 2 from OBS 04
Rec 930 (+ 3 sec) from Event 107 (+ 0 sec), (fftl=512 pts=10.24 sec)
Spectral Difference (dB)
pressure
z-axis
y-axis
x-axis
40
20
0
-20
-40
0.00
5.00
10.00
15.00
20.00
Frequency (Hz)

Figure V.48

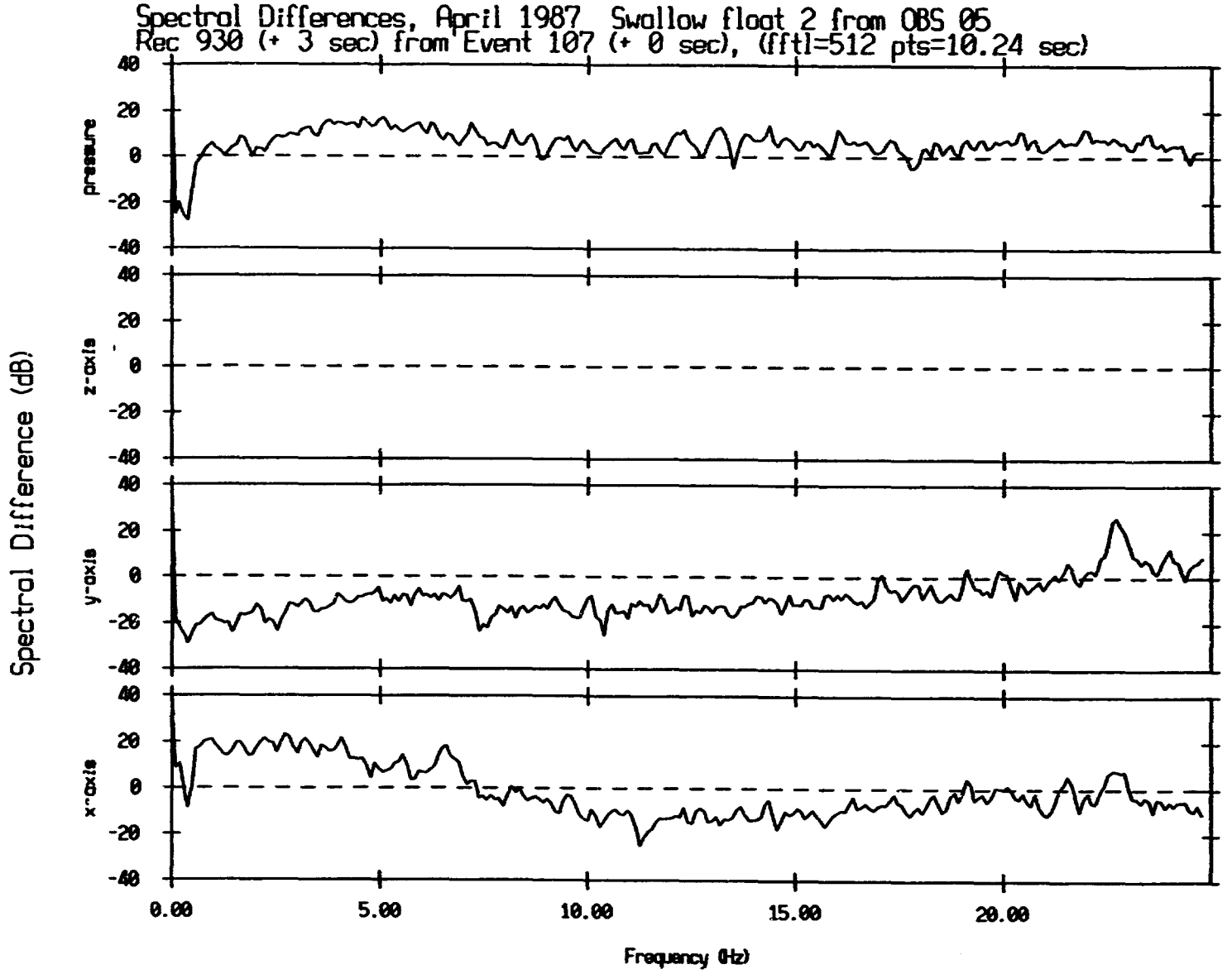
Spectral Differences, April 1987 Swallow float 2 from OBS 05
Rec 930 (+ 3 sec) from Event 107 (+ 0 sec), (fftl=512 pts=10.24 sec)
Spectral Difference (dB)
pressure
z-axis
y-axis
x-axis
40
20
0
-20
-40
0.00
5.00
10.00
15.00
20.00
Frequency (Hz)

Figure V.49

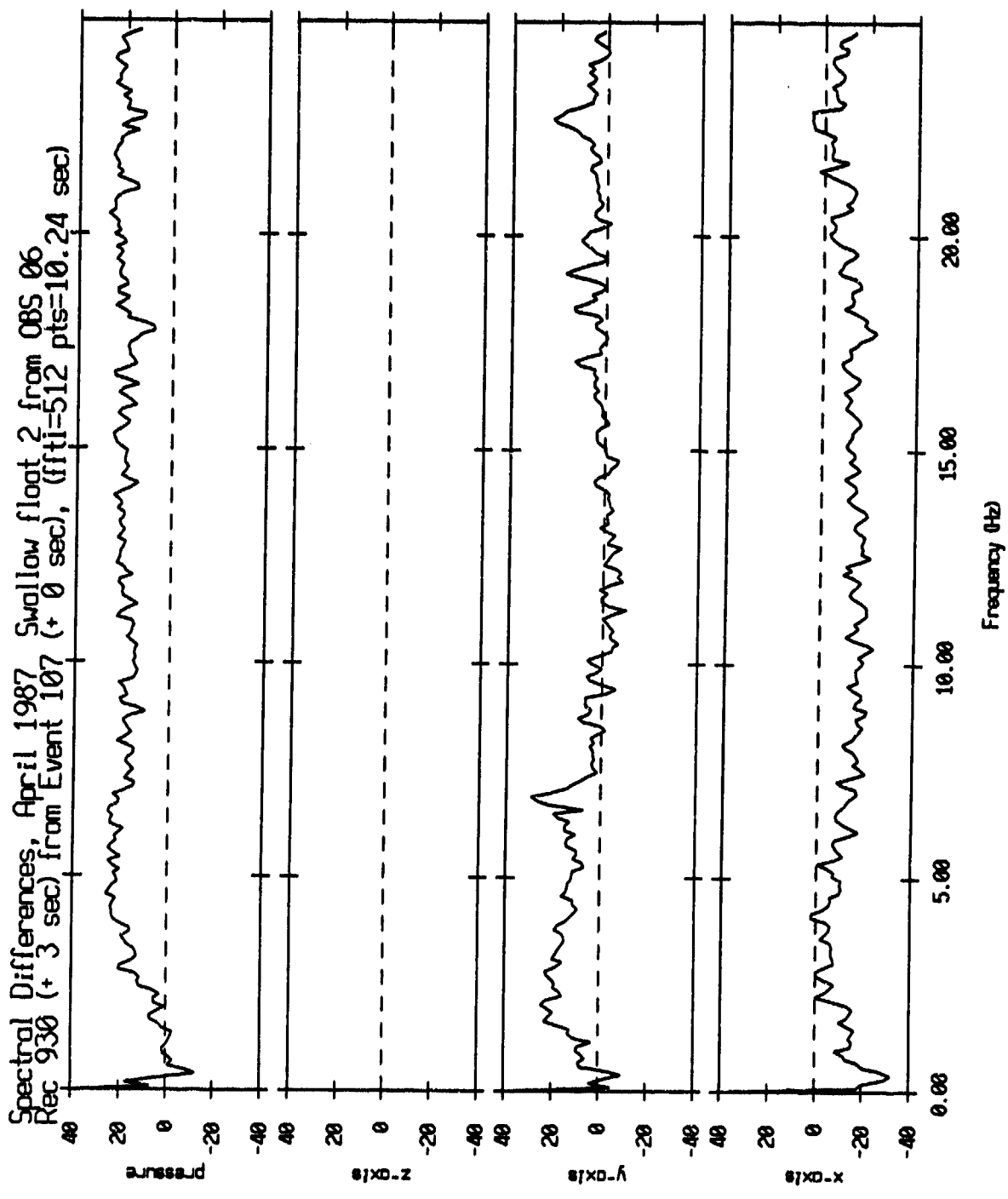
Spectral Differences, April 1987 Swallow float 2 from OBS 06
Rec 930 (+ 3 sec) from Event 107 (+ 0 sec), (fftl=512 pts=10.24 sec)
pressure
z-axis
y-axis
x-axis
40
20
0
-20
-40
0.00
5.00
10.00
15.00
20.00
Frequency (Hz)
Spectral Difference (dB)

Figure V.50

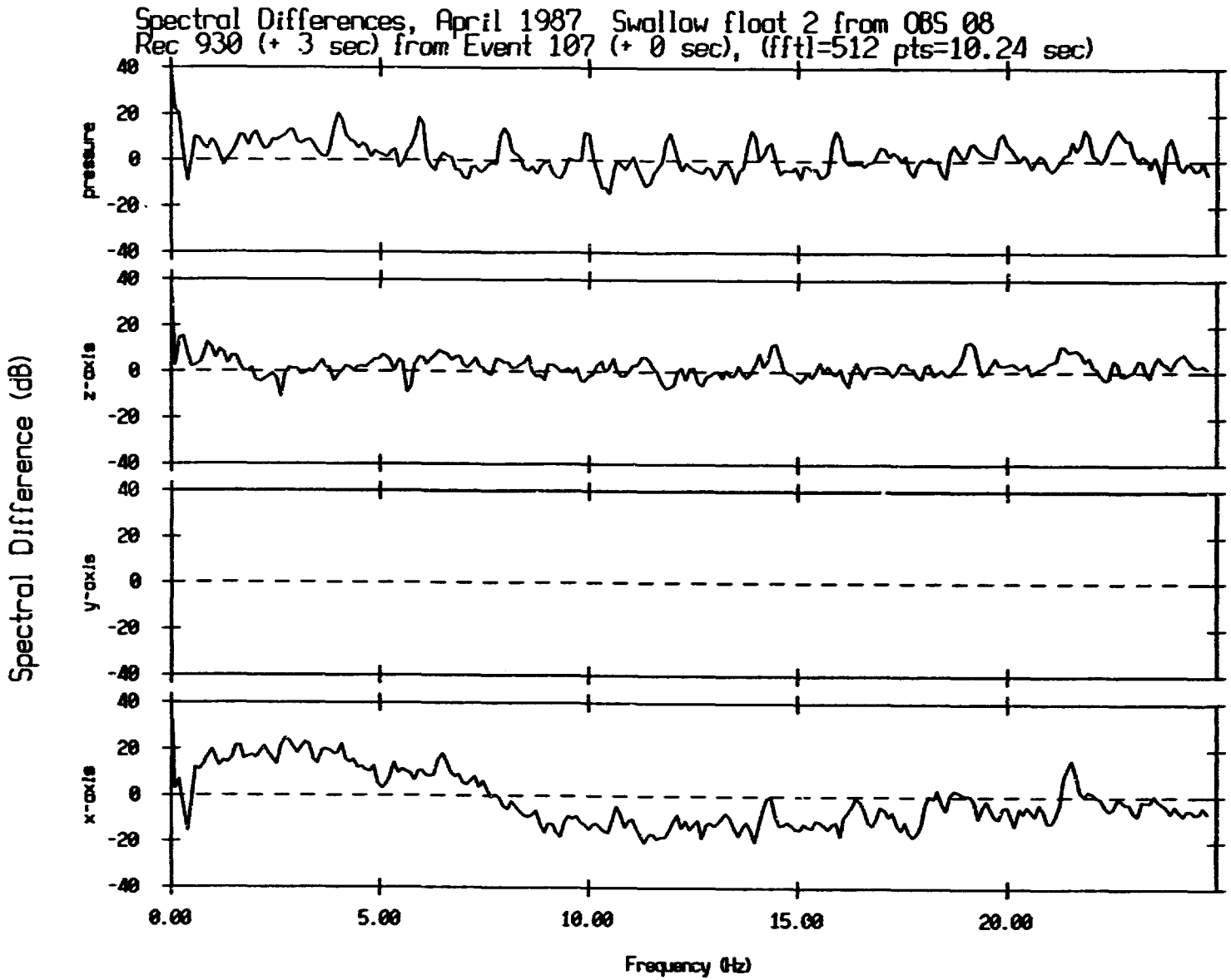
Spectral Differences, April 1987 Swallow float 2 from OBS 08
Rec 930 (+ 3 sec) from Event 107 (+ 0 sec), (fft)=512 pts=10.24 sec)
Spectral Difference (dB)
pressure
z-axis
y-axis
x-axis
40
20
0
-20
-40
0.00
5.00
10.00
15.00
20.00
Frequency (Hz)

Figure V.51

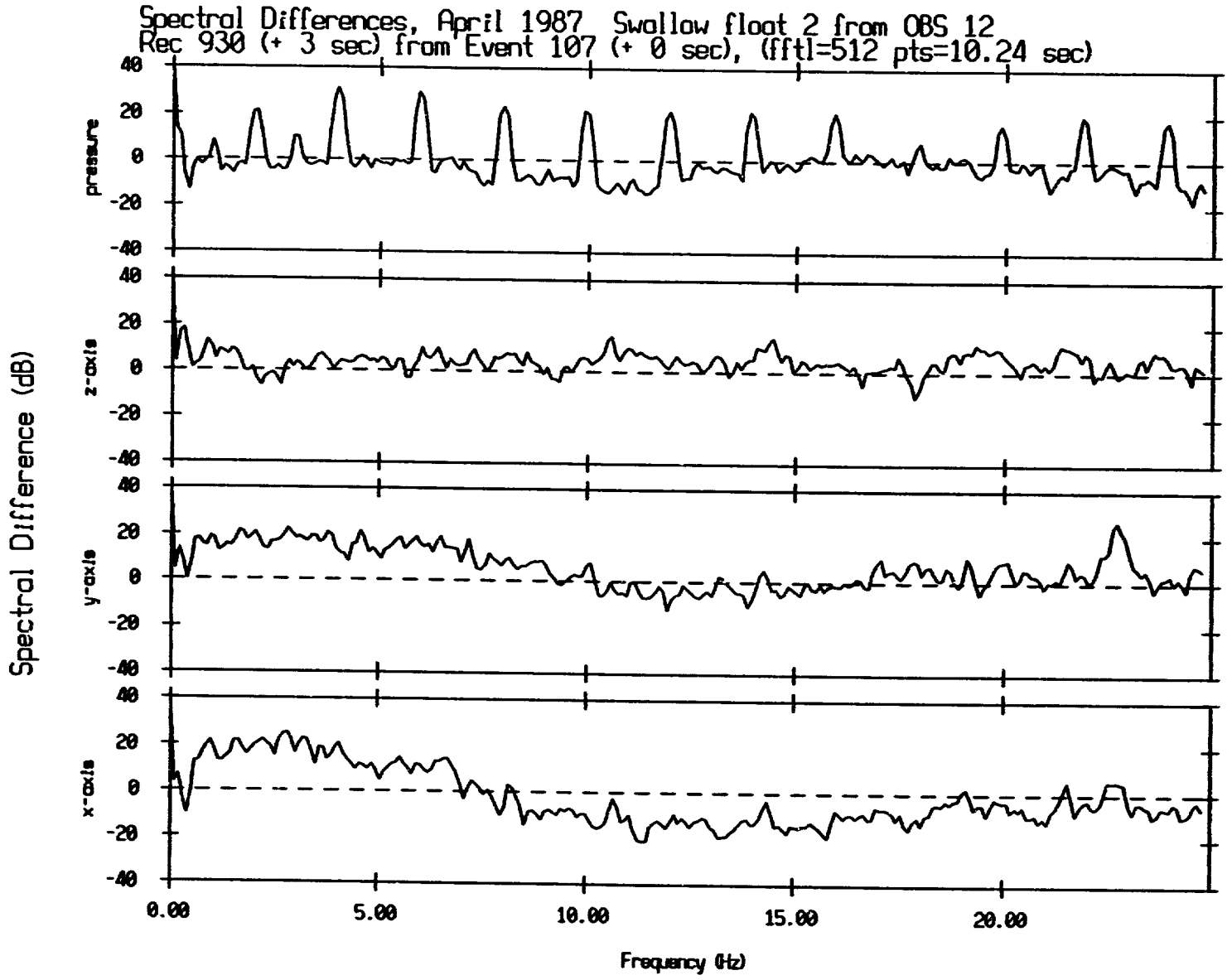
Spectral Differences, April 1987 Swallow float 2 from OBS 12
Rec 930 (+ 3 sec) from Event 107 (+ 0 sec), (fftl=512 pts=10.24 sec)
Spectral Difference (dB)
pressure
z-axis
y-axis
x-axis
40
20
0
-20
-40
0.00
5.00
10.00
15.00
20.00
Frequency (Hz)

Figure V.52

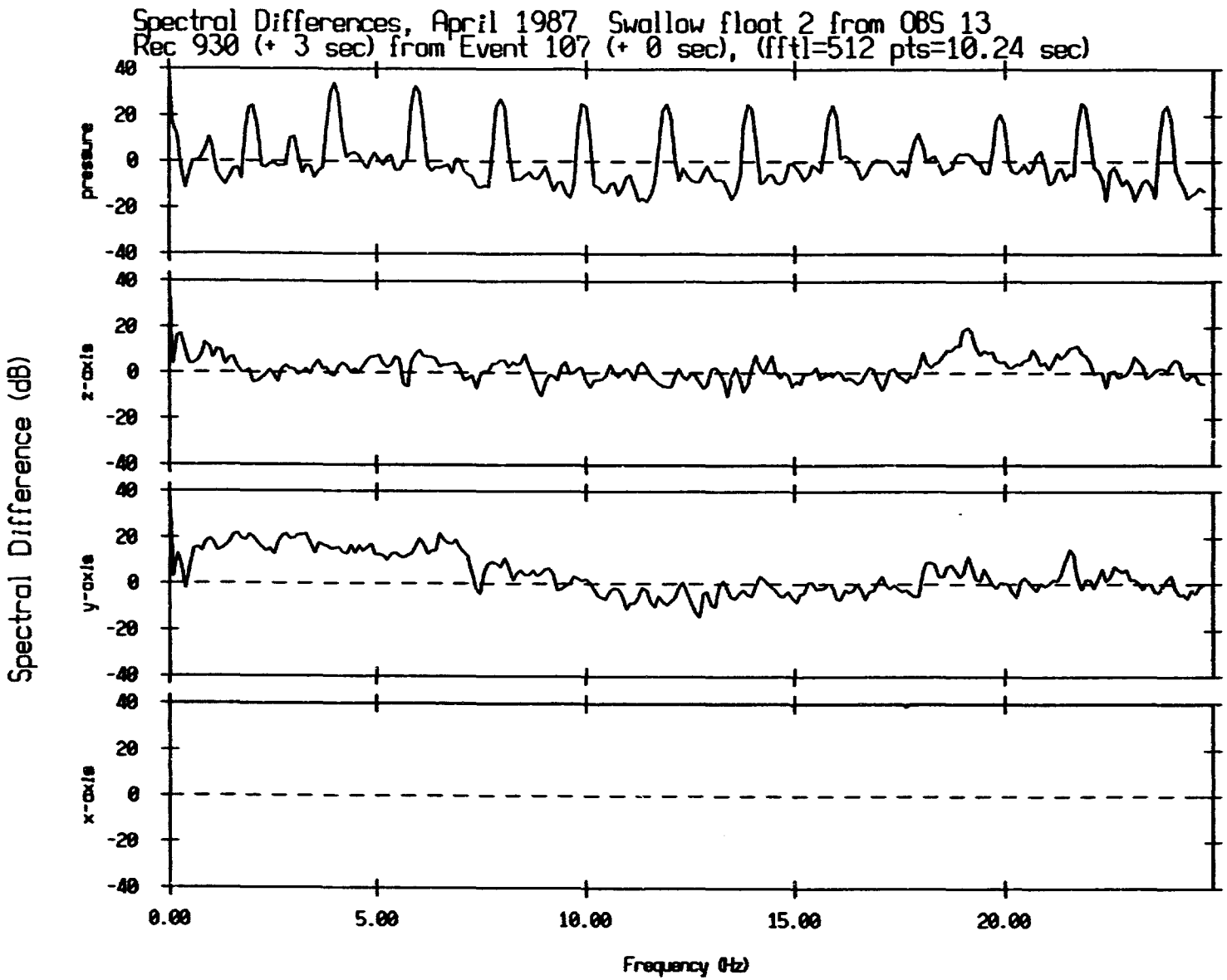
Spectral Differences, April 1987 Swallow float 2 from OBS 13
Rec 930 (+ 3 sec) from Event 107 (+ 0 sec), (fft=512 pts=10.24 sec)
Spectral Difference (dB)
pressure
z-axis
y-axis
x-axis
40
20
0
-20
-40
0.00
5.00
10.00
15.00
20.00
Frequency (Hz)

Figure V.53

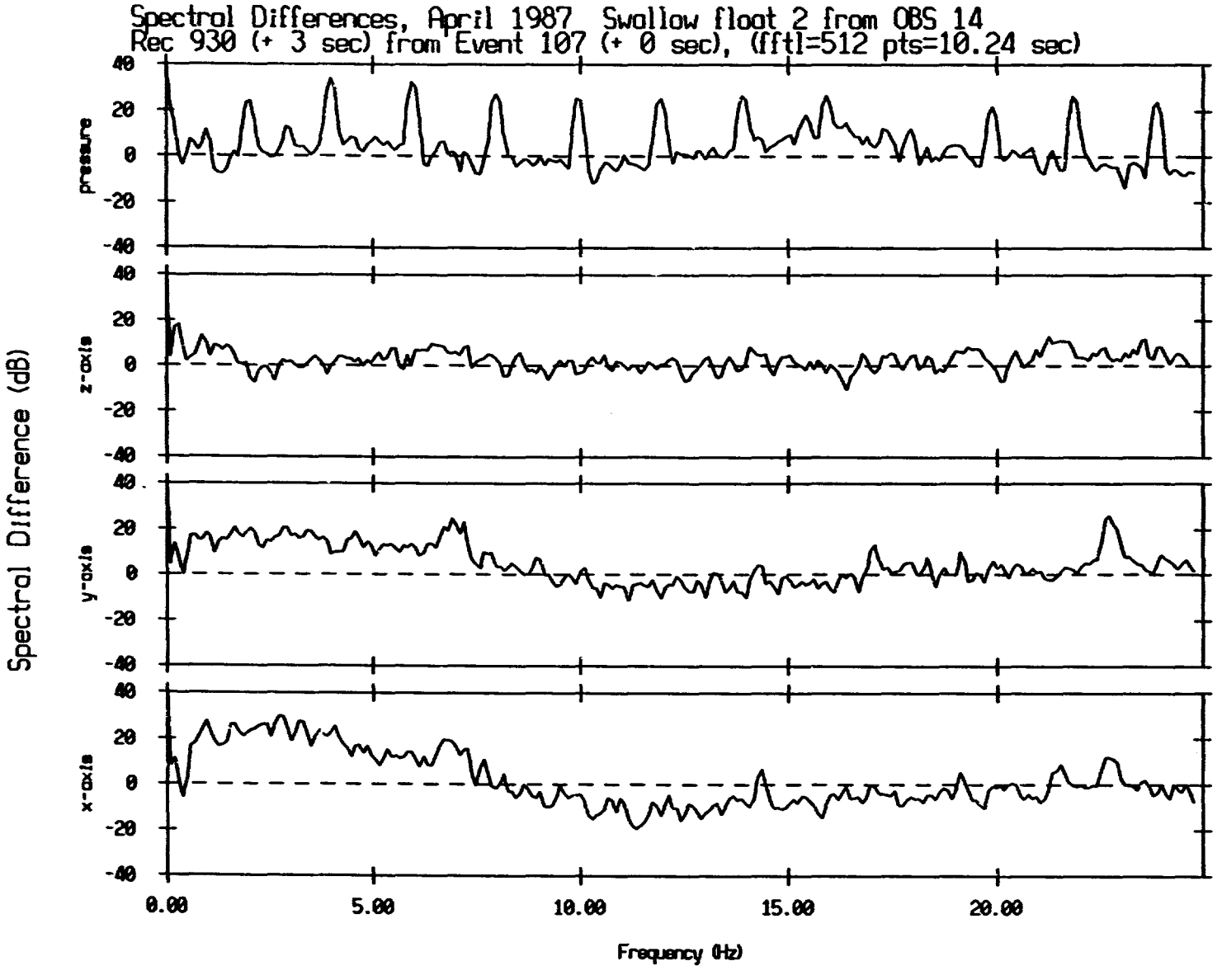
Spectral Differences, April 1987 Swallow float 2 from OBS 14
Rec 930 (+ 3 sec) from Event 107 (+ 0 sec), (fftl=512 pts=10.24 sec)
Spectral Difference (dB)
pressure
z-axis
y-axis
x-axis
40
20
0
-20
-40
0.00
5.00
10.00
15.00
20.00
Frequency (Hz)

Figure V.54

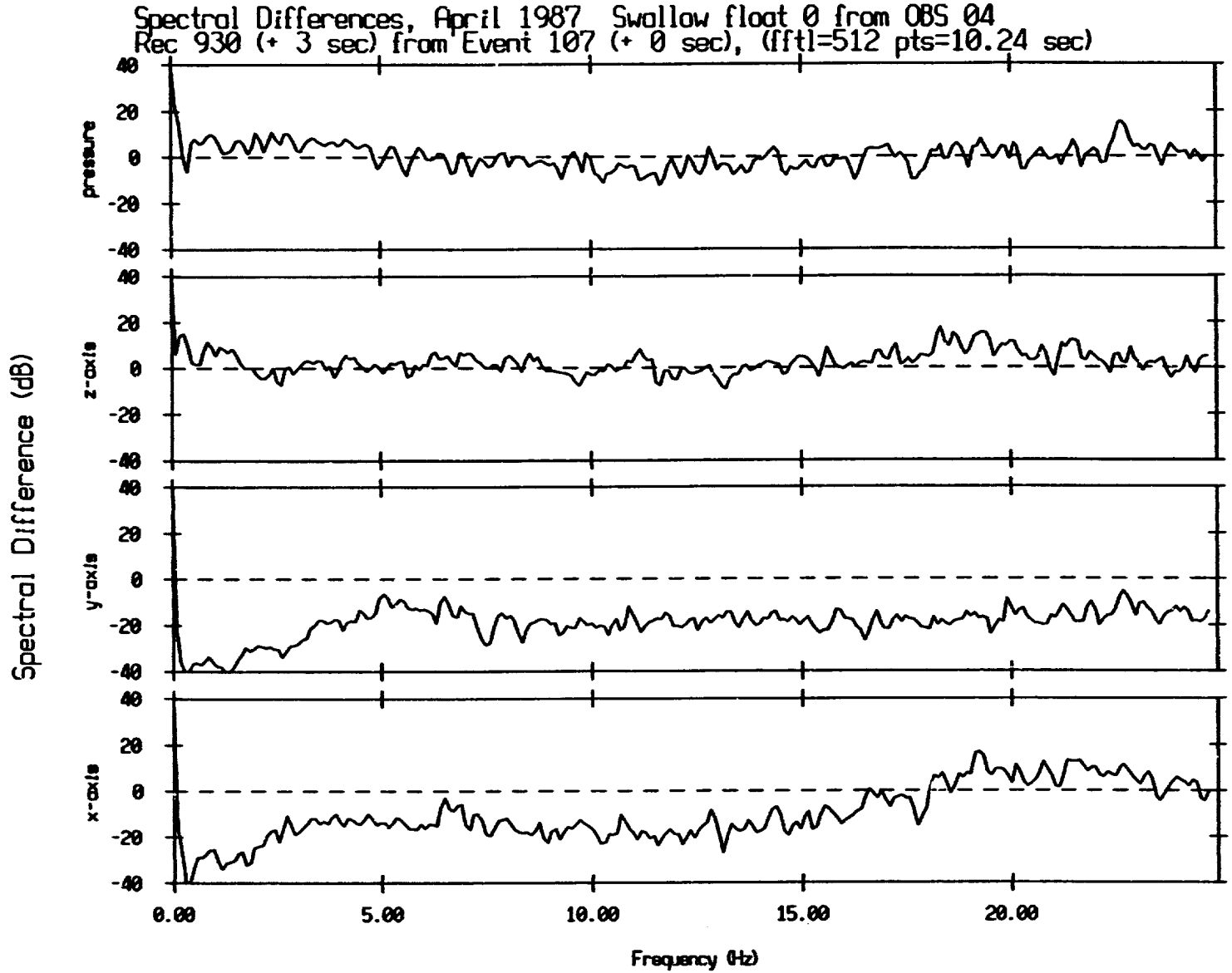
Spectral Differences, April 1987 Swallow float 0 from OBS 04
Rec 930 (+ 3 sec) from Event 107 (+ 0 sec), (fftl=512 pts=10.24 sec)
Spectral Difference (dB)
pressure
z-axis
y-axis
x-axis
40
20
0
-20
-40
0.00
5.00
10.00
15.00
20.00
Frequency (Hz)

Figure V.55

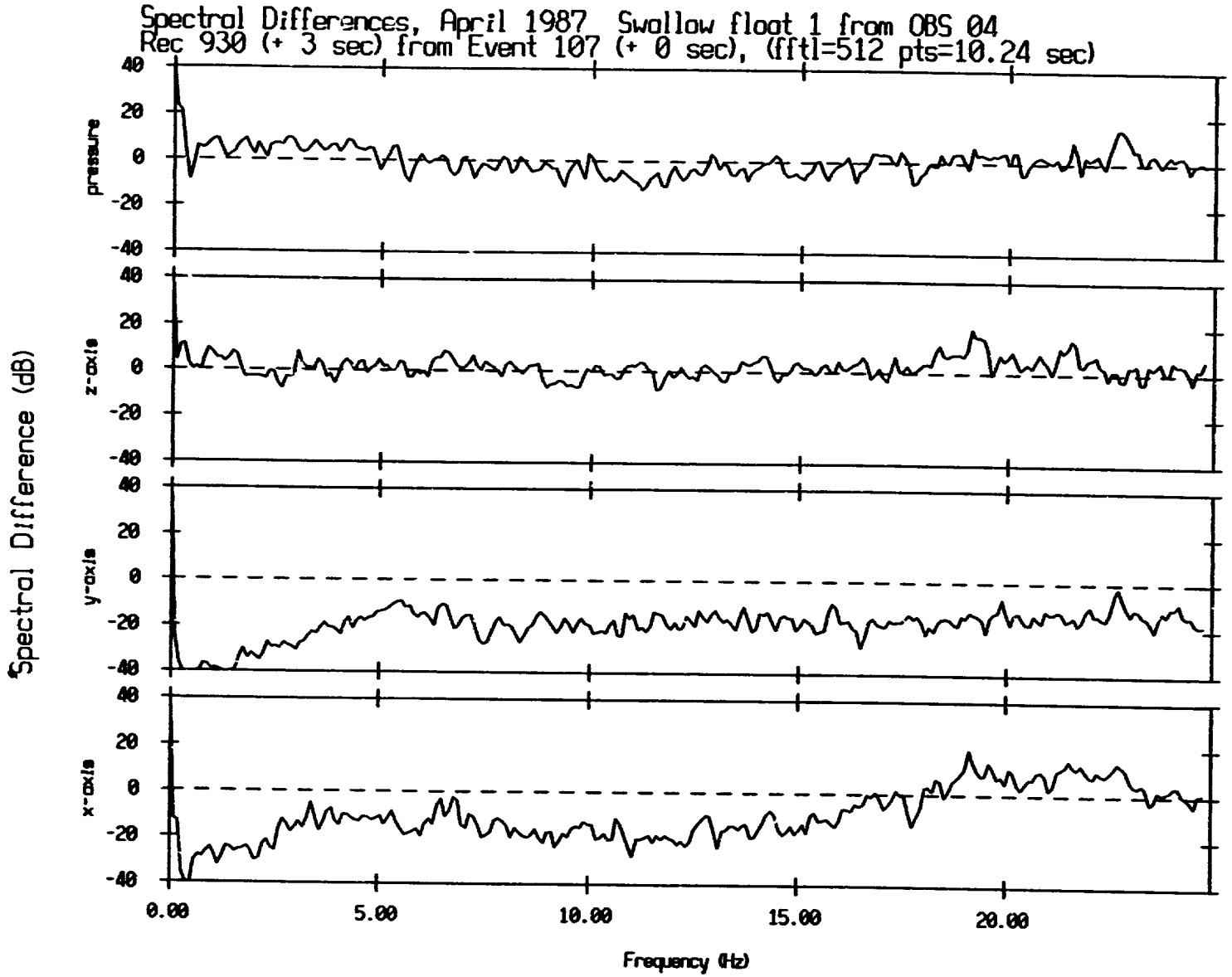
Spectral Differences, April 1987 Swallow float 1 from OBS 04
Rec 930 (+ 3 sec) from Event 107 (+ 0 sec), (fftl=512 pts=10.24 sec)
Spectral Difference (dB)
pressure
z-axis
y-axis
x-axis
40
20
0
-20
-40
0.00
5.00
10.00
15.00
20.00
Frequency (Hz)

Figure V.56

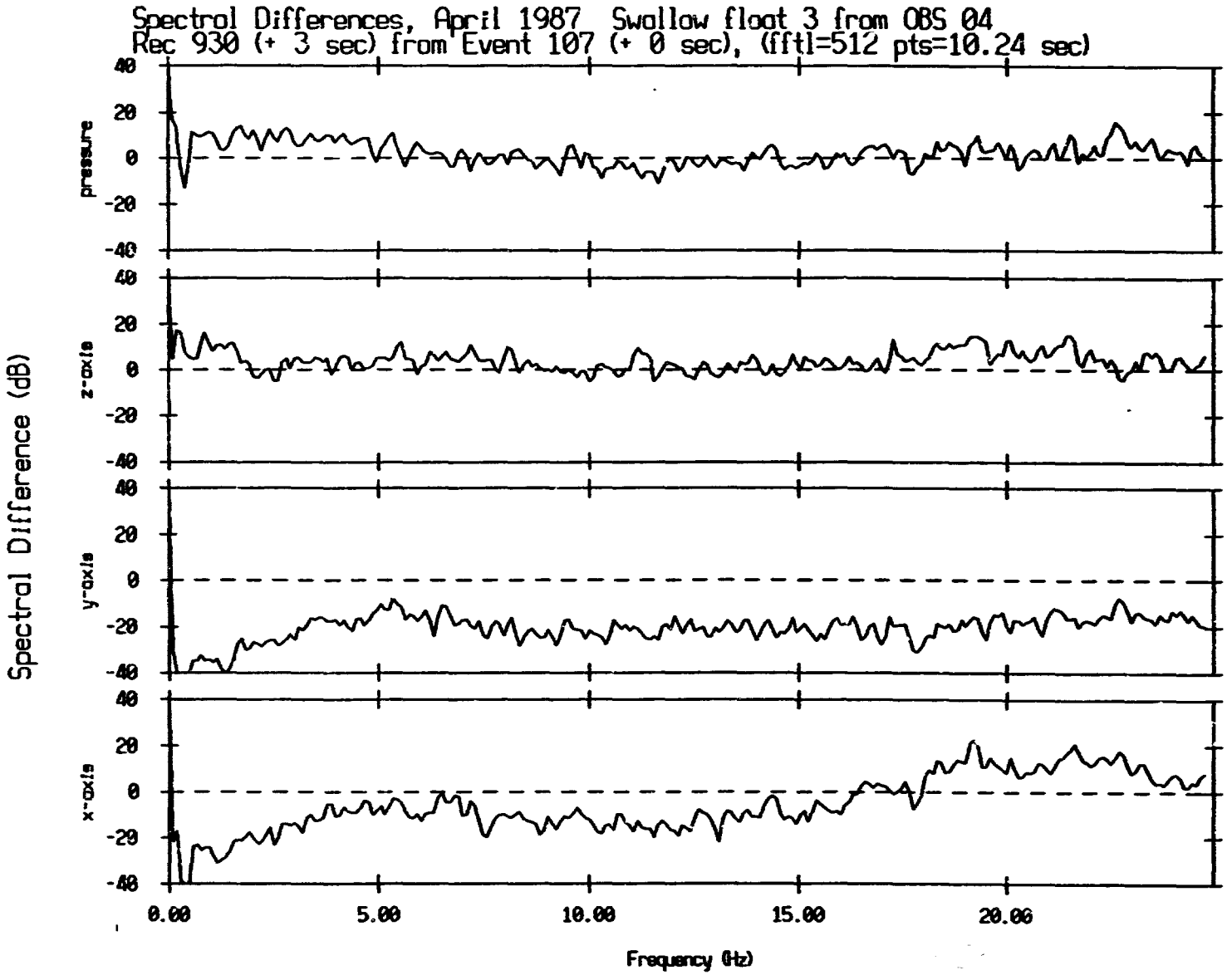
Spectral Differences, April 1987 Swallow float 3 from OBS 04
Rec 930 (+ 3 sec) from Event 107 (+ 0 sec), (fftl=512 pts=10.24 sec)
Spectral Difference (dB)
pressure
z-axis
y-axis
x-axis
40
20
0
-20
-40
0.00
5.00
10.00
15.00
20.00
Frequency (Hz)

Figure V.57

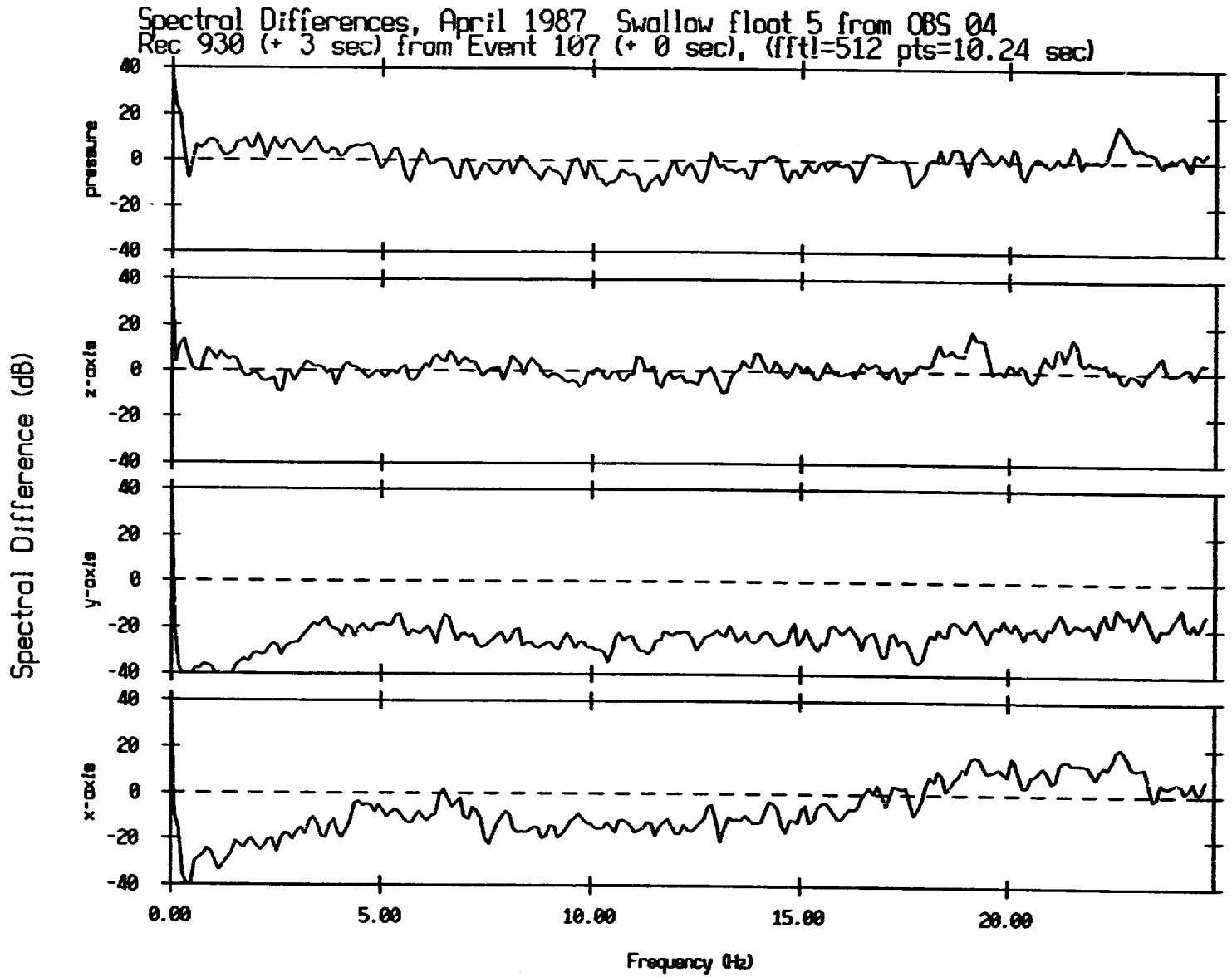
Spectral Differences, April 1987 Swallow float 5 from OBS 04
Rec 930 (+ 3 sec) from Event 107 (+ 0 sec), (fft!=512 pts=10.24 sec)
Spectral Difference (dB)
pressure
z-axis
y-axis
x-axis
40
20
0
-20
-40
0.00
5.00
10.00
15.00
20.00
Frequency (Hz)

Figure V.58

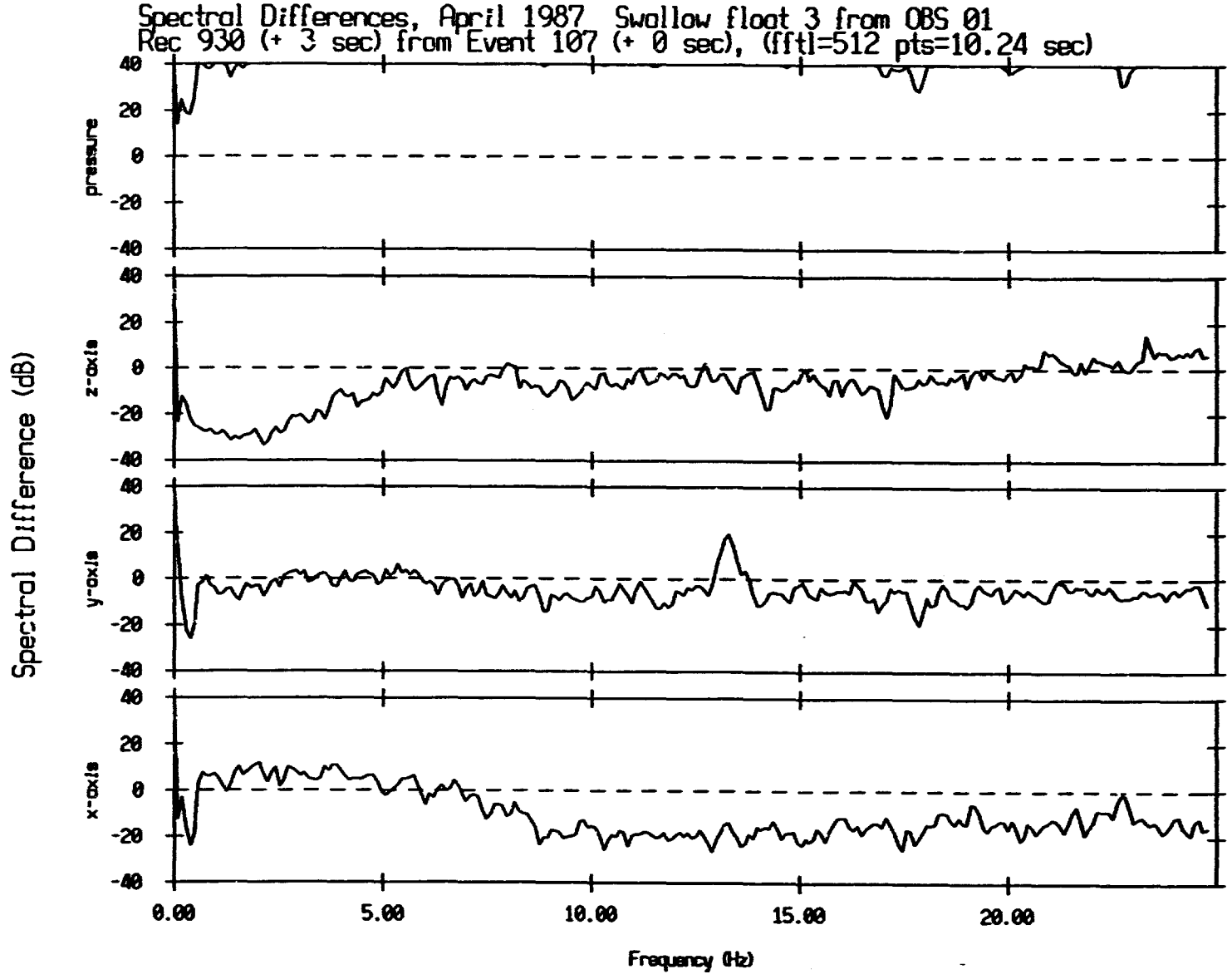
Spectral Differences, April 1987 Swallow float 3 from OBS 01
Rec 930 (+ 3 sec) from Event 107 (+ 0 sec), (fftl=512 pts=10.24 sec)
Spectral Difference (dB)
pressure
z-axis
y-axis
x-axis
40
20
0
-20
-40
0.00
5.00
10.00
15.00
20.00
Frequency (Hz)

Figure V.50

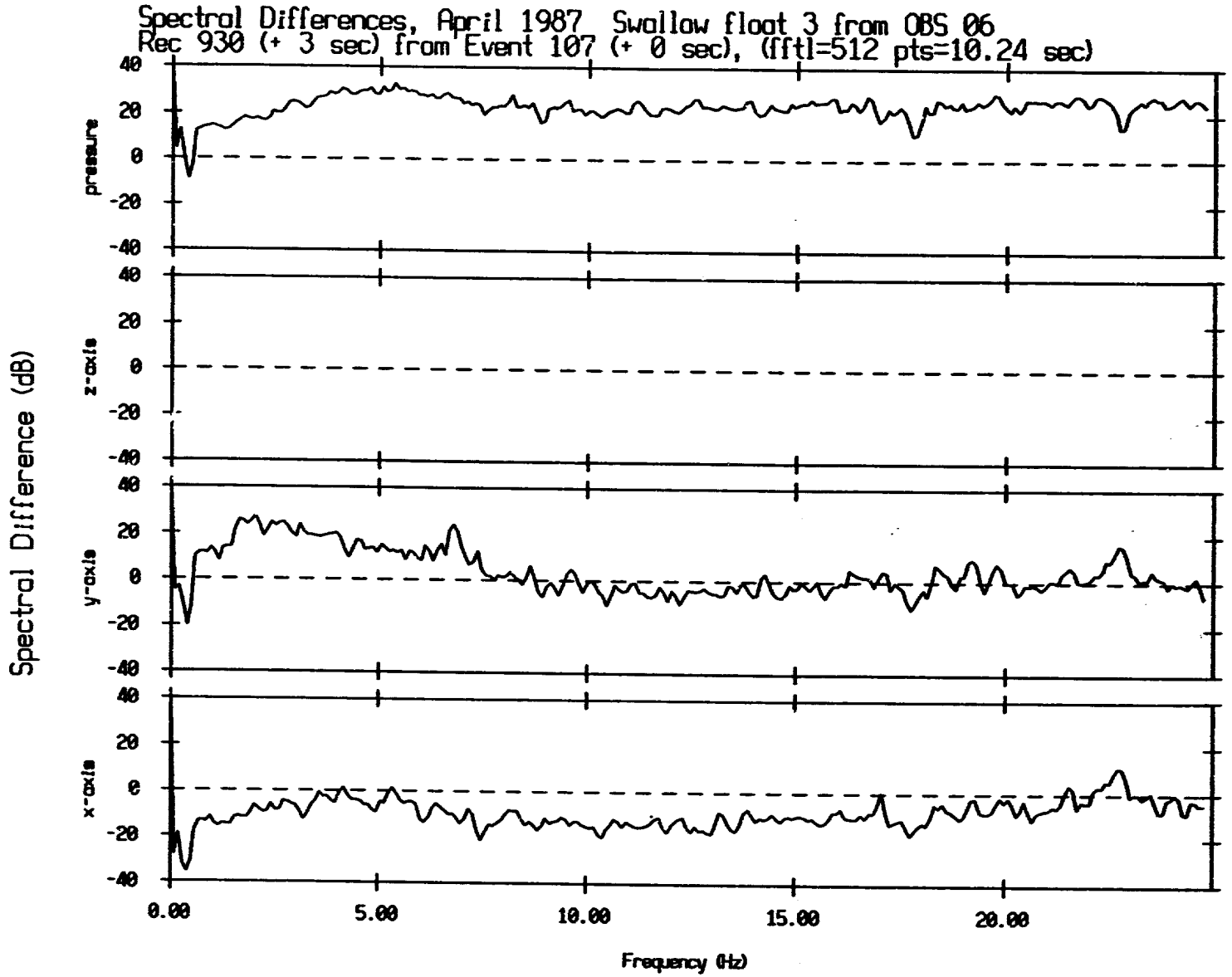
Spectral Differences, April 1987 Swallow float 3 from OBS 06
Rec 930 (+ 3 sec) from Event 107 (+ 0 sec), (fftl=512 pts=10.24 sec)
Spectral Difference (dB)
pressure
z-axis
y-axis
x-axis
40
20
0
-20
-40
0.00
5.00
10.00
15.00
20.00
Frequency (Hz)

Figure V.60

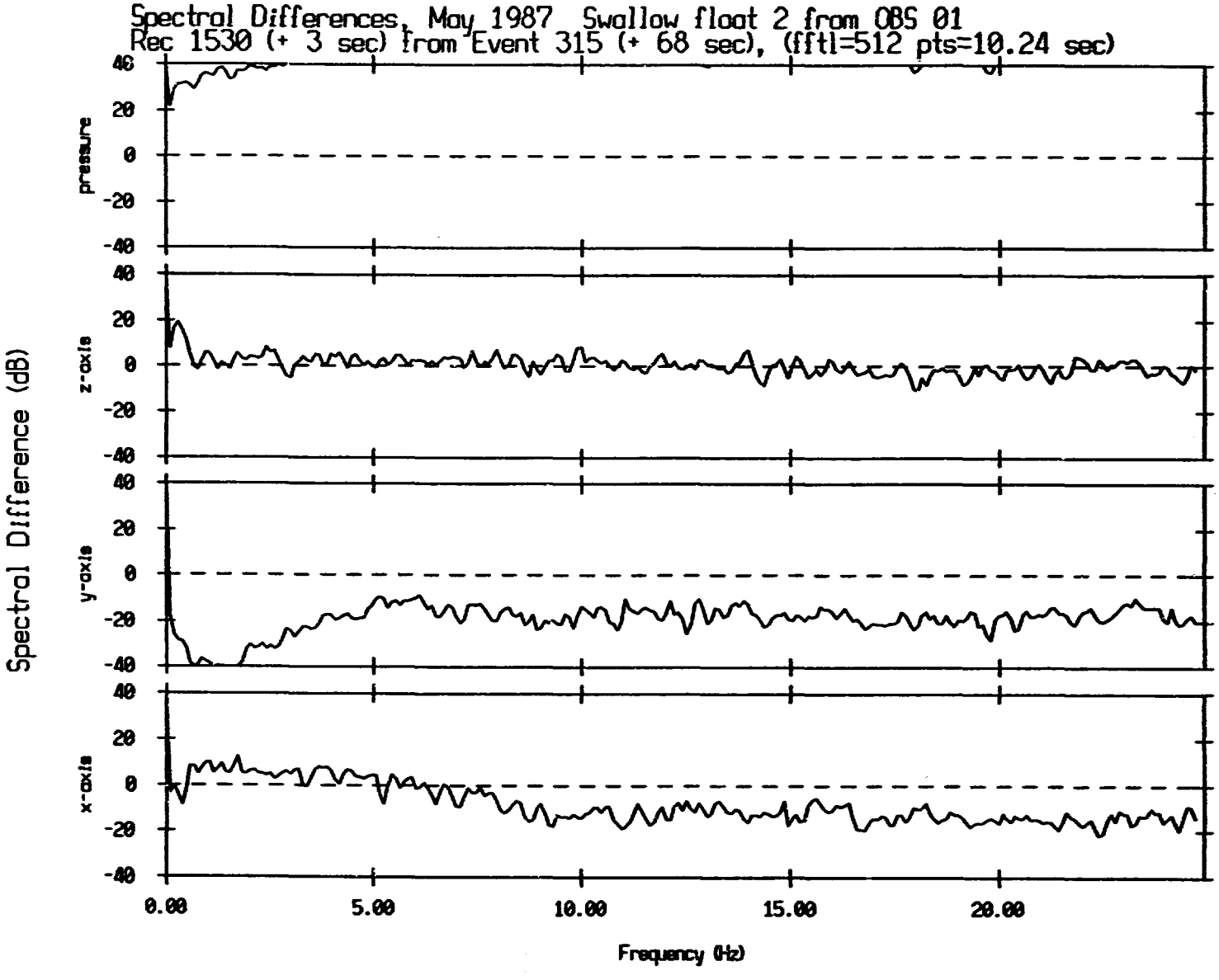
Spectral Differences, May 1987 Swallow float 2 from OBS 01
Rec 1530 (+ 3 sec) from Event 315 (+ 68 sec), (fftl=512 pts=10.24 sec)
Spectral Difference (dB)
pressure
z-axis
y-axis
x-axis
40
20
0
-20
-40
0.00
5.00
10.00
15.00
20.00
Frequency (Hz)

Figure V.01

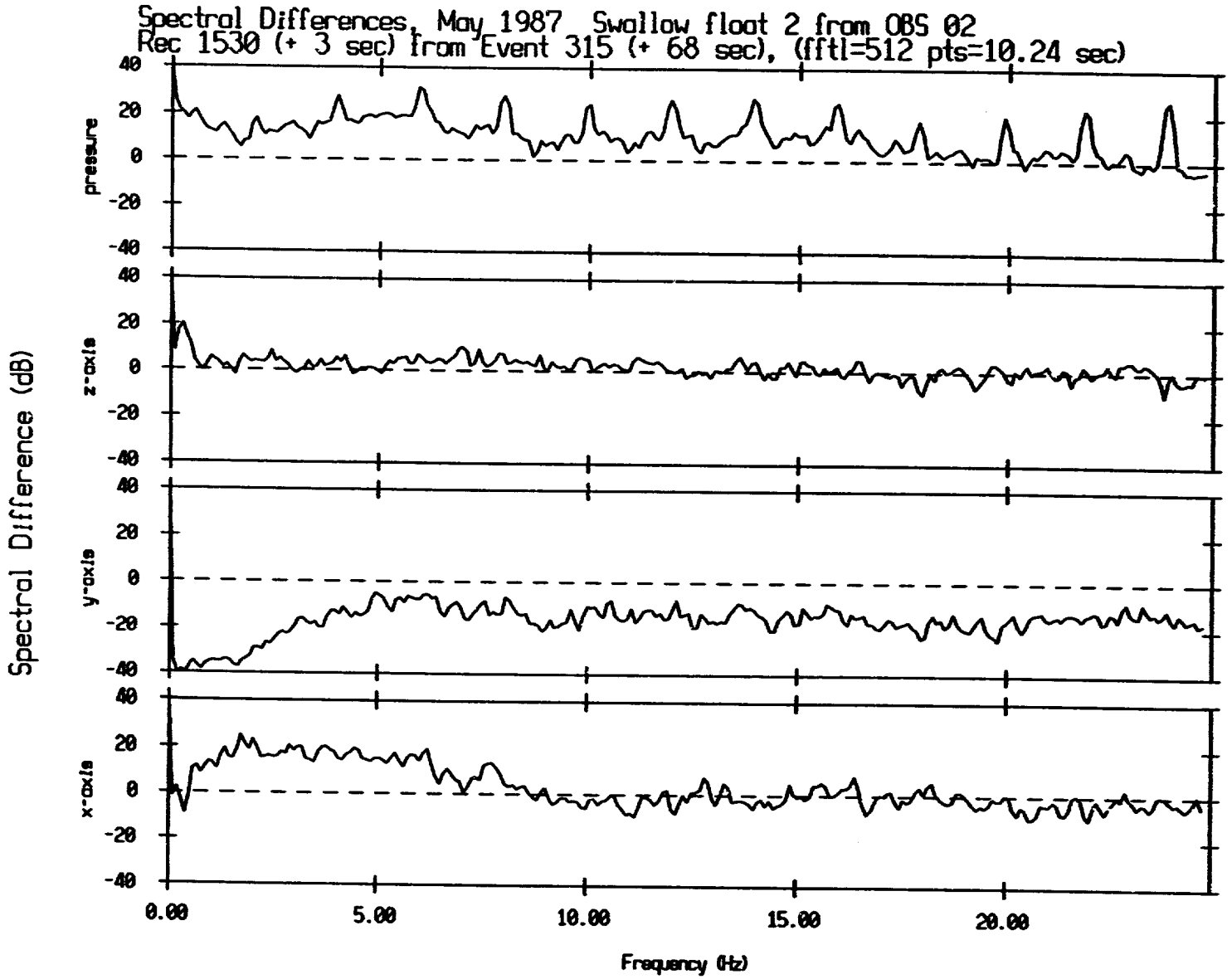
Spectral Differences, May 1987 Swallow float 2 from OBS 02
Rec 1530 (+ 3 sec) from Event 315 (+ 68 sec), (fftl=512 pts=10.24 sec)
Spectral Difference (dB)
pressure
z-axis
y-axis
x-axis
40
20
0
-20
-40
0.00
5.00
10.00
15.00
20.00
Frequency (Hz)

Figure V.62

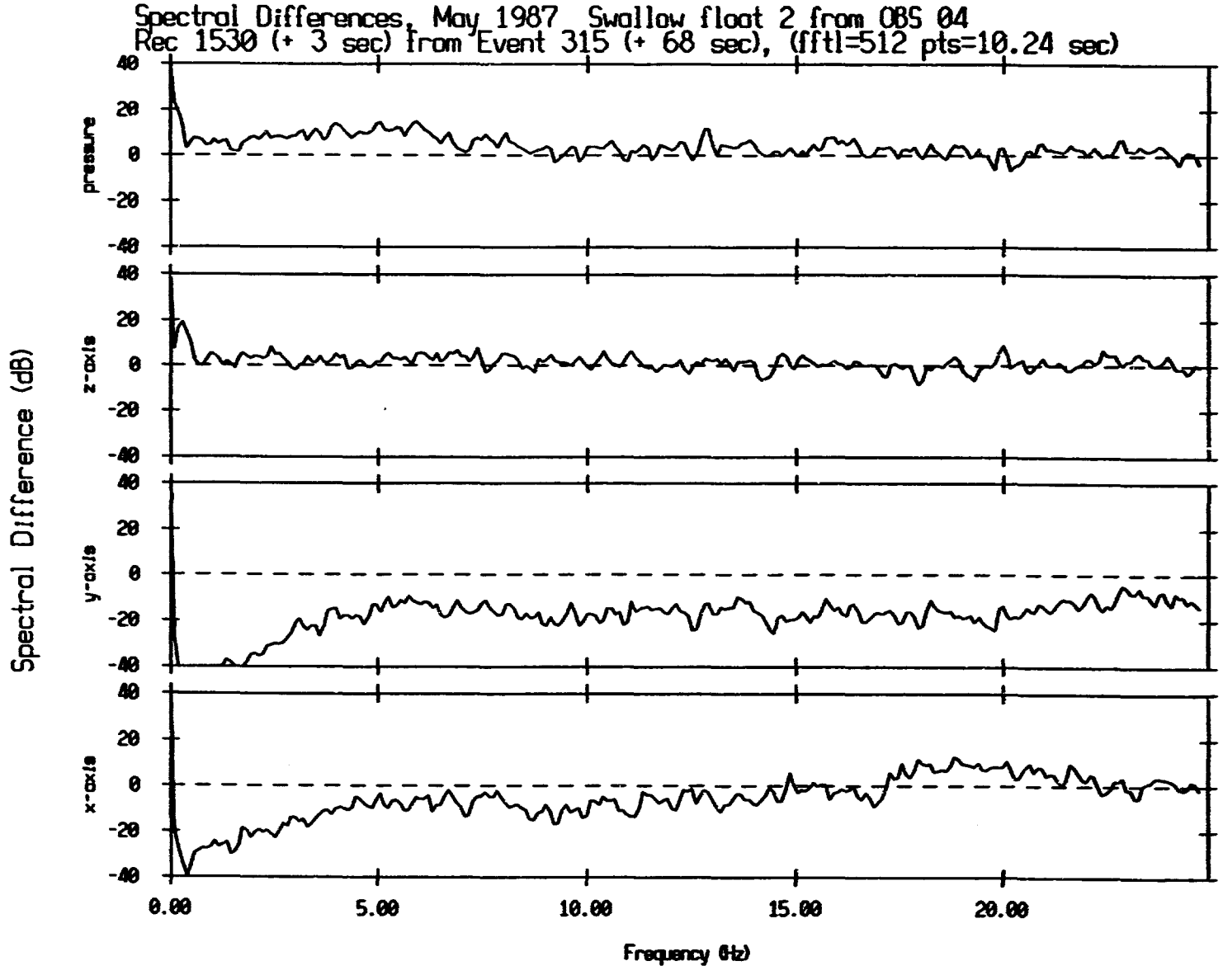
Spectral Differences, May 1987 Swallow float 2 from OBS 04
Rec 1530 (+ 3 sec) from Event 315 (+ 68 sec), (fftl=512 pts=10.24 sec)
Spectral Difference (dB)
pressure
z-axis
y-axis
x-axis
40
20
0
-20
-40
0.00
5.00
10.00
15.00
20.00
Frequency (Hz)

Figure V.63

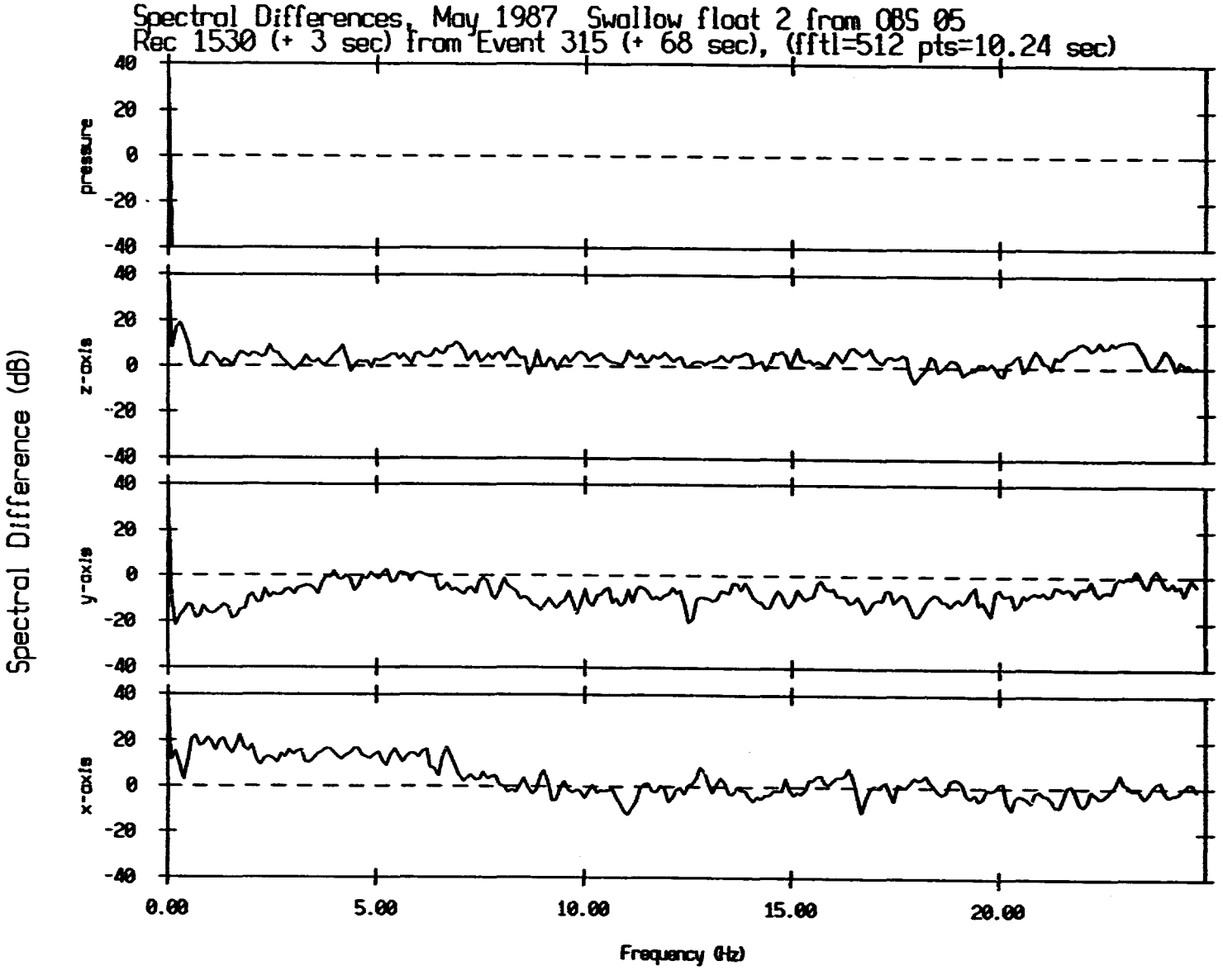
Spectral Differences, May 1987 Swallow float 2 from OBS 05
Rec 1530 (+ 3 sec) from Event 315 (+ 68 sec), (fftl=512 pts=10.24 sec)
Spectral Difference (dB)
pressure
z-axis
y-axis
x-axis
40
20
0
-20
-40
0.00
5.00
10.00
15.00
20.00
Frequency (Hz)

Figure V.64

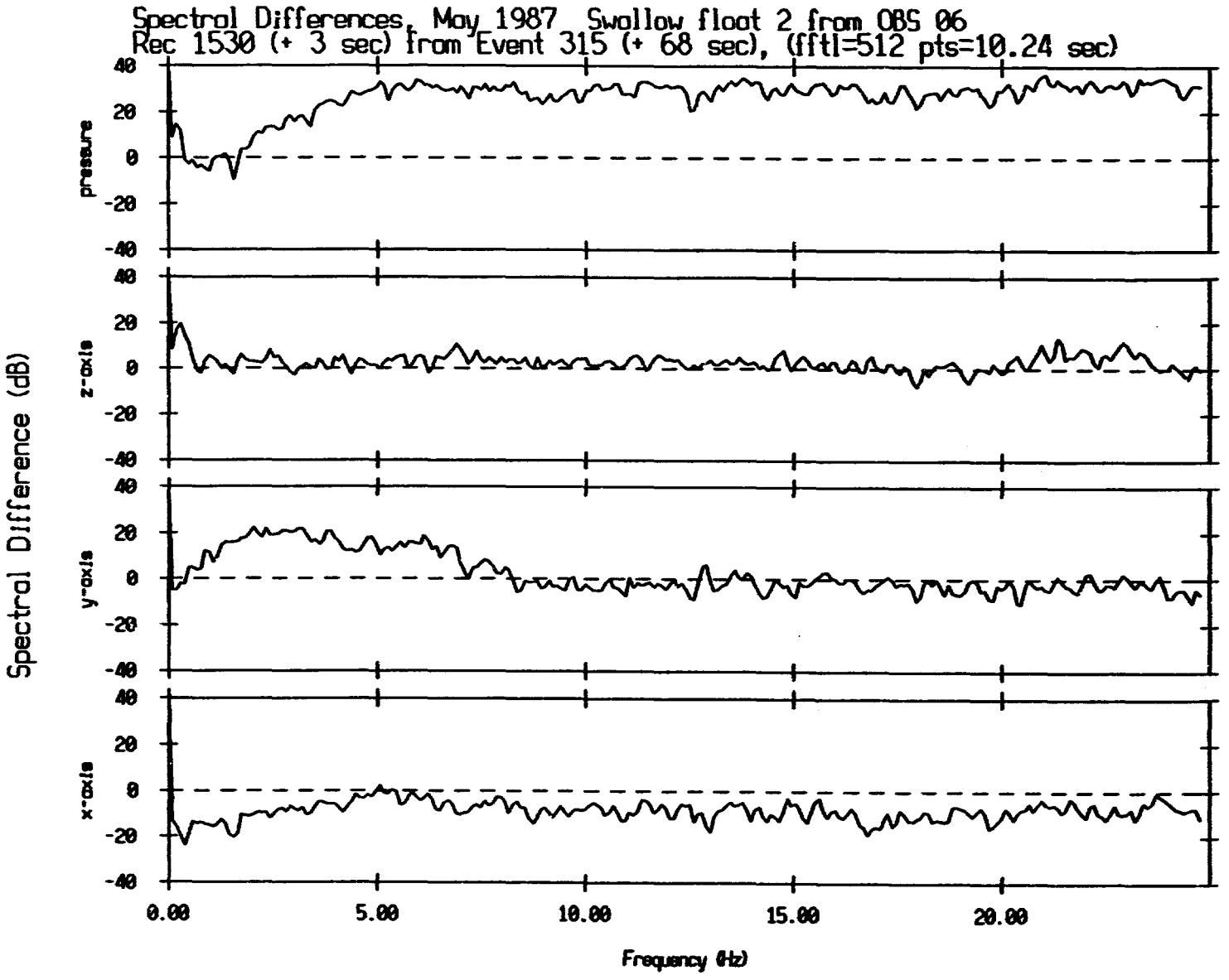
Spectral Differences, May 1987 Swallow float 2 from OBS 06
Rec 1530 (+ 3 sec) from Event 315 (+ 68 sec), (fftl=512 pts=10.24 sec)
Spectral Difference (dB)
pressure
z-axis
y-axis
x-axis
40
20
0
-20
-40
0.00
5.00
10.00
15.00
20.00
Frequency (Hz)

Figure V.65

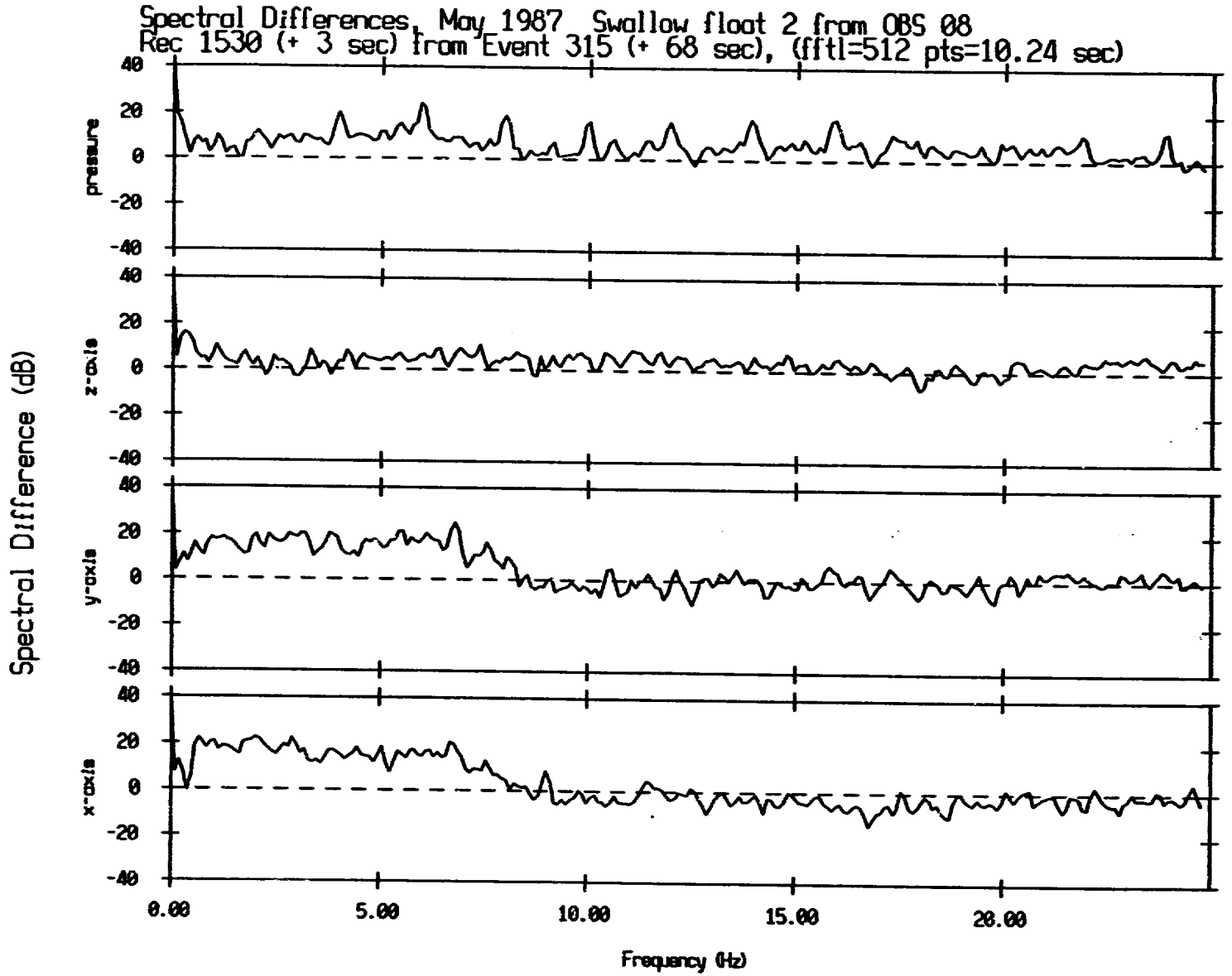
Spectral Differences, May 1987 Swallow float 2 from OBS 08
Rec 1530 (+ 3 sec) from Event 315 (+ 68 sec), (fftl=512 pts=10.24 sec)
Spectral Difference (dB)
pressure
z-axis
y-axis
x-axis
40
20
0
-20
-40
0.00
5.00
10.00
15.00
20.00
Frequency (Hz)

Figure V.06

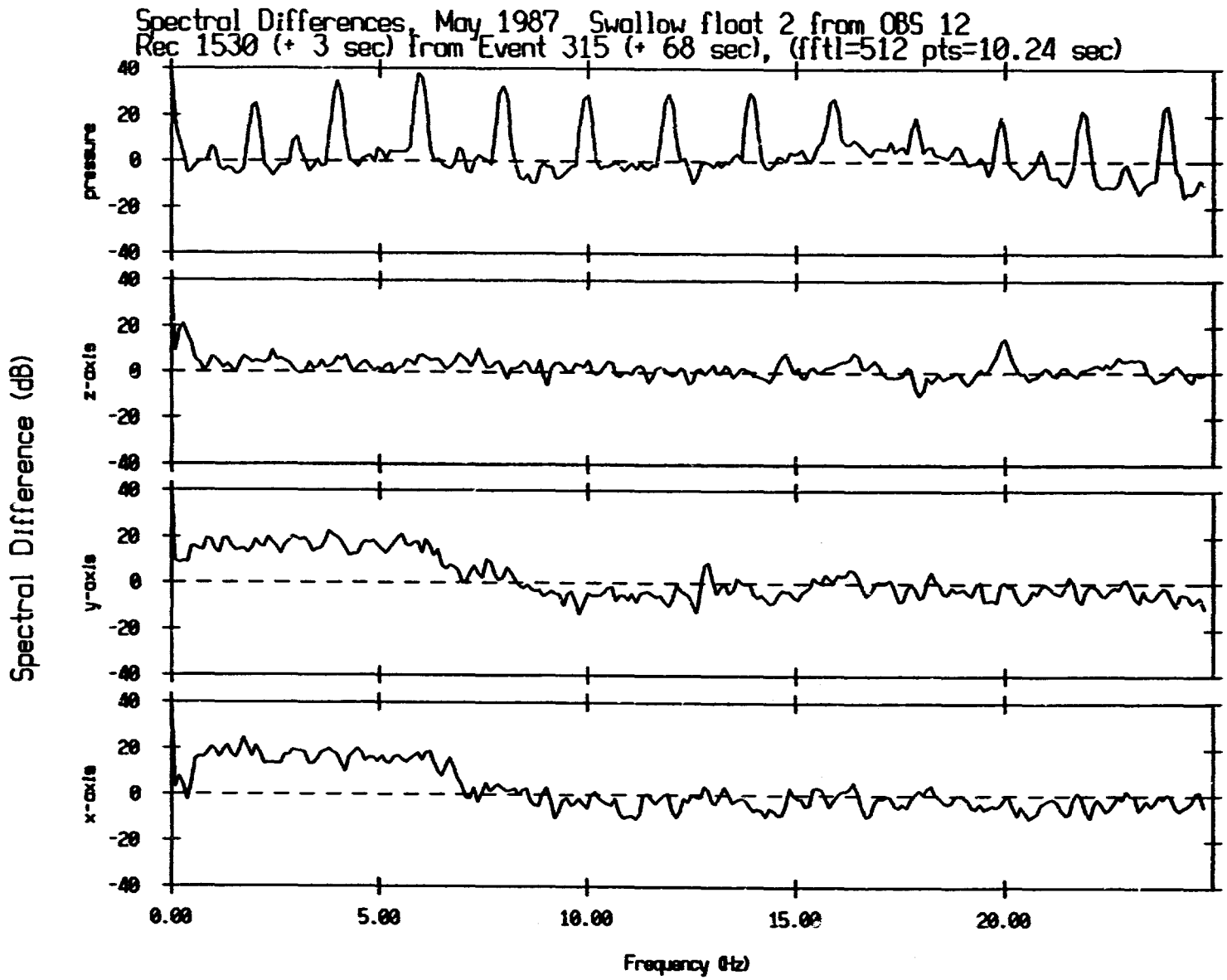
Spectral Differences, May 1987 Swallow float 2 from OBS 12
Rec 1530 (+ 3 sec) from Event 315 (+ 68 sec), (fftl=512 pts=10.24 sec)
Spectral Difference (dB)
pressure
z-axis
y-axis
x-axis
40
20
0
-20
-40
0.00
5.00
10.00
15.00
20.00
Frequency (Hz)

Figure V.87

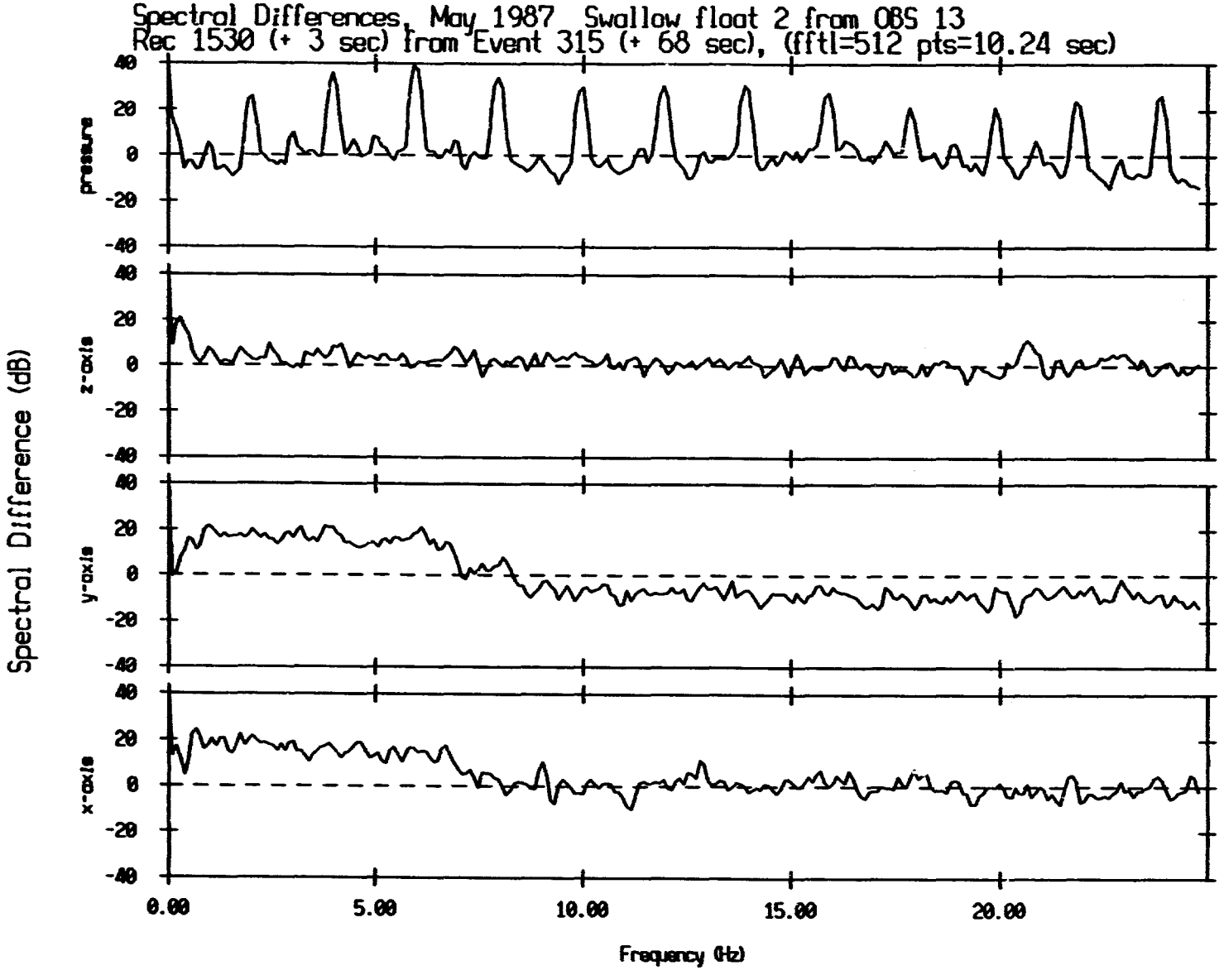
Spectral Differences, May 1987 Swallow float 2 from OBS 13
Rec 1530 (+ 3 sec) from Event 315 (+ 68 sec), (fftl=512 pts=10.24 sec)
Spectral Difference (dB)
pressure
z-axis
y-axis
x-axis
40
20
0
-20
-40
0.00
5.00
10.00
15.00
20.00
Frequency (Hz)

Figure V.88

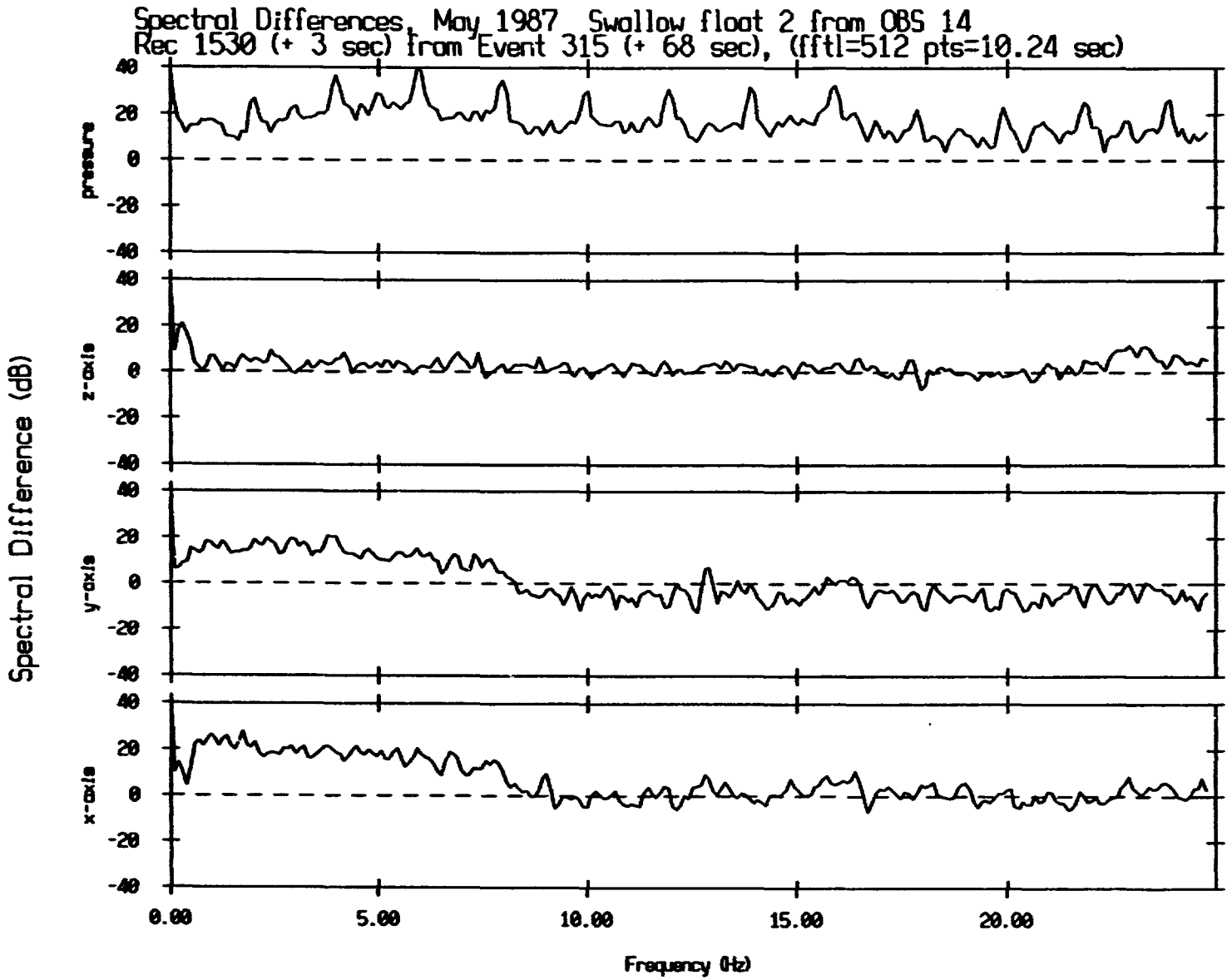
Spectral Differences, May 1987 Swallow float 2 from OBS 14
Rec 1530 (+ 3 sec) from Event 315 (+ 68 sec), (fftl=512 pts=10.24 sec)
Spectral Difference (dB)
pressure
z-axis
y-axis
x-axis
40
20
0
-20
-40
0.00
5.00
10.00
15.00
20.00
Frequency (Hz)

Figure V.09

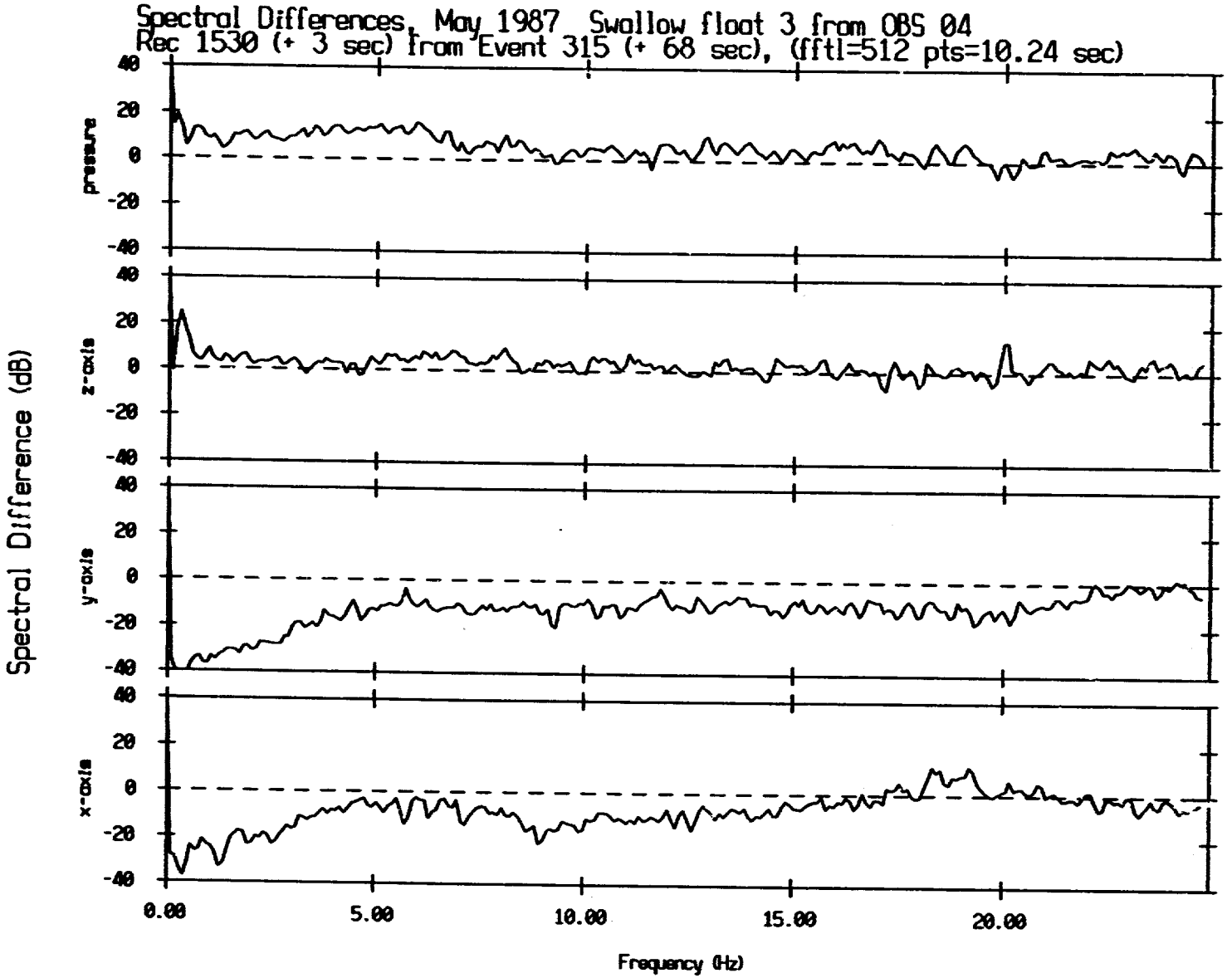
Spectral Differences, May 1987 Swallow float 3 from OBS 04
Rec 1530 (+ 3 sec) from Event 315 (+ 68 sec), (fftl=512 pts=10.24 sec)
Spectral Difference (dB)
pressure
z-axis
y-axis
x-axis
40
20
0
-20
-40
0.00
5.00
10.00
15.00
20.00
Frequency (Hz)

Figure V.7.0

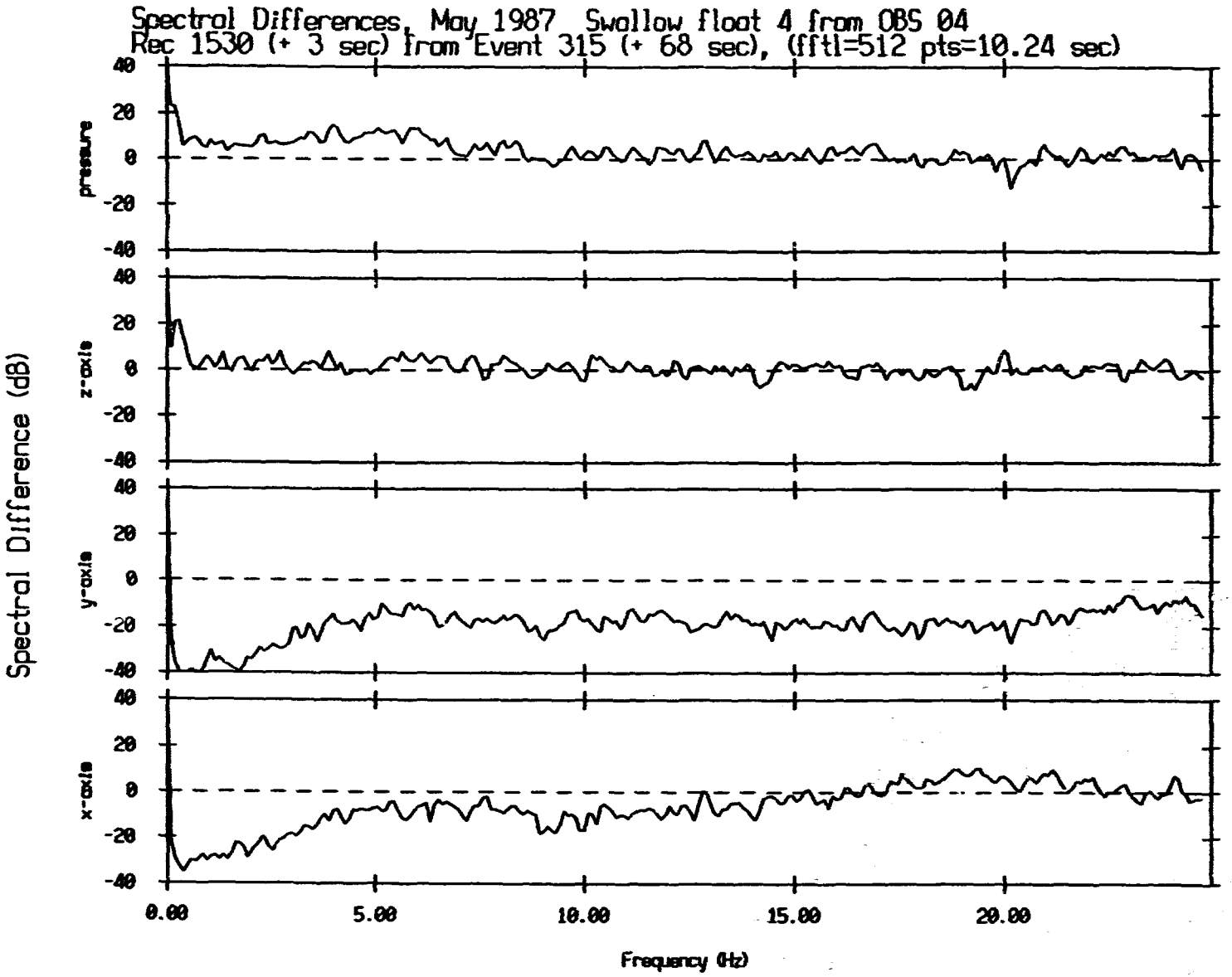
Spectral Differences, May 1987 Swallow float 4 from OBS 04
Rec 1530 (+ 3 sec) from Event 315 (+ 68 sec), (fftl=512 pts=10.24 sec)
Spectral Difference (dB)
pressure
z-axis
y-axis
x-axis
40
20
0
-20
-40
0.00
5.00
10.00
15.00
20.00
Frequency (Hz)

Figure V.71

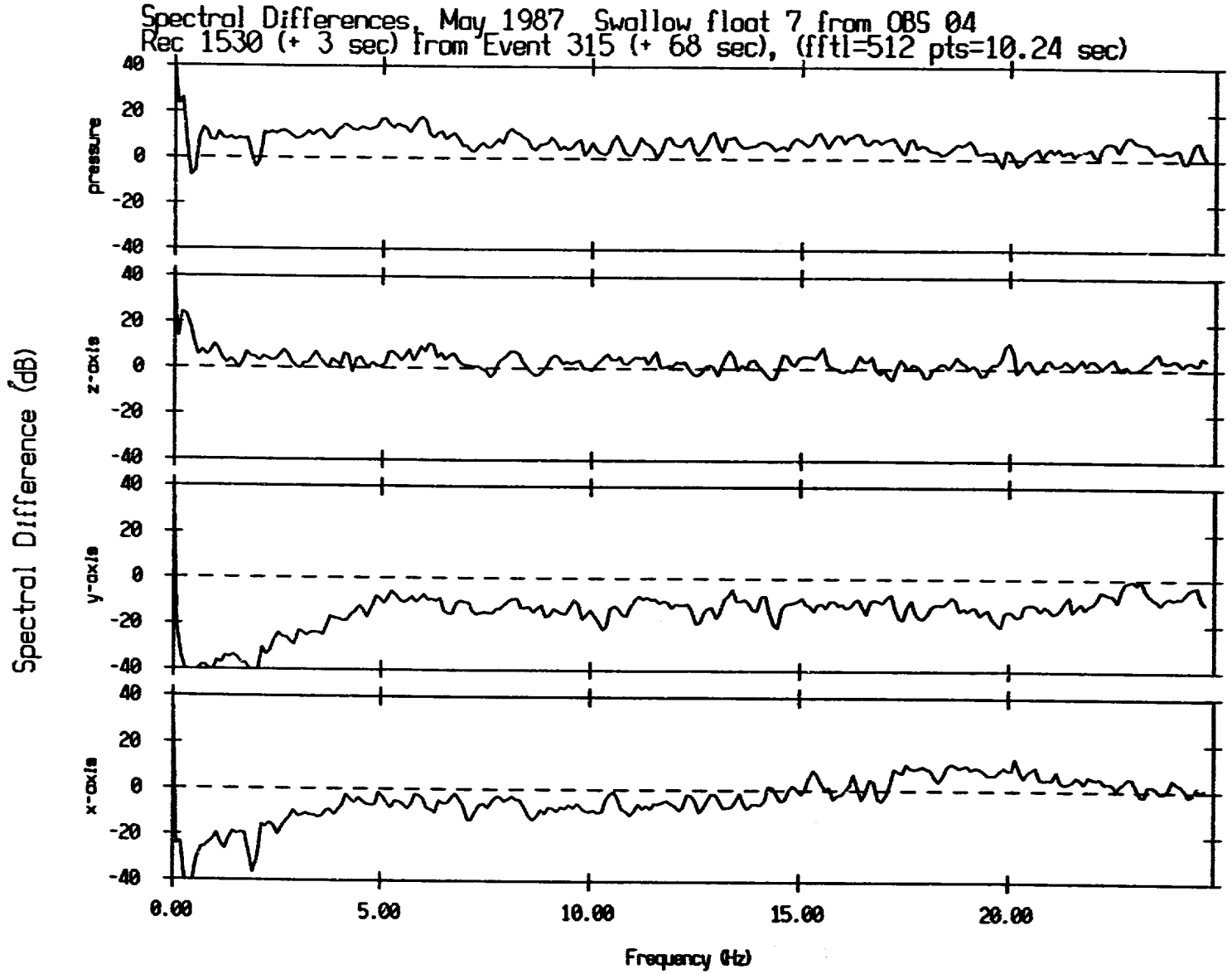
Spectral Differences, May 1987 Swallow float 7 from OBS 04
Rec 1530 (+ 3 sec) from Event 315 (+ 68 sec), (fftl=512 pts=10.24 sec)
Spectral Difference (dB)
pressure
z-axis
y-axis
x-axis
40
20
0
-20
-40
0.00
5.00
10.00
15.00
20.00
Frequency (Hz)

Figure V.72

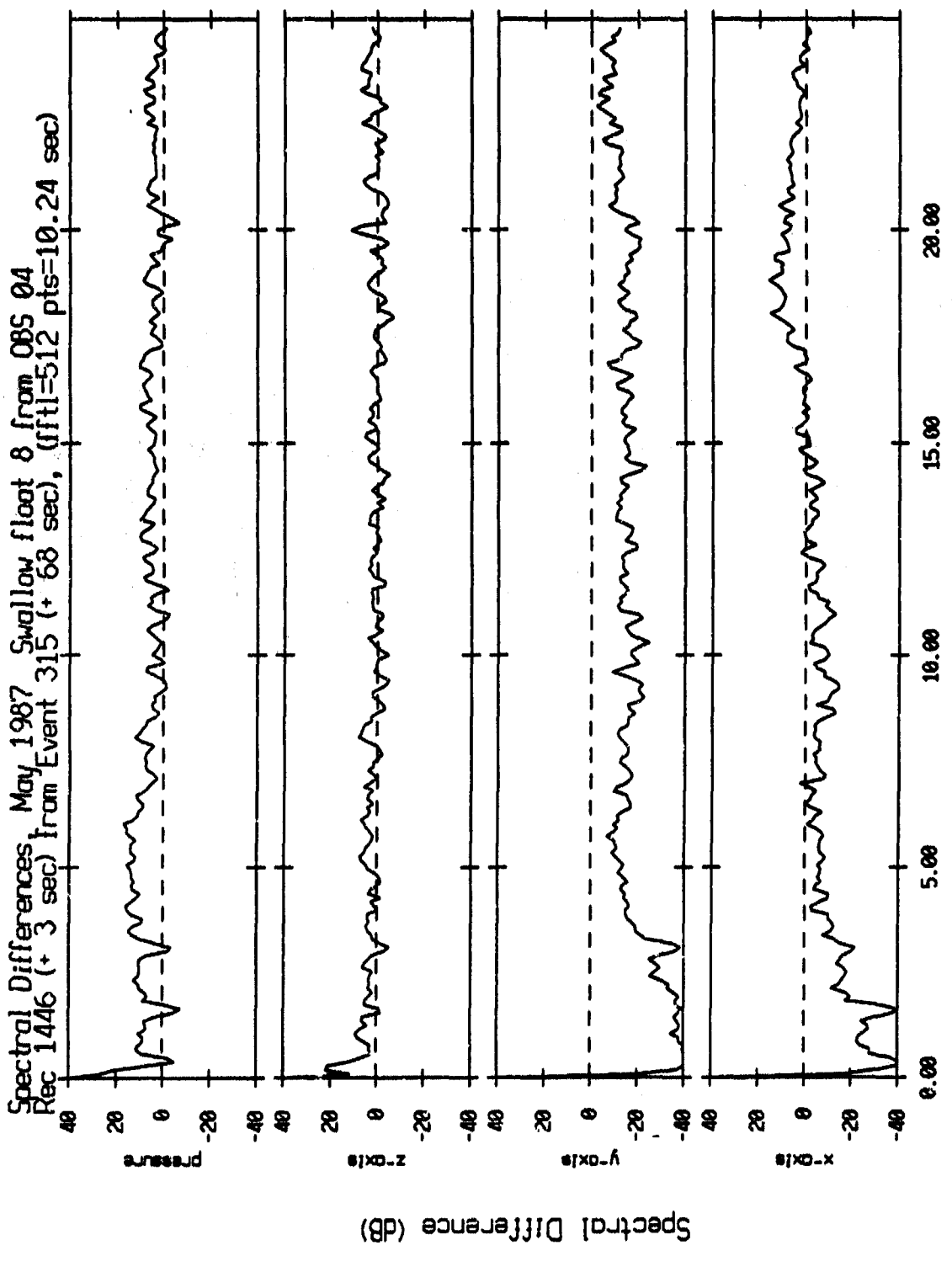
Spectral Differences, May 1987 Swallow float 8 from OBS 04
Rec 1446 (+ 3 sec) from Event 315 (+ 68 sec), (fft1=512 pts=10.24 sec)
pressure
z-axis
y-axis
x-axis
40
20
0
-20
-40
0.00
5.00
10.00
15.00
20.00
Frequency (Hz)
Spectral Difference (dB)

Figure V.73

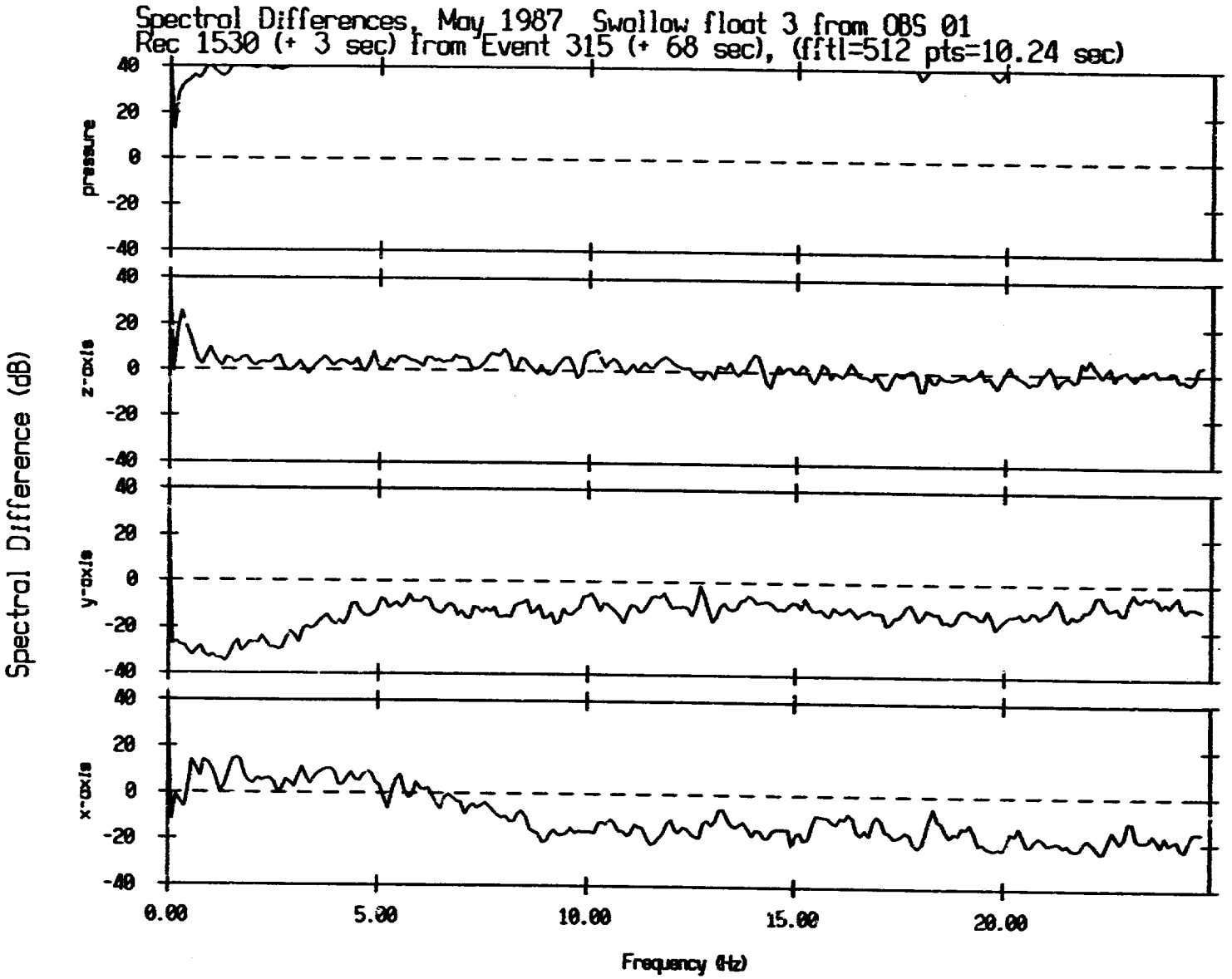
Spectral Differences, May 1987 Swallow float 3 from OBS 01
Rec 1530 (+ 3 sec) from Event 315 (+ 68 sec), (fftl=512 pts=10.24 sec)
Spectral Difference (dB)
pressure
z-axis
y-axis
x-axis
40
20
0
-20
-40
0.00
5.00
10.00
15.00
20.00
Frequency (Hz)

Figure V.74

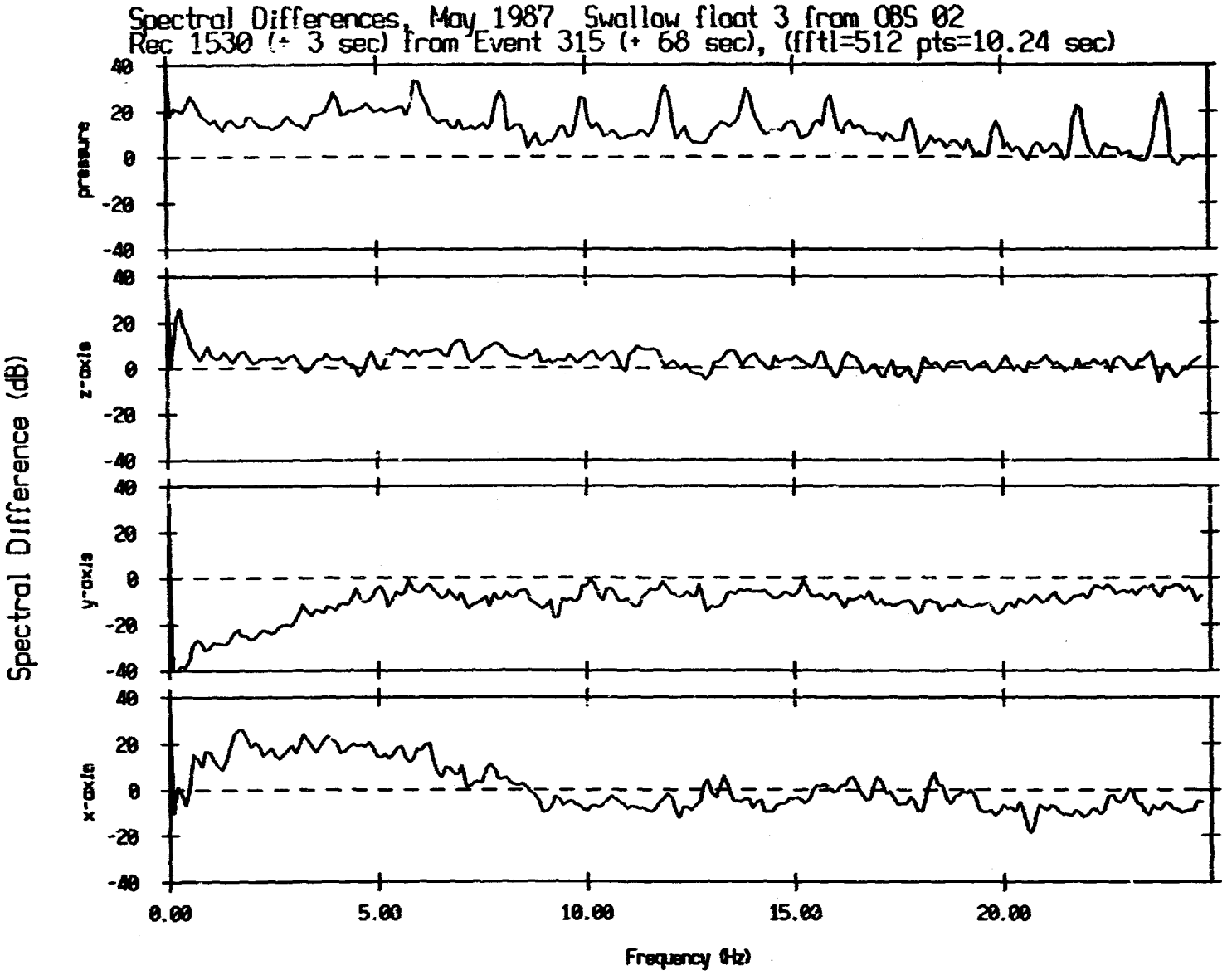
Spectral Differences, May 1987 Swallow float 3 from OBS 02
Rec 1530 (+ 3 sec) from Event 315 (+ 68 sec), (fftl=512 pts=10.24 sec)
Spectral Difference (dB)
pressure
z-axis
y-axis
x-axis
40
20
0
-20
-40
0.00
5.00
10.00
15.00
20.00
Frequency (Hz)

Figure V.75

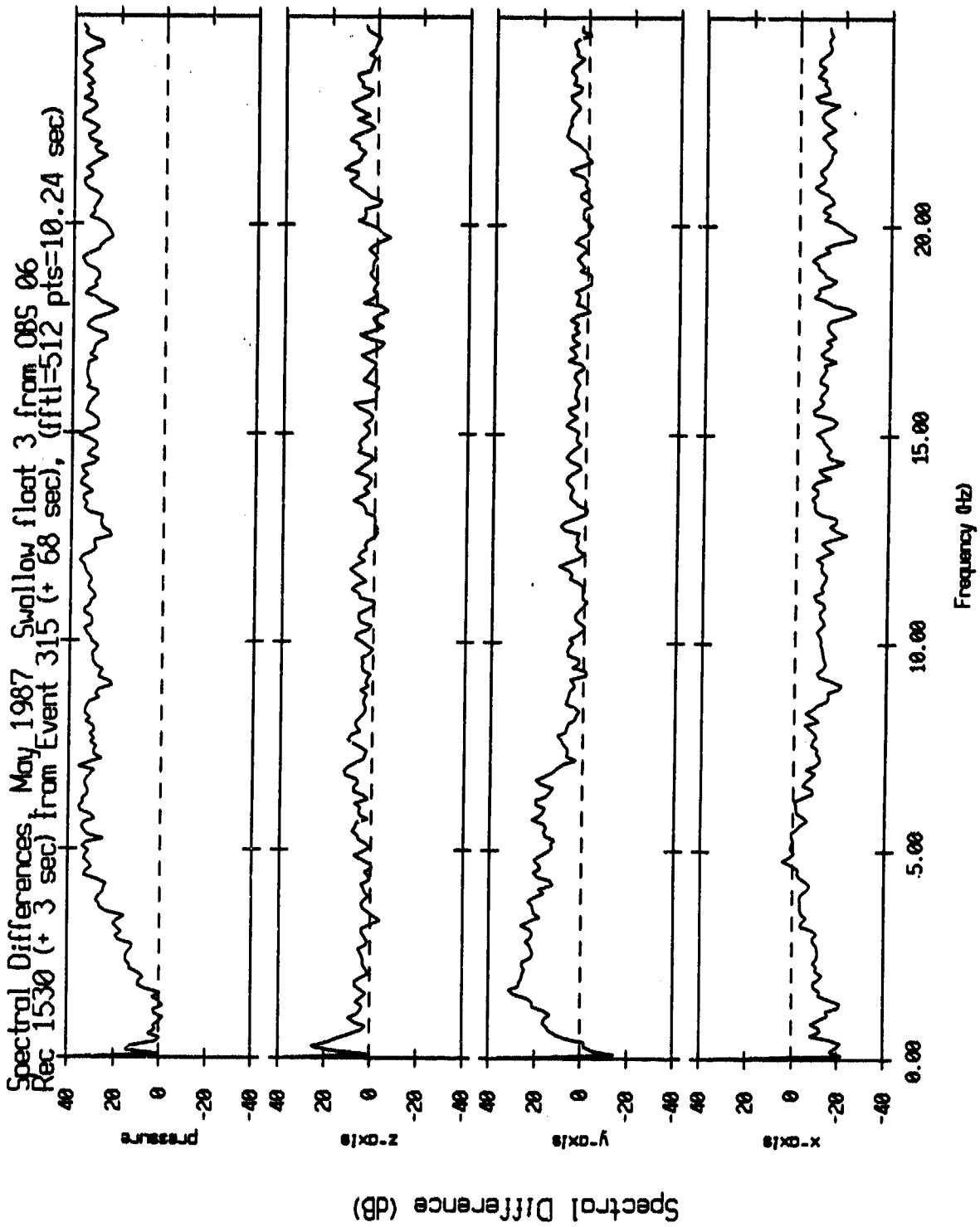
Spectral Differences, May 1987 Swallow float 3 from OBS 06
Rec 1530 (+ 3 sec) from Event 315 (+ 68 sec), (fftl=512 pts=10.24 sec)
pressure
z-axis
y-axis
x-axis
40
20
0
-20
-40
0.00
5.00
10.00
15.00
20.00
Frequency (Hz)
Spectral Difference (dB)

Figure V.76

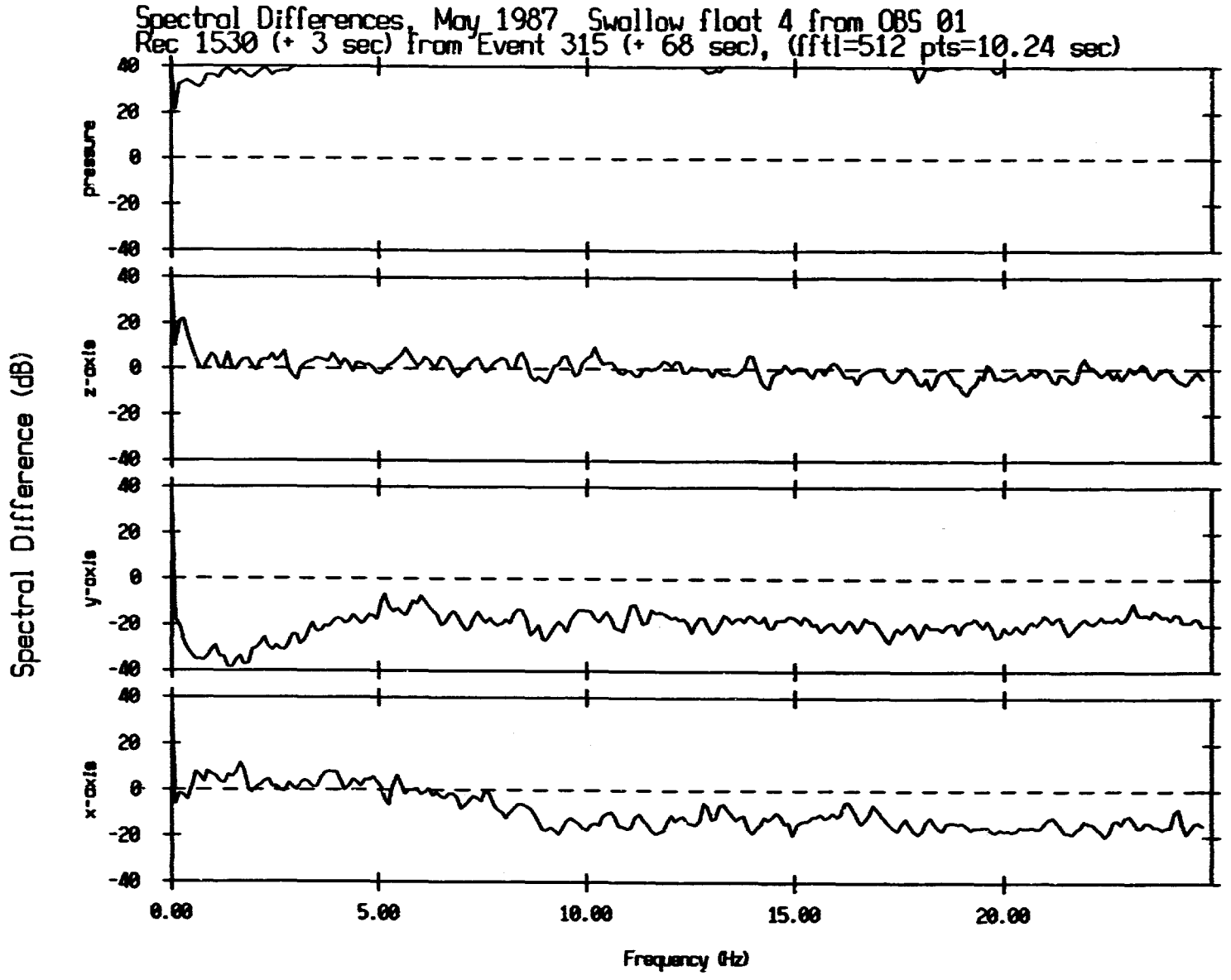
Spectral Differences, May 1987 Swallow float 4 from OBS 01
Rec 1530 (+ 3 sec) from Event 315 (+ 68 sec), (fftl=512 pts=10.24 sec)
Spectral Difference (dB)
pressure
z-axis
y-axis
x-axis
40
20
0
-20
-40
0.00
5.00
10.00
15.00
20.00
Frequency (Hz)

Figure V.17

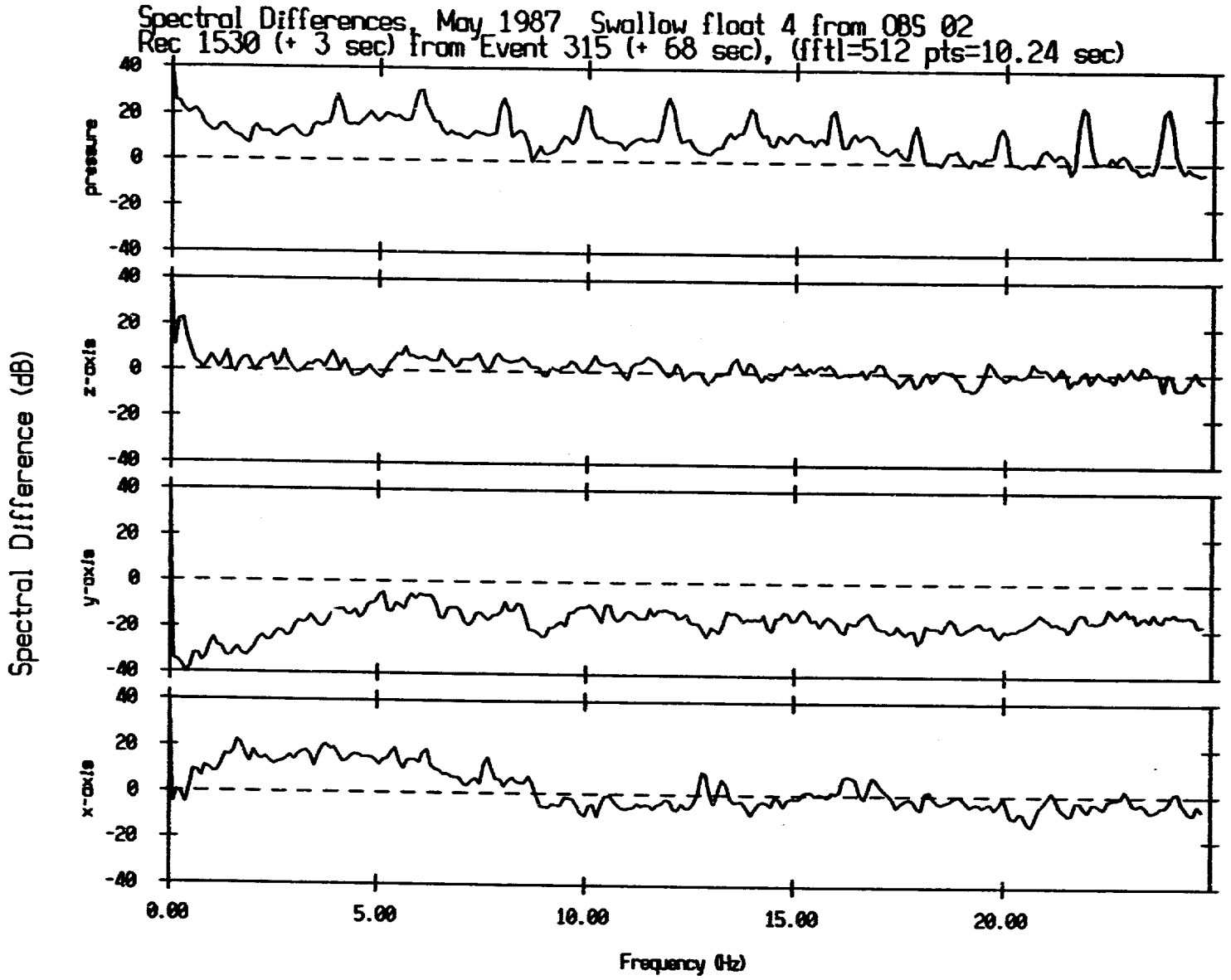
Spectral Differences, May 1987 Swallow float 4 from OBS 02
Rec 1530 (+ 3 sec) from Event 315 (+ 68 sec), (fftl=512 pts=10.24 sec)
Spectral Difference (dB)
pressure
z-axis
y-axis
x-axis
40
20
0
-20
-40
0.00
5.00
10.00
15.00
20.00
Frequency (Hz)

Figure V.78

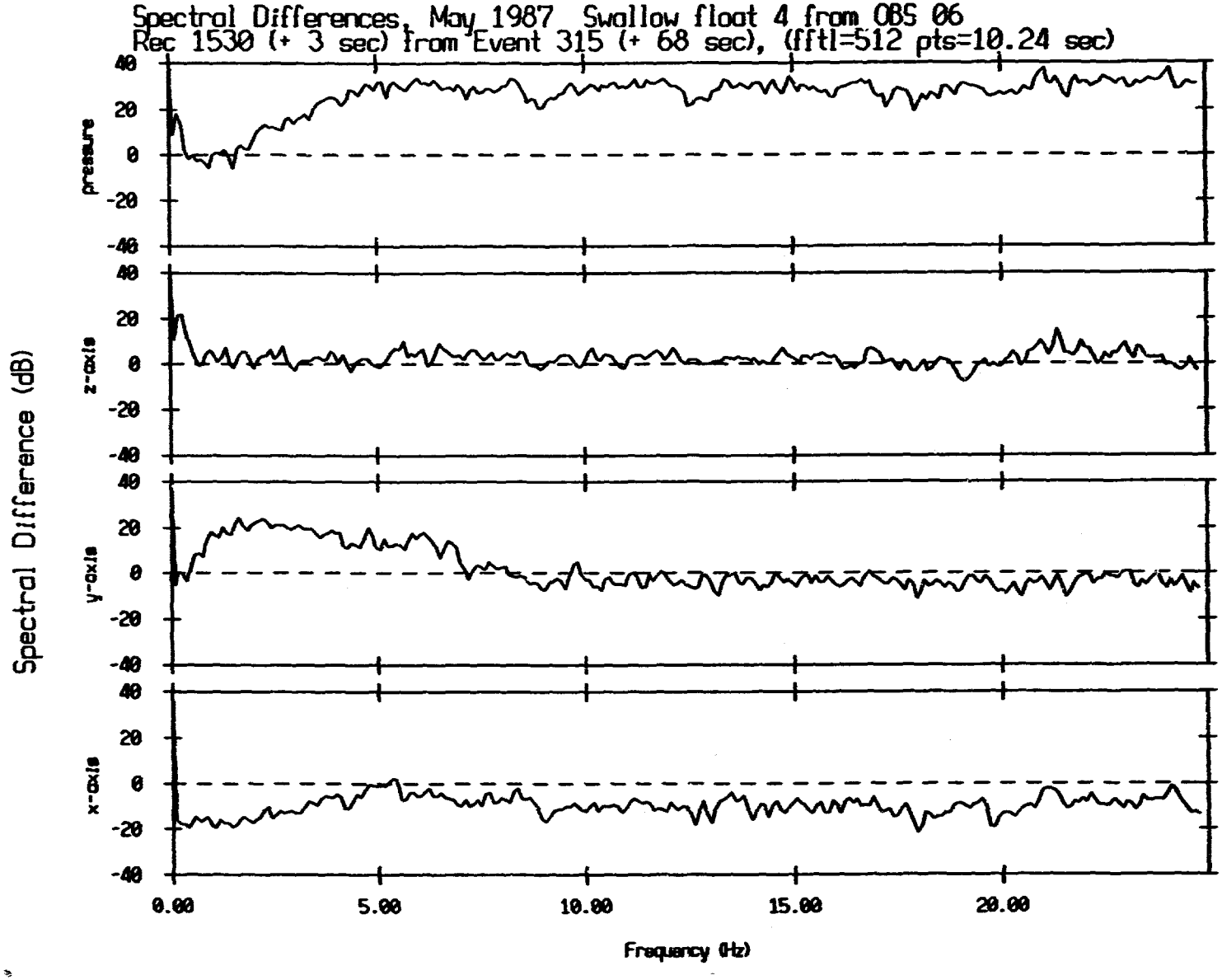
Spectral Differences, May 1987 Swallow float 4 from OBS 06
Rec 1530 (+ 3 sec) from Event 315 (+ 68 sec), (fftl=512 pts=10.24 sec)
Spectral Difference (dB)
pressure
z-axis
y-axis
x-axis
40
20
0
-20
-40
0.00
5.00
10.00
15.00
20.00
Frequency (Hz)

Figure V.70

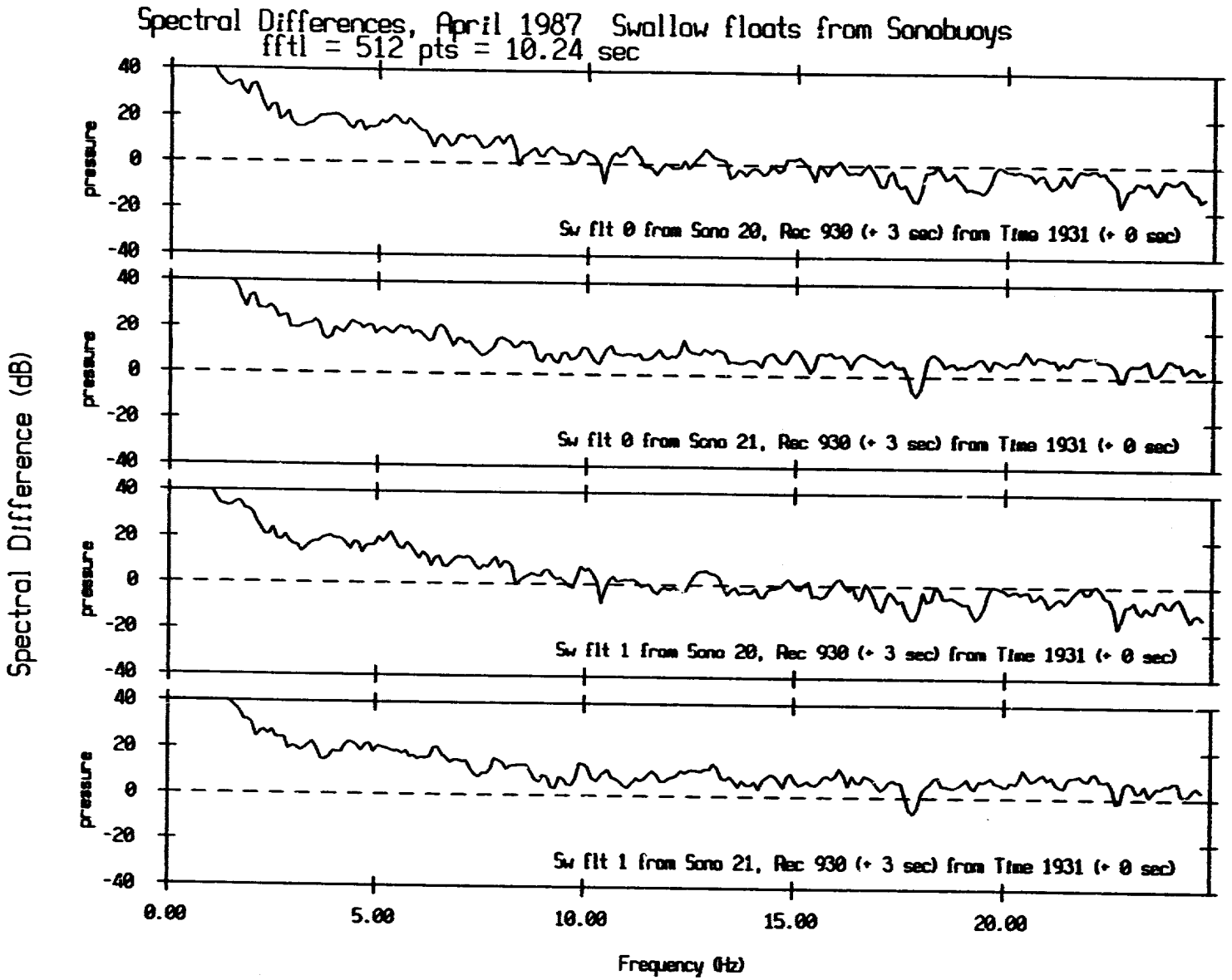
Spectral Differences, April 1987 Swallow floats from Sonobuoys
fftl = 512 pts = 10.24 sec
Spectral Difference (dB)
pressure
Sw flt 0 from Sono 20, Rec 930 (+ 3 sec) from Time 1931 (+ 0 sec)
Sw flt 0 from Sono 21, Rec 930 (+ 3 sec) from Time 1931 (+ 0 sec)
Sw flt 1 from Sono 20, Rec 930 (+ 3 sec) from Time 1931 (+ 0 sec)
Sw flt 1 from Sono 21, Rec 930 (+ 3 sec) from Time 1931 (+ 0 sec)
40
20
0
-20
-40
0.00
5.00
10.00
15.00
20.00
Frequency (Hz)

Figure V.80

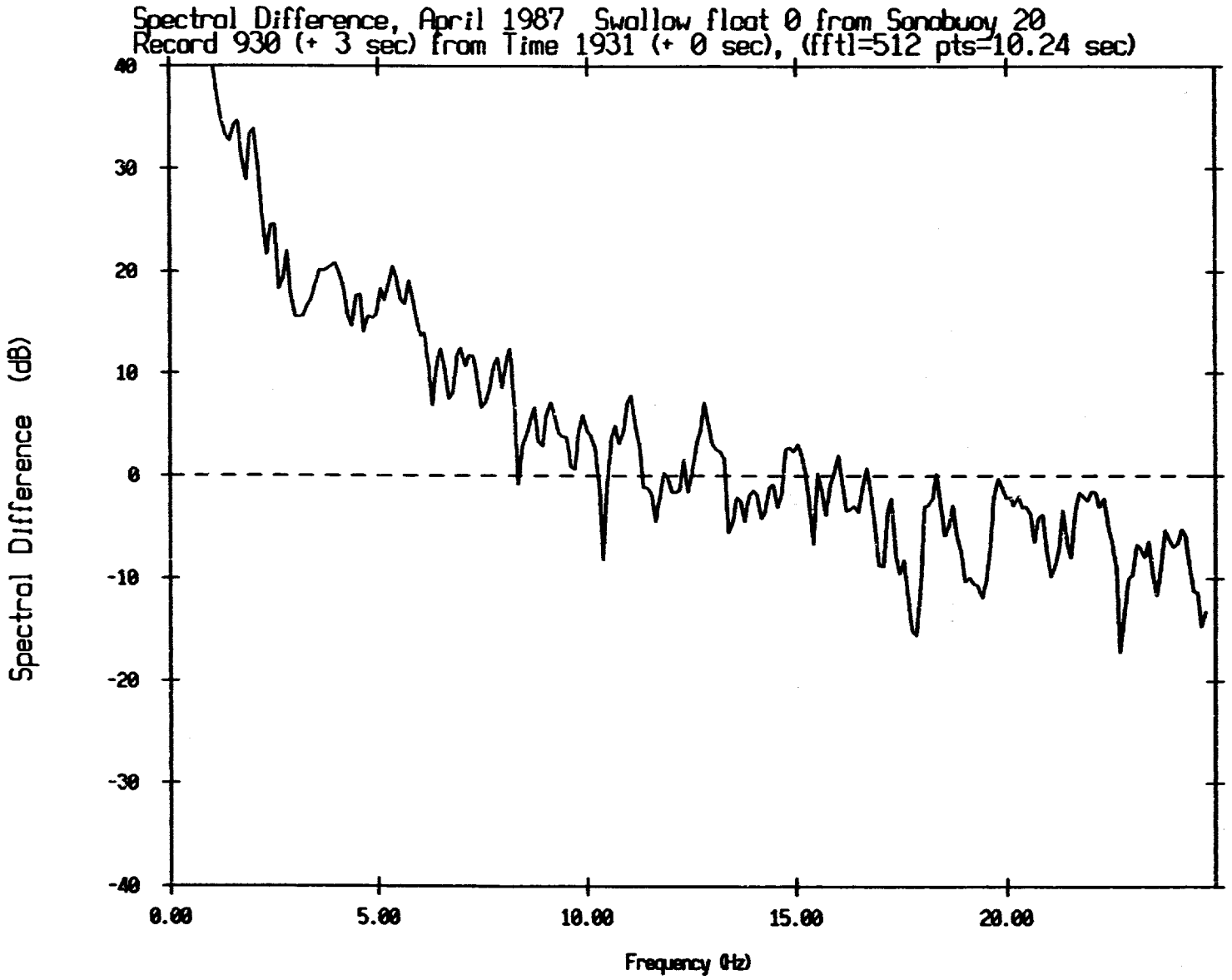
Spectral Difference, April 1987 Swallow float 0 from Sonobuoy 20
Record 930 (+ 3 sec) from Time 1931 (+ 0 sec), (fftl=512 pts=10.24 sec)
Spectral Difference (dB)
40
30
20
10
0
-10
-20
-30
-40
0.00
5.00
10.00
15.00
20.00
Frequency (Hz)

Figure V.81

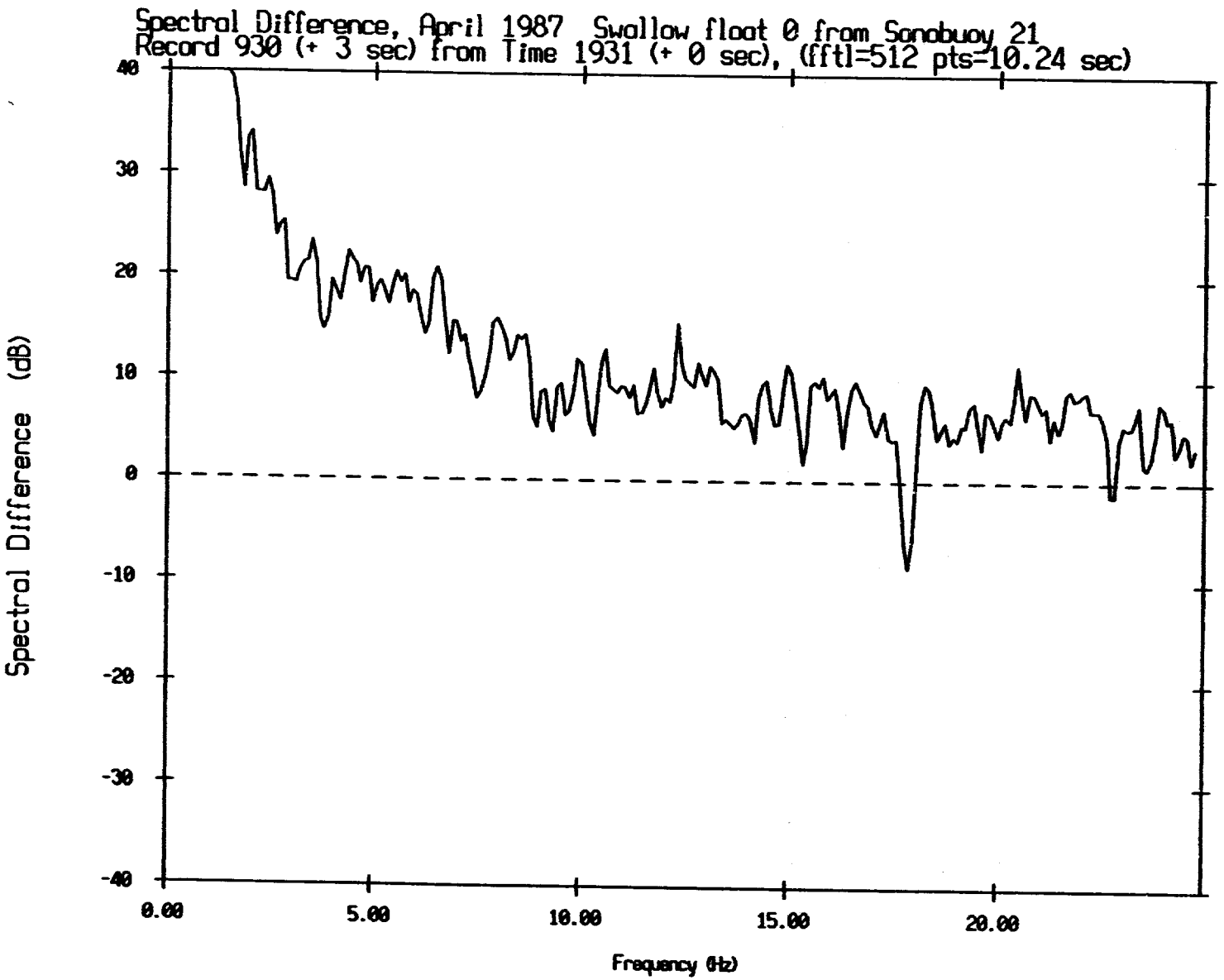
Spectral Difference, April 1987 Swallow float 0 from Sonobuoy 21
Record 930 (+ 3 sec) from Time 1931 (+ 0 sec), (fftl=512 pts=10.24 sec)
Spectral Difference (dB)
40
30
20
10
0
-10
-20
-30
-40
0.00
5.00
10.00
15.00
20.00
Frequency (Hz)

Figure V.82

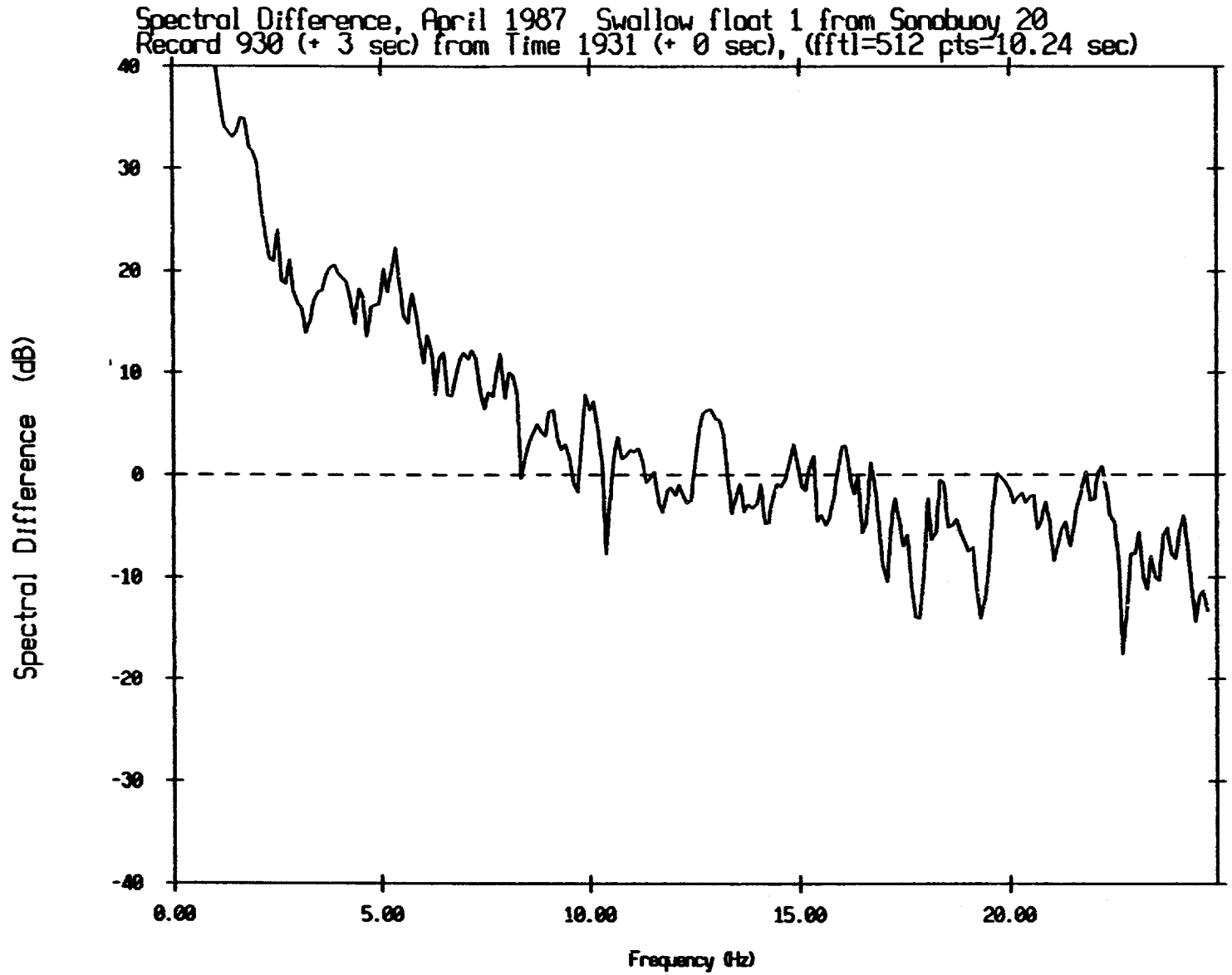
Spectral Difference, April 1987 Swallow float 1 from Sonobuoy 20
Record 930 (+ 3 sec) from Time 1931 (+ 0 sec), (fftl=512 pts=10.24 sec)
Spectral Difference (dB)
40
30
20
10
0
-10
-20
-30
-40
0.00
5.00
10.00
15.00
20.00
Frequency (Hz)

Figure V.83

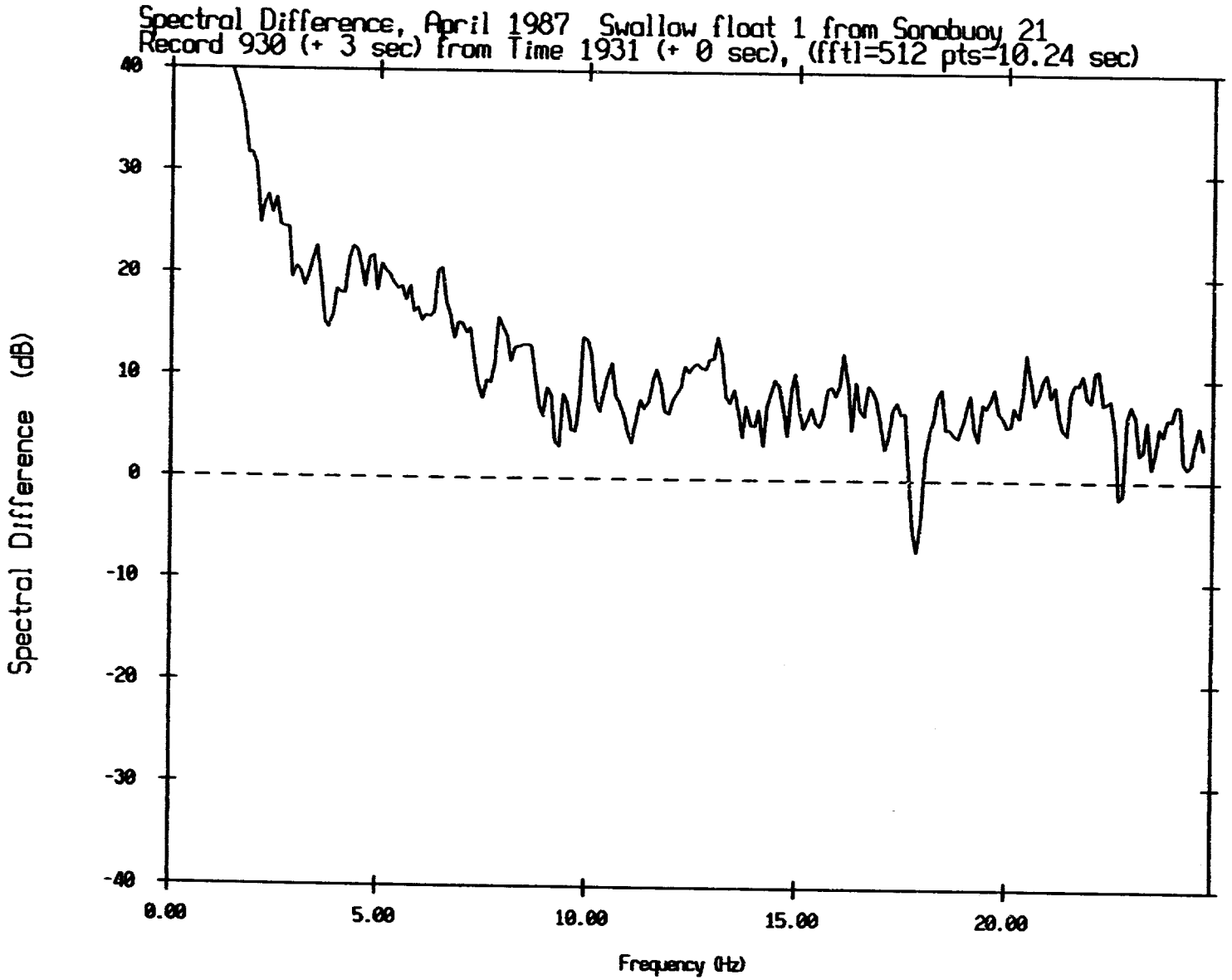
Spectral Difference, April 1987 Swallow float 1 from Sonobuoy 21
Record 930 (+ 3 sec) from Time 1931 (+ 0 sec), (fftl=512 pts=10.24 sec)
Spectral Difference (dB)
40
30
20
10
0
-10
-20
-30
-40
0.00
5.00
10.00
15.00
20.00
Frequency (Hz)

Figure V.84

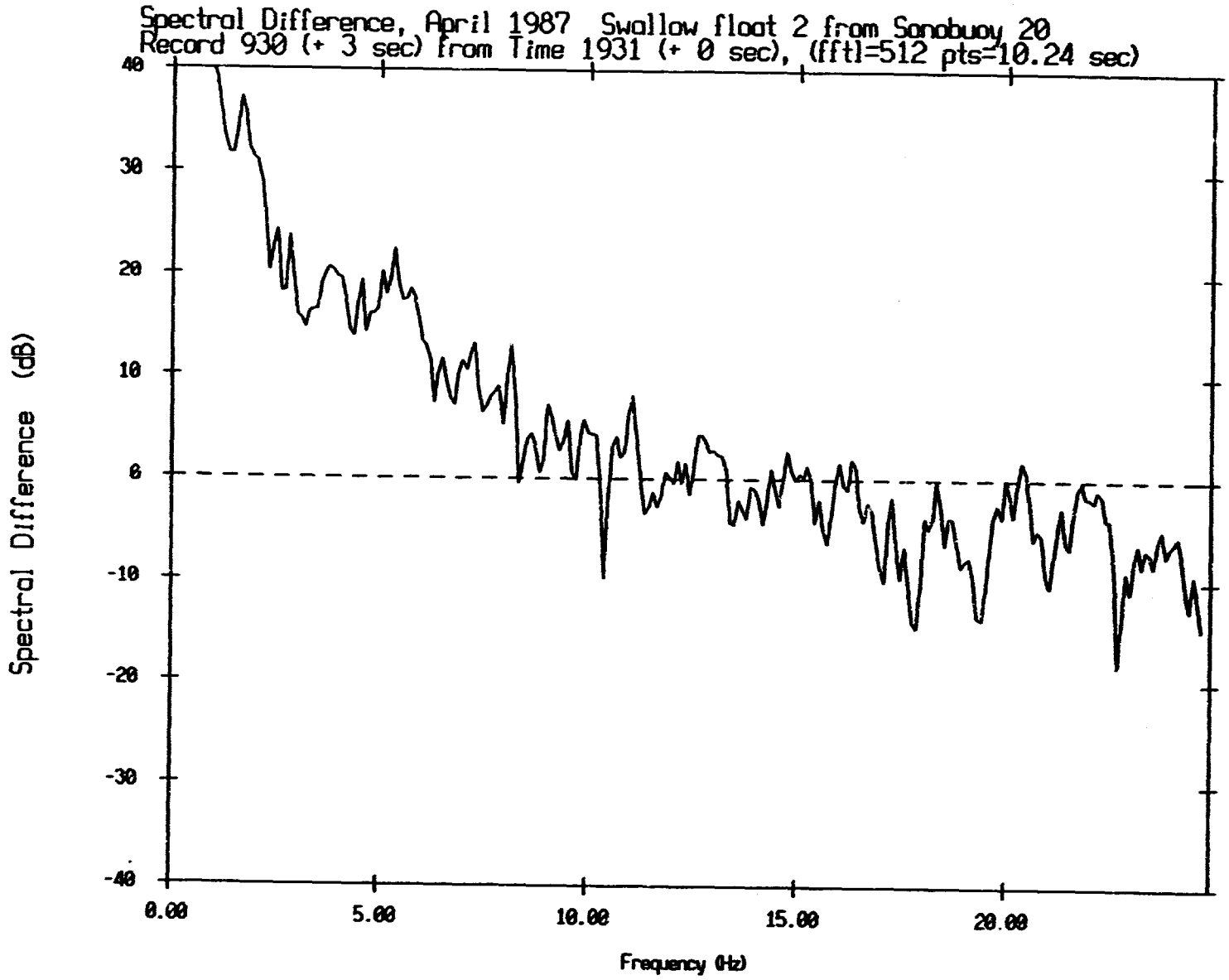
Spectral Difference, April 1987 Swallow float 2 from Sonobuoy 20
Record 930 (+ 3 sec) from Time 1931 (+ 0 sec), (fftl=512 pts=10.24 sec)
Spectral Difference (dB)
40
30
20
10
0
-10
-20
-30
-40
0.00
5.00
10.00
15.00
20.00
Frequency (Hz)

Figure V.85

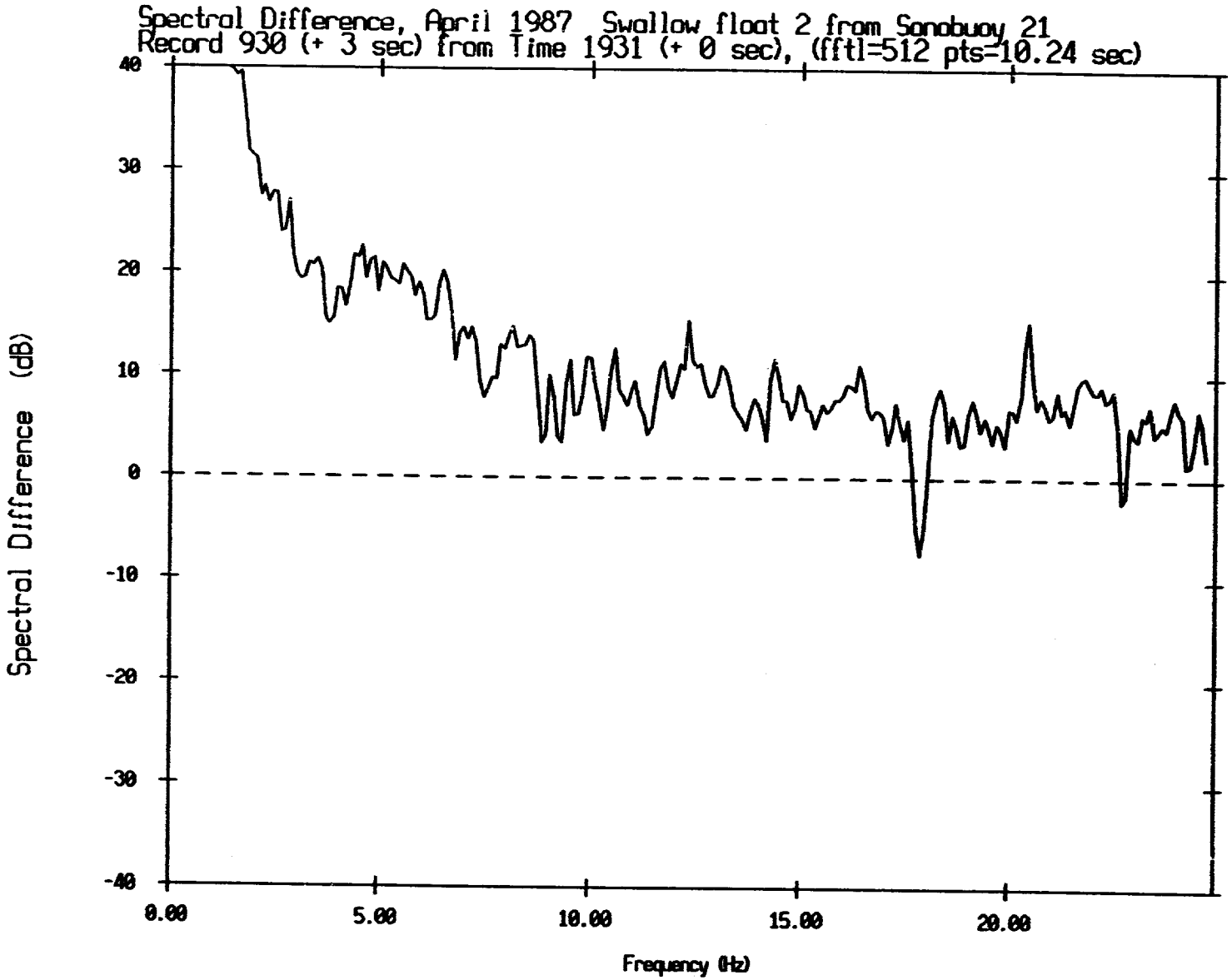
Spectral Difference, April 1987 Swallow float 2 from Sonobuoy 21
Record 930 (+ 3 sec) from Time 1931 (+ 0 sec), (fftl=512 pts=10.24 sec)
Spectral Difference (dB)
40
30
20
10
0
-10
-20
-30
-40
0.00
5.00
10.00
15.00
20.00
Frequency (Hz)

Figure V.86

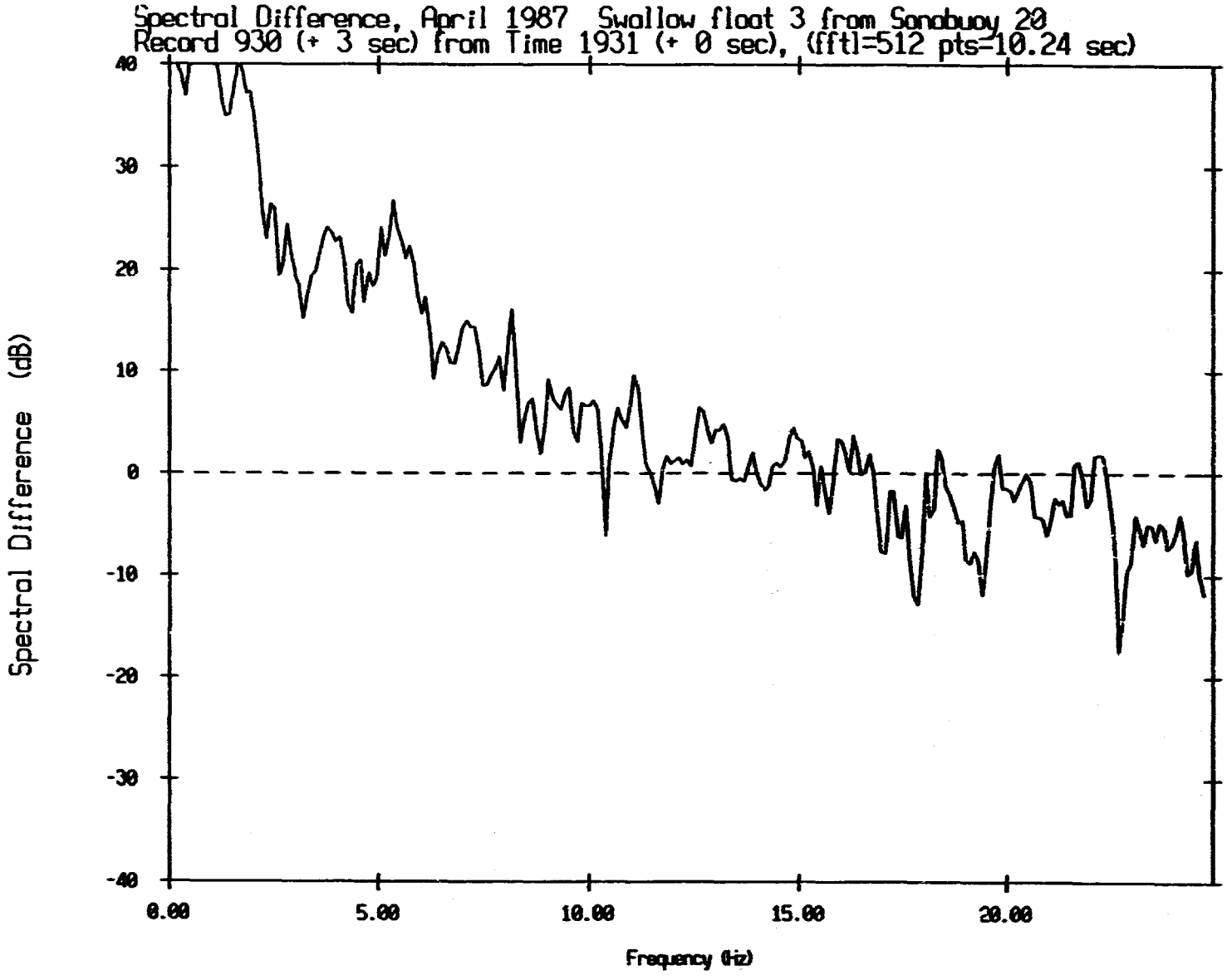
Spectral Difference, April 1987 Swallow float 3 from Sonobuoy 20
Record 930 (+ 3 sec) from Time 1931 (+ 0 sec), (fftl=512 pts=10.24 sec)
Spectral Difference (dB)
40
30
20
10
0
-10
-20
-30
-40
0.00
5.00
10.00
15.00
20.00
Frequency (Hz)

Figure V.87

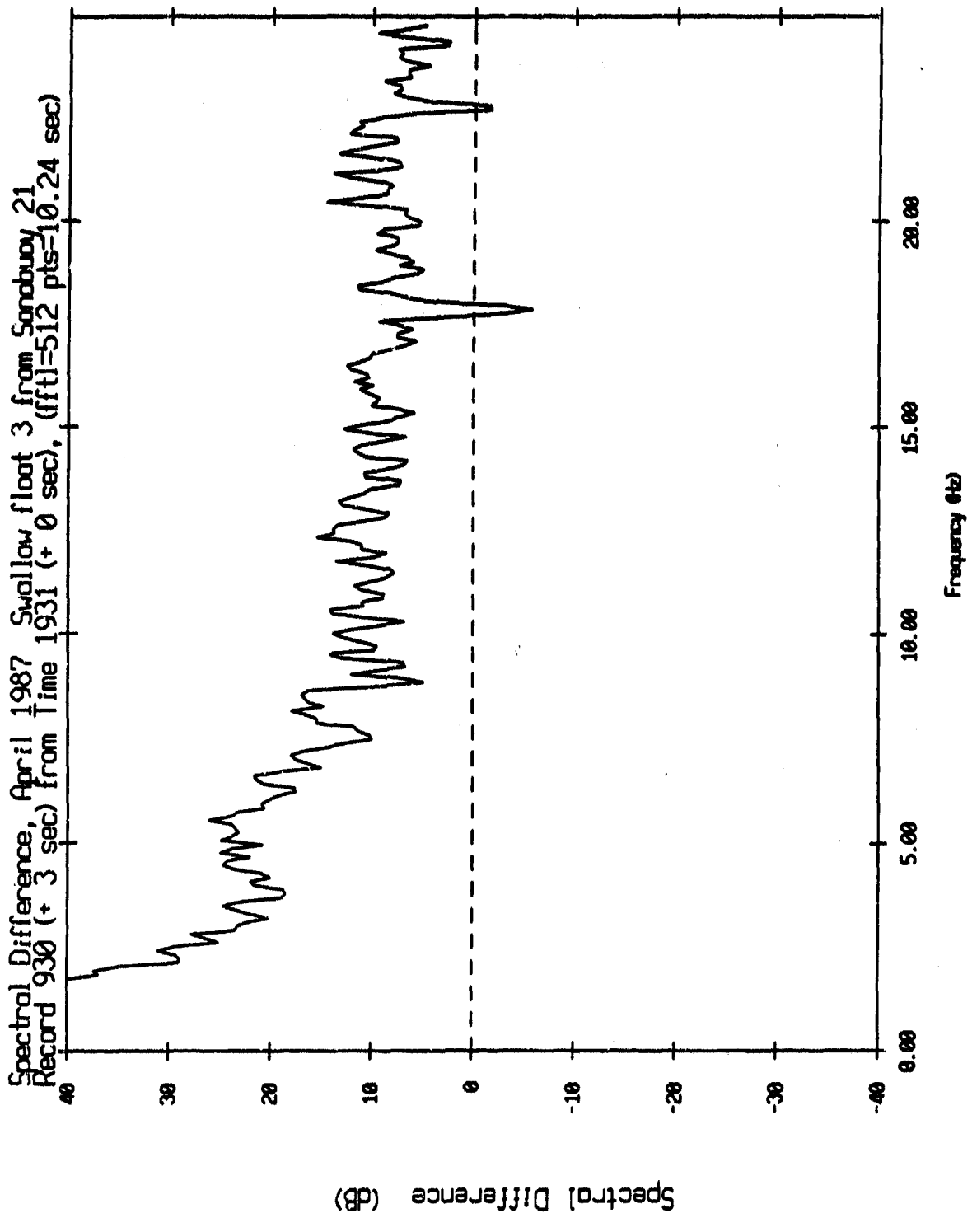
Spectral Difference, April 1987 Swallow float 3 from Sandbuoy 21
Record 930 (+ 3 sec) from Time 1931 (+ 0 sec), (fftl=512 pts=10.24 sec)
40
30
20
10
0
-10
-20
-30
-40
0.00
5.00
10.00
15.00
20.00
Frequency (Hz)
Spectral Difference (dB)

Figure V.88

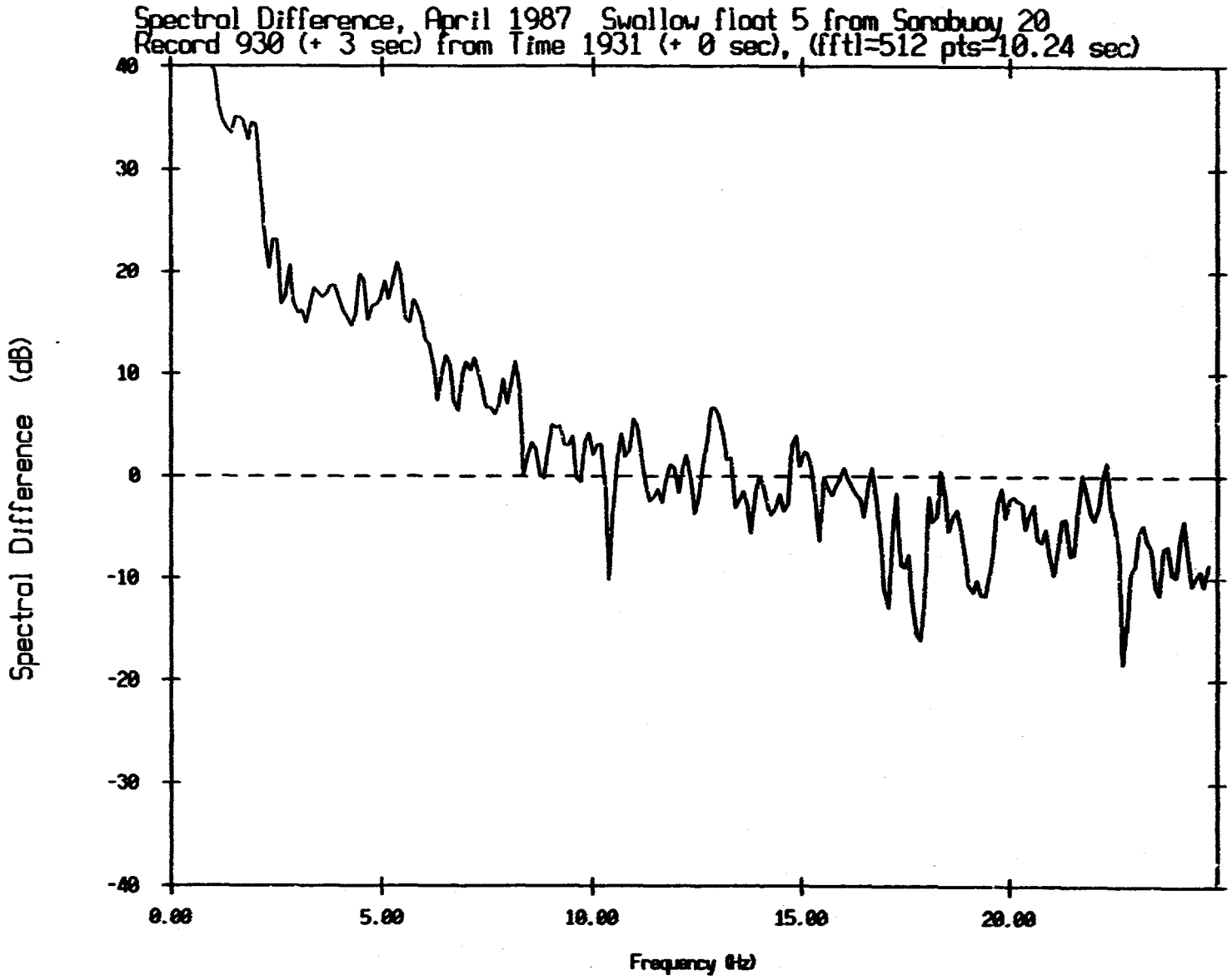
Spectral Difference, April 1987 Swallow float 5 from Sonobuoy 20
Record 930 (+ 3 sec) from Time 1931 (+ 0 sec), (fftl=512 pts=10.24 sec)
Spectral Difference (dB)
40
30
20
10
0
-10
-20
-30
-40
0.00
5.00
10.00
15.00
20.00
Frequency (Hz)

Figure V.80

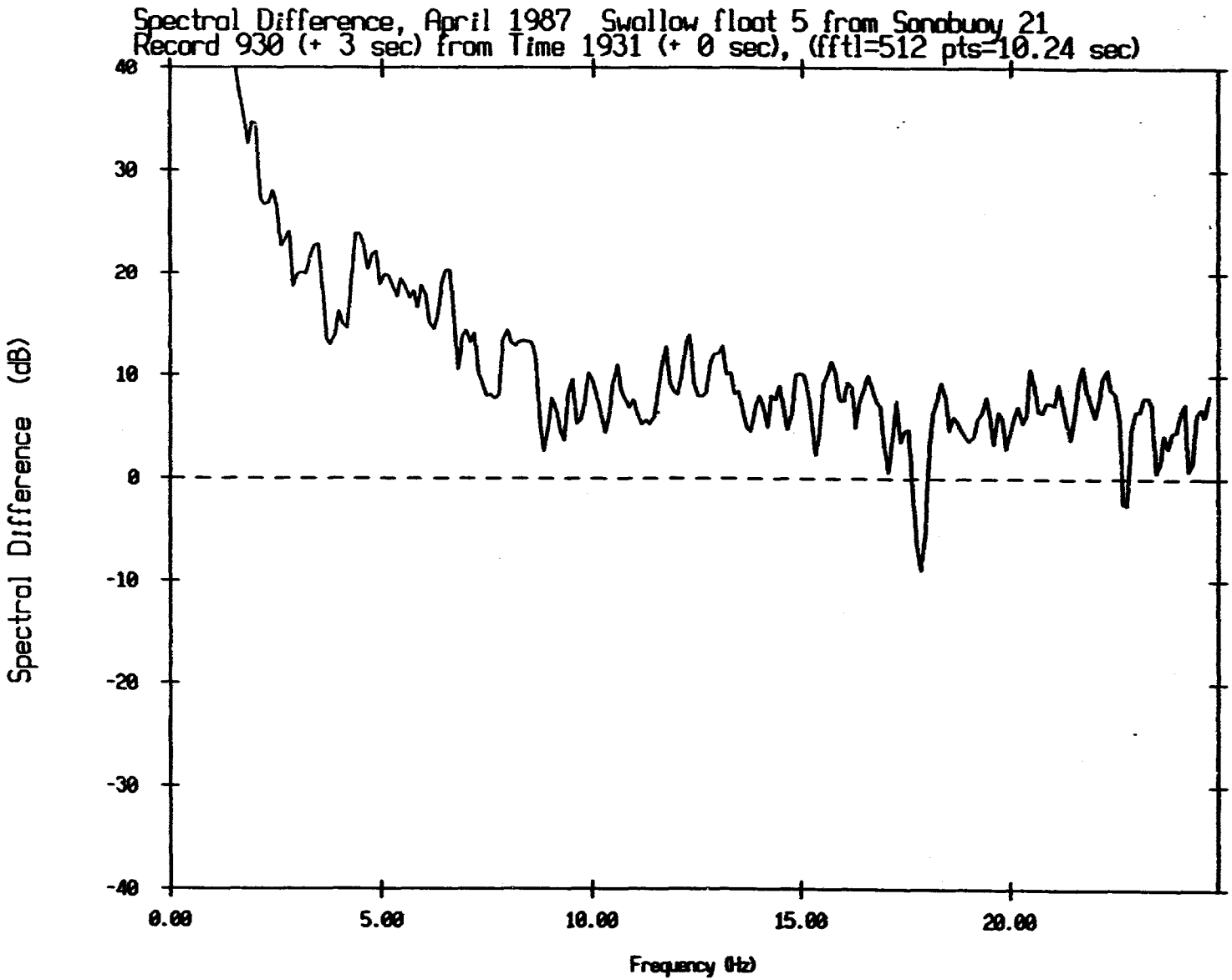
Spectral Difference, April 1987 Swallow float 5 from Sonobuoy 21
Record 930 (+ 3 sec) from Time 1931 (+ 0 sec), (fftl=512 pts=10.24 sec)
Spectral Difference (dB)
40
30
20
10
0
-10
-20
-30
-40
0.00
5.00
10.00
15.00
20.00
Frequency (Hz)

Figure V.90

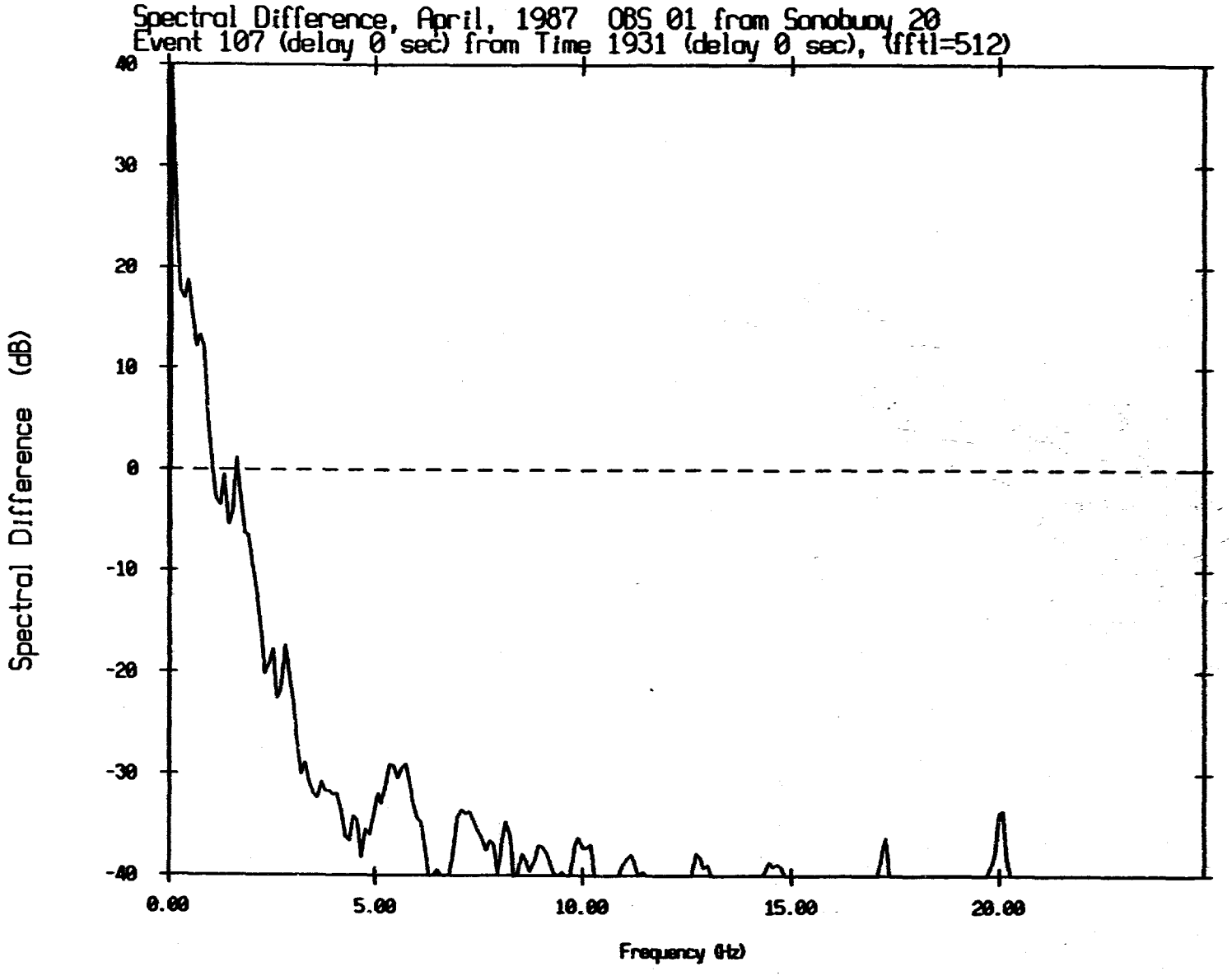
Spectral Difference, April, 1987 OBS 01 from Sonobuoy 20
Event 107 (delay 0 sec) from Time 1931 (delay 0 sec), (fftl=512)
Spectral Difference (dB)
40
30
20
10
0
-10
-20
-30
-40
0.00
5.00
10.00
15.00
20.00
Frequency (Hz)

Figure V.01

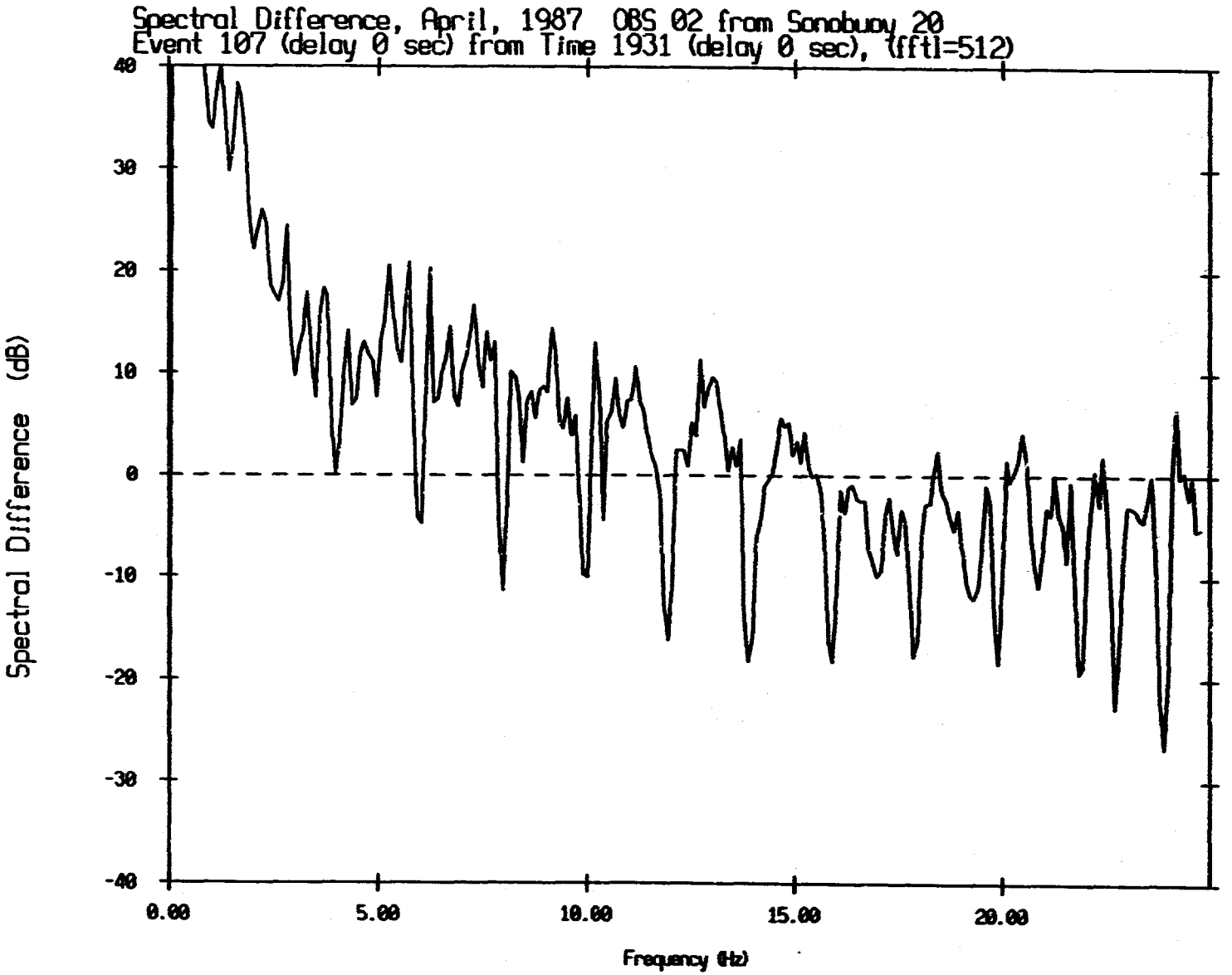
Spectral Difference, April, 1987 OBS 02 from Sonobuoy 20
Event 107 (delay 0 sec) from Time 1931 (delay 0 sec), (fftl=512)
Spectral Difference (dB)
40
30
20
10
0
-10
-20
-30
-40
0.00
5.00
10.00
15.00
20.00
Frequency (Hz)

Figure V.92

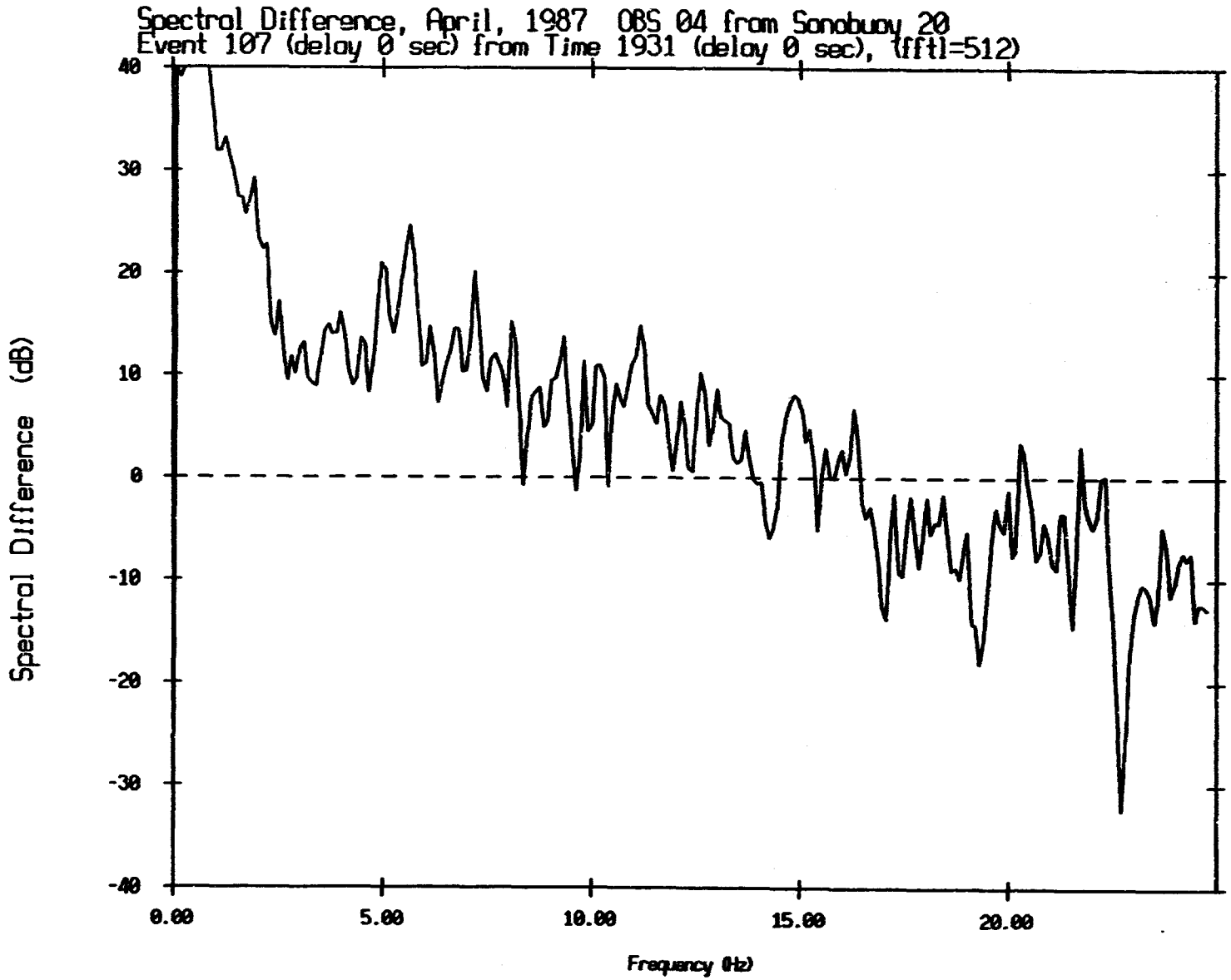
Spectral Difference, April, 1987 OBS 04 from Sonobuoy 20
Event 107 (delay 0 sec) from Time 1931 (delay 0 sec), (fftl=512)
Spectral Difference (dB)
40
30
20
10
0
-10
-20
-30
-40
0.00
5.00
10.00
15.00
20.00
Frequency (Hz)

Figure V.93

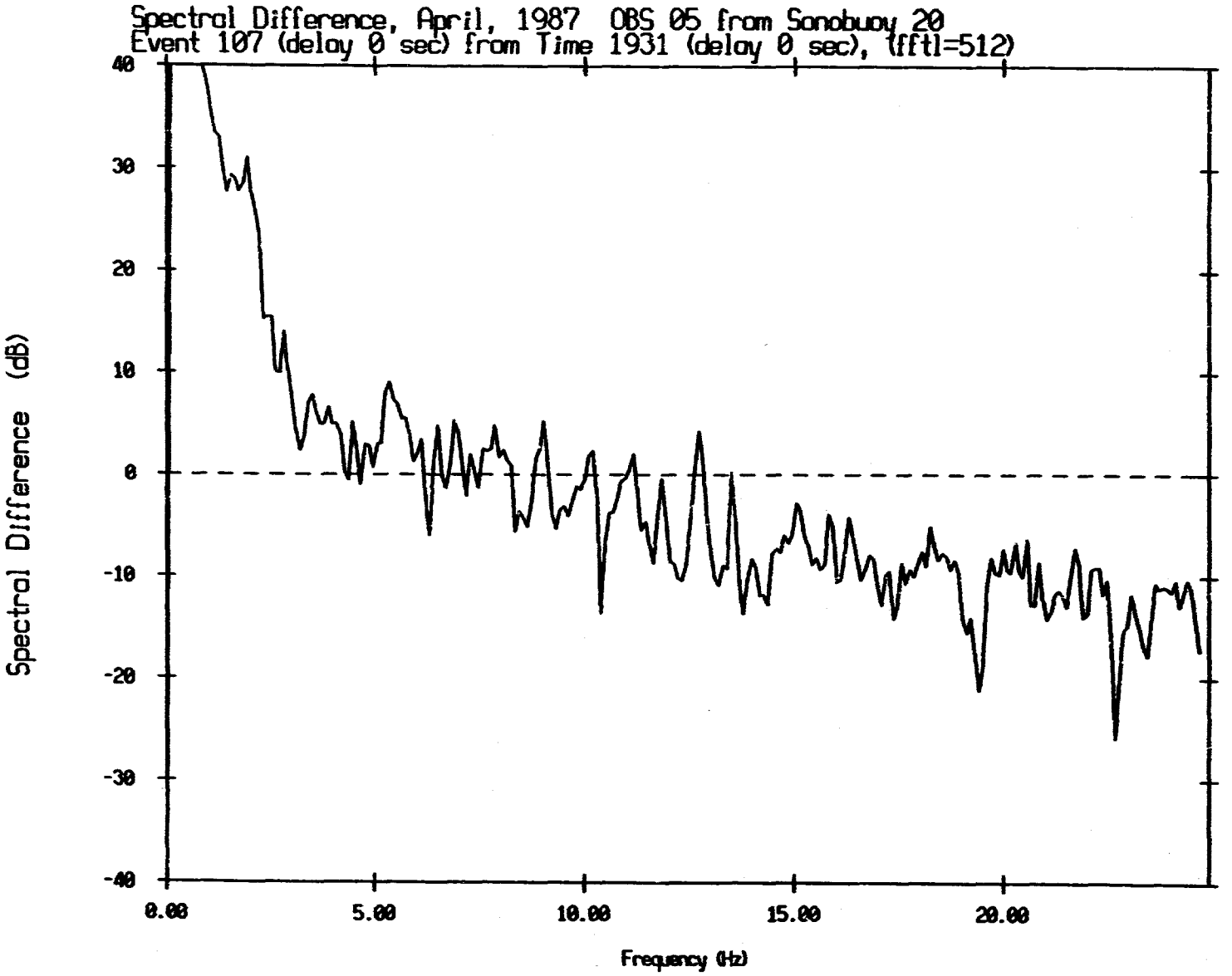
Spectral Difference, April, 1987 OBS 05 from Sonobuoy 20
Event 107 (delay 0 sec) from Time 1931 (delay 0 sec), (fftl=512)
Spectral Difference (dB)
40
30
20
10
0
-10
-20
-30
-40
0.00
5.00
10.00
15.00
20.00
Frequency (Hz)

Figure V.04

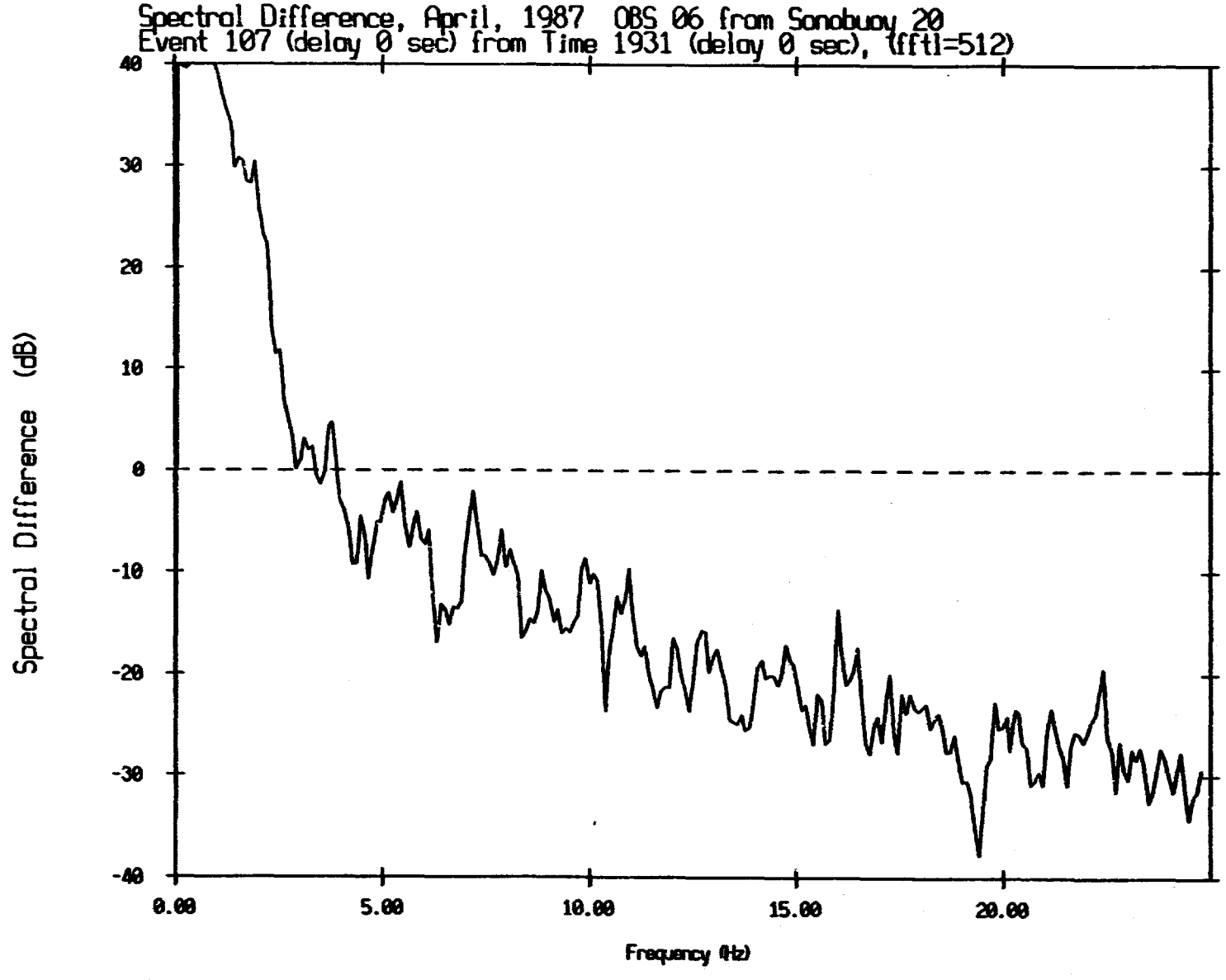
Spectrol Difference, April, 1987 OBS 06 from Sonobuoy 20
Event 107 (delay 0 sec) from Time 1931 (delay 0 sec), (fftl=512)
Spectrol Difference (dB)
40
30
20
10
0
-10
-20
-30
-40
0.00
5.00
10.00
15.00
20.00
Frequency (Hz)

Figure V.35

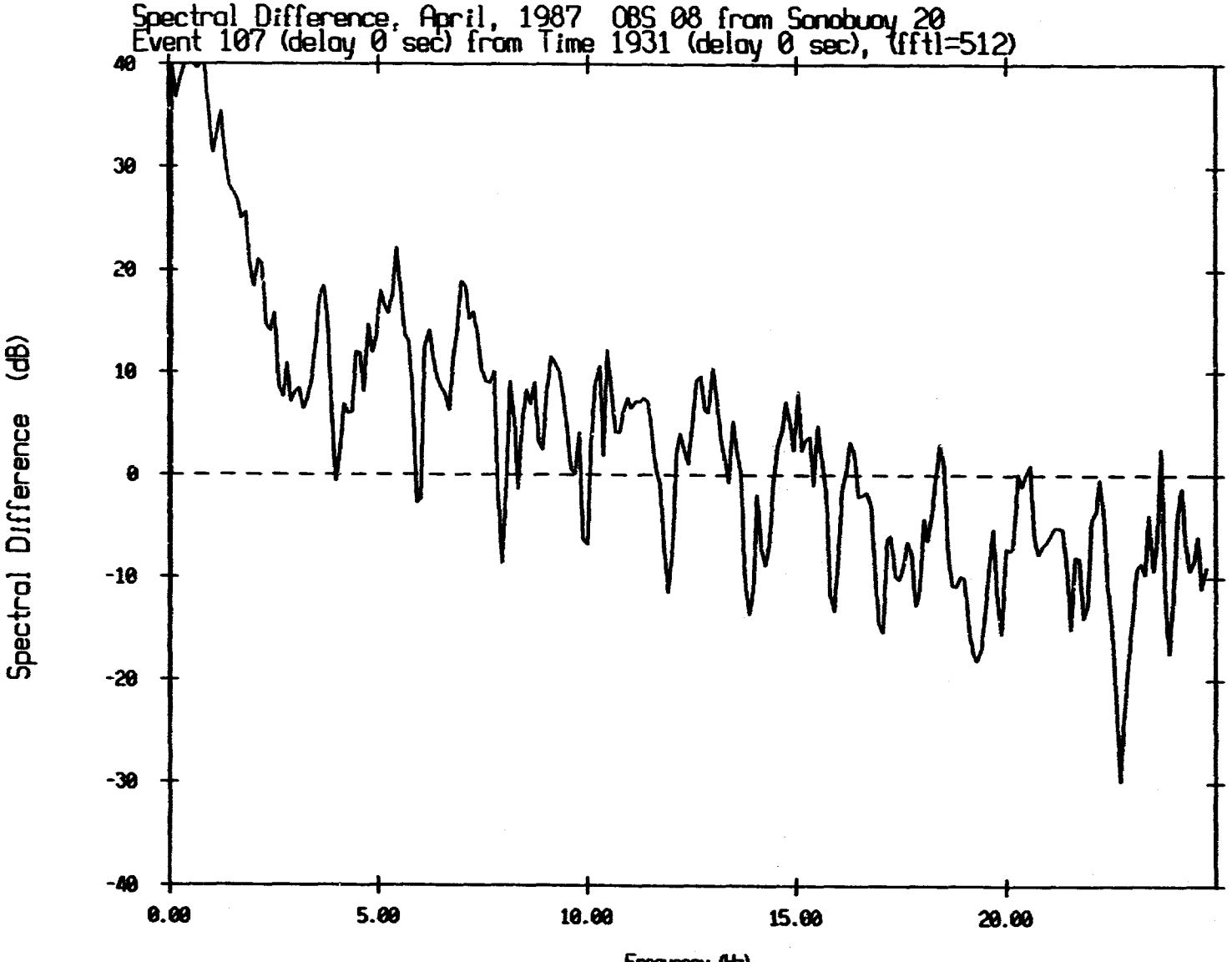
Spectral Difference, April, 1987 OBS 08 from Sonobuoy 20
Event 107 (delay 0 sec) from Time 1931 (delay 0 sec), (fftl=512)
Spectral Difference (dB)
40
30
20
10
0
-10
-20
-30
-40
0.00
5.00
10.00
15.00
20.00
Frequency (Hz)

Figure V.96

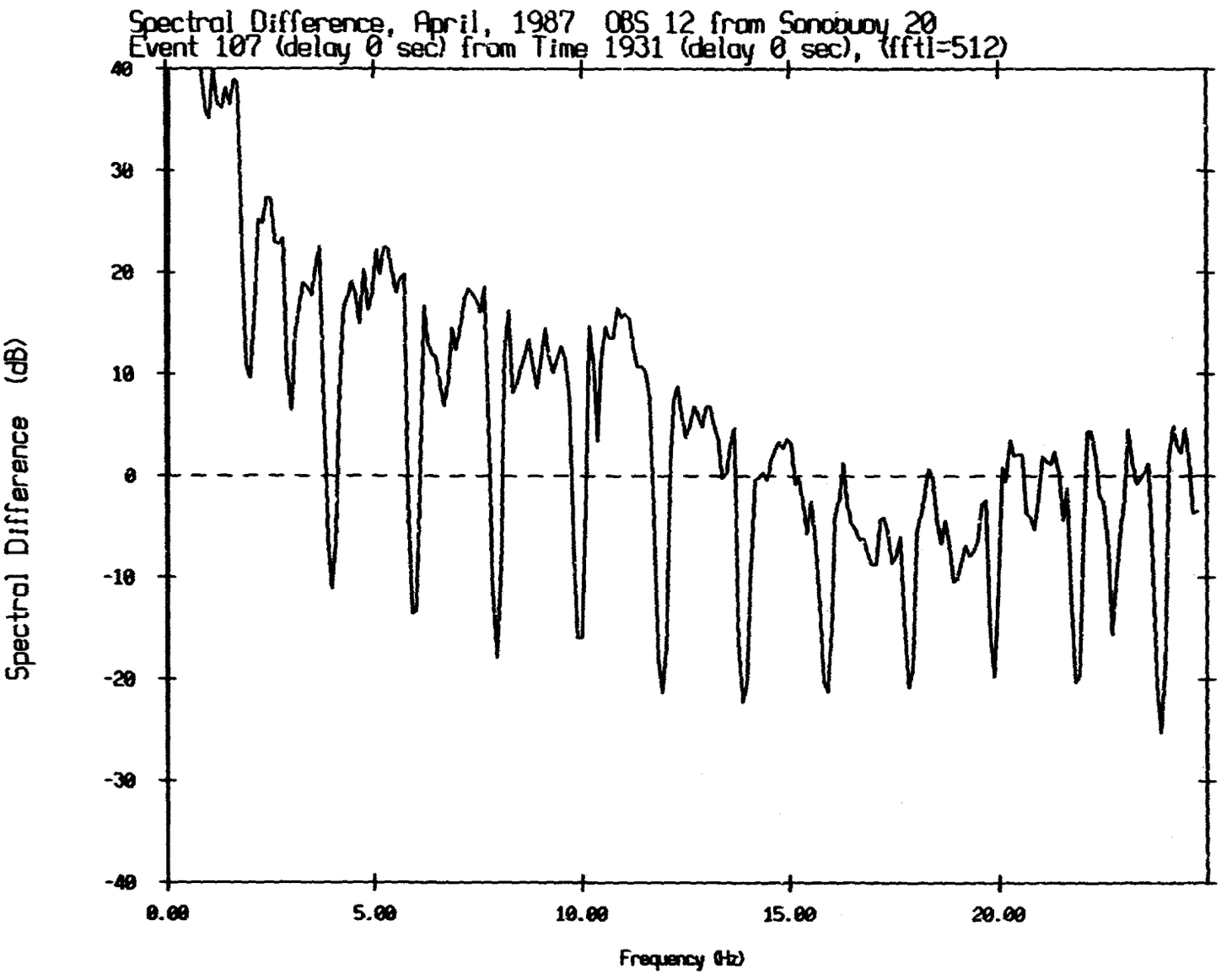
Spectral Difference, April, 1987 OBS 12 from Sonobuoy 20
Event 107 (delay 0 sec) from Time 1931 (delay 0 sec), (fftl=512)
Spectral Difference (dB)
40
30
20
10
0
-10
-20
-30
-40
0.00
5.00
10.00
15.00
20.00
Frequency (Hz)

Figure V.97

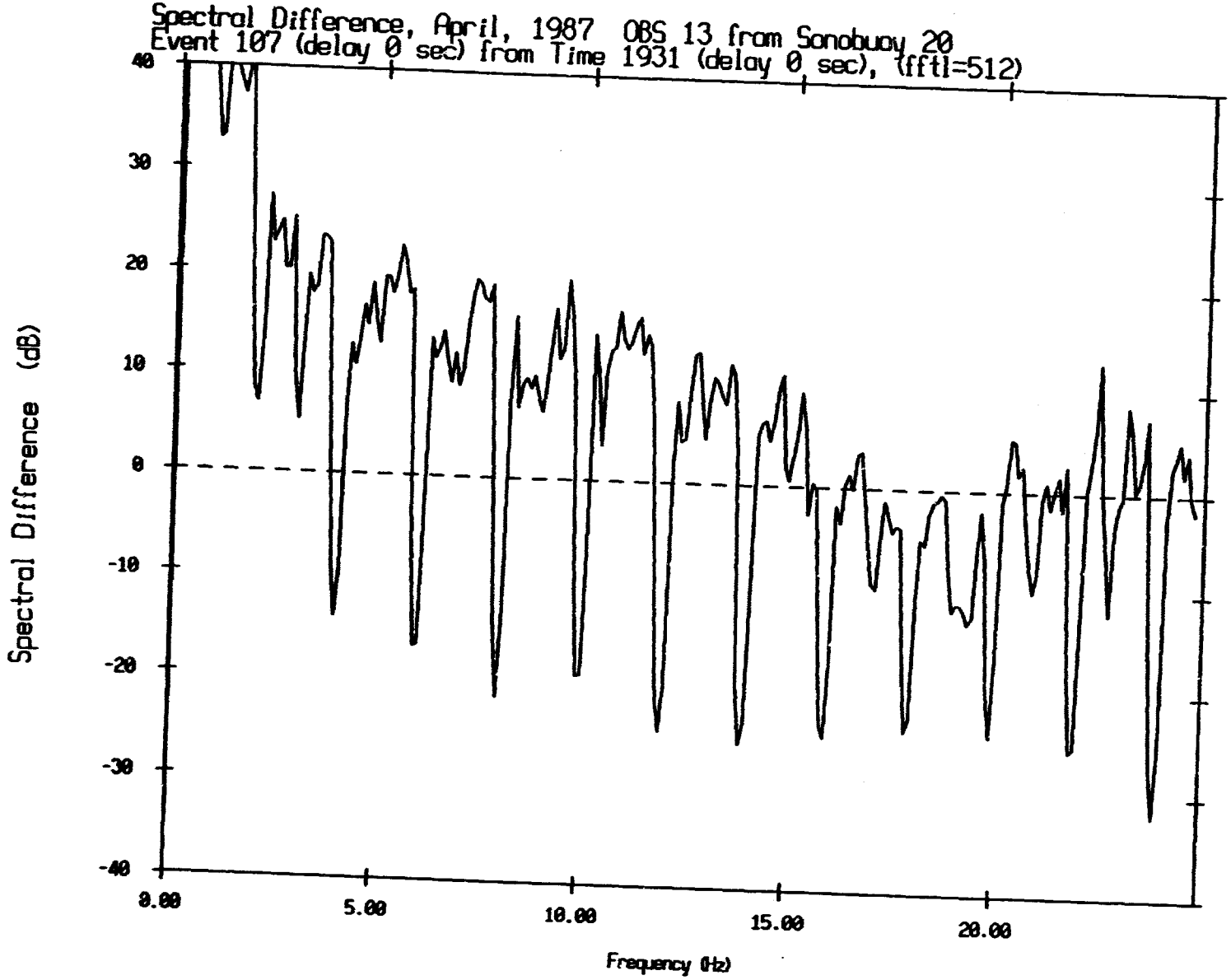
Spectral Difference, April, 1987 OBS 13 from Sonobuoy 20
Event 107 (delay 0 sec) from Time 1931 (delay 0 sec), (fftl=512)
Spectral Difference (dB)
40
30
20
10
0
-10
-20
-30
-40
0.00
5.00
10.00
15.00
20.00
Frequency (Hz)

Figure V.38

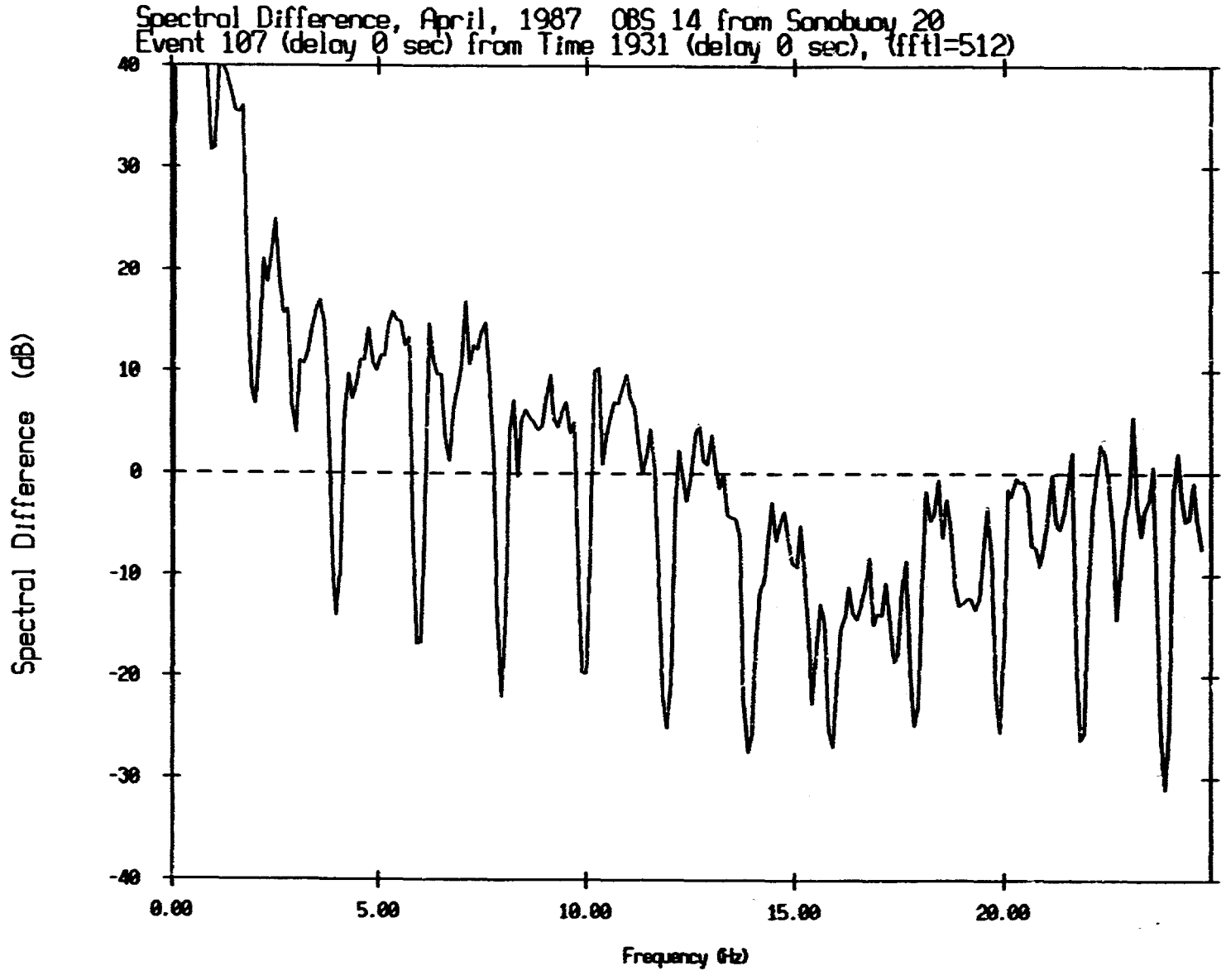
Spectral Difference, April, 1987 OBS 14 from Sonobuoy 20
Event 107 (delay 0 sec) from Time 1931 (delay 0 sec), (fftl=512)
Spectral Difference (dB)
40
30
20
10
0
-10
-20
-30
-40
0.00
5.00
10.00
15.00
20.00
Frequency (Hz)

Figure V.38

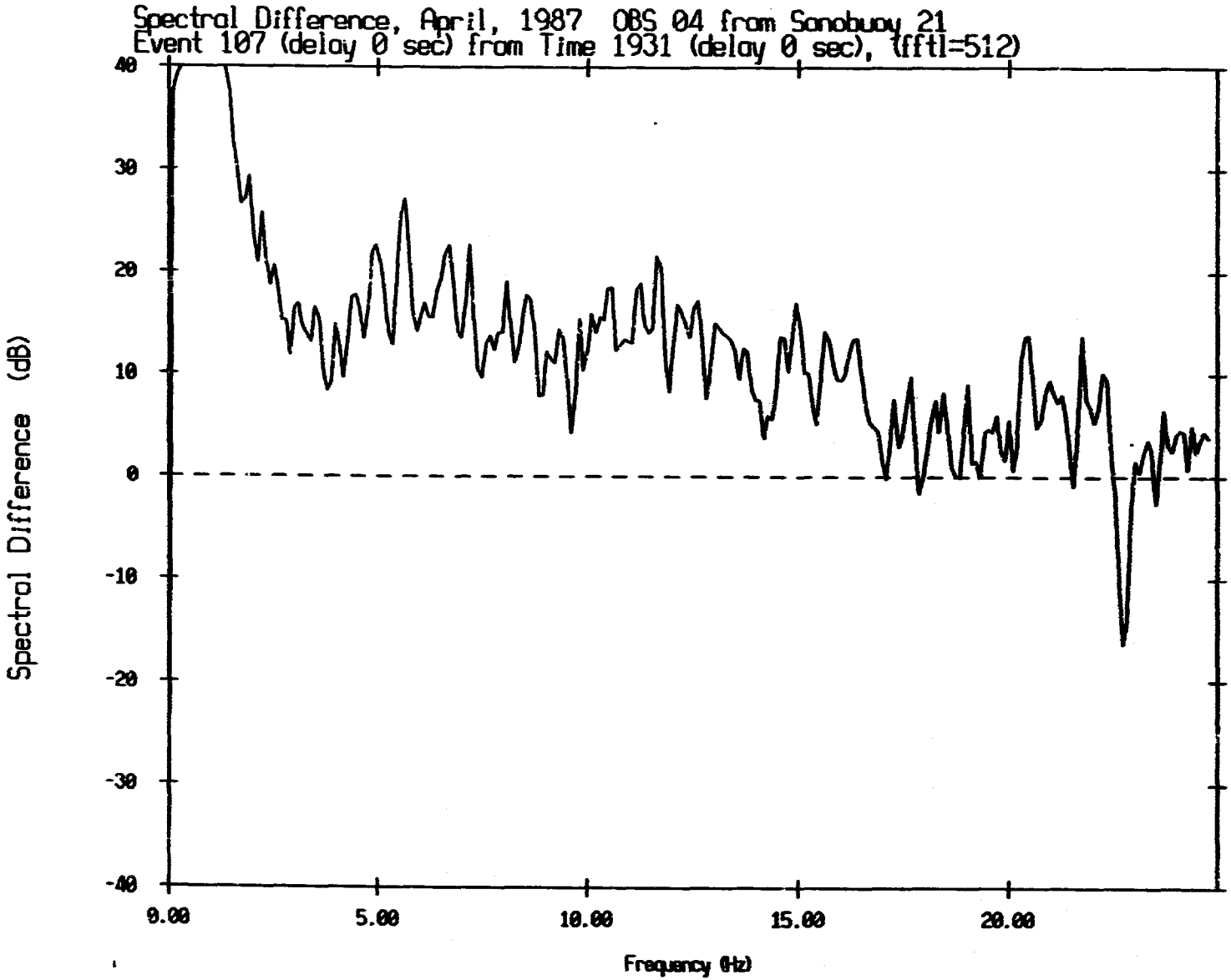
Spectral Difference, April, 1987 OBS 04 from Sonobuoy 21
Event 107 (delay 0 sec) from Time 1931 (delay 0 sec), fftl=512
Spectral Difference (dB)
40
30
20
10
0
-10
-20
-30
-40
0.00
5.00
10.00
15.00
20.00
Frequency (Hz)

Figure V.100

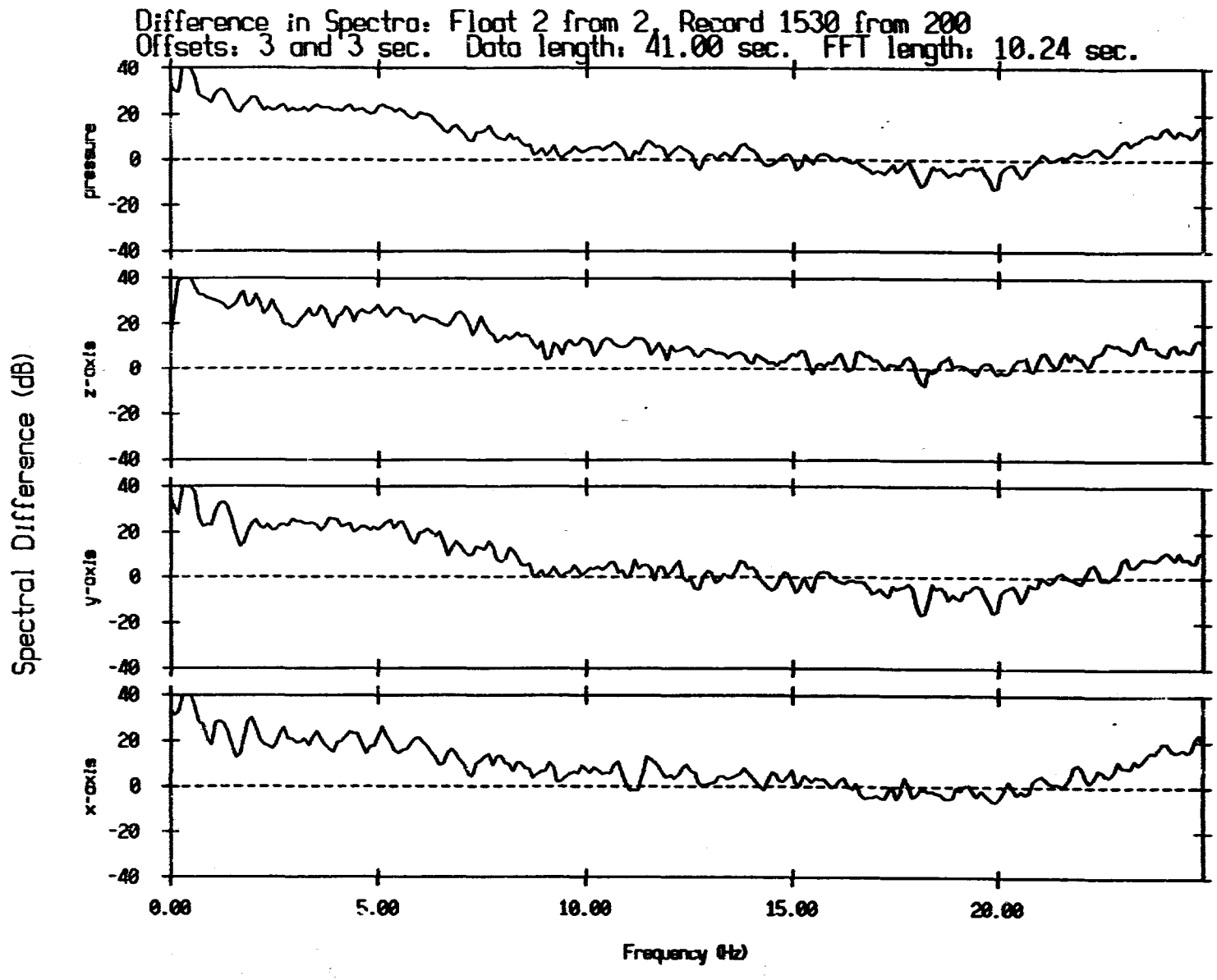
Difference in Spectra: Float 2 from 2, Record 1530 from 200
Offsets: 3 and 3 sec. Data length: 41.00 sec. FFT length: 10.24 sec.
Spectral Difference (dB)
pressure
z-axis
y-axis
x-axis
40
20
0
-20
-40
0.00
5.00
10.00
15.00
20.00
Frequency (Hz)

Figure V.101

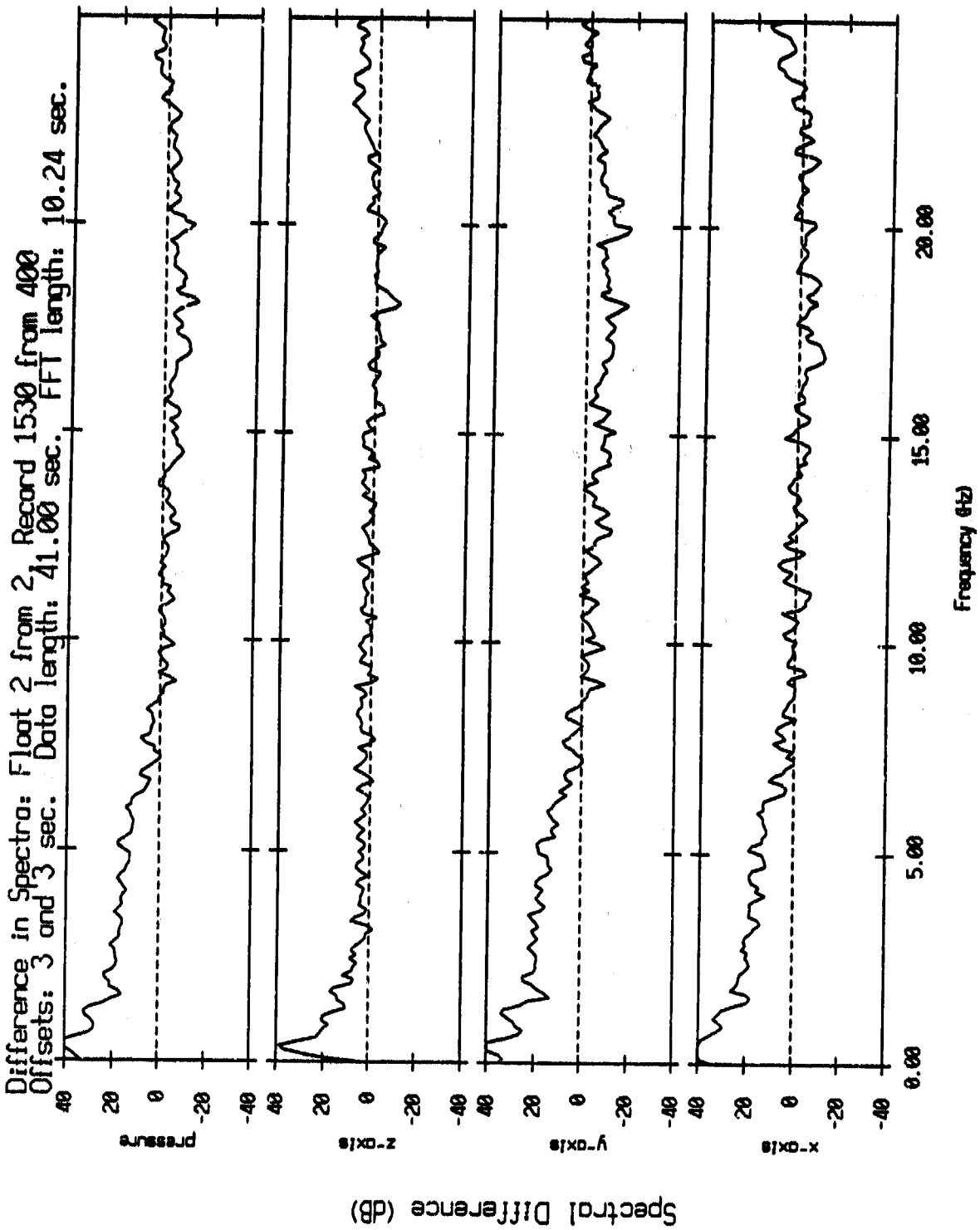
Difference in Spectra: Float 2 from 2, Record 1530 from 400
Offsets: 3 and 3 sec. Data length: 41.00 sec. FFT length: 10.24 sec.
pressure
z-axis
y-axis
x-axis
40
20
0
-20
-40
0.00
5.00
10.00
15.00
20.00
Frequency (Hz)
Spectral Difference (dB)

Figure V.102

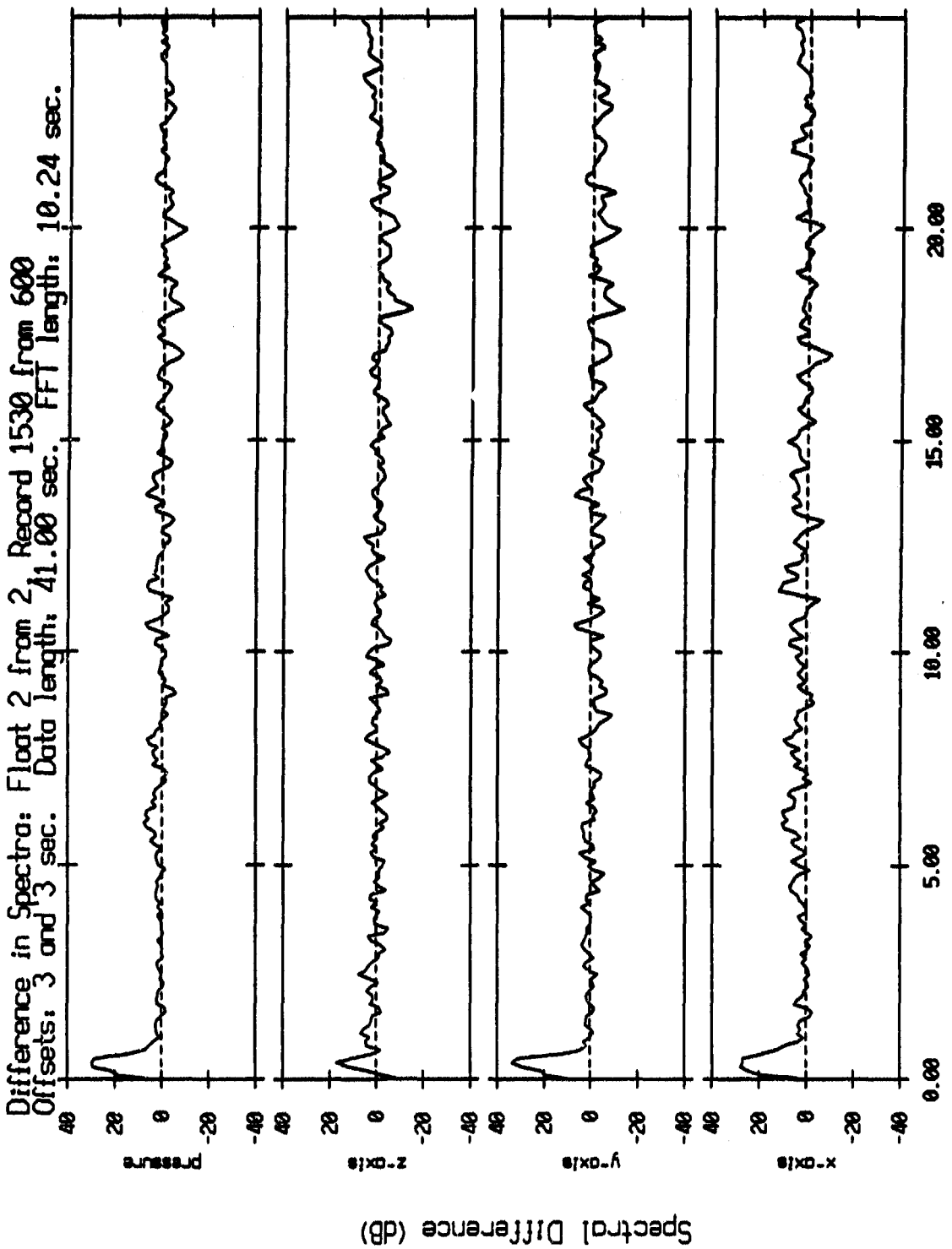
Difference in Spectra: Float 2 from 2, Record 1530 from 600
Offsets: 3 and 3 sec. Data length: 41.00 sec. FFT length: 10.24 sec.
pressure
z-axis
y-axis
x-axis
40
20
0
-20
-40
0.00
5.00
10.00
15.00
20.00
Frequency (Hz)
Spectral Difference (dB)

Figure V.103

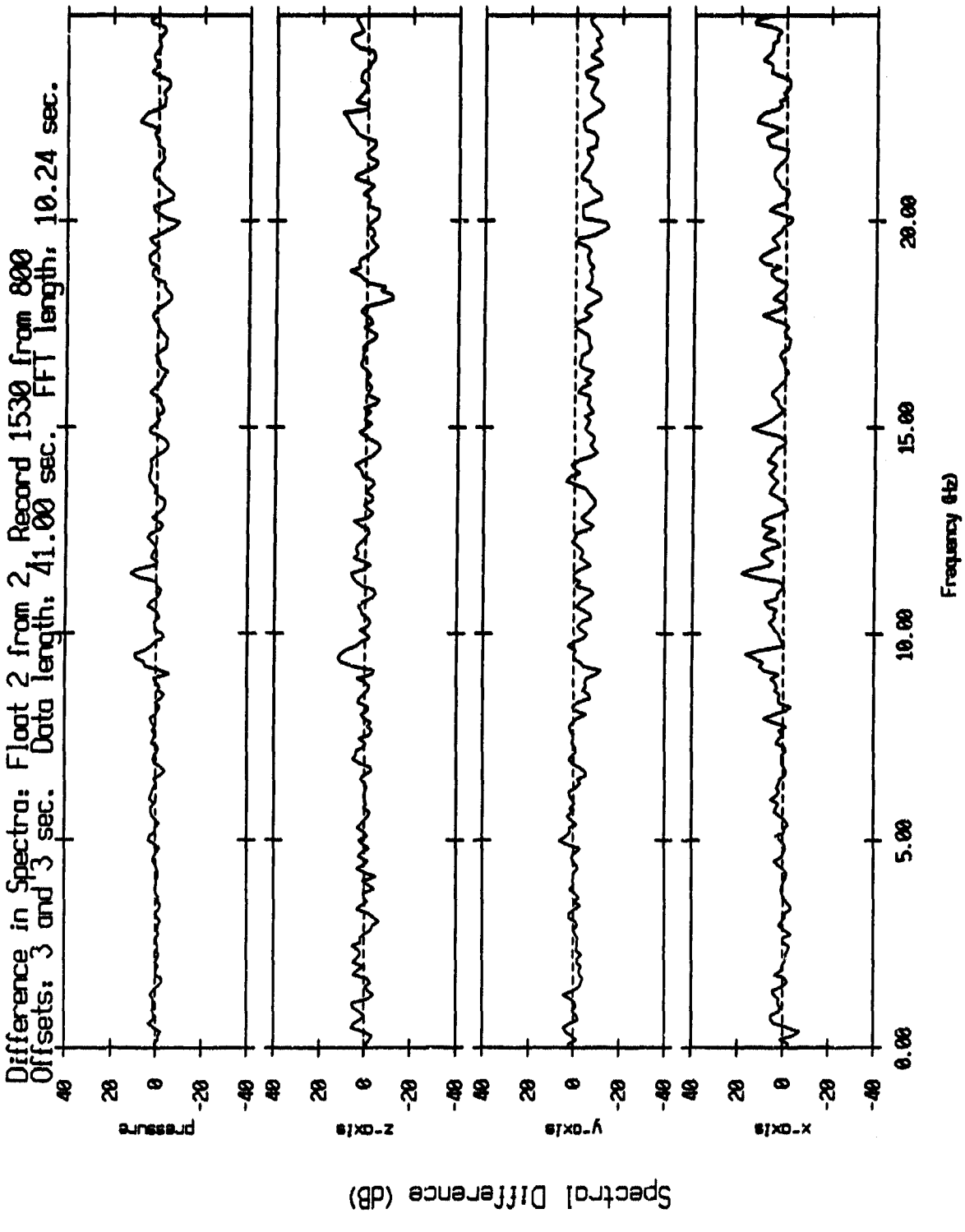
Difference in Spectra: Float 2 from 2, Record 1530 from 800
Offsets: 3 and 3 sec. Data length: 41.00 sec. FFT length: 10.24 sec.
pressure
z-axis
y-axis
x-axis
40
20
0
-20
-40
0.00
5.00
10.00
15.00
20.00
Frequency (Hz)
Spectral Difference (dB)

Figure V.104

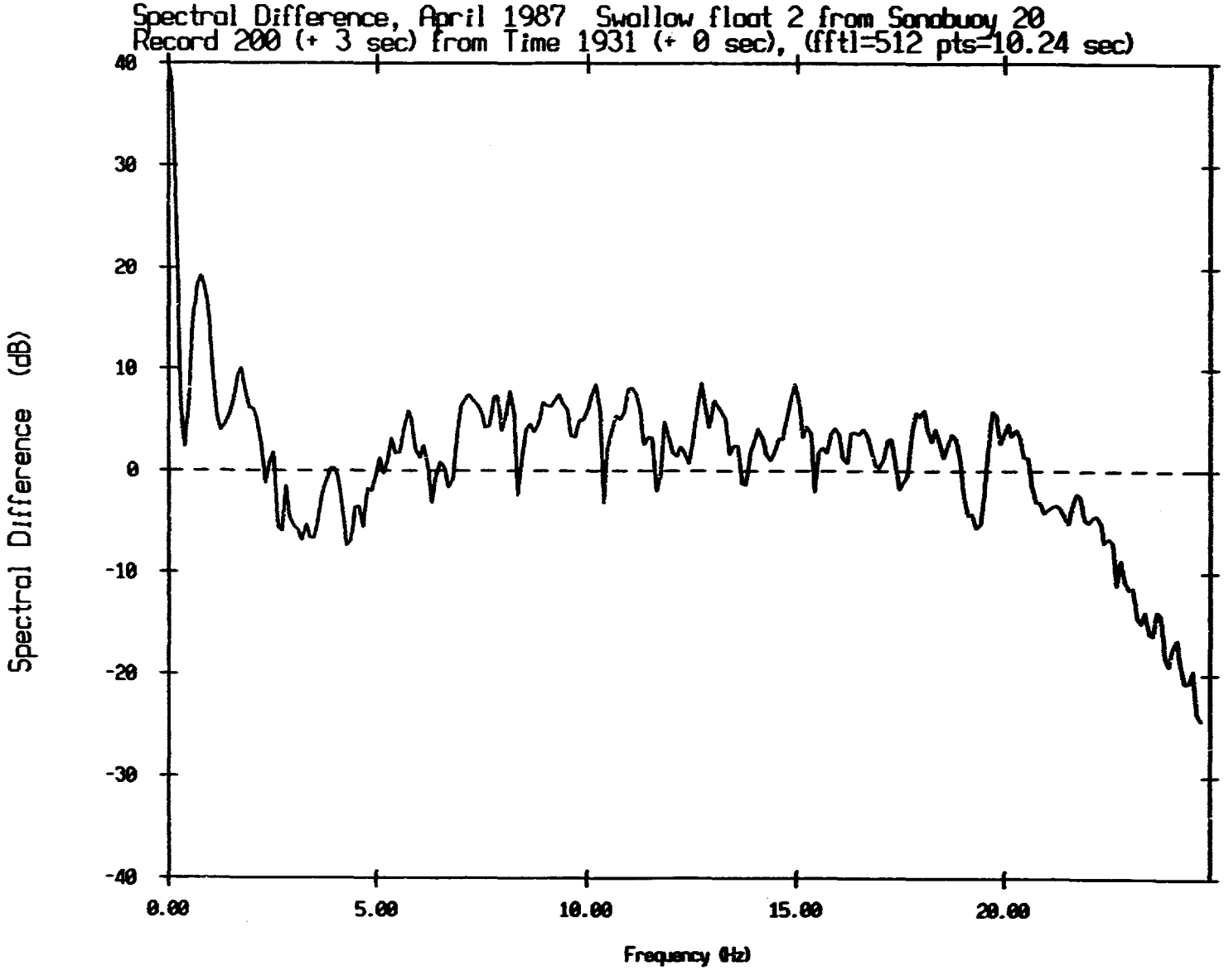
Spectral Difference, April 1987 Swallow float 2 from Sonobuoy 20
Record 200 (+ 3 sec) from Time 1931 (+ 0 sec), (fftl=512 pts=10.24 sec)
Spectral Difference (dB)
40
30
20
10
0
-10
-20
-30
-40
0.00
5.00
10.00
15.00
20.00
Frequency (Hz)

Figure V.105

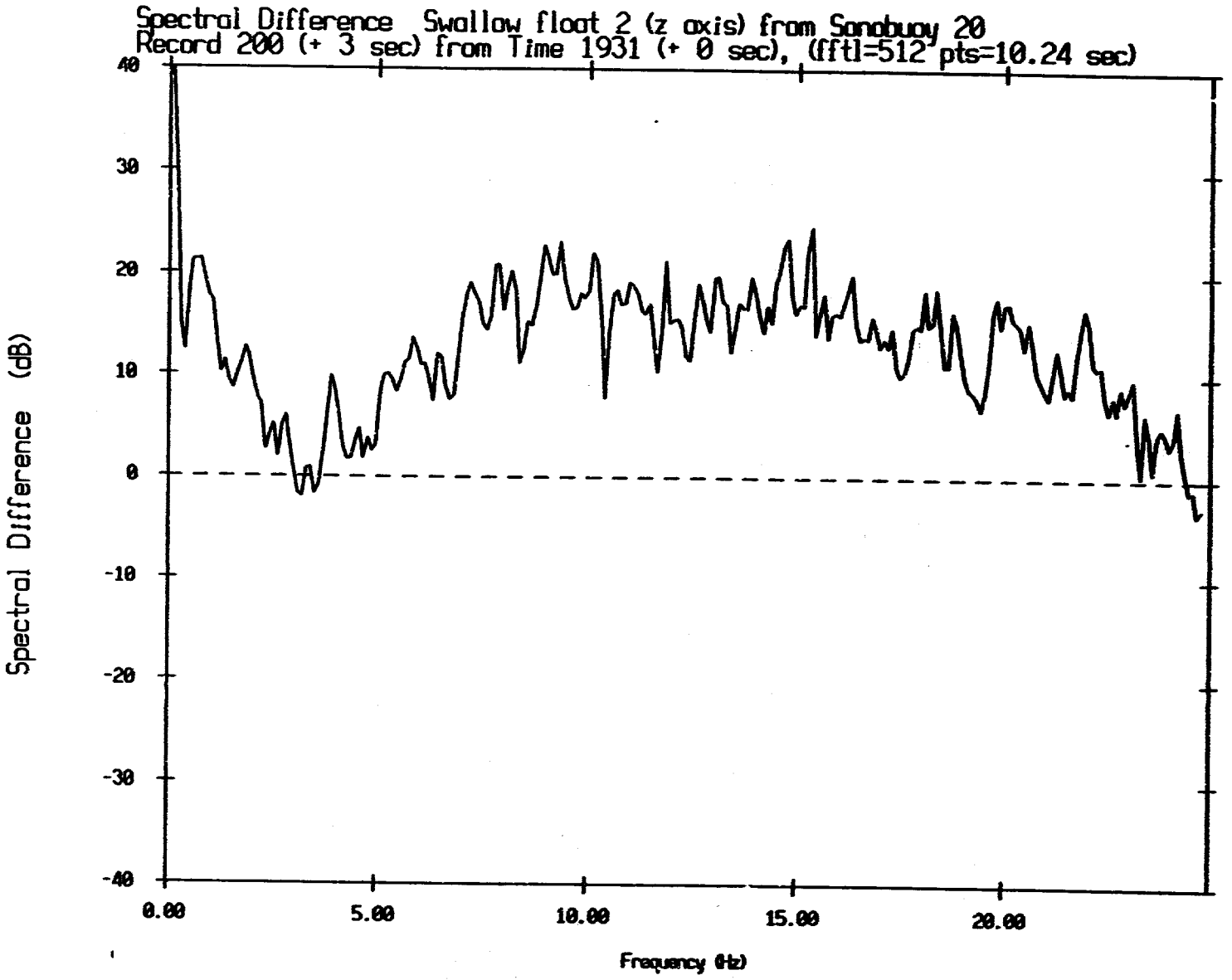
Spectral Difference Swallow float 2 (z axis) from Sonobuoy 20
Record 200 (+ 3 sec) from Time 1931 (+ 0 sec), (fftl=512 pts=10.24 sec)
Spectral Difference (dB)
40
30
20
10
0
-10
-20
-30
-40
0.00
5.00
10.00
15.00
20.00
Frequency (Hz)

Figure V.106

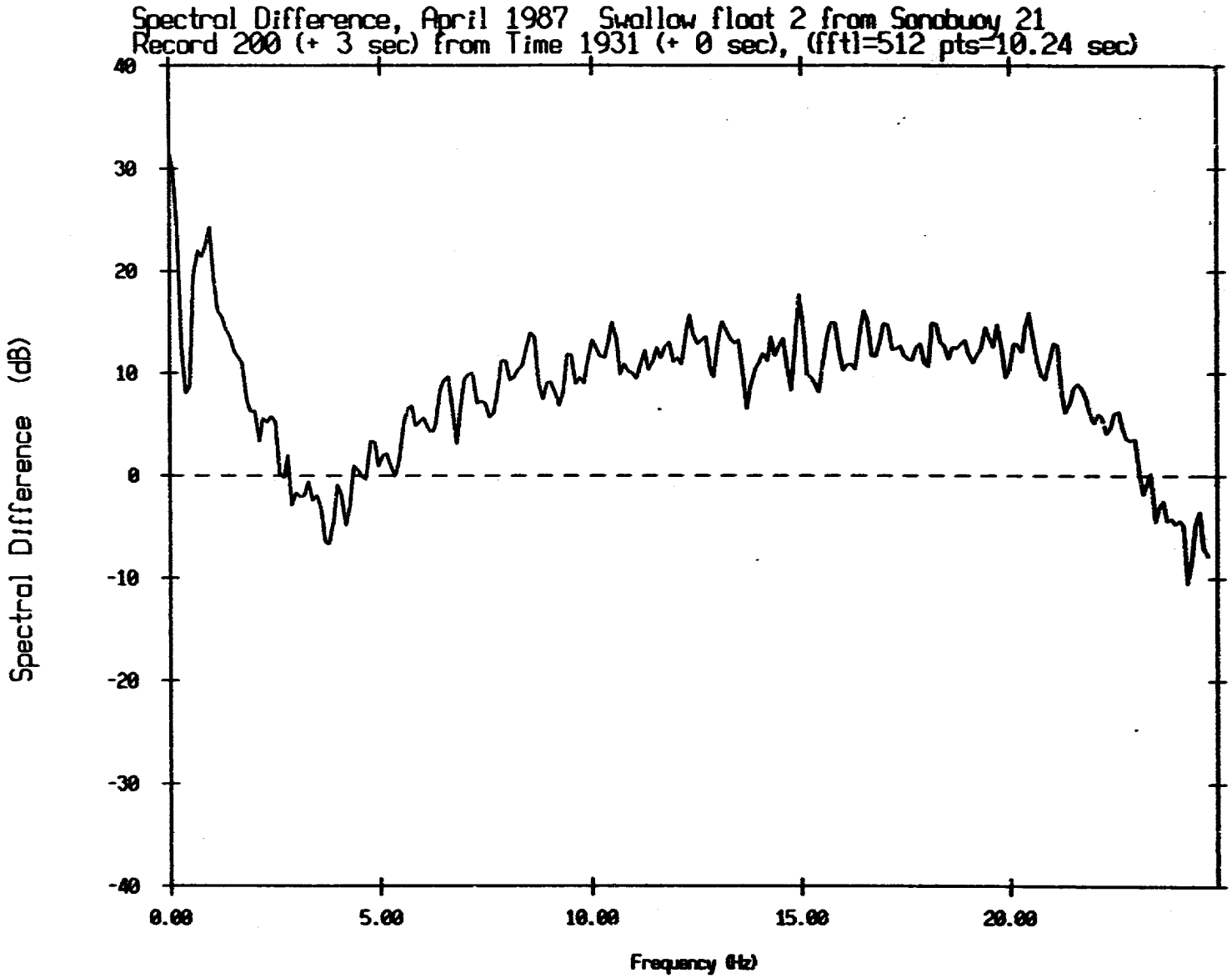
Spectral Difference, April 1987 Swallow float 2 from Sonobuoy 21
Record 200 (+ 3 sec) from Time 1931 (+ 0 sec), (fftl=512 pts=10.24 sec)
Spectral Difference (dB)
40
30
20
10
0
-10
-20
-30
-40
0.00
5.00
10.00
15.00
20.00
Frequency (Hz)

Figure V.107

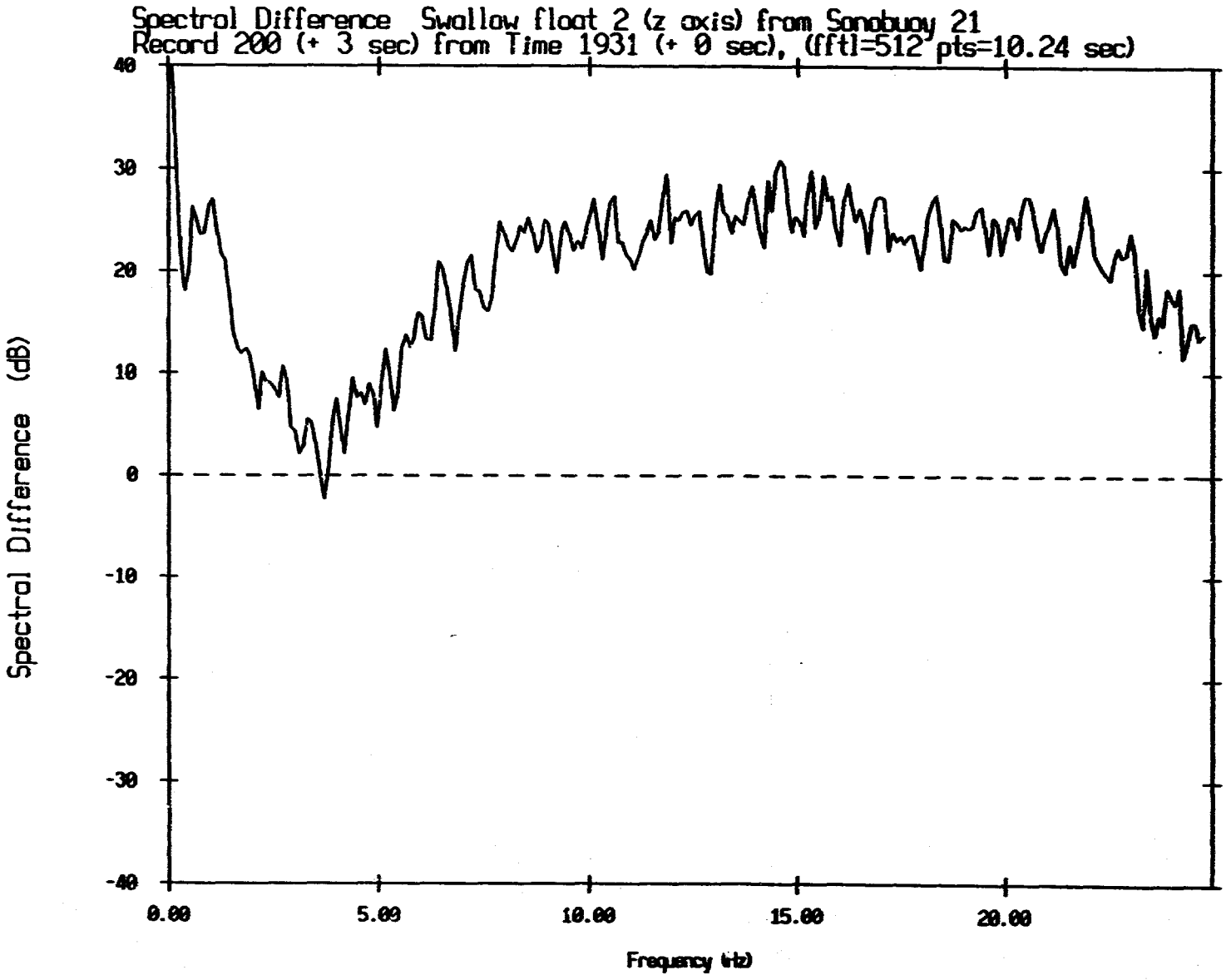
Spectral Difference Swallow float 2 (z axis) from Sonobuoy 21
Record 200 (+ 3 sec) from Time 1931 (+ 0 sec), (fftl=512 pts=10.24 sec)
Spectral Difference (dB)
40
30
20
10
0
-10
-20
-30
-40
0.00
5.00
10.00
15.00
20.00
Frequency (Hz)

Figure V.108

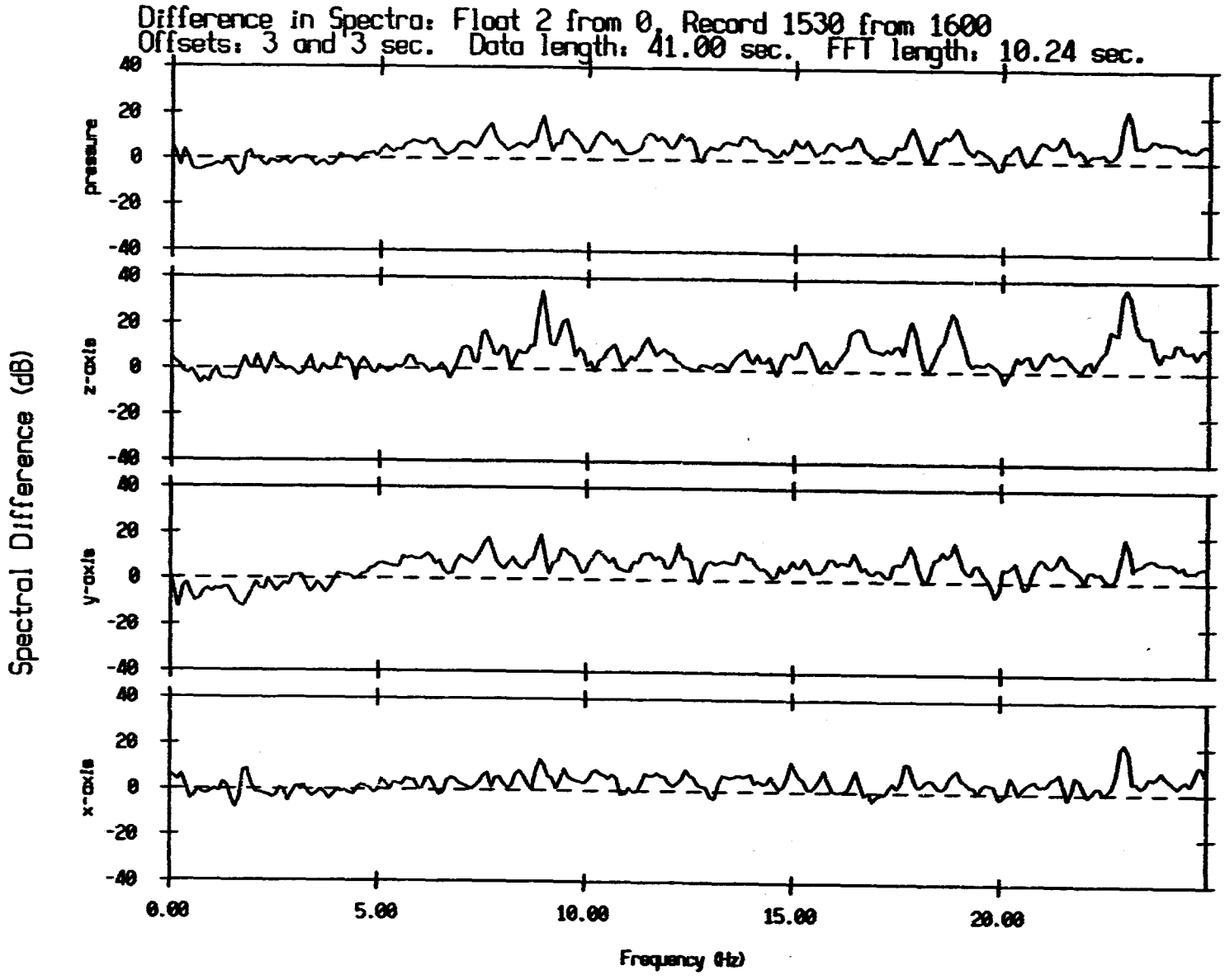
Difference in Spectra: Float 2 from 0, Record 1530 from 1600
Offsets: 3 and 3 sec. Data length: 41.00 sec. FFT length: 10.24 sec.
Spectral Difference (dB)
pressure
z-axis
y-axis
x-axis
40
20
0
-20
-40
0.00
5.00
10.00
15.00
20.00
Frequency (Hz)

Figure V.109

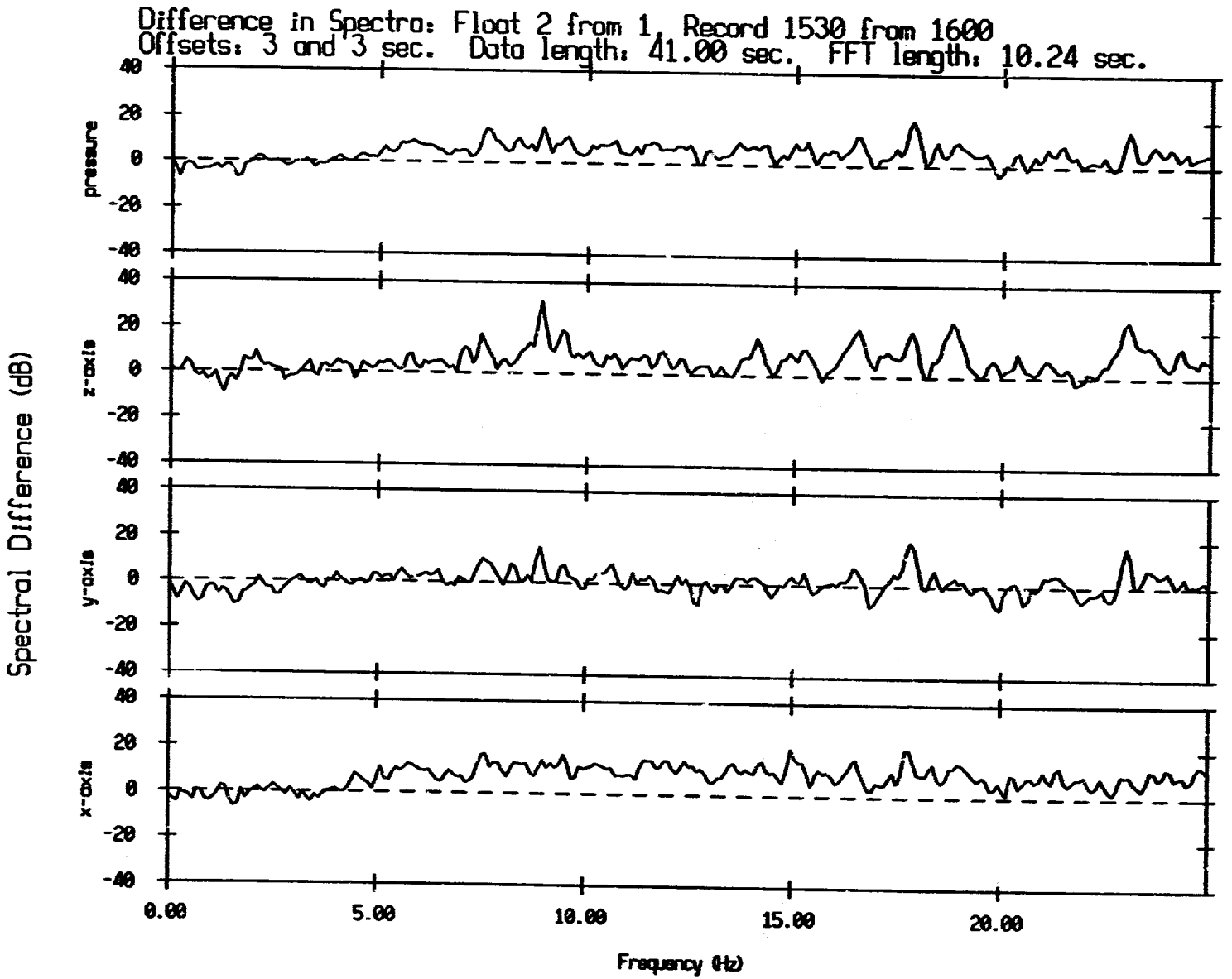
Difference in Spectra: Float 2 from 1, Record 1530 from 1600
Offsets: 3 and 3 sec. Data length: 41.00 sec. FFT length: 10.24 sec.
Spectral Difference (dB)
pressure
z-axis
y-axis
x-axis
40
20
0
-20
-40
0.00
5.00
10.00
15.00
20.00
Frequency (Hz)

Figure V.110

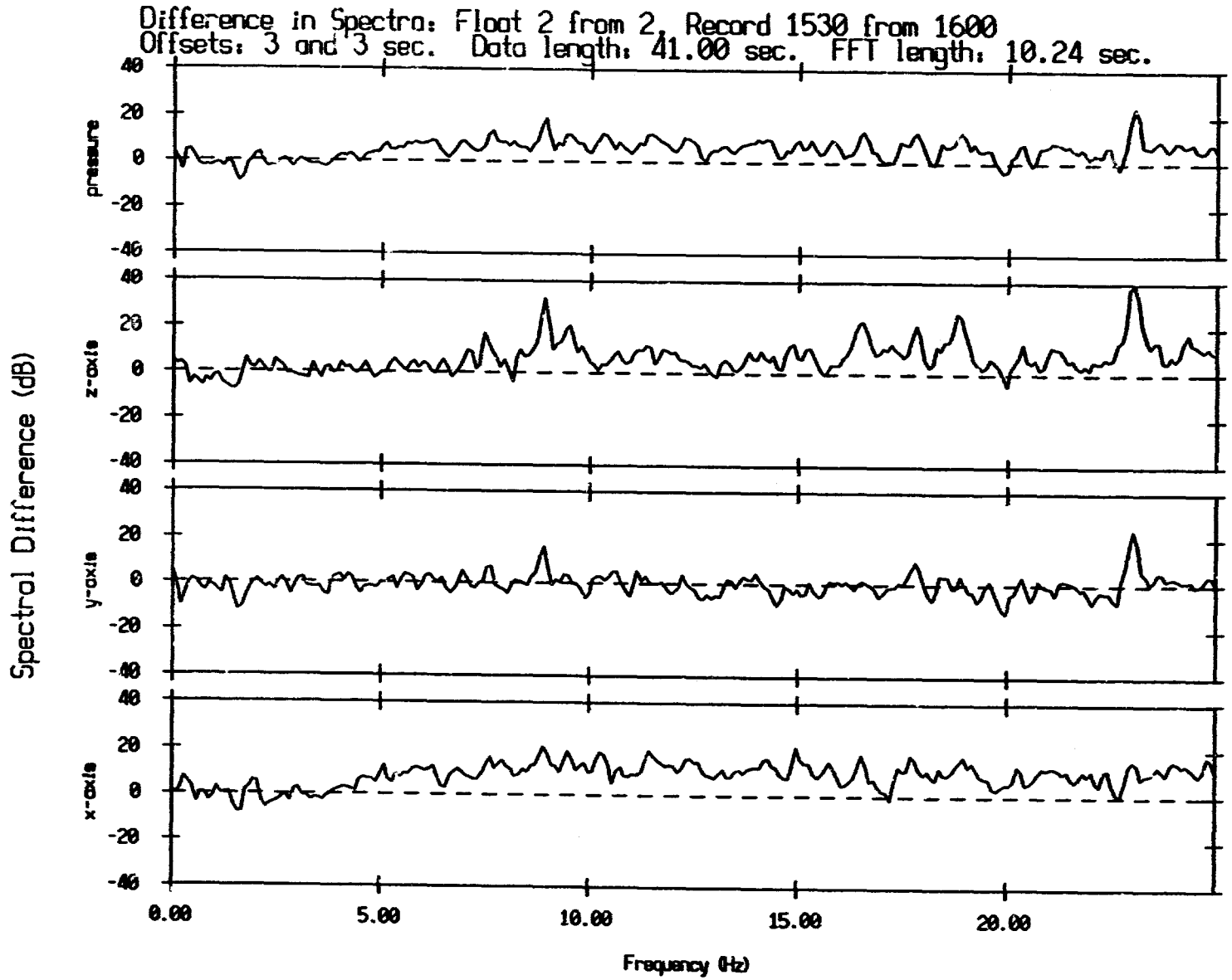
Difference in Spectra: Float 2 from 2, Record 1530 from 1600
Offsets: 3 and 3 sec. Data length: 41.00 sec. FFT length: 10.24 sec.
Spectral Difference (dB)
pressure
z-axis
y-axis
x-axis
40
20
0
-20
-40
0.00
5.00
10.00
15.00
20.00
Frequency (Hz)

Figure V.111

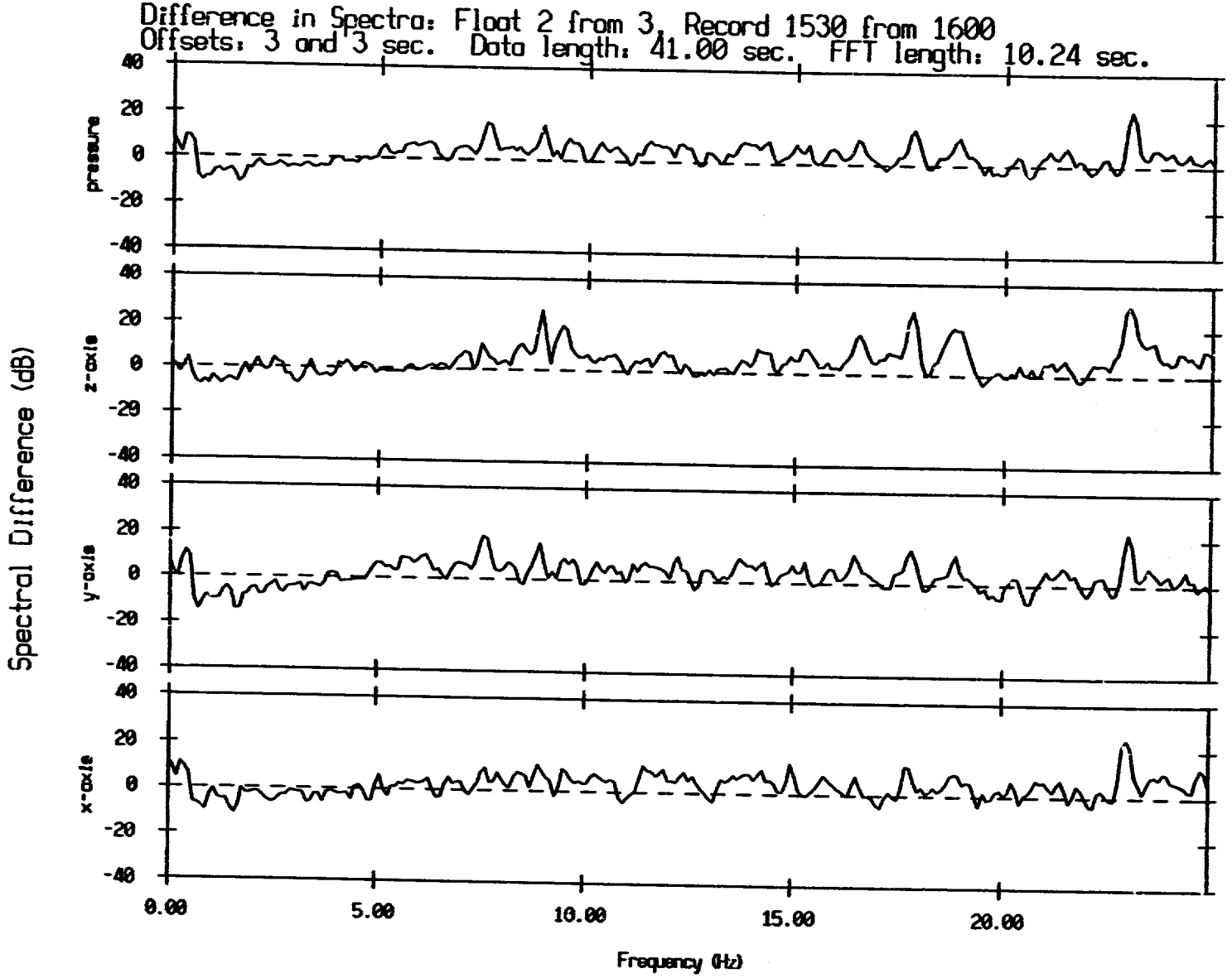
Difference in Spectra: Float 2 from 3, Record 1530 from 1600
Offsets: 3 and 3 sec. Data length: 41.00 sec. FFT length: 10.24 sec.
Spectral Difference (dB)
pressure
z-axis
y-axis
x-axis
40
20
0
-20
-40
0.00
5.00
10.00
15.00
20.00
Frequency (Hz)

Figure V.112

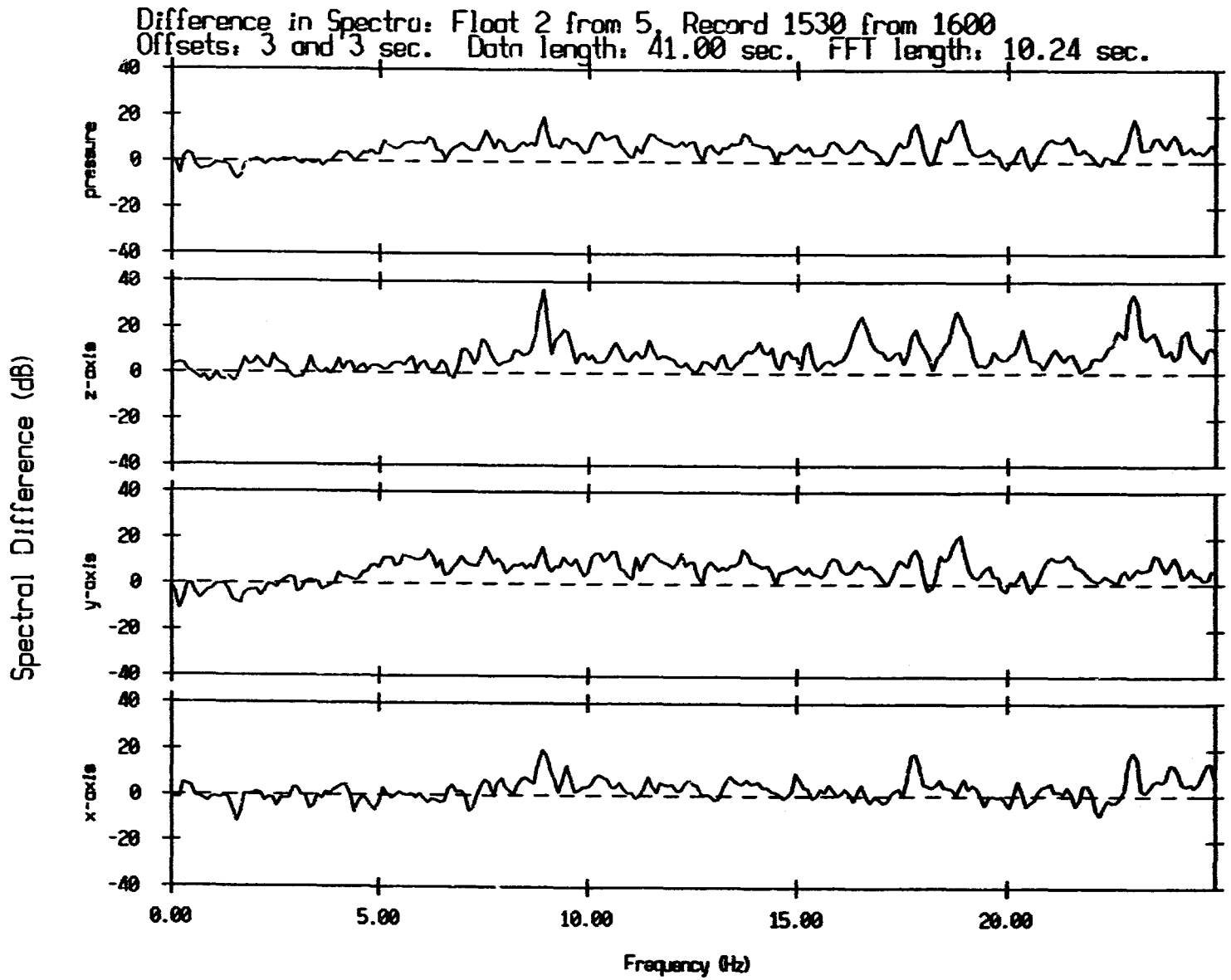
Difference in Spectra: Float 2 from 5, Record 1530 from 1600
Offsets: 3 and 3 sec. Data length: 41.00 sec. FFT length: 10.24 sec.
Spectral Difference (dB)
pressure
z-axis
y-axis
x-axis
40
20
0
-20
-40
0.00
5.00
10.00
15.00
20.00
Frequency (Hz)

Figure V.113

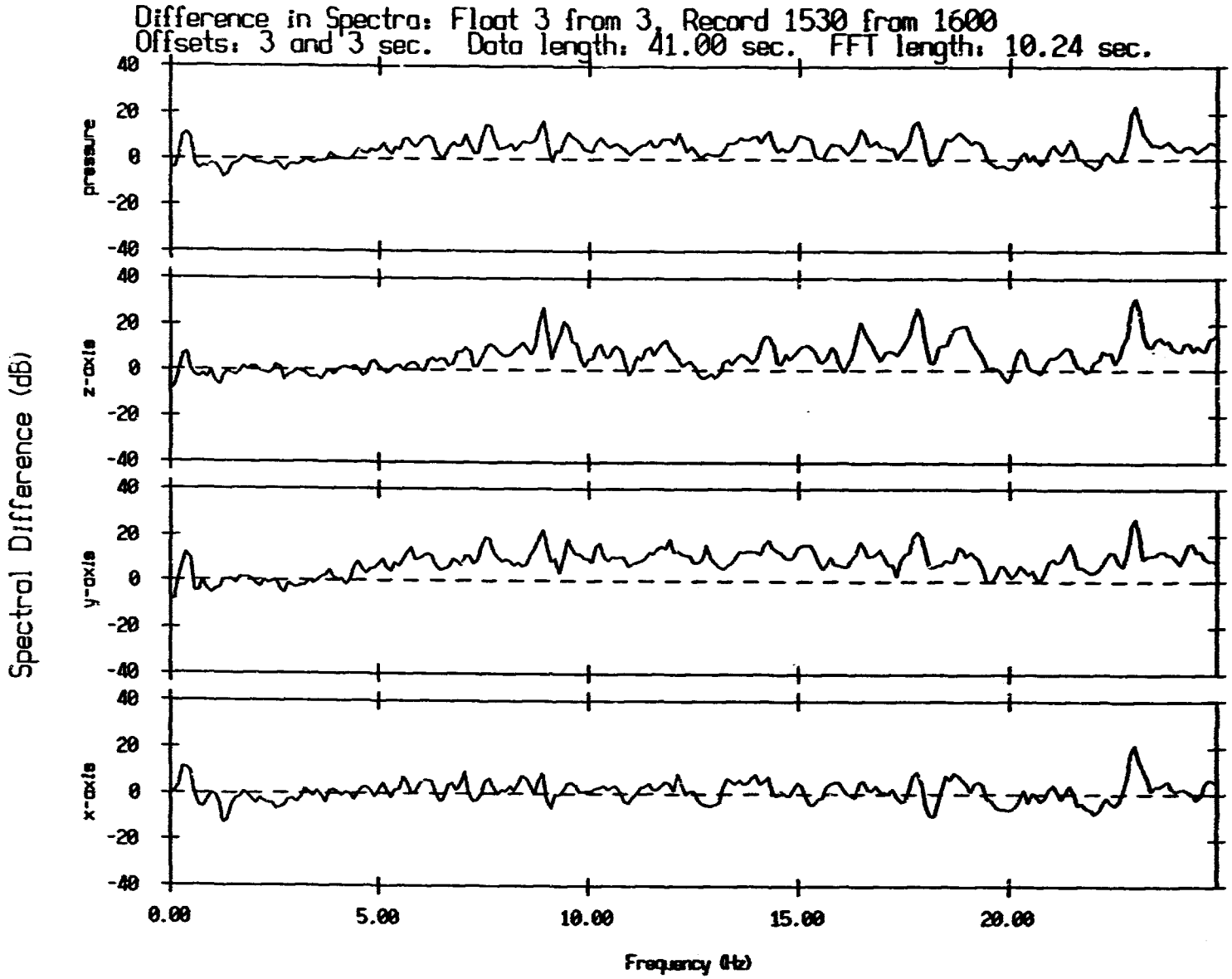
Difference in Spectra: Float 3 from 3, Record 1530 from 1600
Offsets: 3 and 3 sec. Data length: 41.00 sec. FFT length: 10.24 sec.
Spectral Difference (dB)
pressure
z-axis
y-axis
x-axis
40
20
0
-20
-40
0.00
5.00
10.00
15.00
20.00
Frequency (Hz)

Figure V.11.4

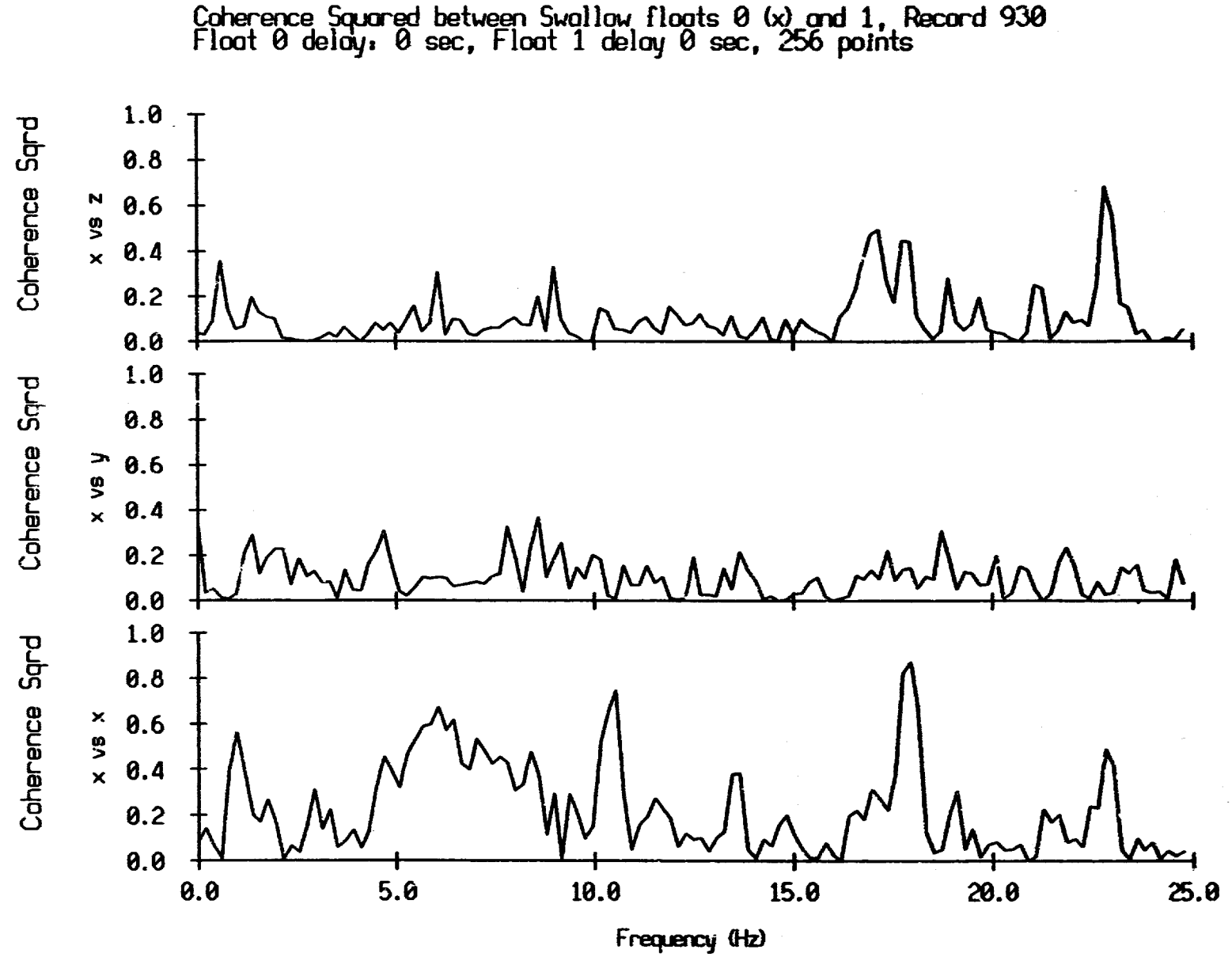
Coherence Squared between Swallow floats 0 (x) and 1, Record 930
Float 0 delay: 0 sec, Float 1 delay 0 sec, 256 points
Coherence Sqrd
x vs z
x vs y
x vs x
1.0
0.8
0.6
0.4
0.2
0.0
0.0
5.0
10.0
15.0
20.0
25.0
Frequency (Hz)

Figure VI.1i

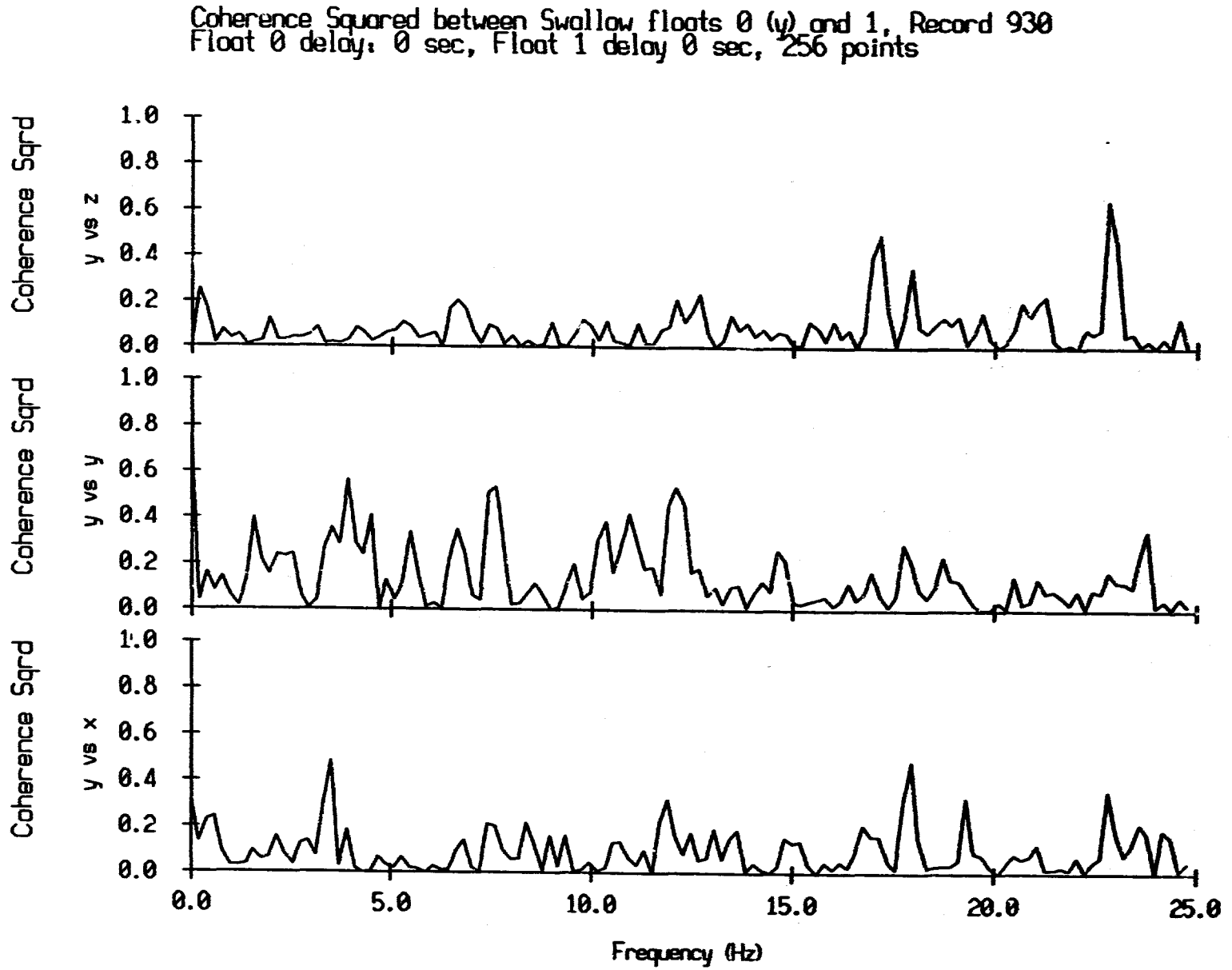
Coherence Squared between Swallow floats 0 (y) and 1, Record 930
Float 0 delay: 0 sec, Float 1 delay 0 sec, 256 points
Coherence Sqrd
y vs z
y vs y
y vs x
1.0
0.8
0.6
0.4
0.2
0.0
0.0
5.0
10.0
15.0
20.0
25.0
Frequency (Hz)

Figure VI.1j

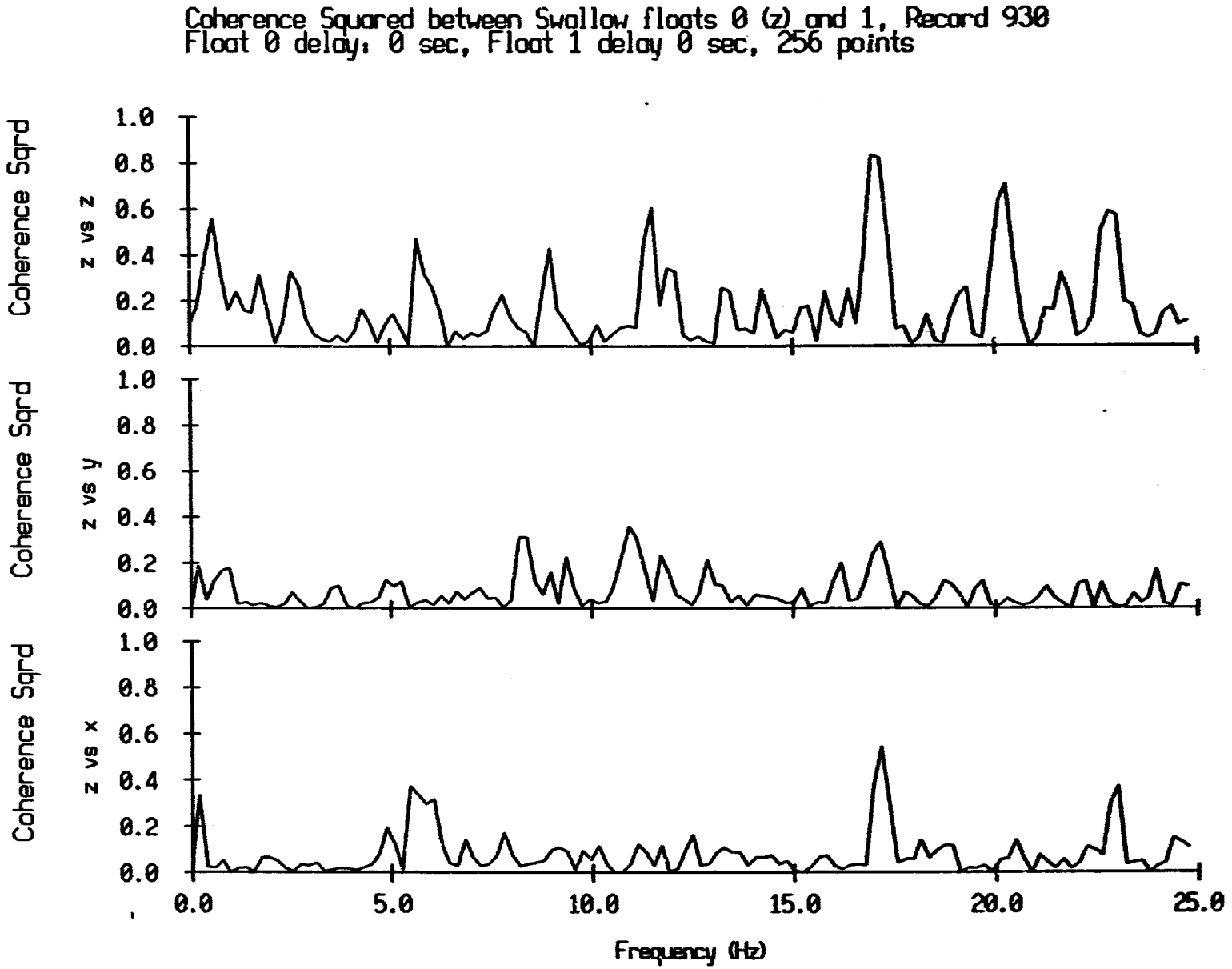
Coherence Squared between Swallow floats 0 (z) and 1, Record 930
Float 0 delay: 0 sec, Float 1 delay 0 sec, 256 points
Coherence Sqrd
z vs z
z vs y
z vs x
1.0
0.8
0.6
0.4
0.2
0.0
0.0
5.0
10.0
15.0
20.0
25.0
Frequency (Hz)

Figure VI.1k

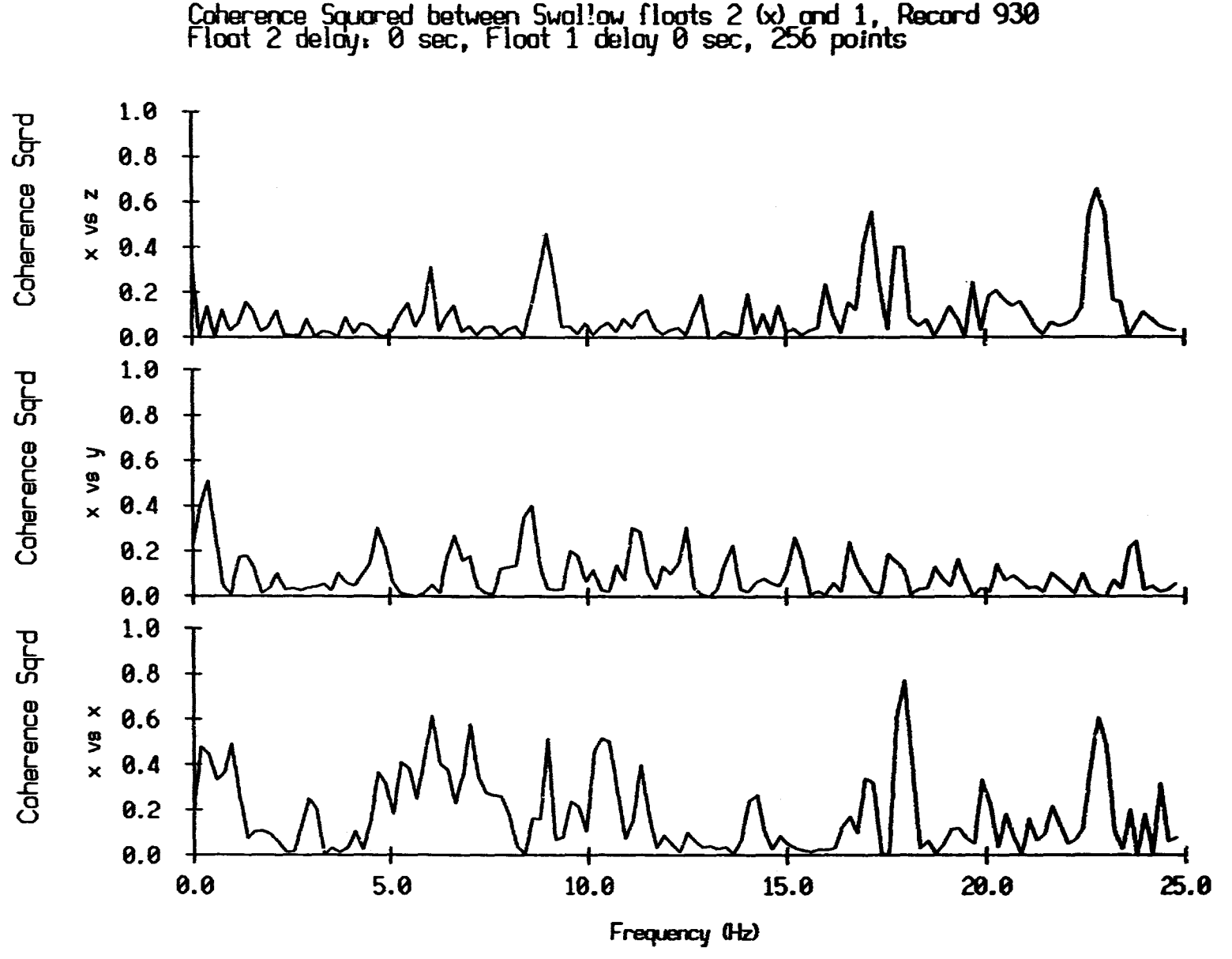
Coherence Squared between Swallow floats 2 (x) and 1, Record 930
Float 2 delay: 0 sec, Float 1 delay 0 sec, 256 points
Coherence Sqrd
x vs z
x vs y
x vs x
1.0
0.8
0.6
0.4
0.2
0.0
0.0
5.0
10.0
15.0
20.0
25.0
Frequency (Hz)

Figure VI.21

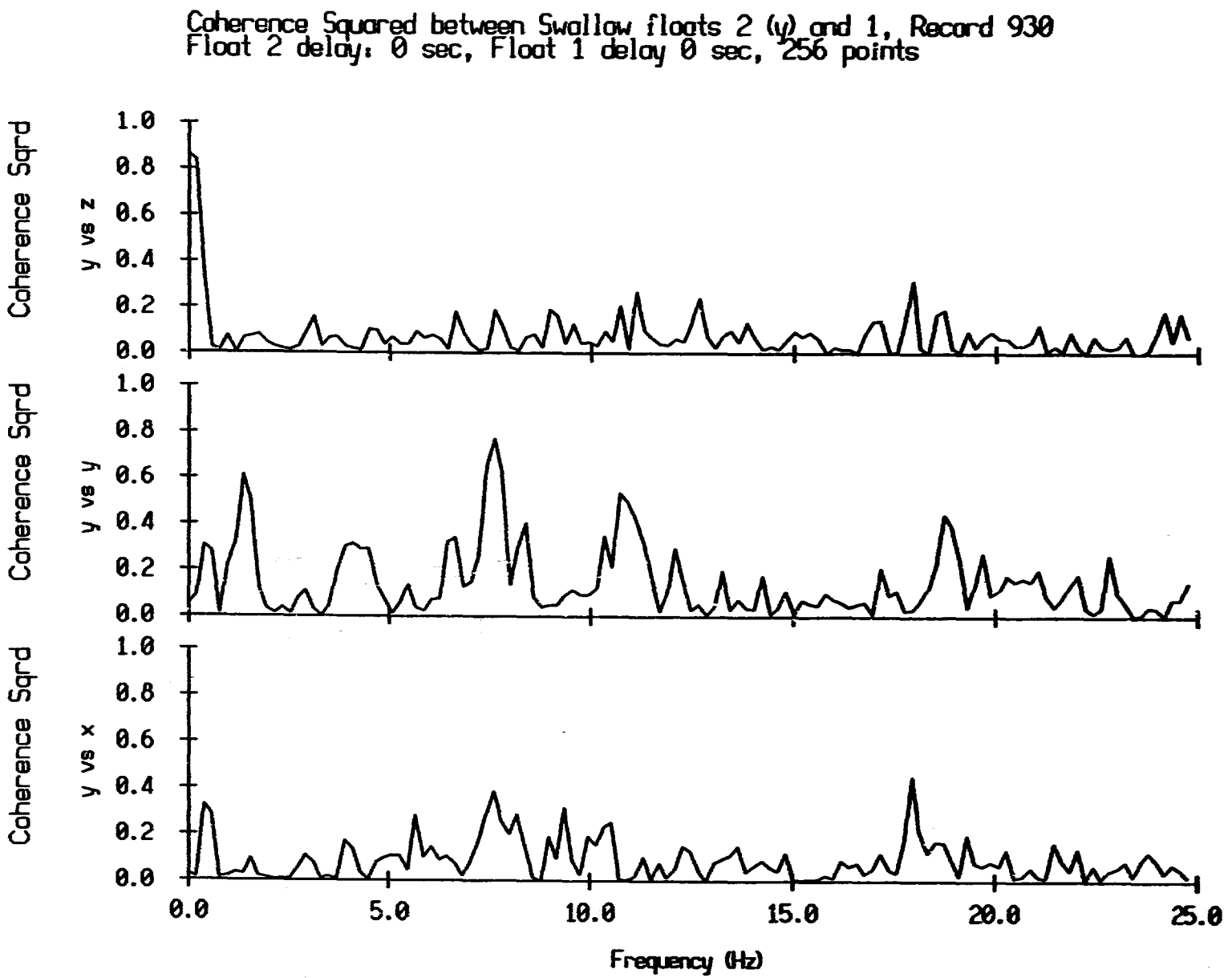
Coherence Squared between Swallow floats 2 (y) and 1, Record 930
Float 2 delay: 0 sec, Float 1 delay 0 sec, 256 points
Coherence Sqrd
y vs z
y vs y
y vs x
1.0
0.8
0.6
0.4
0.2
0.0
0.0
5.0
10.0
15.0
20.0
25.0
Frequency (Hz)

Figure VI.2j

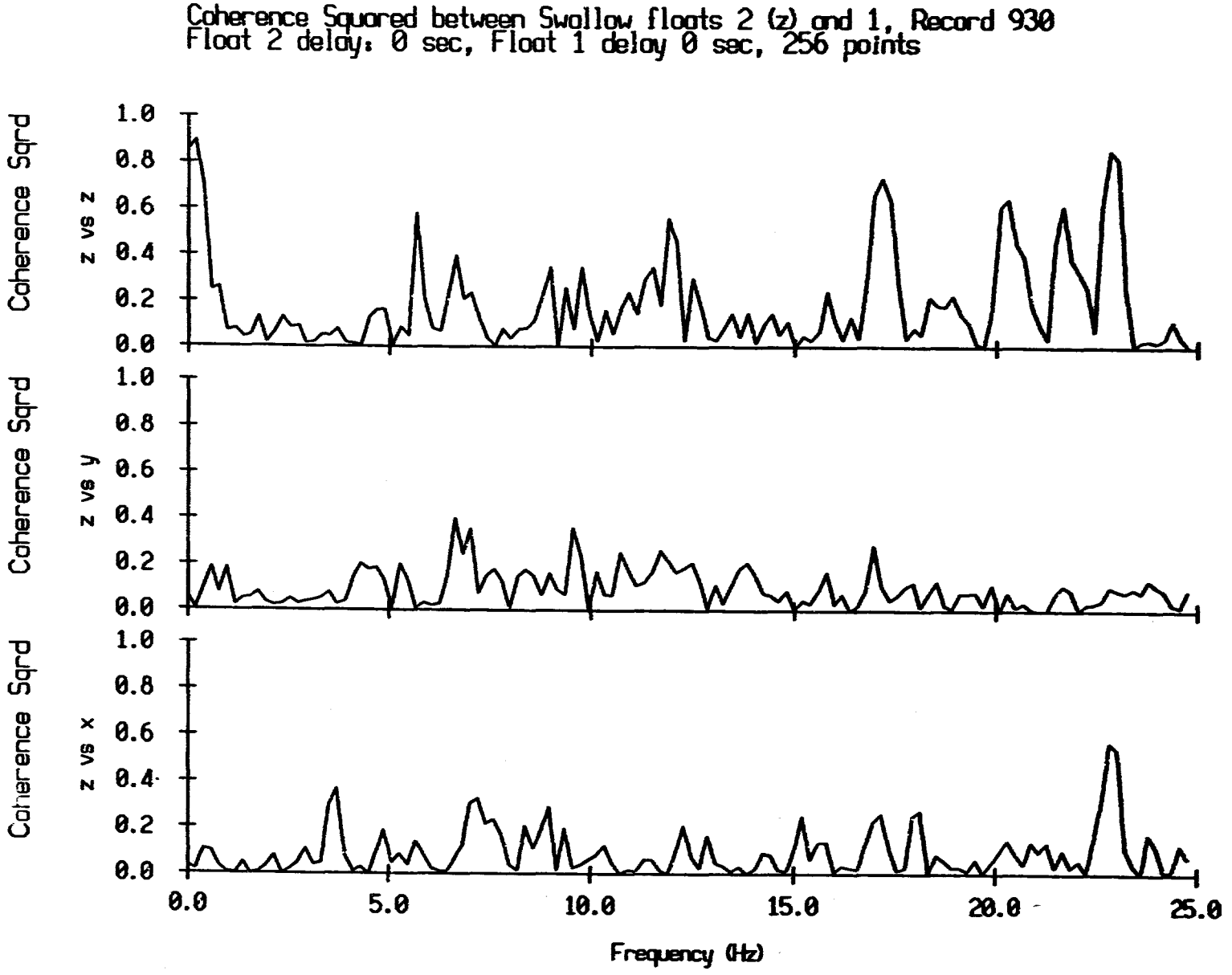
Coherence Squared between Swallow floats 2 (z) and 1, Record 930
Float 2 delay: 0 sec, Float 1 delay 0 sec, 256 points
Coherence Sqrd
z vs z
z vs y
z vs x
1.0
0.8
0.6
0.4
0.2
0.0
0.0
5.0
10.0
15.0
20.0
25.0
Frequency (Hz)

Figure VI.2k

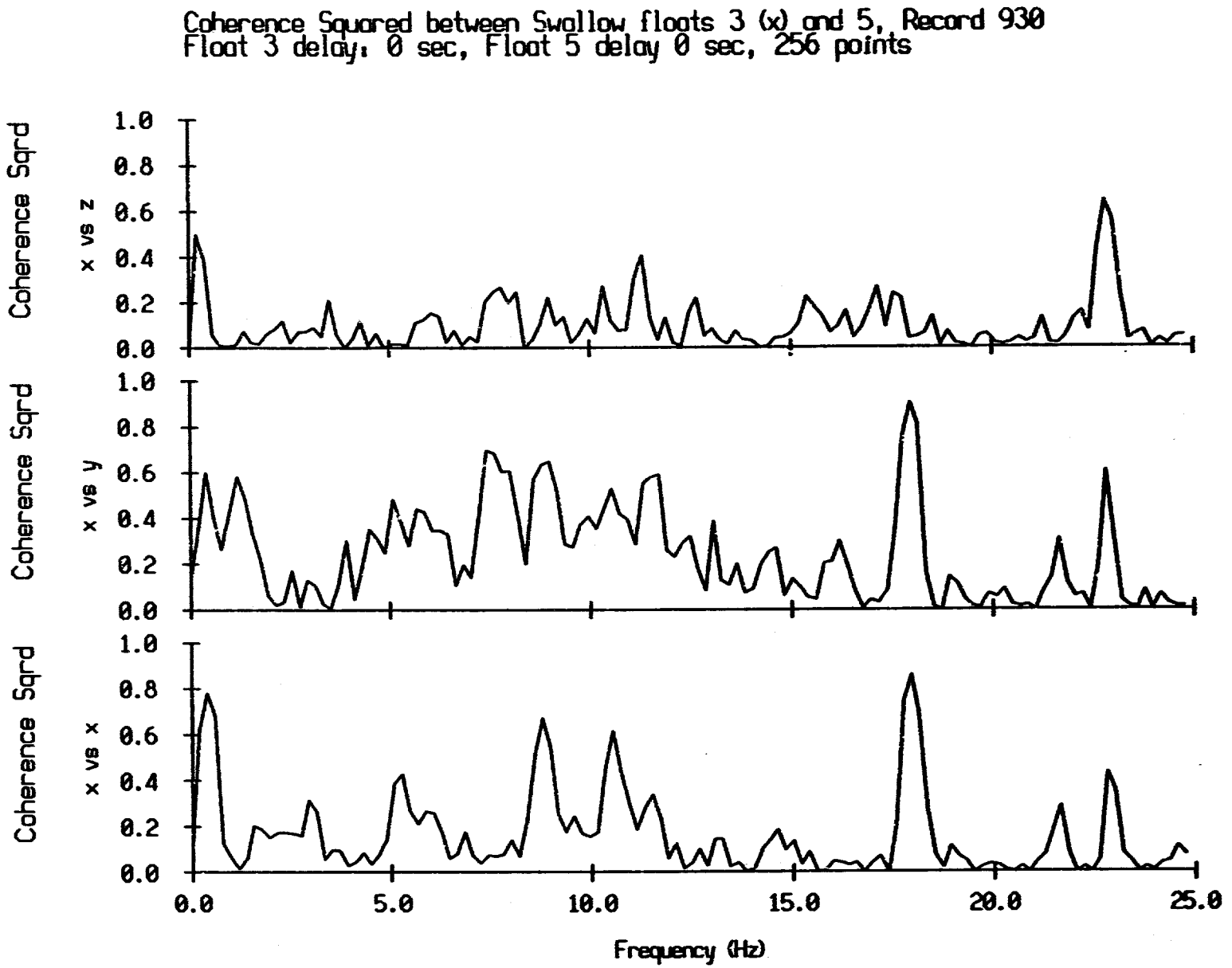
Coherence Squared between Swallow floats 3 (x) and 5, Record 930
Float 3 delay: 0 sec, Float 5 delay 0 sec, 256 points
Coherence Sqrd
x vs z
x vs y
x vs x
1.0
0.8
0.6
0.4
0.2
0.0
0.0
5.0
10.0
15.0
20.0
25.0
Frequency (Hz)

Figure VI.3i

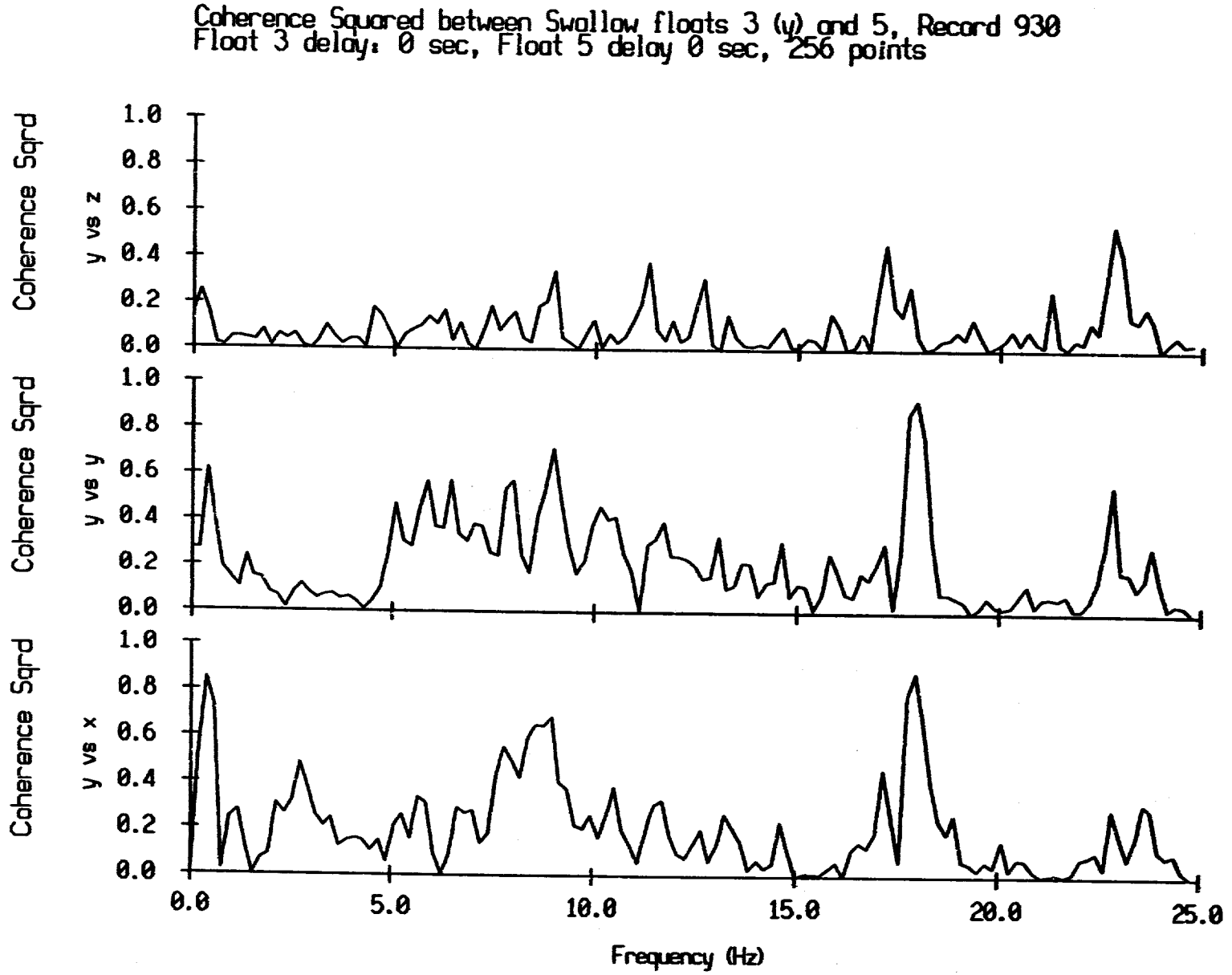
Coherence Squared between Swallow floats 3 (y) and 5, Record 930
Float 3 delay: 0 sec, Float 5 delay 0 sec, 256 points
Coherence Sqrd
y vs z
y vs y
y vs x
1.0
0.8
0.6
0.4
0.2
0.0
0.0
5.0
10.0
15.0
20.0
25.0
Frequency (Hz)

Figure VI.3j

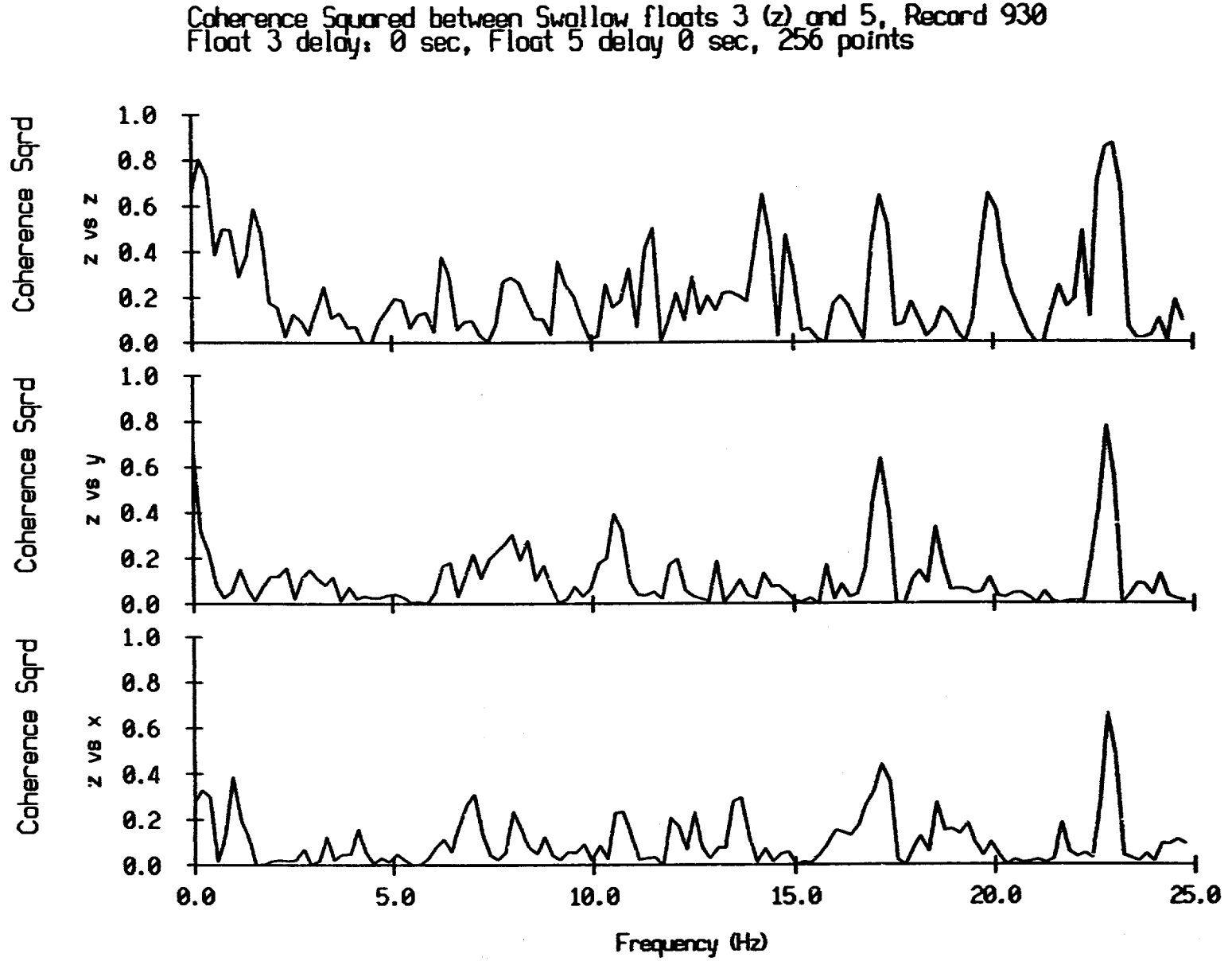
Coherence Squared between Swallow floats 3 (z) and 5, Record 930
Float 3 delay: 0 sec, Float 5 delay 0 sec, 256 points
Coherence Sqrd
z vs z
z vs y
z vs x
1.0
0.8
0.6
0.4
0.2
0.0
0.0
5.0
10.0
15.0
20.0
25.0
Frequency (Hz)

Figure VI.3k

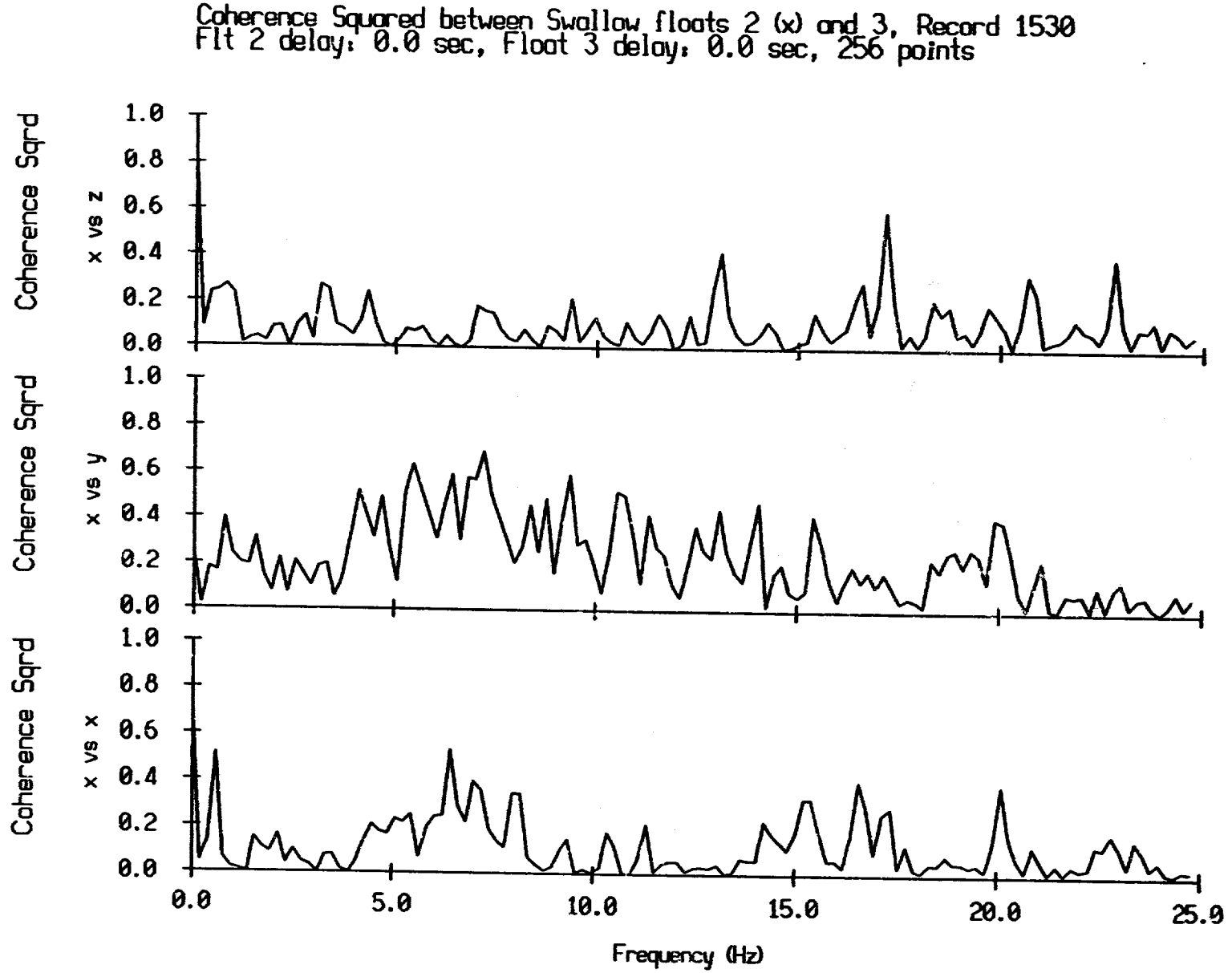
Coherence Squared between Swallow floats 2 (x) and 3, Record 1530
Flt 2 delay: 0.0 sec, Float 3 delay: 0.0 sec, 256 points
Coherence Sqrd
x vs z
Coherence Sqrd
x vs y
Coherence Sqrd
x vs x
1.0
0.8
0.6
0.4
0.2
0.0
0.0
5.0
10.0
15.0
20.0
25.0
Frequency (Hz)

Figure VI.4i

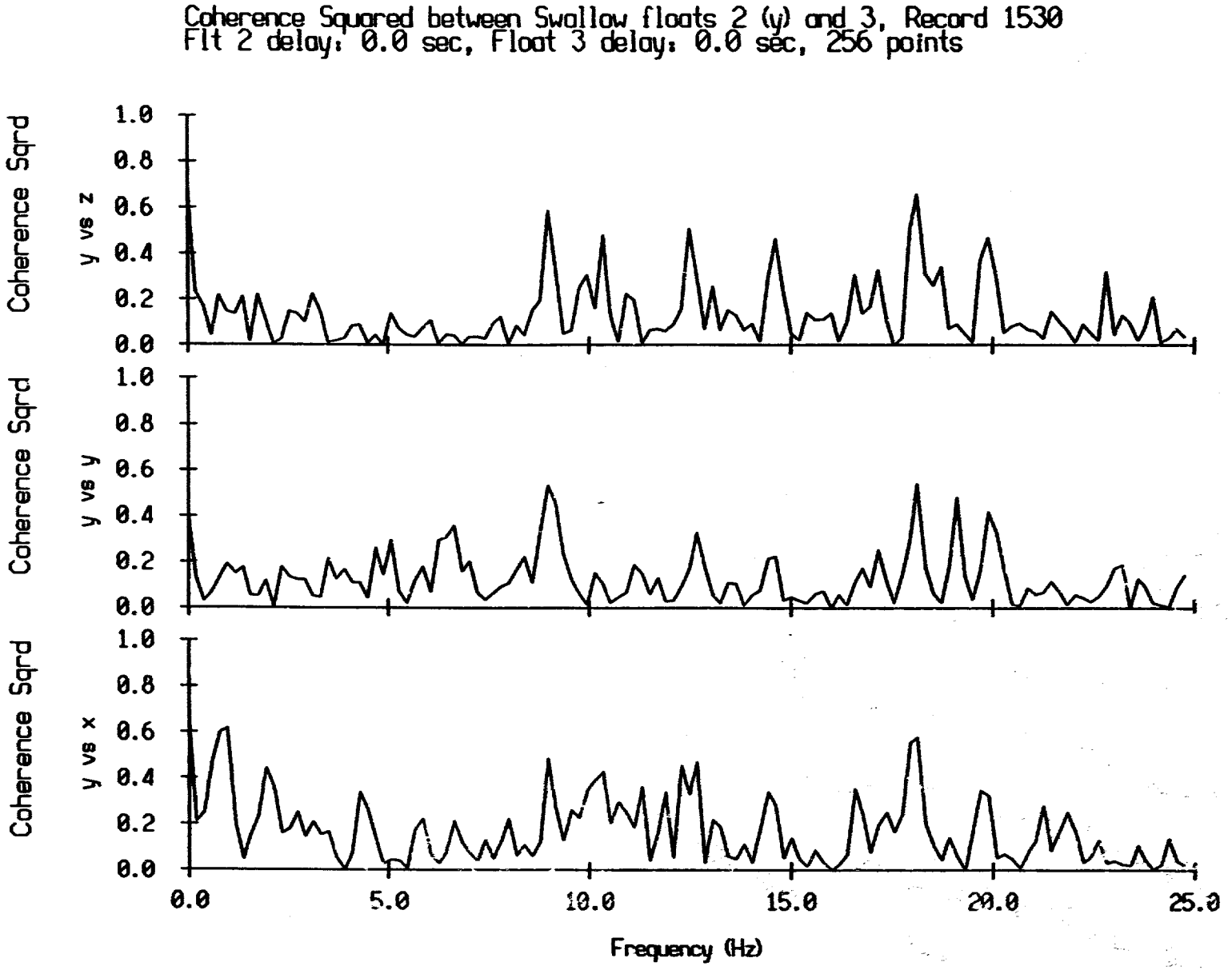
Coherence Squared between Swallow floats 2 (y) and 3, Record 1530
Flt 2 delay: 0.0 sec, Float 3 delay: 0.0 sec, 256 points
Coherence Sqrd
y vs z
Coherence Sqrd
y vs y
Coherence Sqrd
y vs x
1.0
0.8
0.6
0.4
0.2
0.0
0.0
5.0
10.0
15.0
20.0
25.0
Frequency (Hz)

Figure VI.4j

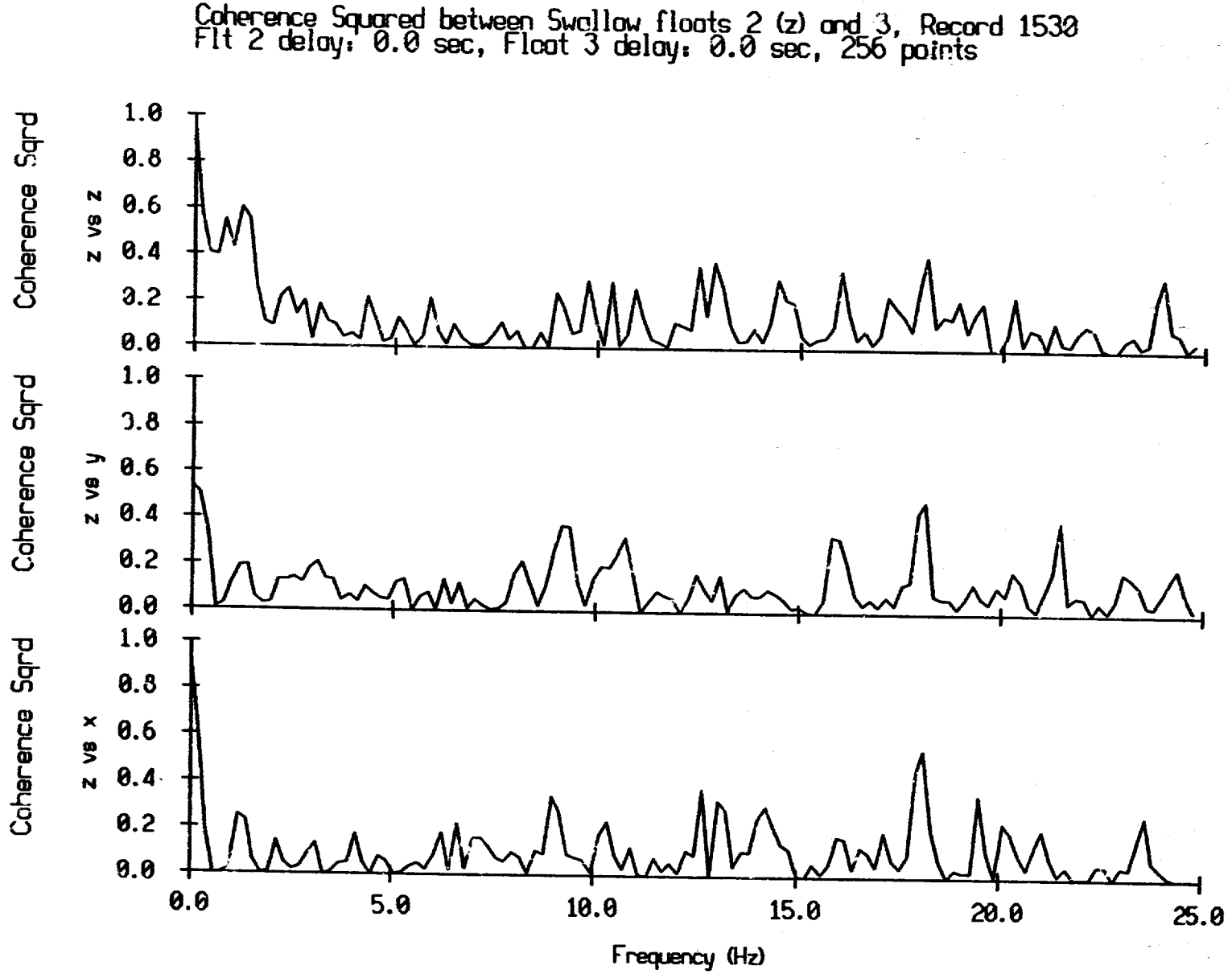
Coherence Squared between Swallow floats 2 (z) and 3, Record 1530
Flt 2 delay: 0.0 sec, Float 3 delay: 0.0 sec, 256 points
Coherence Sqrd
z vs z
z vs y
z vs x
1.0
0.8
0.6
0.4
0.2
0.0
0.0
5.0
10.0
15.0
20.0
25.0
Frequency (Hz)

Figure VI.4k

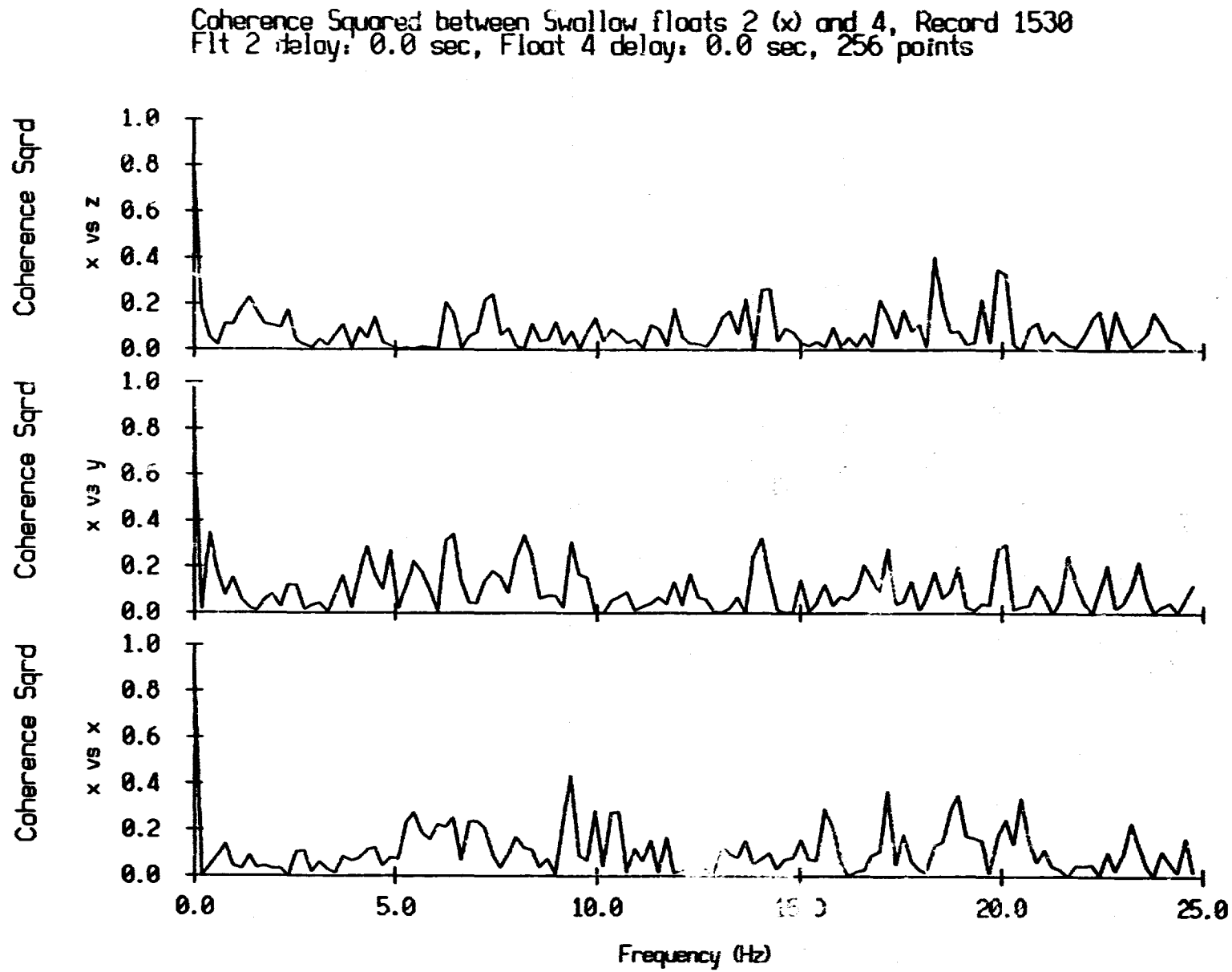
Coherence Squared between Swallow floats 2 (x) and 4, Record 1530
Flt 2 delay: 0.0 sec, Float 4 delay: 0.0 sec, 256 points
Coherence Sqrd
x vs z
x vs y
x vs x
1.0
0.8
0.6
0.4
0.2
0.0
0.0
5.0
10.0
20.0
25.0
Frequency (Hz)

Figure V1.5i

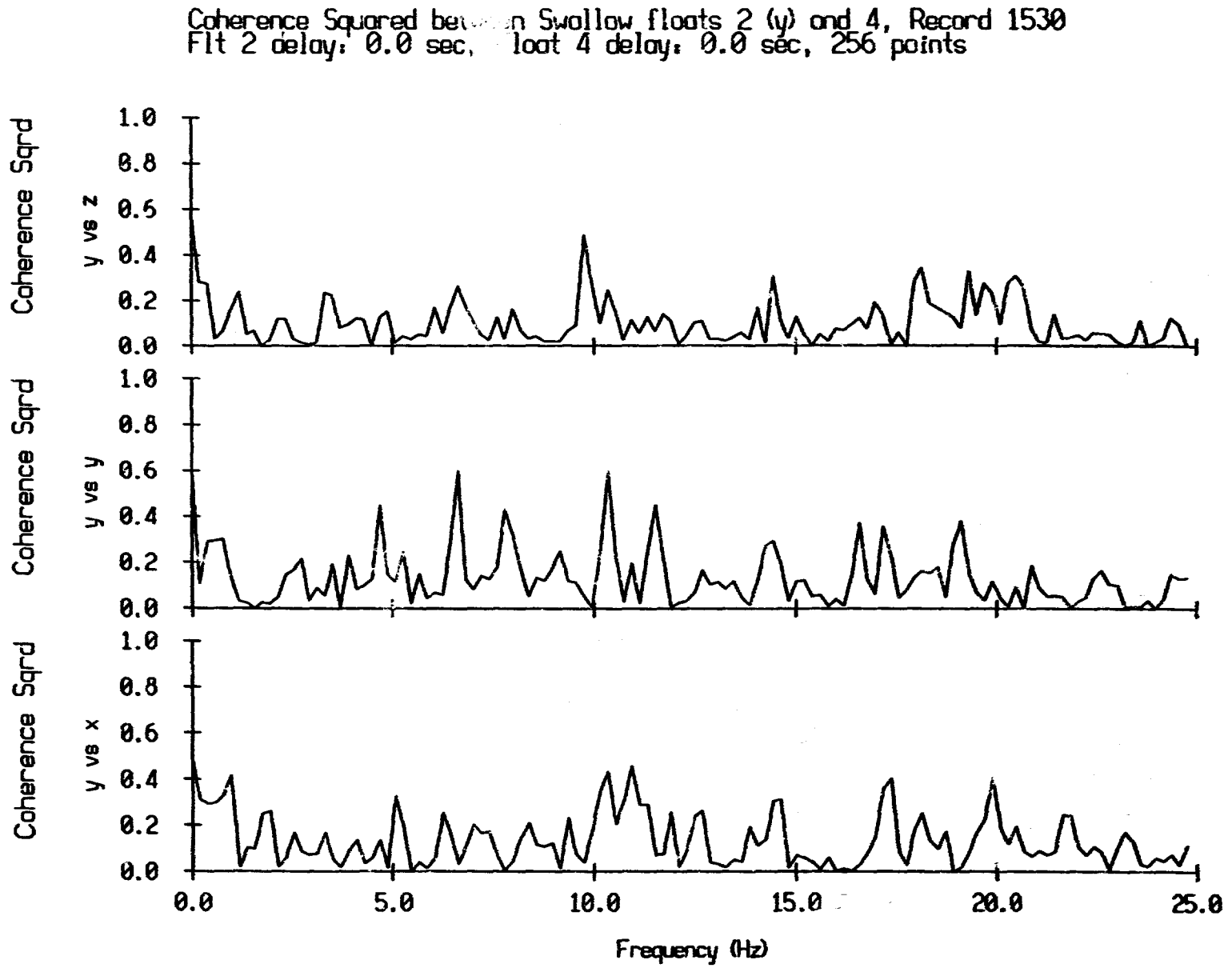
Coherence Squared between Swallow floats 2 (y) and 4, Record 1530
Flt 2 delay: 0.0 sec, float 4 delay: 0.0 sec, 256 points
Coherence Sqrd
y vs z
y vs y
y vs x
1.0
0.8
0.6
0.5
0.4
0.2
0.0
0.0
5.0
10.0
15.0
20.0
25.0
Frequency (Hz)

Figure VI.5j

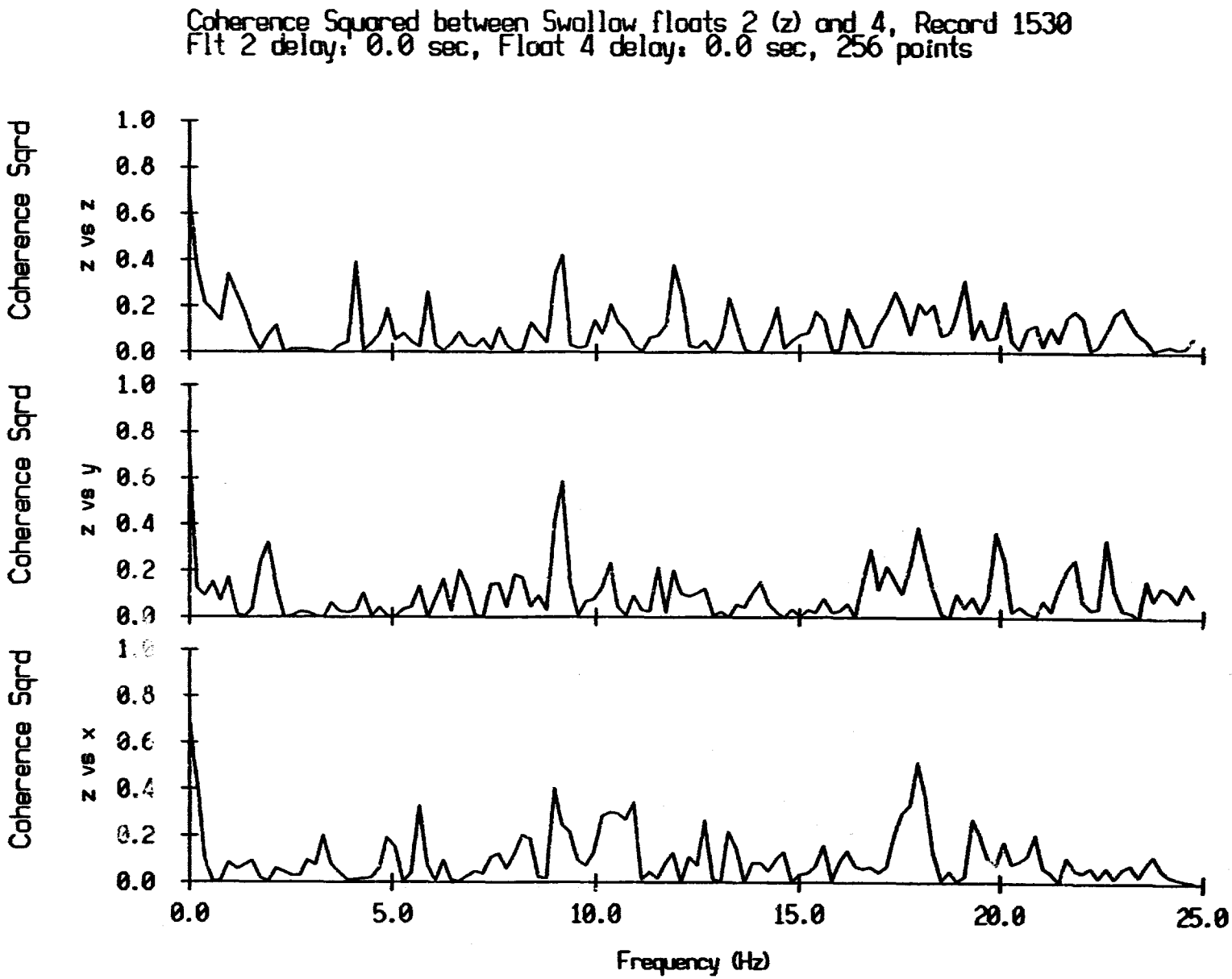
Coherence Squared between Swallow floats 2 (z) and 4, Record 1530
Flt 2 delay: 0.0 sec, Float 4 delay: 0.0 sec, 256 points
Coherence Sqrd
z vs z
z vs y
z vs x
1.0
0.8
0.6
0.4
0.2
0.0
0.0
5.0
10.0
15.0
20.0
25.0
Frequency (Hz)

Figure VI.5k

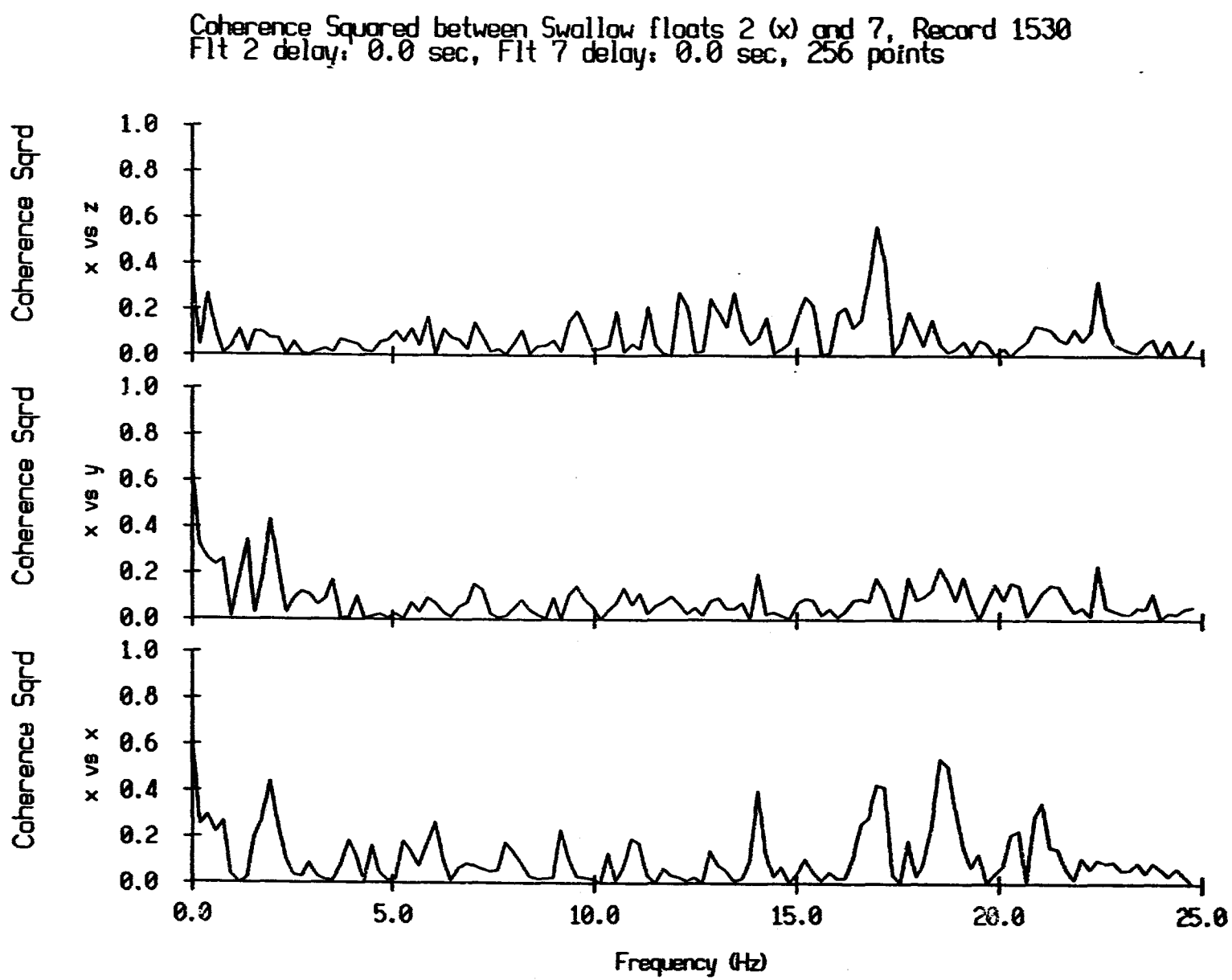
Coherence Squared between Swallow floats 2 (x) and 7, Record 1530
Flt 2 delay: 0.0 sec, Flt 7 delay: 0.0 sec, 256 points
Coherence Sqrd
x vs z
x vs y
x vs x
1.0
0.8
0.6
0.4
0.2
0.0
0.0
5.0
10.0
15.0
20.0
25.0
Frequency (Hz)

Figure VI.6i

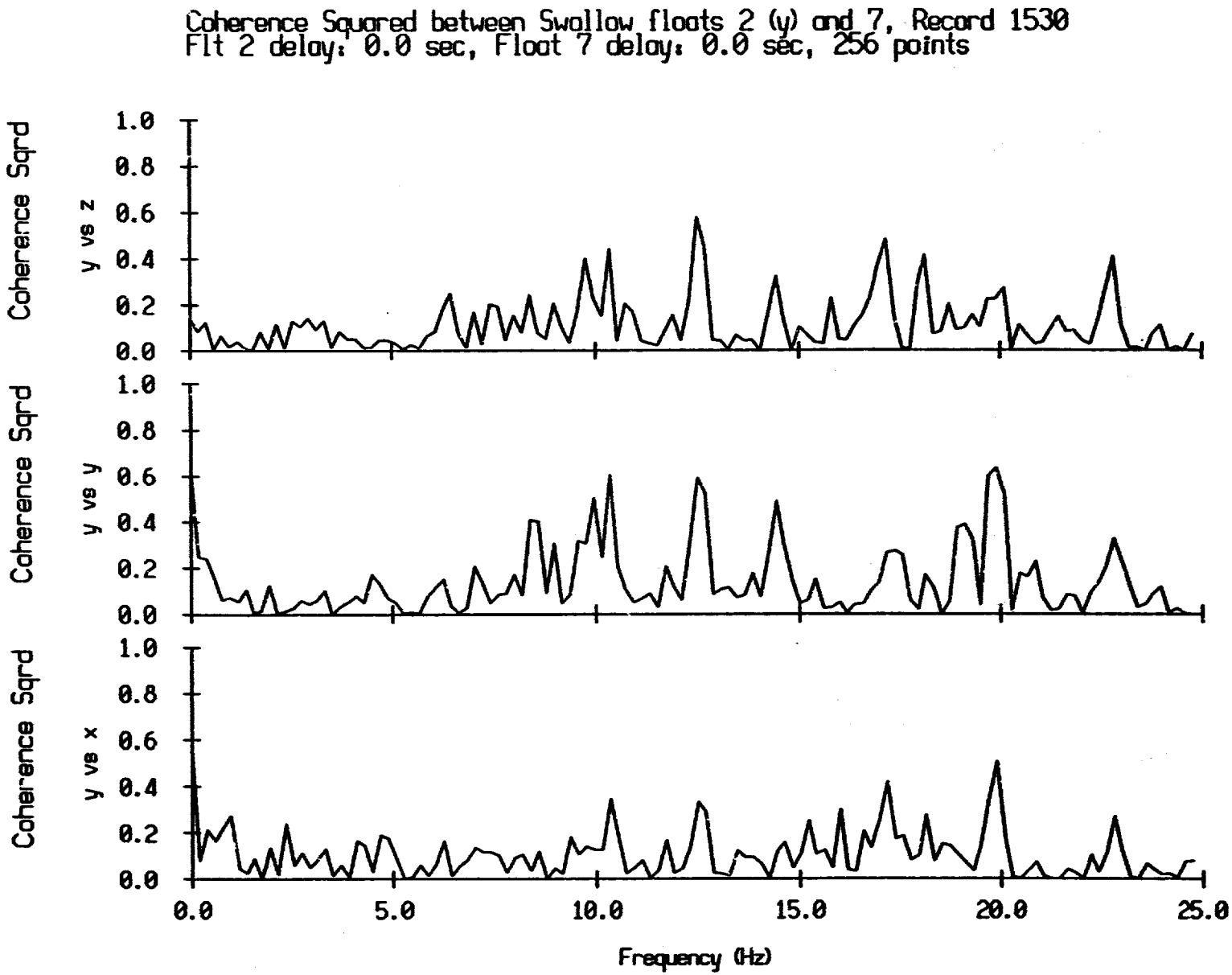
Coherence Squared between Swallow floats 2 (y) and 7, Record 1530
Flt 2 delay: 0.0 sec, Float 7 delay: 0.0 sec, 256 points
Coherence Sqrd
y vs z
y vs y
y vs x
1.0
0.8
0.6
0.4
0.2
0.0
0.0
5.0
10.0
15.0
20.0
25.0
Frequency (Hz)

Figure VI.6j

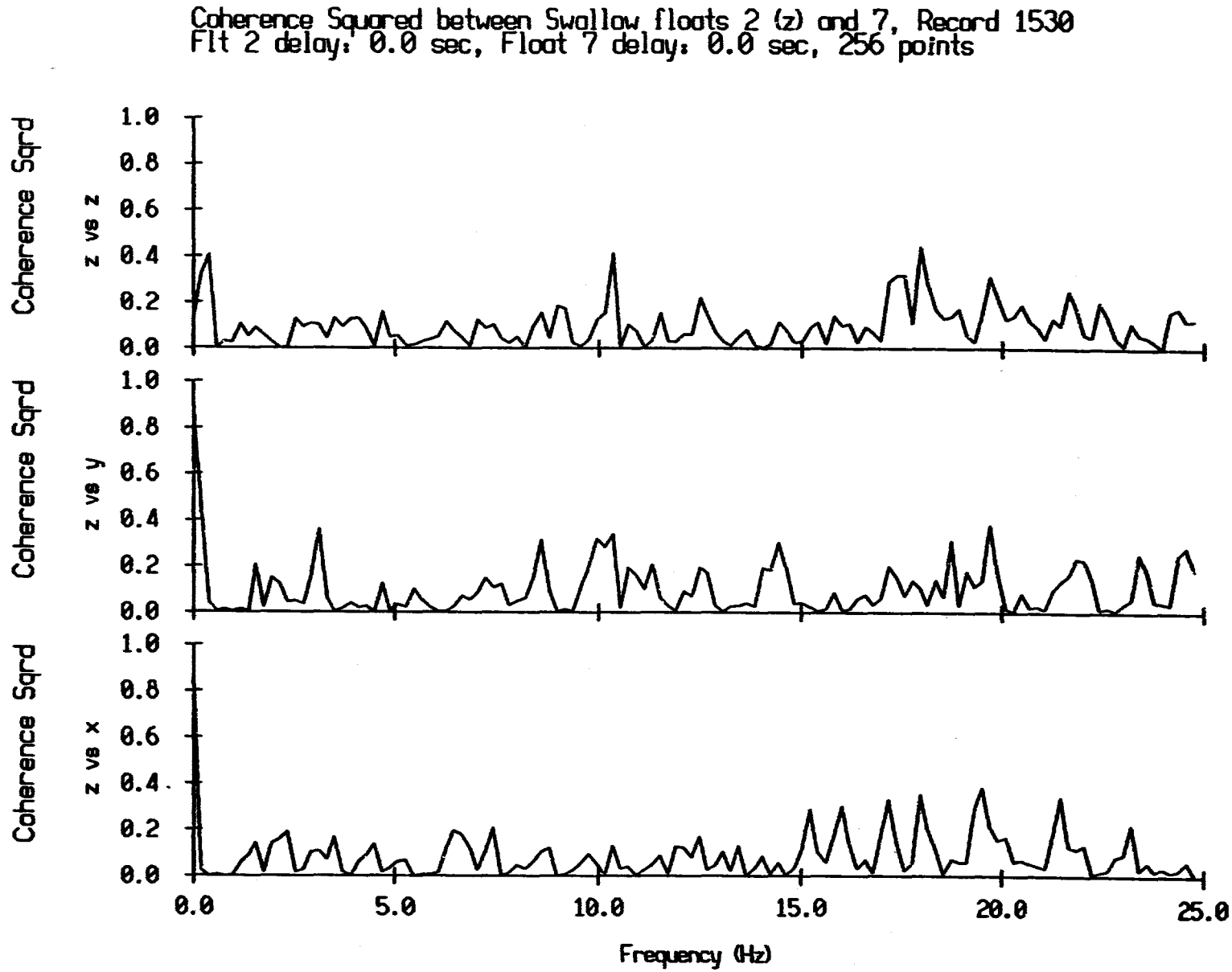
Coherence Squared between Swallow floats 2 (z) and 7, Record 1530
Flt 2 delay: 0.0 sec, Float 7 delay: 0.0 sec, 256 points
Coherence Sqrd
z vs z
z vs y
z vs x
1.0
0.8
0.6
0.4
0.2
0.0
0.0
5.0
10.0
15.0
20.0
25.0
Frequency (Hz)

Figure VI.6k

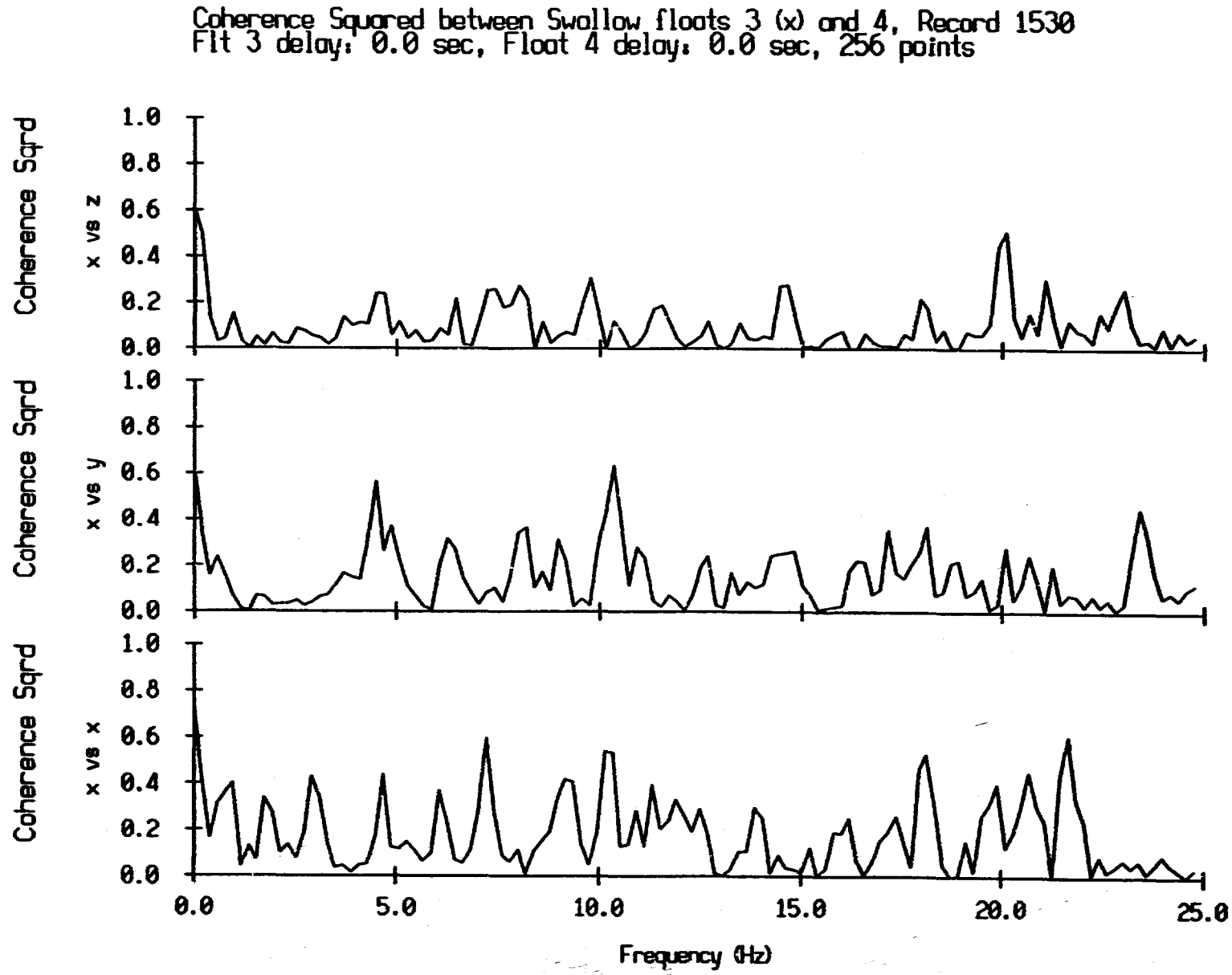
Coherence Squared between Swallow floats 3 (x) and 4, Record 1530
Flt 3 delay: 0.0 sec, Float 4 delay: 0.0 sec, 256 points
Coherence Sqrd
x vs z
x vs y
x vs x
1.0
0.8
0.6
0.4
0.2
0.0
0.0
5.0
10.0
15.0
20.0
25.0
Frequency (Hz)

Figure VI.7i

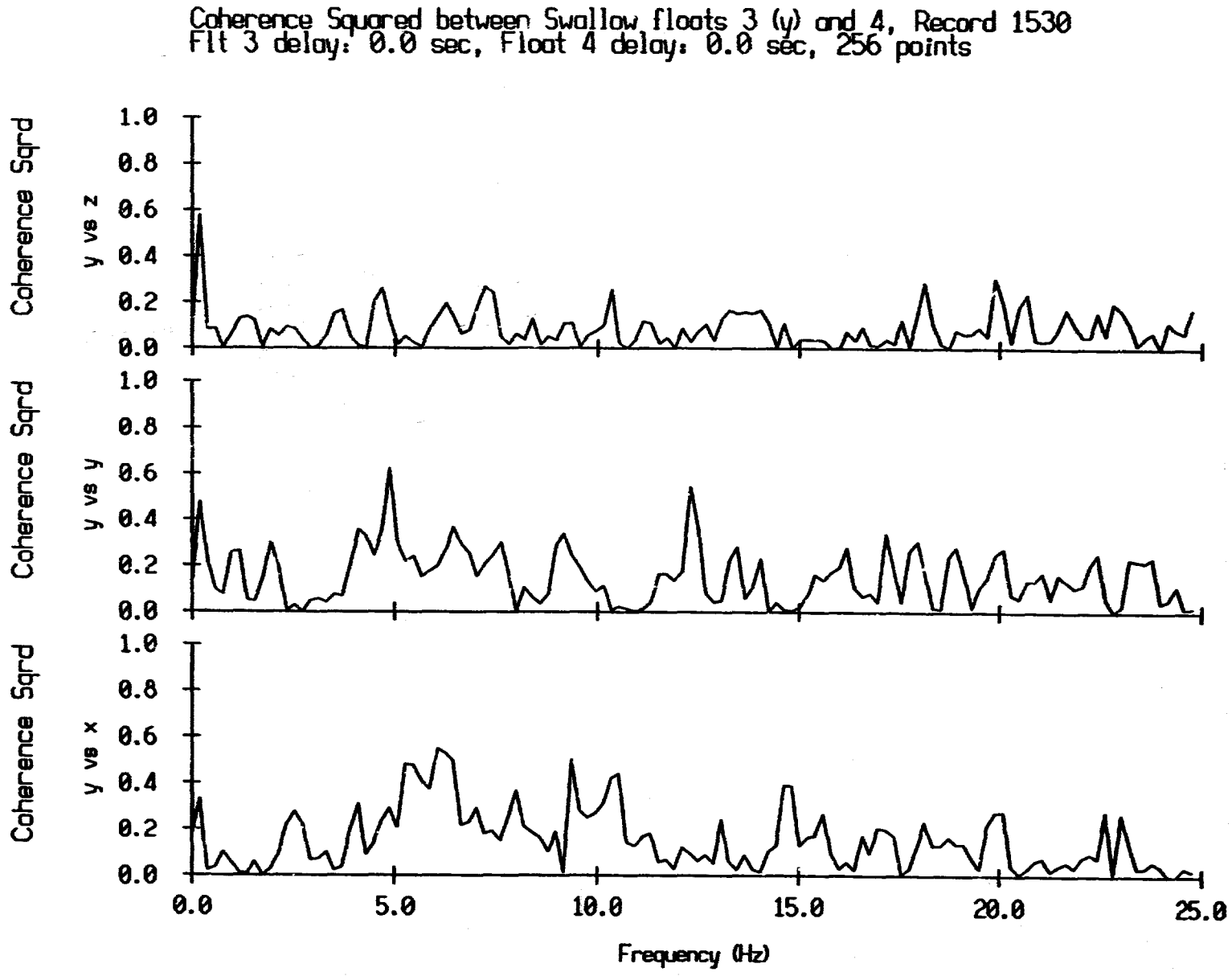
Coherence Squared between Swallow floats 3 (y) and 4, Record 1530
Flt 3 delay: 0.0 sec, Float 4 delay: 0.0 sec, 256 points
Coherence Sqrd
y vs z
y vs y
y vs x
1.0
0.8
0.6
0.4
0.2
0.0
0.0
5.0
10.0
15.0
20.0
25.0
Frequency (Hz)

Figure VI.7j

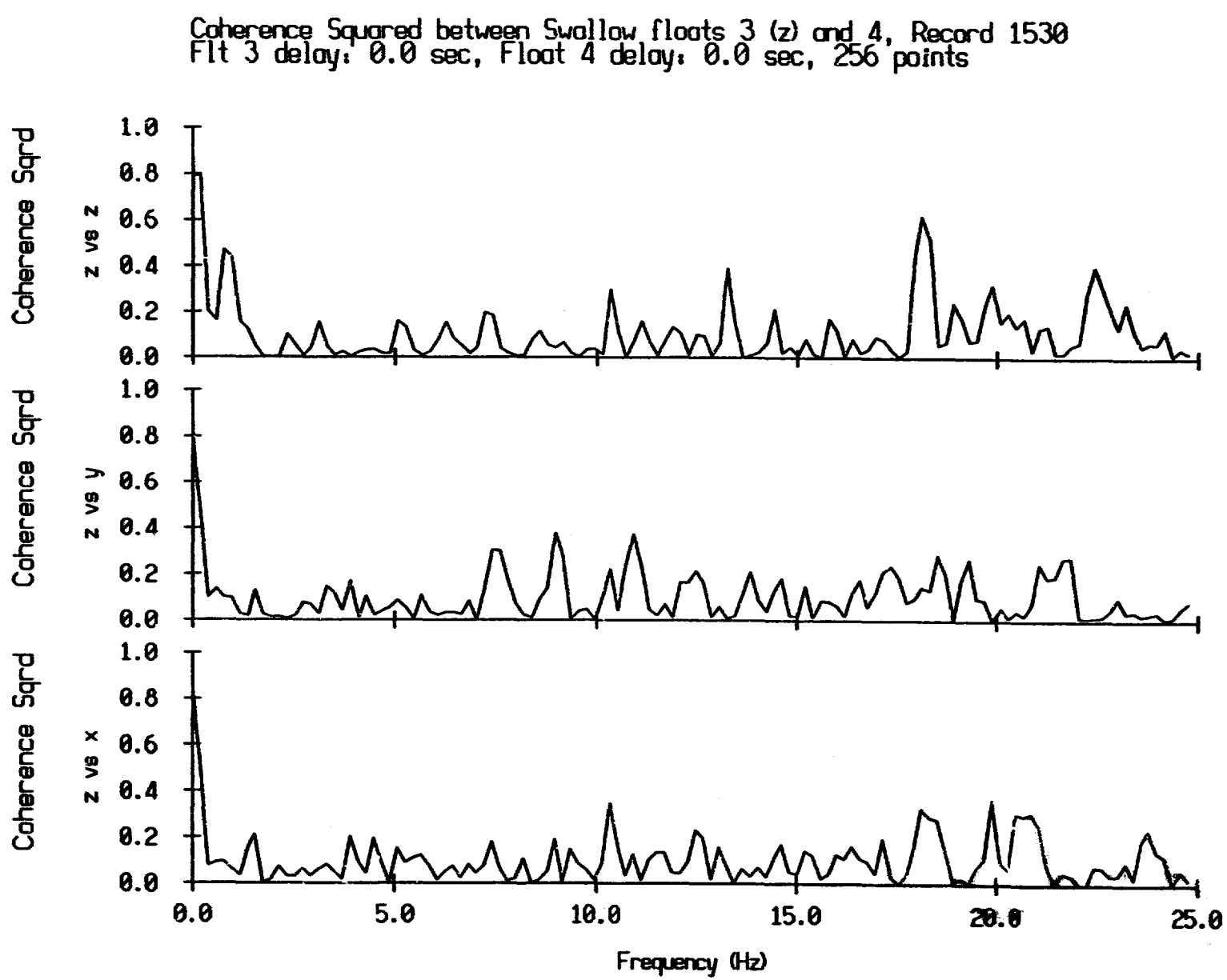
Coherence Squared between Swallow floats 3 (z) and 4, Record 1530
Flt 3 delay: 0.0 sec, Float 4 delay: 0.0 sec, 256 points
Coherence Sqrd
z vs z
z vs y
z vs x
1.0
0.8
0.6
0.4
0.2
0.0
0.0
5.0
10.0
15.0
20.0
25.0
Frequency (Hz)

Figure VI.7k

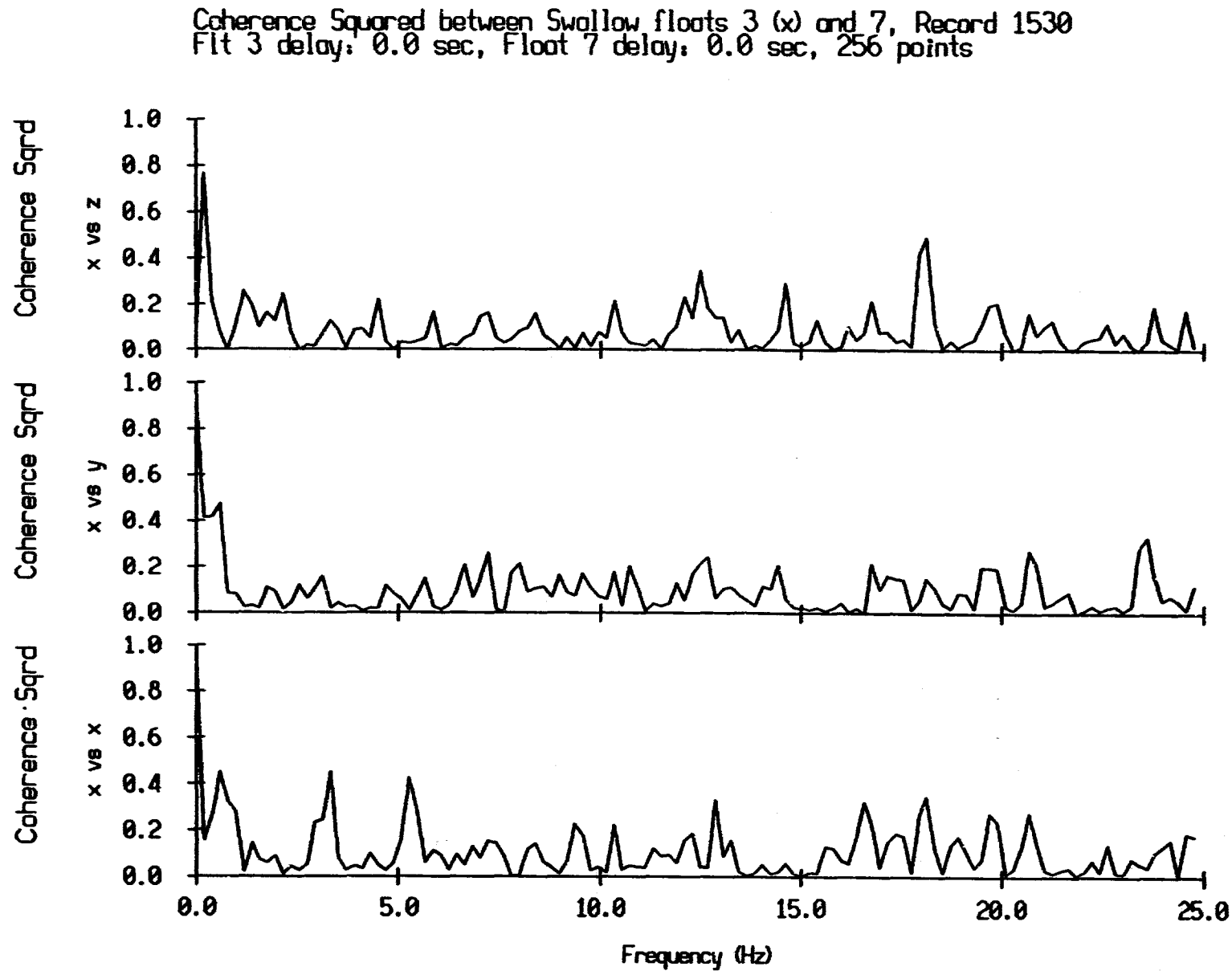
Coherence Squared between Swallow floats 3 (x) and 7, Record 1530
Flt 3 delay: 0.0 sec, Float 7 delay: 0.0 sec, 256 points
Coherence Sqrd
x vs z
Coherence Sqrd
x vs y
Coherence Sqrd
x vs x
1.0
0.8
0.6
0.4
0.2
0.0
0.0
5.0
10.0
15.0
20.0
25.0
Frequency (Hz)

Figure VI.8i

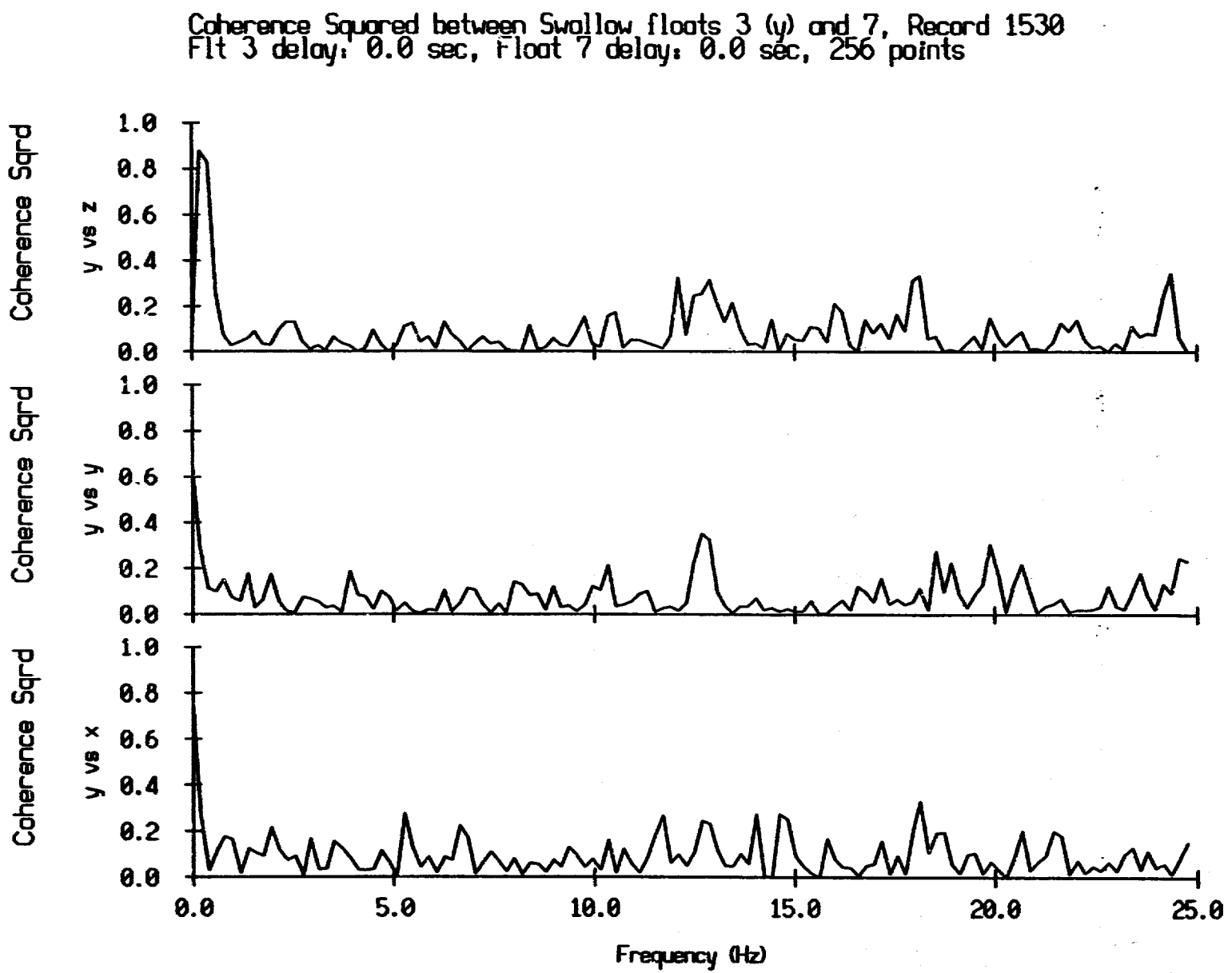
Coherence Squared between Swallow floats 3 (y) and 7, Record 1530
Flt 3 delay: 0.0 sec, Float 7 delay: 0.0 sec, 256 points
Coherence Sqrd
y vs z
y vs y
y vs x
1.0
0.8
0.6
0.4
0.2
0.0
0.0
5.0
10.0
15.0
20.0
25.0
Frequency (Hz)

Figure VI.8j

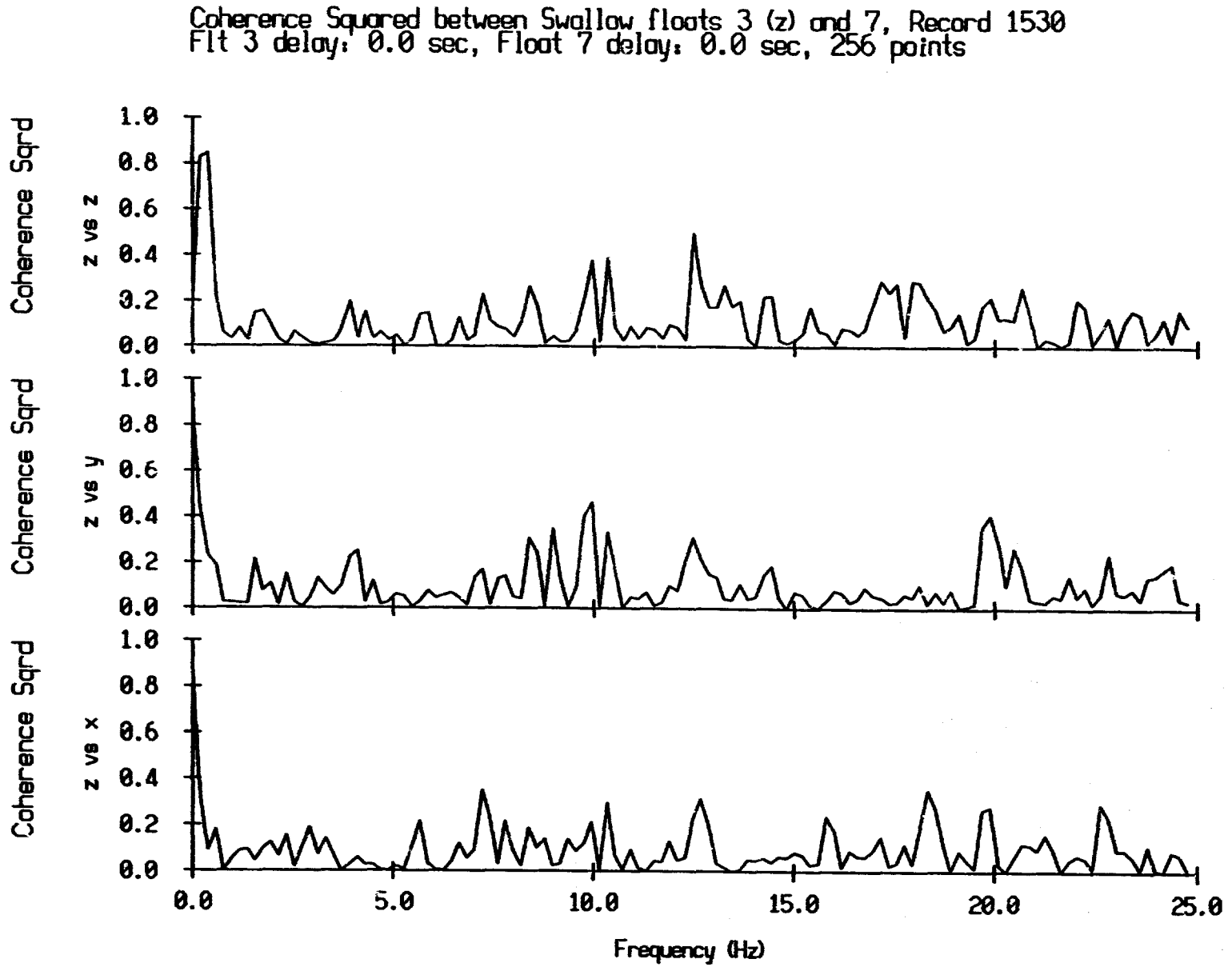
Coherence Squared between Swallow floats 3 (z) and 7, Record 1530
Flt 3 delay: 0.0 sec, Float 7 delay: 0.0 sec, 256 points
Coherence Sqrd
z vs z
Coherence Sqrd
z vs y
Coherence Sqrd
z vs x
1.0
0.8
0.6
0.4
0.2
0.0
0.0
5.0
10.0
15.0
20.0
25.0
Frequency (Hz)

Figure V.18k

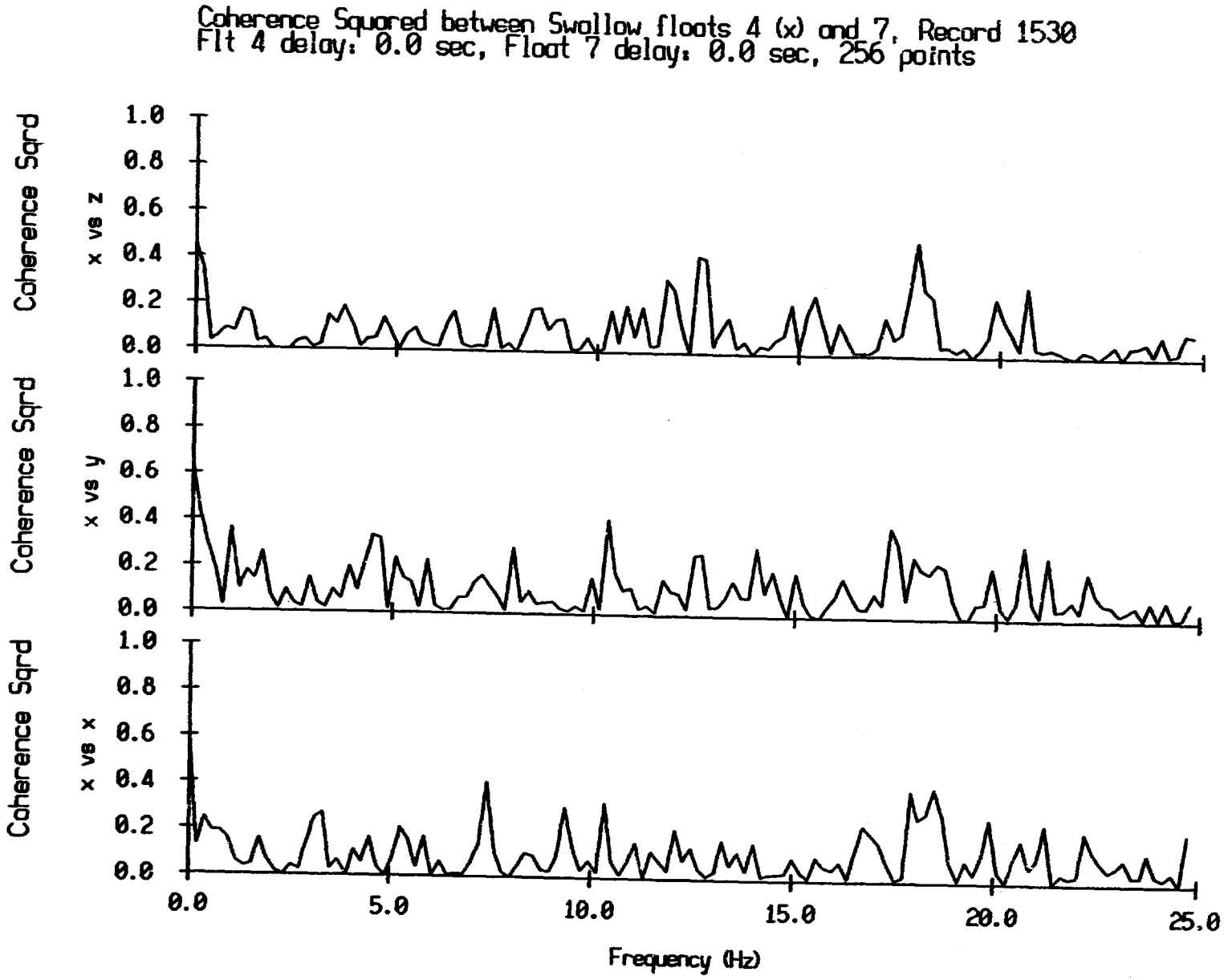
Coherence Squared between Swallow floats 4 (x) and 7, Record 1530
Flt 4 delay: 0.0 sec, Float 7 delay: 0.0 sec, 256 points
Coherence Sqrd
x vs z
x vs y
x vs x
1.0
0.8
0.6
0.4
0.2
0.0
0.0
5.0
10.0
15.0
20.0
25.0
Frequency (Hz)

Figure VI.9i

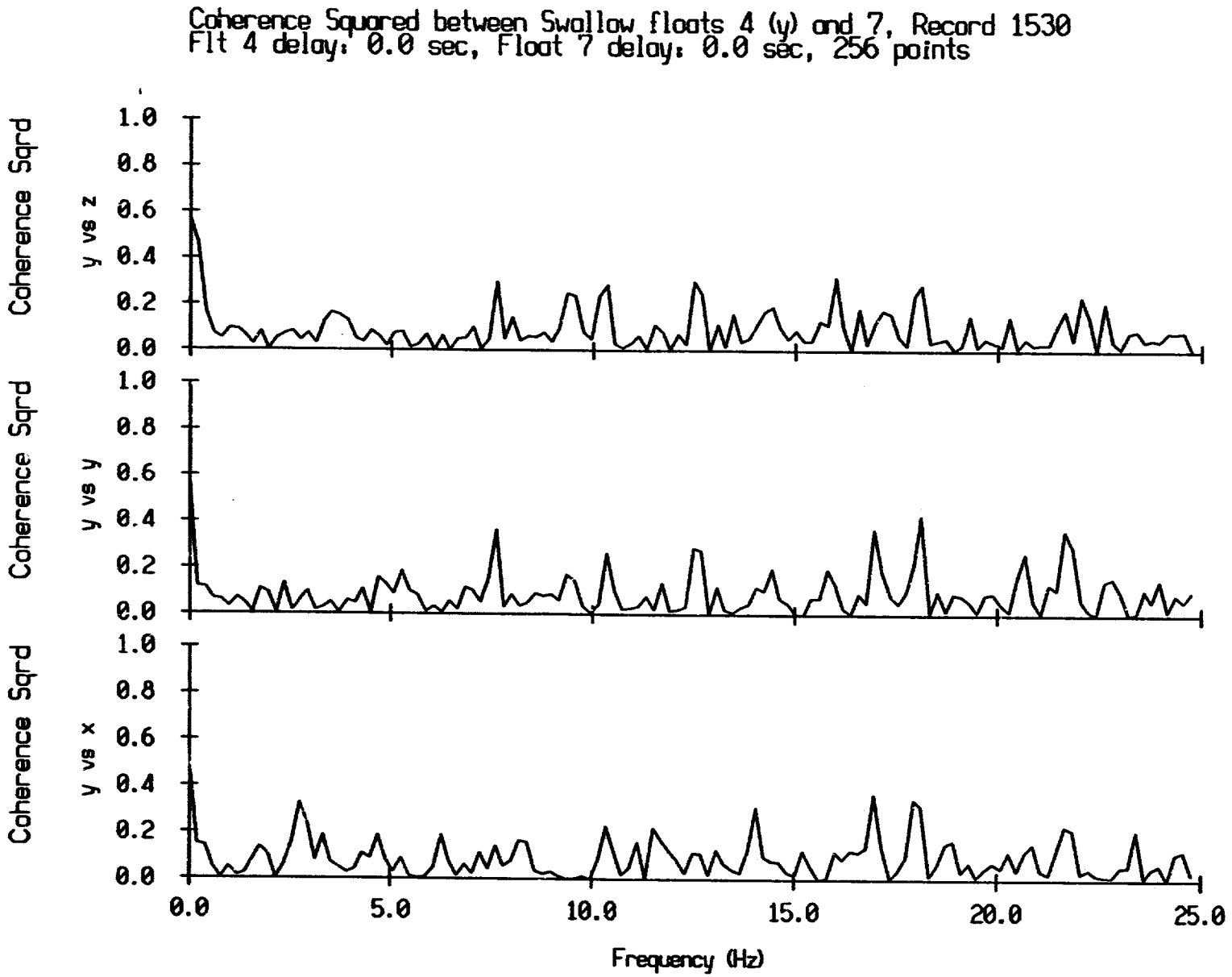
Coherence Squared between Swallow floats 4 (y) and 7, Record 1530
Flt 4 delay: 0.0 sec, Float 7 delay: 0.0 sec, 256 points
Coherence Sqrd
y vs z
Coherence Sqrd
y vs y
Coherence Sqrd
y vs x
1.0
0.8
0.6
0.4
0.2
0.0
0.0
5.0
10.0
15.0
20.0
25.0
Frequency (Hz)

Figure VI.9j

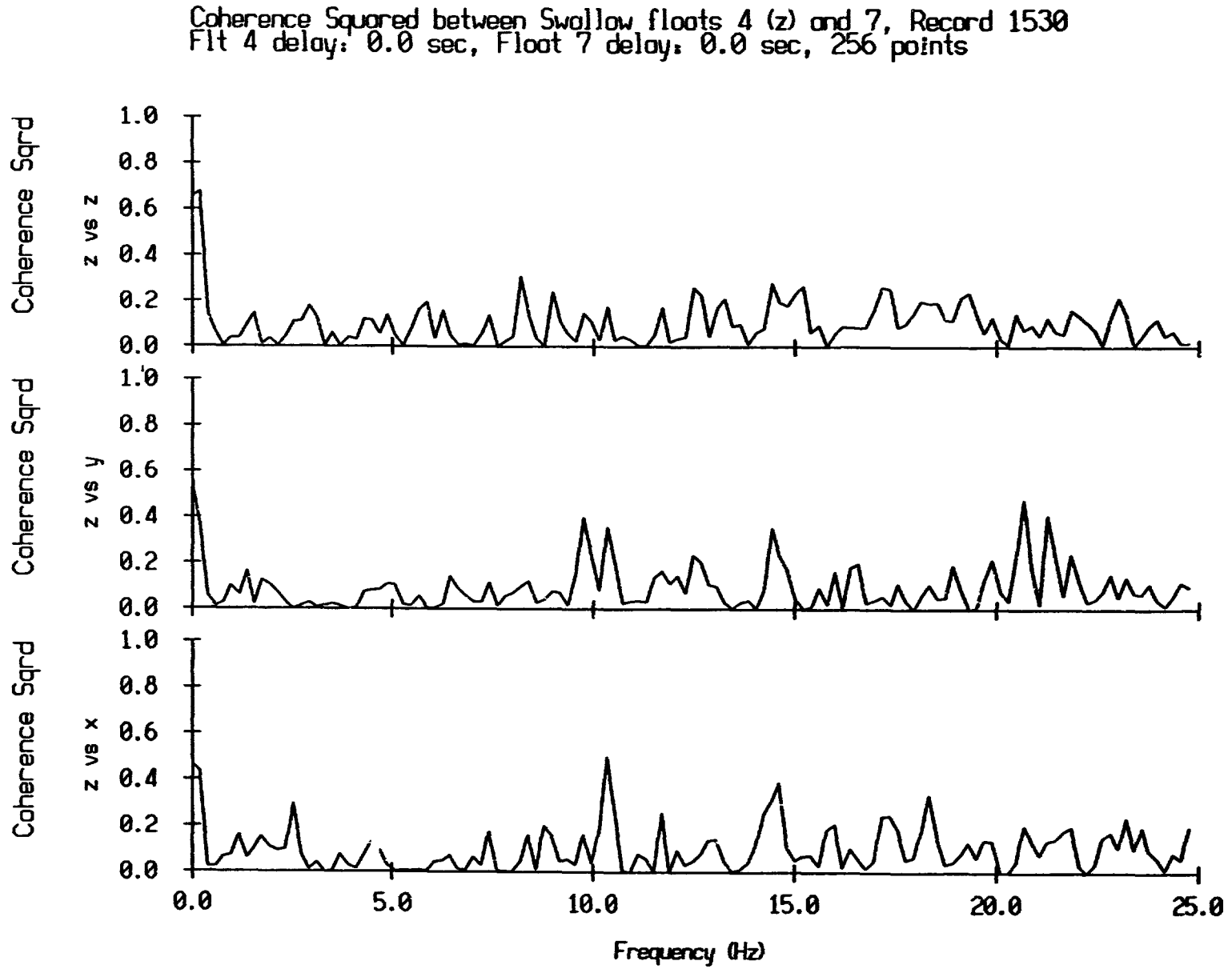
Coherence Squared between Swallow floats 4 (z) and 7, Record 1530
Flt 4 delay: 0.0 sec, Float 7 delay: 0.0 sec, 256 points
Coherence Sqrd
z vs z
z vs y
z vs x
1.0
0.8
0.6
0.4
0.2
0.0
0.0
5.0
10.0
15.0
20.0
25.0
Frequency (Hz)

Figure VI.9k

Individual OBS Data Recording Times April, May 1987

Time (sec) of First Sample for Each OBS

Event	1	2	4	5	6	8	12	13	14
073	----	57.057	57.488	56.559	56.825	58.441	57.310	57.695	57.452
097	----	57.054	57.488	56.572	56.826	58.470	57.313	57.698	57.461
105	57.504	57.053	57.488	56.576	56.827	58.480	57.314	57.699	57.464
106	57.504	57.053	57.488	56.577	56.827	58.481	57.314	57.699	57.465
107	57.504	57.053	57.488	56.577	56.827	58.483	57.314	57.699	57.465
108	57.504	57.053	57.488	56.578	56.827	58.484	57.314	57.699	57.466
109	57.504	57.053	57.488	56.579	56.827	58.485	57.314	57.699	57.466
110	57.504	57.053	57.488	56.579	56.827	58.486	57.315	57.700	57.466
111	57.504	57.053	57.488	56.580	56.827	58.487	57.315	57.700	57.467
112	57.504	57.052	57.488	56.580	56.827	58.489	57.315	57.700	57.467
113	57.504	57.052	57.488	56.581	56.827	58.490	57.315	57.700	57.468
114	57.504	57.052	57.488	56.581	56.827	58.491	57.315	57.700	57.468
115	57.505	57.052	57.488	56.582	56.827	58.492	----	57.700	57.468
116	57.505	57.052	57.488	56.582	56.827	58.494	57.315	57.700	57.469
117	57.505	57.052	57.488	56.583	56.827	58.495	----	57.700	57.469
118	57.505	57.052	57.488	56.583	56.827	58.496	57.316	57.701	57.470
119	57.505	57.052	57.488	56.584	56.828	58.497	57.316	57.701	57.470
120	57.505	57.052	57.488	56.585	56.828	58.498	57.316	57.701	57.470
121	57.505	57.051	57.488	56.585	56.828	58.500	57.316	57.701	57.471
145	57.507	57.049	57.488	56.598	56.829	58.529	57.319	57.704	57.481
309	60.609	59.913	60.485	60.235	59.887	62.964	60.474	60.864	60.955
311	60.611	*	60.485	60.248	59.888	62.994	60.477	60.867	60.965
313	60.613	59.907	60.485	60.261	59.889	*	----	60.870	60.975
315	60.615	59.905	60.485	60.274	59.891	*	60.484	60.873	60.984
317	60.617	59.902	60.485	60.287	59.892	63.082	60.487	60.877	60.994

* For obs 2, event 311 was recorded about 42 minutes earlier, at 16:18 32.910, than for the other instruments; for obs 8, event 313 was recorded about 12 minutes earlier, at 22:48 44.022, and event 315 was recorded 31 minutes early, at 04:30 04.050. The cause of these premature recordings of an event is thought to be due to misinterpretation of the clock signal.

Figure VI.10

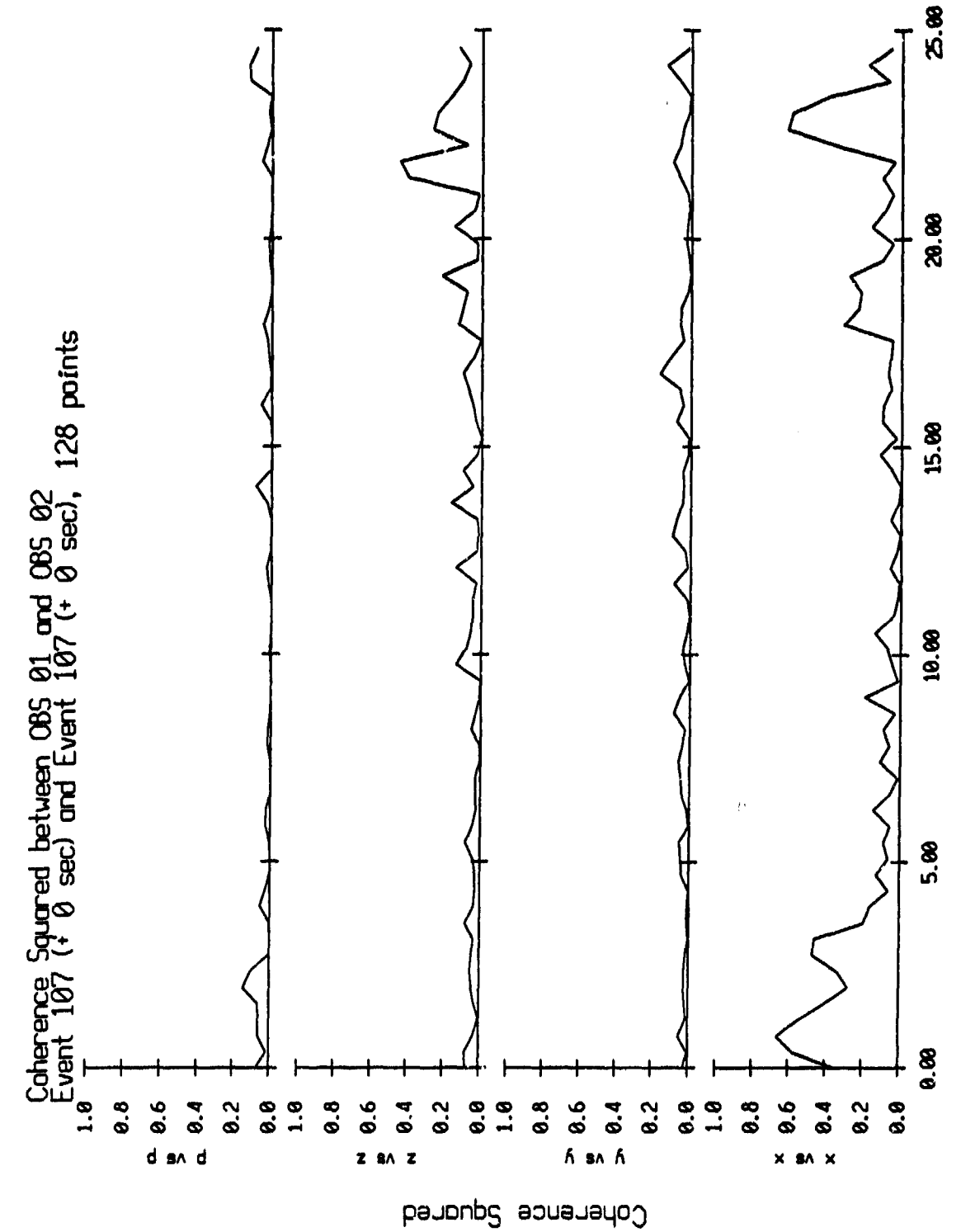
Coherence Squared between OBS 01 and OBS 02
Event 107 (+ 0 sec) and Event 107 (+ 0 sec), 128 points
Coherence Squared
p vs p
z vs z
y vs y
x vs x
1.0
0.8
0.6
0.4
0.2
0.0
0.00
5.00
10.00
15.00
20.00
25.00
Frequency (Hz)

Figure VI.11

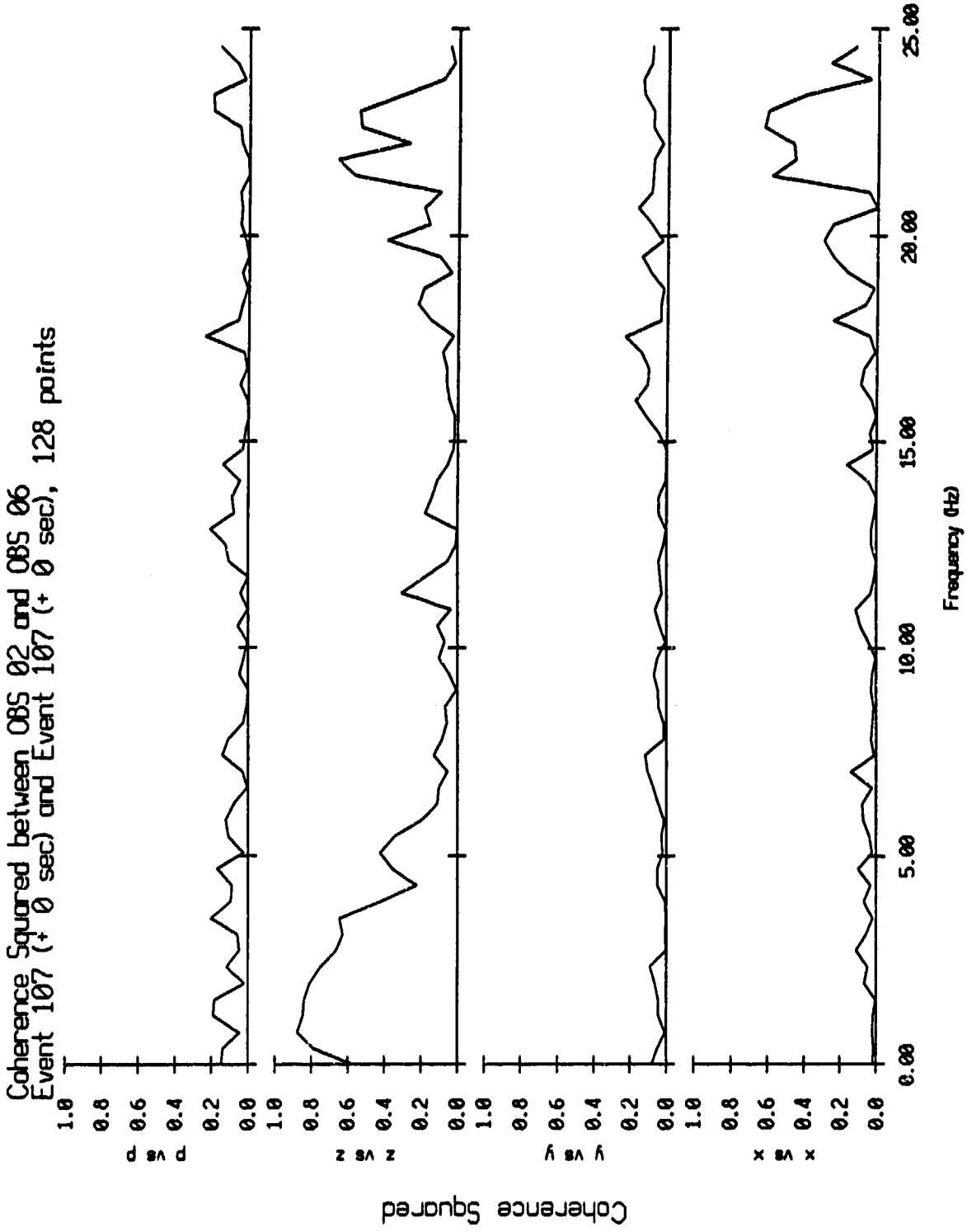
Coherence Squared between OBS 02 and OBS 06
Event 107 (+ 0 sec) and Event 107 (+ 0 sec), 128 points
Coherence Squared
p vs p
z vs z
y vs y
x vs x
1.0
0.8
0.6
0.4
0.2
0.0
0.00
5.00
10.00
15.00
20.00
25.00
Frequency (Hz)

Figure VI.12

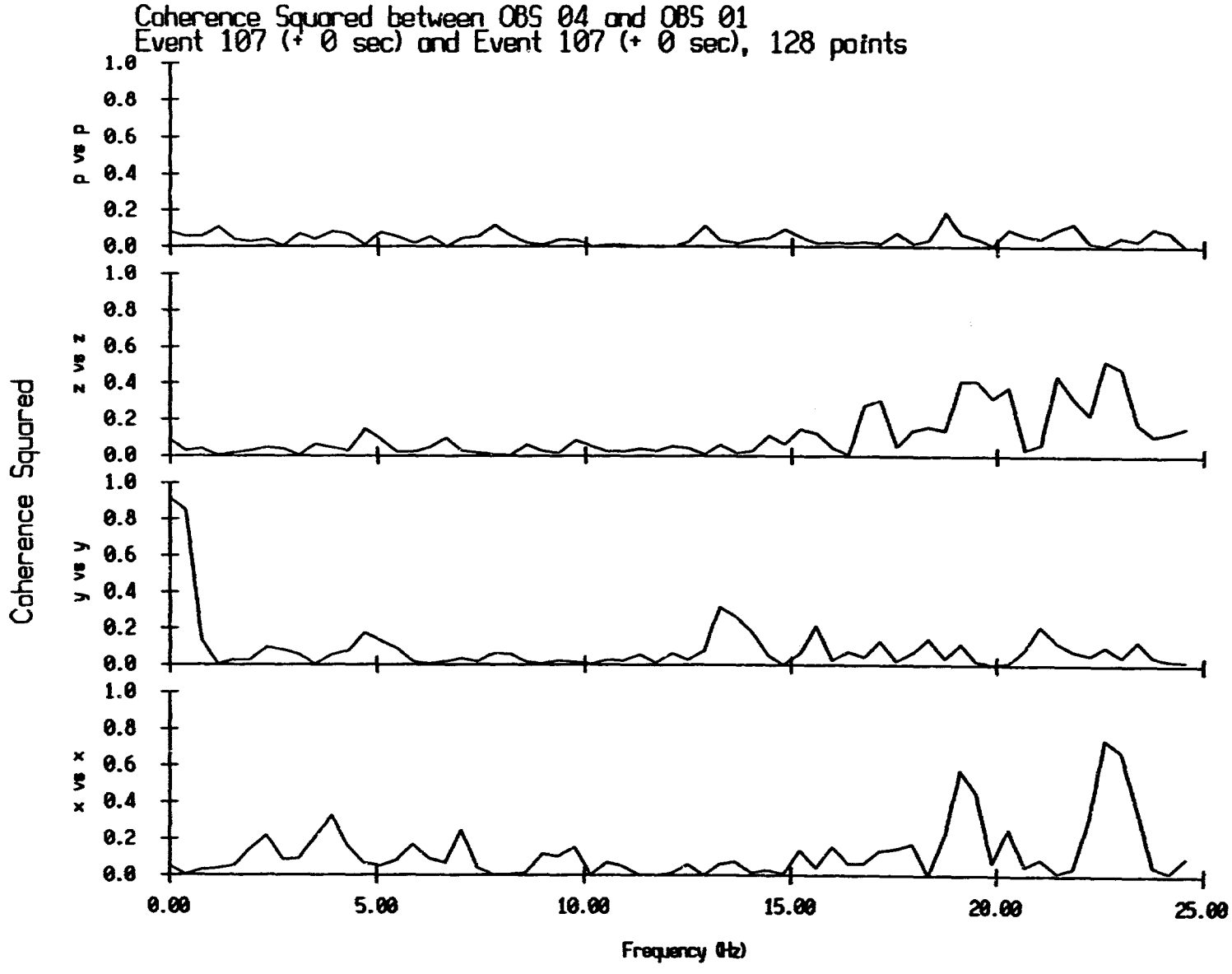
Coherence Squared between OBS 04 and OBS 01
Event 107 (+ 0 sec) and Event 107 (+ 0 sec), 128 points
Coherence Squared
p vs p
z vs z
y vs y
x vs x
1.0
0.8
0.6
0.4
0.2
0.0
0.00
5.00
10.00
15.00
20.00
25.00
Frequency (Hz)

Figure VI.13

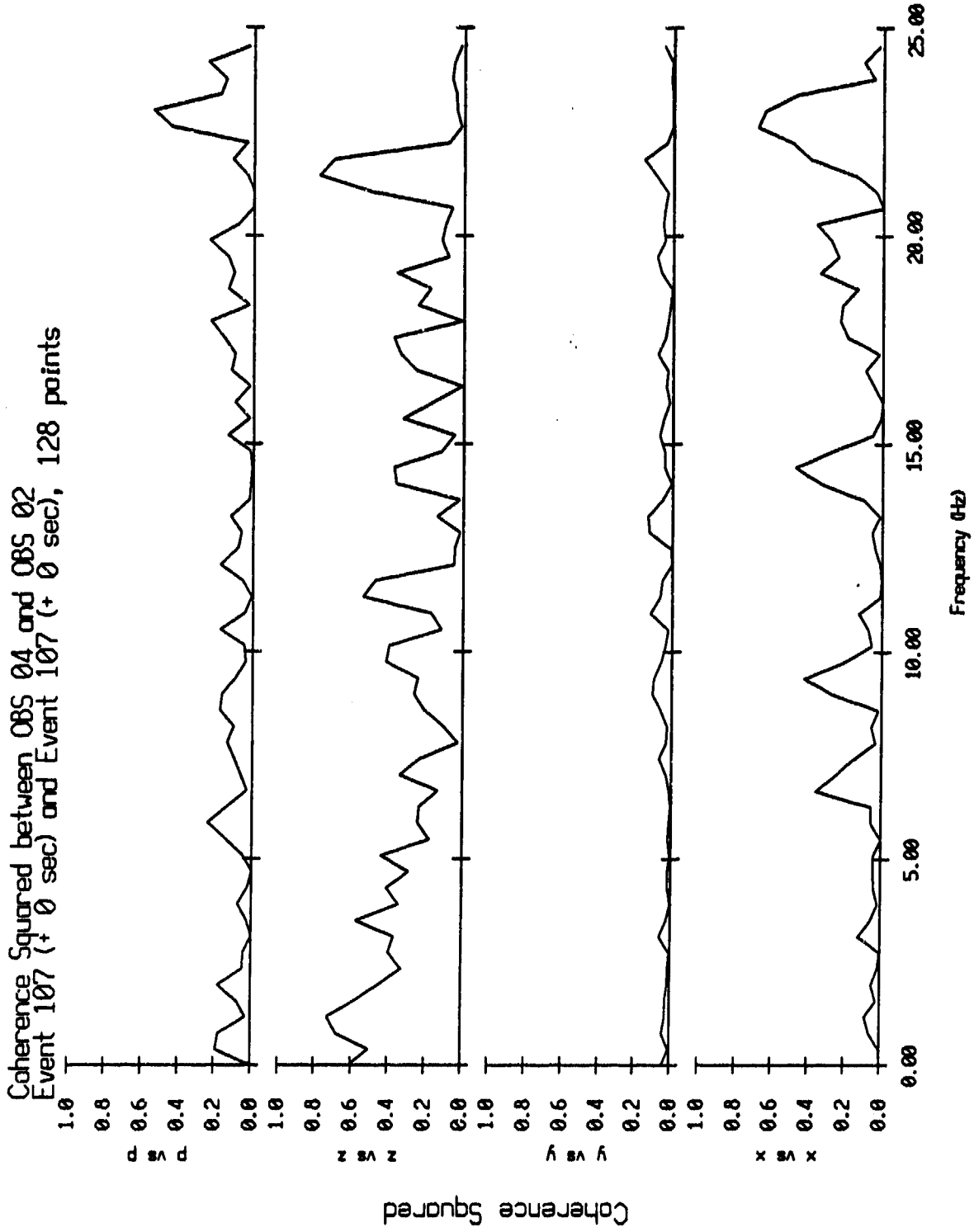
Coherence Squared between OBS 04 and OBS 02
Event 107 (+ 0 sec) and Event 107 (+ 0 sec), 128 points
p vs p
z vs z
y vs y
x vs x
1.0
0.8
0.6
0.4
0.2
0.0
0.00
5.00
10.00
15.00
20.00
25.00
Coherence Squared
Frequency (Hz)

Figure VI.14

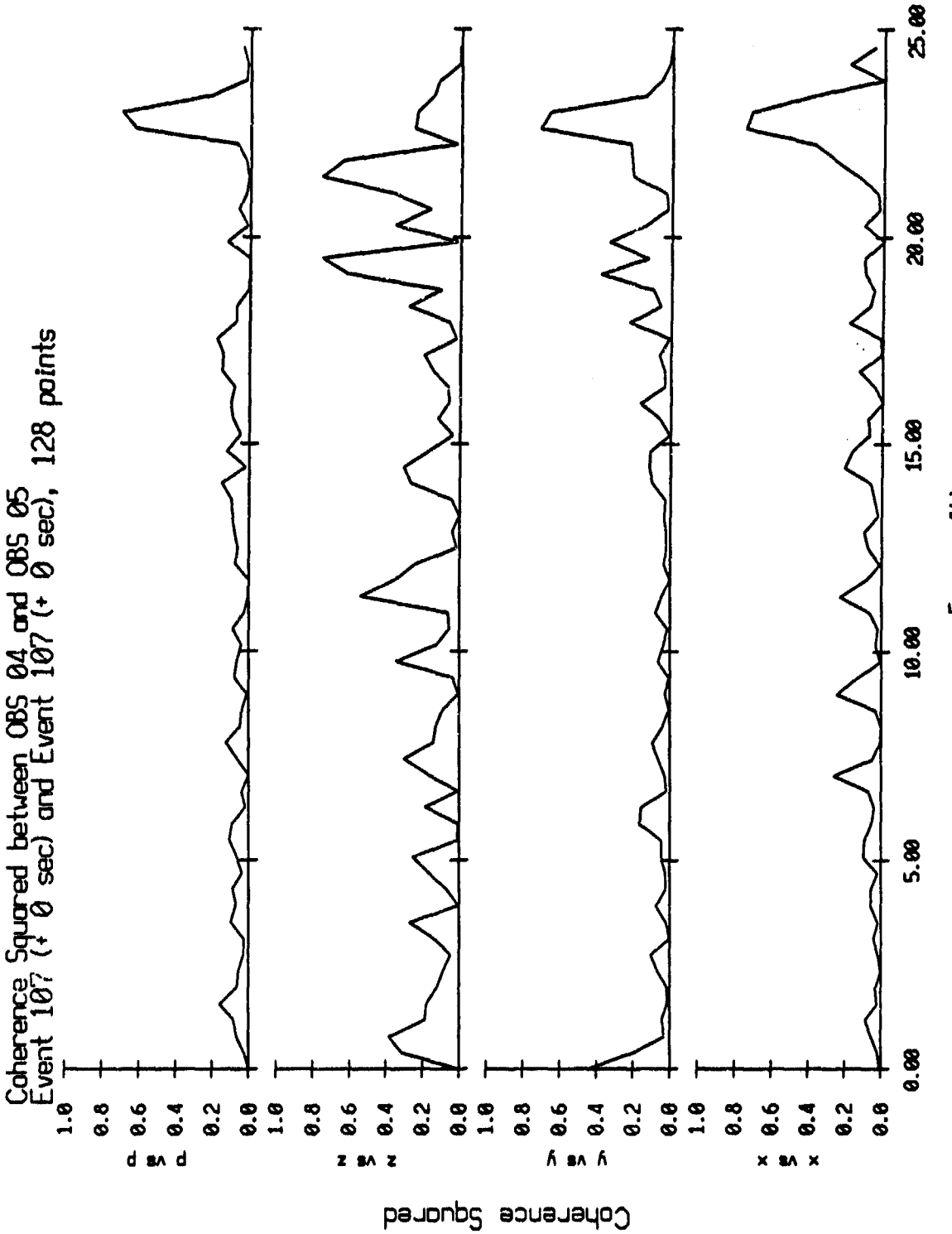
Coherence Squared between OBS 04 and OBS 05
Event 107 (+ 0 sec) and Event 107 (+ 0 sec), 128 points
Coherence Squared
P vs P
Z vs Z
Y vs Y
X vs X
1.0
0.8
0.6
0.4
0.2
0.0
0.00
5.00
10.00
15.00
20.00
25.00
Frequency (Hz)

Figure VI.15

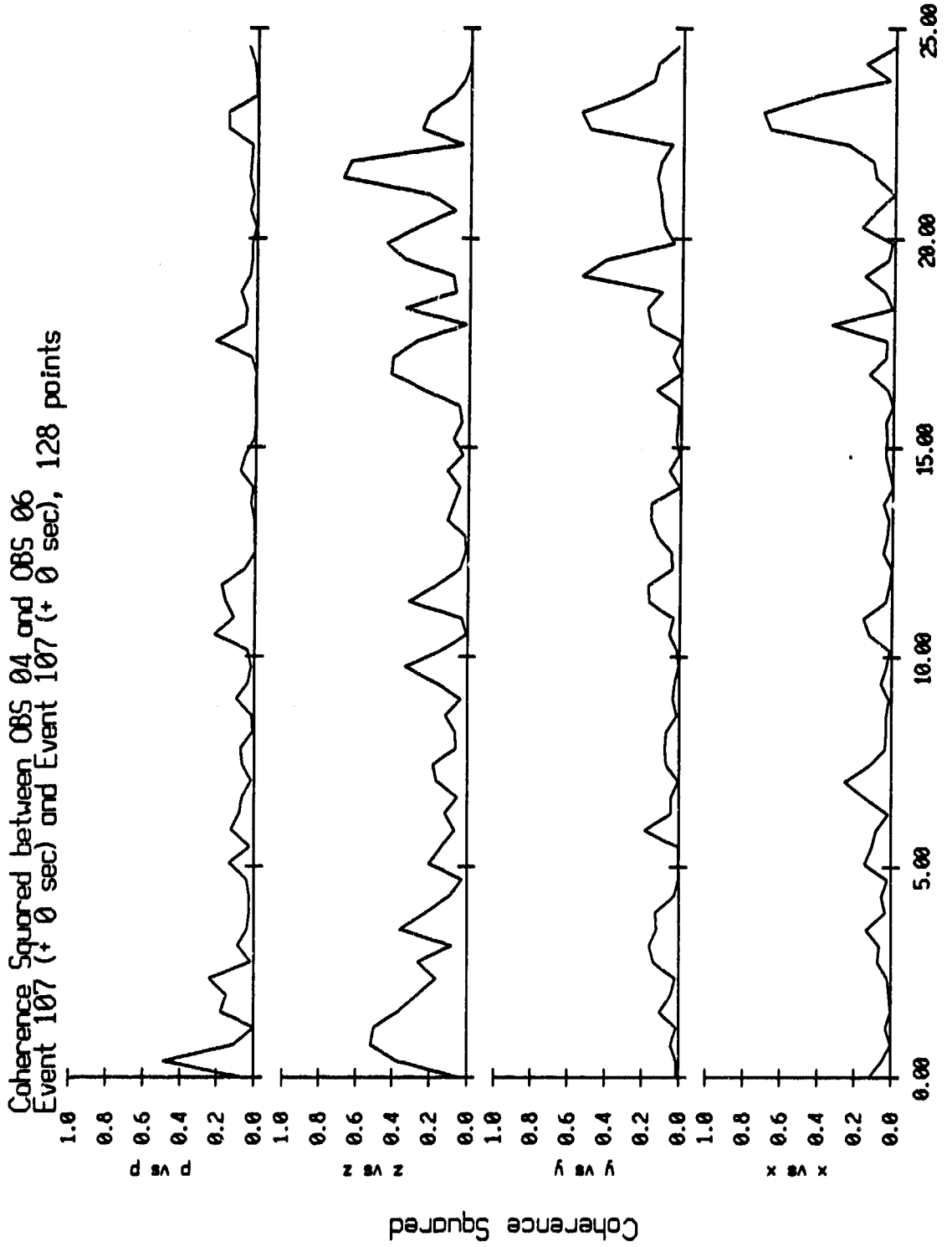
Coherence Squared between OBS 04 and OBS 06
Event 107 (+ 0 sec) and Event 107 (+ 0 sec), 128 points
p vs p
z vs z
y vs y
x vs x
1.0
0.8
0.6
0.4
0.2
0.0
0.00
5.00
10.00
15.00
20.00
25.00
Frequency (Hz)
Coherence Squared

Figure VI.16

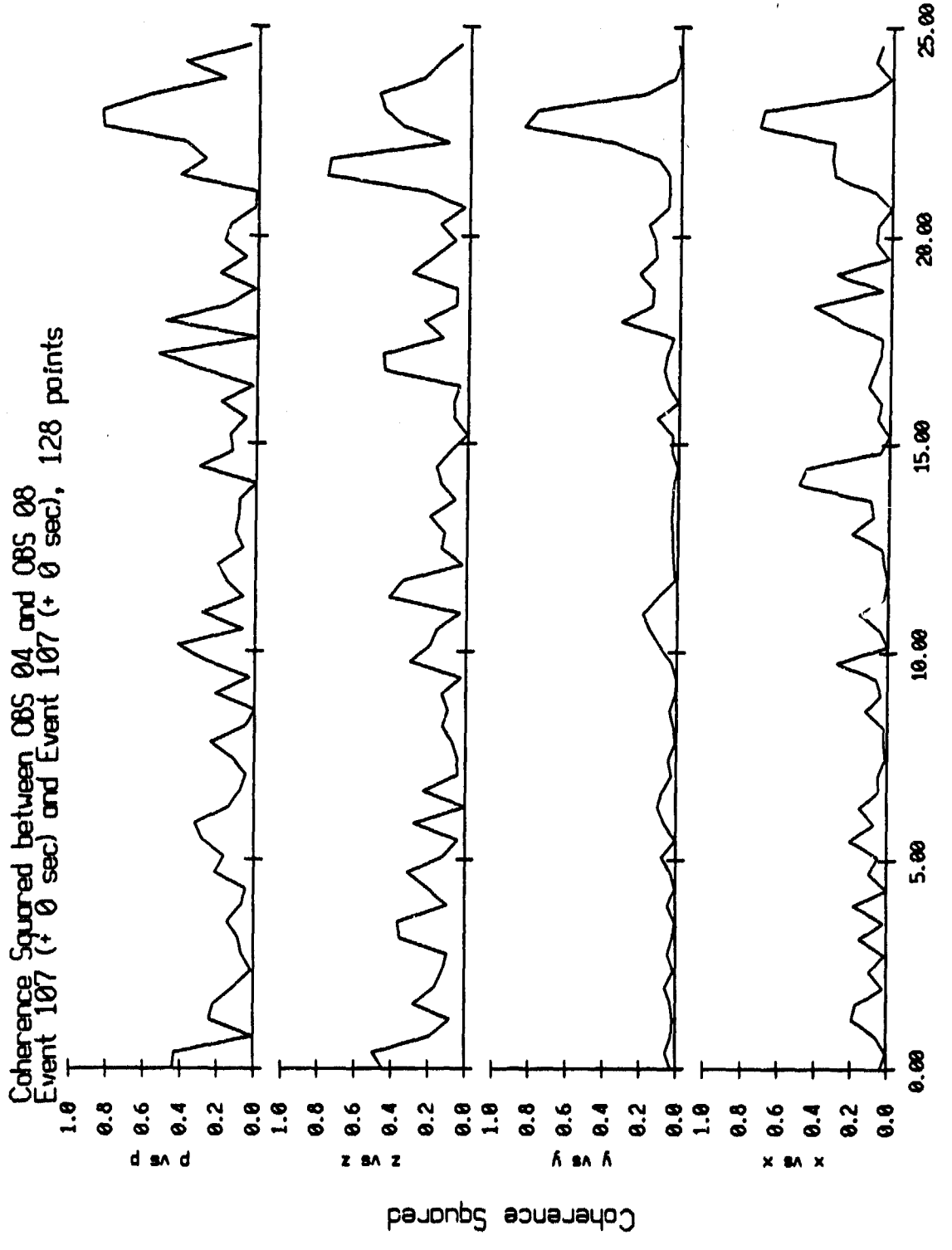
Coherence Squared between OBS 04 and OBS 08
Event 107 (+ 0 sec) and Event 107 (+ 0 sec), 128 points
p vs p
z vs z
y vs y
x vs x
1.0
0.8
0.6
0.4
0.2
0.0
0.00
5.00
10.00
15.00
20.00
25.00
Frequency (Hz)
Coherence Squared

Figure VI.17

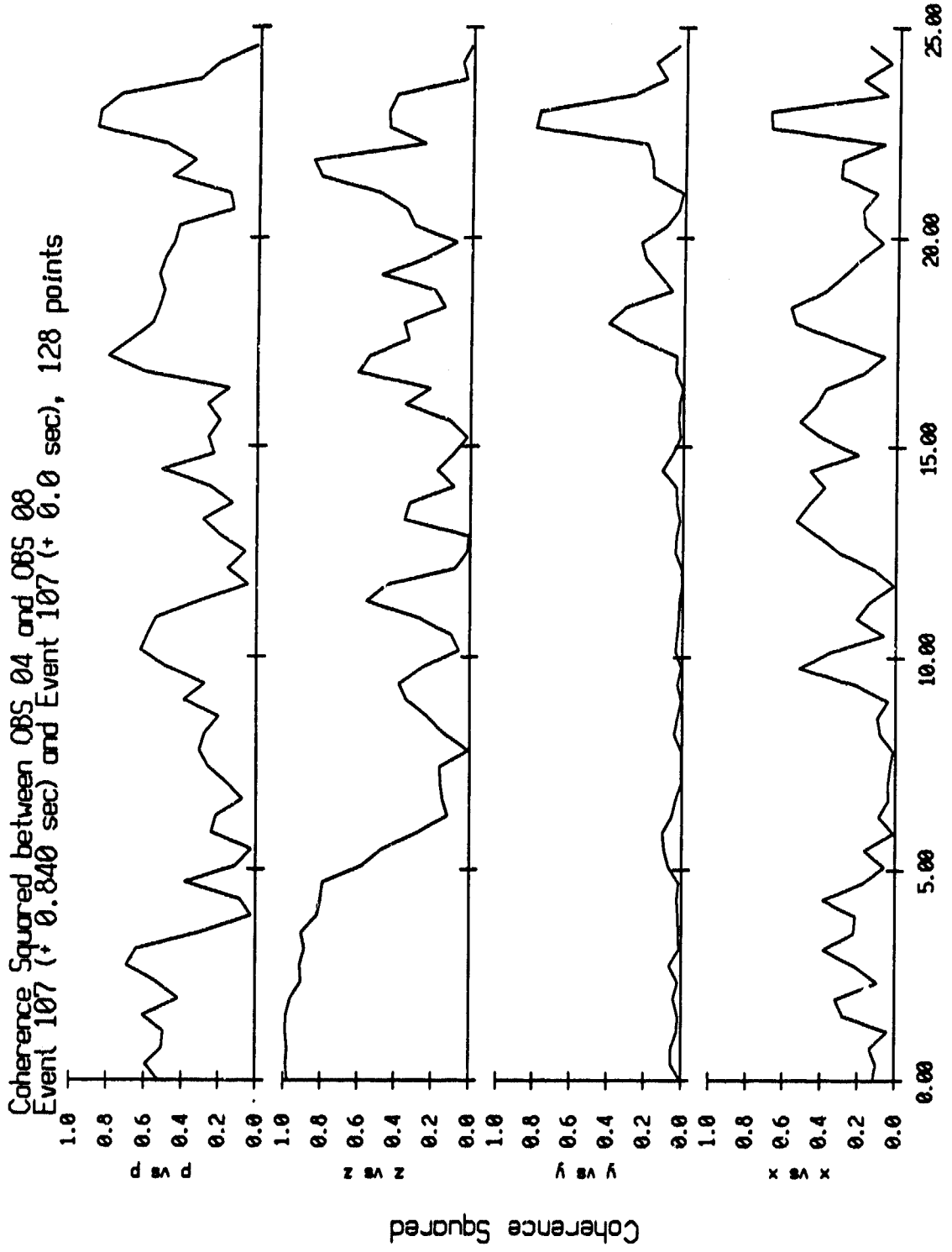
Coherence Squared between OBS 04 and OBS 08
Event 107 (+ 0.840 sec) and Event 107 (+ 0.0 sec), 128 points
P vs P
Z vs Z
Y vs Y
X vs X
1.0
0.8
0.6
0.4
0.2
0.0
0.00
5.00
10.00
15.00
20.00
25.00
Frequency (Hz)
Coherence Squared

Figure VI.18

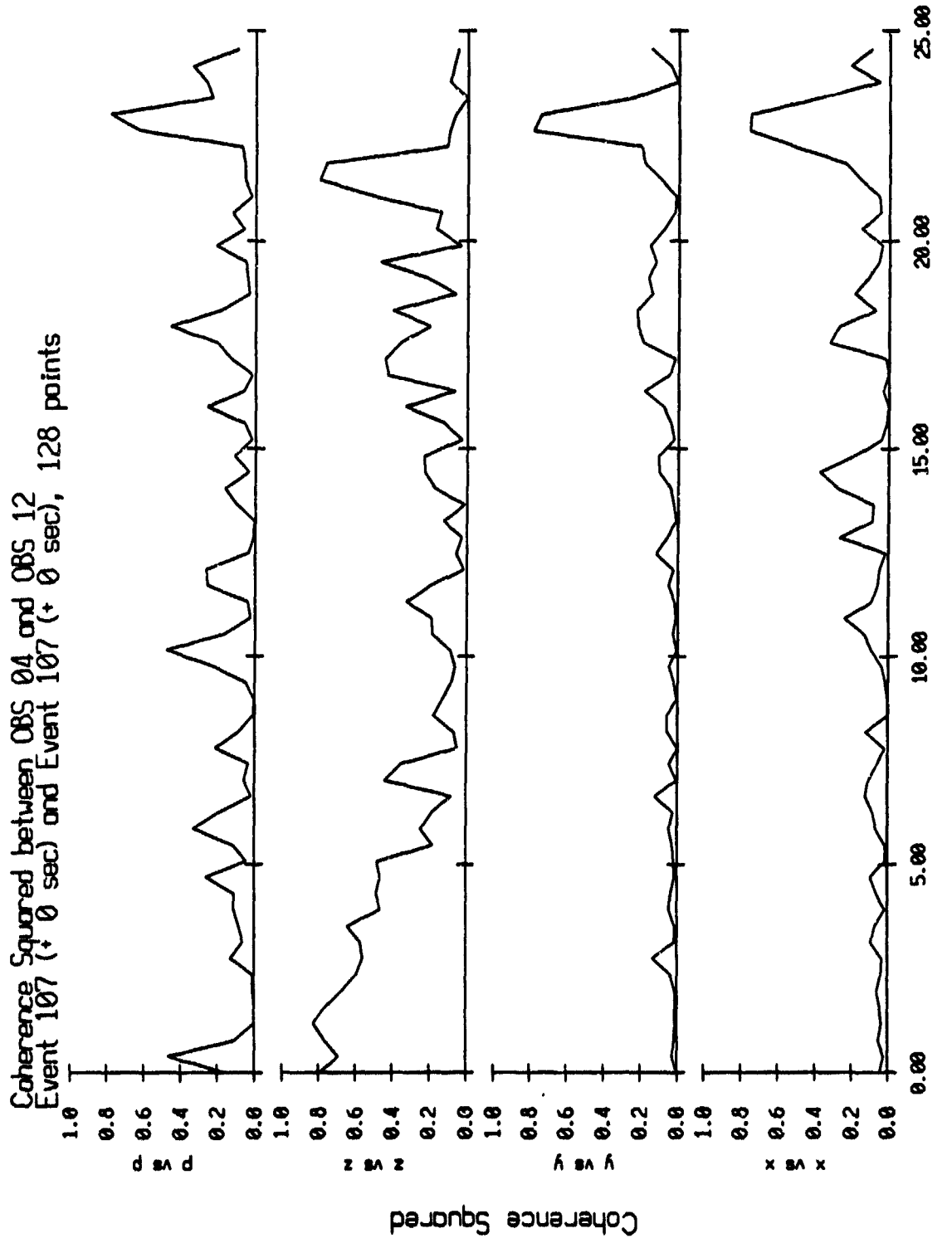
Coherence Squared between OBS 04 and OBS 12
Event 107 (+ 0 sec) and Event 107 (+ 0 sec), 128 points
Coherence Squared
p vs p
z vs z
y vs y
x vs x
1.0
0.8
0.6
0.4
0.2
0.0
0.00
5.00
10.00
15.00
20.00
25.00
Frequency (Hz)

Figure VI.19

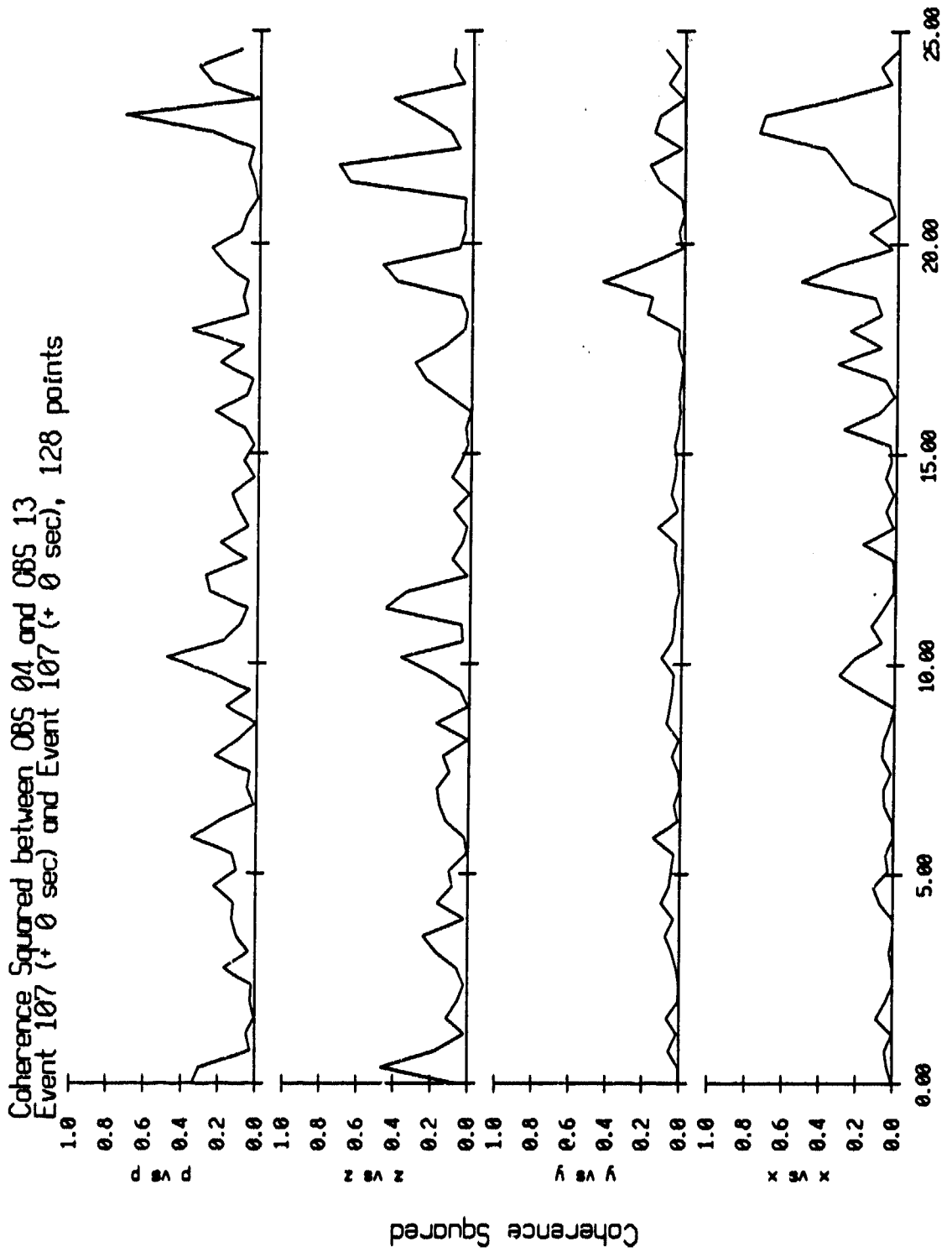
Coherence Squared between OBS 04 and OBS 13
Event 107 (+ 0 sec) and Event 107 (+ 0 sec), 128 points
P vs P
Z vs Z
Y vs Y
X vs X
Coherence Squared
1.0
0.8
0.6
0.4
0.2
0.0
0.00
5.00
10.00
15.00
20.00
25.00
Frequency (Hz)

Figure VI.20

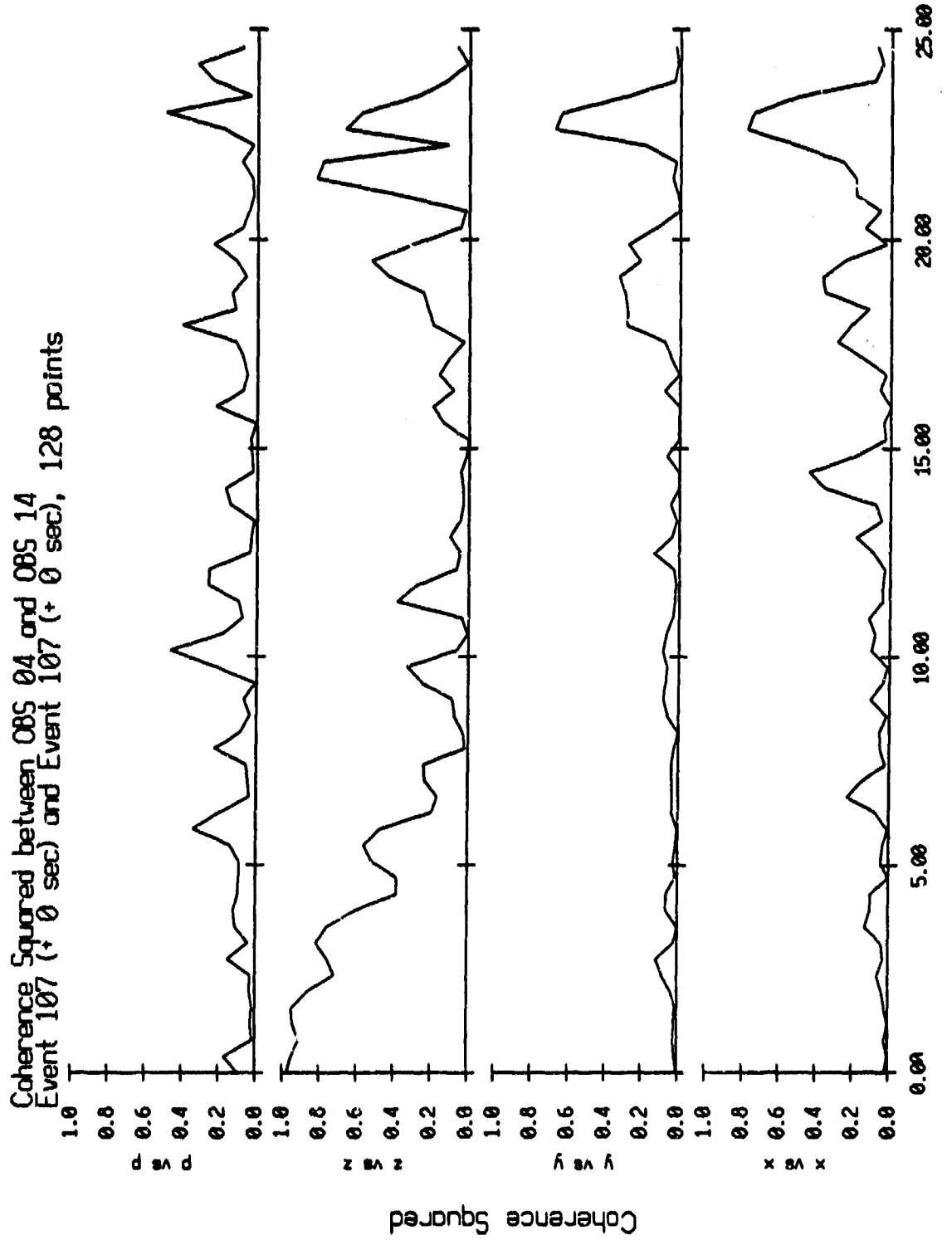
Coherence Squared between OBS 04 and OBS 14
Event 107 (+ 0 sec) and Event 107 (+ 0 sec), 128 points
Coherence Squared
p vs p
z vs z
y vs y
x vs x
1.0
0.8
0.6
0.4
0.2
0.0
0.00
5.00
10.00
15.00
20.00
25.00
Frequency (Hz)

Figure VI.21

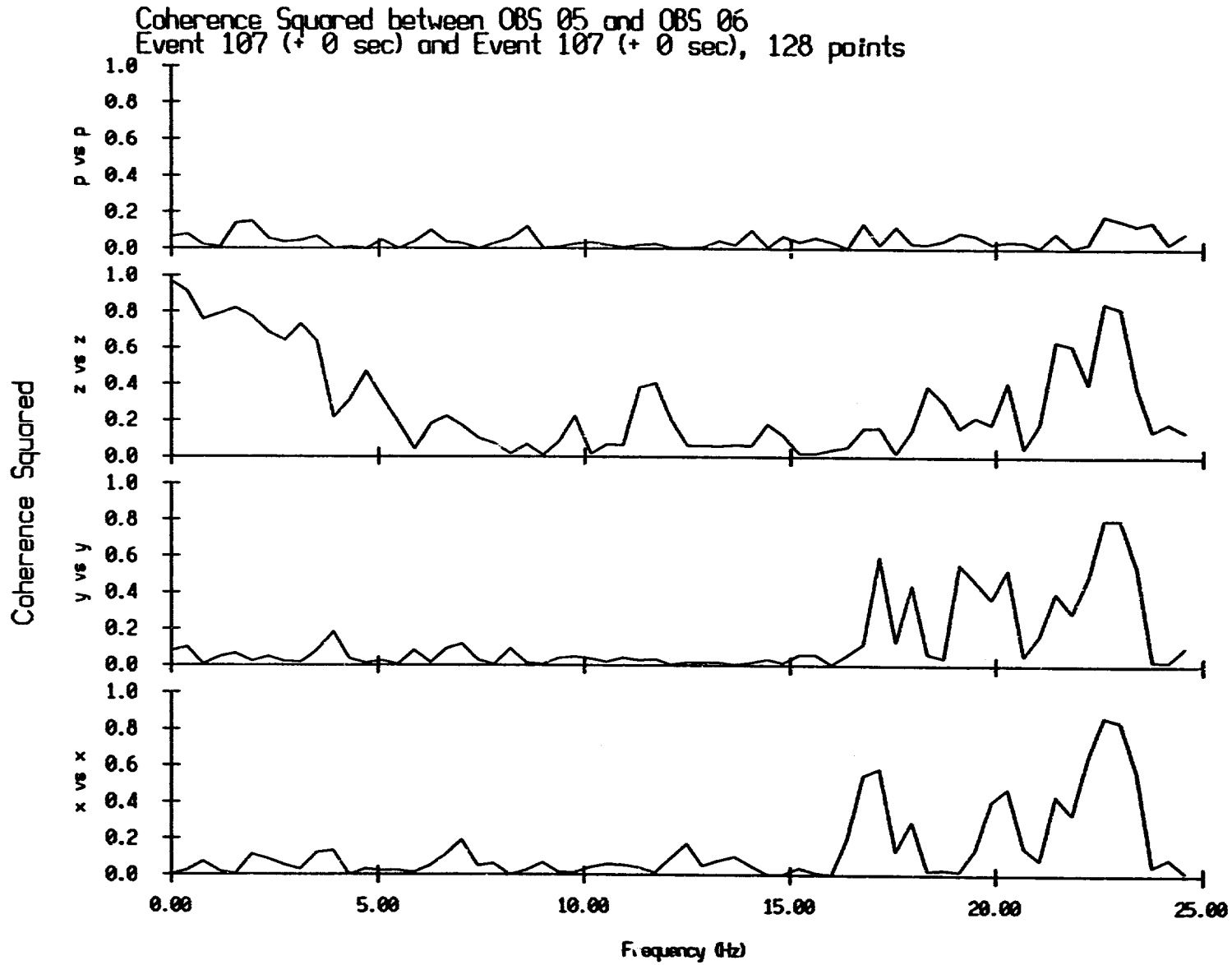
Coherence Squared between OBS 05 and OBS 06
Event 107 (+ 0 sec) and Event 107 (+ 0 sec), 128 points
Coherence Squared
p vs p
z vs z
y vs y
x vs x
1.0
0.8
0.6
0.4
0.2
0.0
0.00
5.00
10.00
15.00
20.00
25.00
Frequency (Hz)

Figure VI.22

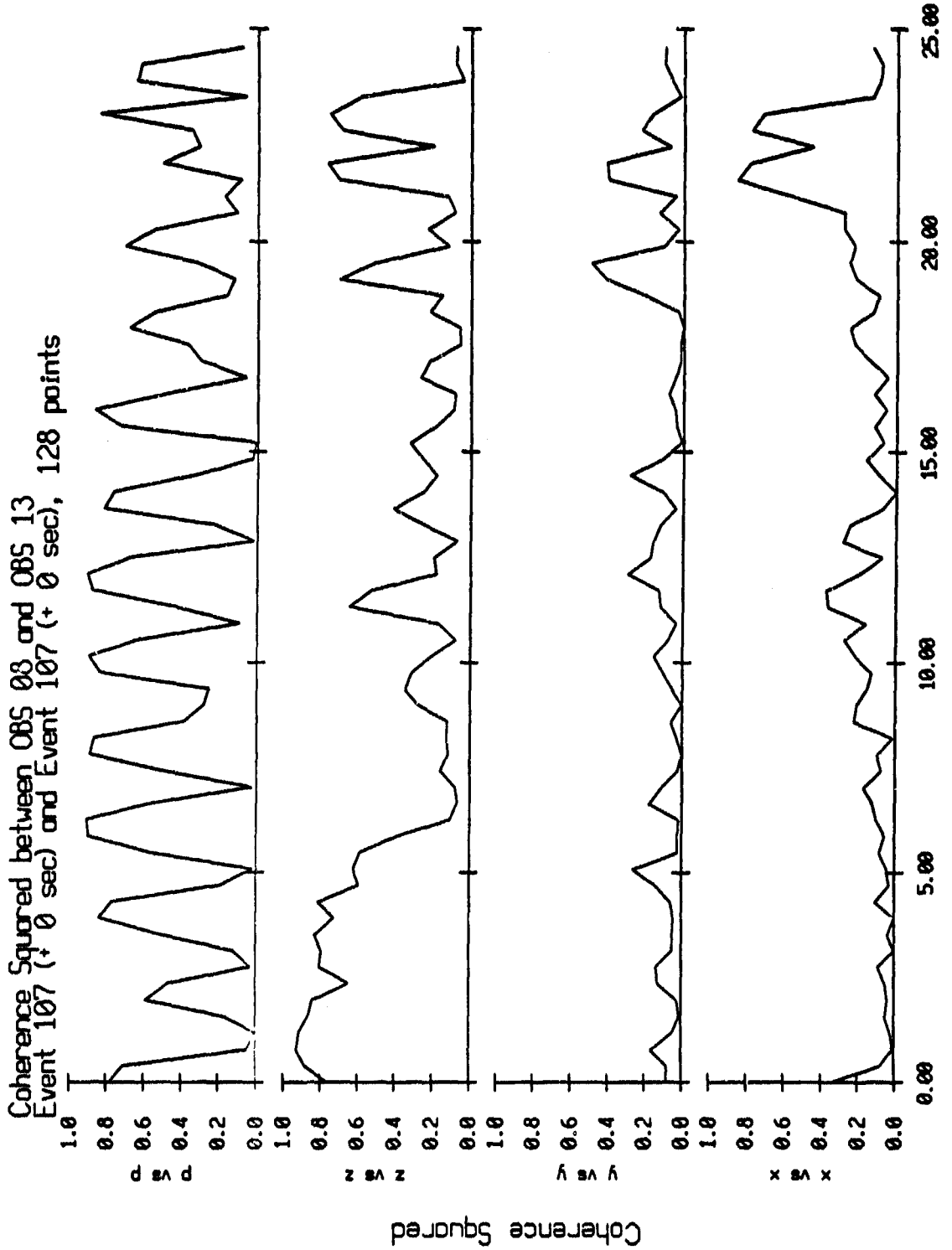
Coherence Squared between OBS 03 and OBS 13
Event 107 (+ 0 sec) and Event 107 (+ 0 sec), 128 points
Coherence Squared
p vs p
z vs z
y vs y
x vs x
1.0
0.8
0.6
0.4
0.2
0.0
0.00
5.00
10.00
15.00
20.00
25.00
Frequency (Hz)

Figure VI.23

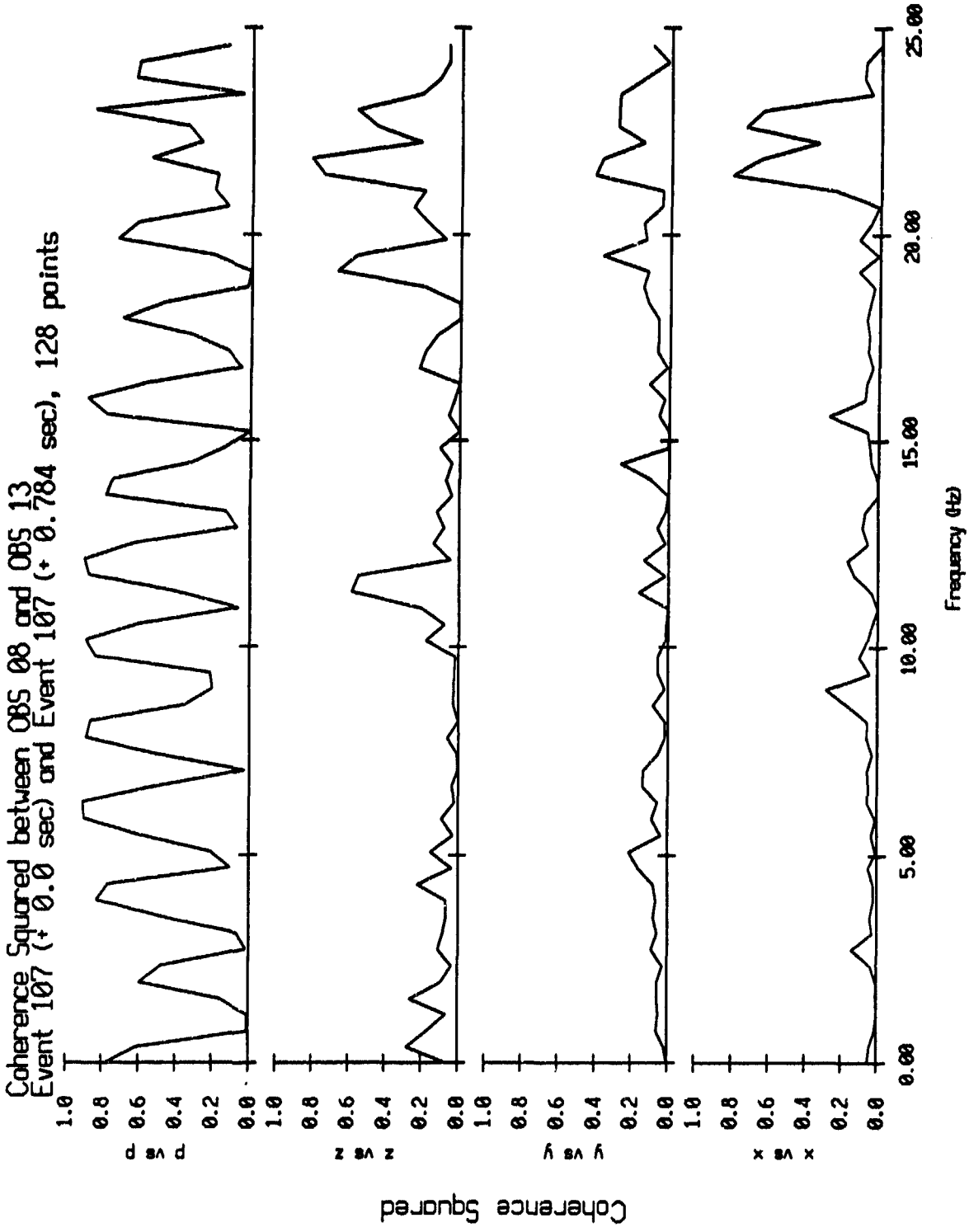
Coherence Squared between OBS 08 and OBS 13
Event 107 (+ 0.0 sec) and Event 107 (+ 0.784 sec), 128 points
p vs p
z vs z
y vs y
x vs x
1.0
0.8
0.6
0.4
0.2
0.0
0.00
5.00
10.00
15.00
20.00
25.00
Frequency (Hz)
Coherence Squared

Figure VI.24

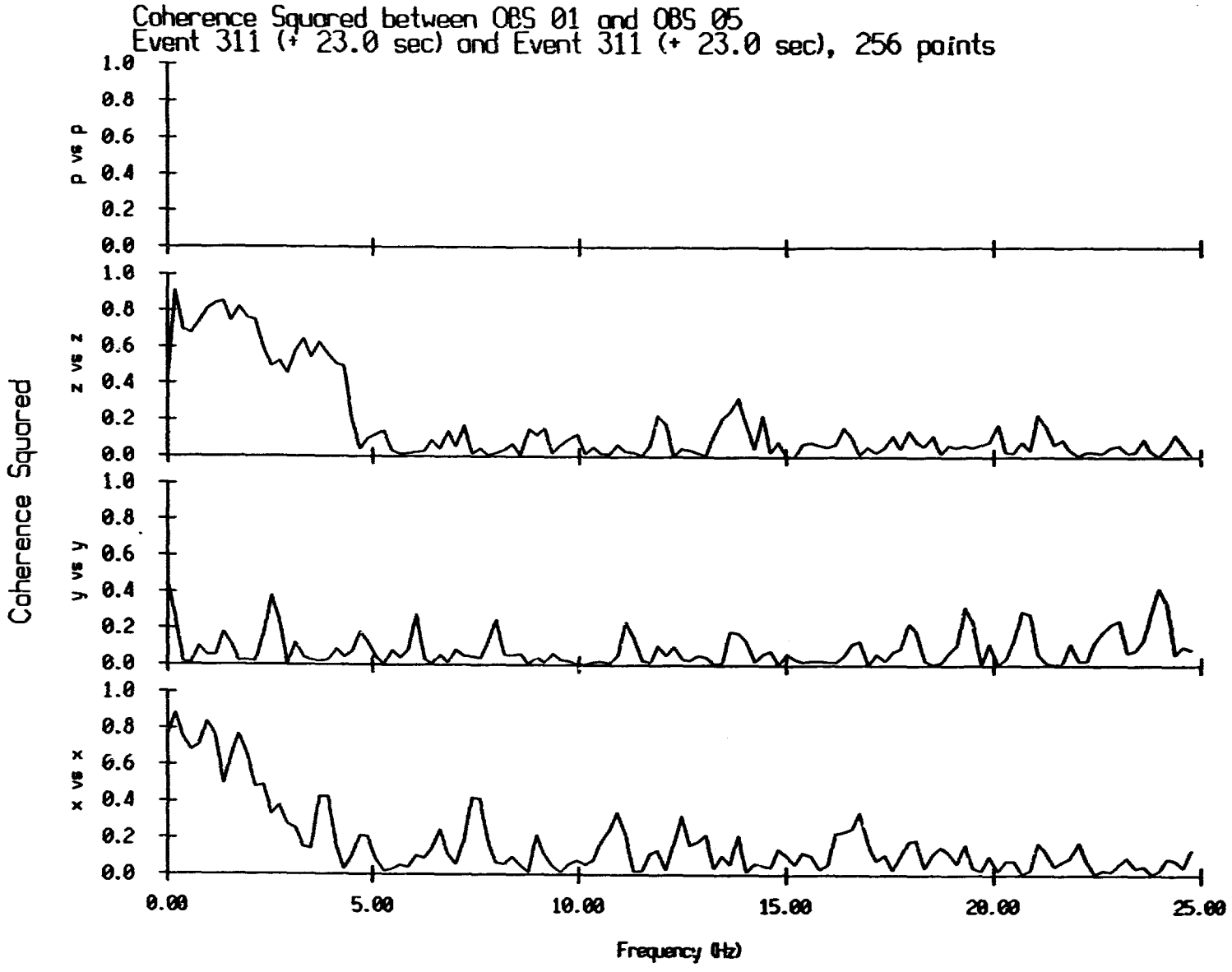
Coherence Squared between OBS 01 and OBS 05
Event 311 (+ 23.0 sec) and Event 311 (+ 23.0 sec), 256 points
Coherence Squared
p vs p
z vs z
y vs y
x vs x
1.0
0.8
0.6
0.4
0.2
0.0
0.00
5.00
10.00
15.00
20.00
25.00
Frequency (Hz)

Figure VI.25

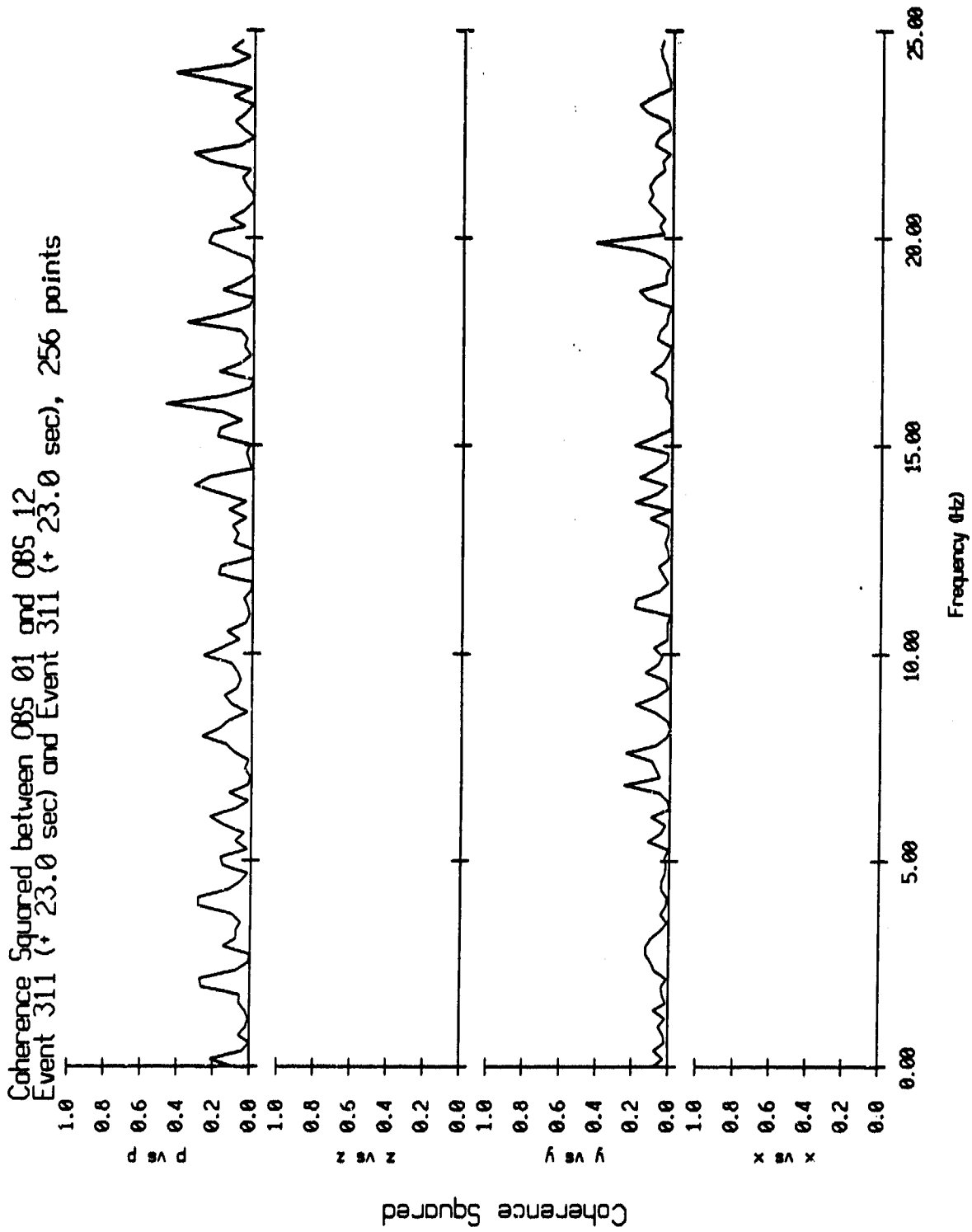
Coherence Squared between OBS 01 and OBS 12
Event 311 (+ 23.0 sec) and Event 311 (+ 23.0 sec), 256 points
Coherence Squared
P vs P
Z vs Z
Y vs Y
X vs X
1.0
0.8
0.6
0.4
0.2
0.0
0.5
0.00
5.00
10.00
15.00
20.00
25.00
Frequency (Hz)

Figure VI.26

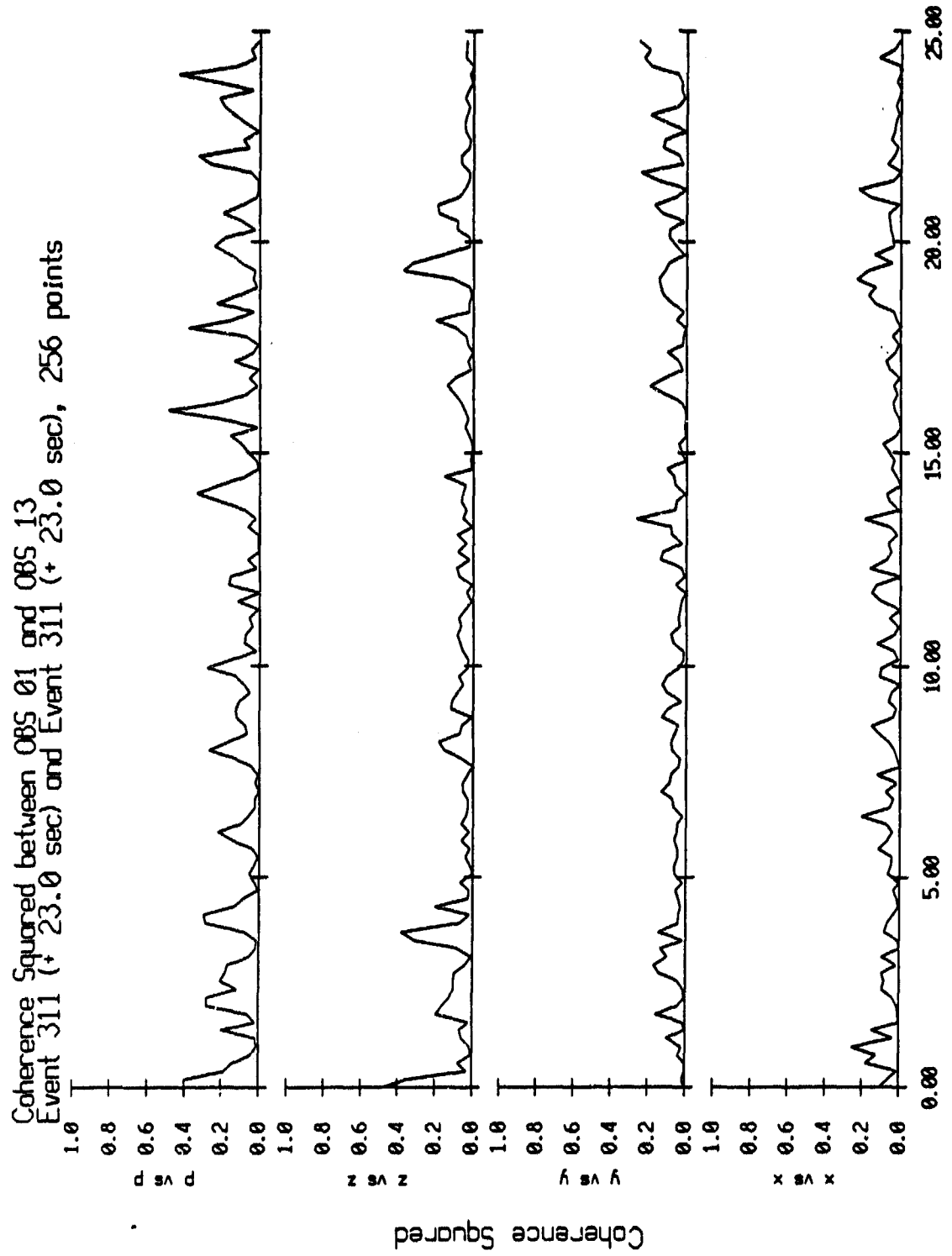
Coherence Squared between OBS 01 and OBS 13
Event 311 (+ 23.0 sec) and Event 311 (+ 23.0 sec), 256 points
Coherence Squared
P vs P
Z vs Z
Y vs Y
X vs X
1.0
0.8
0.6
0.4
0.2
0.0
0.00
5.00
10.00
15.00
20.00
25.00
Frequency (Hz)

Figure VI.27

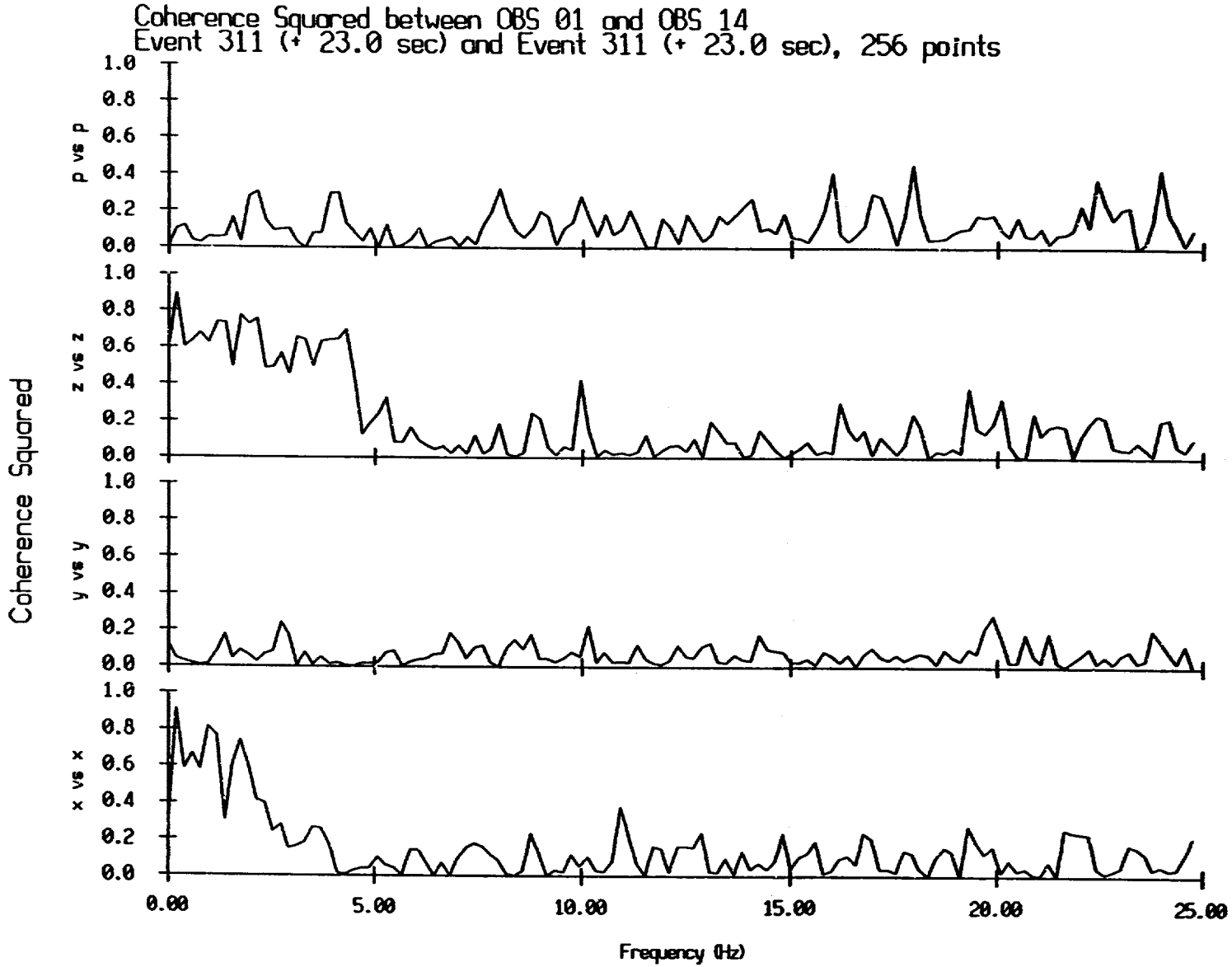
Coherence Squared between OBS 01 and OBS 14
Event 311 (+ 23.0 sec) and Event 311 (+ 23.0 sec), 256 points
Coherence Squared
p vs p
z vs z
y vs y
x vs x
1.0
0.8
0.6
0.4
0.2
0.0
0.00
5.00
10.00
15.00
20.00
25.00
Frequency (Hz)

Figure VI.28

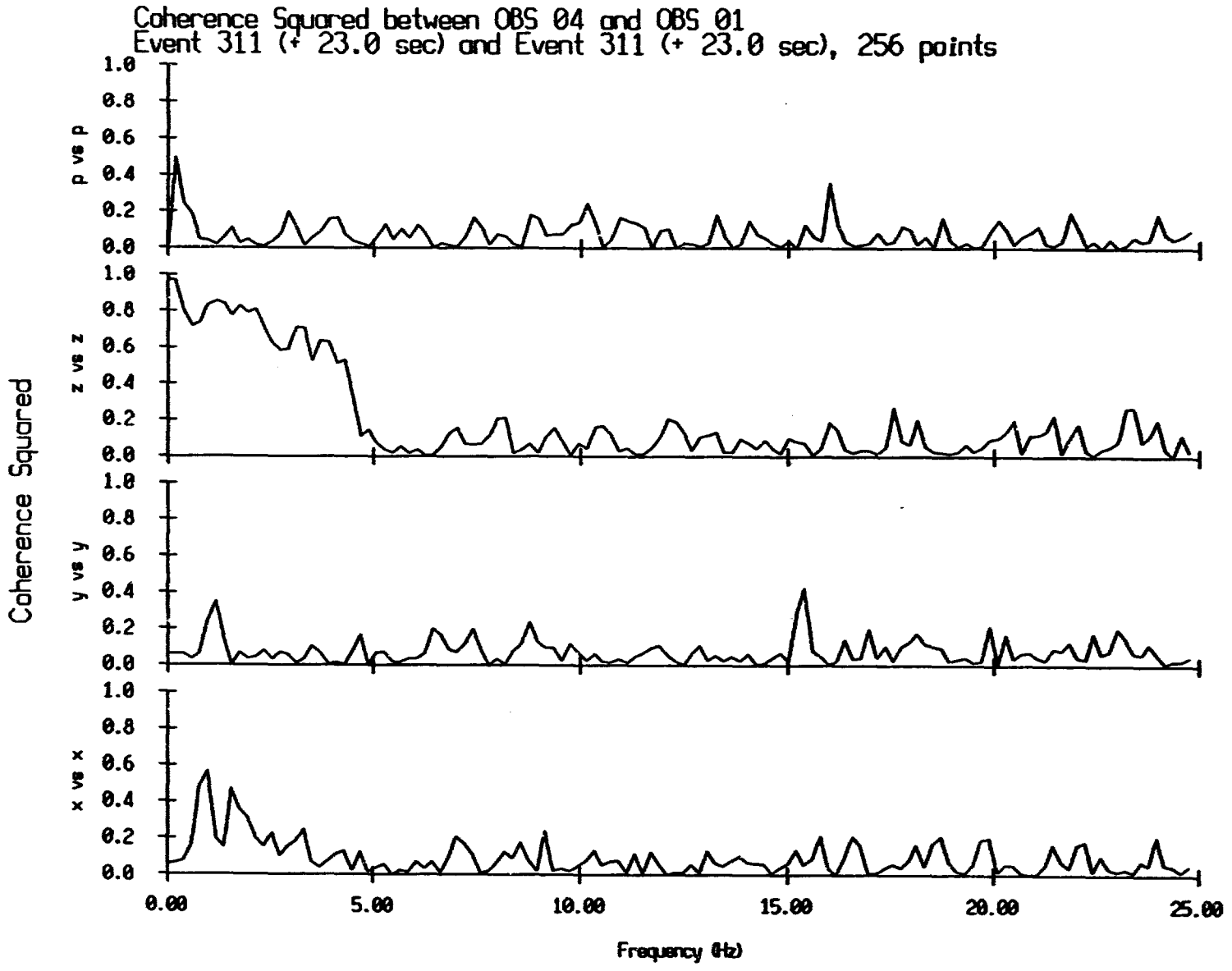
Coherence Squared between OBS 04 and OBS 01
Event 311 (+ 23.0 sec) and Event 311 (+ 23.0 sec), 256 points
Coherence Squared
p vs p
z vs z
y vs y
x vs x
1.0
0.8
0.6
0.4
0.2
0.0
0.00
5.00
10.00
15.00
20.00
25.00
Frequency (Hz)

Figure VI.29

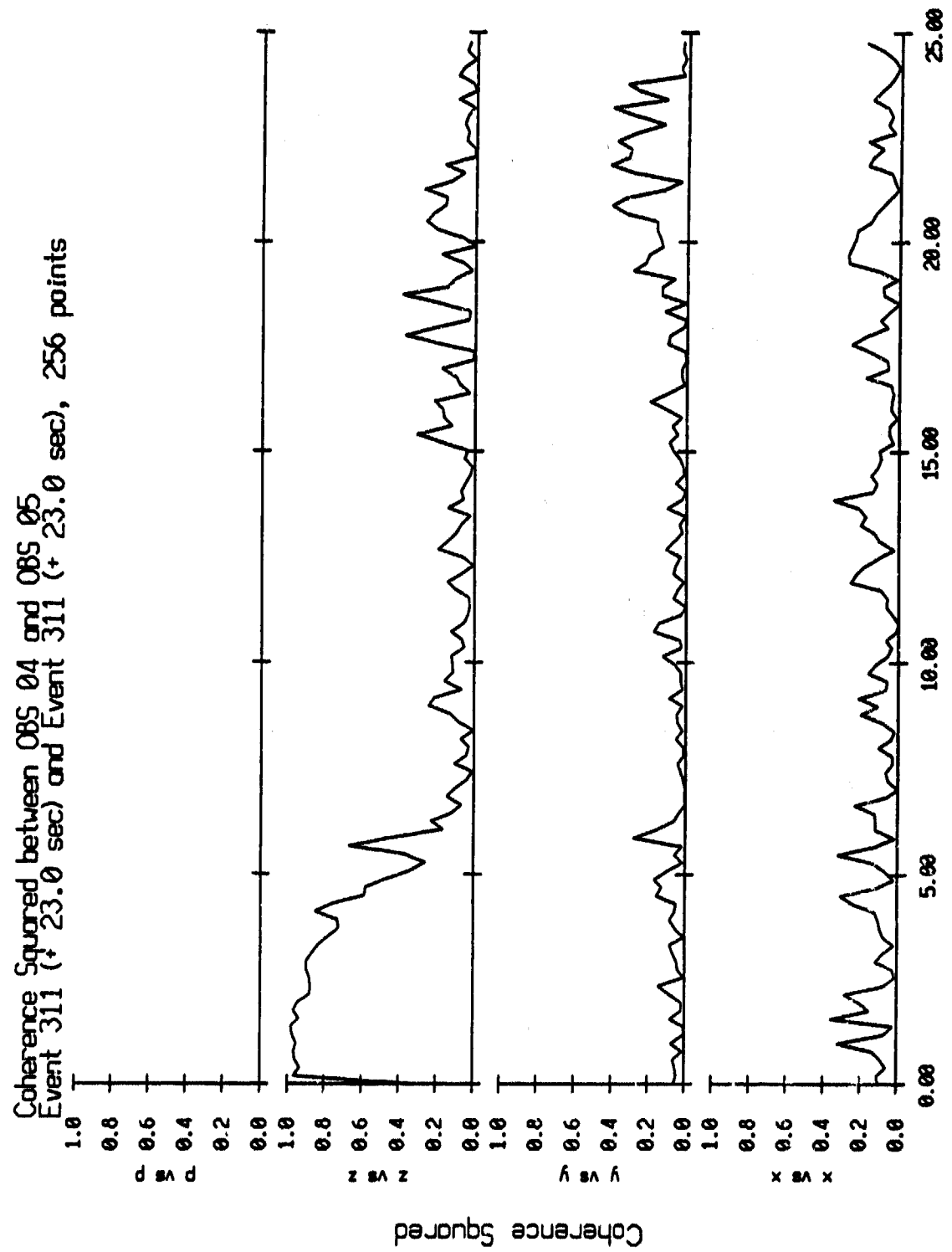
Coherence Squared between OBS 04 and OBS 05
Event 311 (+ 23.0 sec) and Event 311 (+ 23.0 sec), 256 points
Coherence Squared
p vs p
z vs z
y vs y
x vs x
1.0
0.8
0.6
0.4
0.2
0.0
0.00
5.00
10.00
15.00
20.00
25.00
Frequency (Hz)

Figure VI.30

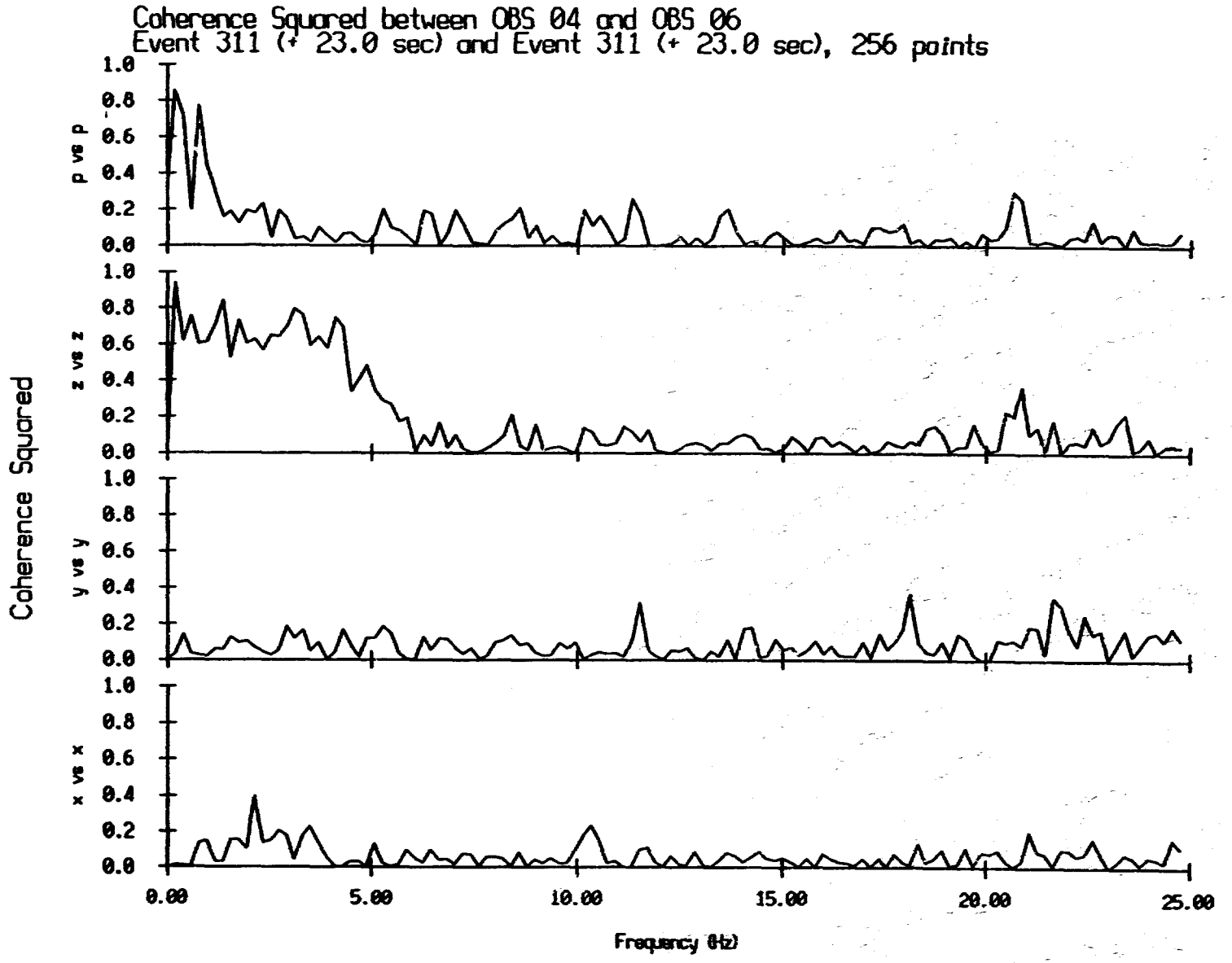
Coherence Squared between OBS 04 and OBS 06
Event 311 (+ 23.0 sec) and Event 311 (+ 23.0 sec), 256 points
Coherence Squared
p vs p
z vs z
y vs y
x vs x
1.0
0.8
0.6
0.4
0.2
0.0
0.00
5.00
10.00
15.00
20.00
25.00
Frequency (Hz)

Figure VI.31

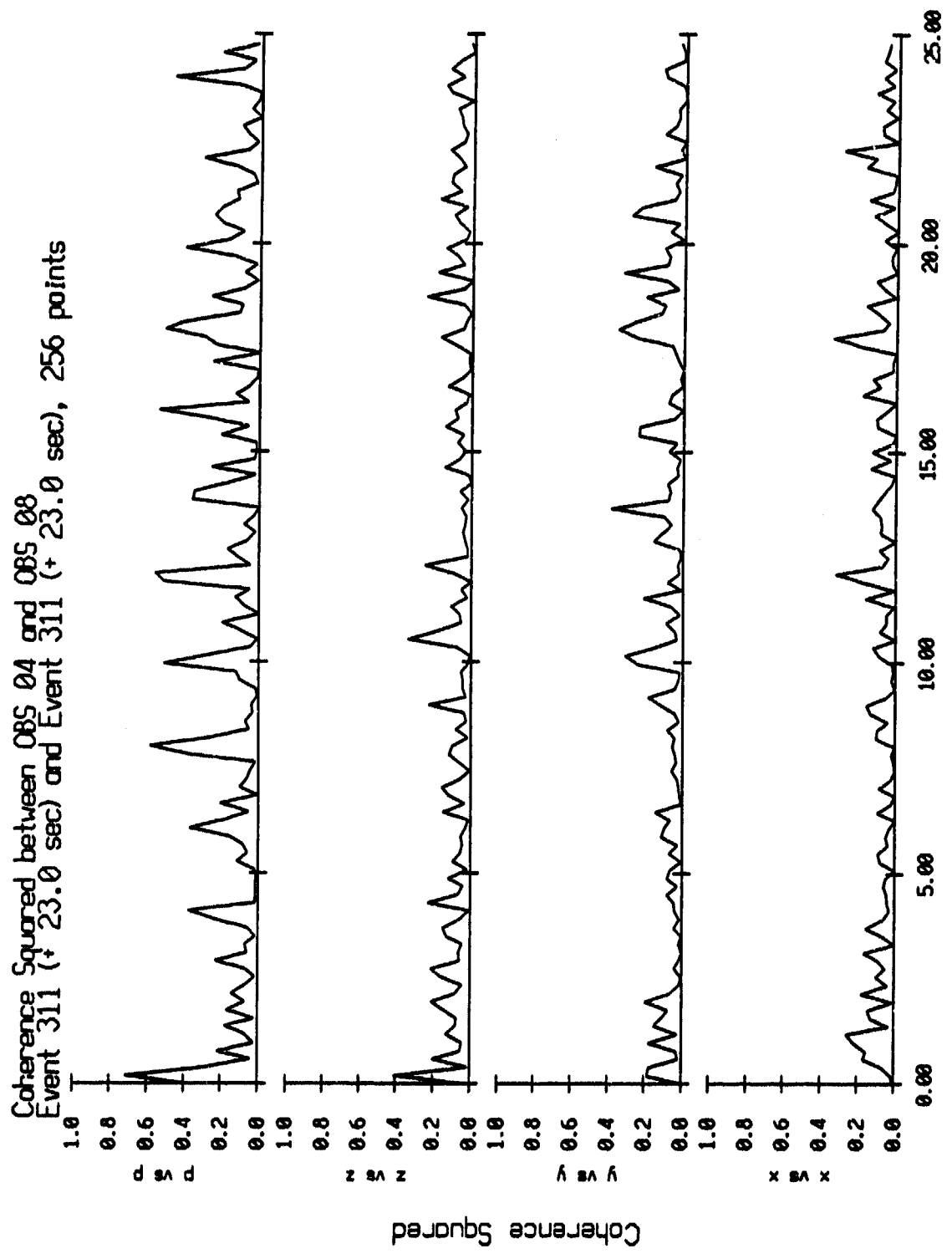
Coherence Squared between OBS 04 and OBS 08
Event 311 (+ 23.0 sec) and Event 311 (+ 23.0 sec), 256 points
p vs p
z vs z
y vs y
x vs x
1.0
0.8
0.6
0.4
0.2
0.0
0.00
5.00
10.00
15.00
20.00
25.00
Frequency (Hz)
Coherence Squared

Figure VI.32

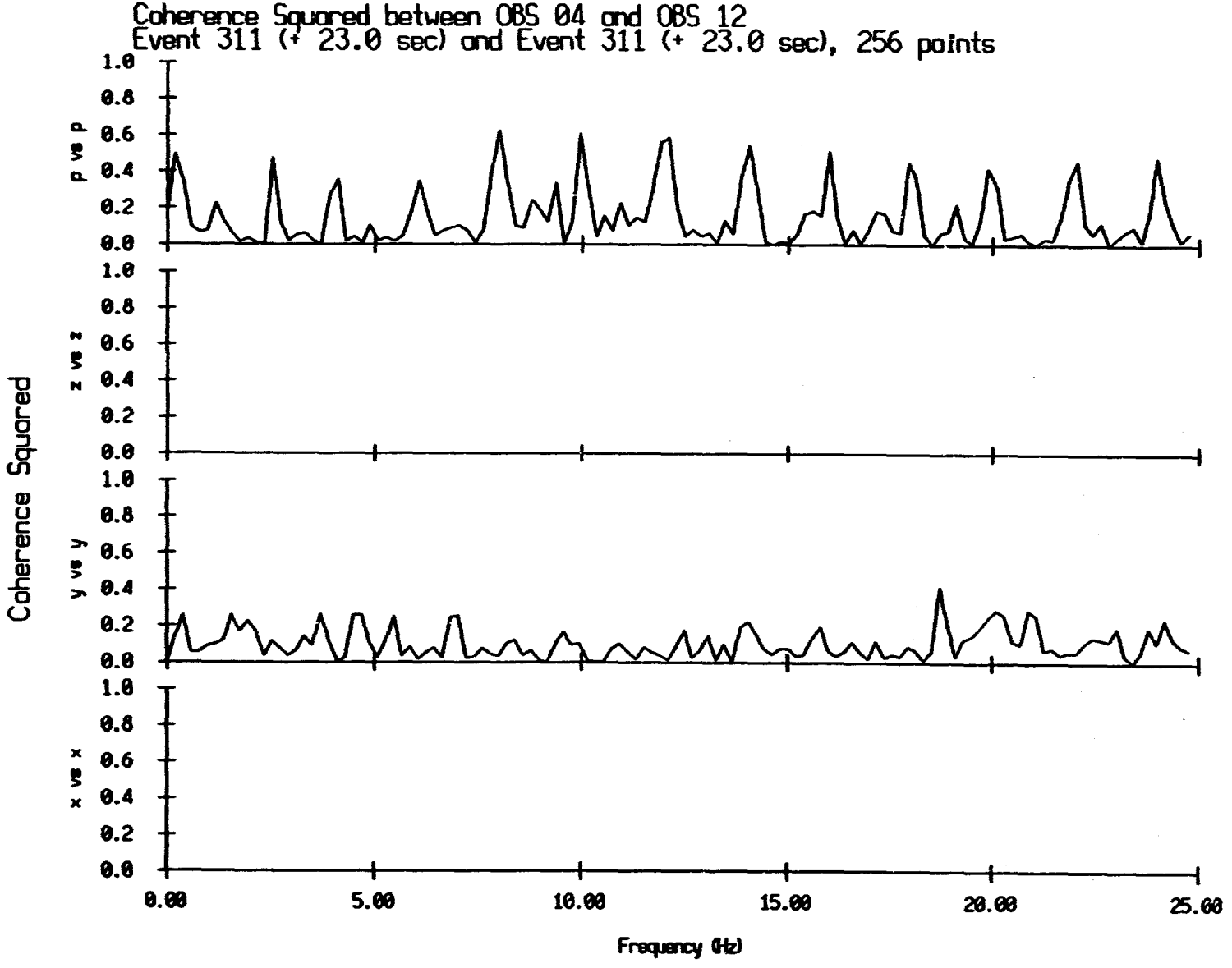
Coherence Squared between OBS 04 and OBS 12
Event 311 (+ 23.0 sec) and Event 311 (+ 23.0 sec), 256 points
Coherence Squared
p vs p
z vs z
y vs y
x vs x
1.0
0.8
0.6
0.4
0.2
0.0
0.00
5.00
10.00
15.00
20.00
25.00
Frequency (Hz)

Figure VI.33

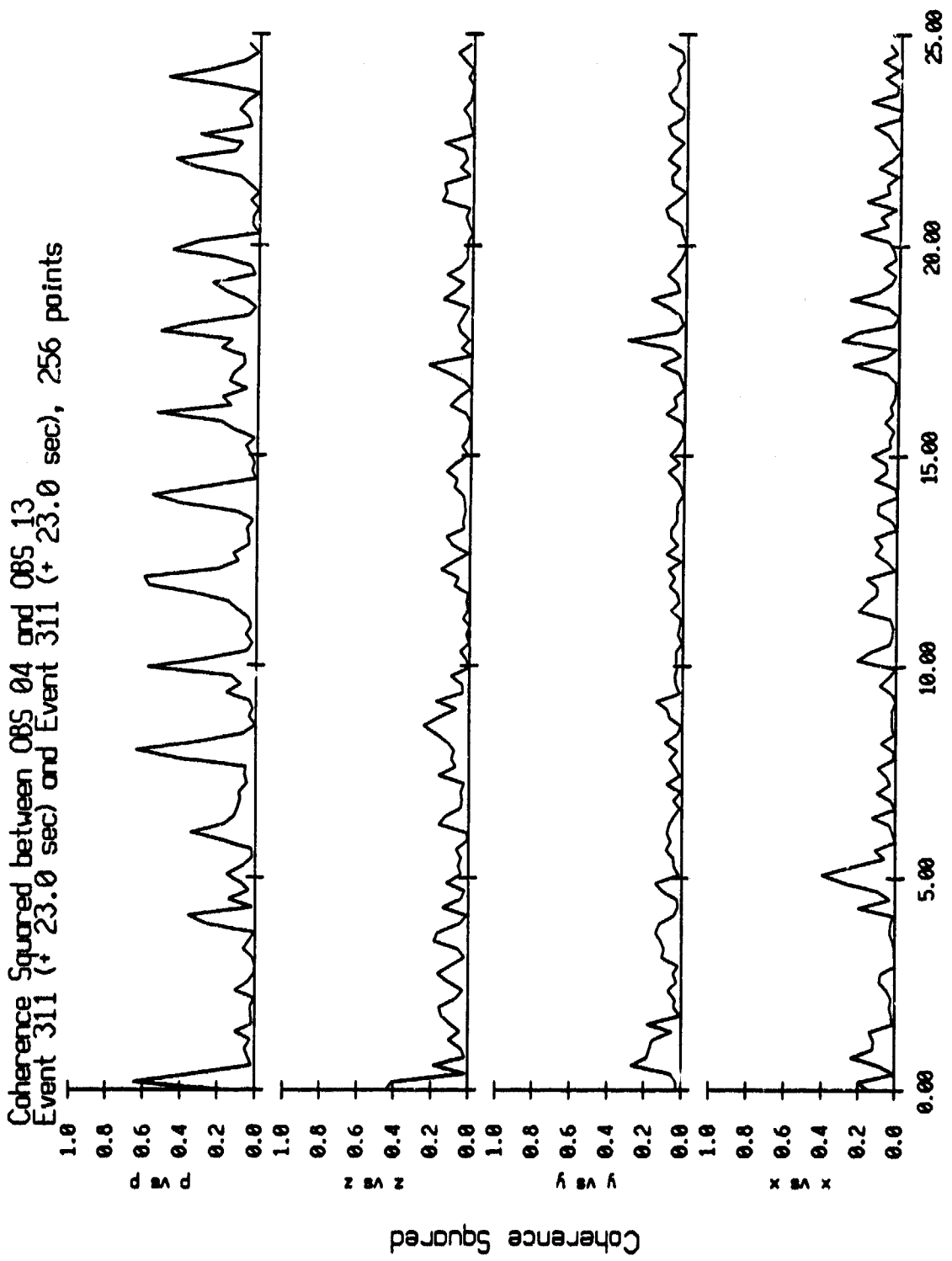
Coherence Squared between OBS 04 and OBS 13
Event 311 (+ 23.0 sec) and Event 311 (+ 23.0 sec), 256 points
Coherence Squared
p vs p
z vs z
y vs y
x vs x
1.0
0.8
0.6
0.4
0.2
0.0
0.00
5.00
10.00
15.00
20.00
25.00
Frequency (Hz)

Figure VI.34

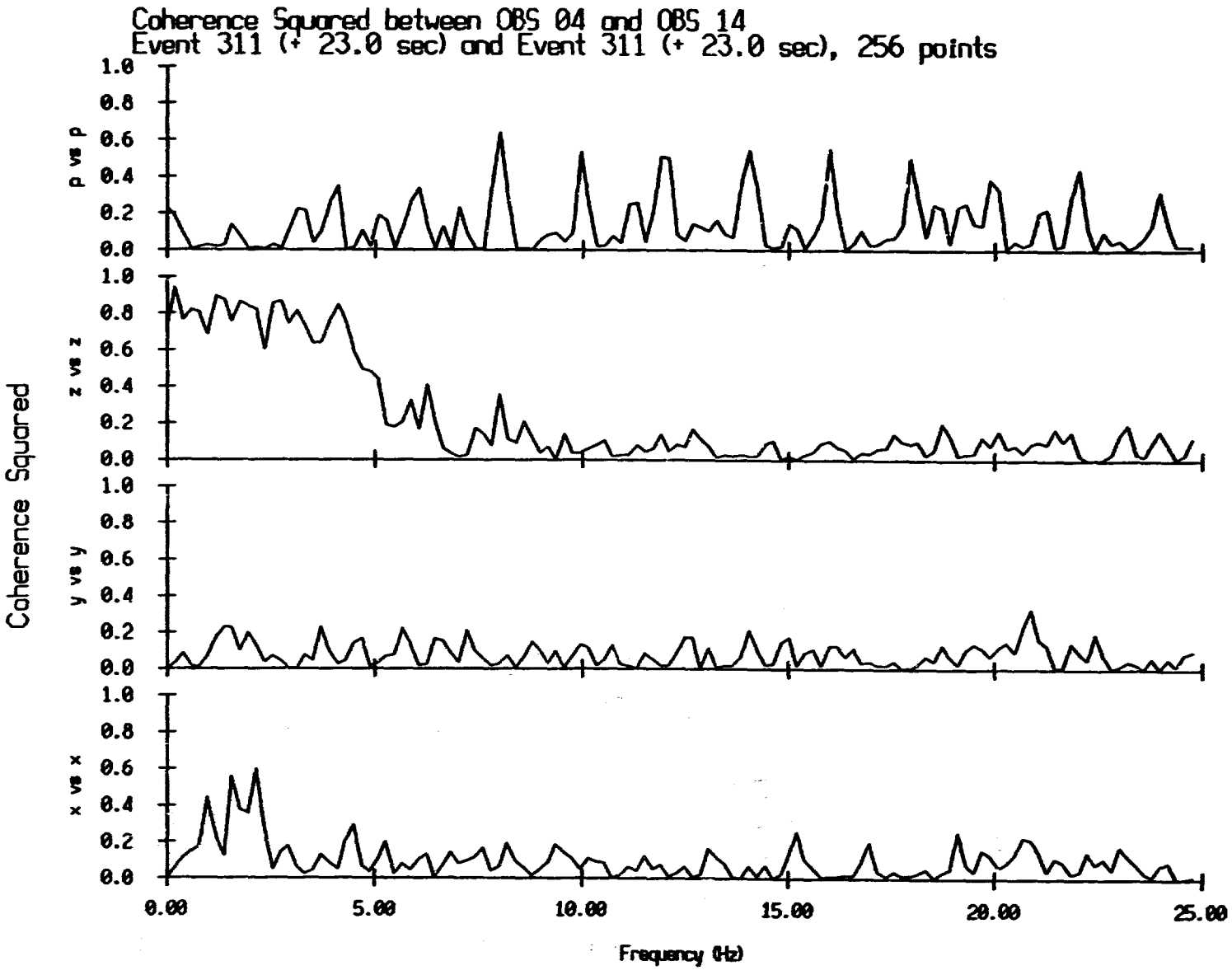
Coherence Squared between OBS 04 and OBS 14
Event 311 (+ 23.0 sec) and Event 311 (+ 23.0 sec), 256 points
Coherence Squared
p vs p
z vs z
y vs y
x vs x
1.0
0.8
0.6
0.4
0.2
0.0
0.00
5.00
10.00
15.00
20.00
25.00
Frequency (Hz)

Figure VI.35

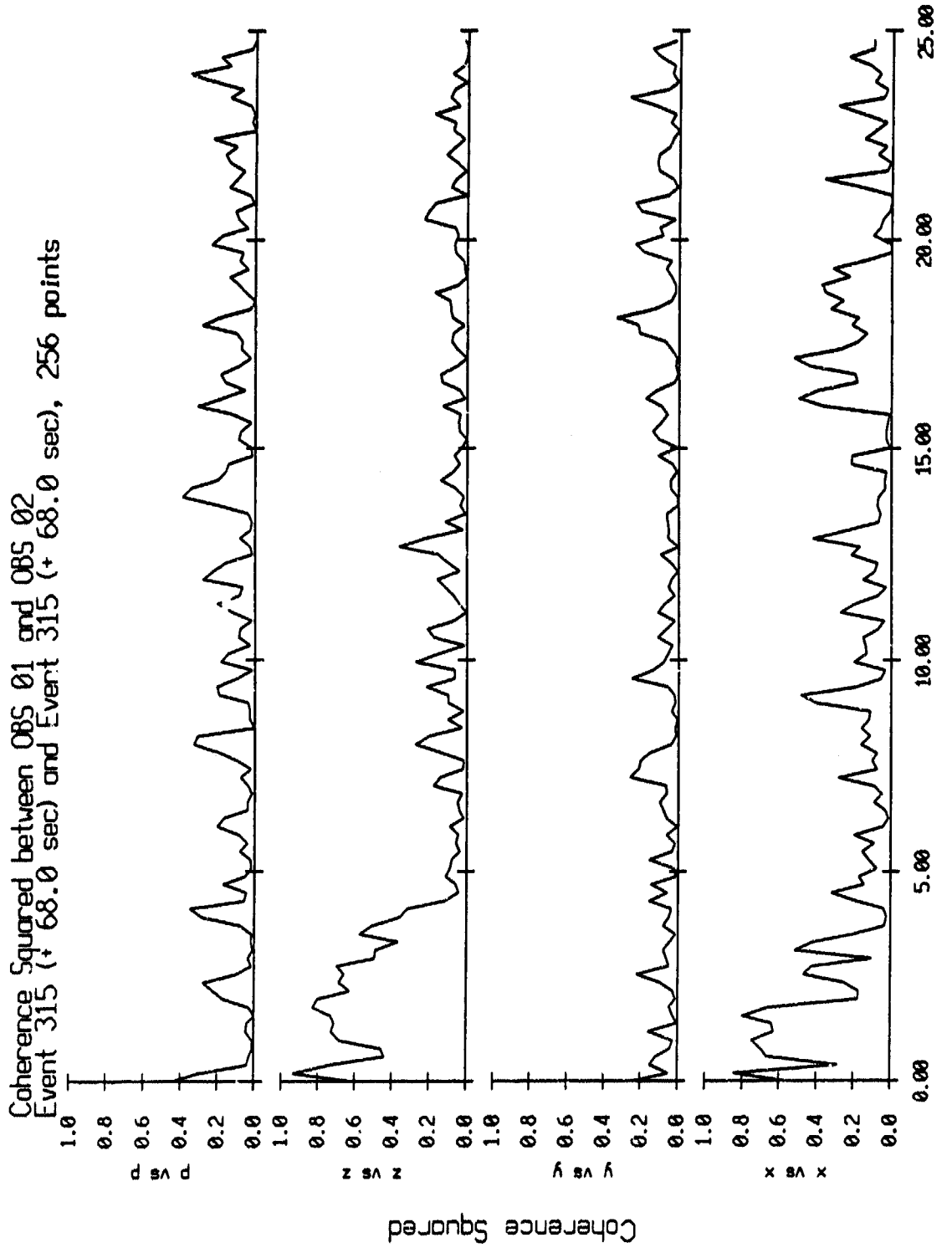
Coherence Squared between OBS 01 and OBS 02
Event 315 (+ 68.0 sec) and Event 315 (+ 68.0 sec), 256 points
P vs P
Z vs Z
Y vs Y
X vs X
Coherence Squared
1.0
0.8
0.6
0.4
0.2
0.0
0.00
5.00
10.00
15.00
20.00
25.00
Frequency (Hz)

Figure VI.36

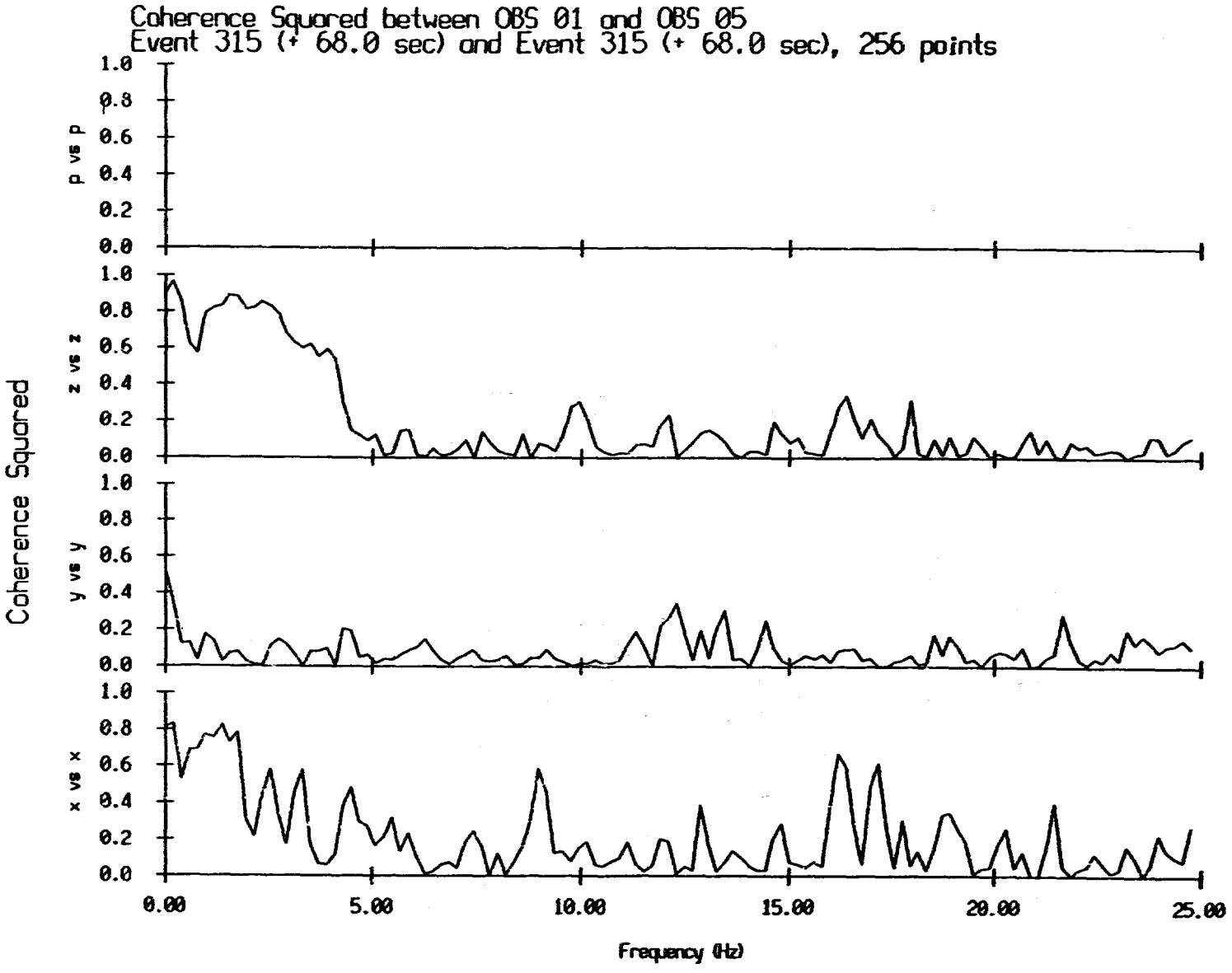
Coherence Squared between OBS 01 and OBS 05
Event 315 (+ 68.0 sec) and Event 315 (+ 68.0 sec), 256 points
Coherence Squared
p vs p
z vs z
y vs y
x vs x
1.0
0.8
0.6
0.4
0.2
0.0
0.00
5.00
10.00
15.00
20.00
25.00
Frequency (Hz)

Figure VI.37

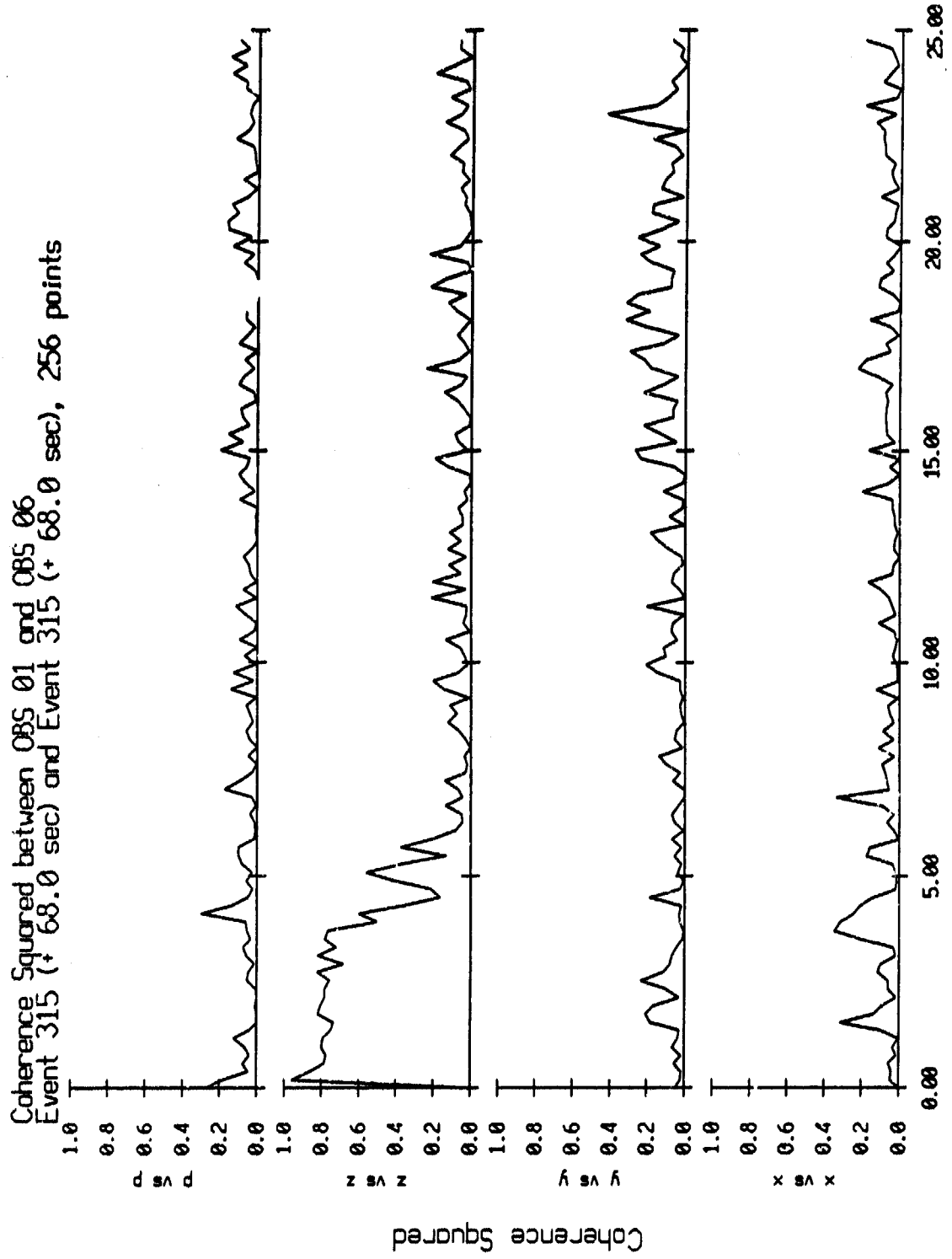
Coherence Squared between OBS 01 and OBS 06
Event 315 (+ 68.0 sec) and Event 315 (+ 68.0 sec), 256 points
P vs P
Z vs Z
Y vs Y
X vs X
1.0
0.8
0.6
0.4
0.2
0.0
0.00
5.00
10.00
15.00
20.00
25.00
Coherence Squared
Frequency (Hz)

Figure VI.38

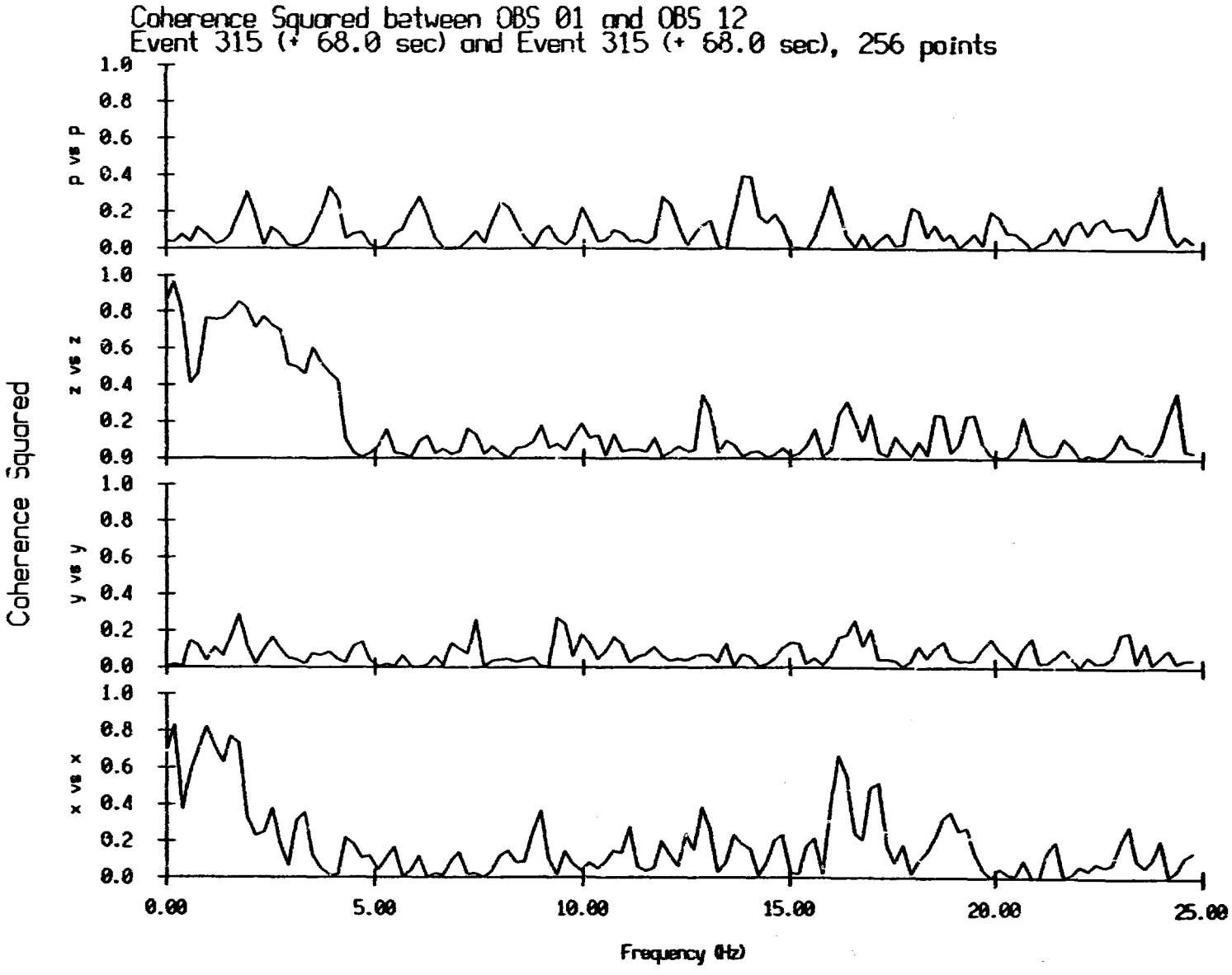
Coherence Squared between OBS 01 and OBS 12
Event 315 (+ 68.0 sec) and Event 315 (+ 68.0 sec), 256 points
Coherence Squared
p vs p
z vs z
y vs y
x vs x
1.0
0.8
0.6
0.4
0.2
0.0
0.00
5.00
10.00
15.00
20.00
25.00
Frequency (Hz)

Figure VI.39

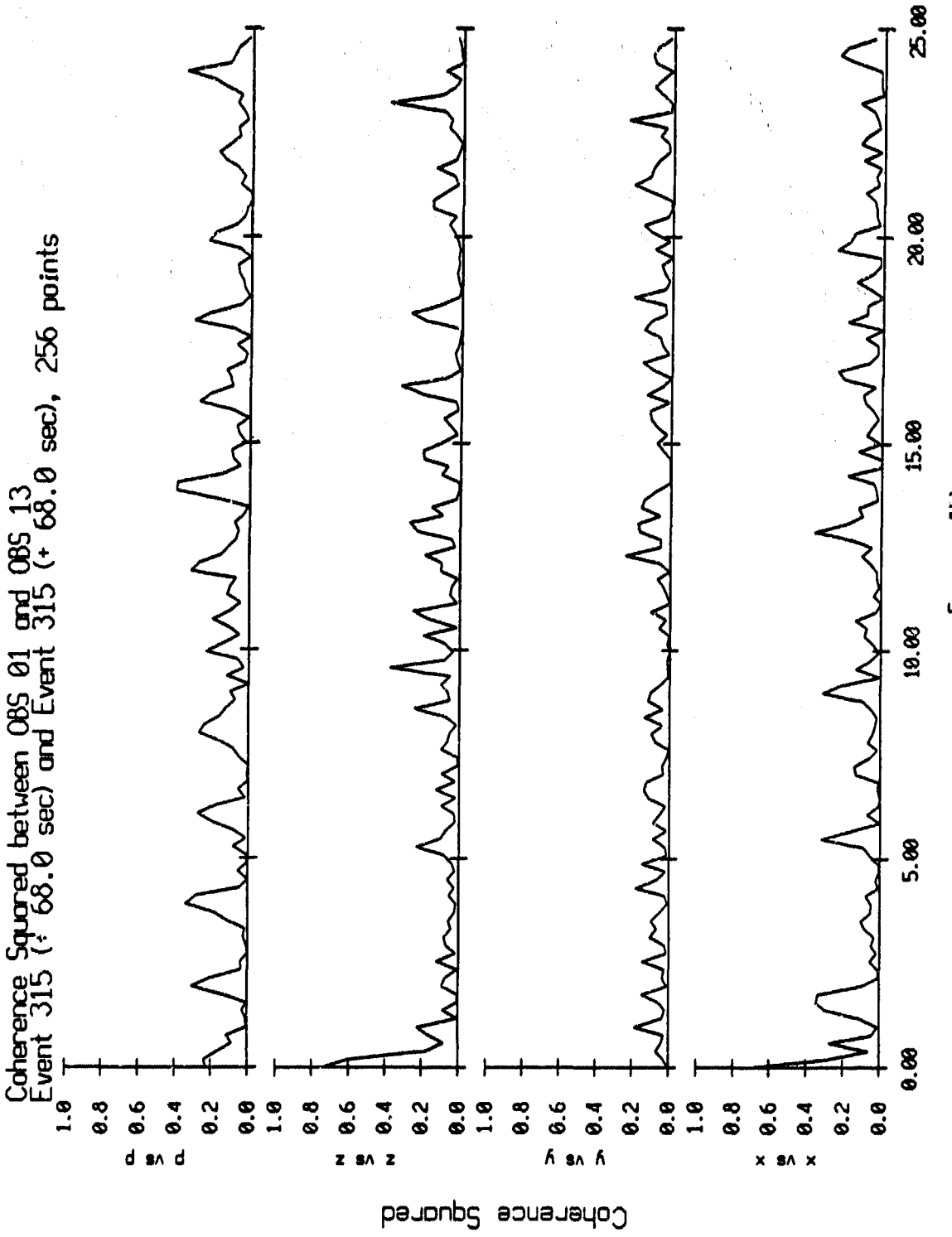
Coherence Squared between OBS 01 and OBS 13
Event 315 (+ 68.0 sec) and Event 315 (+ 68.0 sec), 256 points
P vs P
Z vs Z
Y vs Y
X vs X
Coherence Squared
1.0
0.8
0.6
0.4
0.2
0.0
0.00
5.00
10.00
15.00
20.00
25.00
Frequency (Hz)

Figure VI.40

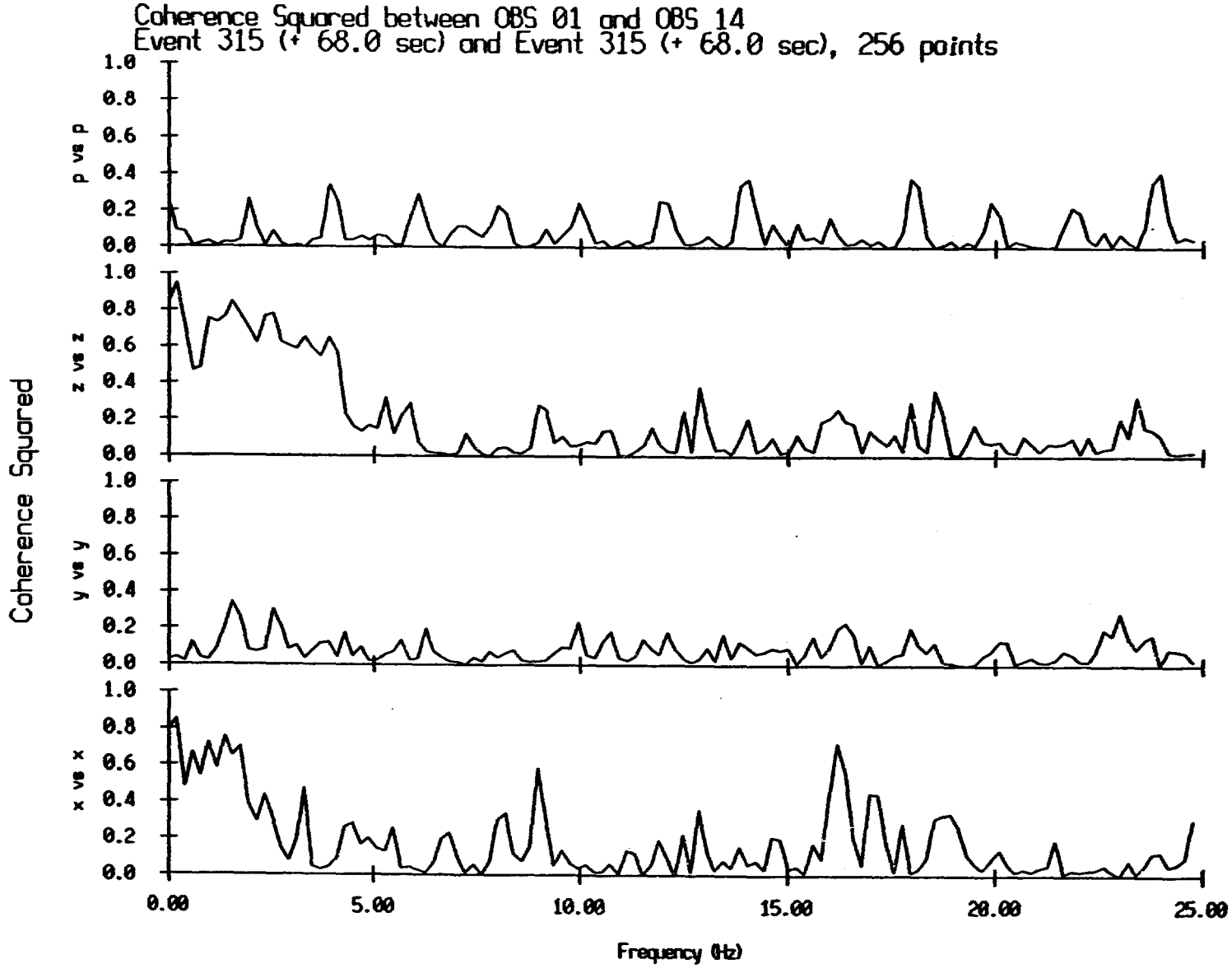
Coherence Squared between OBS 01 and OBS 14
Event 315 (+ 68.0 sec) and Event 315 (+ 68.0 sec), 256 points
Coherence Squared
p vs p
z vs z
y vs y
x vs x
1.0
0.8
0.6
0.4
0.2
0.0
0.00
5.00
10.00
15.00
20.00
25.00
Frequency (Hz)

Figure VI.41

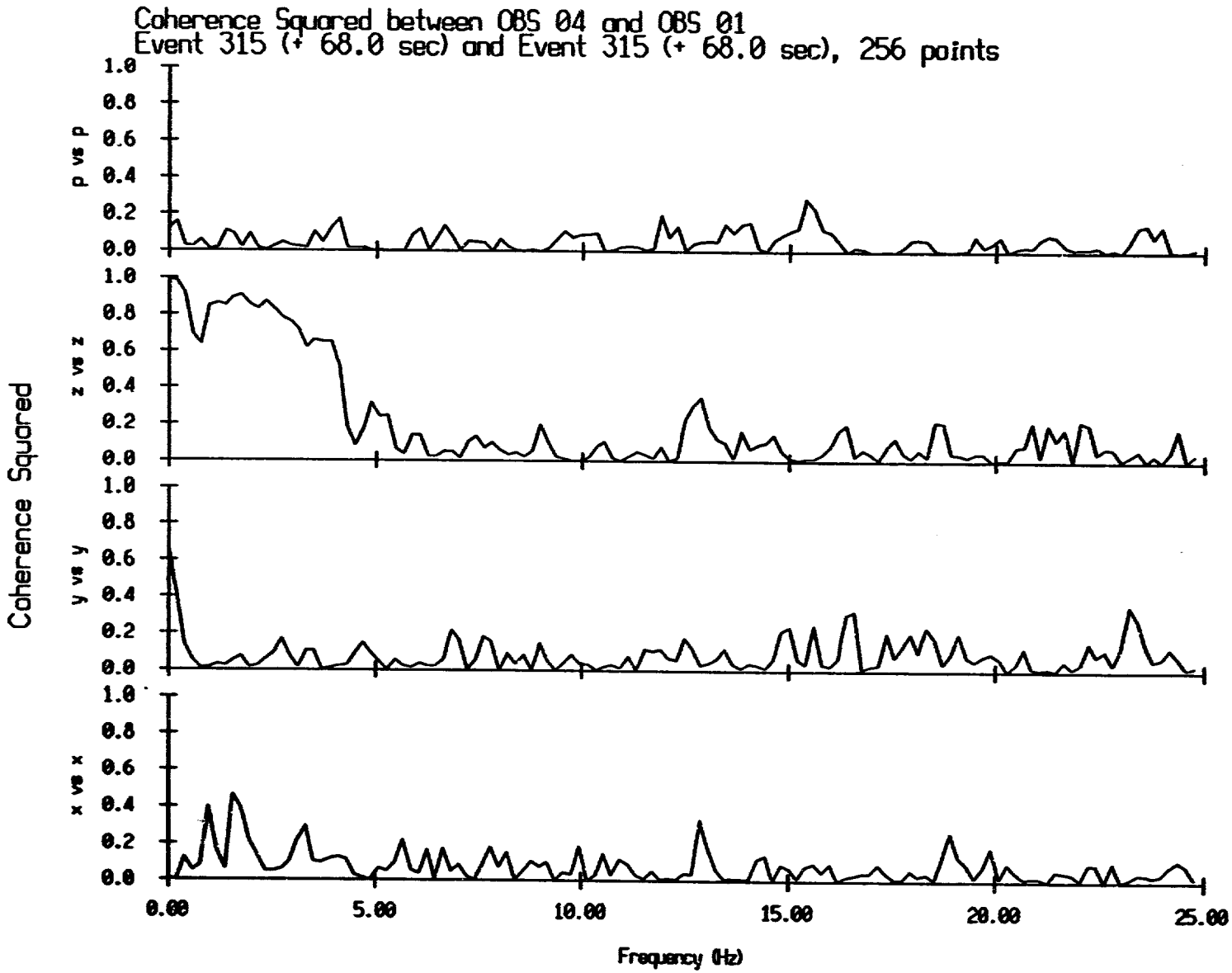
Coherence Squared between OBS 04 and OBS 01
Event 315 (+ 68.0 sec) and Event 315 (+ 68.0 sec), 256 points
Coherence Squared
p vs p
z vs z
y vs y
x vs x
1.0
0.8
0.6
0.4
0.2
0.0
0.00
5.00
10.00
15.00
20.00
25.00
Frequency (Hz)

Figure VI.42

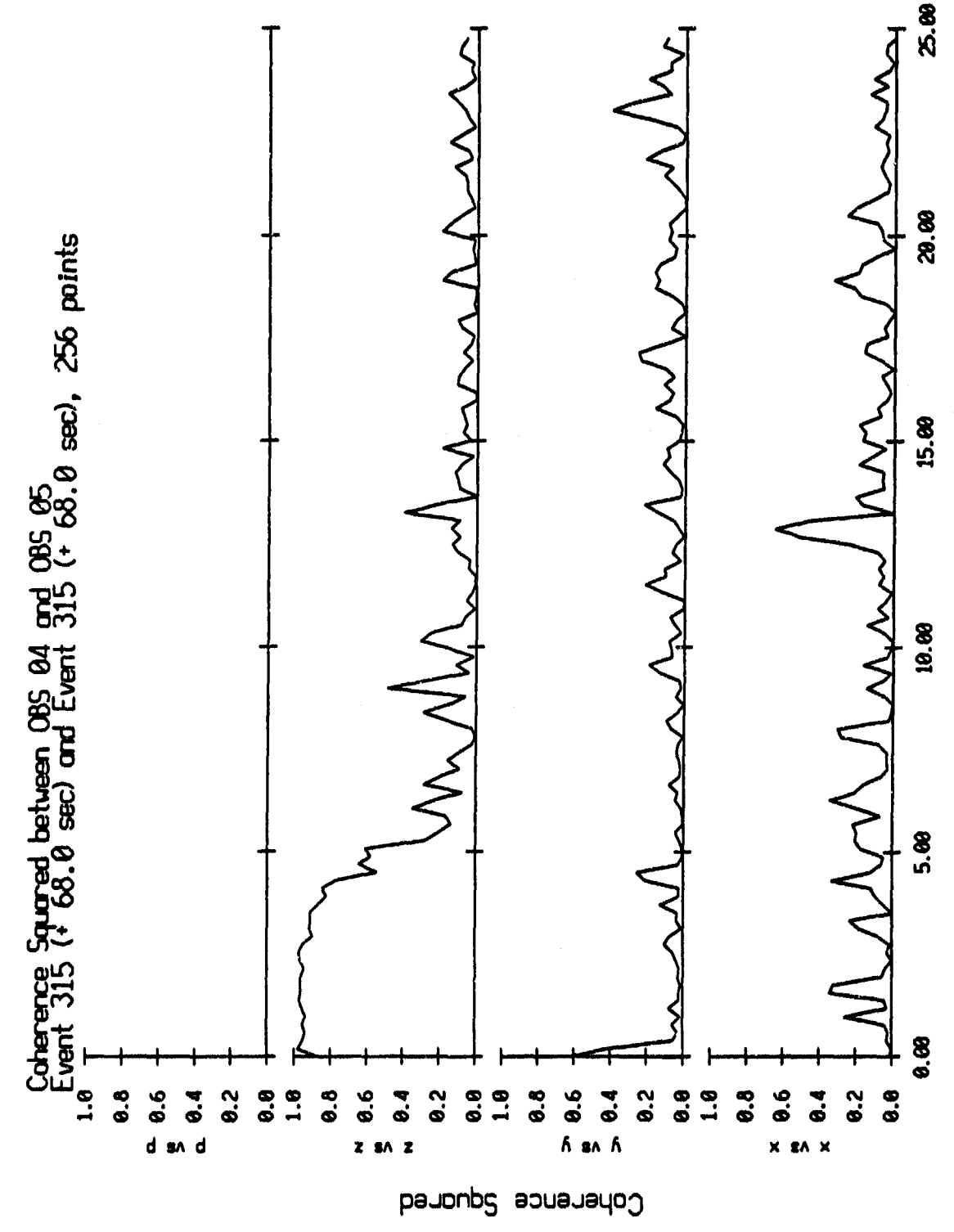
Coherence Squared between OBS 04 and OBS 05
Event 315 (+ 68.0 sec) and Event 315 (+ 68.0 sec), 256 points
Coherence Squared
p vs p
z vs z
y vs y
x vs x
1.0
0.8
0.6
0.4
0.2
0.0
0.00
5.00
10.00
15.00
20.00
25.00
Frequency (Hz)

Figure VI.43

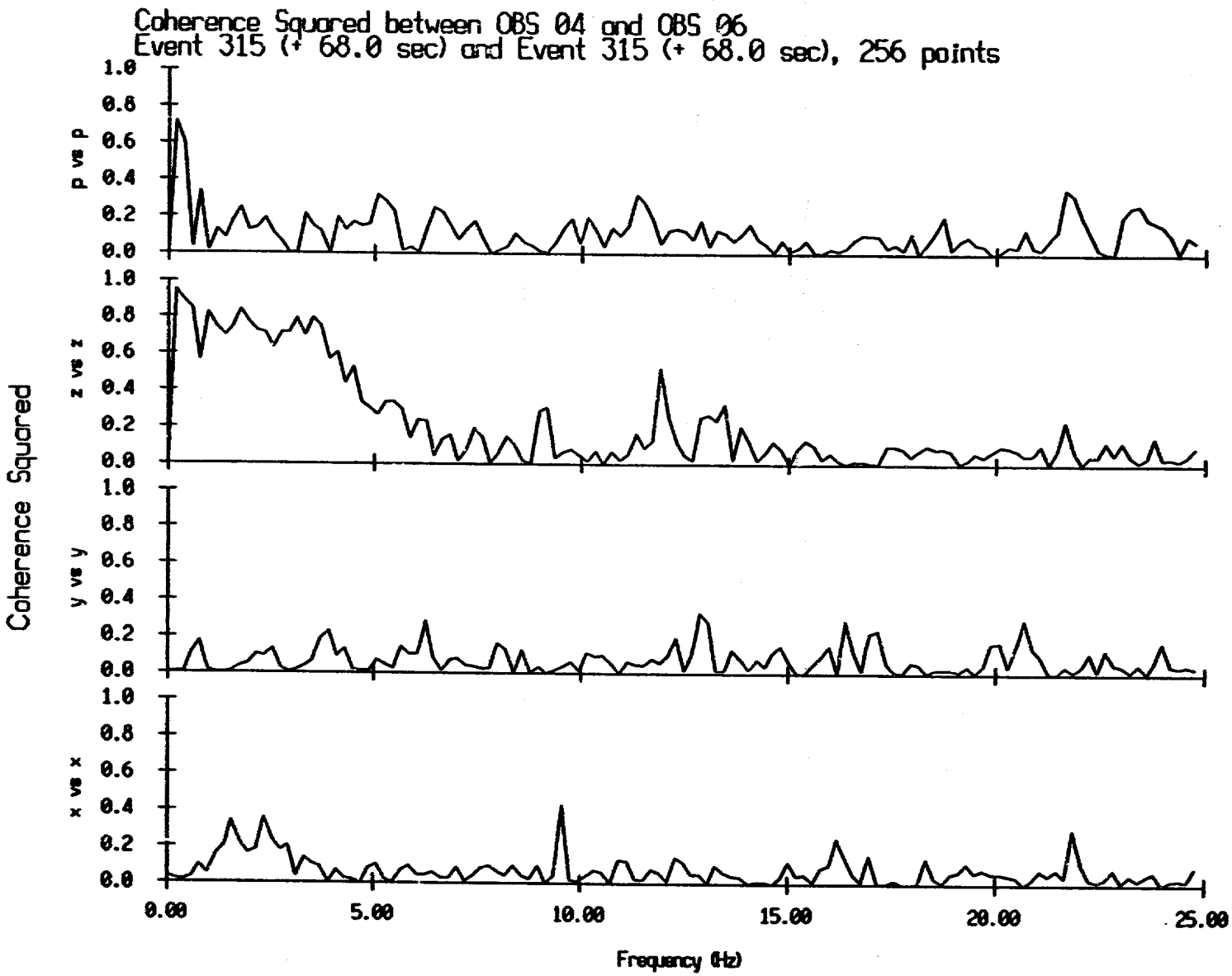
Coherence Squared between OBS 04 and OBS 06
Event 315 (+ 68.0 sec) and Event 315 (+ 68.0 sec), 256 points
Coherence Squared
p vs p
z vs z
y vs y
x vs x
1.0
0.8
0.6
0.4
0.2
0.0
0.00
5.00
10.00
15.00
20.00
25.00
Frequency (Hz)

Figure VI.44

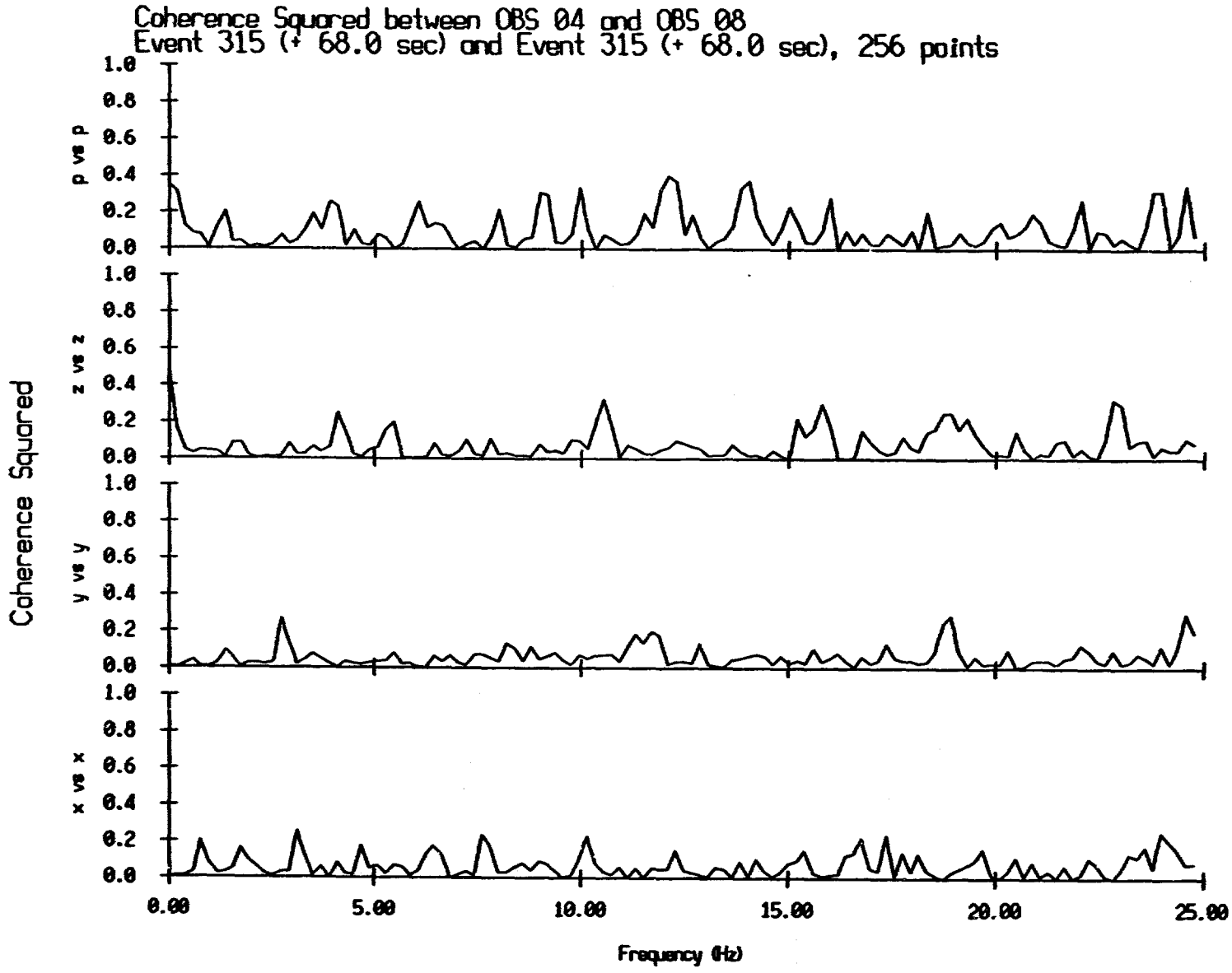
Coherence Squared between OBS 04 and OBS 08
Event 315 (+ 68.0 sec) and Event 315 (+ 68.0 sec), 256 points
Coherence Squared
p vs p
z vs z
y vs y
x vs x
1.0
0.8
0.6
0.4
0.2
0.0
0.00
5.00
10.00
15.00
20.00
25.00
Frequency (Hz)

Figure VI.45

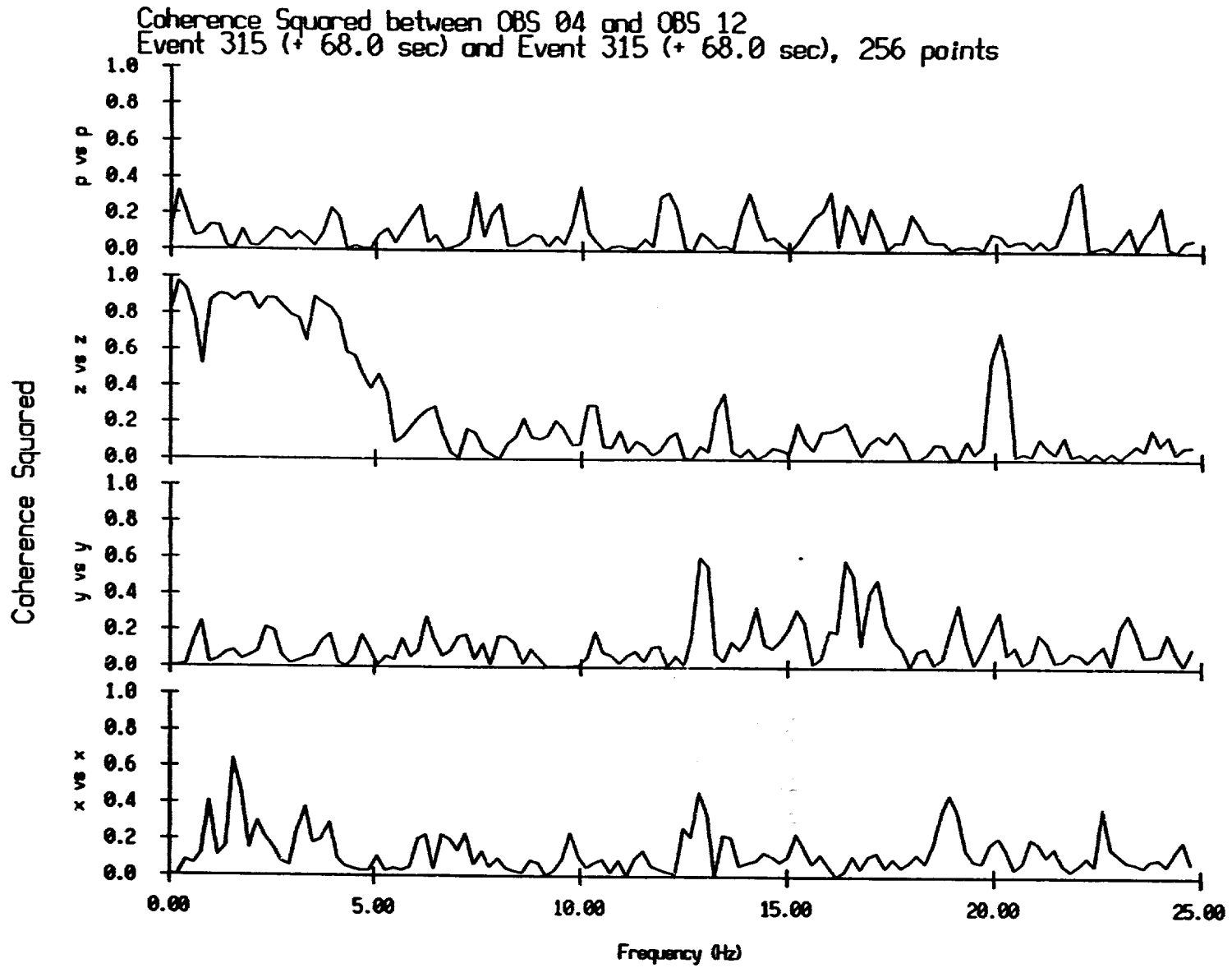
Coherence Squared between OBS 04 and OBS 12
Event 315 (+ 68.0 sec) and Event 315 (+ 68.0 sec), 256 points
Coherence Squared
p vs p
z vs z
y vs y
x vs x
1.0
0.8
0.6
0.4
0.2
0.0
0.00
5.00
10.00
15.00
20.00
25.00
Frequency (Hz)

Figure VI.48

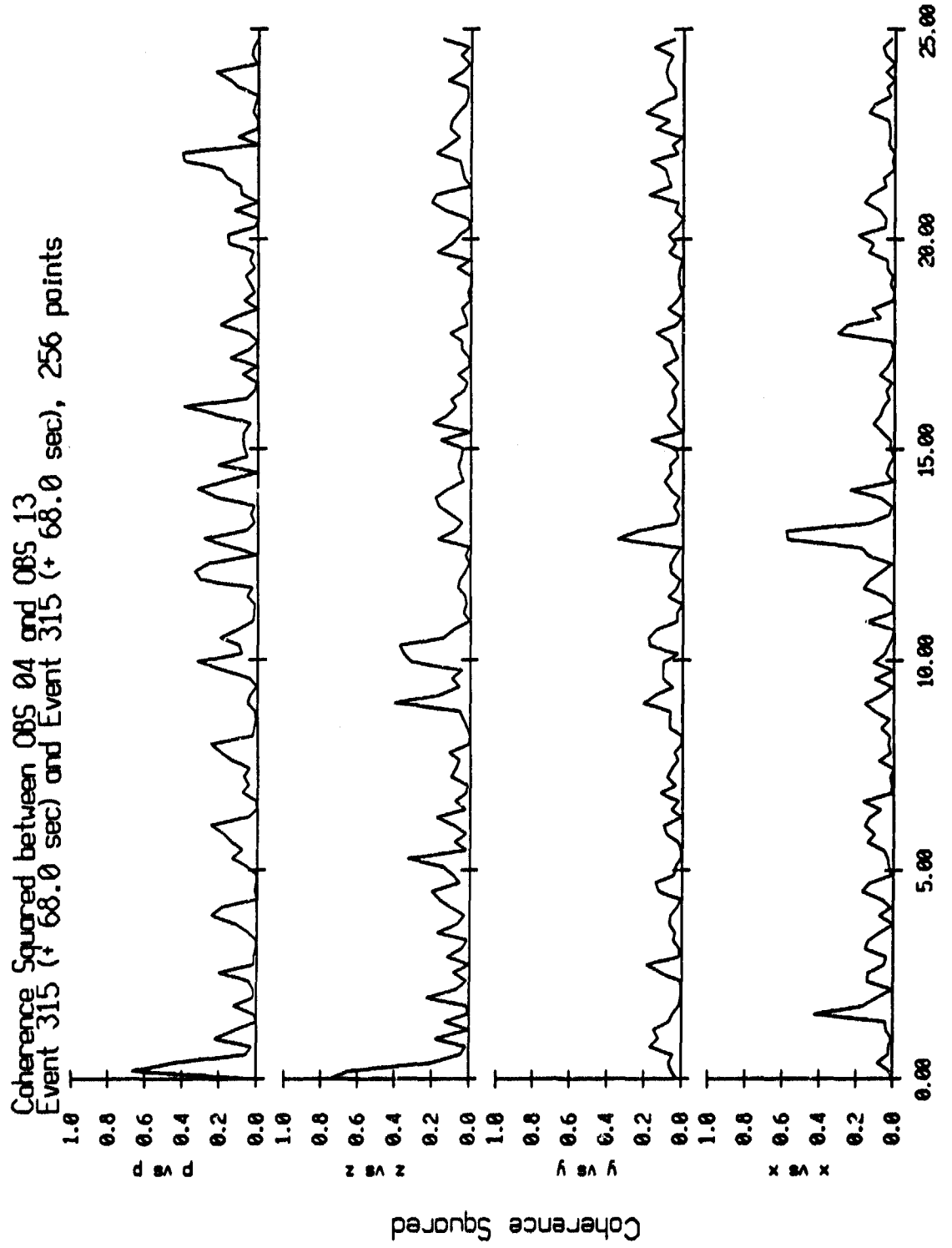
Coherence Squared between OBS 04 and OBS 13
Event 315 (+ 68.0 sec) and Event 315 (+ 68.0 sec), 256 points
Coherence Squared
p vs p
z vs z
y vs y
x vs x
1.0
0.8
0.6
0.4
0.2
0.0
0.00
5.00
10.00
15.00
20.00
25.00
Frequency (Hz)

Figure VI.47

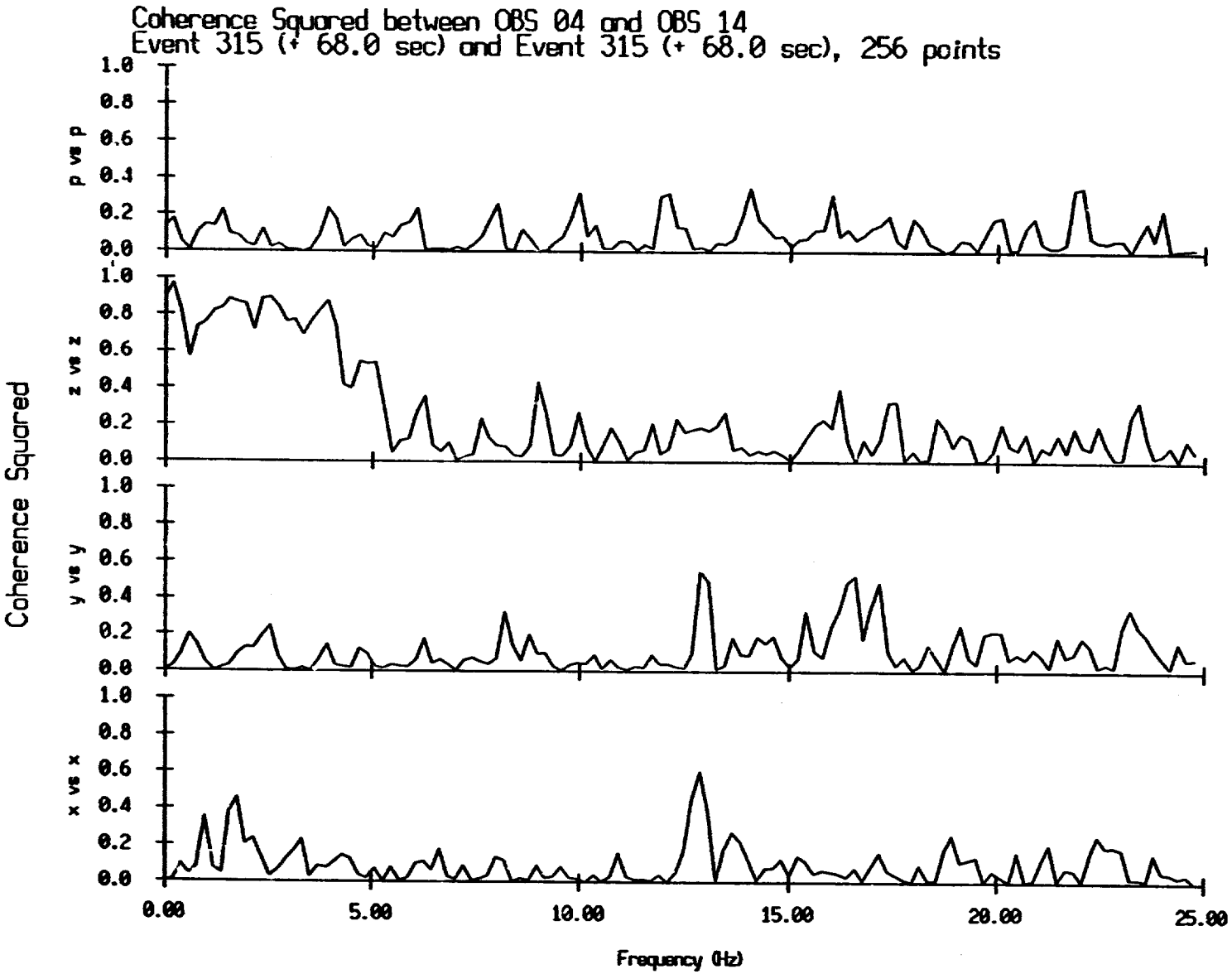
Coherence Squared between OBS 04 and OBS 14
Event 315 (+ 68.0 sec) and Event 315 (+ 68.0 sec), 256 points
Coherence Squared
p vs p
z vs z
y vs y
x vs x
1.0
0.8
0.6
0.4
0.2
0.0
0.00
5.00
10.00
15.00
20.00
25.00
Frequency (Hz)

Figure VI.48

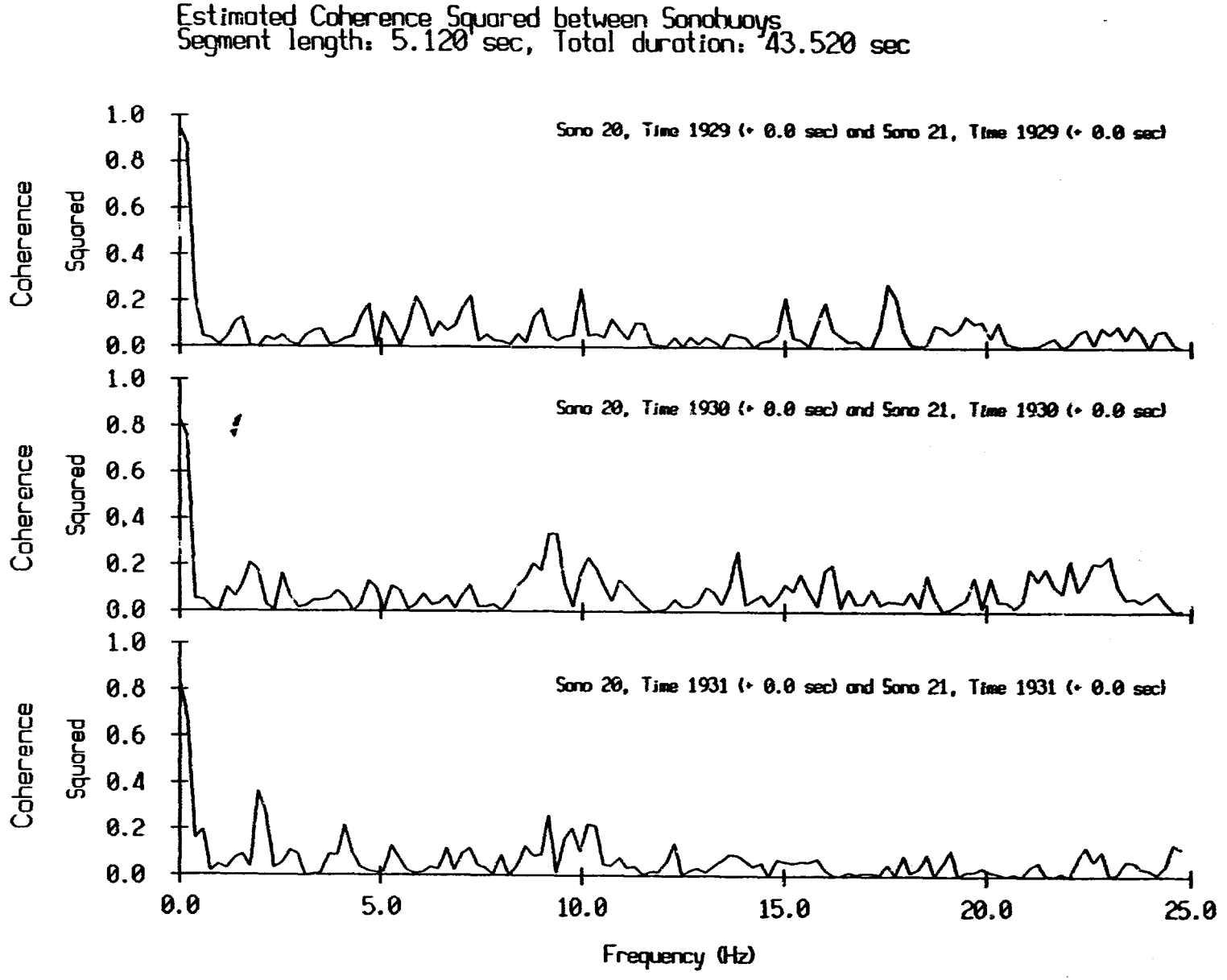
Estimated Coherence Squared between Sonobuoys
Segment length: 5.120 sec, Total duration: 43.520 sec
Sono 20, Time 1929 (+ 0.0 sec) and Sono 21, Time 1929 (+ 0.0 sec)
Sono 20, Time 1930 (+ 0.0 sec) and Sono 21, Time 1930 (+ 0.0 sec)
Sono 20, Time 1931 (+ 0.0 sec) and Sono 21, Time 1931 (+ 0.0 sec)
Coherence Squared
1.0
0.8
0.6
0.4
0.2
0.0
0.0
5.0
10.0
15.0
20.0
25.0
Frequency (Hz)

Figure VI.49

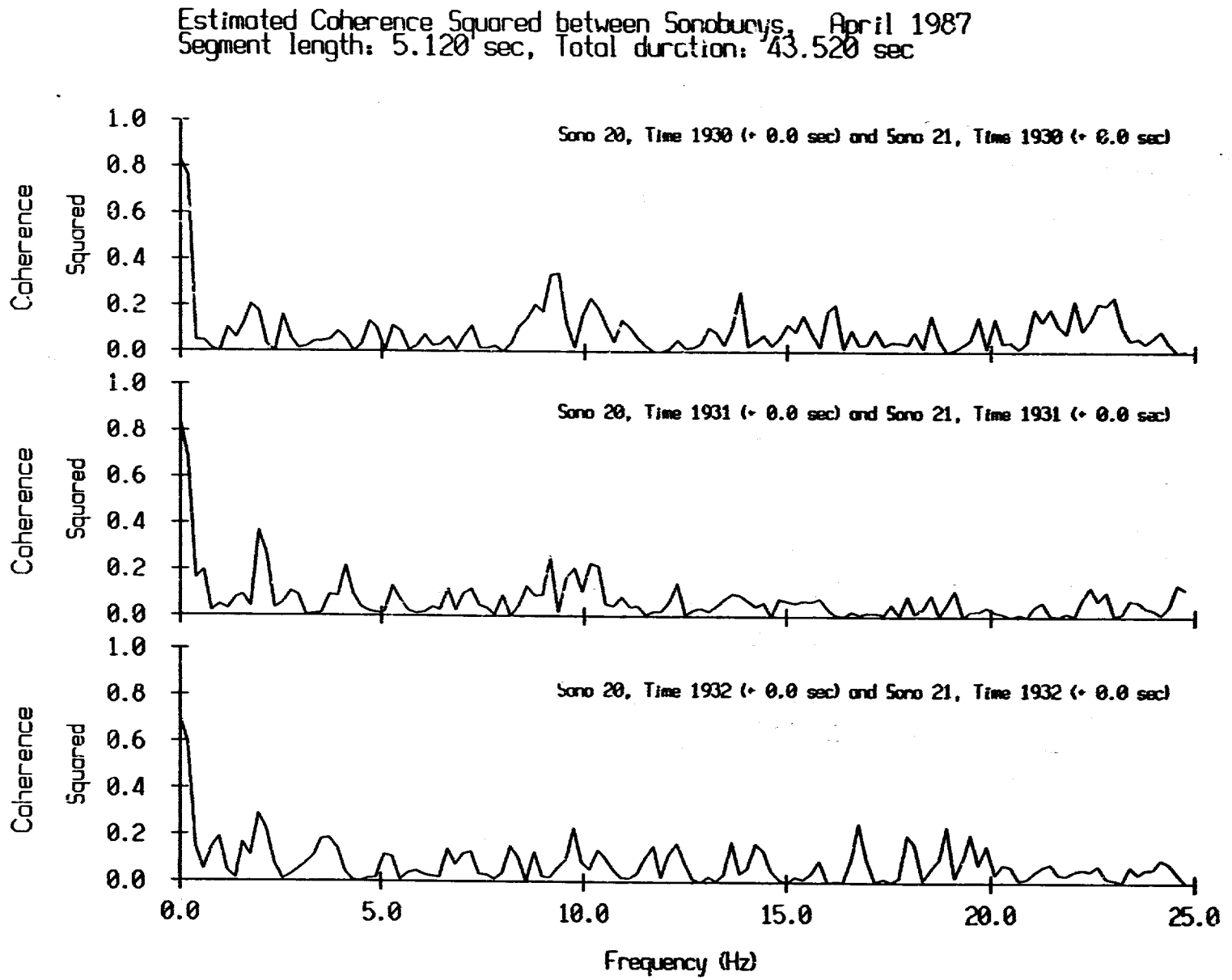
Estimated Coherence Squared between Sonobuoys, April 1987
Segment length: 5.120 sec, Total duration: 43.520 sec
Sono 20, Time 1930 (+ 0.0 sec) and Sono 21, Time 1930 (+ 0.0 sec)
Sono 20, Time 1931 (+ 0.0 sec) and Sono 21, Time 1931 (+ 0.0 sec)
Sono 20, Time 1932 (+ 0.0 sec) and Sono 21, Time 1932 (+ 0.0 sec)
Coherence Squared
1.0
0.8
0.6
0.4
0.2
0.0
0.0
5.0
10.0
15.0
20.0
25.0
Frequency (Hz)

Figure VI.50

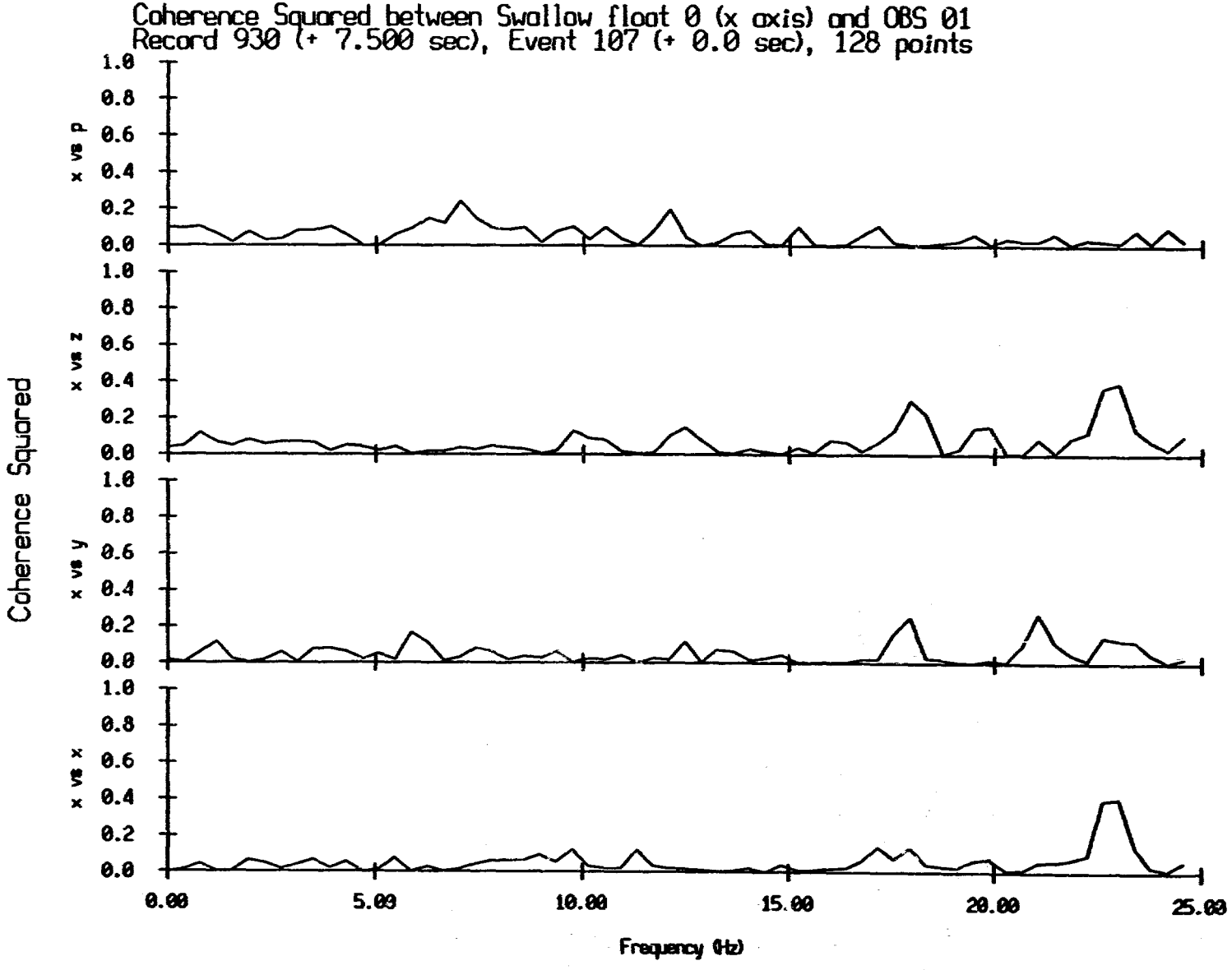

Figure VI.51i

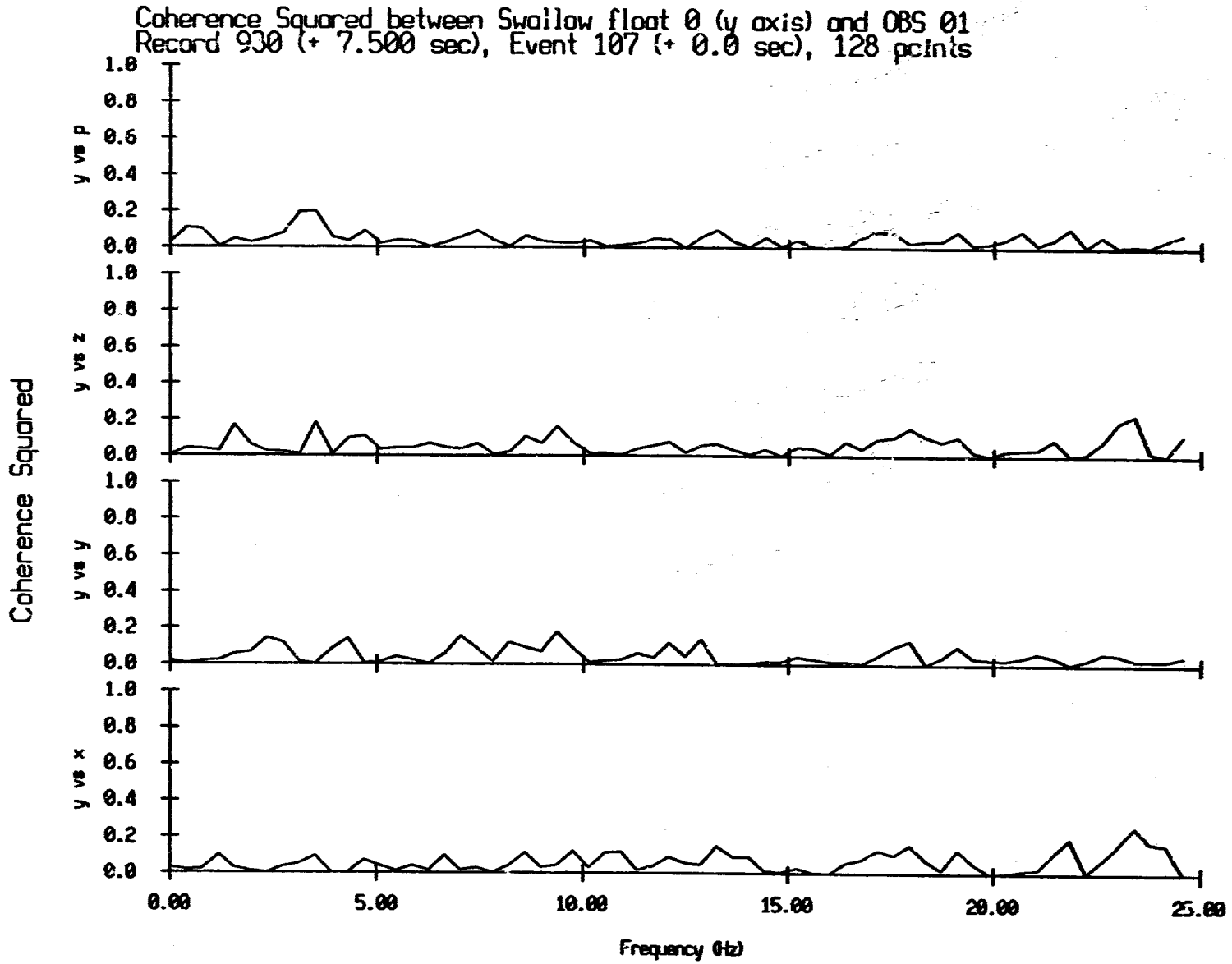

Figure VI.51j

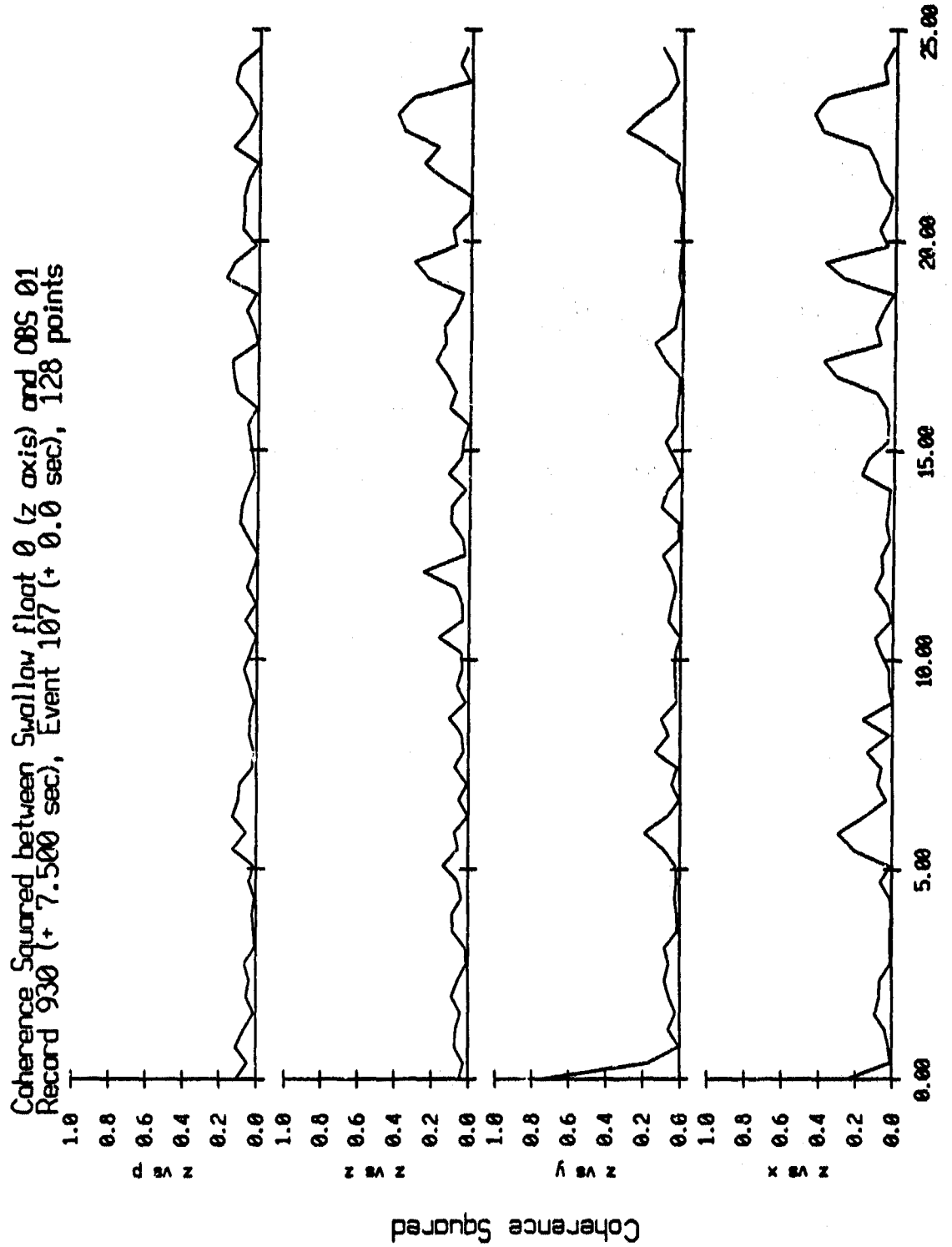

Figure VI.51k

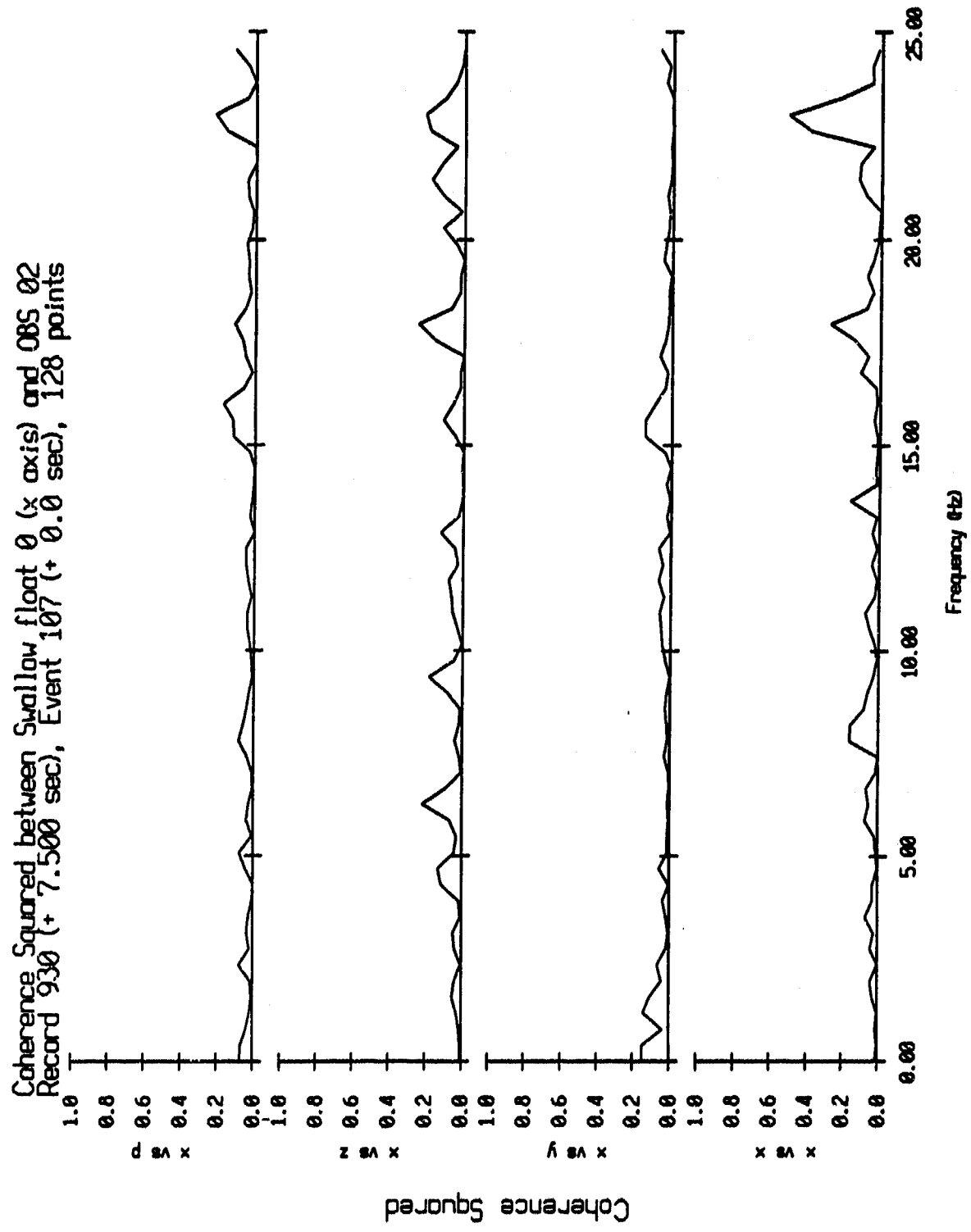

Figure VI.52i

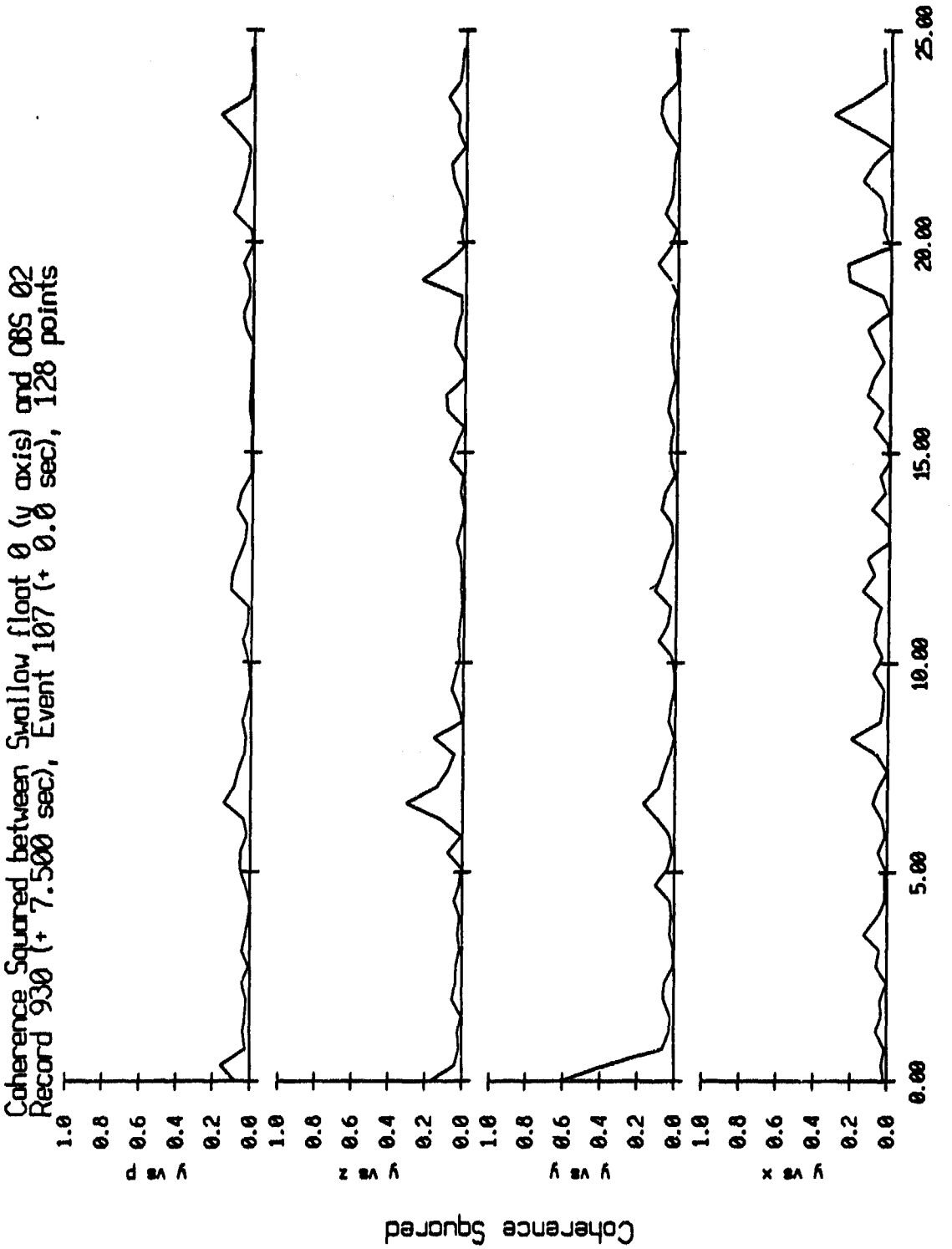

Figure VI.52j

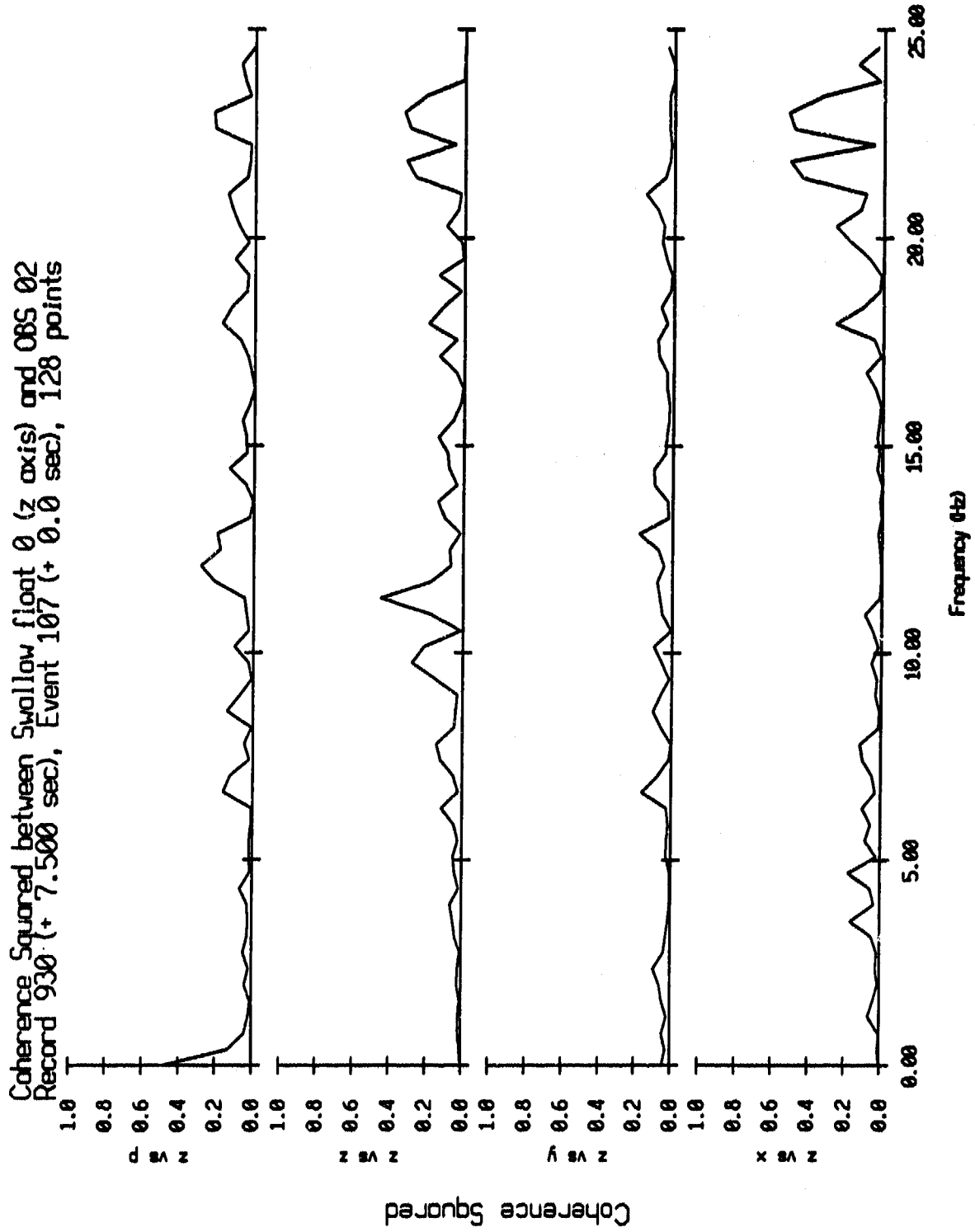

Figure VI.52k

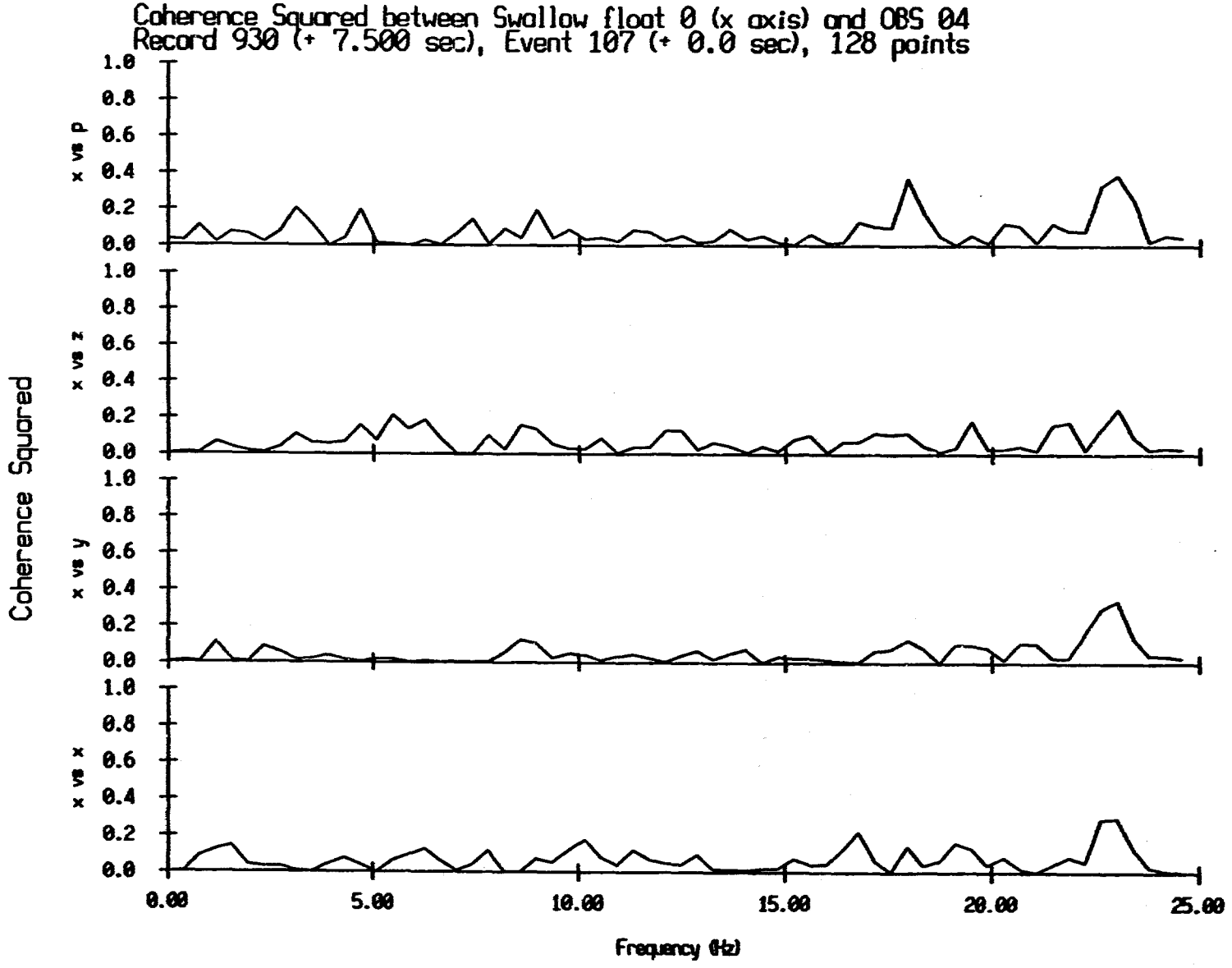

Figure VI.53i

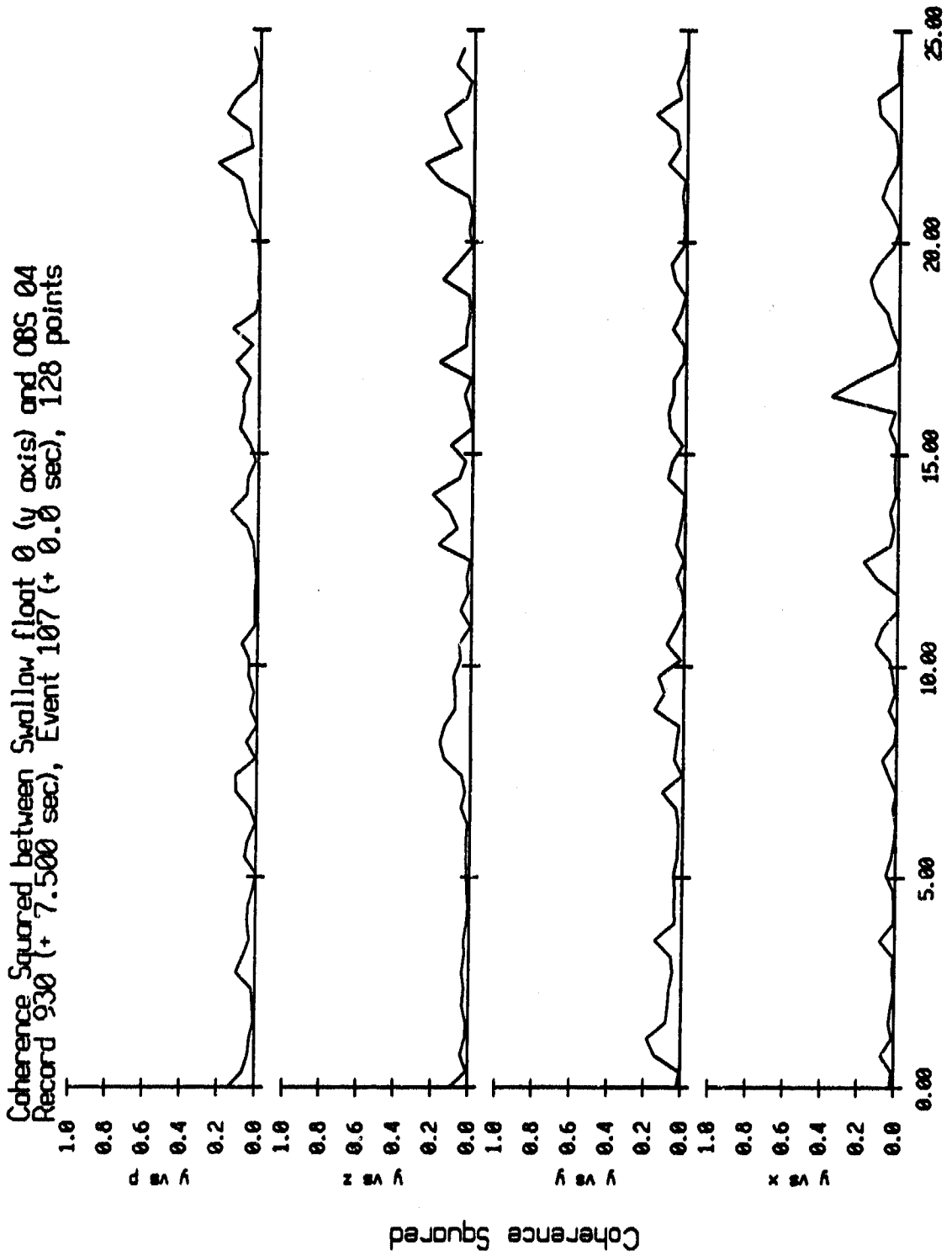

Figure VI.53j

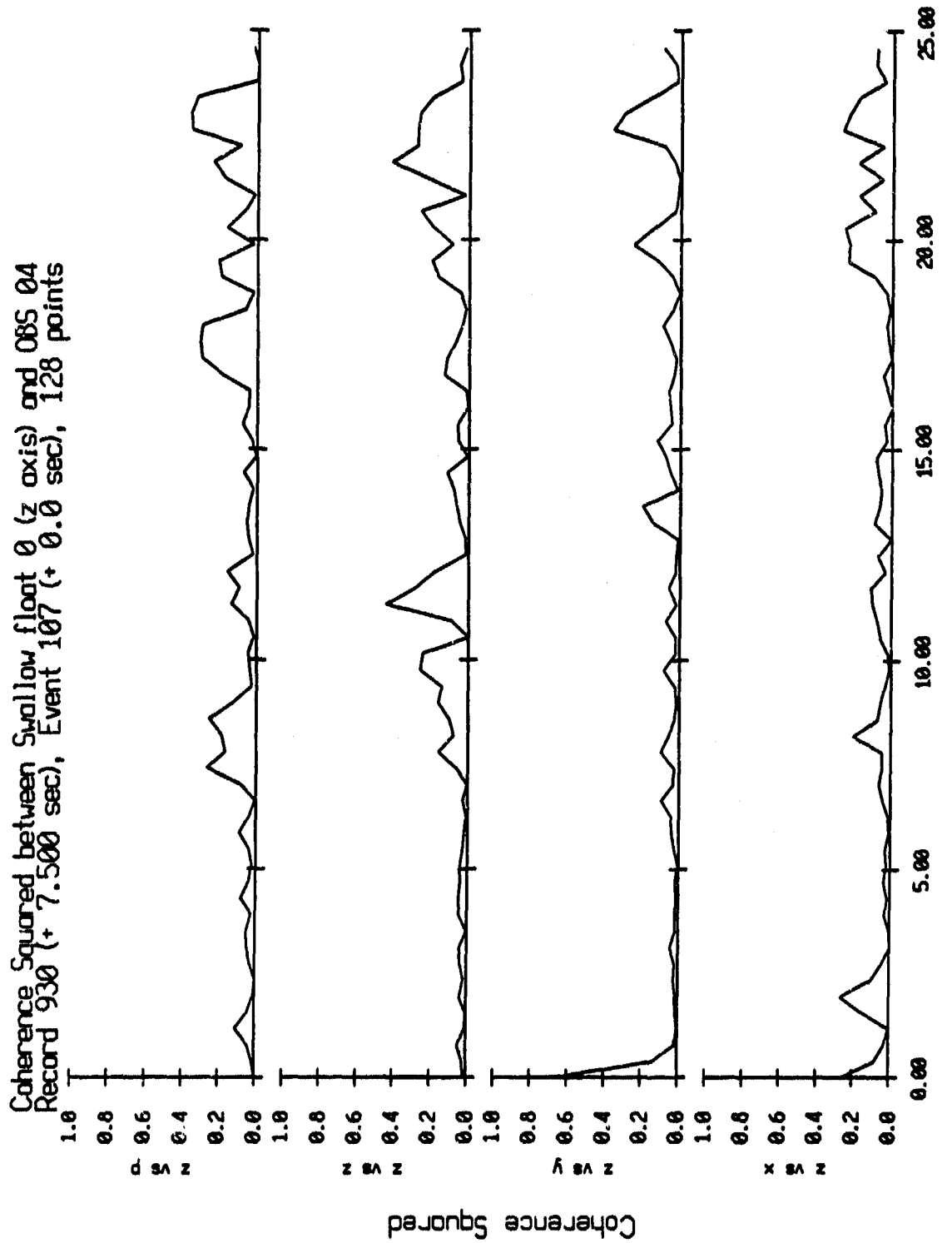

Figure VI.53k

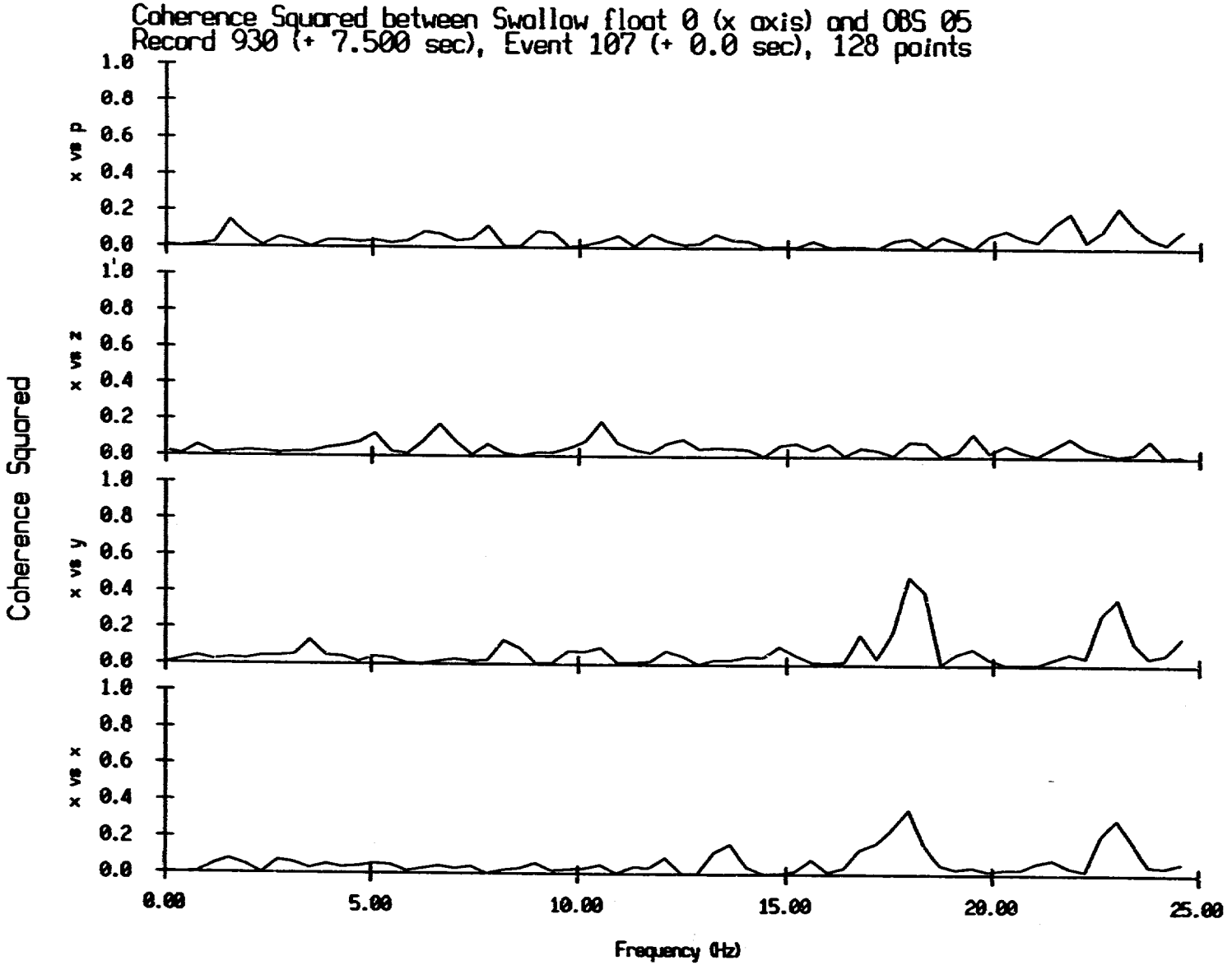

Figure VI.54i

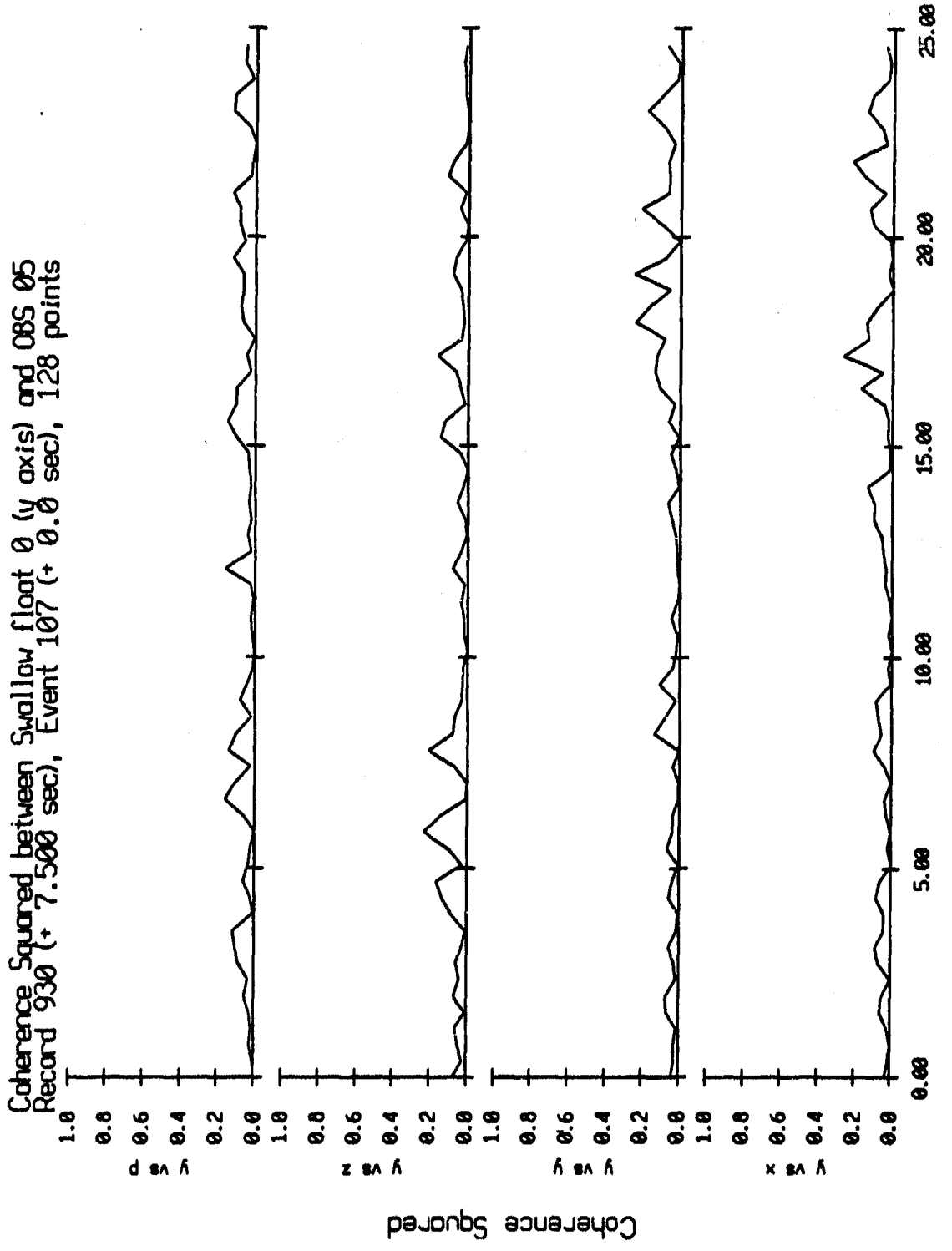

Figure VI.54j

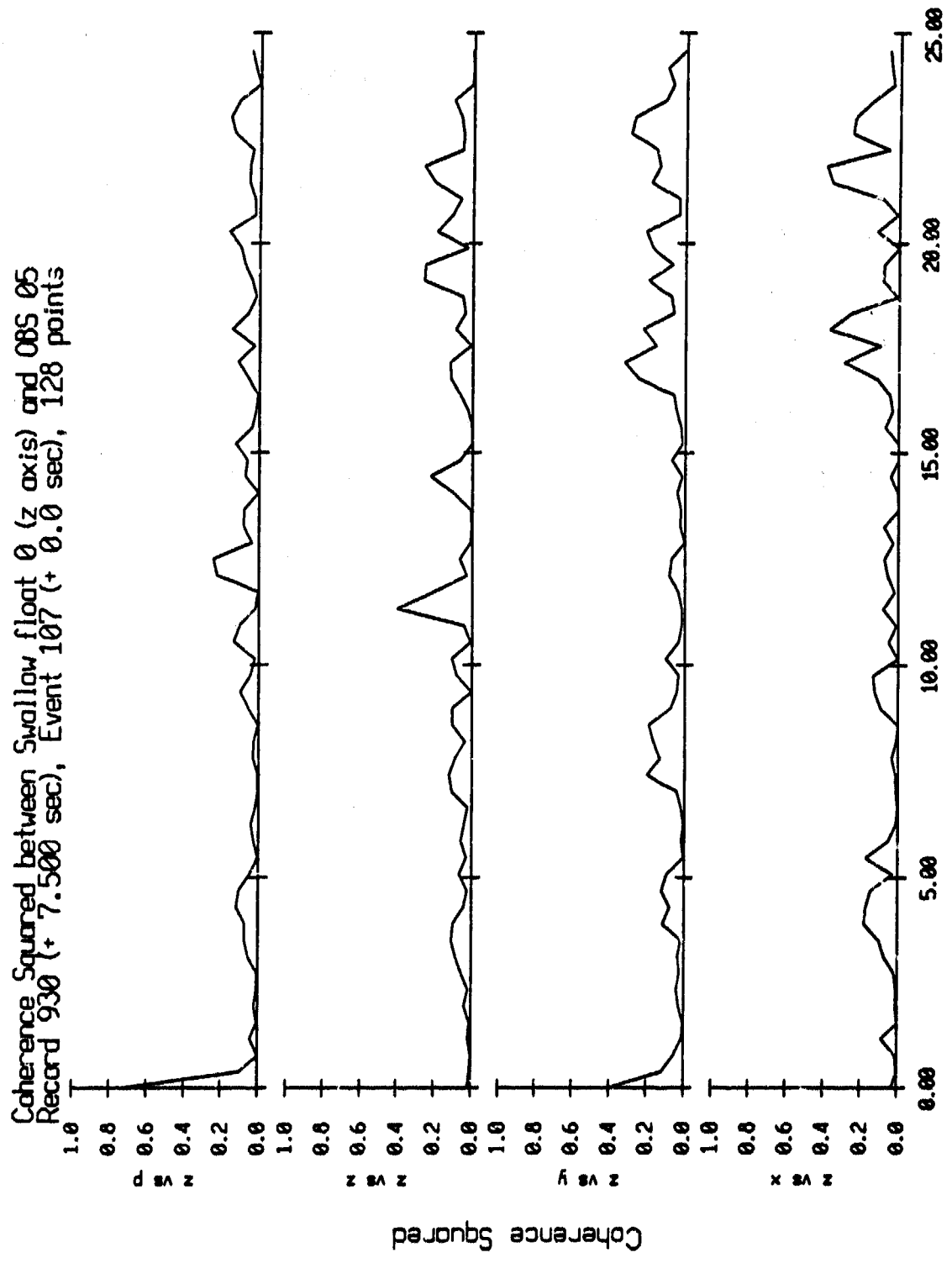

Figure VI.54k

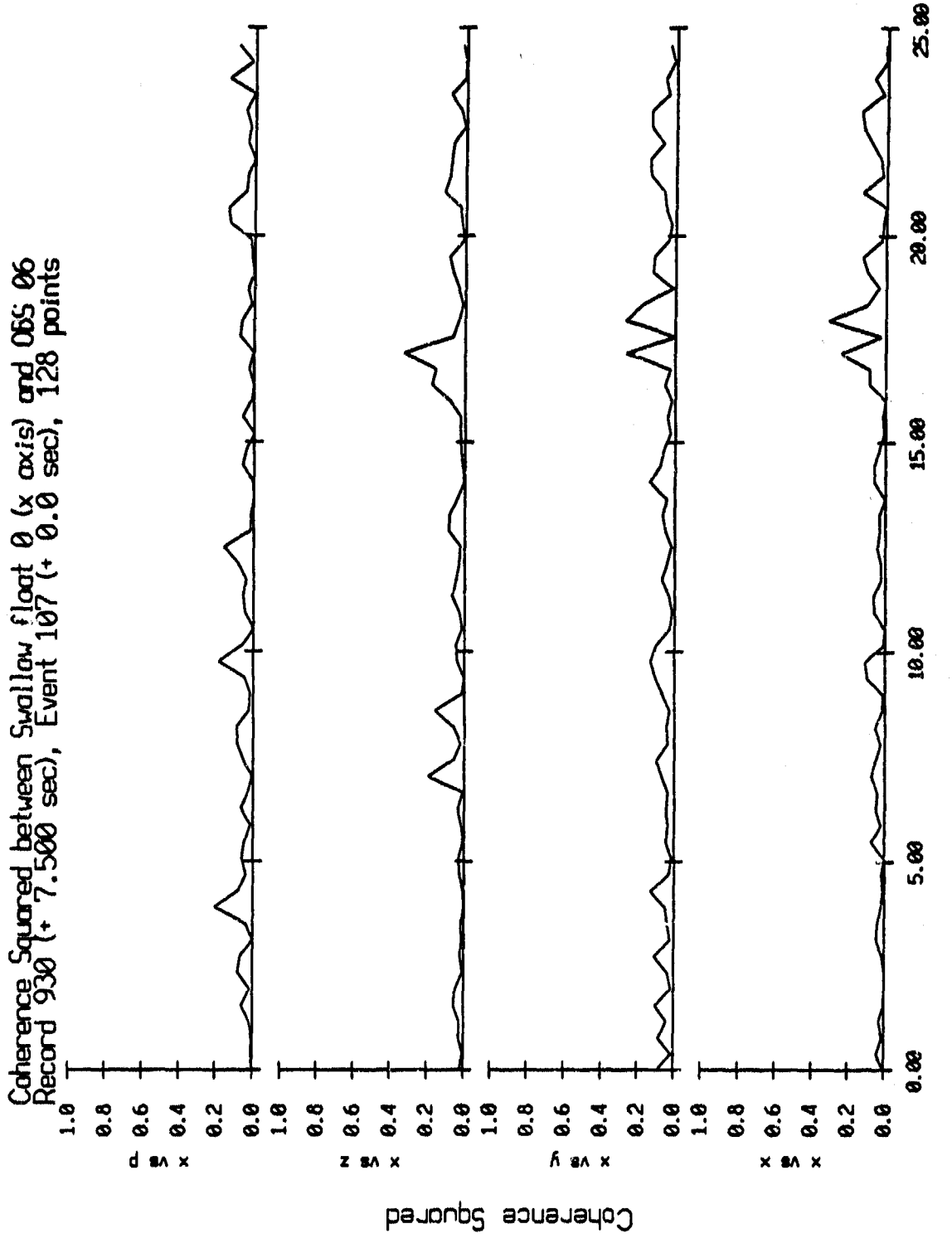

Figure VI.55i

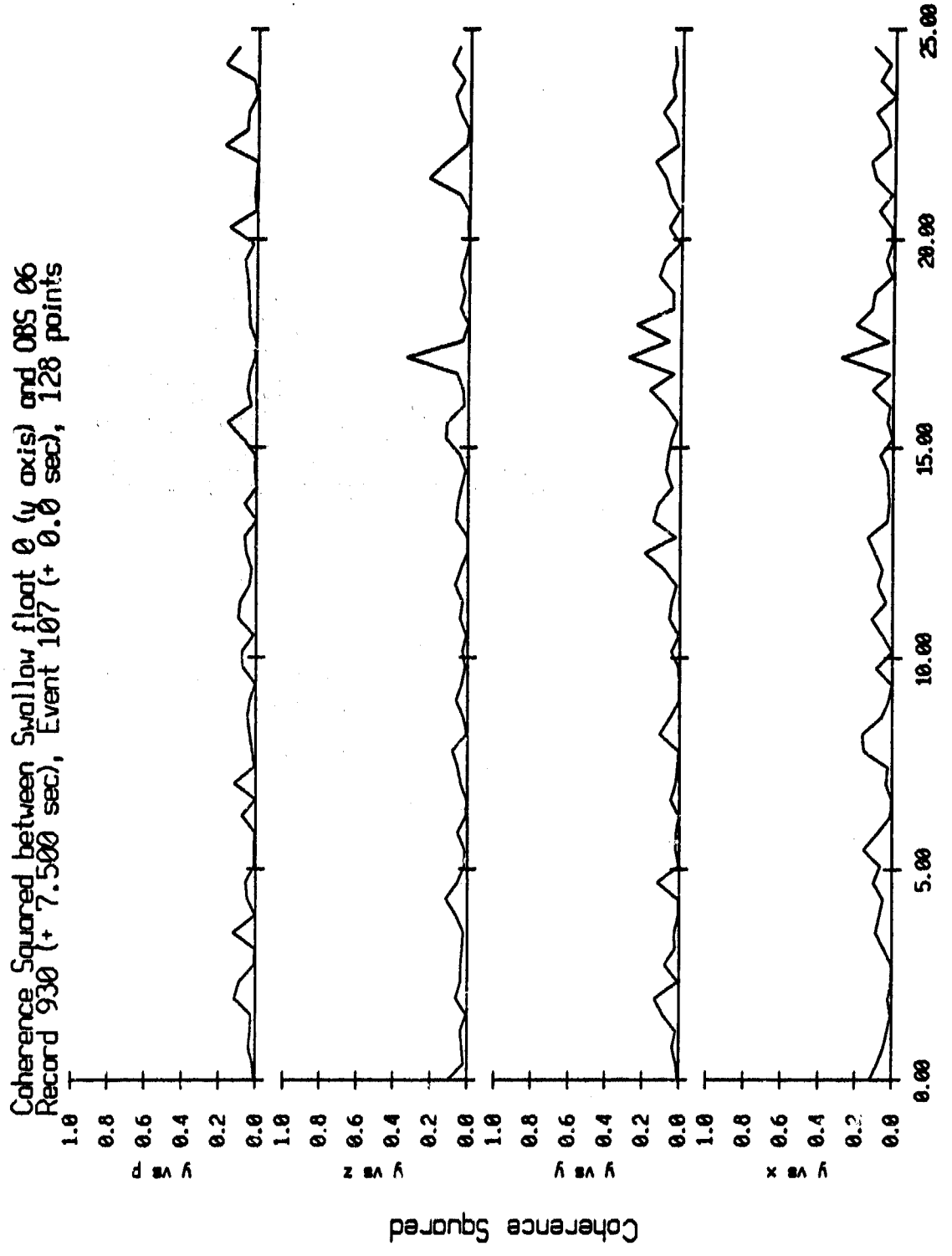

Figure VI.55j

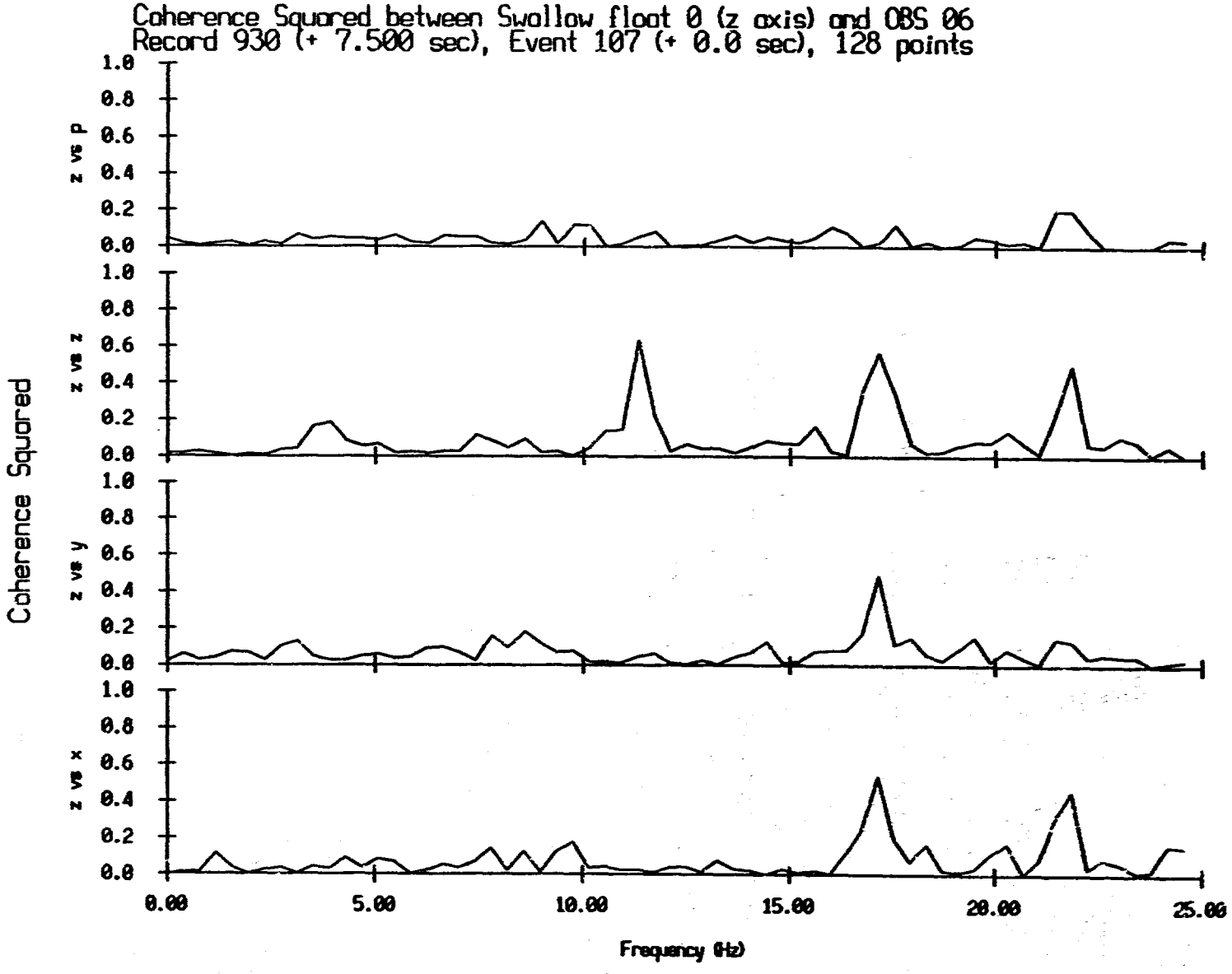

Figure VI.55k

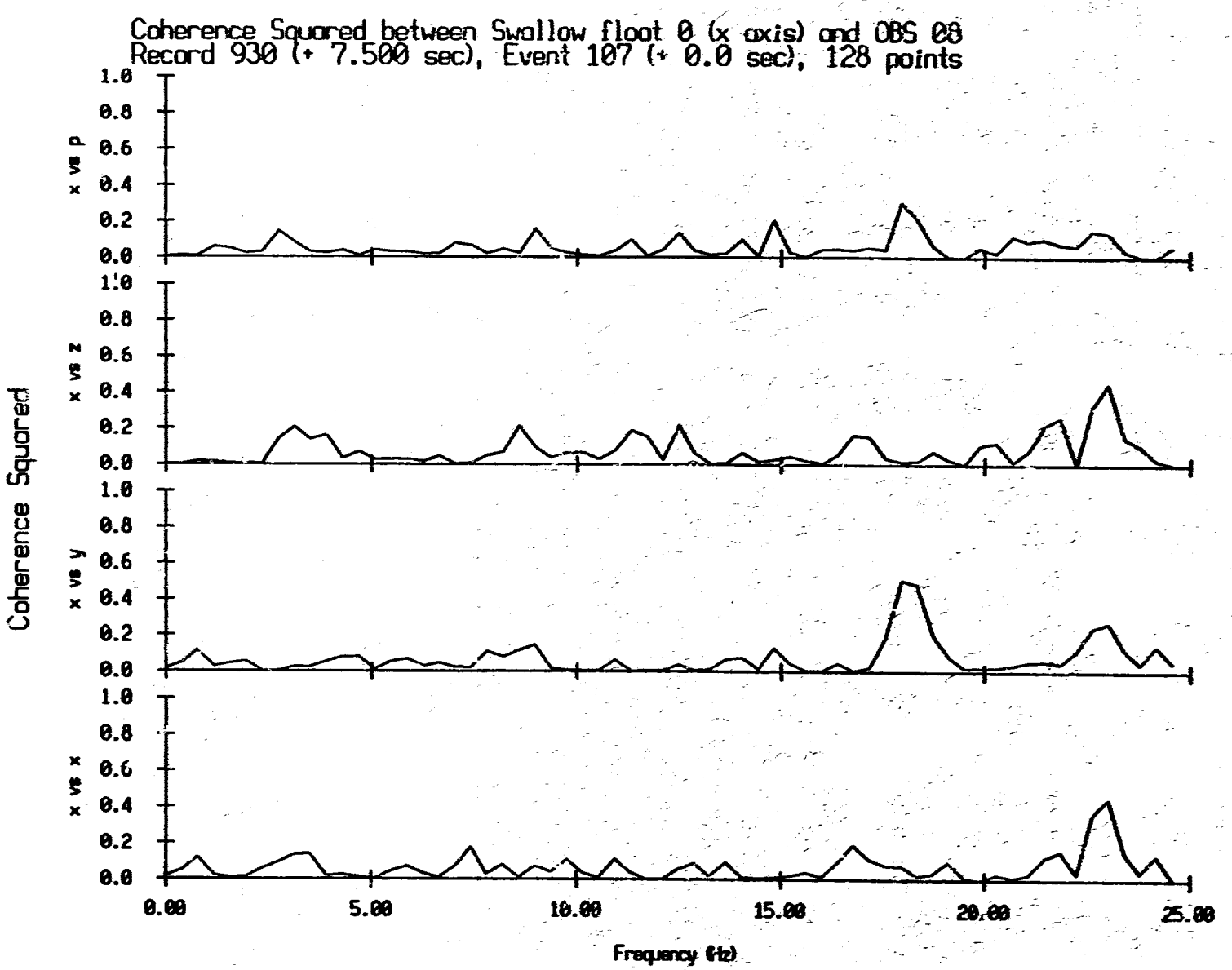

Figure VI.56i

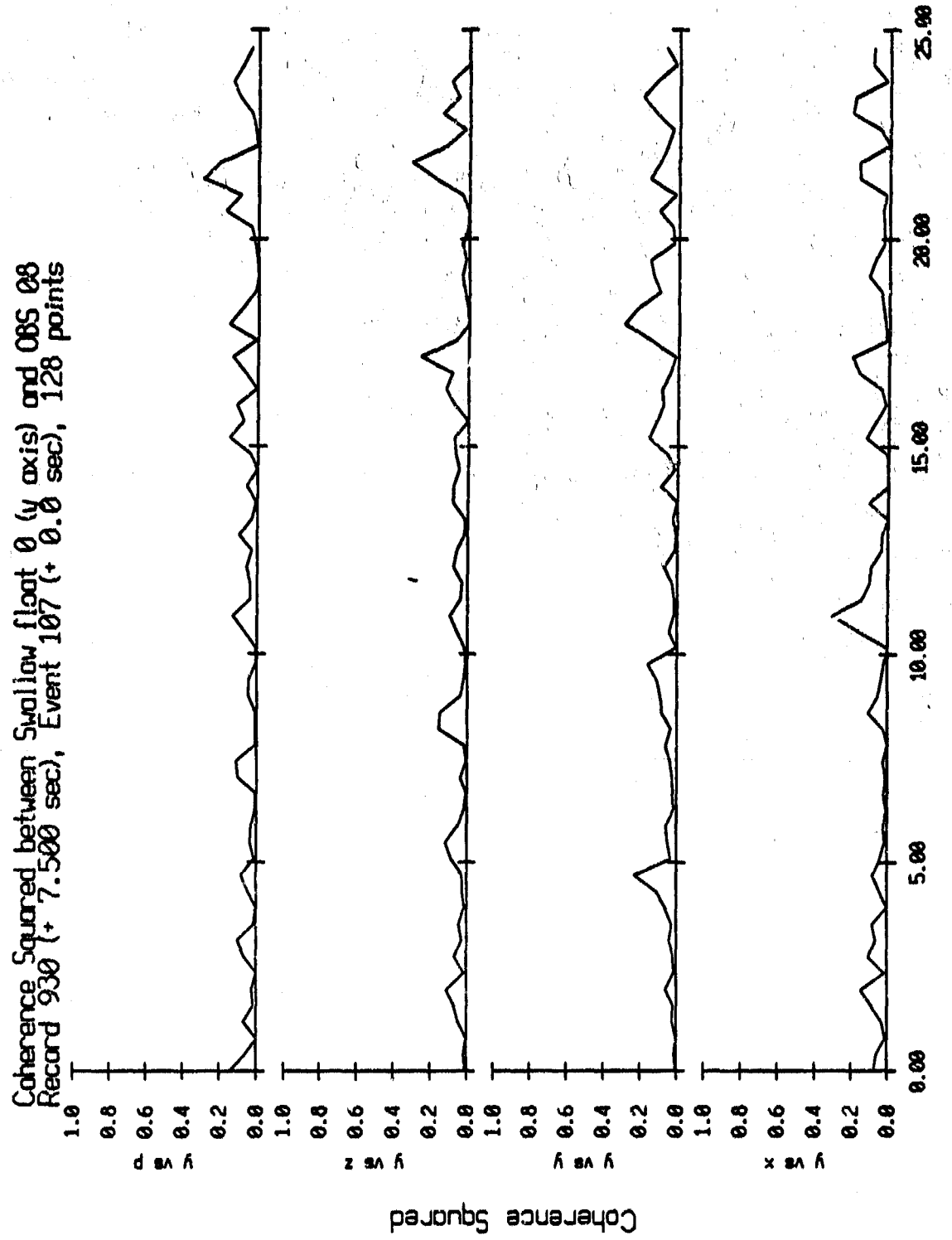

Figure VI.56j

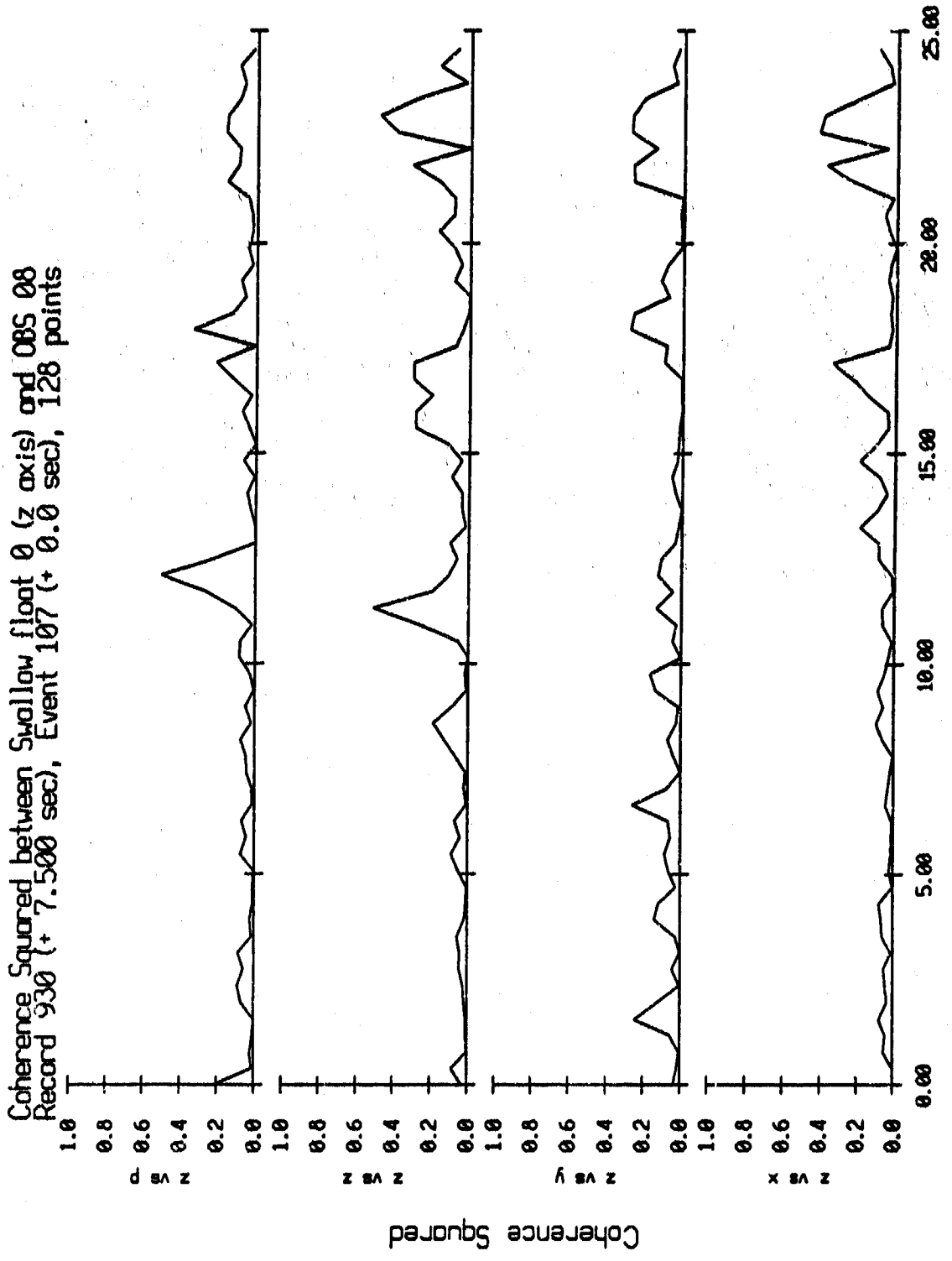

Figure VI.56k

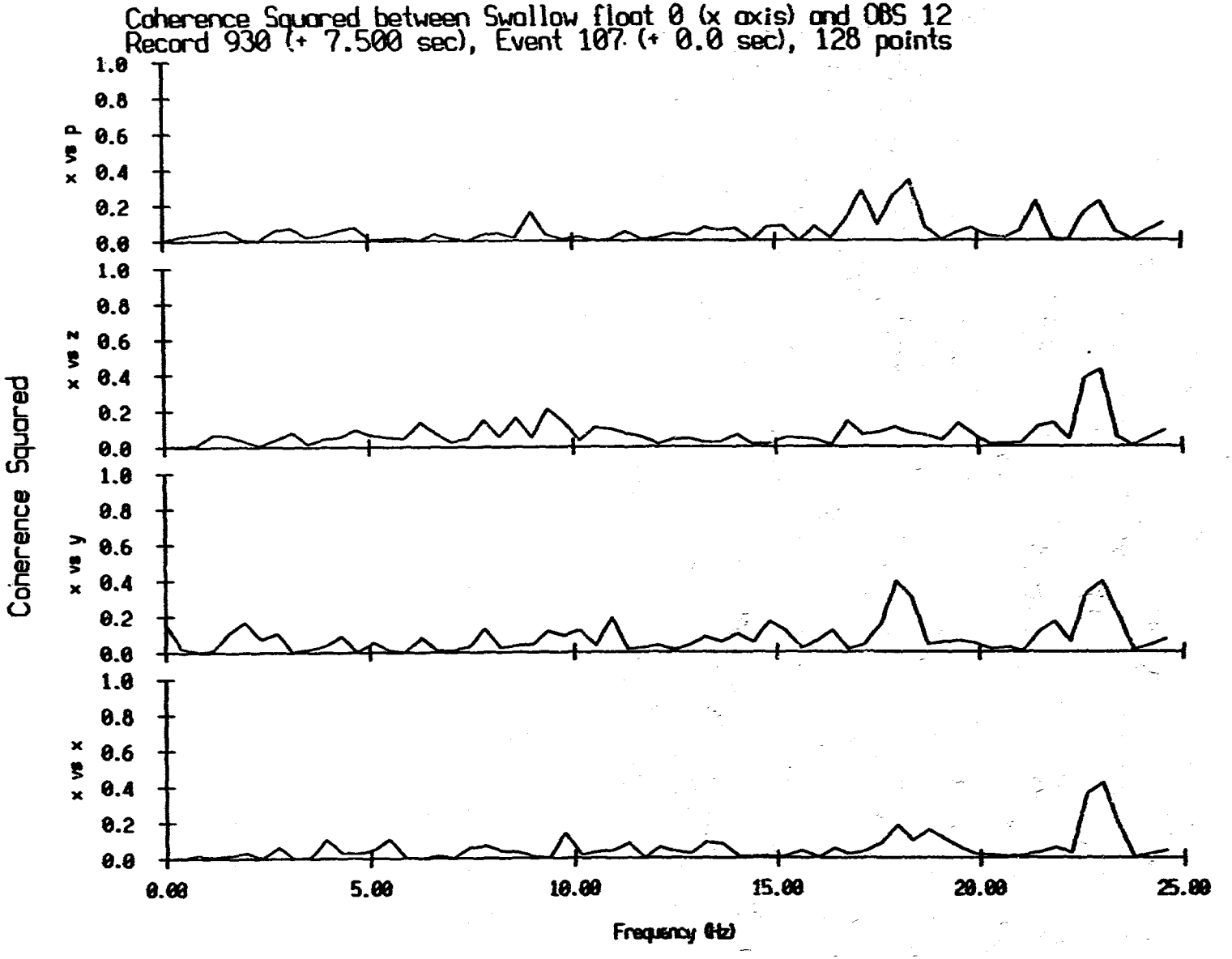

Figure VI.57i

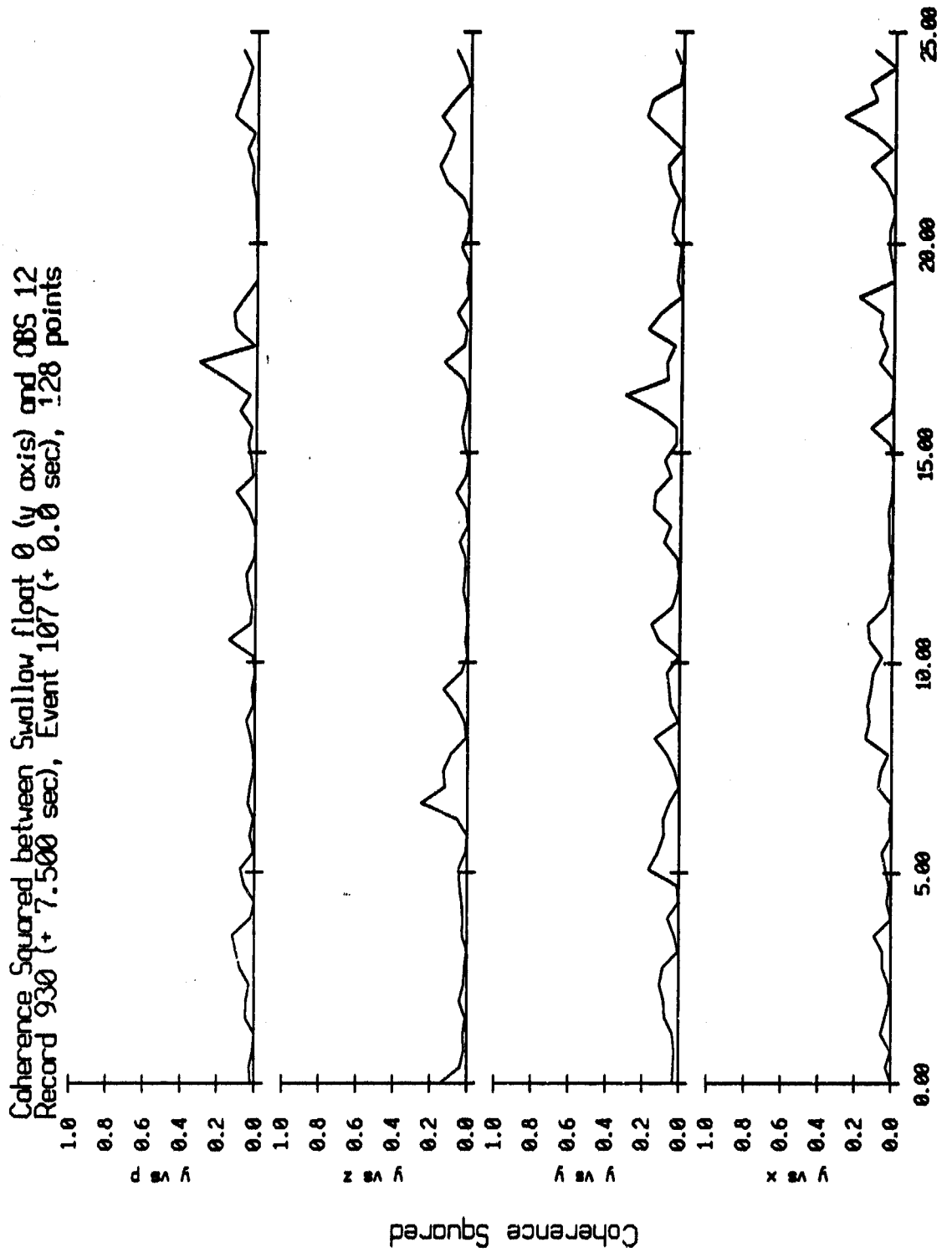

Figure VI.57j

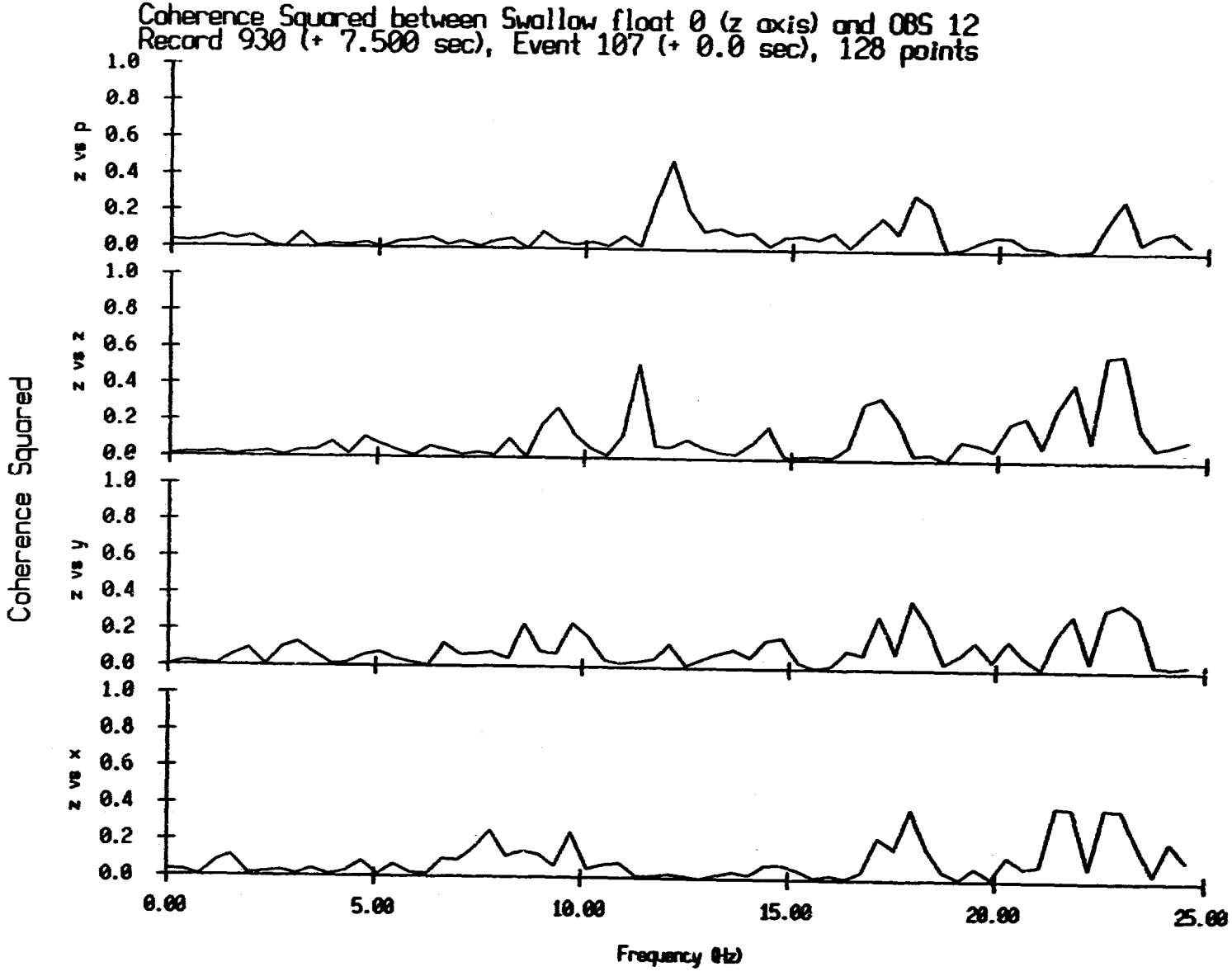

Figure VI.57k

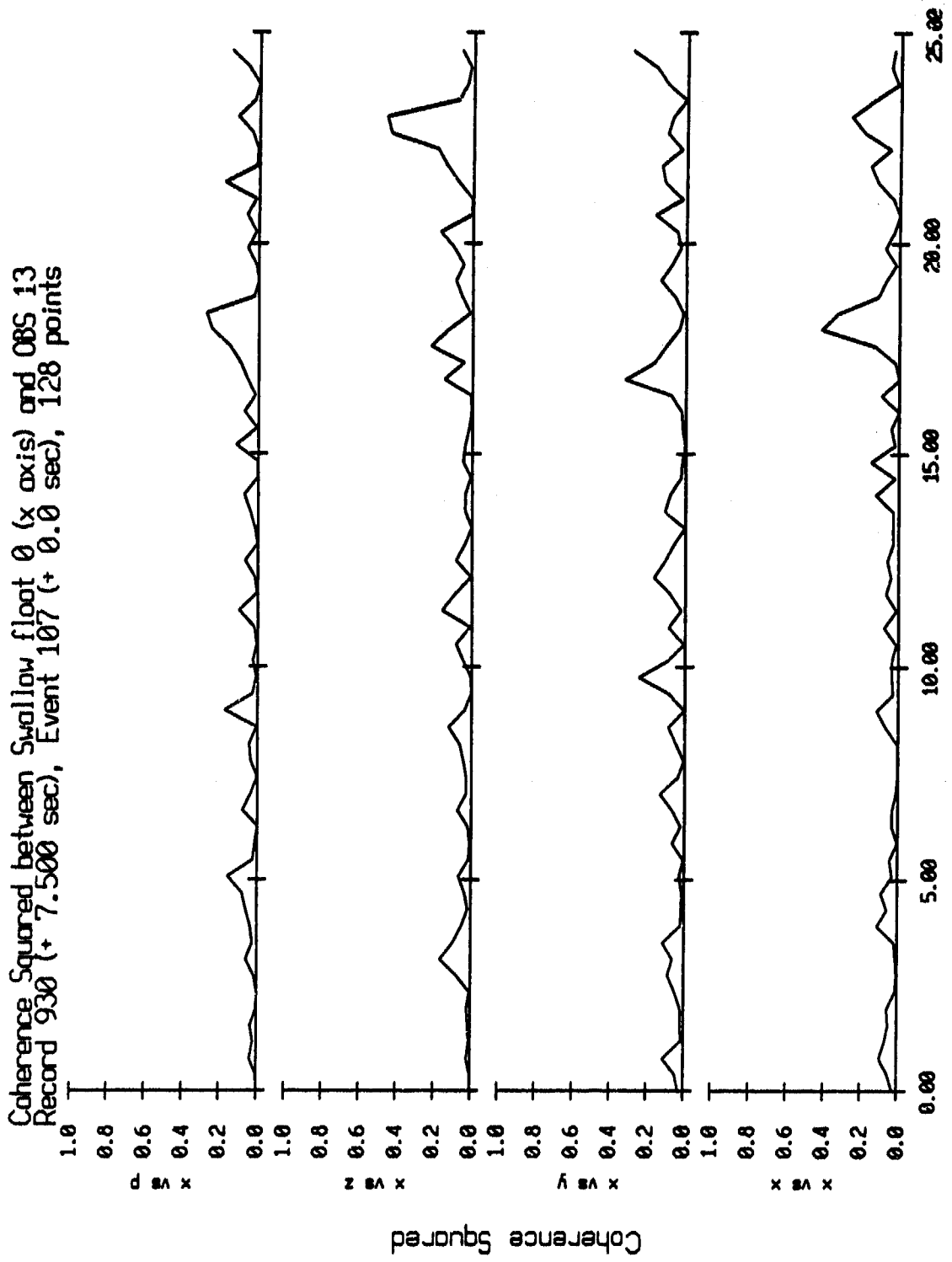

Figure VI.58i

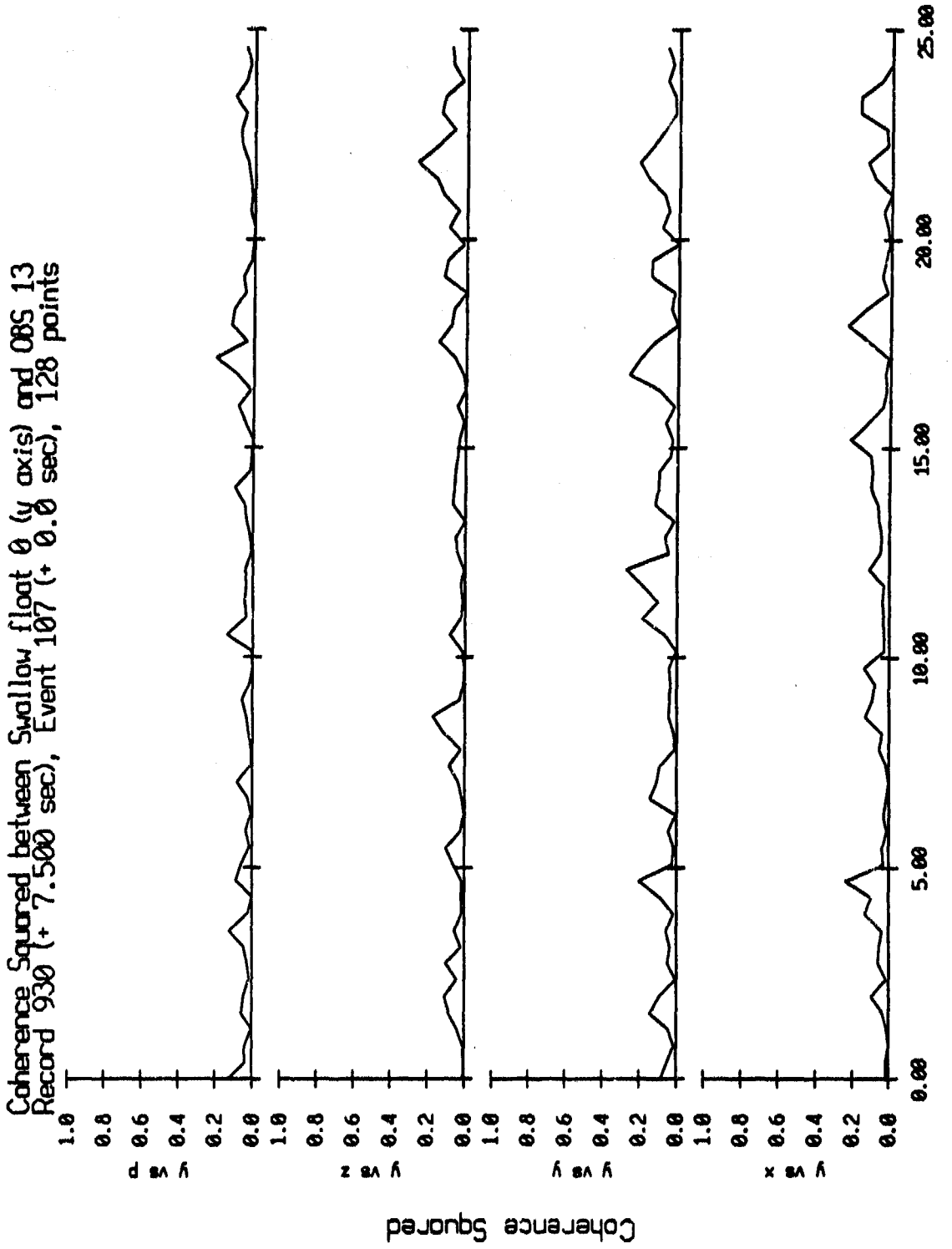

Figure VI.58j

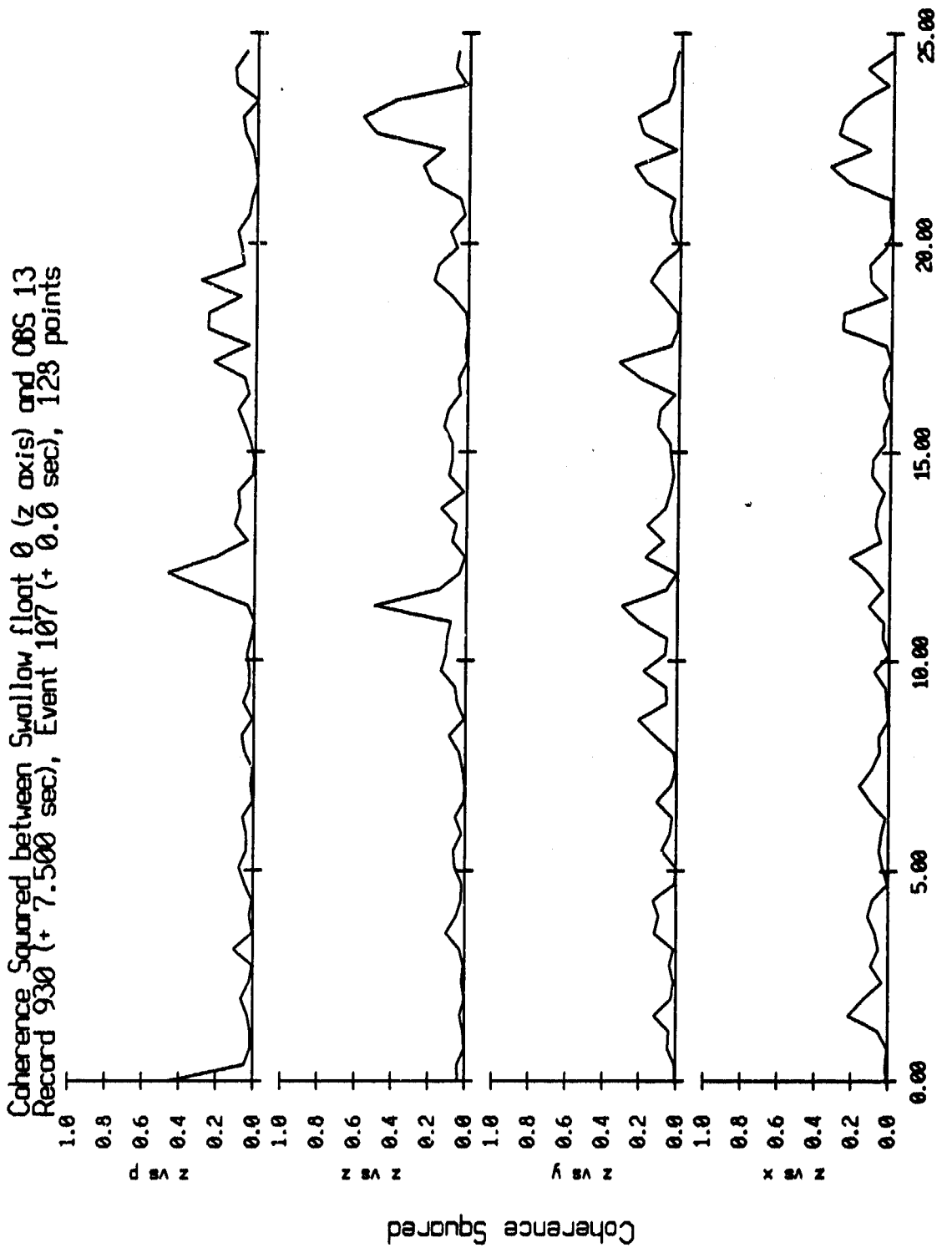

Figure VI.58k

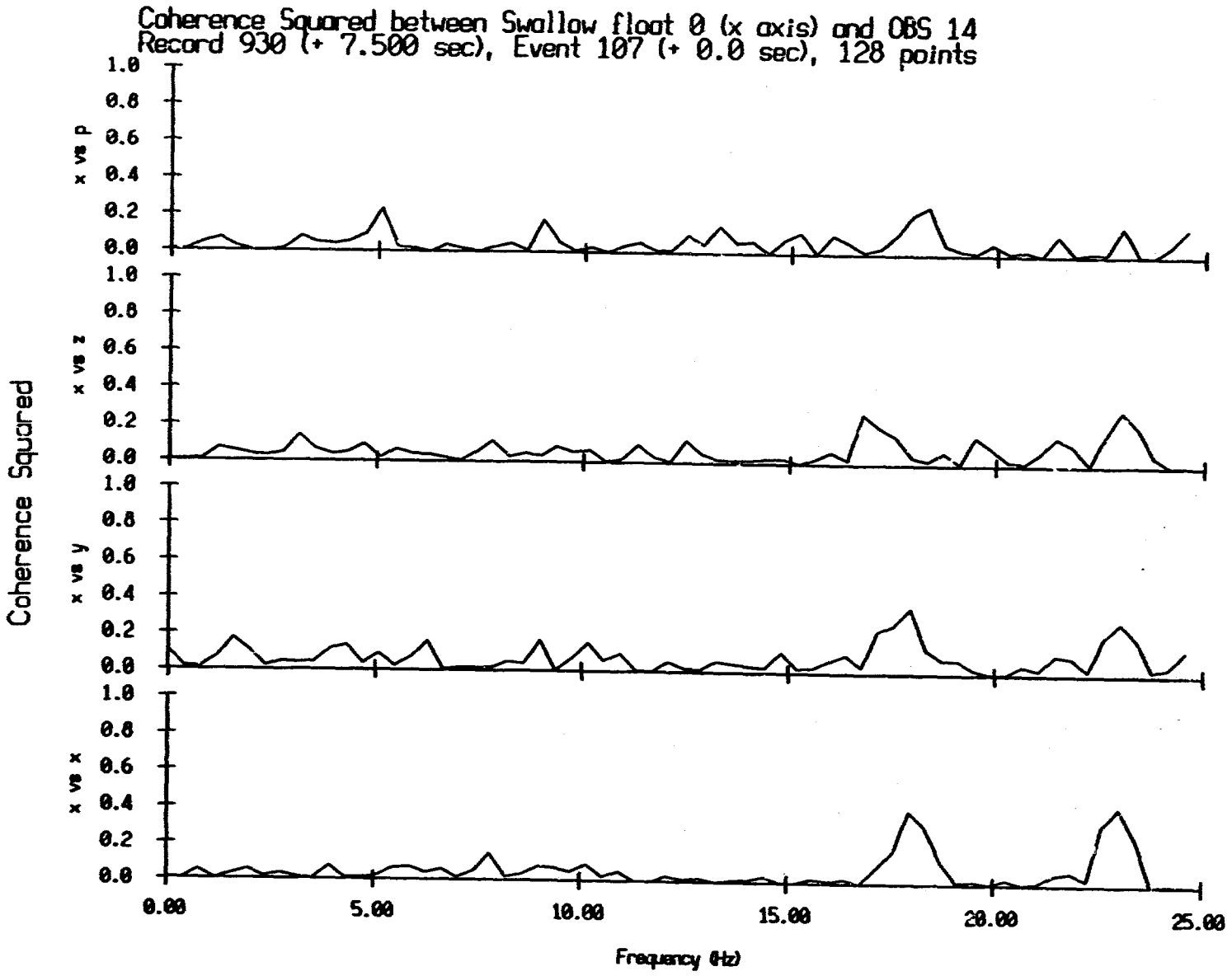

Figure VI.59i

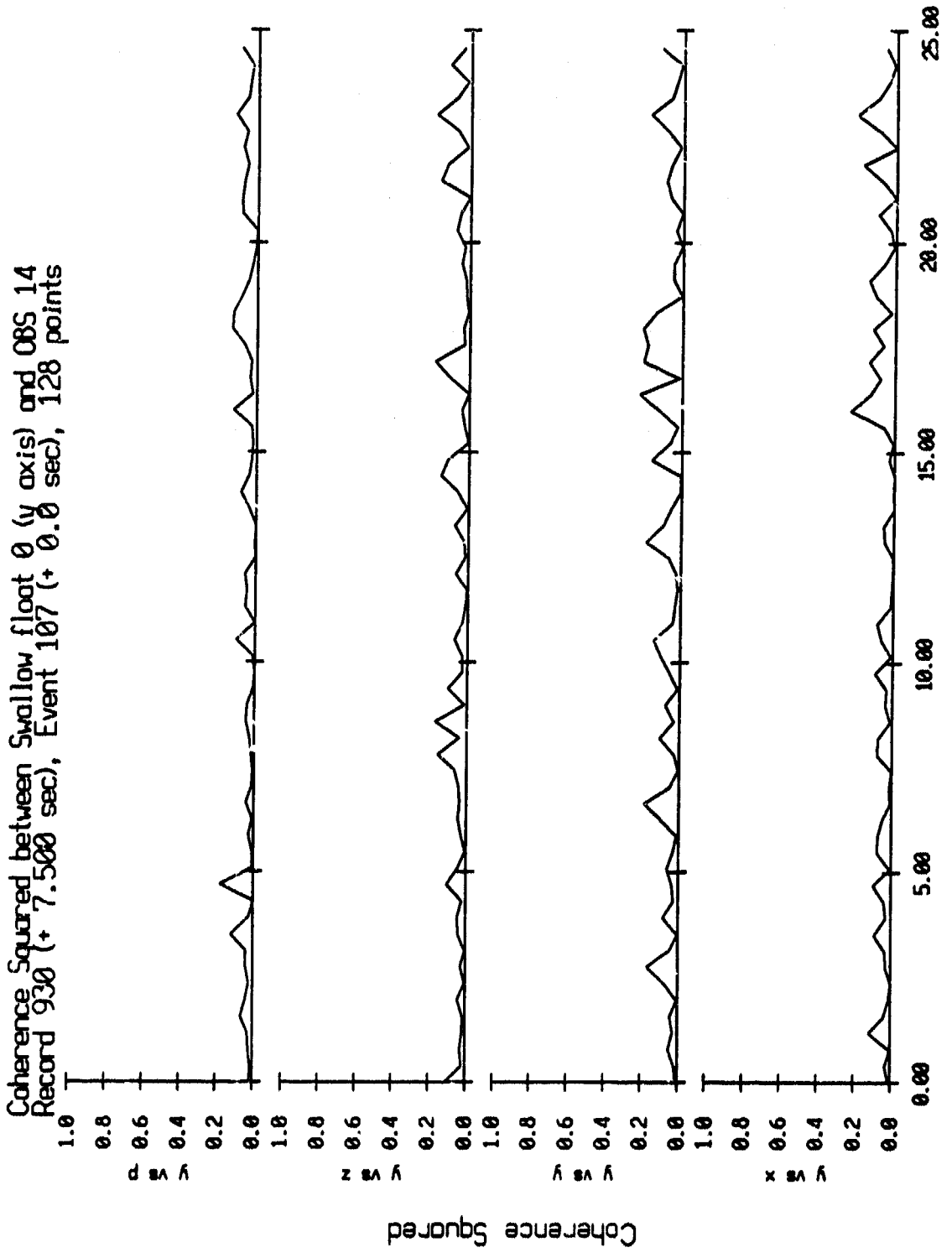

Figure VI.59j

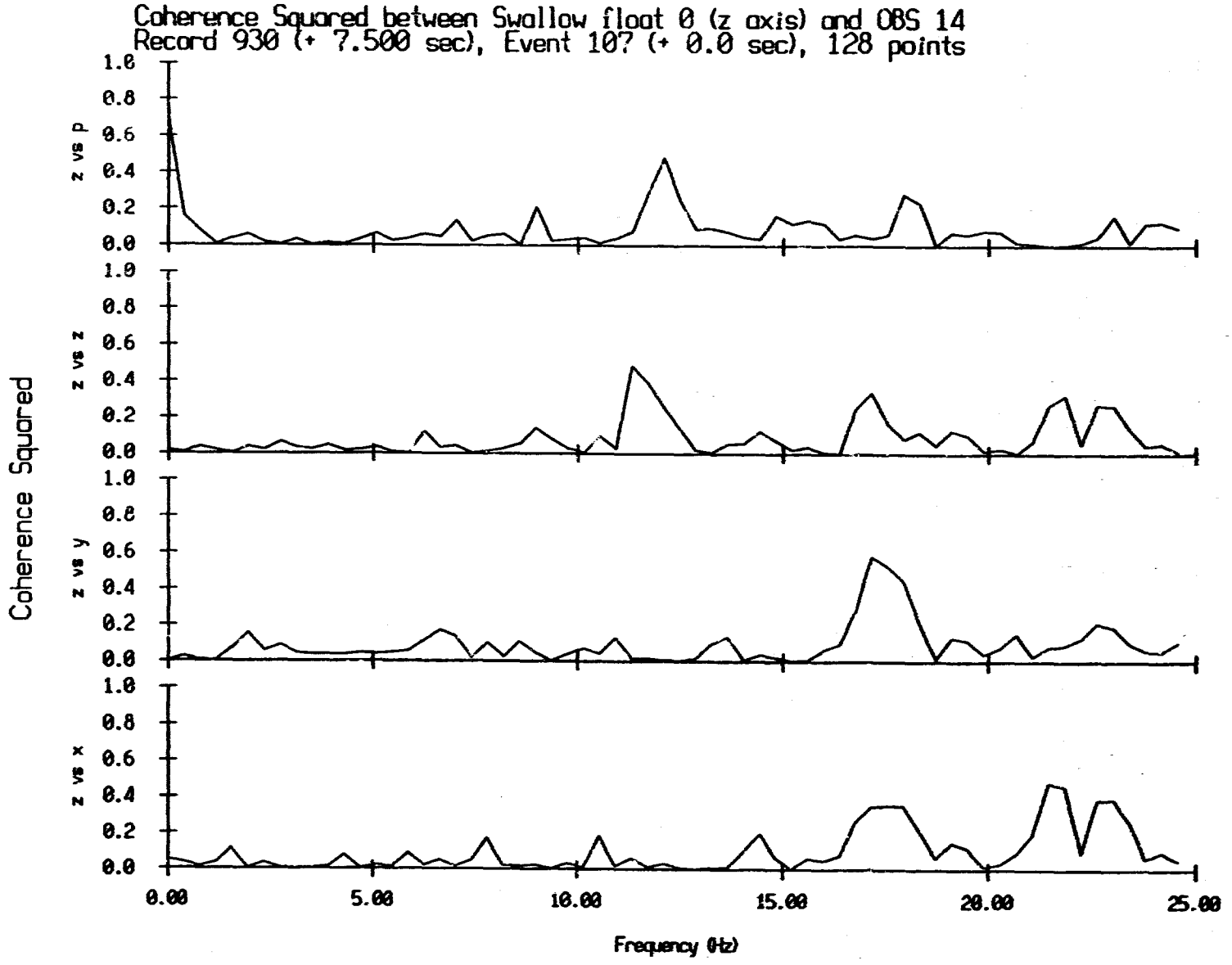

Figure V1.59k

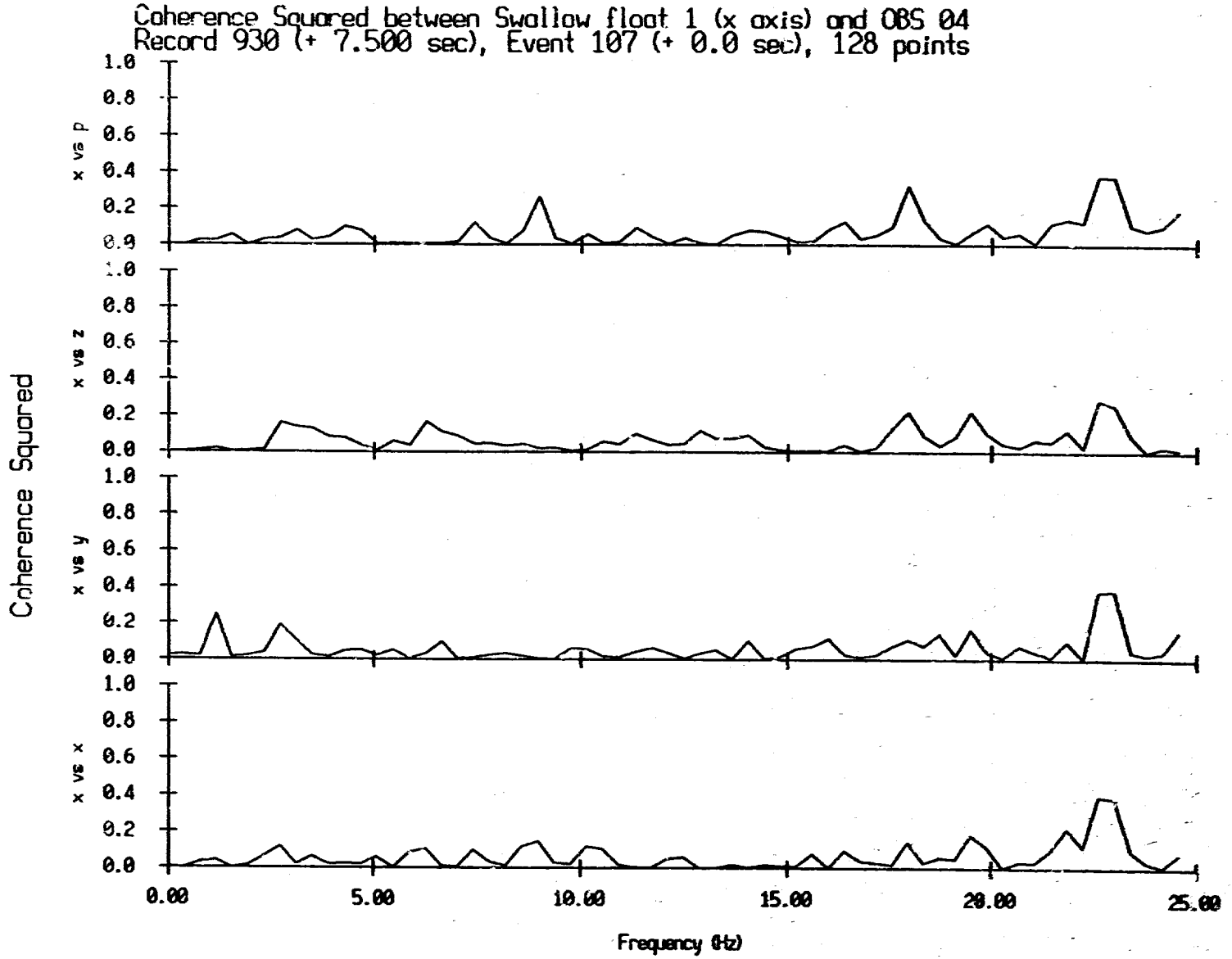

Figure VI.60i

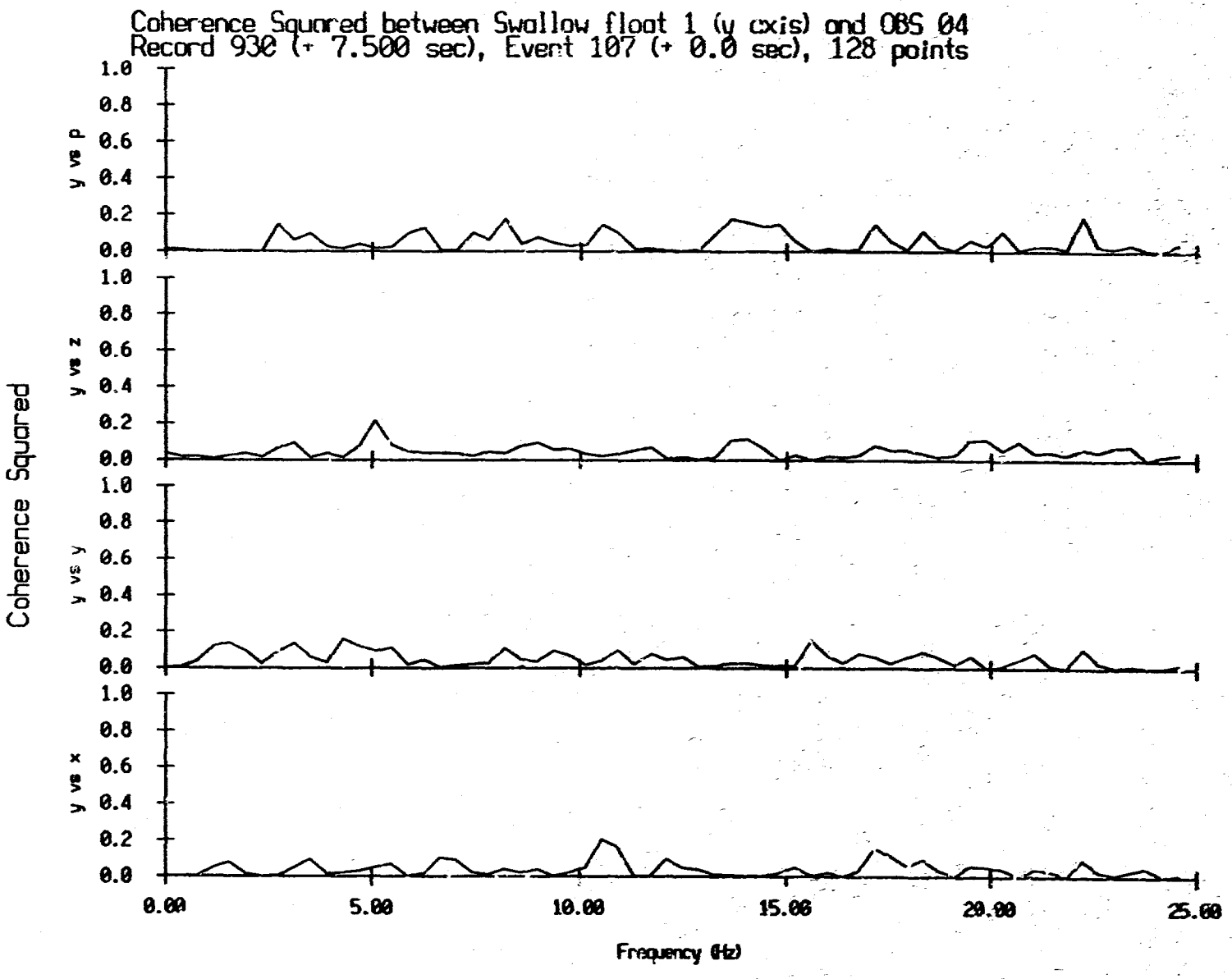

Figure VI.60j

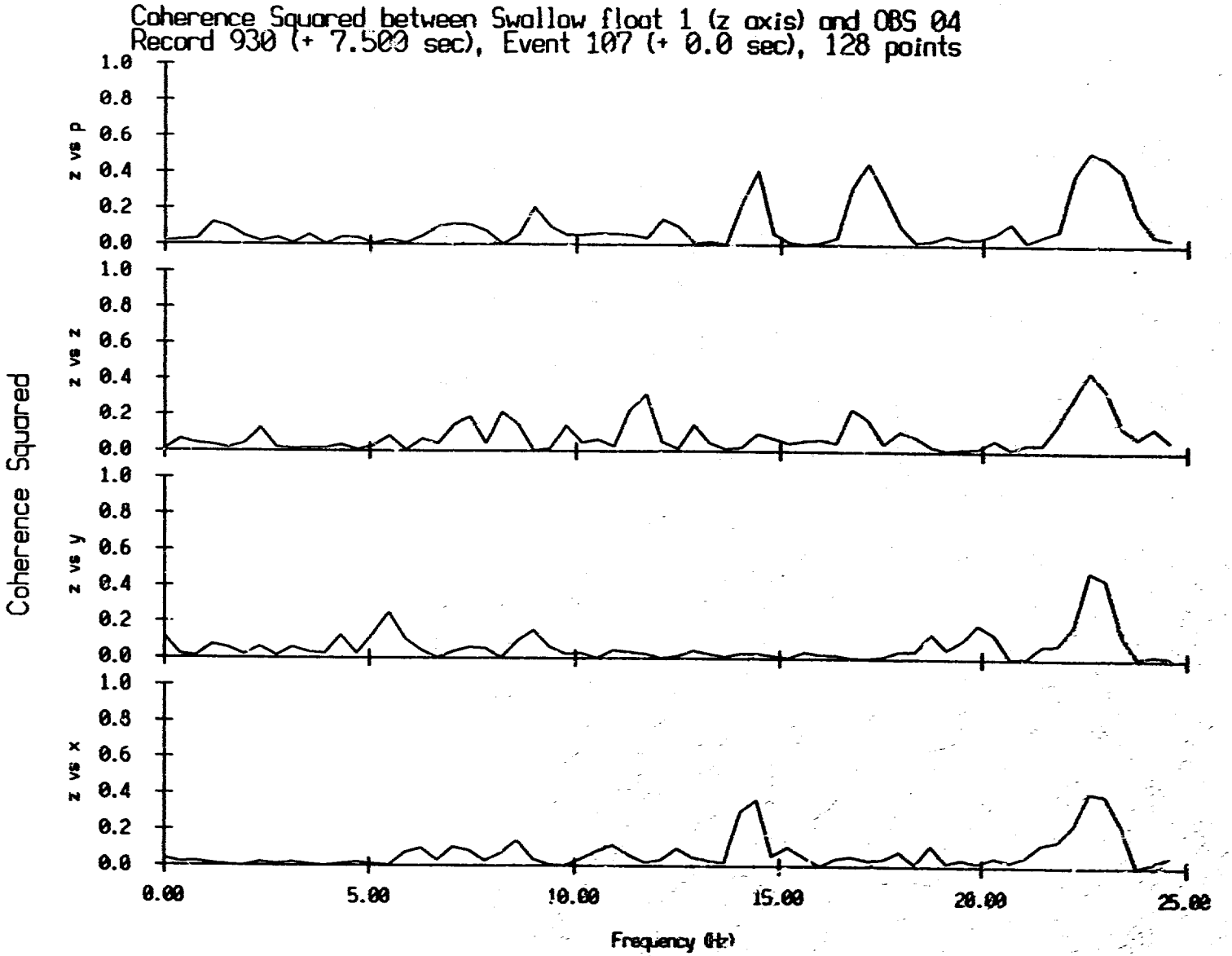

Figure VI.60k

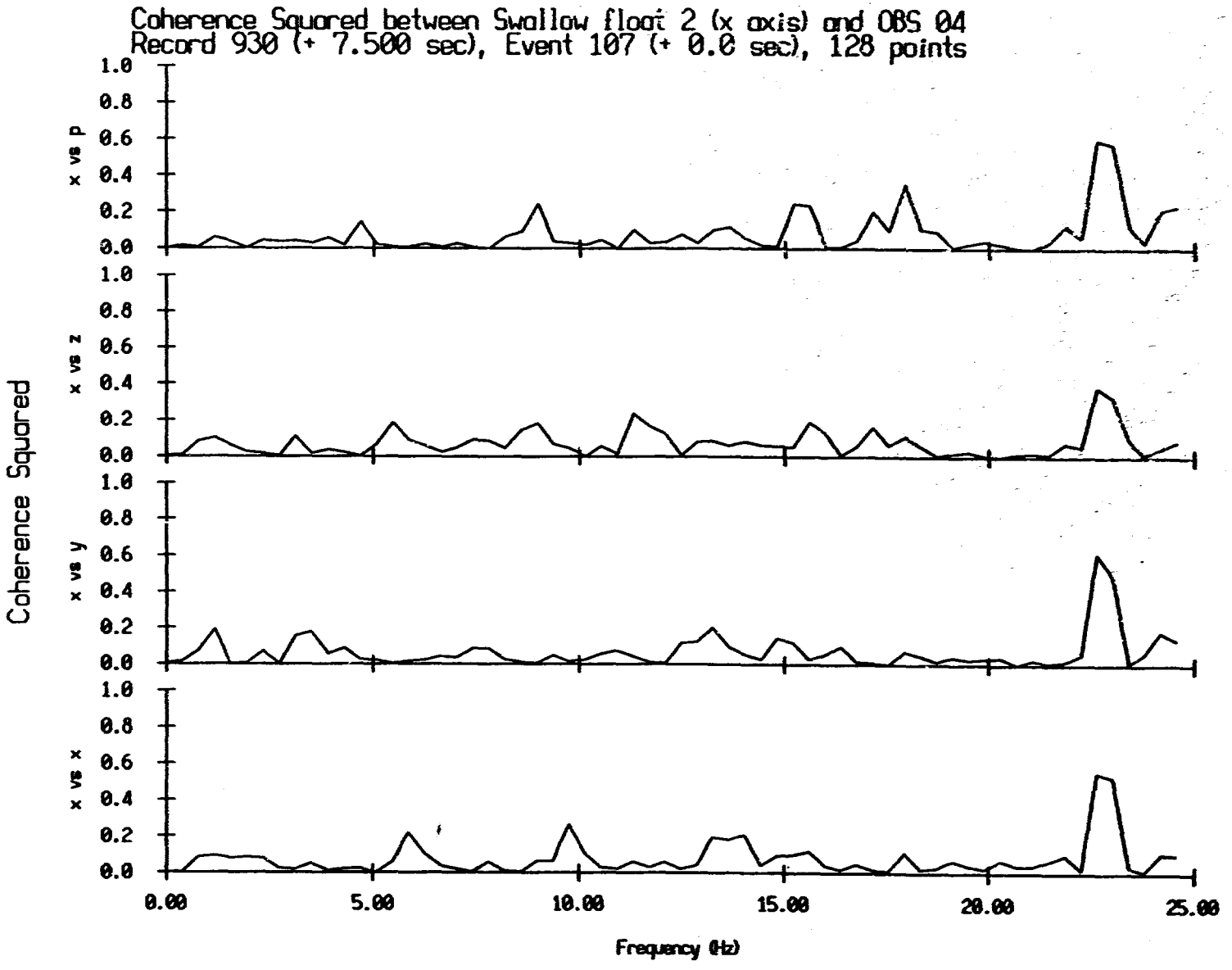

Figure VI.61i

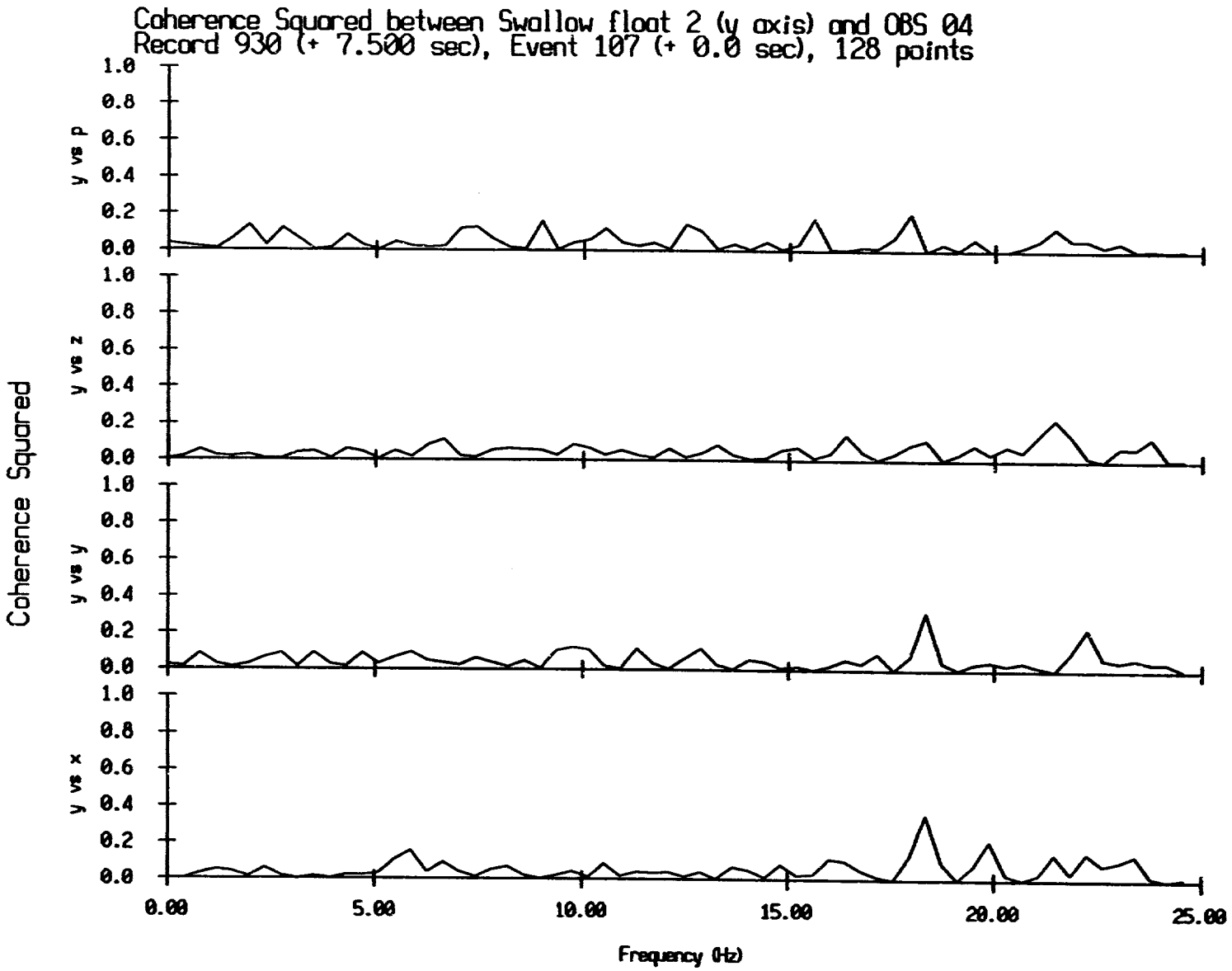

Figure VI.81j

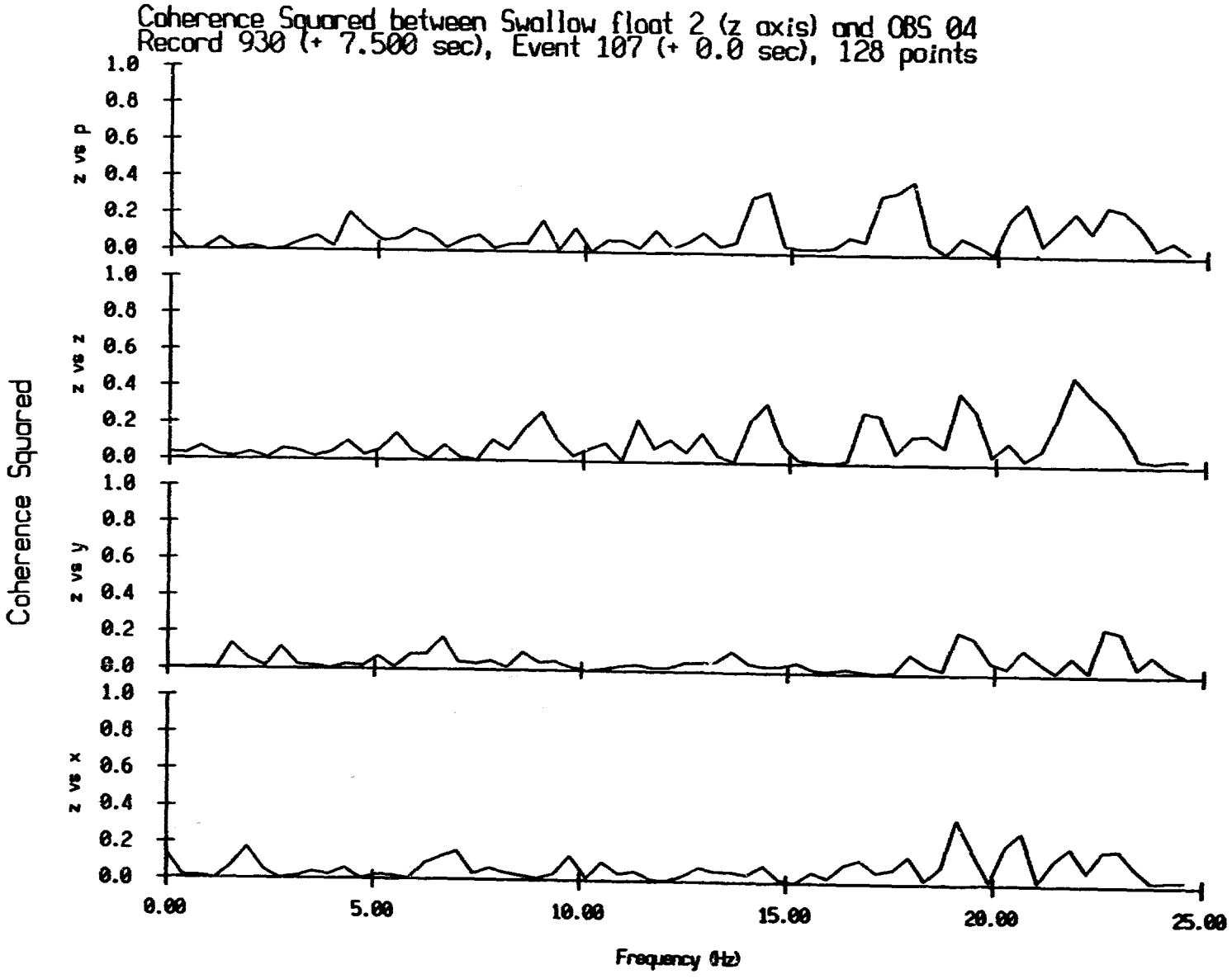

Figure VI.61k

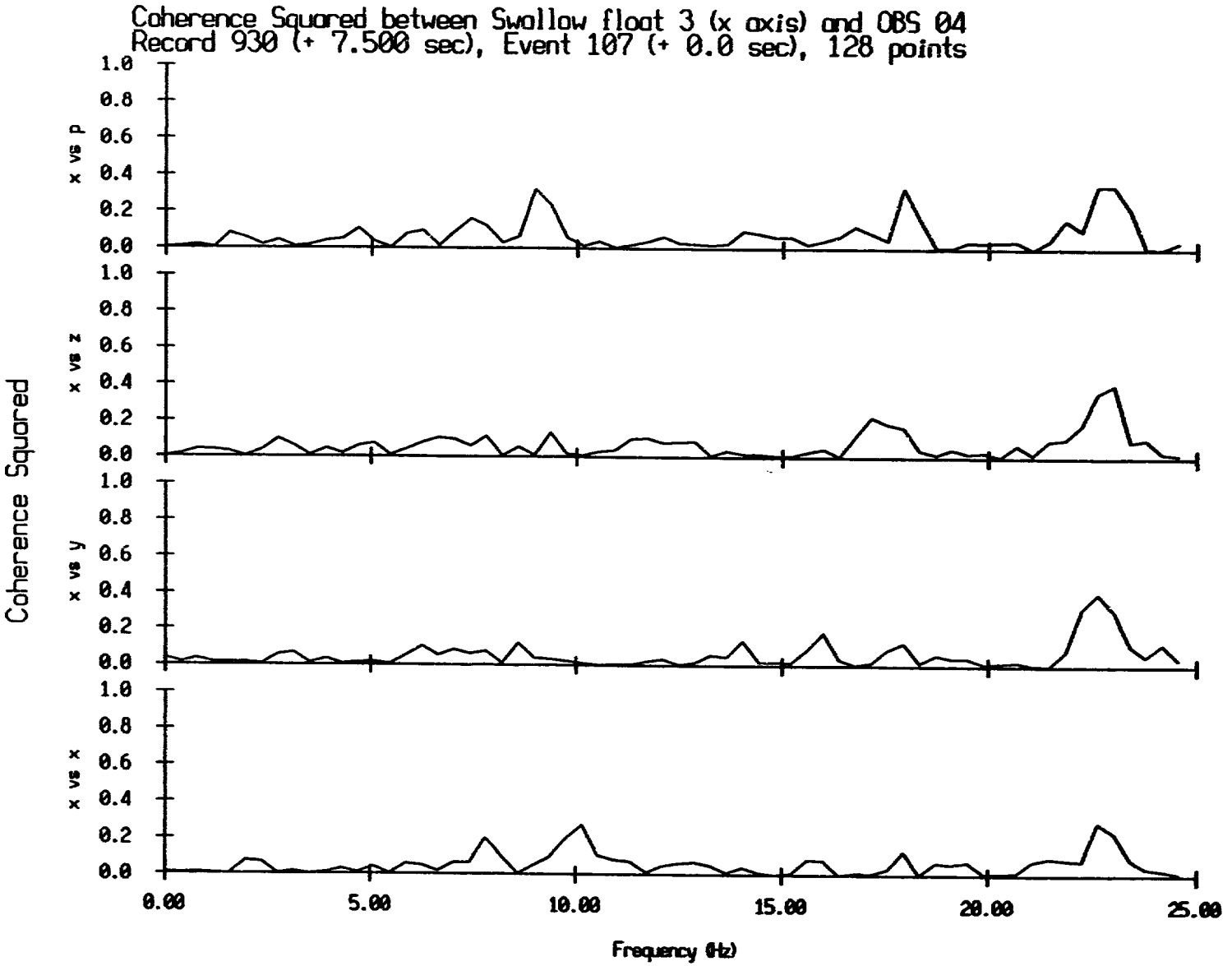

Figure VI.62i

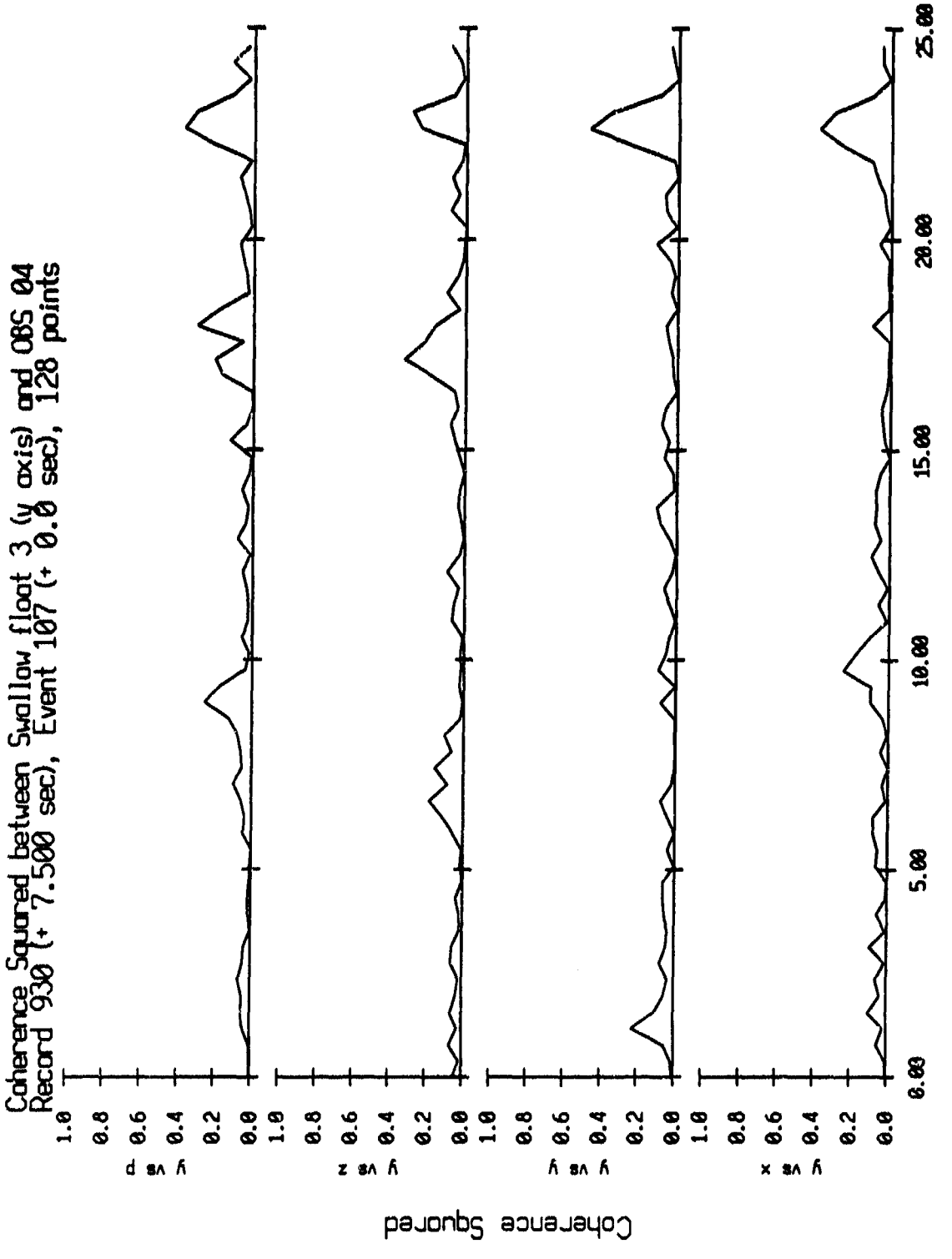

Figure VI.62j

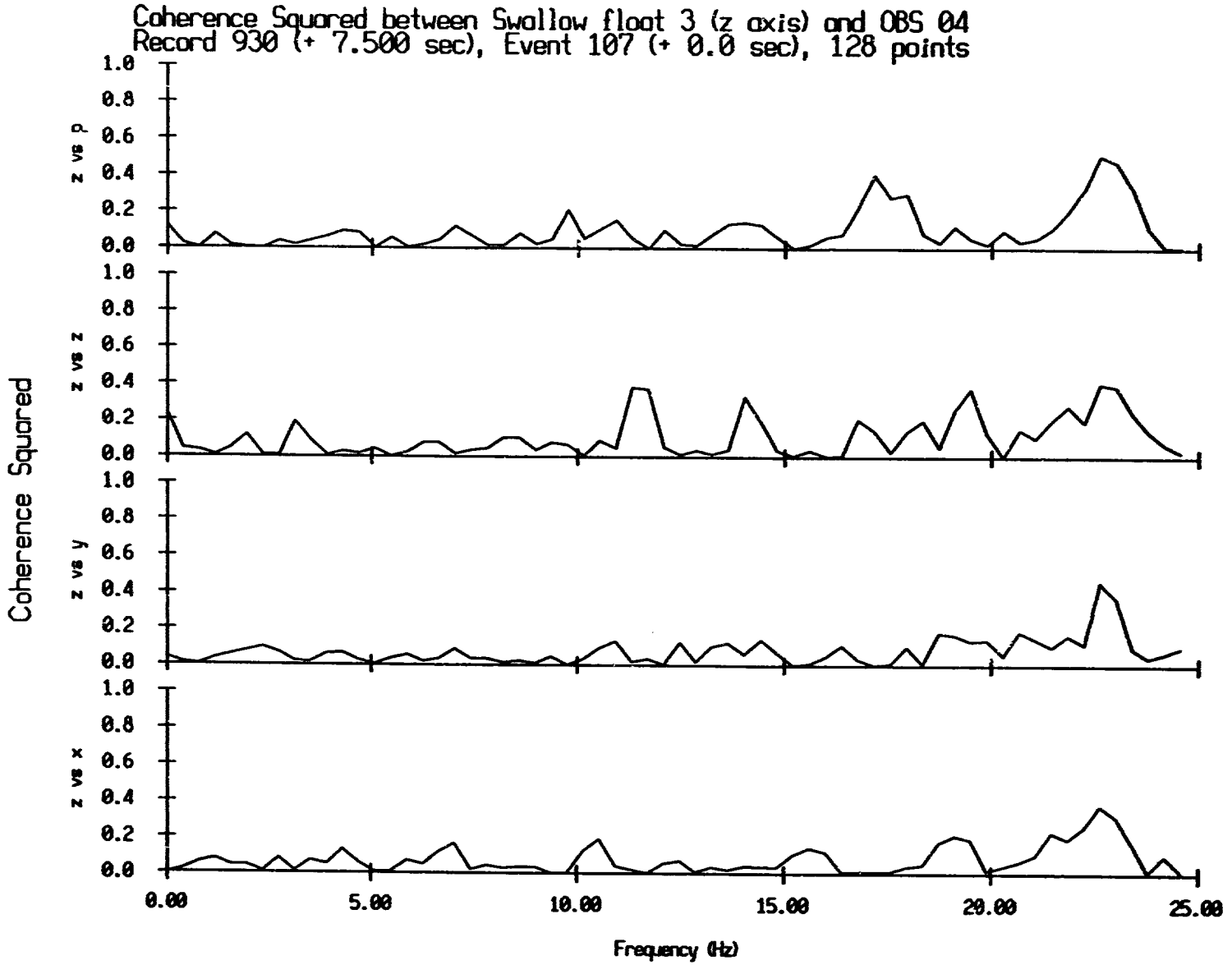

Figure VI.62k

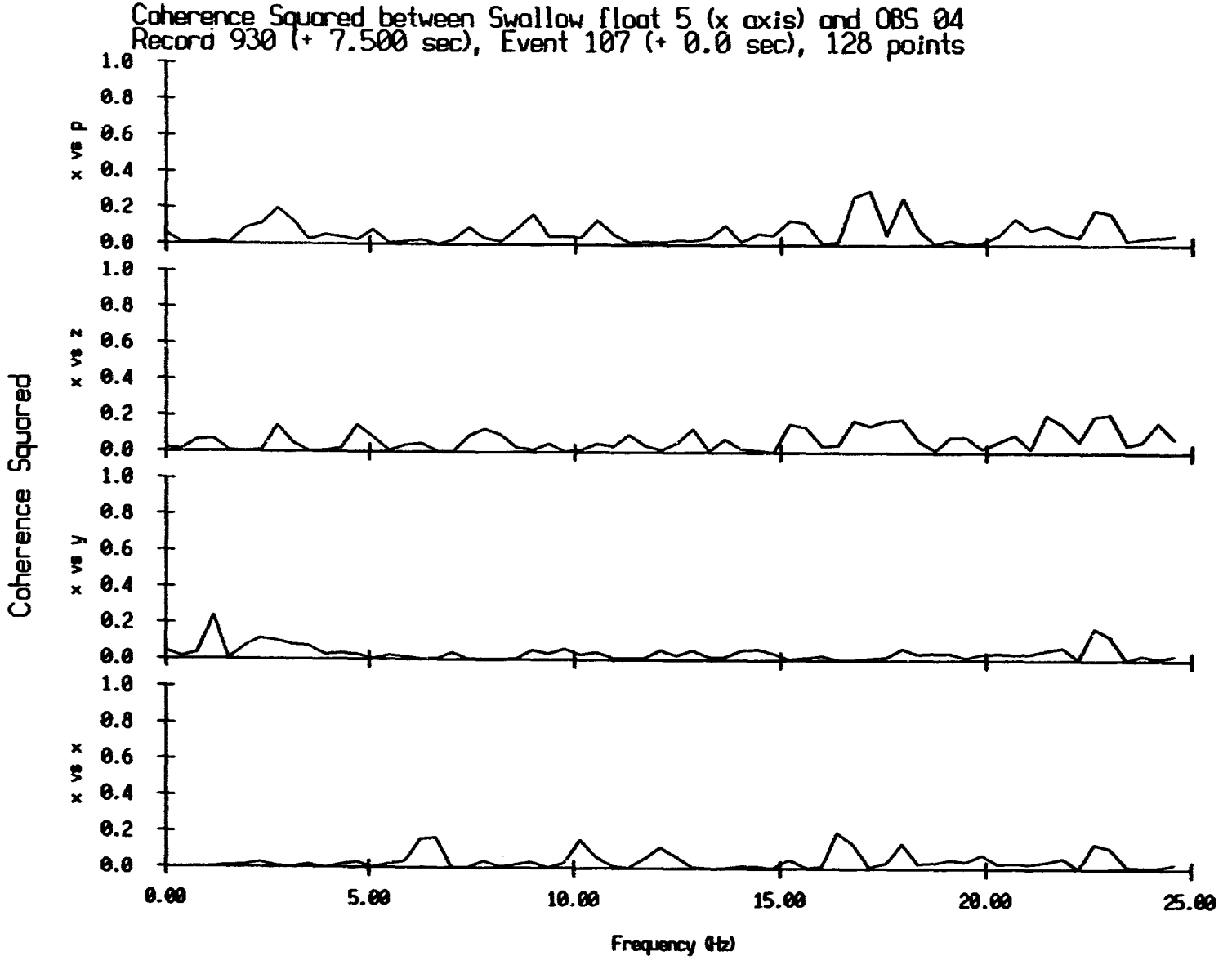

Figure VI.63i

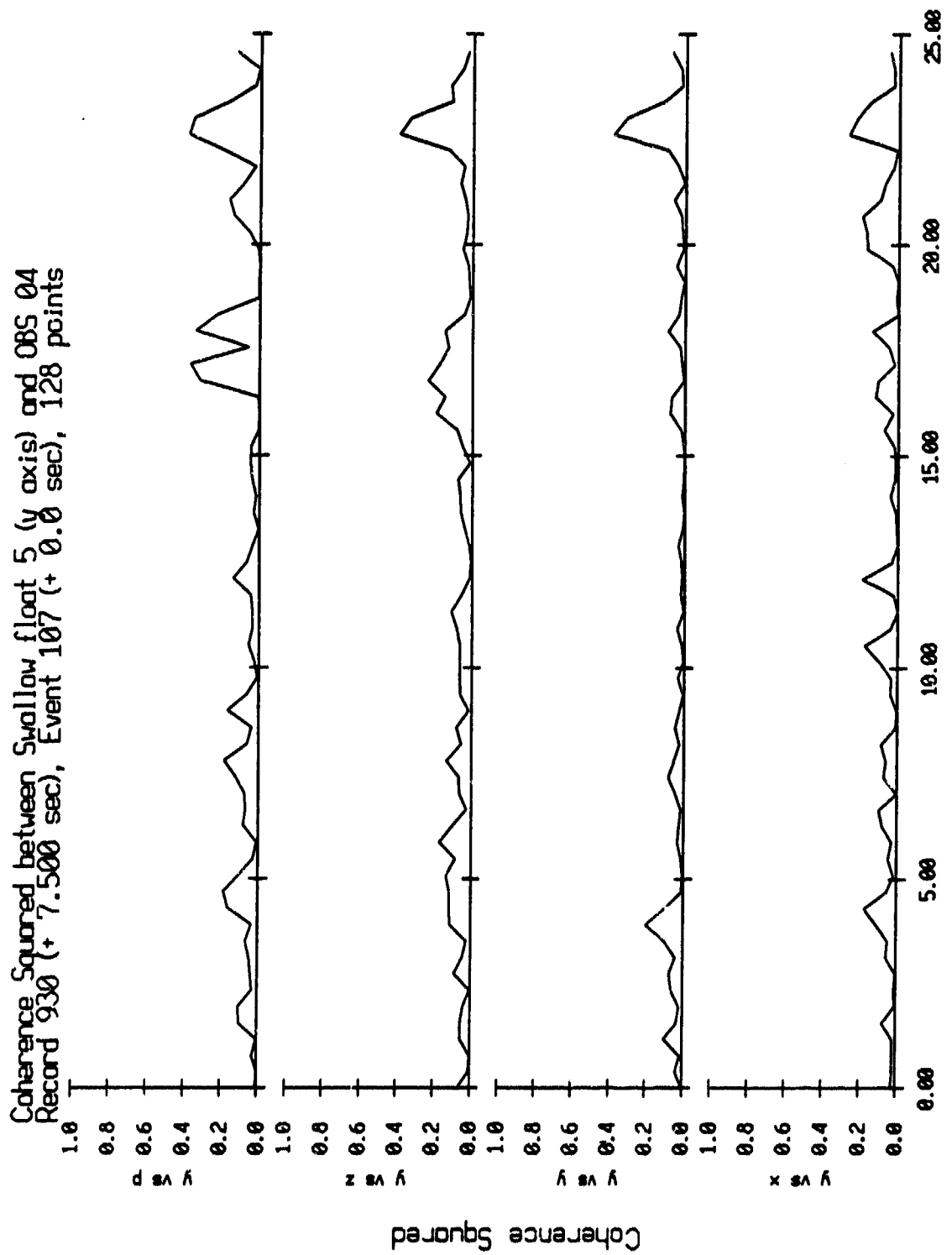

Figure VI.63j

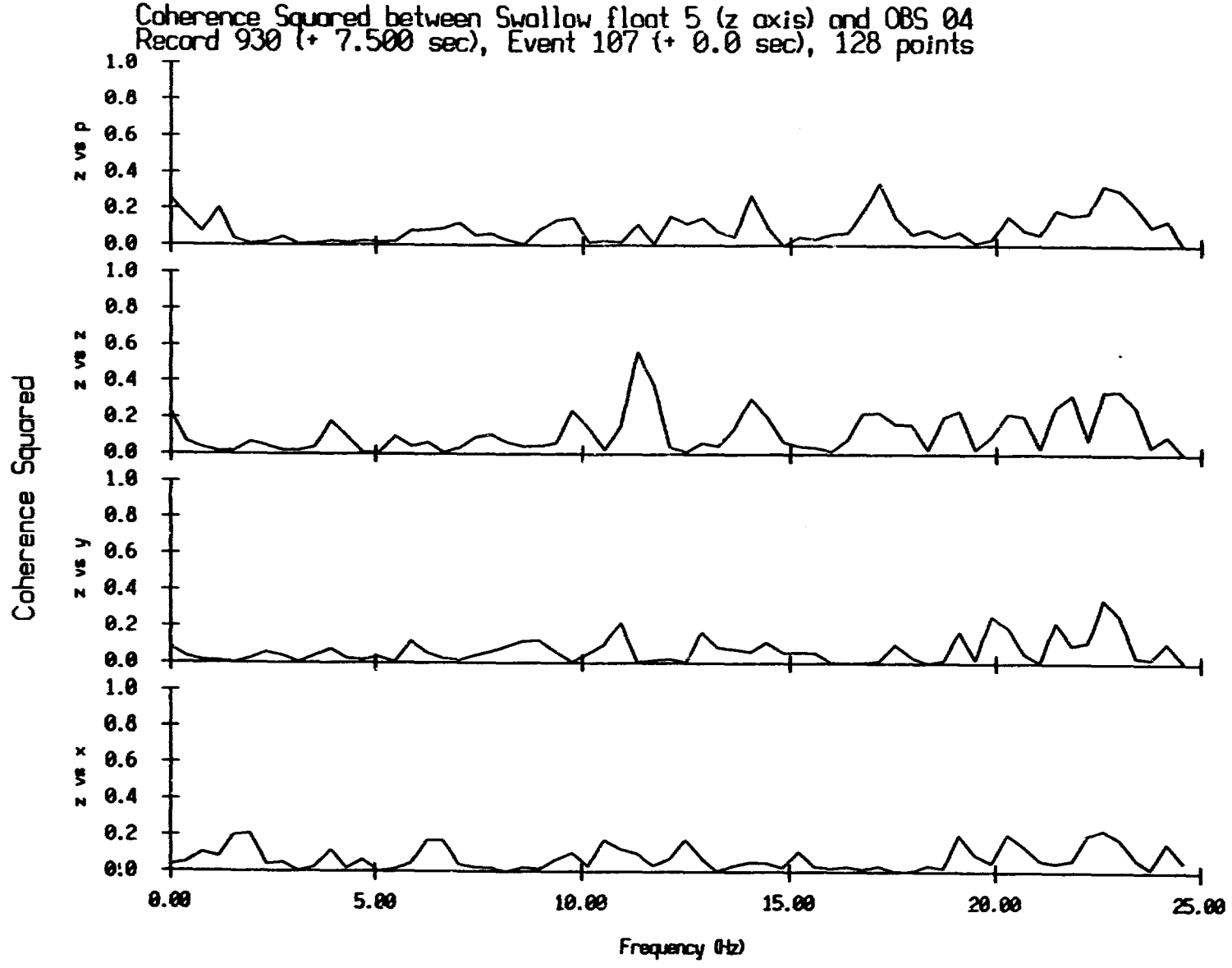

Figure VI.03k

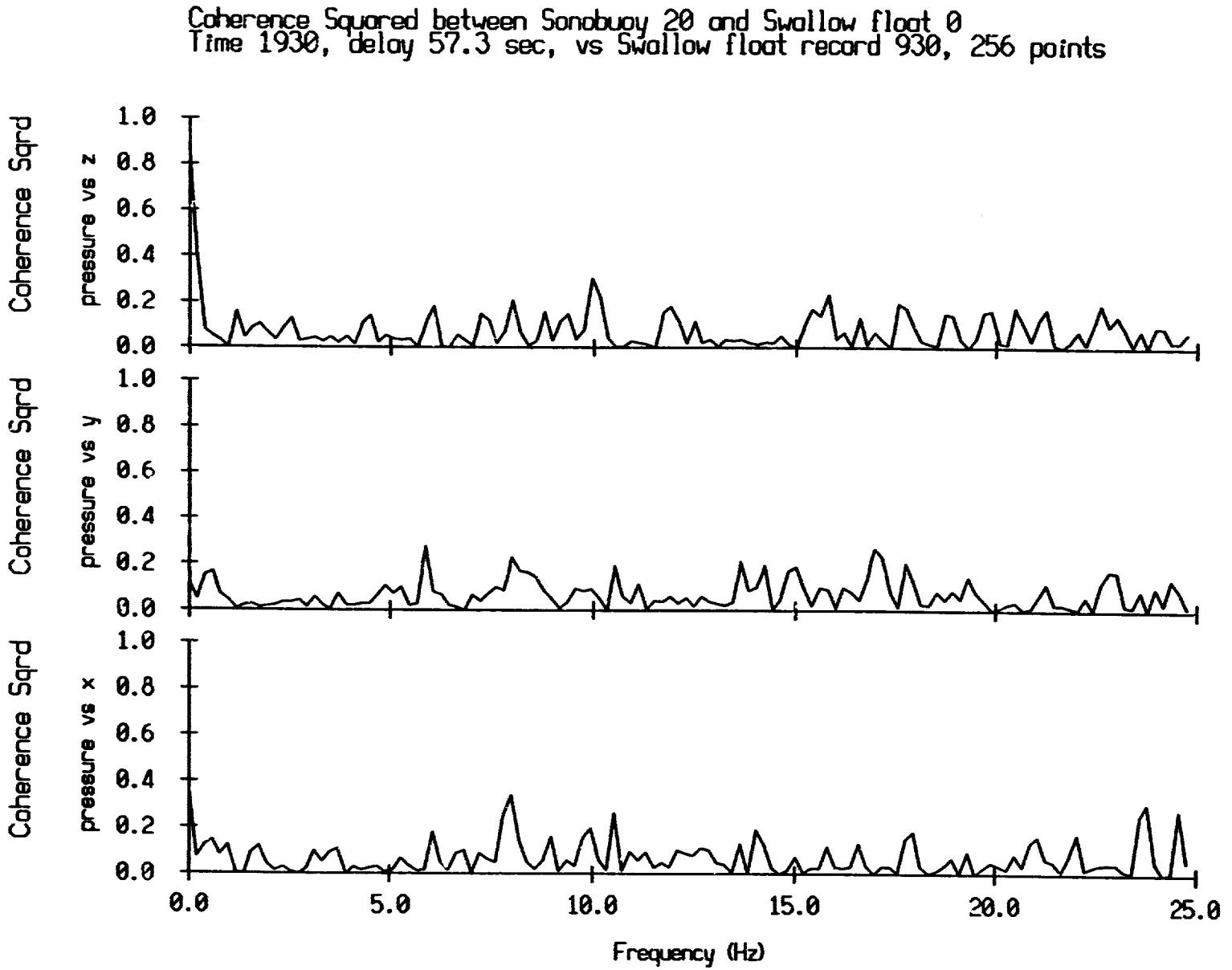
Coherence Squared between Sonobuoy 20 and Swallow float 0
Time 1930, delay 57.3 sec, vs Swallow float record 930, 256 points
Coherence Sqrd
pressure vs z
pressure vs y
pressure vs x
1.0
0.8
0.6
0.4
0.2
0.0
0.0
5.0
10.0
15.0
20.0
25.0
Frequency (Hz)

Figure VI.64

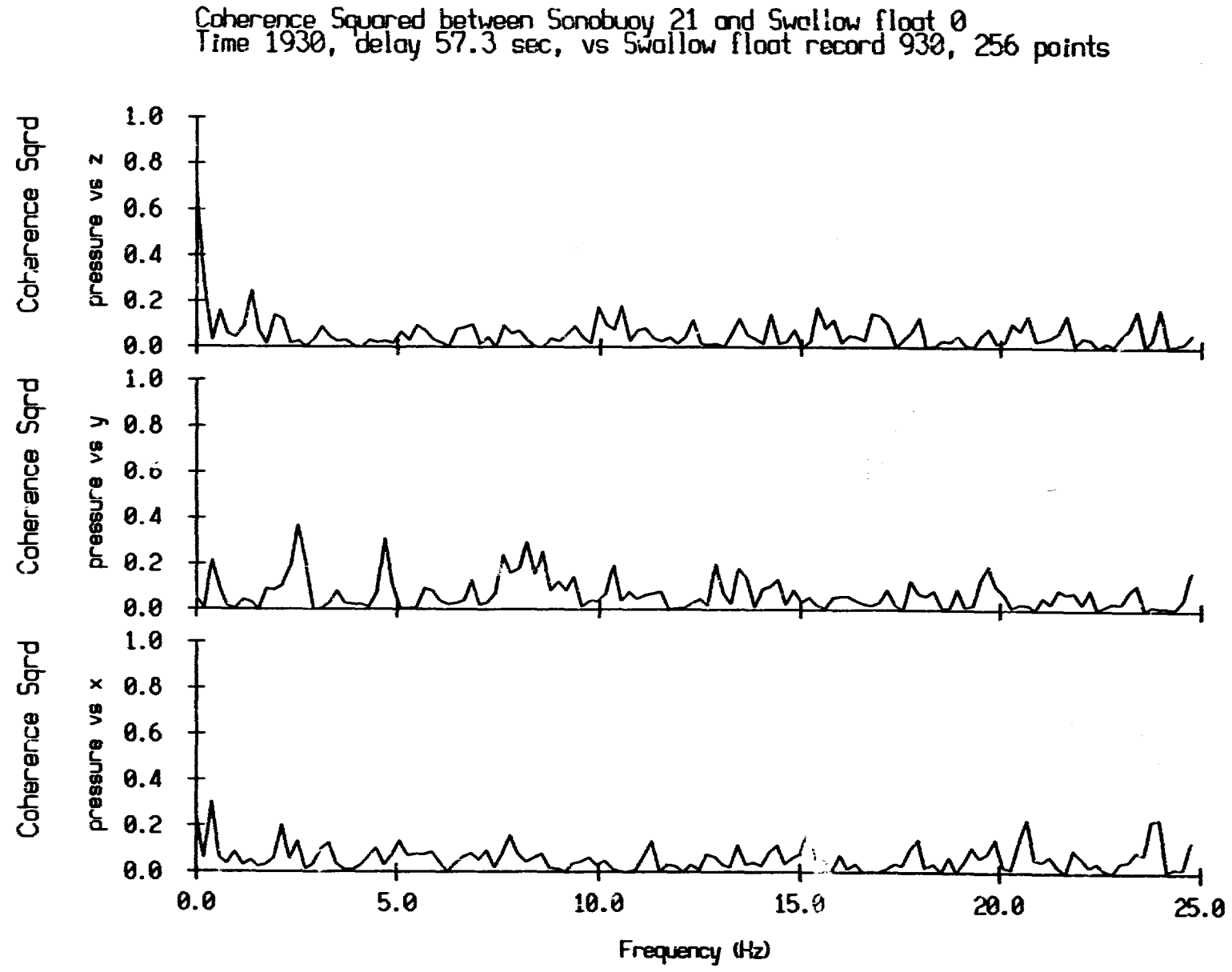
Coherence Squared between Sonobuoy 21 and Swallow float 0
Time 1930, delay 57.3 sec, vs Swallow float record 930, 256 points
Coherence Sqrd
pressure vs z
pressure vs y
pressure vs x
1.0
0.8
0.6
0.4
0.2
0.0
0.0
5.0
10.0
15.0
20.0
25.0
Frequency (Hz)

Figure VI.65

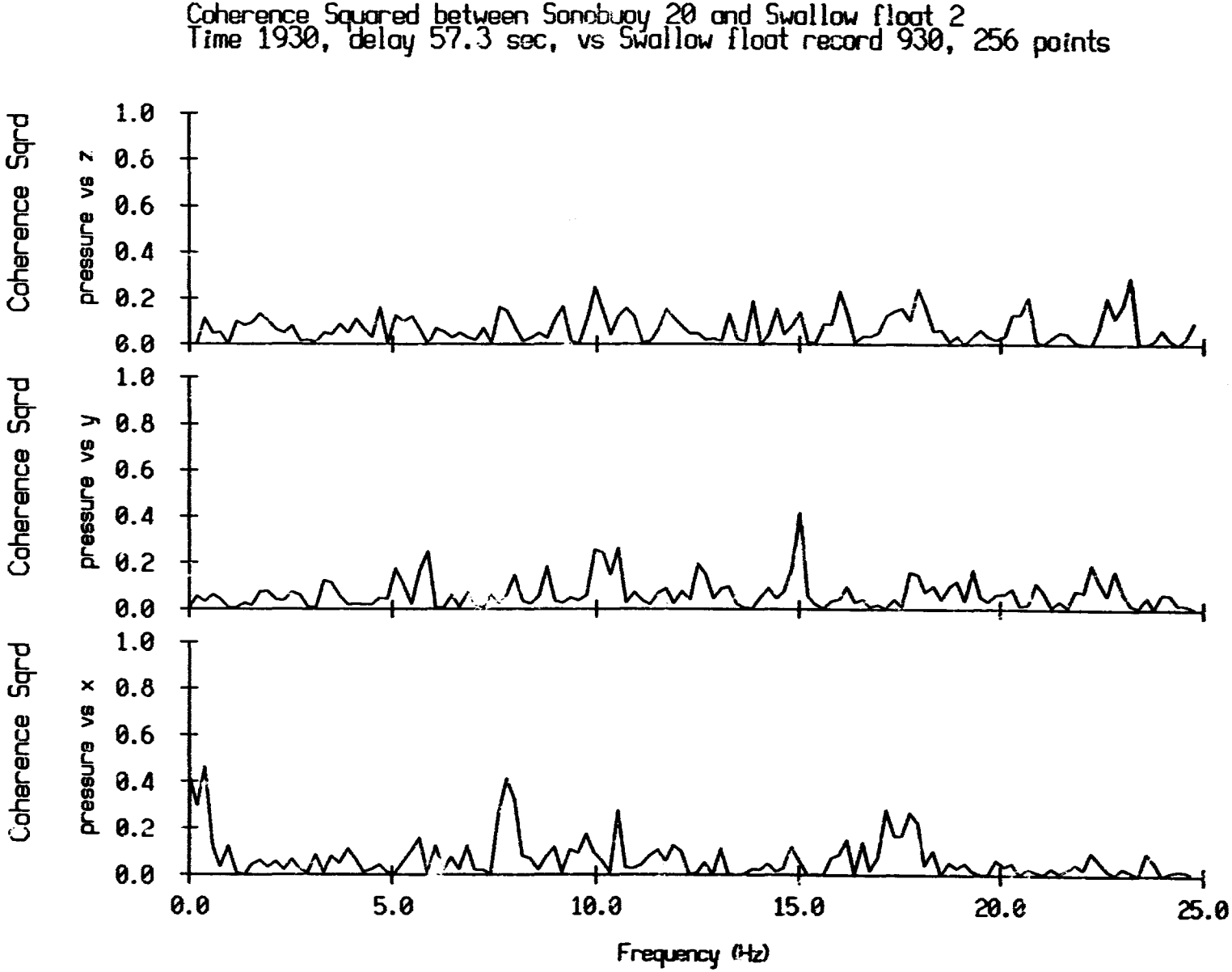
Coherence Squared between Sonobuoy 20 and Swallow float 2
Time 1930, delay 57.3 sec, vs Swallow float record 930, 256 points
Coherence Sqrd
pressure vs z
1.0
0.8
0.6
0.4
0.2
0.0
Coherence Sqrd
pressure vs y
1.0
0.8
0.6
0.4
0.2
0.0
Coherence Sqrd
pressure vs x
1.0
0.8
0.6
0.4
0.2
0.0
0.0
5.0
10.0
15.0
20.0
25.0
Frequency (Hz)

Figure VI.08

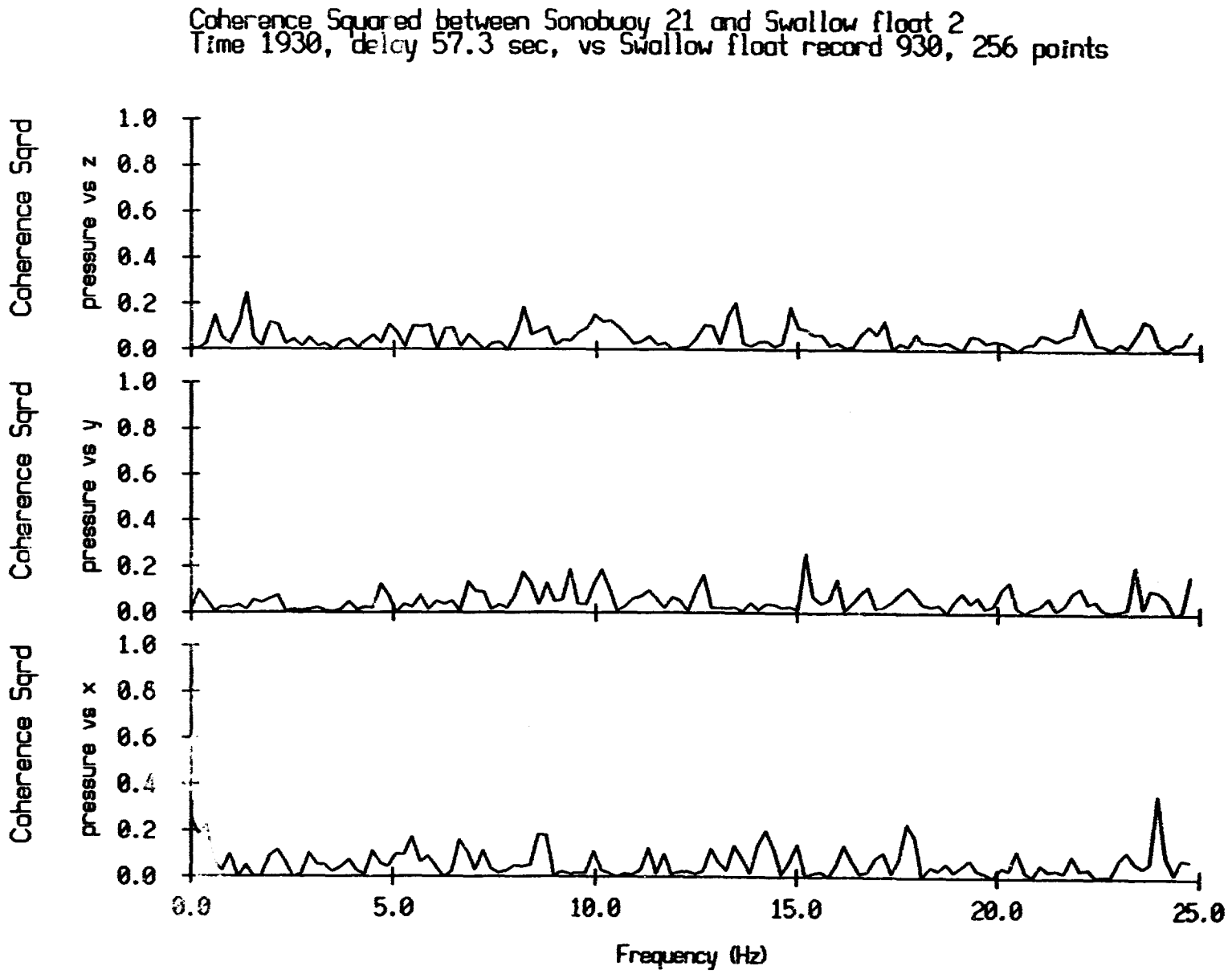
Coherence Squared between Sonobuoy 21 and Swallow float 2
Time 1930, delay 57.3 sec, vs Swallow float record 930, 256 points
Coherence Sqrd
pressure vs z
Coherence Sqrd
pressure vs y
Coherence Sqrd
pressure vs x
1.0
0.8
0.6
0.4
0.2
0.0
0.0
5.0
10.0
15.0
20.0
25.0
Frequency (Hz)

Figure V.87

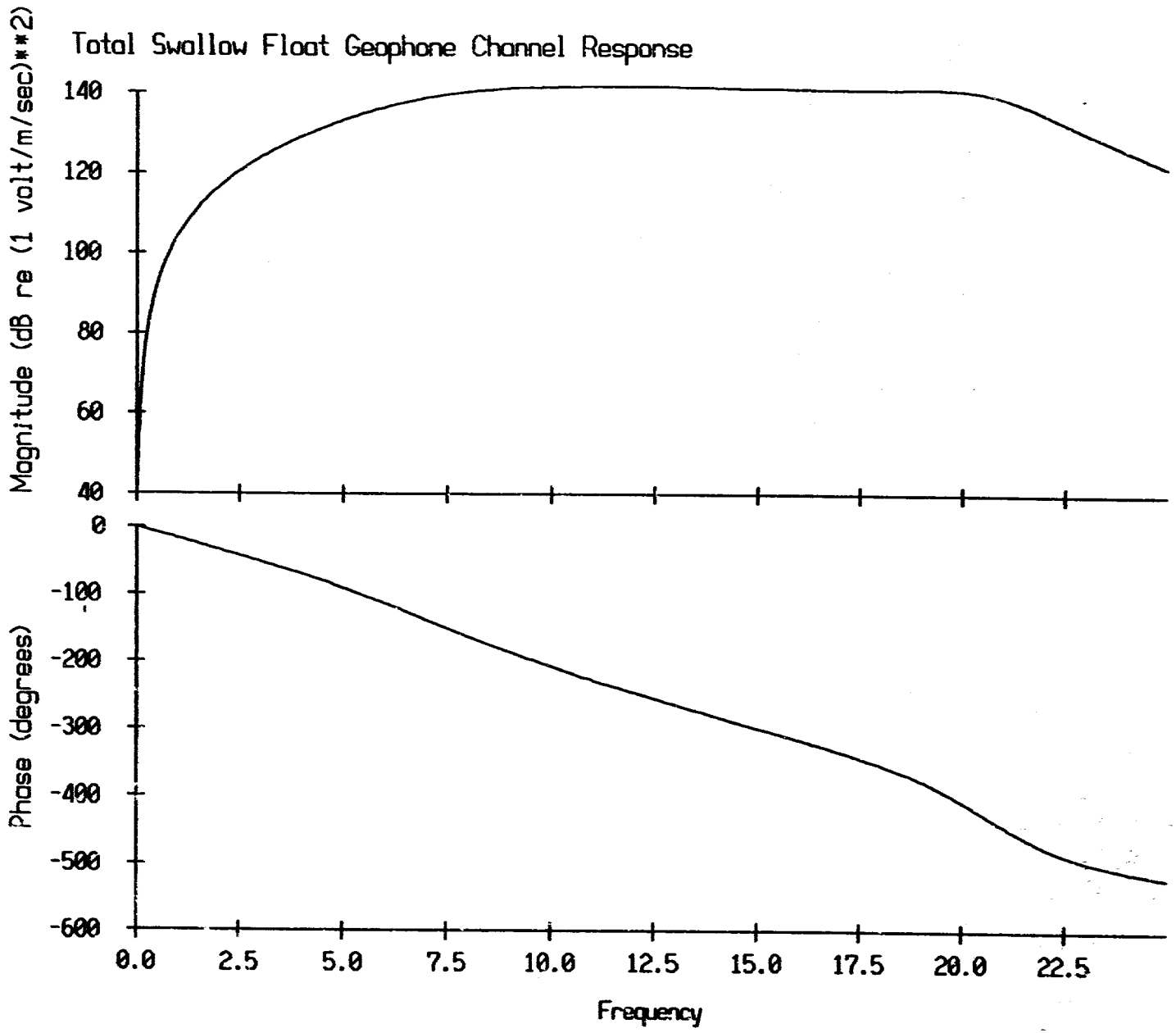
Total Swallow Float Geophone Channel Response
Magnitude (dB re (1 volt/m/sec)**2)
140
120
100
80
60
40
0
-100
-200
-300
-400
-500
-600
Phase (degrees)
0.0
2.5
5.0
7.5
10.0
12.5
15.0
17.5
20.0
22.5
Frequency

Figure A1

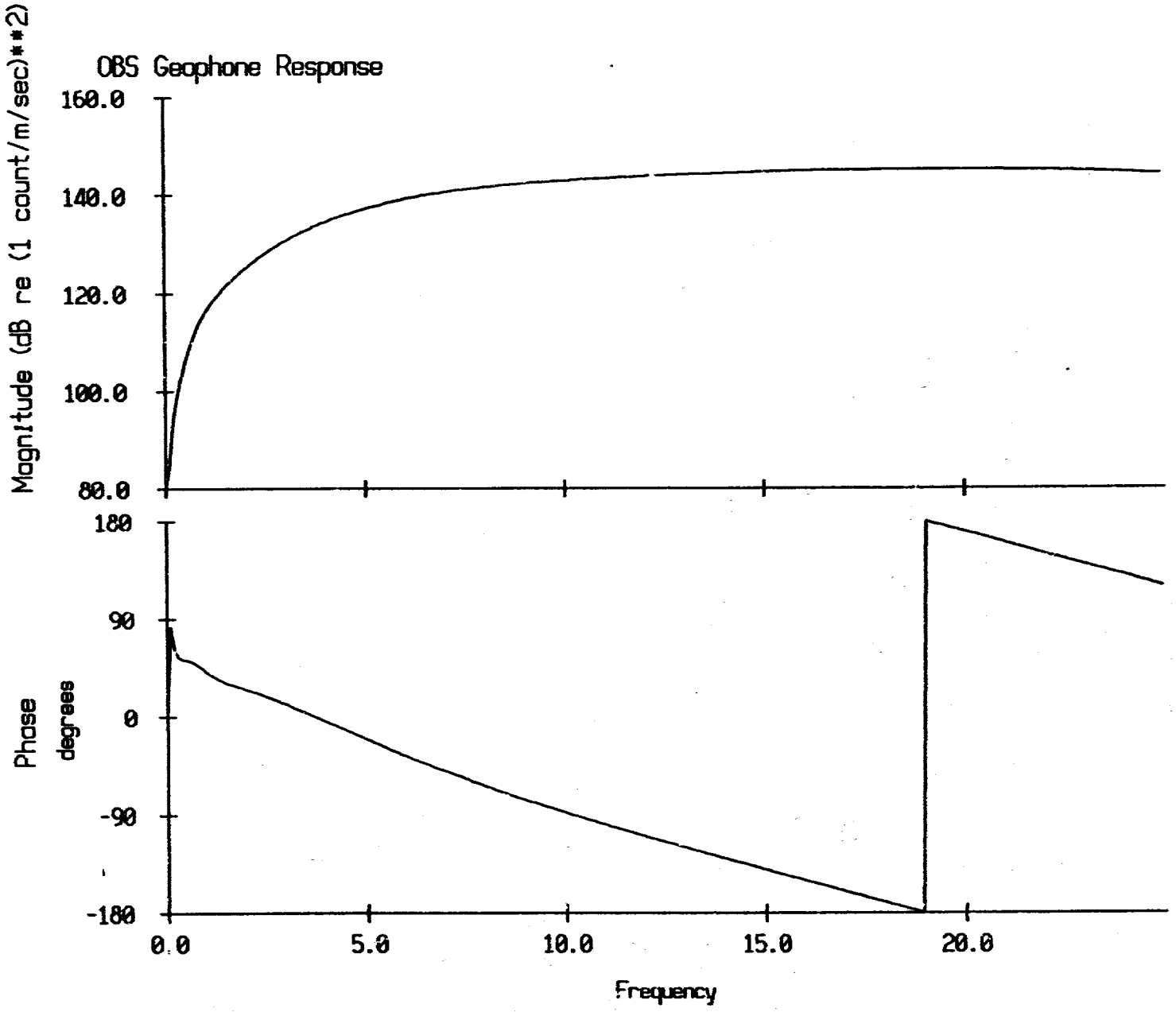
OBS Geophone Response
Magnitude (dB re (1 count/m/sec)**2)
160.0
140.0
120.0
100.0
80.0
180
90
0
-90
-180
Phase
degrees
0.0
5.0
10.0
15.0
20.0
Frequency

Figure A2

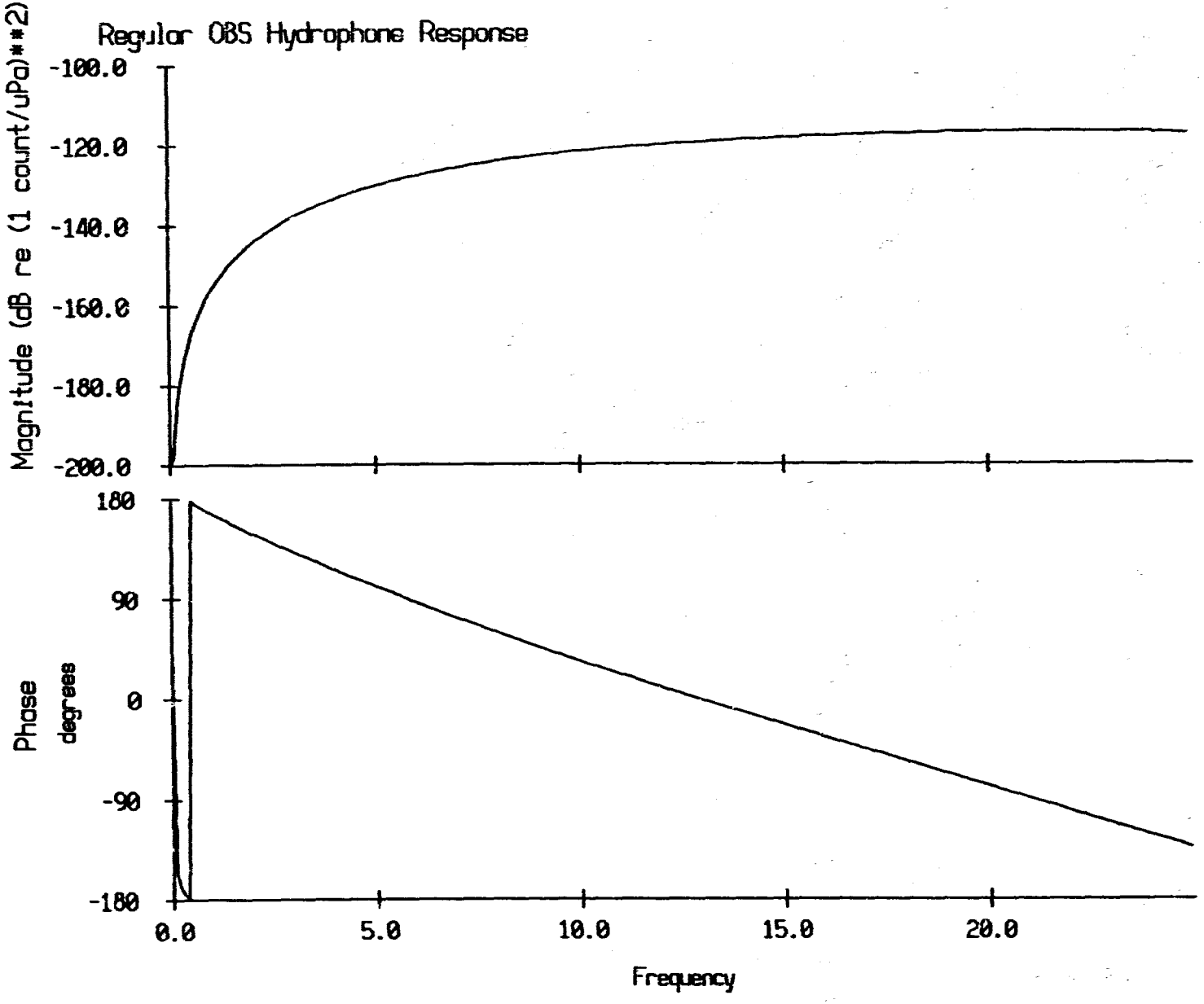
Regular OBS Hydrophone Response
Magnitude (dB re (1 count/uPa)**2)
-100.0
-120.0
-140.0
-160.0
-180.0
-200.0
180
90
0
-90
-180
Phase
degrees
0.0
5.0
10.0
15.0
20.0
Frequency

Figure A3

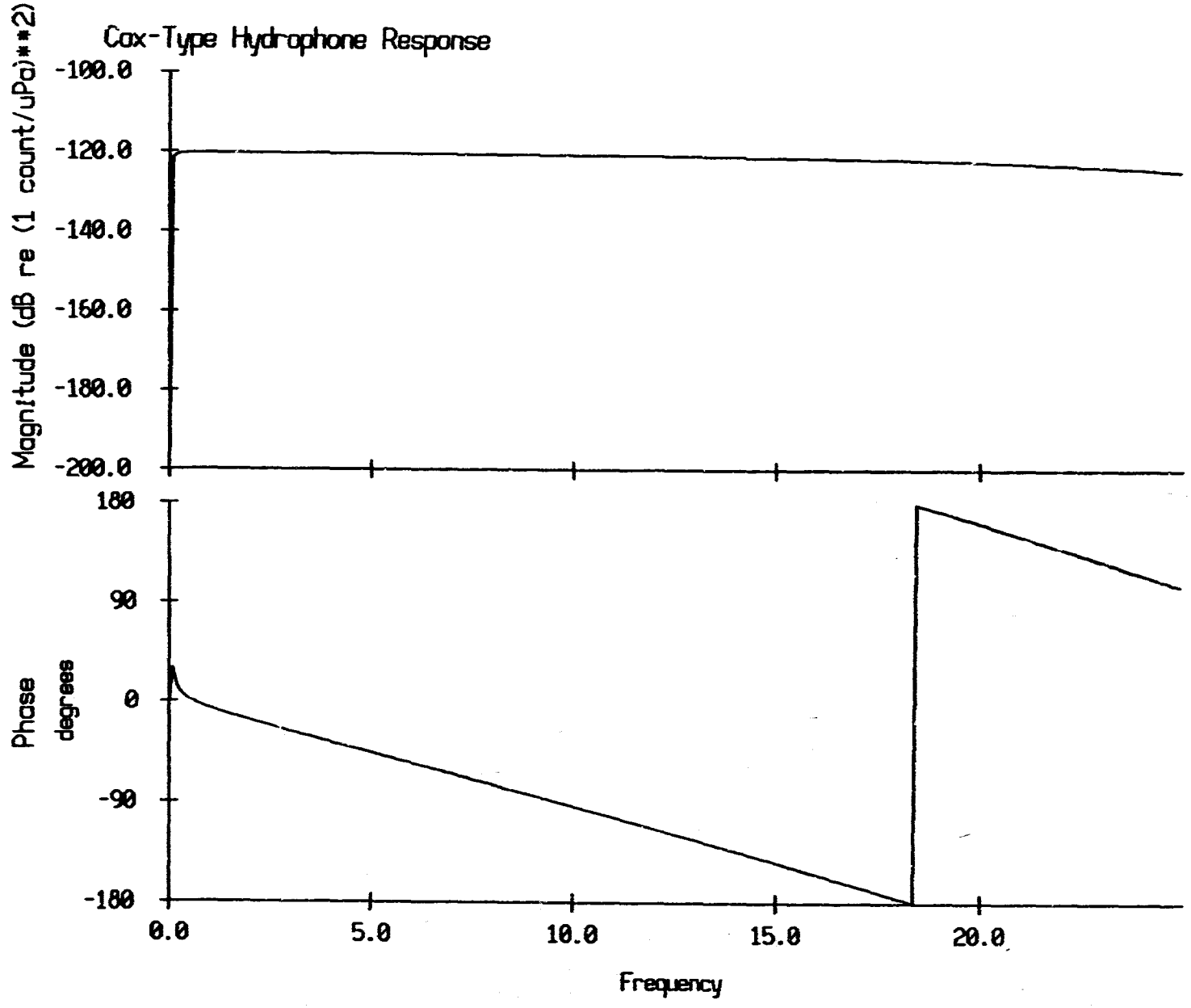
Cox-Type Hydrophone Response
Magnitude (dB re (1 count/uPa)**2)
-100.0
-120.0
-140.0
-160.0
-180.0
-200.0
Phase
degrees
180
90
0
-90
-180
0.0
5.0
10.0
15.0
20.0
Frequency

Figure A4

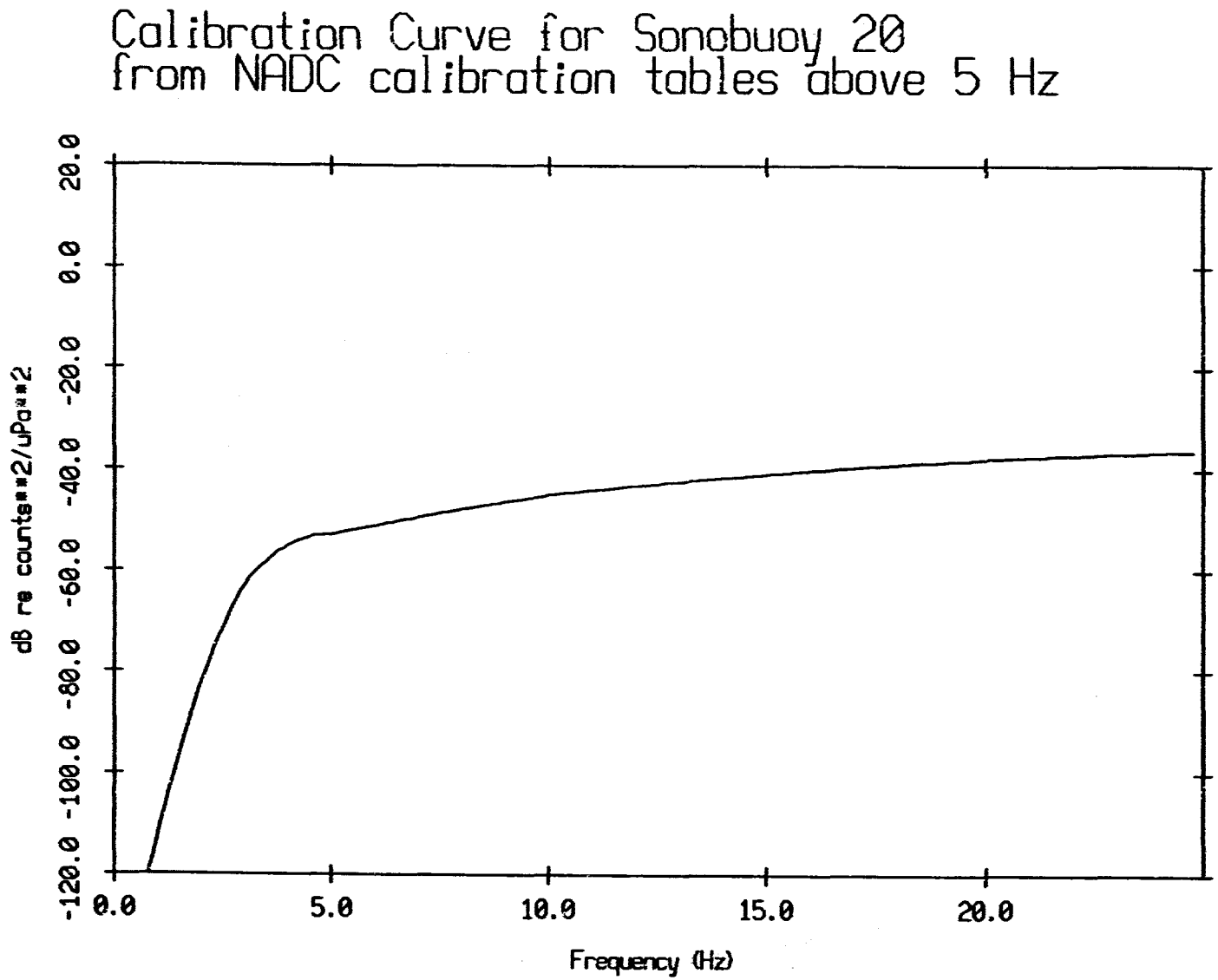
Calibration Curve for Sonobuoy 20
from NADC calibration tables above 5 Hz
dB re counts**2/uPa**2
20.0
0.0
-20.0
-40.0
-60.0
-80.0
-100.0
-120.0
0.0
5.0
10.0
15.0
20.0
Frequency (Hz)

Figure A5